

©

Advanced Topics of Theoretical Physics II

Advanced Solid-State Theory

Peter E. Blöchl

don't panic!

© Peter Blöchl, 2000-April 23, 2026
Source: https://phisx.org/

Permission to make digital or hard copies of this work or portions thereof for personal or classroom use is granted provided that copies are not made or distributed for profit or commercial advantage and that copies bear this notice and the full citation. To copy otherwise requires prior specific permission by the author.

[1]

[1] To the title page: What is the meaning of ΦSX? Firstly, it sounds like "Physics". Secondly, the symbols stand for the three main pillars of theoretical physics: "X" is the symbol for the coordinate of a particle and represents Classical Physics. "Φ" is the symbol for the wave function and represents Quantum Physics "S" is the symbol for the entropy and represents Statistical Physics.

Foreword and Outlook

A word of caution, before I start: This book is work in progress. You can use this book as a basis for following through the material presented in the course. But, you should never blindly copy formulas and apply them. The chances that there are still errors is still too large. However, the goal of this lecture is that the reader is able to convince themself, whether it is correct what he learns. For this purpose, I provide explicit derivations of all the material presented in this lecture and I make an effort to provide guidance to make careful reading as easy as possible.

My aim is to include all proofs in a comprehensive and hopefully water-tight manner. I am also avoiding special systems of units. I consider this important in view of a large variety of notations, differing definitions etc. While the proofs have the advantage to train the student to perform the typical operations, it clutters the course with material far from applications. Therefore, I have placed many of the more detailed derivations into appendices. It is strongly recommended to follow through the derivations. On the graduate level, the student should be able to follow the proofs without problem.

This book provides an introduction into the quantum mechanics of the interacting electron gas. It aims at students at the graduate level, that already have a good understanding on one-particle quantum mechanics.

The goal of the lecture is that the student

- understands language of many-particle quantum mechanics using many-particle wave functions, field operators and Green's functions.
- understands the approach to many-particle physics both using Green's functions as well as from the point of view of density-functional theory.
- is familiar with many-electron Green's functions, their meaning and properties
- understands the main theorems underlying the perturbation expansion of Green's functions, including Feynman diagrams.
- understands both time-dependent as well as finite-temperature formulation of Green's functions

In the online version of my lecture notes, there are many hyperreferences that allow one to jump to the relevant information in the book. The hyperlinks do not stand out because they have a different color. Thus, it is important to know where the hyperlinks are. The following items are hyperlinks:

- items in the list of contents will take you to the corresponding section.
- references to equation numbers, figures, tables, sections, appendices, etc. will take you to the indicated object.
- citations will take you to the corresponding position in the list of references

It is recommended that the student is already familiar with the one-particle description of the electronic structure of solids, because the present text implicitly builds on these concepts. These

foundations are provided in the preceding volume of the ΦSX series *"Introduction to solid-state theory"*[1].

My lectures do not follow a particular text, but they reflect my personal approach to the problem. Nevertheless it is useful and it will often be necessary to consult other text books. For the section on Green's function, I strongly recommend the book by Stefanucci and van Leeuwen[2]. It makes use of a unified view of zero-temperature, finite-temperature and non-equilibrium Green's functions, which is similar to the present text. A solid, rather detailed, reference employing the more traditional view is the text by Fetter and Walecka [3]. The book of Mattuck [4] presents a very intuitive approach to Feynman diagrams. The book of P. Fulde[5] provides a wealth of physical insight and, in addition, it connects to the quantum chemical point of view.

Here a incomplete chronological list of textbooks:

- Kadanoff, Baym (1962) "Quantum Statistical Mechanics: Green's function Methods in Equilibrium and Nonequilibirum Problems"[6]
- Abrikosov, Gorkov, Dzyaloshinski (1965) *"Methods of Quantum Field Theory in Statistical Physics"*[7]
- Mattuck (1967) *"A guide to Feynman diagrams in the many-body problem"*[4]
- Fetter, Walecka (1971) *"Quantum theory of many-particle systems"* [3]
- Stefanucci, van Leeuwen, (2013) *"Nonequilibrium Many-Body theory of Quantum systems"*[2]

Another excellent book on many-particle physics, which, however, concentrates on path integrals, a quite different approach from the one used in my text, is the book by Negele and Orland [8]. A recommended reading are the Lecture notes[9] by Wolf-Dieter Schöne.

With the present lecture notes, I hope to provide a solid ground on the subject of many-electron Green' functions. In order to make use of it, it will be necessary to specialize and extend this background. For this purpose, I recommend the lecture notes of the Julich autumn schools on correlated electrons. The lecture notes of these schools are freely available at

`https://www.cond-mat.de/events/correl.html`

Some Thoughts

The emphasis of this book is on the structure of the theory and the underlying concepts. For this reason I often refer to the real-space and time representation rather than starting from momenta and energies. The latter are derived from the former after introducing the corresponding symmetries. Making the underlying principles evident is also the reason for describing non-equilibrium Green's functions, from which the zero-temperature and finite-temperature (Matsubara) formalism can be derived.

Many-particle quantum mechanics comes in several flavors, the most prominent being the following.

- So-called wave function approaches, which directly deal with many-particle wave functions. Wave function approaches are commonly used by quantum chemists.
- Many-particle Green's-function approaches. Green's-function approaches are best known from Feynman diagrams, which are one of the prominent tools in this methodology. Many-particle Green's function are close to spectroscopic measurements of excitations.
- effective independent-particle descriptions such as density-functional theory. Here, the physical description is very similar to that of non-interacting electrons, while the interaction are taken into account approximately as in the Hartree-Fock approximation, or exactly as in the density-functional theory. Density-functional theory is the basis of first-principle calculations of solids.

While the focus of this lecture is on Green's functions, the intent of this lecture is to also show the link to other descriptions.

Contents

I Lecture notes **1**

1 Non-interacting electrons **3**

1.1 One-particle quantum mechanics . . . 3
1.1.1 One-particle Schrödinger equation . . . 3
1.1.2 Notation . . . 3
1.1.3 Spin orbitals . . . 4
1.1.4 Frequently used observables . . . 5
1.1.5 Discrete and continuous spectra of quantum states . . . 8
1.1.6 Momentum eigenstates . . . 9
1.1.7 Non-orthonormal and local orbitals . . . 10
1.1.8 Bloch theorem . . . 12
1.2 Functionals and their derivatives . . . 17
1.3 N-particle wave functions . . . 19
1.3.1 N-particle states . . . 19
1.3.2 Product states . . . 19
1.3.3 Slater determinants . . . 20
1.4 Many-particle states and Fock space . . . 22
1.4.1 Occupation-number representation . . . 23
1.4.2 Many-particle states of non-interacting electrons . . . 24
1.4.3 Size of Hilbert spaces . . . 24
1.5 Home study and practice: Simple one-particle problems . . . 25
1.5.1 Hydrogen molecule . . . 26
1.5.2 General diatomic molecule . . . 28
1.5.3 Linear chain of hydrogen atoms . . . 33
1.5.4 Insulating linear chain . . . 36
1.5.5 Free-electron gas or jellium model . . . 41

2 Weakly interacting electrons **47**

2.1 The setting . . . 48
2.2 Expectation values of Slater determinants . . . 49
2.2.1 One- and two-particle operators . . . 49
2.2.2 Expectation value of a one-particle operator with a Slater determinant . . . 50
2.2.3 One-particle-reduced density matrix . . . 52
2.2.4 Expectation value of a two-particle operator with a Slater determinant . . . 55
2.3 Total energy of a Slater determinant . . . 58
2.3.1 Hartree energy . . . 58

2.3.2 Exchange energy . . . 59
2.3.3 Non-interacting energy . . . 60
2.3.4 Total energy of a Slater determinant . . . 60
2.4 Exchange-correlation hole . . . 60
2.4.1 Two-particle density and exchange-correlation hole . . . 60
2.4.2 Properties of the exchange-correlation hole . . . 62
2.5 Energetics and thermodynamics in the Hartree-Fock approximation . . . 64
2.5.1 Ensembles of quantum states . . . 64
2.5.2 von-Neumann entropy . . . 65
2.5.3 Thermal ensembles and maximum-entropy principle . . . 66
2.5.4 Ensembles of Slater determinants . . . 67
2.5.5 Thermal ensembles of Slater determinants . . . 68
2.5.6 Boltzmann entropy . . . 70
2.5.7 Grand potential in the thermal Hartree-Fock approximation . . . 71
2.5.8 Selfconsistency . . . 72
2.5.9 Thermal ensemble in the THFA (optional) . . . 74
2.5.10 Misconceptions . . . 75
2.6 Spectral properties . . . 78
2.6.1 Excited states and the averaged-phase approximation (APA) . . . 78
2.6.2 Spectroscopies . . . 81
2.6.3 Energy balance in the inverse photoemission process . . . 84
2.6.4 Energy balance in optical absorption . . . 85
2.6.5 More or less approximations . . . 86
2.6.6 Spectral properties of the free-electron gas . . . 87
2.7 What is the Hartree-Fock approximation? . . . 91
2.8 Beyond Slater determinants . . . 92
2.9 Summary . . . 95
2.10 Further reading . . . 96
2.11 Home study and Practice . . . 97
2.11.1 Boltzmann entropy and Fermi distribution . . . 97
2.11.2 The hydrogen atom in the Hartree-Fock approximation . . . 99
2.11.3 Two one-dimensional particles in a box . . . 105
2.11.4 Two fermions in a 1d-box . . . 112
2.11.5 Toy model for the exchange-correlation hole . . . 121

3 Second quantization 129
3.1 Fock space . . . 129
3.2 Occupation-number representation . . . 130
3.3 Creation and annihilation operators . . . 132
3.4 Anticommutator relations . . . 135
3.5 Slater-Condon rules . . . 138
3.6 Operators expressed by creation and annihilation operators . . . 140
3.6.1 One-particle-reduced density matrix in second quantization . . . 141
3.7 Real-space-and-spin representation of field operators . . . 142
3.7.1 Anticommutator relations in real space . . . 143
3.7.2 One-particle operators in real space . . . 144

3.7.3 Interaction operator in real space . . . 145
3.7.4 Many-electron Hamiltonian in real space . . . 146
3.8 Creation and annihilation operators in a non-orthonormal representation . . . 146
3.9 From Hilbert space to Fock space and back . . . 146
3.9.1 From Hilbert space to Fock space and back . . . 146
3.10 Summary . . . 147
3.11 Home study and practice . . . 148
3.11.1 Hydrogen molecule with interacting electrons . . . 148
3.11.2 Spin eigenstates . . . 160
3.11.3 Ground state of the linear chain in second quantization . . . 165

4 Green's functions in one-particle quantum mechanics 167
4.1 Green's function as inverse of a differential operator . . . 167
4.1.1 Definition . . . 167
4.1.2 Two simple examples: . . . 168
4.1.3 Boundary conditions . . . 170
4.2 Green's function of a time-independent Hamiltonian . . . 170
4.2.1 In the time representation . . . 170
4.2.2 In the energy representation . . . 171
4.3 Green's function as propagator . . . 174
4.3.1 Definition of the propagator . . . 174
4.3.2 Relation between Green's function and propagator . . . 176
4.3.3 Propagator as time-ordered exponential . . . 176
4.4 Density of States . . . 178
4.4.1 Density of states from the Green's function . . . 179
4.4.2 Total density of states . . . 180
4.4.3 Electron density . . . 180
4.4.4 Green's function from the density of states . . . 180
4.5 Summary . . . 181
4.6 Home study and practice . . . 182
4.6.1 Role of boundary conditions . . . 182
4.6.2 Green's function for a Lorentzian-shaped density of states . . . 182

5 Composite and open systems: down-folding and retarded potentials 187
5.1 Systems in contact: down-folding . . . 187
5.1.1 Effective Schrödinger equation for an embedded system: . . . 190
5.2 Green's function of a system coupled to a bath . . . 194
5.2.1 Coupling to a bath in the energy representation . . . 195
5.2.2 Coupling to a bath in the time represenation . . . 196
5.3 Retarded and time-dependent potentials . . . 198
5.3.1 Time-independent Schrödinger equation with a retarded potential . . . 198
5.3.2 Time-dependent potential in an energy representation . . . 199
5.3.3 Summary . . . 200
5.3.4 Other uses of retarded or energy-dependent potentials . . . 200
5.4 Home study and practice . . . 201
5.4.1 Energy dependent Hamiltonian in the time representation . . . 201

5.4.2 Minimal model for a quantum system coupled to a bath . . . 201
5.4.3 System in contact with a bath having a finite life time . . . 208
5.4.4 Surface Green's function of a one-dimensional linear chain . . . 211
5.4.5 Construction . . . 219
5.4.6 Fano-Anderson model . . . 225
5.4.7 Construction: Downfold the positronic degrees of freedom in the Dirac equation 236
5.4.8 Construction: Inelastic tunneling . . . 237

6 Dynamics in Fock space and complex time 239
6.1 Propagator in Fock space . . . 239
6.2 Time as complex variable . . . 241
6.2.1 Motivation . . . 241
6.2.2 Definitions and working rules . . . 242
6.2.3 Memory hook . . . 243
6.2.4 Contour time-ordering operator . . . 245
6.2.5 Heisenberg operators . . . 246
6.3 Home study and practice . . . 247

7 Green's functions in many-particle physics 249
7.1 One-particle Green's functions in second quantization . . . 249
7.2 Propagate electrons in a non-interacting electron gas . . . 250
7.3 From the propagator of non-interacting electrons to the Green's function . . . 252
7.4 Propagate interacting electrons at finite temperature . . . 253
7.5 Contour-ordered Green's function of non-interacting particles . . . 254
7.6 Generality of the problem . . . 259
7.6.1 Initial state: . . . 259
7.7 Home study and practice . . . 260
7.7.1 Non-interacting contour Green's function for the non-interacting hydrogen molecule . . . 260
7.7.2 Bare contour Green's function of the homogeneous electron gas . . . 262

8 Exact properties of the many-particle Green's function 265
8.1 Equation of motion for the many-particle Green's function . . . 265
8.2 Self energy . . . 269
8.3 Expectation value of one-particle operators . . . 271
8.4 Migdal-Galitskii-Koltun (MGK) sum rule and total energy . . . 272
8.5 Home study and practice . . . 274
8.5.1 Self-energy and contour Green's function of the Hubbard atom . . . 274

9 Spectral properties 277
9.1 Lehmann amplitudes . . . 277
9.1.1 Motivation: Green's function in terms of Lehmann amplitudes . . . 277
9.1.2 What are Lehmann amplitudes? . . . 279
9.1.3 Lehmann amplitudes for ensembles of Slater determinants . . . 282
9.1.4 Lehmann amplitudes vs. quasi-particles vs. Dyson's orbitals . . . 283
9.2 Spectral function . . . 283
9.2.1 Definition . . . 283

9.2.2 Spectral function in Lehmann amplitudes: . . . 284
9.2.3 From the spectral function to the Green's function and back . . . 285
9.3 Energy representation for thermal ensembles . . . 287
9.3.1 Lehmann amplitudes . . . 287
9.3.2 Spectral function . . . 287
9.3.3 Green's function . . . 289
9.4 Home-study and practice . . . 291
9.4.1 Satellites in the spectral function . . . 291
9.4.2 Model for strongly retarded Green's function . . . 296
9.4.3 One-particle spectrum of the Hubbard dimer . . . 299
9.4.4 Anderson impurity model . . . 301
9.4.5 Spectral function and momentum density of a 1d chain . . . 302

10 Diagrammatic expansion of the Green's function 309
10.1 Interacting Green's function expressed by non-interacting ground states . . . 309
10.1.1 From Heisenberg to interaction picture: . . . 309
10.1.2 S-matrix . . . 311
10.1.3 Interacting from non-interacting ensemble: complex-time contour . . . 313
10.2 Wick's theorem . . . 316
10.2.1 Notation: incoming and outgoing indices . . . 317
10.2.2 Time order inside the interaction . . . 317
10.2.3 Alternating order inside the interaction . . . 318
10.2.4 Single step of Wick's theorem . . . 319
10.2.5 Sequence of Wick's iterations: . . . 322
10.2.6 Generalized Wick's theorem: Summary . . . 324
10.3 Perturbation expansion of the Green's function . . . 325
10.3.1 Outline . . . 325
10.3.2 Expansion of the S-matrix . . . 325
10.3.3 Expansion of the denominator of the Green's function . . . 326
10.3.4 Diagrams of the denominator . . . 327
10.3.5 Feynman diagrams . . . 327
10.4 Diagrams of the numerator of the Green's function . . . 329
10.4.1 Numerator from Wick's theorem . . . 329
10.4.2 Numerator from functional derivative of denominator . . . 331
10.5 Home study and practice . . . 337
10.5.1 Green's function from generating functional . . . 337

11 Diagrammatics of the generating functional 343
11.1 Classes of diagrams . . . 343
11.1.1 Green's function diagram . . . 343
11.1.2 Interaction diagram . . . 343
11.1.3 Self-energy diagrams . . . 344
11.1.4 Polarization diagram . . . 344
11.1.5 Vertex diagram . . . 344
11.1.6 Closed diagrams . . . 344
11.1.7 Linked diagrams . . . 344

11.1.8 One-particle-irreducible (1PI) diagrams . . . 344
11.1.9 Two-particle irreducible (2PI) diagrams . . . 345
11.1.10 Named diagrams . . . 345
11.2 Systematic construction of closed diagrams . . . 347
11.2.1 Construct all permutation vectors . . . 347
11.2.2 First-order diagrams . . . 348
11.2.3 Second-order diagrams . . . 349
11.3 Sign theorem . . . 350
11.4 Linked-cluster theorem . . . 353
11.5 Topologically-equivalent diagrams and symmetry factors . . . 358
11.5.1 Hand's-on for the evaluation of symmetry factors . . . 363
11.6 Systematic rule to construct all topologically distinct, linked, closed diagrams . . . 364
11.7 Systematic rule to evaluate Feynman diagrams . . . 365
11.7.1 Contour time and orbital basisset . . . 365
11.7.2 Contour time and real-space-and-spin representation . . . 367
11.8 Exploit the symmetry of the problem . . . 369
11.8.1 Exploit time-translation symmetry . . . 369
11.8.2 Exploit spatial translation symmetry . . . 370
11.8.3 Exploit spin-inversion symmetry . . . 370
11.8.4 Exploit Bloch theorem . . . 371
11.9 Zoo of diagrams . . . 371
11.9.1 First-order Hartree Fock . . . 371
11.9.2 Random-phase approximation (RPA) . . . 371
11.9.3 Ladder- or T-matrix approximation . . . 372
11.9.4 Fluctuation-exchange (FLEX) approximation . . . 372
11.10 Home study and practice . . . 373
11.10.1 Enumerate permutations . . . 373
11.10.2 Feynman diagrams from permutation vectors . . . 374
11.10.3 Evaluate symmetry factors . . . 377
11.10.4 Value of a given Feynman diagrams . . . 381
11.10.5 Example: Evaluate the Green's function for a specific example . . . 381
11.11 Summary . . . 381

II Additional topics 383

12 Luttinger-Ward functional 385
12.1 Compact notation: Generalized matrix algebra . . . 385
12.2 From our generating functional $\mathcal{Q}_{T,\mu}[G^{(0)}]$ to the Luttinger-Ward functional . . . 386
12.2.1 Domain of the Luttinger-Ward functional . . . 389
12.3 Skeleton expansion: diagrams of the Luttinger-Ward functional . . . 391
12.4 Summary on the Luttinger-Ward functional . . . 394

13 Shift the reference 397
13.1 Separating out the Hartree term . . . 397
13.2 Density-functional theory as reference . . . 398
13.2.1 DFT Green's function . . . 400

14 Common approximations **403**
14.1 Hartree-Fock approximation . . . 403
14.1.1 First-order skeleton diagrams . . . 403
14.1.2 Luttinger-Ward functional in the Hartree-Fock approximation . . . 404
14.2 Second-order Born approximation . . . 405
14.3 Diagrammatic sequences that can be summed up analytically . . . 406
14.4 Random-Phase approximation . . . 408
14.5 T-matrix approximation . . . 410
14.6 Fluctuating-exchange approximation (FLEX) . . . 410
14.7 Compact notations . . . 410
14.7.1 Combined vertex indices . . . 410

15 Functional of the Green's function and the screened interaction **413**

16 Linear response and Kubo formula **417**
16.1 Linear-response theory . . . 417

17 Models in many-particle theory **421**
17.1 Jellium model . . . 422
17.1.1 The model . . . 422
17.1.2 Fermi-liquid theory . . . 423
17.1.3 Landau expansion . . . 423
17.1.4 Long lifetime of low-energy quasi-particles . . . 426
17.1.5 Spectral function of Fermi-liquid theory . . . 428
17.1.6 Some background material on Fermi liquid theory . . . 431
17.1.7 A brief outlook to Fermi-Liquid theory . . . 431
17.2 Hubbard model . . . 435
17.2.1 Physics of the Hubbard model . . . 435
17.2.2 Hubbard atom . . . 436
17.2.3 Hubbard dimer . . . 444
17.2.4 Hubbard chain . . . 448
17.3 Heisenberg model . . . 450
17.3.1 The model . . . 450
17.3.2 Outlook on phenomena . . . 451
17.3.3 Quantum fluctuations in the antiferromagnetic ground state . . . 451
17.3.4 Magnons . . . 457
17.4 Anderson impurity model . . . 460
17.4.1 Anderson dimer . . . 460
17.4.2 Weak-contact limit of the Anderson impurity model . . . 463
17.5 Holstein model for polarons . . . 466
17.5.1 Holstein monomer . . . 467
17.5.2 Holstein dimer . . . 468
17.5.3 Extended Holstein model . . . 469
17.6 Bardeen-Cooper-Schrieffer model for superconductivity . . . 469
17.7 Su-Schrieffer-Heeger model for solitons and topological insulators . . . 470
17.7.1 Electronic structure with frozen displacements . . . 471
17.8 Light-matter interaction . . . 474

17.8.1 Introduction . . . 474
17.8.2 Jaynes-Cummings model . . . 474
17.8.3 Wigner-Weisskopf theory . . . 478
17.8.4 Related models . . . 482
17.8.5 Quantization of photons . . . 482

18 Organization and examination 487
18.1 Teaching goals . . . 487
18.2 Examination . . . 487
18.3 Summary . . . 489
18.4 Todo . . . 491
18.5 Distribution of the teaching load . . . 491
18.6 List of exercises . . . 493
18.7 Timeline 2024 . . . 495
18.8 Timeline 2026 . . . 496

III Appendices 497

A Mathematical expressions 499
A.1 Crazy idea: representation of the entropy . . . 499
A.2 Laplace expansion theorem (not needed) . . . 500
A.3 Fourier transforms . . . 501
A.3.1 Choices . . . 501
A.3.2 Fourier transform of the step function . . . 501
A.4 Wirtinger derivatives . . . 502
A.5 Cauchy relation . . . 504
A.6 Imaginary part of a pole and spectral density . . . 504
A.7 Padé approximation . . . 505
A.7.1 Problems . . . 506
A.7.2 Least-square Padé . . . 506
A.8 Baker-Hausdorff Theorem . . . 508
A.8.1 Baker-Hausdorff Theorem . . . 508
A.8.2 Hadamard Lemma . . . 509
A.9 Sum rules related to the f-sum rule . . . 510
A.9.1 General derivation by Wang . . . 510
A.9.2 f-sum rule or Thomas-Reiche-Kuhn sum rule . . . 511
A.9.3 Bethe sum rule . . . 512
A.10 Friedel sum rule . . . 512
A.11 Sherman-Morrison Formula . . . 515

B Non-orthonormal basissets 517
B.1 Creation and annihilation operators for non-orthonormal orbitals . . . 517
B.1.1 Operators and matrix elements . . . 519

C Fermions and bosons 523

D Hubbard dimer and hydrogen molecule **527**
D.1 Asymmetric two-site model . . . 527
D.1.1 Symmetry-adapted many-particle states . . . 528
D.2 Hubbard dimer . . . 534
D.2.1 Symmetry-adapted many-particle states . . . 535
D.2.2 Spectral function of the Hubbard dimer . . . 538
D.3 Anderson dimer . . . 540
D.3.1 Many-particle eigenstates . . . 541
D.3.2 Spectrum . . . 543
D.3.3 Andersen dimer and the Hartree-Fock method . . . 543
D.4 Hydrogen atom . . . 549
D.5 Hydrogen molecule . . . 552
D.5.1 Two-center integral of spherical functions . . . 553
D.5.2 Overlap . . . 553
D.5.3 Coulomb repulsion between the protons . . . 555
D.5.4 Electron-proton interaction matrix elements . . . 555
D.5.5 Electron-nucleus Coulomb matrix elements . . . 555
D.5.6 U-tensor . . . 555
D.6 Dihydrogen cation . . . 560

E Homogeneous electron gas **561**
E.1 Energy contributions of the homogeneous electron gas . . . 561
E.2 Non-interacting homogeneous electron gas . . . 561
E.2.1 Gradient correction of the kinetic energy . . . 563
E.3 Hartree-Fock description of the free-electron gas . . . 565
E.3.1 Exchange potential as non-local potential . . . 565
E.3.2 Exchange energy of the homogeneous electron gas . . . 568
E.3.3 Energy-level shifts by the exchange potential . . . 569
E.3.4 Density of states of the free-electron gas . . . 572
E.3.5 Exchange hole of the free-electron gas . . . 574
E.4 Polarization insertion . . . 575
E.4.1 Polarisation insertion for homogeneous systems . . . 576
E.4.2 Material-specific term $K_{\vec{q}}(\epsilon, \epsilon')$ . . . 579
E.4.3 Geometric problem . . . 580
E.4.4 Free electron gas at zero temperature . . . 582
E.4.5 Frequency moments of the polarization . . . 590
E.4.6 Fourier transform of the Coulomb potential . . . 593
E.4.7 Screened interaction and dielectric constant . . . 596

F Additional topics on Downfolding **599**
F.1 Embedding in the time domain . . . 599

G Hartree-Fock approximation **603**
G.1 Boltzmann entropy . . . 603
G.1.1 Definition . . . 603
G.1.2 Maximum-entropy ensemble for a one-particle-reduced density matrix . . . 604
G.1.3 Functional form of the Boltzmann entropy . . . 607

G.1.4 Fermi and Bose distribution . . . 608
G.1.5 Dilute limit (Boltzman distribution) . . . 608
G.1.6 Summary . . . 609
G.2 Averaged-phase approximation . . . 610
G.3 Correlated occupation-number fluctuations . . . 611
G.3.1 Two-orbital model . . . 611
G.3.2 Attempt to construct a new density-matrix functional . . . 615
G.4 Hartree-Fock equations in the zero-temperature case . . . 616
G.4.1 Prologue to this section . . . 616
G.4.2 Hartree-Fock equations . . . 616
G.4.3 Zero-temperature Hartree Fock in second quantization . . . 620
G.5 Contributions to exchange . . . 621
G.5.1 Decompose the exchange term into local orbitals . . . 622
G.5.2 Long-range exchange . . . 622
G.5.3 On-site exchange . . . 623
G.5.4 Bond-exchange . . . 627
G.6 Self-consistent Hartree-Fock code for finite temperatures . . . 631
G.6.1 Theoretical background . . . 632
G.6.2 Calculating one step of the HF loop . . . 638
G.6.3 Source code . . . 639
G.6.4 Generalization to periodic systems . . . 648
G.7 Spectral function in the Hartree-Fock approximation . . . 653
G.7.1 Spectral function of Hartree-Fock at finite temperatures . . . 653
G.7.2 Spectral function beyond the mean-field spectral function . . . 654
G.8 Excitations in the thermal Hartree-Fock approximation . . . 655
G.8.1 Green's function in the thermal Hartree-Fock approximation . . . 656
G.9 Post Hartree-Fock methods: Quantum chemistry . . . 658
G.9.1 Coupled cluster: . . . 658

H Density-functional theory **661**
H.1 Existence of a density functional for the energy . . . 661
H.1.1 The many-particle Hamiltonian . . . 661
H.1.2 The proof: constrained search . . . 662
H.2 More explicit proof at finite temperature . . . 663
H.2.1 Grand potential . . . 664
H.2.2 Helmholtz potential . . . 664
H.2.3 Density as fundamental variable . . . 665
H.2.4 Constrained search . . . 665
H.2.5 Exchange and correlation energy . . . 666
H.2.6 Kinetic-energy functional . . . 668
H.2.7 Self-consistent equations . . . 668
H.3 One-particle density matrices and two-particle densities . . . 670
H.3.1 Pair-correlation function and hole function . . . 670
H.4 Adiabatic connection . . . 671
H.5 Ideas that guide the construction of density functionals . . . 673
H.5.1 Screened interaction . . . 673

H.5.2 Hybrid functionals . . . 674
H.6 Scaling of with a fixed shape of the XC-hole function . . . 675
H.7 Local density functionals . . . 676
H.8 Local spin-density approximation . . . 678
H.8.1 Non-collinear local spin-density approximation . . . 678
H.9 Generalized gradient functionals . . . 678
H.10 Additional material . . . 682
H.10.1 Relevance of the highest occupied Kohn-Sham orbital . . . 682
H.10.2 Correlation inequality and lower bound of the exact density functional . . . 682
H.11 Reliability of DFT . . . 682
H.12 Deficiencies of DFT . . . 682

I Derivation of Slater-Condon rules 685
I.1 Maximum coincidence and orthonormality . . . 685
I.2 Matrix elements with identical Slater determinants . . . 685
I.2.1 Expectation value of a one-particle operator . . . 685
I.2.2 Expectation value of a two-particle operator . . . 687
I.3 Slater determinants differing by one orbital . . . 688
I.3.1 One-particle operator . . . 688
I.3.2 Two-particle operator . . . 689
I.4 Slater determinants differing by two orbitals . . . 691
I.4.1 One-particle operator . . . 691
I.4.2 Two-particle operator . . . 691
I.5 Slater determinants differing by more than two orbitals . . . 691

J One- and two-particle operators expressed by field operators 693
J.1 Matrix elements between identical Slater determinants . . . 694
J.2 Matrix elements between Slater determinants differing by one orbital . . . 695
J.3 Matrix elements between Slater determinants differing by two orbitals . . . 697

K Addenda to the equation of motion for the Green's function 699

L Derivation of Wick's theorem 703
L.1 Field operators in the interaction picture for complex time . . . 704
L.1.1 Proof for a time-dependent non-interacting Hamiltonian in the complex time plane . . . 704
L.1.2 Sanity check: One-orbital model . . . 709
L.2 Anticommutators of field operators in the interaction picture . . . 712
L.3 Commutating a field operator with the density matrix . . . 713
L.4 Contract the trace . . . 716
L.4.1 Single step of Wick's theorem . . . 716
L.4.2 Sequence of Wick's iterations: . . . 722
L.4.3 Wick's theorem for a product that is not time ordered . . . 723
L.4.4 Alternating order of annihilation an creation operators . . . 724
L.4.5 Final form of Wick's theorem . . . 725
L.4.6 Why is the time-ordered Green's function important? . . . 725
L.5 Non-interacting grand potential . . . 725

L.5.1 Grand potential of non-interacting electrons . . . 725
L.5.2 Fermi distribution from the grand potential of non-interacting fermions . . . 726
L.5.3 Grand potential of non-interacting fermions as functional of the non-interacting Green's function . . . 728

M Code for the construction of Feynman diagrams 731
M.1 Procedure to exclude disconnected diagrams . . . 731
M.2 Procedure to single out skeleton diagrams . . . 732
M.2.1 Skeleton diagrams last . . . 733
M.3 Procedure to single out interaction-skeleton diagrams . . . 733
M.3.1 Insertions . . . 733
M.4 Installation: . . . 734
M.5 Example: . . . 734
M.6 Code Description . . . 734
M.7 Source code: . . . 735
M.8 Low-order diagrams with symmetry factor and sign . . . 750
M.8.1 First order . . . 750
M.8.2 Second order . . . 751
M.8.3 Third order . . . 751
M.8.4 Fourth order . . . 752

N Second-order perturbation theory 757
N.1 Perturbation theory . . . 757
N.2 Ensembles of Slater determinants . . . 761

O Further material about Lehmann amplitudes 763
O.1 Equation of motion for Lehmann amplitudes . . . 763
O.1.1 Lehmann amplitudes and wave functions . . . 764
O.1.2 Spectral function in the average-phase approximation (APA) . . . 766
O.1.3 Comparison with Stefanucci . . . 768

P Dictionary and Symbols 773
P.1 English-German Dictionary . . . 773
P.2 Explanations . . . 773
P.3 Symbols . . . 773
P.4 Mathematical Symbols . . . 774
P.5 Vectors, matrices, operators, functions, etc. . . . 775
P.6 Generic conventions . . . 775
P.7 Symbols of physical quantities . . . 775
P.8 Comparison with Fetter Walecka . . . 777
P.9 Greek Alphabet . . . 777

Q About the PhiSX Series 779
Q.1 Philosophy of the PhiSX Series . . . 779
Q.2 About the Author . . . 780

Bibliography 783

Index **793**

Part I

Lecture notes

Chapter 1

Non-interacting electrons

In this section, I will remind of some concepts from quantum mechanics. While the material in this chapter is rather elementary, I will use it to make the reader familiar with my notation and the mathematical language, that will be used in the later chapters. A more detailed coverage is found in Blöchl, *ΦSX: Introduction to Solid-State Theory*.[1]

1.1 One-particle quantum mechanics

1.1.1 One-particle Schrödinger equation

The wave function of a single particle is described by a time-dependent Schrödinger equation.

$$i\hbar\partial_t|\psi(t)\rangle = \hat{h}(t)|\psi(t)\rangle \tag{1.1}$$

where $|\psi(t)\rangle$ is the quantum state and $\hat{h}(t)$ is the time-dependent Hamiltonian.

If the Hamiltonian $\hat{h}$ is time-independent, the problem is invariant under time translations. Time-translation symmetry, in turn, results in energy conservation, which implies that the general solution can be expressed in terms of energy eigenstates $|\varphi_n\rangle$ with arbitrary, complex-valued coefficients c_n.

$$|\psi(t)\rangle = \sum_n |\varphi_n\rangle \mathrm{e}^{-\frac{i}{\hbar}\epsilon_n t} c_n \tag{1.2}$$

The coefficients are determined by the initial conditions as $c_n = \langle\varphi_n|\psi(t=0)\rangle$.

The energy eigenstates $|\varphi_n\rangle$ obey the time-independent Schrödinger equation

$$\hat{h}|\varphi_n\rangle = |\varphi_n\rangle\epsilon_n \tag{1.3}$$

and the orthonormality condition[1]

$$\langle\varphi_m|\varphi_n\rangle = \delta_{m,n} \tag{1.4}$$

To ensure normalization of the wave function $|\psi(t)\rangle$ in Eq. 1.2, the coefficients need to satisfy $\sum_n c_n^* c_n = 1$.

1.1.2 Notation

In my lecture notes, I make an effort to be explicit in notation and units.

[1] The orthogonality of non-degenerate states is automatically satisfied, but the orthogonality between states from the same degenerate multiplet must be imposed.

- vectors are indicated by an upper arrow such as $\vec{r}$.
- matrices are indicated by a bold-face symbol $\boldsymbol{A}$. On the blackboard, I use a double underscore $\underline{\underline{A}}$ instead.
- A quantum state is written in bra-ket notation as $|\psi\rangle$.
- a quantum operator, such as $\hat{A}$, acting on a ket is indicated by a hat. There is a distinction between a quantum operator and a differential operator. Let me demonstrate the difference on the example of a momentum operator.
  - Do not write $\frac{\hbar}{i}\vec{\nabla}|\psi\rangle$, nor $\hat{p}\Psi(\vec{r})$,
  - but

$$\hat{p}|\psi\rangle = \int d^3r|\vec{r}\rangle\frac{\hbar}{i}\vec{\nabla}\langle\vec{r}|\psi\rangle \qquad \text{or} \tag{1.5}$$

$$\frac{\hbar}{i}\vec{\nabla}\langle\vec{r}|\psi\rangle = \frac{\hbar}{i}\vec{\nabla}\psi(\vec{r}) = \langle\vec{r}|\hat{p}|\psi\rangle \tag{1.6}$$

- For the matrix elements of a function of a matrix, taking the inverse as an example for a function, I use

$$A^{-1}_{\alpha,\beta} \stackrel{\text{def}}{=} (A^{-1})_{\alpha,\beta} \neq (A_{\alpha,\beta})^{-1} \tag{1.7}$$

- I do not distinguish between column and row vectors. Rather, I distinguish between two different products, the scalar product and the dyadic product.
  - The **dot product** $\vec{a}\cdot\vec{b} = \vec{a}\vec{b} = \sum_j a_j b_j$ is also called **scalar product** or **inner product**. The dot is often omitted. The dot product of two vectors is a scalar. It corresponds to a product of a row vector on the left with a column vector on the right.
  - **dyadic product** $\vec{a}\otimes\vec{b}$, defined by $(\vec{a}\otimes\vec{b})_{m,n} = a_m b_n$ is also called **outer product**.

1.1.3 Spin orbitals

The electron is properly described by the **Dirac equation**, which is a relativistic equation for spin-$\frac{1}{2}$ particles. The wave function of the Dirac equation has four components, which make up a four-component Dirac spinor. Each component is a complex wave function in real space. The four components describe electrons with two spin directions and positrons with two spin directions. In the non-relativistic limit, the Dirac equation separates into two **Pauli equations**, one for the electron components and one for the positron components. The Pauli equation describes spin-$\frac{1}{2}$ particles with two spin-components.

I will describe electrons here on the level of the Pauli equation: An electron is characterized by a position $\vec{r}$ in space and a spin index σ. The spin index can have the values [2] $\sigma \in \{\uparrow,\downarrow\}$. Often we will refer to the numerical values of σ, namely $\uparrow \mathrel{\hat{=}} +1$ and $\downarrow \mathrel{\hat{=}} -1$.

The wave function of an electron consists of two distinct functions in space and time, namely $\psi(\vec{r},\uparrow,t)$ and $\psi(\vec{r},\downarrow,t)$. The wave function is thus a so-called **spin orbital** or a **two-component spinor**.

[2] The notation using arrows is mathematical slang. It is very intuitive but not according the rules. What it means is that a spin-$\frac{1}{2}$ has a two-dimensional Hilbert space. As basisset for this Hilbert space, I can use the two eigenstates of $\hat{S}_z$

$$\hat{S}_z|\psi_1\rangle = |\psi_1\rangle\left(+\frac{\hbar}{2}\right) \quad \text{and} \quad \hat{S}_z|\psi_2\rangle = |\psi_2\rangle\left(-\frac{\hbar}{2}\right) \tag{1.8}$$

A more pictorial way of distinguishing the two states uses arrows, i.e. $|\uparrow\rangle \stackrel{\text{def}}{=} |\psi_1\rangle$, respectively $|\downarrow\rangle \stackrel{\text{def}}{=} |\psi_2\rangle$. The sum over these two states is written as $\sum_{\sigma\in\{\uparrow,\downarrow\}}$, rather than $\sum_{\sigma=1}^{2}$ or $\sum_{\sigma\in\{1,2\}}$.

REAL-SPACE-AND-SPIN BASISSET

The states $|\vec{r},\sigma\rangle$ form a complete basis for a single electron. The states in this basis are characterized by the eigenvalue equations

$$\begin{aligned}\hat{\vec{r}}|\vec{r},\sigma\rangle &= |\vec{r},\sigma\rangle\vec{r}\\ \hat{S}_z|\vec{r},\sigma\rangle &= |\vec{r},\sigma\rangle\frac{\hbar}{2}\sigma = |\vec{r},\sigma\rangle\begin{cases}+\frac{\hbar}{2} & \text{for } \sigma=+1=\uparrow\\ -\frac{\hbar}{2} & \text{for } \sigma=-1=\downarrow\end{cases}.\end{aligned} \tag{1.9}$$

The states obey the orthonormality condition

$$\langle\vec{r},\sigma|\vec{r'},\sigma'\rangle = \delta(\vec{r}-\vec{r'})\delta_{\sigma,\sigma'} \tag{1.10}$$

and the completeness relation in the one-electron Hilbert space

$$\hat{1} = \sum_{\sigma\in\{\uparrow,\downarrow\}}\int d^3r\ |\vec{r},\sigma\rangle\langle\vec{r},\sigma|\ . \tag{1.11}$$

The one-electron wave function is obtained as

$$\psi(\vec{r},\sigma,t) = \langle\vec{r},\sigma|\psi(t)\rangle \tag{1.12}$$

so that

$$|\psi(t)\rangle = \sum_{\sigma\in\{\uparrow,\downarrow\}}\int d^3r\ |\vec{r},\sigma\rangle\langle\vec{r},\sigma|\psi(t)\rangle = \sum_{\sigma\in\{\uparrow,\downarrow\}}\int d^3r\ |\vec{r},\sigma\rangle\psi(\vec{r},\sigma,t) \tag{1.13}$$

Combined position and spin argument

In order to simplify the notation, we combine the continuous position $\vec{r}$ and discrete spin coordinate σ into a single "four-dimensional" quantity

$$\vec{x} \stackrel{\text{def}}{=} (\vec{r},\sigma) \qquad \text{with } \vec{r}\in\mathbb{R}^3 \text{ and } \sigma\in\{\uparrow,\downarrow\} \tag{1.14}$$

In this notation, the integral is defined as

$$\int d^4x \stackrel{\text{def}}{=} \sum_{\sigma\in\{\uparrow,\downarrow\}}\int d^3r \tag{1.15}$$

and the δ function is

$$\delta(\vec{x}-\vec{x'}) \stackrel{\text{def}}{=} \delta(\vec{r}-\vec{r'})\delta_{\sigma,\sigma'} \tag{1.16}$$

Often, I need to refer to a specific component of $\vec{x}$ such as either the position $\vec{r}$ or the spin index σ. Then, I use the components with the same indices, that is $\vec{x}=(\vec{r},\sigma)$, $\vec{x'}=(\vec{r'},\sigma')$, $\vec{x}_1=(\vec{r}_1,\sigma_1)$, and so on. Let me give a small warning beforehand: I will use the symbol σ also as occupation-number eigenvalues $\sigma\in\{0,1\}$. This notation may be confusing.

1.1.4 Frequently used observables

Let me remind you of the most relevant observables. I will provide here, both, the operator and the corresponding expectation value.

- probability density $n(\vec{r},t)$ for the electron to be at position $\vec{r}$

$$\hat{n}(\vec{r}) \stackrel{\text{def}}{=} \sum_{\sigma\in\{\uparrow,\downarrow\}} |\vec{r},\sigma\rangle\langle\vec{r},\sigma| \tag{1.17}$$

$$n(\vec{r},t) \stackrel{\text{def}}{=} \langle\psi(t)|\hat{n}(\vec{r})|\psi(t)\rangle = \sum_{\sigma\in\{\uparrow,\downarrow\}} |\psi(\vec{r},\sigma,t)|^2 \tag{1.18}$$

The probability density at $\vec{r}$ is sum of the absolute-squared wave-function amplitudes for both spin directions. In one-particle quantum mechanics, the operator $\hat{n}(\vec{r})$ is the real-space projection operator.

- (average) position $\hat{r}$

$$\hat{r} \stackrel{\text{def}}{=} \sum_{\sigma\in\{\uparrow,\downarrow\}} \int d^3r\ |\vec{r},\sigma\rangle\vec{r}\langle\vec{r},\sigma|$$

$$\vec{r}(t) \stackrel{\text{def}}{=} \langle\psi(t)|\hat{\vec{r}}|\psi(t)\rangle = \int d^3r\ \vec{r} \sum_{\sigma\in\{\uparrow,\downarrow\}} |\psi(\vec{r},\sigma,t)|^2 \tag{1.19}$$

The average position is used, for example, to determine the electric dipole $\vec{d} = q\langle\psi|\hat{\vec{r}} - \vec{r}_0\hat{1}|\psi\rangle$ of a molecule, where $q = -e$ is the electron charge. In an optical excitation, the dipole couples to the electric field of the light wave.

- probability P_σ for having a spin $\frac{\hbar}{2}\sigma$ pointing along the z-axis. $\hat{P}_\sigma$ is the spin-projection operator.

$$\hat{P}_\sigma(t) = \int d^3r\ |\vec{r},\sigma\rangle\langle\vec{r},\sigma|$$

$$P_\sigma(t) \stackrel{\text{def}}{=} \langle\psi(t)|\hat{P}_\sigma|\psi(t)\rangle = \int d^3r\ |\psi(\vec{r},\sigma,t)|^2\ , \tag{1.20}$$

For example, $P_\uparrow = \int d^3r\ |\psi(\vec{r},\uparrow,t)|^2$.

- Spin along an axis $\vec{e}$ with $\vec{e}^2 = 1$

$$\vec{e}\hat{\vec{S}} \stackrel{\text{def}}{=} \sum_{\sigma,\sigma'\in\{\uparrow,\downarrow\}} \int d^3r\ |\vec{r},\sigma\rangle \sum_{j=1}^{3} e_j \frac{\hbar}{2}\sigma_{j,\sigma,\sigma'}\langle\vec{r},\sigma'|$$

$$\vec{e}\vec{S}(t) = \langle\psi(t)|\vec{e}\hat{\vec{S}}|\psi(t)\rangle = \int d^3r \sum_{j=1}^{3} e_j \frac{\hbar}{2} \sum_{\sigma,\sigma'\in\{\uparrow,\downarrow\}} \psi^*(\vec{r},\sigma,t)\sigma_{j,\sigma,\sigma'}\psi(\vec{r},\sigma',t) \tag{1.21}$$

where the (2×2) matrices $\boldsymbol{\sigma}_j$ are the **Pauli matrices**.

PAULI MATRICES

The Pauli matrices are

$$\boldsymbol{\sigma}_x \hat{=} \begin{pmatrix} 0 & 1 \\ 1 & 0 \end{pmatrix} \quad \text{and} \quad \boldsymbol{\sigma}_y \hat{=} \begin{pmatrix} 0 & -i \\ i & 0 \end{pmatrix} \quad \text{and} \quad \boldsymbol{\sigma}_z \hat{=} \begin{pmatrix} 1 & 0 \\ 0 & -1 \end{pmatrix} \tag{1.22}$$

so that

$$\vec{e}\vec{\boldsymbol{\sigma}} \hat{=} \begin{pmatrix} e_z & e_x - ie_y \\ e_x + ie_y & -e_z \end{pmatrix} \tag{1.23}$$

The most general hermitian 2×2 matrix is $\sum_{j\in\{0,x,y,z\}} a_j\boldsymbol{\sigma}_j$ with a 4-dimensional, real-valued vector $\vec{a}$ with indices $j \in \{0,x,y,z\}$ and the 2-dimensional unit matrix $\boldsymbol{\sigma}_0 = \mathbf{1}$.

I recommend to memorize the Pauli matrices.

- spin density: The spin density $\vec{n}_s(\vec{r},t)$ is defined as the electron density[3] of unpaired electrons.[10].

$$\hat{n}_{s,j}(\vec{r}) = \sum_{\sigma,\sigma'\in\{\uparrow,\downarrow\}} |\vec{r},\sigma\rangle\sigma_{j,\sigma,\sigma'}\langle\vec{r},\sigma'| \qquad \text{for } x\in\{x,y,z\} \tag{1.24}$$

so that

$$n_{s,j}(\vec{r},t) = \sum_{\sigma,\sigma'\in\{\uparrow,\downarrow\}} \psi^*(\vec{r},\sigma,t)\sigma_{j,\sigma,\sigma'}\psi(\vec{r},\sigma',t) \tag{1.25}$$

To avoid ambiguities, let me write down an example, namely the x-component of the spin density:

$$\begin{aligned}\hat{n}_{s,x} &= \begin{pmatrix}|\vec{r},\uparrow\rangle\\|\vec{r},\downarrow\rangle\end{pmatrix}\begin{pmatrix}0&1\\1&0\end{pmatrix}\begin{pmatrix}\langle\vec{r},\uparrow|\\\langle\vec{r},\downarrow|\end{pmatrix} = |\vec{r},\uparrow\rangle\langle\vec{r},\downarrow| + |\vec{r},\downarrow\rangle\langle\vec{r},\uparrow|\\ n_{s,x}(\vec{r},t) &= \psi^*(\vec{r},\uparrow)\psi(\vec{r},\downarrow) + \psi^*(\vec{r},\downarrow)\psi(\vec{r},\uparrow)\end{aligned} \tag{1.26}$$

The spin contribution of the angular-momentum density is obtained from the spin density by multiplication with the spin $\hbar/2$ of the electron

$$\vec{s}(\vec{r},t) \stackrel{\text{def}}{=} \frac{\hbar}{2}\vec{n}_s(\vec{r},t) \tag{1.27}$$

The **magnetization** $\vec{m}(\vec{r},t)$ is obtained from the spin density $\vec{n}_s(\vec{r},t)$ by multiplication with the **electron magnetic moment** $\mu_e = \frac{1}{2}g_e\mu_B$, where $g_e = 2.002319\ldots$ is the electron Landé **g-factor** of the free electron and $\mu_B \stackrel{\text{def}}{=} e\hbar/(2m_e)$ is the **Bohr magneton**.[11]

$$\vec{m}(\vec{r},t) \stackrel{\text{def}}{=} -\mu_e\vec{n}_s(\vec{r},t) \tag{1.28}$$

Because of the negative charge of the electron, its magnetic moment is oriented opposite to the spin direction, which explains the minus sign in the equation Eq. 1.28 above[4].

- momentum: The momentum operator, expressed in a real-space-and-spin basisset, has the following form

[3] According to the definition in the Gold book[10], the spin density would be $|\vec{n}_s(\vec{r},t)|$ rather then the vectorial quantity. I consider this as an oversight, because usually only collinear spin distributions with an axis along the z-direction are considered.

[4] Some caution is needed regarding which quantities carry the minus sign and which do not. This is not always handled on the same way.

MOMENTUM OPERATOR

$$\hat{\vec{p}} = \sum_{\sigma\in\{\uparrow,\downarrow\}} \int d^3r\ |\vec{r},\sigma\rangle \frac{\hbar}{i}\vec{\nabla}\langle\vec{r},\sigma| \tag{1.29}$$

which has matrix elements [a]

$$\langle\vec{r},\sigma|\hat{\vec{p}}|\vec{r}',\sigma'\rangle = \frac{\hbar}{i}\vec{\nabla}_r\delta(\vec{r}-\vec{r}')\delta_{\sigma,\sigma'} = \delta(\vec{r}-\vec{r}')\delta_{\sigma,\sigma'}\frac{\hbar}{i}\vec{\nabla}_{r'} \tag{1.32}$$

where the gradient $\vec{\nabla}$ acts on the spatial argument $\vec{r}$.

[a] Like the δ-function, also $\vec{\nabla}\delta(\vec{r})$ is not a regular function, but a **distribution** (see for example [12]). It is defined by the integral identity

$$\int d^3r\ f(\vec{r})\vec{\nabla}\delta(\vec{r}) = -\vec{\nabla}|_{\vec{r}=\vec{0}}\, f \tag{1.30}$$

where $f(\vec{r})$ can be any differentiable function. One can also construct $\vec{\nabla}\delta(\vec{r})$ as the limit of a sequence of functions, or via the differential quotient from the δ-function

$$\vec{e}\,\vec{\nabla}\delta(\vec{r}) = \lim_{\Delta\to 0}\frac{\delta(\vec{r}+\vec{e}\Delta)-\delta(\vec{r}-\vec{e}\Delta)}{2\Delta} \tag{1.31}$$

where $\vec{e}$ is an arbitrary unit vector. This vector specifies the direction along which the derivative is taken.

The momentum expectation value at time t is

$$\begin{aligned}\vec{p}(t) = \langle\psi(t)|\hat{\vec{p}}|\psi(t)\rangle &\overset{\text{Eq. 1.29}}{=} \sum_{\sigma\in\{\uparrow,\downarrow\}}\int d^3r\ \langle\psi(t)|\vec{r},\sigma\rangle\frac{\hbar}{i}\vec{\nabla}\langle\vec{r},\sigma|\psi(t)\rangle \\ &= \int d^3r \sum_{\sigma\in\{\uparrow,\downarrow\}} \psi^*(\vec{r},\sigma,t)\frac{\hbar}{i}\vec{\nabla}\psi(\vec{r},\sigma,t)\end{aligned} \tag{1.33}$$

- current density: The particle-current density is calculated from the velocity $\vec{v} = \dot{\vec{r}} = \vec{\nabla}_p H(\vec{p},\vec{r})$. For the Hamilton operator $H(\vec{p},\vec{r},t) = \frac{1}{2m}(\vec{p}-q\vec{A}(\vec{r},t))^2 + q\Phi(\vec{r},t)$ of a charged particle with charge q and mass m in an electromagnetic field with an electric potential $\Phi(\vec{r},t)$ and a vector potential $\vec{A}(\vec{r},t)$, the current density is

$$\hat{\vec{j}}(\vec{r}) = \frac{1}{2m_e}\sum_{\sigma\in\{\uparrow,\downarrow\}}\left[\left(\hat{p}-q\vec{A}(\hat{\vec{r}})\right)|\vec{r},\sigma\rangle\langle\vec{r},\sigma| + |\vec{r},\sigma\rangle\langle\vec{r},\sigma|\left(\hat{p}-q\vec{A}(\hat{\vec{r}})\right)\right]. \tag{1.34}$$

Two terms are required to ensure that the observable is represented by a hermitian operator. The charge current is obtained from the particle current by multiplication with the charge q.

1.1.5 Discrete and continuous spectra of quantum states

The spectrum of an operator is the set of its eigenvalues. Quantum states may have discrete and continuous spectra, and, even worse, they may have spectra consisting of discrete eigenvalues and regions, where they are continuous. An example is the hydrogen atom, which has a discrete energy spectrum at negative energies, but a continuous spectrum of scattering states at positive energies. A common mistake is to forget the continuous part of the spectrum.

Rather than dealing with these difficulties, I am avoiding them by introducing what I call a **finite universe**. A continuous spectrum can result, when the norm is defined on an infinite region. When this region is replaced by a finite region, like a very large box, the spectrum becomes discrete. I call this box my finite universe.

As a consequence of the finite extent, all states have the regular normalization and all spectra are discrete. The advantage of this choice is that I can treat localized and extended states on the very same footing. While the spectrum of a finite system is discrete, the eigenvalues may be extremely close. Furthermore, states that extend over the entire box, may have a very small wave function amplitude.

The limit to a truly infinite system, is postponed to the final result, rather than done during the derivations. Given that an infinite system is usually an idealization, I consider this approach appealing.

For infinite periodic systems, which are described with periodic boundary conditions and Bloch's theorem (see below in section 1.1.8), we proceed slightly differently: Rather than choosing a finite volume, we choose a large supercell and require the wave function (not only the potential) to be strictly periodic with the supercell lattice vectors. This requirement leads to a discrete energy spectrum just as in the case described above. The wave functions are normalized within this supercell. Once the final equations have been obtained, we increase the size of the supercell to infinity and normalize within the regular unit cell of the crystal.

1.1.6 Momentum eigenstates

The eigenstates of the momentum are plane waves, which extend over an infinite volume. The momentum eigenvalues are continuous.

I define the basis states as eigenvalues of momentum operator Eq. 1.29 and spin (with $\uparrow \hat{=} 1$ and $\downarrow \hat{=} -1$)

$$\begin{aligned} \hat{\vec{p}}|\vec{p},\sigma\rangle &= |\vec{p},\sigma\rangle\vec{p} \\ \hat{S}_z|\vec{p},\sigma\rangle &= |\vec{p},\sigma\rangle\frac{\hbar}{2}\sigma \end{aligned} \tag{1.35}$$

The eigenvalue equation of the momentum operator Eq. 1.29 and the normalization $\langle\vec{p},\sigma|\vec{p},\sigma\rangle = 1$ define the basis states of the momentum representation as

$$\underbrace{\langle\vec{x}|\vec{p},\sigma'\rangle}_{\langle\vec{r},\sigma|\vec{p},\sigma'\rangle} = \frac{1}{\sqrt{\Omega}}\mathrm{e}^{\frac{i}{\hbar}\vec{p}\vec{r}}\delta_{\sigma,\sigma'} \tag{1.36}$$

where $\Omega = L^3$ is the size of the integration volume, which also defines the periodic boundary condition for the wave function. For periodic boundary conditions in a cubic box of side length L, the set of momentum eigenvalues $\vec{p}_{i,j,k} = (i,j,k)\Delta p$ is discrete with integer i,j,k and the spacing of the momentum eigenvalues is $\Delta p = \frac{2\pi\hbar}{L}$ in each of the three spatial directions.

Note, that I define momentum eigenstates which are normalized within a finite, even though very large, box. I name the box jokingly the "finite universe". The consequence of this choice is that the sum over all states is a discrete sum, rather than an integral. This simplifies the notation considerable. The limit to an infinite box needs to be done, but here it is done at the very end of a calculations, or where it becomes convenient, and not right in the beginning. Adopting this style requires that the reader is familiar with executing this limit.[5]

[5] One advantage is that one may capture problems, when another limiting case is to be done, which may not be interchangeable with that to an infinitely large system. In this context, it is also important to distinguish between periodic boundary conditions and that of a true finite box.

NORMALIZATION OF MOMENTUM EIGENSTATES

The overlap matrix elements of momentum eigenstates are[a]

$$\langle \vec{p},\sigma|\vec{p'},\sigma'\rangle \overset{\text{Eq. 1.36}}{=} \delta_{\sigma,\sigma'} \int_\Omega d^3r\, \frac{1}{\Omega} e^{\frac{i}{\hbar}(\vec{p}-\vec{p'})\vec{r}} = \delta_{\vec{p},\vec{p'}}\delta_{\sigma,\sigma'} \quad \overset{\Omega\to\infty}{\to} \quad \frac{(2\pi\hbar)^3}{\Omega}\delta(\vec{p}-\vec{p'})\delta_{\sigma,\sigma'} \quad (1.38)$$

The completeness relation has the form

$$\hat{1} = \sum_{\{\vec{p}\},\sigma\in\{\uparrow,\downarrow\}} |\vec{p},\sigma\rangle\langle\vec{p},\sigma| \quad \overset{\Omega\to\infty}{\to} \quad \sum_{\sigma\in\{\uparrow,\downarrow\}} \Omega \int \frac{d^3p}{(2\pi\hbar)^3}\, |\vec{p},\sigma\rangle\langle\vec{p},\sigma| \quad (1.39)$$

[a] In the limit $\Omega\to\infty$, I use

$$1 = \sum_{\{\vec{p'}\}} \delta_{\vec{p},\vec{p'}} \overset{\Delta p = 2\pi\hbar/L}{=} \Omega \sum_{\{\vec{p'}\}} \frac{(\Delta p)^3}{(2\pi\hbar)^3}\delta_{\vec{p},\vec{p'}} \rightsquigarrow \Omega\int \frac{d^3p'}{(2\pi\hbar)^3}\, \frac{(2\pi\hbar)^3}{\Omega}\delta(\vec{p}-\vec{p'}) = 1\,. \quad (1.37)$$

The factors are verified by performing the sum, respectively, the integral, which, both, give 1 as result. I express this as $\delta_{p,p'} \rightsquigarrow \frac{(2\pi\hbar)^3}{\Omega}\delta(\vec{p}-\vec{p'})$.

1.1.7 Non-orthonormal and local orbitals

When studying atoms, it is often convenient to use local orbitals $|\chi_\alpha\rangle$. The local orbitals are reminiscent of **atomic orbitals**, because they usually have the same quantum numbers as the atomic wave functions. The quantum numbers of atomic orbitals are the **principal quantum number** n, the **angular-momentum quantum number** ℓ, the **magnetic quantum number** m, and **spin quantum number** σ. In addition, there is a site index R referring to a particular atom. Thus, the index $\alpha = (R, n, \ell, m, \sigma)$ is a composite index of all these quantum numbers.

The principal quantum number is often suppressed, because the main interest of many-particle problems is related to the valence states, to which only one main quantum number contributes for a given site R and angular momentum ℓ.

Often, but not always, we will assume that the local orbitals are orthonormal among each other, that is $\langle\chi_\alpha|\chi_\beta\rangle = \delta_{\alpha,\beta}$. This orthonormality is not compatible with true atomic orbitals, when orbitals from different sites are considered. However, in a solid, one can construct so-called **Wannier orbitals**[13], which are localized and at the same time orthonormal to each other.

In practice, however, also Wannier orbitals are often too extended to be of use. Furthermore the Wannier orbitals often have a complex shape. Therefore, it is often advantageous to work in a non-orthonormal basisset, which provides more flexibility. This is shown in the present section.

We consider a basisset of orbitals $|\chi_\alpha\rangle$, which has an overlap matrix

$$S_{\alpha,\beta} \overset{\text{def}}{=} \langle\chi_\alpha|\chi_\beta\rangle \quad (1.40)$$

The unit operator[6] expressed in the non-orthonormal basis has the form

$$\hat{1} = \sum_{\alpha,\beta} |\chi_\alpha\rangle \left(\boldsymbol{S}^{-1}\right)_{\alpha,\beta} \langle\chi_\beta| \quad (1.41)$$

We can define a **projector function** $\langle\pi_\alpha| = \sum_\beta \left(\boldsymbol{S}^{-1}\right)_{\alpha,\beta}\langle\chi_\beta|$, so that

$$\hat{1} = \sum_\alpha |\chi_\alpha\rangle\langle\pi_\alpha|\,. \quad (1.42)$$

[6] For a finite basisset, the unit operator below is defined as unity within this basisset. In the more extended Hilbert space of all square-integrable functions, the expression is a projection operator onto the basisset spanned by the local orbitals.

The projector function probes the state for a certain character. This character is quantified by the "weight" $\langle\pi_\alpha|\psi\rangle$ of a local orbital $|\chi_\alpha\rangle$ in the state $|\psi\rangle$. I consider the projector function as probe function.

In practical applications, the overlap matrix $\boldsymbol{S}$ is often singular[7], which implies that its inverse $\boldsymbol{S}^{-1}$ does not exist, respectively that it is not unique. This is the case whenever one works with finite, and therefore incomplete basissets. The ambiguity in the inverse reflects in a similar ambiguity for the projector functions. To make this ambiguity explicit, we use the projector functions as the fundamental quantity, as opposed to the $\boldsymbol{S}^{-1}$, and specify only the requirement for the projector function, namely the **bi-orthogonality condition**.

$$\langle\pi_\alpha|\chi_\beta\rangle = \delta_{\alpha,\beta} \tag{1.43}$$

The inverse of the overlap matrix becomes a quantity that is derived from the projector functions via

$$\langle\pi_\alpha|\pi_\beta\rangle = \langle\pi_\alpha|\hat{1}|\pi_\beta\rangle \overset{\text{Eq. 1.41}}{=} \sum_{\gamma,\delta}\langle\pi_\alpha|\chi_\gamma\rangle\left(\boldsymbol{S}^{-1}\right)_{\gamma,\delta}\langle\chi_\delta|\pi_\beta\rangle \overset{\text{Eq. 1.43}}{=} \left(\boldsymbol{S}^{-1}\right)_{\alpha,\beta} \tag{1.44}$$

NON-ORTHONORMAL ORBITALS

The wave function can be represented in terms of local orbitals $|\chi_\alpha\rangle$ as

$$|\psi(t)\rangle = \sum_\alpha |\chi_\alpha\rangle\langle\pi_\alpha|\psi(t)\rangle \tag{1.45}$$

where the state $|\pi_\alpha\rangle$ is the **projector function**[a], which extracts the contribution of a particular local orbital $|\chi_\alpha\rangle$ from the wave function $|\psi\rangle$.
The projector functions obey the bi-orthonormality condition

$$\langle\pi_\alpha|\chi_\beta\rangle \overset{\text{Eq. 1.43}}{=} \delta_{\alpha,\beta} \tag{1.46}$$

as well as

$$\begin{aligned}\langle\chi_\alpha|\chi_\beta\rangle &\overset{\text{Eq. 1.40}}{=} S_{\alpha,\beta}\\ \langle\pi_\alpha|\pi_\beta\rangle &\overset{\text{Eq. 1.44}}{=} \left(\boldsymbol{S}^{-1}\right)_{\alpha,\beta}\end{aligned} \tag{1.47}$$

Convention:

- observables $\hat{A}$ are written with the projector functions outward

$$\hat{A} = \sum_{\alpha,\beta} |\pi_\alpha\rangle \underbrace{\langle\chi_\alpha|\hat{A}|\chi_\beta\rangle}_{A_{\alpha,\beta}}\langle\pi_\beta| \tag{1.48}$$

- states $|\psi\rangle$, density matrices $\hat{\rho}$ and densities of states are written with the orbitals pointing outward

$$\hat{\rho} = \sum_{\alpha,\beta} |\chi_\alpha\rangle \underbrace{\langle\pi_\alpha|\hat{\rho}|\pi_\beta\rangle}_{\rho_{\alpha,\beta}}\langle\chi_\beta| \tag{1.49}$$

Non-orthonormal basissets are summarized in appendix B on p. 517.

[a] I introduced the terminology of a projector function in my paper on the projector augmented wave method[14].

[7] A matrix is singular, when it has a vanishing (left or right) eigenvalue.

One can easily verify that the projector functions extract the appropriate coefficients for any state $|\psi\rangle$ that is contained within the Hilbert space spanned by the local orbitals: Consider a wave function that can be represented by the local orbitals with some coefficients c_α

$$|\psi\rangle = \sum_\alpha |\chi_\alpha\rangle c_\alpha \tag{1.50}$$

A particular coefficient c_β can be obtained from the scalar product of the wave function $|\psi\rangle$ with the projector function

$$\langle\pi_\beta|\psi\rangle = \sum_\alpha \langle\pi_\beta|\chi_\alpha\rangle c_\alpha \overset{\text{Eq. 1.46}}{=} c_\beta \qquad q.e.d. \tag{1.51}$$

If the basis set is orthonormal, that is $\langle\chi_\alpha|\chi_\beta\rangle = \delta_{\alpha,\beta}$, the orbitals themselves can act as projector functions. This is what is done in nearly all text books. Distinguishing orbitals and projector functions, however, provides a lot of additional freedom.

The treatment of non-orthonormal orbitals is mathematically analogous to that of vectors using oblique coordinate systems. Distinguishing orbitals and projector functions is analogous to **covariant** and **contravariant** vectors in **skewed coordinate systems**. A comparison between bra-ket notation and the co- and contravariant notation is given in table 1.1.

Each one-particle orbital defines a coordinate axis[8] $|\chi_\mu\rangle \hat{=} \vec{e}_\mu$ in the Hilbert space. The overlap matrix between the basis states plays the role of a metric tensor $S_{\mu,\nu} = \langle\chi_\mu|\chi_\nu\rangle \hat{=} g_{\mu,\nu} = \vec{e}_\mu\vec{e}_\nu$. On the one hand, co- and contra-variant indices distinguish between states and projector functions, a distinction which is not explicit in the bra-ket notation. On the other hand, the co- and contravariant notation does not distinguish between complex conjugate partners such as the distinction between bras and kets in the bra-ket notation: such a distinction is not required for real-valued vectors.

More detail can be found in section 5.4 of ΦSX:Classical Mechanics[15].

1.1.8 Bloch theorem

I provided derivations of **Bloch's theorem** earlier in ΦSX: Quantum Physics[16]. and in ΦSX: Introduction to Solid-State Theory[1]. This section is not meant as an independent derivation but as a brief reminder and the presentation of a "cooking recipe".

Let me first revisit some notions regarding symmetries in physical systems: Noether's theorem for classical particles or classical fields says that a conserved quantity emerges from of every continuous symmetry. In quantum mechanics, this translates into the notion that the Hamiltonian becomes block-diagonal when represented in terms of eigenstates of a commutating set of its symmetry operators. As a consequence, the matrix diagonalization of a big matrix is broken down in many diagonalization problems with smaller dimensions. Each block is characterized by the set eigenvalues from the commutating set of symmetry operators, i.e. the quantum numbers.

This concept is now applied to the lattice translation symmetry. **Bloch theorem** exploits the discrete lattice-translation symmetry of a lattice of atoms. Lattice-translation symmetry implies that the Hamiltonian is invariant under a lattice translation, i.e. $\langle\vec{r}-\vec{t},\sigma|\hat{h}|\vec{r'}-\vec{t},\sigma'\rangle = \langle\vec{r},\sigma|\hat{h}|\vec{r'},\sigma'\rangle$. The **lattice translation vectors** $\vec{t}$ are integer multiples of the **primitive lattice translation vectors** $\vec{T}_1, \vec{T}_2, \vec{T}_3$.

The conserved quantity resulting from the lattice-translation symmetry is the **crystal momentum** $\hbar\vec{k}$ or **Bloch vector** $\vec{k}$, simply called the k-point. The eigenstates of the lattice translation are **Bloch states**

$$\psi_{\vec{k}}(\vec{r},\sigma) = u_{\vec{k}}(\vec{r},\sigma)e^{i\vec{k}\vec{r}} \tag{1.52}$$

[8] The cartesian coordinate axes in three dimensions are defined by three orthonormal unit vectors $\vec{e}_x$, $\vec{e}_y$, $\vec{e}_z$. A tripel of numbers (x,y,z) defines the vector $\vec{r} = \vec{e}_x x + \vec{e}_y y + \vec{e}_z z$. In the covariant notation for skewed coordinate axis, the axes are defined by the contra-variant vectors $\vec{e}_\mu$ and the coordinates are defined by the co-variant vectors u^μ.

Table 1.1: Comparison of Dirac's bra-ket notation for quantum states and the co-and contravariant vector notation. I do not use Einstein notation, but use explicit sums.

Bra-Ket notation		co and contravariant notation	
		Basis	
basis-state	$\|\chi_\mu\rangle$	$\vec{e}_\mu$	contravariant vector
projector-function	$\langle\pi_\alpha\|$	$\vec{e}^\mu$	co-variant vector
		Scalar product and metric tensor $g_{\mu,\nu}$	
bi-orthogonality	$\langle\pi_\mu\|\chi_\nu\rangle = \delta_{\mu,\nu}$	$g^\mu{}_\nu = \vec{e}^\mu\vec{e}_\nu = \delta_{\mu,\nu}$	
overlap matrix	$S_{\mu,\nu} = \langle\chi_\mu\|\chi_\nu\rangle$	$g_{\mu,\nu} = \vec{e}_\mu\vec{e}_\nu$	contravariant metric tensor
inverse overlap	$\left(S^{-1}\right)_{\mu,\nu} = \langle\pi_\mu\|\pi_\nu\rangle$	$g^{\mu,\nu} = \vec{e}^\mu\vec{e}^\nu$	
scalar product	$\langle\psi\|\phi\rangle$	$\vec{r}\vec{s} = \sum_\mu u_\mu u^\mu$	
completeness	$\hat{1} = \sum_{\mu,\nu}\|\chi_\mu\rangle S^{-1}{}_{\mu,\nu}\langle\chi_\nu\|$	$\mathbf{1} = \sum_{\mu,\nu} g^{\mu,\nu}\vec{e}_\mu\otimes\vec{e}_\nu$	
		States and projector-functions	
state	$\|\psi\rangle = \sum_\mu\|\chi_\mu\rangle c_\mu$	$\vec{r} = \sum_\mu \vec{e}_\mu u^\mu$	vector
coefficient	$c_\mu = \langle\pi_\mu\|\psi\rangle$	$u^\mu = \vec{e}^\mu\vec{r}$	co-variant coefficient
	$c_\mu = \sum_\nu S^{-1}_{\mu,\nu}\langle\chi_\nu\|\psi\rangle$	$u^\mu = \sum_\nu g^{\mu,\nu}u_\nu$	
	$\langle\chi_\mu\|\psi\rangle$	$u_\mu = \vec{e}_\mu\vec{r}$	

where $u_{\vec{k}}(\vec{r})$ is periodic with the lattice. In words, *the wave functions are periodic functions* $u_{n,k}(\vec{r})$ *that are modulated by a plane wave* $e^{i\vec{k}\vec{r}}$.

As a result of the lattice symmetry, the Hamilton operator does not mix wave functions with different Bloch vectors $\vec{k} \neq \vec{k'}$ in the same reciprocal unit cell, i.e. $\langle\psi_{\vec{k}}|\hat{h}|\psi_{\vec{k'}}\rangle = 0$.[9] As a consequence, the eigenstates of the Hamiltonian can be written as Bloch states.

A Bloch vector can be any vector in the reciprocal unit cell. In order to avoid the complications of an infinite space region and the corresponding continuous Bloch-vectors, one imposes periodic boundary conditions

$$\psi_{\vec{k}}(\vec{r} + \vec{T}_j^{\text{super}}) = \psi_{\vec{k}}(\vec{r}) \; . \tag{1.53}$$

on a large, but finite, supercell, with supercell lattice vectors $\vec{T}_1^{\text{super}} = \vec{T}_1 N_1$, $\vec{T}_2^{\text{super}} = \vec{T}_2 N_2$, $\vec{T}_3^{\text{super}} = \vec{T}_3 N_3$. N_1, N_2, N_3 are very large, but finite, integers. The limit $N_j \to \infty$ is taken typically towards the end of a calculation.

A discrete set of Bloch-vectors $\vec{k}$ is specified via the **quantization condition** imposed by periodic boundary conditions: The periodicity of the Bloch wave function Eq. 1.52 implies

$$\begin{aligned} & e^{i\vec{k}\vec{T}_q^{\text{super}}} = 1 \qquad \text{for } q \in \{1,2,3\} \\ \Rightarrow \qquad & \vec{k}_{j_1,j_2,j_3} = \sum_{q=1}^{3} \vec{g}_q \frac{j_q}{N_q} \qquad \text{with } j_q \in \{0,1,\ldots,N_q\} \end{aligned} \tag{1.54}$$

where the **primitive reciprocal lattice vectors** $\vec{g}_j$ are defined by

$$\vec{g}_i \vec{T}_j = 2\pi\delta_{i,j} \qquad \text{for } i,j \in \{1,2,3\} \tag{1.55}$$

The discrete k-point set are the reciprocal lattice points of the supercell.

[9] The eigenvalues and eigenstates are periodic with the reciprocal lattice. Therefore, the Hamilton matrix elements do not necessarily vanish for two Bloch vectors related by a reciprocal-lattice translation vector.

Table 1.2: Symbols used for real and reciprocal lattice vectors

real space lattice	
$\vec{T}_1, \vec{T}_2, \vec{T}_3$	primitive lattice vectors
$\boldsymbol{T}$	matrix made from the three primitive lattice vectors
$\vec{t}$	general lattice vector
reciprocal space lattice	
$\vec{g}_1, \vec{g}_2, \vec{g}_3$	primitive lattice vectors
$\boldsymbol{g}$	matrix made from the three primitive lattice vectors
$\vec{G}$	general lattice vector
$\vec{g}_i \vec{T}_j = 2\pi\delta_{i,j}$ or $\boldsymbol{G}^\dagger \boldsymbol{T} = 2\pi \mathbf{1}$	

For atom-centered basissets $\{|\chi_{\alpha,\vec{t}}\rangle\}$, Bloch's theorem has an appearance that differs slightly from Eq. 1.52, namely

$$\begin{aligned} \psi_{\vec{k}}(\vec{r},\sigma) &\overset{\text{Eq. 1.52}}{=} \overbrace{\frac{1}{\sqrt{\sum_{\vec{t}}}} \sum_{\vec{t},\alpha} \chi_{\alpha,\vec{t}}(\vec{r},\sigma) \mathrm{e}^{-i\vec{k}(\vec{r}-\vec{t})} c_\alpha(\vec{k})}^{u_{n,k}(\vec{r})} \mathrm{e}^{i\vec{k}\vec{r}} \\ &= \frac{1}{\sqrt{\sum_{\vec{t}}}} \sum_{\vec{t},\alpha} \chi_{\alpha,\vec{t}}(\vec{r},\sigma) c_\alpha(\vec{k}) \mathrm{e}^{i\vec{k}\vec{t}} \end{aligned} \tag{1.56}$$

where $\vec{t}_{i_1,i_2,i_3} = \vec{T}_1 i_1 + \vec{T}_2 i_2 + \vec{T}_3 i_3$ is an arbitrary real-space lattice vector. The orbital $|\chi_{\alpha,\vec{t}}\rangle$ is centered at site $\vec{R}_\alpha + \vec{t}$, where R_α is the position of the equivalent atom in the first unit cell. The orbital index α identifies the orbitals of a specific site and may consist of the angular-momentum and spin quantum numbers (ℓ, m, σ). The complex-valued coefficients are denoted by $c_\alpha(\vec{k})$.

In the normalization factor, I use the symbol $\sum_{\vec{t}}$, meaning $\sum_{\vec{t}\in\mathbb{T}} 1 = N_1, N_2, N_3$, which counts the lattice translation vectors $\vec{t} \in \mathbb{T}$ in the supercell [10] used in Eq. 1.53. The set $\mathbb{T}$ is usually not made explicit.

Eq. 1.56 corresponds to constructing first a basisset of Bloch states $|\chi_{\alpha,\vec{k}}\rangle$ out of the individual local orbitals $|\chi_{\alpha,\vec{t}}\rangle$ and their corresponding projector functions $|\pi_{\alpha,\vec{k}}\rangle$.

$$\begin{aligned} |\chi_{\alpha,\vec{k}}\rangle &= \frac{1}{\sqrt{\sum_{\vec{t}}}} \sum_{\vec{t}} |\chi_{\alpha,\vec{t}}\rangle \mathrm{e}^{i\vec{k}\vec{t}} \\ |\pi_{\alpha,\vec{k}}\rangle &= \frac{1}{\sqrt{\sum_{\vec{t}}}} \sum_{\vec{t}} |\pi_{\alpha,\vec{t}}\rangle \mathrm{e}^{i\vec{k}\vec{t}} \end{aligned} \tag{1.57}$$

which satisfy the bi-orthogonality condition

$$\langle \pi_{\alpha,\vec{k}} | \chi_{\beta,\vec{k}'} \rangle = \delta_{\alpha,\beta} \delta_{\vec{k},\vec{k}'} \ . \tag{1.58}$$

Caution is required because the same symbol is used for the Bloch waves $|\chi_{\alpha,\vec{k}}\rangle$ and the site-centered orbitals $|\chi_{\alpha,\vec{t}}\rangle$. The two basissets are distinguished by the type of their indices, namely $\vec{t}$ versus $\vec{k}$. The Kronecker symbol $\delta_{\vec{k},\vec{k}'}$ refers to the discrete set of k-points, which result from the quantization condition, respectively, the periodic boundary conditions for a large but finite supercell.

[10] The set $\mathbb{T}$ is contains all lattice translation vectors $\vec{t}_{j_1,j_2,j_3} = \vec{T}_1 j_1 + \vec{T}_2 j_2 + \vec{T}_3 j_3$ with $j_1 \in \{0, 1, \ldots, N_1\}$, $j_2 \in \{0, 1, \ldots, N_2\}$, and $j_3 \in \{0, 1, \ldots, N_3\}$. where N_1, N_2, N_3 define, together with the primitive lattice translations, the supercell.

In the basis of Bloch orbitals, the Ansatz for the eigenstates of the Hamiltonian has the form

$$|\varphi_{n,\vec{k}}\rangle = \sum_{\alpha} |\chi_{\alpha,\vec{k}}\rangle c_{\alpha,n}(\vec{k}) \tag{1.59}$$

A k-dependent Hamiltonian in the discrete basis is obtained by transforming onto k-dependent orbitals given in Eq. 1.57.

Let me now rewrite the Schrödinger equation for a Bloch wave function $|\varphi_n(\vec{k})\rangle$. I represent Hamilton and overlap matrix elements in the form[11]

$$\begin{aligned}
\hat{h} &= \underbrace{\sum_{\alpha,\vec{t}} |\pi_{\alpha,\vec{t}}\rangle\langle\chi_{\alpha,\vec{t}}|}_{=\hat{1}}\, \hat{h} \underbrace{\sum_{\beta,\vec{t}'} |\chi_{\beta,\vec{t}'}\rangle\langle\pi_{\beta,\vec{t}'}|}_{=\hat{1}} = \sum_{\alpha,\beta}\sum_{\vec{t},\vec{t}'} |\pi_{\alpha,\vec{t}}\rangle \underbrace{\langle\chi_{\alpha,\vec{t}}|\hat{h}|\chi_{\beta,\vec{t}'}\rangle}_{h_{\alpha,\vec{t},\beta,\vec{t}'}} \langle\pi_{\beta,\vec{t}'}| \\
\hat{1} &= \underbrace{\sum_{\alpha,\vec{t}} |\pi_{\alpha,\vec{t}}\rangle\langle\chi_{\alpha,\vec{t}}|}_{=\hat{1}}\, \hat{1} \underbrace{\sum_{\beta,\vec{t}'} |\chi_{\beta,\vec{t}'}\rangle\langle\pi_{\beta,\vec{t}'}|}_{=\hat{1}} = \sum_{\alpha,\beta}\sum_{\vec{t},\vec{t}'} |\pi_{\alpha,\vec{t}}\rangle \underbrace{\langle\chi_{\alpha,\vec{t}}|\chi_{\beta,\vec{t}'}\rangle}_{S_{\alpha,\vec{t},\beta,\vec{t}'}} \langle\pi_{\beta,\vec{t}'}|
\end{aligned} \tag{1.60}$$

and I exploit lattice-translation symmetry of $\hat{h}$, namely $h_{\alpha,\vec{t},\beta,\vec{t}'} = h_{\alpha,\vec{0},\beta,\vec{t}'-\vec{t}}$.

Let me now set up the generalized eigenvalue for the periodic Hamiltonian:

$$\begin{aligned}
0 &= \left(\hat{h} - \epsilon_n(\vec{k})\hat{1}\right)|\varphi_n(\vec{k})\rangle \\
&\overset{\text{Eq. 1.56}}{=} \underbrace{\left(\sum_{\alpha,\beta}\sum_{\vec{t},\vec{t}'} |\pi_{\alpha,\vec{t}}\rangle h_{\alpha,\vec{t},\beta,\vec{t}'}\langle\pi_{\beta,\vec{t}'}|\right)}_{\hat{h}} - \epsilon_n(\vec{k}) \underbrace{\sum_{\alpha,\beta}\sum_{\vec{t},\vec{t}'} |\pi_{\alpha,\vec{t}}\rangle \overbrace{\langle\chi_{\alpha,\vec{t}}|\chi_{\beta,\vec{t}'}\rangle}^{S_{\alpha,\vec{t},\beta,\vec{t}'}} \langle\pi_{\beta,\vec{t}'}|}_{\hat{1}} \Big) \underbrace{\sum_{\gamma,\vec{t}''} |\chi_{\gamma,\vec{t}''}\rangle e^{i\vec{k}\vec{t}''} \frac{1}{\sqrt{\sum_{\vec{t}}}} c_{\gamma,n}(\vec{k})}_{|\varphi_n(\vec{k})\rangle} \\
&= \sum_{\alpha}\sum_{\vec{t}} |\pi_{\alpha,\vec{t}}\rangle \sum_{\beta,\gamma}\sum_{\vec{t}',\vec{t}''} \Big(h_{\alpha,\vec{t},\beta,\vec{t}'} - \epsilon_n(\vec{k}) S_{\alpha,\vec{t},\beta,\vec{t}'}\Big) \underbrace{\langle\pi_{\beta,\vec{t}'}|\chi_{\gamma,\vec{t}''}\rangle}_{\delta_{\beta,\gamma}\delta_{\vec{t}',\vec{t}''}} e^{i\vec{k}\vec{t}''} \frac{1}{\sqrt{\sum_{\vec{t}}}} c_{\gamma,n}(\vec{k}) \\
&= \sum_{\alpha,\vec{t}} |\pi_{\alpha,\vec{t}}\rangle e^{i\vec{k}\vec{t}} \frac{1}{\sqrt{\sum_{\vec{t}}}} \sum_{\beta} \left[\sum_{\vec{t}'} \Big(h_{\alpha,\vec{0},\beta,\vec{t}'-\vec{t}} - \epsilon_n(\vec{k}) S_{\alpha,\vec{0},\beta,\vec{t}'-\vec{t}}\Big) e^{i\vec{k}(\vec{t}'-\vec{t})}\right] c_{\beta,n}(\vec{k}) \\
&= \sum_{\alpha} \underbrace{\sum_{\vec{t}} |\pi_{\alpha,\vec{t}}\rangle e^{i\vec{k}\vec{t}} \frac{1}{\sqrt{\sum_{\vec{t}}}}}_{|\pi_{\alpha,\vec{k}}\rangle \text{ Eq. 1.57}} \sum_{\beta} \left[\underbrace{\sum_{\vec{t}''} h_{\alpha,\vec{0},\beta,\vec{t}''} e^{i\vec{k}\vec{t}''}}_{=:h_{\alpha,\beta}(\vec{k})} - \epsilon_n(\vec{k}) \underbrace{\sum_{\vec{t}''} S_{\alpha,\vec{0},\beta,\vec{t}''} e^{i\vec{k}\vec{t}''}}_{=:S_{\alpha,\beta}(\vec{k})}\right] c_{\beta,n}(\vec{k}) \\
&= \sum_{\alpha} |\pi_{\alpha,\vec{k}}\rangle \sum_{\beta} \Big[h_{\alpha,\beta}(\vec{k}) - \epsilon_n(\vec{k}) S_{\alpha,\beta}(\vec{k})\Big] c_{\beta,n}(\vec{k})
\end{aligned} \tag{1.61}$$

Given that the projector functions are linear independent, all coefficients must vanish so that we obtain the Schrödinger equation in matrix form

$$\sum_{\beta} \Big[h_{\alpha,\beta}(\vec{k}) - \epsilon_n(\vec{k}) S_{\alpha,\beta}(\vec{k})\Big] c_{\beta,n}(\vec{k}) = 0 \tag{1.62}$$

with

$$h_{\alpha,\beta}(\vec{k}) \overset{\text{def}}{=} \langle\chi_{\alpha,\vec{k}}|\hat{h}|\chi_{\beta,\vec{k}}\rangle \overset{\text{Eq. 1.57}}{=} \sum_{\vec{t}} h_{\alpha,\vec{0},\beta,\vec{t}} e^{i\vec{k}\vec{t}} \quad \text{and} \tag{1.63}$$

$$S_{\alpha,\beta}(\vec{k}) \overset{\text{def}}{=} \langle\chi_{\alpha,\vec{k}}|\chi_{\beta,\vec{k}}\rangle \overset{\text{Eq. 1.57}}{=} \sum_{\vec{t}} S_{\alpha,\vec{0},\beta,\vec{t}} e^{i\vec{k}\vec{t}}\,. \tag{1.64}$$

[11] It is often difficult to decide where the orbitals go and where the projector functions. The notation is completely symmetric with respect to an interchange between the two. As a rule of thumb, one uses orbitals to expand the wave functions, and since operators act on wave functions, operators are expanded in projector functions.

Notably, there is no coupling of states having a different Bloch vectors, which is the essence of Bloch's theorem.

We are almost done: Let us now impose the normalization on the eigenstates $\langle\varphi_m(\vec{k})|\varphi_n(\vec{k'})\rangle = \delta_{m,n}\delta_{\vec{k},\vec{k'}}$

$$\begin{aligned}
\langle\varphi_m(\vec{k})|\varphi_n(\vec{k'})\rangle &= \sum_{\alpha,\beta} c^*_{\alpha,m}(\vec{k})\langle\chi_\alpha(\vec{k})|\chi_\beta(\vec{k'})\rangle c_{\beta,n}(\vec{k'}) \\
&\overset{\text{Eq. 1.57}}{=} \sum_{\alpha,\beta} c^*_{\alpha,m}(\vec{k})\frac{1}{\sum_{\vec{t}}}\sum_{\vec{t},\vec{t'}} \mathrm{e}^{-i\vec{k}\vec{t}}\langle\chi_{\alpha,\vec{t}}|\chi_{\beta,\vec{t'}}\rangle \mathrm{e}^{i\vec{k'}\vec{t'}} c_{\beta,n}(\vec{k'}) \\
&= \sum_{\alpha,\beta} c^*_{\alpha,m}(\vec{k}) \underbrace{\frac{1}{\sum_{\vec{t}}}\sum_{\vec{t}} \mathrm{e}^{-i(\vec{k}-\vec{k'})\vec{t}}}_{\delta_{\vec{k},\vec{k'}}} \underbrace{\sum_{\vec{t'}}\langle\chi_{\alpha,\vec{t}}|\chi_{\beta,\vec{t'}}\rangle \mathrm{e}^{i\vec{k'}(\vec{t'}-\vec{t})}}_{S_{\alpha,\beta}(\vec{k'})} c_{\beta,n}(\vec{k'}) \\
&= \delta_{\vec{k},\vec{k'}} \sum_{\alpha,\beta} c^*_{\alpha,m}(\vec{k}) S_{\alpha,\beta}(\vec{k}) c_{\beta,n}(\vec{k}) \qquad (1.65)
\end{aligned}$$

The orthonormality between states having different Bloch-vector is inherent in the Ansatz of Bloch wave function.[12] The orthonormality of states with the same Bloch-vector needs to be enforced by setting

$$\sum_{\alpha,\beta} c^*_{\alpha,m}(\vec{k}) S_{\alpha,\beta}(\vec{k}) c_{\beta,n}(\vec{k}) = \delta_{m,n} \qquad (1.66)$$

[12] States with different Bloch vector have different eigenvalues of the symmetry operator and are, therefore, orthogonal.

COOKING RECIPE FOR NON-INTERACTING ELECTRONS ON A LATTICE

This implies the following recipe to construct the eigenvalues and eigenstates of the Hamiltonian of a lattice.

1. Extract the real-space Hamilton $h_{\alpha,\vec{0},\beta,\vec{t}'}$ and overlap $S_{\alpha,\vec{0},\beta,\vec{t}'}$ matrix elements connecting the orbitals in the first unit cell $\vec{t} = \vec{0}$ to those in a unit cell displaced by a real-space lattice translation vector $\vec{t}'$.

2. Determine the k-dependent Hamiltonian and overlap matrix from the matrix elements in real space

$$h_{\alpha,\beta}(\vec{k}) = \sum_{\vec{t}} h_{\alpha,\vec{0},\beta,\vec{t}} e^{i\vec{k}\vec{t}} \tag{1.67}$$

$$S_{\alpha,\beta}(\vec{k}) = \sum_{\vec{t}} S_{\alpha,\vec{0},\beta,\vec{t}} e^{i\vec{k}\vec{t}} \tag{1.68}$$

3. Solve the generalized eigenvalue problem and obtain k-dependent energies $\epsilon_n(\vec{k})$ and the eigenvectors $c_{\alpha,n}(\vec{k})$

$$0 = \sum_{\beta} \left[h_{\alpha,\beta}(\vec{k}) - \epsilon_n(\vec{k}) S_{\alpha,\beta}(\vec{k}) \right] c_{\beta,n}(\vec{k}) \tag{1.69}$$

with the normalization condition

$$\sum_{\alpha,\beta} c^*_{\alpha,m}(\vec{k}) S_{\alpha,\beta}(\vec{k}) c_{\beta,n}(\vec{k}) = \delta_{m,n} \tag{1.70}$$

4. Construct eigenstates of the Hamiltonian from the eigenvectors

$$|\varphi_n(\vec{k})\rangle = \sum_{\alpha} \underbrace{\sum_{\vec{t}} |\chi_{\alpha,\vec{t}}\rangle e^{i\vec{k}\vec{t}} \frac{1}{\sqrt{\sum_{\vec{t}'}}}}_{|\chi_{\alpha,\vec{k}}\rangle} c_{\alpha,n}(\vec{k}) \tag{1.71}$$

1.2 Functionals and their derivatives

In the lecture notes, I also use derivatives of a functional with respect to the bra or ket of a wave function. This is a straightforward, but uncommon generalization of functional derivatives. Let me motivate the notation here.

I found it convenient to write down the variation of functionals, which define functional derivatives, rather than using the usual rules for functional derivatives.

1. **normal derivative:** For a simple function $f(\vec{r})$ of a vector argument $\vec{r}$, the first variation is

$$\delta f(\vec{r}) = \sum_j \frac{\delta f}{\delta r_j} \delta r_j + O(\delta r^2) \tag{1.72}$$

The derivative is defined as the prefactor of the variation of the argument.

$$\frac{\partial f}{\partial r_j} \stackrel{\text{def}}{=} \frac{\delta f}{\delta r_j} \tag{1.73}$$

2. **functional derivative:** Making the index of the argument continuous, i.e. $j \rightsquigarrow s$, turns the vector $\vec{r}$ into a function $r(s)$ and the function $f(\vec{r})$ into a functional $F[r]$.

$$\delta F[r] = \int ds \underbrace{\frac{\delta F}{\delta r(s)}}_{=\partial F/\partial r(s)} \delta r(s) + O(\delta r^2) \tag{1.74}$$

which defines the functional derivative

$$\frac{\partial F}{\partial r(s)} \stackrel{\text{def}}{=} \frac{\delta F}{\delta r(s)} \tag{1.75}$$

It is common to differentiate a derivative from a functional derivative using the symbol ∂ for a partial derivative, δ for functional derivatives and d for total derivatives. Because I consider these as variations of the same theme, I do not follow this distinction, at least not rigorously. Rather I use δ, when I have infinitesimal, but discrete displacements of a variable in mind, and ∂ for derivatives.

3. **Wirtinger derivative:** For complex-valued arguments, the concept of **Wirtinger derivatives** is useful. The concept is described in more detail in appendix A.4 on p. 502. It shows that the variation of a general function of a complex number, can be expressed by the variations with respect to those of the complex number and its complex conjugate. The complex number and its complex conjugate are treated as if they were independent. This is, however, only a formal "trick". It reflects that a complex number consists of two independent real numbers.

   In the following, I demonstrate the principle writing a function $f(c)$ once as function of complex-valued argument, and once as function with two real arguments, which represent real and imaginary part of c.

$$\begin{aligned}
f(\vec{c}) &= \bar{f}(\mathrm{Re}[c], \mathrm{Im}[c]) \\
\delta f(\vec{c}) &= \frac{\delta \bar{f}}{\delta \mathrm{Re}[c]} \delta \mathrm{Re}[c] + \frac{\delta \bar{f}}{\delta \mathrm{Im}[c]} \delta \mathrm{Im}[c] \\
&= \frac{\delta \bar{f}}{\delta \mathrm{Re}[c]} \frac{\delta c + \delta c^*}{2} + \frac{\delta \bar{f}}{\delta \mathrm{Im}[c]} \frac{\delta c - \delta c^*}{2i} \\
&= \underbrace{\frac{1}{2}\Big(\frac{\delta \bar{f}}{\delta \mathrm{Re}[c]} - i \frac{\delta \bar{f}}{\delta \mathrm{Im}[c]}\Big)}_{\frac{\delta f}{\delta c}} \delta c + \underbrace{\frac{1}{2}\Big(\frac{\delta \bar{f}}{\delta \mathrm{Re}[c]} + i \frac{\delta \bar{f}}{\delta \mathrm{Im}[c]}\Big)}_{\frac{\delta f}{\delta c^*}} \delta c^*
\end{aligned} \tag{1.76}$$

   This motivates the definition of the Wirtinger derivatives

$$\begin{aligned}
\frac{\partial f}{\partial c} &\stackrel{\text{def}}{=} \frac{1}{2}\Big(\frac{\delta \bar{f}}{\delta \mathrm{Re}[c]} - i \frac{\delta \bar{f}}{\delta \mathrm{Im}[c]}\Big) \\
\frac{\partial f}{\partial c^*} &\stackrel{\text{def}}{=} \frac{1}{2}\Big(\frac{\delta \bar{f}}{\delta \mathrm{Re}[c]} + i \frac{\delta \bar{f}}{\delta \mathrm{Im}[c]}\Big)
\end{aligned} \tag{1.77}$$

4. **Derivative with respect to a bra or ket:** Next we talk about functionals of complex functions such as quantum mechanical wave functions.

$$\begin{aligned}
\delta F[\phi(\vec{x}), \phi^*(\vec{x})] &= \int d^4x \underbrace{\frac{\delta F}{\delta \phi(\vec{x})}}_{\frac{\delta F}{\delta \langle \vec{x}|\phi\rangle}} \underbrace{\delta\phi(\vec{x})}_{\langle \vec{x}|\delta\phi\rangle} + \int d^4x \underbrace{\frac{\delta F}{\delta \phi^*(\vec{x})}}_{\frac{\delta F}{\delta \langle \phi|\vec{x}\rangle}} \underbrace{\delta\phi^*(\vec{x})}_{\langle \delta\phi|\vec{x}\rangle} + O(\delta\phi^2) \\
&= \int d^4x \left\langle \frac{\delta F}{\delta|\phi\rangle}\middle|\vec{x}\right\rangle \langle \vec{x}|\delta\phi\rangle + \int d^4x \langle \delta\phi|\vec{x}\rangle \left\langle \vec{x}\middle| \frac{\delta F}{\delta\langle\phi|}\right\rangle + O(\delta\phi^2) \\
&= \frac{\delta F}{\delta|\phi\rangle}|\delta\phi\rangle + \langle\delta\phi|\frac{\delta F}{\delta\langle\phi|} + O(\delta|\phi\rangle^2)
\end{aligned} \tag{1.78}$$

This motivates the following definition of the derivative with respect to a bra or a ket.

$$\begin{aligned}\frac{\delta F}{\delta|\phi\rangle} &\stackrel{\text{def}}{=} \int d^4x\ \frac{\delta F}{\delta\langle\vec{x}|\phi\rangle}\langle\vec{x}| = \int d^4x\ \frac{\delta F}{\delta\phi(\vec{x})}\langle\vec{x}| \\ \frac{\delta F}{\delta\langle\phi|} &\stackrel{\text{def}}{=} \int d^4x\ |\vec{x}\rangle\frac{\delta F}{\delta\langle\phi|\vec{x}\rangle} = \int d^4x\ |\vec{x}\rangle\frac{\delta F}{\delta\phi^*(\vec{x})}\end{aligned} \tag{1.79}$$

The same principles can be carried further to include derivatives with respect to operators or other objects.

1.3 N-particle wave functions

1.3.1 N-particle states

In order to describe N particles instead of only one, we need N position coordinates and N spin indices. Thus, the wave function of a N-particle state is

$$\psi(\vec{x}_1,\ldots,\vec{x}_N) = \langle\vec{x}_1,\ldots,\vec{x}_N|\psi\rangle \tag{1.80}$$

The absolute square of a two-particle wave function is the probability density for the first electron to be at $\vec{x}_1$ with position $\vec{r}_1$ with spin σ_1 and another one to be at $\vec{x}_2$ with position $\vec{r}_2$ with spin σ_2.

One basis set, which spans the N-particle Hilbert space, is $\{|\vec{x}_1,\ldots,\vec{x}_N\rangle\}$. The orthonormality has the form

$$\langle\vec{x}_1,\ldots,\vec{x}_N|\vec{x'}_1,\ldots,\vec{x'}_N\rangle = \delta(\vec{x}_1-\vec{x'}_1)\cdots\delta(\vec{x}_N-\vec{x'}_N) \tag{1.81}$$

and the completeness relation is

$$\hat{1} = \int d^4x_1\cdots\int d^4x_N\ |\vec{x}_1,\ldots,\vec{x}_N\rangle\langle\vec{x}_1\ldots,\vec{x}_N| \tag{1.82}$$

1.3.2 Product states

A **product state** of a set with N one-particle wave functions has the form

$$\Psi_{a,\ldots,z}(\vec{x}_1,\ldots,\vec{x}_N) = \langle\vec{x}_1,\ldots,\vec{x}_N|\Psi_{a,\ldots,z}\rangle = \varphi_a(\vec{x}_1)\cdots\varphi_z(\vec{x}_N) \tag{1.83}$$

Product states are useful, because they can be expressed simply by specifying N one-particle wave functions $|\varphi_j\rangle$.

Product states are often written in the form of a $\otimes$.

$$\begin{aligned}|\vec{x}_1,\vec{x}_2,\ldots,\vec{x}_N\rangle &= |\vec{x}_1\rangle\otimes|\vec{x}_2\rangle\otimes\cdots\otimes|\vec{x}_N\rangle \\ |\varphi_a,\varphi_b,\ldots,\varphi_z\rangle &= |\varphi_a\rangle\otimes|\varphi_b\rangle\otimes\cdots\otimes|\varphi_z\rangle\end{aligned} \tag{1.84}$$

I will not use the form on the right-hand side.

The set of all N-particle product states, that can be formed from a complete-and-orthonormal one-particle basisset, is again a complete-and-orthonormal basis set in the N-particle Hilbert space. Note, however, that the most general N-particle state is a superposition of all these product states.

An attempt to visualize the restrictions of product states is given in figure 1.1.

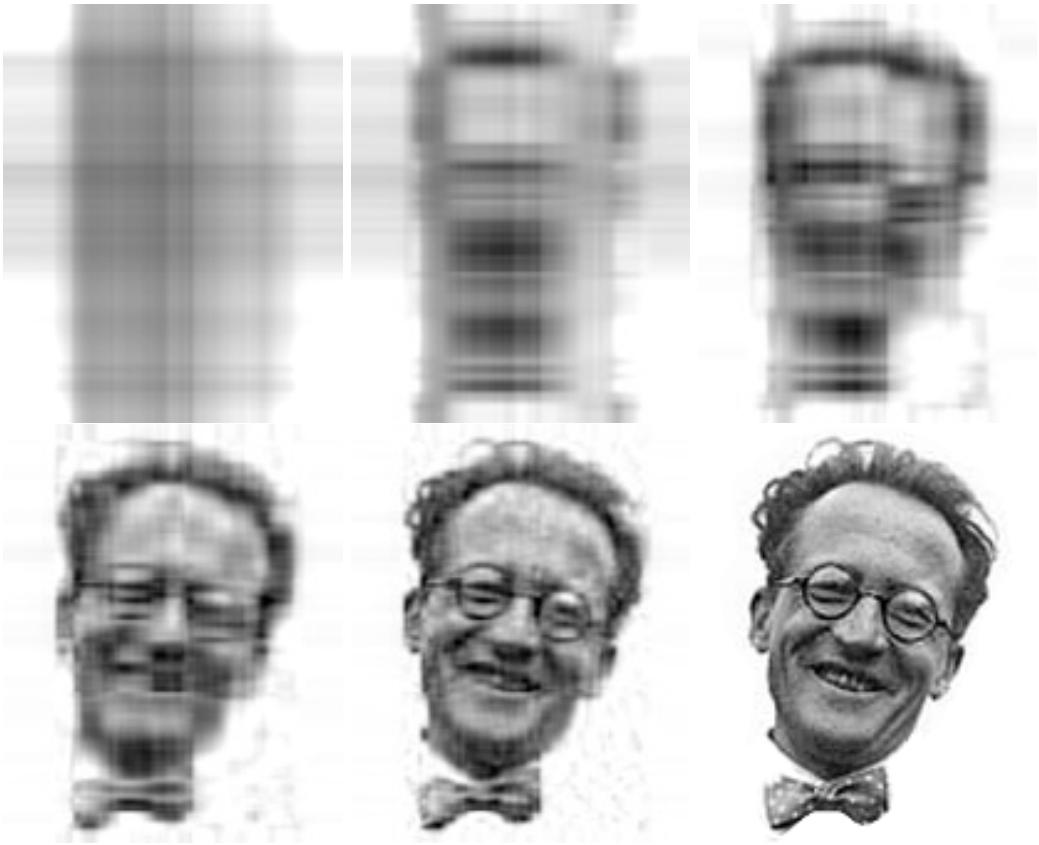


Fig. 1.1: Demonstration of product states and the superposition of product states. The grey-scale values $F(x, y)$ of the picture of Erwin Schrödinger is approximated by finite sums of product wave functions in the form $F(x, y) = \sum_{j=1}^{M} f_j(x) g_j(y)$ for $M = 1, 2, 4$ in the top row and for $M = 8, 16$ and the original figure in the bottom row. The functions $f_j(x)$ and $g_j(y)$ have been optimized individually to minimize the mean square deviation from the grey-scale values.

1.3.3 Slater determinants

The particles can be divided into classes of **identical particles**. Any physical Hamilton operator is symmetric under exchange of two identical particles. If that were not the case, it would be possible to distinguish the two particles which would make them non-identical.

Thus, the physical wave function is an eigenstate of the **permutation operator** between two identical particles. The permutation operator has the eigenvalues $+1$ and -1. Particles described by the permutation eigenvalue $+1$ are **bosons**, and those with permutation eigenvalue -1 are **fermions**. Fermionic wave functions are antisymmetric under exchange of two particles, while bosonic wave functions are symmetric under particle exchange.

Fermionic wave functions can be constructed from N one-particle wave functions $\varphi_i(\vec{x})$ with $i \in \{1, \ldots, N\}$ as antisymmetrized product state.

$$\underbrace{\Psi^F(\vec{x}_1, \ldots, \vec{x}_N)}_{\langle \vec{x}_1, \ldots, \vec{x}_N | \Psi^F \rangle} = \frac{1}{\sqrt{N!}} \sum_{i_1, \ldots, i_N = 1}^{N} \epsilon_{i_1, \ldots, i_N} \varphi_{i_1}(\vec{x}_1) \cdots \varphi_{i_N}(\vec{x}_N) \tag{1.85}$$

where $\epsilon_{i_1, \ldots, i_N}$ is the fully antisymmetric tensor.

The **fully antisymmetric tensor**, also called **Levi-Civita symbol**, is defined by

- It has the value 1 if the indices are in ascending order.

$$\epsilon_{1,2,\ldots,N} = 1 \tag{1.86}$$

- any permutation of two indices of the fully antisymmetric tensor changes its sign.
- the antisymmetric tensor is zero whenever two indices are equal.

Thus, every non-zero matrix element of the antisymmetric tensor corresponds to a permutation of the numbers $(1, 2, \ldots, N)$. Because there are $N!$ permutation of the indices $1, 2, \ldots, N$, the sum contributes $N!$ non-zero terms. Whenever the one-particle states $\varphi_j(\vec{x})$ are orthonormal, all terms in the sum Eq. 1.85 are orthonormal. Thus, the factor $1/\sqrt{N!}$ establishes the normalization of the final function. Non-orthonormal one-particle states can be used as well, but then the resulting many-particle wave function is not normalized.

The fully antisymmetric tensor can be used to evaluate the determinant of a matrix $\boldsymbol{A}$ via

$$\det|\boldsymbol{A}| = \sum_{i_1,\ldots,i_N=1}^{N} \epsilon_{i_1,\ldots,i_N} A_{i_1,1} A_{i_2,2} \cdots A_{i_N,N} \tag{1.87}$$

Thus, the antisymmetrized product wave function can also be expressed as a determinant of the matrix with elements $A_{i,j} = \varphi_i(\vec{x}_j)$.

$$\begin{aligned}\Psi^F(\vec{x}_1, \ldots, \vec{x}_N) &= \frac{1}{\sqrt{N!}} \sum_{i_1,\ldots,i_N} \epsilon_{i_1,\ldots,i_N} \varphi_{i_1}(\vec{x}_1) \cdots \varphi_{i_N}(\vec{x}_N) \\ &= \frac{1}{\sqrt{N!}} \det \begin{vmatrix} \varphi_1(\vec{x}_1) & \varphi_1(\vec{x}_2) & \ldots & \varphi_1(\vec{x}_N) \\ \varphi_2(\vec{x}_1) & \varphi_2(\vec{x}_2) & \ldots & \varphi_2(\vec{x}_N) \\ \vdots & \vdots & & \vdots \\ \varphi_N(\vec{x}_1) & \varphi_N(\vec{x}_2) & \ldots & \varphi_N(\vec{x}_N) \end{vmatrix}\end{aligned} \tag{1.88}$$

This is the reason for calling the antisymmetrized product wave functions **Slater determinants**.

The normalization factor $1/\sqrt{N!}$ makes sense[13] only for orthonormal one-particle wave functions $|\varphi_j\rangle$. While it is perfectly allowed to construct antisymmetrized wave functions from non-orthonormal one-particle wave functions, it is very inconvenient in practice. For example, the normalization of the resulting wave function is much more complicated.

For bosons, we need to symmetrize, rather than antisymmetrize, the product state under particle exchange, which can be accomplished by replacing the determinant by the **permanent** replacing the fully antisymmetric tensor by its absolute value.

$$\begin{aligned}\Psi^B(\vec{x}_1, \ldots, \vec{x}_N) &= \frac{1}{\sqrt{N! \prod_{k=1}^{N_d}(n_k!)}} \sum_{i_1,\ldots,i_N} \left|\epsilon_{i_1,\ldots,i_N}\right| \varphi_{i_1}(\vec{x}_1) \cdots \varphi_{i_N}(\vec{x}_N) \\ &= \frac{1}{\sqrt{N! \prod_{k=1}^{N_d}(n_k!)}} \mathrm{perm} \begin{vmatrix} \varphi_1(\vec{x}_1) & \varphi_1(\vec{x}_2) & \ldots & \varphi_1(\vec{x}_N) \\ \varphi_2(\vec{x}_1) & \varphi_2(\vec{x}_2) & \ldots & \varphi_2(\vec{x}_N) \\ \vdots & \vdots & & \vdots \\ \varphi_N(\vec{x}_1) & \varphi_N(\vec{x}_2) & \ldots & \varphi_N(\vec{x}_N) \end{vmatrix}\end{aligned} \tag{1.89}$$

The normalization of the permanent is non-trivial[14], because some of the orbitals may be identical to each other. Let me assume that the permanent is made out of N_d distinct orbitals. The multiplicity of the k-th set of distinct orbitals shall be n_k, saying that the k-th orbital is occupied by n_k particles. The total number of particles in the permanent is $\sum_{k=1}^{N_d} n_k = N$.

[13] For a non-orthonormal basisset, the resulting Slater determinant would not me normalized.
[14] No derivative of this factor is provided here.

The bosonic wave function is non-zero also if two orbitals are identical. For example, if $|\varphi_\alpha\rangle = |\varphi_\beta\rangle$, the permanent is

$$\langle \vec{x}_1, \vec{x}_2 | \psi^B_{\alpha,\beta} \rangle = \frac{1}{\sqrt{2}} \left[\varphi_\alpha(\vec{x}_1)\varphi_\beta(\vec{x}_2) + \varphi_\beta(\vec{x}_1)\varphi_\alpha(\vec{x}_2) \right] \quad \Rightarrow \quad \langle \vec{x}_1, \vec{x}_2 | \psi^B_{\alpha,\alpha} \rangle = \varphi_\alpha(\vec{x}_1)\varphi_\alpha(\vec{x}_2) \neq 0$$

For fermions, on the other hand, the Slater determinant of two identical one-particle orbitals is the zero state

$$\langle \vec{x}_1, \vec{x}_2 | \psi^F_{\alpha,\beta} \rangle = \frac{1}{\sqrt{2}} \left[\varphi_\alpha(\vec{x}_1)\varphi_\beta(\vec{x}_2) - \varphi_\beta(\vec{x}_1)\varphi_\alpha(\vec{x}_2) \right] \quad \Rightarrow \quad \langle \vec{x}_1, \vec{x}_2 | \psi^F_{\alpha,\alpha} \rangle = 0$$

1.4 Many-particle states and Fock space

Many-particle physics deals with situations where the particle number changes or where the wave function consists of contributions with different particle numbers. Therefore, we need to overcome the limitation of wave functions with fixed particle numbers. This extension will lead us to the concept of the Fock space.

Examples of problems which require states with different particle numbers are the following:

- A physical process may change the number of particles. An example would be an electron-positron collision, where two particles disappear while two photons are created.
- The number of particles in a so-called **open system** may change as particles migrate from the system under study and into the environment and vice versa.
- The number of particles may be variable, because the system is coupled to a thermodynamic particle reservoir. The situation is analogous to that of an open system, mentioned above. The main difference is that the coupling to the particle reservoir is considered infinitesimally small, so that the time scale of the particle exchange is considered infinite.

In order to describe systems with variable particle numbers, we need to generalize the concept of the N-particle Hilbert space to that of the **Fock space**. The Fock space is the union of all Hilbert spaces with N particles, where N can vary from zero to infinity. The zero-particle state is the so-called **vacuum state**. The vacuum state describes a system without particles, which is the true vacuum.[15]

The problem of the Fock space is that its states can no more be represented as wave functions in real space, because we cannot construct a function with a variable number of arguments. In order to describe a wave function in Fock space, we need to form the projection of the state onto each N-particle channel. For each N-particle channel we obtain a normalized N-particle wave function and a complex factor. The absolute square of this factor is the probability for the system to contain N particles. The phase factor describes the phase relations or the **entanglement**[17][16] between different N particle channels.

A basis for the Fock space is

$$\underbrace{|\mathcal{O}\rangle}_{\text{vacuum st.}} \cup \underbrace{\{|\vec{x}_1\rangle\}}_{\text{1p-Hilbert space}} \cup \underbrace{\{|\vec{x}_1, \vec{x}_2\rangle\}}_{\text{2p-Hilbert space}} \cup \underbrace{\{|\vec{x}_1, \vec{x}_2, \vec{x}_3\rangle\}}_{\text{3p-Hilbert space}} \cup \ldots \tag{1.91}$$

[15] The vacuum state is a normalized state and describes a physical situation, namely the vacuum, which does not have any particles in it. Thus, it is different from the zero state, which has a norm equal to 0, and which does not describe any physical situation.

[16] Two subsystems are called entangled, when the state of the combined system is a sum of the wave functions of the two parts $|\Psi\rangle = |\Psi_A\rangle + |\Psi_B\rangle e^{i\varphi}$ with a defined relative phase φ. The expectation values of an observable $\hat{O}$ depends on the relative phase

$$\langle \Psi | \hat{O} | \Psi \rangle = \langle \Psi_A | \hat{O} | \Psi_A \rangle + \langle \Psi_B | \hat{O} | \Psi_B \rangle + \mathrm{Re}\left[\langle \Psi_A | \hat{O} | \Psi_B \rangle e^{i\varphi} \right] \tag{1.90}$$

In an ensemble of wave functions, in which all relative phases contribute equally, the last term in the observable vanishes. This implies that the quantum mechanical coupling between the subsystems is absent and the two subsystems are not entangled. The phase relation is unimportant also, when the system is described by a product state $|\Psi\rangle = |\Psi_A, \Psi_B\rangle$.Editor: This is a first draft. Clean this up.

where the $\vec{x}_j = (\vec{r}_j, \sigma_j)$ denotes the combined position-and-spin argument. With $A \cup B$, I denote the union of the two sets A and B.

The basisset is orthonormal, that is, (1) two states with the same particle number N satisfy the same orthonormality conditions as those in the N-particle Hilbert space. (2) States with different particle numbers are orthonormal.

$$\langle \vec{x}_1, \ldots, \vec{x}_N | \vec{x'}_1, \ldots, \vec{x'}_{N'} \rangle = \begin{cases} 0 & \text{for } N \neq N' \\ \delta(\vec{x}_1 - \vec{x'}_1) \cdots \delta(\vec{x}_N - \vec{x'}_N) & \text{for } N = N' \end{cases} \tag{1.92}$$

One way to rationalize the orthonormality between states with differing particle number is that states with a given particle number are eigenstates of a particle-number operator. Eigenstates of a hermitian operator with different eigenvalues are orthonormal.[17]

The completeness relation in Fock space has the form

$$\hat{1} = \sum_{N=0}^{\infty} \int d^4x_1 \ldots \int d^4x_N \, |\vec{x}_1, \ldots, \vec{x}_N\rangle\langle \vec{x}_1, \ldots, \vec{x}_N| \tag{1.93}$$

1.4.1 Occupation-number representation

The Slater determinants formed from a given complete, ortho-normal one-particle basis set span the complete Fock space. The occupation-number representation is a convenient notation to describe this basis of many-particle states.

We start from an orthonormal set of one-particle basis functions $|\varphi_j\rangle$ which are arranged in a well-defined order, that is with indices increasing from left to right. Each subset of these functions specifies one Slater determinant. This subset is specified by a vector $\vec{\sigma}$ of occupation numbers $\sigma_1, \sigma_2, \ldots$. The index j of the occupation number σ_j refers to one of the one-particle wave functions $|\psi_j\rangle$. Each occupation number σ_j can be either zero or one. The one-particle states with occupation number equal to one are used to build the Slater determinant $|\vec{\sigma}\rangle$.

OCCUPATION NUMBERS AND SLATER DETERMINANTS

The occupation-number representation is defined such the one-particle orbitals in the Slater-determinant are arranged in the same order as the non-zero occupation numbers in the string $\vec{\sigma}$ of occupation numbers.

The Slater determinants formed in this way form a complete and orthonormal basis set of the Fock space, that is

$$\hat{1} = \sum_{\vec{\sigma}} |\vec{\sigma}\rangle\langle\vec{\sigma}| = \sum_{\sigma_1=0}^{1} \sum_{\sigma_2=0}^{1} \cdots |\sigma_1, \sigma_2, \ldots\rangle\langle\sigma_1, \sigma_2, \ldots| \tag{1.94}$$

The fact that Slater determinants form a complete basis in Fock space is the reason why Slater determinants are relevant even for interacting electron systems. Typically the eigenstates of the Hamiltonian for non-interacting electrons are Slater determinants. This is, however, not the case for interacting electrons.

A general many-particle state must be represented by a superposition of such Slater determinants. A general state in the Fock space has the form

$$|\Phi\rangle = \sum_{\vec{\sigma}} |\vec{\sigma}\rangle \underbrace{\langle\vec{\sigma}|\Phi\rangle}_{c_{\vec{\sigma}}} = \sum_{\vec{\sigma}} |\vec{\sigma}\rangle c_{\vec{\sigma}} \tag{1.95}$$

[17] This may not be a proof, because we probably need the orthonormality before we can define a hermitian particle-number operator.

1.4.2 Many-particle states of non-interacting electrons

If the one-particle basis used to define the Slater determinants are the eigenstates $|\varphi_j\rangle$ of the non-interacting Hamiltonian $\hat{h}$, the Slater determinants are eigenstates of that Hamiltonian and the particle-number operator[18] $\hat{N}$

$$\hat{h}|\vec{\sigma}\rangle = |\vec{\sigma}\rangle E_{\vec{\sigma}} \qquad \text{and} \qquad \hat{N}|\vec{\sigma}\rangle = |\vec{\sigma}\rangle N_{\vec{\sigma}} \tag{1.96}$$

with

$$E_{\vec{\sigma}} = \sum_j \epsilon_j \sigma_j \qquad \text{and} \qquad N_{\vec{\sigma}} = \sum_j \sigma_j \ . \tag{1.97}$$

The energy levels ϵ_j are the eigenvalues of the Hamiltonian $\hat{h}$ in the one-particle Hilbert space, i.e.

$$\hat{h}|\varphi_j\rangle = |\varphi_j\rangle \epsilon_j \ . \tag{1.98}$$

1.4.3 Size of Hilbert spaces

Consider a finite set of n one-particle states. The one-particle Hilbert space has n dimensions. The N-particle Hilbert space of distinguishable orbitals has N^n dimensions. The N-particle Hilbert space of fermionic wave functions has[19] $\frac{n(n-1)\ldots(n-N+1)}{1\cdot 2\cdots N} = \frac{n!}{(n-N)!(N!)} = \binom{n}{N}$ dimensions. The bosonic N-particle Hilbert space is larger and has $d = \frac{(N+n-1)!}{N!(n-N)!}$ dimensions.[20]

Table 1.3: Dimensions d of different spaces of quantum mechanical wave functions based on a n-dimensional one-particle Hilbert space. N is the number of particles in the N-particle wave function.

one-particle Hilbert space	$d = n$
N-particle Hilbert space, distinguishable particles	$d = n^N$
N-particle Hilbert space, fermions	$d = n!/[(n-N)!N!]$
N-particle Hilbert space, bosons	$d = (N+n-1)!/[N!(n-1)!]$
Fock space, fermions	$d = 2^n$

We see that the Fock space formed by a one-particle basisset of only 10 orbitals has dimension 1024. This is appropriate to describe the d-shell of a transition metal atom. The Hamiltonian for such a system has one million matrix elements, which can still be handled on a computer. If we consider 10 such atoms, i.e. 100 one-particle orbitals, the Fock space has dimension of order $d > 10^{30}$. This is beyond the capability of any computer. The rapid increase of the dimensionality of the problem has been coined as **dimensional bottleneck** of many-particle physics. It implies that, when dealing with many-particle physics, it is not sufficient to wait for larger computers: Each additional one-particle orbital doubles dimension of the problem and usually increases the computational by a factor four or eight.

[18] The eigenstates of the Hamiltonian can be represented as eigenstates of the particle-number operator, if the Hamiltonian commutates with the particle-number operator. In that case, the Hamilton operator conserves the particle number. Examples for a Hamilton operator, that does not conserve the particle number are the following: (1) A Hamiltonian that describes the annihilation of an electron-positron pair under creation of two photons. (2) A Hamiltonian describing a subsystem embedded into a bath, which can provide particles to the subsystem or accept particles leaving the subsystem.

[19] We can pick from n one-particle states as the first orbital. The second orbital can be picked from the $(n-1)$ remaining one-particle states, because each orbital may occur at most once in the Slater determinant. In the set of two-particle wave functions obtained in this way, each wave function is included twice. One of them has the orbitals in the reversed order. Therefore, I need to divide by two. In the end there are $n!/(n-N)!$ product states of N distinct orbitals irrespective of their order. This number is divided by the number $N!$ of permutations of the N orbitals, which yields the final dimension of the fermionic N-particle Hilbert space formed in a n-dimensional one-particle basisset.

[20] For bosons the dimension of a N-particle state is $d = \frac{(N+n-1)!}{N!(n-N)!}$. See `https://everettyou.github.io/teaching/PHYS212B/SecondQuantization.pdf`

1.5 Home study and practice: Simple one-particle problems

In order to explore the role of the formalism described in the book, we need a few simple systems with non-interacting particles as model systems.

The models are selected to be **minimal models**. A minimal model is the most simple model describing a certain effect. The idea is to capture the essence of an effect without obscuring it by the complexity of the calculations.

One of the most important models for the many-particle physics of extended systems is the so-called **Hubbard model**.[18, 19, 20] This model consists of a regular grid of hydrogen atoms, with electrons that strongly interact when they meet on the same hydrogen atom. While the purpose of the Hubbard model is to study interacting systems, in the models discussed here, we will discard the interaction. As we proceed towards interacting systems, we will study the role of interactions. Here, we will select two variants of the Hubbard model, namely the hydrogen molecule and the linear chain.

The **jellium model** is our model for a continuous system. In contrast to the Hubbard model, the atomic structure is absent in this model.

1.5.1 Hydrogen molecule

Introduction

The hydrogen molecule is the smallest non-trivial system for the study of electron correlation. Most calculations for this system can be done analytically, which makes it an ideal system to test the understanding and the workings of new concepts. It is also a cross link between the study of strong correlations in physics and chemistry. On the one-hand, the hydrogen dimer is the smallest Hubbard model.[18] As the interaction between the electrons is increased, one can study the mechanisms behind the so-called Mott-Hubbard insulator. On the other hand, when the hopping parameter is reduced in size, the hydrogen model describes the dissociation of a chemical bond. Because the ratio of interaction and hopping is large in this limit, one arrives at basically the same effects of strong correlations.

The first exercise is meant as an appetizer. We will frequently return to the hydrogen molecule during this lecture. Here, we study the hydrogen molecule without electron-electron interactions.

Problem

Consider a simplified hydrogen molecule. On each of the two sites, two orbitals are considered, one for spin up and the other for spin down.
The Hamiltonian has the form

$$\hat{h} = \underbrace{\sum_{\sigma\in\{\uparrow,\downarrow\}}\sum_{R=1}^{2} |\pi_{R,\sigma}\rangle\, \bar{\epsilon}\, \langle\pi_{R,\sigma}|}_{\text{atomic energies}} \underbrace{- \sum_{\sigma\in\{\uparrow,\downarrow\}} \Big(|\pi_{1,\sigma}\rangle\, \bar{t}\, \langle\pi_{2,\sigma}| + |\pi_{2,\sigma}\rangle\, \bar{t}\, \langle\pi_{1,\sigma}| \Big)}_{\text{hopping}} \tag{1.99}$$

where $\bar{\epsilon}$ is the so-called **atomic level** and $\bar{t}$ is the so-called **hopping parameter**[a] The orbital index $\alpha = (R, \sigma)$ selects a particular atom $R \in \{1, 2\}$ and a spin index $\sigma \in \{\uparrow, \downarrow\}$. The $|\pi_\alpha\rangle$ are the **projector functions**, which correspond to the local orbitals $|\chi_\alpha\rangle$, i.e. $\langle\pi_\alpha|\chi_\beta\rangle \overset{\text{Eq. 1.43}}{=} \delta_{\alpha,\beta}$. Despite the fact that we distinguish orbitals $|\chi_\alpha\rangle$ and projector functions $\langle\pi_\alpha|$, we consider orthonormal local orbitals $|\chi_\alpha\rangle$, that is $\langle\chi_\alpha|\chi_\beta\rangle = \delta_{\alpha,\beta}$.

1 Determine the eigenvalues and eigenstates of the Hamiltonian in the basis of local orbitals $|\chi_{R,\sigma}\rangle$, that is with the ansatz $|\psi_n\rangle = \sum_\alpha |\chi_\alpha\rangle c_{\alpha,n}$. The state index n is a composite index containing a spin quantum number and a non-spin index $j \in \{b, a\}$.

[a] I will use the sign convention that the hopping parameter has the same sign as the overlap matrix element of the orbitals. That is, the hopping parameter $\bar{t}$ between two s-orbitals is positive, while that between two p-orbitals pointing along the bond axis is negative. Editor: Caution: this adjustment may not be uniform in the lecture notes.

Solution

1 Determine the eigenvalues and eigenstates of the Hamiltonian in the basis of local orbitals $|\chi_{R,\sigma}\rangle$, that is with the ansatz $|\varphi_n\rangle = \sum_\alpha |\chi_\alpha\rangle c_{\alpha,n}$. The state index n is a composite index containing a spin quantum number and a non-spin index $j \in \{b, a\}$.

The result is as follows: The single-electron levels are

- the two lower, **b**onding states $|\varphi_{b,\sigma}\rangle$ for the two spin directions with energy $\epsilon_b = \bar{\epsilon} - |\bar{t}|$

$$|\varphi_{b,\sigma}\rangle = \frac{1}{\sqrt{2}}\Big(|\chi_{1,\sigma}\rangle + |\chi_{2,\sigma}\rangle \mathrm{sgn}(\bar{t}) \Big) \tag{1.100}$$

- and the two upper, **a**ntibonding states $|\varphi_{a,\sigma}\rangle$ with energy $\epsilon_a = \bar{\epsilon} + |\bar{t}|$.

$$|\varphi_{a,\sigma}\rangle = \frac{1}{\sqrt{2}}\Big(|\chi_{1,\sigma}\rangle - |\chi_{2,\sigma}\rangle \mathrm{sgn}(\bar{t})\Big) \tag{1.101}$$

For the hydrogen molecule, the orbitals are s orbitals, which have a positive overlap along the bond. Per our convention[21], the hopping parameter $\bar{t}$ has the same sign as the overlap matrix element. For the hydrogen molecule, the hopping parameter $\bar{t}$ is therefore positive.[22]

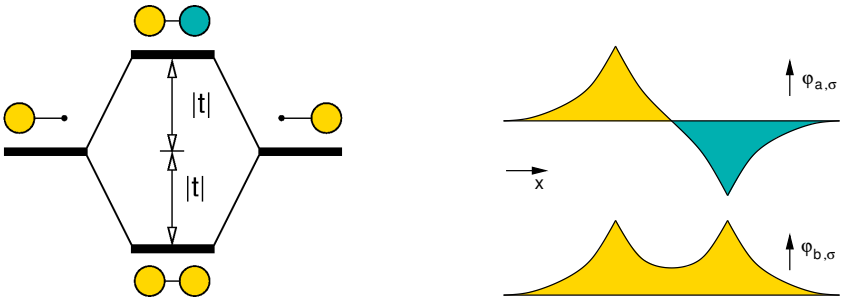


Fig. 1.2: Schematic representation of the energy level diagram (left) and the orbitals (left and right) of a hydrogen molecule. The atomic energy levels (outer bars) are split into a bonding (lower bar) and an antibonding (upper bar) state as the distance between the atoms approaches the bond distance. The orbital representation on the left is derived from an iso-contour plot of the wave function, with the color selecting the positive or negative contour value. Yellow and blue represent two signs of the wave function. On the right, the bonding state $|\varphi_{b,\sigma}\rangle$ and the antibonding state $|\varphi_{a,\sigma}\rangle$ are drawn along the bond axis.

[21] The convention that the sign of the hopping parameter $\bar{t}$ is equal to that of the overlap matrix element between the two orbitals, is not generally adapted.

[22] In contrast, the overlap between two p-orbitals, which are oriented along the bond, is negative. Consequently, also the hopping matrix element $\bar{t} < 0$ is negative. In this case, Eq. 1.100, would describe the upper, rather than the lower orbital, and it would be called the antibonding orbital. Analogously, Eq. 1.101 would be lower in energy and would be called the bonding orbital.

1.5.2 General diatomic molecule

Introduction

The general diatomic molecule is the model for a general 2-dimensional Hamiltonian. This problem is so important that its behavior should be known, even without doing the calculations. Whenever the coupling between two states stands out one can approximate the behavior by a 2-dimensional problem.

This problem will also make you familiar with a couple general rules, which do not require any calculation.

- Level repulsion: The presence of an off-diagonal matrix element between two states will lead to a repulsion of the energy levels. This repulsion will become weaker with the initial energy separation of the orbitals.
- Charge sum rule: The weight of an orbital summed over all eigenstates adds up to unity.
- Energy sum rule: the sum of all energy levels is equal to the sum of diagonal elements of the Hamiltonian.
- The character of an eigenstate is dominated by that basis-orbital, which is closest in energy.

These rules appear very simple, but later they will be key to understand the workings of Green's functions, which will be the topic of this course.

Problems with two orbitals will be important in these lecture notes, where we try to experience many-particle physics with minimal problems.

Problem

Exercise: Generalize the hydrogen molecule to a molecule with two distinct orbitals. That is, the "atomic energy levels" $\bar{\epsilon}_\alpha$ of both sites are distinct. Determine energy levels and eigenstates. Plot the energy levels as function of the hopping parameter. Identify the degenerate and the non-degenerate limit. What are the characteristic energy scales of the problem? Observe and describe the character of the wave functions in the limit of small and large hopping parameters, i.e. $\bar{t} \to 0$ and $\bar{t} \to \infty$.

Solution

The solution can also be found in section 2.3 of ΦSX:Quantum mechanics of the chemical bond[21].

In the following, I often suppress the spin index. Editor: Caution! The order of site and spin indices, respectively k- and spin indices is not consistent in the following. The spin index as quantum number is part of the orbital index, which should stand in front of the lattice translation.

The model Hamiltonian, we investigate, is

$$\boldsymbol{h} = \begin{pmatrix} \bar{\epsilon}_1 & -\bar{t} \\ -\bar{t} & \bar{\epsilon}_2 \end{pmatrix} \qquad \text{and} \qquad \boldsymbol{S} = \mathbf{1} = \begin{pmatrix} 1 & 0 \\ 0 & 1 \end{pmatrix} \tag{1.102}$$

Eigenvalues

We diagonalize the Hamiltonian by finding the zeros of the determinant of $\mathbf{H} - \epsilon\mathbf{1}$.[23]

[23] The condition that the determinant vanishes, that is $\det[\mathrm{H} - \epsilon\mathrm{O}] = 0$ determines the eigenvalues of the system. We need to determine the zeros of a polynomial of the energy. This polynomial is called the **characteristic polynomial**

The zero's of the characteristic polynomial

$$0 = (\bar{\epsilon}_1 - \epsilon)(\bar{\epsilon}_2 - \epsilon) - \bar{t}^2 \tag{1.103}$$

determine the eigenvalues ϵ_- and ϵ_+ of the two-center bond

$$\epsilon_\pm = \frac{\bar{\epsilon}_1 + \bar{\epsilon}_2}{2} \pm \sqrt{\left(\frac{\bar{\epsilon}_1 - \bar{\epsilon}_2}{2}\right)^2 + \bar{t}^2} \tag{1.104}$$

The eigenvalues are shown in fig. 1.3 for an **avoided crossing**: The hopping parameter $\bar{t}$ is fixed and the diagonal elements $\bar{\epsilon}_1(x)$ and $\bar{\epsilon}_2(x)$ depend on some unspecified variable x.

- To the left and to the right of the graph, the spacing $|\bar{\epsilon}_2(x) - \bar{\epsilon}_1(x)|$ is large compared to the hopping $\bar{t}$, which is the **non-degenerate limit**, $|\bar{\epsilon}_1 - \bar{\epsilon}_2| \gg \bar{t}$.
- In the center of the graph, the diagonal Hamilton elements cross as function of x. This is the **degenerate limit**, $|\bar{\epsilon}_1 - \bar{\epsilon}_2| \ll |\bar{t}|$.

The effect sees is, what I call **level repulsion**: Without hopping, the eigenvalues are equal to the diagonal elements. As the absolute value of the hopping is increased, the energy levels are displaced away from each other. The displacement is large when the energy levels are close, and it becomes negligible if the initial states are separated by a large amount.

- In the degenerate limit the spacing of the Hamilton eigenvalues are is twice the hopping parameter $\bar{t}$, i.e.

$$\epsilon_\pm \approx \bar{\epsilon}_{1/2} \pm |\bar{t}| \tag{1.105}$$

- In the non-degenerate limit the eigenvalues are shifted, in second-order perturbation theory of the Hopping parameter, by $\frac{|\bar{t}|^2}{|\bar{\epsilon}_2 - \bar{\epsilon}_1|}$ away from each other, i.e

$$\epsilon_\pm \approx \bar{\epsilon}_{1/2} \pm \frac{|\bar{t}|^2}{|\bar{\epsilon}_1 - \bar{\epsilon}_2|} \tag{1.106}$$

  where $\bar{\epsilon}_{1/2}$ is the lower atomic energy level for the bonding state with $\pm = -$ and the upper atomic energy level for the antibonding state with $\pm = +$. This equation is worth to remember for back-on-the-envelope considerations.

The mean value of the energy levels remains unchanged.[24]

If we start from one electron in each orbital, the energy gain consists of two parts. First we gain an amount $\bar{\epsilon}_2 - \bar{\epsilon}_1$ by transferring the electron from the upper orbital at $\bar{\epsilon}_2$ to the lower orbital at $\bar{\epsilon}_1$. This is the **ionic contribution**, because a cation and an anion are formed. Secondly, the lower orbital is lowered through **hybridization** with the higher orbital and we gain $\frac{2\bar{t}^2}{\bar{\epsilon}_2 - \bar{\epsilon}_1}$ for the electron pair. This covalent contribution becomes smaller the larger the initial energy separation. Thus, if the ionic contribution is large, the covalent contribution is usually small.

Eigenvectors

The eigenvectors are obtained from

$$\begin{pmatrix} \bar{\epsilon}_1 - \epsilon_\pm & -\bar{t} \\ -\bar{t} & \bar{\epsilon}_2 - \epsilon_\pm \end{pmatrix} \begin{pmatrix} c_{1,\pm} \\ c_{2,\pm} \end{pmatrix} = 0 \tag{1.107}$$

[24] This holds exactly, when the overlap matrix is the unity. It does not hold when the overlap matrix deviates from unity.

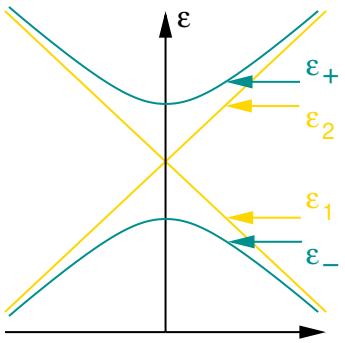


Fig. 1.3: Energy levels ϵ_-, ϵ_+ (green) as function of some parameter, which tunes the diagonal elements $\bar{\epsilon}_1$, $\bar{\epsilon}_1$ of the Hamiltonian at a fixed hopping parameter $\bar{t}$. Note the **level repulsion**, which is strongest, when the diagonal elements come close. The nature of the wave functions far from the avoided crossing, is as if the coupling of the states were absent.

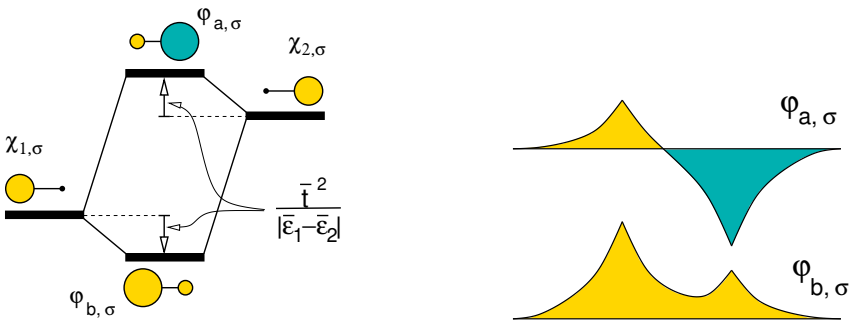


Fig. 1.4: Orbital diagram (left)and schematic cut through the bonding wave function and antibonding wave function for a non-degenerate bond. The level shifts $\frac{\bar{t}^2}{|\epsilon_1-\epsilon_2}$ are approximate, and become accurate in the non-degenerate limit.

where we insert the corresponding eigenvalues. For a two-dimensional Hamiltonian it is convenient to choose an ansatz that directly guarantees the orthonormality of the two eigenstates.

Namely, we exploit $\cos^2(x) + \sin^2(x) = 1$ $(x \in \mathbb{R})$

$$\begin{pmatrix} c_{1,-} \\ c_{2,-} \end{pmatrix} = \begin{pmatrix} \cos(\gamma \\ \sin(\gamma) \end{pmatrix} \quad \text{and} \quad \begin{pmatrix} c_{1,+} \\ c_{2,+} \end{pmatrix} = \begin{pmatrix} -\sin(\gamma \\ \cos(\gamma) \end{pmatrix} \tag{1.108}$$

Insertion of this Ansatz yields

$$\begin{aligned} 0 &\stackrel{!}{=} (\bar{\epsilon}_1 - \epsilon_-)\cos(\gamma) - \bar{t}\sin(\gamma) \\ \tan(\gamma) &= \frac{\bar{\epsilon}_1 - \epsilon_-}{\bar{t}} \\ &\stackrel{\text{Eq. 1.104}}{=} -\frac{1}{\bar{t}}\left(\frac{\bar{\epsilon}_1 + \bar{\epsilon}_2}{2} - \sqrt{\left(\frac{\bar{\epsilon}_1 - \bar{\epsilon}_2}{2}\right)^2 + \bar{t}^2} - \bar{\epsilon}_1\right) \\ &= -\left(\frac{\bar{\epsilon}_2 - \bar{\epsilon}_1}{2\bar{t}} - \sqrt{1 + \left(\frac{\bar{\epsilon}_2 - \bar{\epsilon}_1}{2\bar{t}}\right)^2}\right) \\ \gamma &= \operatorname{atan}\left\{-\left(\frac{\bar{\epsilon}_2 - \bar{\epsilon}_1}{2\bar{t}} - \sqrt{1 + \left(\frac{\bar{\epsilon}_2 - \bar{\epsilon}_1}{2\bar{t}}\right)^2}\right)\right\} \end{aligned} \tag{1.109}$$

Insertion of γ into the Ansatz leads to the desired result. This result appears cumbersome because of the trigonometric functions. However, the expression avoids divisions by zero, which otherwise tend to show up.

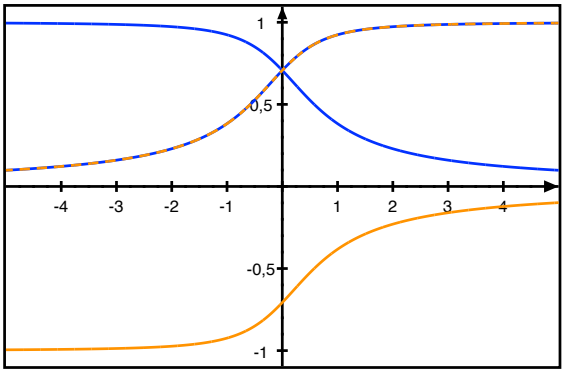


Fig. 1.5: Coefficients for the bonding (blue) and antibonding (orange) states of a two-center bond as function of $\frac{\bar{\epsilon}_2 - \bar{\epsilon}_1}{2\bar{t}}$. The blue-orange dashed line is $\cos(\gamma)$, the full blue line is $\sin(\gamma)$ and the full orange line is $\sin(\gamma)$. $\gamma\left(\frac{\bar{\epsilon}_2 - \bar{\epsilon}_1}{2\bar{t}}\right)$ is the mixing angle of the two orbitals. See text for discussion.

Let me summarize a few general observations, which are worth remembering. They will come up again later on. The reader may verify them for the example at hand. (The intention here is not to provide a derivation.)

- The eigenvectors are determined completely by the ratio $|\frac{\epsilon_1 - \epsilon_2}{2\bar{t}}|$. $|\epsilon_1 - \epsilon_2|$ is the relevant energy scale of the extreme non-degenerate limit, while $2|\bar{t}|$ is the energy-level spacing in the degenerate limit, the relevant energy scale in that limit.

- In the degenerate limit, the weight of the orbitals is equally distributed over both sides, i.e. $|c_{\alpha,\pm}| = \frac{1}{\sqrt{2}}$ for $\alpha \in \{1, 2\}$.

- In the lower (bonding) wave function, the two atomic orbitals add up in the bonding region between the two atoms, while the upper (antibonding) wave function has a node plane in the bonding region. The energy difference between the bonding and antibonding orbitals is due to the difference in kinetic energy, which is proportional to the squared gradient of the wave function: The kinetic energy of a wave function is $\int d^4x\, \psi^*(\vec{x}) \frac{-\hbar^2\vec{\nabla}^2}{2m_e}\psi(\vec{x}) = \frac{+\hbar^2}{2m_e}\int d^4x\, \left|\vec{\nabla}\psi(\vec{x})\right|^2$.

This shows up in our calculation as follows: For a positive hopping $\bar{t} = -h_{1,2} > 0$, the bonding orbital has coefficients with equal sign, while the coefficients of antibonding orbital have opposite sign. For negative hopping $\bar{t} = -h_{12} < 0$, the coefficients of the bonding orbital change sign and the antibonding orbitals have the same sign. The hopping is positive if the atomic orbitals point towards each other with the same sign as in the hydrogen molecule. When two orbitals point towards each other with the opposite sign, such as two p-orbitals pointing along the bond axis, the hopping parameter is negative.

- In a given wave function, the weight of that atomic orbital dominates, which has the closest atomic energy level. That is, for $\bar{\epsilon}_1 < \bar{\epsilon}_2$, the wave function of the bonding state (at ϵ_-) is concentrated on orbital 1, and the contribution of orbital 2 is smaller. The antibonding orbital (at ϵ_+) has its main contribution on atom 2.

- There are sum rules, namely that the sum $\epsilon_- + \epsilon_+$ of the energy eigenvalues is identical to the sum of the atomic levels $\bar{\epsilon}_1 + \bar{\epsilon}_2$. It can be shown that, for orthonormal atomic levels, the sum of eigenvalues is equal to the trace of the Hamiltonian matrix, i.e. $\sum_n \epsilon_n = \sum_n \bar{\epsilon}_n = \mathrm{Tr}[\boldsymbol{h}] = \mathrm{Tr}[\hat{h}]$ for arbitrary dimensions. This implies that the energy gain of the bonding orbital is compensated by the energy loss of the antibonding orbitals, when both are equally occupied.

- A second sum rule is that the total weight of each orbital, counting its contribution to all eigenstates, filled and empty, is the same before and after the bond formation. In our case, this implies $c_{\alpha,-}^2 + c_{\alpha,+}^2 = 1$ for both atomic orbitals $|\chi_\alpha\rangle$ with $\alpha \in \{1, 2\}$. Also this is a general result, which holds when the overlap matrix is unity.

What we observed are examples for two sum rules that are generally valid. They are presented here without proof.

NOTIONS ON DIAGONALIZATION

For an eigenvalue problem with a hermitian Hamiltonian $\boldsymbol{h}$

$$\Big(\boldsymbol{h} - \epsilon_n \mathbf{1})\vec{c}_n = 0 \tag{1.110}$$

with eigenvalues ϵ_n and eigenvectors $\vec{c}_n$, the following statements hold:

- **energy sum rule**:

$$\sum_n \epsilon_n = \mathrm{Tr}[\boldsymbol{h}] \tag{1.111}$$

- **charge sum rule**:

$$\sum_n |c_{j,n}|^2 = 1 \qquad \forall_j \tag{1.112}$$

Important note: This statements do not hold for a generalized eigenvalue problem, that is in the presence of an overlap matrix that differs from the unit matrix.

1.5.3 Linear chain of hydrogen atoms

The most simple model for an extended system is the linear chain. The linear chain describes hydrogen atoms placed on an equi-spaced one-dimensional grid with spacing a_{lat}. The spacing a_{lat} is the **lattice constant**.

We impose **periodic boundary conditions**. That is, we require the wave function to become identical after n beads. This describes either (1) a ring with N_s beads or (2) an infinite system with n k-points. Consider orthonormal local orbitals $|\chi_{j,\sigma}\rangle$ with $j = 1, \ldots N_s$, where N_s is the number of sites. Choose, whether the calculated eigenstates are normalized per one-atom unit cell of the linear chain or for the N_s-bead ring.

Problem

The linear chain has the Hamiltonian

$$\hat{h} = \underbrace{\sum_{\sigma\in\{\uparrow,\downarrow\}}\sum_{j=-\infty}^{\infty} |\pi_{\sigma,j}\rangle\bar{\epsilon}\langle\pi_{\sigma,j}|}_{\text{atomic energies}} - \underbrace{\sum_{\sigma\in\{\uparrow,\downarrow\}}\sum_{j=-\infty}^{\infty}\left(|\pi_{\sigma,j}\rangle\bar{t}\langle\pi_{\sigma,j+1}| + |\pi_{\sigma,j+1}\rangle\bar{t}\langle\pi_{\sigma,j}|\right)}_{\text{hopping}} \tag{1.113}$$

where j is the site index.

1. determine the eigenstates and eigenvalues of the linear chain with periodic boundary conditions with a repeat unit of N_s beads.

Solution

1. determine the eigenstates and eigenvalues of the linear chain with periodic boundary conditions with a repeat unit of N_s beads.

The linear chain is a worked example in section 6.7 of ΦSX:Quantum mechanics of the chemical bond.[21]. Here, I follow the recipe described in section 1.1.8 on p. 12.

In our problem, the primitive real-space lattice vector is $\vec{T} = a_{\text{lat}}\vec{e}_x$, where the lattice constant a_{lat} is the distance between the beads and $\vec{e}_x$ is a unit vector pointing along the chain (which is oriented in x-direction). The general lattice vectors are $\vec{t}_j = \vec{T}\cdot j = \vec{e}_x a_{\text{lat}}\cdot j$ with integer j.

In our problem, there are only two spin orbitals per unit cell. Therefore, the orbital index (α) is the same as the spin index σ. Bloch theorem already determines the wave functions, namely

$$|\varphi_{n,\vec{k}}\rangle = \sum_{\sigma\in\{\uparrow,\downarrow\}} \frac{1}{\sqrt{N_s}} \sum_{j=-\infty}^{\infty} |\chi_{\sigma,j}\rangle e^{i\vec{k}\vec{e}_x a_{\text{lat}}\cdot j} c_{\sigma,n}(\vec{k}) \tag{1.114}$$

N_s is the number of sites in the unit cell, which determines the set of k-points and the normalization of the wave functions.

In order to practice the recipe described in section 1.1.8 on p. 12, let me proceed in small steps. I leave out many explanations, because they are already given in section 1.1.8.

The recipe goes as follows:

1. *"Extract the real-space Hamilton $h_{\alpha,\vec{0},\beta,\vec{t}'}$ and overlap $S_{\alpha,\vec{0},\beta,\vec{t}'}$ matrix elements connecting the orbitals in the first unit cell $\vec{t} = \vec{0}$ to those in a unit cell displaced by a real-space lattice translation vector $\vec{t}'$."*

I obtain

$$\begin{aligned} h_{0,\sigma,0,\sigma'} &= \bar{\epsilon}\delta_{\sigma,\sigma'} \\ h_{0,\sigma,1,\sigma'} &= -\bar{t}\delta_{\sigma,\sigma'} \\ h_{0,\sigma,-1,\sigma'} &= -\bar{t}\delta_{\sigma,\sigma'} \end{aligned}$$

$$S_{0,\sigma,j,\sigma'} = \delta_{\sigma,\sigma'}\delta_{j,0} \tag{1.115}$$

2. *"Determine the k-dependent Hamiltonian and overlap matrix from the matrix elements in real space"*

$$\begin{aligned} h_{\sigma,\sigma'}(\vec{k}) &\overset{\text{Eq. 1.67}}{=} \sum_{j=-\infty}^{\infty} h_{\sigma,0,\sigma',j} e^{ik_x a_{\text{lat}} j} = \delta_{\sigma,\sigma'}\left(\bar{\epsilon} - 2\bar{t}\cos(k_x a_{\text{lat}})\right) \\ S_{\sigma,\sigma'}(\vec{k}) &\overset{\text{Eq. 1.68}}{=} \sum_{j=-\infty}^{\infty} S_{\sigma,0,\sigma',j} e^{ik_x a_{\text{lat}} j} = \delta_{\sigma,\sigma'} \end{aligned} \tag{1.116}$$

3. *"Solve the generalized eigenvalue problem and obtain k-dependent energies $\epsilon_n(\vec{k})$ and the eigenvectors $c_{\alpha,n}(\vec{k})$ satisfying the normalization condition"*

   The k-dependent energy levels are

$$\epsilon_n(\vec{k}) = \bar{\epsilon} - 2\bar{t}\cos(k_x a_{\text{lat}}) \tag{1.117}$$

   and the eigenvectors $\vec{c}_n(k_x) = (c_{\uparrow,n}(k_x), c_{\downarrow,n}(k_x))$ are $\vec{c}_1(k_x) = (1,0)$ and $\vec{c}_2(k_x) = (0,1)$. The first band (n=1) refers to the states with spin $\uparrow$ and the second band (n=2) has the spin $\downarrow$.

   The normalization condition

$$\sum_{\sigma,\sigma' \in \{\uparrow,\downarrow\}} c^*_{\sigma,m}(\vec{k}) S_{\sigma,\sigma'}(\vec{k}) c_{\sigma',n}(\vec{k}) = \delta_{m,n} \tag{1.118}$$

   is satisfied.

4. *"Construct eigenstates of the Hamiltonian from the eigenvectors"*

   The wave function is

$$|\varphi_n(\vec{k})\rangle \overset{\text{Eq. 1.71}}{=} \sum_{\sigma} \underbrace{\frac{1}{\sqrt{\sum_{\vec{t}'}}} \sum_{\vec{t}} |\chi_{\sigma,\vec{t}}\rangle e^{i\vec{k}\vec{t}}}_{|\chi_{\sigma,\vec{k}}\rangle} c_{\sigma,n}(\vec{k}) = \sum_j |\chi_{\sigma,j}\rangle \frac{1}{\sqrt{N_s}} e^{ik_x a_{\text{lat}} j} \tag{1.119}$$

   where N_s is the number of beads in the (super) unit cell, which defines the quantization condition for the k-points and the normalization of the eigenstates. The wave function extends over all space, but the wave function repeats every N_s sites.

The dispersion relation $\epsilon_n(k_x)$ of the linear chain and the resulting density of states is shown in figure 1.6. The shape of the density of states with the raised band edges is characteristic for quasi-one-dimensional structures in the material. This shape explains, why one-dimensional system tend to distort in order to open the band gap, such as in a **Peierls distortion**.

Editor: This concept needs to be explained. Consider the following line of thought: Consider the G vector connecting the two k-points for which the bands intersect the Fermi level. If a perturbation has a contribution with this G-vector, a band gap opens at the Fermi level. Out of the plane waves $e^{i\frac{G}{2}r}$ and $e^{-i\frac{G}{2}r}$, we can form a lower state of the form $\cos(\frac{G}{2}r)$ and an upper state $\sin(\frac{G}{2}r)$. The density of the lower state is proportional to $\cos(Gr)$, which is a charge density wave with a wave vector G. If

the electrons interact, this charge-density wave produces a perturbing potential with the same wave length, namely G, which was the perturbation causing the charge density wave in the first place. The band edges on both sides of the Fermi level have the spiked form of a one-dimensional density of states. This tells that the charge density wave is strong, stronger than in higher dimensions. This is the underlying reason for the observation that one-dimensional problems tend to undergo phase transitions.

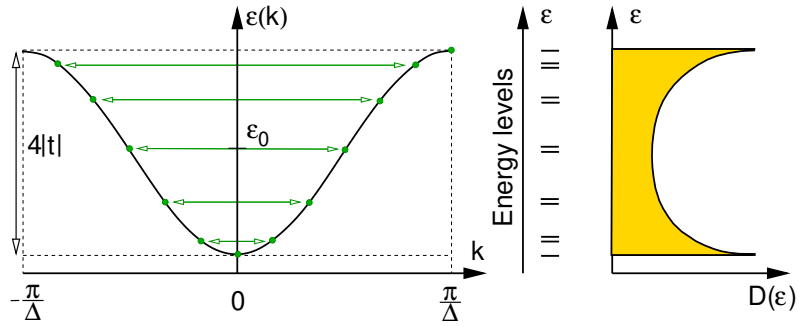


Fig. 1.6: Dispersion relation of linear chain of hydrogen atoms with periodic boundary conditions. The green points correspond to the energy levels of a ring with 14 atoms. In the middle figure we show the energy levels, and on the right the schematic density of states $D(\epsilon)$ for the infinite chain.

The boundary condition imposes

$$\langle \pi_{\sigma,N_s} | \varphi_n(k) \rangle = \langle \pi_{\sigma,0} | \varphi_n(k) \rangle \overset{\text{Eq. 1.114}}{\Rightarrow} e^{ik_x a_{\text{lat}} \cdot N_s} = 1 \quad \Rightarrow k_x a_{\text{lat}} \cdot N_s = 2\pi m$$
$$\Rightarrow \vec{k}_m = \vec{e}_x \frac{2\pi}{N_s a_{\text{lat}}} \cdot m \tag{1.120}$$

Only the k-points from the interval $-\frac{\pi}{a_{\text{lat}}} < k_m \leq \frac{\pi}{a_{\text{lat}}}$ are considered, because the wave functions of k_m and $k_m + N_s$ are identical.

1.5.4 Insulating linear chain

Introduction

While the linear chain is the minimal problem for a metallic system, we can also form the minimal model for an insulating system by doubling the periodicity of the half-filled linear chain.

In the most general form, this is the so-called **Rice-Mele model**[22], which is used to describe ferroelectric materials. When the atomic energy levels alternate, but the hopping parameters remain constant, the model describes an ionic insulator. If the hopping parameters vary, but the energy levels are constant, the model describes a covalent insulator. This latter special case, alternating hopping but constant energy levels, leads to the so-called **Su-Schrieffer-Heeger (SSH) model** [23], which is the minimal model system for a topological insulator.

One purpose of this exercise is to train Bloch-theorem for a case with more than one atom in the unit cell. Secondly, we become familiar with a frequently used toy model, for which we can investigate the role of interactions. Later, we will see that there are insulators, so-called Mott insulators, which turn insulating only due to interaction. The model described here allows to set the Mott insulator apart from the regular "band" insulators.

Problem

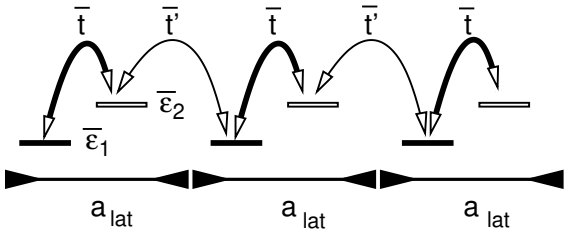


Fig. 1.7: Scheme to demonstrate the Hamiltonian of the alternating linear chain. It describes a chain with two atoms per unit cell with different ionicity, that is atomic energy levels $\bar{\epsilon}_1$ and $\bar{\epsilon}_2$. The atoms are connected by weak and strong bonds as characterized by the two hopping parameters $\bar{t}$ and $\bar{t}'$. With a_{lat} I denote the lattice constant.

1 Calculate the band structure of the linear chain with two distinct sites per unit cell. Both, the "atomic energies" $\bar{\epsilon}_1, \bar{\epsilon}_2$ and the hopping parameters $\bar{t}, \bar{t}'$ alternate. Alternating atomic levels describe a material with ionic character, while alternating hoppings describe materials with covalent bonds.

2 Determine the k-dependent wave functions.

Discussion

1 Calculate the band structure of the linear chain with two distinct sites per unit cell. Both, the "atomic energies" $\bar{\epsilon}_1, \bar{\epsilon}_2$ and the hopping parameters $\bar{t}, \bar{t}'$ alternate. Alternating atomic levels describe a material with ionic character, while alternating hoppings describe materials with covalent bonds.

The solution is a worked example in section **??** in ΦSX: Introduction to Solid-State Theory[1], which has been included below. In contrast to the previous exercise for the linear chain, I do not express the Hamiltonian as abstract operator using the projector and orbital states, but I go directly to the matrix equation.

Let us consider the example of a linear chain made from atoms with one s-type orbital. There shall be two atoms per unit cell. The lattice constant shall be a_{lat}. The orbitals are denoted by (α, j), where $\alpha \in \{1, 2\}$ denote the two orbitals and j is the number of lattice displacements by a_{lat} from the origin to the current site.

The two atoms in the unit cell have orbital energies $\bar{\epsilon}_1$ and $\bar{\epsilon}_2$. We denote the hopping matrix element between orbitals $(1, j)$ and $(2, j)$ by $\bar{t}$ and the one between $(2, j)$ and $(1, j+1)$ by $\bar{t}'$. In the context of Slater-Koster matrix elements, both are matrix elements of the type $-h_{ss\sigma}$.

The difference of the atomic energy levels $\bar{\epsilon}_2 - \bar{\epsilon}_1$ describes relative **electronegativity** of the two atoms. The atom with the lower electron level is more electronegative than the one with the higher level. Without hopping, the electrons would accumulate at the more electronegative atom. This is analogous to rock salt (NaCl), where the sodium atom holds on only weakly to its valence electron, while the lowest unoccupied orbital of the chlorine atom is much stronger bound to the atom core. Therefore, sodium donates its electron to the chlorine atom, so that two ions Na^+ and Cl^- are formed.

The different hopping parameters describe that two of the atoms are pairwise closer together. That is, we describe a chain of molecules.

For the sake of simplicity, we only consider wave functions with one spin direction. The bands of the two spin direction are identical, because there is no magnetic field. When we consider one spin direction, the wave-function component of the other spin direction is zero.

The infinite Hamiltonian has the form

$$\mathbf{h} = \left(\begin{array}{c|cc|cc|cc|c} & \vdots & \vdots & \vdots & & & & \\ \hline \dots & \bar{\epsilon}_1 & -\bar{t} & 0 & 0 & \dots & & \\ \dots & -\bar{t} & \bar{\epsilon}_2 & -\bar{t}' & 0 & \dots & & \\ \hline \dots & 0 & -\bar{t} & \bar{\epsilon}_1 & -\bar{t} & 0 & 0 & \dots \\ \dots & 0 & 0 & -\bar{t} & \bar{\epsilon}_2 & -\bar{t}' & 0 & \dots \\ \hline & & \dots & 0 & -\bar{t}' & \bar{\epsilon}_1 & -\bar{t} & \dots \\ & & \dots & 0 & 0 & -\bar{t} & \bar{\epsilon}_2 & \dots \\ \hline & & & \vdots & \vdots & \vdots & \vdots & \end{array}\right) \tag{1.121}$$

The Hamilton matrix elements can also be written as

$$\boldsymbol{h}_{i,j} = \begin{pmatrix} \bar{\epsilon}_1 & -\bar{t} \\ -\bar{t} & \bar{\epsilon}_2 \end{pmatrix} \delta_{i,j} + \begin{pmatrix} 0 & 0 \\ -\bar{t}' & 0 \end{pmatrix} \delta_{i+1,j} + \begin{pmatrix} 0 & -\bar{t}' \\ 0 & 0 \end{pmatrix} \delta_{i-1,j} \tag{1.122}$$

where i and j are the indices of the lattice translations $\vec{t}_j = a_{\text{lat}} \cdot j$. The components of the 2×2 matrices $\boldsymbol{h}_{i,j}$ refer to the orbital indices in the primitive unit cell, while i, j identify a particular unit cell.

When we transform the Hamiltonian into the Bloch representation using Eq. 1.67, we obtain the k-dependent Hamiltonian with $\vec{t}_j = a_{\text{lat}} \cdot j$

$$\boldsymbol{h}(\vec{k}) \overset{\text{Eq. 1.67}}{=} \sum_j \boldsymbol{h}(0, j) \mathrm{e}^{ika_{\text{lat}}j} = \begin{pmatrix} \bar{\epsilon}_1 & -\bar{t} - \bar{t}'\mathrm{e}^{-ika_{\text{lat}}} \\ -\bar{t} - \bar{t}'\mathrm{e}^{ika_{\text{lat}}} & \bar{\epsilon}_2 \end{pmatrix} \tag{1.123}$$

The eigenvalues $\epsilon_n(k)$ and eigenvectors $c_\alpha(k)$ are obtained from the characteristic equation

$$\det|\boldsymbol{h}(k) - \epsilon\mathbf{1}| = 0.$$

$$\begin{aligned}
(\bar{\epsilon}_1 - \epsilon)(\bar{\epsilon}_2 - \epsilon) - \left(-\bar{t} - \bar{t}'\mathrm{e}^{-ika_{\mathrm{lat}}}\right)\left(-\bar{t} - \bar{t}'\mathrm{e}^{+ika_{\mathrm{lat}}}\right) &= 0 \\
\epsilon^2 - 2\frac{\bar{\epsilon}_1 + \bar{\epsilon}_2}{2}\epsilon + \left(\frac{\bar{\epsilon}_1 + \bar{\epsilon}_2}{2}\right)^2 - \left(\frac{\bar{\epsilon}_1 + \bar{\epsilon}_2}{2}\right)^2 + \bar{\epsilon}_1\bar{\epsilon}_2 &= \bar{t}^2 + \bar{t}'^2 + 2\bar{t}\bar{t}'\cos(ka_{\mathrm{lat}}) \\
\left(\epsilon - \frac{\bar{\epsilon}_1 + \bar{\epsilon}_2}{2}\right)^2 &= \left(\frac{\bar{\epsilon}_1 - \bar{\epsilon}_2}{2}\right)^2 + \bar{t}^2 + \bar{t}'^2 + 2\bar{t}\bar{t}'\cos(ka_{\mathrm{lat}}) \\
\epsilon_n(k) &= \frac{\bar{\epsilon}_1 + \bar{\epsilon}_2}{2} \pm \sqrt{\left(\frac{\bar{\epsilon}_1 - \bar{\epsilon}_2}{2}\right)^2 + \bar{t}^2 + \bar{t}'^2 + 2\bar{t}\bar{t}'\cos(ka_{\mathrm{lat}})}
\end{aligned} \tag{1.124}$$

The first band $n = 1$ is obtained with $\pm = -$ and the second band is obtained with $\pm = +$.

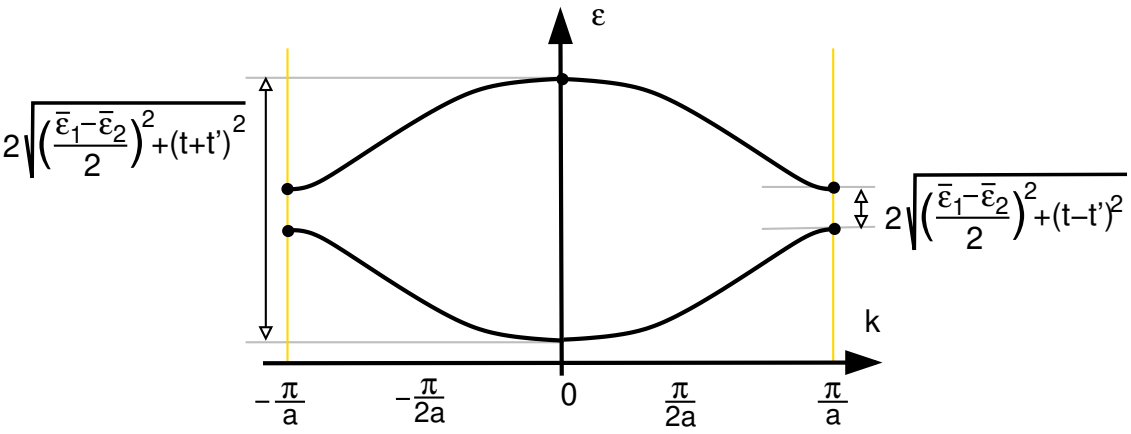


Fig. 1.8: Band structure of the alternating linear chain. See text for the definition of the symbols. The indices of the hopping parameters have been dropped. Editor: the hopping parameters in the figure need a bar

Let us investigate some special cases

- chain of decoupled molecules: We set one hopping parameter to zero, i.e. $\bar{t}' = 0$. The result are two k-independent bands for the molecular orbitals

$$\epsilon_n(k) = \frac{\bar{\epsilon}_1 + \bar{\epsilon}_2}{2} \pm \sqrt{\left(\frac{\bar{\epsilon}_1 - \bar{\epsilon}_2}{2}\right)^2 + \bar{t}^2} \tag{1.125}$$

- both atoms and hopping parameters are identical, i,e, $\bar{\epsilon}_1 = \bar{\epsilon}_2$ and $\bar{t} = \bar{t}'$.

$$\begin{aligned}
\epsilon_n(k) &= \bar{\epsilon}_1 \pm \sqrt{2\bar{t}^2 + 2\bar{t}^2\cos(ka_{\mathrm{lat}})} = \bar{\epsilon}_1 \pm |\bar{t}|\underbrace{\sqrt{2 + 2\cos(ka_{\mathrm{lat}})}}_{\sqrt{4\cos^2(ka_{\mathrm{lat}}/2)}} \\
&= \bar{\epsilon}_1 \pm \left|2\bar{t}\cos\left(\frac{1}{2}ka_{\mathrm{lat}}\right)\right|
\end{aligned} \tag{1.126}$$

This is the band structure of a mono-atomic chain

$$\epsilon(k) = \bar{\epsilon}_1 + 2\bar{t}\cos\left(\frac{ka_{\mathrm{lat}}}{2}\right)$$

folded back into the first Brillouin zone.

- for alternating orbital energies or alternating hopping matrix elements, The band gap at the zone boundary opens, so that an insulator is obtained if the orbitals are half filled.

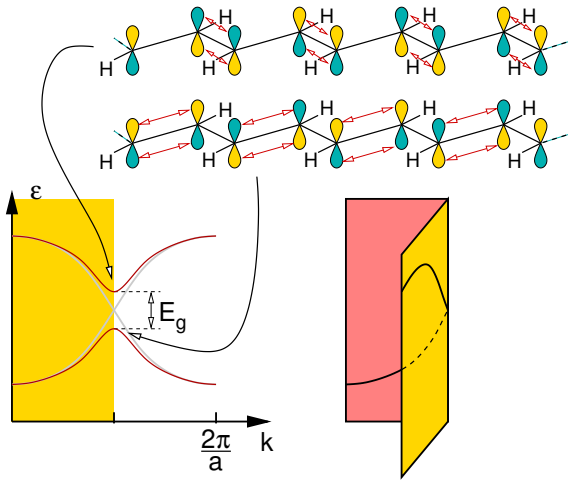


Fig. 1.9: Folding back of the band structure into the reciprocal cell of a doubled real-space unit cell. The example is shown for the one-dimensional molecule acetylene, which undergoes a Peierls distortion, which doubles the unit cell. Only the p-orbitals perpendicular to the molecular plane are considered. Editor: The commonly used picture of folding back is not exactly how the band structure is deformed. Rather it is a shift of the band structure by $\pi/2$. A new graph may be useful.

Note that $\bar{t}$ and $\bar{t}'$ are negative, because it is approximately equal to the overlap matrix element multiplied with the potential in the bond-center. The potential is negative.

2 Determine the k-dependent wave functions.

The eigenvectors $\vec{c}_\pm$ are obtained from

$$\Big[\boldsymbol{h}(k) - \epsilon_\pm(k)\mathbf{1}\Big]\vec{c}_\pm(\vec{k}) = 0 \tag{1.127}$$

where the k-dependent Hamiltonian is taken from Eq. 1.123. We parameterize the eigenstates in terms of a mixing angle $\gamma(\vec{k})$, i.e.

$$\begin{pmatrix} c_{1,-}(k) \\ c_{2,-}(k) \end{pmatrix} = \begin{pmatrix} \cos(\gamma(k)) \\ \sin(\gamma(k))\mathrm{e}^{i\phi(k)} \end{pmatrix} \quad \text{and} \quad \begin{pmatrix} c_{1,+}(k) \\ c_{2,+}(k) \end{pmatrix} = \begin{pmatrix} -\sin(\gamma(k))\mathrm{e}^{-i\phi(k)} \\ \cos(\gamma(k)) \end{pmatrix} \tag{1.128}$$

which ensures the normalization and the orthonormality of the two states

We use the k-dependent Hamiltonian Eq. 1.123 and the eigenvalue Eq. 1.124.

$$\begin{aligned} 0 &= \Big[h_{11}(k) - \epsilon_-(k)\Big]\cos(\gamma(k)) + h_{12}(k)\sin(\gamma(k))\mathrm{e}^{i\phi(k)} \\ &= \left(\frac{\bar{\epsilon}_1 - \bar{\epsilon}_2}{2} + \sqrt{\left(\frac{\bar{\epsilon}_1 - \bar{\epsilon}_2}{2}\right)^2 + \bar{t}^2 + \bar{t}'^2 + 2\bar{t}\bar{t}'\cos(k a_{\mathrm{lat}})}\right)\cos(\gamma(k)) + \left(-\bar{t} - \bar{t}'\mathrm{e}^{-ika_{\mathrm{lat}}}\right)\sin(\gamma(k))\mathrm{e}^{i\phi(k)} \end{aligned} \tag{1.129}$$

$$\begin{aligned} \mathrm{e}^{i\phi(k)} &= \left(\frac{\bar{t} + \bar{t}'\mathrm{e}^{-ika_{\mathrm{lat}}}}{|\bar{t} + \bar{t}'\mathrm{e}^{-ika_{\mathrm{lat}}}|}\right)^* \\ \phi(k) &= -\mathrm{atan}\left(\frac{\mathrm{Im}(\bar{t} + \bar{t}'\mathrm{e}^{-ika_{\mathrm{lat}}})}{\mathrm{Re}(\bar{t} + \bar{t}'\mathrm{e}^{-ika_{\mathrm{lat}}})}\right) = -\mathrm{atan}\left(\frac{\bar{t}'\sin(-ka_{\mathrm{lat}})}{\bar{t} + \bar{t}'\cos(-ka_{\mathrm{lat}})}\right) = \mathrm{atan}\left(\frac{\sin(ka_{\mathrm{lat}})}{\bar{t}/\bar{t}' + \cos(ka_{\mathrm{lat}})}\right) \end{aligned} \tag{1.130}$$

$$\left(\frac{\bar{\epsilon}_1-\bar{\epsilon}_2}{2}+\sqrt{\left(\frac{\bar{\epsilon}_1-\bar{\epsilon}_2}{2}\right)^2+\bar{t}^2+\bar{t}'^2+2\bar{t}\bar{t}'\cos(ka_{\text{lat}})}\right)\cos(\gamma(k))=\left|\bar{t}+\bar{t}'e^{-ika_{\text{lat}}}\right|\sin(\gamma(k)) \tag{1.131}$$

$$\begin{aligned}\gamma(k)&=\operatorname{atan}\left(\frac{\frac{\bar{\epsilon}_1-\bar{\epsilon}_2}{2}+\sqrt{\left(\frac{\bar{\epsilon}_1-\bar{\epsilon}_2}{2}\right)^2+\bar{t}^2+\bar{t}'^2+2\bar{t}\bar{t}'\cos(ka_{\text{lat}})}}{\left|\bar{t}+\bar{t}'e^{-ika_{\text{lat}}}\right|}\right)\\&=\operatorname{atan}\left(\frac{\bar{\epsilon}_1-\bar{\epsilon}_2}{2\sqrt{\bar{t}^2+\bar{t}'^2+2\bar{t}\bar{t}'\cos(ka_{\text{lat}})}}+\sqrt{1+\left(\frac{\bar{\epsilon}_1-\bar{\epsilon}_2}{2\sqrt{\bar{t}^2+\bar{t}'^2+2\bar{t}\bar{t}'\cos(ka_{\text{lat}})}}\right)^2}\right)\end{aligned} \tag{1.132}$$

Editor: finish it by inserting it into the expression for the eigenvectors
Editor: exploit

$$|\bar{t}\pm\bar{t}'e^{ika_{\text{lat}}}|^2=\bar{t}^2+\bar{t}'^2\pm2\bar{t}\bar{t}'\cos(ka_{\text{lat}}) \tag{1.133}$$

1.5.5 Free-electron gas or jellium model

Introduction

The **jellium model**, also called **free-electron gas**, describes a system of electrons with a homogeneous charge background ensuring overall charge neutrality.

In the jellium model, the atom-cores are smeared out into a neutralizing charge background, which effectively removes the effects of the atomic structure. We can still exploit the complete translational and rotational symmetry of free space. The Coulomb potential from the neutralizing charge background is described by a constant potential V_0, which acts on the electrons. Usually, V_0 is set to zero by using it as the zero of the energy scale. A global constant can be added to the potential because of the gauge symmetry of electric potential.[25]

The Hamiltonian for the free-electron gas is

$$\hat{h} = \sum_{\sigma\in\{\uparrow,\downarrow\}} \Big(\frac{\hat{\vec{p}}^2}{2m_e} + V_0 \Big) \tag{1.134}$$

where m_e is the electron mass.

When the Fermi level lies within the spectrum of the free-electron gas, i.e. $\mu > V_0$ (or better $\mu - V_0 \gg k_B T$), we call it a **degenerate electron gas**.[26] The degenerate electron gas is a model for a metal.

The free-electron gas is not only useful to describe the behavior of metals, but it is also valuable to understand semi-conductors and insulators. In those cases, the free-electron gas is a model for electrons near the band edges, where the bands can be approximated by parabolic bands. These situations are described by a **dilute electron gas**, as opposed to the degenerate electron gas. A dilute electron gas is characterized by a Fermi level that lies below the bottom of the band, i.e. $\mu < V_0$ (or better $V_0 - \mu \gg k_B T$).

By changing the sign of the kinetic energy, for example by using a negative mass, the free-electron gas is a model for holes (missing electrons) in the valence band of a semiconductor.

This exercise provides a fundamental insight into **magnetism**. While the kinetic energy favors non-magnetic states, the Coulomb repulsion between electrons favors magnetic states. Whether an electron gas is magnetic or not is decided by the balance between kinetic energy and the Coulomb interaction. In this exercise we will explore the kinetic energy as function of the magnetization of the electron gas. This will lead to the **magnetic suszeptibility** of the free electron gas. In a later exercise, we will estimate the Coulomb repulsion between electrons in an electron gas as function of the magnetization.

The electron repulsion favors electrons with parallel spin, because the Pauli principle keeps electrons with the same spins at a distance. This reduces their Coulomb repulsion compared to electrons with opposite spin. One consequence is **Hund's rule**, which says that electrons in a angular momentum shell of an atom tend to align with parallel spin.

Problem

Let us describe the free-electron gas with **periodic boundary conditions** in a cubic box with side length L. The wave functions shall be normalized with in the box. As we approach the final result, we let L go to infinity.

[25] See gauge symmetry of the electromagnetic potentials in ΦSX: Elektrodynamik.[24]. The gauge symmetry says that such a global potential shift has no effect on the observable properties of the system.

[26] The term *"degenerate"* is not related to degeneracy of quantum states. Rather it means "ill-formed" or "degenerated", referring to its fundamental differences from a regular gas of molecules.

1 Calculate the band structure of the free-electron gas

2 Calculate the density of states of the free-electron gas with a specified electron density.

3 Calculate the energy of the non-magnetic electron gas

4 Calculate the energy of the spin-polarized electron gas as function of the spin polarization n_s/n_t, where $n_s = n_\uparrow - n_\downarrow$ is the spin density and $n_t = n_\uparrow + n_\downarrow$ is the total electron density. Without restriction of generality (WroG), the magnetization is oriented along the z-direction.

Discussion

Band structure

1 Calculate the band structure of the free-electron gas

The wave functions are

$$|\psi_{\vec{k},\sigma}\rangle = \sum_{\sigma' \in \{\uparrow,\downarrow\}} \int_V d^3r \, |\vec{r},\sigma'\rangle \underbrace{\frac{1}{\sqrt{L^3}} e^{i\vec{k}\vec{r}} \delta_{\sigma,\sigma'}}_{\psi_{\vec{k},\sigma}(\vec{r},\sigma')} \tag{1.135}$$

The integration region V is a three-dimensional cubic box of side-length L. The box is both, (1) the normalization volume, and (2) the supercell defining the periodic boundary conditions

$$\psi(\vec{r} + \vec{e}_j L, \sigma) = \psi(\vec{r}, \sigma) \tag{1.136}$$

where $\vec{e}_j$ is the unit vector pointing along the j-th cartesian coordinate.

The boundary conditions limit the wave vectors to a discrete set

$$\vec{k}_{i_1,i_2,i_3} = \frac{2\pi}{L} \begin{pmatrix} i_1 \\ i_2 \\ i_3 \end{pmatrix} \qquad \text{with integer } i_1, i_2, i_3 \in \mathbb{I} \tag{1.137}$$

The one-particle energies are

$$\epsilon_\sigma(\vec{k}) = \langle \psi_{\vec{k},\sigma} | \hat{h} | \psi_{\vec{k},\sigma} \rangle = V_0 + \frac{\hbar^2 \vec{k}^2}{2m_e} \tag{1.138}$$

This defines the dispersion relation, i.e. the band structure of the free-electron gas.

Density of states

2 Calculate the density of states of the free-electron gas

The **density of states** $D(\epsilon)$ is best evaluated[1] indirectly from the number-of-states function [27] $\mathcal{N}(\epsilon)$ as $D(\epsilon) = \partial_\epsilon \mathcal{N}(\epsilon)$.

The number of states $\mathcal{N}(\mu)$ of the free-electron gas is obtained from the occupied region of k-space. In a free electron gas, the occupied states lie within a sphere with $(\hbar\vec{k})^2/2m_e < \mu$, where μ

[27]

$$D(\epsilon) = \sum_n \delta(\epsilon - \epsilon_n) = \sum_n \partial_\epsilon \theta(\epsilon - \epsilon_n) = \partial_\epsilon \sum_n \theta(\epsilon - \epsilon_n) = \partial_\epsilon \mathcal{N}(\epsilon) \tag{1.139}$$

The number-of-states function $\mathcal{N}(\epsilon)$ is defined as the number of states with energy below ϵ. The particle number $N_{T,\mu}$ is only loosely related to the number of states function $\mathcal{N}(\epsilon)$. The relation is $N_{T=0,\mu} = \mathcal{N}(\mu)$.

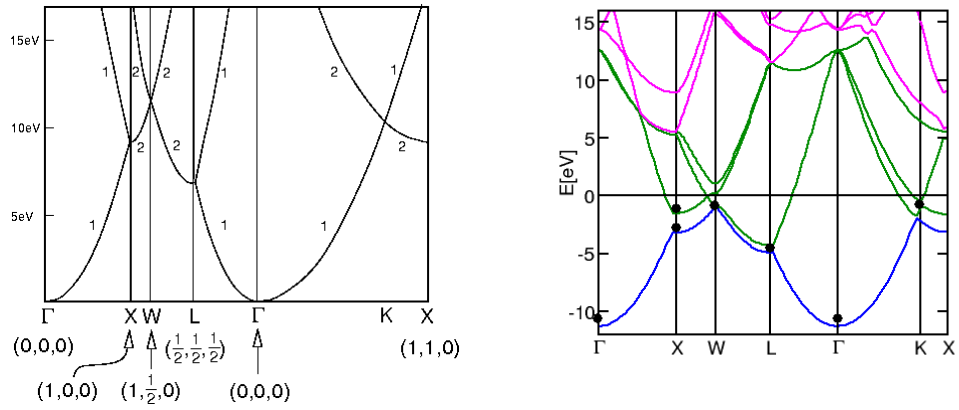


Fig. 1.10: Band structure of free, non-interacting electrons. The lattice is an fcc-cell with a lattice constant of 4.05 Å corresponding to aluminum. The high symmetry points are given in units of $\frac{2\pi}{a_{\text{lat}}}$. The numbers indicate the degeneracy beyond spin-degeneracy. On the right-hand side, the band structure of aluminum is shown in comparison.

is the Fermi level, the chemical potential for the electrons. For the purpose of obtaining the density of states, we determine $\mathcal{N}(\epsilon)$ for all possible chemical potentials and denote them by the symbol ϵ.

The k-points are determined by the periodic boundary conditions. The reciprocal-space volume per k-point is $\Delta k^3 = (2\pi/L)^3$.

$$\begin{aligned}\mathcal{N}(\epsilon) &= \underbrace{\left(\sum_{\sigma\in\{\uparrow,\downarrow\}}\right)}_{2} \overbrace{\frac{4\pi}{3}\Big(\underbrace{\frac{1}{\hbar}\sqrt{2m_e(\epsilon-V_0)}}_{k_F(\epsilon)}\Big)^3}^{\text{occupied rec.space volume}} \underbrace{\left(\frac{2\pi}{L}\right)^{-3}}_{\Delta k^{-3}} \theta(\epsilon-V_0) \\ &= \underbrace{V}_{L^3}\underbrace{\left(\sum_{\sigma\in\{\uparrow,\downarrow\}}\right)}_{2}\left(\frac{\sqrt{2m_e}}{2\pi\hbar}\right)^3\frac{4\pi}{3}(\epsilon-V_0)^{\frac{3}{2}}\theta(\epsilon-V_0) \qquad (1.140)\end{aligned}$$

k_F is the so-called **Fermi-momentum**, which is the radius of the Fermi sphere.[28]

The Heaviside step function $\theta(\epsilon - V_0)$ has been included because the number of states is zero for energies below the parabola $\epsilon_\sigma(k)$ in Eq. 1.138, i.e. for $\epsilon \leq V_0$.

The density of states is thus

$$D(\epsilon) = \partial_\epsilon \mathcal{N}(\epsilon) = \underbrace{V}_{L^3}\underbrace{\left(\sum_{\sigma\in\{\uparrow,\downarrow\}}\right)}_{2}\left(\frac{\sqrt{2m_e}}{2\pi\hbar}\right)^3 2\pi\theta(\epsilon-V_0)\sqrt{\epsilon-V_0} \qquad (1.141)$$

My convention to define the number of states and the density of states as extensive quantities is uncommon. Usually, the numbers are divided by volume or calculated for a specified unit cell of a crystal. I have chosen my convention to avoid ambiguity: Because of the volume occurring in the expression, it is apparent that it is an extensive quantity. By scaling the result, one obtains the other choices.

[28] The sphere in reciprocal space, which contains the occupied states of the free electron gas.

The square-root behavior of the density of states in Eq. 1.141 is characteristic for the density of states of parabolic bands in three dimensions. This behavior is regularly observed near band edges in three dimensions.[29]

Let us now turn to the thermodynamic properties.

Energy of the non-magnetic electron gas

3 Calculate the energy of the non-magnetic electron gas with a specified electron density.

Editor:

$$E(N) = \operatorname*{stat}_{\mu} E(\mu) - \mu(\mathcal{N}(\mu) - N)$$
$$E(N_t, N_s) = \operatorname*{stat}_{B,V} E(\mu_\uparrow, \mu_\downarrow) - \mu_e B(N_\uparrow - N_\downarrow - N_s) + V(N_\uparrow + N_\downarrow - N_t) \tag{1.142}$$

The energy calculated from the density of states depends on the chemical potential μ. The particle number as function of chemical potential allows one to obtain the chemical potential.

Let me express particle number and the energy as an integral over the density of states, that has obtained earlier in Eq. 1.141. The chemical potential is the Fermi level.

$$\mathcal{N}(\mu) = \int_{-\infty}^{\mu} d\epsilon\, D(\epsilon) \quad \text{and} \quad E(\mu) = \int_{-\infty}^{\mu} d\epsilon\, D(\epsilon)\epsilon \tag{1.143}$$

The density of states of the free-electron gas in three dimensions, Eq. 1.141, can be written as

$$D(\epsilon) = C\theta(\epsilon - V_0)\sqrt{\epsilon - V_0} \qquad \text{with} \quad C = L^3 \underbrace{\left(\sum_{\sigma\in\{\uparrow,\downarrow\}}\right)}_{2} \left(\frac{\sqrt{2m_e}}{2\pi\hbar}\right)^3 2\pi \tag{1.144}$$

$$\mathcal{N}(\mu) \overset{\text{Eq. 1.143}}{=} C \underbrace{\frac{2}{3}(\mu - V_0)^{\frac{3}{2}}}_{\int_{V_0}^{\mu} d\epsilon\, \sqrt{\epsilon - V_0}} \qquad \Rightarrow \qquad \mu - V_0 = \left(\frac{3\mathcal{N}(\mu)}{2C}\right)^{\frac{2}{3}}$$

$$E(\mu) \overset{\text{Eq. 1.143}}{=} \underbrace{V_0\mathcal{N}(\mu) + \frac{2}{5}C(\mu - V_0)^{\frac{5}{2}}}_{C\int_{V_0}^{\mu} d\epsilon\, \epsilon\sqrt{\epsilon - V_0}}$$

$$= V_0\mathcal{N}(\mu) + \frac{2C}{5}\left(\frac{3\mathcal{N}(\mu)}{2C}\right)^{\frac{5}{3}} = V_0\mathcal{N}(\mu) + \frac{2}{5}C^{-\frac{2}{3}}\left(\frac{3\mathcal{N}(\mu)}{2}\right)^{\frac{5}{3}}$$

$$\overset{\text{Eq. 1.144}}{=} V_0\mathcal{N}(\mu) + \underbrace{\left[L^3\left(\sum_{\sigma\in\{\uparrow,\downarrow\}}\right)\left(\frac{\sqrt{2m_e}}{2\pi\hbar}\right)^3 2\pi\right]^{-\frac{2}{3}}}_{C} \frac{2}{5}\left(\frac{3}{2}\right)^{\frac{5}{3}} L^5\left(\frac{\mathcal{N}(\mu)}{L^3}\right)^{\frac{5}{3}}$$

$$= V_0\mathcal{N}(\mu) + L^3\left(\frac{1}{2}\sum_{\sigma\in\{\uparrow,\downarrow\}}\right)^{-\frac{2}{3}}\left[2\left(\frac{2}{4\pi^2}\right)^{\frac{3}{2}}2\pi\right]^{-\frac{2}{3}} \underbrace{\frac{3}{10}2}_{\frac{2}{5}\cdot\frac{3}{2}} \underbrace{\left(\frac{2}{3}\right)^{-\frac{2}{3}}}_{\frac{2}{3}\left(\frac{3}{2}\right)^{\frac{5}{3}}} \frac{\hbar^2}{m_e}\left(\frac{\mathcal{N}(\mu)}{L^3}\right)^{\frac{5}{3}}$$

$$= \underbrace{V_0\mathcal{N}(\mu)}_{E_{pot}} + \underbrace{L^3\frac{3}{10}\left(\frac{1}{2}\sum_{\sigma\in\{\uparrow,\downarrow\}}\right)^{-\frac{2}{3}}\left(3\pi^2\right)^{\frac{2}{3}}\frac{\hbar^2}{m_e}\left(\frac{\mathcal{N}(\mu)}{L^3}\right)^{\frac{5}{3}}}_{E_{kin}} \tag{1.145}$$

[29] The dimensionality has a large impact in the shape of the density of states.

I use the factor $\frac{1}{2}\sum_{\sigma\in\{\uparrow,\downarrow\}}$ to make the spin-degeneracy explicit, while keeping the expression for a non-spin polarized electron gas simple, because this factor equals unity.

Thus, the potential energy per volume is

$$\frac{1}{L^3}E_{\text{pot}} = V_0 n_t \tag{1.146}$$

and the kinetic energy per volume is

$$\frac{1}{L^3}E_{\text{kin}}(n_t) = \frac{3}{10}\left(3\pi^2\right)^{\frac{2}{3}}\frac{\hbar^2}{m_e}n_t^{\frac{5}{3}} \tag{1.147}$$

where $n_t \stackrel{\text{def}}{=} \frac{1}{L^3}\mathcal{N}(\mu)$ is the total (both spin directions) electron density.

Energy functional for the spin-polarized electron gas

4 Calculate the energy of the spin-polarized electron gas as function of the spin polarization n_s/n_t, where $n_s = n_\uparrow - n_\downarrow$ is the spin density and $n_t = n_\uparrow + n_\downarrow$ is the total electron density. Without restriction of generality (WroG), the magnetization is oriented along the z-direction.

Next we can also determine the energy as function of the spin polarization. The spin polarization is the ratio between the spin density n_s and the total density n_t. The spin density for an electron gas polarized in z direction is $n_s = n_\uparrow - n_\downarrow$.

$$\frac{1}{L^3}\left(E_{\text{kin}}(n_\uparrow) + E_{\text{kin}}(n_\downarrow)\right) \stackrel{\text{Eq. 1.147}}{=} \frac{3}{10}\left(3\pi^2\right)^{\frac{2}{3}}\frac{\hbar^2}{m_e}\frac{1}{2}\left((2n_\uparrow)^{\frac{5}{3}} + (2n_\downarrow)^{\frac{5}{3}}\right) \tag{1.148}$$

With $n_\uparrow = \frac{1}{2}(n_t + n_S)$ and $n_\downarrow = \frac{1}{2}(n_t - n_S)$, we obtain

KINETIC ENERGY OF THE NON-INTERACTING FREE ELECTRON GAS

This is the Thomas-Fermi expression for the kinetic energy of a non-interacting homogeneous electron gas at zero Kelvin.

$$\frac{1}{L^3}E_{\text{kin}}(n_t, n_s) = \underbrace{\frac{3}{10}\left(3\pi^2\right)^{\frac{2}{3}}\frac{\hbar^2}{m_e}n_t^{\frac{5}{3}}}_{E(n_t,0)/L^3} \cdot \underbrace{\frac{1}{2}\left(\left(1+\frac{n_s}{n_t}\right)^{\frac{5}{3}} + \left(1-\frac{n_s}{n_t}\right)^{\frac{5}{3}}\right)}_{\approx 1+(2^{\frac{2}{3}}-1)\left(\frac{n_s}{n_t}\right)^2} \tag{1.149}$$

where $n_t \stackrel{\text{def}}{=} \frac{1}{L^3}\mathcal{N}(\mu) = n_\uparrow + n_\downarrow$ is the **total electron density** (both spin directions)and $n_s = n_\uparrow - n_\downarrow$ is the **spin density** .
The spin dependence of the kinetic energy is shown in Fig. 1.11. The dependence of the spin polarization can fairly well be approximated by a simple parabola.

This expression is significant to understand the interacting homogeneous electron gas. It is further used in the Thomas-Fermi approximation of electrons. The Thomas-Fermi approximation is a predecessor of the Density-Functional Theory (DFT), for which its inventor Walter Kohn received the Nobel price in chemistry 1998.

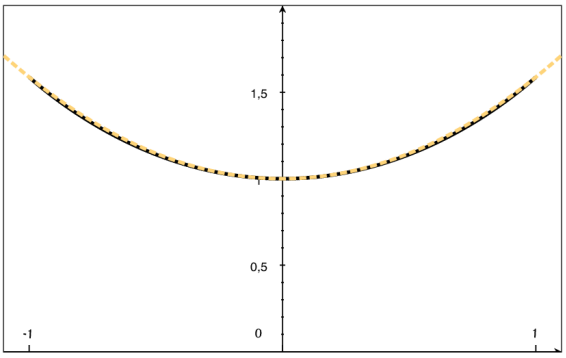


Fig. 1.11: Dependence of the kinetic energy of the free-electron gas on the spin polarization n_s/n_t. The dashed line is the approximation by a simple parabola, which is surprisingly accurate.

Chapter 2

Weakly interacting electrons

In order to explore the role of interactions, let us start with small interactions. The interaction energy can be obtained in first-order perturbation theory using the wave functions of the non-interacting system, namely Slater determinants. Slater determinants have a particularly simple structure, which allows one to express most quantities in terms of one-particle wave functions.

Because the Coulomb interaction between electrons is strong, one may question the reliability of such an approach. This concern is justified. However, in practice we do not start the perturbation theory from a truly non-interacting system: Rather, we choose an effective one-particle potential and a renormalized interaction. The effective potential considers also the electron-electron repulsion and the renormalized interaction takes into account that the interaction is screened by the electron gas between two charges. Both effects lead to a substantially reduced effective interaction, which usually can be well described by perturbation theory.

One such description using one-particle wave functions is the self-consistent Hartree-Fock method. The **Hartree-Fock method** [25, 26, 27] is an electronic-structure method that is the work-horse of quantum chemistry. Today it plays an important role as a starting point of more accurate and involved methods.

Let me quote P.W. Anderson, noble laureate and probably the father of strong correlations in solid-state phyics: *"One may get the impression that modern many-body theory, of which one hears so much, goes far beyond Hartree-Fock, and that, therefore, we should not bother with such old-fashioned stuff. This is not at all true– in fact, modern many-body theory has mostly just served to show us how, where, and when to use Hartree-Fock theory and how flexible and useful a technique it can be."* P.W. Anderson, 1963[28]

Another description using one-particle wave functions is **density-functional theory**(DFT). In contrast to the Hartree-Fock approximation, density-functional theory is formally exact, albeit limited to ground states, respectively equilibrium ensembles. This method is the workhorse for first-principles calculations and widely used for quantitative calculations of materials and molecules considering the quantum nature of the electronic structure. Despite the different foundation of density-functional theory and the Hartree-Fock method, they exhibit many similarities that provide a insights for first-principles calculations.

Let me return to the Hartree-Fock method discussed in this chapter: The basic idea of the Hartree-Fock method is to restrict the wave functions to Slater determinants[25]. The wave function is borrowed from a non-interacting system, but one chooses the very best non-interacting system for that purpose.

After having defined Slater determinants in the previous chapter, in this chapter we will gain some familiarity with them. We will see, how non-interacting many-particle systems can be described by a set of one-particle wave functions. Furthermore, we will become familiar with the most important contributions of the electron interaction, namely **Hartree energy** and **exchange energy**.

Then we will explore the energetics. I will directly step into the finite-temperature formalism, in

order to prepare the ground for the finite-temperature Green's-function formalism discussed later. While being slighly more complex, the finite-temperature point of view avoids a number of difficulties inherent in the zero-temperature formalism. We will learn the implications of the mean-field approximation, which is inherent in Hartree-Fock approximation. While density-functional theory does not make the mean-field approximation, the understanding of the Hartree-Fock approximation sheds light onto concepts of density-functional theory.

In this chapter, I will also introduce the concept **spectral function**, which can be probed experimentally. Besides determining the state the system is in, understanding the response of the system to an external perturbation is the second most important goal of theoretical solid-state physics, if not of all physics.

- The state is often determined assuming thermal equilibrium.[1] Thermal equilibrium is based on the energy of the system.
- The response of the system requires the understanding of excited states. The latter are described by the spectral function.

2.1 The setting

In this book, we investigate interacting electrons in a solid or a molecule. Specifically, we consider the Born-Oppenheimer Hamiltonian[2] which acts on the electrons. The Born-Oppenheimer Hamiltonian depends on the atomic positions. It is important to understand that the description of the electronic Hamiltonian does not make any simplifying assumption on the atom dynamics. It simply does not talk about it.[3] Nevertheless, it provides the ingredients required for the complete combined quantum dynamics of the nuclei and electrons. The equation of motion for nuclei and electrons is described in another booklet within the PhiSX series, namely ΦSX: Introduction to Solid-State Theory[1].

The Born-Oppenheimer Hamiltonian for a system with M atoms at positions $\vec{R}_j$ and N electrons at positions-and-spin $\vec{x}_j = (\vec{r}_j, \sigma_j)$ is

$$\hat{H}^{BO}(\vec{R}_1,\ldots,\vec{R}_M) = \underbrace{\underbrace{\underbrace{\sum_{j=1}^{N}\frac{\hat{\vec{p}}_j^2}{2m_e}}_{\text{kinetic energy}} + \underbrace{\sum_{i=1}^{N}\sum_{j=1}^{M}\frac{-e^2 Z_j}{4\pi\epsilon_0|\hat{\vec{r}}_i-\vec{R}_j|}}_{v_{ext}(\vec{r}_i)}}_{\text{external potential energy}}}_{\text{non-interacting Hamiltonian }\hat{h}} + \underbrace{\frac{1}{2}\sum_{i\neq j}^{M}\frac{e^2 Z_i Z_j}{4\pi\epsilon_0|\vec{R}_i-\vec{R}_j|}}_{\text{Coulomb repulsion between nuclei}} + \underbrace{\frac{1}{2}\sum_{i\neq j=1}^{N}\frac{e^2}{4\pi\epsilon_0|\hat{\vec{r}}_i-\hat{\vec{r}}_j|}}_{\text{electron-electron interaction }\hat{W}} \tag{2.1}$$

We use explicit fundamental constants for the elementary charge e, the (reduced) Plank quantum $\hbar$, the electron mass m_e and the electric constant ϵ_0. The Z_j are the atomic numbers of the nuclei.

The details of the Hamiltonian will not be relevant. The offset by the Coulomb repulsion of the nuclei does not depend on the electrons and is not mentioned again. The Hamiltonian will be written in the following as

$$\hat{H} = \hat{h} + \hat{W} \tag{2.2}$$

[1] Non-equilibrium states are usually constructed by a controlled perturbation of thermal equilibrium state.

[2] We consider here the Born-Oppenheimer Hamiltonian $\hat{H}^{BO}(R)$ Eq. **??** of ΦSX: Introduction to Solid-State Theory.

[3] I stress this point because people even introduced a "clamped atom approximation" to claim the presence of hidden approximation. I consider this as nonsense.

where $\hat{H}$ is the full Hamiltonian acting on the electrons, $\hat{h}$ is the non-interacting part and $\hat{W}$ is the interaction term.

2.2 Expectation values of Slater determinants

The development of a suitable notation had a large impact on many-partcle physics. We will later use the occupation-number representation and, creation and annihilation operators. Until then, we need to live with a conventional notation, which is a bit clumsy for many-particle physics. This means that it may not be worth trying to memorize formulas in this notation. Nevertheless, it will remain important to be able to translate the expressions from the elegant, but also abstract, notations into the conventional wave function notation.

In the following, I will use the unit operator in Fock space

$$\hat{1} = \sum_{N=0}^{\infty} \int d^4x_1 \cdots \int d^4x_N \, |\vec{x}_1, \ldots, \vec{x}_N\rangle\langle \vec{x}_1, \ldots, \vec{x}_N| \tag{2.3}$$

where $|\vec{x}_1, \ldots, \vec{x}_N\rangle = |\vec{x}_1\rangle \otimes \ldots \otimes |\vec{x}_N\rangle$ is a product state.[4] The term for $N = 0$ is the **vacuum state** $|\mathcal{O}\rangle$. The vacuum state cannot be described by a wave function, but only by a single complex number.

2.2.1 One- and two-particle operators

The Hamiltonian $\hat{h}$ is called a **one-particle operator**, because it acts on all particles, but only on one at a time. To make the distinction to an operator in one-particle Hilbert space explicit, I will call such operators also **one-particle-at-a-time operators** .[5]

$$\hat{h} = \underbrace{\sum_{N=1}^{\infty} \underbrace{\sum_{j=1}^{N} \underbrace{\int d^4x_1 \cdots \int d^4x_N \, |\vec{x}_1, \ldots, \vec{x}_N\rangle \left[\frac{-\hbar^2}{2m_e}\vec{\nabla}_j^2 + v_{ext}(\vec{r}_j)\right] \langle \vec{x}_1, \ldots, \vec{x}_N|}_{\text{acts on the j-th electron in a state with } N \text{ electrons}}}_{\text{acts on all electrons in states with N-electrons}}}_{\text{acts on all electrons without restriction}} \tag{2.5}$$

The second operator in Eq. 2.2, $\hat{W}$, describes the Coulomb interaction between the electrons. The Coulomb interaction cannot be decomposed in a sum over all electrons. Rather, we need to consider electron pairs

$$\hat{W} = \underbrace{\sum_{N=2}^{\infty} \underbrace{\frac{1}{2} \sum_{i \neq j}^{N} \underbrace{\int d^4x_1 \cdots \int d^4x_N \, |\vec{x}_1, \ldots, \vec{x}_N\rangle \frac{e^2}{4\pi\epsilon_0 |\vec{r}_i - \vec{r}_j|} \langle \vec{x}_1, \ldots, \vec{x}_N|}_{\text{interaction between electron } i \text{ and electron } j}}_{\text{interaction between all electron pairs in states with } N\text{-particles}}}_{\text{interaction between all electron pairs without restriction}} \tag{2.6}$$

Each pair of electrons occurs twice in the sum, which is corrected by the factor $\frac{1}{2}$. As above, the indices i and j denote the two interacting electrons. Because two particles need to be considered at

[4] Some caution is required to distinguish product states from Slater determinants and permanents.

[5] A general one-particle-at-a-time operator $\hat{A}$ has the form

$$\hat{A} = \sum_{N=1}^{\infty} \sum_{j=1}^{N} \int d^4x_1 \cdots \int d^4x_N \int d^4x'_j \, |\vec{x}_1, \cdots, \vec{x}_N\rangle\langle \vec{x}_j|\hat{A}|\vec{x'}_j\rangle\langle \vec{x}_1, \ldots, \vec{x'}_j, \cdots \vec{x}_N| \tag{2.4}$$

All particle coordinates except the one experiencing the operator are integrated out. The equation comes from $\hat{A} = \hat{1}\hat{A}\hat{1}$ with the unit operator expressed by Eq. 2.3. The matrix elements for the operator acting on the j-th particle have the form $\langle \vec{x}_1|\vec{x'}_1\rangle \cdots \langle \vec{x}_j|\hat{A}|\vec{x'}_j\rangle \cdots \langle \vec{x}_N|\vec{x'}_N\rangle$. The double integrations $\int dx \int dx' \, \langle \vec{x}|\vec{x'}\rangle$ for "bystander" particles reduce to single integrations.

a time, the operator $\hat{W}$ is called a **two-particle operator**. The two-particle term is the cause for the dazzling complexity of many-particle physics.

The term "one-particle operator" is ambiguous, which makes it confusing.

- On the one hand, it may be a **true one-particle operator** in the one-particle Hilbert space. It acts on states that describe exactly a single electron.

- On the other hand, it may be a **one-particle-at-a-time operator** in the N-particle Hilbert space or the Fock space. Such an operator acts on many-particle states, but it acts on one electron at a time. The result is a sum over the contributions from the individual particles.

Let us now work out the expectation values for the one-particle and two-particle operators for a Slater determinant.

2.2.2 Expectation value of a one-particle operator with a Slater determinant

Here, we will work out the expectation value of a one-particle-at-a-time operator for a Slater determinant. An example for such a one-particle operator is the non-interacting part of the Hamiltonian.

Explicit example for the two-particle wave function

The two-particle Slater determinant $|\Psi\rangle$ of two one-particle orbitals $|\varphi_a\rangle$ and $|\varphi_b\rangle$ has the form

$$\underbrace{\langle \vec{x}_1, \vec{x}_2 | \Psi \rangle}_{\Psi(\vec{x}_1,\vec{x}_2)} = \frac{1}{\sqrt{2}} \underbrace{\Big[\langle \vec{x}_1 | \varphi_a \rangle \langle \vec{x}_2 | \varphi_b \rangle - \langle \vec{x}_1 | \varphi_b \rangle \langle \vec{x}_2 | \varphi_a \rangle \Big]}_{\varphi_a(\vec{x}_1)\varphi_b(\vec{x}_2) - \varphi_b(\vec{x}_1)\varphi_a(\vec{x}_2)} \tag{2.7}$$

As a specific example for a one-particle-at-a-time operator, I choose the particle-density operator $\hat{n}(\vec{r})$ defined as

$$\hat{n}(\vec{r}) = \sum_{\sigma \in \{\uparrow,\downarrow\}} \int d^4x_1 \int d^4x_2 \; |\vec{x}_1, \vec{x}_2\rangle \Big[\delta(\underbrace{\vec{x}}_{(\vec{r},\sigma)} - \vec{x}_1) + \delta(\underbrace{\vec{x}}_{(\vec{r},\sigma)} - \vec{x}_2) \Big] \langle \vec{x}_1, \vec{x}_2 | \tag{2.8}$$

The electron density $n(\vec{r})$ at position $\vec{r}$ of a Slater determinant $|\Psi\rangle$ with two particles in the

one-particle orbitals $\varphi_a(\vec{x})$ and $\varphi_b(\vec{x})$ is

$$
\begin{aligned}
n(\vec{r}) &= \langle\Psi|\hat{n}(\vec{r})|\Psi\rangle \\
&\overset{\text{Eq. 2.8}}{=} \sum_{\sigma\in\{\uparrow,\downarrow\}} \int d^4x_1 \int d^4x_2\; \Psi^*(\vec{x}_1,\vec{x}_2)\Big[\delta(\vec{x}-\vec{x}_1)+\delta(\vec{x}-\vec{x}_2)\Big]\Psi(\vec{x}_1,\vec{x}_2) \\
&\overset{\Psi(\vec{x}_1,\vec{x}_2)=-\Psi(\vec{x}_2,\vec{x}_1)}{=} \sum_{\sigma\in\{\uparrow,\downarrow\}} \Bigg\{ \int d^4x_1 \int d^4x_2\; \Psi^*(\vec{x}_1,\vec{x}_2)\delta(\vec{x}-\vec{x}_1)\Psi(\vec{x}_1,\vec{x}_2) \\
&\qquad + \int d^4x_1 \int d^4x_2\; \overbrace{\Psi^*(\vec{x}_2,\vec{x}_1)}^{-\Psi^*(\vec{x}_1,\vec{x}_2)}\delta(\vec{x}-\vec{x}_2)\overbrace{\Psi(\vec{x}_2,\vec{x}_1)}^{-\Psi(\vec{x}_1,\vec{x}_2)} \Bigg\} \\
&\overset{\vec{x}_1\leftrightarrow\vec{x}_2}{=} \sum_{\sigma\in\{\uparrow,\downarrow\}} 2\int d^4x_1 \int d^4x_2\; \Psi^*(\vec{x}_1,\vec{x}_2)\delta(\vec{x}-\vec{x}_1)\Psi(\vec{x}_1,\vec{x}_2) \\
&\overset{\text{Eq. 2.7}}{=} \sum_{\sigma\in\{\uparrow,\downarrow\}} \Bigg\{ 2\int d^4x_1 \int d^4x_2\; \frac{1}{\sqrt{2}}\Big[\varphi_a(\vec{x}_1)\varphi_b(\vec{x}_2)-\varphi_b(\vec{x}_1)\varphi_a(\vec{x}_2)\Big]^* \\
&\qquad \times \delta(\vec{x}-\vec{x}_1)\frac{1}{\sqrt{2}}\Big[\varphi_a(\vec{x}_1)\varphi_b(\vec{x}_2)-\varphi_b(\vec{x}_1)\varphi_a(\vec{x}_2)\Big] \Bigg\} \\
&= \sum_{\sigma\in\{\uparrow,\downarrow\}} \Bigg\{ \int d^4x_1 \int d^4x_2\; \varphi_a^*(\vec{x}_1)\varphi_b^*(\vec{x}_2)\delta(\vec{x}-\vec{x}_1)\varphi_a(\vec{x}_1)\varphi_b(\vec{x}_2) \\
&\qquad - \int d^4x_1 \int d^4x_2\; \varphi_a^*(\vec{x}_1)\varphi_b^*(\vec{x}_2)\delta(\vec{x}-\vec{x}_1)\varphi_b(\vec{x}_1)\varphi_a(\vec{x}_2) \\
&\qquad - \int d^4x_1 \int d^4x_2\; \varphi_b^*(\vec{x}_1)\varphi_a^*(\vec{x}_2)\delta(\vec{x}-\vec{x}_1)\varphi_a(\vec{x}_1)\varphi_b(\vec{x}_2) \\
&\qquad + \int d^4x_1 \int d^4x_2\; \varphi_b^*(\vec{x}_1)\varphi_a^*(\vec{x}_2)\delta(\vec{x}-\vec{x}_1)\varphi_b(\vec{x}_1)\varphi_a(\vec{x}_2) \Bigg\} \\
&= \sum_{\sigma\in\{\uparrow,\downarrow\}} \Bigg\{ \langle\varphi_a|\vec{x}\rangle\langle\vec{x}|\varphi_a\rangle \underbrace{\langle\varphi_b|\varphi_b\rangle}_{=1} - \langle\varphi_a|\vec{x}\rangle\langle\vec{x}|\varphi_b\rangle \underbrace{\langle\varphi_b|\varphi_a\rangle}_{=0} \\
&\qquad - \langle\varphi_b|\vec{x}\rangle\langle\vec{x}|\varphi_a\rangle \underbrace{\langle\varphi_a|\varphi_b\rangle}_{=0} + \langle\varphi_b|\vec{x}\rangle\langle\vec{x}|\varphi_b\rangle \underbrace{\langle\varphi_a|\varphi_a\rangle}_{=1} \Bigg\} \\
&= \sum_{\sigma\in\{\uparrow,\downarrow\}} \Big(\varphi_a^*(\vec{x})\varphi_a(\vec{x}) + \varphi_b^*(\vec{x})\varphi_b(\vec{x})\Big) \qquad (2.9)
\end{aligned}
$$

This result can be generalized to arbitrary one-particle-at-a-time operators. The derivation of the general result is provided in appendix I.2.1 on 685. It is summarized as follows:

EXPECTATION VALUE OF A ONE-PARTICLE-AT-A TIME OPERATOR WITH A SLATER DETERMINANT

The expectation value of a general one-particle-at-a-time operator $\hat{A}$ with a Slater determinant $|\vec{\sigma}\rangle$ built from an orthonormal set of one-particle orbitals $|\varphi_n\rangle$ with occupation numbers σ_n is a sum over occupied one-particle states. That is

$$\langle\vec{\sigma}|\hat{A}|\vec{\sigma}\rangle \overset{\text{Eq. I.5}}{=} \sum_{n=1}^{\infty}\sigma_n\langle\varphi_n|\hat{A}|\varphi_n\rangle \qquad \text{for one-particle-at-a-time operators } \hat{A}. \qquad (2.10)$$

Occupied are the one-particle orbitals with occupation numbers $\sigma_n = 1$.

Let me mention a few observations:

- The number of terms is drastically reduced just because we have used an orthonormal set of

one-particle wave functions. A Slater determinant for N electrons is a sum of $N!$ product states. An expectation value has $(N!)^2$ terms, not even considering the number (N) of terms in the operator itself. This is a daunting large number of terms. By exploiting the orthonormality of the one-particle orbitals, the number of terms for a N-particle system is reduced from $N(N!)^2$ to only N. For large systems, this is an enormous simplification. This simplification is the sole reason for (often) using orthonormal basissets in many-particle physics.

- The *sum over particles* is turned into a *sum over orbitals*. Eq. 2.10 is the reason that the sum of orbitals is often considered as a sum over electrons. The term "sum over electrons" in this context is, however, a misnomer, because we cannot attribute an electron to a specific one-particle orbital. Nevertheless, it offers a physical intuitive picture, which may be useful as long as one is aware of its limitations.

- The anti symmetry of the wave function ensures that the same expectation value is obtained, whether we work out a property of the first, the second, or any other electron.[6]

2.2.3 One-particle-reduced density matrix

The physics of non-interacting and weakly interacting particles can be described well by the **one-particle-reduced density matrix** $\hat{\rho}^{(1)}$. The superscript "(1)" distinguishes the one-particle-reduced density matrix from the von-Neumann density matrix $\hat{\rho}^{vN}$ introduced earlier in Eq. 2.49.

The **one-particle-reduced density matrix** of a general ensemble of many-particle wave functions $|\Phi_q\rangle$ with probabilities P_q is defined such that the ensemble expectation value $\langle A \rangle$ of any one-particle-at-a-time operator $\hat{A}$ is obtained as trace of the product of the operator $\hat{A}$ and the one-particle-reduced density matrix $\hat{\rho}^{(1)}$, i.e.

$$\underbrace{\langle A \rangle}_{\sum_q P_q \langle \Phi_q | \hat{A} | \Phi_q \rangle} = \mathrm{Tr}\left[\hat{\rho}^{(1)} \hat{A}\right] . \tag{2.11}$$

The operator $\hat{A}$ in the matrix element $\langle \Phi_q | \hat{A} | \Phi_q \rangle$ is a one-particle-at-a-time operator in Fock space, while the operator $\hat{A}$ on the right is a true one-particle operator in the one-particle Hilbert space. Unlike the similar Eq. 2.51 with the von-Neumann density matrix, the expression Eq. 2.11 above is limited to one-particle-at-a-time operators.

For the sake of completeness, let me extract the expression for the one-particle-reduced density matrix for an ensemble $\{P_q, |\Phi_q\rangle\}$ of many-particle wave functions. We insert a general one-particle-at-a-time operator $\hat{A}$ into the equation Eq. 2.11 defining the one-particle-reduced density matrix

[6] The wave function is, up to a sign, the same when the coordinates of the coordinates of the first and the second electron are interchanged. The sign drops out for expectation values, because the wave function enters twice. Example: Using the anti symmetry of the wave function $\psi(x,x') = -\psi(x',x)$ one can convert the density ρ_1 of the first particle $\rho_1(x) = \int dx'\, \psi^*(x,x')\psi(x,x') = (-1)^2 \int dx'\, \psi^*(x',x)\psi(x',x) = \rho_2(x)$ into the density $\rho_2(x)$ of the second.

$\hat{\rho}^{(1)}$.

$$\begin{aligned}
\langle A\rangle &= \sum_q P_q \langle\Phi_q| \overbrace{\sum_{N=1}^{\infty}\sum_{j=1}^{N}\int d^4x_1\cdots\int d^4x_N\int d^4x'_j}^{\hat{A}} |\vec{x}_1,\ldots,\vec{x}_N\rangle\langle\vec{x}_j|\hat{A}|\vec{x'}_j\rangle\langle\vec{x}_1,\ldots,\vec{x'}_j,\ldots\vec{x}_N| |\Phi_q\rangle \\
&= \sum_q P_q \sum_{N=1}^{\infty} N\int d^4x_1 \int d^4x_2\cdots\int d^4x_N\int d^4x'_1\ \langle\Phi_q|\vec{x}_1,\vec{x}_2,\ldots,\vec{x}_N\rangle\langle\vec{x}_1|\hat{A}|\vec{x'}_1\rangle\langle\vec{x'}_1,\vec{x}_2,\ldots,\vec{x}_N|\Phi_q\rangle \\
&= \mathrm{Tr}\Big\{\int d^4x_1\int d^4x'_1 \\
&\quad\times|\vec{x'}_1\rangle \underbrace{\sum_{N=1}^{\infty} N\int d^4x_2\cdots\int d^4x_N\ \sum_q\langle\vec{x'}_1,\vec{x}_2\ldots,\vec{x}_N|\Phi_q\rangle P_q\langle\Phi_q|\vec{x}_1,\vec{x}_2\ldots,\vec{x}_N\rangle}_{\rho^{(1)}(\vec{x'}_1,\vec{x}_1)}\langle\vec{x}_1|\hat{A}\Big\} \\
&= \mathrm{Tr}[\hat{\rho}^{(1)}\hat{A}]
\end{aligned} \tag{2.12}$$

with

$$\begin{aligned}
\hat{\rho}^{(1)} &= \int d^4x\int d^4x' \\
&\quad\times|\vec{x}\rangle\Big\{\sum_{N=1}^{\infty} N\int d^4x_2\cdots\int d^4x_N\ \sum_q\langle\vec{x},\vec{x}_2\ldots,\vec{x}_N|\Phi_q\rangle P_q\langle\Phi_q|\vec{x'},\vec{x}_2\ldots,\vec{x}_N\rangle\Big\}\langle\vec{x'}|
\end{aligned} \tag{2.13}$$

All particles except the first are traced out. The result is then multiplied with N to account for the contribution from all other particles. The scalar product between states with distinct particle numbers vanish. Hence, $\langle\vec{x}_1,\vec{x}_2\ldots,\vec{x}_N|\Phi_q\rangle$ is only sensitive on the N-particle contribution in $|\Phi_q\rangle$.

The language of second quantization introduced later will offer a much more elegant and intuitive expression Eq. 3.57 for the one-particle-reduced density matrix.

Natural orbitals and occupations: The one-particle-reduced density matrix is an operator in the one-particle Hilbert space. Because it is hermitian, it has real-valued eigenvalues and orthonormal eigenstates. The eigenstates $|\varphi_n\rangle$ of the one-particle-reduced density matrix are called **natural orbitals**[29, 30] and the eigenvalues f_n are called **occupations**[29].

$$\hat{\rho}^{(1)}|\varphi_n\rangle = |\varphi_n\rangle f_n \tag{2.14}$$

ONE-PARTICLE-REDUCED DENSITY MATRIX

Expressed in terms of natural orbitals $|\varphi_n\rangle$ and occupations f_n, the one-particle-reduced density matrix of a general ensemble of many-particle wave functions can be written as

$$\hat{\rho}^{(1)} = \sum_n |\varphi_n\rangle f_n\langle\varphi_n| \ . \tag{2.15}$$

The **occupations** f_n are the eigenvalues and the **natural orbitals** $|\varphi_n\rangle$ are the eigenstates of the one-particle-reduced density matrix as defined in Eq. 2.14.

The expectation values of one-particle operators are obtained by the well-known form

$$\Big\langle A\Big\rangle = \mathrm{Tr}\Big[\hat{\rho}^{(1)}\hat{A}\Big] = \sum_n f_n\langle\varphi_n|\hat{A}|\varphi_n\rangle \tag{2.16}$$

For a thermal ensemble of non-interacting electrons, the occupations are given by the **Fermi distribution**

$$f_{T,\mu}(\epsilon) \stackrel{\text{def}}{=} \left(1 + e^{\beta(\epsilon-\mu)}\right)^{-1} \tag{2.17}$$

shown in figure 2.1.

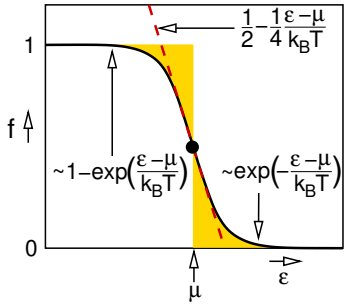


Fig. 2.1: Fermi distribution function Eq. 2.17 and common limits.

Slater determinants and idempotency of the one-particle-reduced density matrix: The comparison of Eq. 2.10 with Eq. 2.16 shows that the one-particle-reduced density matrix of a Slater determinant is

$$\hat{\rho}^{(1)} = \sum_{n=0}^{\infty} |\varphi_n\rangle \sigma_n \langle\varphi_n| \tag{2.18}$$

where σ_n is the occupation number of the n-th orbital, from which the Slater determinant is built. The comparison shows also that these one-particle orbitals are also the natural orbitals. Furthermore, the occupations f_n of a Slater determinant are the occupation numbers $\sigma_n \in \{0, 1\}$, which have integer values.

Because the occupations of a Slater determinant are either zero or one, the one-particle-reduced density matrix of a Slater determinant is **idempotent**[7], i.e.

$$\left(\hat{\rho}^{(1)}\right)^2 = \hat{\rho}^{(1)} \ . \tag{2.20}$$

The reverse is also true: An idempotent one-particle-reduced density matrix corresponds to a single Slater determinant.

Notice a possible confusion with the idempotency of the von-Neumann density matrix $\hat{\rho}^{vN} = \sum_q |\Phi_q\rangle P_q \langle\Phi_q|$. Idempotency of the von-Neumann density matrix implies that the system is in a **pure state** [8]. Idempotency of the one-particle-reduced density matrix is a stronger statement: It not only says that we deal with a single many-particle wave function, but also that this wave function can be expressed as a single Slater determinant.

The one-particle orbitals, from which the Slater determinant is built, are also its natural orbitals.[9]

[7]

$$\left(\hat{\rho}^{(1)}\right)^2 = \sum_{m,n} |\varphi_m\rangle \sigma_m \underbrace{\langle\varphi_m|\varphi_n\rangle}_{\delta_{m,n}} \sigma_n \langle\varphi_n| = \sum_n |\varphi_n\rangle \sigma_n^2 \langle\varphi_n| \stackrel{\sigma_n \in \{0,1\}}{=} \sum_n |\varphi_n\rangle \sigma_n \langle\varphi_n| = \hat{\rho}^{(1)} \ . \tag{2.19}$$

[8] A pure state is an ensemble with only a single many-particle wave function $|\Phi_q\rangle$

[9] Because the occupations are highly degenerate, there is a large flexibility of choosing the natural orbitals.

N-representability: The occupations for a general fermionic many-particle wave function or any ensemble of them lie in the interval between zero and one[31]. That is,

$$0 \leq f_n \leq 1 \tag{2.21}$$

for any fermionic many-particle wave function or any ensemble of them. The converse statement is also true: any hermitian matrix with eigenvalues between zero and one can be represented as one-particle-reduced density matrix of a fermionic wave function.[31] A matrix with this property is called *N*-**representable**.

For bosons and for distinguishable particles the occupations can have any non-negative value.

Real-space-and-spin representation: Below, I will express the one-particle-reduced density matrix in terms of their real-space-and-spin components $\vec{x} = (\vec{r}, \sigma)$ respectively $\vec{x'} = (\vec{r'}, \sigma')$, with position $\vec{r}$ and spin index $\sigma \in \{\uparrow, \downarrow\}$

$$\rho^{(1)}(\vec{x}, \vec{x'}) = \langle \vec{x} | \hat{\rho}^{(1)} | \vec{x'} \rangle \tag{2.22}$$

Caution is required because the same symbol "σ" is used for the spin index and the occupation number of a Slater determinant.

The electron density can be obtained from the one-particle-reduced density matrix as

$$n(\vec{r}) = \sum_{\sigma \in \{\uparrow,\downarrow\}} \rho^{(1)}(\vec{x}, \vec{x}) \tag{2.23}$$

To become familiar with the expressions, let me write down the expectation values of a few common operators.

- electron density

$$\begin{aligned} n(\vec{r}) = \mathrm{Tr}\Big[\hat{\rho}^{(1)} \underbrace{\sum_{\sigma \in \{\uparrow,\downarrow\}} |\vec{r}, \sigma\rangle\langle\vec{r}, \sigma|}_{\hat{n}(\vec{r})}\Big] &\overset{\text{Eq. 2.15}}{=} \sum_{\sigma \in \{\uparrow,\downarrow\}} \sum_n \langle \vec{r}, \sigma | \varphi_n \rangle f_n \langle \varphi_n | \vec{r}, \sigma \rangle \\ &= \sum_{\sigma \in \{\uparrow,\downarrow\}} \sum_n f_n \varphi_n^*(\vec{r}, \sigma) \varphi_n(\vec{r}, \sigma) \end{aligned} \tag{2.24}$$

- kinetic energy

$$E_{\mathrm{kin}} = \mathrm{Tr}\Big[\hat{\rho}^{(1)} \frac{\hat{\vec{p}}^2}{2m}\Big] \overset{\text{Eq. 2.15}}{=} \sum_n f_n \Big\langle \varphi_n \Big| \frac{\hat{\vec{p}}^2}{2m_e} \Big| \varphi_n \Big\rangle \tag{2.25}$$

2.2.4 Expectation value of a two-particle operator with a Slater determinant

Let us now turn to the two-particle term. We introduce the symbol [10] $\hat{W}$ for the interaction operator. For the Coulomb interaction, the interaction acts pairwise on two particles at a time. The two-particle matrix elements $W(\vec{x}, \vec{x'})$ of the Coulomb interaction is

$$W(\vec{x}, \vec{x'}) = \frac{e^2}{4\pi\epsilon_0 |\vec{r} - \vec{r'}|} \tag{2.26}$$

[10] The letter W stems for the German word *"Wechselwirkung"* for interaction.

where e is the elementary charge and ϵ_0 is the **electric constant** or **vacuum permittivity**. The Coulomb interaction is independent of the spin index. Furthermore it is local in the two coordinates.[11]

While a general derivation for the interaction energy of a Slater determinant is given in the appendix, let me work out here the interaction energy for a two-particle Slater determinant.

$$
\begin{aligned}
E_{int} &= \langle\Psi|\hat{W}|\Psi\rangle \\
&= \int d^4x_1 \int d^4x_2\ \Psi^*(\vec{x}_1,\vec{x}_2)\frac{1}{2}\Big[W(\vec{x}_1,\vec{x}_2)+W(\vec{x}_2,\vec{x}_1)\Big]\Psi(\vec{x}_1,\vec{x}_2) \\
&\overset{\Psi(\vec{x}_1,\vec{x}_2)=-\Psi(\vec{x}_2,\vec{x}_1)}{=} \int d^4x_1 \int d^4x_2\ \Psi^*(\vec{x}_1,\vec{x}_2)W(\vec{x}_1,\vec{x}_2)\Psi(\vec{x}_1,\vec{x}_2) \\
&\overset{\text{Eq. 2.7}}{=} \int d^4x_1 \int d^4x_2\ \frac{1}{\sqrt{2}}\Big[\varphi_a(\vec{x}_1)\varphi_b(\vec{x}_2)-\varphi_a(\vec{x}_2)\varphi_b(\vec{x}_1)\Big]^* \\
&\qquad\qquad \cdot W(\vec{x}_1,\vec{x}_2)\frac{1}{\sqrt{2}}\Big[\varphi_a(\vec{x}_1)\varphi_b(\vec{x}_2)-\varphi_a(\vec{x}_2)\varphi_b(\vec{x}_1)\Big] \\
&= \frac{1}{2}\int d^4x_1 \int d^4x_2\ \varphi_a^*(\vec{x}_1)\varphi_b^*(\vec{x}_2)W(\vec{x}_1,\vec{x}_2)\varphi_a(\vec{x}_1)\varphi_b(\vec{x}_2) \\
&- \frac{1}{2}\int d^4x_1 \int d^4x_2\ \varphi_a^*(\vec{x}_1)\varphi_b^*(\vec{x}_2)W(\vec{x}_1,\vec{x}_2)\varphi_a(\vec{x}_2)\varphi_b(\vec{x}_1) \\
&- \frac{1}{2}\int d^4x_1 \int d^4x_2\ \varphi_a^*(\vec{x}_2)\varphi_b^*(\vec{x}_1)W(\vec{x}_1,\vec{x}_2)\varphi_a(\vec{x}_1)\varphi_b(\vec{x}_2) \\
&+ \frac{1}{2}\int d^4x_1 \int d^4x_2\ \varphi_a^*(\vec{x}_2)\varphi_b^*(\vec{x}_1)W(\vec{x}_1,\vec{x}_2)\varphi_a(\vec{x}_2)\varphi_b(\vec{x}_1) \\
&= \int d^4x_1 \int d^4x_2\ \varphi_a^*(\vec{x}_1)\varphi_b^*(\vec{x}_2)\frac{1}{2}\Big[W(\vec{x}_1,\vec{x}_2)+W(\vec{x}_2,\vec{x}_1)\Big]\varphi_a(\vec{x}_1)\varphi_b(\vec{x}_2) \\
&- \int d^4x_1 \int d^4x_2\ \varphi_a^*(\vec{x}_1)\varphi_b^*(\vec{x}_2)\frac{1}{2}\Big[W(\vec{x}_1,\vec{x}_2)+W(\vec{x}_2,\vec{x}_1)\Big]\varphi_a(\vec{x}_2)\varphi_b(\vec{x}_1) \\
&= \underbrace{\frac{1}{2}\sum_{i,j\in\{a,b\}}\int d^4x_1 \int d^4x_2\ \varphi_i^*(\vec{x}_1)\varphi_j^*(\vec{x}_2)\frac{1}{2}\Big[W(\vec{x}_1,\vec{x}_2)+W(\vec{x}_2,\vec{x}_1)\Big]\varphi_i(\vec{x}_1)\varphi_j(\vec{x}_2)}_{\text{Hartree}} \\
&- \underbrace{\frac{1}{2}\sum_{i,j\in\{a,b\}}\int d^4x_1 \int d^4x_2\ \varphi_i^*(\vec{x}_1)\varphi_j^*(\vec{x}_2)\frac{1}{2}\Big[W(\vec{x}_1,\vec{x}_2)+W(\vec{x}_2,\vec{x}_1)\Big]\varphi_j(\vec{x}_1)\varphi_i(\vec{x}_2)}_{\text{exchange}}
\end{aligned}
\tag{2.28}
$$

In the last step, I added terms with $i = j$ to the first term and subtracted them again from the second term. As shown in section 2.3.1 below, this has the advantage that the first term is simply the electrostatic selfenergy of the electron density.

Interesting is the term with the negative sign. It differs from the first term in that the arguments of the orbitals on the right-hand side are interchanged. This is why the term is called the **exchange**

[11] A general two-particle operator has the form

$$
\begin{aligned}
\hat{W}_{1,2} &= \int dx_1 \cdots \int dx_N \int dx'_1 \cdots \int dx'_N |\vec{x}_1,\ldots,\vec{x}_N\rangle\langle\vec{x}_1,\ldots,\vec{x}_N|\hat{W}_{1,2}|\vec{x'}_1,\ldots,\vec{x'}_N\rangle\langle\vec{x'}_1,\ldots,\vec{x'}_N| \\
&= \int dx_1 \cdots \int dx_N \int dx'_1 \int dx'_2 |\vec{x}_1,\ldots,\vec{x}_N\rangle\langle\vec{x}_1,\ldots,\vec{x}_N|\hat{W}_{1,2}|\vec{x'}_1,\vec{x'}_2,\vec{x}_3,\ldots,\vec{x}_N\rangle\langle\vec{x'}_1,\vec{x'}_2,\vec{x}_3,\ldots,\vec{x}_N| \\
&= \int dx_1 \cdots \int dx_N \int dx'_1 \int dx'_2 |\vec{x}_1,\ldots,\vec{x}_N\rangle\langle\vec{x}_1,\vec{x}_2|\hat{W}_{1,2}|\vec{x'}_1,\vec{x'}_2\rangle\langle\vec{x'}_1,\vec{x'}_2,\vec{x}_3,\ldots,\vec{x}_N|
\end{aligned}
\tag{2.27}
$$

Thus, a general two-particle operator is nonlocal in the two particle coordinates and, therefore, its matrix elements depends on four arguments.

term. The exchange term is a direct consequence of the Pauli principle, that is, the antisymmetry of the wave function.

The general expectation value for a two-particle operator with a Slater determinant is worked out in appendix I.2.2 on p. 687. The result for the expectation value of the interaction energy is as follows.

EXPECTATION VALUE OF THE INTERACTION WITH A SLATER DETERMINANT

The expectation value of an interaction $\hat{W}$ with a Slater determinant[a] $|\vec{\sigma}\rangle$ built from orthonormal one-particle orbitals $|\varphi_j\rangle$ with occupation numbers σ_j is

$$\langle\vec{\sigma}|\hat{W}|\vec{\sigma}\rangle \overset{\text{Eq. I.7}}{=} \frac{1}{2}\sum_{i,j=1}^{\infty}\sigma_i\sigma_j\Big[\underbrace{\langle\varphi_i,\varphi_j|\hat{W}|\varphi_i,\varphi_j\rangle}_{\text{Hartree}}-\underbrace{\langle\varphi_i,\varphi_j|\hat{W}|\varphi_j,\varphi_i\rangle}_{\text{exchange}}\Big] \tag{2.29}$$

The terms with $i=j$ have been included in the sum, because the two terms cancel each other. The matrix elements used in the above equation Eq. 2.29 are matrix elements of two-particle product wave functions with the, e.g., Coulomb interaction

$$\langle\varphi_a,\varphi_b|\hat{W}|\varphi_c,\varphi_d\rangle \overset{\text{Eq. I.8}}{=} \sum_{\sigma,\sigma'\in\{\uparrow,\downarrow\}}\int d^3r\int d^3r'\;\varphi_a^*(\vec{r},\sigma)\varphi_b^*(\vec{r'},\sigma')\frac{e^2}{4\pi\epsilon_0|\vec{r}-\vec{r'}|}\varphi_c(\vec{r},\sigma)\varphi_d(\vec{r'},\sigma') \tag{2.30}$$

[a] The occupation-number representation $|\vec{\sigma}\rangle$ of Slater determinants has been introduced in section 1.4.1.

We can already look ahead and inspect the Feynman diagrams related to exchange and correlation. The diagrams related to the scattering processes are shown in fig. 2.2 on p. 57. The corresponding energy diagrams are shown in figure 11.1 on p. 350.

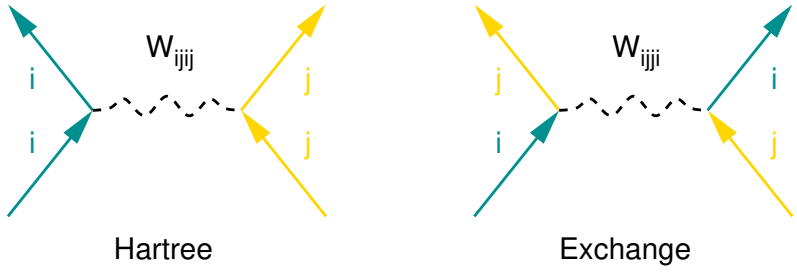


Fig. 2.2: The left diagram describes that two particles are scattered by the Coulomb interaction. The right diagram describes the same process, but the two electrons are exchanged. The second process is possible, because the two electrons are indistinguishable so that we cannot detect if the two electrons are still the same or not.

The equations that trace the matrix elements between Slater determinants to one-particle orbitals, such as Eq. 2.10 and Eq. 2.30, are the so-called **Slater-Condon rules**. The expectation values shown here are due to Slater, while Condon generalized the expression to matrix elements between two different Slater determinants. They will be summarized in section 3.5 on p. 138 and they are derived in appendix I on p. 685.

2.3 Total energy of a Slater determinant

TOTAL ENERGY OF A SLATER DETERMINANT

The total energy of a Slater determinant $|\vec{\sigma}\rangle$ formed from orthonormal one-particle orbitals $|\varphi_j\rangle$ with occupation numbers σ_j is obtained by combining Eq. 2.10 and Eq. 2.29

$$\langle\vec{\sigma}|\hat{h}+\hat{W}|\vec{\sigma}\rangle = \underbrace{\sum_{j=1}^{\infty}\sigma_j\langle\varphi_j|\hat{h}|\varphi_j\rangle}_{\text{kinetic energy and external potential}} + \underbrace{\frac{1}{2}\sum_{i,j=1}^{\infty}\sigma_i\sigma_j\overbrace{\int d^4x\int d^4x'\,\frac{e^2\varphi_i^*(\vec{x})\varphi_j^*(\vec{x'})\varphi_i(\vec{x})\varphi_j(\vec{x'})}{4\pi\epsilon_0|\vec{r}-\vec{r'}|}}^{=\langle\varphi_i,\varphi_j|\hat{W}|\varphi_i,\varphi_j\rangle\quad\text{(Eq. 2.30)}}}_{\text{Hartree energy}}$$
$$\underbrace{-\frac{1}{2}\sum_{i,j=1}^{\infty}\sigma_i\sigma_j\overbrace{\int d^4x\int d^4x'\,\frac{e^2\varphi_i^*(\vec{x})\varphi_j^*(\vec{x'})\varphi_j(\vec{x})\varphi_i(\vec{x'})}{4\pi\epsilon_0|\vec{r}-\vec{r'}|}}^{=\langle\varphi_i,\varphi_j|\hat{W}|\varphi_j,\varphi_i\rangle\quad\text{(Eq. 2.30)}}}_{\text{exchange energy}} \tag{2.31}$$

The exchange term differs from the Hartree term by the sign and the order of the last two indices. $\hat{h}$ is the one-particle Hamiltonian, which describes the kinetic energy and the external potential imposed by the nuclei. $\hat{W}$ is the interaction term of the Hamiltonian.

The surprising fact of Eq. 2.31, respectively Eq. 2.29, is the appearance of two terms for the interaction. Therefore, let us try to give some physical meaning to the two contributions.

2.3.1 Hartree energy

The first interaction term in Eq. 2.29 is the so-called **Hartree energy**. The Hartree energy turns out to be the classical electrostatic interaction of the electron density.

$$\begin{aligned}E_H &= \frac{1}{2}\sum_{i,j=1}^{\infty}\sigma_i\sigma_j\int d^4x\int d^4x'\,\varphi_i^*(\vec{x})\varphi_j^*(\vec{x'})\frac{e^2}{4\pi\epsilon_0|\vec{r}-\vec{r'}|}\varphi_i(\vec{x})\varphi_j(\vec{x'})\\ &= \frac{1}{2}\int d^3r\int d^3r'\,\underbrace{\left[\sum_{i=1}^{\infty}\sigma_i\sum_{\sigma\in\{\uparrow,\downarrow\}}\varphi_i^*(\vec{x})\varphi_i(\vec{x})\right]}_{n(\vec{r})}\frac{e^2}{4\pi\epsilon_0|\vec{r}-\vec{r'}|}\underbrace{\left[\sum_{j=1}^{\infty}\sigma_j\sum_{\sigma'\in\{\uparrow,\downarrow\}}\varphi_j^*(\vec{x'})\varphi_j(\vec{x'})\right]}_{n(\vec{r'})}\end{aligned} \tag{2.32}$$

The sum over orbitals can be combined to the electron density Eq. 2.24. The occupations of a Slater determinant are either zero or one, so that the sum is limited to N-orbitals. Thus, w obtain the final expression for the Hartree energy expressed in terms of the electron density $\vec{n}(\vec{r})$

HARTREE ENERGY

$$E_H = \frac{1}{2}\int d^3r\int d^3r'\,\frac{e^2n(\vec{r})n(\vec{r'})}{4\pi\epsilon_0|\vec{r}-\vec{r'}|} \tag{2.33}$$

The Hartree energy corresponds to the electrostatic self energy[12] of a charge density $\rho(\vec{r}) = -en(\vec{r})$.

[12] The electrostatic expression is based on infinitesimal charges making up the charge density, so that the interaction

The **Hartree potential** is defined as functional derivative of the Hartree energy with respect to the electron density $v_H(\vec{r}) = \delta E_H[n]/\delta n(\vec{r})$, which results in

$$v_H(\vec{r}) = \int d^3r' \, \frac{e^2 n(\vec{r'})}{4\pi\epsilon_0 |\vec{r} - \vec{r'}|} \qquad \text{or as operator} \qquad \hat{V}_H = \int d^4x \, |\vec{x}\rangle v_H(\vec{r}) \langle\vec{x}| \tag{2.34}$$

2.3.2 Exchange energy

The Hartree energy is clearly not the correct electrostatic energy of an N-electron system, because it describes the interaction of N electrons with N electrons. Instead, each electron can only interact with $N-1$ other electrons. Thus, the Hartree term also includes, incorrectly, the interaction of each electron with itself. This so-called **self interaction** is subtracted by the so-called **exchange energy**, the second interaction term in Eq. 2.29

$$\begin{aligned} E_X &= -\frac{1}{2} \sum_{i,j=1}^{\infty} \sigma_i \sigma_j \int d^4x \int d^4x' \; \varphi_i^*(\vec{x}) \varphi_j^*(\vec{x'}) \frac{e^2}{4\pi\epsilon_0 |\vec{r} - \vec{r'}|} \varphi_j(\vec{x}) \varphi_i(\vec{x'}) \\ &= -\frac{1}{2} \int d^4x \int d^4x' \; \underbrace{\left[\sum_{i=1}^{\infty} \sigma_i \varphi_i(\vec{x'}) \varphi_i^*(\vec{x}) \right]}_{\rho^{(1)}(\vec{x'}, \vec{x})} \frac{e^2}{4\pi\epsilon_0 |\vec{r} - \vec{r'}|} \underbrace{\left[\sum_{j=1}^{\infty} \sigma_j \varphi_j(\vec{x}) \varphi_j^*(\vec{x'}) \right]}_{\rho^{(1)}(\vec{x}, \vec{x'})} \end{aligned} \tag{2.35}$$

With the one-particle-reduced density matrix $\hat{\rho}^{(1)}$ defined in Eq. 2.15[13], we arrive at the final expression for the exchange energy

EXCHANGE ENERGY

$$E_X = -\frac{1}{2} \int d^4x \int d^4x' \; \frac{e^2 \rho^{(1)}(\vec{x}, \vec{x'}) \rho^{(1)}(\vec{x'}, \vec{x})}{4\pi\epsilon_0 |\vec{r} - \vec{r'}|} \tag{2.36}$$

The **exchange potential** is defined as functional derivative of the exchange energy with respect to the one-particle-reduced density matrix $v_X(\vec{x}, \vec{x'}) = \delta E_X[\rho^{(1)}]/\delta\rho(\vec{x'}, \vec{x})$, which results in

$$v_X(\vec{x}, \vec{x'}) = -\frac{e^2 \rho^{(1)}(\vec{x}, \vec{x'})}{4\pi\epsilon_0 |\vec{r} - \vec{r'}|} \qquad \text{or as operator} \qquad \hat{V}_X = \int d^4x \int d^4x' \; |\vec{x}\rangle v_X(\vec{x}, \vec{x'}) \langle\vec{x'}| \tag{2.37}$$

Attraction vs. repulsion: It may be puzzling in the discussion of the exchange energy, that electrons tend arrange themselves preferably in "similar" orbitals despite the facts that (1) they stay away from each other due to the Pauli principle, and that (2) they repel each other via the Coulomb repulsion. The puzzle is resolved by noting that the repulsive features are captured by the Hartree energy, while the exchange energy compensates for the **self-interaction** of electrons that is included in the Hartree term. Because an electron does not interact with itself, this self interaction is removed again by the exchange energy. By considering changes that leave the Hartree term unaffected, we turn the focus on the attractive exchange term, which is responsible for the seemingly attractive behavior of electrons.

of the charges with themselves can be ignored. The contribution due to the finite charge of an electron is considered in the exchange term discussed below.

[13] The occupations f_n of a Slater determinant are equal to its occupation numbers σ_n.

2.3.3 Non-interacting energy

The non-interacting energy in Eq. 2.31 describes the kinetic energy and the potential energy in an external potential. Because its Hamiltonian $\hat{h}$ is a one-particle operator, it is conveniently expressed in terms of the one-particle-reduced density matrix as

$$E_{1P} \overset{\text{Eq. 2.31}}{=} \sum_{j=1}^{\infty} \sigma_j \langle \varphi_j | \hat{h} | \varphi_j \rangle = \text{Tr}[\hat{\rho}^{(1)} \hat{h}] \tag{2.38}$$

2.3.4 Total energy of a Slater determinant

The preceding sections show that the total energy of a Slater determinant can be expressed as **density-matrix functional**: the energy is a functional of the one-particle-reduced density matrix $\hat{\rho}^{(1)}$.

TOTAL ENERGY OF A SLATER DETERMINANT

The total energy of a Slater determinant $|\vec{\sigma}\rangle$ formed from orthonormal one-particle orbitals $|\varphi_j\rangle$ is

$$\langle \vec{\sigma} | \hat{h} + \hat{W} | \vec{\sigma} \rangle = \underbrace{\text{Tr}\left[\hat{\rho}^{(1)} \hat{h}\right]}_{E_{1P}} + \underbrace{\frac{1}{2} \int d^3r \int d^3r' \, \frac{e^2 n(\vec{r}) n(\vec{r'})}{4\pi\epsilon_0 |\vec{r} - \vec{r'}|}}_{E_H} \underbrace{- \frac{1}{2} \int d^4x \int d^4x' \, \frac{e^2 \rho^{(1)}(\vec{x}, \vec{x'}) \rho^{(1)}(\vec{x'}, \vec{x})}{4\pi\epsilon_0 |\vec{r} - \vec{r'}|}}_{E_X} \tag{2.39}$$

$\hat{h}$ is the one-particle Hamiltonian, which describes the kinetic energy and the external potential imposed by the nuclei.
The one-particle-reduced density matrix

$$\hat{\rho}^{(1)} \overset{\text{Eq. 2.15}}{=} \sum_{j=1}^{\infty} |\varphi_j\rangle f_j \langle \varphi_j| \tag{2.40}$$

can be expressed in terms of occupations f_j and natural orbitals $|\varphi_j\rangle$. For Slater determinants, the one-particle-reduced density matrix is idempotent, $\left(\hat{\rho}^{(1)}\right)^2 = \hat{\rho}^{(1)}$. In other words, the occupations for a Slater determinant are either zero or one, i.e. $f_j \in \{0, 1\}$ and they are equal to the occupation numbers σ_j.
The density is obtained from the one-particle-reduced density matrix as $n(\vec{r}) = \sum_{\sigma \in \{\uparrow, \downarrow\}} \rho^{(1)}(\vec{x}, \vec{x})$.

2.4 Exchange-correlation hole

2.4.1 Two-particle density and exchange-correlation hole

The first term of the interaction energy of a Slater determinant, the Hartree energy, is fairly easy to understand. The second term, the exchange energy, is, however, puzzling. Nevertheless, it can be expressed in intuitive manner in terms an **exchange hole**. Let me describe the underlying physics behind this term.

The notion of an exchange(-correlation) hole is not limited to the Hartree-Fock Theory. Let me therefore introduce this concept from a general point of view.

The **exchange** captures the effects described within the Hartree-Fock approximation, while the

terms beyond Hartree-Fock approximation are called **correlation**. Both effects together are called "exchange-and-correlation". You will often find the subscript "xc" for exchange-and-correlation and "X" for exchange only. Analogously, there is an exchange hole, a correlation hole[14] and the sum, the exchange-correlation hole.

Consider the distribution of electrons when one of the electrons is at a specific location and has a specific spin. I call this electron the spectator electron and denote its position with $\vec{r}_0$. If the system contains N electrons in total, there will only be $N-1$ other electrons. Thus, the spectator electron will not see the total density, but only the density of the $N-1$ other electrons. The difference between the total density and that of the other $N-1$ electrons is the exchange-correlation hole.

The interaction energy of a system of interacting electrons can be expressed rigorously by the **two-particle density** $n^{(2)}(\vec{r},\vec{r'})$. Like the electron density $n^{(1)}(\vec{r})$ describes the density of electrons at a given point in space, the two-particle density describes the density of (oriented) pairs of electrons[15], with one electron at $\vec{r}$ and the other one at $\vec{r'}$. The two-particle density is thus a density in six-dimensional space.

TWO-PARTICLE DENSITY

For a N-particle wave function $|\Phi\rangle$, the two-particle density is[a]

$$n^{(2)}(\vec{r},\vec{r'}) = \int d^4x_1 \cdots \int d^4x_N \left|\Phi(\vec{x}_1,\ldots,\vec{x}_N)\right|^2 \left(\sum_{\substack{i,j=1\\ i\neq j}}^{N} \delta(\vec{r}-\vec{r}_i)\delta(\vec{r'}-\vec{r}_j)\right) \tag{2.41}$$

The two-particle density is twice the density in the 6-dimensional coordinate space of electron pairs disregarding their orientation. This factor 2 originates from counting oriented pairs. The integral is $\int d^3r \int d^3r' n^{(2)}(\vec{r},\vec{r'}) = N(N-1)$.

For an N-particle state, the conditional density given by $\frac{n^{(2)}(\vec{r}_0,\vec{r})}{n^{(1)}(\vec{r}_0)}$ is the electron density of the remaining $N-1$ electrons at position $\vec{r'}$, as "seen" by an spectator electron at site $\vec{r}_0$.

[a] For a many-particle state having contributions with different particle numbers, the state is first decomposed into its N particle contributions as shown below:

$$n^{(2)}(\vec{r},\vec{r'}) = \left\langle \Phi \middle| \sum_{N=2}^{\infty} \int d^4x_1 \cdots \int d^4x_N \middle|\vec{x}_1,\ldots,\vec{x}_N\right\rangle \left(\sum_{\substack{i,j=1\\ i\neq j}}^{N} \delta(\vec{r}-\vec{r}_i)\delta(\vec{r'}-\vec{r}_j)\right) \left\langle \vec{x}_1,\ldots,\vec{x}_N \middle| \Phi \right\rangle$$

With the two-particle density $n^{(2)}(\vec{r},\vec{r'})$, the interaction energy can be written rigorously as

$$\begin{aligned} E_{int} &\overset{\text{def}}{=} \langle\Phi|\hat{W}|\Phi\rangle = \frac{1}{2}\int d^3r \int d^3r' \, \frac{e^2 n^{(2)}(\vec{r},\vec{r'})}{4\pi\epsilon_0|\vec{r}-\vec{r'}|} \\ &\overset{\text{Eq. 2.33}}{=} E_H + \overbrace{\int d^3r \, n^{(1)}(\vec{r}) \frac{1}{2}\int d^3r' \, \frac{e^2}{4\pi\epsilon_0|\vec{r}-\vec{r'}|} \underbrace{\left(\frac{n^{(2)}(\vec{r},\vec{r'})}{n^{(1)}(\vec{r})} - n^{(1)}(\vec{r'})\right)}_{\text{hole density } h_{xc}(\vec{r},\vec{r'})}}^{=:U_{xc}} \end{aligned} \tag{2.42}$$

while the Hartree energy can be expressed by the one-particle density $n^{(1)}(\vec{r})$ as

$$E_H \overset{\text{Eq. 2.33}}{=} \frac{1}{2}\int d^3r \int d^3r' \, \frac{e^2 n^{(1)}(\vec{r}) n^{(1)}(\vec{r'})}{4\pi\epsilon_0|\vec{r}-\vec{r'}|} \, . \tag{2.43}$$

[14] The correlation hole is not a hole in the literal sense, because it integrates to zero

[15] There are different definitions of the two-particle density, which differ by a factor 2. In our case, the two-particle density counts the pair $(1,2)$ and the pair $(2,1)$ as distinct. Thus, our two-particle density integrates up to twice the number of electron pairs, i.e. to $N(N-1)$. This definition is suitable for both, distinguishable and indistinguishable, particles. Other definitions normalize the two-particle density so that it integrates to the number of electron pairs, namely $N(N-1)/2$.

The symbol U_{xc} in Eq. 2.42 has been used to discriminate the "potential energy of exchange and correlation" U_{xc} from the "exchange and correlation energy" E_{xc}. The exchange and correlation energy (of DFT) has an additional kinetic-energy contribution, that describes the loss of kinetic energy while adapting the exchange correlation hole for a finite interaction. This kinetic energy contribution is only present in the correlation, but not for exchange.

HOLE DENSITY

The hole density $h_{xc}(\vec{r}_0, \vec{r'})$ for the spectator electron at site $\vec{r}_0$ is

$$h_{xc}(\vec{r}_0, \vec{r'}) \stackrel{\text{def}}{=} \frac{n^{(2)}(\vec{r}_0, \vec{r'})}{n^{(1)}(\vec{r}_0)} - n^{(1)}(\vec{r'}) \tag{2.44}$$

POTENTIAL ENERGY OF EXCHANGE AND CORRELATION

$$U_{xc} = \int d^3r \; n^{(1)}(\vec{r}) \; \underbrace{\frac{1}{2} \int d^3r' \; \frac{e^2 h_{xc}(\vec{r}, \vec{r'})}{4\pi\epsilon_0 |\vec{r} - \vec{r'}|}}_{\text{potential XC-energy per electron}} \tag{2.45}$$

It is as if each electron at $\vec{r}$ is surrounded by a positive charge density, namely $\frac{1}{2} e h(\vec{r}, \vec{r'})$. This positive charge density counteracts the Coulomb repulsion described by the Hartree energy.

The exchange-correlation hole of a real material, namely silicon, is shown in fig. 2.3.

What has been gained? Once the exchange and correlation hole is known, the interaction energy can be evaluated without any approximations. In order to know the exchange-correlation hole, one needs to solve the complete many-particle problem. However, already rather simple models for its shape are quite successful to estimate the exchange-correlation energy.

The successes of **Density-Functional Theory**(DFT) [33, 34], one of the most successful theories for quantitative electronic-structure calculations of real materials from first principles, rests on the successful modeling of the exchange-correlation hole.

2.4.2 Properties of the exchange-correlation hole

The most important features of the exchange correlation hole are the following

- **charge sum rule**: The integrated exchange-correlation hole corresponds exactly to one hole.

$$\int d^3r' \; h_{xc}(\vec{r}, \vec{r'}) = -1 \tag{2.46}$$

- **negativity:** The exchange correlation hole must not exceed the electron density

$$-n(\vec{r}) \leq h_{xc}(\vec{r}, \vec{r'}) \leq 0 \tag{2.47}$$

  The reason is that the density of the remaining $N-1$ electrons must not be negative.

- **nearsightedness:** The exchange correlation hole vanishes at large distances of $|\vec{r} - \vec{r'}|$. There is no proof and violations are not excluded.

Size of the exchange-correlation hole

The size of the exchange-correlation hole in a material is typically that of a chemical bond, that is, of an atomic distance. The size can be seen in fig. 2.3, which shows the exchange hole in silicon. The

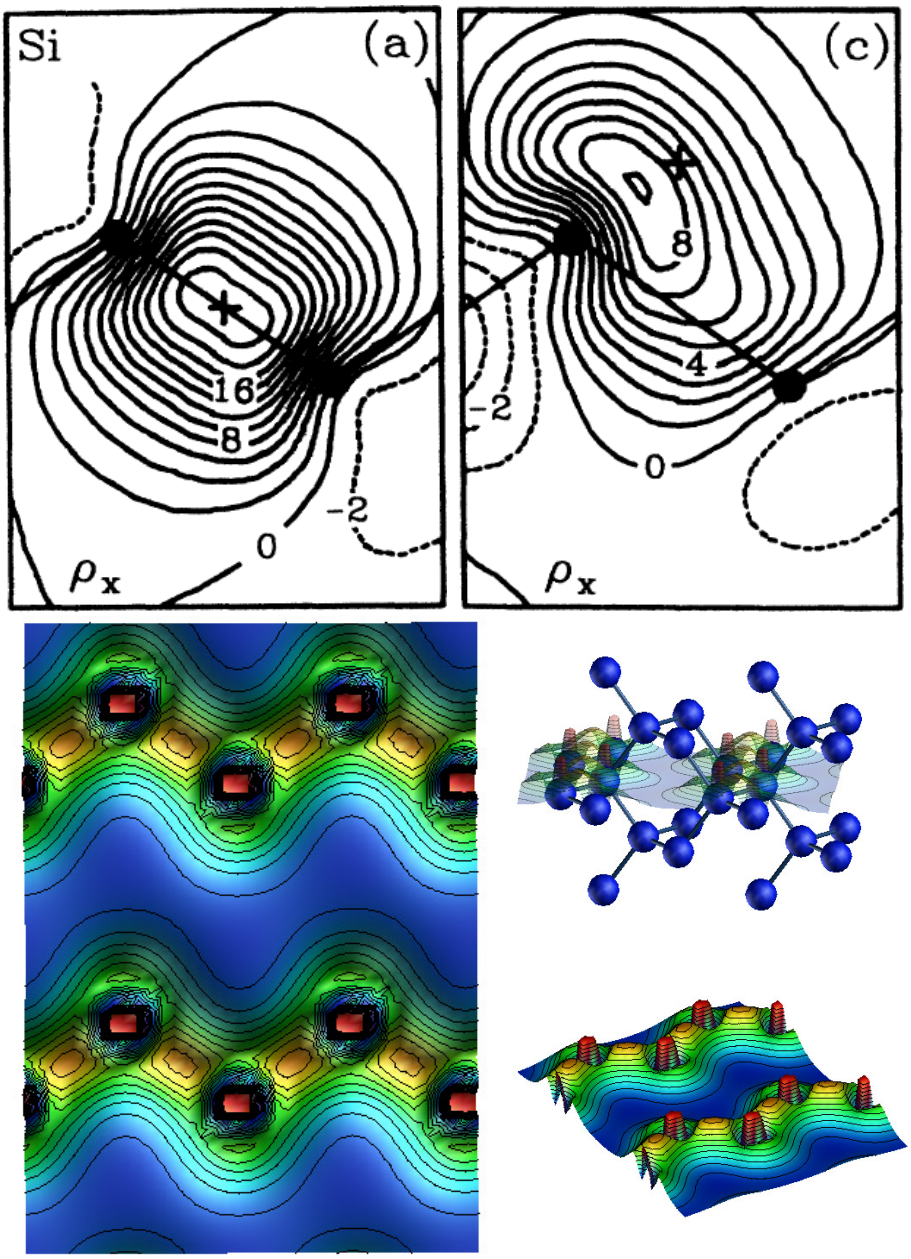


Fig. 2.3: Top: exchange hole in the 110 plane of silicon[32]. The cross indicates the position of the reference electron. In the bond, the exchange-correlation hole is centered on the reference electron, while in the tail region it is located off-center. Bottom: Valence charge density of silicon in the (110) plane. (With friendly permission by Mark Hybertsen)

size can be rationalized by the fact that a chemical bond typically has one electron per spin, which is the charge in the exchange-correlation hole according to the charge sum rule.

Far away from a molecule or a piece of material, the electron density is small. Hence, the exchange-correlation hole must be very extended to satisfy the charge sum rule. This is because the density of the $N-1$ other electrons can never be negative and thus, the hole density can never be larger in absolute value than the electron density, i.e. $n(\vec{r}) + h_{xc}(\vec{r}, \vec{r}_0) \geq 0$.

If the material nearest to the reference electron is an atom or a molecule, the reference electron "sees" a positive ion. Thus, the exchange-correlation hole is the difference between the atom or molecule and its singly positive cation. A rough estimate for this density is the density of the highest occupied natural orbital of that atom or molecule.

If the reference electron is far away from a material and the next material is a surface, the exchange correlation hole is located at the surface.

These considerations provide an intuitive understanding of the exchange correlation hole, but they also indicate that the shape of the exchange correlation hole can depend in a complicated manner on the environment of the reference electron.

A lot more is understood about the exchange-correlation hole. For further information on the properties of the exchange-correlation hole see, for example Burke[35]. Accurate calculations of the exchange-correlation hole have been performed by quantum Monte Carlo calculations[36].

2.5 Energetics and thermodynamics in the Hartree-Fock approximation

In this section, we explore the energetics in the Hartree-Fock approximation. In the previous section, we learned in Eq. 2.31 that the total energy of an interacting system can be expressed in terms of one-particle wave functions, if the wave function is a Slater determinant. Slater determinants are wave functions of non-interacting systems. The Hartree-Fock approximation attempts to describe an interacting system in terms of wave functions of non-interacting systems. The goal is to find that non-interacting system, which is suited best for that purpose.

Let me directly venture into the finite-temperature formalism. This will prepare for the later chapters, which rest on the finite-temperature description. The finite-temperature formalism using ensembles avoids a number of nagging conceptional problems related to degenerate ground states and symmetry breaking.

Let me start this section with an introduction to thermodynamics of quantum systems. For this lecture, it will be important that we find a common language for some fundamental concepts from thermodynamics.

2.5.1 Ensembles of quantum states

ENSEMBLE

The fundamental entity of statistical mechanics is the **ensemble** $\{(|\Phi_q\rangle, P_q)\}$. An ensemble is a set of many-particle wave functions $|\Phi_q\rangle$ with their probabilities P_q. Each many-particle wave function describes a possible state of the system. Its probability P_q describes the likelihood that the system is in this specific state $|\Phi_q\rangle$.
The wave functions of the ensemble are normalized. The probabilities are non-negative and add up to one.

$$\langle\Phi_q|\Phi_q\rangle = 1 \quad \text{and} \quad P_q \geq 0 \quad \text{and} \quad \sum_q P_q = 1 \,. \tag{2.48}$$

The many-particle wave functions $|\Phi_q\rangle$ are called the **micro states**. The ensemble itself is called the **macro state**. Note, that the terms "micro" and "macro" do **not** distinguish small and large systems in this context!

An ensemble is represented completely by its **von-Neumann density matrix** [37] (Eq. 6.1 of

ΦSX: Statistical Physics[38]).

$$\hat{\rho}^{vN} = \sum_q |\Phi_q\rangle P_q \langle\Phi_q| \tag{2.49}$$

The von-Neumann density matrix is (1) hermitean, (2) positive semi-definite, and (3) has a unit trace, i.e.

$$\hat{\rho}^{vN} = \left(\hat{\rho}^{vN}\right)^\dagger \qquad \text{and} \qquad \forall_{|\Psi\rangle}\ \langle\Psi|\hat{\rho}^{vN}|\Psi\rangle \geq 0 \qquad \text{and} \qquad \mathrm{Tr}\left[\hat{\rho}^{vN}\right] = 1\ . \tag{2.50}$$

The von-Neumann density matrix contains the complete physical information on the system. The expectation value of any operator $\hat{A}$ is obtained from

$$\langle A\rangle = \sum_q P_q \langle\Phi_q|\hat{A}|\Phi_q\rangle = \mathrm{Tr}\left[\hat{\rho}^{vN}\hat{A}\right]\ . \tag{2.51}$$

Two sets $\{P_q, |\Phi_q\rangle\}$ of probabilities and micro-states with the same von-Neumann density matrix are equivalent, even though their micro states and probabilities may differ. They describe the same ensemble. They are equivalent, because there is no physical observable that could differentiate between them.[16] This leaves some freedom in choosing the probabilities P_q and micro states $|\Phi_q\rangle$.

A special choice for the micro states for a given ensemble are the eigenstates of the von-Neumann density matrix, so that $\hat{\rho}^{vN}|\Phi_q\rangle = |\Phi_q\rangle P_q$. The resulting micro states are orthonormal. The corresponding probabilities, which are now the eigenvalues of the von-Neumann density matrix, are also specific for this choice. Each ensemble may therefore also be represented by a set of orthonormal micro states and their probabilities[17], that satisfy

$$\langle\Phi_q|\Phi_{q'}\rangle = \delta_{q,q'} \quad \text{and} \quad P_q \geq 0 \quad \text{and} \quad \sum_q P_q = 1\ . \tag{2.52}$$

2.5.2 von-Neumann entropy

Thermodynamics in the sense of equilibrium statistical physics is rooted in the concept of **thermal equilibrium**. Thermal equilibrium lives from the basic assumption that all states are in principle accessible and equally likely. This means that a system, which is left alone for a sufficiently long time, will end up in a maximally unbiased ensemble. This connection between statistics and dynamics is the **ergodic theorem**.[39] (See also [40])

In order to discuss bias, we need to quantify the amount of uncertainty about the state of a system. This measure of uncertainty is the entropy. The entropy of a quantum system is the **von-Neumann entropy** S [37] (Eq. 6.8 of ΦSX: Statistical Physics[38]).

$$S\left(\hat{\rho}^{vN}\right) = -k_B \mathrm{Tr}\left[\hat{\rho}^{vN} \ln\left(\hat{\rho}^{vN}\right)\right] \tag{2.53}$$

k_B is the **Boltzmann constant**, which connects the temperature scale with that of energies.

If the micro states $|\Phi_q\rangle$ are chosen as the eigenstates of the von-Neumann density matrix, they are orthonormal, which allows to express the von-Neumann entropy in terms of the corresponding probabilities P_q as

$$S\Big(\overbrace{\sum_q |\Phi_q\rangle P_q \langle\Phi_q|}^{\hat{\rho}^{vN}}\Big) \overset{\text{Eq. 2.53}}{=} -k_B \sum_q P_q \ln(P_q) \qquad \text{only, if } \langle\Phi_q|\Phi_{q'}\rangle = \delta_{q,q'} \tag{2.54}$$

This is, up to a factor, equivalent to **Shannon's entropy** [41] obtained from information theory. (See section 1.4 of ΦSX: Statistical Physics[38]).

[16] Two ensembles with the same von-Neumann density matrix yield the same expectation values for any observable,

[17] One possible strategy is to first define the ensemble in terms of general non-orthonormal microstates. From these, one constructs the von-Neumann density matrix, which is then diagonalized to obtain a new set of orthogonal micro-states and their probabilites. The main advantage of this special choice is that, as shown below, the entropy can be evaluated from the new probabilities alone.

2.5.3 Thermal ensembles and maximum-entropy principle

Finding the most unbiased ensemble is the essence of the **maximum-entropy principle**. [42, 43]. (See also Section 1.5 of ΦSX: Statistical Physics[38]). In order to determine the most unbiased ensemble, we maximize the **von-Neumann entropy** under constraints, that describe the state of our knowledge about the system. The ensemble that maximimizes the entropy under these constraints defines thermal equilibrium and is called a **thermal ensemble**. It is the most unbiased ensemble considering everything that we know about the system.[18]

Given the thermal energy expectation value $\bar{E}$ and the thermal expectation value of the particle number $\bar{N}$, the maximum-entropy principle produces the **grand-canonical ensemble** with an appropriate temperature $T(\bar{E},\bar{N})$ and chemical potential $\mu(\bar{E},\bar{N})$.

The maximum entropy $S_{max}(\bar{E},\bar{N})$ for a system with a known thermal expectation value $\bar{E}$ for the energy and $\bar{N}$ for the particle number[19] , is obtained by a **constrained search** over all ensembles, respectively all allowed[20] von-Neumann density matrices, that are consistent with our knowledge of $\bar{E}$ and $\bar{N}$.[21]

$$\begin{aligned} S_{max}(\bar{E},\bar{N}) &= \max_{\hat{\rho}^{vN}} \operatorname*{stat}_{T,\mu,\lambda} \Bigg\{ \underbrace{\overbrace{-k_B \mathrm{Tr}\left[\hat{\rho}^{vN} \ln\left(\hat{\rho}^{vN}\right)\right]}^{S(\hat{\rho}^{vN})}}_{\text{entropy}} - \frac{1}{T} \underbrace{\left(\overbrace{\mathrm{Tr}\left[\hat{\rho}^{vN}(\hat{h}+\hat{W})\right]}^{E(\hat{\rho}^{vN})} - \bar{E} \right)}_{\text{energy constraint}} \\ &\qquad + \frac{\mu}{T} \underbrace{\left(\overbrace{\mathrm{Tr}\left[\hat{\rho}^{vN}\hat{N}\right]}^{N(\hat{\rho}^{vN})} - \bar{N} \right)}_{\text{particle number constraint}} + \lambda \underbrace{\left(\mathrm{Tr}\left[\hat{\rho}^{vN}\right] - 1 \right)}_{\text{norm constraint}} \Bigg\} \\ &\overset{\text{Eq. 2.56}}{=} \operatorname*{stat}_{T,\mu} \left[-\frac{1}{T} \left\{ \Omega_{T,\mu} - \bar{E} + \mu\bar{N} \right\} \right] \end{aligned} \tag{2.55}$$

The grand potential $\Omega_{T,\mu}$ is defined in Eq. 2.56 below. The constraints are enforced using the method of Lagrange multipliers. The Lagrange multipliers $\frac{1}{T}$ and $\frac{\mu}{T}$ are expressed by the temperature T and chemical potential μ.

The grand potential $\Omega_{T,\mu}$ in Eq. 2.55 is obtained as an ensemble minimum:

$$\Omega_{T,\mu} = \min_{\hat{\rho}^{vN}} \operatorname*{stat}_{\lambda} \left\{ \overbrace{\mathrm{Tr}[\hat{\rho}^{vN}(\hat{h}+\hat{W})]}^{E(\hat{\rho}^{vN})} \overbrace{+k_B T\ \mathrm{Tr}\left[\hat{\rho}^{vN}\ln\left(\hat{\rho}^{vN}\right)\right]}^{-TS(\hat{\rho}^{vN})} \overbrace{-\mu \mathrm{Tr}[\hat{\rho}^{vN}\hat{N}]}^{-\mu N(\hat{\rho}^{vN})} + \lambda \overbrace{\left(\mathrm{Tr}\left[\hat{\rho}^{vN}\right]-1\right)}^{\text{norm constraint}} \right\} \tag{2.56}$$

The minimum condition for the grand potential $\Omega_{T,\mu}$ yields the **thermal von-Neumann density matrix** [22] , which describes a system in thermal equilibrium with a **heat bath** and a **particle reservoir**.

$$\hat{\rho}^{vN}_{T,\mu} \overset{\text{Eq. 2.56}}{=} \frac{1}{Z_{T,\mu}} \mathrm{e}^{-\frac{1}{k_B T}\left(\hat{h}+\hat{W}-\mu\hat{N}\right)} \tag{2.57}$$

where the **partition function** is

$$Z_{T,\mu} \overset{\text{def}}{=} \mathrm{Tr}\left[\mathrm{e}^{-\frac{1}{k_B T}\left(\hat{h}+\hat{W}-\mu\hat{N}\right)}\right] \tag{2.58}$$

[18] The reader may notice that I adhere to the subjective interpretation of probabilities: The probabilities describe the state of our mind, rather than a physical property of the system. A system does not care about what we know about it.

[19] The particle-number operator can be defined in terms of a complete set of Slater determinants $|\vec{\sigma}\rangle$ as $\hat{N} = \sum_{\vec{\sigma}} |\vec{\sigma}\rangle \left(\sum_{\vec{\sigma}} \sigma_n\right) \langle\vec{\sigma}|$

[20] A von-Neumann density matrix is hermitean, positive semi-definite and has a unit trace, as stated in Eq. 2.50.

[21] With "stat", I denote the stationary condition, which is analogous to the maximum and minimum conditions, but also allows for saddle points.

[22] The term "thermal" refers to thermal equilibrium in general and is not limited to a specific choice of reservoirs.

The ensemble for the parameters $(\bar{E}, \bar{N})$ as opposed to (T, μ) is then obtained from the stationary principle

$$S(\bar{E}, \bar{N}) = -\operatorname*{stat}_{T,\mu} \frac{1}{T}\Big(\Omega_{T,\mu} - \bar{E} + \mu\bar{N}\Big) \tag{2.59}$$

which provides the intrinsic variables (T, μ) for a specific set of extrinsic variables $(\bar{E}, \bar{N})$. The ensemble, respectively the von-Neumann density matrix, is then obtained via Eq. 2.57 as $\rho^{vN}_{T(\bar{E},\bar{N}),\mu(\bar{E},\bar{N})}$.

As a side remark: The thermal (optimized) grand potential can be obtained from the partition function as[23]

$$\Omega_{T,\mu} \overset{\text{Eq. 2.60}}{=} -k_B T \ln\big(Z_{T,\mu}\big) \ . \tag{2.61}$$

In terms of (orthonormal) eigenstates of the Hamiltonian and particle number, the thermal von-Neumann density matrix Eq. 2.57 can be expressed in terms of Boltzmann factors.

$$\hat{\rho}^{vN}_{T,\mu} \overset{\text{Eq. 2.57}}{=} \sum_q \Big|\Phi_q\Big\rangle \underbrace{\frac{\mathrm{e}^{-\frac{1}{k_B T}\left(E_q - \mu N_q\right)}}{\sum_{q'} \mathrm{e}^{-\frac{1}{k_B T}\left(E_{q'} - \mu N_{q'}\right)}}}_{P_q(T,\mu)} \Big\langle\Phi_q\Big|$$
$$\text{with } (\hat{h} + \hat{W})|\Phi_q\rangle = |\Phi_q\rangle E_q \text{ and } \hat{N}|\Phi_q\rangle = |\Phi_q\rangle N_q \tag{2.62}$$

So much to the reminder of the Statistical Mechanics of quantum systems.

2.5.4 Ensembles of Slater determinants

For weak interactions, we may obtain approximate solutions by limiting the wave functions to those of non-interacting systems, namely Slater determinants.

In a world, where we can only evaluate expectation values of single Slater determinants, the natural choice for an approximation is to limit the search for the maximum entropy to ensembles of Slater determinants. Let me investigate this approximation and, furthermore, let me only consider ensembles of Slater determinants that are constructed from one common one-particle basis.[24]

Let me work out the energy for this subclass of ensembles. The ensemble is characterized by Slater determinants $|\vec{\sigma}\rangle$ and their probabilities $P_{\vec{\sigma}}$. A Slater determinant is characterized by $\vec{\sigma}$, the sequence of its occupation numbers. The Slater determinants are in a basis of arbitrary orthonormal one-particle orbitals $|\varphi_n\rangle$. The energy of the ensemble is the weighted sum of the energies Eq. 2.31

[23] The thermal (optimized) density matrix is inserted into the defining equation Eq. 2.56

$$\begin{aligned}
\Omega_{T,\mu} &\overset{\text{Eq. 2.56}}{=} \mathrm{Tr}\Big[\hat{\rho}^{vN}_{T,\mu}(\hat{h} + \hat{W})\Big] + k_B T\ \mathrm{Tr}\Big[\hat{\rho}^{vN}_{T,\mu} \ln\Big(\hat{\rho}^{vN}_{T,\mu}\Big)\Big] - \mu \mathrm{Tr}\Big[\hat{\rho}^{vN}_{T,\mu}\hat{N}\Big] \\
&\overset{\text{Eq. 2.57}}{=} \mathrm{Tr}\Big[\hat{\rho}^{vN}_{T,\mu}\Big(\hat{h} + \hat{W} + k_B T \overbrace{\Big(-\ln[Z_{T,\mu}] - \frac{1}{k_B T}(\hat{h} + \hat{W} - \mu\hat{N})\Big)}^{\ln\left(\hat{\rho}^{vN}_{T,\mu}\right)} - \mu\hat{N}\Big)\Big] = -k_B T \ln\big(Z_{T,\mu}\big) \underbrace{\mathrm{Tr}\Big[\hat{\rho}^{vN}_{T,\mu}\Big]}_{=1} \\
&= \quad -k_B T \ln\big(Z_{T,\mu}\big)
\end{aligned} \tag{2.60}$$

[24] This additional limitation to Slater determinants from a common one-particle basis is taken for convenience. It might be interesting to explore the consequences of lifting this limitation.

of the individual Slater determinants

$$
\begin{aligned}
E &= \sum_{\vec{\sigma}} P_{\vec{\sigma}} \langle \vec{\sigma} | \hat{h} + \hat{W} | \vec{\sigma} \rangle \\
&\overset{\text{Eq. 2.31}}{=} \underbrace{\sum_{n=1}^{\infty} \overbrace{\sum_{\vec{\sigma}} P_{\vec{\sigma}} \sigma_n}^{f_n} \langle \varphi_n | \hat{h} | \varphi_n \rangle}_{\text{kinetic energy and external potential}} + \underbrace{\frac{1}{2} \sum_{m,n=1}^{\infty} \overbrace{\sum_{\vec{\sigma}} P_{\vec{\sigma}} \sigma_m \sigma_n}^{\langle \sigma_m \sigma_n \rangle} \left(\overbrace{\langle \varphi_m \varphi_n | \hat{W} | \varphi_m \varphi_n \rangle}^{\rightsquigarrow \text{Hartree}} - \overbrace{\langle \varphi_m \varphi_n | \hat{W} | \varphi_n \varphi_m \rangle}^{\rightsquigarrow \text{exchange}} \right)}_{\text{interaction energy}} \\
&\overset{\text{Eq. 2.39}}{=} \underbrace{\underbrace{\overbrace{\sum_{n=1}^{\infty} f_n \langle \varphi_n | \hat{h} | \varphi_n \rangle}^{\mathrm{Tr}\left[\hat{\rho}^{(1)} \hat{h}\right]}}_{\text{one-particle energy}} + \underbrace{\overbrace{\frac{1}{2} \sum_{m,n=1}^{\infty} f_m f_n \left(\langle \varphi_m \varphi_n | \hat{W} | \varphi_m \varphi_n \rangle - \langle \varphi_m \varphi_n | \hat{W} | \varphi_n \varphi_m \rangle \right)}^{\frac{1}{2} \int d^3r \int d^3r' \frac{e^2 n(\vec{r}) n(\vec{r}')}{4\pi\epsilon_0 |\vec{r} - \vec{r}'|}} - \underbrace{\frac{1}{2} \int d^4x \int d^4x' \frac{e^2 \rho^{(1)}(\vec{x}, \vec{x}') \rho^{(1)}(\vec{x}', \vec{x})}{4\pi\epsilon_0 |\vec{r} - \vec{r}'|}}_{\text{exchange energy}}}_{\text{Hartree energy}}}_{\text{mean-field energy}} \\
&\quad + \underbrace{\frac{1}{2} \sum_{m,n=1; m \neq n}^{\infty} \Big(\langle \sigma_m \sigma_n \rangle - \langle \sigma_m \rangle \langle \sigma_n \rangle \Big) \Big(\langle \varphi_m \varphi_n | \hat{W} | \varphi_m \varphi_n \rangle - \langle \varphi_m \varphi_n | \hat{W} | \varphi_n \varphi_m \rangle \Big)}_{\text{energy due to correlated occupation-number fluctuations}}
\end{aligned}
\tag{2.63}
$$

I introduced the notation $\langle \sigma_m \sigma_n \rangle \overset{\text{def}}{=} \sum_{\vec{\sigma}} P_{\vec{\sigma}} \sigma_m \sigma_n$ and $\langle \sigma_n \rangle \overset{\text{def}}{=} \sum_{\vec{\sigma}} P_{\vec{\sigma}} \sigma_n = f_n$.[25] The one-particle orbitals $|\varphi_n\rangle$ are the natural orbitals[26] of the ensemble. The f_n are the occupations. The electron density $n(\vec{r}) = \sum_n f_n \sum_{\sigma \in \{\uparrow,\downarrow\}} \varphi_n^*(\vec{x}) \varphi_n(\vec{x})$ and the one-particle-reduced density matrix $\rho^{(1)}(\vec{x}, \vec{x}') = \sum_n \langle \vec{x} | \varphi_n \rangle f_n \langle \varphi_n | \vec{x}' \rangle$ are those of the ensemble.

The first term, marked **mean-field energy**, has the same form as the total energy of a single Slater determinant given in Eq. 2.39 on p. 60. It differs only by the fact that the occupations f_n of the ensemble are fractional, while the occupations σ_n of a single Slater determinants are either zero or one.

The second term, which is due to **correlated occupation-number fluctuations**,

$$
\sum_{\vec{\sigma}} P_{\vec{\sigma}} \sigma_m \sigma_n - \Big(\sum_{\vec{\sigma}} P_{\vec{\sigma}} \sigma_m \Big) \Big(\sum_{\vec{\sigma}} P_{\vec{\sigma}} \sigma_n \Big) = \underbrace{\langle \sigma_m \sigma_n \rangle - \langle \sigma_m \rangle \langle \sigma_n \rangle}_{\left\langle \left(\sigma_m - f_m\right) \left(\sigma_n - f_n\right) \right\rangle} , \tag{2.64}
$$

is easily overlooked, because it magically drops out of many expressions. There is no such term in the energy Eq. 2.39 of a single Slater determinant: Slater determinants do not have fractional occupations and, therefore, they do do not exhibit occupation-number fluctuations.

2.5.5 Thermal ensembles of Slater determinants

For an ensemble of Slater determinants $|\vec{\sigma}\rangle$ with probabilities $P_{\vec{\sigma}}$, one can proceed along two distinct routes:

- In the so-called **Thermal Single-Determinant Approximation (TSDA)** [44], one proceeds as described above and arrives at Eq. 2.63: The maximum-entropy search is limited to ensembles of Slater determinants constructed from a common one-particle basisset. The energy is the ensemble average of the energies $\langle \vec{\sigma} | \hat{h} + \hat{W} | \vec{\sigma} \rangle$, Eq. 2.31 and Eq. 2.39, of the Slater determinants.

[25] I am introducing the notation $\langle \sigma_n \rangle$ and $\langle \sigma_m \sigma_n \rangle$, because it reminds on average value and variance. It will be used only in the present context.

[26] The natural orbitals are the eigenstates of the one-particle-reduced density matrix of the ensemble.

Let me denote the one-particle-reduced density matrix of the Slater determinant $|\vec{\sigma}\rangle$ by $\hat{\rho}^{(1)}_{\vec{\sigma}}$. Eq. 2.63 can be written in the form

$$E = \sum_{\vec{\sigma}} P_{\vec{\sigma}} \underbrace{E^{HF}\left[\hat{\rho}^{(1)}_{\vec{\sigma}}\right]}_{\langle\vec{\sigma}|\hat{h}+\hat{W}|\vec{\sigma}\rangle} \tag{2.65}$$

where[27]

$$E^{HF}[\hat{\rho}^{(1)}] \stackrel{\text{def}}{=} \mathrm{Tr}\left[\hat{\rho}^{(1)}\hat{h}\right] + \frac{1}{2}\int d^3r \int d^3r' \, \frac{e^2 n(\vec{r}) n(\vec{r'})}{4\pi\epsilon_0|\vec{r}-\vec{r'}|} - \frac{1}{2}\int d^4x \int d^4x' \, \frac{e^2\rho^{(1)}(\vec{x},\vec{x'})\rho^{(1)}(\vec{x'},\vec{x})}{4\pi\epsilon_0|\vec{r}-\vec{r'}|} \tag{2.66}$$

- Less accurate[28], but much easier is to handle, is the **mean-field approximation** called the **Thermal Hartree-Fock Approximation (THFA)** [45]. Here, one restricts the search for the maximum-entropy state to ensembles of Slater determinants and, furthermore, to those with **vanishing correlated occupation-number fluctuations**, that is, with $\langle\sigma_m\sigma_n\rangle = \langle\sigma_m\rangle\langle\sigma_n\rangle$ for[29] $m \neq n$.

  [30]

  This energy amounts to

$$E = E^{HF}\Big[\underbrace{\sum_{\vec{\sigma}} P_{\vec{\sigma}}\hat{\rho}^{(1)}_{\vec{\sigma}}}_{\hat{\rho}^{(1)}}\Big] \tag{2.67}$$

  with E^{HF} from Eq. 2.66. Eq. 2.67 is a **mean-field approximation**. The averaged (mean) one-particle-reduced density matrix is simply that of the ensemble. The reader is encouraged to compare this expression Eq. 2.67 to the one Eq. 2.65 for the TSDA. In the TSDA the energy is averaged, while in the THFA, the argument of the energy functional is averaged.

  The mean-field approximation exists in many different contexts. Therefore, it is important to always specify the quantity that becomes the mean field. In this case, the mean field is the one-particle-reduced density matrix averaged over the Slater determinants, respectively the averaged potential. In the Thermal Hartree-Fock Approximation (THF) all electrons experience the same mean potential, while in the Thermal Single-Determinant Approximation (TSDA), each Slater determinant experiences its own potential.

  The mean-field approximation can be described in two different ways:

  - ensembles with correlated occupation-number fluctuations are excluded from the constrained search for the maximum-entropy ensemble.
  - all Slater determinants in the ensemble experience the same effective potential.

  Both statements are equivalent. They are different points of view on the same procedure.

A comparison of Thermal Hartree-Fock theory and the Thermal Single-Determinant Approximation is done by Gu and Hirata[46, 47].

[27] The electron density is given by the one-particle-reduced density matrix as $n(\vec{r}) = \sum_{\sigma\in\{\uparrow,\downarrow\}} \rho^{(1)}(\vec{r},\sigma,\vec{r},\sigma)$.

[28] It is less accurate, because the search of the maximum-entropy principle is restricted by an additional constraint as compared to the TSDA.

[29] The diagonal terms $\langle\sigma_n^2\rangle - \langle\sigma_n\rangle$ are not restricted. They do not contribute to the energy, because the Coulomb integrals in Eq. 2.63 vanish. The requirement that the diagonal terms vanish as well would limit the search to a single Slater determinant rather than ensembles of them.

[30] Editor: check this: This implies that the probabilities factorize into a product of probabilities for the individual one-particle orbitals, i.e. $P_{\vec{\sigma}} = \prod_{n=1}^{\infty} p_n(\sigma_n)$.

2.5.6 Boltzmann entropy

In the mean-field approximation Eq. 2.67, the energy depends only on the one-particle-reduced density matrix. Much of the information contained in the von-Neumann density matrix does not enter the mean-field energy.

In order to determine the maximum-entropy ensemble, we need the von-Neumann entropy. However, the von-Neumann entropy Eq. 2.53 depends on the full von-Neumann density matrix, which is not available from only the one-particle-reduced density matrix. How do we then arrive at the equilibrium ensemble?

The best we can do[31] is to choose the most unbiased ensemble for a specific one-particle-reduced density matrix $\hat{\rho}^{(1)}$. The resulting maximum entropy is what I call the **Boltzmann entropy**[32] $S^B[\hat{\rho}^{(1)}]$. The Boltzmann entropy is discussed in detail in the appendix G.1 on p. 603.

The Boltzmann entropy $S^B[\hat{\rho}^{(1)}]$ is the maximum von-Neumann entropy Eq. 2.53 for ensembles with a specified one-particle-reduced density matrix.[33]

$$S^B[\hat{\rho}^{(1)}] \stackrel{\text{def}}{=} \max_{\hat{\rho}^{vN}} \operatorname*{stat}_{\boldsymbol{B}} \left\{ -k_B \mathrm{Tr}\left[\hat{\rho}^{vN} \ln\left(\hat{\rho}^{vN}\right)\right] - \sum_{\alpha,\beta} k_B B_{\alpha,\beta} \Big(\mathrm{Tr}\left[\hat{\rho}^{vN} \hat{c}_\alpha^\dagger \hat{c}_\beta\right] - \underbrace{\langle \pi_\beta | \hat{\rho}^{(1)} | \pi_\alpha \rangle}_{\rho^{(1)}_{\beta,\alpha}} \Big) \right\} \tag{2.68}$$

The search for the maximum is performed over all allowed[34] von-Neumann density matrices $\hat{\rho}^{vN}$. The matrix $k_B\boldsymbol{B}$ is a Lagrange multiplier and $\mathrm{Tr}\left[\hat{\rho}^{vN} \hat{c}_\alpha^\dagger \hat{c}_\beta\right]$ is the expectation value for the one-particle-reduced density matrix element $\rho^{(1)}_{\beta,\alpha}$ of the corresponding ensemble. The expectation value is expressed in terms of creation and annihilation operators $\hat{c}_\alpha^\dagger$ and $\hat{c}_\alpha$, that will be introduced only later. For the time being, it is sufficient to know that the one-particle-reduced density matrix can be obtained as expectation value of an operator in Fock space. The $\langle \pi_\alpha |$ are the projector functions for the orbitals $|\chi_\alpha\rangle$, that define the one-particle basis for the creation and annihilation operators.

For fermions, the Boltzmann entropy[35] is

$$S^B\left[\hat{\rho}^{(1)}\right] \stackrel{\text{Eq. } G.31}{=} -k_B \mathrm{Tr}\left[\hat{\rho}^{(1)} \ln\left(\hat{\rho}^{(1)}\right) + \left(\hat{1} - \hat{\rho}^{(1)}\right) \ln\left(\hat{1} - \hat{\rho}^{(1)}\right)\right] \tag{2.69}$$

The fermionic Boltzmann entropy is known better in the form expressed in terms of occupations f_n.

$$S^B[\{f_n\}] = -k_B \sum_n \Big[f_n \ln(f_n) + (1 - f_n) \ln(1 - f_n) \Big] \tag{2.70}$$

where the occupations f_n are the eigenvalues of the one-particle-reduced density matrix.

Interestingly, the maximum-entropy principle defining the Boltzmann entropy Eq. 2.68 establishes a unique mapping of the one-particle-reduced density matrix to the corresponding ensemble, respectively, to the von-Neumann density matrix

$$\hat{\rho}^{(1)} \qquad \stackrel{\text{Eq. 2.68}}{\longrightarrow} \qquad \hat{\rho}^{vN}\left[\hat{\rho}^{(1)}\right] \stackrel{\text{Eq. } G.32}{=} \sum_{\vec{\sigma}} |\vec{\sigma}\rangle \underbrace{\left[\prod_{n=1}^{\infty} f_n^{\sigma_n} (1 - f_n)^{1-\sigma_n}\right]}_{\vec{P}_{\vec{\sigma}}} \langle \vec{\sigma}| \tag{2.71}$$

where the Slater determinants $|\vec{\sigma}\rangle$ are constructed from the natural orbitals $|\varphi_n\rangle$, the eigenstates of the one-particle-reduced density matrix.

[31] This is not an additional approximation. The minimization over all von-Neumann density matrices is only broken up in two steps: first we determin the optimum von-Neumann density matrix for each one-particle-reduced density matrix. Second, we minimize over all one-particle-reduced density matrices.

[32] The name "Boltzmann entropy" for this object is not common.

[33] See e.g. Eq. **??** of ΦSX:Introduction to Solid-State Theory[1] or Eq. 8.26 of ΦSX: Statistical Physics.[38].

[34] Allowed, in this context, are positive semidefinite, hermitean operators with unit trace in the fermionic Fock space.

[35] See e.g. Eq. **??** of ΦSX:Introduction to Solid-State Theory[1] or Eq. 8.26 of ΦSX: Statistical Physics.[38].

The fact that the probabilities $P_{\vec{\sigma}}$ in Eq. 2.71 are products of probabilities for each orbital shows already that the occupation-number fluctuations between different natural orbitals are uncorrelated. A more explicit proof is provided in appendix G.1.2 on p. 606.

The absence of correlated occupation-number fluctuations establishes that the equilibrium ensemble satisfies the conditions of the thermal Hartree-Fock approximation (THFA) despite using an extended search space.

2.5.7 Grand potential in the thermal Hartree-Fock approximation

The physical state (ensemble) and its grand potential is determined by a minimization in Eq. 2.56.

$$\Omega_{T,\mu} \overset{\text{Eq. 2.56}}{=} \min_{\hat{\rho}^{vN}} \left\{ \overbrace{\mathrm{Tr}[\hat{\rho}^{vN}(\hat{h}+\hat{W})]}^{E(\hat{\rho}^{vN})} \overbrace{+k_B T\ \mathrm{Tr}\left[\hat{\rho}^{vN} \ln\left(\hat{\rho}^{vN}\right)\right]}^{-TS^{vN}(\hat{\rho}^{vN})} \overbrace{-\mu \mathrm{Tr}[\hat{\rho}^{vN}\hat{N}]}^{-\mu N(\hat{\rho}^{vN})} \right\} \tag{2.72}$$

In the thermal Hartree-Fock approximation (THFA), this search is limited (1) to ensembles of Slater-determinants and, further, (2) to such ensembles without correlated occupation-number fluctuations Eq. 2.64.[36] This so-called "constrained minimization" defines a the grand potential $\Omega_{T,\mu}^{THF}$ of the thermal Hartree-Fock approximation.

In Eq. 2.63, I have shown that energy and particle number for this limited set of ensembles are determined already by the one-particle-reduced density matrix. The entropy term $-TS^{vN}$, however, poses a problem, because it still depends explicitly on the von-Neumann density matrix.

For each one-particle-reduced density matrix, there are many ensembles with different entropies S^{vN}. The maximum entropy for a given one-particle-reduced density matrix defines the Boltzmann entropy via Eq. 2.68. Its value is given in Eq. 2.69.

Thus, the minimum grand potential of the thermal Hartree-Fock approximation can be obtained by a minimization over one-particle-reduced density matrices.[37] In other words, the grand potential of the thermal Hartree-Fock approximation is determined by a minimum principle of a **density-matrix functional**.[38]

[36] The restriction to ensembles of Slater determinants without correlated occupation-number fluctuations implies

$$\sum_{m,n} P_{\vec{\sigma}} \sigma_m \sigma_n - \Big(\sum_m P_{\vec{\sigma}} \sigma_m\Big)\Big(\sum_n P_{\vec{\sigma}} \sigma_n\Big) = 0 \tag{2.73}$$

(see discussion of Eq. 2.63) I am still looking for an expression to constrain von-Neumann density matrix to ensembles of Slater determinants.

[37] The minimization over von-Neumann density matrices $\hat{\rho}^{vN}$ is divided into two steps: First one minimizes the grand potential over all von-Neumann density matrices with a specific one-particle-reduced density matrix $\hat{\rho}^{(1)}$. This replaces the von-Neumann entropy $S^{vN}[\hat{\rho}^{vN}]$ in the grand potential by the Boltzmann entropy $S^{B}[\hat{\rho}^{(1)}]$. What is left, is the minimization over the one-particle-reduced density matrices.

[38] An early review article on density matrix functional theory is from McWeeny[48].

GRAND POTENTIAL OF THE THERMAL HARTREE-FOCK APPROXIMATION (THFA)

The grand potential $\Omega_{T,\mu}^{THFA}$ of the THFA is the minimum of a functional of the one-particle-reduced density matrix $\hat{\rho}^{(1)}$. The electron density $n(\vec{r}) = \sum_{\sigma\in\{\uparrow,\downarrow\}} \langle\vec{x}|\rho^{(1)}|\vec{x}\rangle$ and $\rho^{(1)}(\vec{x},\vec{x'}) = \langle\vec{x}|\rho^{(1)}|\vec{x'}\rangle$ are functionals of the one-particle-reduced density matrix.
The grand potential is

$$\begin{aligned}\Omega_{T,\mu}^{THF} = \min_{\hat{\rho}^{(1)}}\Bigg\{ & \underbrace{\mathrm{Tr}\left[\hat{\rho}^{(1)}\hat{h}\right]}_{E_{1P}} \\ & + \underbrace{\frac{1}{2}\int d^3r \int d^3r' \, \frac{e^2 n(\vec{r}) n(\vec{r'})}{4\pi\epsilon_0|\vec{r}-\vec{r'}|}}_{\text{Hartree energy } E_H} \underbrace{-\frac{1}{2}\int d^4x \int d^4x' \, \frac{e^2\rho^{(1)}(\vec{x},\vec{x'})\rho^{(1)}(\vec{x'},\vec{x})}{4\pi\epsilon_0|\vec{r}-\vec{r'}|}}_{\text{exchange energy } E_X} \\ & + \underbrace{k_B T \, \mathrm{Tr}\left[\hat{\rho}^{(1)} \ln\left(\hat{\rho}^{(1)}\right) + \left(\hat{1}-\hat{\rho}^{(1)}\right)\ln\left(\hat{1}-\hat{\rho}^{(1)}\right)\right]}_{-TS^B \quad \text{heat bath}} \underbrace{-\mu \mathrm{Tr}\left[\hat{\rho}^{(1)}\right]}_{\text{particle-reservoir}} \Bigg\} \end{aligned} \tag{2.74}$$

The minimum obeys the N-representability constraint $0 \leq f_n \leq 1$ because of the special choice of the entropy term. This will be confirmed by the final result.

In practice, the functional is expressed in terms of natural orbitals and occupations rather than directly by the one-particle-reduced density matrix operator $\hat{\rho}^{(1)} = \sum_n |\varphi_n\rangle f_n \langle\varphi_n|$.

The density matrix functional of the thermal Hartree-Fock approximation is a model for other functional theories, such as density-functional theory (DFT) or reduced-density-matrix-functional theory (rDMFT). In contrast to the THFA, the latter are, in principle, exact theories. They differ from the THFA by the exchange energy, which is replaced by an exchange-correlation functional $E_{xc}[n]$ in DFT and a exchange functional $U_{xc}[\hat{\rho}^{(1)}]$ in rDMFT. To be specific, the grand potential of density-functional theory is given in Eq. 13.6 on p. 398 with the exchange-correlation functional $E_{xc,T}[n]$ defined in Eq. 13.8. Also in these exact theories, approximations are done in practice to make problem solving managable. But, the approximation are done on a well defined quantity, which allows a systematic improvement to reach the desired balance between feasibility and accuracy.

2.5.8 Selfconsistency

Let me determine the minimum of the grand potential in Eq. 2.74. I will use the variational calculus, which I find convenient to determine the derivatives with respect to more complex objects such as functions and operators.[39] The equilibrium condition is the requirement that the first variation of the functional with respect to the one-particle-reduced density matrix vanishes. It is analogous to the requirement that the gradient vanishes at an extremum of a function.

For the following discussion, I need a name for the density-matrix functional inside the curly brackets of Eq. 2.74. Let me call it $\mathcal{F}_{T,\mu}[\hat{\rho}^{(1)}]$. Thus, Eq. 2.74 is written as $\Omega_{T,\mu}^{HF} = \min_{\hat{\rho}^{(1)}} \mathcal{F}_{T,\mu}[\hat{\rho}^{(1)}]$. The first variation $\delta\mathcal{F}_{T,\mu}$ of $\mathcal{F}_{T,\mu}$ with respect to the one-particle-reduced density matrix $\hat{\rho}^{(1)}$ is obtained via a Taylor expansion.

$$\mathcal{F}_{T,\mu}[\hat{\rho}^{(1)} + \delta\hat{\rho}^{(1)}] = \mathcal{F}_{T,\mu}[\hat{\rho}^{(1)}] + \underbrace{\sum_{\alpha,\beta} \delta\rho_{\alpha,\beta}^{(1)} \frac{\delta\mathcal{F}_{T,\mu}}{\delta\rho_{\alpha,\beta}^{(1)}}}_{\delta\mathcal{F}_{T,\mu}} + O\left([\delta\hat{\rho}^{(1)}]^2\right) \tag{2.75}$$

At the minimum of $\mathcal{F}_{T,\mu}$, the first variation $\delta\mathcal{F}_{T,\mu}$ vanishes. To minimize $\mathcal{F}_{T,\mu}[\hat{\rho}^{(1)}]$, let me therefore

[39] The first variation of a function $f(\vec{x})$ with respect to an argument $\vec{x}$ is the first-order term of $f(\vec{x}+\delta\vec{x}) - f(x) = \delta f + O(\delta\vec{x}^2)$. It can be expressed in terms of the derivative $\delta f = \delta\vec{x}\vec{\nabla} f$

identify the zeros of the first variation.

$$
\begin{aligned}
0 \quad &\stackrel{!}{=} \quad \delta\mathcal{F}_{T,\mu} \\
&\stackrel{\text{Eq. 2.74}}{=} \delta\Big\{ \mathrm{Tr}\Big[\hat{\rho}^{(1)}\hat{h}\Big] + \frac{1}{2}\int d^4x \int d^4x' \, \frac{e^2\langle\vec{x}|\hat{\rho}^{(1)}|\vec{x}\rangle\langle\vec{x}'|\hat{\rho}^{(1)}|\vec{x}'\rangle}{4\pi\epsilon_0|\vec{r}-\vec{r}'|} - \frac{1}{2}\int d^4x \int d^4x' \, \frac{e^2\langle\vec{x}|\hat{\rho}^{(1)}|\vec{x}'\rangle\langle\vec{x}'|\hat{\rho}^{(1)}|\vec{x}\rangle}{4\pi\epsilon_0|\vec{r}-\vec{r}'|} \\
&\qquad\qquad + k_BT\,\mathrm{Tr}\Big[\hat{\rho}^{(1)}\ln\Big(\hat{\rho}^{(1)}\Big) + \Big(\hat{1}-\hat{\rho}^{(1)}\Big)\ln\Big(\hat{1}-\hat{\rho}^{(1)}\Big)\Big] - \mu\mathrm{Tr}\big[\hat{\rho}^{(1)}\big]\Big\} \\
&= \quad \mathrm{Tr}\Big\{\delta\hat{\rho}^{(1)}\Big[\hat{h} + \underbrace{\int d^4x|\vec{x}\rangle\Big(\int d^4x' \, \frac{e^2\langle\vec{x}'|\hat{\rho}^{(1)}|\vec{x}'\rangle}{4\pi\epsilon_0|\vec{r}-\vec{r}'|}\Big)\langle\vec{x}|}_{\hat{V}_H} - \underbrace{\int d^4x \int d^4x' \, |\vec{x}\rangle\Big(\frac{e^2\langle\vec{x}|\hat{\rho}^{(1)}|\vec{x}'\rangle}{4\pi\epsilon_0|\vec{r}-\vec{r}'|}\Big)\langle\vec{x}'|}_{\hat{V}_X} \\
&\qquad\qquad + k_BT\Big[\ln\Big(\hat{\rho}^{(1)}\Big) + \hat{1} - \ln\Big(\hat{1}-\hat{\rho}^{(1)}\Big) - \hat{1}\Big] - \mu\hat{1}\Big]\Big\} \\
&= \quad \mathrm{Tr}\Big\{\delta\hat{\rho}^{(1)}\Big[\underbrace{\hat{h}+\hat{V}_H+\hat{V}_X}_{\text{Fock operator } \hat{F}} + k_BT\ln\Big(\hat{\rho}^{(1)}\Big(\hat{1}-\hat{\rho}^{(1)}\Big)^{-1}\Big) - \mu\hat{1}\Big]\Big\}
\end{aligned}
\tag{2.76}
$$

The Hartree potential V_H and the exchange potential $\hat{V}_X$ have been defined in Eq. 2.34 and Eq. 2.37, respectively. The Fock operator $\hat{F}[\hat{\rho}^{(1)}] = \hat{h} + \hat{V}_H[\hat{\rho}^{(1)}] + \hat{V}_X[\hat{\rho}^{(1)}]$ is that obtained from the current one-particle-reduced density matrix and electron density. Remember, that the Fock operator, unlike "normal" operators, is itself a functional of the one-particle-reduced density matrix.

FOCK OPERATOR

$$
\begin{aligned}
\hat{F} &\stackrel{\text{def}}{=} \hat{h} + \hat{V}_H + \hat{V}_X \\
&= \hat{h} + \overbrace{\int d^4x \, \big|\vec{x}\big\rangle \underbrace{\int d^3r' \, \frac{e^2 n(\vec{r}')}{4\pi\epsilon_0|\vec{r}-\vec{r}'|}}_{v_H(\vec{r})} \big\langle\vec{x}\big|}^{\hat{V}_H} \overbrace{- \int d^4x \int d^4x' \, \big|\vec{x}\big\rangle \underbrace{\frac{e^2\rho^{(1)}(\vec{x},\vec{x}')}{4\pi\epsilon_0|\vec{r}-\vec{r}'|}}_{-v_X(\vec{x},\vec{x}')} \big\langle\vec{x}'\big|}^{\hat{V}_X}
\end{aligned}
\tag{2.77}
$$

The Fock operator is a one-particle operator, which depends on density and one-particle-reduced density matrix.

The first variation of $\mathcal{F}_T$ vanishes only when the operator in brackets in Eq. 2.76 is the zero-operator. This yields the following operator identity, which can be resolved for the one-particle-reduced density matrix

$$
\begin{aligned}
\hat{0} &= \hat{h} + \hat{V}_H + \hat{V}_X + k_BT\ln\Big(\hat{\rho}^{(1)}\Big(\hat{1}-\hat{\rho}^{(1)}\Big)^{-1}\Big) - \mu\hat{1} \\
\Rightarrow \qquad \hat{\rho}^{(1)}_{T,\mu} &= \Big[\hat{1} + \mathrm{e}^{\frac{1}{k_BT}\left(\hat{h}+\hat{V}_H+\hat{V}_X-\mu\hat{1}\right)}\Big]^{-1}
\end{aligned}
\tag{2.78}
$$

The result is the Fermi distribution evaluated for the Fock operator. To make this more evident, let me represent the one-particle-reduced density matrix in an eigenbasis $\{|\varphi_n\rangle\}$ of the Fock operator,

$$
\Big(\hat{h} + \hat{V}_H + \hat{V}_X\Big)|\varphi_n\rangle = |\varphi_n\rangle\epsilon_n \, , \tag{2.79}
$$

which yields the one-particle-reduced density matrix in THFA as

$$
\hat{\rho}^{(1)}_{T,\mu} \stackrel{\text{Eq. 2.78}}{=} \sum_n |\varphi_n\rangle \underbrace{f_{T,\mu}(\epsilon_n)}_{\frac{1}{1+e^{\beta(\epsilon_n-\mu)}}} \langle\varphi_n| \tag{2.80}
$$

where $f_{T,\mu}(\epsilon) = \left(1 + \mathrm{e}^{\frac{1}{k_B T}(\epsilon-\mu)}\right)^{-1}$ is the Fermi function. This one-particle-reduced density matrix Eq. 2.78 is hermitian and N-representable, i.e. $0 \leq f_n \leq 1$.

The one-particle-reduced density matrix $\hat{\rho}^{(1)}_{T,\mu}$ in Eq. 2.78 cannot be calculated directly, because the Fock operator, respectively $\hat{V}_H + \hat{V}_X$, depends itself on the one-particle-reduced density matrix.

SELF-CONSISTENT EQUATION FOR THERMAL HARTREE FOCK

Thus, the two equations

$$\hat{\rho}^{(1)}_{T,\mu}\big[\hat{F}\big] \overset{\text{Eq. 2.78}}{=} \left[\hat{1} + \mathrm{e}^{\frac{1}{k_B T}\left(\hat{F}-\mu\hat{1}\right)}\right]^{-1} \qquad \text{and} \qquad \hat{F}[\hat{\rho}^{(1)}_{T,\mu}] = \hat{h} + \hat{V}_H[\hat{\rho}^{(1)}_{T,\mu}] + \hat{V}_X[\hat{\rho}^{(1)}_{T,\mu}] \tag{2.81}$$

need to be solved simultaneously, i.e. self-consistently.
In practice, one makes an initial guess for the Fock operator and diagonalizes it. This yields one-particle wave functions $|\varphi_n\rangle$ and energies ϵ_n. These are used to set up the one-particle-reduced density matrix $\hat{\rho}^{(1)} = \sum_n |\varphi_n\rangle f_{T,\mu}(\epsilon_n)\langle\varphi_n|$ using occupations given by the Fermi distribution $f_{T,\mu}(\epsilon) = [1 + \mathrm{e}^{\frac{1}{k_B T}(\epsilon-\mu)}]^{-1}$. An improved Fock operator is calculated from this one-particle-reduced density matrix. This cycle is iterated until the quantities do not change any more.

2.5.9 Thermal ensemble in the THFA (optional)

The minimum principle in Eq. 2.74 specifies the one-particle-reduced density matrix $\hat{\rho}^{(1)}_{T,\mu}$. To avoid the limitation to predictions for one-particle-at-a-time observables, we need to know also the corresponding ensemble, respectively its von-Neumann density matrix.

In the THFA, the von-Neumann density matrix is implicitly specified via the maximum-entropy principle employed to obtain the Boltzmann entropy Eq. 2.69. The ensemble of many-particle states is that, which maximizes the entropy for the specified one-particle-reduced density matrix, and which is given in Eq. 2.71. The von-Neumann density matrix of the THFA is thus obtained by inserting Eq. 2.80 into Eq. 2.71 as shown in appendix G.1.2 on p. 604.

The thermal von-Neumann density matrix in the THFA is

$$\begin{aligned}
\hat{\rho}^{vN,THFA}_{T,\mu} &= \hat{\rho}^{vN}[\hat{\rho}^{(1)}_{T,\mu}] \\
&\overset{\text{Eq. 2.71}}{=} \sum_{\vec{\sigma}} |\vec{\sigma}\rangle \left[\prod_{n=1}^{\infty} \Big(f_{T,\mu}(\epsilon_n)\Big)^{\sigma_n} \Big(1 - f_{T,\mu}(\epsilon_n)\Big)^{1-\sigma_n}\right] \langle\vec{\sigma}| \\
&= \frac{\sum_{\vec{\sigma}} |\vec{\sigma}\rangle \mathrm{e}^{-\frac{1}{k_B T}\sum_n \sigma_n(\epsilon_n-\mu)} \langle\vec{\sigma}|}{\sum_{\vec{\sigma}} \mathrm{e}^{-\frac{1}{k_B T}\sum_n \sigma_n(\epsilon_n-\mu)}} = \frac{\mathrm{e}^{-\beta(\hat{h}+\hat{V}_H+\hat{V}_X-\mu\hat{N})}}{\mathrm{Tr}\big[\mathrm{e}^{-\beta(\hat{h}+\hat{V}_H+\hat{V}_X-\mu\hat{N})}\big]}
\end{aligned} \tag{2.82}$$

In the last equation, I used the Fock operator $\hat{h} + \hat{V}_H + \hat{V}_X$ as a one-particle-at-a-time operator in Fock space.

The corresponding probabilities of the Slater determinants $|\vec{\sigma}\rangle$ are

$$P^{THFA}_{T,\mu,\vec{\sigma}} = \frac{1}{Z_{T,\mu}} \mathrm{e}^{-\beta\sum_n \sigma_n(\epsilon_n-\mu)} = \frac{1}{Z_{T,\mu}} \mathrm{e}^{-\beta\langle\vec{\sigma}|\hat{F}-\mu\hat{N}|\vec{\sigma}\rangle} \tag{2.83}$$

where $Z_{T,\mu}$ is the partition function, which normalizes the probability distribution, and ϵ_n are the eigenvalues of the self-consistent Fock operator $\hat{F} = \hat{h} + \hat{V}_X + \hat{V}_H$. It is understood, that the Slater determinants are formed from the eigenstates of the Fock operator.

As already mentioned while discussing the Boltzmann entropy in section 2.5.6 above, the occupation-number fluctuations in the resulting ensemble are uncorrelated, i.e. $\langle\sigma_m\sigma_n\rangle - \langle\sigma_m\rangle\langle\sigma_n\rangle = 0$ for $m \neq n$, so that the contribution of correlated occupation-number fluctuations to the energy of the ensemble

vanishes. [40]

2.5.10 Misconceptions

There is some confusion between the interacting Hamiltonian

$$\hat{H} = \hat{h} + \hat{W} \tag{2.85}$$

and the Fock-operator

$$\hat{F}[\hat{\rho}^{(1)}] = \frac{\delta E^{HF}}{\delta \hat{\rho}^{(1)}} = \hat{h} + \hat{V}_H + \hat{V}_X \ . \tag{2.86}$$

which is an operator in the one-particle Hilbert space.

To complete the confusion, there is a valid approximation *–albeit not necessarily a good one–* of the many-particle Hamiltonian involving the Fock operator, treating the latter as one-particle-at-a-time operator in Fock space. Namely,

$$\hat{H} \approx \hat{1}\ \mathrm{Tr}\Big[\hat{\rho}^{vN,THF}_{T,\mu}\Big(\underbrace{\hat{h} + \hat{W} - \big(\hat{h} + \hat{V}_H + \hat{V}_X\big)}_{\hat{W}-\hat{V}_H-\hat{V}_X}\Big)\Big] + \hat{h} + \hat{V}_H + \hat{V}_X \tag{2.87}$$

where $\hat{\rho}^{vN,THF}_{T,\mu}$ is the von-Neumann density matrix Eq. 2.82 of the Thermal Hartree-Fock approximation.

Sometimes, the Fock operator is also called the Hartree-Fock Hamiltonian, which I consider a misnomer. Let me *"vaccinate"* the reader with a few facts against these misunderstandings.

Energy: The energy E differs in a fundamental way from the expectation value of the Fock operator $\hat{F}$.

$$E = \mathrm{Tr}\Big[\hat{\rho}^{vN}\Big(\hat{h} + \hat{W}\Big)\Big] \neq \mathrm{Tr}\Big[\hat{\rho}^{vN}\underbrace{\Big(\hat{h} + \hat{V}_H[\hat{\rho}^{(1)}] + \hat{V}_X[\hat{\rho}^{(1)}]\Big)}_{\text{Fock operator}}\Big] \tag{2.88}$$

The energy is different, even if the Fock operator is obtained from the same ensemble $\hat{\rho}^{vN} \to \hat{\rho}^{(1)} \to \hat{V}_H + \hat{V}_X \to \hat{F}$. Instead, in the thermal Hartree-Fock approximation THFA, we can use a variant of the Galitski-Migdal-Koltun sum rule Eq. 8.36 to calculate the energy, which, however, introduces some factors one-half.

$$E^{THFA} \overset{\text{Eq. 2.74}}{=} \mathrm{Tr}\Big[\hat{\rho}^{vN}_{T,\mu}\Big(\hat{h} + \frac{1}{2}\hat{V}_H + \frac{1}{2}\hat{V}_X\Big)\Big] \tag{2.89}$$

This shows, that the energy is fundamentally different from the expectation value of the Fock operator. Using the identity anyway is a misunderstanding, not an approximation.

[40] Occupation-number fluctuations in the thermal ensemble of a non-interacting system are uncorrelated.

$$\begin{aligned}\langle\sigma_m\sigma_n\rangle_{T,\mu} &= \sum_{\vec{\sigma}} \underbrace{\frac{\mathrm{e}^{-\beta\sum_j \sigma_j(\epsilon_j-\mu)}}{\sum_{\vec{\sigma}'}\mathrm{e}^{-\beta\sum_j \sigma'_j(\epsilon_j-\mu)}}}_{=P_{\vec{\sigma}}}\sigma_m\sigma_n = \frac{\sum_{\vec{\sigma}}\sigma_m\sigma_n\prod_j \mathrm{e}^{-\beta\sigma_j(\epsilon_j-\mu)}}{\sum_{\vec{\sigma}'}\prod_j \mathrm{e}^{-\beta\sigma'_j(\epsilon_j-\mu)}} \\ &\overset{m\neq n}{=} \frac{\sum_{\sigma_m}\sigma_m \mathrm{e}^{-\beta\sigma_m(\epsilon_m-\mu)}}{\sum_{\sigma_m}\mathrm{e}^{-\beta\sigma_m(\epsilon_j-\mu)}}\frac{\sum_{\sigma_n}\sigma_n \mathrm{e}^{-\beta\sigma_n(\epsilon_n-\mu)}}{\sum_{\sigma_n}\mathrm{e}^{-\beta\sigma_n(\epsilon_j-\mu)}} = \underbrace{\langle\sigma_m\rangle}_{f_m}\underbrace{\langle\sigma_n\rangle}_{f_n} \qquad \text{for } m\neq n\end{aligned} \tag{2.84}$$

Density matrix: In contrast, the thermal von-Neumann density matrix Eq. 2.82 of the Thermal Hartree-Fock Approximation is given by the Fock operator, as opposed to the full Hamiltonian. Remember, that the Fock operator is normally a one-particle operator in the one-particle Hilbert space, while it is used here as a one-particle-at-a-time operator in the Fock space.

$$\hat{\rho}^{\nu N,\mathrm{THFA}}_{T,\mu} \overset{\text{Eq. 2.82}}{=} \frac{\mathrm{e}^{-\beta(\hat{h}+\hat{V}_H+\hat{V}_X-\mu\hat{N})}}{\mathrm{Tr}\left[\mathrm{e}^{-\beta(\hat{h}+\hat{V}_H+\hat{V}_X-\mu\hat{N})}\right]} \neq \frac{\mathrm{e}^{-\beta(\hat{h}+\hat{W}-\mu\hat{N})}}{\mathrm{Tr}\left[\mathrm{e}^{-\beta(\hat{h}+\hat{W}-\mu\hat{N})}\right]} \overset{\text{Eq. 2.57}}{=} \hat{\rho}^{\nu N}_{T,\mu} \tag{2.90}$$

The left-hand side is a valid approximation of the right-hand side, namely the thermal Hartree-Fock approximation. Often, it even is a fairly good approximation.

Why is the replacement in this case reasonable, but not for the energy? The reason is that the maximum-entropy ensemble, i.e. the von-Neumann density matrix, is determined by the gradient of the grand potential and not by its value, nor by the value of the energy.

Expectation values: Often, one extracts thermal expectation values as derivatives of the grand potential in the **extended Hamiltonian** technique. In the extended Hamiltonian technique, the physical Hamiltonian is augmented by an additional term $\gamma\hat{A}$, namely the observable $\hat{A}$ scaled by a coupling constant γ. The expectation value is then obtained as derivative of the grand potential with respect to the coupling constant. Editor: The naming extended or augmented Hamiltonian is not uniform and also used for other things. Is there a generally accepted term?

The relation can be shown as follows:

$$\begin{aligned}
\langle A\rangle_{T,\mu} &= \mathrm{Tr}\left[\hat{A}\,\hat{\rho}^{\nu N}_{T,\mu}\right] = \mathrm{Tr}\left[\hat{A}\,\underbrace{\left.\frac{\mathrm{e}^{-\beta(\hat{H}+\gamma\hat{A}-\mu\hat{N})}}{\mathrm{Tr}\left[\mathrm{e}^{-\beta(\hat{H}+\gamma\hat{A}-\mu\hat{N})}\right]}\right|_{\gamma=0}}_{\hat{\rho}^{\nu N}_{T,\mu}}\right] = \left.\frac{\mathrm{Tr}\left[\overbrace{\hat{A}\,\mathrm{e}^{-\beta(\hat{H}+\gamma\hat{A}-\mu\hat{N})}}^{-k_BT\partial_\gamma \mathrm{e}^{-\beta(\hat{H}+\gamma\hat{A}-\mu\hat{N})}}\right]}{\mathrm{Tr}\left[\mathrm{e}^{-\beta(\hat{H}+\gamma\hat{A}-\mu\hat{N})}\right]}\right|_{\gamma=0} \\
&\overset{\partial\hat{H}/\partial\gamma=0}{=} \left.\frac{\partial}{\partial\gamma}\right|_{\gamma=0} \underbrace{\left[-k_BT\ln\mathrm{Tr}\left(\mathrm{e}^{-\beta(\hat{H}+\gamma\hat{A}-\mu\hat{N})}\right)\right]}_{\Omega_{T,\mu,\gamma}} = \left.\frac{\partial}{\partial\gamma}\right|_{\gamma=0}\Omega_{T,\mu,\gamma}
\end{aligned} \tag{2.91}$$

Similarly[41] , one can derive from Eq. 2.74 the identity for the expectation value in the thermal Hartree-Fock approximation.

$$\langle A\rangle^{THF}_{T,\mu} = \left.\frac{\partial}{\partial_\gamma}\right|_{\gamma=0}\Omega^{THF}_{T,\mu,\gamma} \tag{2.93}$$

[41] The expectation value of a one-particle-at-a-time operator $\hat{A}$ is obtained from the extended grand potential in the THF approximation as follows. Caution: I am using the same symbol $\Omega^{THF}_{T,\mu,\gamma}$ and $\Omega^{THF}_{T,\mu,\gamma}[\hat{\rho}^{(1)}]$ for the grand potential after and before the minimization.

$$\begin{aligned}
\Omega^{THF}_{T,\mu,\gamma}[\hat{\rho}^{(1)}] &\overset{\text{Eq. 2.74}}{=} \underbrace{\mathrm{Tr}\left[\hat{\rho}^{(1)}(\hat{h}+\gamma\hat{A})\right]}_{E_{1P}} + \underbrace{\frac{1}{2}\int d^3r\int d^3r'\,\frac{e^2n(\vec{r})n(\vec{r}')}{4\pi\epsilon_0|\vec{r}-\vec{r}'|}}_{\text{Hartree energy } E_H} \underbrace{-\frac{1}{2}\int d^4x\int d^4x'\,\frac{e^2\rho^{(1)}(\vec{x},\vec{x}')\rho^{(1)}(\vec{x}',\vec{x})}{4\pi\epsilon_0|\vec{r}-\vec{r}'|}}_{\text{exchange energy } E_X} \\
&+ \underbrace{k_BT\,\mathrm{Tr}\left[\hat{\rho}^{(1)}\ln\left(\hat{\rho}^{(1)}\right)+\left(\hat{1}-\hat{\rho}^{(1)}\right)\ln\left(\hat{1}-\hat{\rho}^{(1)}\right)\right]}_{-TS^B\quad\text{heat bath}} \underbrace{-\mu\mathrm{Tr}\left[\hat{\rho}^{(1)}\right]}_{\text{particle-reservoir}} \\
\Omega^{THF}_{T,\mu,\gamma} &= \min_{\hat{\rho}^{(1)}}\Omega^{THF}_{T,\mu,\gamma}[\hat{\rho}^{(1)}] = \Omega^{THF}_{T,\mu,\gamma}[\hat{\rho}^{(1)}_{T,\mu,\gamma}] \\
\left.\frac{\partial\Omega^{THF}_{T,\mu,\gamma}}{\partial\gamma}\right|_{\gamma=0} &= \left.\frac{d}{d\gamma}\right|_{\gamma=0}\Omega^{THF}_{T,\mu,\gamma}[\hat{\rho}^{(1)}_{T,\mu,\gamma}] = \underbrace{\left.\frac{\partial\Omega^{THF}_{T,\mu,\gamma}[\hat{\rho}^{(1)}]}{\partial\gamma}\right|_{\hat{\rho}^{(1)}=\hat{\rho}^{(1)}_{T,\mu,0}}}_{\mathrm{Tr}[\hat{\rho}^{(1)}_{T,\mu,0}\hat{A}]} + \mathrm{Tr}\left[\underbrace{\left.\frac{\delta\Omega^{THF}_{T,\mu,0}[\hat{\rho}^{(1)}]}{\delta\hat{\rho}^{(1)}}\right|_{\hat{\rho}^{(1)}_{T,\mu,0}}}_{=0}\left.\frac{d\hat{\rho}^{(1)}_{T,\mu,\gamma}}{d\gamma}\right|_{\gamma=0}\right] \\
&= \mathrm{Tr}[\rho^{(1)}_{T,\mu,0}\hat{A}] = \langle A\rangle_{T,\mu}
\end{aligned} \tag{2.92}$$

$\rho^{(1)}_{T,\mu,\gamma=0}$ is the minimizer of the grand potential.

for an augmented Hamiltonian $\hat{h}(\gamma) = \hat{h} + \gamma\hat{A}$, if $\hat{A}$ is a one-particle operator.[42]

A common misconception is to express the grand potential of the thermal Hartree-Fock approximation by the partition sum of the Fock operator (treated as one-particle-at-a-time operator). We need to live with the inequalities[43]

$$\Omega^{THF}_{T,\mu,\gamma} \neq -k_B T \ln \mathrm{Tr}\left[\mathrm{e}^{-\beta(\hat{F}_{T,\mu,\gamma}-\mu\hat{1})}\right] \tag{2.95}$$

respectively

$$Z^{THF}_{T,\mu,\gamma} \neq \mathrm{Tr}\left[\mathrm{e}^{-\beta(\hat{F}_{T,\mu,\gamma}-\mu\hat{1})}\right] . \tag{2.96}$$

Energies of Slater determinants: The Galitski-Migdal-Koltun sum rule Eq. 8.36 allows one to express the energy with the help of the Fock operator. The Fock operator depends on the state, and it is essential to use the correct Fock operator for the problem at hand.

While it is a poor habit[44] to describe the Hartree and exchange energies as expectation values such as $E_H = \frac{1}{2}\langle\vec{\sigma}|\hat{V}_H|\vec{\sigma}\rangle$, let me nevertheless do it in this section for the sake of the "vaccination".

We may calculate the energy expectation value for each Slater determinant using the Hartree and exchange energy from that Slater determinant, namely $\hat{V}_{H,\vec{\sigma}}$ and $\hat{V}_{X,\vec{\sigma}}$.

$$E_{\vec{\sigma}} = \langle\vec{\sigma}|\hat{h} + \hat{W}|\vec{\sigma}\rangle \overset{\text{Eq. 2.39}}{=} \langle\vec{\sigma}|\underbrace{\hat{h} + \frac{1}{2}\hat{V}_{H,\vec{\sigma}} + \frac{1}{2}\hat{V}_{X,\vec{\sigma}}}_{\frac{1}{2}\left(\hat{h}+\hat{F}\right)}|\vec{\sigma}\rangle \tag{2.97}$$

There are no correlated occupation-number fluctuations in the expectation value of a single Slater determinant.

However, when the Hartree and exchange potentials of the ensemble are used, namely $\hat{V}_H^{\mathrm{THFA}} = \sum_{\vec{\sigma}} P_{\vec{\sigma}}^{\mathrm{THFA}}\hat{V}_{H,\vec{\sigma}}$ and $\hat{V}_X^{\mathrm{THFA}} = \sum_{\vec{\sigma}} P_{\vec{\sigma}}^{\mathrm{THFA}}\hat{V}_{X,\vec{\sigma}}$, the correlated occupation-number fluctuations are no more negligible, so that

$$E_{\vec{\sigma}} \neq \langle\vec{\sigma}|\hat{h} + \frac{1}{2}\hat{V}_H^{THFA} + \frac{1}{2}\hat{V}_X^{THFA}|\vec{\sigma}\rangle \tag{2.98}$$

What is missing can be expressed in terms of correlated occupation-number fluctuations as shown in Eq. 2.63.

When we add up the total energy of the thermal ensemble of the thermal Hartree-Fock approximation, the correlated occupation-number fluctuations miraculously drop out.

$$\sum_{\vec{\sigma}} P_{\vec{\sigma}}^{\mathrm{THFA}}\langle\vec{\sigma}|\hat{h} + \hat{W}|\vec{\sigma}\rangle = \sum_{\vec{\sigma}} P_{\vec{\sigma}}^{\mathrm{THFA}}\langle\vec{\sigma}|\hat{h} + \frac{1}{2}\hat{V}_H^{\mathrm{THFA}} + \frac{1}{2}\hat{V}_X^{\mathrm{THFA}}|\vec{\sigma}\rangle \tag{2.99}$$

The miracle is actually constructed, because we imposed the requirement on the THFA that the correlated occupation-number fluctuations vanish.

[42] The derivation rests on the minimum principle with respect to the one-particle-reduced density matrix. I am not aware of a generalization to general many-particle operators. A proof would require a constrained minimum principle in terms of von-Neumann density matrices.

[43] Unlike the Hamiltonian $\hat{H}$, the Fock operator depends itself on γ. Therefore, one does not obtain the expectation value as derivative of the thermodynamic potential.

$$\frac{d}{d\gamma}\Big|_{\gamma=0}\underbrace{\left[-k_B T \ln \mathrm{Tr}\left[\mathrm{e}^{-\beta(F(\gamma)+\gamma\hat{A})}\right]\right]}_{\Omega_{T,\mu}(\gamma)} = \frac{\mathrm{Tr}\left[\left(\frac{d\hat{F}(\gamma)}{d\gamma}+\hat{A}\right)\mathrm{e}^{-\beta(\hat{F}(\gamma)+\gamma\hat{A})}\right]}{\mathrm{Tr}\left[\mathrm{e}^{-\beta(\hat{F}(\gamma)+\gamma\hat{A})}\right]}\Bigg|_{\gamma=0} \neq \mathrm{Tr}\left[\hat{\rho}^{\nu N,HF}_{T,\mu}\hat{A}\right] \tag{2.94}$$

[44] The Hartree potential $\hat{V}_H$ and the exchange potential V_X are operators in the one-particle Hilbert space.

2.6 Spectral properties

For non-interacting electrons, the one-particle energies determine both the thermodynamic properties of the system as well as its spectral properties such as optical absorption and emission. For interacting electrons, this connection of spectral and thermodynamic properties is broken.

2.6.1 Excited states and the averaged-phase approximation (APA)

In this section, I do not aim at an exact description of spectral properties, but I will stick to the level of Slater determinants. We use the natural orbitals $|\varphi_n\rangle$ of the equilibrium ensemble[45] and approximate the excited states by the corresponding Slater determinants.

This corresponds to the **averaged-phase approximation** described in appendix G.2 on p. 610.

$$\hat{H} \overset{\text{Eq. } G.37}{\approx} \hat{H}^{APA} = \sum_{\vec{\sigma}} |\vec{\sigma}\rangle \underbrace{E\big(|\vec{\sigma}\rangle\big)}_{\langle\vec{\sigma}|\hat{h}+\hat{W}|\vec{\sigma}\rangle} \langle\vec{\sigma}| \tag{2.100}$$

The eigenvalues of the APA Hamiltonian are the energy expectation values of Slater determinants. The energy of a Slater determinant has been worked out in Eq. 2.31 on p. 58. Let me repeat it here for convenience:

$$\underbrace{E\big(|\vec{\sigma}\rangle\big)}_{\langle\vec{\sigma}|\hat{h}+\hat{W}|\vec{\sigma}\rangle} \overset{\text{Eq. } 2.31}{=} \sum_{j=1}^{\infty} \sigma_j \langle\varphi_j|\hat{h}|\varphi_j\rangle + \frac{1}{2}\sum_{i,j=1}^{\infty} \sigma_i\sigma_j \Big(\langle\varphi_i\varphi_j|\hat{W}|\varphi_i\varphi_j\rangle - \langle\varphi_i\varphi_j|\hat{W}|\varphi_j\varphi_i\rangle \Big) \tag{2.101}$$

The APA limits the approximation to one object, namely the underlying many-particle Hamiltonian. The approximation made is the neglect of the off-diagonal Hamilton matrix elements $\langle\vec{\sigma}|\hat{H}|\vec{\sigma'}\rangle$ between distinct Slater determinants.[46] For this Hamiltonian,The complete theory can then be carried through. The interaction between electrons is retained. The APA removes the *entanglement between* the Slater determinants, while it retains *entanglement within* the Slater determinants. The APA also keeps electron correlations, which go beyond the **mean-field approximation** for excited states, often attributed to the Hartree-Fock approximation. This will be useful to elucidate the effects of the mean-field approximation.

From electrons to quasiparticles

The energy Eq. 2.101 can also be expressed in terms of **quasi-particles**. For this purpose, one decomposes the occupation number $\sigma_j = f_j + (\sigma_j - f_j)$ of the Slater determinant $|\vec{\sigma}\rangle$ at hand into the thermal occupation f_j of the equilibrium ensemble [47] and its deviation $\sigma_j - f_j$ from the thermal occupation.

[45] The natural orbitals of the equilibrium ensemble are the eigenstates of its one-particle-reduced density matrix.

[46] Part of defining the approximation Eq. 2.100 is the choice of the one-particle basisset for the Slater determinants. The one-particle-reduced density matrix defines the basis as its natural orbitals. The approximate Hamiltonian in Eq. 2.100 is therefore itself a functional $H^{APA}[\hat{\rho}^{(1)}_{T,\mu}]$ of the thermal one-particle-reduced density matrix of the *interacting* electrons. In order to obtain the one-particle-reduced density matrix, one could resort to the thermal Hartree-Fock (THF) approximation, which implies choosing the eigenstates of the corresponding Fock operator. As a consequence, the approximate Hamiltonian Eq. 2.100 depends on the temperature and chemical potential as well as, for example, atomic positions.

[47] The identity between the energies given in Eq. 2.101 and Eq. 2.102 holds for arbitrary (N-representable) occupations. The occupations used here need not result from a thermal ensemble as $f_j = \sum_{\vec{\sigma}} P_{\vec{\sigma}}\sigma_j$ nor from the Hartree-Fock approximation. Thus, one may choose a single Slater determinant as the reference ensemble and treat the deviation of the occupation numbers from this reference like quasi-particles.

ENERGY OF A QUASIPARTICLE DISTRIBUTION IN THE APA

The energy Eq. 2.101 of a Slater determinant with occupation numbers $\vec{\sigma}$ can be expressed in terms of a reference ensemble, indicated by occupations $\vec{f}$, and the energy of a quasi-particle distribution. The one-particle orbitals of the Slater determinant must be identical tp the natural orbitals $\{\varphi_n\rangle\}$ of the reference ensemble. Typically the reference ensemble is the thermal ensemble of the thermal Hartree-Fock approximation.

$$\begin{aligned}\underbrace{E\big(|\vec{\sigma}\rangle\big)}_{\langle\vec{\sigma}|\hat{h}+\hat{V}|\vec{\sigma}\rangle} &\overset{\text{Eq. 2.101}}{=} \underbrace{\sum_{n=1}^{\infty} f_n\langle\varphi_n|\hat{h}|\varphi_n\rangle + \frac{1}{2}\sum_{n,j=1}^{\infty} f_n f_j\Big(\langle\varphi_n\varphi_j|\hat{W}|\varphi_n\varphi_j\rangle - \langle\varphi_n\varphi_j|\hat{W}|\varphi_j\varphi_n\rangle\Big)}_{\text{mean-field energy of the reference ensemble}} \\ &+ \underbrace{\sum_{n=1}^{\infty}\Big(\sigma_n - f_n\Big)\overbrace{\langle\varphi_n|\hat{h}+\hat{V}_H^{(\vec{f})}+\hat{V}_X^{(\vec{f})}|\varphi_n\rangle}^{\epsilon_n^{(\vec{f})}}}_{\text{energy of non-interacting quasi-particles}} \\ &+ \overbrace{\underbrace{\frac{1}{2}\sum_{n,j=1}^{\infty}\Big(\sigma_n - f_n\Big)\big(\sigma_j - f_j\big)\Big(\langle\varphi_n\varphi_j|\hat{W}|\varphi_n\varphi_j\rangle - \langle\varphi_n\varphi_j|\hat{W}|\varphi_j\varphi_n\rangle\Big)}_{\text{Interaction between quasi-particles}}}^{\frac{1}{2}\sum_n(\sigma_n-f_n)\left\langle\varphi_n\middle|\hat{V}_H^{(\vec{\sigma})}+\hat{V}_X^{(\vec{\sigma})}-\hat{V}_H^{(\vec{f})}-\hat{V}_X^{(\vec{f})}\middle|\varphi_n\right\rangle} \qquad (2.102)\end{aligned}$$

The Hartree and exchange potentials in Eq. 2.102 are those of the reference ensemble, which is indicated by the superscript $(\vec{f})$.

$$\begin{aligned}\hat{V}_H^{(\vec{f})} &= \sum_k |\varphi_k\rangle\Big(\sum_j f_j\langle\varphi_k\varphi_j|\hat{W}|\varphi_k\varphi_j\rangle\Big)\langle\varphi_k| \qquad \text{and} \\ \hat{V}_X^{(\vec{f})} &= \sum_k |\varphi_k\rangle\Big(-\sum_j f_j\langle\varphi_k\varphi_j|\hat{W}|\varphi_j\varphi_k\rangle\Big)\langle\varphi_k| \qquad (2.103)\end{aligned}$$

The quasi-particle energy $\epsilon_n^{(f)}$ is an eigenstate of the Fock operator Eq. 2.77 for the equilibrium ensemble.
The Hartree and exchange potentials $\hat{V}_H^{(\vec{\sigma})}, \hat{V}_H^{(\vec{\sigma})}$ are defined analogously, but with the occupation numbers $\vec{\sigma}$ of the actual Slater determinant replacing the occupations $\vec{f}$ of the reference ensemble.

Usually, one deals with excited states for which only few electrons are lifted into higher-lying orbitals. That is, most occupation numbers σ_n are equal to the occupations $f_n = \sum_{\vec{\sigma}} P_{T,\mu;\vec{\sigma}}\sigma_n$ of the equilibrium ensemble. As a result, only few non-vanishing terms are left in the quasi-particle summations.

From Eq. 2.102 emerges an intuitive picture of a

- **Fermi sea**, the electrons in the equilibrium ensemble, with additional
- **quasi-particles**, namely electrons and holes, and the
- **quasi-particle interaction** between them.

The energy and the interactions *within* the Fermi sea are combined in one term, the internal energy of the reference ensemble. Each quasi-particle contributes, in addition, its own quasi-particle energy $\epsilon_n^{(\vec{f})}$, which is an eigenvalue of the Fock operator. Furthermore, the Coulomb interaction between the quasi-particles, electrons and holes, needs to be accounted for.

The charge of the quasi-particle can be positive or negative, depending on the sign of $\sigma_n - f_n$. If $\sigma_n - f_n$ is positive, the quasi-particle is called an **electron** and it is called a **hole**, if it is negative.

Interestingly, the quasi-particles next to the Fermi-level occur with a fractional charge $q_n^{QP} = q_e|\sigma_n - f_n|$, where $q_e = -e$ is the charge of an electron. The fractional charge (as opposed to the full charge) leads to a smaller interaction.

In chapter 9 below (p. 277), this quasi-particle concept is generalized beyond the average phase approximation (APA). I will call this generalized concept the "Lehmann amplitudes" Eq. 9.3.

Energy differences of Slater determinants

In spectroscopy, one excites the system into an excited state and senses the intensity and energy of the transition. Hence, one needs to access the energy differences between eigenstates of the Hamiltonian, which, in the average phase approximation (APA), are Slater determinants.

We begin with Eq. 2.102 obtained above

$$
\begin{aligned}
E\big(|\vec{\sigma}\rangle\big) - E\big(|\vec{\sigma'}\rangle\big) \overset{\text{Eq. 2.102}}{=} & \sum_{j=1}^{\infty}\Big(\sigma_j - \sigma'_j\Big)\epsilon_j^{(\vec{f})} \\
& + \frac{1}{2}\sum_{i,j=1}^{\infty}\Bigg[\underbrace{\Big(\sigma_i - f_i\Big)\Big(\sigma_j - f_j\Big) - \Big(\sigma'_i - f_i\Big)\Big(\sigma'_j - f_j\Big)}_{\Big(\sigma_i-\sigma'_i+\sigma'_i-f_i\Big)\Big(\sigma_j-\sigma'_j+\sigma'_j-f_j\Big)-\Big(\sigma'_i-f_i\Big)\Big(\sigma'_j-f_j\Big)}\Bigg]\Big(\langle\varphi_i\varphi_j|\hat{W}|\varphi_i\varphi_j\rangle - \langle\varphi_i\varphi_j|\hat{W}|\varphi_j\varphi_i\rangle\Big) \\
& \qquad\qquad \underbrace{\qquad\qquad\qquad\qquad\qquad\qquad\qquad\qquad}_{\Big(\sigma_i-\sigma'_i\Big)\Big(\sigma_j-\sigma'_j\Big)+2\Big(\sigma_i-\sigma'_i\Big)\Big(\sigma'_j-f_j\Big)} \\
& = \sum_{j=1}^{\infty}\Big(\sigma_j - \sigma'_j\Big)\underbrace{\Big\{\epsilon_j^{(\vec{f})} + \sum_k\big(\sigma'_k - f_k\big)\Big(\langle\varphi_j\varphi_k|\hat{W}|\varphi_j\varphi_k\rangle - \langle\varphi_j\varphi_k|\hat{W}|\varphi_k\varphi_j\rangle\Big)\Big\}}_{\epsilon_j^{(\vec{\sigma'})}} \\
& + \frac{1}{2}\sum_{j,k}^{\infty}\Big(\sigma_j - \sigma'_j\Big)\Big(\sigma_k - \sigma'_k\Big)\Big(\langle\varphi_j\varphi_k|\hat{W}|\varphi_j\varphi_k\rangle - \langle\varphi_j\varphi_k|\hat{W}|\varphi_k\varphi_j\rangle\Big) \qquad (2.104)
\end{aligned}
$$

The energy difference for the addition of a set of quasi-particles , described by $\vec{\sigma} - \vec{\sigma'}$, to an initial state $|\vec{\sigma'}\rangle$ probes

1. the energy of the added quasi-particles in the Coulomb potential of the quasi-particle distribution of the initial state and the

2. Coulomb interaction of the added quasi-particles among each other. The latter term is absent, if only a single quasi-particle is added or removed.

Notation

NOTATION

In order to describe states with additional quasi-particles, let me use already the notation of second quantization. I will only use certain aspects of it ahead of time. A detailed motivation and description of this notation will be given only in the next chapter.

- a Slater determinant $|\vec{\sigma'}\rangle$ obtained from $|\vec{\sigma}\rangle$ by adding an electron to an unoccupied one-particle orbital $|\varphi_n\rangle$ is described by

$$|\vec{\sigma'}\rangle = \hat{a}_n^\dagger |\vec{\sigma}\rangle \tag{2.105}$$

  The operator $\hat{a}_n^\dagger$ is called **creation operator** for the n-th orbital. If the n-th orbital is already occupied, i.e. $\sigma_n = 1$, the result is the **zero state** $|\varnothing\rangle$, i.e. $\hat{a}_n^\dagger|\vec{\sigma}\rangle = |\varnothing\rangle$. Otherwise the occupation number σ_n is raised from zero to one.

  The energy of the new Slater determinant is denoted as $E\big(\hat{a}_n^\dagger|\vec{\sigma}\rangle\big) = E(|\vec{\sigma'}\rangle)$ as defined in Eq. 2.101

- a Slater determinant $|\vec{\sigma'}\rangle$ obtained from $|\vec{\sigma}\rangle$ by removing an electron from an occupied one-particle orbital $|\varphi_n\rangle$ is described by

$$|\vec{\sigma'}\rangle = \hat{a}_n |\vec{\sigma}\rangle \tag{2.106}$$

  The operator $\hat{a}_n$ is called **annihilation operator** for the n-th orbital. If there is no electron in the n-th orbital, the result is the zero state, i.e. $\hat{a}_n|\vec{\sigma}\rangle = |\varnothing\rangle$. Otherwise the occupation number σ_n is lowered from one to zero.

- a Slater determinant $|\vec{\sigma'}\rangle$ obtained from $|\vec{\sigma}\rangle$ by removing an electron from the one-particle orbital $|\varphi_m\rangle$ and by adding it into the one-particle orbital $|\varphi_n\rangle$ is

$$|\vec{\sigma'}\rangle = \hat{a}_n^\dagger \hat{a}_m |\vec{\sigma}\rangle \tag{2.107}$$

  The annihilation and creation operators are applied in sequence as described above.

2.6.2 Spectroscopies

Our discussion rests on **Fermi's golden rule** for the transition rate of an excitation, which is discussed, for example, in section 13.4.5 of PhiSX: Quantum Physics[16]. The transition rate is given there in Eq. 13.52 as follows:

FERMI'S GOLDEN RULE

The **transition rate** (transition probability per unit time) from an initial state $|\Phi_i\rangle$ to a final state $|\Phi_f\rangle$ due to approximately monochromatic pulses with shape $\hat{W}(t) = \hat{W}_0 \mathrm{e}^{-i\omega_0 t}\chi_k(t)$, having a smooth pulse shape $\chi_k(t)$ and a total intensity $\frac{1}{T}\int_0^T dt\ \sum_k |\chi_k(t)|^2 = 1$ is

$$\Lambda_{f\leftarrow i} = \frac{1}{T}\Gamma_{f\leftarrow i} = \frac{2\pi}{\hbar}|\langle\phi_f|\hat{W}_0|\phi_i\rangle|^2 \delta\left(E_f - E_i - \hbar\omega_0\right) + O(\hat{W}_0^3) \tag{2.108}$$

Fermi's golden rule says that an excitation with monochromatic light is only possible if the incident light beam has exactly that energy $\hbar\omega_0$ that is necessary to lift the system into a higher-, or lower-energetic state.

While the equation above has been derived in the context of single-particle quantum mechanics, it is

equally valid for many-particle wave functions.

The absorption probability for an initial ensemble $\{P_q, |\Phi_q\rangle\}$ is as sum over all final states $|F\rangle$, i.e. all eigenstates of the many-particle Hamiltonian in the absence of the exciting pulse.

$$Q(\hbar\omega) = \frac{2\pi}{\hbar} \sum_F \sum_q P_q \langle \phi_q | \hat{W}_0 | F \rangle \delta \left(E_{|F\rangle} - E_q - \hbar\omega \right) \langle F | \hat{W}_0 | \phi_q \rangle \tag{2.109}$$

I will not consider all existing spectroscopies, but rather concentrate on three representative examples that capture the most relevant effects for our purpose.

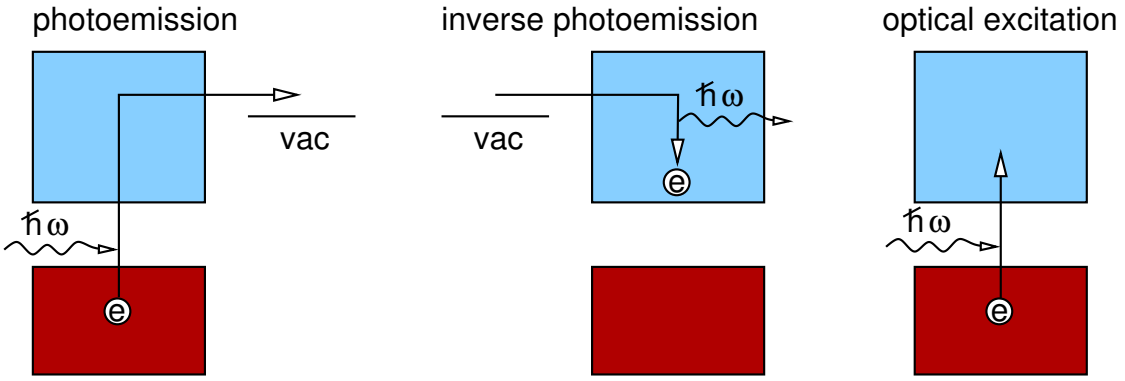


Fig. 2.4: Energy vs. position sketch of the photoemmission, inverse photoemission and optical excitation process. The red square represents the valence band, while the blue square represents the conduction band. The vacuum level is denoted by *"vac"*.

For sketches of the different spectroscopic techniques mentioned here, see figure 2.4.

- **photoemission**: a photon is absorbed, while an electron is emitted out of the system. The kinetic energy E_{kin} of the electron, which escapes from the system, is measured. The energy of the emitted electron is $E_{vac} + E_{\text{kin}}$, where the vacuum energy E_{vac} is the energy of an electron at rest in the vacuum. The energy difference of the emitted electron and the absorbed photon $\hbar\omega$ is the energy of the electron before the photon absorption, because it is due to the removal (annihilation) of an electron from the valence band. The photoemission process thus detects the density of states of the occupied states.[48]
- **inverse photoemission**: The system captures an electron while emitting a photon. The electron injected drops from a high-lying energy level into a low-lying empty orbital. The energy difference of the emitted photon $\hbar\omega$ and the injected electron $E_{vac} + E_{\text{kin}}$ is due to the addition (creation) of an electron to the conduction band. The inverse photoemission process thus detects the density of states of the conduction band.
- **optical spectroscopy**: a photon is absorbed, while an electron-hole pair is created. That is, an electron is lifted from a filled orbital into an empty one. It is described by a simultaneous removal (annihilation) of an electron from the valence bands and and the simultaneous addition (creation) of an electron in the conduction bands. While photo-emission and inverse photo-emmission are **one-particle excitations**, the optical absorption is an example for a **two-particle excitation**.

Energy balance of the photoemission process

In the photoemission process, an electron is ejected from an occupied state $|\varphi_n\rangle$ and lifted into the vacuum. The energy of the emitted electron is the sum of **vacuum level** ϵ_{vac} and the kinetic energy

[48] Damascelli et al.[49] provide a insightful introduction to angular resolved photoemission spectroscopy (ARPES).

E_{kin} of the emitted electron. The vacuum level ϵ_{vac} is the potential energy of an electron far above the surface of the material.

The energy balance between the initial state, consisting of the incident photon with energy $\hbar\omega$ and the ground state $|\vec{\sigma}\rangle$ of the target, and the final state[49] consisting of the target after removal of one electron from the n-th orbital $\hat{a}_n|\vec{\sigma}\rangle$ and the emitted electron in the vacuum, is

$$\underbrace{\hbar\omega + E\big(|\vec{\sigma}\rangle\big)}_{\text{initial state}} = \underbrace{E\big(\hat{a}_n|\vec{\sigma}\rangle\big) + \epsilon_{\text{vac}} + E_{\text{kin}}}_{\text{final state}} \tag{2.110}$$

The energy loss ΔE_{loss} of the photoemission process, the energy absorbed by the material, is the energy cost for annihilating an electron in the material

$$\Delta E_{\text{loss}} \overset{\text{def}}{=} \hbar\omega - \Big(\epsilon_{\text{vac}} + E_{\text{kin}}\Big) \overset{\text{Eq. 2.110}}{=} E\big(\hat{a}_n|\vec{\sigma}\rangle\big) - E\big(|\vec{\sigma}\rangle\big) \tag{2.111}$$

An important concept is that spectral properties are related to the addition or removal of quasi-particles. Because, in the present case, only a single quasi-particle is added, a hole, the resulting spectral function is called a one-particle spectral function. The optical excitation discussed below is an example for the addition of two quasi-particles, an electron-hole pair.

The energy difference between the initial electron configuration $|\vec{\sigma}\rangle$ with an electron in orbital $|\varphi_n\rangle$, i.e. $\sigma_n = 1$, and the final one $\hat{a}_n|\vec{\sigma}\rangle$ after remobing the electron is

$$\begin{aligned}\Delta E_{\text{loss}} \quad &= \quad E\big(\hat{a}_n|\vec{\sigma}\rangle\big) - E\big(|\vec{\sigma}\rangle\big) \overset{\text{Eq. 2.101}}{=} -\epsilon_n^{(\vec{\sigma})} \\ &\overset{\text{Eq. 2.104}}{=} \underbrace{-}_{(\sigma_n-1)-\sigma_n} \underbrace{\left\{\epsilon_n^{(\vec{f})} + \sum_k \big(\sigma_k - f_k\big)\Big(\langle\varphi_n\varphi_k|\hat{W}|\varphi_n\varphi_k\rangle - \langle\varphi_n\varphi_k|\hat{W}|\varphi_k\varphi_n\rangle\Big)\right\}}_{\epsilon_n^{(\vec{\sigma})}}\end{aligned} \tag{2.112}$$

The energy loss during photoemission can directly be related[50] to the eigenvalues $\epsilon_n^{(\vec{\sigma})}$ of the Fock operator $\hat{F}^{(\vec{\sigma})} = \hat{h} + \hat{V}_H^{(\vec{\sigma})} + \hat{V}_X^{(\vec{\sigma})}$ *obtained from the initial Slater determinant* $|\vec{\sigma}\rangle$.

$$\epsilon_n^{(\vec{\sigma})} = \big\langle\varphi_n\big|\hat{h} + \hat{V}_H^{(\vec{\sigma})} + \hat{V}_X^{(\vec{\sigma})}\big|\varphi_n\big\rangle \tag{2.113}$$

If the the state $|\varphi_n\rangle$ is already empty in the initial state $|\vec{\sigma}\rangle$, no transition can occur. The filled eigenvalues of the Fock operator are related, up to the sign, to **electron-removal energies**.

For an ensemble of Slater determinants, the loss is a distribution a, often slightly different, contributions to the loss.

$$\mathcal{A}_n^{PE}(\hbar\omega) = \sum_{\vec{\sigma}} P_{\vec{\sigma}}\sigma_n\delta\big(\hbar\omega - \epsilon_n^{(\vec{\sigma})}\big) \tag{2.114}$$

The occupation number σ_n ensures that only Slater determinants are considered, for which $|\varphi_n\rangle$ is occupied.

Each Slater determinant contributes with a different energy

$$\epsilon_n^{(\vec{\sigma})} = \epsilon_n^{(\vec{f})} + \overbrace{\underbrace{\sum_k \big(\sigma_k - f_k\big)\Big(\langle\varphi_n\varphi_k|\hat{W}|\varphi_n\varphi_k\rangle - \langle\varphi_n\varphi_k|\hat{W}|\varphi_k\varphi_n\rangle\Big)}_{\text{level shift due to a fluctuation of the Coulomb potential}}}^{\langle\varphi_n|\hat{V}_H^{\vec{\sigma}} + \hat{V}_X^{\vec{\sigma}} - \hat{V}_H^{\vec{f}} - \hat{V}_X^{\vec{f}}|\varphi_n\rangle} \tag{2.115}$$

[49] The final state may be written in the form $\hat{a}_n|\vec{\sigma}\rangle \otimes |\vec{k},\sigma\rangle$, where $|\vec{k},\sigma\rangle$ describes the emitted electron in the vakuum.

[50] Gauge invariance: The vacuum level must be specified on the same energy axis as the Fock operator. Due to the gauge invariance of electrodynamics, all observables must be independent of an additional spatially invariant electrostatic potential. Such a potential shifts the Fock operator, but also the vacuum level, so that $\epsilon_{vac} - \epsilon_n^{\sigma}$ is gauge invariant.

to the spectral function. While the first term $\epsilon_n^{(\vec{f})}$ is the same for the entire ensemble, the second term describes the potential of **charge fluctuations**[51] acting on the orbital $|\varphi_n\rangle$. The electron to be removed in the excitation process experiences the interaction with the quasi-particles already present in the initial state. Because the electron experiences a spread of potentials, one from each Slater determinant, the spectral peak is broadened. The width of a spectral peak is related to the life-time, respectively to a exponential decay of the intensity on the time axis. It is therefore called the **lifetime broadening**. The relation of the spectral-peak width and the lifetime can already be explored using the damped, driven harmonic oscillator as shown in section 3.10.2 of ΦSX: Klassische Mechanik[15].

For a band structure $\epsilon_n(\vec{k})$, the lifetime broadening implies that the bands are no more sharp. Thus one describes the band structure by a k- and energy-dependent spectral function $\mathcal{A}(\vec{k},\epsilon)$. In the **mean-field theory**, the charge fluctuations are averaged out, so that the band structure becomes sharp and the spectral function consists of delta peaks at $\epsilon(\vec{k})$.

The spectral functions for distinct orbitals can be combined into an operator

$$\hat{\mathcal{A}}^{PE}(\hbar\omega) = \sum_n |\varphi_n\rangle \mathcal{A}_n^{PE}(\hbar\omega)\langle\varphi_n| = \sum_n |\varphi_n\rangle \Big\{ \sum_{\vec{\sigma}} P_{\vec{\sigma}}\sigma_n \delta\big(\hbar\omega - \epsilon_n^{(\vec{\sigma})}\big)\Big\}\langle\varphi_n| \tag{2.116}$$

The connection to the well known density of states becomes evident when one considers an ensemble with a single Slater determinant $|\vec{\sigma}\rangle$, i.e. $P_{\vec{\sigma}} = 1$.

$$\hat{\mathcal{A}}^{PE}(\hbar\omega) \overset{P_{\vec{\sigma}}=1}{=} \sum_n \sigma_n\, |\varphi_n\rangle \delta\big(\hbar\omega - \epsilon_n^{(\vec{\sigma})}\big)\langle\varphi_n| \tag{2.117}$$

2.6.3 Energy balance in the inverse photoemission process

Let me now consider the inverse photoemission process, in which an electron is absorbed by the material and a photon is emitted, while the electron settles into a previously unoccupied orbital.

Let me denote the Slater determinant of the final state by $\hat{a}_n^\dagger|\vec{\sigma}\rangle$. Compared to the initial state $|\vec{\sigma}\rangle$, it has an additional electron in state $|\varphi_n\rangle$.

The energy conservation requires that the initial and final energies are the same

$$\underbrace{E\big(|\vec{\sigma}\rangle\big) + E_{\text{vac}} + E_{\text{kin}}}_{\text{initial state}} = \underbrace{E\big(\hat{a}_n^\dagger|\vec{\sigma}\rangle\big) + \hbar\omega}_{\text{final state}} \tag{2.118}$$

The energy loss ΔE_{loss}, the energy $\epsilon_{\text{vac}} + E_{\text{kin}}$ of the injected electron minus the energy $\hbar\omega$ of the emitted photon, can be calculated as energy difference of the initial and final Slater determinants.

$$\begin{aligned} \Delta E_{\text{loss}} \quad &= \quad \epsilon_{\text{vac}} + E_{\text{kin}} - \hbar\omega \overset{\text{Eq. 2.118}}{=} E(\hat{a}_n^\dagger|\vec{\sigma}\rangle) - E(|\vec{\sigma}\rangle) \\ &\overset{\text{Eq. 2.104}}{=} \underbrace{\epsilon_n^{(\vec{f})} + \sum_j (\sigma_j - f_j)\Big(\langle\varphi_n\varphi_j|\hat{W}|\varphi_n\varphi_j\rangle - \langle\varphi_n\varphi_j|\hat{W}|\varphi_j\varphi_n\rangle\Big)}_{\epsilon_n^{(\vec{\sigma})}} \end{aligned} \tag{2.119}$$

The unoccupied eigenvalues of the Fock operator are **electron-addition energies**.

Proceeding analogous to photoemission process, we obtain the **spectral function for electron addition** as

$$\hat{\mathcal{A}}^{IPE}(\hbar\omega) = \sum_n |\varphi_n\rangle \Big\{ \sum_{\vec{\sigma}} P_{\vec{\sigma}}(1-\sigma_n)\delta(\hbar\omega - \epsilon_n^{(\vec{\sigma})})\langle\varphi_n| \tag{2.120}$$

[51] The term *"fluctuations"* seems to refer to a dynamical process. The connection is not immediately obvious. The underlying picture is that of a particle passing through the material, which is not in an eigenstate of a system, but in a superposition of many eigenstates of the Hamiltonian contributing to the same peak. The electron distribution of the electrons surrounding the traveling particle is therefore not stationary and produces time-dependent potential fluctuations at the site of the particle.

The spectral function for the IPE probes the empty states ($\sigma_n = 0$).

The **total spectral function** is the sum of the spectral function for electron addition and electron removal.

$$\hat{\mathcal{A}}(\hbar\omega) = \hat{\mathcal{A}}_n^{PE}(\hbar\omega) + \hat{\mathcal{A}}_n^{IPE}(\hbar\omega) = \sum_n |\varphi_n\rangle \left\{ \sum_{\vec{\sigma}} P_{\vec{\sigma}} \delta\Big(\hbar\omega - \epsilon_n^{(\vec{\sigma})}\Big) \right\} \langle\varphi_n| \tag{2.121}$$

The energy level $\epsilon_n^{(\vec{\sigma})}$ is the energy to add or –with the opposite sign– to remove an electron.

$$\epsilon_n^{(\vec{\sigma})} = \underbrace{\Big(E[\hat{a}_n^\dagger|\vec{\sigma}\rangle] - E[|\vec{\sigma}\rangle]\Big)(1-\sigma_n)}_{\text{Eq. 2.119}} \underbrace{-\Big(E[\hat{a}_n|\vec{\sigma}\rangle] - E[|\vec{\sigma}\rangle]\Big)\sigma_n}_{\text{Eq. 2.112}} \tag{2.122}$$

Eq. 2.121 will occur again, in somewhat different shape, but without the restriction to the average-phase approximation, in Eq. 9.24 on p. 284.

2.6.4 Energy balance in optical absorption

Let us now consider the energy required to lift an electron from an occupied state $|\varphi_m\rangle$ into an empty orbital $|\varphi_n\rangle$. Let me denote the state with the electron-hole pair as $\hat{a}_m^\dagger \hat{a}_n |\vec{\sigma}\rangle$.

The energy loss for optical absorption is the energy of the absorbed photon. The energy balance is

$$\underbrace{\hbar\omega + E(|\vec{\sigma}\rangle)}_{\text{initial state}} = \underbrace{E(\hat{a}_m^\dagger \hat{a}_n |\vec{\sigma}\rangle)}_{\text{final state}} \tag{2.123}$$

Thus, the energy loss upon formation of an **electron-hole pair**, that is upon removal of an electron from orbital $|\varphi_n\rangle$ and addition of an electron in orbital $|\varphi_n\rangle$ is

$$\begin{aligned}
\Delta E_{\text{loss}} = \hbar\omega &= E\big(\hat{a}_m^\dagger \hat{a}_n |\vec{\sigma}\rangle\big) - E\big(|\vec{\sigma}\rangle\big) \\
\overset{\text{Eq. 2.104}}{=} & \underbrace{\left\{ \epsilon_m^{(\vec{f})} + \sum_j (\sigma_j - f_j) \Big(\langle\varphi_m\varphi_j|\hat{W}|\varphi_m\varphi_j\rangle - \langle\varphi_m\varphi_j|\hat{W}|\varphi_j\varphi_m\rangle \Big) \right\}}_{\epsilon_m^{(\vec{\sigma})}} \\
- & \underbrace{\left\{ \epsilon_n^{(\vec{f})} + \sum_j (\sigma_j - f_j) \Big(\langle\varphi_n\varphi_j|\hat{W}|\varphi_n\varphi_j\rangle - \langle\varphi_n\varphi_j|\hat{W}|\varphi_j\varphi_n\rangle \Big) \right\}}_{\epsilon_n^{(\vec{\sigma})}} \\
& \underbrace{- \Big(\langle\varphi_m\varphi_n|\hat{W}|\varphi_m\varphi_n\rangle - \langle\varphi_m\varphi_n|\hat{W}|\varphi_n\varphi_m\rangle \Big)}_{\text{exciton binding energy}} \\
= & \quad \epsilon_n^{(\vec{\sigma})} - \epsilon_m^{(\vec{\sigma})} - \underbrace{\Big(\langle\varphi_m\varphi_n|\hat{W}|\varphi_m\varphi_n\rangle - \langle\varphi_m\varphi_n|\hat{W}|\varphi_n\varphi_m\rangle \Big)}_{\text{exciton binding energy (E)}}
\end{aligned} \tag{2.124}$$

The one-particle energies $\epsilon_n^{(\vec{\sigma})}$ and $\epsilon_m^{(\vec{\sigma})}$ are the eigenvalues of the Fock-operator of the initial state $|\vec{\sigma}\rangle$.

The first two terms in Eq. 2.124 are simply the electron-addition and removal energies, which are given by the one-particle spectrum. The last term is the electrostatic attraction of electron and hole. The picture emerges of quasi-electrons that can be added to the system with their own energies. The quasiparticle energies are the eigenvalues of the Fock operator of the initial Slater determinant. The interaction with the other electrons in the ground state does not show up. However, the added quasi-particles interact with each other.

The interaction energy for an electron-hole pair is the so-called **exciton binding energy**.[52] The second interaction term, the exchange term, counteracts the first, but it is only present when both orbitals have the same spin direction. Therefore, the Coulomb interaction between wave functions with opposite spin are much stronger than those with equal spin.

Optical absorption is considered a two-particle process, because one electron is removed and one is added. Unlike one-particle processes, two-particle processes need to take the interaction of quasi-particle into account.

To describe the spectrum for optical absorption, we need a **two-particle spectral function**.

$$\begin{aligned}\hat{\mathcal{A}}^{eh}(\hbar\omega) = \sum_{m,n} |\varphi_m\varphi_n\rangle \sum_{\vec{\sigma}} P_{\vec{\sigma}}\ (1-\sigma_m)\sigma_n \\ \times\delta\Big(\hbar\omega - \big[\epsilon_n^{(\vec{\sigma})} - \epsilon_m^{(\vec{\sigma})} - \big(\langle\varphi_m\varphi_n|\hat{W}|\varphi_m\varphi_n\rangle - \langle\varphi_m\varphi_n|\hat{W}|\varphi_n\varphi_m\rangle\big)\big]\langle\varphi_m\varphi_n| \quad (2.125)\end{aligned}$$

When the exciton-binding energy can be ignored, the spectral function for optical absorption is

$$\begin{aligned}\mathcal{A}^{eh}_{m,n}(\hbar\omega) &= \int d\epsilon \int d\epsilon'\ \mathcal{A}^{IPE}_m(\epsilon)\mathcal{A}^{PE}_n(\epsilon')\delta(\hbar\omega - (\epsilon-\epsilon')) \\ &= \int d\epsilon\ \mathcal{A}^{IPE}_m(\epsilon)\mathcal{A}^{PE}_n(\epsilon-\hbar\omega) \\ &\overset{T,\mu}{=} \int d\epsilon\ \big(1-f_{T,\mu}(\epsilon)\big) f_{T,\mu}(\epsilon-\hbar\omega)\mathcal{A}^{tot}_m(\epsilon)\mathcal{A}^{tot}_n(\epsilon-\hbar\omega) \\ &\overset{T=0}{=} \int_\mu^{\mu+\hbar\omega} d\epsilon\ \mathcal{A}^{tot}_m(\epsilon)\mathcal{A}^{tot}_n(\epsilon-\hbar\omega) \qquad (2.126)\end{aligned}$$

2.6.5 More or less approximations

Editor: This section is being cleaned up.

Spectral function in the mean-field approximation: The most common approximations, used for example to calculate band structures, do not exhibit a lifetime broadening. Due to a misunderstanding, this is often attributed to the neglect of interactions. Rather it is due to a mean-field approximation: For a given ensemble or many-particle wave function, an electron added or removed experiences the same average one-particle potential, irrespective of the charge distribution in a specific Slater determinant contributing to the ensemble of initial states.

As a result of the mean-field approximation, the one-particle spectral properties are given by an effective one-particle operator such as the Fock operator in the thermal Hartree-Fock approximation or the Kohn-Sham Hamiltonian in Density-Functional Theory (DFT).[53]

In the Hartree-Fock approximation of spectral properties, the interaction between quasi-particles is ignored. When the interaction between quasi-particles is ignored, the electron in an orbital $|\varphi_n\rangle$ experiences the average electron distribution of the reference ensemble, irrespective of the specific initial Slater determinant $|\vec{\sigma}\rangle$ present before the excitation. As a result the broadening of the excitation levels due to the charge fluctuations is not present in the Hartree-Fock approximation.

$$\hat{\mathcal{A}}^{HF}(\hbar\omega) = \sum_n |\varphi_n\rangle\delta\Big(\hbar\omega - \epsilon_n^{(\vec{f})}\Big)\langle\varphi_n| \qquad (2.127)$$

For each one-particle state $|\varphi_n\rangle$, The Hartree-Fock approximation yields a single, sharp δ-peak in the spectrum.

[52] In a complete description, the exciton binding energy also contains the kinetic energy cost required to localize electron and hole in the same region.

[53] Density-Functional Theory (DFT) does not predict spectral properties and it is not a mean field theory. Nevertheless, in analogy to the Hartree Fock approximation or the GW approximation, the spectrum is often, *illegally* but very successful, calculated from the Kohn-Sham Hamiltonian.

The average-phase approximation goes beyond the mean-field approximation and retains the quasi-particle interactions. While the excitation spectrum of the APA is given, like that of the HFA, by single Slater determinants, the APA captures many-particle effects such as finite lifetime of quasi-particles, satellites and many more. The APA thus forms a bridge between the mean-field approximation on the one side and the full description of spectral function discussed later in chapter 9.

The comparison of the APA with the Hartree-Fock approximation sheds light on a long-standing discussion regarding the mean-field nature of spectra calculated with numerical first-principles calculations based on density-functional theory. In contrast the Hartree-Fock approximation, density-functional theory is an exact theory. Nevertheless, the structures of the two theories are so similar, that the discussion can be analyzed on the simpler Hartree-Fock approximation. I will not discuss density-functional theory in detail, but I will return to it in section 13.2 on p. 398 and in appendix H on p. 661.

Relation to the Density of States: The spectral function is the same as the **density-of-states** $D(\epsilon)$. The term density-of-states is common in combination with effectively non-interacting quasi-particles, such as Density-Functional Theory. The term spectral function emphasises the experiment and is common in many-particle physics.

$$\hat{D}(\epsilon) = \sum_n |\varphi_n\rangle \delta(\epsilon - \epsilon_n) \langle \varphi_n| \tag{2.128}$$

For non-interacting electrons, the Fock operator is just the one-particle Hamiltonian $\hat{h}$.

The term density of states alludes to a density of one-particle states on an energy axis, where each one-particle state has a specific energy as in a mean-field theory. Usually the term density of states and spectral functions are used interchangeably.

Relation to the self energy: We will learn that the dynamics of an electron in an electron gas can be described by the one-particle Green's function.

The equation of motion Eq. 8.16 of the Green's function is

$$\left[\epsilon - \hat{h} - \hat{\Sigma}(\epsilon)\right] \hat{G}(\epsilon) = \hat{1} \tag{2.129}$$

with a self-energy $\hat{\Sigma}(\epsilon)$ from Eq. 8.15. This equation of motion is general and not limited to weak interactions. In the Hartree-Fock approximation, the self energy is given by Hartree and exchange potentials.

$$\hat{\Sigma}^{HF}(\epsilon) = \hat{V}_H^{(\vec{f})} - \hat{V}_X^{(\vec{f})} \tag{2.130}$$

where the occupations $\vec{f}$ are those of the thermal ensemble of Hartree Fock. With the self energy, we encounter already one of the most fundamental quantities in many-particle physics.

The self energy acts like an energy-dependent potential. In the time representation, this corresponds to a retarded potential, analogous to an echo: The electron perturbs the surrounding electron gas. This perturbation propagates through the electron gas, until it acts back on the travelling electron at a later time. In the Hartree-Fock approximation, the potentials are energy independent and hence not retarded.

2.6.6 Spectral properties of the free-electron gas

Let me describe here the qualitative changes undergone by the band structure of the electron gas due to the interaction between electrons. I will summarize the main effects also beyond the Hartree-Fock limit. It shall provide an outlook for correlation effects related to a particularly simple system, the free electron gas.

Within the Hartree-Fock method, the free-electron gas can be treated analytically. This is shown in appendix E.3 on p. 565. The findings are not only relevant for the Hartree-Fock method but also beyond. Here, I will only discuss the main findings.

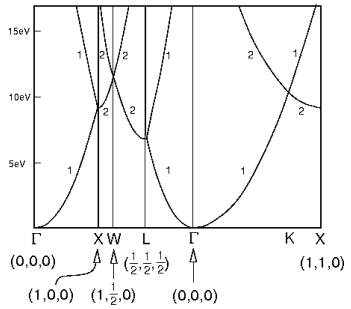


Fig. 2.5: Dispersion of free electrons in the reduced zone scheme for an fcc lattice, Eq. 2.131. See also figure 1.10 on p. 43.

1. **Non-interacting electrons:** the dispersion relation $\epsilon(\vec{k})$ of the non-interacting, free-electron gas is a simple parabola.

$$\epsilon(\vec{k}) = \frac{\hbar^2 \vec{k}^2}{2m_e} \tag{2.131}$$

   In a crystal lattice with primitive lattice vectors $\vec{T}_1, \vec{T}_2, \vec{T}_2$, a parabola is centered at each general reciprocal lattice vector $\vec{G}_n$, i.e.

$$\epsilon_n(\vec{k}) = \frac{\hbar^2}{2m_e}\left(\vec{k} - \vec{G}_n\right)^2 \tag{2.132}$$

   The resulting dispersion relation has several bands and the band structure is periodic in the periodic lattice. The band structure of the free-electron gas in the **reduced zone scheme** is shown in figure 2.5

2. **Hartree Fock:** The exchange potential $\hat{V}_X$ shifts the band structure down in energy. This is the so-called **quasi-particle shift**. The quasi-particle shift is large for the filled states, and vanishes for high kinetic energy $\epsilon(\vec{k})$. This can be attributed to the fact that the exchange term stabilizes states that are similar to filled states[54]

   . The empty states far above the Fermi level are little affected by the exchange hole. Loosely speaking, this is because the electrons are so fast that the exchange hole cannot properly form, respectively that the electron escapes the exchange hole.

   The Fermi-momentum $\hbar k_F$ is unchanged by a weak interaction. The Hartree-Fock approximation produces an **artifact at the Fermi surface**: as shown in figure 2.6, the slope of the dispersion relation becomes infinite and the spectral function drops to zero.

[54] The notion that the exchange term stabilizes states, which are similar to already filled states, is a common observation. One way to do this qualitative argument is based on the dominant contribution of exchange, the self-interaction correction.

$$E_{SIC} = -\frac{1}{2}\sum_n f_n^2 \int d^4x \int d^4x' \; \frac{e^2 |\varphi_n^*(\vec{x})|^2 |\varphi_n^*(\vec{x'})|^2}{4\pi\epsilon_0 |\vec{r} - \vec{r'}|} \tag{2.133}$$

The corresponding potential is (Using Janak's theorem $\epsilon_n = \frac{\partial E}{\partial f_n}$)

$$\hat{v}_{SIC} = \sum_n |\varphi_n\rangle \left[-f_n \int d^4x \int d^4x' \; \frac{e^2 |\varphi_n^*(\vec{x})|^2 |\varphi_n^*(\vec{x'})|^2}{4\pi\epsilon_0 |\vec{r} - \vec{r'}|} \right] \langle\varphi_n| \tag{2.134}$$

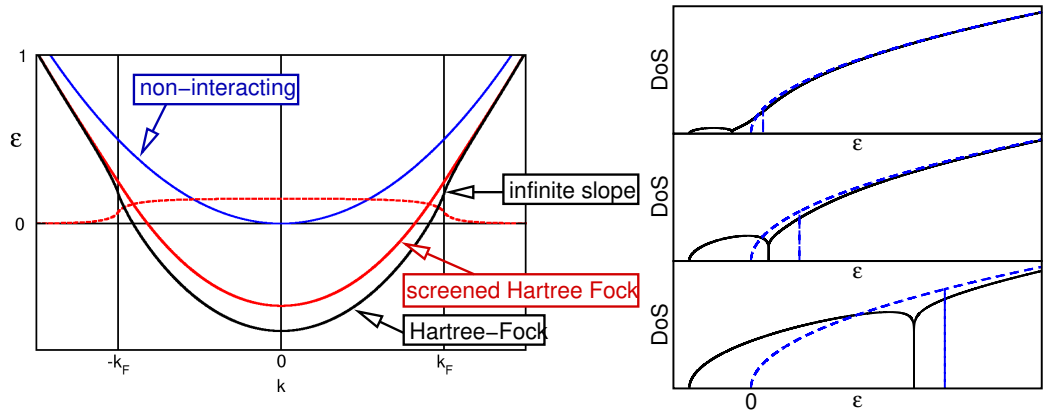


Fig. 2.6: Left: dispersion relation $\epsilon(k)$ of the free-electron gas as calculated without interactions (blue), with Hartree-Fock (black) and with screened Hartree-Fock (red). The Fermi momentum has been chosen as $k_F = 1/a_0$ and the screening length for the screened Hartree-Fock calculation has been 6 a_0, where a_0 is the Bohr radius. The red, dashed line is the quasi-particle shift due to screening. Only the bands of unscreened Hartree-Fock exhibit an infinite slope at the Fermi level. The Fermi level is at $\epsilon(k_F)$. Right: density of states of the free-electron gas without interactions (blue) and in the Hartree-Fock approximation. The Fermi level of the non-interacting electron gas is indicated by the straight line. The electron density increases from top to bottom. The density of states for the Hartree-Fock calculation drops to zero at the Fermi level. The energy of the bottom of the band is independent of the electron density and depends only on the strength of the interaction.

3. **Screened Hartree Fock:** The artifact at the Fermi surface (infinite slope and vanishing density of states) is due to long-ranged nature of the Coulomb interaction. In the presence of a Fermi-gas, the Coulomb interaction is screened: The electric field polarizes the electron density. This can be described by the formation of electron-hole pairs, forming electric dipoles, that oppose the electric field. This effect is described by a momentum- and frequency-dependent dielectric constant. The resulting screened Coulomb interaction is replaced by an approximate **Yukawa potential**[55] with finite range. The picture just described is the essence of the so-called **random-phase approximation (RPA)** [50, 51, 52]. Screening removes the infinite slope of the energy bands at the Fermi level, which was an artifact of the Hartree-Fock approximation.

   Furthermore, screening generally decreases the net quasiparticle shift compared to the Hartree-Fock description. Thus it affects the **band width** of metals, the energy distance from the bottom of the valence band to the Fermi level. For potassium, the band width of the free-electron gas is 2 eV, somewhat larger than the experimental result of 1.5-1.6 eV. The Hartree-Fock approximation yields a far too large value of 5.3 eV. (See lecture notes by Wolf-Dieter Schöne. 2001)

4. **Life-time broadening:** An interacting electron travelling through an electron gas may collide with other electrons and thus transfer energy and momentum to electron-hole excitations in the surrounding electron gas. This energy dissipation acts like an effective friction which is responsible for the finite conductivity.

   The same effect results in a life-time broadening of the delta peaks $\delta(\epsilon - \epsilon(k))$ of the k-resolved spectral function. The electron level hybridizes with electron-hole excitations and mixes the

[55] A Yukawa potential has the form

$$v(\vec{r}) = \frac{C}{|\vec{r}|} e^{-\lambda|\vec{r}|} \tag{2.135}$$

where C is some prefactor and $1/lambda$ is the range of the interaction.

electron-hole excitations into the electron spectral function.

When one adds or removes an electron during spectroscopy, one may simultaneously create an electron-hole pair. Its energy affects the addition- or removal energy. Thus, instead of a single energy level, there are many possible energy levels, which describe the addition or removal of an electron in combination with a formation or recombination of an electron-hole pair. In the spectral function one observes a broadening of the original delta-peak at $\epsilon(\vec{k})$.

The total weight of the peak is conserved because of the **charge sum rule**[56]

Editor: Include a figure showing the life-time broadening in a Fermi liquid.

5. **Satellites and plasmons:** Satellites are spectral features, which are separated from the main electron addition and removal energies as sketched in figure 2.7. They are due to the mixing of one-particle excitations with other particle-number conserving excitations. In the free-electron gas, an example for such a particle-number conserving excitation is a **plasmon**, a kind of collective charge fluctuation. If the electron removal leaves another excitation behind, the energy of the latter adds to the excitation energy. Therefore, additional spectral features are observed for the composite excitations at energies corresponding to the sum of the energies of its contributions.

   Due to the charge sum rule, the total weight of the spectrum of an orbital must sum up to one. The weight lost to the satellite is lost from the main peak. This leads to the so-called **quasi-particle weight** Z, which is less than one.

   A minimal model for a satellite is the topic of the exercise 9.4.1 on p. 291.

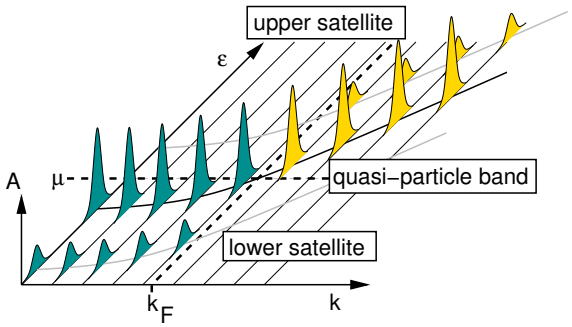


Fig. 2.7: Spectral function $A(\epsilon, k)$ of the free-electron gas with a single particle-conserving excitation with energy Δ and zero momentum producing satellite bands. The green shaded region denotes the occupied part of the spectral function, while the yellow shaded region denotes the unoccupied part. (This figure is repeated as figure 9.3.

   A spectral function of the free-electron gas with the satellite due to plasmons is shown in Caruso et al.[53]. (`https://doi.org/10.48550/arXiv.1606.08573.pdf`) The satellite structure of silicon has been investigated, both experimentally and theoretically, by Lischner et al. [54].

   Editor: see `Figs/Fortran/Lundquist/src/code.f90`

6. **Phase transitions:** (Ferromagnet, Mott insulator?) If the interaction becomes large enough, the changes are not only gradual, but abrupt. The system undergoes phase transitions.

   Among the phase transitions and corresponding effects are

   - Ferromagnet, Antiferromagnet

[56] As the weight of the original orbital is decreased by admixing the excitation, the electron-hole pair will also obtain a contribution from the electron removal or electron addition. The net weight of the electron removal or addition is conserved.

- Mott insulator
- Superconductor
- Kondo effect
- colossal magnetoresistance

Editor: include a figure showing the band structure or the density of states after a phase transition. Mott insulator, Ferromagnet, antiferromagnet or something.

2.7 What is the Hartree-Fock approximation?

Some confusion is caused because the name **Hartree-Fock approximation** is used in different contexts for quite distinct concepts. Worse, closely related theories use different names and fairly different theories appear similar to what is called Hartree-Fock approximation.

The common ground for all such theories is that the energy eigenstates are Slater determinants as opposded to superpositions of several Slater determinants.

The versions of Hartree-Fock approximations can be divided into two groups:

- One group targets the ground state or the thermal ensemble. It aims at thermodynamics or the equilibrium properties of a material. This group can be divided further into theories that use single wave functions (i.e. pure states) and those dealing with ensembles.
- The other group targets excited states and aims at spectral properties.

Let me briefly list various concepts of Hartree-Fock approximations.

- One version of the Hartree-Fock approximation is connected to first-order perturbation theory in the interaction. The wave functions in this description are those of the non-interacting system, which are Slater determinants. This works for both, ground- and excited states.
- Probably the most commen version of the Hartree-Fock approximation targets the zero-temperature ground state. The ground state is the "best possible" Slater determinant, namely the one that minimizes the total energy $\langle\Phi|\hat{h}+\hat{W}|\Phi\rangle$ including the interaction. Because the true ground-state energy is the minimum for all wave functions including superpositions of Slater determinants, this Hartree-Fock approximation provides a rigorous upper bound for the ground-state total energy.

  The limitation to a single Slater determinant can produce artifacts, so-called broken-symmetry states. The symmetry is restored by using ensembles of several Slater determinants as in the zero-temperature limit of the thermal single-determinant approximation (TSDA) and of the thermal Hartree-Fock approximation (THFA).
- The thermal single-determinant approximation (TSDA) extends the zero-temperature Hartree-Fock approximation to finite temperatures. Rather than optimizing a single Slater determinant, the TSDA optimizes a thermal ensemble of Slater determinant so that it minimizes the grand potential $\Omega_{T,\mu}$. The grand potential obtained from the TSDA is thus a rigorous upper bound for the true grand potential.
- The thermal Hartree-Fock approximation (THFA) extends the zero-temperature Hartree-Fock approximation to finite temperatures like the TSDA, but it furthermore requires, in addition, the **correlated occupation-number fluctuations** to vanish. In contrast to the TSDA, the THFA is widely distributed. Also the THFA provides a rigorous upper bound to the true grand potential and furthermore to that of the TSDA.

For a given ground state or thermal ensemble, several ways are available to calculate excitation spectra on the level of Slater determinants.

- The conventional Hartree-Fock approximation approximates the excited states by the Slater determinants formed from the eigenstates of the Fock operator. One can construct a many-particle Hamiltonian $\hat{H}^{HF}$, which produces the equilibrium ensemble ensemble and the mean-field approximation for the excited states as follows:

$$\hat{H}^{HF} = \sum_{\vec{\sigma}} |\vec{\sigma}\rangle \left(\Delta + \underbrace{\langle\vec{\sigma}|\hat{h} + \hat{V}_H^{(\vec{f})} + \hat{V}_X^{(\vec{f})}|\vec{\sigma}\rangle}_{\sum_n \sigma_n \epsilon_n^{\vec{f}}}\right) \langle\vec{\sigma}|$$

$$\text{with} \quad \Delta \stackrel{\text{def}}{=} \sum_{\vec{\sigma}'} P_{\vec{\sigma}',T,\mu}\big(\langle\vec{\sigma}'|\hat{h} + \hat{W}|\vec{\sigma}'\rangle - \langle\vec{\sigma}'|\hat{h} + \hat{V}_H + \hat{V}_X|\vec{\sigma}'\rangle\big) \tag{2.136}$$

  and $f_n = \sum_{\vec{\sigma}} P_{\vec{\sigma},T,\mu}\sigma_n$. Similar to non-interacting electrons, the energies of the HFA are thus obtained by summing over the occupied energy levels. Δ is a global shift of the excitation energies, which ensures that the ground-state energy of the HF approximation is recovered as the ground state of $\hat{H}^{HF}$, i.e. $E_G = \langle\Phi_G^{HF}|\hat{H}^{HF}|\Phi_G^{HF}\rangle = \langle\Phi_G^{HF}|\hat{h} + \hat{W}|\Phi_G^{HF}\rangle$.

- More rigorous is the averaged-phase approximation (APA). It uses the same excited-state wave functions $|\vec{\sigma}\rangle$ as the Hartree-Fock approximation, but it includes the correct interaction energy.

$$\hat{H}^{APA} = \sum_{\vec{\sigma}} |\vec{\sigma}\rangle \langle\vec{\sigma}|\hat{h} + \hat{W}|\vec{\sigma}\rangle \langle\vec{\sigma}| \tag{2.137}$$

  Note, however that the APA can be defined for an arbitrary orthonormal one-particle basisset. Using the natural orbitals of the thermal Hartree-Fock approximation (THFA) is just one of the possible choices. Any many-particle state (or ensemble) has a set of natural orbitals, which in turn can be used to define a specific version of the APA.

2.8 Beyond Slater determinants

Slater determinants are more easily understood than entangled many-particle wave functions, because they can be traced back to one-particle orbitals. Ensembles of Slater determinants are more easily understood than entangled many-particle wave functions, because they are related to a classical average over sets of configurations (Slater determinants). Thus, a description is desirable, that firstly approximates a many-particle wave function by an ensemble of Slater determinants and secondly includes the missing entanglement as additional quantum feature.

This goal has one caveat: An ensemble of states is fundamentally different from a superposition of states. The more important it is, not to mix up these puzzling quantum effects with familiar effects already present in classical ensembles. The goal of this section is to provide a "language" to discuss this topic in a clearcut manner.

There is a useful physical picture behind the comparison of ensembles and superpositions of Slater determinants. While thermal ensembles exhibit thermally created electron hole pairs, interacting system exhibit, in addition, quantum fluctuations, which are due to the Coulomb interaction. Like the zero-point vibrations of a harmonic oscillator, the quantum fluctuations persist even at zero temperature. These fluctuations can be attributed to electron-hole pairs, which screen the Coulomb interaction and thus lower the energy of the interacting electrons.

Consider a general many-particle wave function

$$|\Phi\rangle = \sum_{\vec{\sigma}} |\vec{\sigma}\rangle c_{\vec{\sigma}}\,, \tag{2.138}$$

which is expanded in a complete set of Slater determinants $|\vec{\sigma}\rangle$. In this section, the Slater determinants are built from the **natural orbitals**[57] , Eq. 2.14, $|\varphi_n\rangle$ of the many-particle wave function.

[57] The natural orbitals are the eigenstates of the one-particle-reduced density matrix.

The energy is

$$E \stackrel{\text{def}}{=} \langle\Phi|\hat{h}+\hat{W}|\Phi\rangle \stackrel{\text{Eq. 2.138}}{=} \sum_{\vec{\sigma},\vec{\sigma'}} c^*_{\vec{\sigma}} c_{\vec{\sigma'}} \langle\vec{\sigma}|\hat{h}+\hat{W}|\vec{\sigma'}\rangle$$

$$= \overbrace{\underbrace{\sum_{\vec{\sigma}} \underbrace{c^*_{\vec{\sigma}} c_{\vec{\sigma}}}_{P_{\vec{\sigma}}} \langle\vec{\sigma}|\hat{h}+\hat{W}|\vec{\sigma}\rangle}_{\text{ensemble of Slater determinants}}}^{\text{diagonal in } \vec{\sigma},\vec{\sigma'}} + \overbrace{\underbrace{\sum_{\vec{\sigma},\vec{\sigma'}:\vec{\sigma}\neq\vec{\sigma'}} \underbrace{c^*_{\vec{\sigma}} c_{\vec{\sigma'}}}_{\sqrt{P_{\vec{\sigma}}P_{\vec{\sigma'}}}e^{i(\phi_{\vec{\sigma'}}-\phi_{\vec{\sigma}})}} \langle\vec{\sigma}|\hat{h}+\hat{W}|\vec{\sigma'}\rangle}_{\text{entanglement energy}}}^{\text{off diagonal in } \vec{\sigma},\vec{\sigma'}} \tag{2.139}$$

The absolute squares of the coefficients $c_{\vec{\sigma}}$ act like probabilities $P_{\vec{\sigma}}$ of the orthonormal set of Slater determinants: They are positive semi-definite and they add up to one. The coefficients $c_{\vec{\sigma}} = \sqrt{P_{\vec{\sigma}}}e^{i\phi_{\vec{\sigma}}}$ can be expressed by their absolute value $\sqrt{P_{\vec{\sigma}}}$ and a phase factor $e^{i\phi_{\vec{\sigma}}}$.

The decomposition allows us to compare a **pure state** [58] $|\Phi\rangle$ with an ensemble $\{(P_{\vec{\sigma}}, |\vec{\sigma}\rangle)\}$ of Slater determinants. A pure state can be represented as **superposition** of Slater determinants. A superposition is very different from an ensemble, even if it consist of the same states: This is already evident from the entropy: A pure state has zero entropy, while an ensemble has a non-zero entropy, unless it is a pure state.

The comparison between a pure state and an ensemble of Slater determinants is useful, (1) because the energy of an ensemble of Slater determinants more easy to evaluate than that of the superposition and (2) because the ensemble captures already the dominant energy contribution. The division of the energy in Eq. 2.139 above allows a systematic comparison between effective one-particle theories and many-particle quantum mechanics.

As shown above in Eq. 2.63, the energy of an ensemble of Slater determinants can further be divided into the mean-field energy and the energy of the correlated occupation-number fluctuations. Thus, the energy expectation value of an arbitrary many-particle wave functions can be decomposed into the following three contributions, namely the **mean-field energy** , the energy due to **correlated occupation-number fluctuations**, and the **entanglement energy**. Remember, though, the requirement that the Slater determinants used in this analysis are made from natural orbitals!

$$E = \langle\Phi|\hat{h}+\hat{W}|\Phi\rangle$$

$$= \underbrace{\overbrace{\sum_{n=1}^{\infty} f_n \langle\varphi_n|\hat{h}|\varphi_n\rangle}^{\text{one-particle energy}} + \overbrace{\frac{1}{2}\int d^3r \int d^3r' \, \frac{e^2 n(\vec{r}) n(\vec{r'})}{4\pi\epsilon_0|\vec{r}-\vec{r'}|}}^{\text{Hartree energy}} \overbrace{-\frac{1}{2}\int d^4x \int d^4x' \, \frac{e^2 \rho^{(1)}(\vec{x},\vec{x'})\rho^{(1)}(\vec{x'},\vec{x})}{4\pi\epsilon_0|\vec{r}-\vec{r'}|}}^{\text{exchange energy}}}_{\text{mean-field energy}}$$

$$+ \underbrace{\frac{1}{2}\sum_{m,n=1;m\neq n}^{\infty} \overbrace{\left(\langle\sigma_m\sigma_n\rangle - \langle\sigma_m\rangle\langle\sigma_n\rangle\right)}^{\sum_{\vec{\sigma}} P_{\vec{\sigma}}\sigma_m\sigma_n - \left(\sum_{\vec{\sigma}} P_{\vec{\sigma}}\sigma_m\right)\left(\sum_{\vec{\sigma}} P_{\vec{\sigma}}\sigma_n\right)} \left(\langle\varphi_m\varphi_n|\hat{W}|\varphi_m\varphi_n\rangle - \langle\varphi_m\varphi_n|\hat{W}|\varphi_n\varphi_m\rangle\right)}_{\text{energy due to correlated occupation-number fluctuations}}$$

$$+ \underbrace{\sum_{\vec{\sigma},\vec{\sigma'}:\vec{\sigma}\neq\vec{\sigma'}} \sqrt{P_{\vec{\sigma}}P_{\vec{\sigma'}}}e^{i(\phi_{\vec{\sigma'}}-\phi_{\vec{\sigma}})}\langle\vec{\sigma}|\hat{h}+\hat{W}|\vec{\sigma'}\rangle}_{\text{entanglement energy}} \tag{2.140}$$

1. The first line denoted as **mean-field energy** is the energy expression used in the Hartree-Fock approximation. However, the occupations and natural orbitals differ from those of thermal Hartree-Fock approximation (THFA). Rather than thermally excited electron-hole pairs present in the finite-temperature ensemble, the correlated many-particle wave function has quantum

[58] A pure state corresponds to a single many-particle wave function as opposed to an ensemble, which contains many micro states along with their probabilities. A pure state can also be described as an ensemble with probability one for a specific many-particle wave function.

fluctuations. The quantum fluctuations may, for example, be electron-hole pairs formed to screen the Coulomb interaction between electrons.

2. The second term describes the contribution from **correlated occupation-number fluctuations**. They vanish for a single Slater determinant and, per construction, for the equilibrium ensemble of the thermal Hartree-Fock approximation. However, they are present in (1) a general ensemble of Slater determinants and (2) in a general many-particle wave function or their ensembles.

   The factors $\langle\varphi_m,\varphi_n|\hat{W}|\varphi_m,\varphi_n\rangle - \langle\varphi_m,\varphi_n|\hat{W}|\varphi_n,\varphi_m\rangle$ are non-negative for all values (m,n)[59] and they vanish for $m=n$. They are large for electron pairs with opposite spin, because, for pairs with equal spin, the exchange term (2nd) counteracts the Hartree term (1st). In contrast, for electron pairs with opposite spin, the exchange term vanishes, while the Hartree term maintains its full weight.

   The correlated occupation-number fluctuations $\sum_{\vec{\sigma}} P_{\vec{\sigma}}(\sigma_m - f_m)(\sigma_n - f_n)$ vanish

   - for completely filled $f_n = 1$ and completely empty $f_n = 0$ orbitals, and
   - for statistically independent occupations, i.e. for

$$\Big(\langle\sigma_m\sigma_n\rangle = \Big) \sum_{\vec{\sigma}} P_{\vec{\sigma}}\sigma_m\sigma_n = \underbrace{\Big(\sum_{\vec{\sigma}} P_{\vec{\sigma}}\sigma_m\Big)}_{f_m}\underbrace{\Big(\sum_{\vec{\sigma}} P_{\vec{\sigma}}\sigma_n\Big)}_{f_n}\Big(= \langle\sigma_m\rangle\langle\sigma_n\rangle\Big) \tag{2.141}$$

   For a given set of occupations $f_n = \sum_{\vec{\sigma}} P_{\vec{\sigma}}\sigma_m$, a wave function with small **double occupancy**

$$d_{m,n} \stackrel{\text{def}}{=} \sum_{\vec{\sigma}} P_{\vec{\sigma}}\sigma_m\sigma_n\Big(= \langle\sigma_m\sigma_n\rangle\Big) \tag{2.142}$$

   will have a lower energy. That is, electrons with strong Coulomb repulsion try to get out of each other's way. The role of correlated occupation-number fluctuations and the double occupancy are discussed in more detail in appendix G.3 on p. 611.

3. The third term describes the **entanglement** of the Slater determinants. Let me call it **entanglement energy**. It describes the **hybridization**[60] of Slater determinants. This is the only term that depends on the relative phases of the coefficients ($c_{\vec{\sigma}}$ in Eq. 2.138) of different Slater determinants in the wave function.

   Imagine a special case with only two relevant Slater determinants $|\vec{\sigma}_1\rangle$ and $|\vec{\sigma}_2\rangle$, so that the many-particle wave functions have the form $|\Phi\rangle = |\vec{\sigma}_1\rangle c_1 + |\vec{\sigma}_2\rangle c_2$. Let us treat the two Slater determinants as basisset in Fock space and evaluate the matrix elements of the interacting 2×2 Hamiltonian. (assuming orthonormality)

$$H_{\alpha,\beta} = \langle\vec{\sigma}_\alpha|\hat{h} + \hat{W}|\vec{\sigma}_\beta\rangle \qquad \text{for } \alpha,\beta \in \{1,2\}. \tag{2.143}$$

   We obtain a 2×2 Schrödinger equation.[61] We will obtain two eigenvectors $\vec{c}_\pm$ for two different energies $E_\pm$, where $\pm \in \{+,-\}$ identifies one or the other eigenstate. The complex coefficients

[59] This follows from the fact that the electrostatic energy of any two-particle system is positive. This is also true if the two electrons are in a two-particle Slater determinant with the two orbitals $|\varphi_m\rangle$ and $|\varphi_n\rangle$. The factor mentioned is twice the Coulomb energy of this Slater determinant.

[60] Hybridization is the formation of a superposition of orbitals to form a bond orbital or an antibonding orbital. The difference between a bond and an antibond can be attributed to a phase factor between the two orbitals forming the bonding and antibonding orbitals. The bond orbital of a hydrogen molecule is $(|\chi_1\rangle+\chi_2\rangle)/\sqrt{2}$ while that of an antibond is $(|\chi_1\rangle-\chi_2\rangle)/\sqrt{2}$. The plus and minus signs can be described by a relative phase factor $e^{i\varphi}$ with a real-valued phase of $\varphi = 0$ for the bond and $\varphi = \pi$ for the antibond. In the present case, it is Slater determinants rather than one-particle states that hybridize. The underlying concept is the matrix diagonalization, which is common to both cases.

[61] The problem of diagonalizing the 2×2 matrix is the same as that for the diatomic molecule. The difference to the diatomic molecule is that the Hamiltonian is formed from many-particle Slater determinants and the Hamiltonian contains also the interaction $\hat{W}$. As in the diatomic molecule, there will be **level repulsion** and superpositions of the two Slater determinants analogous to the bonding and the antibonding states of the diatomic molecule.

of the eigenvectors $c_{\alpha,\pm} = \sqrt{P_\pm} e^{i\phi_{\alpha,\pm}}$ contain the phase relation $\phi_{2,\pm} - \phi_{1,\pm}$ between the two Slater determinants. When the two Slater determinants with different phases contribute with distinct weight, i.e. $P_{\vec{\sigma}_1} \neq P_{\vec{\sigma}_2}$, there will be a finite entanglement energy.

The entanglement energy is the energy gain from optimizing the relative phases of the Slater determinants as compared to an averaged phases. The neglect of the entanglement energy can be described as an **averaged-phase approximation** as described in appendix G.2 on p. 610.

An estimate of the entanglement energy based on second-order perturbation theory is given in Eq. N.29 on p. 762.

$$\Delta E_{\text{entangle}} \approx -\frac{1}{2} \sum_{\vec{\sigma},\vec{\sigma}'} \Big(P_{\vec{\sigma}} - P_{\vec{\sigma}'} \Big) \frac{\big| \langle \vec{\sigma} | \hat{h} + \hat{W} | \vec{\sigma}' \rangle \big|^2}{\langle \vec{\sigma} | \hat{h} + \hat{W} | \vec{\sigma} \rangle - \langle \vec{\sigma}' | \hat{h} + \hat{W} | \vec{\sigma}' \rangle} \tag{2.144}$$

2.9 Summary

- The eigenstates of non-interacting Hamiltonians $\hat{h}$ are Slater determinants $|\vec{\sigma}\rangle$

$$\hat{h}|\varphi_n\rangle = |\varphi_n\rangle \epsilon_n \qquad \text{and} \qquad \hat{h}|\vec{\sigma}\rangle = |\vec{\sigma}\rangle \underbrace{\sum_n \sigma_n \epsilon_n}_{E_{\vec{\sigma}}} \tag{2.145}$$

- expectation value of the interacting Hamiltonian with a Slater determinant.
- one-particle operator, one-particle-at-a-time operator, two-particle operator
- expectation values of one-particle-at-a-time operators are obtained as sum over occupied one-particle orbitals.

$$\langle A \rangle = \langle \vec{\sigma} | \hat{A} | \vec{\sigma} \rangle = \sum_n \sigma_n \langle \varphi_n | \hat{A} | \varphi_n \rangle = \text{Tr}[\hat{\rho}^{(1)} \hat{A}] \tag{2.146}$$

- Hartree- and exchange energy. Hartree- and exchange potentials.
- occupations and natural orbitals and their relation to one-particle-reduced density matrix $\hat{\rho}^{(1)}$.
- ensemble, probabilities, micro states and their relation to the von-Neumann density matrix.
- von-Neumann and Boltzmann entropy
- exchange hole (some properties)
- Thermal Hartree-Fock Approximation
- grand potential in the thermal Hartree-Fock approximation
- Fock operator.
- mean-field energy, Correlated occupation-number fluctuations, entanglement energy.
- spectroscopy: photoemission, inverse photoemission, optical absorption
- one-particle excitations: Electron addition and removal. Two-particle excitations: e.g. formation of an electron-hole pair.
- one-particle spectral function or density-of-states. Relation to the Fock operator. Thermal broadening and mean-field approximation.
- Two-particle excitations have, in addition, a correction from the interaction of the two particles, such as the Coulomb attraction of electrons and holes.

2.10 Further reading

Let me refer to the appendix G on p. 603, where I collected some material that I found interesting in this context.

2.11 Home study and Practice

2.11.1 Boltzmann entropy and Fermi distribution

Introduction

This exercise serves to strengthen the understanding of the origin of the Fermi distribution function and its connection to the Boltzmann entropy. The second part shall refresh how to deal with functions of operators.

Problem

Derive the Fermi-distribution function as thermal occupation of non-interacting fermions. The Hamiltonian of a non-interacting system can be represented in terms of its eigenstates and eigenvalues as $\hat{h} = \sum_n |\varphi_m\rangle \bar{\epsilon}_n \langle\varphi_n|$.

1 Minimize the grand canonical potential of a non-interacting system with the Boltzmann entropy

$$S^B[\{f_n\}] = -k_B \sum_n \Big[f_n \ln(f_n) + (1 - f_n) \ln(1 - f_n) \Big] \tag{2.147}$$

and show that the resulting thermal occupations are identical to the Fermi distribution.

2 Show, how the Boltzmann entropy expressed in terms of occupations is obtained from the more general expression using the one-particle-reduced density matrix

$$S^B[\hat{\rho}^{(1)}] = -k_B \mathrm{Tr} \Big[\hat{\rho}^{(1)} \ln(\hat{\rho}^{(1)}) + (\hat{1} - \hat{\rho}^{(1)}) \ln(\hat{1} - \hat{\rho}^{(1)}) \Big] \tag{2.148}$$

Solution

1 Minimize the grand canonical potential of a non-interacting system with the Boltzmann entropy

$$S^B[\{f_n\}] = -k_B \sum_n \Big[f_n \ln(f_n) + (1-f_n)\ln(1-f_n) \Big] \tag{2.149}$$

and show that the resulting thermal occupations are identical to the Fermi distribution.

$$\begin{aligned}
\Omega_{T,\mu} &= \min_{\{f_n\}} \Big\{ \sum_n f_n \bar{\epsilon}_n - T S^B[\{f_n\}] - \mu N[\{f_n\}] \Big\} \\
&= \min_{\{f_n\}} \Big\{ \sum_n f_n \bar{\epsilon}_n + k_B T \sum_n \Big[f_n \ln(f_n) + (1-f_n)\ln(1-f_n) \Big] - \mu \sum_n f_n \Big\} \\
\delta\Omega_{T,\mu} &= \sum_n \delta f_n \Big\{ \bar{\epsilon}_n + k_B T \Big[\ln(f_n) + f_n \frac{1}{f_n} - \ln(1-f_n) - (1-f_n)\frac{1}{1-f_n} \Big] - \mu \Big\} \stackrel{!}{=} 0 \\
0 &= \bar{\epsilon}_n + k_B T \ln\left[\frac{f_n}{1-f_n} \right] - \mu \\
\ln\Big[\frac{f_n}{1-f_n} \Big] &= -\frac{1}{k_B T}(\bar{\epsilon}_n - \mu) \\
f_n &= \mathrm{e}^{-\frac{1}{k_B T}(\bar{\epsilon}_n - \mu)} \Big(1 - f_n \Big) \\
f_n &= \frac{\mathrm{e}^{-\frac{1}{k_B T}(\bar{\epsilon}_n - \mu)}}{1 + \mathrm{e}^{-\frac{1}{k_B T}(\bar{\epsilon}_n - \mu)}} = \frac{1}{1 + \mathrm{e}^{+\frac{1}{k_B T}(\epsilon_n - \mu)}} = f_{T,\mu}(\bar{\epsilon})
\end{aligned} \tag{2.150}$$

This is the Fermi distribution function.

2 Show, how the Boltzmann entropy expressed in terms of occupations is obtained from the more general expression using the one-particle-reduced density matrix

$$S^B[\hat{\rho}^{(1)}] = -k_B \mathrm{Tr}\Big[\hat{\rho}^{(1)} \ln(\hat{\rho}^{(1)}) + (\hat{1} - \hat{\rho}^{(1)}) \ln(\hat{1} - \hat{\rho}^{(1)}) \Big] \tag{2.151}$$

I represent the one-particle-reduced density matrix in term of occupations and natural orbitals

$$\hat{\rho}^{(1)} = \sum_n |\varphi_n\rangle f_n \langle\varphi_n| \tag{2.152}$$

$$\begin{aligned}
S^B[\hat{\rho}^{(1)}] &= -k_B \, \mathrm{Tr}\Big[\hat{\rho}^{(1)} \ln(\hat{\rho}^{(1)}) + (\hat{1} - \hat{\rho}^{(1)}) \ln(\hat{1} - \hat{\rho}^{(1)}) \Big] \\
&= -k_B \mathrm{Tr}\Big[\Big(\sum_n |\varphi_n\rangle f_n \langle\varphi_n| \Big) \ln\Big(\sum_n |\varphi_n\rangle f_n \langle\varphi_n| \Big) \\
&\quad + \Big(\sum_n |\varphi_n\rangle (1-f_n) \langle\varphi_n| \Big) \ln\Big(\sum_n |\varphi_n\rangle (1-f_n) \langle\varphi_n| \Big) \Big]
\end{aligned} \tag{2.153}$$

Now, I exploit that a function $g(x)$ of an operator $\hat{x} = \sum_n |\varphi_n\rangle x_n \langle\varphi_n|$ in its diagonal form has the same eigenstates and its eigenvalues are the functions of the eigenvalues of the operator in the argument.

$$g\Big(\sum_n |\varphi_n\rangle x_n \langle\varphi_n| \Big) = \sum_n |\varphi_n\rangle g(x_n) \langle\varphi_n| \tag{2.154}$$

This statement follows from the similar relation for power-series expansions

$$g(x) = \sum_j a_j x^j \tag{2.155}$$

which can be proven recursively. The step from a power series expansion to general functions is done by using (local) Taylor expansions of the function g.

$$\begin{aligned} S^B[\hat{\rho}^{(1)}] &\overset{\text{Eq. 2.153}}{=} -k_B \mathrm{Tr}\Big[\Big(\sum_n |\varphi_n\rangle f_n \langle\varphi_n|\Big)\Big(\sum_{n'} |\varphi_{n'}\rangle \ln(f_{n'})\langle\varphi_{n'}|\Big) \\ &\quad + \Big(\sum_n |\varphi_n\rangle (1-f_n)\langle\varphi_n|\Big)\Big(\sum_{n'} |\varphi_{n'}\rangle \ln(1-f_{n'})\langle\varphi_{n'}|\Big)\Big] \\ &= -k_B \mathrm{Tr}\Big[\sum_{n,n'}\Big(|\varphi_n\rangle f_n \underbrace{\langle\varphi_n|\varphi_{n'}\rangle}_{\delta_{n,n'}} \ln(f_{n'})\langle\varphi_{n'}| + |\varphi_n\rangle(1-f_n)\underbrace{\langle\varphi_n|\varphi_{n'}\rangle}_{\delta_{n,n'}} \ln(1-f_{n'})\langle\varphi_{n'}|\Big)\Big)\Big] \end{aligned} \tag{2.156}$$

Finally, I exploit the orthonormality of the natural orbitals and resolve the trace.

$$\begin{aligned} S^B[\hat{\rho}^{(1)}] &= -k_B \mathrm{Tr}\Big[\sum_n |\varphi_n\rangle \Big(f_n \ln(f_n) + (1-f_n)\ln(1-f_n)\Big)\langle\varphi_n|\Big] \\ &= -k_B \sum_n \Big(f_n \ln(f_n) + (1-f_n)\ln(1-f_n)\Big) \end{aligned} \tag{2.157}$$

2.11.2 The hydrogen atom in the Hartree-Fock approximation

Introduction

This is a little but extremely useful exercise, which clarifies some notions regarding many-particle physics and the Hartree-Fock approximation. It may be surprising that we study the hydrogen atom in a course on solid-state theory. However, many concepts from solid state theory are already there in the hydrogen atom and the hydrogen atom is the minimal problem for quite a few solid-state effects.

The hydrogen atom represents Hubbard atom, the monomer of the Hubbard model. The Hubbard atom is thus the zero-coupling limit of the extended Hubbard model.

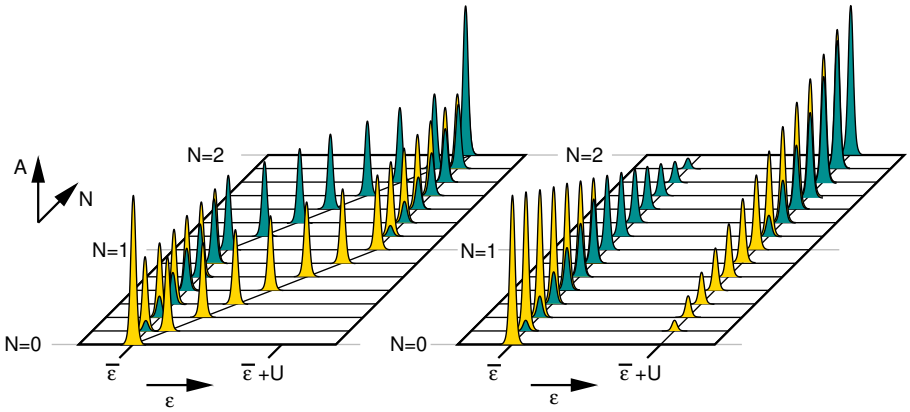


Fig. 2.8: Schematic figure of the spectral function $A_{tot}(\epsilon) = A_\uparrow(\epsilon) + A_\downarrow(\epsilon)$ of the Hubbard atom for several values of the particle number N. The occupied states are shown in green, while the unoccupied states are shown in yellow. On the left hand side, the spectral function from the mean-field Hartree-Fock approximation is shown. On the right-hand side the correct spectral function is shown. In the mean-field approximation the peaks have the same height, but their position adapts to the number of electrons. In the correct spectrum, the position of the peaks is independent of the number of electrons, but their weight adjusts.

Problem

We will use here hydrogen 1s orbitals as one-particle basisset for the hydrogen atom.

$$\chi_\sigma(\vec{r},\sigma') \overset{\text{Eq. D.60}}{=} \frac{1}{\pi a_0^3} e^{-|\vec{r}|/a_0} \delta_{\sigma,\sigma'} \tag{2.158}$$

The shape of the orbital is not important for the problem at hand and is provided only for the sake of completeness. The Bohr radius $a_0 = \frac{4\pi\epsilon_0\hbar^2}{e^2 m_e}$ and the Hartree $E_h = H = \frac{m_e e^4}{(4\pi\epsilon_0)^2\hbar^2}$, used below, are the units for length and energy in the Hartree-atomic-unit system. The **Hartree atomic units** are defined by[62] $\hbar = e = m_e = 4\pi\epsilon_0 = 1$.

The matrix elements for the hydrogen atom have been worked out in the appendix D.4 on p. 549.

The two states Eq. 2.158 are eigenstates of the non-interacting part $\hat{h}$ of the Hamiltonian.

$$\hat{h}|\chi_\alpha\rangle = |\chi_\alpha\rangle\bar{\epsilon} \qquad \text{with } \bar{\epsilon} = -\frac{1}{2}H \qquad \text{for } \alpha \in \{\uparrow,\downarrow\} \tag{2.159}$$

The value $\bar{\epsilon}$ has been set equal to the $\epsilon_{1s} = -\frac{1}{2}E_h$ level of the hydrogen atom (See table D.8 on p. 550). We used the energy unit **Hartree** $1E_h = m_e\left(e^2/(4\pi\epsilon_0\hbar)\right)^2 \approx 27.211$ eV from the **Hartree atomic unit system** defined by[63] $e = \hbar = m_e = 4\pi\epsilon_0 = 1$.

The interaction matrix element is

$$W_{\alpha,\beta,\gamma,\delta} \overset{\text{Eq. 2.30}}{=} \int d^4x \int d^4x' \, \frac{e^2 \chi^*_\alpha(\vec{x})\chi^*_\beta(\vec{x'})\chi_\gamma(\vec{x})\chi_\delta(\vec{x'})}{4\pi\epsilon_0|\vec{r}-\vec{r'}|} \qquad \text{with } U \overset{\text{def}}{=} W_{\uparrow,\uparrow,\uparrow,\uparrow} = \frac{5}{8}H \tag{2.160}$$

1 Determine all 2^4 interaction matrix elements:

2 Specify the Hartree and exchange energy for the two-particle state.

3 Determine the total energy of the zero-particle state $|0\rangle$, the one-particle states $|\uparrow\rangle$ and $|\downarrow\rangle$, and two-particle state $|\uparrow\downarrow\rangle$ of the hydrogen atom using the one-particle Hilbert space described above.

4 Write down the Fock operator for the four many-particle eigenstates of the hydrogen atom.

5 Editor: Check this: Plot the density of states projected onto one of the one-particle orbitals for a many-particle system at low temperature.

6 Compare the density of states of an ensemble of eigenstates of the hydrogen atom with that of the mean-field Fock operator.

Discussion

1 Determine all 2^4 matrix interaction matrix elements:

$$\begin{aligned} W_{\alpha,\beta,\gamma,\delta} &= \begin{cases} U & \text{for } \sigma_\gamma = \sigma_\alpha \text{ and } \sigma_\delta = \sigma_\beta \\ 0 & \text{else} \end{cases} \\ &= U\delta_{\alpha,\gamma}\delta_{\beta,\delta} \end{aligned} \tag{2.161}$$

[62] ϵ_0 is the electric constant, e is the elementary charge, m_e is the electron mass and $\hbar = h/(2\pi)$ is the reduced Planck constant.

[63] ϵ_0 is the electric constant, e is the elementary charge, m_e is the electron mass and $\hbar = h/(2\pi)$ is the reduced Planck constant.

The U-parameter is one of the **Kanamori parameters**.[19] (See appendix G.5.3 on p. 624) Kanamori defined a set of parameters with which the interaction-tensor matrix elements of, for example, d-orbitals of a transition metal ion can be expressed. The interaction of the d-shell ($\ell = 2$) has $10^4 = 10000$ matrix elements. However, they can all be expressed by Editor: four? (check!) independent Kanamori parameters. While the selection of a Kanamori parameter for a s-orbital shell is trivial, this is our first contact with this important concept.

2 Specify the Hartree and exchange energy for the two-particle state.

The two orbitals of the hydrogen atom are characterized by their spin quantum number, i.e. $\alpha \in \{\uparrow, \downarrow\}$. In the two-particle state, both orbitals are occupied so that $f_\uparrow = f_\downarrow = 1$.

$$
\begin{aligned}
n(\vec{r}) &= \sum_{\sigma\in\{\uparrow,\downarrow\}} \sum_{\alpha\in\{\uparrow,\downarrow\}} f_\alpha |\chi_\alpha(\vec{r},\sigma)|^2 \\
E_H &\overset{\text{Eq. 2.33}}{=} \frac{1}{2}\int d^3r \int d^3r' \frac{e^2 n(\vec{r}) n(\vec{r'})}{4\pi\epsilon_0 |\vec{r}-\vec{r'}|} \\
&= \frac{1}{2}\sum_{\alpha,\beta\in\{\uparrow,\downarrow\}} f_\alpha f_\beta \underbrace{\int d^4x \int d^4x' \frac{e^2 \chi_\alpha^*(\vec{x})\chi_\beta^*(\vec{x'})\chi_\alpha(\vec{x})\chi_\beta(\vec{x'})}{4\pi\epsilon_0|\vec{r}-\vec{r'}|}}_{W_{\alpha,\beta,\alpha,\beta}} \\
&= \frac{1}{2}\sum_{\alpha,\beta\in\{\uparrow,\downarrow\}} \underbrace{f_\alpha f_\beta}_{=1} \underbrace{W_{\alpha,\beta,\alpha,\beta}}_{U} \overset{\text{Eq. 2.161}}{=} 2U \\
\rho^{(1)}(\vec{x},\vec{x'}) &= \sum_{\alpha\in\{\uparrow,\downarrow\}} f_\alpha \chi_\alpha(\vec{x})\chi_\alpha^*(\vec{x'}) \\
E_X &\overset{\text{Eq. 2.36}}{=} -\frac{1}{2}\int d^4x \int d^4x' \frac{e^2 \rho^{(1)}(\vec{x},\vec{x'})\rho^{(1)}(\vec{x'},\vec{x})}{4\pi\epsilon_0|\vec{r}-\vec{r'}|} \\
&= -\frac{1}{2}\sum_{\alpha,\beta\in\{\uparrow,\downarrow\}} f_\alpha f_\beta \underbrace{\int d^4x \int d^4x' \frac{e^2 \chi_\alpha^*(\vec{x})\chi_\beta^*(\vec{x'})\chi_\beta(\vec{x})\chi_\alpha(\vec{x'})}{4\pi\epsilon_0|\vec{r}-\vec{r'}|}}_{W_{\alpha,\beta,\beta,\alpha}} \\
&= -\frac{1}{2}\sum_{\alpha,\beta\in\{\uparrow,\downarrow\}} \underbrace{f_\alpha f_\beta}_{=1} \underbrace{W_{\alpha,\beta,\beta,\alpha}}_{U\delta_{\alpha,\beta}} \overset{\text{Eq. 2.161}}{=} -U
\end{aligned}
\tag{2.162}
$$

3 Determine the total energy of the zero-particle state $|0\rangle$, the one-particle states $|\uparrow\rangle$ and $|\downarrow\rangle$, and two-particle state $|\uparrow\downarrow\rangle$ of the hydrogen atom using the one-particle Hilbert space described above.

The total energy can be evaluated using Eq. 2.39.

$$
\begin{aligned}
E_{|0\rangle} &= \langle 0|\hat{H}|0\rangle = 0 \\
E_{|\uparrow\rangle} &= \langle\uparrow|\hat{H}|\uparrow\rangle = \bar{\epsilon} = -\frac{1}{2}H \\
E_{|\downarrow\rangle} &= \langle\downarrow|\hat{H}|\downarrow\rangle = \bar{\epsilon} = -\frac{1}{2}H \\
E_{|\uparrow\downarrow\rangle} &= \langle\uparrow\downarrow|\hat{H}|\uparrow\downarrow\rangle = 2\bar{\epsilon} + U = -\frac{3}{8}H
\end{aligned}
\tag{2.163}
$$

4 Write down the Fock operator for the four many-particle eigenstates of the hydrogen atom.

The Fock operator is

$$\hat{F} = \hat{h} + \hat{V}_H + \hat{V}_X \tag{2.164}$$

with the Hartree potential $\hat{V}_H$ and the exchange potential $\hat{V}_X$, which depend on the density, respectively on the on-particle-reduced density matrix.

The density and one-particle-reduced density matrix is

$$\begin{aligned} n(\vec{r}) &= \sum_{\sigma\in\{\uparrow,\downarrow\}} \sum_{\alpha} f_\alpha \chi^*_\alpha(\vec{r},\sigma)\chi_\alpha(\vec{r},\sigma) \\ \rho^{(1)}(\vec{x},\vec{x'}) &= \sum_{\alpha} f_\alpha \chi_\alpha(\vec{x})\chi^*_\alpha(\vec{x'}) \end{aligned} \tag{2.165}$$

Below, I am using the projector functions $\langle\pi_\alpha|$ to represent the unit operator in an orbital basis $\{|\chi_\alpha\rangle\}$ as

$$\hat{1} = \sum_{\alpha,\beta} |\chi_\alpha\rangle S^{-1}_{\alpha,\beta}\langle\pi_\beta| = \sum_{\alpha} |\chi_\alpha\rangle \underbrace{\sum_{\beta} S^{-1}_{\alpha,\beta}\langle\chi_\beta|}_{=:\langle\pi_\alpha|} = \sum_{\alpha} |\chi_\alpha\rangle\langle\pi_\alpha| \tag{2.166}$$

With $S^{-1}_{\alpha,\beta}$, I denote the matrix elements of the inverse overlap matrix, which satisfy $\sum_\gamma S^{-1}_{\alpha,\gamma}\langle\chi_\gamma|\chi_\beta\rangle = \delta_{\alpha,\beta}$. If you find the notation with the projector functions $\langle\pi_\alpha|$ confusing, you can use the expression without the projector functions, but including the inverse overlap matrix.

$$\begin{aligned} \hat{V}_H &\overset{\text{Eq. 2.34}}{=} \int d^4x\, |\vec{x}\rangle \left(\int d^3r'\, \frac{e^2 n(\vec{r'})}{4\pi\epsilon_0|\vec{r}-\vec{r'}|} \right) \langle\vec{x}| \\ &\overset{\text{Eq. 2.166}}{=} \underbrace{\sum_\beta |\pi_\beta\rangle\langle\chi_\beta|}_{\hat{1}} \int d^4x\, |\vec{x}\rangle \int d^4x'\, \frac{e^2 \sum_\alpha f_\alpha \chi^*_\alpha(\vec{x'})\chi_\alpha(\vec{x'})}{4\pi\epsilon_0|\vec{r}-\vec{r'}|} \langle\vec{x}| \underbrace{\sum_\gamma |\chi_\gamma\rangle\langle\pi_\gamma|}_{\hat{1}} \\ &= \sum_{\beta,\gamma} |\pi_\beta\rangle \sum_\alpha f_\alpha \int d^4x \int d^4x'\, \frac{e^2 \chi^*_\beta(\vec{x})\chi^*_\alpha(\vec{x'})\chi_\gamma(\vec{x})\chi_\alpha(\vec{x'})}{4\pi\epsilon_0|\vec{r}-\vec{r'}|} \langle\pi_\gamma| \\ &= \sum_{\alpha,\beta,\gamma} |\pi_\beta\rangle f_\alpha \underbrace{W_{\beta,\alpha,\gamma,\alpha}}_{U\delta_{\beta,\gamma}\delta_{\alpha,\alpha}} \langle\pi_\gamma| \\ &\overset{\text{Eq. 2.161}}{=} \sum_\beta |\pi_\beta\rangle U \sum_\alpha f_\alpha \langle\pi_\beta| \end{aligned} \tag{2.167}$$

$$\begin{aligned} \hat{V}_X &\overset{\text{Eq. 2.37}}{=} -\int d^4x \int d^4x'\, |\vec{x}\rangle \frac{e^2 \rho^{(1)}(\vec{x},\vec{x'})}{4\pi\epsilon_0|\vec{r}-\vec{r'}|} \langle\vec{x'}| \\ &\overset{\text{Eq. 2.166}}{=} -\underbrace{\sum_\beta |\pi_\beta\rangle\langle\chi_\beta|}_{\hat{1}} \int d^4x\, |\vec{x}\rangle \int d^4x'\, \frac{e^2 \sum_\alpha \chi_\alpha(\vec{x}) f_\alpha \chi^*_\alpha(\vec{x'})}{4\pi\epsilon_0|\vec{r}-\vec{r'}|} \langle\vec{x'}| \underbrace{\sum_\gamma |\chi_\gamma\rangle\langle\pi_\gamma|}_{\hat{1}} \\ &= -\sum_{\beta,\gamma} |\pi_\beta\rangle \sum_\alpha f_\alpha \int d^4x \int d^4x'\, \frac{e^2 \chi^*_\beta(\vec{x})\chi^*_\alpha(\vec{x'})\chi_\alpha(\vec{x})\chi_\gamma(\vec{x'})}{4\pi\epsilon_0|\vec{r}-\vec{r'}|} \langle\pi_\gamma| \\ &= -\sum_{\alpha,\beta,\gamma} |\pi_\beta\rangle f_\alpha \underbrace{W_{\beta,\alpha,\alpha,\gamma}}_{U\delta_{\beta,\alpha}\delta_{\alpha,\gamma}} \langle\pi_\gamma| \\ &\overset{\text{Eq. 2.161}}{=} -\sum_\alpha |\pi_\alpha\rangle f_\alpha U \langle\pi_\alpha| \end{aligned} \tag{2.168}$$

The Fock operator $\hat{F}$ has the form

$$\hat{F} = \hat{h} + \hat{V}_H + \hat{V}_X = \sum_{\alpha\in\{\uparrow,\downarrow\}} |\pi_\alpha\rangle \Big(\bar{\epsilon} + U\Big(\sum_{\gamma\in\{\uparrow,\downarrow\}} f_\gamma \Big) - U f_\alpha \Big) \langle\pi_\alpha| \tag{2.169}$$

For the individual states, the Fock operator is

- For the vacuum state $|0\rangle$, the occupations $f_\uparrow = f_\downarrow = 0$ are zero. The Fock operator is

$$\hat{F} = |\pi_\uparrow\rangle \bar{\epsilon} \langle\pi_\uparrow| + |\pi_\downarrow\rangle \bar{\epsilon} \langle\pi_\downarrow| \tag{2.170}$$

- For the one-particle state $|\uparrow\rangle$ with a spin-up electron, the occupations are $f_\uparrow = 1$, $f_\downarrow = 0$.

$$\hat{F} = |\pi_\uparrow\rangle \bar{\epsilon} \langle\pi_\uparrow| + |\pi_\downarrow\rangle \Big(\bar{\epsilon} + U \Big) \langle\pi_\downarrow| \tag{2.171}$$

- For the one-particle state $|\downarrow\rangle$ with a spin-down electron, the occupations are $f_\uparrow = 0$, $f_\downarrow = 1$

$$\hat{F} = |\pi_\uparrow\rangle \Big(\bar{\epsilon} + U \Big) \langle\pi_\uparrow| + |\pi_\downarrow\rangle \bar{\epsilon} \langle\pi_\downarrow| \tag{2.172}$$

- For the two-particle state $|\uparrow\downarrow\rangle$, the occupations are $f_\uparrow = 1$, $f_\downarrow = 1$

$$\hat{F} = |\pi_\uparrow\rangle \Big(\bar{\epsilon} + U \Big) \langle\pi_\uparrow| + |\pi_\downarrow\rangle \Big(\bar{\epsilon} + U \Big) \langle\pi_\downarrow| \tag{2.173}$$

Lessons to be learned: We recognize, that the one-particle systems has two different energy levels, which are separated by the Coulomb repulsion U. The lower level is the energy gained by removing an electron, while the upper level is the energy required to add an electron. When an electron is added, also the Coulomb repulsion with the electron, which already resides on the atom, has to be overcome. The electron-addition energy is called **electron affinity** and the electron-removal energy is the **ionization potential**.

The spectral function for general interacting electrons is discussed below in section 9.2.

5 Plot the density of states projected onto one of the one-particle orbitals for a one-particle system at low temperature.

The density-of-states of non-interacting electrons has been used previously in section 1.5.5. See *ΦSX: Introduction to Solid-State Theory* for more information.[1].

The density-of-states for an ensemble of many-particle states is obtained as the ensemble average over the density-of-states functions calculated for the eigenstates of the many-particle Hamiltonian.

$$D(\epsilon) = \sum_q P_q D^{(q)}(\epsilon) \tag{2.174}$$

where $D^{(q)}$ is the density of states obtained for the particular many-particle wave function $|\Psi_q\rangle$.

For a non-interacting electron gas, the spectrum is the same for all many-particle states.

Therefore, the density of states is simply a sum of δ-functions on the eigenstates of the one-particle Hamiltonian. In the Hartree-Fock approximation, the density-of-states is given by the eigenvalues of the Fock operator. Because the Fock operator depends on the particular Slater-determinant chosen, the ensemble average needs to be performed.

The probability for the system to be in one of the many-particle states is

$$\begin{aligned}
P_{|\Phi\rangle} &= \frac{1}{Z}\mathrm{e}^{-\beta(E_{|\Phi\rangle}-\mu N_{|\Phi\rangle})} \\
&= \frac{1}{Z}\times\begin{cases}1 & \text{for } |\Phi\rangle = |0\rangle \\ \mathrm{e}^{-\beta(\bar{\epsilon}-\mu)} & \text{for } |\Phi\rangle = |\uparrow\rangle \text{ or } |\Phi\rangle = |\downarrow\rangle \\ \mathrm{e}^{-\beta(2\bar{\epsilon}+U-2\mu)} & \text{for } |\Phi\rangle = |\uparrow\downarrow\rangle\end{cases} \\
Z &= \sum_{\Phi\in\{|0\rangle,|\uparrow\rangle,|\downarrow\rangle,|\uparrow,\downarrow\rangle\}} \mathrm{e}^{-\beta(E_{|\Phi\rangle}-\mu N_{|\Phi\rangle})} \\
&= \mathrm{e}^{-\beta(0-\mu 0)} + \mathrm{e}^{-\beta(\bar{\epsilon}-\mu)} + \mathrm{e}^{-\beta(\bar{\epsilon}-\mu)} + \mathrm{e}^{-\beta(2\bar{\epsilon}+U-2\mu)} \\
&= \left(1+\mathrm{e}^{-\beta(\bar{\epsilon}-\mu)}\right)^2 + \mathrm{e}^{-\beta(2\bar{\epsilon}+U-2\mu)} - \mathrm{e}^{-\beta(2\bar{\epsilon}-2\mu)} \\
&= \left(1+\mathrm{e}^{-\beta(\bar{\epsilon}-\mu)}\right)^2 + \mathrm{e}^{-\beta(2\bar{\epsilon}-2\mu)}\left(\mathrm{e}^{-\beta U}-1\right)
\end{aligned} \tag{2.175}$$

The density of states is the weighted sum of the density of states obtained from the many-particle states in the ensemble.

$$\begin{aligned}
D_\uparrow(\epsilon) &= P_{|0\rangle}\delta(\epsilon-\bar{\epsilon}) + P_{|\uparrow\rangle}\delta(\epsilon-\bar{\epsilon}) + P_{|\downarrow\rangle}\delta(\epsilon-\bar{\epsilon}-U) + P_{|\uparrow\downarrow\rangle}\delta(\epsilon-\bar{\epsilon}-U) \\
&= \left(P_{|0\rangle}+P_{|\uparrow\rangle}\right)\delta(\epsilon-\bar{\epsilon}) + \left(P_{|\downarrow\rangle}+P_{|\uparrow\downarrow\rangle}\right)\delta(\epsilon-\bar{\epsilon}-U) \\
D_\downarrow(\epsilon) &= \left(P_{|0\rangle}+P_{|\downarrow\rangle}\right)\delta(\epsilon-\bar{\epsilon}) + \left(P_{|\uparrow\rangle}+P_{|\uparrow\downarrow\rangle}\right)\delta(\epsilon-\bar{\epsilon}-U)
\end{aligned} \tag{2.176}$$

See section 17.2.2 and in particular figure 17.4 on p. 439.

6 Compare the density of states of an ensemble of eigenstates of the hydrogen atom with the mean-field Fock operator.

For an ensemble of eigenstates, we superimpose the density of states of the individual many-particle states weighted with their probabilities. The density of states consists of peaks at $\bar{\epsilon}$ and at $\bar{\epsilon}+U$. While the energy-level positions are unchanged, the weights of the peaks in the density of states depend on the specific ensemble.

For each orbital, there are contributions from both energies. These two energies can be interpreted as upper and lower **Hubbard band**. This is the underlying mechanism for the physics of **Mott insulators**.

In the mean-field solution, the position of the energy levels change with the ensemble

$$\hat{F}^{mf} \overset{\text{Eq. } 2.169}{=} \sum_{\alpha\in\{\uparrow,\downarrow\}} |\pi_\alpha\rangle\left(\bar{\epsilon}+U\sum_\gamma f_\gamma - U f_\alpha\right)\langle\pi_\alpha| \tag{2.177}$$

Thus, the density of states has peaks at $\bar{\epsilon}+UN_e-Uf_\alpha$, where N_e is the total number of electrons. If the occupations are equal, the two orbitals are degenerate. If the occupations are different the two energy levels are separated by $U|f_\uparrow - f_\downarrow|$. The mean value of the two energy levels shift upward with the particle number as UN_e. The weights of the peaks are always equal to one. I.e. there is one spin-up level and one spin-down level.

2.11.3 Two one-dimensional particles in a box

Introduction

One example, which allows one to demonstrate many-particle effects in a most simple way, are two one-dimensional particles in a box. This system is mathematically identical to one two-dimensional particle in a box. This problem allows one to work out and visualize many-particle effects in a well known territory. The antisymmetry of the fermionic wave function is easily enforced and the interaction between two one-dimensional particles is analogous to an external one-particle potential for the two-dimensional particle. Then main interest is to work out the exchange hole, which will be central to the description of the interaction energy.

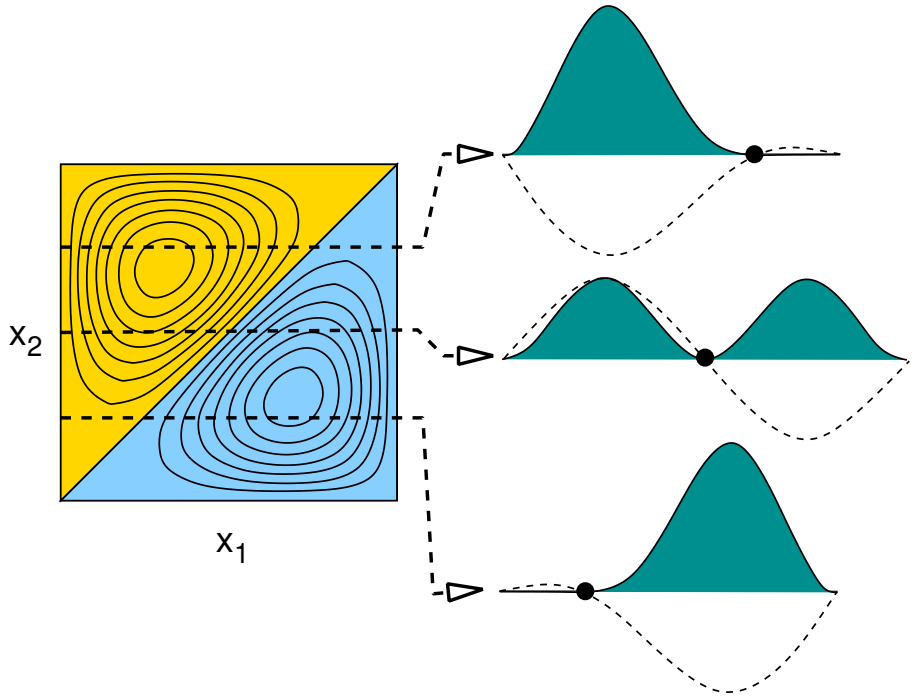


Fig. 2.9: Many-particle wave function of two spin-less fermions in a one-dimensional box. Left: Many-particle wave function (Slater determinant) $\Phi(x_1, x_2)$ of the ground state. The two colors distinguish regions with positive and negative signs of the wave functions. (Note, that x is the one-dimensional coordinate and does not refer to the combined position-and-spin representation.) Right: The dashed lines show the wave functions $\Phi(x_1, x_2)$ as function of x_1 for a three different fixed position x_2 of the second particle. The full function is the density of the first particle, while the second particle is fixed at position x_2. Notice, the exchange hole. Editor: include also the total density so that the exchange hole becomes evident.

Problem

Let me introduce the notation I will use to describe spin-$\frac{1}{2}$ particles in one dimension. The position along the box will be denoted by the scalar r. The box ranges from $r = 0$ to $r = L$. The combined real-space-and-spin coordinate is $\vec{x} = (r, \sigma)$.

1. Calculate the electron density $n(r)$ of the two electrons as function of the position in the box of side length L. The exchange hole $h(r, \sigma, r', \sigma')$ is the difference between electron density of the other electron(s), given that one electron is at position r and has the spin $\sigma \in \{\uparrow, \downarrow\}$ and the total electron density. Consider first two electrons with the same spin. Then consider electrons with opposite spin and discuss changes.

   Plot the exchange hole,

   - for an electron close to the boundary of the box and in the center of the box
   - for two different sizes L of the box. (i.e. for different electron densities.
   - Consider the case of two electrons with opposite spin. What are the differences?

   Remark: I found it useful to work out the expressions for two abstract orbitals $\varphi_a(\vec{x})$ and $\varphi_b(\vec{x})$. Then, I calculated the one-particle orbitals in order to insert them into the expressions obtained previously. Finally, I used a plotting program.

2. Construct the two-particle wave function with lowest kinetic energy of two electrons with equal spin in a box of side-length L.

3. Construct the two-particle density for the wave function with lowest kinetic energy of two electrons with equal spin in a box of side-length L. Calculate the one-particle density. For example, from the two-particle density.

4. Construct the exchange hole for the wave function with lowest kinetic energy of two electrons with equal spin in a box of side-length L.

5. Calculate the density for the state with lowest energy for two electrons with opposite spin

6. Calculate the two-particle density for the state with lowest energy for two electrons with opposite spin

7. Calculate the exchange hole for the state with lowest energy for two electrons with opposite spin

Discussion

1. Calculate the electron density $n(r)$ of the two electrons as function of the position in the box of side length L. The exchange hole $h(r, \sigma, r', \sigma')$ is the difference between electron density of the other electron(s), given that one electron is at position r and has the spin $\sigma \in \{\uparrow, \downarrow\}$ and the total electron density. Consider first two electrons with the same spin. Then consider electrons with opposite spin and discuss changes.

   Plot the exchange hole,

   - for an electron close to the boundary of the box and in the center of the box
   - for two different sizes L of the box. (i.e. for different electron densities.
   - Consider the case of two electrons with opposite spin. What are the differences?

   Remark: I found it useful to work out the expressions for two abstract orbitals $\varphi_a(\vec{x})$ and $\varphi_b(\vec{x})$. Then, I calculated the one-particle orbitals in order to insert them into the expressions obtained previously. Finally, I used a plotting program.

2. Construct the two-particle wave function with lowest kinetic energy of two electrons with equal spin in a box of side-length L.

Let me first construct the one-particle orbitals relevant for this case. We use the two one-particle orbitals with lowest kinetic energy, namely

$$\begin{aligned}\varphi_a(r, \sigma) &= \sqrt{\frac{2}{L}} \sin(\pi r/L)\delta_{\sigma,\uparrow} \\ \varphi_b(r, \sigma) &= \sqrt{\frac{2}{L}} \sin(2\pi r/L)\delta_{\sigma,\uparrow}\end{aligned} \tag{2.178}$$

Notice that the spatial part of the two orbitals differs φ_a is node-less, while φ_b has one node in the spatial wave function.

The Slater determinant formed by these orbitals is

$$\begin{aligned}\Psi(\vec{x}_1, \vec{x}_2) &= \frac{1}{\sqrt{2}}\Big(\varphi_a(\vec{x}_1)\varphi_b(\vec{x}_2) - \varphi_b(\vec{x}_1)\varphi_a(\vec{x}_2)\Big) \\ &= \frac{1}{\sqrt{2}}\left(\sqrt{\frac{2}{L}} \sin(\pi r_1/L)\delta_{\sigma_1,\uparrow}\sqrt{\frac{2}{L}} \sin(2\pi r_2/L)\delta_{\sigma_2,\uparrow} - \sqrt{\frac{2}{L}} \sin(2\pi r_1/L)\delta_{\sigma_1,\uparrow}\sqrt{\frac{2}{L}} \sin(\pi r_2/L)\delta_{\sigma_2,\uparrow}\right)\end{aligned} \tag{2.179}$$

Side remark: Chemists like to take the spatial and spin parts apart. With the one-particle orbitals

$$\begin{aligned}\varphi_a(\vec{r}, \sigma) &= f(\vec{r})\delta_{\sigma\uparrow} \\ \varphi_b(\vec{r}, \sigma) &= g(\vec{r})\delta_{\sigma,\uparrow}\end{aligned} \tag{2.180}$$

one constructs a two-particle Slater determinant

$$\begin{aligned}\Psi(\vec{x}_1, \vec{x}_2) &= \frac{1}{\sqrt{2}}\Big(\phi_a(\vec{x}_1)\phi_b(\vec{x}_2) - \phi_b(\vec{x}_1)\phi_1(\vec{x}_2)\Big)\Big) \\ &= \frac{1}{\sqrt{2}}\Big(f(\vec{r}_1)g(\vec{r}_2)\delta_{\sigma_1,\uparrow}\delta_{\sigma_2,\uparrow} - g(\vec{r}_1)f(\vec{r}_2)\delta_{\sigma_1,\uparrow}\delta_{\sigma_2,\uparrow}\Big) \\ &= \underbrace{\frac{1}{\sqrt{2}}\Big(f(\vec{r}_1)g(\vec{r}_2) - g(\vec{r}_1)f(\vec{r}_2)\Big)}_{\text{spatial part}}\underbrace{\Big(\delta_{\sigma_1,\uparrow}\delta_{\sigma_2,\uparrow}\Big)}_{\text{spin part}}\end{aligned} \tag{2.181}$$

One notices that the spin part by itself is symmetric under particle exchange and that the spatial part by itself is antisymmetric under particle exchange. For particle with opposite spin, the spatial part is symmetric and the spin-part is antisymmetric.

3. Construct the two-particle density for the wave function with lowest kinetic energy of two electrons with equal spin in a box of side-length L. Calculate the one-particle density. For example, from the two-particle density.

The two-particle density is obtained as the square of the wave function

$$\begin{aligned} n^{(2)}(\vec{r},\vec{r}') &\overset{\text{Eq. 2.41}}{=} \underbrace{2}_{N(N-1)} \langle\Psi| \left(\int d^4x_1 \int d^4x_2 \, \big|\vec{x}_1,\vec{x}_2\big\rangle \delta(\vec{r}-\vec{r}_1)\delta(\vec{r}'-\vec{r}_2) \big\langle \vec{x}_1,\vec{x}_2\big| \right) |\Psi\rangle \\ &= 2 \int d^4x_1 \int d^4x_2 \, \delta(\vec{r}-\vec{r}_1)\delta(\vec{r}'-\vec{r}_2) \big\langle\Psi\big|\vec{x}_1,\vec{x}_2\big\rangle \big\langle \vec{x}_1,\vec{x}_2\big|\Psi\big\rangle \\ &= 2 \sum_{\sigma_1,\sigma_2} \Big| \big\langle \vec{r},\sigma_1,\vec{r}',\sigma_2\big|\Psi\big\rangle \Big|^2 \end{aligned} \tag{2.182}$$

This expression is valid for three dimensional position space. To go to the one-dimensional case, I use the scalar quantity r as the one-dimensional position and the two-dimensional $\vec{x} = (r,\sigma)$ as the composite real-space-and-spin coordinate.

$$\begin{aligned} n^{(2)}(r,r') &\overset{\text{Eq. 2.182}}{=} \underbrace{2}_{N(N-1)} \sum_{\sigma_1,\sigma_2} \left[\frac{1}{\sqrt{2}} \left(\frac{2}{L} \sin(\pi r/L)\sin(2\pi r'/L) - \frac{2}{L}\sin(2\pi r/L)\sin(\pi r'/L) \right) \delta_{\sigma_1,\uparrow}\delta_{\sigma_2,\uparrow} \right]^2 \\ &= \underbrace{2}_{N(N-1)} \left[\frac{1}{\sqrt{2}} \left(\frac{2}{L} \sin(\pi r/L)\sin(2\pi r'/L) - \frac{2}{L}\sin(2\pi r/L)\sin(\pi r'/L) \right) \right]^2 \underbrace{\sum_{\sigma_1,\sigma_2} \delta_{\sigma_1,\uparrow}\delta_{\sigma_2,\uparrow}}_{=1} \\ &= \frac{4}{L^2} \left(\sin(\pi r/L)\sin(2\pi r'/L) - \sin(2\pi r/L)\sin(\pi r'/L) \right)^2 \end{aligned} \tag{2.183}$$

The density is obtained by integrating over all positions of the second particle.

$$n(\vec{r}) = \int d^3r' \; n^{(2)}(\vec{r},\vec{r}') = \frac{2}{L}\sin^2(\pi r/L) + \frac{2}{L}\sin^2(2\pi r/L) \tag{2.184}$$

I exploited the orthogonality of the spatial parts of the one-particle orbitals. The orthonormality can be seen from the symmetry properties. One orbital is symmetric under reflection at the box-center, while the other is antisymmetric.

4. Construct the exchange hole for the wave function with lowest kinetic energy of two electrons with equal spin in a box of side-length L.

$$h(\vec{r},\vec{r}') = \frac{1}{n^{(1)}(\vec{r})} \Big(n^{(2)}(\vec{r},\vec{r}') - n^{(1)}(\vec{r}) n^{(1)}(\vec{r}') \Big) \tag{2.185}$$

$n^{(2)}$:Eq. 2.183

$$\begin{aligned} h(r,r') &= \underbrace{\frac{1}{\frac{2}{L}\sin^2(\pi r/L)+\frac{2}{L}\sin^2(2\pi r/L)}}_{1/n(r)} \\ &\quad\times\Bigg(\underbrace{\frac{4}{L^2}\Big[\sin(\pi r/L)\sin(2\pi r'/L)-\sin(2\pi r/L)\sin(\pi r'/L)\Big]^2}_{n^{(2)}(r,r')} \\ &\quad-\underbrace{\left[\frac{2}{L}\sin^2(\pi r/L)+\frac{2}{L}\sin^2(2\pi r/L)\right]}_{n(r)}\underbrace{\left[\frac{2}{L}\sin^2(\pi r'/L)+\frac{2}{L}\sin^2(2\pi r'/L)\right]}_{n(r')}\Bigg) \\ &= \underbrace{\frac{1}{\frac{2}{L}\sin^2(\pi r/L)+\frac{2}{L}\sin^2(2\pi r/L)}}_{1/n(r)} \\ &\quad\times\Bigg(\underbrace{\frac{4}{L^2}\Big[\sin(\pi r/L)\sin(2\pi r'/L)-\sin(2\pi r/L)\sin(\pi r'/L)\Big]^2}_{n^{(2)}(r,r')} \\ &\quad-\underbrace{\left[\frac{2}{L}\sin^2(\pi r/L)+\frac{2}{L}\sin^2(2\pi r/L)\right]}_{n(r)}\underbrace{\left[\frac{2}{L}\sin^2(\pi r'/L)+\frac{2}{L}\sin^2(2\pi r'/L)\right]}_{n(r')}\Bigg) \end{aligned} \tag{2.186}$$

The hole for different positions of the reference electron is shown in figure 2.9.

5. Calculate the density for the state with lowest energy for two electrons with opposite spin

For two electrons with opposite spin the two-particle wave function is

$$\begin{aligned} \Psi(x_1,\sigma_1,x_2,\sigma_2) &= \frac{1}{\sqrt{2}}\Bigg[\underbrace{\sqrt{\frac{2}{L}}\sin(\pi x_1/L)\delta_{\sigma_1,\uparrow}}_{\varphi_a(x_1,\sigma_1)}\underbrace{\sqrt{\frac{2}{L}}\sin(\pi x_2/L)\delta_{\sigma_2,\downarrow}}_{\varphi_b(x_2,\sigma_2)}-\underbrace{\sqrt{\frac{2}{L}}\sin(\pi x_1/L)\delta_{\sigma_1,\downarrow}}_{\varphi_b(x_1,\sigma_1)}\underbrace{\sqrt{\frac{2}{L}}\sin(\pi x_2/L)\delta_{\sigma_2,\uparrow}}_{\varphi_a(x_2,\sigma_2)}\Bigg] \\ &= \frac{2}{L}\sin(\pi x_1/L)\sin(\pi x_2/L)\frac{1}{\sqrt{2}}\Big(\delta_{\sigma_1,\uparrow}\delta_{\sigma_2,\downarrow}-\delta_{\sigma_1,\downarrow}\delta_{\sigma_2,\uparrow}\Big) \end{aligned} \tag{2.187}$$

The density can directly be evaluated using Eq. 2.10 by summing over the densities of the one-particle orbitals, because the precondition that the two one-particle orbitals are orthonormal is satisfied. The orthogonality is shown as follows:

$$\langle\varphi_a|\varphi_b\rangle = \sum_\sigma\int d^3r\left(\sqrt{\frac{2}{L}}\sin(\pi x/L)\delta_{\sigma,\uparrow}\right)\left(\sqrt{\frac{2}{L}}\sin(\pi x/L)\delta_{\sigma,\downarrow}\right)=0 \tag{2.188}$$

because $\delta_{\sigma,\uparrow}\delta_{\sigma,\downarrow}=0$ for all σ.

I now insert the orbitals into Eq. 2.10

$$n(\vec{r}) = \sum_{\alpha\in\{a,b\}}\sum_{\sigma\in\{\uparrow,\downarrow\}}|\varphi_\alpha(\vec{r},\sigma)|^2 \tag{2.189}$$

6. Calculate the two-particle density for the state with lowest energy for two electrons with opposite spin

The two-particle density is obtained as the square of the wave function

$$\begin{aligned} n^{(2)}(\vec{r},\vec{r'}) &\overset{\text{Eq. 2.41}}{=} \underbrace{2}_{N(N-1)} \langle\Psi|\left(\int d^4x_1 \int d^4x_2 \left|\vec{x}_1,\vec{x}_2\right\rangle\delta(\vec{r}-\vec{r_1})\delta(\vec{r'}-\vec{r_2})\left\langle\vec{x}_1,\vec{x}_2\right|\right)|\Psi\rangle \\ &= 2\int d^4x_1 \int d^4x_2\, \delta(\vec{r}-\vec{r_1})\delta(\vec{r'}-\vec{r_2})\left\langle\Psi\middle|\vec{x}_1,\vec{x}_2\right\rangle\left\langle\vec{x}_1,\vec{x}_2\middle|\Psi\right\rangle \\ &= 2\sum_{\sigma_1,\sigma_2}\left|\left\langle\vec{r},\sigma_1,\vec{r'},\sigma_2\middle|\Psi\right\rangle\right|^2 \end{aligned} \tag{2.190}$$

This expression is valid for three dimensional position space. To go to the one-dimensional case, I use the scalar quantity r as the one-dimensional position and the two-dimensional $\vec{x} = (r,\sigma)$ as the composite real-space-and-spin coordinate.

$$\begin{aligned} n^{(2)}(r,r') &\overset{\text{Eq. 2.41}}{=} \underbrace{2}_{N(N-1)} \sum_{\sigma_1,\sigma_2}\left(\frac{2}{L}\sin(\pi r_1/L)\sin(\pi r_2/L)\frac{1}{\sqrt{2}}\left(\delta_{\sigma_1,\uparrow}\delta_{\sigma_2,\downarrow}-\delta_{\sigma_1,\downarrow}\delta_{\sigma_2,\uparrow}\right)\right)^2 \\ &= 2\frac{4}{L^2}\sin^2(\pi r_1/L)\sin^2(\pi r_2/L)\underbrace{\sum_{\sigma_1,\sigma_2}\frac{1}{2}\left(\delta_{\sigma_1,\uparrow}\delta_{\sigma_2,\downarrow}-\delta_{\sigma_1,\downarrow}\delta_{\sigma_2,\uparrow}\right)^2}_{=1} \\ &= 2\underbrace{\frac{2}{L}\sin^2(\pi r/L)}_{n_1(r)}\underbrace{\frac{2}{L}\sin^2(\pi r_2/L)}_{n_2(r)} \end{aligned} \tag{2.191}$$

The density is obtained by integrating over all positions of the second particle.

$$n(\vec{r}) = \int d^3r'\, n^{(2)}(\vec{r},\vec{r'}) = 2\cdot\frac{2}{L}\sin^2(\pi r/L) \tag{2.192}$$

7. Calculate the exchange hole for the state with lowest energy for two electrons with opposite spin

The exchange-correlation hole is the difference of the total density $n(\vec{r'})$ and the density, in this case $n^{(2)}(\vec{r},\vec{r'})$ of the remaining particles, given that the first is at a specific position $\vec{r}$

$$h_{xc}(\vec{r},\vec{r'}) \overset{\text{Eq. 2.44}}{=} \frac{1}{n(\vec{r})}\left(n^{(2)}(\vec{r},\vec{r'}) - n(\vec{r})n(\vec{r'})\right) \tag{2.193}$$

$$\begin{aligned} h(r,r') &\overset{\text{Eq. 2.191}}{=} \frac{2}{L}\sin^2(\pi r'/L) - \underbrace{2\cdot\frac{2}{L}\sin^2(\pi r/L)}_{n(r')} \\ &= -\frac{2}{L}\sin^2(\pi r'/L) = -\frac{1}{2}n(r') \end{aligned} \tag{2.194}$$

Observations:

- Noticeable is the behavior of the hole for the opposite-spin wave function as the reference electron approaches one of the boundaries. The hole is not centered on the reference electron but displaced inside the box. This is because the density of the other electron must not be negative and thus the hole cannot exceed the density in absolute value. The hole must be, where the electrons are. The shape of the hole is governed by the electron density and thus remains unchanged until the reference electron moves sufficiently far into the box.

- The spin part of the wave function of the wave function for opposite spin electrons is that of a singlet term. One easily makes the mistake assuming that one has a singlet, whenever an $\uparrow$ orbital is combined with a $\downarrow$ orbital. This, however, only says that $S_z = 0$. It can still be a triplet $\frac{1}{\sqrt{2}}(\delta_{\sigma_1,\uparrow}\delta_{\sigma_2,\downarrow} + \delta_{\sigma_1,\downarrow}\delta_{\sigma_2,\uparrow})$ with $S^2 = \hbar^2 S(S+1) = 2\hbar^2$ and the spin perpendicular to the z axis. A simple product $\delta_{\sigma_1,\uparrow}\delta_{\sigma_2,\downarrow}$ is not a spin eigenstate, i.e. an eigenstate of $\hat{S}^2$, but a superposition of a singlet and a triplet state.

- The spatial wave function is symmetric under exchange of the two positions. If one forms a Slater determinant of two opposite-spin orbitals with different spatial parts, the result is not a spin eigenstate, but a superposition of a singlet and a triplet state. This is shown as follows.

$$\begin{aligned}\psi(x_1,\sigma_1,x_2,\sigma_2) &= \frac{1}{\sqrt{2}}\Big(f(x_1)\delta_{\sigma_1,\uparrow}g(x_2)\delta_{\sigma_2,\downarrow} - g(x_1)\delta_{\sigma_1,\downarrow}f(x_2)\delta_{\sigma_2,\uparrow}\Big)\\ &= \frac{1}{2}\Big\{\Big(f(x_1)g(x_2) + g(x_1)f(x_2)\Big)\frac{1}{\sqrt{2}}\Big(\delta_{\sigma_1,\uparrow}\delta_{\sigma_2,\downarrow} - \delta_{\sigma_1,\downarrow}\delta_{\sigma_2,\uparrow}\Big)\\ &+ \Big(f(x_1)g(x_2) - g(x_1)f(x_2)\Big)\frac{1}{\sqrt{2}}\Big(\delta_{\sigma_1,\uparrow}\delta_{\sigma_2,\downarrow} + \delta_{\sigma_1,\downarrow}\delta_{\sigma_2,\uparrow}\Big)\Big\} \quad (2.195)\end{aligned}$$

  A spatial part of a singlet wave function is always symmetric under particle exchange, while that of a triplet wave function is antisymmetric under particle exchange.

- Unlike two electrons with equal spin, electrons with opposite spin do not go out of each other's way. The exchange hole is equal in absolute value to the density of the corresponding one-particle orbital.

2.11.4 Two fermions in a 1d-box

Introduction and background

The goal of this exercise is to provide an understanding of many-particle wave functions and of identical particles. This exercise will also show the underlying reasons why non-interacting electrons are often a good model to describe interacting electrons despite their strong interaction and the breakdown of a perturbation theory.

Consider two non-interacting spin-less particles in a 1-dimensional box with side-length L. This problem is analogous to a single particle in a two-dimensional box, which can be solved analytically. The symmetry under permutation of particles, which defines fermions and bosons, is translated into a simple geometrical mirror symmetry.

To investigate the role of interactions, I introduce a hard-core repulsion of extent s

$$W(x,x') = \begin{cases} W_0 & \text{for } |x-x'| < s \\ 0 & \text{for } |x-x'| \geq s \end{cases} \tag{2.196}$$

in the limit $W_0 \to \infty$.

The hard-core repulsion is appropriate for the description of the fermionic Helium-3 and the bosonic Helium-4.

Tasks

1 Determine the wave functions and energy eigenvalues for a particle with mass m in a N-dimensional square box with side-length L.

2 Use the result from the previous question to determine the wave functions and the spectrum for N distinguishable particles in a one-dimensional box. Notice that the wave functions are single product wave functions formed from one-particle wave functions.

3 Discuss under the guidance of the tutor the following puzzles: (1) What is the wave function of a zero particle state? (2) What is the scalar product of two states with different particle numbers.

4 The real-space basis functions for two particles is $\{|x_1, x_2\rangle\}$, where x_1, x_2 denote the two coordinates of the particles.

$$\langle x_1, x_2 | x_1', x_2' \rangle = \delta(x_1 - x_1')\delta(x_2 - x_2')$$
$$\hat{1} = \int dx_1 \int dx_2 \, |x_1, x_2\rangle\langle x_1, x_2| \tag{2.197}$$

The particle-permutation operator for two one-dimensional particles is

$$\hat{P}_{1,2} = \int dx_1 \int dx_2 \, |x_2, x_1\rangle\langle x_1, x_2| \tag{2.198}$$

Show that the particle-permutation operator is unitary. Determine the eigenvalues and eigenstates of the particle-permutation operator.

5 Determine the wave functions and spectra for two fermions in a 1-d box and for two bosons. Show that bosonic and fermionic wave functions span the complete Hilbert space. (There are no other types of identical particles.) From the multiplicity of the states, respectively the spectra argue, why two identical fermions cannot be in one orbital (Pauli principle) and why bosons are preferably in the same orbital. That is, show that the probability to find two particles in the same orbital is higher for bosons than for distinguishable particles. (Bunching and anti-bunching.)

6 The wave functions for two particles with a hard-core interaction can be expressed in terms of the wave function of two non-interacting fermionic wave functions with side-length $L - s$, where s is the range of the interaction. In the case of an interaction the wave functions are zero in a strip of width s along the main diagonal $x_1 = x_2$. Such wave functions can be constructed by dividing the non-interacting wave function at the node-line, and by separating the two pieces out of the interaction region.

- Sketch the interaction in the two-dimensional box
- Use this principle to construct the exact fermionic and bosonic wave functions for the hard-core interaction.
- Determine the eigenvalue spectrum for fermions and for bosons.
- Estimate the eigenvalue spectrum using first-order perturbation theory in the interaction. (Use approximations)

Solution

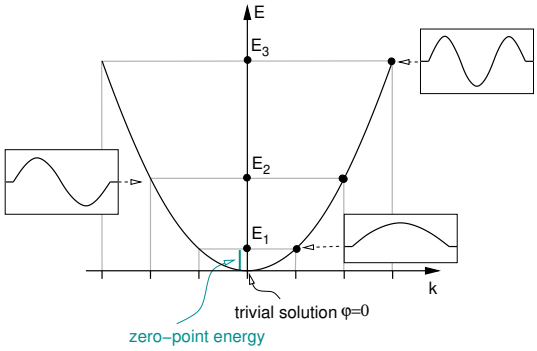
1 Determine the wave functions and energy eigenvalues for a particle with mass m in a N-dimensional square box with side-length L.

1. **Particle in a one-dimensional box**

$$\varphi_n^{(1)}(x) = \sqrt{\frac{2}{L}} \sin\left(\frac{n\pi}{L}x\right)$$

The energy of this state is

$$\epsilon_n = \frac{\hbar^2\pi^2}{2m_e L^2} n^2$$



2. **Particle in a two-dimensional box** The two-dimensional box with side-length L covers the area $[0, L] \times [0, L]$.

The wave functions for a particle in a 2-dimensional box are of the form

$$\varphi_{n,m}(x, y) = \varphi_n(x)\varphi_m(y) = \frac{2}{L} \sin\left(\frac{n\pi}{L}x\right) \sin\left(\frac{m\pi}{L}y\right) \tag{2.199}$$

The energy of such a state is due to the kinetic energy. It is

$$E_{n,m} = \epsilon_n + \epsilon_m = \frac{\hbar^2\pi^2}{2m_e L^2}(n^2 + m^2) \tag{2.200}$$

3. **Particle in a N-dimensional box**

$$\varphi_{n_1,n_2,\ldots,n_N}(x_1, x_2, \ldots, x_N) = \prod_{j=1}^{N} \varphi_{n_j}(x_j) = \left(\frac{2}{L}\right)^{\frac{N}{2}} \prod_{j=1}^{N} \sin\left(\frac{n_j\pi}{L}x_j\right)$$

$$E_{n_1,n_2,\ldots,n_N} = \sum_{j=1}^{N} \epsilon_j = \frac{\hbar^2\pi^2}{2m_e L^2} \sum_{j=1}^{N} n_j^2$$

2 Use the result from the previous question to determine the wave functions and the spectrum for N distinguishable particles in a one-dimensional box. Notice that the wave functions are single product wave functions formed from one-particle wave functions.

The Schrödinger equation for a one-dimensional particle in a N-dimensional box is identical to that

for N particles in a one-dimensional box. Thus, the wave functions and energy levels are equivalent.

$$\varphi_{n_1,n_2,\ldots,n_N}(x_1,x_2,\ldots,x_N) \overset{\text{Eq. 2.201}}{=} \prod_{j=1}^{N}\varphi_{n_j}(x_j) = \left(\frac{2}{L}\right)^{\frac{N}{2}}\prod_{j=1}^{N}\sin\left(\frac{n_j\pi}{L}x_j\right) \tag{2.201}$$

$$E_{n_1,n_2,\ldots,n_N} = \sum_{j=1}^{N}\epsilon_j \overset{\text{Eq. 2.201}}{=} \frac{\hbar^2\pi^2}{2m_eL^2}\sum_{j=1}^{N}n_j^2 \tag{2.202}$$

3 Discuss under the guidance of the tutor the following puzzles: (1) What is the wave function of a zero particle state? (2) What is the scalar product of two states with different particle numbers.

There is no zero-particle wave function, because it would not have any arguments. The zero-particle state, however, has a phase. Therefore, the zero particle state is a complex number.

A common mistake is to describe the zero particle state as a function of some particle coordinates, albeit with constant value. This mistake happens usually when trying to add a zero particle state and a one-particle state. The result cannot be simplified to a single function.

The scalar product of two states with different particle numbers can not be formed in real space, because the two functions have different numbers of arguments.

One can form the integral of two functions with different number of arguments such as $f(\vec{x}) = \int d^4x'\ \phi(\vec{x'})\psi(\vec{x},\vec{x'}$, which is a function of the additional argument. Such a construction will occur later in the context of quasi-particle wave functions. This is, however, not the scalar product. The scalar product $\langle\phi|\psi\rangle = 0$ of this example would be zero.

The scalar product can be given in the Fock space, because then the particle number is not a parameter but an observable represented by a hermitian operator. Since eigenstates of a hermitian operator to different eigenvalues are orthogonal, the scalar product of states with different particle numbers is zero.

4 The real-space basis functions for two particles is $\{|x_1,x_2\rangle\}$, where x_1, x_2 denote the two coordinates of the particles.

$$\langle x_1,x_2|x_1',x_2'\rangle = \delta(x_1-x_1')\delta(x_2-x_2')$$
$$\hat{1} = \int dx_1\int dx_2\ |x_1,x_2\rangle\langle x_1,x_2| \tag{2.203}$$

The particle-permutation operator for two one-dimensional particles is

$$\hat{P}_{1,2} = \int dx_1\int dx_2\ |x_2,x_1\rangle\langle x_1,x_2| \tag{2.204}$$

Show that the particle-permutation operator is unitary. Determine the eigenvalues and eigenstates of the particle-permutation operator.

1. **Show that the particle permutation operator is unitary:** The permutation operator is

$$\hat{P}_{12} = \int dx_1\int dx_2\ |x_2,x_1\rangle\langle x_1,x_2| \tag{2.205}$$

This implies for wave functions

$$|\Psi'\rangle \overset{\text{def}}{=} \hat{P}_{12}|\Psi\rangle$$
$$\Psi'(x_1,x_2) = \langle x_1,x_2|\hat{P}_{12}|\Psi\rangle = \langle x_2,x_1|\Psi\rangle = \Psi(x_2,x_1) \tag{2.206}$$

An operator is unitary, if its adjoint is its inverse. That is, it is unitary if $\hat{P}\hat{P}^\dagger = \hat{1}$.
The adjoint can be obtained by exchanging bra's and kets.

$$\hat{P}_{12}^\dagger = \int dx_1 \int dx_2 \, |x_1, x_2\rangle\langle x_2, x_1| \tag{2.207}$$

The equation above also shows that the permutation operator is furthermore hermitian, i.e.

$$\hat{P}_{12}^\dagger = \hat{P}_{12} \tag{2.208}$$

Now we can show that particle permutation operator is unitary

$$\begin{aligned}
\hat{P}_{12}\hat{P}_{12}^\dagger &\stackrel{?}{=} 1 \\
\hat{P}_{12}\hat{P}_{12}^\dagger &= \underbrace{\int dx_1 \int dx_2 \, |x_2, x_1\rangle\langle x_1, x_2|}_{\hat{P}_{12}} \underbrace{\int dx_1' \int dx_2' \, |x_1', x_2'\rangle\langle x_2', x_1'|}_{\hat{P}_{12}^\dagger} \\
&= \int dx_1 \int dx_2 \int dx_1' \int dx_2' \, |x_2, x_1\rangle \underbrace{\langle x_1, x_2 | x_1', x_2'\rangle}_{\delta(x_1 - x_1')\delta(x_2 - x_2')} \langle x_2', x_1'| \\
&= \int dx_1 \int dx_2 \, |x_2, x_1\rangle\langle x_2, x_1| = \hat{1} \qquad \text{q.e.d}
\end{aligned} \tag{2.209}$$

Thus, the permutation operator is unitary.

2. Eigenvalues of the permutation operator: As shown above, the permutation operator is unitary and hermitian. Hence, the permutation operator is cyclic $\hat{P}_{12}^2 = \hat{P}_{12}\hat{P}_{12}^\dagger = \hat{1}$.
   Because $\hat{P}_{12}^2 = 1$, the eigenvalues of $\hat{P}_{12}$ are $+1$ and -1.
3. Eigenstates of the permutation operator:
   - The eigenstates $|\Psi^B\rangle$ for eigenvalue $+1$ are bosonic states

$$\begin{aligned}
|\Psi^B\rangle &\stackrel{\text{Eq. 1.89}}{=} |\Psi^D\rangle + \hat{P}_{12}|\Psi^D\rangle \\
\Psi^B(x_1, x_2) &= \Psi^D(x_1, x_2) + \Psi^D(x_2, x_1)
\end{aligned} \tag{2.210}$$

     where $\Psi^D(x_1, x_2)$ is an arbitrary wave function (for two distinguishable (D) particles). The resulting state is not normalized. It can occur that symmetrized wave function vanishes. (This occurs when Ψ is antisymmetric.)
   - The eigenstates Ψ^F for eigenvalue -1 are fermionic states

$$\begin{aligned}
|\Psi^F\rangle &= |\Psi^D\rangle - \hat{P}_{12}|\Psi^D\rangle \\
\Psi^F(x_1, x_2) &= \Psi^D(x_1, x_2) - \Psi^D(x_2, x_1)
\end{aligned} \tag{2.211}$$

     where $\Psi^D(x_1, x_2)$ is an arbitrary wave function (for two distinguishable particles). The resulting state is not normalized. It can occur that antisymmetrized wave function vanishes. (This occurs when Ψ is symmetric.)

5 Determine the wave functions and spectra for two fermions in a 1-d box and for two bosons. Show that bosonic and fermionic wave functions span the complete Hilbert space. (There are no other types of identical particles.) From the multiplicity of the states, respectively the spectra argue, why two identical fermions cannot be in one orbital (Pauli principle) and why bosons are preferably in the same orbital. That is, show that the probability to find two particles in the same orbital is higher for bosons than for distinguishable particles. (Bunching and anti-bunching.)

1. **Construct the fermionic (anti symmetric) and bosonic (symmetric) eigenstates of the Hamiltonian**

Fermions:

$$|\Psi^F_{n,m}\rangle = \frac{1}{\sqrt{2}}\Big(|\Psi^D_{n,m}\rangle - \hat{P}_{12}|\Psi^D_{n,m}\rangle\Big)$$
$$\psi^F_{n,m}(x,y) = \frac{\sqrt{2}}{L}\left(\sin\left(\frac{n\pi}{L}x\right)\sin\left(\frac{m\pi}{L}y\right) - \sin\left(\frac{m\pi}{L}x\right)\sin\left(\frac{n\pi}{L}y\right)\right) \qquad \text{for } n > m \tag{2.212}$$

If a fermionic two-particle wave function $|\Psi_{nm}\rangle$ is constructed from two one-particle states $|\varphi_n\rangle$, $|\Psi_{n,m}\rangle$ is a Slater determinant.

$$\Psi^F_{n,m}(x,y) = \frac{\sqrt{2}}{L}\det\begin{vmatrix}\sin\left(\frac{n\pi}{L}x\right); & \sin\left(\frac{m\pi}{L}x\right)\\ \sin\left(\frac{n\pi}{L}y\right); & \sin\left(\frac{m\pi}{L}y\right)\end{vmatrix} \tag{2.213}$$

We find that the wave function with two electrons in the same orbital vanishes, $|\Psi^F_{n,n}\rangle = |\varnothing\rangle$, which says that there is no fermionic state with two identical fermions in the same one-particle state. This is one consequence of the Pauli principle.

We find $|\Psi^F_{n,m}\rangle = -|\Psi^F_{m,n}\rangle$. Interchanging the quantum numbers of a fermionic state does not produce a new state.

The energies are

$$E_{n,m} = \sum_{j=1}^{2}\epsilon_j = \frac{\hbar^2\pi^2}{2m_eL^2}(n^2+m^2) \qquad \text{for } n > m \tag{2.214}$$

Note that the states with $n < m$ are, up to a phase factor identical to the one with exchanged quantum numbers. States with two equal quantum numbers are zero states and therefore excluded from the sum. This indicates that fermions try to stay away from each other (anti bunching).

Bosons:

$$|\psi^B_{n,m}\rangle = \begin{cases}|\psi^D_{n,n}\rangle & \text{for } n = m\\ \frac{1}{\sqrt{2}}\big(|\Psi^D_{n,m}\rangle + \hat{P}_{12}|\Psi^D_{n,m}\rangle\big) & \text{for } m < n\end{cases}$$
$$\psi^B_{n,m}(x,y) = \begin{cases}\frac{2}{L}\sin\left(\frac{n\pi}{L}x\right)\sin\left(\frac{n\pi}{L}y\right) & \text{for } n = m\\ \frac{\sqrt{2}}{L}\left(\sin\left(\frac{n\pi}{L}x\right)\sin\left(\frac{m\pi}{L}y\right) + \sin\left(\frac{m\pi}{L}x\right)\sin\left(\frac{n\pi}{L}y\right)\right) & \text{for } m < n\end{cases} \tag{2.215}$$

The energies are

$$E_{n,m} = \sum_{j=1}^{2}\epsilon_j = \frac{\hbar^2\pi^2}{2m_eL^2}(n^2+m^2) \qquad \text{for } m \le n \tag{2.216}$$

Note here, that the states with equal quantum numbers are present. Per state with unequal quantum numbers, there are twice as many states with equal quantum numbers as in the case of distinguishable particles. This is an indication that bosons prefer to be next to each other (bunching).

2. **Show that, for two-particle systems, bosonic and fermionic wave functions span the complete Hilbert space for distinguishable particles.** Observe that the bosonic and fermionic

wave basis functions taken together again span the complete two-particle Hilbert space. Compare the energy spectrum and degeneracies for fermionic and bosonic wave functions separately.

$$|\Psi^D_{n,m}\rangle = \begin{cases} \frac{1}{\sqrt{2}}\left(|\Psi^F_{n,m}\rangle + |\Psi^B_{n,m}\rangle\right) & \text{for } m \neq n \\ |\Psi^B_{n,m}\rangle & \text{for } m = n \end{cases} \tag{2.217}$$

Remark: bosonic and fermionic wave functions do however **not** span the complete space for distinguishable particles for three or more particles. Let me demonstrate that for three particles. The group of permutations can be generated from two permutations $P_{1,2}$ and $P_{2,3}$. The permutation $P_{1,3} = P_{1,2}P_{2,3}P_{1,2}$ can be expressed in terms of the other two permutations.
Editor: This needs to be expanded?

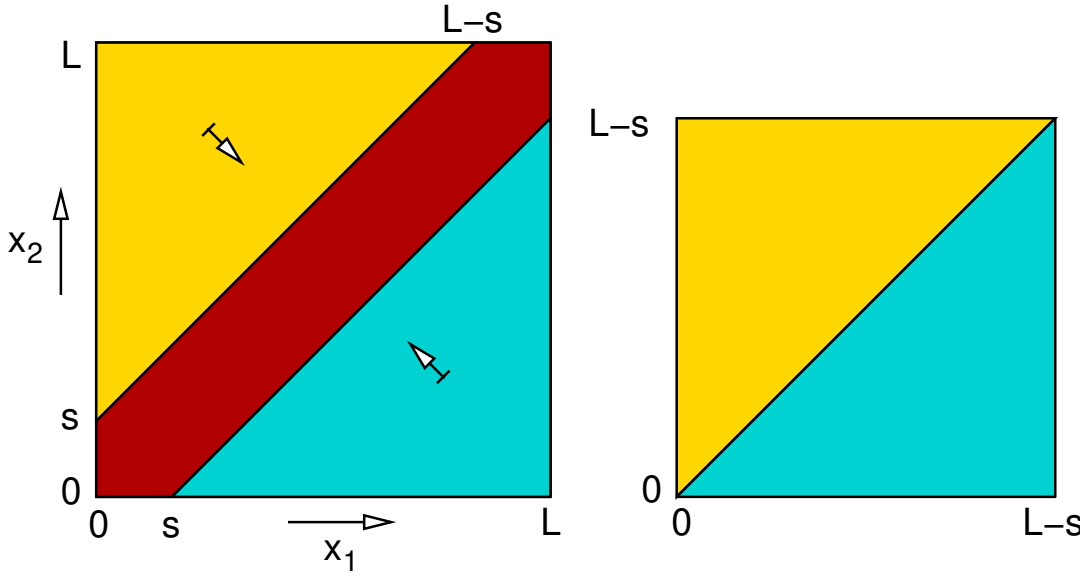
6 The wave functions for two particles with a hard-core interaction can be expressed in terms of the wave function of two non-interacting fermionic wave functions with side-length $L-s$, where s is the range of the interaction. In the case of an interaction the wave functions are zero in a strip of width s along the main diagonal $x_1 = x_2$. Such wave functions can be constructed by dividing the non-interacting wave function at the node-line, and by separating the two pieces out of the interaction region.

- Sketch the interaction in the two-dimensional box
- Use this principle to construct the exact fermionic and bosonic wave functions for the hard-core interaction.
- Determine the eigenvalue spectrum for fermions and for bosons.
- Estimate the eigenvalue spectrum using first-order perturbation theory in the interaction. (Use approximations)

Firstly, we introduce a mapping which cuts space in the main diagonal and shifts the two halfs apart by s.

Two particles at x_1 and x_2 interact if $|x_2 - x_1| < s$.

The wave function in the interaction region i.e. for $|x_2 - x_1|$ vanishes. At the boundary of the interaction region, the wave function vanishes just like the fermionic wave function vanishes at the node-line $x_1 = x_2$.



The wave function $|\Psi^{L,W}\rangle$ of the interacting system in a box of length L can be obtained from

that $|\Psi^{L-s,0}\rangle$ of the non-interacting system with a smaller box-length $L-s$.

$$\Psi^{L,W}(x_1,x_2) = \Psi^{L-s,0}(x_1',x_2') \tag{2.218}$$

where the mapping from (x_1,x_2) to (x_1',x_2') is described below.

"Above" the interaction region, i.e. for $x_2 > x_1 + s$, I need to look up

$$\begin{pmatrix} x_1' \\ x_2' \end{pmatrix} = \begin{pmatrix} x_1 \\ x_2 \end{pmatrix} - s \begin{pmatrix} 0 \\ 1 \end{pmatrix} \tag{2.219}$$

and "below" the interaction region i.e. for $x_2 < x_1 - s$, I need to look up

$$\begin{pmatrix} x_1' \\ x_2' \end{pmatrix} = \begin{pmatrix} x_1 \\ x_2 \end{pmatrix} - s \begin{pmatrix} 1 \\ 0 \end{pmatrix} \tag{2.220}$$

This maps the points at the boundaries of the interaction region onto the node plane of the non-interacting system.

The non-interacting fermions in the box, which has been shrunk by the range of the interaction is

$$\Psi^{L-s,0}_{n,m}(x_1,x_2) = \frac{\sqrt{2}}{L-s}\left(\sin\left(\frac{n\pi}{L-s}x_1\right)\sin\left(\frac{m\pi}{L-s}x_2\right) - \sin\left(\frac{m\pi}{L-s}x_1\right)\sin\left(\frac{n\pi}{L-s}x_2\right)\right) \tag{2.221}$$

where $0 < x_{1/2} < L-s$.

The interacting fermionic wave function is

$$\Psi^{W}(x_1,x_2) = \begin{cases} \Psi^0(x_1,x_2-s) & \text{for } x_2 > x_1+s \\ 0 & \text{for } x_1 - s < x_2 < x_1 + s \\ \Psi^0(x_1-s,x_2) & \text{for } x_2 < x_1 - s \end{cases} \tag{2.222}$$

with $m > n$ and the energies are

$$E^{L,W}_{m,n} = E^{L-s,0}_{m,n} = \frac{\hbar^2\pi^2}{2m_e(L-s)}(n^2+m^2) \tag{2.223}$$

We see that the energies of the interacting system are obtained from those of the non-interacting system by

$$\begin{aligned} E^{L,W}_{m,n} &= \frac{L}{L-s}E^{L,0}_{m,n} = \frac{1}{1-\frac{s}{L}}E^{L,0}_{m,n} \\ \Rightarrow \quad E^{L,W}_{m,n} - E^{L,0}_{m,n} &\approx \frac{s}{L}E^{L,0}_{m,n} \end{aligned} \tag{2.224}$$

This shows that the energy increases strongly with the density of the system. A very dilute system has a small collision probability and therefore the energy increase is negligible.

Interestingly there is a one-to-one correspondence between bosonic and fermionic eigenstates of the system in the limit of a hard-core repulsion. The energies are identical and the wave function is identical, except that there is no sign change under particle permutation of two bosons.

Gnuplot example

Fig. 2.9 has been drawn by graphical tool Gnuplot. Here, a small script is provided for gnuplot. Simply paste it into a file '`boxtwopartcle.gnu`' and run the command '`gnuplot boxtwopartcle.gnu`'

```
#Set terminal postscript
#set output "boxtwoparticle.eps"
```

```
set terminal png
set output "boxtwoparticle.png"
#set terminal latex
#set terminal fig
#set output "boxtwoparticle.fig"
#set size 1.0,1.0
set size ratio 1.0
set nokey
set contour
set view 30, 20
#set view 0, 0
set contour surface
set hidden3d
set isosamples 40, 40
set ticslevel -0.5
#unset surface
unset xtics
unset ytics
unset ztics
set cntrparam cubicspline
set cntrparam levels auto 20
splot[0:1][0:1](-sin(x*pi)*sin(2*y*pi)+sin(2*x*pi)*sin(y*pi))
```

2.11.5 Toy model for the exchange-correlation hole

Introduction

In this section, I will exploit only the two, probably most important properties of the exchange-correlation hole, to construct an extremely simple toy model for the exchange-correlation hole. Despite its simplicity, one can already rationalize a few physical effects. We will demonstrate, how solid-state magnetism can be understood in these terms.

The exchange-correlation hole of this model is a homogeneously charged sphere.

$$h_{xc}(\vec{r},\vec{r}') = \overbrace{h_X(\vec{r},\vec{r})}^{\text{on-top value}}\ \theta\Big(R - |\vec{r}' - \vec{r}|\Big) \tag{2.225}$$

where $\theta(x)$ is the Heaviside function and R is the sphere radius. Consult the figure 2.10 on p. 121.

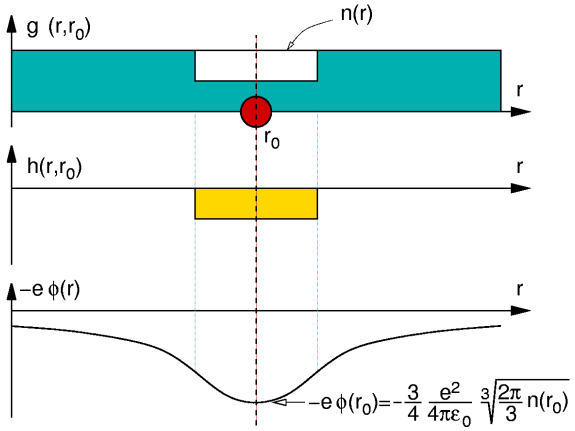


Fig. 2.10: Sketch of the construction of a simple model-density functional.

64

The charge on the sphere is determined from the **charge sum rule** Eq. 2.46. The size of the sphere is then obtained using the **on-top value**[65] of the exchange hole of the free-electron gas. Without interactions, the exchange hole for the spin-up electrons depends only on the spin-up density and the exchange hole for the spin-down electrons depends only on the spin-down density. I use the same assumption for the model of the exchange hole, which provides a spin-dependence of the this on-top value. The extension of the on-top value of the exchange hole to correlation can be found in the literature[35]

Working out the interaction energy then becomes a simple exercise of electrodynamics. This approximate interaction energy can then be combined with the kinetic energy of the free-electron gas, which we evaluated in a prior exercise, section 1.5.5 on p. 41. This will allow us to analyze, in this approximate model, how the electron gas will turn, at low density, into a ferromagnet.

Editor: Show the comparison of the exchange-correlation energy of the toy model with exact Hartree-Fock and quantum Monte Carlo calculations of the polarized and non-spinpolarized electron gas.

Editor: Compare the exact exchange hole of the free-electron gas as function of radius with the toy model. See figure E.2 on p.568.

[64] The first argument of $h_X(\vec{r},\vec{r}')$ is the position of the spectator electron, which experiences the Coulomb potential of the exchange hole. The second argument is value at which the hole-density is evaluated.

[65] The on-top value of the exchange hole is the value $h_X(\vec{r},\vec{r})$ of the exchange hole right at the position of the "spectator electron".

On-top value of the exchange hole

We will also need the **on-top value** $h_X(\vec{r},\vec{r})$ of the exchange hole. The on-top value is the value of the hole $h_x(\vec{r},\vec{r})$ right at the position of the spectator electron, i.e. for $\vec{r}=\vec{r'}$.

While the discussion of the exchange-correlation hole has been completely general so far, we can calculate the on-top value only for the exchange hole. The extension to correlation can be found in the literature[35]

The two-particle density $n^{(2)}$ of a Slater determinant is obtained analogously to the exchange energy E_X obtained in Eq. 2.36.

$$n^{(2)}(\vec{r},\vec{r'}) = n^{(1)}(\vec{r})n^{(1)}(\vec{r'}) - \sum_{\sigma,\sigma'} \rho^{(1)}(\vec{x},\vec{x'})\rho^{(1)}(\vec{x'},\vec{x}) \tag{2.226}$$

The corresponding hole density is

$$h_X(\vec{r},\vec{r'}) = -\frac{1}{n^{(1)}(\vec{r})} \sum_{\sigma,\sigma'\in\{\uparrow,\downarrow\}} \rho^{(1)}(\vec{x},\vec{x'})\rho^{(1)}(\vec{x'},\vec{x}) \tag{2.227}$$

The subscript X shall denote that this expression only considers the exchange contribution and ignores the correlation contribution.

The on-top value of the exchange hole is the hole for $\vec{r}=\vec{r'}$.

$$h_X(\vec{r},\vec{r}) = -\frac{1}{n^{(1)}(\vec{r})} \sum_{\sigma,\sigma'\in\{\uparrow,\downarrow\}} \rho^{(1)}(\vec{r},\sigma,\vec{r},\sigma')\rho^{(1)}(\vec{r},\sigma',\vec{r},\sigma) \tag{2.228}$$

The on-top value of the one-particle-reduced density matrix can be expressed in terms of total density n_t, i.e. $n^{(1)}$, and spin density $\vec{n}_S(\vec{r})$ and the Pauli matrices in the two-dimensional spin space as[66]

$$\begin{aligned}\rho^{(1)}(\vec{r},\sigma,\vec{r},\sigma') &\hat{=} \frac{1}{2}\left[n_t(\vec{r}) \underbrace{\begin{pmatrix}1&0\\0&1\end{pmatrix}}_{\mathbf{1}} + n_{S,x}(\vec{r}) \underbrace{\begin{pmatrix}0&1\\1&0\end{pmatrix}}_{\boldsymbol{\sigma}_x} + n_{S,y}(\vec{r}) \underbrace{\begin{pmatrix}0&-i\\i&0\end{pmatrix}}_{\boldsymbol{\sigma}_y} + n_{S,z}(\vec{r}) \underbrace{\begin{pmatrix}1&0\\0&-1\end{pmatrix}}_{\boldsymbol{\sigma}_z} \right] \\ &= \frac{1}{2}\begin{pmatrix} n_t + n_{S,z} & n_{S,x} - i n_{S,y} \\ n_{S,x} + i n_{S,y} & n_t - n_{S,z} \end{pmatrix} \end{aligned} \tag{2.230}$$

I will use the identity

$$\begin{aligned} \boldsymbol{A} &\overset{\text{def}}{=} a_0\mathbf{1} + \vec{a}\vec{\boldsymbol{\sigma}} \hat{=} \begin{pmatrix} a_0 + a_z & a_x - i a_y \\ a_x + i a_y & a_0 - a_z \end{pmatrix} \qquad \text{with } a_0 \in \mathbb{R}, \vec{a} \in \mathbb{R}^3 \\ &\Rightarrow \sum_{\sigma,\sigma'} A_{\sigma,\sigma'}A_{\sigma',\sigma} \overset{\boldsymbol{A}=\boldsymbol{A}^\dagger}{=} \sum_{\sigma,\sigma'} |A_{\sigma,\sigma'}|^2 = 2(a_0^2 + \vec{a}^2) \end{aligned} \tag{2.231}$$

and apply it to Eq. 2.228 with the one-particle-reduced density matrix $\rho^{(1)}$ from Eq. 2.230.

[66] In order to verify the factors, consider a spin density, which is fully polarized in z-direction. In that case $n_{S,z} = n_\uparrow - n_\downarrow = n_t$. The corresponding density matrix evaluated with Eq. 2.230 is

$$\rho^{(1)}(\vec{r},\sigma,\vec{r},\sigma') = \begin{pmatrix} n_t(\vec{r}) & 0 \\ 0 & 0 \end{pmatrix} \tag{2.229}$$

which is the anticipated result.

ON-TOP VALUE OF THE EXCHANGE HOLE

$$h_X(\vec{r},\vec{r}) = -\frac{1}{n_t(\vec{r})}\frac{1}{2}\left(\left(n_t(\vec{r})\right)^2 + \left(\vec{n}_s(\vec{r})\right)^2\right) = -n_t(\vec{r})\left[\frac{1}{2} + \frac{1}{2}\left(\frac{\vec{n}_S(\vec{r})}{n_t(\vec{r})}\right)^2\right] \qquad (2.232)$$

The on-top value of the exchange hole varies between half the density, for a non-spin polarized system, and once the density for a fully spin-polarized system.

The significance of this result is the dependence on the spin density. When, for a given total density, the spin density is increased, the hole becomes more compact. Because the hole is now closer to the reference electron, the energy is lowered. Hence, the exchange term favors spin polarization. This is the origin of magnetism in solid materials.

Problem:

1 Determine the size of the exchange correlation hole

2 Use the on-top value Eq. 2.232 to construct the exchange correlation hole as function of the electron density and the spin density.

3 Combine the approximate exchange energy with the kinetic energy to determine the total energy as function of electron density and spin density. Estimate the energy difference between an electron gas in the paramagnetic and the ferromagnetic state. Estimate the electron density where the transition occurs. Estimate the electron density for real materials considering only the valence electrons.

? Editor: Sketch only: Estimate the entropy of the electron gas to estimate the Curie temperature of a free-electron gas.

Solution

1 Determine the size of the exchange correlation hole

The density value is obtained from the on-top value Eq. 2.232 for a Slater determinant and the radius is obtained from the sum rule Eq. 2.46. This yields

$$\overbrace{-n_t(\vec{r})\left[\frac{1}{2} + \frac{1}{2}\left(\frac{\vec{n}_S(\vec{r})}{n_t(\vec{r})}\right)^2\right]}^{\text{on-top value Eq. 2.232}} \cdot \frac{4\pi}{3}R^3 = -1 \quad \Rightarrow \quad R = \sqrt[3]{\frac{3}{4\pi}}\left[\frac{1}{2} + \frac{1}{2}\left(\frac{\vec{n}_S(\vec{r})}{n_t(\vec{r})}\right)^2\right]^{-\frac{1}{3}} [n_t(\vec{r})]^{-\frac{1}{3}} \qquad (2.233)$$

2 Use the on-top value Eq. 2.232 to construct the exchange correlation hole as function of the electron density and the spin density.

Next, we evaluate the exchange energy

The interaction of an electron with its exchange correlation hole is the electrostatic potential of the hole multiplied with the charge of the electron.[67] Integration over all electrons, yields the exchange-

[67] The potential acting on electrons of a homogeneously charged sphere with charge $+e$ and radius R is

$$v(|\vec{r}|) = -\frac{e^2}{4\pi\epsilon_0 R}\begin{cases}\frac{3}{2} - \frac{1}{2}\left(\frac{r}{R}\right)^2 & \text{for } |\vec{r}| < R \\ \left(\frac{r}{R}\right)^{-1} & \text{for } |\vec{r}| > R\end{cases} \qquad (2.234)$$

correlation (here only the exchange energy) energy. In contrast to the exchange-correlation energy, the exchange energy does not have a kinetic energy contribution, so that the exchange energy E_X has only a potential energy contribution U_X.

$$\begin{aligned} E_X &\overset{\text{Eq. 2.45}}{=} \int d^3r\, n^{(1)}(\vec{r}) \frac{1}{2} \int d^3r' \, \frac{e^2 h_X(\vec{r},\vec{r'})}{4\pi\epsilon_0 |\vec{r}-\vec{r'}|} \\ &= \frac{1}{2}\frac{e^2}{4\pi\epsilon_0} \int d^3r\, n^{(1)}(\vec{r}) \frac{-3}{2R} \\ &\overset{\text{Eq. 2.233}}{=} -\frac{1}{2}\frac{e^2}{4\pi\epsilon_0}\frac{3}{2} \int d^3r\, n^{(1)}(\vec{r}) \left\{ \sqrt[3]{\frac{3}{4\pi}} \left[\frac{1}{2} + \frac{1}{2}\left(\frac{\vec{n}_S(\vec{r})}{n_t(\vec{r})} \right)^2 \right]^{-\frac{1}{3}} \left[n^{(1)}(\vec{r}) \right]^{-\frac{1}{3}} \right\}^{-1} \\ &= -\frac{1}{2}\frac{e^2}{4\pi\epsilon_0}\frac{3}{2}\sqrt[3]{\frac{4\pi}{3}} \int d^3r \, \left(n^{(1)}(\vec{r}) \right)^{\frac{4}{3}} \left[\frac{1}{2} + \frac{1}{2}\left(\frac{\vec{n}_S(\vec{r})}{n_t(\vec{r})} \right)^2 \right]^{+\frac{1}{3}} \end{aligned} \tag{2.235}$$

Despite its simplicity, the model captures many features of the real system. This is because it correctly captures the charge sum rule Eq. 2.46.

Because the system is charge neutral, the Hartree energy, the electrostatic self energy of the charge background and the interaction of electrons with the background cancel exactly. Hence only the kinetic energy and the exchange-correlation energy need to be considered.

3 Combine the approximate exchange energy with the kinetic energy to determine the total energy as function of electron density and spin density. Estimate the energy difference between an electron gas in the paramagnetic and the ferromagnetic state. Estimate the electron density where the transition occurs. Estimate the electron density for real materials considering only the valence electrons.

The total energy of the model is

$$\begin{aligned} E_{\text{tot}}(n_t, \vec{n}_S) = & \underbrace{\int d^3r \, \underbrace{\frac{3}{10}\left(3\pi^2\right)^{\frac{2}{3}} \frac{\hbar^2}{m_e} n_t^{\frac{5}{3}}}_{E(n_t,0)/L^3} \cdot \underbrace{\frac{1}{2}\left(\left(1+\frac{|\vec{n}_S|}{n_t}\right)^{\frac{5}{3}} + \left(1-\frac{|\vec{n}_S|}{n_t}\right)^{\frac{5}{3}} \right)}_{\approx 1+(2^{\frac{2}{3}}-1)\left(\frac{n_S}{n_t}\right)^2}}_{E_{kin} \quad \text{Eq. 1.149}} \\ & \underbrace{-\frac{1}{2}\frac{e^2}{4\pi\epsilon_0}\frac{3}{2}\sqrt[3]{\frac{4\pi}{3}} \int d^3r \, \left(n_t(\vec{r})\right)^{\frac{4}{3}} \left[\frac{1}{2} + \frac{1}{2}\left(\frac{\vec{n}_S(\vec{r})}{n_t(\vec{r})} \right)^2 \right]^{+\frac{1}{3}}}_{U_{xc} \quad \text{Eq. 2.235}} \end{aligned} \tag{2.236}$$

The resulting total energy

Editor: The model artificially stabilizes the ferromagnetic electron gas. This is probably due to the lack of correlation, the Coulomb hole. It may also be due to the kinetic energy. The kinetic energy correction can be estimated from excluded volume in a hard sphere model. The ferromagnetic electron gas becomes favorable only at very low densities with $r_s >>$ look up thesis of Graham George Spink 2017 in the group of Richard Needs. spink17_thesis.pdf

In the following, we will resort to the exchange-correlation hole to rationalize the findings related to the electron-electron interaction in real materials.

Hund's rule and Stoner parameter

The model provides the underlying reason for Hund's rule, which says that electrons will align their spin, unless the kinetic-energy cost is too large.

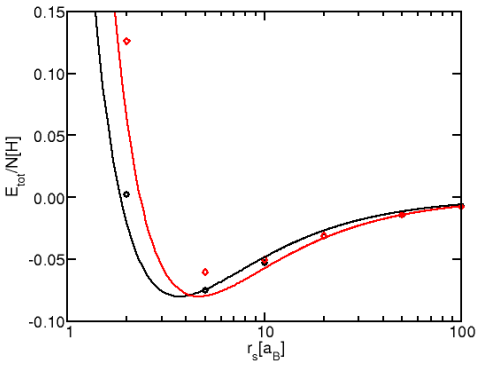


Fig. 2.11: Total energy per electron $(E_{kin} + U_{xc})/N$ of the paramagnetic free-electron gas (black) and of the ferromagnetic free-electron gas (red). The lines are obtained from Eq. 2.236. Circles and diamonds are from accurate quantum-Monte-Carlo calculations by Ceperley and Alder[55]. Compare also to ["*Energy, Specific Heat, and Magnetic Properties of the Low-Density Electron Gas*", W. J. Carr, Jr., Phys. Rev. **122**, 1437 (1961), https://doi.org/10.1103/PhysRev.122.1437].

HUND'S RULE AND FERROMAGNETISM

Exchange acts only between electrons pairs with the same spin. Because exchange counteracts the Coulomb repulsion, it favors electrons with the same spin.

A result is **Hund's 1st rule**: *"For a given electron configuration, the term with maximum multiplicity has the lowest energy. The multiplicity is equal to* $2S+1$*, where* S *is the total spin angular momentum for all electrons. The term with lowest energy is also the term with maximum* S*."* [a] To be precise, the spin angular momentum is $\hbar S$.
Consider a set of degenerate one-particle states. Hund's rule says that the electrons will occupy this set so that the total spin is maximized. (The state with maximum spin has the largest multiplicity, namely $2S + 1$.) If many electrons have the same spin, the energy gain from the exchange term is large.

The same effect is responsible for the tendency of some solids to become **ferromagnetic**. Due to the finite band width of metals, spin-alignment leads to some loss of kinetic energy. The balance of kinetic energy and exchange determines whether ferromagnetism wins.

[a] Source `https://en.wikipedia.org/wiki/Hund%27s_rules`, retrieved Mar. 24, 2017.

Closely related to Hund's rule, which is useful for atoms, is Stoner's criterion for Ferromagnetism.

STONER CRITERION

If the density of states at the Fermi level of a non-magnetic metal obeys

$$D(\epsilon_F) I_{Stoner} > 1 \tag{2.237}$$

it exhibits an instability towards a ferromagnetism. I_{Stoner} is Stoner's exchange parameter.

While the concept underlying the tendency of electrons to arrange ferromagnetically is more general, studying this effect for our model as a specific example shall make the explanation more transparent. For this purpose, we can combine the exchange energy of the model-hole function Eq. 2.235 with the kinetic energy from Eq. 1.149 on p. 45.[68] This is a reasonably good model for

[68] The Hartree contribution of the electron interaction, the energy of the external potential (from the positive charge

a free-electron gas with interaction. It is able to describe, at least qualitatively, the transition to a ferromagnet with increasing interaction.

In the model, one can evaluate the energy as function of spin polarization $x = |\vec{n}_s|/n_t$ relative to the non-magnetic case. For the sake of simplicity, kinetic and exchange energies are scaled so that the kinetic energy is constant and the exchange energy can be scaled by the parameter a.

$$y(x) = \underbrace{\frac{1}{2}\left[(1+x)^{\frac{5}{3}} + (1-x)^{\frac{5}{3}}\right]}_{\sim \text{ kinetic energy Eq. 1.149}} \underbrace{-a(1+x^2)^{\frac{1}{3}}}_{\sim \text{exchange Eq. 2.235}} + a - 1 \tag{2.238}$$

The parameter a is a dimension-less ratio of the constants for the kinetic energy and exchange energy, which we will not work out in detail. The result Eq. 2.238 is shown figure 2.12. The model predicts a transition to a ferromagnet for $a = 5/3$.

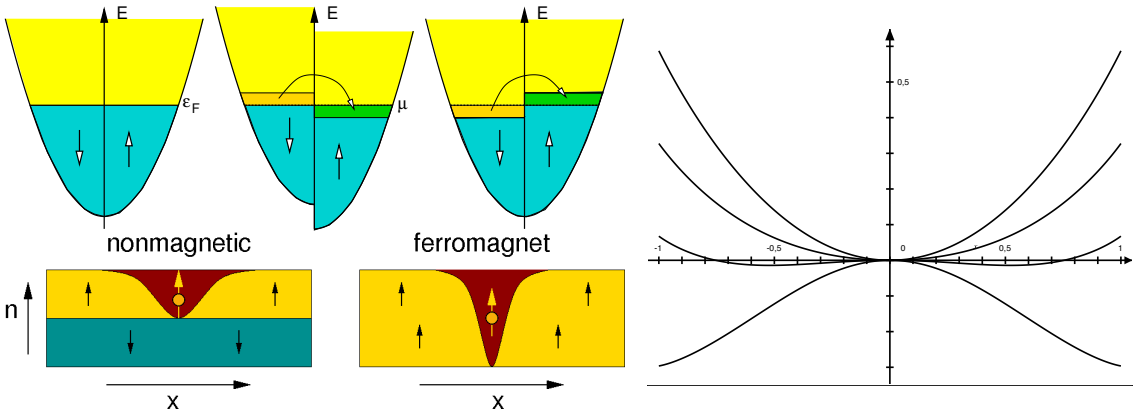


Fig. 2.12: Left, top: Scheme to explain the increasing kinetic energy with spin-polarization: density of states of a free-electron gas for spin-up and spin-down electrons. A magnetic moment can be induced, for example, by applying an external magnetic field, which makes the electrons of one spin direction more favorable than those with opposite spin. The kinetic energy increase is seen by removing the external field but maintaining the occupations of the spin-polarized system. Left,bottom: Scheme to explain the gain of interaction energy through spin polarization. The exchange hole of a ferromagnet has a higher density, namely $-n_t$ rather than $-n_t/2$. Considering the sum rule, the radius of the exchange hole is thus smaller. Thus, the interaction of electrons with the exchange hole is larger. Right: total energy Eq. 2.238 of the jellium model as function of the spin polarization $|\vec{n}_s|/n_t$ for different values of the interaction strength. The exchange energy is obtained with the model hole function of Eq. 2.235. The results are shown for $a = 0, 1, 2, 3$ from top to bottom. Without interaction, the Fermi gas is non-magnetic. For $a > 5/3$, however, the system becomes ferromagnetic.

The tendency towards ferromagnetism is a general feature of electrons, which is captured by the **Stoner criterion** for ferromagnetism:

When the kinetic energy dominates, the system strongly resists a spin polarization. We can say that the spin polarization requires electron-hole pairs, with the electron in the majority-spin channel and the hole in the minority-spin channel. When the density of states is small, as in a system in a large kinetic energy, a specific spin polarization requires electron-hole pairs with large energy. This energy cost must be overcome by the energy gain from the exchange energy. When the bands narrow, i.e. fairly flat, the density of states is high, and one can create many electron-hole pairs with small energy. In that case, ferromagnetism is favorable.

background) and the electrostatic self energy of the positive charge background cancel each other exactly and are therefore not accounted for. They cancel each other because they sum up to the total density of electrons and charge background. This total density vanishes per construction.

This is one explanation, why just the elemental 3-d transition-metals Fe, Co, Ni exhibit magnetism. Despite their energy position in the valence-band region, 3d-states have a radial extent similar to the 3s- and 3p-core states. Thus, they have a small hopping parameters and form fairly narrow bands with large density of states. For the heavier transition metals, of row 5 and 6 in the periodic table, the valence d-bands are wider. The larger radial extent of the 5d and 6d-states is due to the **Pauli repulsion**[69] with the lower 3d-states, which pushes the 4d and 5d states outward from the nucleus. The larger overlap with the neighboring atoms, which causes larger hopping parameters, and thus increases the band width.

[69] The Pauli repulsion describes an upward shift due to the orthogonality requirement with lower lying states.

Chapter 3

Second quantization

In this chapter, I will introduce the notion of creation and annihilation operators. This will lead to an elegant formulation of quantum mechanics in the Fock space.

I will place some emphasis on the definitions and the relations between different notations. The connection is easily lost. In particular, I consider the connection to wave functions (in real space) important for two reasons: Firstly, it connects to our knowledge base of one-particle quantum mechanics. Secondly, it allows one to connect to first-principles calculations, which employ explicit wave functions.

3.1 Fock space

There are several ways towards second quantization. The most simple one is to define the Fock space. The **Fock space** is the combination of the Hilbert spaces for 0-particle states, 1-particle states, 2-particle states, etc. Let $\mathcal{H}_N$ be the Hilbert space of all N-particle states. The Fock space $\mathcal{F}$ is the union[1] of all N-particle Hilbert spaces $\mathcal{H}^N$, that is

$$\mathcal{F} \stackrel{\text{def}}{=} \bigcup_{N=0}^{\infty} \mathcal{H}_N \tag{3.1}$$

The definition of the scalar product is that of the Hilbert spaces. What is missing is a definition of the scalar product between states with different particle numbers. We postulate that the scalar product of states with different particle numbers vanishes.[2]

As a curiosity, we introduced here also the 0-particle state, called **vacuum state**, that is not represented by a wave function at all.

Another way to define the Fock space[3] is the following.

1. Starting from a one-particle Hilbert space $\mathcal{H}$ one constructs the Hilbert space $\mathcal{H}^{\otimes N}$ of general N-particle states as tensor product of N one-particle states.

2. For identical particles these states are antisymmetrized (for fermions) or symmetrized (for bosons). The resulting space of fermionic N-particle wave functions is denoted by $\mathcal{H}^{-,\otimes N}$ –denoted above as $\mathcal{H}_N$ – and the one for bosonic N-particle wave functions is denoted by $\mathcal{H}^{+,\otimes N}$

[1] germ.:union=Vereinigung

[2] This postulate is non-trivial and can be derived more naturally from the second quantization via introducing wave functions in the space of the fields describing the wave functions.

[3] Taken from `https://en.wikipedia.org/wiki/Fock_space`.

3. The direct sum of all fermionic N-particle Hilbert spaces is the Fock space

$$\mathcal{F}^{(-)} = \bigoplus_{N=0}^{\infty} \mathcal{H}^{-,\otimes N} , \tag{3.2}$$

denoted above simply as $\mathcal{F}$. The definition for the bosonic Fock space is analogous.

$$\mathcal{F}^{(+)} = \bigoplus_{N=0}^{\infty} \mathcal{H}^{+,\otimes N} \tag{3.3}$$

3.2 Occupation-number representation

We are entering a new level of abstraction and it turned out to be useful to introduce a special notation for it. This will lead us to the occupation-number representation and to creation and annihilation operators.

In order to work within the Fock space, we need to select a suitable basis set. We have already learned that Slater determinants, which are constructed from a complete orthonormal one-particle basis, form a complete set of many-particle wave functions.

Each Slater determinant is uniquely defined, up to a sign, by the one-particle states used in its construction. Therefore, the Slater determinants can be written economically in the **occupation-number representation**. For a given, ordered, one-particle basisset, we form a vector, where each position corresponds to a particular one-particle orbital. Each entry can be zero or one, and describes if that particular orbital is present in the Slater determinant or not. If the occupation number is one, we say that the orbital is occupied, and if the occupation-number is zero, we say that it is unoccupied or empty. Thus, a Slater determinant can be expressed in a form like

$$|0,0,0,\underbrace{1}_{i_1},0,\underbrace{1}_{i_2},0,\ldots\rangle = |S_{i_1,i_2,\ldots}\rangle \qquad \text{with} \quad i_1 < i_2 < \ldots \tag{3.4}$$

where $S_{i_1,i_2,\ldots}$ is a Slater determinant made of the one-particle orbitals $|\varphi_{i_1}\rangle, |\varphi_{i_2}\rangle, \ldots$.

Because the Slater determinant changes its sign under permutation of two one-particle wave functions, we need to define the sign convention. The sign is fixed such that the one-particle orbitals must occur in the corresponding Slater determinant in the order of increasing index, that is $i_1 < i_2, \ldots$. Thus,

$$|1,1,0,0,\ldots\rangle = |S_{1,2}\rangle = -|S_{2,1}\rangle \tag{3.5}$$

$$\langle \vec{r}, \vec{r'}|1,1,0,0,\ldots\rangle = \frac{1}{\sqrt{2!}}\left[\varphi_1(\vec{r})\varphi_2(\vec{r'}) - \varphi_2(\vec{r})\varphi_1(\vec{r'})\right] \tag{3.6}$$

Note also, that there is an explicit **vacuum state**

$$|\mathcal{O}\rangle \stackrel{\text{def}}{=} |0,0,0,0,0,0,0,0,0,0,\ldots\rangle \tag{3.7}$$

The vacuum state describes a system without particles. Note that the vacuum state, which we denote by a calligraphic "O", $|\mathcal{O}\rangle$, is different from the zero state $|\varnothing\rangle$. The latter is obtained by multiplying an arbitrary state with zero.

The most general antisymmetric wave function has the form

$$|\Phi\rangle = \sum_{\vec{\sigma}} |\vec{\sigma}\rangle c_{\vec{\sigma}} = \sum_{\sigma_1,\sigma_2,\ldots=0}^{1} |\sigma_1,\sigma_2,\ldots\rangle c_{\sigma_1,\sigma_2,\ldots} \tag{3.8}$$

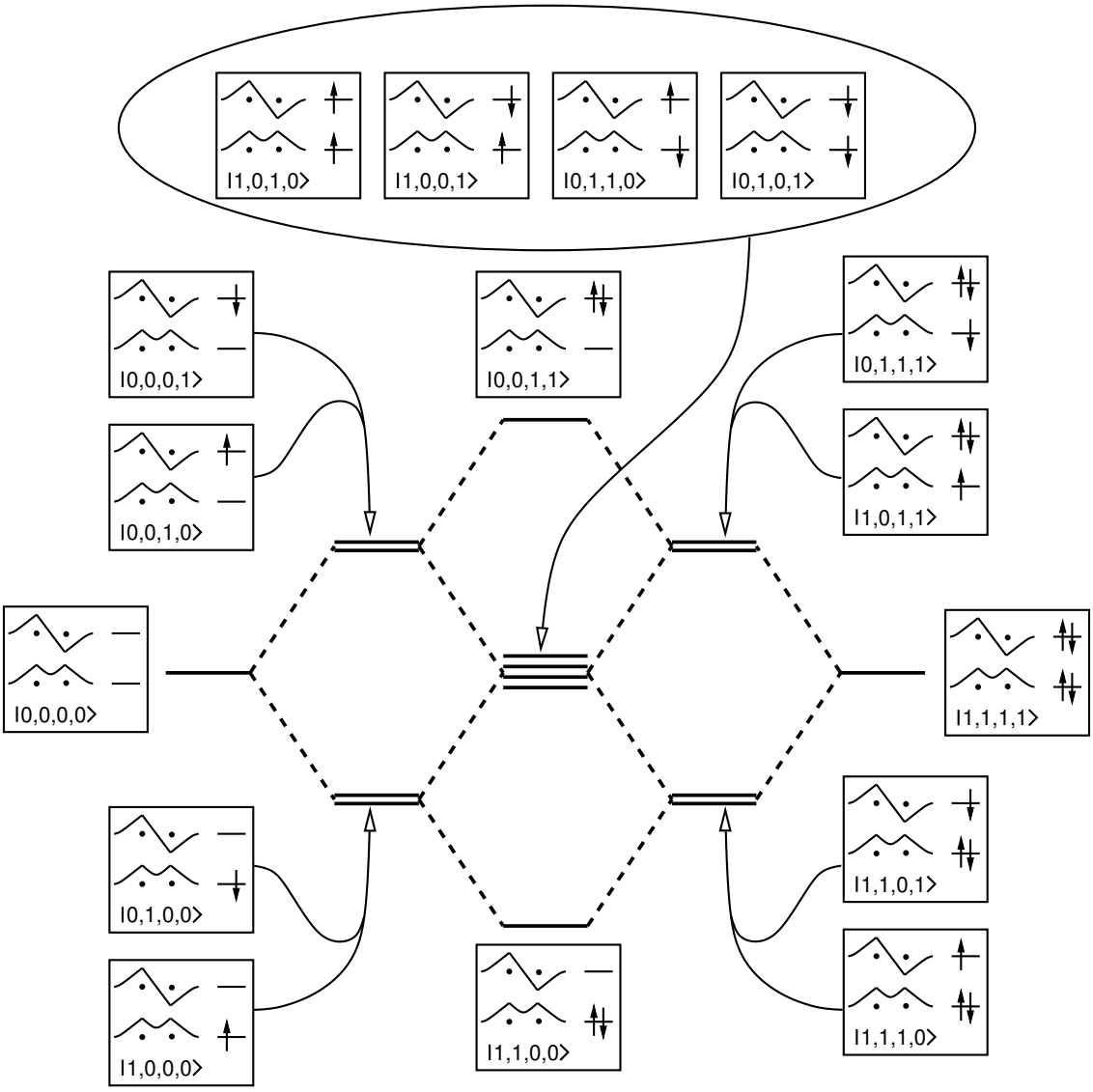


Fig. 3.1: Schematic representation of the Fock space build from the bonding and antibonding states of the hydrogen molecule. The middle diagram represents the many-particle energy levels assuming non-interacting electrons and with $\epsilon_a = -\epsilon_b$, where ϵ_a is the one-particle energy of the antibonding level and ϵ_b is the energy level of the bonding orbital. The insets correspond to the occupation-number representation and the corresponding one-electron energy level diagram. On the left it contains a schematic drawing of the one-particle wave functions.

Example: hydrogen molecule

Let us consider a hydrogen molecule with only one s-orbital per site. The s-orbitals shall be combined into bonding and an antibonding orbitals. The ordered one-particle basis is $|b,\uparrow\rangle, |b,\downarrow\rangle, |a,\uparrow\rangle, |a,\downarrow\rangle$, where $|b,\sigma\rangle$ describes the bonding and $|a,\sigma\rangle$ describes the antibonding orbital.

Now, we can form the limited Fock space for this model. There are $2^4 = 16$ Slater determinants as shown in Fig. 3.1.

- $|0000\rangle$ is the zero-particle state. It describes just the two protons without electrons.
- $|1000\rangle$, $|0100\rangle$, $|0010\rangle$ and $|0001\rangle$ are the one-particle states. Thus, they describe the H_2^+ ion.

The states $|1000\rangle$ and $|0100\rangle$ correspond to the bound H_2^+ ion, while the remaining two states correspond to the electron in the antibonding state. The molecule in the latter configuration would be unstable.

- $|1100\rangle$ corresponds to the ground state of the H_2 molecule with two paired electrons in the bonding orbital. There are in total 6 two-electron Slater determinants of which 5 are excited states.
- There are four three-electron states, namely $|1110\rangle$ $|1101\rangle$, $|1011\rangle$,$|01111\rangle$. The three particle states describe the negative H_2^- ion.
- finally there is one four-electron state, $|1111\rangle$ which describes the H_2^{2-} ion.

Excursion: Integer representation representation of Slater determinants

Note that the sequence can be considered as a binary number with the digits. This allows one to identify each Slater determinant uniquely with one integer number.

The conversion of an integer into the number representation is

$$\begin{aligned} 0 &\rightarrow |0,0,0,0,0,0,0,0,0,0,\ldots\rangle \\ 1 &\rightarrow |1,0,0,0,0,0,0,0,0,0,\ldots\rangle \\ 2 &\rightarrow |0,1,0,0,0,0,0,0,0,0,\ldots\rangle \\ 3 &\rightarrow |1,1,0,0,0,0,0,0,0,0,\ldots\rangle \\ 4 &\rightarrow |0,0,1,0,0,0,0,0,0,0,\ldots\rangle \\ \mathcal{I}(\vec{\sigma}) \stackrel{\text{def}}{=} \sum_j \sigma_j 2^{j-1} &\rightarrow |\sigma_1,\sigma_2,\ldots\rangle \end{aligned} \tag{3.9}$$

In FORTRAN, bits can be handled in a simple manner. If $\mathcal{I}$ is the integer representation of a Slater determinant and i is the position of a particular one-particle orbital, we obtain its occupation number by

$$\sigma_i = \texttt{BTEST}(\mathcal{I}-1, i-1) \tag{3.10}$$

The bits can be manipulated using the FORTRAN functions

$$\begin{aligned} \mathcal{I}' &= \texttt{IBCLR}(\mathcal{I}-1, i-1) \\ \mathcal{I}'' &= \texttt{IBSET}(\mathcal{I}-1, i-1) \end{aligned} \tag{3.11}$$

where $\mathcal{I}'$ is obtained from $\mathcal{I}(\vec{\sigma})$ by setting the occupation σ_i to zero, and $\mathcal{I}''$ is obtained by setting it to one.

In order to see the difficulty of many-particle physics let us count the number of states. When we truncate the one-particle basisset to M orbitals, there are 2^M many-particle basisfunctions, because any one-particle state can be occupied or unoccupied. For $M = 10$ there are already $2^{10} = 1024$ states, which requires a kilobyte of memory to hold the coefficients. For $M = 20$ we already require a Megabyte and for 30 orbitals we need a gigabyte.

3.3 Creation and annihilation operators

We define **creation operators** $\hat{a}_i^\dagger$ that increase the particle number in a given one-particle state. Using creation operators, we can create all many-particle states from the vacuum state.

. . . from Slater determinants

DEFINITION OF A CREATION OPERATOR IN TERMS OF SLATER DETERMINANTS

We define the creation operator for a particular orbital as follows: When we apply a creation operator to a Slater determinant, it adds a row with the new orbital at the top of the corresponding matrix, and introduces a column with a new coordinate to the right.
This definition is the link between wave functions and the operator algebra used in the following.

It is important to watch the sign of the state. Let us consider an example where a third particle in state $|\varphi_2\rangle$ is created in a state that contains two particles, one in $|\varphi_1\rangle$ and one in $|\varphi_3\rangle$.

$$\begin{aligned}\hat{a}_2^\dagger \overbrace{\frac{1}{\sqrt{2!}}\det\begin{vmatrix}\varphi_1(\vec{x}_1) & \varphi_1(\vec{x}_2)\\ \varphi_3(\vec{x}_1) & \varphi_3(\vec{x}_2)\end{vmatrix}}^{|1,0,1,0,\ldots\rangle} &= \overbrace{\frac{1}{\sqrt{3!}}\det\begin{vmatrix}\varphi_2(\vec{x}_1) & \varphi_2(\vec{x}_2) & \varphi_2(\vec{x}_3)\\ \varphi_1(\vec{x}_1) & \varphi_1(\vec{x}_2) & \varphi_1(\vec{x}_3)\\ \varphi_3(\vec{x}_1) & \varphi_3(\vec{x}_2) & \varphi_3(\vec{x}_3)\end{vmatrix}}^{\hat{a}_2^\dagger|1,0,1,0,\ldots\rangle}\\ &= (-1)\cdot\underbrace{\frac{1}{\sqrt{3!}}\det\begin{vmatrix}\varphi_1(\vec{x}_1) & \varphi_1(\vec{x}_2) & \varphi_1(\vec{x}_3)\\ \varphi_2(\vec{x}_1) & \varphi_2(\vec{x}_2) & \varphi_2(\vec{x}_3)\\ \varphi_3(\vec{x}_1) & \varphi_3(\vec{x}_2) & \varphi_3(\vec{x}_3)\end{vmatrix}}_{|1,1,1,0,\ldots\rangle}\end{aligned} \tag{3.12}$$

. . . from the occupation-number representation

Each state $|\vec{\sigma}\rangle$ of the occupation-number representation can be translated uniquely into a Slater determinant. This translation rule requires the choice of an ordered, complete orthonormal set of one-particle wave functions $|\varphi_j\rangle$. Once we have this translation, we can translate the definition of creation operators into the occupation-number representation.

For the example Eq. 3.12 above, we obtain

$$\hat{a}_2^\dagger|1,0,1,0,0,\ldots\rangle = -|1,1,1,0,0,\ldots\rangle \tag{3.13}$$

The added one-particle state needs to be moved to the correct position in the Slater determinant. Each occupied orbital, one passes during that process, contributes a sign change. Thus, we need to count the number of occupied orbitals left of the final position. The net number of sign changes for adding an electron in orbital $|\varphi_i\rangle$ is thus $\sum_{j<i}\sigma_j$.

Generalizing this principle leads to

$$\begin{aligned}\hat{a}_i^\dagger|\sigma_1,\sigma_2,\ldots,\underbrace{0}_{\text{pos } i},\ldots\rangle &= |\sigma_1,\sigma_2,\ldots,\underbrace{1}_{\text{pos } i},\ldots\rangle\ \left[(-1)^{\sum_{j<i}\sigma_j}\right]\\ \hat{a}_i^\dagger|\sigma_1,\sigma_2,\ldots,\underbrace{1}_{\text{pos } i},\ldots\rangle &= |\varnothing\rangle\end{aligned} \tag{3.14}$$

In short, we may write

$$\hat{a}_i^\dagger = \sum_{\vec{\sigma}} \underbrace{\left|\sigma_1,\sigma_2,\ldots,\sigma_i+1,\ldots\right\rangle}_{=|\varnothing\rangle \text{ for } \sigma_i=1}\left(\left[(-1)^{\sum_{j<i}\sigma_j}\right]\ \underbrace{\sqrt{1-\sigma_i}}_{=0 \text{ for } \sigma_i=1}\right)\left\langle\sigma_1,\sigma_2,\ldots,\sigma_i,\ldots\right| \tag{3.15}$$

The factor $\sqrt{1-\sigma_i}$ ensures that Eq. 3.15 does not produce states with occupations $\sigma_i \geq 2$. The square root has been chosen to be consistent with the case of bosons, discussed later: The factor for bosons is $\sqrt{1+\sigma}$. For fermions σ_j can only have values zero and one, for which $\delta_{\sigma,1} = \sigma = \sqrt{\sigma}$, so that the result is unchanged from $1-\sigma$ to $\sqrt{1-\sigma}$.

The hermitian conjugate of the creation operator is calculated from Eq. 3.15 using the general operator identity

$$\hat{A} = \sum_{m,n} |m\rangle A_{m,n} \langle n| \qquad \Leftrightarrow \qquad \hat{A}^\dagger = \sum_{m,n} |n\rangle A^*_{m,n} \langle m| = \sum_{m,n} |m\rangle A^*_{n,m} \langle n| \tag{3.16}$$

which yields for $\hat{a}_i = (\hat{a}_i^\dagger)^\dagger$

$$\begin{aligned} \hat{a}_i &\overset{\text{Eq. 3.15}}{=} \sum_{\vec{\sigma}} \Big|\sigma_1, \sigma_2, \ldots, \sigma_i, \ldots\Big\rangle \left(\left[(-1)^{\sum_{j<i}\sigma_j}\right] \sqrt{1-\sigma_i}\right)^* \Big\langle \sigma_1, \sigma_2, \ldots, \sigma_i + 1, \ldots\Big| \\ &= \sum_{\vec{\sigma}} \Big|\sigma_1, \sigma_2, \ldots, \sigma_i - 1, \ldots\Big\rangle \left(\left[(-1)^{\sum_{j<i}\sigma_j}\right] \sqrt{\sigma_i}\right) \Big\langle \sigma_1, \sigma_2, \ldots, \sigma_i, \ldots\Big| \end{aligned} \tag{3.17}$$

We see that $\hat{a}_i$ annihilates electrons and is thus named **annihilator**.

The last step in Eq. 3.17 is a little tricky. In first line of Eq. 3.17, the factor $\sqrt{1-\sigma}$ excludes the terms with $\sigma_i = 1$. In the second line, the factor $\sqrt{\sigma}$ excludes terms with $\sigma_i = 0$.

CREATION AND ANNIHILATION OPERATORS FOR FERMIONS

The definition of creation operators $\hat{a}_i^\dagger$ and annihilation operators $\hat{a}_i$ for fermions is

$$\begin{aligned} \hat{a}_i^\dagger &\overset{\text{Eq. 3.15}}{=} \sum_{\vec{\sigma}} \Big|\sigma_1, \sigma_2, \ldots, \sigma_i + 1, \ldots\Big\rangle \left(\left[(-1)^{\sum_{j<i}\sigma_j}\right] \sqrt{1-\sigma_i}\right) \Big\langle \sigma_1, \sigma_2, \ldots, \sigma_i, \ldots\Big| \\ \hat{a}_i &\overset{\text{Eq. 3.17}}{=} \sum_{\vec{\sigma}} \Big|\sigma_1, \sigma_2, \ldots, \sigma_i - 1 \ldots\Big\rangle \left(\left[(-1)^{\sum_{j<i}\sigma_j}\right] \sqrt{\sigma_i}\right) \Big\langle \sigma_1, \sigma_2, \ldots, \sigma_i, \ldots\Big| \end{aligned} \tag{3.18}$$

The sum is performed over all vectors $|\vec{\sigma}\rangle$ with $\sigma_i \in \{0, 1\}$, where the indices j refer to a ordered, complete and orthonormal one-particle basisset.

It may disturb that states with forbidden occupations σ_i turn up with $\sigma_i < 0$ or $\sigma_i > 1$. This formal difficulty can be healed by simply defining those states as being the zero state $|\varnothing\rangle$. Thus,

$$|\sigma_1, \sigma_2, \ldots\rangle \overset{\text{def}}{=} |\varnothing\rangle \qquad \text{if there is an} \qquad \sigma_i \notin \{0, 1\} \tag{3.19}$$

Note, that the zero state $|\varnothing\rangle$ is different from the vacuum state $|\mathcal{O}\rangle$. The vacuum state describes a physical situation, namely one without particles. The zero state does not describe any physical situation. In a superposition of states, it can simply be left out.

Building up the Fock space from the vacuum state

The creation and annihilation operators lead us to one other representation of the basis states, which is distinct from the occupation-number representation and the Slater determinants. Each state can be identified with a product of creation operators.

We start out from the **vacuum state** defined in Eq. 3.7

$$|\mathcal{O}\rangle \overset{\text{def}}{=} |0, 0, 0, \ldots\rangle \tag{3.20}$$

The vacuum state is a zero-particle state. It represents the vacuum, which is a system without particles.[4]

Then, we fill electrons into the vacuum using the creation operators:

[4] Note, that the vacuum state differs from a zero state.

OCCUPATION-NUMBER REPRESENTATION AND CREATION OPERATORS

A state characterized in the occupation-number representation by a string $\vec{\sigma}$ of occupation numbers, i.e. a Slater determinant, can be constructed by successively applying creation operators to the vacuum state $|\mathcal{O}\rangle$ in the form

$$|\vec{\sigma}\rangle = \prod_{j=1}^{\infty} \left(\hat{a}_j^\dagger\right)^{\sigma_j} |\mathcal{O}\rangle$$

$$\langle\vec{\sigma}| = \langle\mathcal{O}| \underbrace{\prod_{j=1}^{\infty}}_{\text{Caution!}} (\hat{a}_j)^{\sigma_j} \tag{3.21}$$

For the ket, the indices in the product increase from the left to the right. This avoids sign changes as particles are created. A different order may induce sign changes. For the bra the order of the operator is opposite, i.e. from right to left. The reversed order of the product is indicated with an uncommon notation, namely by interchanging the lower and upper bound of the index in the product. As a special case, we obtain a representation of one-particle orbitals in terms of the vacuum state and the corresponding creation operator.

$$|\varphi_j\rangle = \hat{a}_j^\dagger |\mathcal{O}\rangle \tag{3.22}$$

A general quantum state $|\Psi\rangle$ is a superposition of Slater determinants $|\vec{\sigma}\rangle$. Also such a state can be built up from the vacuum state with the help of creation operators.

$$|\Psi\rangle = \sum_{\vec{\sigma}} |\vec{\sigma}\rangle c_{\vec{\sigma}} = \left(\sum_{\vec{\sigma}} c_{\vec{\sigma}} \prod_{j=1}^{\infty} \left(\hat{a}_j^\dagger\right)^{\sigma_j}\right) |\mathcal{O}\rangle \tag{3.23}$$

This is an important step: From this point on, not only the operators, but even the states, are represented by operators. Because there is only one vacuum state, the sequence of creation operators is sufficient to uniquely define a state. All expectation values are finally ones calculated with the vacuum state.

3.4 Anticommutator relations

Commutator relations play an important role in quantum mechanics. In the case of quantum field theory of fermions, it is the anticommutator relations between fermionic creation and annihilation operators.

We determine the anticommutator relation[5] between creation and annihilation operators in the following.

The origin of the anticommutator rules is Pauli's principle, i.e. the antisymmetry of the fermionic wave function.

- From the definition of the creation operators in terms of Slater determinants, i.e. Eq. 3.12, we know that an interchange of two particles changes the sign of the wave function, i.e.

$$\hat{a}_i^\dagger \hat{a}_j^\dagger |\Phi\rangle = -\hat{a}_j^\dagger \hat{a}_i^\dagger |\Phi\rangle \qquad \Rightarrow \qquad [\hat{a}_i^\dagger, \hat{a}_j^\dagger]_+ |\Phi\rangle = |\varnothing\rangle \tag{3.24}$$

  $|\varnothing\rangle$ is the null state. Because the equation holds for any fermionic wave function $|\Phi\rangle$, it can

[5] The anticommutator of two operators $\hat{A}$ and $\hat{B}$ is denoted as $[\hat{A}, \hat{B}]_+ \stackrel{\text{def}}{=} \hat{A}\hat{B} + \hat{B}\hat{A}$.

simply be written as operator relation

$$\left[\hat{a}_i^\dagger, \hat{a}_j^\dagger\right]_+ = 0 \tag{3.25}$$

- The anticommutator for two annihilation operators is obtained as hermitian conjugate[6] of Eq. 3.25.

$$\left[\hat{a}_i, \hat{a}_j\right]_+ = 0 \tag{3.26}$$

- What happens if we interchange a creation and an annihilation operator?

  Let me start writing out the products using the definition Eq. 3.18.

  To simplify the derivation, I use Eq. 3.18 for the annihilation operator $\hat{a}_n$, and generate the creator $\hat{a}_n^\dagger$ by hermitean conjugation of the annihilator.

  The annihilator converts some of the Slater-determinants into the null state. The creation operator cannot revive this state because $\hat{a}_m^\dagger|\varnothing\rangle = |\varnothing\rangle$. It is the matrix element in the middle, $\sqrt{\sigma_n}$ that ensures that the corresponding term does not occur in the final result.

$$\begin{aligned}
\hat{a}_n^\dagger \hat{a}_n \overset{\text{Eq. 3.18}}{=} & \sum_{\vec{\sigma}'} \underbrace{\left|\sigma_1', \sigma_2', \ldots, \sigma_n', \ldots\right\rangle \left(\left[(-1)^{\sum_{k<n}\sigma_k'}\right]\sqrt{\sigma_n'}\right)\left\langle\sigma_1', \sigma_2', \ldots, \sigma_n' - 1, \ldots\right|}_{(\hat{a}_n)^\dagger} \\
\times & \underbrace{\sum_{\vec{\sigma}} \left|\sigma_1, \sigma_2, \ldots, \sigma_n - 1, \ldots\right\rangle \left(\left[(-1)^{\sum_{k<n}\sigma_k}\right]\sqrt{\sigma_n}\right)\left\langle\sigma_1, \sigma_2, \ldots, \sigma_n, \ldots\right|}_{\hat{a}_n \text{ (Eq. 3.18)}} \\
= & \sum_{\vec{\sigma}} \left|\vec{\sigma}\right\rangle \left[(-1)^{\sum_{k<n}\sigma_k}\right]^2 \sigma_n \left\langle\vec{\sigma}\right| \\
= & \sum_{\vec{\sigma}} \left|\vec{\sigma}\right\rangle \sigma_n \left\langle\vec{\sigma}\right|
\end{aligned} \tag{3.27}$$

  We proceed analogously with the product in reverse order. Here, I use the expression for the creation operator and generate the one for the annihilation operator by hermitean conjugation.

$$\begin{aligned}
\hat{a}_n \hat{a}_n^\dagger \overset{\text{Eq. 3.18}}{=} & \sum_{\vec{\sigma}'} \left|\sigma_1', \sigma_2', \ldots, \sigma_n', \ldots\right\rangle \left(\left[(-1)^{\sum_{k<n}\sigma_k'}\right]\sqrt{1-\sigma_n'}\right)\left\langle\sigma_1', \sigma_2', \ldots, \sigma_n' + 1, \ldots\right| \\
\times & \sum_{\vec{\sigma}} \left|\sigma_1, \sigma_2, \ldots, \sigma_n + 1, \ldots\right\rangle \left(\left[(-1)^{\sum_{k<n}\sigma_k}\right]\sqrt{1-\sigma_n}\right)\left\langle\sigma_1, \sigma_2, \ldots, \sigma_n, \ldots\right| \\
= & \sum_{\vec{\sigma}} \left|\vec{\sigma}\right\rangle \left[(-1)^{\sum_{k<n}\sigma_k}\right]^2 (1-\sigma_n) \left\langle\vec{\sigma}\right| \\
= & \sum_{\vec{\sigma}} \left|\vec{\sigma}\right\rangle (1-\sigma_n) \left\langle\vec{\sigma}\right|
\end{aligned} \tag{3.28}$$

  Thus, we obtain the anticommutator relation by adding Eqs. 3.27 and 3.28.

$$\left[\hat{a}_n^\dagger, \hat{a}_n\right]_+ \overset{\text{Eqs. 3.27,3.28}}{=} 1 \tag{3.29}$$

  On the way, we also obtained another useful operator, namely the one that provides the occupation of a specific orbital.

[6] Use $(\hat{A}\hat{B})^\dagger = \hat{B}^\dagger \hat{A}^\dagger$

OCCUPATION-NUMBER OPERATOR

.

$$\hat{n}_j \overset{\text{def}}{=} \hat{a}_j^\dagger \hat{a}_j \overset{\text{Eq. 3.27}}{=} \sum_{\vec{\sigma}} |\vec{\sigma}\rangle \sigma_j \langle \vec{\sigma}| \tag{3.30}$$

The expectation value of the occupation-number operator $\hat{n}_j$ is the mean number of particles in the j-th orbital.

Let me now turn to the products $\hat{a}_m^\dagger \hat{a}_n$ and $\hat{a}_n \hat{a}_m^\dagger$ with $m \neq n$. I use Eq. 3.18 to express the operators in the occupation-number representation.

In each of the two products below, only few terms are non-zero because of the factors $\sqrt{1-\sigma'_m}$ and $\sqrt{\sigma_n}$. I use the short-hand notation[7], that $\sum_{m \leq k < n}$ stands for $\sum_{\min(m,n) \leq k < \max(m,n)}$.

$$\begin{aligned}
\hat{a}_m^\dagger \hat{a}_n &\overset{\text{Eq. 3.18}}{=} \sum_{\vec{\sigma}'} \Big| \dots, \underbrace{\sigma'_m + 1}_{\rightsquigarrow \sigma_m + 1}, \dots, \underbrace{\sigma'_n}_{\rightsquigarrow \sigma_n - 1}, \dots \Big\rangle \Bigg(\underbrace{\Big[(-1)^{\sum_{k<m} \sigma'_k}\Big]}_{\rightsquigarrow \mathrm{sgn}(n-m)(-1)^{\sum_{k<m}\sigma_k}} \underbrace{\sqrt{1-\sigma'_m}}_{=\delta_{\sigma'_m,0} \rightsquigarrow \delta_{\sigma_m,0}} \Bigg) \Big\langle \dots, \underbrace{\sigma'_m}_{\rightsquigarrow \sigma_m}, \dots, \underbrace{\sigma'_n}_{\rightsquigarrow \sigma_n - 1}, \dots \Big| \\
&\times \sum_{\vec{\sigma}} \Big| \dots, \sigma_m, \dots, \sigma_n - 1, \dots \Big\rangle \Big(\Big[(-1)^{\sum_{k<n} \sigma_k}\Big] \underbrace{\sqrt{\sigma_n}}_{\delta_{\sigma_n,1}} \Big) \Big\langle \dots, \sigma_m, \dots, \sigma_n, \dots \Big| \\
&\overset{\text{Eq. 3.32}}{=} \sum_{\vec{\sigma}} \Big| \dots, \sigma_m + 1, \dots, \sigma_n - 1, \dots \Big\rangle \Big[\delta_{\sigma_m,0} \delta_{\sigma_n,1} \mathrm{sgn}(n-m) (-1)^{\sum_{m \leq k < n} \sigma_k} \Big] \Big\langle \vec{\sigma} \Big|
\end{aligned} \tag{3.33}$$

Now, I rewrite the product in reverse order analogously:

$$\begin{aligned}
\hat{a}_n \hat{a}_m^\dagger &\overset{\text{Eq. 3.18}}{=} \sum_{\vec{\sigma}'} \Big| \dots, \underbrace{\sigma'_m}_{\rightsquigarrow \sigma_m + 1}, \dots, \underbrace{\sigma'_n - 1}_{\rightsquigarrow \sigma_n - 1}, \dots \Big\rangle \Bigg(\underbrace{\Big[(-1)^{\sum_{k<n} \sigma'_k}\Big]}_{\rightsquigarrow \mathrm{sgn}(m-n)(-1)^{\sum_{k<n}\sigma_k}} \underbrace{\sqrt{\sigma'_n}}_{=\delta_{\sigma'_n,1} \rightsquigarrow \delta_{\sigma_n,1}} \Bigg) \Big\langle \dots, \underbrace{\sigma'_m}_{\rightsquigarrow \sigma_m + 1}, \dots, \underbrace{\sigma'_n}_{\rightsquigarrow \sigma_n}, \dots \Big| \\
&\times \sum_{\vec{\sigma}} \Big| \dots, \sigma_m + 1, \dots, \sigma_n, \dots \Big\rangle \Big(\Big[(-1)^{\sum_{k<m} \sigma_k}\Big] \underbrace{\sqrt{1-\sigma_m}}_{\delta_{\sigma_m,0}} \Big) \Big\langle \dots, \sigma_m, \dots, \sigma_n, \dots \Big| \\
&= \sum_{\vec{\sigma}} \Big| \dots, \sigma_m + 1, \dots, \sigma_n - 1, \dots \Big\rangle \Big[\delta_{\sigma_m,0} \delta_{\sigma_n,1} \underbrace{\mathrm{sgn}(m-n)}_{-\mathrm{sgn}(n-m)} (-1)^{\sum_{m \leq k < n} \sigma_k} \Big] \Big\langle \vec{\sigma} \Big|
\end{aligned} \tag{3.34}$$

Thus, the two operator products Eq. 3.33 and Eq. 3.34 are identical except for a sign change resulting from the different arguments of the sign function, so that

$$\left[\hat{a}_m^\dagger, \hat{a}_n\right]_+ = 0 \tag{3.35}$$

Eqs. 3.29 and 3.35 can be combined to

$$\left[\hat{a}_m^\dagger, \hat{a}_n\right]_+ = \delta_{m,n} \tag{3.36}$$

[7] Below, I exploit the orthonormality of the Slater determinants in the occupation-number representation, so that

$$\langle \dots, \sigma'_m, \dots \sigma'_n, \dots | \dots, \sigma_m, \dots, \sigma_n - 1, \dots \rangle = \delta_{\sigma'_m,\sigma_m} \delta_{\sigma'_n,1-\sigma_n} \prod_{k \notin \{m,n\}} \delta_{\sigma'_k,\sigma_k} = \delta_{\sigma'_n,1-\sigma_n} \prod_{k \notin \{n\}} \delta_{\sigma'_k,\sigma_k} \tag{3.31}$$

Thus, in the double sum over $\vec{\sigma}, \vec{\sigma}'$, all σ'_k can be replaced by σ_k, except for $k = n$.

$$\Big[(-1)^{\sum_{k<m} \sigma'_k}\Big] \Big\langle \dots, \sigma'_m, \dots \sigma'_n, \dots \Big| \dots, \sigma_m, \dots, \sigma_n - 1, \dots \Big\rangle = \mathrm{sgn}(n-m) \Big[(-1)^{\sum_{k<m} \sigma_k}\Big] \delta_{\sigma'_n,1-\sigma_n} \prod_{k \notin \{n\}} \delta_{\sigma'_k,\sigma_k} \tag{3.32}$$

The exchange of the primed σ'_n by the un-primed σ_n introduces a sign change, if $n < m$. The sign change is absent for $n > m$ because then it is not considered in the sign factor $(-1)^{\sum_{k<m} \sigma'_k}$. Thus, we can account the sign change when going from primed to un-primed numbers by an additional factor $\mathrm{sgn}(n-m)$.

The rules, we arrive at, are

ANTICOMMUTATION RULES FOR FERMIONIC CREATION AND ANNIHILATION OPERATORS

$$[\hat{a}_i^\dagger, \hat{a}_j^\dagger]_+ \overset{\text{Eq. 3.25}}{=} 0 \qquad \text{and} \qquad [\hat{a}_i, \hat{a}_j]_+ \overset{\text{Eq. 3.26}}{=} 0 \qquad \text{and} \qquad [\hat{a}_i^\dagger, \hat{a}_j]_+ \overset{\text{Eq. 3.36}}{=} \delta_{i,j} \tag{3.37}$$

The anticommutators Eq. 3.37 between creation and annihilation operators are numbers.[8] No such rule exists for the commutators of fermionic creation and annihilation operators: the commutators of fermion operators are still operators.

For bosons, similar relations exist, but for commutators, rather than for anticommutators.

Commutator relations in first quantization: The reader will remember that the commutator relations

$$\begin{aligned} [\hat{x}_i, \hat{x}_j]_- &= 0 \\ [\hat{p}_i, \hat{p}_j]_- &= 0 \\ [\hat{p}_i, \hat{x}_j]_- &= \frac{\hbar}{i}\delta_{i,j} \ , \end{aligned} \tag{3.38}$$

between positions and momenta have been central to formulation of quantum mechanics. In the second quantization of fermions, the anticommutator relations above play a similarly important role.

Commutator relations for the quantized harmonic oscillator: If we consider the harmonic oscillator, we found the commutator relations

$$\begin{aligned} [\hat{b}_i^\dagger, \hat{b}_j^\dagger]_- &= 0 \\ [\hat{b}_i, \hat{b}_j]_- &= 0 \\ [\hat{b}_i, \hat{b}_j^\dagger]_- &= \delta_{i,j} \end{aligned} \tag{3.39}$$

where the index refers to certain vibrational mode of a multidimensional harmonic oscillator. The resulting energy spectrum was equidistant and only bounded from below. In the second quantization of bosons, we say that the creation operator $b_i^\dagger$ creates a particle in a certain vibrational mode. We can construct any number of excitations, or particles, in a given vibration. The quantization of bosons follows naturally when one applies the **correspondence principle** to the wave function itself. Since the Lagrangian and the Hamiltonian of a one-particle system is quadratic in the wave function, it is natural that the quantization of a field leads to a harmonic oscillator. The difference between fermions and bosons is that the creation and annihilation operators obey an anticommutator relation in the fermionic case and a commutator relation in bosonic case.

3.5 Slater-Condon rules

The next step towards a description solely by creation and annihilation operators is to express one- and two-particle operators in terms of creation and annihilation operators.

For this purpose, we need to evaluate first the matrix elements $O_{\vec{\sigma},\vec{\sigma'}}$ of operators between Slater determinants $|\vec{\sigma}\rangle$.

$$\hat{O} = \sum_{\vec{\sigma},\vec{\sigma'}} |\vec{\sigma}\rangle O_{\vec{\sigma},\vec{\sigma'}} \langle\vec{\sigma'}| \tag{3.40}$$

[8] If an operator is an identity times a number, we call it a number.

In a next step, the matrix elements between Slater determinants can be expressed in terms of creation and annihilation operators. When we exploit that a set of all Slater determinants, which are formed from a complete orthonormal one-particle basisset, is a complete basis of Fock space, we can then represent a general one-particle or two-particle operator in terms of creation and annihilation operators.

While determining the matrix elements looks like a daunting task, it can be achieved in an elegant way as shown by Slater and Condon, when using an orthonormal set of one-particle orbitals. The resulting rules are the so-called **Slater-Condon rules**[25, 56]. A derivation of the Slater-Condon rules is given in appendix I on p. 685. I recommend, that the reader works through the derivation of at least one of the Slater-Condon rules.

The matrix elements can reasonably be worked out only using an orthonormal one-particle basisset. This is probably the sole reason, one almost exclusively works with orthonormal basissets in many-particle physics. Using orthonormal one-particle orbitals, is, however, by no means a requirement. Once the matrix elements are obtained in one basis, the results can be transformed into any other, even non-orthonormal basisset.

The Slater-Condon rules have been generalized to non-orthonormal basissets by Löwdin[29].

I only summarize the Slater-Condon rules here. The derivation is provided in appendix I on p. 685.

SLATER-CONDON RULES

The Slater-Condon rules provide the matrix elements of one-particle operators $\hat{A}$ and two-particle operators $\hat{W}$, between Slater determinants $|\Phi\rangle$ and $\Psi\rangle$. The Slater determinants must be expressed in an **orthonormal one-particle basisset** $\{|\varphi_j\rangle\}$ and they must be in **maximum coincidence**, which requires that any one-particle orbitals, which are present in both Slater determinants, must be in the same position in both Slater determinants (see also appendix I.1 on p. 685).

- Identical Slater determinants, i.e. $|\Psi\rangle = |\Phi\rangle$

$$\langle\Psi|\hat{A}|\Phi\rangle \overset{\text{Eq. I.5}}{=} \sum_{n=1}^{N}\langle\varphi_n|\hat{A}|\varphi_n\rangle$$

$$\langle\Psi|\hat{W}|\Phi\rangle \overset{\text{Eq. I.7}}{=} \frac{1}{2}\sum_{n,m}^{N}\Big(\underbrace{\langle\varphi_n\varphi_m|\hat{W}|\varphi_n\varphi_m\rangle}_{\rightsquigarrow\text{Hartree}} - \underbrace{\langle\varphi_n\varphi_m|\hat{W}|\varphi_m\varphi_n\rangle}_{\rightsquigarrow\text{exchange}}\Big) \tag{3.41}$$

  Notice, that the two terms in the sum for the two-particle term cancel each other for $n = m$.

  Eq. 3.41 are the so-called Slater rules[25]. They provide the expectation value with a Slater determinant. A general many-particle wave function is a superposition of many Slater determinants. To evaluate the expectation value with such a general, correlated, wave function also the off-diagonal matrix elements are required, which are obtained via the Condon rules[56] provided below.

- Slater determinants that differ by a single one-particle orbital φ_a and φ_b

$$\langle\Psi|\hat{A}|\Phi\rangle \overset{\text{Eq. I.15}}{=} \langle\varphi_a|\hat{A}|\varphi_b\rangle \tag{3.42}$$

$$\langle\Psi|\hat{W}|\Phi\rangle \overset{\text{Eq. I.22}}{=} \sum_{n=1;n\neq a,b}^{N-1}\Big(\langle\varphi_a\varphi_n|\hat{W}|\varphi_b\varphi_n\rangle - \langle\varphi_a\varphi_n|\hat{W}|\varphi_n\varphi_b\rangle\Big) \tag{3.43}$$

- Slater determinants that differ by two one-particle orbitals φ_a, φ_b and φ_c, φ_d

$$\langle\Psi|\hat{A}|\Phi\rangle \overset{\text{Eq. I.23}}{=} 0 \tag{3.44}$$

$$\langle\Psi|\hat{W}|\Phi\rangle \overset{\text{Eq. I.25}}{=} \langle\varphi_a\varphi_b|\hat{W}|\varphi_c\varphi_d\rangle - \langle\varphi_a\varphi_b|\hat{W}|\varphi_d\varphi_c\rangle \tag{3.45}$$

- Slater determinants that differ by more than two one-particle orbitals

$$\langle\Psi|\hat{A}|\Phi\rangle = 0 \tag{3.46}$$

$$\langle\Psi|\hat{W}|\Phi\rangle = 0 \tag{3.47}$$

The matrix elements of two-particle operators, such as an interaction $\hat{W}(\vec{x},\vec{x'})$, are defined as

$$\langle\varphi_a\varphi_b|\hat{W}|\varphi_c\varphi_d\rangle \overset{\text{def}}{=} \int d^4x \int d^4x'\ \varphi_a^*(\vec{x})\varphi_b^*(\vec{x'})W(\vec{x},\vec{x'})\varphi_c(\vec{x})\varphi_d(\vec{x'}) \tag{3.48}$$

3.6 Operators expressed by creation and annihilation operators

We have seen that all states of the Fock space can be expressed by creation operators and the vacuum state. Hence, the creation and annihilation operators also provide a means to transform the

states of the Fock space into each other, which is what a general operator does. This shows that each operator acting on the Fock space can be expressed by creation and annihilation operators.

In the previous section, we derived the Slater-Condon rules, which provide the matrix elements of one- and two-particle operators in terms of the Slater determinants that form the many-particle basisset. In appendix J on p. 693, we use the Slater-Condon rules to derive the explicit expressions for the one- and two-particle operators in this representation. Here, we just provide the results:

OPERATORS IN SECOND QUANTIZATION

A one-particle operator $\hat{A}$ has the form

$$\hat{A} = \sum_{i,j} A_{i,j} \hat{a}_i^\dagger \hat{a}_j \tag{3.49}$$

and a two-particle operator $\hat{W}$ has the form

$$\hat{W} = \frac{1}{2} \sum_{i,j,k,l} W_{i,j,k,l} \hat{a}_i^\dagger \hat{a}_j^\dagger \hat{a}_l \hat{a}_k \tag{3.50}$$

Note the reversed order of the annihilators relative to the indices.
The matrix elements are

$$\begin{aligned} A_{a,b} &\overset{\text{def}}{=} \langle \varphi_a | \hat{A} | \varphi_b \rangle \quad \overset{\text{def}}{=} \int d^4x \; \varphi_a^*(\vec{x}) \hat{A} \varphi_b(\vec{x}) \\ W_{a,b,c,d} &\overset{\text{def}}{=} \langle \varphi_a \varphi_b | \hat{W} | \varphi_c \varphi_d \rangle \overset{\text{Eq. 3.48}}{=} \int d^4x \int d^4x' \; \varphi_a^*(\vec{x}) \varphi_b^*(\vec{x'}) W(\vec{x}, \vec{x'}) \varphi_c(\vec{x}) \varphi_d(\vec{x'}) \end{aligned} \tag{3.51}$$

Conventions: Often, the interaction matrix elements are defined differently from Eq. 3.51.They differ in the order of the indices in the tensor $\boldsymbol{W}$. Our choice is consistent with the "physicist notation" $< ab|cd >= W_{a,b,c,d}$ as used in the book of Szabo and Ostlund [57] (See their section 2.3.2 "Notations for One- and Two-Electron Integrals"). It is also consistent with the notation used in the lecture notes *Theoretische Festkörperphysik* (p.63, Eq. 15.47) by Franz Wegener. Szabo and Ostlund also refer to the "chemist notation" $[ij|kl]$ defined as $< ik|jl >= [ij|kl]$, which lists first both x coordinates and then both x' coordinates. This chemists notation is also used by Mahan's Book[58] (see Eq. 1.157).

$$\text{Physicist notation} \qquad < ab|cd > \overset{\text{def}}{=} W_{a,b,c,d} \tag{3.52}$$

$$\text{Chemist notation} \qquad [ac|bd] \overset{\text{def}}{=} W_{a,b,c,d} \tag{3.53}$$

3.6.1 One-particle-reduced density matrix in second quantization

The one-particle-reduced density matrix follows from Eq. 3.49. It has been defined so that a the expectation value of a general, one-particle operator $\hat{A}$ is obtained as

$$A = \mathrm{Tr}[\hat{\rho}^{(1)} \hat{A}] = \sum_{i,j} \rho_{i,j}^{(1)} A_{j,i} \tag{3.54}$$

From Eq. 3.49 the expectation value of a one-particle operator with general ensemble of many-particle states $|\Phi_q\rangle$ in Fock space and their probabilities P_q is

$$\langle A \rangle = \sum_q P_q \langle \Phi_q | \sum_{i,j} A_{i,j} \hat{a}_i^\dagger \hat{a}_j | \Phi_q \rangle = \sum_{i,j} A_{i,j} \underbrace{\sum_q P_q \langle \Phi_q | \hat{a}_i^\dagger \hat{a}_j | \Phi_q \rangle}_{\rho_{j,i}^{(1)}} \tag{3.55}$$

This provides us with the one-particle-reduced density matrix as

ONE-PARTICLE-REDUCED DENSITY MATRIX IN SECOND QUANTIZATION

$$\rho^{(1)}_{m,n} = \sum_q P_q \langle \Phi_q | \hat{a}^\dagger_n \hat{a}_m | \Phi_q \rangle \tag{3.56}$$

$$\hat{\rho}^{(1)} = \sum_{m,n} |\varphi_m\rangle \sum_q P_q \langle \Phi_q | \hat{a}^\dagger_n \hat{a}_m | \Phi_q \rangle \langle \varphi_n | \tag{3.57}$$

Note, that the indices m, n on the right side of the equation are in the opposite order than on the left side.

3.7 Real-space-and-spin representation of field operators

We obtained the basic elements of the theory, namely states, Eq. 3.21, and operators, Eq. 3.49 and Eq. 3.50. The formulation rests on the choice of a particular set of one-particle orbitals $|\varphi_i\rangle$. Here, we change the representation from this set of one-particle orbitals to the real-space-and-spin representation. The real-space-and-spin representation is then the reference, from which formulation can be transformed into any other basisset of one-particle orbitals.

Let me start with the representation of the orthonormal one-particle basis functions $|\varphi_j\rangle$ in terms of vacuum state and creation operator

$$\hat{a}^\dagger_j |\mathcal{O}\rangle \overset{\text{Eq. 3.22}}{=} |\varphi_j\rangle \tag{3.58}$$

Any one-particle state $|f\rangle$ can be expanded into the chosen one-particle basis $|\varphi_j\rangle$.

$$|f\rangle = \sum_j |\varphi_j\rangle\langle\varphi_j|f\rangle \overset{\text{Eq. 3.58}}{=} \sum_j \underbrace{\hat{a}^\dagger_j |\mathcal{O}\rangle}_{|\varphi_j\rangle} \langle\varphi_j|f\rangle = \Big(\sum_j \hat{a}^\dagger_j \langle\varphi_j|f\rangle\Big)|\mathcal{O}\rangle \tag{3.59}$$

Because the state $|f\rangle$ is arbitrary, we can insert a basisstate of the real-space-and-spin representation $|\vec{x}\rangle$, which yields

$$|\vec{x}\rangle = \underbrace{\Big(\sum_j \hat{a}^\dagger_j \langle\varphi_j|\vec{x}\rangle\Big)}_{=:\hat{\psi}^\dagger(\vec{x})} |\mathcal{O}\rangle \tag{3.60}$$

This defines the field operators

FIELD OPERATORS

$$\begin{aligned} \hat{\psi}^\dagger(\vec{x}) &\overset{\text{def}}{=} \sum_j \hat{a}^\dagger_j \langle\varphi_j|\vec{x}\rangle = \sum_j \varphi^*_j(\vec{x}) \hat{a}^\dagger_j \\ \hat{\psi}(\vec{x}) &= \sum_j \langle\vec{x}|\varphi_j\rangle \hat{a}_j = \sum_j \varphi_j(\vec{x}) \hat{a}_j \end{aligned} \tag{3.61}$$

An arbitrary one-particle state can then be written in the form

$$|f\rangle \overset{\text{Eq. 3.59}}{=} \Big(\sum_j \hat{a}_j^\dagger \langle\varphi_j|f\rangle\Big)|\mathcal{O}\rangle = \Big(\int d^4x \underbrace{\sum_j \hat{a}_j^\dagger \langle\varphi_j|\vec{x}\rangle}_{\hat{\psi}^\dagger(\vec{x})} \underbrace{\langle\vec{x}|f\rangle}_{f(\vec{x})}\Big)|\mathcal{O}\rangle$$
$$\overset{\text{Eq. 3.61}}{=} \Big(\int d^4x\, \hat{\psi}^\dagger(\vec{x}) f(\vec{x})\Big)|\mathcal{O}\rangle \tag{3.62}$$

Insertion of the basis function $|\varphi_j\rangle$ in place of the general state $|f\rangle$ yields the back transform.

$$\hat{a}_j^\dagger|\mathcal{O}\rangle \overset{\text{Eq. 3.58}}{=} |\varphi_j\rangle \overset{\text{Eq. 3.62}}{=} \Big(\int d^4x\, \hat{\psi}^\dagger(\vec{x})\varphi_j(\vec{x})\Big)|\mathcal{O}\rangle \tag{3.63}$$

ORBITAL CREATION AND ANNIHILATION OPERATORS FROM FIELD OPERATORS

$$\hat{a}_i^\dagger = \int d^4x\, \hat{\psi}^\dagger(\vec{x})\, \langle\vec{x}|\varphi_i\rangle = \int d^4x\, \hat{\psi}^\dagger(\vec{x})\varphi_i(\vec{x})$$
$$\hat{a}_i = \int d^4x\, \langle\varphi_i|\vec{x}\rangle\, \hat{\psi}(\vec{x}) = \int d^4x\, \varphi_i^*(\vec{x})\hat{\psi}(\vec{x}) \tag{3.64}$$

The symbol "psi" for the field operator $\hat{\psi}^\dagger(\vec{x})$ is not a space holder for a specific field. We would not write something like $\varphi^\dagger(\vec{x})$. This is different from the notation $\hat{a}_i^\dagger$ or $\hat{c}_j^\dagger$, for which the letters may indicate the choice of one or another basisset. For the field operators the basisset is already chosen: It is $\{|\vec{x}\rangle\}$.

3.7.1 Anticommutator relations in real space

The anti-commutator relations of the field operators in real space are obtained by insertion.

$$\begin{aligned}
\big[\hat{\psi}^\dagger(\vec{x}), \hat{\psi}(\vec{x'})\big]_+ &\overset{\text{Eq. 3.61}}{=} \big(\sum_j \hat{a}_j^\dagger \langle\varphi_j|\vec{x}\rangle\big)\big(\sum_k \langle\vec{x'}|\varphi_k\rangle \hat{a}_k\big) + \big(\sum_k \langle\vec{x'}|\varphi_k\rangle \hat{a}_k\big)\big(\sum_j \hat{a}_j^\dagger \langle\varphi_j|\vec{x}\rangle\big) \\
&= \sum_{j,k} \langle\vec{x'}|\varphi_k\rangle \underbrace{\big(\hat{a}_j^\dagger \hat{a}_k + \hat{a}_k \hat{a}_j^\dagger\big)}_{=[\hat{a}_j^\dagger, \hat{a}_k]_+ = \delta_{j,k}} \langle\varphi_j|\vec{x}\rangle\big) \\
&= \langle\vec{x'}| \underbrace{\Big(\sum_j \varphi_j\rangle\langle\varphi_j|\Big)}_{=\hat{1}} |\vec{x}\rangle \\
&= \underbrace{\delta(\vec{x} - \vec{x'})}_{\delta(\vec{r}-\vec{r'})\delta_{\sigma,\sigma'}}
\end{aligned} \tag{3.65}$$

For a continuous variable such as the position we need to remember that we have to use the delta-function instead of the Kronecker delta.

3.7.2 One-particle operators in real space

Let us now transform a general one-particle operator $\hat{A}$ into the real-space representation

$$\begin{aligned}
\hat{A} &\overset{\text{Eq. 3.49}}{=} \sum_{i,j} \langle \varphi_i | \hat{A} | \varphi_j \rangle \hat{a}_i^\dagger \hat{a}_j \\
&= \sum_{i,j} \langle \varphi_i | \underbrace{\int d^4x \, |\vec{x}\rangle\langle\vec{x}|}_{=1} \hat{A} \underbrace{\int d^4x' \, |\vec{x'}\rangle\langle\vec{x'}|}_{=1} |\varphi_j\rangle \hat{a}_i^\dagger \hat{a}_j \\
&= \int d^4x \int d^4x' \sum_{i,j} \underbrace{\langle \varphi_i | \vec{x} \rangle}_{\varphi_i^*(\vec{x})} \underbrace{\langle \vec{x} | \hat{A} | \vec{x'} \rangle}_{A(\vec{x},\vec{x'})} \underbrace{\langle \vec{x'} | \varphi_j \rangle}_{\varphi_j(\vec{x'})} \hat{a}_i^\dagger \hat{a}_j \\
&= \int d^4x \int d^4x' \, A(\vec{x},\vec{x'}) \underbrace{\sum_i \varphi_i^*(\vec{x}) \hat{a}_i^\dagger}_{\hat{\psi}^\dagger(\vec{x})} \underbrace{\sum_j \varphi_j(\vec{x'}) \hat{a}_j}_{\hat{\psi}(\vec{x'})} \\
&\overset{\text{Eq. 3.61}}{=} \int d^4x \int d^4x' \, A(\vec{x},\vec{x'}) \hat{\psi}^\dagger(\vec{x}) \hat{\psi}(\vec{x'})
\end{aligned} \tag{3.66}$$

Note that we deal here with two different types of operators: The creators and annihilators act on the Fock space. The operator $\hat{A}$ acts on a one-particle state if it is bracketed between two one-particle states.

Example: one-particle Hamiltonian

The one-particle part of the Hamiltonian has the form

$$\hat{h} = \int d^4x \int d^4x' \, |\vec{x}\rangle \underbrace{\delta(\vec{x}-\vec{x'}) \left(\frac{-\hbar^2}{2m_e} \vec{\nabla}'^2 + v_{ext}(\vec{x'}) \right)}_{h(\vec{x},\vec{x'}) = \langle \vec{x} | \hat{h} | \vec{x'} \rangle} \langle \vec{x'} | \tag{3.67}$$

with

$$h(\vec{x},\vec{x'}) = \delta(\vec{x}-\vec{x'}) \left(\frac{-\hbar^2}{2m_e} \vec{\nabla}'^2 + v_{ext}(\vec{x'}) \right) . \tag{3.68}$$

The corresponding one-particle-at-a-time Hamiltonian has the form[9]

$$\begin{aligned}
\hat{h} &\overset{\text{Eq. 3.66}}{=} \int d^4x \int d^4x' \, \delta(\vec{x}-\vec{x'}) \left(\frac{-\hbar^2}{2m_e} \vec{\nabla}'^2 + v_{ext}(\vec{x'}) \right) \hat{\psi}^\dagger(\vec{x}) \hat{\psi}(\vec{x'}) \\
&= \int d^4x \, \hat{\psi}^\dagger(\vec{x}) \left(\frac{-\hbar^2}{2m_e} \vec{\nabla}^2 + v_{ext}(\vec{x}) \right) \hat{\psi}(\vec{x})
\end{aligned} \tag{3.69}$$

The expression just looks like a normal expectation value of the one-particle Hamiltonian. However, since the wave functions are replaced by the creation and annihilation operators, the expression is an operator in Fock space.

[9] It may be puzzling to have a differential operator, the Laplacian, act on an operator. This object is to be interpreted as for normal functions as the differential quotient of the operator in the limit of small displacements.

3.7.3 Interaction operator in real space

Analogously, we can determine the interaction operator in real space as

$$\begin{aligned}
\hat{W} &\overset{\text{Eq. 3.50}}{=} \frac{1}{2}\sum_{i,j,k,l} W_{i,j,k,l}\hat{a}_i^\dagger \hat{a}_j^\dagger \hat{a}_l \hat{a}_k \\
&\overset{\text{Eq. 3.64}}{=} \frac{1}{2}\sum_{i,j,k,l} W_{i,j,k,l} \underbrace{\int d^4x_1\ \varphi_i(\vec{x_1})\hat{\psi}^\dagger(\vec{x}_1)}_{\hat{a}_i^\dagger} \underbrace{\int d^4x_2\ \varphi_j(\vec{x_2})\hat{\psi}^\dagger(\vec{x}_2)}_{\hat{a}_j^\dagger} \\
&\quad \underbrace{\int d^4x_4\ \varphi_l^*(\vec{x_4})\hat{\psi}(\vec{x}_4)}_{\hat{a}_l} \underbrace{\int d^4x_3\ \varphi_k^*(\vec{x_3})\hat{\psi}(\vec{x}_3)}_{\hat{a}_k} \\
&= \frac{1}{2}\int d^4x_1 \int d^4x_2 \int d^4x_3 \int d^4x_4 \underbrace{\sum_{i,j,k,l} W_{i,j,k,l}\varphi_i(\vec{x_1})\varphi_j(\vec{x_2})\varphi_k^*(\vec{x_3})\varphi_l^*(\vec{x_4})}_{W(\vec{x}_1,\vec{x}_2,\vec{x}_3,\vec{x}_4)} \\
&\quad \cdot\hat{\psi}^\dagger(\vec{x}_1)\hat{\psi}^\dagger(\vec{x}_2)\hat{\psi}(\vec{x}_4)\hat{\psi}(\vec{x}_3)
\end{aligned} \tag{3.70}$$

We use the expression for the matrix elements in the orbital basis

$$W_{i,j,k,l} \overset{\text{Eq. 3.51}}{=} \int d^4x \int d^4x'\ \varphi_i^*(\vec{x})\varphi_j^*(\vec{x'})v_{int}(\vec{x},\vec{x'})\varphi_k(\vec{x})\varphi_l(\vec{x'}) \tag{3.71}$$

to work out the real-space matrix elements of the interaction in Eq. 3.70. For our purposes the interaction potential is the Coulomb potential

$$v_{int}(\vec{x},\vec{x'}) = v_{int}(\vec{r},\sigma,\vec{r'},\sigma') = \frac{e^2}{4\pi\epsilon_0|\vec{r}-\vec{r'}|} \tag{3.72}$$

$$\begin{aligned}
W(\vec{x}_1,\vec{x}_2,\vec{x}_3,\vec{x}_4) &\overset{\text{def}}{=} \sum_{i,j,k,l} W_{i,j,k,l}\varphi_i(\vec{x_1})\varphi_j(\vec{x_2})\varphi_k^*(\vec{x_3})\varphi_l^*(\vec{x_4}) \\
&\overset{\text{Eq. 3.71}}{=} \sum_{i,j,k,l} \underbrace{\int d^4x \int d^4x' \left[\varphi_i^*(\vec{x})\varphi_j^*(\vec{x'})v_{int}(\vec{x},\vec{x'})\varphi_k(\vec{x})\varphi_l(\vec{x'})\right]}_{W_{i,j,k,l}} \left[\varphi_i(\vec{x_1})\varphi_j(\vec{x_2})\varphi_k^*(\vec{x_3})\varphi_l^*(\vec{x_4})\right] \\
&= \int d^4x \int d^4x' \underbrace{\sum_i \varphi_i^*(\vec{x})\varphi_i(\vec{x_1})}_{\delta(\vec{x}-\vec{x}_1)} \underbrace{\sum_j \varphi_j^*(\vec{x'})\varphi_j(\vec{x_2})}_{\delta(\vec{x'}-\vec{x}_2)} \\
&\qquad \times v_{int}(\vec{x},\vec{x'}) \underbrace{\sum_k \varphi_k(\vec{x})\varphi_k^*(\vec{x_3})}_{\delta(\vec{x}-\vec{x}_3)} \underbrace{\sum_l \varphi_l(\vec{x'})\varphi_l^*(\vec{x_4})}_{\delta(\vec{x'}-\vec{x}_4)} \\
&= v_{int}(\vec{x}_1,\vec{x}_2)\delta(\vec{x}_1-\vec{x}_3)\delta(\vec{x}_2-\vec{x}_4)
\end{aligned} \tag{3.73}$$

We insert this result into the above expression Eq. 3.70

$$\begin{aligned}
\hat{W} &\overset{Eqs.\ 3.70,3.73}{=} \frac{1}{2}\int d^4x_1 \int d^4x_2 \int d^4x_3 \int d^4x_4\ v_{int}(\vec{x}_1,\vec{x}_2)\delta(\vec{x}_1-\vec{x}_3)\delta(\vec{x}_2-\vec{x}_4) \\
&\quad \cdot\hat{\psi}^\dagger(\vec{x}_1)\hat{\psi}^\dagger(\vec{x}_2)\hat{\psi}(\vec{x}_4)\hat{\psi}(\vec{x}_3) \\
&= \frac{1}{2}\int d^4x_1 \int d^4x_2\ v_{int}(\vec{x}_1,\vec{x}_2)\hat{\psi}^\dagger(\vec{x}_1)\hat{\psi}^\dagger(\vec{x}_2)\hat{\psi}(\vec{x}_2)\hat{\psi}(\vec{x}_1) \\
&= \frac{1}{2}\int d^4x \int d^4x'\ \hat{\psi}^\dagger(\vec{x})\hat{\psi}^\dagger(\vec{x'})v_{int}(\vec{x},\vec{x'})\hat{\psi}(\vec{x'})\hat{\psi}(\vec{x})
\end{aligned} \tag{3.74}$$

3.7.4 Many-electron Hamiltonian in real space

The Hamiltonian has the form

MANY-PARTICLE HAMILTONIAN

$$\hat{H} = \int d^4x\, \hat{\psi}^\dagger(\vec{x}) \left(\frac{-\hbar^2}{2m_e} \vec{\nabla}^2 + v_{ext}(\vec{x}) \right) \hat{\psi}(\vec{x}) + \frac{1}{2} \int d^4x \int d^4x'\, \hat{\psi}^\dagger(\vec{x}) \hat{\psi}^\dagger(\vec{x'}) \underbrace{\frac{e^2}{4\pi\epsilon_0 |\vec{r} - \vec{r'}|}}_{v_{int}(\vec{x},\vec{x'})} \hat{\psi}(\vec{x'}) \hat{\psi}(\vec{x}) \tag{3.75}$$

Notice the order of the annihilation operators on the right-hand side of the interaction term!

3.8 Creation and annihilation operators in a non-orthonormal representation

The extension of creation and annihilation operators to non-orthonormal orbitals is possible. It is discussed in appendix B on p. 517.

3.9 From Hilbert space to Fock space and back

Often we encounter a problem expressed in one-particle wave functions and we want to express it in second quantization or vice versa. In this section, I am collecting examples and advice on how this can be done.

3.9.1 From Hilbert space to Fock space and back

I find it very useful to start with the representation of a one-particle state in the language of second quantization. I provide equations for orthonormal orbitals $|\varphi_n\rangle$, non-orthonormal states $|\chi_\alpha\rangle$ and the real-space-and-spin representation.

In a orthonormal basisset, each orbital $|\chi_\alpha\rangle$ is accompanied by a projector function $\langle\pi_\alpha|$. Projector functions and orbitals satisfy a bi-orthogonality condition $\langle\pi_\alpha|\chi_\beta\rangle = \delta_{\alpha,\beta}$ so that $|\psi\rangle = \sum_\alpha |\chi_\alpha\rangle\pi_\alpha|\psi\rangle$ if $|\psi\rangle$ lies in the Hilbert space spanned by the orbitals.

ONE-PARTICLE ORBITALS IN SECOND QUANTIZATION

$$|\varphi_n\rangle = \hat{a}_n^\dagger|\mathcal{O}\rangle \tag{3.76}$$

$$|\pi_\alpha\rangle \overset{\text{Eq. } B.5}{=} \hat{c}_\alpha^\dagger|\mathcal{O}\rangle \tag{3.77}$$

$$|\chi_\alpha\rangle = \sum_\beta \hat{c}_\beta^\dagger|\mathcal{O}\rangle\langle\chi_\beta|\chi_\alpha\rangle \tag{3.78}$$

$$|\vec{x}\rangle = \hat{\psi}^\dagger(\vec{x})|\mathcal{O}\rangle \tag{3.79}$$

Similarly, two-particle Slater determinants can be written in the form

$$|\varphi_\alpha, \varphi_\beta\rangle = \hat{a}_\alpha^\dagger\hat{a}_\beta^\dagger|\mathcal{O}\rangle \quad \text{respectively} \quad |\pi_\alpha, \pi_\beta\rangle = \hat{c}_\alpha^\dagger\hat{c}_\beta^\dagger|\mathcal{O}\rangle \tag{3.80}$$

respectively

$$|\vec{x}, \vec{x'}\rangle = \hat{\psi}^\dagger(\vec{x})\hat{\psi}^\dagger(\vec{x'})|\mathcal{O}\rangle \tag{3.81}$$

A one-particle operator acting on the one-particle Hilbert space can be rewritten as follows:

$$\begin{aligned}\hat{A} &= \sum_{\alpha,\beta} |\pi_\alpha\rangle \underbrace{\langle\chi_\alpha|\hat{A}|\chi_\beta\rangle}_{A_{\alpha,\beta}}\langle\pi_\beta| = \sum_{\alpha,\beta} |\pi_\alpha\rangle A_{\alpha,\beta}\langle\pi_\beta| = \sum_{\alpha,\beta} \underbrace{\hat{c}_\alpha^\dagger|\mathcal{O}\rangle}_{|\pi_\alpha\rangle} A_{\alpha,\beta} \underbrace{\langle\mathcal{O}|\hat{c}_\beta}_{\langle\pi_\beta|} \\ &= \sum_{\alpha,\beta} A_{\alpha,\beta}\hat{c}_\alpha^\dagger \underbrace{|\mathcal{O}\rangle\langle\mathcal{O}|}_{\hat{P}_{|\mathcal{O}\rangle}} \hat{c}_\beta\end{aligned} \tag{3.82}$$

In the middle we have the projection operator $\hat{P}_{|\mathcal{O}\rangle}$ onto the zero-particle state, which limits the action of the operator to the one-particle channel. In order to generalize this result to the Fock space, we replace the projection operator by the unit operator in Fock space

$$\hat{A} = \sum_{\alpha,\beta} A_{\alpha,\beta}\hat{c}_\alpha^\dagger \underbrace{\sum_{\vec{\sigma}} |\vec{\sigma}\rangle\langle\vec{\sigma}|}_{\hat{1}} \hat{c}_\beta = \sum_{\alpha,\beta} A_{\alpha,\beta}\hat{c}_\alpha^\dagger\hat{c}_\beta \tag{3.83}$$

Despite the fact that we use the same symbols, the operators $\hat{A}$ Eq. 3.82 and Eq. 3.83 are in principle two different operators, because they act on different spaces.

Similarly, we can go backwards from Eq. 3.83 to Eq. 3.82, as long as the operator $\hat{A}$ is a one-particle operator, that is, it can be built up from products $\hat{a}_m^\dagger\hat{a}_n$.

3.10 Summary

In this chapter, we introduced creation and annihilation operators, and showed how many-particle wave functions and operators can be expressed by them. In addition to the creation and annihilation operators, only a single state, the vacuum state $|\mathcal{O}\rangle$ is required.

Field operators $\hat{\psi}^\dagger(\vec{x})$ and $\hat{\psi}(\vec{x})$ have been introduced by selecting the space-and-spin basisset. In this representation the Hamilton operator looks like the energy expectation value in one-particle quantum mechanics, with the difference that the wave function is replaced by the field operator. Special care is required, because of the anticommutator relation of the field operators, their order is not arbitrary.

The formulation given in this section can be extended to incomplete and non-orthonormal basis sets. This is shown in the appendix B on p. 517.

3.11 Home study and practice

3.11.1 Hydrogen molecule with interacting electrons

Introduction

Here, we extend the earlier exercise on the hydrogen molecule in section 1.5.1 on p. 26 to interacting electrons. This example will give us a first glance on a number of electron-correlation effects. It may be helpful to inspect figure 3.1 on p. 131 which schematically shows the many-particle states of a hydrogen atom with non-interacting electrons.

A number of many-particle effects attributed to solids are already present in the hydrogen molecule.

- One of the main correlation effects is the concept of a Mott insulator. A **Mott insulator** is a system that, without interaction, would be a metal, but it becomes an insulator because of the Coulomb interaction. Of particular interest is the corresponding **metal-insulator transition**.

- The most simple model for a Mott insulator is the **Hubbard model**. The ground state of a half-filled Hubbard model is an antiferromagnetic singlet state. While this state has no local (nor non-local) magnetization $\vec{M}_z(\vec{r})$, it has an nevertheless antiferromagnetic correlations.

- For the low-energy excitations with strong Coulomb repulsion, the half-occupied Hubbard model maps onto **Heisenberg model**. The Heisenberg model describes a lattice of spins that interact via an exchange coupling $E = -\sum_j J\vec{S}_j\vec{S}_{j+1}$. Interestingly, this exchange coupling is not due to magnetic interactions, but it is a result of the Coulomb repulsion between electrons and quantum fluctuations of electrons to neighboring sites. The low-energy excitations of the half-filled Hubbard model in the strongly interacting limit are spin flips.

- The **exchange coupling**, which describes the antiferromagnetic coupling of neighboring spins is proportional to by $J \sim t^2/U$: It depends on hopping t and the onsite Coulomb repulsion U as opposed to magnetic interactions.

- The one-particle excitations, which determine the one-particle spectral function exhibits a band gap for the half-filled Hubbard model. The electron addition energies of the half-filled Hubbard model are higher by U as the electron removal energies. This is because the addition of an electron leads to a double occupied site, where the two electrons repell each other, while the removing an electron does not change the on-site Coulomb energy. The electron addition energies form the **upper Hubbard band**, which is separated by approximately U from the **lower Hubbard band** resulting from the electron-removal energies.

Problem

1 Translate the non-interacting Hamiltonian for the hydrogen molecule from section 1.5.1 on p. 26 into second quantization using atomic hydrogen 1s orbitals.

2 Use a one-particle basisset of atomic hydrogen 1s orbitals. Ignore the non-orthonormality of the one-particle wave functions. List the two-particle Slater determinants of the hydrogen molecule and express them in terms of creation and annihilation operators and the vacuum state.

3 Consider the Hamiltonian

$$\hat{H} = \sum_{\alpha,\beta} h_{\alpha,\beta} \hat{c}_\alpha^\dagger \hat{c}_\beta + \frac{1}{2} \sum_{\alpha,\beta,\gamma,\delta} W_{\alpha,\beta,\gamma\delta} \hat{c}_\alpha^\dagger \hat{c}_\beta^\dagger \hat{c}_\delta \hat{c}_\gamma \tag{3.84}$$

with

$$h_{\alpha,\beta} = \bar{\epsilon}\delta_{\alpha,\beta} - t\delta_{\sigma_\alpha,\sigma_\beta}\left(1 - \delta_{R_\alpha,R_\beta}\right) \tag{3.85}$$

and

$$W_{\alpha,\beta,\gamma,\delta} = \delta_{\alpha,\gamma}\delta_{\beta,\delta}\Big[U\delta_{R_\alpha,R_\beta} + V(1 - \delta_{R_\alpha,R_\beta})\Big] \tag{3.86}$$

where the indices $\alpha, \beta, \ldots$ are combined indices $\alpha = (R, \sigma)$ holding a site index $R \in \{1, 2\}$ and a spin index $\sigma \in \{\uparrow, \downarrow\}$.

The on-site Coulomb parameter U describes the Coulomb repulsion of two electrons on the same site and the parameter V describes the Coulomb repulsion of two electrons on neighboring sites. We use the assumption $U > V$ which will be useful to avoid considering distinct cases.

Determine the Hamiltonian for the (4×4) subblock of two-particle states with $S_z = 0$. I recommend to first write out the Hamiltonian with the specific indices of the hydrogen molecule. Try to combine creation and annihilation operators to occupation-number operators $\hat{n}_j$. Then act with the Hamiltonian onto the four two-particle basis states and extract the matrix elements.

4 Exploit the reflection symmetry $\hat{P}$ of the hydrogen molecule to block-diagonalize the Hamiltonian in the two-particle channel. That is, construct the eigenstates of the parity operator under reflection symmetry of the molecule. These parity eigenstates are superpositions of the two-particle Slater determinants $|\Phi_i\rangle$ obtained previously. The Hamiltonian in terms of the symmetrized states[a] will "fall apart" into one 2×2 matrix and 1×1 blocks.

[a] With symmetrized states, I mean eigenstates of the symmetry operator. In the case of the parity operator, these eigenstates may be symmetric or antisymmetric.

Discussion

1 Translate the non-interacting Hamiltonian for the hydrogen molecule from section 1.5.1 on p. 26 into second quantization using atomic hydrogen 1s orbitals.

The one-particle Hamilton operator in the one-particle Hilbert space given earlier has the form

$$\hat{h} = \underbrace{\sum_{\sigma\in\{\uparrow,\downarrow\}} \sum_{R=1}^{2} |\pi_{R,\sigma}\rangle\, \bar{\epsilon}\, \langle\pi_{R,\sigma}|}_{\text{atomic energies}} \underbrace{- \sum_{\sigma\in\{\uparrow,\downarrow\}} \Big(|\pi_{1,\sigma}\rangle\, t\, \langle\pi_{2,\sigma}| + |\pi_{2,\sigma}\rangle\, t\, \langle\pi_{1,\sigma}|\Big)}_{\text{hopping}} \tag{3.87}$$

For an operator in Fock space, the term one-particle means *"one particle at a time"*. The corre-

sponding one-particle operator in Fock space is

$$\hat{h} = \underbrace{\sum_{\sigma\in\{\uparrow,\downarrow\}} \sum_{R=1}^{2} \bar{\epsilon} \hat{c}^{\dagger}_{R,\sigma} \hat{c}_{R,\sigma}}_{\text{atomic energies}} - \underbrace{\sum_{\sigma\in\{\uparrow,\downarrow\}} t\left(\hat{c}^{\dagger}_{1,\sigma} \hat{c}_{2,\sigma} + \hat{c}^{\dagger}_{2,\sigma} \hat{c}_{1,\sigma}\right)}_{\text{hopping}} \tag{3.88}$$

2 Use a one-particle basisset of atomic hydrogen 1s orbitals. Ignore the non-orthonormality of the one-particle wave functions. List the two-particle Slater determinants of the hydrogen molecule and express them in terms of creation and annihilation operators and the vacuum state.

Let me first set up the one-particle basisset and specify an order.

$$\begin{aligned}
|\uparrow, 0\rangle &= |1000\rangle = \hat{c}^{\dagger}_{1,\uparrow}|\mathcal{O}\rangle \\
|\downarrow, 0\rangle &= |0100\rangle = \hat{c}^{\dagger}_{1,\downarrow}|\mathcal{O}\rangle \\
|0, \uparrow\rangle &= |0010\rangle = \hat{c}^{\dagger}_{2,\uparrow}|\mathcal{O}\rangle \\
|0, \downarrow\rangle &= |0001\rangle = \hat{c}^{\dagger}_{2,\downarrow}|\mathcal{O}\rangle
\end{aligned} \tag{3.89}$$

The notation for the kets on the very left of the equation above follows a convention that has not been used or defined before. Here, the two entries refer to the two sites of the hydrogen molecule. The arrows indicate which orbitals on that molecule are occupied, namely none for 0, only the spin-up orbital for $\uparrow$, only the spin-down orbital for $\downarrow$, or both spin orbitals for $\uparrow\downarrow$. The notation is very intuitive for certain systems, but, in contrast to the occupation-number representation, it is not suitable in general.

The two-particle states are, with Eq. 3.21,

$$\begin{aligned}
|\Phi_1\rangle &= |\uparrow\downarrow, 0\rangle = |1100\rangle = \hat{c}^{\dagger}_{1,\uparrow}\hat{c}^{\dagger}_{1,\downarrow}|\mathcal{O}\rangle \\
|\Phi_2\rangle &= |0, \uparrow\downarrow\rangle = |0011\rangle = \hat{c}^{\dagger}_{2,\uparrow}\hat{c}^{\dagger}_{2,\downarrow}|\mathcal{O}\rangle \\
|\Phi_3\rangle &= |\uparrow, \downarrow\rangle = |1001\rangle = \hat{c}^{\dagger}_{1,\uparrow}\hat{c}^{\dagger}_{2,\downarrow}|\mathcal{O}\rangle \\
|\Phi_4\rangle &= |\downarrow, \uparrow\rangle = |0110\rangle = \hat{c}^{\dagger}_{1,\downarrow}\hat{c}^{\dagger}_{2,\uparrow}|\mathcal{O}\rangle \\
|\Phi_5\rangle &= |\uparrow, \uparrow\rangle = |1010\rangle = \hat{c}^{\dagger}_{1,\uparrow}\hat{c}^{\dagger}_{2,\uparrow}|\mathcal{O}\rangle \\
|\Phi_6\rangle &= |\downarrow, \downarrow\rangle = |0101\rangle = \hat{c}^{\dagger}_{1,\downarrow}\hat{c}^{\dagger}_{2,\downarrow}|\mathcal{O}\rangle
\end{aligned} \tag{3.90}$$

Please note the order of the operators, respectively the sign.

Let me check the number of two-particle states. With $n = 4$ one-particle orbitals, I can form $n(n-1)/2 = 6$ two-particle states.[10] Thus, the number of orbitals in our basisset is correct.

Discussion:

The first two two-particle states, $|\Phi_1\rangle$, $|\Phi_2\rangle$ have a doubly occupied hydrogen atom. They describe an ionic pair H^-H^+. The second pair of two-particle states $|\Phi_3\rangle$, $|\Phi_4\rangle$ describe antiferromagnetic electron distributions. The last two states $|\Phi_5\rangle$, $|\Phi_6\rangle$ are states with parallel spins along the z-axis.

The two antiferromagnetic states $|\Phi_3\rangle$, $|\Phi_4\rangle$ can be superimposed to give a **singlet state** or a **triplet state**. The singlet state has a total spin of zero, while the triplet state has a total spin S=1, while $S_z = 0\hbar$. This last state is called a *"triplet state"*, because there are three degenerate states with $S = 1$. The singlet state is called *"singlet"* because it has an energy different from the triplet state and it is non-degenerate.

[10] There are four possibilities to select the first orbital. Because the second orbital must be different, there are only 3 possibilities to choose the second orbital. Now, however, each pair of orbitals has been selected twice, namely once for each order of the two orbitals. This is corrected by the division by two.

3 Consider the Hamiltonian

$$\hat{H} = \sum_{\alpha,\beta} h_{\alpha,\beta} \hat{c}_\alpha^\dagger \hat{c}_\beta + \frac{1}{2} \sum_{\alpha,\beta,\gamma,\delta} W_{\alpha,\beta,\gamma\delta} \hat{c}_\alpha^\dagger \hat{c}_\beta^\dagger \hat{c}_\delta \hat{c}_\gamma \tag{3.91}$$

with

$$h_{\alpha,\beta} = \bar{\epsilon}\delta_{\alpha,\beta} - t\delta_{\sigma_\alpha,\sigma_\beta}\left(1 - \delta_{R_\alpha,R_\beta}\right) \tag{3.92}$$

and

$$W_{\alpha,\beta,\gamma,\delta} = \delta_{\alpha,\gamma}\delta_{\beta,\delta}\Big[U\delta_{R_\alpha,R_\beta} + V(1 - \delta_{R_\alpha,R_\beta})\Big] \tag{3.93}$$

The parameter U describes the Coulomb matrix elements of two electrons on the same site and the parameter V describes that of two electrons on different sites. We use the assumption $U > V$ which will be useful to avoid considering distinct cases.

Determine the Hamiltonian for the (4×4) subblock of two-particle states with $S_z = 0$. I recommend to first write out the Hamiltonian with the specific indices of the hydrogen molecule. Try to combine creation and annihilation operators to occupation-number operators $\hat{n}_j$. Then act with the Hamiltonian onto the four two-particle basis states and extract the matrix elements.

For the curious I am also including two additional states, which is not requested for this task.

$$\begin{aligned}
\hat{h} &\overset{\text{Eq. 3.49}}{=} \sum_{\alpha,\beta} h_{\alpha,\beta} \hat{c}_\alpha^\dagger \hat{c}_\beta \\
&= \bar{\epsilon} \sum_{\sigma\in\{\uparrow,\downarrow\}} \sum_{R\in\{1,2\}} \underbrace{\hat{c}_{R,\sigma}^\dagger \hat{c}_{R,\sigma}}_{\hat{n}_{R,\sigma}} - t \sum_{\sigma\in\{\uparrow,\downarrow\}} \left(\hat{c}_{1,\sigma}^\dagger \hat{c}_{2,\sigma} + \hat{c}_{2,\sigma}^\dagger \hat{c}_{1,\sigma}\right) \\
\hat{W} &\overset{\text{Eq. 3.50}}{=} \frac{1}{2} \sum_{\alpha,\beta,\gamma,\delta} W_{\alpha,\beta,\gamma,\delta} \hat{c}_\alpha^\dagger \hat{c}_\beta^\dagger \hat{c}_\delta \hat{c}_\gamma \\
&= \frac{1}{2} U \sum_{R\in\{1,2\}} \sum_{\sigma,\sigma'\in\{\uparrow,\downarrow\}} \underbrace{\hat{c}_{R,\sigma}^\dagger \hat{c}_{R,\sigma'}^\dagger \hat{c}_{R,\sigma'} \hat{c}_{R,\sigma}}_{\text{see point A below}} + \frac{1}{2} V \sum_{R\neq R'\in\{1,2\}} \sum_{\sigma,\sigma'\in\{\uparrow,\downarrow\}} \hat{c}_{R,\sigma}^\dagger \hat{c}_{R',\sigma'}^\dagger \hat{c}_{R',\sigma'} \hat{c}_{R,\sigma} \qquad (3.94) \\
&= U \sum_{R\in\{1,2\}} \underbrace{\underbrace{\hat{c}_{R,\uparrow}^\dagger \hat{c}_{R,\uparrow}}_{\hat{n}_{R,\uparrow}} \underbrace{\hat{c}_{R,\downarrow}^\dagger \hat{c}_{R,\downarrow}}_{\hat{n}_{R,\downarrow}}}_{\text{double occupancy}} + V \sum_{\sigma,\sigma'\in\{\uparrow,\downarrow\}} \underbrace{\hat{c}_{1,\sigma}^\dagger \hat{c}_{2,\sigma'}^\dagger \hat{c}_{2,\sigma'} \hat{c}_{1,\sigma}}_{\hat{n}_{1,\sigma}\hat{n}_{2,\sigma'}} \qquad (3.95)
\end{aligned}$$

Thus, the Hamiltonian has the form

$$\begin{aligned}
\hat{H} \overset{\text{def}}{=} \hat{h} + \hat{W} = \bar{\epsilon} \sum_{R,\sigma} \hat{n}_{R,\sigma} + U \sum_R \hat{n}_{R,\uparrow}\hat{n}_{R,\downarrow} + V\Big(\sum_\sigma \hat{n}_{1,\sigma}\Big)\Big(\sum_{\sigma'} \hat{n}_{2,\sigma'}\Big) \\
- t \sum_\sigma \Big(\hat{c}_{1,\sigma}^\dagger \hat{c}_{2,\sigma} + \hat{c}_{2,\sigma}^\dagger \hat{c}_{1,\sigma}\Big)
\end{aligned} \tag{3.96}$$

Remarks:

- The occupation-number operators $\hat{n}_\alpha = \hat{c}_\alpha^\dagger \hat{c}_\alpha$ are convenient, because the Slater determinants in the same basisset are eigenstates of the occupation-number operator. Furthermore, the occupation-number operator commutates with the creation and annihilation operators in the same basisset.
- The factor $\frac{1}{2}$ in the interaction energy has been absorbed by making specific selections of spins, respectively sites.

- Point A in Eq. 3.95:

$$\hat{c}^\dagger_{R,\sigma}\hat{c}^\dagger_{R,\sigma'}\underbrace{\hat{c}_{R,\sigma'}\hat{c}_{R,\sigma}}_{-\hat{c}_{R,\sigma}\hat{c}_{R,\sigma'}} = -\hat{c}^\dagger_{R,\sigma}\underbrace{\hat{c}^\dagger_{R,\sigma'}\hat{c}_{R,\sigma}}_{\delta_{\sigma,\sigma'}-\hat{c}_{R,\sigma}\hat{c}^\dagger_{R,\sigma'}}\hat{c}_{R,\sigma'} = \underbrace{-\delta_{\sigma,\sigma'}\hat{c}^\dagger_{R,\sigma}\hat{c}_{R,\sigma'}}_{\text{exchange}} + \underbrace{\hat{c}^\dagger_{R,\sigma}\hat{c}_{R,\sigma}\hat{c}^\dagger_{R,\sigma'}\hat{c}_{R,\sigma'}}_{\text{Hartree}}$$
$$= \hat{n}_{R,\sigma}\hat{n}_{R,\sigma'} - \delta_{\sigma,\sigma'}\underbrace{\hat{n}_{R,\sigma}}_{=\hat{n}^2_{R,\sigma}} = \Big(1-\delta_{\sigma,\sigma'}\Big)\hat{n}_{R,\sigma}\hat{n}_{R,\sigma'} \tag{3.97}$$

When the Hamiltonian acts onto the states with $S_z = 0$, namely $|\Phi_j\rangle$ with $j \in \{1,\dots,6\}$ from Eq. 3.90, one obtains

$$\begin{aligned}
\hat{H}\underbrace{\hat{c}^\dagger_{1,\uparrow}\hat{c}^\dagger_{1,\downarrow}|\mathcal{O}\rangle}_{|\Phi_1\rangle} &= \underbrace{\hat{c}^\dagger_{1,\uparrow}\hat{c}^\dagger_{1,\downarrow}|\mathcal{O}\rangle}_{|\Phi_1\rangle}\Big(2\bar{\epsilon}+U\Big) + \overbrace{\underbrace{\hat{c}^\dagger_{2,\uparrow}\hat{c}^\dagger_{1,\downarrow}}_{-\hat{c}^\dagger_{1,\downarrow}\hat{c}^\dagger_{2,\uparrow}}|\mathcal{O}\rangle}^{-|\Phi_4\rangle}\Big(-t\Big) + \underbrace{\hat{c}^\dagger_{1,\uparrow}\hat{c}^\dagger_{2,\downarrow}|\mathcal{O}\rangle}_{|\Phi_3\rangle}\Big(-t\Big)\\
\hat{H}\underbrace{\hat{c}^\dagger_{2,\uparrow}\hat{c}^\dagger_{2,\downarrow}|\mathcal{O}\rangle}_{|\Phi_2\rangle} &= \underbrace{\hat{c}^\dagger_{2,\uparrow}\hat{c}^\dagger_{2,\downarrow}|\mathcal{O}\rangle}_{|\Phi_2\rangle}\Big(2\bar{\epsilon}+U\Big) + \underbrace{\hat{c}^\dagger_{1,\uparrow}\hat{c}^\dagger_{2,\downarrow}|\mathcal{O}\rangle}_{|\Phi_3\rangle}\Big(-t\Big) + \overbrace{\underbrace{\hat{c}^\dagger_{2,\uparrow}\hat{c}^\dagger_{1,\downarrow}}_{-\hat{c}^\dagger_{1,\downarrow}\hat{c}^\dagger_{2,\uparrow}}|\mathcal{O}\rangle}^{-|\Phi_4\rangle}\Big(-t\Big)\\
\hat{H}\underbrace{\hat{c}^\dagger_{1,\uparrow}\hat{c}^\dagger_{2,\downarrow}|\mathcal{O}\rangle}_{|\Phi_3\rangle} &= \underbrace{\hat{c}^\dagger_{1,\uparrow}\hat{c}^\dagger_{2,\downarrow}|\mathcal{O}\rangle}_{|\Phi_3\rangle}\Big(2\bar{\epsilon}+V\Big) + \underbrace{\hat{c}^\dagger_{2,\uparrow}\hat{c}^\dagger_{2,\downarrow}|\mathcal{O}\rangle}_{|\Phi_2\rangle}\Big(-t\Big) + \underbrace{\hat{c}^\dagger_{1,\uparrow}\hat{c}^\dagger_{1,\downarrow}|\mathcal{O}\rangle}_{|\Phi_1\rangle}\Big(-t\Big)\\
\hat{H}\underbrace{\hat{c}^\dagger_{1,\downarrow}\hat{c}^\dagger_{2,\uparrow}|\mathcal{O}\rangle}_{|\Phi_4\rangle} &= \underbrace{\hat{c}^\dagger_{1,\downarrow}\hat{c}^\dagger_{2,\uparrow}|\mathcal{O}\rangle}_{|\Phi_4\rangle}\Big(2\bar{\epsilon}+V\Big) + \overbrace{\underbrace{\hat{c}^\dagger_{2,\downarrow}\hat{c}^\dagger_{2,\uparrow}}_{-\hat{c}^\dagger_{2,\uparrow}\hat{c}^\dagger_{2,\downarrow}}|\mathcal{O}\rangle}^{-|\Phi_2\rangle}\Big(-t\Big) + \overbrace{\underbrace{\hat{c}^\dagger_{1,\downarrow}\hat{c}^\dagger_{1,\uparrow}}_{-\hat{c}^\dagger_{1,\uparrow}\hat{c}^\dagger_{1,\downarrow}}|\mathcal{O}\rangle}^{-|\Phi_1\rangle}\Big(-t\Big)\\
\hat{H}\underbrace{\hat{c}^\dagger_{1,\uparrow}\hat{c}^\dagger_{2,\uparrow}|\mathcal{O}\rangle}_{|\Phi_5\rangle} &= \underbrace{\hat{c}^\dagger_{1,\uparrow}\hat{c}^\dagger_{2,\uparrow}|\mathcal{O}\rangle}_{|\Phi_5\rangle}\Big(2\bar{\epsilon}+V\Big)\\
\hat{H}\underbrace{\hat{c}^\dagger_{1,\downarrow}\hat{c}^\dagger_{2,\downarrow}|\mathcal{O}\rangle}_{|\Phi_6\rangle} &= \underbrace{\hat{c}^\dagger_{1,\downarrow}\hat{c}^\dagger_{2,\downarrow}|\mathcal{O}\rangle}_{|\Phi_6\rangle}\Big(2\bar{\epsilon}+V\Big)
\end{aligned} \tag{3.98}$$

Let $\hat{P}_2$ be the projector onto the two-particle Hilbert space. The results obtained above can be condensed into the following equation for the Hamiltonian in the two-particle Hilbert space.

$$\begin{aligned}
\hat{P}_2\Big(\hat{h}+\hat{W}\Big)\hat{P}_2 &= \sum_{i,j=1}^{6}|\Phi_i\rangle\langle\Phi_i|\hat{h}+\hat{W}|\Phi_j\rangle\langle\Phi_j|\\
&= \begin{pmatrix}\hat{c}^\dagger_{1,\uparrow}\hat{c}^\dagger_{1,\downarrow}|\mathcal{O}\rangle\\ \hat{c}^\dagger_{2,\uparrow}\hat{c}^\dagger_{2,\downarrow}|\mathcal{O}\rangle\\ \hat{c}^\dagger_{1,\uparrow}\hat{c}^\dagger_{2,\downarrow}|\mathcal{O}\rangle\\ \hat{c}^\dagger_{1,\downarrow}\hat{c}^\dagger_{2,\uparrow}|\mathcal{O}\rangle\end{pmatrix}\begin{pmatrix}2\bar{\epsilon}+U & 0 & -t & +t\\ 0 & 2\bar{\epsilon}+U & -t & +t\\ -t & -t & 2\bar{\epsilon}+V & 0\\ +t & +t & 0 & 2\bar{\epsilon}+V\end{pmatrix}\begin{pmatrix}\langle\mathcal{O}|\hat{c}_{1,\downarrow}\hat{c}_{1,\uparrow}\\ \langle\mathcal{O}|\hat{c}_{2,\downarrow}\hat{c}_{2,\uparrow}\\ \langle\mathcal{O}|\hat{c}_{2,\downarrow}\hat{c}_{1,\uparrow}\\ \langle\mathcal{O}|\hat{c}_{2,\uparrow}\hat{c}_{1,\downarrow}\end{pmatrix}\\
&\quad+\begin{pmatrix}\hat{c}^\dagger_{1,\uparrow}\hat{c}^\dagger_{2,\uparrow}|\mathcal{O}\rangle\\ \hat{c}^\dagger_{1,\downarrow}\hat{c}^\dagger_{1,\downarrow}|\mathcal{O}\rangle\end{pmatrix}\begin{pmatrix}2\bar{\epsilon}+V & 0\\ 0 & 2\bar{\epsilon}+V\end{pmatrix}\begin{pmatrix}\langle\mathcal{O}|\hat{c}_{2,\uparrow}\hat{c}_{1,\uparrow}\\ \langle\mathcal{O}|\hat{c}_{2,\downarrow}\hat{c}_{1,\downarrow}\end{pmatrix}\\
&= \begin{pmatrix}|\Phi_1\rangle\\ |\Phi_2\rangle\\ |\Phi_3\rangle\\ |\Phi_4\rangle\\ |\Phi_5\rangle\\ |\Phi_6\rangle\end{pmatrix}\begin{pmatrix}2\bar{\epsilon}+U & 0 & -t & +t & 0 & 0\\ 0 & 2\bar{\epsilon}+U & -t & +t & 0 & 0\\ -t & -t & 2\bar{\epsilon}+V & 0 & 0 & 0\\ +t & +t & 0 & 2\bar{\epsilon}+V & 0 & 0\\ 0 & 0 & 0 & 0 & 2\bar{\epsilon}+V & 0\\ 0 & 0 & 0 & 0 & 0 & 2\bar{\epsilon}+V\end{pmatrix}\begin{pmatrix}\langle\Phi_1|\\ \langle\Phi_2|\\ \langle\Phi_3|\\ \langle\Phi_4|\\ \langle\Phi_5|\\ \langle\Phi_6|\end{pmatrix}
\end{aligned} \tag{3.99}$$

4 Exploit the reflection symmetry $\hat{P}$ of the hydrogen molecule to block-diagonalize the Hamiltonian in the two-particle channel. That is, construct the eigenstates of the parity operator under reflection symmetry of the molecule. These parity eigenstates are superpositions of the two-particle Slater determinants $|\Phi_i\rangle$ obtained previously. The Hamiltonian in terms of the symmetrized states[a] will "fall apart" into one 2×2 matrix and 1×1 blocks.

[a]With symmetrized states, I mean eigenstates of the symmetry operator. In the case of the parity operator, these eigenstates may be symmetric or antisymmetric.

Determine parity eigenstates: Let $\hat{P}$ be the parity operator under space inversion.

$$\begin{aligned}
\hat{P}|\Phi_1\rangle &= \hat{P}\hat{c}^\dagger_{1\uparrow}\hat{c}^\dagger_{1\downarrow}|\mathcal{O}\rangle = \hat{c}^\dagger_{2\uparrow}\hat{c}^\dagger_{2\downarrow}|\mathcal{O}\rangle = |\Phi_2\rangle \\
\hat{P}|\Phi_2\rangle &= \hat{P}\hat{c}^\dagger_{2\uparrow}\hat{c}^\dagger_{2\downarrow}|\mathcal{O}\rangle = \hat{c}^\dagger_{1\uparrow}\hat{c}^\dagger_{1\downarrow}|\mathcal{O}\rangle = |\Phi_1\rangle \\
\hat{P}|\Phi_3\rangle &= \hat{P}\hat{c}^\dagger_{1\uparrow}\hat{c}^\dagger_{2\downarrow}|\mathcal{O}\rangle = \hat{c}^\dagger_{2\uparrow}\hat{c}^\dagger_{1\downarrow}|\mathcal{O}\rangle = -\hat{c}^\dagger_{1\downarrow}\hat{c}^\dagger_{2\uparrow}|\mathcal{O}\rangle = -|\Phi_4\rangle \\
\hat{P}|\Phi_4\rangle &= \hat{P}\hat{c}^\dagger_{1\downarrow}\hat{c}^\dagger_{2\uparrow}|\mathcal{O}\rangle = \hat{c}^\dagger_{2\downarrow}\hat{c}^\dagger_{1\uparrow}|\mathcal{O}\rangle = -\hat{c}^\dagger_{1\uparrow}\hat{c}^\dagger_{2\downarrow}|\mathcal{O}\rangle = -|\Phi_3\rangle \\
\hat{P}|\Phi_5\rangle &= \hat{P}\hat{c}^\dagger_{1\uparrow}\hat{c}^\dagger_{2\uparrow}|\mathcal{O}\rangle = \hat{c}^\dagger_{2\uparrow}\hat{c}^\dagger_{1\uparrow}|\mathcal{O}\rangle = -\hat{c}^\dagger_{1\uparrow}\hat{c}^\dagger_{2\uparrow}|\mathcal{O}\rangle = -|\Phi_5\rangle \\
\hat{P}|\Phi_6\rangle &= \hat{P}\hat{c}^\dagger_{1\downarrow}\hat{c}^\dagger_{2\downarrow}|\mathcal{O}\rangle = \hat{c}^\dagger_{2\downarrow}\hat{c}^\dagger_{1\downarrow}|\mathcal{O}\rangle = -\hat{c}^\dagger_{1\downarrow}\hat{c}^\dagger_{2\downarrow}|\mathcal{O}\rangle = -|\Phi_6\rangle
\end{aligned} \tag{3.100}$$

Just above, we worked out $\hat{P}|\Phi_j\rangle$ for $j = 1, 6$. Now we construct the parity eigenstates $|\Psi_j\rangle$ ($j \in \{a, b, c, d, e, f\}$).

The eigenstates $|\psi_j\rangle$ ($j \in \{a, b\}$) with parity eigenvalue $+1$ are

$$|\Psi_a\rangle \stackrel{\text{def}}{=} \frac{1}{\sqrt{2}}\Big(\hat{c}^\dagger_{1\uparrow}\hat{c}^\dagger_{1\downarrow} + \hat{c}^\dagger_{2\uparrow}\hat{c}^\dagger_{2\downarrow}\Big)|\mathcal{O}\rangle = \Big(|\Phi_1\rangle + |\Phi_2\rangle\Big)\frac{1}{\sqrt{2}} \tag{3.101}$$

$$|\Psi_b\rangle \stackrel{\text{def}}{=} \frac{1}{\sqrt{2}}\Big(\hat{c}^\dagger_{1\uparrow}\hat{c}^\dagger_{2\downarrow} - \hat{c}^\dagger_{1\downarrow}\hat{c}^\dagger_{2\uparrow}\Big)|\mathcal{O}\rangle = \Big(|\Phi_3\rangle - |\Phi_4\rangle\Big)\frac{1}{\sqrt{2}} \tag{3.102}$$

and the eigenstates $|\psi_j\rangle$ ($j \in \{c, d, e, f\}$) with parity eigenvalue -1 are

$$|\Psi_c\rangle \stackrel{\text{def}}{=} \frac{1}{\sqrt{2}}\Big(\hat{c}^\dagger_{1\uparrow}\hat{c}^\dagger_{1\downarrow} - \hat{c}^\dagger_{2\uparrow}\hat{c}^\dagger_{2\downarrow}\Big)|\mathcal{O}\rangle = \Big(|\Phi_1\rangle - |\Phi_2\rangle\Big)\frac{1}{\sqrt{2}} \tag{3.103}$$

$$|\Psi_d\rangle \stackrel{\text{def}}{=} \frac{1}{\sqrt{2}}\Big(\hat{c}^\dagger_{1\uparrow}\hat{c}^\dagger_{2\downarrow} + \hat{c}^\dagger_{1\downarrow}\hat{c}^\dagger_{2\uparrow}\Big)|\mathcal{O}\rangle = \Big(|\Phi_3\rangle + |\Phi_4\rangle\Big)\frac{1}{\sqrt{2}} \tag{3.104}$$

$$|\Psi_e\rangle \stackrel{\text{def}}{=} \hat{c}^\dagger_{1\uparrow}\hat{c}^\dagger_{2\uparrow}|\mathcal{O}\rangle = |\Phi_5\rangle \tag{3.105}$$

$$|\Psi_f\rangle \stackrel{\text{def}}{=} \hat{c}^\dagger_{1\downarrow}\hat{c}^\dagger_{2\downarrow}|\mathcal{O}\rangle = |\Phi_6\rangle \tag{3.106}$$

Determine Hamiltonian for parity eigenstates: Now, we start from the parity eigenstates and apply the Hamiltonian to them. As expected, the result does not contain a contribution of the opposite parity. This means that the Hamiltonian becomes block diagonal in the representation of parity eigenstates.

I use the matrix-vector notation in the basis of the two-particle states $|\Phi_j\rangle$ with $j \in \{1, \ldots, 4\}$ defined in Eq. 3.90. The first term in Eq. 3.112 describes the Hamiltonian in the desired 4-dimensional subspace. To keep things simple, I exclude the states $|\Phi_e\rangle$ and $|\Phi_f\rangle$, because we know already, that they are eigenstates of the Hamiltonian.

I apply the Hamiltonian to the parity eigenstates $|\Psi_j\rangle$ with $j \in \{a, b, c, d\}$ one at a time. Choosing symmetry eigenstates, has the advantage that the result $(\hat{h} + \hat{W})|\Phi_j\rangle$ will be limited to few terms, namely the symmetry eigenstates with the same symmetry eigenvalues.

1. I begin with $|\Psi_a\rangle \overset{\text{Eq. 3.101}}{=} \Big(|\Phi_1\rangle + |\Phi_2\rangle\Big)/\sqrt{2}$

   The state $|\Psi_a\rangle$ is represented in the basis $|\Phi_j\rangle$ with $j \in \{1,\ldots,4\}$ from Eq. 3.90 by the vector $\vec{c}_a = (1,1,0,0)/\sqrt{2}$, i.e.

$$|\Psi_a\rangle = \sum_{j=1}^{4} |\Phi_j\rangle c_{j,a} \tag{3.107}$$

   Let $\boldsymbol{H}$ be the matrix of the Hamiltonian $\hat{h}+\hat{W}$ in the same basis as above

$$\begin{aligned}\boldsymbol{H}\vec{c}_a &= \begin{pmatrix} 2\bar{\epsilon}+U & 0 & -t & +t \\ 0 & 2\bar{\epsilon}+U & -t & +t \\ -t & -t & 2\bar{\epsilon}+V & 0 \\ +t & +t & 0 & 2\bar{\epsilon}+V \end{pmatrix} \begin{pmatrix} 1 \\ 1 \\ 0 \\ 0 \end{pmatrix} \frac{1}{\sqrt{2}} = \begin{pmatrix} 2\bar{\epsilon}+U \\ 2\bar{\epsilon}+U \\ -2t \\ +2t \end{pmatrix} \frac{1}{\sqrt{2}} \\ &= \begin{pmatrix} 1 \\ 1 \\ 0 \\ 0 \end{pmatrix} \frac{1}{\sqrt{2}}\Big(2\bar{\epsilon}+U\Big) + \begin{pmatrix} 0 \\ 0 \\ 1 \\ -1 \end{pmatrix} \frac{1}{\sqrt{2}}\Big(-2t\Big)\end{aligned}$$

$$\Rightarrow \quad (\hat{h}+\hat{W})|\Psi_a\rangle = |\Psi_a\rangle\Big(2\bar{\epsilon}+U\Big) + |\Psi_b\rangle\Big(-2t\Big) \tag{3.108}$$

2. $|\Psi_b\rangle \overset{\text{Eq. 3.102}}{=} \Big(|\Phi_3\rangle - |\Phi_4\rangle\Big)/\sqrt{2}$ with the vector representation $\vec{c}_b = (0,0,1,-1)/\sqrt{2}$ of $|\Psi_b\rangle$.

$$\boldsymbol{H}\vec{c}_b = \begin{pmatrix} 2\bar{\epsilon}+U & 0 & -t & +t \\ 0 & 2\bar{\epsilon}+U & -t & +t \\ -t & -t & 2\bar{\epsilon}+V & 0 \\ +t & +t & 0 & 2\bar{\epsilon}+V \end{pmatrix} \begin{pmatrix} 0 \\ 0 \\ 1 \\ -1 \end{pmatrix} \frac{1}{\sqrt{2}} = \begin{pmatrix} -2t \\ -2t \\ 2\bar{\epsilon}+V \\ -(2\bar{\epsilon}+V) \end{pmatrix} \frac{1}{\sqrt{2}}$$

$$\Rightarrow \quad (\hat{h}+\hat{W})|\Psi_b\rangle = |\Psi_a\rangle\Big(-2t\Big) + |\Psi_b\rangle\Big(2\bar{\epsilon}+V\Big) \tag{3.109}$$

3. $|\Psi_c\rangle \overset{\text{Eq. 3.103}}{=} \Big(|\Phi_1\rangle - |\Phi_2\rangle\Big)/\sqrt{2}$ with the vector representation $\vec{c}_c = (1,-1,0,0)/\sqrt{2}$ of $|\Psi_c\rangle$.

$$\boldsymbol{H}\vec{c}_c = \begin{pmatrix} 2\bar{\epsilon}+U & 0 & -t & +t \\ 0 & 2\bar{\epsilon}+U & -t & +t \\ -t & -t & 2\bar{\epsilon}+V & 0 \\ +t & +t & 0 & 2\bar{\epsilon}+V \end{pmatrix} \begin{pmatrix} 1 \\ -1 \\ 0 \\ 0 \end{pmatrix} \frac{1}{\sqrt{2}} = \begin{pmatrix} 2\bar{\epsilon}+U \\ -(2\bar{\epsilon}+U) \\ 0 \\ 0 \end{pmatrix} \frac{1}{\sqrt{2}}$$

$$\Rightarrow \quad (\hat{h}+\hat{W})|\Psi_c\rangle = |\Psi_c\rangle\Big(2\bar{\epsilon}+U\Big) \tag{3.110}$$

4. $|\Psi_d\rangle \overset{\text{Eq. 3.104}}{=} \Big(|\Phi_3\rangle + |\Phi_4\rangle\Big)/\sqrt{2}$ with the vector representation $\vec{c}_d = (0,0,1,1)/\sqrt{2}$ of $|\Psi_d\rangle$.

$$\boldsymbol{H}\vec{c}_d = \begin{pmatrix} 2\bar{\epsilon}+U & 0 & -t & +t \\ 0 & 2\bar{\epsilon}+U & -t & +t \\ -t & -t & 2\bar{\epsilon}+V & 0 \\ +t & +t & 0 & 2\bar{\epsilon}+V \end{pmatrix} \begin{pmatrix} 0 \\ 0 \\ 1 \\ 1 \end{pmatrix} \frac{1}{\sqrt{2}} = \begin{pmatrix} 0 \\ 0 \\ 2\bar{\epsilon}+V \\ 2\bar{\epsilon}+V \end{pmatrix} \frac{1}{\sqrt{2}}$$

$$\Rightarrow \quad (\hat{h}+\hat{W})|\Psi_d\rangle = |\Psi_d\rangle\Big(2\bar{\epsilon}+V\Big) \tag{3.111}$$

These expressions can be used to express the Hamiltonian Eq. 3.112 in terms of symmetry-adapted orbitals $|\Psi_j\rangle$ with $j \in \{a, b, c, d, e, f\}$.

$$\hat{P}_2(\hat{h}+\hat{W})\hat{P}_2 = \begin{pmatrix} |\Psi_a\rangle \\ |\Psi_b\rangle \\ |\Psi_c\rangle \\ |\Psi_d\rangle \\ |\Psi_e\rangle \\ |\Psi_f\rangle \end{pmatrix} \begin{pmatrix} 2\bar{\epsilon}+U & -2t & 0 & 0 & 0 & 0 \\ -2t & 2\bar{\epsilon}+V & 0 & 0 & 0 & 0 \\ 0 & 0 & 2\bar{\epsilon}+U & 0 & 0 & 0 \\ 0 & 0 & 0 & 2\bar{\epsilon}+V & 0 & 0 \\ 0 & 0 & 0 & 0 & 2\bar{\epsilon}+V & 0 \\ 0 & 0 & 0 & 0 & 0 & 2\bar{\epsilon}+V \end{pmatrix} \begin{pmatrix} \langle\Psi_a| \\ \langle\Psi_b| \\ \langle\Psi_c| \\ \langle\Psi_d| \\ \langle\Psi_e| \\ \langle\Psi_f| \end{pmatrix} \tag{3.112}$$

All this effort has been done to block-diagonalize the Hamiltonian further. For the states with $S_z = 0$, i.e. a-d, we obtain two additional eigenstates of the Hamiltonian, and one 2×2 block.

Diagonalize Hamiltonian in the basis of parity eigenstates: In the basis of eigenstates of the parity operator, the Hamiltonian falls apart into two 1×1 blocks and one 2×2 block. The one-by-one blocks identify $|\Psi_c\rangle$ and $|\Psi_d\rangle$ as eigenstates. The eigenvalues are $E_c = 2\bar{\epsilon}+U$ and $E_d = 2\bar{\epsilon}+V$. The 2×2 block in the space spanned by $|\Psi_j\rangle$ with $j \in \{\Psi_a, \Psi_b\}$ has the form

$$\begin{pmatrix} 2\bar{\epsilon}+U & -2t \\ -2t & 2\bar{\epsilon}+V \end{pmatrix} \tag{3.113}$$

and has eigenvalues

$$E_\pm = 2\bar{\epsilon} + \frac{U+V}{2} \pm \sqrt{\left(\frac{U-V}{2}\right)^2 + 4t^2} \tag{3.114}$$

and eigenstates

$$|\Psi_\pm\rangle = |\Psi_a\rangle \cos(\gamma_\pm) + |\Psi_b\rangle \sin(\gamma_\pm) \tag{3.115}$$

Using cosine and sine takes care of the normalization, because $\cos^2(x) + \sin^2(x) = 1$.

The angle $\gamma_\pm$ is obtained from the eigenvector equation

$$\begin{aligned}
&\begin{pmatrix} 2\bar{\epsilon}+U-E_\pm & -2t \\ -2t & 2\bar{\epsilon}+V-E_\pm \end{pmatrix} \begin{pmatrix} \cos(\gamma_\pm) \\ \sin(\gamma_\pm) \end{pmatrix} = 0 \\
\Rightarrow \quad \tan(\gamma_\pm) &= \frac{\sin(\gamma_\pm)}{\cos(\gamma_\pm)} = \frac{1}{2t}\Big(2\bar{\epsilon}+U-E_\pm\Big) \\
&= \frac{1}{2t}\left(2\bar{\epsilon}+U-2\bar{\epsilon}-\frac{U+V}{2} \mp \sqrt{\left(\frac{U-V}{2}\right)^2+4t^2}\right) \\
&= \frac{1}{2t}\left(\frac{U-V}{2} \mp \sqrt{\left(\frac{U-V}{2}\right)^2+4t^2}\right) \\
&= \frac{U-V}{4t} \mp \sqrt{1+\left(\frac{U-V}{4t}\right)^2} \\
&= q \mp \sqrt{1+q^2} \qquad \text{with} \qquad q = \frac{U-V}{4t} \\
\Rightarrow \quad \gamma_\pm &= \arctan\left(q \mp \sqrt{1+q^2}\right) \qquad \text{with} \qquad q = \frac{U-V}{4t}
\end{aligned} \tag{3.116}$$

The parameter q is a measure for the importance of Coulomb interactions. For strong interaction, that is when hopping is small compared to the Coulomb terms, q is very large. On the other hand, the non-interacting limit is characterized by $q = 0$.

The energy can be expressed in terms of the parameter q.

$$E_\pm = 2\bar{\epsilon} + \frac{U+V}{2} \underbrace{\pm\sqrt{\left(\frac{U-V}{2}\right)^2 + 4t^2}}_{-2t\tan(\gamma_\pm)+\frac{U-V}{2}} = 2\bar{\epsilon} + U - 2t \underbrace{\left(q \mp \sqrt{1+q^2}\right)}_{\tan(\gamma_\pm)} \tag{3.117}$$

Thus, the eigenstates of the Hamiltonian in the two-particle channel are

eigenstate	energy	parity	total spin	S_z	
$\|\Psi_-\rangle$	$2\bar{\epsilon}+U-2t(q+\sqrt{1+q^2})$	+1	0	$0\hbar$	antiferrom. singlet
$\|\Psi_+\rangle$	$2\bar{\epsilon}+U-2t(q-\sqrt{1+q^2})$	+1	0	$0\hbar$	antib. singlet
$\|\Psi_c\rangle$	$2\bar{\epsilon}+U$	-1	0	$0\hbar$	ionized (H^+H^-) state
$\|\Psi_d\rangle$	$2\bar{\epsilon}+V$	-1	1	$0\hbar$	triplet
$\|\Psi_e\rangle$	$2\bar{\epsilon}+V$	-1	1	$1\hbar$	triplet
$\|\Psi_f\rangle$	$2\bar{\epsilon}+V$	-1	1	$-1\hbar$	triplet

The eigenvalues are shown in figure 3.2 on p. 160.

Discuss eigenstates Let me summarize the energy eigenstates and their energy levels. We make the plausible assumption that $U > V$.

1. The lowest state is

$$\begin{aligned}|\Psi_-\rangle &\overset{\text{Eq. 3.115}}{=} |\Psi_a\rangle\cos(\gamma_-) + |\Psi_b\rangle\sin(\gamma_-) \\ &\overset{\text{Eqs. 3.101,3.102}}{=} \left[\frac{\cos\gamma_-}{\sqrt{2}}\left(\hat{c}^\dagger_{1\uparrow}\hat{c}^\dagger_{1\downarrow} + \hat{c}^\dagger_{2\uparrow}\hat{c}^\dagger_{2\downarrow}\right) + \frac{\sin(\gamma_-)}{\sqrt{2}}\left(\hat{c}^\dagger_{1\uparrow}\hat{c}^\dagger_{2\downarrow} - \hat{c}^\dagger_{1\downarrow}\hat{c}^\dagger_{2\uparrow}\right)\right]|\mathcal{O}\rangle\end{aligned} \tag{3.118}$$

   with energy

$$\begin{aligned}E_- &\overset{\text{Eq. 3.117}}{=} 2\bar{\epsilon} + \frac{U+V}{2} - \sqrt{\left(\frac{U-V}{2}\right)^2 + 4t^2} \\ &\overset{\text{Eq. 3.116}}{=} 2\bar{\epsilon} + U - 2t\tan(\gamma_-)\end{aligned} \tag{3.119}$$

   This is corresponds to the bonding configuration of the hydrogen molecule.

   - In the non-interacting limit, i.e. $q = (U-V)/(4t) = 0$ and $\gamma = \pi/4$, the ground-state wave function is a superposition of four Slater determinants, which, however, can be written as a single Slater determinant of two bonding orbitals,.

$$|\Psi_-(q=0)\rangle = \frac{1}{\sqrt{2}}\left(\hat{c}^\dagger_{1,\uparrow} + \hat{c}^\dagger_{2,\uparrow}\right)\frac{1}{\sqrt{2}}\left(\hat{c}^\dagger_{1,\downarrow} + \hat{c}^\dagger_{2,\downarrow}\right)|\mathcal{O}\rangle \tag{3.120}$$

   - In the limit with infinite interaction, i.e. $q = (U-V)/(4t) = \infty$ and $\gamma = \pi/2$, the contribution with double occupancy, namely $|\Psi_a\rangle$ is suppressed and the ground state is an **antiferromagnetic singlet**, namely $|\Psi_b\rangle$.

$$|\Psi_-(q=\infty)\rangle = |\Psi_b\rangle = \frac{1}{\sqrt{2}}\left(\hat{c}^\dagger_{1,\uparrow}\hat{c}^\dagger_{2,\downarrow} - \hat{c}^\dagger_{1,\downarrow}\hat{c}^\dagger_{2,\uparrow}\right)|\mathcal{O}\rangle \tag{3.121}$$

     An antiferromagnetic singlet describes a singlet state, which has no magnetization, but still an antiferromagnetic correlation between the spins on different sites.

- The mechanism that favors an antiferromagnetic alignment of spins over a ferromagnetic[11] alignment is called **superexchange**. The usual explanation for this effect is as follows: When two electrons with equal spin are located on neighboring sites, the Pauli-principle prohibits any delocalization of electrons onto the neighboring site, because no two electrons with the same spin can occupy the same spatial orbital. If the electrons have opposite spin, each electron finds a vacant orbital with the same spin on the other site. The delocalization to the neighboring site requires to overcome the on-site Coulomb repulsion between the electrons, but it also lowers the kinetic energy. The lowering of the kinetic energy can be argued in terms of Heisenberg's uncertainty principle.
- This state expresses the **left-right correlation** of the electrons in a bond. If the spin-up electron is on the left side, the spin-down electron is on the right hand side and vice versa. That is, the electrons get out of each other's way to reduce their Coulomb repulsion. The price to pay, is that the electrons also loose their binding energy, because the electrons are confined to one of the two atoms.
- This left-right-correlated state is also the classical example for **entanglement**: The thought experiment goes as follows: Prepare hydrogen molecule in the left-right correlated state and separate the two hydrogen atoms. Two observers receive one hydrogen atom each. One observer measures the spin of his hydrogen atom. Due to the measurement, the wave function collapses "instantly" into either $\hat{c}_{1,\uparrow}\hat{c}_{2,\downarrow}|\mathcal{O}\rangle$ or $\hat{c}_{1,\downarrow}\hat{c}_{2,\uparrow}|\mathcal{O}\rangle$. This implies that by doing his measurement, he determines what the outcome of the measurement of the other observer will be. This gives the impression of an information transfer, which may even proceed faster than the speed of light, a seeming paradox.

2. The second-lowest state is

$$|\Psi_d\rangle \stackrel{\text{def}}{=} \frac{1}{\sqrt{2}}\left(\hat{c}^\dagger_{1\uparrow}\hat{c}^\dagger_{2\downarrow} + \hat{c}^\dagger_{1\downarrow}\hat{c}^\dagger_{2\uparrow}\right)|\mathcal{O}\rangle \tag{3.122}$$

with energy

$$E_d = 2\bar{\epsilon} + V \tag{3.123}$$

This is actually one of the three triplet states with parallel spins. $|\Psi_d\rangle$ has $S = 1$ and $S_z = 0\hbar$. The other two states of the triplet are

$$|\Psi_{S=1,S_z=+\hbar}\rangle = \hat{c}^\dagger_{1\uparrow}\hat{c}^\dagger_{2\uparrow}|\mathcal{O}\rangle \tag{3.124}$$

$$|\Psi_{S=1,S_z=-\hbar}\rangle = \hat{c}^\dagger_{1\downarrow}\hat{c}^\dagger_{2\downarrow}|\mathcal{O}\rangle \tag{3.125}$$

and have the same energy.

- The energy between the singlet ground state and the triplet is the so-called **singlet-triplet splitting**. It is the smallest excitation energy of a hydrogen molecule.

$$\Delta_{st} = E_d - E_- = \sqrt{\left(\frac{U-V}{2}\right)^2 + 4t^2} - \frac{U-V}{2} \approx \frac{(2t)^2}{U-V} \tag{3.126}$$

  This means that the excitation energy becomes smaller due to the Coulomb interaction.
- The singlet-triplet excitation is not a one-particle excitation and, therefore, it does not show up in the density of states or the spectral function. Rather, it is a two-particle excitation like an optical excitation.

[11] The ferromagnetic states of the hydrogen molecule are the triplet states $|\Psi_d\rangle, |\Psi_e\rangle, |\Psi_f\rangle$, which have parallel spins.

- If we consider only the singlet ground state and the triplet as first excited state, we can describe the hydrogen molecule in the strongly interacting limit by a **Heisenberg model**, which is discussed in greater detail in section 17.3 on p. 450. The Heisenberg model has the Hamiltonian

$$\hat{H}_H = -\sum_{R,R' \in n.n.} J_{R,R'} \hat{\vec{S}}_R \hat{\vec{S}}_{R'} \qquad \text{with}$$

$$J_{R,R'} \stackrel{\text{def}}{=} -\Delta_{st}/\hbar^{-2} \approx -\frac{(2t/\hbar)^2}{U-V} \text{ for } R, R' \text{ next neighbors} \tag{3.127}$$

  The indices R, R' refer to the individual hydrogen atoms. The double sum is executed over all nearest neighbors (n.n.). Each spin operator acts on a spin-one-half system, i.e. the electron on a specific hydrogen atom. The coupling J between two neighboring spins is called **exchange parameter**.[12] Because it is negative, it favors an antiferromagnetic coupling between the sites.

  The elementary excitations of the Heisenberg model are spin-waves, so-called **magnons**. A magnon is yet another elementary excitation of the solid state. Editor: I plan to describe magnons in more detail in appendix 17.3.4 on p. 457.

- In the non-interacting case, the triplet states correspond to a state, where one electron is lifted from the bonding state into the antibonding state. The electron in the antibonding state prefers a parallel spin alignment because of Hund's rule[13]. Therefore, the excitation energy is reduced with increasing interaction and the lowest excitation goes from a singlet to a triplet state.

  Note, however, that the dominant optical excitation in the hydrogen molecule does not lead to the triplet states, but to the "ionized (H^+H^-) state" $|\Phi_c\rangle$ discussed below in Eq. 3.128. This is because the optic excitations, which dominate the absorption spectrum, conserve the spin. This is because the dominant excitations are due to the electric field and preserve the spin, while the excitations due to the magnetic field, which may induce spin flips, are much weaker.

- **Mott-Hubbard insulator**. In our example on the insulating linear chain in section 1.5.4, we learned how a band gap in a metal can be opened by breaking the translational symmetry. This is what is called a band insulator. Interaction does not play a role in the formation of an insulator.

  One important aspect of a non-magnetic band insulator is that it requires an even number of electrons in the unit cell. It was surprising to find that certain transition-metal oxides turned out to be insulating despite having an odd number of electrons. An example is the half-filled Hubbard model. A simple-minded picture is that, in a system with strong interactions, electrons occupy each site with one electron. An excitation must lift an electron from a singly occupied site to one that is already occupied. Therefore, the excitation energy is finite and of order U.

  Editor: This is not clear as such. Show that a band in the band structure must be broken up to create a gap with an odd number of electrons.

- The relevant Coulomb parameter for the excitation spectra is not the onsite Coulomb repulsion U, but the difference $U - V$ between onsite and offsite Coulomb parameters. Thus, the effective Coulomb parameter is smaller than anticipated. In the Hubbard model, the effect of the offsite Coulomb interaction is discarded from the beginning. In the so-called **extended Hubbard model** (see e.g.[60]), the off-site Coulomb interaction is taken into account. (In contrast to the simple Hubbard model with only onsite Coulomb terms, the extended Hubbard model can describe **plasmons** [see Tosatti and Anderson, Japanese

[12] The definition of exchange parameter J is not uniform.[59]

[13] Compare two configurations with one electron in the bonding orbital and another in the antibonding orbital. Both have the same electron density. However, due to the Pauli principle the electrons with parallel spin get out of each other's way, which in turn reduces the Coulomb repulsion. This stabilizes the configuration with parallel spins.

Journal of Applied Physics 13, 381 (1974)] and it can describe **charge ordering**.(see e.g.[61])

3. Above the triplet, we find the ionized (H^+H^-) state $|\Psi_c\rangle$

$$|\Psi_c\rangle \stackrel{\text{def}}{=} \frac{1}{\sqrt{2}}\left(\hat{c}^\dagger_{1\uparrow}\hat{c}^\dagger_{1\downarrow} - \hat{c}^\dagger_{2\uparrow}\hat{c}^\dagger_{2\downarrow}\right)|\mathcal{O}\rangle \tag{3.128}$$

with energy

$$E_c = 2\bar{\epsilon} + U \tag{3.129}$$

- this is a state with double occupancy. It is a superpositions of two Slater determinants, which describe ionic pairs, H^-H^+ and H^+H^-.

4. Finally, we find again a complicated singlet state

$$\begin{aligned}|\Psi_+\rangle &= |\Psi_a\rangle\cos(\gamma_+) + |\Psi_b\rangle\sin(\gamma_+)\\ &= \left[\frac{\cos\gamma_+}{\sqrt{2}}\left(\hat{c}^\dagger_{1\uparrow}\hat{c}^\dagger_{1\downarrow} + \hat{c}^\dagger_{2\uparrow}\hat{c}^\dagger_{2\downarrow}\right) + \frac{\sin(\gamma_+)}{\sqrt{2}}\left(\hat{c}^\dagger_{1\uparrow}\hat{c}^\dagger_{2\downarrow} - \hat{c}^\dagger_{1\downarrow}\hat{c}^\dagger_{2\uparrow}\right)\right]|\mathcal{O}\rangle\end{aligned} \tag{3.130}$$

with energy

$$E_+ = 2\bar{\epsilon} + \frac{U+V}{2} + \sqrt{\left(\frac{U-V}{2}\right)^2 + 4t^2} \approx 2\bar{\epsilon} + U + \frac{4t^2}{U-V} \tag{3.131}$$

- In the non-interacting system, this is a singlet state with both electrons in the antibonding orbitals.
- In the interacting system this state accumulates the contribution with double occupancy in order to compensate the suppression of the double occupancy in the singlet ground state. The total contribution of a given basisstate summed over all eigenstates of the system must be unity.

The many-particle energies are shown as function of the Coulomb interaction in figure 3.2
Let me combine the energy levels of the hydrogen molecule with interaction

$$E_- = \left(2\bar{\epsilon} + V\right) + 2t\left(\frac{U-V}{4t} - \sqrt{1 + \left(\frac{U-V}{4t}\right)^2}\right) \qquad \text{antiferromagnetic singlet} \tag{3.132}$$

$$E_d = \left(2\bar{\epsilon} + V\right) \qquad \text{(ferromagnetic) triplet} \tag{3.133}$$

$$E_c = \left(2\bar{\epsilon} + V\right) + 4t\frac{U-V}{4t} \qquad \text{ionized } (H^+H^-) \text{ state} \tag{3.134}$$

$$E_+ = \left(2\bar{\epsilon} + V\right) + 2t\left(\frac{U-V}{4t} + \sqrt{1 + \left(\frac{U-V}{4t}\right)^2}\right) \qquad \text{two antibonding electrons} \tag{3.135}$$

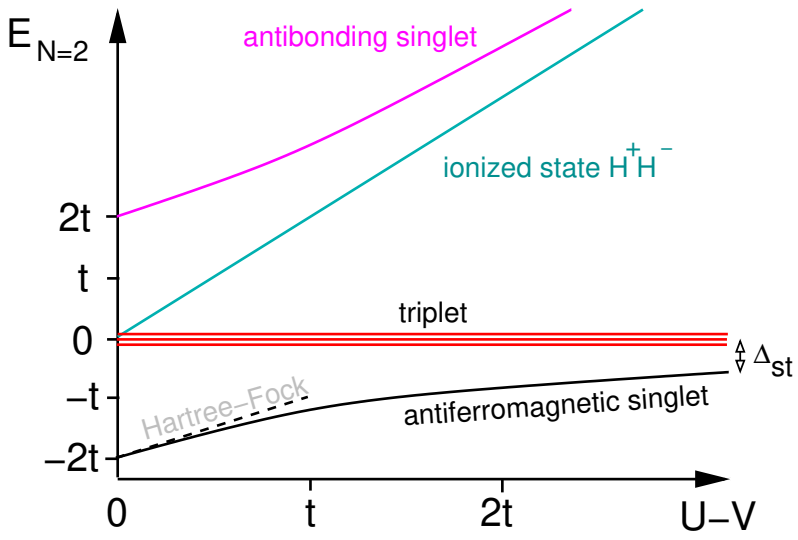


Fig. 3.2: Energies of the hydrogen molecule with two electrons are shown as function of $q = (U - V)/(4t)$ in units of the hopping t. The energies are shifted by $2t - 2\bar{\epsilon} - V$. The energy of the ground state E_-, the antiferromagnetic singlet is shown in black. The energies of the triplet states $|\Psi_d\rangle$, $|\Psi_e\rangle$, and $|\Psi_f\rangle$, (artificially displaced) are shown in red. The energy of the double-occupancy state $|\Psi_c\rangle$ is shown in green and the state $|\Psi_+\rangle$ with two antibonding orbitals is shown in magenta. The black dashed line gives the spin-restricted Hartree-Fock energy with both electrons in the bonding orbital. Note that the Hartree-Fock ground state undergoes a transition to an antiferromagnetic broken-symmetry state for large q. Editor: A copy of this figure is fig. 17.7 on p. 446 Editor: Caution! for the figure $V = 0$ has been used.

3.11.2 Spin eigenstates

Purpose

The main purpose of this exercise is to practice the manipulation of creation and annihilation operators. The secondary purpose is to get used to one rather common two-particle operator, the squared spin. The result obtained here will be required later in section 17.4.1 and in appendix D.1.1.

Introduction

The model used in this exercise is the minimal model derived for an impurity in a metal. Models describing this situation are the famous Andersen model and the Kondo model. The impurity may be a rare-earth ion with a partially filled shell of f-electrons. The metal is described by non-interacting quasi-electrons in a band structure. To arrive at the minimal model we replace the orbitals in the f-shell by two spin orbitals $\{|f, \sigma\rangle\}$, and the orbitals of the metal again by only two spin orbitals $\{|c, \sigma\rangle\}$.

Consider this system with two orbital degrees of freedom and two spin degrees of freedom. The one-particle basis consists of four spin orbitals, namely $|1, \uparrow\rangle$, $|1, \downarrow\rangle$ $|2, \uparrow\rangle$, $|2, \downarrow\rangle$.

The orbital degrees of freedom $\{1, 2\}$ are denoted by symbols f and c. The symbol f is derived from *"f-orbital"* ($\ell = 3$), which is a localized orbital with large Coulomb interaction, and the symbol c is derived from a delocalized *"conduction electron"*. The naming of the spatial orbitals is taken from the **Kondo model**, section 17.4.1.

The corresponding creation operators are denoted as $\hat{c}^\dagger_{1,\uparrow} =: \hat{f}^\dagger_\uparrow$, $\hat{c}_{1,\downarrow} =: \hat{f}_\downarrow$, $\hat{c}_{2,\uparrow} =: \hat{c}_\uparrow$, $\hat{c}_{2,\downarrow} =: \hat{c}_\downarrow$.

That is, we use the letter to discriminate between the two sites of the dimer.[14]

Consider only the two-particle states spanned by the six Slater determinants given in table 3.1. The numbering is related to the integer representation described in section 3.2. **Note, that $\vec{\sigma}$ is the bit representation of $n-1$ rather than of the number n itself. Hence, the vacuum state has the number $n=1$.**

Table 3.1: Two-particle states of the asymmetric dimer with spin orbitals $|f,\uparrow\rangle$ and $|f,\downarrow\rangle$ on the "left" atom and $|c,\uparrow\rangle$ and $|c,\downarrow\rangle$ on the "right" atom.

$\|n\rangle$ with $n = 1 + \sum_{j=1}^{4} \sigma_j 2^{j-1}$	$\|\vec{\sigma}\rangle$	$\prod_{j=1}^{4} (\hat{c}_j^\dagger)^{\sigma_j} \|\mathcal{O}\rangle$
$\|4\rangle$	$\|1100\rangle$	$\hat{f}_\uparrow^\dagger \hat{f}_\downarrow^\dagger \|\mathcal{O}\rangle$
$\|6\rangle$	$\|1010\rangle$	$\hat{f}_\uparrow^\dagger \hat{c}_\uparrow^\dagger \|\mathcal{O}\rangle$
$\|7\rangle$	$\|0110\rangle$	$\hat{f}_\downarrow^\dagger \hat{c}_\uparrow^\dagger \|\mathcal{O}\rangle$
$\|10\rangle$	$\|1001\rangle$	$\hat{f}_\uparrow^\dagger \hat{c}_\downarrow^\dagger \|\mathcal{O}\rangle$
$\|11\rangle$	$\|0101\rangle$	$\hat{f}_\downarrow^\dagger \hat{c}_\downarrow^\dagger \|\mathcal{O}\rangle$
$13\rangle$	$\|0011\rangle$	$\hat{c}_\uparrow^\dagger \hat{c}_\downarrow^\dagger \|\mathcal{O}\rangle$

The main goal of this exercise is to determine matrix elements of $\hat{\vec{S}}^2$ and of $\hat{S}_z$ and their eigenstates. The individual questions shall give some guidance towards this goal.

Problem

1 Express $\hat{S}_x$, $\hat{S}_y$, and $\hat{S}_z$ in terms of creation operators and annihilation operators. Start from the Pauli matrices.

2 Express $\hat{\vec{S}}^2$ in terms of $\hat{S}_j$ with $j = 1, 2, 3$. Then, write it in terms of $\hat{S}_+ = \hat{S}_x + i\hat{S}_y$, $\hat{S}_- = \hat{S}_+^\dagger$ and S_z.

3 Determine the matrix elements of $\hat{S}_+$ and $\hat{S}_z$ with the two-particle states listed in table 3.1 on p.161 above.

4 Determine the matrix elements of $\hat{S}_-$ from those of $\hat{S}_+$ by spin reversal.

5 In the subspace of the two-particle states, express the spin operators $\hat{S}_+$, $\hat{S}_-$, and $\hat{S}_z$ as sum of dyadic products of the two-particle states given above. Use $\hat{P}_2$ as symbol for the projection operator onto the two-particle Hilbert space.

6 Determine the spin eigenstates in the two-particle Hilbert space

Discussion

1 Express $\hat{S}_x$, $\hat{S}_y$, and $\hat{S}_z$ in terms of creation operators and annihilation operators. Start from the Pauli matrices.

[14] While this notation seems a bit clumsy, it is frequently used, which is why I want to expose the reader to it.

The spin operators are given by the Pauli matrices $\boldsymbol{\sigma}_x$, $\boldsymbol{\sigma}_y$ and $\boldsymbol{\sigma}_z$, defined in Eq. 1.22, as

$$\hat{S}_j \overset{\text{Eq. 3.49}}{=} \frac{\hbar}{2} \sum_{\sigma,\sigma' \in \{\uparrow,\downarrow\}} \sigma_{j,\sigma,\sigma'} \left(\hat{f}_\sigma^\dagger \hat{f}_{\sigma'} + \hat{c}_\sigma^\dagger \hat{c}_{\sigma'} \right) \tag{3.136}$$

The spin S_j is obtained by summing over both sites (orbitals).

Hence, the spin operators are

$$\begin{aligned} \hat{S}_z &= \frac{\hbar}{2} \left(\hat{f}_\uparrow^\dagger \hat{f}_\uparrow - \hat{f}_\downarrow^\dagger \hat{f}_\downarrow + \hat{c}_\uparrow^\dagger \hat{c}_\uparrow - \hat{c}_\downarrow^\dagger \hat{c}_\downarrow \right) \\ \hat{S}_x &= \frac{\hbar}{2} \left(\hat{f}_\uparrow^\dagger \hat{f}_\downarrow + \hat{f}_\downarrow^\dagger \hat{f}_\uparrow + \hat{c}_\uparrow^\dagger \hat{c}_\downarrow + \hat{c}_\downarrow^\dagger \hat{c}_\uparrow \right) \\ \hat{S}_y &= \frac{\hbar}{2} \left(-i \hat{f}_\uparrow^\dagger \hat{f}_\downarrow + i \hat{f}_\downarrow^\dagger \hat{f}_\uparrow - i \hat{c}_\uparrow^\dagger \hat{c}_\downarrow + i \hat{c}_\downarrow^\dagger \hat{c}_\uparrow \right) \end{aligned} \tag{3.137}$$

2 Express $\hat{\vec{S}}^2$ in terms of $\hat{S}_j$ with $j = 1, 2, 3$. Then, write it in terms of $\hat{S}_+ = \hat{S}_x + i\hat{S}_y$, $\hat{S}_- = \hat{S}_+^\dagger$ and S_z.

$$\hat{\vec{S}}^2 = \hat{S}_x^2 + \hat{S}_y^2 + \hat{S}_z^2 \tag{3.138}$$

While $\hat{S}_x$, $\hat{S}_y$ $\hat{S}_z$ are one-particle (one-particle-at-a-time) operators, $\hat{\vec{S}}^2$ is a two-particle operator.

It is convenient to introduce the operators

$$\begin{aligned} \hat{S}_+ &\overset{\text{def}}{=} \hat{\vec{S}}_x + i\hat{\vec{S}}_y = \left(\hat{f}_\uparrow^\dagger \hat{f}_\downarrow + \hat{c}_\uparrow^\dagger \hat{c}_\downarrow \right) \hbar \\ \hat{S}_- &\overset{\text{def}}{=} \hat{\vec{S}}_x - i\hat{\vec{S}}_y = \left(\hat{f}_\downarrow^\dagger \hat{f}_\uparrow + \hat{c}_\downarrow^\dagger \hat{c}_\uparrow \right) \hbar \end{aligned} \tag{3.139}$$

$\hat{S}_+$ raises S_z, while $\hat{S}_-$ lowers it. $\hat{S}_+$ annihilates a spin-down electron and, if possible, creates instead the corresponding spin-up electron.

For us, the advantage of the operators $\hat{S}_+$ and $\hat{S}_-$ is that $\hat{S}_+$ and $\hat{S}_-$ have less terms than $\hat{S}_x$ and $\hat{S}_y$, when expressed in terms of creation and annihilation operators.

In order to evaluate $\hat{\vec{S}}^2$, we first form the back transform from $(\hat{S}_x, \hat{S}_y)$ to $(\hat{S}_+, \hat{S}_-)$ before we insert it into the equation Eq. 3.138 above.

$$\begin{aligned} \hat{S}_x &= \frac{1}{2} \left(\hat{\vec{S}}_+ + \hat{\vec{S}}_- \right) \\ \hat{S}_y &= -i \frac{1}{2} \left(\hat{\vec{S}}_+ - \hat{\vec{S}}_- \right) \end{aligned} \tag{3.140}$$

This yields

$$\hat{\vec{S}}^2 \overset{\text{Eq. 3.138}}{=} \frac{1}{2} \left(\hat{S}_+ \hat{S}_- + \hat{S}_- \hat{S}_+ \right) + \hat{S}_z^2 \tag{3.141}$$

3 Determine the matrix elements of $\hat{S}_+$ and $\hat{S}_z$ with the two-particle states listed in table 3.1 on p.161 above.

We apply the operators $\hat{S}_+$ to the two-particle basis states. The idea is to permutate the annihilation operator towards the vacuum state. Each permutation produces a sign change. When the annihilation operator is interchanged with its corresponding creation operator, the anticommutator leaves

a non-zero contribution. The annihilation operator acting on the vacuum state produces the zero state.

$$\hat{\vec{S}}_+|4\rangle = \hbar\Big(\hat{f}_\uparrow^\dagger\hat{f}_\downarrow + \hat{c}_\uparrow^\dagger\hat{c}_\downarrow\Big)\hat{f}_\uparrow^\dagger\hat{f}_\downarrow^\dagger|\mathcal{O}\rangle = \hat{f}_\uparrow^\dagger\hat{f}_\downarrow\hat{f}_\uparrow^\dagger\hat{f}_\downarrow^\dagger|\mathcal{O}\rangle\hbar = |\varnothing\rangle \tag{3.142}$$

$$\hat{\vec{S}}_+|6\rangle = \hbar\Big(\hat{f}_\uparrow^\dagger\hat{f}_\downarrow + \hat{c}_\uparrow^\dagger\hat{c}_\downarrow\Big)\hat{f}_\uparrow^\dagger\hat{c}_\uparrow^\dagger|\mathcal{O}\rangle = |\varnothing\rangle \tag{3.143}$$

$$\hat{\vec{S}}_+|7\rangle = \hbar\Big(\hat{f}_\uparrow^\dagger\hat{f}_\downarrow + \hat{c}_\uparrow^\dagger\hat{c}_\downarrow\Big)\hat{f}_\downarrow^\dagger\hat{c}_\uparrow^\dagger|\mathcal{O}\rangle = \hat{f}_\uparrow^\dagger\hat{f}_\downarrow\hat{f}_\downarrow^\dagger\hat{c}_\uparrow^\dagger|\mathcal{O}\rangle\hbar = \hat{f}_\uparrow^\dagger\hat{c}_\uparrow^\dagger|\mathcal{O}\rangle\hbar = |6\rangle\hbar \tag{3.144}$$

$$\hat{\vec{S}}_+|10\rangle = \hbar\Big(\hat{f}_\uparrow^\dagger\hat{f}_\downarrow + \hat{c}_\uparrow^\dagger\hat{c}_\downarrow\Big)\hat{f}_\uparrow^\dagger\hat{c}_\downarrow^\dagger|\mathcal{O}\rangle = \hat{c}_\uparrow^\dagger\hat{c}_\downarrow\hat{f}_\uparrow^\dagger\hat{c}_\downarrow^\dagger|\mathcal{O}\rangle\hbar = -\hat{c}_\uparrow^\dagger\hat{f}_\uparrow^\dagger|\mathcal{O}\rangle\hbar = \hat{f}_\uparrow^\dagger\hat{c}_\uparrow^\dagger|\mathcal{O}\rangle\hbar = |6\rangle\hbar \tag{3.145}$$

$$\hat{\vec{S}}_+|11\rangle = \hbar\Big(\hat{f}_\uparrow^\dagger\hat{f}_\downarrow + \hat{c}_\uparrow^\dagger\hat{c}_\downarrow\Big)\hat{f}_\downarrow^\dagger\hat{c}_\downarrow^\dagger|\mathcal{O}\rangle = \Big(\hat{f}_\uparrow^\dagger\hat{c}_\downarrow^\dagger - \hat{c}_\uparrow^\dagger\hat{f}_\downarrow^\dagger\Big)|\mathcal{O}\rangle\hbar = \Big(|10\rangle + |7\rangle\Big)\hbar \tag{3.146}$$

$$\hat{\vec{S}}_+|13\rangle = \hbar\Big(\hat{f}_\uparrow^\dagger\hat{f}_\downarrow + \hat{c}_\uparrow^\dagger\hat{c}_\downarrow\Big)\hat{c}_\uparrow^\dagger\hat{c}_\downarrow^\dagger|\mathcal{O}\rangle = \hat{c}_\uparrow^\dagger\hat{c}_\downarrow\hat{c}_\uparrow^\dagger\hat{c}_\downarrow^\dagger|\mathcal{O}\rangle\hbar = -\hat{c}_\uparrow^\dagger\hat{c}_\uparrow^\dagger|\mathcal{O}\rangle\hbar = |\varnothing\rangle \tag{3.147}$$

$$\begin{aligned}
\hat{S}_z|4\rangle &= \frac{\hbar}{2}\Big(\hat{f}_\uparrow^\dagger\hat{f}_\uparrow - \hat{f}_\downarrow^\dagger\hat{f}_\downarrow + \hat{c}_\uparrow^\dagger\hat{c}_\uparrow - \hat{c}_\downarrow^\dagger\hat{c}_\downarrow\Big)\hat{f}_\uparrow^\dagger\hat{f}_\downarrow^\dagger|\mathcal{O}\rangle = |\varnothing\rangle \\
\hat{S}_z|6\rangle &= \hat{S}_z\hat{f}_\uparrow^\dagger\hat{c}_\uparrow^\dagger|\mathcal{O}\rangle = \hat{f}_\uparrow^\dagger\hat{c}_\uparrow^\dagger|\mathcal{O}\rangle\hbar = |6\rangle\hbar \\
\hat{S}_z|7\rangle &= |\varnothing\rangle \\
\hat{S}_z|10\rangle &= |\varnothing\rangle \\
\hat{S}_z|11\rangle &= |11\rangle(-\hbar) \\
\hat{S}_z|13\rangle &= |\varnothing\rangle
\end{aligned} \tag{3.148}$$

4 Determine the matrix elements of $\hat{S}_-$ from those of $\hat{S}_+$ by spin reversal.

Other matrix elements can be obtained by exchanging simultaneously

- $\uparrow$ and $\downarrow$ as well as
- $\hat{S}_+$ with $\hat{S}_-$ and
- $\hat{S}_z$ with $-\hat{S}_z$.

This yields

$$\begin{aligned}
-\hat{S}_-|4\rangle &\overset{\text{Eq. } 3.142}{=} |\varnothing\rangle \\
\hat{S}_-|11\rangle &\overset{\text{Eq. } 3.143}{=} |\varnothing\rangle \\
\hat{S}_-|10\rangle &\overset{\text{Eq. } 3.144}{=} |11\rangle\hbar \\
\hat{S}_-|7\rangle &\overset{\text{Eq. } 3.145}{=} |11\rangle\hbar \\
\hat{S}_-|6\rangle &\overset{\text{Eq. } 3.146}{=} \Big(|7\rangle + |10\rangle\Big)\hbar \\
-\hat{S}_-|13\rangle &\overset{\text{Eq. } 3.147}{=} |\varnothing\rangle
\end{aligned} \tag{3.149}$$

5 In the subspace of the two-particle states, express the spin operators $\hat{S}_+$, $\hat{S}_-$, and $\hat{S}_z$ as sum of dyadic products of the two-particle states given above. Use $\hat{P}_2$ as symbol for the projection operator onto the two-particle Hilbert space.

$$\begin{aligned}
\hat{S}_+\hat{P}_2 = \hat{P}_2\hat{S}_+ &= \Big(|6\rangle\langle 10| + |6\rangle\langle 7| + |10\rangle\langle 11| + |7\rangle\langle 11|\Big)\hbar \\
\hat{P}_2\hat{S}_- = \hat{S}_-\hat{P}_2 &= \Big(|10\rangle\langle 6| + |7\rangle\langle 6| + |11\rangle\langle 10| + |11\rangle\langle 7|\Big)\hbar \\
\hat{P}_2\hat{S}_z = \hat{S}_z\hat{P}_2 &= \Big(|6\rangle\langle 6| - |11\rangle\langle 11|\Big)\hbar
\end{aligned} \tag{3.150}$$

$$\begin{aligned}
\hat{P}_2\hat{\vec{S}}^2\hat{P}_2 &= \frac{\hbar^2}{2}\Big(|6\rangle\langle 10| + |6\rangle\langle 7| + |10\rangle\langle 11| + |7\rangle\langle 11|\Big)\Big(|10\rangle\langle 6| + |7\rangle\langle 6| + |11\rangle\langle 10| + |11\rangle\langle 7|\Big) \\
&+ \frac{\hbar^2}{2}\Big(|10\rangle\langle 6| + |7\rangle\langle 6| + |11\rangle\langle 10| + |11\rangle\langle 7|\Big)\Big(|6\rangle\langle 10| + |6\rangle\langle 7| + |10\rangle\langle 11| + |7\rangle\langle 11|\Big) \\
&+ \hbar^2\Big(|6\rangle\langle 6| - |11\rangle\langle 11|\Big)^2 \\
&= \frac{\hbar^2}{2}\Big(|6\rangle\langle 6| + |6\rangle\langle 6| + |10\rangle\langle 10| + |10\rangle\langle 7| + |7\rangle\langle 10| + |7\rangle\langle 7|\Big) \\
&+ \frac{\hbar^2}{2}\Big(|10\rangle\langle 10| + |10\rangle\langle 7| + |7\rangle\langle 10| + |7\rangle\langle 7| + |11\rangle\langle 11| + |11\rangle\langle 11|\Big) \\
&+ \hbar^2\Big(|6\rangle\langle 6| + |11\rangle\langle 11|\Big) \\
&= 2\hbar^2\Big(|6\rangle\langle 6| + |11\rangle\langle 11|\Big) + \hbar^2\Big(|7\rangle\langle 7| + |7\rangle\langle 10| + |10\rangle\langle 7| + |10\rangle\langle 10|\Big)
\end{aligned} \tag{3.151}$$

6 Determine the spin eigenstates in the two-particle Hilbert space

We recognize the eigenvalues having the form $\hbar^2 S(S+1)$ with the main spin angular-momentum quantum number S.

Thus, we obtain three states with spin quantum number $S = 1$, namely

$$\begin{aligned}
|6\rangle &= \hat{f}_\uparrow^\dagger \hat{c}_\uparrow^\dagger |\mathcal{O}\rangle \\
|11\rangle &= \hat{f}_\downarrow^\dagger \hat{c}_\downarrow^\dagger |\mathcal{O}\rangle \\
\frac{1}{\sqrt{2}}\Big(|7\rangle + |10\rangle\Big) &= \frac{1}{\sqrt{2}}\Big(\hat{f}_\downarrow^\dagger \hat{c}_\uparrow^\dagger + \hat{f}_\uparrow^\dagger \hat{c}_\downarrow^\dagger\Big)|\mathcal{O}\rangle
\end{aligned} \tag{3.152}$$

and three states with $S = 0$, namely

$$\begin{aligned}
|4\rangle &= \hat{f}_\uparrow^\dagger \hat{f}_\downarrow^\dagger |\mathcal{O}\rangle \\
|13\rangle &= \hat{c}_\uparrow^\dagger \hat{c}_\downarrow^\dagger |\mathcal{O}\rangle \\
\frac{1}{\sqrt{2}}\Big(|7\rangle - |10\rangle\Big) &= \frac{1}{\sqrt{2}}\Big(\hat{f}_\downarrow^\dagger \hat{c}_\uparrow^\dagger - \hat{f}_\uparrow^\dagger \hat{c}_\downarrow^\dagger\Big)|\mathcal{O}\rangle
\end{aligned} \tag{3.153}$$

The three states with $S = \hbar$ are degenerate in a system with spin rotation symmetry. Therefore, they are called **triplet states**. In contrast, the states with spin $S = 0$ are called **singlet states**.

3.11.3 Ground state of the linear chain in second quantization

Purpose

The purpose of this exercise is to, firstly, practice the translation between expressions in bra-ket notation of one-particle quantum mechanics and the notation of second quantization using creation and annihilation operators. Furthermore, it reminds of the transformation between one-particle basissets, in this case, local states versus Bloch states.

Introduction

In the first chapter we analyzed in section 1.5.3 on p. 33 the linear chain of hydrogen atoms.

Problem

We found that the eigenstates of the Hamiltonian for the linear chain

$$\hat{h} \overset{\text{Eq. 1.113}}{=} \underbrace{\sum_{\sigma\in\{\uparrow,\downarrow\}}\sum_{j=-\infty}^{\infty} |\pi_{j,\sigma}\rangle\epsilon_0\langle\pi_{j,\sigma}|}_{\text{atomic energies}} \underbrace{-\sum_{\sigma}\sum_{j=-\infty}^{\infty} |\pi_{j,\sigma}\rangle t\langle\pi_{j+1,\sigma}| - |\pi_{j,\sigma}\rangle t\langle\pi_{j-1,\sigma}|}_{\text{hopping}} \tag{3.154}$$

are

$$|\varphi_\sigma(k)\rangle \overset{\text{Eq. 1.114}}{=} \sum_j |\chi_{j,\sigma}\rangle \underbrace{\mathrm{e}^{ika_{\text{lat}}j}\frac{1}{\sqrt{n}}}_{\langle\pi_\sigma(k)|\varphi_\sigma(k)\rangle} \qquad \text{with } k_m = \frac{2\pi}{na_{\text{lat}}}m \tag{3.155}$$

where periodic boundary conditions after n beads are assumed.
The energies are

$$\epsilon_\sigma(k_m) \overset{\text{Eq. 1.117}}{=} \epsilon_0 - 2t\cos(k_m a_{\text{lat}}) \tag{3.156}$$

.
As in the first chapter, we assume that the basis functions are orthonormal.

1 Write the Hamiltonian in second quantization

2 Represent the ground state wave function of the half-filled linear chain in terms of creation and annihilation operators of local orbitals.

Discussion

1 Write the Hamiltonian in second quantization

In second quantization, the Hamiltonian is

$$\hat{h} = \sum_{j=1}^{n}\left\{\sum_{\sigma\in\{\uparrow,\downarrow\}}\epsilon_0\hat{c}^\dagger_{j,\sigma}\hat{c}_{j,\sigma} - t\sum_{\sigma\in\{\uparrow,\downarrow\}}\left(\hat{c}^\dagger_{j,\sigma}\hat{c}_{j+1,\sigma} + \hat{c}^\dagger_{j,\sigma}\hat{c}_{j-1,\sigma}\right)\right\} \tag{3.157}$$

2 Represent the ground state wave function of the half-filled linear chain in terms of creation and annihilation operators of local orbitals.

The wave function is a Slater determinant of all occupied eigenstates of the Hamiltonian. The creator for an eigenstate $|\varphi_m\rangle$ of the Hamiltonian is the superposition of the orbital creation operators multiplied with the coefficients of the eigenstate in the orbital representation.

$$|\varphi_\sigma(\vec{k})\rangle \overset{\text{Eq. } 1.119}{=} \sum_\alpha \underbrace{\sum_{\vec{t}} |\chi_{\alpha,\vec{t}}\rangle e^{i\vec{k}\vec{t}}}_{|\chi_{\alpha,\vec{k}}\rangle} c_{\alpha,n}(\vec{k}) = \sum_j |\chi_{\sigma j}\rangle e^{ik_x a_{\text{lat}} j} \frac{1}{\sqrt{n}} \tag{3.158}$$

$$\begin{aligned}
|\Phi\rangle &= \left\{ \prod_{m=1}^{n/2} \left(\hat{a}^\dagger_{m,\sigma} \right)^{\gamma_{j,\sigma}} \right\} |\mathcal{O}\rangle \\
&\overset{\text{Eq. } 3.64}{=} \left\{ \prod_{m=1}^{n/2} \left(\int d^4x \, \hat{\psi}^\dagger(\vec{x}) \langle \vec{x} | \varphi_{m,\sigma} \rangle \right)^{\gamma_{j,\sigma}} \right\} |\mathcal{O}\rangle \\
&\overset{\text{Eq. } B.17}{=} \left\{ \prod_{m=1}^{n/2} \left(\int d^4x \underbrace{\sum_{j,\sigma} \hat{c}^\dagger_{j,\sigma} \langle \chi_{j,\sigma} | \vec{x} \rangle}_{\hat{\psi}^\dagger(\vec{x})} \langle \vec{x} | \varphi_{m,\sigma} \rangle \right)^{\gamma_{j,\sigma}} \right\} |\mathcal{O}\rangle \\
&= \left\{ \prod_{m=1}^{n/2} \left(\sum_{j,\sigma} \hat{c}^\dagger_{j,\sigma} \langle \chi_{j,\sigma} | \varphi_{m,\sigma} \rangle \right)^{\gamma_{j,\sigma}} \right\} |\mathcal{O}\rangle \\
&\overset{\text{Eq. } 3.155}{=} \left\{ \prod_{m=1}^{n/2} \left(\sum_j \hat{c}^\dagger_{j,\sigma} \sum_{j'} \underbrace{\langle \chi_{j,\sigma} | \chi_{j',\sigma} \rangle}_{\delta_{j,j'}\delta_{\sigma,\sigma}} \underbrace{e^{ika_{\text{lat}}j'} \frac{1}{\sqrt{n}}}_{\langle \pi_{j',\sigma} | \varphi_{m,\sigma} \rangle} \right)^{\gamma_{j,\sigma}} \right\} |\mathcal{O}\rangle \\
&\overset{\text{Eq. } 3.155}{=} \left\{ \prod_{m=1}^{n/2} \left(\sum_j \hat{c}^\dagger_{j,\sigma} e^{ika_{\text{lat}}j} \frac{1}{\sqrt{n}} \right)^{\gamma_{j,\sigma}} \right\} |\mathcal{O}\rangle
\end{aligned} \tag{3.159}$$

$\gamma_{j,\sigma} \in \{0, 1\}$ are the occupation numbers of the Bloch states

$$\gamma_\sigma(k_m) = \theta(\mu - \epsilon_\sigma(k_m)) \tag{3.160}$$

where μ is the chemical potential. $\theta(x)$ is the Heaviside step function. $\gamma_\sigma(k_m)$ is unity, if the energy of the eigenstate is below the Fermi level, and zero, if it is above. In the limit $n \to \infty$ the chemical potential for a half filled linear chain lies at $\mu = \epsilon_0$.

Remark on a side: We have made the assumption that the orbitals $|\chi_{j,\sigma}\rangle$ are orthonormal. Without this assumption, the Bloch wave function would have a different form, when they are required to be orthonormal themselves. Specifically, they would carry the inverse square root of the overlap matrix as additional factor in Eq. 3.155. This factors would compensate the overlap matrix in the derivation above.

Chapter 4

Green's functions in one-particle quantum mechanics

Green's functions[1] are a powerful tool of many-particle physics. However, they also play an important role in one-particle quantum mechanics. Even more, we use Green's functions in many contexts, often without realizing it.

Because explaining Green's functions in the context of many-particle physics is a double difficulty, let us first become familiar with Green's function in the context of one-particle quantum mechanics.

4.1 Green's function as inverse of a differential operator

Let me first lay out the general concept of Green's functions: In short, Green's functions are useful

- to solve inhomogeneous linear differential equations,
- to solve boundary value problems of linear differential equations,
- to propagate solutions of differential equations in time,
- to describe the effective influence of one subsystem onto another.

4.1.1 Definition

Consider a differential operator $D(\vec{x}, \vec{\nabla})$. $D(\vec{x}, \vec{y})$ is a normal function of two (vector-) arguments, which is turned into a differential operator by supplying derivatives as argument. The vector $\vec{x}$ shall be an n-dimensional vector, where n may also be one. The vector $\vec{x}$ may contain time coordinates, spatial coordinates, both, or any other set of variables.

GREEN'S FUNCTION AS INVERSE OF A DIFFERENTIAL OPERATOR

The Green's function $G(\vec{x}, \vec{x'})$ is defined as the inverse of the differential operator $D(\vec{x}, \vec{\nabla})$

$$D(\vec{x}, \vec{\nabla})G(\vec{x}, \vec{x}_0) = \delta(\vec{x} - \vec{x}_0) \tag{4.1}$$

and a suitable set of boundary conditions.(see section 4.1.3 below!)

[1] Green's functions have been invented by the George Green in 1828[62].

GREEN'S FUNCTION AND INHOMOGENEOUS DIFFERENTIAL EQUATIONS

An inhomogeneous differential equation can be solved with the help of the Green's function by

$$D(\vec{x},\vec{\nabla})f(\vec{x}) = I(\vec{x}) \quad \Leftrightarrow \quad f(\vec{x}) = \int d^n x'\, G(\vec{x},\vec{x'})I(\vec{x'}) \tag{4.2}$$

Hereby, $I(\vec{x})$ is the inhomogeneity.

The Green's function can be considered as an inverse of the differential operator. It behaves like an inverse matrix while solving a linear system of equations. Consider the solution of such a linear system of equations, expressed in terms of a matrix $\boldsymbol{A}$, an unknown vector $\vec{y}$ and a known vector $\vec{b}$.

$$\begin{aligned} \text{With} \qquad & \boldsymbol{A}\boldsymbol{A}^{-1} = \mathbf{1} \qquad \text{one obtains} \\ & \boldsymbol{A}\vec{y} = \vec{b} \qquad \Rightarrow \qquad \vec{y} = \boldsymbol{A}^{-1}\vec{b} \end{aligned} \tag{4.3}$$

On a more abstract level, the system of equations is identical to the differential equation Eq. 4.2: The matrix $\boldsymbol{A}$ replaces the differential operator $D(\vec{x},\vec{\nabla})$, the vector $\vec{y}$ replaces the function $f(\vec{x})$, the vector $\vec{b}$ the inhomogeneity $I(\vec{x})$ and the inverse $\boldsymbol{A}^{-1}$ replaces the Green's function $G(\vec{x},\vec{x'})$. The indices of matrix $\boldsymbol{A}$ and the vectors $\vec{y}$ and $\vec{b}$ in the system of equations replaces the continuous variable $\vec{x}$ in the differential equation.

4.1.2 Two simple examples:

Let me demonstrate the principle of the Green's function for a few well-known examples, the driven harmonic oscillator and the Poisson equation.

Driven harmonic oscillator

The Green's function can be used to solve the driven harmonic oscillator with damping

$$m\ddot{x} = -cx - \alpha\dot{x} + f(t) \tag{4.4}$$

Here, $x(t)$ is the particle position, m is the mass of the particle, c the force constant, α the friction coefficient and $f(t)$ is the driving force.

The differential operator of this problem is

$$D(t,\partial_t) = m\partial_t^2 + \alpha\partial_t + c \tag{4.5}$$

and the force $f(t)$ is the inhomogeneity.

According to the definition Eq. 4.1, the Green's function fulfills

$$\underbrace{\left(m\partial_t^2 + c + \alpha\partial_t\right)}_{D(t,\partial_t)} G(t,t_0) = \delta(t-t_0) \tag{4.6}$$

The boundary conditions are chosen so that value and derivative of the Green's function vanish at $t = -\infty$.

The Green's function is (see e.g. ΦSX: Klassische Mechanik[15])

$$\begin{aligned} G(t,t') &= \frac{-i}{m(\omega_1-\omega_2)}\left(\mathrm{e}^{i\omega_1(t-t')} - \mathrm{e}^{i\omega_2(t-t')}\right)\theta(t-t') \\ &= \frac{1}{m\sqrt{\frac{c}{m} - \left(\frac{\alpha}{2m}\right)^2}} \sin\left(\sqrt{\frac{c}{m} - \left(\frac{\alpha}{2m}\right)^2}\,(t-t')\right) \mathrm{e}^{-\frac{\alpha}{2m}(t-t')}\theta(t-t') \end{aligned} \tag{4.7}$$

where ω_1 and ω_2 are the complex eigenfrequencies of the damped harmonic oscillator.[2] The Green's function is shown in figure 4.1.

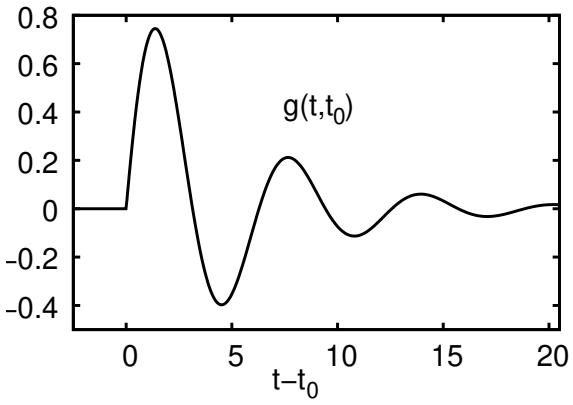


Fig. 4.1: Green's function for the driven harmonic oscillator with damping. Editor: Replace the symbol g by uppercase G.

Once the Green's function is known, we can immediately write down the solution for the driven harmonic oscillator, which fulfills the corresponding inhomogeneous equations of motion. The solution is

$$\begin{aligned} x(t) &= \int dt'\, G(t,t') f(t') \\ &\overset{\text{Eq. 4.7}}{=} \int_{-\infty}^{t} dt'\, \frac{\sin\left(\omega(t-t')\right) e^{-\frac{\alpha}{2m}(t-t')}}{m\omega} f(t') \qquad \text{with } \omega = \sqrt{\frac{c}{m} - \left(\frac{\alpha}{2m}\right)^2} \end{aligned} \tag{4.8}$$

In this case, the Green's function is the response to a Kraftstoß[3] The integral for the position in the presence of a driving force may still be difficult to evaluate, but an integration is usually much simpler than solving a differential equation.

Poisson equation

The Green's function has been used to solve the Poisson equation for the electrostatic potential $\Phi(\vec{r})$ in the presence of a charge density $\rho(\vec{r})$

$$\nabla^2 \Phi(\vec{r}) = -\frac{1}{\epsilon_0} \rho(\vec{r}) \tag{4.9}$$

The Green's function for this problem obeys

$$\nabla^2 G(\vec{r}, \vec{r'}) = \delta(\vec{r} - \vec{r'}) \tag{4.10}$$

which yields the Green's function

$$G(\vec{r}, \vec{r'}) = \frac{-1}{4\pi |\vec{r} - \vec{r'}|} \tag{4.11}$$

Natural boundary conditions have been used.

The solution of Poisson's equation is thus

$$\Phi(\vec{r}) = \int d^3r'\, G(\vec{r}, \vec{r'}) \left(\frac{-\rho(\vec{r'})}{\epsilon_0} \right) = \int d^3r'\, \frac{\rho(\vec{r'})}{4\pi\epsilon_0 |\vec{r} - \vec{r'}|} \tag{4.12}$$

[2] For the undamped harmonic oscillator the frequencies are $\omega_1 = \sqrt{\frac{c}{m}}$ and $\omega_2 = -\sqrt{\frac{c}{m}}$

[3] There does not seem to exist an English word for the German word "Kraftstoß". It describes a force peak in the form of a δ function, which transfers a finite momentum in an infinitesimal time interval.

4.1.3 Boundary conditions

An aspect which is often overlooked is that the definition of the Green's function is only complete when, besides the differential equation, also the boundary conditions are defined.

Let me go back to a differential equation. In order to determine a solution of a linear differential equation unambiguously, we need to define the boundary conditions. Given that one solution of the inhomogeneous differential equation has been found, one can immediately construct another one by adding an arbitrary solution of the homogeneous differential equation. A set of boundary conditions needs to be defined such that any such addition of a homogeneous differential equation would violate the boundary conditions. Only then the solution found is unique.

The same set of boundary conditions must be imposed on the Green's function in the defining equation Eq. 4.1 to make the Green's function unique and appropriate to the problem at hand.

4.2 Green's function of a time-independent Hamiltonian

4.2.1 In the time representation

Consider a time-independent Hamiltonian $\hat{h}$, which has eigenstates $|\varphi_n\rangle$ with eigenvalues ϵ_n. The differential operator[4] describing the Schrödinger equation has the form

$$\hat{D}(t,\partial_t) = \left[\hat{1} i\hbar\partial_t - \hat{h}\right] = \hat{1} i\hbar\partial_t - \underbrace{\sum_n |\varphi_n\rangle \epsilon_n \langle\varphi_n|}_{\hat{h}} = \sum_n |\varphi_n\rangle \left(i\hbar\partial_t - \epsilon_n\right) \langle\varphi_n| \tag{4.13}$$

The Green's function is obtained from Eq. 4.1, which we adapt to the problem at hand.

EQUATION OF MOTION FOR THE GREEN'S FUNCTION OF A SINGLE PARTICLE

$$\left[\hat{1} i\hbar\partial_t - \hat{h}\right] \hat{G}(t,t') = \hat{1}\delta(t-t') \tag{4.14}$$

The boundary condition is $\hat{G}(-\infty, t') = 0$, which implies $\hat{G}(t,t') = 0$ for $t < t'$. This requirement is attributed to **causality**.

Let me work out the Green's function from Eq. 4.14 by introducing eigenstates of the Hamiltonian.

$$\begin{aligned}
&\overbrace{\sum_j |\varphi_j\rangle \left(i\hbar\partial_t - \epsilon_j\right) \langle\varphi_j|}^{=\hat{D}\quad(\text{See Eq. 4.13})} \overbrace{\sum_{n,m} |\varphi_n\rangle G_{n,m}(t,t') \langle\varphi_m|}^{\hat{G}} = \overbrace{\sum_{n,m} |\varphi_n\rangle \delta_{n,m} \langle\varphi_m|}^{\hat{1}} \delta(t-t') \\
\Rightarrow \quad &\sum_{j,n,m} |\varphi_j\rangle \left(i\hbar\partial_t - \epsilon_j\right) \underbrace{\langle\varphi_j|\varphi_n\rangle}_{\delta_{j,n}} G_{n,m}(t,t') \langle\varphi_m| = \sum_{n,m} |\varphi_n\rangle \delta_{n,m} \delta(t-t') \langle\varphi_m| \\
&\Rightarrow \quad \left(i\hbar\partial_t - \epsilon_n\right) G_{n,m}(t,t') = \delta_{n,m}\delta(t-t')
\end{aligned} \tag{4.15}$$

In the last step, I exploited that the eigenstates are linear independent, which implies that each operator cannot be represented by two different sets of matrix elements.

Thus, we arrived at an ordinary differential equation for the matrix elements, namely Eq. 4.15,

[4] Here, we use the bra-ket notation rather than the differential operator.

which has the solution[5]

$$G_{n,m}(t,t') = \frac{1}{i\hbar} e^{-\frac{i}{\hbar}\epsilon_n(t-t')}\theta(t-t')\delta_{n,m} \,. \tag{4.16}$$

where $\theta(t-t')$ is the Heaviside step function. With the matrix elements $G_{n,m}(t,t')$, we can also express the Green's function in the operator form Eq. 4.17 below

GREEN'S FUNCTION OF A SINGLE PARTICLE

$$\hat{G}(t,t') = \frac{1}{i\hbar}\theta(t-t')\sum_n |\varphi_n\rangle e^{-\frac{i}{\hbar}\epsilon_n(t-t')}\langle\varphi_n| = \frac{1}{i\hbar}\theta(t-t')e^{-\frac{i}{\hbar}\hat{h}(t-t')} \tag{4.17}$$

The wave functions $|\varphi_n\rangle$ are eigenstates of the Hamiltonian $\hat{h}$ with eigenvalues ϵ_n, i.e. $\hat{h}|\varphi_n\rangle = |\varphi_n\rangle\epsilon_n$. The states are chosen to be orthonormal,i.e. $\langle\varphi_m|\varphi_n\rangle = \delta_{m,n}$

The Green's function in real-space-and-spin representation is

$$\begin{aligned} G(\vec{x},t,\vec{x'},t') &\overset{\text{def}}{=} \langle\vec{x}|\hat{G}(t,t')|\vec{x'}\rangle = \sum_n \langle\vec{x}|\varphi_n\rangle \frac{1}{i\hbar}\theta(t-t_0)e^{-\frac{i}{\hbar}\epsilon_n(t-t')}\langle\varphi_n|\vec{x'}\rangle \\ &= \frac{1}{i\hbar}\sum_n \varphi_n(\vec{x})\varphi_n^*(\vec{x'})\theta(t-t_0)e^{-\frac{i}{\hbar}\epsilon_n(t-t')} \end{aligned} \tag{4.18}$$

4.2.2 In the energy representation

Because the Hamiltonian is time independent, the problem is time-translationally invariant and the Green's function depends only on the difference of its time arguments, i.e.

$$G(\vec{x},t,\vec{x'},t_0) = G(\vec{x},t-t_0,\vec{x'},0) \tag{4.19}$$

This allows one to Fourier transform the Green's function in the time-difference argument.

$$\begin{aligned} G(\vec{x},\vec{x'},\epsilon) &\overset{\text{def}}{=} \int_{-\infty}^{\infty} dt\; G(\vec{x},t,\vec{x'},0)\; e^{\frac{i}{\hbar}\epsilon t} \\ &\overset{\text{Eq. 4.17}}{=} \frac{1}{i\hbar}\sum_n \varphi_n(\vec{x})\varphi_n^*(\vec{x'}) \int_{-\infty}^{\infty} dt\; \theta(t) e^{-\frac{i}{\hbar}(\epsilon_n-\epsilon)t} \\ &= \frac{1}{i\hbar}\sum_n \varphi_n(\vec{x})\varphi_n^*(\vec{x'}) \int_0^{\infty} dt\; e^{-\frac{i}{\hbar}(\epsilon_n-\epsilon)t} \end{aligned} \tag{4.20}$$

The integral does not converge if we let the upper limit of the integral go to infinity, while ϵ is real-valued. If we consider the energy argument of the Green's function to be a complex number, we

[5] Let us make the test (proof may continue on the next page):

$$\begin{aligned} & [i\hbar\partial_t - \epsilon_n]\frac{1}{i\hbar}e^{-\frac{i}{\hbar}\epsilon_n(t-t')}\theta(t-t')\delta_{n,m} \\ &= \left(\partial_t e^{-\frac{i}{\hbar}\epsilon_n(t-t')}\right)\theta(t-t')\delta_{n,m} + e^{-\frac{i}{\hbar}\epsilon_n(t-t')}\left(\partial_t\theta(t-t')\right)\delta_{n,m} - \frac{1}{i\hbar}\epsilon_n e^{-\frac{i}{\hbar}\epsilon_n(t-t')}\theta(t-t')\delta_{n,m} \\ &= \underbrace{\left(\frac{1}{i\hbar}\epsilon_n e^{-\frac{i}{\hbar}\epsilon_n(t-t')}\right)\theta(t-t')\delta_{n,m}}_{X} + \underbrace{e^{-\frac{i}{\hbar}\epsilon_n(t-t')}}_{=1 \text{ for } t=t'}\left(\delta(t-t')\right)\delta_{n,m} - \underbrace{\frac{1}{i\hbar}\epsilon_n e^{-\frac{i}{\hbar}\epsilon_n(t-t')}\theta(t-t')\delta_{n,m}}_{X} \\ &= \underbrace{\delta(t-t')}_{\partial_t\theta(t-t')}\delta_{n,m} \end{aligned}$$

see that the integral converges only, if the imaginary part of ϵ is positive. If it is real-valued or if it has a negative imaginary part, the result is undefined.

$$\begin{aligned} G(\vec{x},\vec{x'},\epsilon+i\eta) &\overset{\text{Eq. 4.20}}{=} \frac{1}{i\hbar}\sum_n \varphi_n(\vec{x})\varphi_n^*(\vec{x'})\int_0^\infty dt'\; \mathrm{e}^{-\frac{i}{\hbar}(\epsilon_n-\epsilon-i\eta)t'} \\ &= \frac{1}{i\hbar}\sum_n \varphi_n(\vec{x})\varphi_n^*(\vec{x'})\left[\frac{i\hbar}{\epsilon_n-\epsilon-i\eta}\mathrm{e}^{-\frac{i}{\hbar}(\epsilon_n-\epsilon-i\eta)t'}\right]_0^\infty \\ &\overset{\eta\geq 0}{=} \frac{1}{i\hbar}\sum_n \varphi_n(\vec{x})\varphi_n^*(\vec{x'})\frac{-i\hbar}{\epsilon_n-\epsilon-i\eta} \\ &= -\sum_n \frac{\varphi_n(\vec{x})\varphi_n^*(\vec{x'})}{\epsilon_n-\epsilon-i\eta} \\ &= \sum_n \frac{\varphi_n(\vec{x})\varphi_n^*(\vec{x'})}{\epsilon-\epsilon_n+i\eta} \qquad \text{for } \eta>0 \end{aligned} \tag{4.21}$$

Notice the restriction that the imaginary part of $\epsilon+i\eta$ must be positive. The Green's function is only defined in the upper half-plane of the complex plane. While we can evaluate the final expression also in the lower half plane, the Green's function is simply not defined there and the numbers are meaningless.[6]

Thus, we can express the Green's function as

GREEN'S FUNCTION IN THE ENERGY REPRESENTATION

$$\begin{aligned} \hat{G}(\epsilon) &\overset{\text{Eq. 4.21}}{=} \lim_{\eta\to 0^+}\sum_n |\varphi_n\rangle\frac{1}{\epsilon-\epsilon_n+i\eta}\langle\varphi_n| \\ &= \lim_{\eta\to 0^+}\left((\epsilon+i\eta)\hat{1}-\hat{h}\right)^{-1} \end{aligned} \tag{4.22}$$

The notation $\eta\to 0^+$ indicates $\eta>0$.

The imaginary part of the Green's function provides (up to a factor $-1/\pi$) the density of states. A pole of the Green's function contributes a Lorentzian at the real axis, which turns into a delta-function, if the pole approaches the real-ϵ axis.[7]

EQUATION OF MOTION FOR THE SINGLE-PARTICLE GREEN'S FUNCTION IN THE ENERGY REPRESENTATION

The Green's function as function of the energy obeys the equation

$$\left(\epsilon-\hat{h}\right)\hat{G}(\epsilon)=\hat{1} \qquad \text{with } \mathrm{Im}(\epsilon)>0. \tag{4.24}$$

where the energy ϵ is considered as complex variable

[6] The part with $\eta<0$ describes an anti-causal Green's function.

[7]

$$\begin{aligned} \mathrm{Im}\left[\frac{1}{\epsilon-\epsilon_n+i\eta}\right] &= \frac{-\eta}{(\epsilon-\epsilon_n)^2+\eta^2} \\ \int_{-\infty}^{\infty} d\epsilon\;\frac{-\eta}{(\epsilon-\epsilon_n)^2+\eta^2} &= -\int_{-\infty}^{\infty} dx\;\frac{1}{x^2+1} = -\,\mathrm{atan}(x)|_{-\infty}^{\infty} = -\pi \\ \Rightarrow \lim_{\eta\to 0^+}\mathrm{Im}\left[\frac{1}{\epsilon-\epsilon_n+i\eta}\right] &= -\pi\delta(\epsilon-\epsilon_n) \end{aligned} \tag{4.23}$$

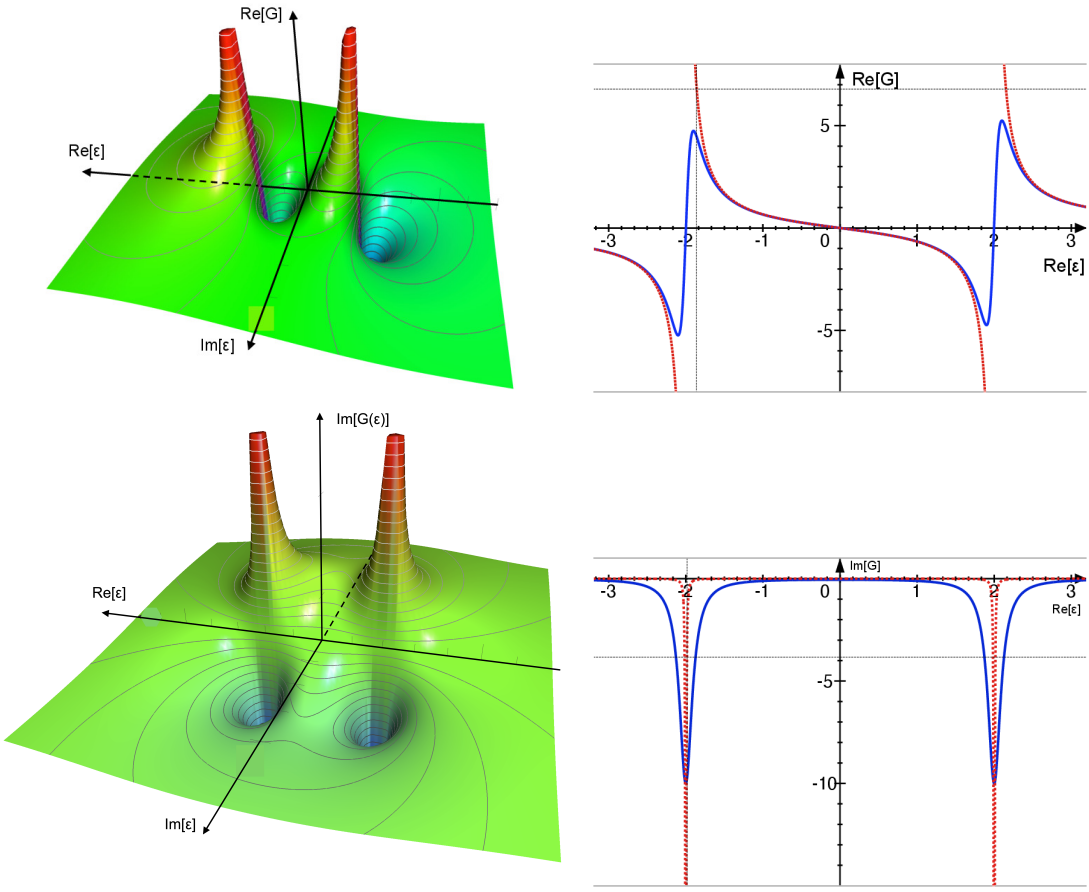


Fig. 4.2: Green's function for a system with two eigenvalues $\epsilon_\pm = \pm 2$ a.u. This example describes one spin component of a non-interacting hydrogen molecule and hopping $t = 2$. Left: Green's function $G(\epsilon)$ in the complex-ϵ plane. Caution: The Re[ϵ]-axis points towards the left and the Im(ϵ)-axis points forward. The energy-dependent Green's function is meaningful only in the half-plane with Im(ϵ) > 0. Right: Green's function $G(\epsilon + i\eta)$ as function of real-valued ϵ with a small, positive η. The full, blue line is with $\eta = 0.1$ while the dashed,red line is for $\eta = 10^{-4}$. Top: real part of $G(\epsilon)$. Bottom: imaginary part.

which can be verified by insertion

$$\left(\epsilon - \hat{h}\right) \hat{G}(\epsilon) = \left(\epsilon - \hat{h}\right) \sum_n |\varphi_n\rangle \frac{1}{\epsilon - \epsilon_n} \langle\varphi_n| = \sum_n |\varphi_n\rangle \frac{\epsilon - \epsilon_n}{\epsilon - \epsilon_n} \langle\varphi_n| = \sum_n |\varphi_n\rangle\langle\varphi_n| = \hat{1} \quad (4.25)$$

Editor: Suggestion: Make already here the contact to level repulsion (Re part of G)

Editor: Suggestion: Make contact to life time η, resulting in peaks with a given width. Explain lifetime from the point of view of an electron on an adsorbed atom. Initial state is not an energy eigenstate, but a superposition of all states from the broad peak. Each contributes with a different frequency, which, over time, results in destructive interference. This destructive interference of the amplitudes on the adsorbed atom forms a decaying exponential.

4.3 Green's function as propagator

There is a very close relationship between the Green's function and the propagator. With these relations we can proceed to Green's functions for time-dependent Hamilton operators.

Below, we will generalize the time to a complex-valued quantity. This is due to an mathematical "trick" to include finite temperature. A wave function will therefore not only be propagated along the real-valued time axis but on a more complicated path in the complex plane. This means that we cannot make use of common properties that, however, hold only on the real-valued time axis. The concept behind that complex-time-contour trick will be explained in detail below.

4.3.1 Definition of the propagator

Let me define the **propagator** [8] $\hat{U}(t,t')$, which transforms an initial state at time t' into a final state at time t according to

$$|\psi(t)\rangle = \hat{U}(t,t')|\psi(t')\rangle \tag{4.26}$$

where $|\psi(t)\rangle$ obeys the time-dependent Schrödinger equation with the Hamiltonian $\hat{h}(t)$.

DEFINING EQUATIONS FOR THE PROPAGATOR

The propagator operator $\hat{U}(t,t')$ obeys the differential equation

$$\Big(i\hbar\partial_t - \hat{h}(t)\Big)\hat{U}(t,t') = \hat{0} \tag{4.27}$$

with the boundary condition

$$\hat{U}(t,t) = \hat{1}\ . \tag{4.28}$$

How can we construct the propagator $\hat{U}(t,t')$? We begin with solving the time-dependent Schrödinger equations for a number of different initial conditions. This yields a set of time-dependent wave functions $|\varphi_n(t)\rangle$ that satisfy the time-dependent Schrödinger equation

$$\Big(i\hbar\partial_t - \hat{h}(t)\Big)|\varphi_n(t)\rangle = 0\ . \tag{4.29}$$

These wave functions need not be eigenstates of the Hamiltonian $\hat{h}(t)$ at any time t.

Because the propagator for equal times $\hat{U}(t,t) = \hat{1}$, let me represent the identity in terms of these solutions of the Schrödinger equation.

$$\hat{1} = \sum_{m,n} |\varphi_m(t)\rangle O^{-1}_{m,n}(t)\langle\varphi_n(t)| \tag{4.30}$$

where $O_{m,n}(t') = \langle\varphi_m(t')|\varphi_n(t')\rangle$ is the time-dependent overlap matrix. I use the notation $O^{-1}_{m,n}(t) = \big(O^{-1}(t)\big)_{m,n}$. While the overlap matrix is time independent on the real-valued time axis, this dies not hold for time contours that move out into the complex plane.

The Schrödinger equation and the initial conditions can simultaneously be satisfied by

$$\hat{U}(t,t_0) = \sum_{m,n} |\varphi_m(t)\rangle O^{-1}_{m,n}(t_0)\langle\varphi_n(t_0)| \tag{4.31}$$

which can be verified by inserting $\hat{U}(t,t_0)|\psi(t_0)\rangle$ with a general wave function $|\psi(t_0)\rangle = \sum_n |\varphi_n(t_0)\rangle c_n$ into the Schrödinger equation and its initial conditions. Notice that the overlap operator is evaluated

[8] in German: Zeitentwicklungsoperator

from the initial state. This apparent asymmetry between initial and final state is OK because the propagator must not be symmetric under interchange of initial and final time arguments.

PROPAGATOR

The propagator can be written in closed form as[a]

$$\hat{U}(t,t') = \sum_m \Big|\varphi_m(t)\Big\rangle \underbrace{\sum_n \Big(\boldsymbol{O}^{-1}(t')\Big)_{m,n} \Big\langle\varphi_n(t')\Big|}_{\langle\pi_m(t')|} \quad \text{with } O_{m,n}(t') = \Big\langle\varphi_m(t')\Big|\varphi_n(t')\Big\rangle \tag{4.32}$$

where each of the states $|\varphi_n(t)\rangle$ obeys the time-dependent Schrödinger equation and where the set $\{|\varphi_n(t')\rangle\}$ spans the complete, but not necessarily orthonormal, one-particle Hilbert space. [b]

[a] It is not a mistake that the expression is not symmetric with respect to exchanging t and t'. For times t, t' on the real axis, the overlap operator is time independent.

[b] On the real time axis, the overlap matrix is time-independent.

$$\begin{aligned}\partial_t O_{m,n}(t) &= \langle\partial_t\varphi_m(t)|\varphi_n(t)\rangle + \langle\varphi_m(t)|\partial_t\varphi_n(t)\rangle = \langle\partial_t\varphi_m(t)|\frac{-1}{i\hbar}\hat{h}^\dagger|\varphi_n(t)\rangle + \langle\varphi_m(t)|\frac{1}{i\hbar}\hat{h}(t)|\varphi_n(t)\rangle \\ &= \frac{1}{i\hbar}\langle\partial_t\varphi_m(t)|(\hat{h}^\dagger - \hat{h})|\varphi_n(t)\rangle = 0\end{aligned} \tag{4.33}$$

From Eq. 4.32, we can immediately extract some properties of $\hat{U}_I(t)$

PROPERTIES OF THE PROPAGATOR

$$\hat{U}(t,t) \overset{\text{Eq. 4.32}}{=} \hat{1} \qquad \text{initial condition} \tag{4.34}$$

$$\hat{U}(t_2,t_3)\hat{U}(t_3,t_1) \overset{\text{Eq. 4.32}}{=} \hat{U}(t_2,t_1) \qquad \text{transitivity} \tag{4.35}$$

$$\hat{U}(t_1,t_2)\hat{U}(t_2,t_1) \overset{Eqs.\ 4.35,4.34}{=} \hat{1} \qquad \text{time inversion} \tag{4.36}$$

$$\hat{U}(t_2,t_1) \overset{\text{Eq. 4.36}}{=} \hat{U}^{-1}(t_1,t_2) \qquad \text{inverse} \tag{4.37}$$

Another property, namely that the propagator is unitary[9] , holds **only for real-valued time arguments**.

$$\hat{U}^\dagger(t_2,t_1) \overset{\text{Eqs. 4.32 4.37}}{=} \hat{U}^{-1}(t_2,t_1) \qquad \text{for } t_1, t_2 \in \mathbb{R}\text{; unitarity} \tag{4.39}$$

Later, we will also use complex-valued time arguments, where they the propagator is no more unitary. Caution is required, because this property is widely used and taken for granted.

[9] For the proof of the unitarity we make use of the form Eq. 4.32 of the propagator together with the fact Eq. 4.33 that the overlap matrix does not change when propagated along the real-valued time axis.

$$\begin{aligned}\hat{U}^\dagger(t,t')\hat{U}(t,t') &= \Big(\sum_{m,n}|\varphi_m(t)\rangle O^{-1}_{m,n}(t')\langle\varphi_n(t')|\Big)^\dagger \sum_{p,q}|\varphi_p(t)\rangle O^{-1}_{p,q}(t')\langle\varphi_q(t')| \\ &= \sum_{m,n}|\varphi_n(t')\rangle O^{-1,*}_{m,n}(t')\langle\varphi_m(t)|\sum_{p,q}|\varphi_p(t)\rangle O^{-1}_{p,q}(t')\langle\varphi_q(t')| \\ &= \sum_{m,n,p,q}|\varphi_n(t')\rangle O^{-1}_{n,m}(t')O_{m,p}(t)O^{-1}_{p,q}(t')\langle\varphi_q(t')| \\ &\overset{\boldsymbol{O}(t)=\boldsymbol{O}(t')}{=} \sum_{m,n,p,q}|\varphi_n(t')\rangle O^{-1}_{n,q}(t')\langle\varphi_q(t')| = \hat{1} \qquad \Rightarrow \quad \hat{U}^\dagger(t,t') = \hat{U}^{-1}(t,t') \quad \text{q.e.d}\end{aligned} \tag{4.38}$$

4.3.2 Relation between Green's function and propagator

GREEN'S FUNCTION AND PROPAGATOR

The Green's function can be expressed by the propagator $\hat{U}$ as

$$\hat{G}(t,t') = \frac{1}{i\hbar}\theta(t-t')\hat{U}(t,t') \tag{4.40}$$

where $\theta(x)$ is the Heaviside step function.
In return, the propagator can be extracted from the Green's function

$$U(t,t') = i\hbar G(t,t') \qquad \text{for } t > t' \tag{4.41}$$

The propagator going backward in time must be recovered using $U(t',t) \overset{\text{Eq. 4.37}}{=} U^{-1}(t,t')$. On the real-valued time axis, the propagator is unitary, and the inverse is equal to the hermitean conjugate.

The relation is proven by inserting ansatz Eq. 4.40 into the equation of motion Eq. 4.14 of the Green's function. Note that the derivative of the Heaviside step function is the delta function.

$$\begin{aligned}\Big(i\hbar\partial_t - \hat{h}(t)\Big)\hat{G}(t,t') &\overset{\text{Eq. 4.40}}{=} \Big(i\hbar\partial_t - \hat{h}(t)\Big)\underbrace{\frac{1}{i\hbar}\theta(t-t')\hat{U}(t,t')}_{\hat{G}(t,t')} \\ &= \underbrace{\Big(i\hbar\partial_t \frac{1}{i\hbar}\theta(t-t')\Big)}_{\delta(t-t')}\hat{U}(t,t') + \frac{1}{i\hbar}\theta(t-t')\underbrace{\Big(i\hbar\partial_t - \hat{h}(t)\Big)\hat{U}(t,t')}_{=0 \quad \text{(Eq. 4.27)}} \\ &\overset{\text{Eq. 4.27}}{=} \underbrace{\hat{U}(t,t')}_{=\hat{1} \quad \text{for } t=t'}\delta(t-t') \overset{\text{Eq. 4.34}}{=} \hat{1}\delta(t-t')\end{aligned} \tag{4.42}$$

The comparison with the equation of motion Eq. 4.14 of the Green's function completes the proof of Eq. 4.40.

4.3.3 Propagator as time-ordered exponential

Evaluating the propagator using Eq. 4.32 requires the knowledge of the wave functions at all times. This is of little practical value. Here, I will derive an expression that refers to the Hamiltonian, namely

PROPAGATOR AS TIME-ORDERED EXPONENTIAL

$$\hat{U}(t_2,t_1) = \mathcal{T}_{\mathcal{D}} \exp\left(-\frac{i}{\hbar}\int_{t_1}^{t_2} dt'\ \hat{h}(t')\right) \tag{4.43}$$

where $\mathcal{T}_D$ is Dyson's time-ordering operator defined below. [a]

[a] Compare with Eq. 31 of[63]

Consider the propagation of a wave function with a time-dependent Hamiltonian.

$$\Big[i\hbar\partial_t\hat{1} - \hat{h}(t)\Big]|\psi(t)\rangle = 0 \tag{4.44}$$

Let me build up an iterative equation, by replacing the derivative by its differential quotient.

$$\begin{aligned}
\frac{|\psi(t+\Delta)\rangle - |\psi(t)\rangle}{\Delta} &= -\frac{i}{\hbar}\hat{h}(t)|\psi(t)\rangle + O(\Delta) \\
\Rightarrow \qquad |\psi(t+\Delta)\rangle &= |\psi(t)\rangle - \frac{i}{\hbar}\hat{h}(t)|\psi(t)\rangle\Delta + O(\Delta^2) \\
&= \Big(\hat{1} - \frac{i}{\hbar}\hat{h}(t)\Delta\Big)|\psi(t)\rangle + O(\Delta^2) \\
&= \exp\Big(-\frac{i}{\hbar}\hat{h}(t)\Delta\Big)|\psi(t)\rangle + O(\Delta^2) \\
\Rightarrow \qquad |\psi(t)\rangle &= \underbrace{\lim_{\Delta\to 0}\left[\prod_{N-1}^{j=0}\exp\Big(-\frac{i}{\hbar}\hat{h}(t_j)\Delta\Big)\right]}_{\hat{U}(t,0)}|\psi(0)\rangle
\end{aligned} \tag{4.45}$$

where $t_j = j\Delta$ and $\Delta = t/N$.

I have introduced the product sign with the reversed positions of initial and final value of the running index to indicate that the terms are arranged in the opposite order than normal, namely

$$\prod_{j=0}^{N} X_j \stackrel{\text{def}}{=} X_1 X_2 \cdots X_N \qquad \text{and} \qquad \prod_{N}^{j=0} X_j \stackrel{\text{def}}{=} X_N X_{N-1} \cdots X_1 \tag{4.46}$$

Now comes the difficult point: It is desirable to combine the exponentials of Eq. 4.45 in a single exponential of an integral. For this purpose, I need the rule $\mathrm{e}^a\mathrm{e}^b = \mathrm{e}^{a+b}$. This rule is valid for numbers, but not for operators that do not commutate. The reason is that a and b occur in different orders for the left-hand and the right-hand side. For the left-hand side

$$\mathrm{e}^a\mathrm{e}^b = \left(\sum_{n=0}^{\infty}\frac{1}{n!}a^n\right)\left(\sum_{m=0}^{\infty}\frac{1}{m!}b^m\right) \tag{4.47}$$

the terms a are always left of the terms b. For the right-hand side

$$\mathrm{e}^{a+b} = \sum_{n=0}^{\infty}\frac{1}{n!}(a+b)^n \tag{4.48}$$

the terms a and b are in a different order.

This problem that $\mathrm{e}^{\hat{a}+\hat{b}}$ differs from $\mathrm{e}^{\hat{a}}\mathrm{e}^{\hat{b}}$ for non-commutating operators $\hat{a}$ and $\hat{b}$, is solved by a simple trick: We simply define a recipe $\mathcal{T}_{ab}$ that places the $\hat{a}$ terms in every product of the expansion of $\mathrm{e}^{\hat{a}+\hat{b}}$ in front of the $\hat{b}$ terms. This leads to the identity

$$\mathrm{e}^{\hat{a}}\mathrm{e}^{\hat{b}} = \mathcal{T}_{ab}\mathrm{e}^{\hat{a}+\hat{b}} \tag{4.49}$$

For the problem at hand, we need a recipe that arranges the Hamiltonians $h(t_j)$ in ascending order from right to left. This recipe is Dyson's time-ordering operator.

DYSON'S TIME-ORDERING OPERATOR

Dyson's time-ordering operator rearranges the operators in a product $\prod_j \hat{A}_j(t_j)$ such that they appear in increasing order from right to left.
Dyson's time-ordering operator $\mathcal{T}_D$ (named P-product in Eq. 29 of [63]) is

$$\begin{aligned}\mathcal{T}_D\hat{A}(t)\hat{B}(t') &= \begin{cases}\hat{A}(t)\hat{B}(t') & \text{for } t \geq t' \\ \hat{B}(t')\hat{A}(t) & \text{for } t < t'\end{cases} \\ &= \theta(t-t')\hat{A}(t)\hat{B}(t') + \theta(t'-t)\hat{B}(t')\hat{A}(t) \end{aligned} \tag{4.50}$$

$\theta(x)$ is Heaviside's step function. The time-ordering operator is not an operator in the conventional sense: Namely, it does not act on states in the Hilbert or Fock space to map them onto other states. Rather, it is a prescription for manipulating a mathematical expression.

Later, we will learn about another time-ordering operator, namely **Wick's time-ordering operator**[64] . Wick's time-ordering operator is similar to Dyson's time-ordering operator, but it introduces a sign change for every interchange of fermionic operators.

With the time-ordering operator, the propagator can be expressed as

$$\begin{aligned}\hat{U}(t,0) &\overset{\text{Eq. 4.45}}{=} \lim_{\Delta\to 0}\left[\prod_{N-1}^{j=0}\exp\Big(-\frac{i}{\hbar}\hat{h}(t_j)\Delta\Big)\right] \\ &= \mathcal{T}_D \lim_{\Delta\to 0}\left[\prod_{N-1}^{j=0}\exp\Big(-\frac{i}{\hbar}\hat{h}(t_j)\Delta\Big)\right] \\ &= \mathcal{T}_D \lim_{\Delta\to 0}\left[\exp\Big(-\frac{i}{\hbar}\sum_{j=0}^{N}\hat{h}(t_j)\Delta\Big)\right] \\ &= \mathcal{T}_D \exp\left(-\frac{i}{\hbar}\int_0^t dt\ \hat{h}(t)\right)\end{aligned} \tag{4.51}$$

With this, we arrived at the desired form Eq. 4.43 for the propagator as a time-ordered exponential.

Finally, we can express the Green's function in terms of a time-ordered exponential

GREEN'S FUNCTION AND TIME-ORDERED EXPONENTIAL

$$\hat{G}(t_2,t_1) \overset{\text{Eq. 4.40}}{=} \frac{1}{i\hbar}\theta(t_2-t_1)\mathcal{T}_D \exp\left(-\frac{i}{\hbar}\int_{t_1}^{t_2} dt'\ \hat{h}(t')\right) \tag{4.52}$$

For this expression to be meaningful, the operator in the integral must have a time attribute. Without a time attribute, the time-ordering operator does not know what to do. The time attribute has therefore two functions: (1) it defines the operator to be inserted into the expression. (2) It furthermore directs the time ordering operaor to arrange the operators in the desired order.

4.4 Density of States

So far, the Green's function is still a fairly abstract object. Let us therefore show a few physical quantities that can be obtained from the Green's function. With the density of states $\hat{D}(\epsilon)$, we gain access to the excitation spectrum of the Hamiltonian.

On the one hand, the projected **density of states** is an extremely useful quantity which can be obtained from the Green's function. On the other hand, the Green's function can be obtained from

a known density of states $D(\epsilon)$.

The density of states has been defined discussed extensively in ΦSX: Introduction to solid-state theory.[1][10]. The role of the density of states will be taken over by the **spectral function**, when we deal with interacting electron systems.

4.4.1 Density of states from the Green's function

PROJECTED DENSITY OF STATES

For a system with time-translation symmetry, the Green's function provides us with the **density of states**

$$\hat{D}(\epsilon) = \underbrace{\sum_n |\varphi_n\rangle\delta(\epsilon-\epsilon_n)\langle\varphi_n|}_{\sum_{\alpha,\beta}|\chi_\alpha\rangle D_{\alpha,\beta}(\epsilon)\langle\chi_\beta|} = -\frac{1}{2\pi i}\lim_{\eta\to 0^+}\left(\hat{G}(\epsilon+i\eta)-\hat{G}^\dagger(\epsilon+i\eta)\right). \tag{4.53}$$

This result follows[a] from the better known equation for the density of states projected onto a state $|\psi\rangle$, namely

$$D_\psi(\epsilon) = \sum_n \langle\psi|\varphi_n\rangle\delta(\epsilon-\epsilon_n)\langle\varphi_n|\psi\rangle \overset{\text{Eq. 4.22}}{=} -\frac{1}{\pi}\lim_{\eta\to 0^+}\mathrm{Im}[\langle\psi|\hat{G}(\epsilon+i\eta)|\psi\rangle] \tag{4.54}$$

[a] Eq. 4.53 follows from Eq. 4.54, because two operators are identical, when all conceivable expectation values are identical.

Proof of Eq. 4.54 In appendix A.6 on p. 504, we show that the imaginary part of a pole in the complex plane is a Lorentzian[11] and that the Lorentzian turns into a delta function when the pole approaches the real axis, that is

$$\lim_{\eta\to 0^+}\mathrm{Im}\left(-\frac{1}{\pi}\frac{1}{x+i\eta}\right) = \delta(x)\,. \tag{4.56}$$

This will be required in the following.

Let me begin the proof with the right-hand side of Eq. 4.54.

$$\begin{aligned}
-\frac{1}{\pi}\lim_{\eta\to 0^+}\mathrm{Im}\left(\langle\psi|\hat{G}(\epsilon+i\eta)|\psi\rangle\right) &\overset{\text{Eq. 4.22}}{=} -\frac{1}{\pi}\lim_{\eta\to 0^+}\mathrm{Im}\left(\sum_n\langle\psi|\varphi_n\rangle\frac{1}{\epsilon-\epsilon_n+i\eta}\langle\varphi_n|\psi\rangle\right)\\
&\overset{\langle\psi|\varphi_n\rangle\langle\varphi_n|\psi\rangle\in\mathbb{R}}{=} \sum_n\langle\psi|\varphi_n\rangle\left\{-\frac{1}{\pi}\lim_{\eta\to 0^+}\mathrm{Im}\left(\frac{1}{\epsilon-\epsilon_n+i\eta}\right)\right\}\langle\varphi_n|\psi\rangle\\
&\overset{\text{Eq. 4.56}}{=} \sum_n\langle\psi|\varphi_n\rangle\delta(\epsilon-\epsilon_n)\langle\varphi_n|\psi\rangle = \langle\psi|\hat{D}(\epsilon)|\psi\rangle \qquad \text{q.e.d.}
\end{aligned} \tag{4.57}$$

Thus, we arrived at the expression for the density of states projected onto the orbital $|\psi\rangle$. This concludes the proof of Eq. 4.54.

[10] The density of states is defined in Eq. **??** of ΦSX: Introduction to solid-state physics. The projected density of states is defined in Eq. **??** therein.

[11] A Lorentzian is a function of the form

$$L_{\bar{\epsilon},\Gamma}(\epsilon) = \frac{1}{\pi}\frac{\frac{1}{2}\Gamma}{(\epsilon-\bar{\epsilon})^2+(\frac{1}{2}\Gamma)^2} \tag{4.55}$$

The function is normalized and has a peak at position $\bar{\epsilon}$ of width Γ. It is the prototypical spectral line shape. Editor: The definition here is consistent with https://mathworld.wolfram.com/LorentzianFunction.html. It differs from the definition in Eq. A.27 on p. 504 by a factor 2 in the width parameter.

Proof of Eq. 4.53 From Eq. 4.54 proven just before, we obtain

$$\begin{aligned}\langle\psi|\hat{D}(\epsilon)|\psi\rangle &= \sum_n \langle\psi|\varphi_n\rangle\delta(\epsilon-\epsilon_n)\langle\varphi_n|\psi\rangle \overset{\text{Eq. 4.54}}{=} -\frac{1}{\pi}\lim_{\eta\to 0^+}\mathrm{Im}[\langle\psi|\hat{G}(\epsilon+i\eta)|\psi\rangle] \\ &= -\frac{1}{\pi}\lim_{\eta\to 0^+}\frac{\langle\psi|\hat{G}(\epsilon+i\eta)|\psi\rangle - \langle\psi|\hat{G}(\epsilon+i\eta)|\psi\rangle^*}{2i} \\ &= \left\langle\psi\middle|\left\{-\frac{1}{\pi}\lim_{\eta\to 0^+}\frac{\hat{G}(\epsilon+i\eta)-\hat{G}^\dagger(\epsilon+i\eta)}{2i}\right\}\middle|\psi\right\rangle \end{aligned} \tag{4.58}$$

The equation above holds for any state $|\psi\rangle$. Now, I exploit that if an identity holds for arbitrary expectation values, then also the underlying operator identity holds.

This

$$\hat{D}(\epsilon) = \sum_n |\varphi_n\rangle\delta(\epsilon-\epsilon_n)\langle\varphi_n| = -\frac{1}{2\pi i}\lim_{\eta\to 0^+}\left(\hat{G}(\epsilon+i\eta)-\hat{G}^\dagger(\epsilon+i\eta)\right). \tag{4.59}$$

which proves Eq. 4.53.

4.4.2 Total density of states

The total density of states[12] can be obtained

$$\begin{aligned} D_{\text{tot}}(\epsilon) &\overset{\text{def}}{=} \sum_n \delta(\epsilon-\epsilon_n) \\ &= \sum_n \int d^4x\ \langle\vec{x}|\varphi_n\rangle\delta(\epsilon-\epsilon_n)\langle\varphi_n|\vec{x}\rangle \\ &\overset{\text{Eq. 4.54}}{=} -\frac{1}{\pi}\mathrm{Im}\left[\int d^4x\ \langle\vec{x}|\hat{G}(\epsilon+i\eta)|\vec{x}\rangle\right] \\ &= -\frac{1}{\pi}\lim_{\eta\to 0^+}\mathrm{Im}\Big(\mathrm{Tr}[\hat{G}(\epsilon+i\eta)]\Big) \end{aligned} \tag{4.60}$$

4.4.3 Electron density

Integration over the occupied states provides us with the probability that an electron is in a given orbital. The orbital $|\psi\rangle$ could also be $|\vec{x}\rangle$, in which case we obtain the electron density.

$$\begin{aligned} n(\vec{r}) &= \sum_\sigma\sum_n \int_{-\infty}^{\infty} d\epsilon\ f_{T,\mu}(\epsilon)\langle\vec{r},\sigma|\varphi_n\rangle\delta(\epsilon-\epsilon_n)\langle\varphi_n|\vec{r},\sigma\rangle \\ &= -\frac{1}{\pi}\sum_\sigma\int_{-\infty}^{\infty} d\epsilon\ f_{T,\mu}(\epsilon)\mathrm{Im}\left(\langle\vec{r},\sigma|\hat{G}(\epsilon)|\vec{r},\sigma\rangle\right) \end{aligned} \tag{4.61}$$

The equation considers thermal equilibrium with the Fermi distribution $f_{T,\mu}(\epsilon) = \left(1+\mathrm{e}^{\beta(\epsilon-\mu)}\right)^{-1}$

4.4.4 Green's function from the density of states

The density of states can be defined as an energy-dependent operator

$$\hat{D}(\epsilon) = \sum_n |\varphi_n\rangle\delta(\epsilon-\epsilon_n)\langle\varphi_n| \tag{4.62}$$

[12] The total density of states is defined in Eq. **??** of ΦSX: Introduction to solid-state physics[1]

where $|\varphi_n\rangle$ and ϵ_n are eigenstates and eigenvalues of the Hamiltonian.

Because the Green's function is itself a sum over the states of the system, we can represent the Green's function in terms of the density of states. This implies that we should be able to work with the density of states or the spectral function as the fundamental quantity, from which the Green's function is constructed in the desired form when it is required.

GREEN'S FUNCTION FROM THE DENSITY OF STATES

With the density of states Eq. 4.62 the one-particle Green's function is

$$\hat{G}(t,t') \overset{\text{Eq. 4.17}}{=} \frac{1}{i\hbar}\int d\epsilon\, \hat{D}(\epsilon)\,\theta(t-t')\mathrm{e}^{-\frac{i}{\hbar}\epsilon(t-t')}$$
$$\hat{G}(\epsilon+i\eta) \overset{\text{Eq. 4.22}}{=} \int d\epsilon'\, \frac{\hat{D}(\epsilon')}{\epsilon-\epsilon'+i\eta} \tag{4.63}$$

4.5 Summary

- The Green's function is the inverse of a differential operator:
- The propagator can be constructed from the Green's function and vice versa.
- The spectral function (Density of States) can be constructed from the Green's function and vice versa.

For an introduction to Greens function and few simple examples, see "The pedagogical introduction to equilibrium Green's function" by Odashima et al.[65].

4.6 Home study and practice

4.6.1 Role of boundary conditions

Editor: This needs to be done: show in an exercise why and how boundary conditions for Green's functions are considered

4.6.2 Green's function for a Lorentzian-shaped density of states

Introduction

The band structure $\bar{\epsilon}_n(\vec{k})$ of a solid describes the position of the poles of the Green's function. For a non-interacting system, the poles of the Green's function lie on the real axis. For every k-point, the k-resolved density of states, respectively the spectral function $\mathcal{A}(\epsilon, \vec{k})$, is a sequence of delta-peaks at the corresponding one-particle energies $\bar{\epsilon}_n(\vec{k})$.

$$\mathcal{A}(\epsilon, \vec{k}) = \sum_n \Omega \int \frac{d^3k}{(2\pi)^3} \delta(\epsilon - \bar{\epsilon}_n(\vec{k})) \tag{4.64}$$

As the interaction between the electrons is switched on, the electrons scatter at other electrons. As a result neither the energy nor the crystal momentum of the electron is a conserved quantity any more. A scattering process is described by annihilating the electron and by creating it again with a new energy and momentum. This implies that the electrons obtain a finite life time. The finite life time $\tau = \hbar/\Gamma(\vec{k})$ results in a broadening of the band structure. The poles of the Green's function move away from the real energy axis into the complex plane and the delta-peaks of the spectral functions turn into Lorentzians.

$$\mathcal{A}(\epsilon, \vec{k}) = \sum_n \Omega \int \frac{d^3k}{(2\pi)^3} \frac{1}{\pi} \frac{\Gamma_n(\vec{k})}{(\epsilon - \bar{\epsilon}_n(\vec{k}))^2 + \Gamma_n^2(k)} \tag{4.65}$$

As a result, each band obtains a width inversely proportional to its life time. Note, that the description via single poles breaks down, when the interaction become sufficiently strong.

The occurrence of finite life times and the corresponding broadening of spectral densities is a general feature of systems coupled to a continuous spectrum of states. In this exercise, we will explore a single state with finite life time.

Problem

Exercise: A very general observation is that a finite line width of an absorption or emission band is related to a finite life time of an excitation. The prototypical shape of a band with a finite line width is a Lorentzian. Here, we determine the corresponding Green's function.
A Lorentzian shaped density of states has the form

$$\langle\pi|\hat{D}(\epsilon)|\pi\rangle = \frac{1}{\pi}\frac{\Gamma}{(\epsilon-\bar{\epsilon})^2+\Gamma^2} \tag{4.66}$$

The density of states is normalized so that its weight integrated to one. The peak is centered at energy $\bar{\epsilon}$, and it has a **full-width-at-half-maximum** (**FWHM**)[a] of 2Γ.
The Green's function for the Lorentzian-shaped density of states has a surprisingly simple form of a single damped oscillation.

$$\langle\pi|\hat{G}(t,t')|\pi\rangle = \frac{1}{i\hbar}\theta(t-t')\mathrm{e}^{-\frac{i}{\hbar}(\bar{\epsilon}-i\Gamma)(t-t')} \tag{4.67}$$

This result can be represented by a single pole in the complex plane at $\epsilon = \bar{\epsilon} - i\Gamma$.
Problem:

1. Derive Eq. 4.67 from Eq. 4.66. (Hint: I used residue theorem.)
2. determine the Green's function in energy representation.

[a] The german expression for FWHM is *"Halbwertsbreite"*.

Discussion

1. Derive Eq. 4.67 from Eq. 4.66. (Hint: I used residue theorem.)

$$\begin{aligned}
\langle\pi|G(t,t')|\pi\rangle &\overset{\text{Eq. ??}}{=} \frac{1}{i\hbar}\int d\epsilon\ \langle\pi|\hat{D}(\epsilon)|\pi\rangle\ \theta(t-t')\mathrm{e}^{-\frac{i}{\hbar}\epsilon(t-t')} \\
&\overset{\text{Eq. 4.66}}{=} \frac{1}{i\hbar}\int_{-\infty}^{\infty} d\epsilon\ \frac{1}{\pi}\frac{\Gamma}{(\epsilon-\bar{\epsilon})^2+\Gamma^2}\theta(t-t')\mathrm{e}^{-\frac{i}{\hbar}\epsilon(t-t')} \\
&= \theta(t-t')\frac{\Gamma}{i\pi\hbar}\int_{-\infty}^{\infty} d\epsilon\ \frac{1}{(\epsilon-\bar{\epsilon}+i\Gamma)(\epsilon-\bar{\epsilon}-i\Gamma)}\mathrm{e}^{-\frac{i}{\hbar}\epsilon(t-t')}
\end{aligned} \tag{4.68}$$

These integrals can be solved with the **residue theorem**:

RESIDUE THEOREM

When $f(z)$ is holomorphic in the region Ω of the complex plane, i.e. $\frac{\partial f}{\partial z^*} = 0$, with the exception of discrete points, the counterclockwise integral about the boundary $\partial\Omega$ of Ω can be mapped to the sum of the residues of the poles in Ω.

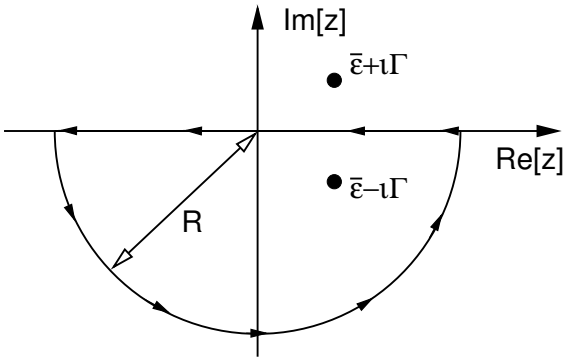
$$\oint_{\partial\Omega} f(z) = 2\pi i \sum_j \mathrm{Res}_{z_j}[f] \tag{4.69}$$

The residual for a simple pole is $\mathrm{Res}_{z_j}[f] = \lim_{z\to z_j}(z-z_j)f(z)$.

The function $f(\epsilon) = \frac{1}{(\epsilon-\bar{\epsilon}+i\Gamma)(\epsilon-\bar{\epsilon}-i\Gamma)} e^{-\frac{i}{\hbar}\epsilon(t-t')}$ has two poles at $\epsilon = \bar{\epsilon} \mp \Gamma$. The residuals are

$$\begin{aligned} \mathrm{Res}_{\bar{\epsilon}+i\Gamma}[f] &= \frac{1}{2i\Gamma} e^{-\frac{i}{\hbar}(\bar{\epsilon}+i\Gamma)(t-t')} \\ \mathrm{Res}_{\bar{\epsilon}-i\Gamma}[f] &= \frac{-1}{2i\Gamma} e^{-\frac{i}{\hbar}(\bar{\epsilon}-i\Gamma)(t-t')} \end{aligned} \tag{4.70}$$

The exponential function $e^{-\frac{i}{\hbar}\epsilon(t-t')}$ damps out the function for $\mathrm{Im}(\epsilon) \to -\infty$. Therefore, we choose a contour for the residual theorem, that proceeds along the real axis from $+R+\bar{\epsilon}$ to $-R+\bar{\epsilon}$ and closes via a half-circle passing through $-iR+\bar{\epsilon}$.



1. In the limit $R \to \infty$, the integral of the half circle goes to zero. This is because the function values fall off like $\frac{1}{R^2}$, while the length of the half-circle expands like πR. I describe the half-circle as $r(s) = \bar{\epsilon} + R\, e^{is} = \bar{\epsilon} + R\, \cos(s) + iR\, \sin(s)$

$$\left| \int_0^\pi ds\, \frac{dr}{ds} f(r(s)) \right| = \left| \int_0^\pi ds\, iR\, e^{is} \underbrace{\frac{1}{|r(s)-\bar{\epsilon}+i\Gamma|^2}}_{1/\left|Re^{is}+i\Gamma|^2\right|^2} \underbrace{e^{-\frac{i}{\hbar}r(s)(t-t')}}_{\left|e^{-\frac{i}{\hbar}r(s)(t-t')}\right| \leq 1 \text{ for } \mathrm{Im}(r(s))<0} \right| \tag{4.71}$$

$$\leq \left| \int_0^\pi ds\, iR\, e^{is}\, \frac{1}{R^2} \right| < \frac{\pi}{R} \to 0 \text{ for } R \to \infty \tag{4.72}$$

2. The integral along the closed contour is

$$\int_\gamma d\epsilon\, f(z) = 2\pi i \mathrm{Res}_{\bar{\epsilon}-i\Gamma}[f] = \frac{-\pi}{\Gamma} e^{-\frac{i}{\hbar}(\bar{\epsilon}-i\Gamma)(t-t')} \tag{4.73}$$

3. Thus, the integral along the real axis in the positive direction is

$$\int_{-\infty}^{\infty} d\epsilon\, f(\epsilon) = \frac{\pi}{\Gamma} e^{-\frac{i}{\hbar}(\bar{\epsilon}-i\Gamma)(t-t')} \tag{4.74}$$

Combining this result with the prefactors, I obtain

$$\begin{aligned} \langle \pi | \hat{G}(t,t') | \pi \rangle &= \theta(t-t') \frac{\Gamma}{i\pi\hbar} \int_{-\infty}^{\infty} d\epsilon\, \frac{1}{(\epsilon-\bar{\epsilon}+i\Gamma)(\epsilon-\bar{\epsilon}-i\Gamma)} e^{-\frac{i}{\hbar}\epsilon(t-t')} \\ &= \theta(t-t') \frac{\Gamma}{i\pi\hbar} \frac{\pi}{\Gamma} e^{-\frac{i}{\hbar}(\bar{\epsilon}-i\Gamma)(t-t')} \\ &= \frac{1}{i\hbar} \theta(t-t') e^{-\frac{i}{\hbar}(\bar{\epsilon}-i\Gamma)(t-t')} \end{aligned} \tag{4.75}$$

2. determine the Green's function in energy representation.

The energy representation is obtained via Eq. 4.63. Simpler is, however, the direct backward Fourier

transform of the Green's function from the time representation.

$$\begin{aligned} G(\epsilon) &= \int dt\; G(t,0) \mathrm{e}^{\frac{i}{\hbar}\epsilon t} \\ &= \int_{-\infty}^{\infty} dt \frac{1}{i\hbar} \theta(t) \mathrm{e}^{-\frac{i}{\hbar}(\bar{\epsilon}-i\Gamma)t} \mathrm{e}^{\frac{i}{\hbar}\epsilon t} \\ &= \int_{0}^{\infty} dt\; \frac{1}{i\hbar} \mathrm{e}^{-\frac{i}{\hbar}(\bar{\epsilon}-\epsilon-i\Gamma)t} \\ &= \frac{1}{i\hbar}\; \frac{\mathrm{e}^{-\frac{i}{\hbar}(\bar{\epsilon}-\epsilon-i\Gamma)t}}{-\frac{i}{\hbar}(\bar{\epsilon}-\epsilon-i\Gamma)} \Bigg|_0^{\infty} \\ &= \frac{1}{\epsilon - \bar{\epsilon} + i\Gamma} \end{aligned} \tag{4.76}$$

Thus, the Green's function has a single pole in the complex plane. The pole is displaced from the real energy axis by Γ.

Observations

1. Interesting is that such a complicated density of states such as a Lorentzian yields a simple result, namely a single harmonic contribution.
2. the Green's function falls off exponentially with time. It seems that a perturbation of the system dies out after a certain while, when it is characterized by Lorentzian peaks in the density of states.
3. The Lorentzian shaped density of states has infinite energy moments $\int d\epsilon\; D(\epsilon)(\epsilon - \bar{\epsilon})^n$ with $n \geq 2$. Editor: Discuss problems and how to cope with it.
4. Editor: Is the dynamics still unitary? This question requires the link to the propagator to be established.

Chapter 5

Composite and open systems: down-folding and retarded potentials

Deep down, the purpose of a Green's function is to describe the influence of one subsystem onto another or to describe the influence of an environment onto the system of interest. In many-particle physics, the environment is an electron gas, which affects the motion of electrons and holes in a solid. Let me therefore describe how the Green's function enters the description of open systems.

Consider a composite system consisting of two subsystems.

Examples:

- A molecule A adsorbed to a surface B. We can investigate the broadening of the molecular levels, and thus the spectroscopic properties of the adsorbed molecule.
- A material consisting of two spatially separated materials A and B with an interface in between.
- A traveling electron A that interacts with a phonon B. We may want to understand the transport properties of the electron in the presence of the phonon, which may act as an elastic or inelastic scattering center.
- A open system A in contact with an environment B, called a bath. This problem allows one to investigate questions such as decoherence, dephasing, loss of information.

The coupling may however be also more general: We may consider a finite set of one-particle orbitals to describe main features of a system. The subset of Fock space spanned by Slater determinants from these orbitals is system A. The one-particle orbitals orthogonal to those of subsystem A are used to define system B. The impact of the subsystem B can be incorporated into the description of system A just as an environment can be considered in a physical subsystem.

5.1 Systems in contact: down-folding

Let us consider a Hilbert space, which is divided into an important subspace $A = \{|\chi_\alpha^A\rangle\}$ and an unimportant subspace $B = \{|\chi_\alpha^B\rangle\}$. The subspace A may describe the system of interest, while the system B may describe the **environment**. The latter is often also called the **bath**.

We consider non-interacting electrons and a time-independent Hamiltonian. Furthermore, let me limit the discussion to orthonormal basissets $\{|\chi_\alpha\rangle\}$.

A one-particle wave function of the complete system is a superposition of the one-particle basis states of the system A of interest and the bath B.

$$|\psi\rangle = \sum_{\alpha\in A} |\chi^A_\alpha\rangle c^A_\alpha + \sum_{\beta\in B} |\chi^B_\beta\rangle c^B_\beta \tag{5.1}$$

The stationary Schrödinger equation has the form[1]

$$\begin{pmatrix} \boldsymbol{H}^{AA} - \epsilon \mathbf{1}^{AA} & \boldsymbol{V}^{AB} \\ \boldsymbol{V}^{BA} & \boldsymbol{H}^{BB} - \epsilon \mathbf{1}^{BB} \end{pmatrix} \begin{pmatrix} \vec{c}^A \\ \vec{c}^B \end{pmatrix} = 0 \tag{5.3}$$

with the norm

$$|\vec{c}^A|^2 + |\vec{c}^B|^2 = 1 \tag{5.4}$$

for an orthonormal basisset.

The Hamilton matrix elements are

$$\begin{aligned} H^{AA}_{\alpha,\beta} &= \langle \chi^A_\alpha | \hat{H} | \chi^A_\beta \rangle && \text{with } \alpha,\beta \in A \\ H^{BB}_{\alpha,\beta} &= \langle \chi^B_\alpha | \hat{H} | \chi^B_\beta \rangle && \text{with } \alpha,\beta \in B \\ V^{AB}_{\alpha,\beta} &= \langle \chi^A_\alpha | \hat{H} | \chi^B_\beta \rangle && \text{with } \alpha \in A,\ \beta \in B \\ V^{BA}_{\alpha,\beta} &= \langle \chi^B_\alpha | \hat{H} | \chi^A_\beta \rangle = \left(V^{A,B}_{\beta,\alpha}\right)^* && \text{with } \alpha \in B,\ \beta \in A \end{aligned} \tag{5.5}$$

The matrices $\mathbf{1}^{AA}$, $\mathbf{1}^{BB}$, $\mathbf{0}^{AB}$, and $\mathbf{0}^{BA}$ are the unit and zero-matrices in the respective subspaces.

Down-folding: From the second line of the Schrödinger equation Eq. 5.3, we obtain a relation that links $\vec{c}_B$ to $\vec{c}_A$.

$$\begin{aligned} &\boldsymbol{V}^{BA}\vec{c}^A + (\boldsymbol{H}^{BB} - \epsilon \mathbf{1}^{BB})\vec{c}^B = 0 \\ &\qquad\Rightarrow \qquad \vec{c}^B = (\epsilon \mathbf{1}^{BB} - \boldsymbol{H}^{BB})^{-1} \boldsymbol{V}^{BA}\vec{c}^A \overset{\text{Eq. 4.24}}{=} \bar{\boldsymbol{G}}^{BB}(\epsilon)\boldsymbol{V}^{BA}\vec{c}^A \end{aligned} \tag{5.6}$$

where

$$\bar{\boldsymbol{G}}^{BB}(\epsilon) \overset{\text{def}}{=} (\epsilon \mathbf{1}^{BB} - \boldsymbol{H}^{BB})^{-1} \tag{5.7}$$

is the Green's function of the isolated bath, i.e. of system B. The bar on-top of the symbol for the **bath Green's function** distinguishes it from the BB matrix elements of the Green's function for the entire system.

---

[1]

$$\left(\begin{array}{cccc|ccc} H^{AA}_{1,1}-\epsilon & H^{AA}_{1,2} & \dots & H^{AA}_{1,M} & V^{AB}_{1,1} & \dots & V^{AB}_{1,N} \\ H^{AA}_{2,1} & H^{AA}_{2,2}-\epsilon & \dots & H^{AA}_{2,M} & V^{AB}_{2,1} & \dots & V^{AB}_{2,N} \\ \vdots & \vdots & \ddots & \vdots & \vdots & \ddots & \vdots \\ H^{AA}_{M,1} & H^{AA}_{M,2} & \dots & H^{AA}_{M,M}-\epsilon & V^{AB}_{M,1} & \dots & V^{AB}_{M,N} \\ \hline V^{BA}_{1,1} & V^{BA}_{1,2} & \dots & V^{BA}_{1,M} & H^{BB}_{1,1}-\epsilon & \dots & H^{BB}_{1,N} \\ \vdots & \vdots & \ddots & \vdots & \vdots & \ddots & \vdots \\ V^{BA}_{N,1} & V^{BA}_{N,2} & \dots & V^{BA}_{N,M} & H^{BB}_{N,1} & \dots & H^{BB}_{N,N}-\epsilon \end{array}\right) \left(\begin{array}{c} c^A_1 \\ c^A_2 \\ \vdots \\ c^A_M \\ \hline c^B_1 \\ \vdots \\ c^N_M \end{array}\right) = 0 \tag{5.2}$$

The wave function $|\psi\rangle$ of the complete system can be represented by energy-dependent orbitals $|\tilde{\chi}^A_\alpha(\epsilon)\rangle$ from system A. The tilde distinguishes the energy-dependent orbitals from the original basis-set.

$$\begin{aligned}
|\psi\rangle &= \sum_{\alpha\in A} |\chi^A_\alpha\rangle c^A_\alpha + \sum_{\beta\in B} |\chi^B_\beta\rangle c^B_\beta \\
&\overset{\text{Eq. 5.6}}{=} \sum_{\alpha\in A} |\chi^A_\alpha\rangle c^A_\alpha + \sum_{\beta\in B} |\chi^B_\beta\rangle \underbrace{\sum_{\alpha\in A}\sum_{\gamma\in B} \bar{G}^{BB}_{\beta,\gamma}(\epsilon) V^{BA}_{\gamma,\alpha} c^A_\alpha}_{c^B_\beta} \\
&= \sum_{\alpha\in A} \underbrace{\left(|\chi^A_\alpha\rangle + \sum_{\beta\in B} |\chi^B_\beta\rangle \sum_{\gamma\in B} \bar{G}^{BB}_{\beta,\gamma}(\epsilon) V^{BA}_{\gamma,\alpha} \right)}_{|\tilde{\chi}^A_\alpha(\epsilon)\rangle} c^A_\alpha \\
&= \sum_{\alpha\in A} |\tilde{\chi}^A_\alpha(\epsilon)\rangle c^A_\alpha \qquad (5.8)
\end{aligned}$$

The energy-dependent orbitals $|\tilde{\chi}^A_\alpha(\epsilon)\rangle$ have the contribution of the environment glued on, that is they leak into the environment.

ORBITALS WITH DOWN-FOLDED ENVIRONMENT

$$\begin{aligned}
|\tilde{\chi}^A_\alpha(\epsilon)\rangle &\overset{\text{def}}{=} |\chi^A_\alpha\rangle + \sum_{\beta,\gamma\in B} |\chi^B_\beta\rangle \overbrace{(\epsilon \mathbf{1}^{BB} - H^{BB})^{-1}}^{\text{Eq. 5.7}} \quad V^{BA}_{\gamma,\alpha} \qquad \text{for } \alpha \in A \\
&= \Big(\hat{1} + \sum_{\beta,\gamma\in B,\delta\in A} |\chi^B_\beta\rangle \bar{G}^{BB}_{\beta,\gamma}(\epsilon) V^{BA}_{\gamma,\delta} \langle\pi_\delta|\Big) |\chi^A_\alpha\rangle \qquad \text{for } \alpha \in A \qquad (5.9)
\end{aligned}$$

where $\langle\pi_\delta|\chi_\alpha\rangle = \delta_{\delta,\alpha}$.

To shed some light on this equation, let me consider the minimal problem with a single orbital in A and single orbital in B.

- $\bar{G}^{BB}(\epsilon)V^{BA} = 0$ The zero of the Green's function indicates that the bath does not couple into system A.
- The poles of the Green's function $\bar{G}^{BB}(\epsilon) = \infty$ indicate states that are eigenstates of system B, without a contribution on subsystem A
- a positive value of $\bar{G}^{BB}(\epsilon)V^{BA} = 0$ indicates that the orbitals $|\chi^A\rangle$ and $|\chi^A\rangle$ occur in the wave function with equal sign as in a bonding orbital. A negative value of $\bar{G}^{BB}(\epsilon)V^{BA} = 0$ indicates that the orbitals $|\chi^A\rangle$ and $|\chi^A\rangle$ occur in the wave function with opposite sign as in a anti-bonding orbital. (Caution! This argument depends on the sign of the orbitals $|\chi^A\rangle$ and $|\chi^B\rangle$.)
- An absolute value of $|\bar{G}^{BB}(\epsilon)V^{BA}|$ smaller than one indicates that the wave function is predominantly on system A, while an absolute value of $|\bar{G}^{BB}(\epsilon)V^{BA}|$ larger than one indicates that the wave function is predominantly on system B. (Caution: This argument assumes orthonormal orbitals $|\chi^A\rangle$ and $|\chi^B\rangle$.)

This indicates that the energy imposes already the phase relations between the orbitals. In an energy region with only small relative changes of $\bar{G}^{BB}$, one can ignore the energy dependence of the orbitals, and thus impose fixed phase relations. This leads to an effective system A, which incorporates the effects of the environment B.

Equation for the coefficients in A: The result Eq. 5.6 for the wave-function coefficients $\vec{c}^B$ in subsystem B is inserted back into the first line of the Schrödinger equation Eq. 5.3

$$\begin{aligned} & (\boldsymbol{H}^{AA} - \epsilon \mathbf{1}^{AA})\vec{c}^A + \boldsymbol{V}^{AB}\vec{c}^B = 0 \\ \overset{\text{Eq. 5.6}}{\Rightarrow} \quad & \Big[\boldsymbol{H}^{AA} + \underbrace{\boldsymbol{V}^{AB}\bar{\boldsymbol{G}}^{BB}(\epsilon)\boldsymbol{V}^{BA}}_{\boldsymbol{\Sigma}^{AA}(\epsilon)} - \epsilon \mathbf{1}^{AA}\Big]\vec{c}^A = 0 \\ \overset{\text{Eq. 5.12}}{\Rightarrow} \quad & \Big[\boldsymbol{H}^{AA} + \boldsymbol{\Sigma}^{AA}(\epsilon) - \epsilon \mathbf{1}^{AA}\Big]\vec{c}^A = 0 \end{aligned} \tag{5.10}$$

DOWN-FOLDED WAVE-FUNCTION EQUATION

The energies ϵ and corresponding wave-function coefficients $\vec{c}^A$, in the energy-dependent basis set Eq. 5.9, are obtained from

$$\Big[\boldsymbol{H}^{AA} + \boldsymbol{\Sigma}^{AA}(\epsilon) - \epsilon \mathbf{1}^{AA}\Big]\vec{c}^A \overset{\text{Eq. 5.10}}{=} 0 \tag{5.11}$$

where the **self energy** is defined as follows

$$\boldsymbol{\Sigma}^{AA}(\epsilon) \overset{\text{def}}{=} \boldsymbol{V}^{AB}\bar{\boldsymbol{G}}^{BB}(\epsilon)\boldsymbol{V}^{BA} \,. \tag{5.12}$$

If Eq. 5.11 has a solution $\vec{c}^A$ for a given energy ϵ, the wave function

$$|\psi\rangle \overset{\text{Eq. 5.9}}{=} \sum_{\alpha \in A} |\tilde{\chi}^A_\alpha(\epsilon)\rangle c^A_\alpha \tag{5.13}$$

solves the Schrödinger equation for the complete system with that energy. The orbitals $|\tilde{\chi}^A_\alpha(\epsilon)\rangle$ defined in Eq. 5.9 have contributions, both, in A and in B. For a normalized wave function $|\psi\rangle$, the norm $\sum_{\alpha \in A} |\vec{c}^A_\alpha|^2$ of vector $\vec{c}^A$ differs usually from 1.

Eq. 5.11 looks like a Schrödinger equation with an energy-dependent potential $\boldsymbol{\Sigma}^{AA}(\epsilon)$. This self energy $\boldsymbol{\Sigma}^{AA}(\epsilon)$ will play a central role in the Green's-functions world.

On the positive side, the size of the matrix equation Eq. 5.11 corresponds to only the subsystem A, which is usually much smaller than the complete system. On the negative side, the matrix problem becomes energy dependent.

In order to obtain a solution for Eq. 5.11, one needs to find those energies for which $\boldsymbol{H}^{AA} + \boldsymbol{\Sigma}^{AA}(\epsilon) - \epsilon \mathbf{1}^{AA}$ has a zero eigenvalue. This is the case, when the determinant $\det[\boldsymbol{H}^{AA} + \boldsymbol{\Sigma}^{AA}(\epsilon) - \epsilon \mathbf{1}^{AA}]$ vanishes. In the absence of a energy-dependent self energy, this is equivalent to solving the characteristic equation for the eigenvalues of a matrix. For an energy-dependent self energy, however, the problem of determining the zeros of the characteristic equation and the corresponding zero-eigenvectors quickly becomes a daunting task for larger systems.

Role of the self energy

Editor: Relate the self energy to level repulsion and life time. Use a one-pole model $G(\hbar\omega) = 1/[\hbar\omega - \epsilon + i\Gamma]$. Real part produced energy level shift, Imaginary part produces broadening. This may not be the best place for this discussion.

5.1.1 Effective Schrödinger equation for an embedded system:

One should resist the impetus to simply drop the energy dependence of $\boldsymbol{\Sigma}^{AA}(\epsilon)$ and interprete Eq. 5.11 as an approximate Schrödinger equation. With little extra effort, one can solve a linear-algebraic problem, which is substantially more accurate and which preserves a lot of the physical content of

the non-linear equation Eq. 5.11. In this section, I describe how we arrive at an Schrödinger equation of an open system. This Schrödinger equation is approximate, but in many cases already quite accurate. In this section, I will also show different ways to arrive at this very same Schrödinger equation. Each of these routes emphasizes a different physical aspect of the problem. In practice you will encounter these as seemingly distinct methodologies. It is useful to understand that and how they are related.

Editor: Is it simpler, to first linearize the equation and then show that Hamilton and overlap matrices coincide with the matrix elements with orbitals at fixed energies?

Approximation of an energy-independent basisset

Despite the similarity of Eq. 5.11 to a Schrödinger equation, there is a fundamental difference, namely, that the normalization of the vector $\vec{c}^A$ needs to consider the bath contribution.

In order to make the connection between a Schrödinger equation Eq. 5.11 and an energy-dependent self energy with a "normal" Schrödinger equation evident, let us work out[2] the Hamiltonian and the overlap matrix for the energy-dependent basisset defined in Eq. 5.9.

Before we continue, I need to prepare a few relations:

$$\begin{aligned}\Big(\mathbf{1}^{BB}\epsilon - \boldsymbol{H}^{BB}\Big)\bar{\boldsymbol{G}}^{BB}(\epsilon) = \mathbf{1} \quad &\Leftrightarrow \quad \overbrace{\bar{\boldsymbol{G}}^{BB,\dagger}(\epsilon)\Big(\mathbf{1}^{BB}\epsilon^* - \boldsymbol{H}^{BB}\Big)}^{[\Big(\mathbf{1}^{BB}\epsilon - \boldsymbol{H}^{BB}\Big)\bar{\boldsymbol{G}}^{BB}(\epsilon)]^\dagger} = \mathbf{1} \\ \Leftrightarrow \quad \bar{\boldsymbol{G}}^{BB,\dagger}(\epsilon) &= \bar{\boldsymbol{G}}^{BB}(\epsilon^*)\end{aligned} \tag{5.14}$$

I will need the energy derivative of the self energy. Let me work it out ahead of time. I will need the derivative of the matrix inverse.

$$\boldsymbol{A}\boldsymbol{A}^{-1} = \mathbf{1} \qquad \Rightarrow \qquad \delta\boldsymbol{A}\boldsymbol{A}^{-1} + \boldsymbol{A}\delta\big(\boldsymbol{A}^{-1}\big) = \mathbf{0} \qquad \Rightarrow \qquad \delta\boldsymbol{A}^{-1} = -\boldsymbol{A}^{-1}\delta\boldsymbol{A}\boldsymbol{A}^{-1} \tag{5.15}$$

With this, we obtain the energy derivative of the self energy, which will be required below.

$$\begin{aligned}\Rightarrow \partial_\epsilon \boldsymbol{\Sigma}^{AA}(\epsilon) &\overset{\text{Eq. 5.12}}{=} \partial_\epsilon\Big(\boldsymbol{V}^{AB}\Big(\epsilon\mathbf{1} - \boldsymbol{H}^{BB}\Big)^{-1}\boldsymbol{V}^{BA}\Big) \\ &\overset{\text{Eq. 5.15}}{=} -\boldsymbol{V}^{AB}\Big(\epsilon\mathbf{1} - \boldsymbol{H}^{BB}\Big)^{-1}\underbrace{\mathbf{1}}_{\partial_\epsilon\left(\epsilon\mathbf{1}-\boldsymbol{H}^{BB}\right)}\Big(\epsilon\mathbf{1} - \boldsymbol{H}^{BB}\Big)^{-1}\boldsymbol{V}^{BA} \\ &= \quad -\boldsymbol{V}^{AB}\Big(G^{BB}(\epsilon)\Big)^2\boldsymbol{V}^{BA}\end{aligned} \tag{5.16}$$

Now, we can work out the matrix elements for Hamiltonian and overlap. Let me consider complex-

[2] We use that the Green's function $\bar{\boldsymbol{G}}^{BB}(\epsilon)$ is hermitian, which follows from the defining equation.

valued energies, which implies that energy and Green's function are non-hermitean.[3] [4]

$$
\begin{aligned}
\tilde{H}_{\alpha,\beta}(\epsilon) &\overset{\text{def}}{=} \langle \tilde{\chi}^A_\alpha(\epsilon^*) | \hat{H} | \tilde{\chi}^A_\beta(\epsilon) \rangle \\
&\overset{\text{Eq. 5.9}}{=} \underbrace{\left(\langle \chi^A_\alpha | + \sum_\gamma \left(\boldsymbol{V}^{AB} \overbrace{\bar{\boldsymbol{G}}^{BB,\dagger}(\epsilon^*)}^{=\bar{\boldsymbol{G}}^{BB}(\epsilon)} \right)_{\alpha,\gamma} \langle \chi^B_\gamma | \right)}_{\langle \tilde{\chi}^A_\alpha(\epsilon^*)|} \hat{H} \underbrace{\left(|\chi^A_\beta\rangle + \sum_\delta |\chi^B_\delta\rangle \left(\bar{\boldsymbol{G}}^{BB}(\epsilon) \boldsymbol{V}^{BA} \right)_{\delta,\beta} \right)}_{|\tilde{\chi}^A_\beta(\epsilon)\rangle} \\
&\overset{\text{Eq. 5.5}}{=} \left(\boldsymbol{H}^{AA} + 2\boldsymbol{V}^{AB}\bar{\boldsymbol{G}}^{BB}(\epsilon)\boldsymbol{V}^{BA} + \boldsymbol{V}^{AB}\bar{\boldsymbol{G}}^{BB}(\epsilon) \underbrace{\boldsymbol{H}^{BB}}_{\epsilon\mathbf{1} - \underbrace{(\epsilon\mathbf{1} - \boldsymbol{H}^{BB})}_{(\tilde{G}^{BB})^{-1}}} \bar{\boldsymbol{G}}^{BB}(\epsilon)\boldsymbol{V}^{BA} \right)_{\alpha,\beta} \\
&\overset{\text{Eq. 5.7}}{=} \left(\boldsymbol{H}^{AA} + \boldsymbol{V}^{AB}\bar{\boldsymbol{G}}^{BB}(\epsilon)\boldsymbol{V}^{BA} + \epsilon\, \boldsymbol{V}^{AB}\bar{\boldsymbol{G}}^{BB}(\epsilon)\bar{\boldsymbol{G}}^{BB}(\epsilon)\boldsymbol{V}^{BA} \right)_{\alpha,\beta} \\
&\overset{\text{Eq. 5.16}}{=} \left(\boldsymbol{H}^{AA} + \boldsymbol{\Sigma}^{AA}(\epsilon) - \epsilon\, \frac{d\boldsymbol{\Sigma}^{AA}}{d\epsilon} \right)_{\alpha,\beta} \qquad (5.17) \\
\tilde{O}_{\alpha,\beta}(\epsilon) &\overset{\text{def}}{=} \langle \tilde{\chi}^A_\alpha(\epsilon^*) | \tilde{\chi}^A_\beta(\epsilon) \rangle \\
&\overset{\text{Eq. 5.9}}{=} \left(\langle \chi^A_\alpha | + \sum_\gamma \left(\boldsymbol{V}^{AB}\bar{\boldsymbol{G}}^{BB}(\epsilon) \right)_{\alpha,\gamma} \langle \chi^B_\gamma | \right) \left(|\chi^A_\beta\rangle + \sum_\delta |\chi^B_\delta\rangle \left(\bar{\boldsymbol{G}}^{BB}(\epsilon)\boldsymbol{V}^{BA} \right)_{\delta,\beta} \right) \\
&\overset{\text{Eq. 5.5}}{=} \left(\mathbf{1}^{AA} + \boldsymbol{V}^{AB}\bar{\boldsymbol{G}}^{BB}(\epsilon)\bar{\boldsymbol{G}}^{BB}(\epsilon)\boldsymbol{V}^{BA} \right)_{\alpha,\beta} \\
&\overset{\text{Eq. 5.16}}{=} \left(\mathbf{1}^{AA} - \frac{d\boldsymbol{\Sigma}^{AA}(\epsilon)}{d\epsilon} \right)_{\alpha,\beta} \qquad (5.18)
\end{aligned}
$$

The Schrödinger equation with the matrix elements of the energy-dependent basisset $\{|\tilde{\chi}_\alpha(\epsilon)\rangle\}$ is identical with the down-folded wave-function equation Eq. 5.11 obtained earlier.

$$
\begin{aligned}
\left[\tilde{\boldsymbol{H}}(\epsilon) - \epsilon\tilde{\boldsymbol{O}} \right] \vec{c}^A &= \Big[\underbrace{\boldsymbol{H}^{AA} + \boldsymbol{\Sigma}^{AA}(\epsilon) - \epsilon \frac{d\boldsymbol{\Sigma}^{AA}}{d\epsilon}}_{\tilde{\boldsymbol{H}}(\epsilon)} - \epsilon \underbrace{\left(\mathbf{1}^{AA} - \frac{d\boldsymbol{\Sigma}^{AA}}{d\epsilon} \right)}_{\tilde{\boldsymbol{O}}(\epsilon)} \Big] \vec{c}^A \\
&= \left[\boldsymbol{H}^{AA} + \boldsymbol{\Sigma}^{AA}(\epsilon) - \epsilon \mathbf{1}^{AA} \right] \vec{c}^A = 0 \qquad (5.19)
\end{aligned}
$$

The norm condition of the wave functions can now be expressed conveniently in terms of the overlap matrix

$$
\langle \psi(\epsilon) | \psi(\epsilon) \rangle = \sum_{\alpha,\beta} \left(c^A_\alpha \right)^* \tilde{O}_{\alpha,\beta} c^A_\beta \overset{!}{=} 1 \qquad (5.20)
$$

Towards an algebraic equation: Because of the energy dependence of the matrix elements, we still have a complicated nonlinear problem to solve. However, we can approximate the problem by discardingf the energy dependence of the basisset. We fix the energy of the orbitals $|\tilde{\chi}^A_\alpha(\epsilon)\rangle$ to a specific value ϵ_ν and write down the resulting Schrödinger equation.

$$
\left[\tilde{\boldsymbol{H}}(\epsilon_\nu) - \epsilon\, \tilde{\boldsymbol{O}}(\epsilon_\nu) \right] \vec{c}^A = 0 + O\big((\epsilon - \epsilon_\nu)^2 \big) \qquad (5.21)
$$

This expression is approximate, because it ignores the energy dependence of the basis states $|\tilde{\chi}^A_\alpha(\epsilon)\rangle$ of Eq. 5.9. No other approximations are made.

[3] In order to ensure that the expressions in the time representation are convergent, we need to insert the Bra for the complex-conjugate of the energy. The downfolding in time representation is provided in appendix F.1 on p. 599.

[4] We can make use of $\bar{\boldsymbol{G}}^{BB}(\epsilon^*) = \bar{\boldsymbol{G}}^{BB,\dagger}(\epsilon)$, where we use $\bar{\boldsymbol{G}}^{BB}(\epsilon) = \left(\mathbf{1}^{BB}\epsilon - \boldsymbol{H}^{BB} \right)^{-1}$

Taylor expansion in the energy

There is another approach to the same eigenvalue problem, namely to linearize Eq. 5.11 in the deviation of the energy ϵ from some expansion point ϵ_ν.

$$\begin{aligned}
0 &\overset{\text{Eq. 5.11}}{=} \Big[\boldsymbol{H}^{AA} + \boldsymbol{\Sigma}^{AA}(\epsilon) - \epsilon \mathbf{1}^{AA}\Big]\vec{c}^{A} \\
&\overset{\text{Taylor}}{=} \left[\left(\boldsymbol{H}^{AA} + \boldsymbol{\Sigma}^{AA}(\epsilon_\nu) - \epsilon_\nu \mathbf{1}^{AA}\right) + (\epsilon - \epsilon_\nu)\left.\frac{d\big(\boldsymbol{H}^{AA} + \boldsymbol{\Sigma}^{AA}(\epsilon) - \epsilon \mathbf{1}^{AA}\big)}{d\epsilon}\right|_{\epsilon_\nu} + O\big((\epsilon-\epsilon_\nu)^2\big)\right]\vec{c}^{A} \\
&= \left[\left(\boldsymbol{H}^{AA} + \boldsymbol{\Sigma}^{AA}(\epsilon_\nu) - \epsilon_\nu \mathbf{1}^{AA}\right) + (\epsilon - \epsilon_\nu)\left(\left.\frac{d\boldsymbol{\Sigma}^{AA}}{d\epsilon}\right|_{\epsilon_\nu} - \mathbf{1}^{AA}\right) + O\big((\epsilon-\epsilon_\nu)^2\big)\right]\vec{c}^{A} \\
&= \Bigg[\underbrace{\left(\boldsymbol{H}^{AA} + \boldsymbol{\Sigma}^{AA}(\epsilon_\nu) - \epsilon_\nu \left.\frac{d\boldsymbol{\Sigma}^{AA}}{d\epsilon}\right|_{\epsilon_\nu}\right)}_{\tilde{H}^{AA}(\epsilon_\nu)\quad\text{(Eq. 5.17)}} - \epsilon \underbrace{\left(\mathbf{1}^{AA} - \left.\frac{d\boldsymbol{\Sigma}^{AA}}{d\epsilon}\right|_{\epsilon_\nu}\right)}_{\tilde{O}^{AA}(\epsilon_\nu)\quad\text{(Eq. 5.18)}}\Bigg]\vec{c}^{A} + O\big((\epsilon-\epsilon_\nu)^2\big) \\
&= \Big[\tilde{\boldsymbol{H}}(\epsilon_\nu) - \epsilon\, \tilde{\boldsymbol{O}}(\epsilon_\nu)\Big]\vec{c}^{A} + O\big((\epsilon-\epsilon_\nu)^2\big) \qquad (5.22)
\end{aligned}$$

We obtained an equation, which is identical to Eq. 5.21, but on a completely different route.

- The derivation to first equation Eq. 5.21 establishes the link to the wave functions in Eq. 5.9. Furthermore, it establishes a variational principle for the approximate (linearized) Schrödinger equation.
- The second derivation emphasizes the self energy, and produces the approximate eigenvalue problem without reference to the wave functions in the environment.

EFFECTIVE SCHRÖDINGER EQUATION

A system A, which is coupled to an environment B, can be described by an effective Schödinger equation acting only in A.

$$\Big[\tilde{\boldsymbol{H}}(\epsilon_\nu) - \epsilon\, \tilde{\boldsymbol{O}}(\epsilon_\nu)\Big]\vec{c}^{A} \underbrace{\approx 0}_{=O\left((\epsilon-\epsilon_\nu)^2\right)} \qquad (5.23)$$

and the normalization

$$\vec{c}^{A,*}\tilde{\boldsymbol{O}}(\epsilon_\nu)\vec{c}^{A} = 1\,. \qquad (5.24)$$

The effective Hamiltonian $\tilde{\boldsymbol{H}}(\epsilon_\nu)$ and overlap matrix $\tilde{\boldsymbol{O}}(\epsilon_\nu)$ can be obtained either from the self energy Eq. 5.12 acting on system A or the energy-dependent wave functions from Eq. 5.9.

$$\tilde{H}_{\alpha,\beta}(\epsilon_\nu) \overset{\text{def}}{=} \big\langle \tilde{\chi}^A_\alpha(\epsilon^*_\nu)\big|\hat{H}\big|\tilde{\chi}^A_\beta(\epsilon_\nu)\big\rangle \overset{\text{Eq. 5.17}}{=} H^{AA}_{\alpha,\beta} + \Sigma_{\alpha,\beta}(\epsilon_\nu) - \epsilon_\nu \left.\frac{d\Sigma_{\alpha,\beta}}{d\epsilon}\right|_{\epsilon_\nu} \qquad (5.25)$$

$$\tilde{O}_{\alpha,\beta}(\epsilon_\nu) \overset{\text{def}}{=} \big\langle \tilde{\chi}^A_\alpha(\epsilon^*_\nu)\big|\tilde{\chi}^A_\beta(\epsilon_\nu)\big\rangle \overset{\text{Eq. 5.18}}{=} \delta_{\alpha,\beta} - \left.\frac{d\Sigma_{\alpha,\beta}}{d\epsilon}\right|_{\epsilon_\nu} \qquad (5.26)$$

The eigenvector $\vec{c}^{A}$ obtained from Eq. 5.23 defines the wave function $|\psi\rangle$ via

$$|\psi\rangle = \sum_{\alpha\in A} |\tilde{\chi}^A_\alpha(\epsilon_\nu)\rangle c^A_\alpha \qquad (5.27)$$

with orbitals defined by Eq. 5.9.

The (approximate) equation Eq. 5.23 is of fundamental importance. It describes the down-folding

of the environment contribution into the description of an effective system, which is of the size of the system of interest. Down-folding leads at first to an equation (Eq. 5.11) that is non-linear in the energy. This nonlinear problem is mapped approximately onto an eigenvalue problem (Eq. 5.23), which can be solved with standard methods from linear algebra.

Energies accurate to second order in $(\epsilon - \epsilon_\nu)$: In order to judge the accuracy of the Schrödinger equation, we need to investigate the error introduced by the first-order Taylor expansion in energy. We will see, that the error in the energy is of second order in $(\epsilon - \epsilon_\nu)$.

I start from the assumption that the error of the eigenvector $\vec{c}^A$ is of first order in $(\epsilon - \epsilon_\nu)$. This is a reasonable assumption because the result is correct for $\epsilon = \epsilon_\nu$.

The energy can be obtained from the Schrödinger equation as

$$\left[\tilde{\boldsymbol{H}} - \epsilon\tilde{\boldsymbol{O}}\right]\vec{c}^A = 0 \quad \Rightarrow \quad \vec{c}^{A*}\left[\tilde{\boldsymbol{H}} - \epsilon\tilde{\boldsymbol{O}}\right]\vec{c}^A = 0 \quad \Rightarrow \quad \epsilon = \frac{\vec{c}^{A*}\tilde{\boldsymbol{H}}\vec{c}^A}{\vec{c}^{A*}\tilde{\boldsymbol{O}}\vec{c}^A} \tag{5.28}$$

Next, we consider the energy as a functional of the vector $\vec{c}^A$. We will see that the energy depends only to second order on an error in the $\vec{c}^A$. Given that that $\vec{c}^A$ is accurate to first order in $\epsilon - \epsilon_\nu$, this will show that the energy is only sensitive to second order in $\epsilon - \epsilon_\nu$.

$$\begin{aligned}
\delta\epsilon &= \epsilon + (\delta\vec{c}^A)^*\left[\frac{\tilde{\boldsymbol{H}}\vec{c}^A}{\vec{c}^{A*}\tilde{\boldsymbol{O}}\vec{c}^A} - \frac{\tilde{\boldsymbol{O}}\vec{c}^A\left(\vec{c}^{A*}\tilde{\boldsymbol{H}}\vec{c}^A\right)}{\left(\vec{c}^{A*}\tilde{\boldsymbol{O}}\vec{c}^A\right)^2}\right] + \left[\cdots\right]\delta\vec{c}^A + O((\delta\vec{c}^A)^2) \\
&= \epsilon + \delta\vec{c}^{A*}\left[\frac{\tilde{\boldsymbol{H}}\vec{c}^A}{\vec{c}^{A*}\tilde{\boldsymbol{O}}\vec{c}^A} - \frac{\tilde{\boldsymbol{O}}\vec{c}^A\left(\vec{c}^{A*}\tilde{\boldsymbol{O}}\vec{c}^A\,\epsilon\right)}{\left(\vec{c}^{A*}\tilde{\boldsymbol{O}}\vec{c}^A\right)^2}\right] + \left[\cdots\right]\delta\vec{c}^A + O((\delta\vec{c}^A)^2) \\
&= \epsilon + \frac{\delta\vec{c}^{A*}\overbrace{\left(\tilde{\boldsymbol{H}} - \epsilon\tilde{\boldsymbol{O}}\right)\vec{c}^A}^{=0}}{\vec{c}^{A*}\tilde{\boldsymbol{O}}\vec{c}^A} + \frac{\overbrace{\vec{c}^{A*}\left(\tilde{\boldsymbol{H}} - \epsilon\tilde{\boldsymbol{O}}\right)}^{=0}\delta\vec{c}^A}{\vec{c}^{A*}\tilde{\boldsymbol{O}}\vec{c}^A} + O((\delta\vec{c}^A)^2) \\
&= \epsilon + O((\delta\vec{c}^A)^2) = \epsilon + O((\epsilon - \epsilon_\nu)^2)
\end{aligned} \tag{5.29}$$

Limitations

While the non-linear equation Eq. 5.11 is exact, the Schrödinger equation Eq. 5.23 is only approximate. It is valid in an energy region around the expansion energy ϵ_ν.

Convergence radius: The Taylor expansion has one important caveat: Every Taylor expansion has a convergence radius beyond which the Taylor expansion does no more converge to the correct result. Usually, the convergence radius is given by the distance of the next pole or discontinuity from the expansion point. In the present case, the eigenstates of the isolated subsystem B introduce a singularity into the Green's function $\bar{\boldsymbol{G}}^{BB}$. Thus, the Taylor expansion will usually be reliable within a band gap of the bath B, but the validity will not reach beyond the band edges of its spectrum.

5.2 Green's function of a system coupled to a bath

In the previous section, the embedding has been described based on wave functions. We have seen how the Green's function of the bath enters in the description. While the wave-function based description is more transparent, I want to translate the same into the more abstract language of Green's functions.

One of the main advantages of the Green's-function formalism is that Green's functions are modular building blocks, that can be stacked together to construct the Green's function for more complex systems.

5.2.1 Coupling to a bath in the energy representation

Let me express the equation defining the Green's function for a composite system. We use the same notation as in the previous section.

$$\begin{pmatrix} \epsilon \mathbf{1}^{AA} - \boldsymbol{H}^{AA} & -\boldsymbol{V}^{AB} \\ -\boldsymbol{V}^{BA} & \epsilon \mathbf{1}^{BB} - \boldsymbol{H}^{BB} \end{pmatrix} \begin{pmatrix} \boldsymbol{G}^{AA}(\epsilon) & \boldsymbol{G}^{AB}(\epsilon) \\ \boldsymbol{G}^{BA}(\epsilon) & \boldsymbol{G}^{BB}(\epsilon) \end{pmatrix} \overset{\text{Eq. 4.24}}{=} \begin{pmatrix} \mathbf{1}^{AA} & \mathbf{0}^{AB} \\ \mathbf{0}^{BA} & \mathbf{1}^{BB} \end{pmatrix} \tag{5.30}$$

After performing the matrix multiplication, we select the two equations, which contain both, $\boldsymbol{G}^{AA}(\epsilon)$ and $\boldsymbol{G}^{BA}(\epsilon)$. One equation expresses $\boldsymbol{G}^{BA}(\epsilon)$ by $\boldsymbol{G}^{AA}(\epsilon)$

$$\begin{aligned} -\boldsymbol{V}^{BA}\boldsymbol{G}^{AA}(\epsilon) + \left(\epsilon \mathbf{1}^{BB} - \boldsymbol{H}^{BB}\right) \boldsymbol{G}^{BA}(\epsilon) &\overset{\text{Eq. 5.30}}{=} \mathbf{0}^{BA} \\ \Rightarrow \qquad \boldsymbol{G}^{BA}(\epsilon) &= \left(\epsilon \mathbf{1}^{BB} - \boldsymbol{H}^{BB}\right)^{-1} \boldsymbol{V}^{BA}\boldsymbol{G}^{AA}(\epsilon) \end{aligned} \tag{5.31}$$

The result is used to eliminate $\boldsymbol{G}^{BA}(\epsilon)$ from the other equation

$$\begin{aligned} \left(\epsilon \mathbf{1}^{AA} - \boldsymbol{H}^{AA}\right)\boldsymbol{G}^{AA}(\epsilon) - \boldsymbol{V}^{AB}\boldsymbol{G}^{BA}(\epsilon) &\overset{\text{Eq. 5.30}}{=} \mathbf{1}^{AA} \\ \Rightarrow \qquad \Big(\underbrace{\epsilon \mathbf{1}^{AA} - \boldsymbol{H}^{AA}}_{[\bar{\boldsymbol{G}}^{AA}(\epsilon)]^{-1}} - \underbrace{\boldsymbol{V}^{AB}\left(\epsilon \mathbf{1}^{BB} - \boldsymbol{H}^{BB}\right)^{-1}\boldsymbol{V}^{BA}}_{\boldsymbol{\Sigma}^{AA}(\epsilon)}\Big)\boldsymbol{G}^{AA}(\epsilon) &= \mathbf{1}^{AA} \end{aligned} \tag{5.32}$$

This yields an equation for $\boldsymbol{G}^{AA}(\epsilon)$, the Green's function projected onto the system of interest.

RETARDED POTENTIALS BY COUPLING TO A BATH

$$\left[\epsilon \mathbf{1}^{AA} - \boldsymbol{H}^{AA} - \boldsymbol{\Sigma}^{AA}(\epsilon)\right]\boldsymbol{G}^{AA}(\epsilon) = \mathbf{1}^{AA} \tag{5.33}$$

with the energy-dependent self energy defined in Eq. 5.12

$$\boldsymbol{\Sigma}^{AA}(\epsilon) \overset{\text{Eq. 5.12}}{=} \boldsymbol{V}^{AB}\bar{\boldsymbol{G}}^{BB}(\epsilon)\boldsymbol{V}^{BA} \tag{5.34}$$

$\bar{\boldsymbol{G}}^{BB}$ is the Green's function of the isolated subsystem B.

Isolated Green's function and coupling are sufficient: Eq. 5.33 shows that the Green's function $\boldsymbol{G}^{AA}(\epsilon)$ of the composite system can be constructed from the Green's functions of the isolated systems and the Hamilton matrix elements connecting the two systems. This is convenient because it shows how a complex system can be built up by stacking together the Green's function of its components.

With the Green's function of the isolated systems,

$$\bar{\boldsymbol{G}}^{AA}(\epsilon) \overset{\text{def}}{=} \left(\epsilon \mathbf{1}^{AA} - \boldsymbol{H}^{AA}\right)^{-1} \tag{5.35}$$

and $\bar{\boldsymbol{G}}^{BB}(\epsilon)$ defined in Eq. 5.7, we obtain

$$\boldsymbol{G}^{AA}(\epsilon) \overset{\text{Eq. 5.33}}{=} \left[\left(\bar{\boldsymbol{G}}^{AA}(\epsilon)\right)^{-1} - \boldsymbol{V}^{AB}\bar{\boldsymbol{G}}^{BB}(\epsilon)\boldsymbol{V}^{BA}\right]^{-1} \tag{5.36}$$

Eq. 5.36 is a variant of the so-called **Dyson equation**. It will show up repeatedly in equivalent forms such as

$$\boldsymbol{G}^{AA} \overset{\text{Eq. 5.36}}{=} \left[\left(\bar{\boldsymbol{G}}^{AA}\right)^{-1} - \boldsymbol{\Sigma}\right]^{-1} \tag{5.37}$$

$$\left(\boldsymbol{G}^{AA}\right)^{-1} \overset{\text{Eq. 5.36}}{=} \left(\bar{\boldsymbol{G}}^{AA}\right)^{-1} - \boldsymbol{\Sigma} \tag{5.38}$$

$$\begin{aligned} \boldsymbol{G}^{AA} &\overset{\text{Eq. 5.36}}{=} \bar{\boldsymbol{G}}^{AA} + \bar{\boldsymbol{G}}^{AA}\boldsymbol{\Sigma}\boldsymbol{G}^{AA} \\ &= \bar{\boldsymbol{G}}^{AA} + \bar{\boldsymbol{G}}^{AA}\boldsymbol{\Sigma}\bar{\boldsymbol{G}}^{AA} + \bar{\boldsymbol{G}}^{AA}\boldsymbol{\Sigma}\bar{\boldsymbol{G}}^{AA}\boldsymbol{\Sigma}\bar{\boldsymbol{G}}^{AA} + \bar{\boldsymbol{G}}^{AA}\boldsymbol{\Sigma}\bar{\boldsymbol{G}}^{AA}\boldsymbol{\Sigma}\bar{\boldsymbol{G}}^{AA}\boldsymbol{\Sigma}\bar{\boldsymbol{G}}^{AA} + \ldots \end{aligned} \tag{5.39}$$

The last form shows the principles for the perturbation expansion of the Green's function.

Where are all the bath states: It seems surprising that nearly all the information of a composite system can be mapped onto a small subsystem.

Indeed some information is lost: If the isolated bath has eigenstates that do not couple to the system of interest, so that $\boldsymbol{V}^{A,B}\vec{c}^{B} = 0$, they do not show up in the self energy. Thus, they do not have any effect on the system $\boldsymbol{G}^{AA}$.

Such states however are related to a pole of the bath Green's function. This pole leads to a singularity in the extended orbital defined in Eq. 5.9. If theses singularities are ignored, a large amount of the bath B is unaccounted. However, this is exactly what is desired when focusing on system A.

5.2.2 Coupling to a bath in the time represenation

The energy representation is limited to systems with time-translation symmetry. Furthermore, it obscures the dynamical properties of the system, which is a source of misunderstandings. Therefore, I will repeat the same derivation in the time representation.

Let me consider the defining equation Eq. 4.14 of the Green's function for a composite system. While we do not make the time dependence of the Hamilton matrix elements explicit, the derivation also works for time-dependent problems.

$$\begin{pmatrix} \mathbf{1}^{AA} i\hbar\partial_t - \boldsymbol{H}^{AA} & -\boldsymbol{V}^{AB} \\ -\boldsymbol{V}^{BA} & \mathbf{1}^{BB} i\hbar\partial_t - \boldsymbol{H}^{BB} \end{pmatrix} \begin{pmatrix} \boldsymbol{G}^{AA}(t,t') & \boldsymbol{G}^{AB}(t,t') \\ \boldsymbol{G}^{BA}(t,t') & \boldsymbol{G}^{BB}(t,t') \end{pmatrix} = \begin{pmatrix} \mathbf{1}^{AA} & \mathbf{0}^{AB} \\ \mathbf{0}^{BA} & \mathbf{1}^{BB} \end{pmatrix} \delta(t-t') \tag{5.40}$$

The symbols are defined in Eq. 5.5.

As in the previous section, I select the two equations containing both, $\boldsymbol{G}^{AA}(t,t')$ and $\boldsymbol{G}^{BA}(t,t')$.

Let me collect the upper-left element of this equation Eq. 5.40

$$\left(\mathbf{1}^{AA} i\hbar\partial_t - \boldsymbol{H}^{AA}\right)\boldsymbol{G}^{AA}(t,t') - \boldsymbol{V}^{AB}\boldsymbol{G}^{BA}(t,t') = \mathbf{1}^{AA}\delta(t-t') \tag{5.41}$$

I eliminate $\boldsymbol{G}^{BA}$ in Eq. 5.41 by expressing it in terms of $\boldsymbol{G}^{AA}$. For that purpose, I take the lower-left element of Eq. 5.40, which is the second equation besides Eq. 5.41 containing both Green's functions.

$$\begin{aligned} -\boldsymbol{V}^{BA}\boldsymbol{G}^{AA}(t,t') + \left(\mathbf{1}^{BB} i\hbar\partial_t - \boldsymbol{H}^{BB}\right)\boldsymbol{G}^{BA}(t,t') &= \mathbf{0}^{BA} \\ \Rightarrow \qquad \left(\mathbf{1}^{BB} i\hbar\partial_t - \boldsymbol{H}^{BB}\right)\boldsymbol{G}^{BA}(t,t') &= \boldsymbol{V}^{BA}\boldsymbol{G}^{AA}(t,t') \end{aligned} \tag{5.42}$$

Let me now introduce the bath Green's function defined earlier in Eq. 5.7 in an energy representation. Here, we need a more general definition, which is also valid for time-dependent Hamiltonians.

$$\left(\mathbf{1}^{BB} i\hbar\partial_t - \boldsymbol{H}^{BB}(t)\right)\bar{\boldsymbol{G}}^{BB}(t,t') = \mathbf{1}^{BB}\delta(t-t') \tag{5.43}$$

Insertion of the bath Green's function $\bar{\boldsymbol{G}}^{BB}$ into Eq. 5.42 for $\boldsymbol{G}^{BA}$ yields

$$\overset{\text{Eq. 5.42}}{\Rightarrow} \quad \left(\mathbf{1}^{BB} i\hbar\partial_t - \boldsymbol{H}^{BB}\right)\boldsymbol{G}^{BA}(t,t') \overset{\text{Eq. 5.42}}{=} \int dt'' \overbrace{\left(\mathbf{1}^{BB} i\hbar\partial_t - \boldsymbol{H}^{BB}\right)\bar{\boldsymbol{G}}^{BB}(t,t'')}^{\mathbf{1}^{BB}\delta(t-t'')} \boldsymbol{V}^{BA}\boldsymbol{G}^{AA}(t'',t')$$

$$\overset{\text{Eq. 5.43}}{=} \left(\mathbf{1}^{BB} i\hbar\partial_t - \boldsymbol{H}^{BB}\right)\left[\int dt''\, \bar{\boldsymbol{G}}^{BB}(t,t'')\boldsymbol{V}^{BA}\boldsymbol{G}^{AA}(t'',t')\right]$$

$$\Rightarrow \qquad \boldsymbol{G}^{BA}(t,t') \quad = \quad \int dt''\, \bar{\boldsymbol{G}}^{BB}(t,t'')\boldsymbol{V}^{BA}\boldsymbol{G}^{AA}(t'',t') + \boldsymbol{C}^{BA}_{\text{hom}}(t,t') \quad (5.44)$$

The object $C^{BA}_{\text{hom}}(t,t')$ is any object that obeys the (homogeneous) Schrödinger equation for subsystem B, that is

$$\left(\mathbf{1}^{BB} i\hbar\partial_t - \boldsymbol{H}^{BB}\right)\boldsymbol{C}^{BA}_{\text{hom}}(t,t') = 0 \tag{5.45}$$

It describes contributions from system B, that are not induced by subsystem A. The boundary conditions will determine the specific value of $C^{BA}_{\text{hom}}(t,t')$. As shown below in Eq. 5.48, this value will be $\boldsymbol{C}^{BA}_{hom}(t,t') = \mathbf{0}^{BA}$.

The result for G^{BA} can now be inserted into Eq. 5.41 to obtain an equation for $\boldsymbol{G}^{AA}$

$$\left(\mathbf{1}^{AA} i\hbar\partial_t - \boldsymbol{H}^{AA}\right)\boldsymbol{G}^{AA}(t,t') \underbrace{-\boldsymbol{V}^{AB}\int dt''\, \bar{\boldsymbol{G}}^{BB}(t,t'')\boldsymbol{V}^{BA}\boldsymbol{G}^{AA}(t'',t') - \boldsymbol{V}^{AB}\boldsymbol{C}^{BA}_{\text{hom}}(t,t')}_{-\boldsymbol{V}^{AB}\boldsymbol{G}^{BA}(t,t'')\ \text{Eq. 5.44}} = \mathbf{1}^{AA}\delta(t-t') \tag{5.46}$$

This equation can also be written in the form

$$\int dt'' \left[\left(\mathbf{1}^{AA} i\hbar\partial_t - \boldsymbol{H}^{AA}\right)\delta(t-t'') - \underbrace{\boldsymbol{V}^{AB}\bar{\boldsymbol{G}}^{BB}(t,t'')\boldsymbol{V}^{BA}}_{\boldsymbol{\Sigma}^{AA}(t,t'')}\right]\boldsymbol{G}^{AA}(t'',t') = \mathbf{1}^{AA}\delta(t-t') + \boldsymbol{V}^{AB}\boldsymbol{C}^{BA}_{\text{hom}}(t,t') \tag{5.47}$$

What happens with $\boldsymbol{C}^{BA}_{hom}$? Together with the differential equation Eq. 4.14 defining the Green's function, also the boundary condition has been specified as $\hat{G}(-\infty,t') = \hat{0}$, which implies $\hat{G}(t,t') = \hat{0}$ for $t < t'$. This boundary condition is specific for the causal Green's function.[5]

Because the propagator of the Schrödinger equation (along the real-valued time axis) is unitary, a solution of the (homogeneous) Schrödinger equation $(\mathbf{1}^{BB} i\hbar\partial_t - \boldsymbol{H}^{BB})\vec{c} = 0$ is either zero for all times or non-zero.[6]

Because also $\boldsymbol{G}^{AA}$ and $\bar{\boldsymbol{G}}^{BB}$ are causal, the block $\boldsymbol{G}^{BA}$ of the Green's function is only causal if $\boldsymbol{C}^{BA}_{\text{hom}}$ vanishes for all times.

$$\boldsymbol{C}^{BA}_{\text{hom}}(t,t') = \mathbf{0}^{BA} \tag{5.48}$$

RETARDED POTENTIALS BY COUPLING TO A BATH

$$\int dt'' \left[\left(\mathbf{1}^{AA} i\hbar\partial_t - \boldsymbol{H}^{AA}(t)\right)\delta(t-t'') - \boldsymbol{\Sigma}^{AA}(t,t'')\right]\boldsymbol{G}^{AA}(t'',t') = \mathbf{1}^{AA}\delta(t-t') \tag{5.49}$$

with the retarded potential

$$\boldsymbol{\Sigma}^{AA}(t,t') = \boldsymbol{V}^{AB}(t)\bar{\boldsymbol{G}}^{BB}(t,t')\boldsymbol{V}^{BA}(t') \tag{5.50}$$

$\bar{\boldsymbol{G}}^{BB}$ is the Green's function of the isolated subsystem B, which satisfies Eq. 5.43.

[5] Later, we will see that there are Green's function for which this requirement is modified.
[6] This is evident from the conservation of the norm of the wave function.

Instead of a differential equation for the Green's function, we obtain now an integro-differential equation.

5.3 Retarded and time-dependent potentials

In this section, I want to elaborate on the role of retarded and time-dependent potentials. Both refer to a time dependence of the self energy, which is why they are easily confused. I will show, how a retarded and an energy-dependent potential appears in the energy-based representation.

5.3.1 Time-independent Schrödinger equation with a retarded potential

Consider a Schrödinger equation that has a nonlocal potential in time. That is, it has a Hamiltonian $\hat{h} + \hat{\Sigma}(t, t')$ with a **retarded potential** $\hat{\Sigma}(t, t')$.

$$\left[i\hbar\partial_t - \hat{h}\right] |\psi(t)\rangle - \int dt' \, \hat{\Sigma}(t, t')|\psi(t')\rangle = 0 \tag{5.51}$$

The retarded potential $\hat{\Sigma}(t, t')$ will play an important role as **self energy**.

In order to ensure **causality**, the retarded potential has to obey $\hat{\Sigma}(t, t') = 0$ for $t' > t$.

For a translation-invariant problem in time, for which the potential $\hat{\Sigma}(t, t')$ depends only on the relative time argument $t - t'$, we can go into the energy representation.[7]

$$\hat{\Sigma}(t, t') \overset{\text{Eq. } A.9}{=} \int \frac{d\epsilon}{2\pi\hbar} \, \hat{\Sigma}(\epsilon) \mathrm{e}^{-\frac{i}{\hbar}\epsilon(t-t')} \tag{5.52}$$

and use the following Ansatz for the wave function

$$|\psi(t)\rangle \overset{\text{Eq. } A.9}{=} \int \frac{d\epsilon}{2\pi\hbar} \, |\psi(\epsilon)\rangle \mathrm{e}^{-\frac{i}{\hbar}\epsilon t} \tag{5.53}$$

I insert this potential $\hat{\Sigma}$ into the retarded Schrödinger equation Eq. 5.51

$$\begin{aligned}
\left[i\hbar\partial_t - \hat{h}\right] |\psi(t)\rangle - \int dt' \overbrace{\int \frac{d\epsilon}{2\pi\hbar} \, \hat{\Sigma}(\epsilon) \mathrm{e}^{-\frac{i}{\hbar}\epsilon(t-t')}}^{\hat{\Sigma}(t,t')} |\psi(t')\rangle = 0 \\
\left[i\hbar\partial_t - \hat{h}\right] \underbrace{\int \frac{d\epsilon}{2\pi\hbar} \, |\psi(\epsilon)\rangle \mathrm{e}^{-\frac{i}{\hbar}\epsilon t}}_{|\psi(t)\rangle \quad \text{from Eq. 5.53}} - \int \frac{d\epsilon}{2\pi\hbar} \, \mathrm{e}^{-\frac{i}{\hbar}\epsilon t} \hat{\Sigma}(\epsilon) \underbrace{\int dt' \, \mathrm{e}^{\frac{i}{\hbar}\epsilon t'} |\psi(t')\rangle}_{|\psi(\epsilon)\rangle \quad \text{via Eq. A.8}} = 0 \\
\Rightarrow \qquad \int \frac{d\epsilon}{2\pi\hbar} \, \mathrm{e}^{-\frac{i}{\hbar}\epsilon t} \Big(\epsilon - \hat{h} - \hat{\Sigma}(\epsilon)\Big) |\psi(\epsilon)\rangle = 0
\end{aligned} \tag{5.54}$$

This equation is satisfied for all times only if all coefficients vanish individually, i.e.

$$\left[\epsilon\hat{1} - \hat{h} - \hat{\Sigma}(\epsilon)\right] |\psi(\epsilon)\rangle = 0 \, . \tag{5.55}$$

In the energy representation, the retarded potential is thus turned into an energy-dependent potential. If the potential were local in time, its Fourier transform would be a constant in ϵ and the potential $\Sigma(\epsilon)$ would be energy independent.

In order to solve the above equation, we must satisfy

[7] A word regarding units. $\Sigma(t, t')$ has the unit energy divided by time. $\Sigma(\epsilon)$ has the unit energy.

SCHRÖDINGER EQUATION WITH A RETARDED POTENTIAL

For a system with a retarded potential $\hat{\Sigma}$, which is invariant under time-translations, the Schrödinger equation has the form

$$\left[\epsilon\hat{1} - \hat{h} - \hat{\Sigma}(\epsilon)\right]|\psi(\epsilon)\rangle = 0 \tag{5.56}$$

with an energy-dependent Hamiltonian $\hat{h} + \hat{\Sigma}(\epsilon)$.
An approximate Schödinger equation with an energy-independent potential can be obtained from Eq. 5.56 by a first-order Taylor expansion in the deviation $\epsilon - \epsilon_\nu$ about some reference energy ϵ_ν. This will naturally include an overlap operator.

If we consider the case, where the self energy is due to coupling to another system, the wave function $|\psi(\epsilon)\rangle = \sum_{\alpha\in A}|\chi^A_\alpha\rangle c^A_\alpha$ is localized on the subsystem A. The wave function $|\tilde{\psi}(\epsilon)\rangle$, which also contains the contribution of system B, is recovered using Eq. 5.9.

$$|\tilde{\psi}(\epsilon)\rangle \overset{\text{Eq. 5.9}}{=} \left(\hat{1} + \sum_{\beta,\gamma\in B,\delta\in A}|\chi^B_\beta\rangle\bar{G}^{BB}_{\beta,\gamma}(\epsilon)V^{BA}_{\gamma,\delta}\langle\pi_\delta|\right)|\psi(\epsilon)\rangle \tag{5.57}$$

with $\langle\pi_\alpha|\chi_\beta\rangle = \delta_{\alpha,\beta}$.

Note however, that the energies obtained from this equation are, in general, complex and that the wave functions are not necessarily orthonormal. (I do not have a proof either way.)

5.3.2 Time-dependent potential in an energy representation

In order to make the contrast to the retarded potential clear, let me investigate a time-dependent potential in the same manner.

Let me consider a time-dependent Hamiltonian $\hat{h} + \hat{W}(t)$ with

$$\hat{W}(t) = \sum_n \hat{w}_n \mathrm{e}^{-i\omega_n t} \tag{5.58}$$

and represent the wave function in the form

$$|\psi(t)\rangle = \int \frac{d\epsilon}{2\pi\hbar}\,|\psi(\epsilon)\rangle \mathrm{e}^{-\frac{i}{\hbar}\epsilon t} \tag{5.59}$$

The Schrödinger equation with the time-dependent potential is

$$\begin{aligned} & \left[i\hbar\partial_t\hat{1} - \hat{h} - \hat{W}(t)\right]|\psi(t)\rangle = 0 \\ \Rightarrow \quad & \int \frac{d\epsilon}{2\pi\hbar}\,\mathrm{e}^{-\frac{i}{\hbar}\epsilon t}\left[\left(\epsilon\hat{1} - \hat{h}\right)|\psi(\epsilon)\rangle - \sum_n \hat{w}_n|\psi(\epsilon - \hbar\omega_n)\rangle\right] = 0 \\ \Rightarrow \quad & \left(\epsilon\hat{1} - \hat{h}\right)|\psi(\epsilon)\rangle - \sum_n \hat{w}_n|\psi(\epsilon - \hbar\omega_n)\rangle = 0 \end{aligned} \tag{5.60}$$

The energy components of the wave functions are no more independent of each other. Each Fourier component in the potential introduces a sequence of **overtones** in the wave function, that is, components with $\epsilon + \hbar\omega_n$. The overtones are responsible for a non-trivial dynamics of the wave function beyond a harmonic oscillation.

For further information on strong time-dependent potentials, I refer to Floquet theory. **Floquet theory** studies perturbations that are periodic in time. In this case it is possible to translate Bloch theorem, formulated for potentials that are periodic in space, to potentials that are periodic in time[8]

We can remember, that a wave function having contributions with distinct energies has a non-linear time evolution and is not the result of a Hamiltonian with time-translation symmetry.

[8]Floquet theorem actually predates Bloch theorem. The latter is an application of the Floquet theorem, which is more general.

5.3.3 Summary

In this section we learned that a part of a quantum system can be investigated, if the Green's function of the isolated remaining system, $\hat{\bar{G}}^{BB}$ is available. The remaining system acts on the system of interest with a retarded potential, which we call a self energy $\hat{\Sigma}(t,t')$. The retardation describes the time delay between action on the remaining system and its back-action, like in an echo. In an energy representation, the self energy acts like an energy-dependent potential. If the back-action is instantaneous, the potential is local in time, that is non-retarded, and hence also energy-independent.

Schrödinger equations with an energy-dependent Hamiltonian can be solved by piece-wise linearization in the energy, which yields, for each piece, a generalized eigenvalue problem with an overlap matrix. The overlap matrix differs from unity, because the wave function has a "tail" extending into the remaining system.

The reader should be able to distinguish time-dependent from retarded potentials. The reader should be able to translate each between the time-representation and energy representation.

Editor: This is under construction. Drop this

1. general potential
$$V(\epsilon,\epsilon') = \int dt \int dt'\, V(t,t') \mathrm{e}^{\frac{i}{\hbar}(\epsilon t + \epsilon' t')} \tag{5.61}$$
2. local in time, but time dependent
3. retarded, but time independent
4. constant: time independent and local in time
$$\begin{aligned} \hat{V}(t,t') &= \hat{F} \\ \hat{V}(\epsilon,\epsilon') &= \hat{F}\delta(\epsilon)\delta(\epsilon') \end{aligned} \tag{5.62}$$

Further information about one-particle Green's functions can be found in the Book by Economou[66].

5.3.4 Other uses of retarded or energy-dependent potentials

- In the proximity of the nucleus the kinetic energy of the electrons becomes so large that they become relativistic. In order to describe relativistic effects, one often down-folds the two small components of the four-component spinor in the Dirac equation. The small components can be attributed to positrons, the antiparticles of electrons. As result one obtains an energy-dependent equation for a two-component spinor describing the spin-up and spin-down electrons.

5.4 Home study and practice

5.4.1 Energy dependent Hamiltonian in the time representation

Introduction

The goal of this exercise is to practice the translation of expressions between the energy and the time representation. In this lecture, I am mostly working in the more general time representation. Still the majority of problems has time translation invariance, for which the energy representation is more convenient. Furthermore, it the translation is important for comparisons in the literature. My choice in favor of the time representation is two-fold. Firstly, I feel that it is more direct and thus provides better physical insight. Secondly, in the future, research will increasingly move away from simple problems towards time dependent and non-equilibrium problems.

Problem

Editor: This example is only a sketch: We need to practice retarded, time dependent and non-local potentials. I do not proper questions and solutions.

1 Translate the following retarded Schrödinger equation into the energy representation.

$$\left(i\hbar\partial_t - \left(\frac{-\hbar^2\vec{\nabla}^2}{2m} + \frac{1}{2}cx^2\right)\right)\psi(x,t) - \int dt'\, x\theta(t-t')\mathrm{e}^{-\lambda(t-t')}\psi(x,t') = 0 \quad (5.63)$$

2 Solve the retarded Schrödinger equation in the time representation.

3 Solve the retarded Schrödinger equation in the energy representation.

Solution

Editor: Solution missing

5.4.2 Minimal model for a quantum system coupled to a bath

Introduction

The following set of three problems shall demonstrate different aspects of dealing with composite systems using Green's functions. In problem 5.4.2, I start with two atoms forming a molecule, which has already discussed explicitly in 1.5.1 and 1.5.2. Then, in problem 5.4.3, I replace one of the atoms with one having a finite life time. In the third problem 5.4.6, the second atom is replaced by an explicit extended system.

In order to gain insight into the coupling between systems, let me investigate a minimal model. The model describes a spin-less Hubbard dimer without interaction: The two Hubbard atoms are denoted as A and B. The hopping parameter between the two subsystems is t and the energy of the orbital at A is at zero, i.e. $\bar{\epsilon}_A = 0$. The orbital of the bath site B is at energy $\bar{\epsilon}_B$. In order to practice, how to replace one part of a combined system by another one, we start with a symmetric dimer $\bar{\epsilon}_B = \bar{\epsilon}_A$. An asymmetric dimer is then constructed by replacing atom B by one with a different atomic level, i.e. $\bar{\epsilon}_B \neq \bar{\epsilon}_A$.

This technique is used, for example, to study point defects in crystals. One example is the **Anderson impurity model**[67], which describes a strongly correlated atom, the **Anderson impurity**, in an otherwise perfect crystal, the **bath**[9]. The Anderson model was introduced to explain that

[9] The term *bath* is probably related to that of the *heat bath* of thermodynamics.

impurities in a free-electron-like metal can produce local magnetic moments observed experimentally. The Anderson model has also been used to explain the **Kondo effect**, an unsuspected increase of the electric resistance below the **Kondo temperature**. The Kondo effect is one of the famous quantum effects of interacting electrons. For more information, I refer to chapter 17 on p. 421. The Hubbard dimer can be considered as a minimal Anderson impurity model. The subsystem A represents the Anderson impurity, while the subsystem B represents the bath. In the following problems, I exclude the electron interaction for the sake of simplicity. This turns the Anderson model into the simpler **Fano model**[68], which has been introduced almost simultaneously with the Anderson model. The Fano model has been introduced to study the asymmetric line-shape of absorption lines.

Problem

Consider the spin-less dimer with the Hamiltonian

$$\hat{h} = |\pi_A\rangle\bar{\epsilon}_A\langle\pi_A| + |\pi_B\rangle\bar{\epsilon}_B\langle\pi_B| - t\Big(|\pi_A\rangle\langle\pi_B| + |\pi_B\rangle\langle\pi_A|\Big) \tag{5.64}$$

Without restriction of generality we choose $\bar{\epsilon}_A = 0$.
I use the notation for non-orthonormal local orbitals with local orbitals $|\chi_\alpha\rangle$ and projector functions $|\pi_\alpha\rangle$, that obey the bi-orthogonality condition $\langle\chi_\alpha|\pi_\beta\rangle = \delta_{\alpha,\beta}$. Nevertheless, in this problem the orbitals are assumed to be orthonormal, that is $\langle\chi_\alpha|\chi_\beta\rangle = \delta_{\alpha,\beta}$.

1. Determine the Green's function $\hat{G}(\epsilon)$ for the dimer with a given value for $\bar{\epsilon}_B = 0$. Calculate $G^{AA}(\epsilon)$, $G^{BB}(\epsilon)$ and the Green's function $\bar{G}^{BB}(\epsilon)$ of the isolated atom B.
2. Calculate the retarded potential $\Delta\Sigma^{AA}(\epsilon)$, which acts on system A due to replacing atom B by one with the atomic level at $\bar{\epsilon}_B$.
3. Construct the Green's function for atom A in the asymmetric dimer (with $\bar{\epsilon}_B \neq 0$) from the Green's function of the symmetric dimer and the retarded potentials produced by site B.
4. Determine the density of states on site A
5. Editor: This problem shall describe how the charge oscillates in sites A, when it is in contact with B. The initial condition is that the particle is completely on site A. The charge oscillates on A as it oscillates back and forth between A and B with the excitation frequency. In the next problem we can discuss how a continuous spectrum in B leads to a decay of the occupation in A, as it leaks into an environment with an infinite number of states.

Discussion

1. Determine the Green's function $\hat{G}(\epsilon)$ for the dimer with a given value for $\bar{\epsilon}_B = 0$. Calculate $G^{AA}(\epsilon)$, $G^{BB}(\epsilon)$ and the Green's function $\bar{G}^{BB}(\epsilon)$ of the isolated atom B.

The Hamiltonian of the dimer with $\bar{\epsilon}_B = 0$ is

$$\boldsymbol{h} = \begin{pmatrix} 0 & -t \\ -t & 0 \end{pmatrix} \tag{5.65}$$

The Hamiltonian is at times represented as 2×2-matrix and sometimes as operator. The operator form has the vector of kets attached on the left side to the matrix and the vector of bras on the right side. The operator form has the advantage, that the basisset is made explicit when it is used. In the

exercise at hand, we also deal with one-dimensional Hilbert spaces, namely for the isolated atom A and the isolated atom B. In that case, the matrix becomes a number.

One can evaluate the Green's function by inverting the matrix $\epsilon\mathbf{1} - \boldsymbol{h}$. This can be done either directly, or via eigenstates and eigenvalues. While both methods are demonstrated, only one is required.

- Green's function by inversion of $\epsilon\mathbf{1} - \boldsymbol{h}$

$$\boldsymbol{G}(\epsilon) \overset{\text{Eq. 4.24}}{=} \left(\epsilon\mathbf{1} - \boldsymbol{h}\right)^{-1} = \frac{1}{\epsilon^2 - t^2}\begin{pmatrix} \epsilon & -t \\ -t & \epsilon \end{pmatrix} \tag{5.66}$$

  I have been using the simple formula for the inversion of a 2×2 matrix.[10]

- Green's function by diagonalization: This method is more involved than direct inversion, but it is instructive.

  The eigenstates of $\boldsymbol{h}$ are

$$\begin{aligned} \vec{c}_1 &= \frac{1}{\sqrt{2}}\begin{pmatrix} 1 \\ 1 \end{pmatrix} \qquad \text{with energy } \epsilon_1 = -t \qquad \text{and} \\ \vec{c}_2 &= \frac{1}{\sqrt{2}}\begin{pmatrix} 1 \\ -1 \end{pmatrix} \qquad \text{with energy } \epsilon_2 = +t \end{aligned} \tag{5.68}$$

  The Green's function is (with the dyadic (outer) product $\otimes$)

$$\begin{aligned} \boldsymbol{G}(\epsilon) &= \sum_{n\in\{1,2\}} \frac{\vec{c}_n \otimes \vec{c}_n^*}{\epsilon - \epsilon_n} = \frac{1}{2}\begin{pmatrix} 1 & 1 \\ 1 & 1 \end{pmatrix}\frac{1}{\epsilon + t} + \frac{1}{2}\begin{pmatrix} 1 & -1 \\ -1 & 1 \end{pmatrix}\frac{1}{\epsilon - t} \\ &= \frac{1}{\epsilon^2 - t^2}\left[\frac{1}{2}\begin{pmatrix} 1 & 1 \\ 1 & 1 \end{pmatrix}(\epsilon - t) + \frac{1}{2}\begin{pmatrix} 1 & -1 \\ -1 & 1 \end{pmatrix}(\epsilon + t)\right] \\ &= \frac{1}{\epsilon^2 - t^2}\begin{pmatrix} \epsilon & -t \\ -t & \epsilon \end{pmatrix} \end{aligned} \tag{5.69}$$

From this result, I can directly look up the diagonal elements of the Green's function

$$G^{AA}(\epsilon) = \frac{\epsilon}{\epsilon^2 - t^2} \qquad \text{and} \qquad G^{BB}(\epsilon) = \frac{\epsilon}{\epsilon^2 - t^2} \tag{5.70}$$

respectively, as operators,

$$\hat{G}^{AA}(\epsilon) = |\chi_A\rangle\frac{\epsilon}{\epsilon^2 - t^2}\langle\chi_A| \qquad \text{and} \qquad \hat{G}^{BB}(\epsilon) = |\chi_B\rangle\frac{\epsilon}{\epsilon^2 - t^2}\langle\chi_B| \tag{5.71}$$

The Green's function $\bar{G}^{BB}$ for the isolated bath is obtained directly from the 1×1 Hamiltonian h^{BB} by inverting $\epsilon - h^{BB}$. In our special case, we have set $\bar{\epsilon}_B = \bar{\epsilon}_A = 0$.

$$\bar{G}^{BB}(\epsilon) = \frac{1}{\epsilon} \tag{5.72}$$

[10]

$$\begin{pmatrix} a & b \\ c & d \end{pmatrix}^{-1} = \frac{1}{ad - bc}\begin{pmatrix} d & -b \\ -c & a \end{pmatrix} \tag{5.67}$$

2. Calculate the retarded potential $\Delta\Sigma^{AA}(\epsilon)$, which acts on system A due to replacing atom B by one with the atomic level at $\bar{\epsilon}_B$.

The self energy of the bath site with a specified $\bar{\epsilon}_B$ is

$$\Sigma^{AA}(\epsilon) \overset{\text{Eq. 5.34}}{=} V^{AB}\bar{G}^{BB}(\epsilon)V^{BA} = \frac{t^2}{\epsilon - \bar{\epsilon}_B} \tag{5.73}$$

The site B is replaced by replacing the self energy with that of the new system. This implies that the replacement is represented by a self energy $\Delta\Sigma$, which is the difference of the one with $\bar{\epsilon}_B \neq 0$ and the one with $\bar{\epsilon}_B = 0$

$$\Delta\Sigma(\epsilon) = \frac{t^2}{\epsilon - \bar{\epsilon}_B} - \frac{t^2}{\epsilon} = \frac{\bar{\epsilon}_B t^2}{\epsilon(\epsilon - \bar{\epsilon}_B)} \tag{5.74}$$

3. Construct the Green's function for atom A in the asymmetric dimer $\bar{\epsilon}_B \neq 0$ from the Green's function of the symmetric dimer and the retarded potentials produced by site B.

In the following, I use two arguments for the Green's function: the second is the "normal" energy argument, while the first is the value of $\bar{\epsilon}_B$, which can be either $\bar{\epsilon}_B$ or zero.

The equation for the Green's function on site A is

$$\begin{aligned}
\hat{G}^{AA}(\bar{\epsilon}_B;\epsilon) &= \left[\epsilon\hat{1}^{AA} - \hat{h}^{AA} - \hat{V}^{AB}\hat{\bar{G}}^{BB}(\bar{\epsilon}_B;\epsilon)\hat{V}^{BA}\right]^{-1} \\
&= \Big[\underbrace{\epsilon\hat{1}^{AA} - \hat{h}^{AA} - \hat{V}^{AB}\hat{\bar{G}}^{BB}(0;\epsilon)\hat{V}^{BA}}_{\left(\hat{G}^{AA}(0;\epsilon)\right)^{-1}} - \underbrace{\hat{V}^{AB}\Big(\hat{\bar{G}}^{BB}(\bar{\epsilon}_B;\epsilon) - \hat{\bar{G}}^{BB}(0;\epsilon)\Big)\hat{V}^{BA}}_{\Delta\hat{\Sigma}^{AA}}\Big]^{-1} \\
&= \left[\left(\hat{G}^{AA}(0;\epsilon)\right)^{-1} - \Delta\hat{\Sigma}^{AA}(\epsilon)\right]^{-1}
\end{aligned} \tag{5.75}$$

Let me now insert the "numbers". $G^{AA}(\epsilon)$ is the sole matrix element of $\hat{G}^{AA}(\epsilon) = |\chi_A\rangle G^{AA}(\epsilon)\langle\chi_A|$.

$$\begin{aligned}
G^{AA}(\bar{\epsilon}_B;\epsilon) &\overset{\text{Eqs. 5.70, 5.74}}{=} \Big[\underbrace{\frac{\epsilon^2 - t^2}{\epsilon}}_{\left(G^{AA}(0;\epsilon)\right)^{-1}} - \underbrace{\frac{t^2\bar{\epsilon}_B}{\epsilon(\epsilon - \bar{\epsilon}_B)}}_{\Delta\Sigma^{AA}(\epsilon)}\Big]^{-1} \\
&= \frac{\epsilon(\epsilon - \bar{\epsilon}_B)}{(\epsilon^2 - t^2)(\epsilon - \bar{\epsilon}_B) - t^2\bar{\epsilon}_B} \\
&= \frac{\epsilon(\epsilon - \bar{\epsilon}_B)}{\epsilon^3 - t^2\epsilon - \epsilon^2\bar{\epsilon}_B + t^2\bar{\epsilon}_B - t^2\bar{\epsilon}_B} \\
&= \frac{\epsilon - \bar{\epsilon}_B}{\epsilon^2 - t^2 - \epsilon\bar{\epsilon}_B} \\
&= \frac{\epsilon - \bar{\epsilon}_B}{\left(\epsilon - \frac{1}{2}\bar{\epsilon}_B - \sqrt{\left(\frac{1}{2}\bar{\epsilon}_B\right)^2 + t^2}\right)\left(\epsilon - \frac{1}{2}\bar{\epsilon}_B + \sqrt{\left(\frac{1}{2}\bar{\epsilon}_B\right)^2 + t^2}\right)}
\end{aligned} \tag{5.76}$$

With this result we could in principle stop. However, the expression is still fairly intransparent. Let us therefore divide the result into the sum of the two poles.

Let us perform a **partial-fraction decomposition**[11]

$$\frac{x - c}{(x - a)(x - b)} = \frac{\frac{c-b}{a-b}(x - a) - \frac{c-a}{a-b}(x - b)}{(x - a)(x - b)} = \frac{a - c}{a - b}\frac{1}{x - a} + \frac{c - b}{a - b}\frac{1}{x - b} \tag{5.77}$$

[11] German(partial fraction decomposition)=Partialbruchzerlegung.

with

$$
\begin{aligned}
c &= \bar{\epsilon}_B \\
a &= \frac{1}{2}\bar{\epsilon}_B + \sqrt{\left(\frac{1}{2}\bar{\epsilon}_B\right)^2 + t^2} \\
b &= \frac{1}{2}\bar{\epsilon}_B - \sqrt{\left(\frac{1}{2}\bar{\epsilon}_B\right)^2 + t^2} \\
\Rightarrow \frac{a-c}{a-b} &= \frac{-\bar{\epsilon}_B/2 + \sqrt{(\bar{\epsilon}_B/2)^2 + t^2}}{2\sqrt{(\bar{\epsilon}_B/2) + t^2}} = \frac{1}{2}\left(1 - \frac{\bar{\epsilon}_B/2}{\sqrt{(\bar{\epsilon}_B/2)^2 + t^2}}\right) \\
\frac{c-b}{a-b} &= \frac{\bar{\epsilon}_B/2 + \sqrt{(\bar{\epsilon}_B/2)^2 + t^2}}{2\sqrt{(\bar{\epsilon}_B/2) + t^2}} = \frac{1}{2}\left(1 + \frac{\bar{\epsilon}_B/2}{\sqrt{(\bar{\epsilon}_B/2)^2 + t^2}}\right)
\end{aligned}
\tag{5.78}
$$

$$
G^{AA}(\bar{\epsilon}_B;\epsilon) \overset{\text{Eq. 5.77}}{=} \frac{1}{2}\frac{1 - \frac{\bar{\epsilon}_B/2}{\sqrt{(\bar{\epsilon}_B/2)^2+t^2}}}{\epsilon - \bar{\epsilon}_B/2 - \sqrt{(\bar{\epsilon}_B/2)^2 + t^2}} + \frac{1}{2}\frac{1 + \frac{\bar{\epsilon}_B/2}{\sqrt{(\bar{\epsilon}_B/2)^2+t^2}}}{\epsilon - \bar{\epsilon}_B/2 + \sqrt{(\bar{\epsilon}_B/2)^2 + t^2}} \tag{5.79}
$$

The first term is the pole with the upper energy and the second term is the pole with the lower energy.

The result can be rationalized with the principle of **level repulsion.** which has bneen discussed in section 1.5.2 on p. 28 .

- The coupling, $-t$, leads to a repulsion of the energy levels relative to the diagonal elements of the Hamiltonian. This level repulsion decreases with increasing energy separation of the uncoupled levels.
- the dominant weight of the state is on the state with nearby energy.
- The phase relation between the contribution from both sites changes its sign from one state to the other. If the off-diagonal Hamilton matrix element, in this case $-t$ is negative, the orbitals in the lower state have similar sign, and the opposite sign in the upper state. The sign relation changes, when the hopping parameter changes its sign.
- The poles of the Green's function lie exactly at the energy eigenvalues of the asymmetric dimer. This is a sanity check that the method works. In the non-degenerate case, there is a pole with large weight near $\epsilon = 0$ and a pole with small weight near $\epsilon = \bar{\epsilon}_B$. This leads to a projected density of states for site A with a large delta-peak near near $\epsilon = 0$ and a smaller one near $\bar{\epsilon}_B$.
  - For $\bar{\epsilon} > 0$, the first pole with small weight lies near $\bar{\epsilon}_B$, and the second one is near $\epsilon = 0$ and has the large weight.
  - for $\bar{\epsilon} < 0$, the two poles change their role. The first is the dominant pole on site A and lies near $\epsilon = 0$, while the second is the smaller pole near $\epsilon = \bar{\epsilon}_B$.
- For the symmetric dimer, i.e. for $\bar{\epsilon}_B = 0$, we obtain $G^{(0)}_{AA}(\epsilon)$ obtained previously.
- For $\bar{\epsilon}_B \to \infty$ we obtain the Green's function for the isolated atom A.
- The weights of the two poles add up to one. This demonstrates an important sum rule for the Green's function.

4. Determine the projected density of states on site A

The density of states on site A is obtained as

$$D_A(\epsilon) \overset{\text{Eq. 4.53}}{=} -\frac{1}{\pi} \lim_{\eta\to 0} \mathrm{Im}\left[\langle\pi_A|\hat{G}(\epsilon+i\eta)|\pi_A\rangle\right] \tag{5.80}$$

where the $|\pi_A\rangle$ are the projector functions for the orbitals $|\chi_\alpha\rangle$.

The density of states is a 2×2 matrix in a two-dimensional basisset $\hat{D}(\epsilon) = \sum_{\alpha,\beta\in\{A,B\}} |\chi_\alpha\rangle D_{\alpha,\beta}\langle\chi_\beta|$. The projected density of states for site A is the matrix element $D_{AA}(\epsilon)$ on the diagonal, which I abbreviate as $D_A(\epsilon)$.

In the following, I will use

$$\lim_{\eta\to 0^+} \mathrm{Im}\Big(-\frac{1}{\pi}\frac{1}{x+i\eta}\Big) \overset{\text{Eq. 4.56}}{=} \delta(x) \tag{5.81}$$

The projected density of states is

$$D_A(\epsilon) = -\frac{1}{\pi} \lim_{\eta\to 0^+} \mathrm{Im}\left[\langle\pi_A|\hat{G}(\epsilon+i\eta)|\pi_A\rangle\right] = -\frac{1}{\pi} \lim_{\eta\to 0} \mathrm{Im}\left[G^{AA}(\bar{\epsilon}_B;\epsilon+i\eta)\right] \tag{5.82}$$

We use the Green's function from Eq. 5.79

$$G^{AA}(\bar{\epsilon}_B;\epsilon+i0^+) \overset{\text{Eq. 5.79}}{=} \frac{1}{2}\frac{1-\frac{\bar{\epsilon}_B/2}{\sqrt{(\bar{\epsilon}_B/2)^2+t^2}}}{\epsilon-\bar{\epsilon}_B/2-\sqrt{(\bar{\epsilon}_B/2)^2+t^2}} + \frac{1}{2}\frac{1+\frac{\bar{\epsilon}_B/2}{\sqrt{(\bar{\epsilon}_B/2)^2+t^2}}}{\epsilon-\bar{\epsilon}_B/2+\sqrt{(\bar{\epsilon}_B/2)^2+t^2}} \tag{5.83}$$

to obtain the projected density of states.

$$\begin{aligned} \Rightarrow \quad D_A(\epsilon) = &\frac{1}{2}\left(1-\frac{\bar{\epsilon}_B/2}{\sqrt{(\bar{\epsilon}_B/2)^2+t^2}}\right) \underbrace{\delta\left(\epsilon-\bar{\epsilon}_B/2-\sqrt{(\bar{\epsilon}_B/2)^2+t^2}\right)}_{\text{upper peak}} \\ &+\frac{1}{2}\left(1+\frac{\bar{\epsilon}_B/2}{\sqrt{(\bar{\epsilon}_B/2)^2+t^2}}\right) \underbrace{\delta\left(\epsilon-\bar{\epsilon}_B/2+\sqrt{(\bar{\epsilon}_B/2)^2+t^2}\right)}_{\text{lower peak}} \end{aligned} \tag{5.84}$$

The result is shown in figure 5.1.

When we choose a $|\bar{\epsilon}_B| \gg t$, we recognize one peak of the density of states lies near zero, i.e. near $\bar{\epsilon}_A$, while the other lies near $\bar{\epsilon}_B$. The peak near $\bar{\epsilon}_B$ has the smaller weight compared to the one near zero. For $\bar{\epsilon}_B$ near zero, we can observe the **level repulsion**.

It shows that the spectral function at site A is only affected by site B if the two energies are close to each other.

One can verify that the peaks of the density of states obtained this way coincide precisely with the energies obtained for the asymmetric dimer in the exercise Eq. 1.5.2 on p. 28.

There is a sum rule, which says that the integral of the density of states Eq. 2.128 projected onto one orbital integrates to one, respectively to the norm of that orbital. [12]

$$\int d\epsilon\, \langle\chi|\hat{D}(\epsilon)|\chi\rangle = \langle\chi|\chi\rangle \tag{5.87}$$

[12] One exploits that the density of states

$$\hat{D}(\epsilon) \overset{\text{Eq. 2.128}}{=} \sum_n |\varphi_n\rangle\delta(\epsilon-\epsilon_n)\langle\varphi_n| \tag{5.85}$$

integrates to the unit operator.

$$\int_{-\infty}^{\infty} d\epsilon\, \hat{D}(\epsilon) = \sum_n |\varphi_n\rangle \underbrace{\Big(\int_{-\infty}^{\infty} d\epsilon\, \delta(\epsilon-\epsilon_n)\Big)}_{=1} \langle\varphi| = \sum_n |\varphi_n\rangle\langle\varphi| = \hat{1} \tag{5.86}$$

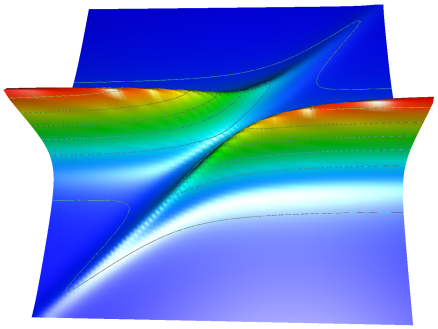


Fig. 5.1: Density of states projected onto orbital A, which is coupled to a second orbital B. The energy axis is the left edge of the graph and the projected density of states is the height. The orbital energy $\bar{\epsilon}_B$ changes from left $\bar{\epsilon}_B \ll \bar{\epsilon}_A$ to right $\bar{\epsilon}_B \gg \bar{\epsilon}_A$. As $\bar{\epsilon}_B$ crosses the energy $\bar{\epsilon}_A$, an avoided band crossing occurs. The positions of the maxima are the positions of the two energy levels. The height is the contribution of of that state at the first atom.

Hence, the weight of a side-peak in the density of states is lost from main peak.

5. Editor: This problem shall describe how the charge oscillates in sites A, when it is in contact with B. The initial condition is that the particle is completely on site A. The charge oscillates on A as it oscillates back and forth between A and B with the excitation frequency. In the next problem we can discuss how a continuous spectrum in B leads to a decay of the occupation in A, as it leaks into an environment with an infinite number of states.

Editor: The following is not finished yet!

$$\begin{aligned}
\hat{G}(t,t') &\overset{\text{Eq. 4.63}}{=} \frac{1}{i\hbar}\theta(t-t')\int d\epsilon\, \hat{D}(\epsilon)\mathrm{e}^{-\frac{i}{\hbar}\epsilon(t-t')} \\
\hat{G}(t,t') &\overset{\text{Eq. 4.40}}{=} \frac{1}{i\hbar}\theta(t-t')\hat{U}(t,t') \\
|\psi(t)\rangle &= \hat{U}(t,t')|\psi(t')\rangle = i\hbar\hat{G}^{AA}(t,t')|\psi(t')\rangle \quad \text{for } t>t' \\
|\psi(t)\rangle &= i\hbar\left(\frac{1}{i\hbar}\int d\epsilon\, \hat{D}(\epsilon)\mathrm{e}^{-\frac{i}{\hbar}\epsilon(t-t')}\right)|\psi(t')\rangle \\
&= \int d\epsilon\, \hat{D}(\epsilon)\mathrm{e}^{-\frac{i}{\hbar}\epsilon(t-t')}|\psi(0)\rangle
\end{aligned} \tag{5.88}$$

$$\langle\pi_A|\psi(t)\rangle = \langle\pi_A|\int d\epsilon\, \hat{D}(\epsilon)\mathrm{e}^{-\frac{i}{\hbar}\epsilon(t-t')}|\psi(0)\rangle \tag{5.89}$$

5.4.3 System in contact with a bath having a finite life time

Introduction

Consider a light-harvesting molecule adsorbed to a surface. A photoexcitation lifts an electron into an orbital $|a\rangle$, from which the excitation energy shall be extracted. The efficiency of this process depends on the rate, with which the energy is extracted, compared to that, with which the energy dissipates. A dissipation mechanism may be the escape of the electron into the supporting surface.

Green's functions can be used to study the transport from the adsorbed orbital into a bath, be it a contact for energy extraction or the environment for a loss mechanism.

The model is an asymmetric dimer as in the preceeding problem. The adsorbed molecule is represented by system A with one orbital $|a\rangle$. In contrast to the preceeding problem the bath is not a single orbital, but an extended system with a continuous energy spectrum. The orbital $|a\rangle$ of the adsorbate shall be coupled to a single orbital $|b\rangle$ of the bath. The coupling is described by a hopping parameter t, so that $\langle a|\hat{h}|b\rangle = -t$.

Rather than treating the extended system B in all detail, we only use only very limited information: Namely, the density of states $D_A(\epsilon)$ projected onto the bath orbital $|b\rangle$, which later is coupled to the orbital A of the adsorbed atom. With the knowledge of the mean energy and the spectral width, the most appropriate shape is that of a Lorentzian.

This leads us to a model related to the asymmetric dimer of the previous exercise, with the main difference that the bath site has a finite lifetime.

By evaluating the Green's function of the coupled system, but projected on the adsorbed site, we can analyze the dynamics of an electron on the adsorbed orbital, while it is in contact with the bath.

Problem

In this problem the spin-degrees of freedom are omitted.

Consider an atom with a single orbital with energy $\bar{\epsilon}_A$ which is coupled to a bath B. Specifically the hopping t connects the adsorbed orbital with a specific orbital of the bath. In the absence of the adsorbed atom, the projected density of states on this orbital shall have the shape of a Lorentzian centered at $\bar{\epsilon}_B$ and having a life-time broadening Γ. The **full-width-at-half-maximum** (**FWHM**) is 2Γ.

The density of states (or spectral function) of a Lorentzian peak at energy $\bar{\epsilon}$ with life time $\hbar/\Gamma$ is (see also Eq. 4.66)

$$D(\epsilon) = \frac{1}{\pi} \frac{\Gamma}{(\epsilon - \bar{\epsilon})^2 + \Gamma^2} \tag{5.90}$$

In Eq. 4.76, we obtained the Green's function for this system as

$$\bar{G}(\epsilon) = \frac{1}{\epsilon - \bar{\epsilon} + i\Gamma} \tag{5.91}$$

1. Consider the Hamiltonian from exercise 5.4.2 and replace the subsystem B by a system with Lorentzian density of states.

1. Determine the Green's function on subsystem A in the time and the energy representation. Plot the result.
2. Determine the energy in subsystem A, the expectation value of the Hamiltonian in the subspace A, as function of time. Discuss energy conservation.
3. Determine the wave function of subsystem A as function of time.

Discussion

1. Determine the Green's function on subsystem A in the time and the energy representation. Plot the result.

$$\begin{aligned}\Sigma^{AA}(\epsilon) &= V^{AB}\bar{G}^{BB}(\epsilon)V^{BA} = \frac{t^2}{\epsilon - \bar{\epsilon}_B + i\Gamma} \\ \Delta\Sigma^{AA}(\epsilon) &= \frac{t^2}{\epsilon - \bar{\epsilon}_B + i\Gamma} - \frac{t^2}{\epsilon} = \frac{t^2(\bar{\epsilon}_B - i\Gamma)}{\epsilon(\epsilon - \bar{\epsilon}_B + i\Gamma)}\end{aligned} \tag{5.92}$$

$$\begin{aligned}G^{AA}(\epsilon) &= \Big(\overbrace{\epsilon - h^{AA}}^{\left(\bar{G}^{AA}\right)^{-1}} - \underbrace{\Sigma^{AA,(0)}(\epsilon)}_{\left(G^{AA}(0;\epsilon)\right)^{-1}} - \Delta\Sigma^{AA}(\epsilon)\Big)^{-1} \\ &= \left(\frac{\epsilon^2 - t^2}{\epsilon} - \frac{t^2(\bar{\epsilon}_B - i\Gamma)}{\epsilon(\epsilon - \bar{\epsilon}_B + i\Gamma)}\right)^{-1} \\ &= \left(\frac{(\epsilon^2 - t^2)(\epsilon - \bar{\epsilon}_B + i\Gamma) - t^2(\bar{\epsilon}_B - i\Gamma)}{\epsilon(\epsilon - \bar{\epsilon}_B + i\Gamma)}\right)^{-1} \\ &= \left(\frac{\epsilon^3 - (\bar{\epsilon}_B - i\Gamma)\epsilon^2 - t^2\epsilon + (\bar{\epsilon}_B - i\Gamma)t^2 - t^2(\bar{\epsilon}_B - i\Gamma)}{\epsilon(\epsilon - \bar{\epsilon}_B + i\Gamma)}\right)^{-1} \\ &= \left(\frac{\epsilon^2 - (\bar{\epsilon}_B - i\Gamma)\epsilon - t^2}{\epsilon - \bar{\epsilon}_B + i\Gamma}\right)^{-1} \\ &= \frac{\epsilon - \bar{\epsilon}_B + i\Gamma}{\epsilon^2 - (\bar{\epsilon}_B - i\Gamma)\epsilon - t^2} \\ &= \frac{\epsilon - \bar{\epsilon}_B + i\Gamma}{\left[\epsilon - (\bar{\epsilon}_B - i\Gamma)/2 - \sqrt{\left(\frac{\bar{\epsilon}_B - i\Gamma}{2}\right)^2 + t^2}\right]\left[\epsilon - (\bar{\epsilon}_B - i\Gamma)/2 + \sqrt{\left(\frac{\bar{\epsilon}_B - i\Gamma}{2}\right)^2 + t^2}\right]}\end{aligned} \tag{5.93}$$

Editor: This is sufficient for plotting. One should continue with the partial fraction decomposition. See Eq. 5.77 on p. 204

Editor: This is nonsense!!!: Let me now transform the Green's function into the time representation:

$$\begin{aligned}G^{AA}(\epsilon) &= \int_{-\infty}^{\infty} d\tau\, \mathrm{e}^{\frac{i}{\hbar}\epsilon\tau} G^{AA}(t+\tau, t) \\ G^{AA}(t+\tau, t) &= \int_{-\infty}^{\infty} d\epsilon\, \mathrm{e}^{-\frac{i}{\hbar}\epsilon\tau} G^{AA}(\epsilon) \\ &= \int_{-\infty}^{\infty} d\epsilon\, \mathrm{e}^{-\frac{i}{\hbar}\epsilon\tau} \frac{1}{\epsilon - \bar{\epsilon}_B + i\Gamma} \\ &= \mathrm{e}^{\frac{1}{\hbar}(i\bar{\epsilon}+\Gamma)\tau} \int_{-\infty}^{\infty} d\epsilon\, \mathrm{e}^{-\frac{i}{\hbar}(\epsilon - \bar{\epsilon} + i\Gamma)\tau} \frac{1}{\epsilon - \bar{\epsilon}_B + i\Gamma}\end{aligned} \tag{5.94}$$

2. Determine the energy in subsystem A, the expectation value of the Hamiltonian in the subspace A, as function of time. Discuss energy conservation.

Editor: This problem is not yet done!

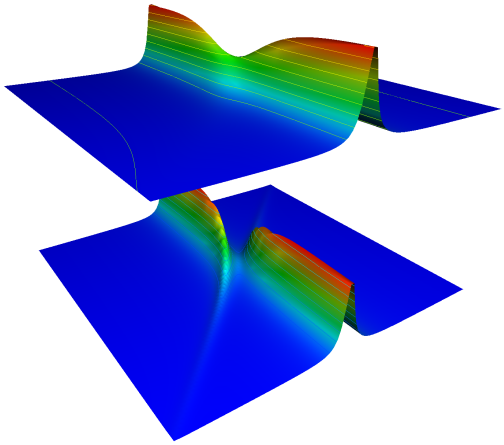


Fig. 5.2: Density of states (up) at an avoided band crossing, where the crossing band has a finite life time (top), compared to that for site B with infinite life time (bottom). Density of states as function of the energy (front-to-back) at the first orbital $|\chi_A\rangle$ in the dimer as function of the energy $\bar{\epsilon}_B$ (left-to-right) of the second orbital. The positions of the maxima are the positions of the two energy levels. The height is the contribution of of that state at the first atom.

3. Determine the wave function of subsystem A as function of time.

Editor: This problem is not yet done!

5.4.4 Surface Green's function of a one-dimensional linear chain

Introduction

In the preceeding exercises, we studied two subsystems A and B in contact, where each subsystem has been modeled, in the spirit of a minimal model, by a single site. In the first exercise of section 5.4.2, we practiced the Green's function machinery on a well known system, the Hubbard dimer. In the second problem of section 5.4.3, we introduced a finite liftime on the bath site. This has been done in an ad-hoc manner without discussing the origin of the bath Green's function or how the finite lifetime emerges.

In the present problem, we will study a minimal problem for an explicit, extended system, which may act as an explicit bath B. To be specific, we study the surface Green's function for the **finite linear chain**. The finite linear chain is analogous to the particle-in-a-box problem from elementary quantum mechanics. For this system, the limit to an infinite system can be done in a controlled manner and will provide additional insight on the transition from finite to infinite systems.

The Green's function of the surface will be a useful model to study (1) adsorbed atoms, (2) two-dimensional band structures of three-dimensional systems and (3) interfaces obtained by glueing two surfaces together.

The surface Green's function and a number of related problems have been investigated by Odashima et al.[65] in her article "The pedagogical introduction to equilibrium Green's function" along with a recommendable introduction to Green's functions.

Problem

Consider a finite one-dimensional chain of atoms with one orbital per site. To keep things simple, consider only a single spin direction. The orbital energy is $\bar{\epsilon}$ and the hopping parameter is $t \in \mathbb{R}$. The Hamiltonian of the finite linear chain is

$$\hat{h} = \sum_{j=1}^{N} |\pi_j\rangle \bar{\epsilon} \langle\pi_j| - \sum_{j=1}^{N-1} \Big(|\pi_j\rangle t \langle\pi_{j+1}| + |\pi_{j+1}\rangle t \langle\pi_j| \Big) \tag{5.95}$$

1. Construct eigenvalues and eigenstates of a finite chain of hydrogen atoms. Inspect the dispersion relation, the quantization of wave vectors, the energy levels, and the density of states in the limit of an infinitely long chain. Ensure that the eigenstates are normalized and describe how. Trick: Extend the chain by one bead in each direction to formulate the boundary conditions.
2. Form the Green's function of the finite chain.
3. Let one of the ends of the chain go to infinity and thus form the Green's function of the half-infinite chain.
4. Calculate the density of states on each atom of the half-infinite chain. Discuss the changes of the density of states as function of distance from the surface. Discuss, how the density of states of the infinite chain is obtained.
5. Calculate the Green's function of the terminal site as function of $\frac{\epsilon-\bar{\epsilon}}{2t}$.

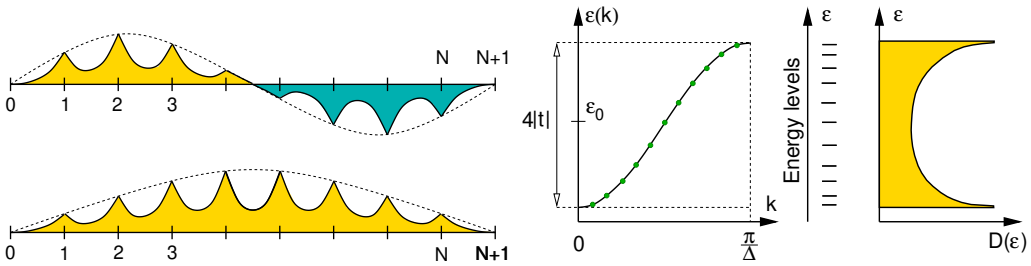
During the calculation, I required the integral formula [Bronstein-Eq. 347 on p.55[69]] below:

$$\int dx \, \frac{1}{a+\cos(x)} = \begin{cases} \frac{2}{\sqrt{a^2-1}} \arctan \frac{(a-1)\tan(x/2)}{\sqrt{a^2-1}} & \text{for } a^2 > 1 \\ \frac{1}{\sqrt{1-a^2}} \ln \frac{(1-a)\tan(x/2)+\sqrt{1-a^2}}{(1-a)\tan(x/2)-\sqrt{1-a^2}} & \text{for } a^2 < 1 \end{cases} \tag{5.96}$$

Discussion

1. Construct eigenvalues and eigenstates of a finite chain of hydrogen atoms. Inspect the dispersion relation, the quantization of wave vectors, the energy levels, and the density of states in the limit of an infinitely long chain. Ensure that the eigenstates are normalized and describe how.

   Trick: Extend the chain by one bead in each direction to formulate the boundary conditions.



Consider a finite chain with N atoms. The distance between the atoms is the lattice constant a_{lat}.

The Hamiltonian is

$$\hat{h} \overset{\text{Eq. 5.95}}{=} \sum_{j=1}^{N} |\pi_j\rangle \bar{\epsilon} \langle \pi_j| - \sum_{j=1}^{N-1} \Big(|\pi_j\rangle t \langle \pi_{j+1}| + |\pi_{j+1}\rangle t \langle \pi_j| \Big) \tag{5.97}$$

The eigenstates can be built up from plane waves with the correct dispersion relation and boundary conditions. The dispersion relation follows from the Schrödinger equation.

$$\begin{aligned} \Big[\hat{h} - \epsilon \hat{1}\Big] \sum_{j=1}^{N} |\chi_j\rangle c_{j,n} &= 0 \\ \Rightarrow \quad -t\Big(c_{j+1} + c_{j-1}\Big) + (\bar{\epsilon} - \epsilon) c_j &= 0 \end{aligned} \tag{5.98}$$

Except for the end-points, the problem has translation invariance which suggests to use the eigenstates of the translation, namely plane waves $c_{j,n} = C e^{i k_n a_{\text{lat}} j}$. Inserting this Ansatz for the coefficients into Eq. 5.98 yields the dispersion relation

$$\begin{aligned} -t\Big(\mathrm{e}^{i k_n a_{\text{lat}}} + \mathrm{e}^{-i k_n a_{\text{lat}}}\Big) + (\bar{\epsilon} - \epsilon_n) &= 0 \\ \Rightarrow \quad \epsilon_n = \bar{\epsilon} - 2t \cos(k_n a_{\text{lat}}) & \end{aligned} \tag{5.99}$$

In the following, we consider the hopping parameter as real-valued quantity.[13]

The boundary conditions can be enforced using the following trick: Extend the chain by one bead in each direction, so that there is one atom at $j = 0$ and one with $j = N+1$. This ensures that none of the true atoms with $j \in \{1, \ldots, N\}$ experience the surface. Then, introduce the boundary condition that the coefficients vanish at the additional fictitious sites by setting $c_{0,n} = 0$ and $c_{N+1,n} = 0$. This ensures that the outermost true atoms, those with $j = 1$ and $j = n$, obey the equation appropriate for the surface. (no contribution from $j = 0$ and $j = N + 1$.)

With this argument, the wave functions can be written down as

$$|\varphi_n\rangle = \sum_{j=1}^{N} |\chi_j\rangle \sin(k_n a_{\text{lat}} j) \sqrt{\frac{2}{N+1}} \tag{5.100}$$

[13] It may be interesting to consider the role of the imaginary part of the hopping parameter. Compare to time inversion symmetry and consider magnetic fields.

and

$$\epsilon_n = \epsilon(k_n) = \bar{\epsilon} - 2t\cos(k_n a_{\text{lat}}) \tag{5.101}$$

with

$$k_n = \frac{\pi}{a_{\text{lat}}(N+1)} n \quad \text{for } n = 1, \ldots, N \tag{5.102}$$

$\epsilon(k)$ is the dispersion relation.

The quantization condition follows from $\sin(k_n a_{\text{lat}}(N+1)) = 0$, so that $k_n = \frac{\pi}{a_{\text{lat}}(N+1)} n$

The normalization follows from[14] $\frac{2}{N}\sum_{j=1}^{N} \sin^2\left(\frac{n\pi}{N+1} j\right) = 1$.

2. Form the Green's function of the finite chain.

The Green's function is

$$\begin{aligned}
\hat{G}(\epsilon + i\eta) &\overset{\text{Eq. 4.22}}{=} \lim_{\eta\to 0^+} \sum_{n=1}^{N} |\varphi_n\rangle \frac{1}{\epsilon - \epsilon_n + i\eta} \langle\varphi_n| \\
&= \sum_{j,j'=1}^{N}\sum_{n=1}^{N} |\chi_j\rangle\langle\pi_j|\varphi_n\rangle \underbrace{\lim_{\eta\to 0^+} \frac{\epsilon - \epsilon_n - i\eta}{(\epsilon-\epsilon_n)^2 + \eta^2}}_{\frac{1}{\epsilon-\epsilon_n} - i\pi\delta(\epsilon-\epsilon_n)} \langle\varphi_n|\pi_{j'}\rangle\langle\chi_{j'}| \\
&= \sum_{j,j'=1}^{N} |\chi_j\rangle \Bigg\{ \underbrace{\sum_{n=1}^{N} \frac{\langle\pi_j|\varphi_n\rangle\langle\varphi_n|\pi_{j'}\rangle}{\epsilon - \epsilon_n}}_{\text{hermitian}} \underbrace{-i\pi \sum_{n=1}^{N} \langle\pi_j|\varphi_n\rangle\delta(\epsilon-\epsilon_n)\langle\varphi_n|\pi_{j'}\rangle}_{\text{anti hermitian}} \Bigg\} \langle\chi_{j'}|
\end{aligned} \tag{5.104}$$

This is a good point to learn about the **Kramers-Kronig relations**. Editor: Provide a link to an explanation of the Kramers-Kronig relations. The equation above shows that the Green's function can be obtained directly from the density of states.

1. Let me extract the density of states using Eq. 4.53.

$$\begin{aligned}
\hat{D}(\epsilon) &\overset{\text{Eq. 4.53}}{=} -\frac{1}{2\pi i} \lim_{\eta\to 0^+} \left(\hat{G}(\epsilon + i\eta) - \hat{G}^\dagger(\epsilon + i\eta)\right) . \\
&= \sum_{j,j'=1}^{N} |\chi_j\rangle \left\{ \sum_{n=1}^{N} \langle\pi_j|\varphi_n\rangle\delta(\epsilon-\epsilon_n)\langle\varphi_n|\pi_{j'}\rangle \right\} \langle\chi_{j'}|
\end{aligned} \tag{5.105}$$

[14]

$$\begin{aligned}
\frac{2}{N+1}\sum_{j=1}^{N} \sin^2\left(\frac{n\pi}{N+1} j\right) &= \frac{2}{N}\sum_{j=1}^{N} \left(\frac{e^{i\pi nj/(N+1)} - e^{-i\pi nj/(N+1)}}{2i}\right)^2 \\
&= \frac{2}{N+1}\frac{-1}{4}\sum_{j=0}^{N} \left(e^{i2\pi nj/(N+1)} - 2 + e^{-i2\pi nj/(N+1)}\right) \\
&= \frac{1}{2(N+1)} 2(N+1) - \frac{1}{2(N+1)}\sum_{j=0}^{N} \left(\left(e^{i2\pi n/(N+1)}\right)^j + \left(e^{-i2\pi n/(N+1)}\right)^j \right) \\
&= 1 - \frac{1}{2(N+1)}\sum_{j=0}^{N} \left(\frac{1 - e^{i2\pi(N+1)/(N+1)}}{1 - e^{i2\pi/(N+1)}} + \frac{1 - e^{-i2\pi(N+1)/(N+1)}}{1 - e^{-i2\pi/(N+1)}} \right) \\
&= 1 - \underbrace{\frac{1}{2(N+1)}\sum_{j=0}^{N} \left(\frac{1-1}{1 - e^{i2\pi/(N+1)}} + \frac{1-1}{1 - e^{-i2\pi/(N+1)}} \right)}_{=0} = 1
\end{aligned} \tag{5.103}$$

I used the rule for the geometric series $\sum_{j=0}^{j} q^j = (1 - q^{j+1})/(1-q)$. Notice the extension of the sum by the term with $j = 0$.

2. Later, we can reconstruct the Green's function from the density of states as

$$\hat{G}(\epsilon + i0^+) = \int d\epsilon' \, \frac{\hat{D}(\epsilon')}{\epsilon - \epsilon' + i0^+} = \int d\epsilon' \, \frac{\hat{D}(\epsilon')}{\epsilon - \epsilon'} - i\pi \hat{D}(\epsilon) \tag{5.106}$$

The last equation uses the **Kramers-Kronig relation**, which allows to construct the real part from the imaginary part of a function that is analytic in the positive half plane.

Now, I work out the density of states. Even though the Green's function, and thus the density of states has been requested only for the terminal site, I will show here the derivation for the full density-of-states matrix, because it will allow me to demonstrate some interesting physical effects lateron.

$$\begin{aligned}
\hat{D}(\epsilon) &= \sum_{j,j'=1}^{N} |\chi_j\rangle \left\{ \sum_{n=1}^{N} \langle \pi_j | \varphi_n \rangle \delta(\epsilon - \epsilon_n) \langle \varphi_n | \pi_{j'} \rangle \right\} \langle \chi_{j'}| \\
&= \sum_{j,j'=1}^{N} |\chi_j\rangle \left\{ \sum_{n=1}^{N} \langle \pi_j | \varphi(k_n) \rangle \delta(\epsilon - \epsilon(k_n)) \langle \varphi(k_n) | \pi_{j'} \rangle \right\} \langle \chi_{j'}| \\
&= \sum_{j,j'=1}^{N} |\chi_j\rangle \left\{ \sum_{n=1}^{N} \frac{2}{N+1} \sin(k_n a_{\rm lat} j) \sin(k_n a_{\rm lat} j') \delta\Big(\epsilon - \bar{\epsilon} + 2t\cos(k_n a_{\rm lat})\Big) \right\} \langle \chi_{j'}| \\
&= \sum_{j,j'=1}^{N} |\chi_j\rangle \Bigg\{ \underbrace{\frac{2a_{\rm lat}}{\pi}}_{2/(N+1)/\Delta k} \underbrace{\sum_{n=1}^{N} \Delta k}_{\to \int_0^{\frac{\pi}{a_{\rm lat}}} dk} \sin(k_n a_{\rm lat} j) \sin(k_n a_{\rm lat} j') \delta\Big(\epsilon - \bar{\epsilon} + 2t\cos(k_n a_{\rm lat})\Big) \Bigg\} \langle \chi_{j'}|
\end{aligned} \tag{5.107}$$

where $k_n \overset{\text{Eq. 5.102}}{=} \frac{n\pi}{a_{\rm lat}(N+1)}$ for $n = 1, \ldots, N$ and, hence, $\Delta k = \frac{\pi}{a_{\rm lat}(N+1)}$.

Let me do the continuum limit $N \to \infty$. I will use $k(\epsilon) = \frac{1}{a_{\rm lat}} \arccos\left(\frac{\epsilon - \bar{\epsilon}}{2t}\right)$, which is obtained from the dispersion relation Eq. 5.101.

$$\begin{aligned}
\hat{D}(\epsilon) &= \sum_{j,j'=1}^{\infty} |\chi_j\rangle \left\{ \frac{2a_{\rm lat}}{\pi} \int_0^{\frac{\pi}{a_{\rm lat}}} dk \, \sin(k a_{\rm lat} j) \sin(k a_{\rm lat} j') \delta\Big(\epsilon - \bar{\epsilon} + 2t\cos(k a_{\rm lat})\Big) \right\} \langle \chi_{j'}| \\
&= \sum_{j,j'=1}^{\infty} |\chi_j\rangle \left\{ \frac{2a_{\rm lat}}{\pi} \int_{\bar{\epsilon}-2t}^{\bar{\epsilon}+2t} d\epsilon \, \left(\frac{d\epsilon}{dk}\right)^{-1} \sin\Big(k(\epsilon) a_{\rm lat} j\Big) \sin\Big(k(\epsilon) a_{\rm lat} j'\Big) \delta\Big(\epsilon - \bar{\epsilon} + 2t\cos(k(\epsilon) a_{\rm lat})\Big) \right\} \langle \chi_{j'}| \\
&= \sum_{j,j'=1}^{\infty} |\chi_j\rangle \left\{ \frac{2a_{\rm lat}}{\pi} \int_{\bar{\epsilon}-2t}^{\bar{\epsilon}+2t} d\epsilon \, \frac{\sin\big(k(\epsilon) a_{\rm lat} j\big) \sin\big(k(\epsilon) a_{\rm lat} j'\big)}{2t a_{\rm lat} \sin\big(k(\epsilon) a_{\rm lat}\big)} \delta\Big(\epsilon - \bar{\epsilon} + 2t\cos(k(\epsilon) a_{\rm lat})\Big) \right\} \langle \chi_{j'}| \\
&= \sum_{j,j'=1}^{\infty} |\chi_j\rangle \left\{ \frac{2}{2\pi t} \frac{\sin\big(k(\epsilon) a_{\rm lat} j\big) \sin\big(k(\epsilon) a_{\rm lat} j'\big)}{\sin\big(k(\epsilon) a_{\rm lat}\big)} \right\} \langle \chi_{j'}|
\end{aligned} \tag{5.108}$$

I will come back to this general result in Eq. 5.121 below. Let me limit the derivation to the terminal site again by selecting $j = j' = 1$. Let me work out the Green's function.

$$\begin{aligned}
\langle \pi_1 | \hat{D}(\epsilon) | \pi_1 \rangle &\overset{\text{Eq. 5.108}}{=} \frac{2}{2\pi t} \sin\Big(k(\epsilon) a_{\rm lat}\Big) = \frac{2}{2\pi t} \sin\left(\arccos\left(\frac{\epsilon - \bar{\epsilon}}{2t}\right)\right) \\
&= \begin{cases} \frac{1}{\pi t} \sqrt{1 - \left(\frac{\epsilon - \bar{\epsilon}}{2t}\right)^2} & \text{for } |\epsilon - \bar{\epsilon}| < 2|t| \\ 0 & \text{for } |\epsilon - \bar{\epsilon}| > 2|t| \end{cases}
\end{aligned} \tag{5.109}$$

The density of states at the terminal site has the form of a half circle $x^2 + y^2 = 1$ with $y(x) = \sqrt{1 - x^2}$. This allows one to verify that the density of states integrates up to one, which is done

below:

$$\int_{\bar{\epsilon}-2t}^{\bar{\epsilon}+2t} d\epsilon \underbrace{\frac{1}{\pi t}\sqrt{1-\left(\frac{\epsilon-\bar{\epsilon}}{2t}\right)^2}}_{D_{1,1}(\epsilon)} = \underbrace{\frac{1}{2}\pi(2t)^2}_{\text{area of half circle}} \underbrace{\frac{1}{2\pi t^2}}_{\text{adjust height to } 1/(\pi t)} = 1 \tag{5.110}$$

The Green's function is then reconstructed from the density of states

$$\hat{G}(\epsilon+i0^+) = \int d\epsilon' \, \frac{\hat{D}(\epsilon')}{\epsilon-\epsilon'+i0^+} = \int d\epsilon' \, \frac{\hat{D}(\epsilon')}{\epsilon-\epsilon'} - i\pi\hat{D}(\epsilon) \tag{5.111}$$

This yields for the surface matrix element $G_{1,1} = \langle\pi_1|\hat{G}|\pi_1\rangle$

$$\begin{aligned} G_{1,1}(\epsilon+i0^+) &= \left[\int_{\bar{\epsilon}-2t}^{\bar{\epsilon}+2t} d\epsilon' \, \frac{1}{\epsilon-\epsilon'} \underbrace{\frac{2}{2\pi t}\sqrt{1-\left(\frac{\epsilon'-\bar{\epsilon}}{2t}\right)^2}}_{D_{1,1}(\epsilon')}\right] - i\pi \underbrace{\frac{2\theta\left(1-\left|\frac{\epsilon-\bar{\epsilon}}{2t}\right|\right)}{2\pi t}\sqrt{1-\left(\frac{\epsilon-\bar{\epsilon}}{2t}\right)^2}}_{D_{1,1}(\epsilon)} \\ &\overset{y=\frac{\epsilon'-\bar{\epsilon}}{2t}}{=} \left[\frac{2}{2\pi t}\int_{-1}^{1} dy \, \frac{\sqrt{1-y^2}}{x-y}\right] - i\frac{\theta(1-|x|)}{t}\sqrt{1-x^2} \quad \text{with } x \overset{\text{def}}{=} \frac{\epsilon-\bar{\epsilon}}{2t} \end{aligned} \tag{5.112}$$

Let me resolve the integral for the real part of the Green's function. I use $a \overset{\text{def}}{=} \frac{\epsilon-\bar{\epsilon}}{2t} (= x)$.

$$\begin{aligned} &\int_{-1}^{1} dy \, \frac{\sqrt{1-y^2}}{x-y} \\ \overset{y=-\cos(z)}{=} &\int_0^{\pi} dz \underbrace{\sin(z)}_{=+\sqrt{1-\cos^2(z)}} \frac{\sqrt{1-\cos^2(z)}}{a+\cos(z)} = \int_0^{\pi} dz \, \frac{1-\cos^2(z)}{a+\cos(z)} \\ = &\int_0^{\pi} dz \, \frac{1-a^2+a^2-\cos^2(z)}{a+\cos(z)} \\ = &(1-a^2)\left(\int_0^{\pi} dz \, \frac{1}{a+\cos(z)}\right) + \left(\int_0^{\pi} dz \, \left(a-\cos(z)\right)\right) \\ = &(1-a^2)\left(\int_0^{\pi} dz \, \frac{1}{a+\cos(z)}\right) + \Big(az-\sin(z)\Big)_0^{\pi} \\ = &a\pi + (1-a^2)\left(\int_0^{\pi} dz \, \frac{1}{a+\cos(z)}\right) \end{aligned} \tag{5.113}$$

The remaining integral is nontrivial. I use Bronstein-Eq. 347 on p.55[69].

$$\int dx \, \frac{1}{a+\cos(x)} \overset{\text{Eq. 5.96}}{=} \begin{cases} \frac{2}{\sqrt{a^2-1}} \arctan \frac{(a-1)\tan(x/2)}{\sqrt{a^2-1}} & \text{for } a^2 > 1 \\ \frac{1}{\sqrt{1-a^2}} \ln \frac{(1-a)\tan(x/2)+\sqrt{1-a^2}}{(1-a)\tan(x/2)-\sqrt{1-a^2}} & \text{for } a^2 < 1 \end{cases} \tag{5.114}$$

The upper bound of the integral requires special care, because the tangens becomes infinite. A proper treatment considers the limit when the upper bound approaches π. As we approach the singularity if the tangens from the left, the tangens approaches $+\infty$.

$$\lim_{x\to\pi^-} \arctan\left(\frac{(a-1)\tan(\frac{x}{2})}{\sqrt{a^2-1}}\right) = \lim_{B\to+\infty} \arctan\left(B\frac{(a-1)}{\sqrt{a^2-1}}\right) \overset{|a|>1}{=} \frac{\pi}{2}\text{sgn}(a) \tag{5.115}$$

Insertion yields

$$\int_0^\pi dx\ \frac{1}{a+\cos(x)} = \begin{cases} \frac{2}{\sqrt{a^2-1}} \overbrace{\arctan\frac{\tan(\pi/2)}{a+1}}^{\frac{\pi}{2}\mathrm{sgn}(a)} & \text{for } a^2>1 \\ \frac{1}{\sqrt{1-a^2}} \underbrace{\Big[\ln[1]-\ln[-1]\Big]}_{=0} & \text{for } a^2<1 \end{cases}$$
$$= \theta(a^2-1)\frac{2}{\sqrt{a^2-1}}\frac{\pi}{2}\mathrm{sgn}(a)$$
$$= \frac{\pi}{\sqrt{a^2-1}}\mathrm{sgn}(a)\theta(a^2-1) \tag{5.116}$$

where $\theta(x)$ is the Heaviside step function.

Let me insert this result for the integral into Eq. 5.113

$$\int_{-1}^{1} dy\ \frac{\sqrt{1-y^2}}{x-y} \overset{\text{Eq. 5.113}}{=} x\pi + (1-x^2)\frac{\pi}{\sqrt{x^2-1}}\mathrm{sgn}(x-1)\theta(x^2-1)$$
$$= \quad \pi\left\{x - \sqrt{x^2-1}\ \mathrm{sgn}(x)\theta(x^2-1)\right\} \tag{5.117}$$

Now, I return to Eq. 5.112 for the surface Green's function obtained previously and insert the expression for the integral just obtained. The resulting Green's function at the terminal site is with $x \overset{\text{def}}{=} \frac{\epsilon-\bar{\epsilon}}{2t}$

$$G_{1,1}(\epsilon+i0^+) \overset{\text{Eq. 5.112}}{=} \left[\frac{2}{2\pi t}\underbrace{\pi\left\{x-\sqrt{x^2-1}\ \mathrm{sgn}(x)\theta(x^2-1)\right\}}_{\int_{-1}^{1} dy\ \frac{\sqrt{1-y^2}}{x-y}}\right] - i\frac{\theta(1-|x|)}{t}\sqrt{1-x^2}$$
$$\overset{x\overset{\text{def}}{=}\frac{\epsilon-\bar{\epsilon}}{2t}}{=} \frac{1}{t}\left\{\frac{\epsilon-\bar{\epsilon}}{2t} - \sqrt{\left(\frac{\epsilon-\bar{\epsilon}}{2t}\right)^2-1}\ \mathrm{sgn}(\epsilon-\bar{\epsilon})\theta\left(\left|\frac{\epsilon-\bar{\epsilon}}{2t|}\right|-1\right)\right.$$
$$\left. -i\theta\left(1-\left|\frac{\epsilon-\bar{\epsilon}}{2t}\right|\right)\sqrt{1-\left(\frac{\epsilon-\bar{\epsilon}}{2t}\right)^2}\right\} \tag{5.118}$$

Because this result is useful for a number of other purposes, let me put it into a box.

GREEN'S FUNCTION FOR THE TERMINAL SITE OF A HALF-INFINITE CHAIN

The Green's function of the half-infinite linear chain projected onto the orbital $|\chi_1\rangle$ of the surface site is

$$\hat{G}(\epsilon+i0^+) \quad = \quad |\chi_1\rangle G_{1,1}(\epsilon+i0^+)\langle\chi_1| \quad \text{with}$$
$$\hat{G}_{1,1}(\epsilon+i0^+) \overset{\text{Eq. 5.118}}{=} \frac{1}{t}\begin{cases} \frac{\epsilon-\bar{\epsilon}}{2t} - i\sqrt{1-\left(\frac{\epsilon-\bar{\epsilon}}{2t}\right)^2} & \text{for } |\epsilon-\bar{\epsilon}|<|2t| \\ \frac{\epsilon-\bar{\epsilon}}{2t}\left(1-\sqrt{1-\left(\frac{2t}{\epsilon-\bar{\epsilon}}\right)^2}\right) & \text{for } |\epsilon-\bar{\epsilon}|>|2t| \end{cases} \tag{5.119}$$

The result Eq. 5.119 is shown below in figure 5.3.

The Green's function of the terminal site is shown in fig. 5.3.

- The real part of the Green's function describes the "quasi-particle shift" of the energy levels of an adsorbate attached to the surface due to the coupling to the half infinite chain.

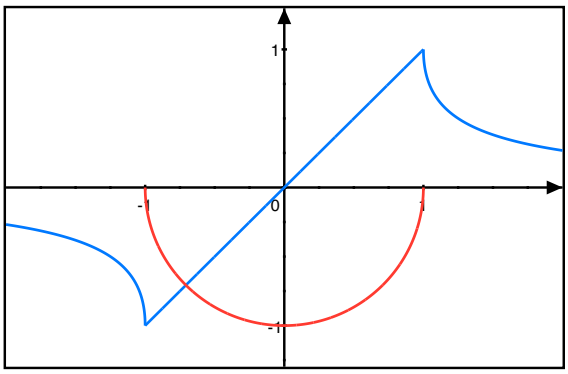


Fig. 5.3: Green's function $G_{1,1}(\epsilon)$ of the half-infinite chain of hydrogen atoms at the terminal site. The real part is shown in blue, and the imaginary part in red. The atomic energy level $\bar{\epsilon}$ is placed to zero and the hopping parameter has been chosen to $t = \frac{1}{2}$.

Given an adsorbate with energy $\bar{\epsilon}_A$ which is coupled to the surface with a hopping parameter V_{AB}, the pole of the Green's functon of the combined system projected on the impurity site A is

$$\begin{aligned} G_{AA}^{-1}(\epsilon) = \epsilon - \bar{\epsilon}_A - |V_{AB}|^2 \bar{G}_{BB}(\epsilon) &\stackrel{!}{=} 0 \\ \epsilon &\approx \bar{\epsilon}_A + \bar{\epsilon}_A |V_{AB}|^2 \bar{G}_{BB}(\bar{\epsilon}_A) \end{aligned} \tag{5.120}$$

The quasi-particle shift is $\delta\epsilon = \mathrm{Tr}[\bar{\epsilon}_A |V_{AB}|^2 \bar{G}_{BB}(\bar{\epsilon}_A)]$. The quasi-particle shift nothing but the **level repulsion**, which we already encountered in the case of the molecular dimer.

- An adsorbate with an energy level below the band of the half-infinite chain will form a bond and will be shifted to lower energies. The antibond will have its main weight in the spectrum of the half-infinite chain.
- An adsorbate with an energy level above the band of the half-infinite chain will form an anti-bond and will be shifted to higher energies. The bond will have its main weight in the spectrum of the half-infinite chain.

- The imaginary part of the Green's function is, up to the prefactor, equal to the density of states on the terminal site. The states at the surface are concentrated closer to the center to the band as compared to the bulk, which can be attributed to the reduced number of nearest neighbors.

- If a wave function of the combined system is in the continuum of bath states, the self energy due to the bath is complex-valued and the adsorbate wave function attains a finite life time. It describes that a particle on the absorbate will disappear over time in the bath, so that its probability amplitude on the adsorbate falls off with time.

If one is familiar with the density of states of a linear chain in the bulk, the density of states on the surface is surprising. In the bulk, the density of states is strongly peaked at the band edges. Here, on the surface, the density of states has its maximum in the center and it falls off at the band edges. This has to do with the fact that the wave functions behave like at the edges like $\sin(kx)$, which has a small slope at the band edges, where ka_{lat} is close to zero or close to π. Because of this small slope, the probability can only rise slowly away from the surface.

Discussion

In Eq. 5.108 we have obtained the density of states for the entire finite chain.

$$\hat{D}(\epsilon) \overset{\text{Eq. 5.108}}{=} \sum_{j,j'=1}^{\infty} |\chi_j\rangle \left\{ \frac{2}{2\pi t} \frac{\sin\left(k(\epsilon) a_{\text{lat}} j\right) \sin\left(k(\epsilon) a_{\text{lat}} j'\right)}{\sin\left(k(\epsilon) a_{\text{lat}}\right)} \right\} \langle \chi_{j'}| \tag{5.121}$$

Let me explore how the density of states changes from the half-circular shape on the surface site to the bulk density of states, which is strongly peaked at the band edges.

$$D_{j,j}(\epsilon) \overset{\text{Eq. 5.121}}{=} \frac{2}{2\pi t} \frac{\sin^2\left(k(\epsilon) a_{\text{lat}} j\right)}{\sin\left(k(\epsilon) a_{\text{lat}}\right)} \tag{5.122}$$

The result is shown in figure 5.4.

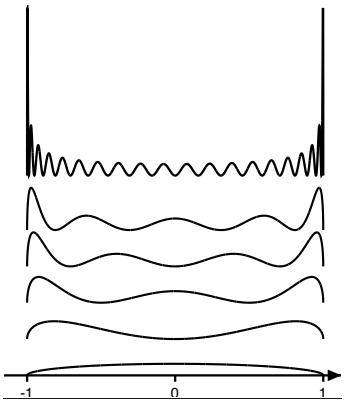


Fig. 5.4: Density of states at the surface of a linear chain of hydrogen atoms. Layers 1,2,3,4,5 and layer 20 are shown from bottom to top and displaced vertically for better visibility. The horizontal axis shows $\frac{\epsilon - \bar{\epsilon}}{2t}$.

The density of states turns into increasingly rapid oscillations, which are modulated by the bulk density of states

$$D_{\text{bulk}}(\epsilon) = \frac{2}{2\pi t} \frac{1}{\sin\left(k(\epsilon) a_{\text{lat}}\right)} \tag{5.123}$$

The oscillations remind of quantized density of states of a finite system with discrete peaks. Here, the origin of the behavior is different. The oscillations are due to the nodeplanes of the wave function. For a given energy, that is for a specific wave length, there is a node at the fictitous site ontop of the surface, and, consequently, at a distance of every half-integer wave length from that fictitious site. Hence there is a node at site $j = \frac{n\pi}{k(\epsilon) a_{lat}}$ for $n = 1, 2, \ldots$.

The oscillatory pattern of the density of states is linked to the coherence length of the electrons. Scattering processes or any perturbing potentials will effectively smear out the density of states, so that the oscillatory pattern vanishes.

5.4.5 Construction

Editor: This is material left over from the exercise on the surface linear chain. This section will be removed after collecting anything that may be useful.

- Next, I decompose the product of the sine functions

$$\begin{aligned}\sin(ax)\sin(bx) &= \frac{e^{iax}-e^{-iax}}{2i}\frac{e^{ibx}-e^{-ibx}}{2i}\\ &= -\frac{1}{4}\Big(e^{i(a+b)x}-e^{i(a-b)x}-e^{-i(a-b)x}+e^{-i(a+b)x}\Big)\\ &= -\frac{1}{2}\Big[\cos\big((a+b)x\big)-\cos\big((a-b)x\big)\Big]\end{aligned} \tag{5.124}$$

-

$$\begin{aligned}\cos(nx) &= \frac{1}{2}\Big(e^{inx}+e^{-inx}\Big) = \frac{1}{2}\Big(\big(e^{ix}\big)^n+\big(e^{-ix}\big)^n\Big) = \mathrm{Re}\Big[\big(e^{ix}\big)^n\Big]\\ &= \mathrm{Re}\Big[\big(\cos(x)+i\sin(x)\big)^n\Big] = \mathrm{Re}\Big[\big(\cos(x)\pm i\sqrt{1-\cos^2(x)}\big)^n\Big]\end{aligned} \tag{5.125}$$

  The sign $\pm$ is undetermined, because $\sin^2(x)+\cos^2(x)=1$ determines only the absolute value of the sinus, not its sign. However, because only the real part of the expression is of interest, the result is independent of the sign chosen.

- Finally, I insert the dispersion relation $\cos\Big(k(\epsilon)\frac{1}{a_{\mathrm{lat}}}\Big) = \frac{\epsilon-\bar{\epsilon}}{2t}$.

- Here, an attempt to obtain the complete Green's function. Skip this

The full Green's function is then obtained from the Kramers-Kronig relation

$$\hat{G}(\epsilon + i0^+) = \int d\epsilon \, \frac{\hat{D}(\epsilon')}{\epsilon - \epsilon'} - i\pi \hat{D}(\epsilon) \tag{5.126}$$

Within the band, the Green's function exhibits a branch cut at the real axis. Therefore, we do not expect to find a closed solution. However, there is a solution only outside the band, that is for $|\epsilon - \bar{\epsilon}| \geq 2t$.
We use the integral formula Bronstein: p68, Eq.25

$$\int_0^\pi dx \frac{\cos(nx)}{1 + b^2 - 2b\cos(x)} = \frac{\pi b^n}{1 - b^2} \quad \Leftrightarrow \quad \int_0^\pi dx \frac{\cos(nx)}{\frac{1+b^2}{2b} - \cos(x)} = \frac{2\pi b^{n+1}}{1 - b^2} \tag{5.127}$$

which yields

$$\frac{1 + b^2}{2b} = \frac{\epsilon - \bar{\epsilon}}{2t} \quad \Rightarrow \quad b^2 - 2\frac{\epsilon - \bar{\epsilon}}{2t} b + 1 = 0 \quad \Rightarrow \quad \left(b - \frac{\epsilon - \bar{\epsilon}}{2t}\right)^2 = \left(\frac{\epsilon - \bar{\epsilon}}{2t}\right)^2 - 1$$

$$b = \frac{\epsilon - \bar{\epsilon}}{2t} \pm \sqrt{\left(\frac{\epsilon - \bar{\epsilon}}{2t}\right)^2 - 1} \overset{|b|\leq 1}{=} \frac{\epsilon - \bar{\epsilon}}{2t}\left(1 - \sqrt{1 - \left(\frac{2t}{\epsilon - \bar{\epsilon}}\right)^2}\right) \tag{5.128}$$

For $|\epsilon - \bar{\epsilon}| \geq 2t$, this yields

$$\begin{aligned}
\hat{G}(\epsilon) &= -\frac{1}{\pi} \sum_{j,j'=1}^{\infty} |\chi_j\rangle \int_0^\pi dy \frac{\cos\left(y(j + j')\right) - \cos\left(y(j - j')\right)}{\epsilon - \bar{\epsilon} - 2t\cos(y)} \langle\chi_j| \\
&= -\frac{1}{2\pi t} \sum_{j,j'=1}^{\infty} |\chi_j\rangle \left(\frac{2\pi(b^{j+j'+1} - b^{j-j'+1})}{1 - b^2}\right) \langle\chi_j| \quad \text{with } b = \frac{\epsilon - \bar{\epsilon}}{2t}\left(1 - \sqrt{1 - \left(\frac{2t}{\epsilon - \bar{\epsilon}}\right)^2}\right) \\
&= -\frac{1}{t} \sum_{j,j'=1}^{\infty} |\chi_j\rangle \left(\frac{b^{j+j'+1} - b^{j-j'+1}}{1 - b^2}\right) \langle\chi_j| \quad \text{with } b = \frac{\epsilon - \bar{\epsilon}}{2t}\left(1 - \sqrt{1 - \left(\frac{2t}{\epsilon - \bar{\epsilon}}\right)^2}\right)
\end{aligned} \tag{5.129}$$

6. Determine the self energy describing the coupling to the half infinite chain

Editor: Remark: the self energy is not hermitian!! Check once again whether this assumption has been made somewhere in the text.

The self-energy at site 0 is

$$\hat{\Sigma}(\epsilon) = \hat{V}^{AB}\hat{\bar{G}}^{BB}\hat{V}^{BA} = |\pi_0\rangle t \langle\pi_1|\hat{G}(\epsilon)|\pi_1\rangle t \langle\pi_0| \tag{5.130}$$

where $\hat{G}(\epsilon)$ is given in Eq. 5.118.

The self energy is has different factors but otherwise it reflects the Green's function on the terminal site of the half-infinite chain shown in Fig. 5.3.

7. Construct the density of states of the adsorbate via the self energy

$$\begin{aligned}
\left(\hat{G}^{AA}(\epsilon)\right)^{-1} &= |\pi_0\rangle\left[\epsilon - \bar{\epsilon}^A - t_A^2\langle\pi_1|\hat{\bar{G}}^{BB}(\epsilon)|\pi_1\rangle\right]\langle\pi_0| \\
\hat{G}^{AA}(\epsilon+i\eta) &= |\chi_0\rangle\frac{1}{\epsilon - \bar{\epsilon}^A - t_A^2\mathrm{Re}\left[\langle\pi_1|\hat{\bar{G}}^{BB}(\epsilon)|\pi_1\rangle\right] - it_A^2\mathrm{Im}\left[\langle\pi_1|\hat{\bar{G}}^{BB}(\epsilon)|\pi_1\rangle\right] + i\eta}\langle\chi_0| \\
&= |\chi_0\rangle\frac{\epsilon - \bar{\epsilon}^A - t_A^2\mathrm{Re}\left[\langle\pi_1|\hat{\bar{G}}^{BB}(\epsilon)|\pi_1\rangle\right] + it_A^2\mathrm{Im}\left[\langle\pi_1|\hat{\bar{G}}^{BB}(\epsilon)|\pi_1\rangle\right] - i\eta}{\left(\epsilon - \bar{\epsilon}^A - t_A^2\mathrm{Re}\left[\langle\pi_1|\hat{\bar{G}}^{BB}(\epsilon)|\pi_1\rangle\right]\right)^2 + \left(t_A^2\mathrm{Im}\left[\langle\pi_1|\hat{\bar{G}}^{BB}(\epsilon)|\pi_1\rangle\right] + \eta\right)^2}\langle\chi_0|
\end{aligned} \tag{5.131}$$

The resulting density of states is obtained from the anti-hermitian part of the Green's function

$$\hat{D}^{AA}(\epsilon) \overset{\text{Eq. 4.53}}{=} -\frac{1}{\pi}\lim_{\eta\to 0}|\chi_0\rangle\frac{t_A^2\mathrm{Im}\left[\langle\pi_1|\hat{\bar{G}}^{BB}(\epsilon)|\pi_1\rangle\right] - \eta}{\left(\epsilon - \bar{\epsilon}^A - t_A^2\mathrm{Re}\left[\langle\pi_1|\hat{\bar{G}}^{BB}(\epsilon)|\pi_1\rangle\right]\right)^2 + \left(t_A^2\mathrm{Im}\left[\langle\pi_1|\hat{\bar{G}}^{BB}(\epsilon)|\pi_1\rangle\right] + \eta\right)^2}\langle\chi_0| \tag{5.132}$$

The small factor η is required to describe any states that result from the adsorbate and lie outside of the spectrum of the half-infinite chain.

The adsorbate contributes an energy level at

$$\epsilon = \bar{\epsilon}^A + t_A^2\mathrm{Re}\left[\langle\pi_1|\hat{\bar{G}}^{BB}(\epsilon)|\pi_1\rangle\right] \tag{5.133}$$

if this energy lies outside the spectrum of the half infinite chain. Then, the imaginary part of the Green's function vanishes at the position of the new energy level, and the width will be governed by the small parameter η. Such a state will contribute a delta function to the density of states.

Because the self energy is a nonlinear function, Eq. 5.133 can have several solutions. For example, when the coupling t^A to the bath is much larger than the band width of the bath, there will be a bonding energy level below the band of the half-infinite chain and one antibonding energy level above. These two states resemble the bonding and antibonding states of a general dimeric molecule, where the terminal site of the half-infinite chain plays the role of one of the atoms in the dimer.

When this energy level falls into the spectrum of the band of the bath, the broadening is due to the coupling to the bath.

8. Determine the wave functions of the adsorbate and chain Editor: This needs to go into the problem formulation.

Here, we explore the tail of the wave function in the half-infinite chain, when an atom is absorbed at the surface.

$$\begin{aligned}
|\tilde{\chi}_\alpha^A(\epsilon)\rangle &\overset{\text{Eq. 5.9}}{=} |\chi_\alpha^A\rangle + \sum_{\beta,\gamma\in B}|\chi_\beta^B\rangle\bar{G}_{\beta,\gamma}^{BB}(\epsilon)V_{\gamma,\alpha}^{BA} \qquad \text{for } \alpha\in A \\
&= \left(\hat{1} + \sum_{\beta,\gamma\in B,\delta\in A}|\chi_\beta^B\rangle\bar{G}_{\beta,\gamma}^{BB}(\epsilon)V_{\gamma,\delta}^{BA}\langle\pi_\delta|\right)|\chi_\alpha^A\rangle \qquad \text{for } \alpha\in A
\end{aligned} \tag{5.134}$$

$$
\begin{aligned}
|\tilde{\chi}^A\rangle &\overset{\text{Eq. 5.9}}{=} \left(|\chi_0^A\rangle + \sum_{j=1}^{N} |\chi_j^B\rangle \bar{G}^{BB}_{j,1}(\epsilon) t^A\right) c^A \\
&= \left(|\chi_0\rangle + \sum_{j=1}^{N} |\chi_j^B\rangle \sum_n \langle \pi_j|\varphi_n\rangle \frac{1}{\epsilon - \epsilon(k_n) + i\eta} \langle \varphi_n|\pi_1\rangle t_A\right) c_A \\
&\overset{\text{Eqs. 5.100 ,5.101}}{=} \left(|\chi_0^A\rangle + \frac{2t_A}{N+1} \sum_{j=1}^{N} |\chi_j^B\rangle \sum_{n=1}^{N} \Delta k \underbrace{\frac{1}{\pi}(N+1)a_{\text{lat}}}_{1/\Delta k} \frac{\sin(k_n a_{\text{lat}} j)\sin(k_n a_{\text{lat}})}{\epsilon - \bar{\epsilon} + 2t\cos(k_n a_{\text{lat}}) + i0^+}\right) c_A \\
&= \left(|\chi_0^A\rangle + \frac{2a_{\text{lat}} t_A}{\pi} \sum_{j=1}^{\infty} |\chi_j^B\rangle \int_0^{\pi} dk \frac{\sin(k a_{\text{lat}} j)\sin(k a_{\text{lat}})}{\epsilon - \bar{\epsilon} + 2t\cos(k a_{\text{lat}}) + i0^+}\right) c_A
\end{aligned}
\tag{5.135}
$$

The coefficient c_A acts as a normalization constant. In order to know a true solution of the Schrödinger equation, we still need to determine the correct energy ϵ.

Let me do a variable transform

$$
y = -2t\cos(k a_{\text{lat}}) \quad \Rightarrow \quad \begin{cases} dy = 2t a_{\text{lat}} \sin(k a_{\text{lat}}) dk \\ k a_{\text{lat}} = \arccos\left(-\frac{y}{2t}\right) \end{cases} \tag{5.136}
$$

$$
|\tilde{\chi}^A_\alpha(\epsilon)\rangle = \left(|\chi_0\rangle + \frac{t_A}{\pi t} \sum_{j=1}^{N} |\chi_j^B\rangle \int_{-2t}^{+2t} dy \frac{\sin\left[j \arccos\left(-\frac{y}{2t}\right)\right]}{\epsilon - \bar{\epsilon} - y + i0^+}\right) c_A \tag{5.137}
$$

Editor: This result shall be analyzed numerically. The shape shall be shown.

- when the energy is far away from the band, the decay of the wave function is expected to be exponential and rapid.
- when the energy lies inside the band, the wave function has a real and an imaginary contribution. The imaginary contribution describes probably the continuum of the half-infinite chain.

Once we found the behavior of the wave function as function of energy, we need to determine the physical energies. For this purpose, we need to determine the poles of the Green's function.

For that purpose, I analyze the adsorbate Green's function $G^{AA}(\epsilon)$. The poles are defined by the equation

Editor: The following is guesswork!

$$
\begin{aligned}
\epsilon - \bar{\epsilon}^A - t_A^2 \langle \pi_1|\bar{G}^{BB}(\epsilon)|\pi_1\rangle &= 0 \\
\frac{\epsilon - \bar{\epsilon}}{2t} - \frac{\bar{\epsilon}^A - \bar{\epsilon}}{2t} + \frac{t_A^2}{t}\left(\frac{\epsilon - \bar{\epsilon}}{2t} - i\pi\sqrt{1 - \left(\frac{\epsilon - \bar{\epsilon}}{2t}\right)^2}\right) &= 0 \\
x - x_A + Bx - i\pi B\sqrt{(1-x^2)} &= 0 \\
(1+B)x - x_A &= i\pi B\sqrt{1-x^2}
\end{aligned}
\tag{5.138}
$$

$$
Re[x] = \frac{x_A}{1+B} \quad \text{and} \quad \text{Im}[x] = \pi\frac{B}{1+B}\sqrt{1 - \left(\frac{x_A}{1+B}\right)^2 - \text{Im}[x]^2} \tag{5.139}
$$

for $|\frac{\epsilon - \bar{\epsilon}}{2t}| < 1$

$$
\begin{aligned}
&|\pi_0\rangle t^2\left[\int d\epsilon'\ \frac{D_{11}(\epsilon')}{\epsilon-\epsilon'} - i\pi D_{11}(\epsilon)\right]\langle\pi_0| \\
&= -\frac{1}{\pi t}|\pi_0\rangle t^2\left[\int_{\bar\epsilon-2t}^{\bar\epsilon+2t} d\epsilon'\ \frac{\sqrt{1-\left(\frac{\epsilon'-\bar\epsilon}{2t}\right)^2}}{\epsilon-\epsilon'} - i\pi\sqrt{1-\left(\frac{\epsilon-\bar\epsilon}{2t}\right)^2}\right]\langle\pi_0| \\
&= -\frac{1}{\pi t}|\pi_0\rangle t^2\left[-\pi\frac{\epsilon-\bar\epsilon}{2t} - i\pi\sqrt{1-\left(\frac{\epsilon-\bar\epsilon}{2t}\right)^2}\right]\langle\pi_0| \\
&= |\pi_0\rangle t\left[\frac{\epsilon-\bar\epsilon}{2t} + i\sqrt{1-\left(\frac{\epsilon-\bar\epsilon}{2t}\right)^2}\right]\langle\pi_0| \\
&= |\pi_0\rangle t\exp\left(i\arccos\left(\frac{\epsilon-\bar\epsilon}{2t}\right)\right)\langle\pi_0| \quad \text{for } |\epsilon-\bar\epsilon|<|2t|
\end{aligned}
\tag{5.140}
$$

This result is apparently only valid for energies within the band.

Bronstein p.55, Eq. 347

$$
\begin{aligned}
\int dx\ \frac{1}{a-\cos(x)} &= \frac{1}{\sqrt{1-a^2}}\ln\left|\frac{(1+a)\tan(x/2)-\sqrt{1-a^2}}{(1+a)\tan(x/2)+\sqrt{1-a^2}}\right| \quad \text{for } a^2<1 \\
\int_0^\pi dx\ \frac{1}{a-\cos(x)} &= \frac{1}{\sqrt{1-a^2}}\Big[\ln|1|-\ln|-1|\Big] = 0
\end{aligned}
\tag{5.141}
$$

For the surface site, the Green's function for $\frac{\epsilon-\bar\epsilon}{2t}|>1$ is

$$
\begin{aligned}
\langle\pi_1|\hat G(\epsilon)|\pi_1\rangle &\overset{\text{Eq. 5.129}}{=} -\frac{1}{t}\left(\frac{b^3-b}{1-b^2}\right) = \frac{1}{t}b \\
&= \frac{1}{t}\frac{\epsilon-\bar\epsilon}{2t} \pm \sqrt{\left(\frac{\epsilon-\bar\epsilon}{2|t|}\right)^2-1} \quad \text{with } |\epsilon-\bar\epsilon|>|2t|
\end{aligned}
\tag{5.142}
$$

Now we combine the two regions of the self energy to

$$
\hat\Sigma(\epsilon) = |t|\begin{cases} |\pi_0\rangle\left[\frac{\epsilon-\bar\epsilon}{2t} + i\sqrt{1-\left(\frac{\epsilon-\bar\epsilon}{2t}\right)^2}\right]\langle\pi_0| & \text{for } |\epsilon-\bar\epsilon|<|2t| \\ |\pi_0\rangle\left[\frac{\epsilon-\bar\epsilon}{2|t|} \pm \sqrt{\left(\frac{\epsilon-\bar\epsilon}{2|t|}\right)^2-1}\right]\langle\pi_0| & \text{for } |\epsilon-\bar\epsilon|>|2t| \end{cases}
\tag{5.143}
$$

Editor: The sign of the hopping parameter is still inconsistent.

$$
\begin{aligned}
\left(G^{AA}(\epsilon)\right)^{-1} &= |\pi_0\rangle\left\{\epsilon-\bar\epsilon^A \pm t_A^2\bar G_{11}^{BB}\right\}\langle\pi_0|] \\
&= \begin{cases} |\pi_0\rangle\left[\epsilon-\bar\epsilon^A - t_A\left(\frac{\epsilon-\bar\epsilon}{2t} + i\sqrt{1-\left(\frac{\epsilon-\bar\epsilon}{2t}\right)^2}\right)\right]\langle\pi_0| & \text{for } |\epsilon-\bar\epsilon|<|2t| \\ |\pi_0\rangle\left[\epsilon-\bar\epsilon^A - t_A\left(\frac{\epsilon-\bar\epsilon}{2|t|} - \sqrt{\left(\frac{\epsilon-\bar\epsilon}{2|t|}\right)^2-1}\right)\right]\langle\pi_0| & \text{for } |\epsilon-\bar\epsilon|>|2t| \end{cases}
\end{aligned}
\tag{5.144}
$$

- For $|\epsilon-\bar\epsilon|<|2t|$ we obtain

$$
\hat G^{AA}(\epsilon) = |\chi_0\rangle\frac{1}{t_A}\left\{\frac{\frac{\epsilon-\bar\epsilon^A}{t_A} - \frac{\epsilon-\bar\epsilon}{2t} + i\sqrt{1-\left(\frac{\epsilon-\bar\epsilon}{2t}\right)^2}}{\left(\frac{\epsilon-\bar\epsilon^A}{t_A} - \frac{\epsilon-\bar\epsilon}{2t}\right)^2 + 1 - \left(\frac{\epsilon-\bar\epsilon}{2t}\right)^2}\right\}\langle\chi_0|
\tag{5.145}
$$

- For $|\epsilon - \bar{\epsilon}| > |2t|$ we obtain (This is still wrong!!!)

$$\hat{G}^{AA}(\epsilon) = |\chi_0\rangle \frac{1}{t_A} \left\{ \frac{1}{\frac{\epsilon-\bar{\epsilon}^A}{t_A} - \frac{\epsilon-\bar{\epsilon}}{2t} + \sqrt{\left(\frac{\epsilon-\bar{\epsilon}}{2t}\right)^2 - 1}} \right\} \langle\chi_0| \tag{5.146}$$

5.4.6 Fano-Anderson model

Introduction

Let us now investigate an adsorbate attached to the surface of the linear chain, which we investigated in the previous exercise of section 5.4.4. This leads us to the one-dimensional version of the well known **Fano-Anderson model** . The **Anderson model** is one of the prime models for systems with strong electron correlations. It describes an impurity with a large onsite interaction within a conductor. The **Fano model** is the non-interacting version of this impurity model, and this is what we wish to study.

The Fano model[15][68] describes an atom which is adsorbed on a metal. It demonstrates the broadening of an energy level when it couples to a continuum.

Editor: Check out

- Coherent Two-Dimensional Spectroscopy of a Fano Model'', by Daniel Finkelstein-Shapiro and Felipe Poulsen and Tõnu Pullerits and Thorsten Hansen, https://arxiv.org/pdf/1605.08572.pdf for introduction and references. See also ''Erratum: Coherent two-dimensional spectroscopy of a Fano model [Phys. Rev. B 94, 205137 (2016)]'' D Finkelstein-Shapiro, F Poulsen, T Pullerits, T Hansen Physical Review B 96 (23), 239906

- ''On the Ubiquity of Beutler-Fano Profiles: from Scattering to Dissipative Processes'' Daniel Finkelstein-Shapiro and Arne Keller, https://arxiv.org/pdf/1710.04800.pdf

- Non-linear Fano Interferences in Open Quantum Systems: an Exactly Solvable Model, https://arxiv.org/pdf/1509.04653.pdf

[15] This exercise follows Stefanucci and van Leeuwen[2], section 2.3.2.

Problem

The Fano model describes a spinless electron with the Hamiltonian

$$\hat{h} = \underbrace{\epsilon_d \hat{d}^\dagger \hat{d}}_{\hat{H}^{AA}} + \underbrace{\sum_{\vec{k}} \epsilon_{\vec{k}} \hat{c}_{\vec{k}}^\dagger \hat{c}_{\vec{k}}}_{\hat{H}^{BB}} + \underbrace{\sum_{\vec{k}} \left(V_{\vec{k}} \hat{d}^\dagger \hat{c}_{\vec{k}} + V_{\vec{k}}^* \hat{c}_{\vec{k}}^\dagger \hat{d} \right)}_{\hat{H}^{AB} + \hat{H}^{BA}} \tag{5.147}$$

The creation operator $\hat{d}^\dagger$ creates a particle on the impurity A. The creation operators $\hat{c}_{\vec{k}}^\dagger$ create particles in the bath B. The index $\vec{k}$ reminds of a Bloch vector, albeit here it can be any label identifying the bath states.
The Hamiltonian corresponds to a non-interacting many-particle system. The one-particle Green's function is an operator in the one-particle Hilbert space, even for a many-particle system. [a]For a non-interacting system, the Green's function is identical to that of the one-particle system.

1. Calculate the Hamilton matrix with elements $h_{\alpha,\beta}$.
2. Determine the bath Green's function. (The Green's function of the isolated system B.)
3. Determine the self energy due to coupling to the bath. Work out real and imaginary part of the self energy in the proximity of the real energy axis.
4. Determine the Green's function at the impurity, when it is coupled to the bath
5. Sketch the density of states at the impurity for two cases:
   - The impurity state lies within the spectrum of the bath
   - The impurity state lies outside the spectrum of the bath

   Consider a rectangular density of states of the bath with a width W and value $\frac{1}{W}$. Let the center of the density of states be $\bar{\epsilon}$. The hopping $V_{\vec{k}} = -t$ shall be constant.

[a]For a many-particle Hamiltonian $\hat{H}$ in Fock space, $(E\hat{1} - \hat{H})^{-1}$ is called **resolvent** rather than Green's function. The resolvent is an operator in Fock space.

Discussion

1. Calculate the Hamilton matrix with elements $h_{\alpha,\beta}$.

The Hamiltonian can be expressed as $\hat{h} = \sum_{\alpha,\beta} h_{\alpha,\beta} \hat{c}_\alpha^\dagger \hat{c}_\beta$ with

$$\boldsymbol{h} = \begin{pmatrix} \epsilon_d & \dots & V_{\vec{k}} & \dots \\ \vdots & \ddots & & 0 \\ V_{\vec{k}}^* & & \epsilon_{\vec{k}} & \\ \vdots & 0 & & \ddots \end{pmatrix} \tag{5.148}$$

The Hamilton operator in one-particle Hilbert space would be

$$\hat{h} = \sum_{\alpha,\beta} |\pi_\alpha\rangle h_{\alpha,\beta} \langle\pi_\beta| \tag{5.149}$$

where $\langle\pi_\alpha|$ are the projector functions for the set of orbitals $|\chi_\alpha\rangle$. In our case, the first orbital is

$|\chi_d\rangle$, while the remaining orbitals $|\chi_{\vec{k}}\rangle$ are Bloch waves in the bath, which are characterized by the Bloch-vector $\vec{k}$.

2. Determine the bath Green's function. (The Green's function of the isolated system B.)

The Green's function of the isolated bath is

$$\hat{\tilde{G}}^{BB}(\epsilon) \overset{\text{Eq. 5.7}}{=} \sum_{\vec{k}} |\chi_{\vec{k}}\rangle \frac{1}{\epsilon - \epsilon_{\vec{k}}} \langle \chi_{\vec{k}}| \tag{5.150}$$

3. Determine the self energy due to coupling to the bath. Work out real and imaginary part of the self energy in the proximity of the real energy axis.

The self energy is

$$\hat{\Sigma}^{AA}(\epsilon) \overset{\text{Eq. 5.34}}{=} \hat{V}^{AB}\hat{\tilde{G}}^{BB}(\epsilon)\hat{V}^{BA} = |\pi_d\rangle \left(\sum_{\vec{k}} \frac{|V_{\vec{k}}|^2}{\epsilon - \epsilon_{\vec{k}}} \right) \langle \pi_d| \tag{5.151}$$

4. Determine the Green's function at the impurity, when it is coupled to the bath

In the complex plane, the Green's function is

$$\hat{G}^{AA}(\epsilon) \overset{\text{Eq. 5.33}}{=} \Big(\underbrace{|\pi_d\rangle(\epsilon - \epsilon_d)\langle\pi_d|}_{\hat{\tilde{G}}^{AA}(\epsilon)} - \hat{\Sigma}^{AA}(\epsilon) \Big)^{-1} \qquad \text{for } \mathrm{Im}(\epsilon) > 0 \tag{5.152}$$

The retarded Green's function is only defined in the half-plane with positive imaginary part of the energy.Editor: refer to where this has been discussed [16]

On the real energy axis,

$$\hat{G}^{AA}(\epsilon) \overset{\text{Eq. 5.33}}{=} \lim_{\eta\to 0^+} \Big(\underbrace{|\pi_d\rangle(\epsilon + i\eta - \epsilon_d)\langle\pi_d|}_{\hat{\tilde{G}}^{AA}(\epsilon+i\eta)} - \hat{\Sigma}^{AA}(\epsilon + i\eta) \Big)^{-1} \qquad \text{for } \epsilon \in \mathbb{R} \tag{5.153}$$

Let me divide the self energy Eq. 5.151 into real part Λ and imaginary part Γ.

$$\hat{\Sigma}^{AA}(\epsilon) = |\pi_d\rangle \Big(\Lambda(\epsilon) + i\Gamma(\epsilon) \Big) \langle \pi_d| \qquad \text{for } \mathrm{Im}(\epsilon) > 0 \tag{5.154}$$

Right on the real axis, the self energy is real-valued, but also ill defined, because the imaginary part of the self energy is discontinuous as one crosses the real energy axis. Because we are interested in the retarded Green's function, we need to select a positive imaginary part of the energy, where the self energy is complex-valued.

[16] The retarded Green's function $G(t_2, t_1) = 0$ vanishes for $t_2 < t_1$. The energy-dependent Green's function is linked to the energy-dependent Green's function via Eq. 4.20 $\hat{G}(\epsilon, t_1) = \int_{-\infty}^{\infty} dt_2 \hat{G}(t_2, t_1) \mathrm{e}^{\frac{i}{\hbar}\epsilon(t_2 - t_1)}$.

The Green's function is[17]

$$\begin{aligned}\hat{G}^{AA}(\epsilon) &= \Big(|\pi_d\rangle\Big(\epsilon-\epsilon_d-\Lambda(\epsilon)-i\Gamma(\epsilon)\Big)\langle\pi_d|\Big)^{-1}\\ &= |\chi_d\rangle\Big(\epsilon-\epsilon_d-\Lambda(\epsilon)-i\Gamma(\epsilon)\Big)^{-1}\langle\chi_d|\\ &= |\chi_d\rangle\frac{\epsilon-\epsilon_d-\Lambda(\epsilon)+i\Gamma(\epsilon)}{\Big(\epsilon-\epsilon_d-\Lambda(\epsilon)\Big)^2+\Gamma^2(\epsilon)}\langle\chi_d| \end{aligned} \tag{5.157}$$

The imaginary part of the self energy is connected[18] to the density of states of the isolated system B weighted with the coupling parameters $|V_{\vec{k}}|^2$ to system A.

$$\lim_{\eta\to 0^+}\Gamma(\epsilon+i\eta)=\lim_{\eta\to 0^+}\mathrm{Im}\left(\sum_{\vec{k}}\frac{|V_{\vec{k}}|^2}{\epsilon+i\eta-\epsilon_{\vec{k}}}\right)\overset{\text{Eq. A.25}}{=}-\pi\sum_{\vec{k}}|V_{\vec{k}}|^2\delta(\epsilon-\epsilon_{\vec{k}}) \tag{5.158}$$

I used Eq. A.25 on p. 504, $\lim_{\eta\to 0^+}\mathrm{Im}(1/(x+i\eta))=-\pi\delta(x)$.

5. Sketch the density of states at the impurity for two cases:
   - The impurity state lies within the spectrum of the bath
   - The impurity state lies outside the spectrum of the bath

   Consider a rectangular density of states of the bath with a width W and value $\frac{1}{W}$. Let the center of the density of states be $\bar{\epsilon}$. The hopping $V_{\vec{k}}=-t$ shall be constant.

The density of states projected onto the atomic orbital of subsystem A is obtained via Eq. 4.54 from[19]

[17] The inverse of an operator $\hat{A}=\sum_{\alpha,\beta}|\pi_\alpha\rangle A_{\alpha,\beta}\langle\pi_\beta|$ is

$$\hat{A}^{-1}=\sum_{\gamma,\delta}|\chi_\gamma\rangle\left(A^{-1}\right)_{\gamma,\delta}\langle\chi_\delta| \tag{5.155}$$

Here, the $\langle\pi_\alpha|$ are the projector functions for the orbitals $|\chi_\alpha\rangle$, which obey the bi-orthogonality condition $\langle\pi_\alpha|\chi_\beta\rangle=\delta_{\alpha,\beta}$. The projector functions can be written as $\langle\pi_\alpha|=\sum_\beta S^{-1}_{\alpha,\beta}\langle\chi_\beta|$, when both span the same Hilbert space. With these definitions, we can test the form of the inverse. We need to show $\hat{A}\hat{A}^{-1}=\hat{1}$.

$$\begin{aligned}\hat{1}&\overset{!}{=}\underbrace{\sum_{\alpha,\beta}|\pi_\alpha\rangle A_{\alpha,\beta}\langle\pi_\beta|}_{\hat{A}}\underbrace{\sum_{\gamma,\delta}|\chi_\gamma\rangle\left(A^{-1}\right)_{\gamma,\delta}\langle\chi_\delta|}_{\hat{A}^{-1}}=\sum_{\alpha,\beta}\sum_{\gamma,\delta}|\pi_\alpha\rangle A_{\alpha,\beta}\underbrace{\langle\pi_\beta|\chi_\gamma\rangle}_{\delta_{\beta,\gamma}}\left(A^{-1}\right)_{\gamma,\delta}\langle\chi_\delta|\\ &=\sum_{\alpha,\delta}|\pi_\alpha\rangle\underbrace{\sum_\beta A_{\alpha,\beta}\left(A^{-1}\right)_{\beta,\delta}}_{\delta_{\alpha,\delta}}\langle\chi_\delta|=\sum_\alpha|\pi_\alpha\rangle\langle\chi_\alpha|=\sum_{\alpha,\beta}|\chi_\beta\rangle S^{-1}_{\beta,\alpha}\langle\chi_\alpha|=\hat{1}\qquad q.e.d\end{aligned} \tag{5.156}$$

[18] The imaginary part of the Green's function of system B is related to its density of states and the self energy is the Green's function times the coupling of the subsystems.

[19] The matrix element is formed with the projector functions $|\pi_d\rangle$ rather than with the orbitals $|\chi_d\rangle$. For an orthonormal set like ours the two can be chosen identical. We have chosen the projector function, because this is the correct choice also for a non-orthonormal basisset. The convention is that matrix elements of observables a built with the orbitals $|\chi\rangle$ and act with the projector functions onto states. The density of states is, like the density matrix, not an observable but it describes a state. Therefore, the matrix elements are build with the projector functions and they act with the orbitals onto observables.

p. 179.

$$\begin{aligned} D_d(\epsilon) &\overset{\text{Eq. 4.54}}{=} -\frac{1}{\pi}\lim_{\eta\to 0^+}\mathrm{Im}\big[\langle\pi_d|\hat{G}(\epsilon+i\eta)|\pi_d\rangle\big] \qquad \text{for } \epsilon\in\mathbb{R} \\ &\overset{\text{Eq. 5.154}}{=} -\frac{1}{\pi}\mathrm{Im}\left[\Big(\epsilon-\epsilon_d-\Lambda(\epsilon)-i\Gamma(\epsilon)\Big)^{-1}\right] \\ &= -\frac{1}{\pi}\left[\frac{\Gamma(\epsilon)}{\Big(\epsilon-\epsilon_d-\Lambda(\epsilon)\Big)^2+\Gamma^2(\epsilon)}\right] \\ &= \frac{1}{\pi}\frac{-\Gamma(\epsilon)}{\Big(\epsilon-\epsilon_d-\Lambda(\epsilon)\Big)^2+\Gamma^2(\epsilon)} \end{aligned} \tag{5.159}$$

Constant density of states in the bath: Let me start the discussion with the most simple case, namely that the self energy is a constant, i.e. energy-independent. Hence, also Λ and Γ are constants. The resulting density of states $D_d(\epsilon)$ of system A in contact with B is a Lorentzian centered at $\epsilon_d+\Lambda$ with a width proportional to $|\Gamma|$. This shows that an energy level broadens, when it is coupled to a continuum of states. The width of the resulting peak is the **life-time broadening**. Its inverse is related to the time, for which the particle remains in system A before it is scattered into the environment, namely system B. The position of the Lorentzian is shifted by the **quasi-particle shift** $\mathrm{Re}\Sigma=\Lambda$ away from the original position of the d-level.

Box-shaped bath density of states: Let me now investigate the next more realistic case: The bath shall have a box-shaped density of states with a finite with. The coupling $V_{\vec{k}}$ shall be, again, constant, i.e. $V_{\vec{k}}=-t$.

$$D^B(\epsilon)=\sum_{\vec{k}}\delta(\epsilon-\bar{\epsilon}_{\vec{k}})=\begin{cases}\frac{1}{W} & \text{for } \bar{\epsilon}-\frac{1}{2}W<\epsilon<\bar{\epsilon}+\frac{1}{2}W\\ 0 & \text{else}\end{cases} \tag{5.160}$$

The result for density of states projected onto the impurity is shown in the lower graph[20] of Fig. 5.5. In the following, I will discuss this figure. Let me consider two limiting cases.

- If the coupling t is small compared to the band width W of system B, we can approximate the system by the limit of infinite band width of system B. In that case, the situation is close to the case of a constant self energy discussed before. The resulting density of states $D_d(\epsilon)$ on system A is a Lorentzian with a life-time broadening that grows with the coupling t between the two systems.
- If the coupling t is large compared to the band width W of system B, the band width of system B can be neglected and system B can be approximated by a single energy level at the center of the band. The situation is close to the case of a dimer, where one atom is the system A and the other is system B. The density of states has one bonding level at low energies and an antibonding level at high energies. For the degenerate case $\bar{\epsilon}_d-\bar{\epsilon}\ll t$ the weight of the two peaks on system A will be similar. In the non-degenerate limit $\bar{\epsilon}_d-\bar{\epsilon}\gg t$, the weight of the state, which is closer to the d-level, will be dominant compared to the other, which is further away.

[20] The graph Fig. 5.5 shows the density of state D_d shifted by $15t$ for better visibility.

$$\begin{aligned} D_d(\epsilon) &= -\frac{1}{\pi}\mathrm{Im}\Big[\frac{1}{\epsilon-\epsilon_d+i\eta+\frac{t^2}{W}\ln\left(\frac{\epsilon-\frac{1}{2}W+i\eta}{\epsilon+\frac{1}{2}W+i\eta}\right)}\Big] \\ \epsilon_d &= \frac{1}{4}; \qquad W=1; \qquad \eta=0.01; \qquad t\in\{0,\frac{1}{10},\frac{2}{10},\frac{3}{10},\frac{4}{10},\frac{5}{10},\frac{6}{10},\frac{7}{10}\} \end{aligned} \tag{5.161}$$

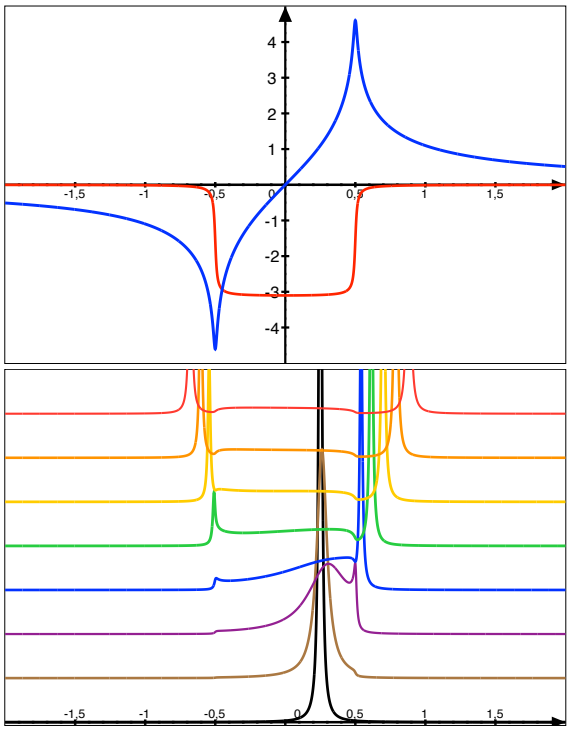
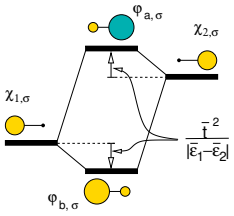


Fig. 5.5: Upper graph: Real part (blue) and imaginary part (red) of the bath Green's function $\bar{G}^{BB}(\epsilon) = -\frac{1}{W}\ln(\frac{\epsilon - W/2 + i\eta}{\epsilon + W/2 + i\eta})$ for $\eta = 0.01$ and $W = 1$ with a constant density of states $D(\epsilon) = 1$ in the energy window between $-\frac{1}{2} \leq \epsilon \leq \frac{1}{2}$. Lower graph: Density of states at atom A in contact with the bath B for $\epsilon_d = \frac{1}{4}$ and hopping parameters $t \in \{0, \frac{1}{10}, \ldots, \frac{7}{10}\}$.

Let me now walk you through the individual results in figure 5.5 step by step: For small hopping $t = 0.1$ the density of states of the d-level broadens due to the hybridization with the bath. As the coupling increases, the d-level broadens further. A peak emerges beyond the band of the bath, which inherits the life time from the original energy level. Also at the lower end of the bath spectrum a second peak emerges. The two peaks correspond to the bonding states and the antibonding states between the two systems. The weight that enters into the separated peaks i removed from the density of states in within the spectrum of the bath.

Analogy with the dimer: I find it useful to rationalize the findings considering one bath state at a time. A pair of states is analogous to the di-atomic molecule investigated in exercises 1.5.1 and 1.5.2. For the following discussion, I recommend to inspect figure 1.4 on p. 30, which I am repeating here for your convenience.



Let me identify the orbital $|\chi_1\rangle$ on the left atom with the impurity A, and the orbital $|\chi_2\rangle$ on the right with the bath B. Let me leave the obvious level repulsion aside and let us focus on the wave functions. As the two states $|\chi_1\rangle$ and $|\chi_2\rangle$ hybridize and form the bonding and antibonding states.

Some weight from site A is transferred from the bonding to the antibonding state. That is, also the antibonding state $|\varphi_a\rangle$ has a contribution from $|\chi_1\rangle$. The density of states projected onto the impurity has a large contribution at the energy of the impurity level and a smaller contribution at the energy of the bath level. The charge sum rule ensures that the total weight from the impurity is still equal to unity. When we take many bath states into account in a similar way, we will notice that the density of states projected onto the impurity is smeared out. Because the hybridization becomes smaller when the initial levels are more distant, the density of states is peaked close to the position of the original impurity level and it falls of further away. This effect is the **life-time broadening**.

Editor: Why is it called life-time broadening? Imagine a wave function which is completely localized on the impurity site A. If the impurity is coupled to the bath, the initial state is not an eigenstate of the combined system. The wave function is

$$|\psi(t)\rangle = \sum_{n\in\{a,b\}} |\varphi_n\rangle e^{-\frac{i}{\hbar}\epsilon_n t}\langle\varphi_n|\chi_1\rangle \tag{5.162}$$

The time-dependent probability on site A is thus... Editor: This argument needs to be completed

Editor: Are the limiting cases covered? (1) impurity level in the continuum of bath states. (2) impurity level separated far from the bath states. (3) strong coupling: impurity and surface site form a dimer, which is weakly coupled to the continuum.

Sanity check: Correspondence with Fano's paper

Editor: This section is not meant for the reader.

The exercise presented here is closely connected to the original paper by Fano[68]. As a sanity check of the derivations, am adding here a one-to-one correspondence of the most relevant equations from Fano's paper and the formulas above.

1. Fano-Eq.2 is Eq. 5.1

$$\begin{aligned} |\Psi_E\rangle &= |\varphi\rangle a + \int d\epsilon'\, |\psi_{E'}\rangle b(E') \qquad \text{Fano-Eq.2} \\ |\psi\rangle &= |\chi^A\rangle c^A + \sum_{\beta\in B} |\chi^B_\beta\rangle c^B_\beta \qquad \text{This text Eq. 5.1} \end{aligned} \tag{5.163}$$

2. Fano-Eq.3a,b is my Eq. 5.3. The definitions $E_\varphi = \langle\varphi|\hat{H}|\varphi\rangle$ and $V_E = \langle\varphi|\hat{H}|\psi(E)\rangle$ are used.

$$\begin{aligned} \langle\varphi|\Big(\hat{H} - E\hat{1}\Big)\Big(|\varphi\rangle a + \int dE'\, |\psi(E')\rangle b(E')\Big) &= 0 \\ \Rightarrow \qquad (E_\varphi - E)a + \int dE'\, V^*_{E'} b(E') &= 0 \qquad \text{Fano-Eq.3a} \\ \langle\psi_{E''}|\Big(\hat{H} - E\hat{1}\Big)\Big(|\varphi\rangle a + \int dE'\, |\psi(E')\rangle b(E')\Big) &= 0 \\ \Rightarrow \qquad V_{E''} a + \int dE'\, (E'' - E)\delta(E'' - E') b(E') &= 0 \\ \Rightarrow \qquad V_{E'} a + (E' - E) b(E') &= 0 \qquad \text{Fano-Eq.3b} \end{aligned} \tag{5.164}$$

3. Fano-Eq.4 is my Eq. 5.6.

$$\begin{aligned} b_{E'} &= \left[\frac{1}{E - E'} + z(E)\delta(E - E')\right] V_{E'} a \qquad \text{Fano-Eq.4} \\ \vec{c}^B &= (\epsilon \mathbf{1}^{BB} - \boldsymbol{H}^{BB})^{-1} \boldsymbol{V}^{BA} \vec{c}^A \qquad \text{This work Eq. 5.6} \end{aligned} \tag{5.165}$$

Fano introduces the quantity $z(E)$. Fano refers to the PhD thesis of van Kampen[70]. (Check chapter 6, p 50). We may add to $\vec{c}^B$ any state from the bath, for which $(\epsilon \mathbf{1}^{BB} - \boldsymbol{H}^{BB})\vec{c}^B = 0$. This solution of the homogeneous equation is described by Fano by adding $z(E)$

Fano obtains $z(E)$ by inserting his Eq.4 into his Eq.3a.

$$\begin{aligned} E_\varphi a + \int dE'\, V^*_{E'} \left[\frac{1}{E-E'} + z(E)\delta(E-E') \right] V_{E'} a = Ea \\ E_\varphi + \left(\int dE'\, \frac{|V_{E'}|^2}{E-E'} \right) + z(E)|V_E|^2 = E \\ z(E) = \frac{1}{|V_E|^2} \left(E - E_\varphi + \int dE'\, \frac{|V_{E'}|^2}{E-E'} \right) \qquad \text{Fano-Eq.9 with Fano-Eq.8} \end{aligned} \tag{5.166}$$

Let me repeat this in my notation

$$\begin{aligned} \Big(\boldsymbol{H}^{AA} - \epsilon \mathbf{1}^{AA} \Big) \vec{c}^A + V^{AB} \vec{c}^B = 0 \\ \Big(\boldsymbol{H}^{AA} - \epsilon \mathbf{1}^{AA} \Big) \vec{c}^A + V^{AB} \left[(\epsilon \mathbf{1}^{BB} - \boldsymbol{H}^{BB})^{-1} \boldsymbol{V}^{BA} \vec{c}^A + \vec{c}^{B,hom} \right] = 0 \\ \Big(\boldsymbol{H}^{AA} - \epsilon \mathbf{1}^{AA} + V^{AB} (\epsilon \mathbf{1}^{BB} - \boldsymbol{H}^{BB})^{-1} \boldsymbol{V}^{BA} \Big) \vec{c}^A + V^{AB} \vec{c}^{B,hom} = 0 \end{aligned} \tag{5.167}$$

Let me now write $\vec{c}^{B,hom} = \boldsymbol{V}^{AB} \boldsymbol{z}(E) \boldsymbol{V}^{\boldsymbol{BA}} \vec{c}^A$.

$$\begin{aligned} \Big(\boldsymbol{H}^{AA} - \epsilon \mathbf{1}^{AA} + \boldsymbol{V}^{AB} (\epsilon \mathbf{1}^{BB} - \boldsymbol{H}^{BB})^{-1} \boldsymbol{V}^{BA} \Big) \vec{c}^A + \boldsymbol{V}^{AB} \boldsymbol{z} \boldsymbol{V}^{BA} \vec{c}^A = 0 \\ \boldsymbol{V}^{AB} \boldsymbol{z} \boldsymbol{V}^{BA} = - \Big(\boldsymbol{H}^{AA} - \epsilon \mathbf{1}^{AA} + \boldsymbol{V}^{AB} (\epsilon \mathbf{1}^{BB} - \boldsymbol{H}^{BB})^{-1} \boldsymbol{V}^{BA} \Big) \end{aligned} \tag{5.168}$$

$$\begin{aligned} |\Psi_E\rangle &= |\varphi\rangle + \int dE'\, |\psi_{E'}\rangle \frac{|V_{E'}|^2}{E-E'} + \int dE'\, |\psi_{E'}\rangle V^*_{E'} z(E) \delta(E-E') V_{E'} \\ &= |\varphi\rangle + \int dE'\, |\psi_{E'}\rangle \frac{|V_{E'}|^2}{E-E'} + |\psi_E\rangle V^*_E z(E) V_E \\ &= |\varphi\rangle + \int dE'\, |\psi_{E'}\rangle \frac{|V_{E'}|^2}{E-E'} - |\psi_E\rangle \underbrace{\left(E - E_\varphi - \int dE'\, \frac{|V_{E'}|^2}{E-E'} \right)}_{|V_E|^2 z(E)} \end{aligned} \tag{5.169}$$

$$\begin{aligned} |\Psi(E)\rangle &= |\varphi\rangle + \int dk\, |\psi_k\rangle \frac{|V_k|^2}{E-E_k} + \int dk\, |\psi_k\rangle |V_k|^2 z(k) \delta(E-E_k) \\ &= |\varphi\rangle + \int dk\, |\psi_k\rangle \frac{|V_k|^2}{E-E_k} + |\psi_{k(E)}\rangle V^*_{k(E)} z(E) V_{k(E)} \\ &= |\varphi\rangle + \int dk\, |\psi_k\rangle \frac{|V_k|^2}{E-E_k} - |\psi_{k(E)}\rangle \underbrace{\left(E - E_\varphi - \int dk\, \frac{|V_k|^2}{E-E_k} \right)}_{|V_{k(E)}|^2 z(E(k))} \\ &= |\varphi\rangle + |\psi_{k(E)}\rangle \Big(E - E_\varphi \Big) + \int dk\, \Big(|\psi_k\rangle - |\psi_{k(E)}\rangle \Big) \frac{|V_k|^2}{E-E_k} \end{aligned} \tag{5.170}$$

Fano-Anderson model by direct diagonalization

Editor: This is not finished. It is not meant for the reader.

In this section, I perform a numerical calculation on the Fano model with a finite number of bath states. The goal is to explore in detail, how the surface states separate from the continuum.

Editor: Caution: Here, I am using the symbol $\bar{\epsilon}_a$, rather than $\bar{\epsilon}_d$ used before.

I start from the Hamiltonian

$$\begin{aligned}\hat{h} &= |\pi_a\rangle\bar{\epsilon}_a\langle\pi_a| + \sum_k |\pi_k\rangle\bar{\epsilon}_k\langle\pi_k| + \sum_k \Big(|\pi_a\rangle V_k\langle\pi_k| + |\pi_k\rangle V_k^*\langle\pi_a|\Big)\\ \hat{h} &= \bar{\epsilon}_a\hat{c}_a^\dagger\hat{c}_a + \sum_k \bar{\epsilon}_k\hat{c}_k^\dagger\hat{c}_k + \sum_k \Big(V_k\hat{c}_a^\dagger\hat{c}_k + V_k^*\hat{c}_k^\dagger\hat{c}_a\Big)\\ &= \begin{pmatrix}\hat{c}_a^\dagger\\ \hat{c}_1^\dagger\\ \hat{c}_2^\dagger\\ \vdots\end{pmatrix}\begin{pmatrix}\bar{\epsilon}_a & V_1 & V_2 & \cdots\\ V_1^* & \bar{\epsilon}_1 & 0 & \cdots\\ V_2^* & 0 & \bar{\epsilon}_2 & \cdots\\ \vdots & \vdots & \vdots & \vdots\end{pmatrix}\begin{pmatrix}\hat{c}_a\\ \hat{c}_1\\ \hat{c}_2\\ \vdots\end{pmatrix}\end{aligned} \tag{5.171}$$

The first Hamiltonian in the equation above is a one-particle Hamiltonian, while the second, despite using the same symbol, is a one-particle-at-a-time Hamiltonian, which acts in Fock space.

Eigenvalues The characteristic equation is

$$\Big(\bar{\epsilon}_a - \epsilon - \sum_k \frac{|V_k|^2}{\bar{\epsilon}_k - \epsilon}\Big)\prod_k(\bar{\epsilon}_k - \epsilon) = 0 \Rightarrow \qquad \epsilon - \bar{\epsilon}_a - \overbrace{\sum_k \frac{|V_k|^2}{\epsilon - \bar{\epsilon}_k}}^{\Sigma(\epsilon)} = 0 \tag{5.172}$$

The zeros of the function determine the positions of the eigenstates.

It is convenient to take the arcus tangens of this function to avoid the infinities. We name the resulting function $y(\epsilon)$

$$y(\epsilon) \stackrel{\text{def}}{=} -\frac{1}{\pi}\arctan\left(\sum_k \frac{V_k^2}{\epsilon - \bar{\epsilon}_k} + \bar{\epsilon}_a - \epsilon\right) \tag{5.173}$$

This function is shown in figure 5.6 for the case at hand.

To be concrete, let me choose a specific coupling V_k between bath and impurity: The system B shall be a metallic system with band edges at A and B. The squared coupling parameters shall sum up to t, an effective hopping parameter. First an energy-dependent coupling parameter $V(\epsilon)$ is defined. It has the shape of an inverted parabola, with zeros at the band edges and with the desired norm $\int_A^B d\epsilon\, V^2(\epsilon) = t$. Then we choose a specific number M of bath sites and obtain the coupling parameters as $V_k^2 = \frac{1}{M}V(\epsilon_k)$

The bare energies $\bar{\epsilon}_k$ of the bath sites are placed on an equi-spaced grid with $M-1$ points with $A < \bar{\epsilon}_k < B$. (The value $\bar{\epsilon}_M = B$ does not contribute, because $V_M = 0$.)

$$\begin{aligned}\bar{\epsilon}_k &= A + (B-A)\frac{k}{M}\\ V_k &= t\sqrt{\frac{(\bar{\epsilon}_k - A)(B - \bar{\epsilon}_k) + 10^{-3}}{-AB(B-A) - \frac{1}{3}(B^3 - A^3) + \frac{1}{2}(B^2 - A^2)(A+B)}}\end{aligned} \tag{5.174}$$

A good guidance is obtained by an approximation of the real system, where the continuum of states is replaced by a single state at $\bar{\epsilon}_b$, the center of gravity of the spectrum of system B,

$$\bar{\epsilon}_b = \frac{\sum_k |V_k|^2\bar{\epsilon}_k}{\sum_k |V_k|^2}\,, \tag{5.175}$$

with a hopping term equal to $t = \frac{1}{M}\sum_{k=1}^M V_k^2$.

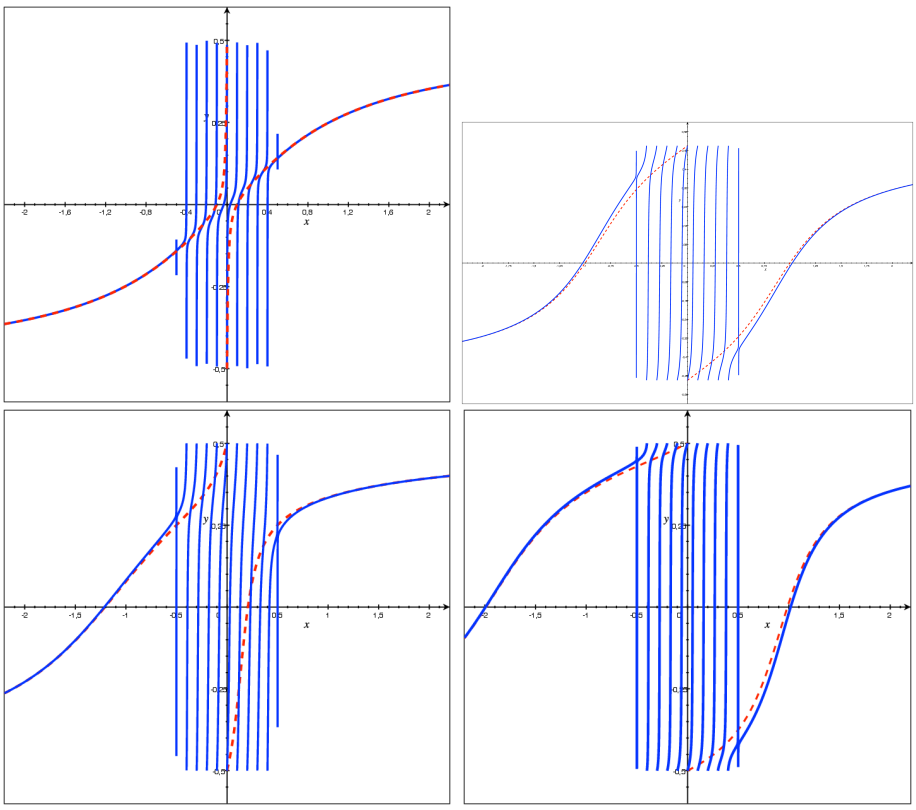


Fig. 5.6: $y(\epsilon) = -\frac{1}{\pi}\arctan\left(\frac{1}{M}\sum_{j=1}^{M}\frac{V^2(\epsilon_j)}{\epsilon-\bar{\epsilon}_k} + \bar{\epsilon}_a - \epsilon\right)$ as function of energy. The dashed line replaces the "continuum" by a single state in its center. (1) $\bar{\epsilon}_a = 0$, $t = 0.2$, $A = -0.5$, $B = 0.5$, $M = 10$ Bonding and antibonding states with the impurity inside the continuum. (2) $\bar{\epsilon}_a = 0$, $t = 1$, $A = -0.5$, $B = 0.5$, $M = 10$ Bonding and antibonding states with the impurity outside the continuum. (3) $\bar{\epsilon}_a = -1$, $t = 0.5$, $A = -0.5$, $B = 0.5$, $M = 10$ (3) $\bar{\epsilon}_a = -1$, $t = 0.5$, $A = -0.5$, $B = 0.5$, $M = 10$ (4) $\bar{\epsilon}_a = -1$, $t = 1.4$, $A = -0.5$, $B = 0.5$, $M = 10$

The eigenstates of the approximate system are determined by the zeros of the function $\bar{y}(\epsilon)$, which is shown as dashed red line

$$\bar{y}(\epsilon) = -\frac{1}{\pi}\arctan\left(\frac{t^2}{\epsilon - \frac{1}{2}(A+B)} + \bar{\epsilon}_a - \epsilon\right) \tag{5.176}$$

whose zeros describe the eigenstates of the approximate system shown in figure 5.6.

There are three possible cases

- Weak coupling: bonding and antibonding state of the two-state problem lie in the continuum. The impurity level is broadened into a resonance inside the continuum.
- one of the two states of the two-state problem lies inside the continuum and the other outside.
- Strong coupling: the bonding state of the two-state problem lies below the continuum and a the antibonding state lies outside. Two sharp states lie outside the continuum.

Level repulsion by the impurity level displaces the energy levels in the continuum, but the continuum levels cannot be displaced beyond the neighboring energy level. Thus, the displacement in the continuum is of order $\frac{1}{M}$. In the limit $M \to \infty$, the displacement approaches zero, but the overall

displacement of the weight $\sim M\frac{1}{M}$ remains finite. This is also important to satisfy the sumrule that the trace of the Hamiltonian is invariant under unitary transformation, which says that the sum of the energy levels is equal to the trace.

Eigenstates

$$|\psi\rangle = |\chi_a\rangle a + \sum_k |\chi_k\rangle b_k$$
$$(\hat{h}-\epsilon)|\psi\rangle = |\chi_a\rangle \underbrace{\Big((\bar{\epsilon}_a-\epsilon)a + \sum_k V_k b_k\Big)}_{(A)} + \sum_k |\varphi_k\rangle \underbrace{\Big(V_k a + (\bar{\epsilon}_k-\epsilon)b_k\Big)}_{(B)} \stackrel{!}{=} 0 \qquad (5.177)$$

This equation can only be satisfied at the zeros of the characteristic equation, respectively of $y(\epsilon)$, defined earlier.

Let me satisfy the equation above by finding the zeros of (B) and then of (A).

$$\underbrace{V_k a + (\bar{\epsilon}_k-\epsilon)b_k}_{(B)} = 0 \qquad \Rightarrow \qquad b_k = \frac{1}{\epsilon-\bar{\epsilon}_k} V_k a$$
$$|\psi\rangle = \Big[|\chi_a\rangle + \sum_k |\varphi_k\rangle \frac{1}{\epsilon-\bar{\epsilon}_k} V_k\Big] a = \frac{|\chi_a\rangle + \sum_k |\varphi_k\rangle \frac{1}{\epsilon-\bar{\epsilon}_k} V_k}{\sqrt{1+\sum_k \frac{|V_k|^2}{(\epsilon-\bar{\epsilon}_k)^2}}} \qquad (5.178)$$

The second equation,

$$0 = \underbrace{(\bar{\epsilon}_a-\epsilon)a + \sum_k V_k b_k}_{(A)} = \Big[(\bar{\epsilon}_a-\epsilon) + \underbrace{\sum_k V_k \frac{1}{\epsilon-\bar{\epsilon}_k} V_k}_{\Sigma(\epsilon)}\Big] a\,, \qquad (5.179)$$

is, in essence, identical to the characteristic equation and determines the positions of the energy levels of the combined system.

The energy of the impurity level in contact with system B is estimated by a Taylor expansion of (A) about the bare impurity level $\bar{\epsilon}_a$

$$0 = (\bar{\epsilon}_a-\epsilon) + \underbrace{\sum_k V_k \frac{1}{\bar{\epsilon}_a-\bar{\epsilon}_k} V_k}_{\Sigma(\bar{\epsilon}_a)} - \underbrace{\sum_k V_k \frac{1}{(\bar{\epsilon}_a-\bar{\epsilon}_k)^2} V_k}_{\partial_\epsilon \Sigma(\bar{\epsilon}_a)} (\epsilon-\bar{\epsilon}_a) + O(\epsilon-\bar{\epsilon}_a)^2$$
$$\epsilon = \bar{\epsilon}_a + \frac{\Sigma(\bar{\epsilon}_a)}{1+\partial_\epsilon|_{\bar{\epsilon}_a}\Sigma} \qquad \text{for small } |\epsilon-\bar{\epsilon}_a| \qquad (5.180)$$

This energy is the next zero of the characteristic polynomial, respectively of $y(\epsilon)$, which lies next to $\bar{\epsilon}_a$. In the continuum limit for the spectrum of subsystem B, the energy derivative of the self energy approaches infinity inside the spectrum of B. This result is not meaningful. Thus, the expression above provides an approximation for the shift of the impurity level, only if the bare level lies outside the spectrum of system B.

Editor: This is open ended...

5.4.7 Construction: Downfold the positronic degrees of freedom in the Dirac equation

Editor: This is only a collection of stuff to formulate a problem later.

Electrons are described by the Dirac equation which describes an electron by a four-component spinor wave function.

$$\left(\gamma^\mu i\hbar\partial_\mu - mc\right)\psi(\vec{x}) = 0 \tag{5.181}$$

with

$$\gamma^0 = \begin{pmatrix} \mathbf{1} & \mathbf{0} \\ \mathbf{0} & -\mathbf{1} \end{pmatrix} \qquad \text{and} \qquad \gamma^j = \begin{pmatrix} \mathbf{0} & \boldsymbol{\sigma}_j \\ -\boldsymbol{\sigma}_j & \mathbf{0} \end{pmatrix} \tag{5.182}$$

Minimal coupling

$$E \to E - q\Phi \tag{5.183}$$
$$\vec{p} \to \vec{p} - q\vec{A} \tag{5.184}$$

$$\epsilon \stackrel{\text{def}}{=} E - m_0 c^2 \tag{5.185}$$
$$M \stackrel{\text{def}}{=} m_0 + \frac{\epsilon - q\Phi}{2c^2} \tag{5.186}$$

$$\begin{pmatrix} q\Phi - \epsilon & \sum_{j\in\{x,y,z\}} \sigma_j(p_i - qA_i)c \\ \sum_{j\in\{x,y,z\}} \sigma_j(p_i - qA_i)c & -2Mc^2 \end{pmatrix} \begin{pmatrix} |\phi\rangle \\ |\chi\rangle \end{pmatrix} = 0 \tag{5.187}$$

$$(\vec{\boldsymbol{\sigma}}\vec{A})(\vec{\boldsymbol{\sigma}}\vec{B}) = \mathbf{1}\vec{A}\vec{B} + i\vec{\boldsymbol{\sigma}}(\vec{A}\times\vec{B}) \tag{5.188}$$

5.4.8 Construction: Inelastic tunneling

Editor: Skip this. It is only a sketch

M. Galperin and MarC Ratner and Nitxzan, Arxiv, *Inelastic electromn tunneling spectroscopy in molecular junctions: Peaks and dips*
S. Tikhodeev et al. Surf. Sci. 493,63 (2001)
T. Mii, S. Tikhodeev et al., Surf. Sci. 502-503, 26 (2002)
B.N.J. Persson and A. Baratovv, PRL 59,339 (1987)
B.N.J. Persson, Physica Scripta 38, 282 (1988)
A. Baratoff and Persson, J. Vacuum Science and Technology A 6, 331 (1988)

Consider an electron traveling along a Hubbard chain, which interacts on a single site with a two-state system. The two-site system could be any system that may accept from or donate energy to the traveling electron.

The Hamiltonian of the Hubbard chain is

$$H_{i,j}^{AA} = \begin{cases} t & \text{for } j = i \pm 1 \\ 0 & \text{else} \end{cases} \tag{5.189}$$

The two-state system has the Hamiltonian

$$\boldsymbol{H}^{BB} = \begin{pmatrix} 0 & 0 \\ 0 & \Delta \end{pmatrix} \tag{5.190}$$

The only non-zero element of the coupling is $V_{0,2}^{AB} = \lambda$.

Solution:

$$\boldsymbol{G}^{BB}(\epsilon) = \begin{pmatrix} \frac{1}{\epsilon} & 0 \\ 0 & \frac{1}{\epsilon - \Delta} \end{pmatrix} \tag{5.191}$$

The retarded potential has the form

$$\boldsymbol{\Sigma}_{0,0}^{AA} = \frac{\lambda^2}{\epsilon - \Delta} \tag{5.192}$$

Chapter 6

Dynamics in Fock space and complex time

In this chapter, we step again into many-particle physics. We prepare the ground the unified formulation of Green's functions in many-particle physics, namely the original ground-state Green's functions for spectroscopy, temperature (Matsubara) Green's functions for thermodynamics, and non-equilibrium Green's functions. The key to this generality is to use a time variable that evolves along a time contour in the complex plane. The various Green's function approaches can then be related to a particular choice of the time contour.

1. propagator in Fock space
2. ensembles
3. complex time contour
4. linear response
5. Heisenberg operators

6.1 Propagator in Fock space

In section 4.3.1, we introduced the propagator in the one-particle Hilbert space. As we proceed to many-particle systems, we need to generalize it to the complete Fock space. The definition is analogous: Instead of a complete basis of one-particle wave functions, we use now a complete basis in the Fock space.

In order to make the distinction between one-particle and many-particle quantities evident, I will use, as much as as possible, uppercase symbols for the many-particle properties and quantities that refer to interacting systems.

Consider the time evolution for any many-particle state $|\Psi(t)\rangle$ which is governed by the many-particle Schrödinger equation

$$\Big[i\hbar\partial_t - \hat{H}(t)\Big]|\Psi(t)\rangle = 0 \tag{6.1}$$

with the many-particle Hamiltonian $\hat{H} = \hat{h} + \hat{W}$.

The time evolution for any many-particle state $|\Psi(t)\rangle$ can be expressed by the propagator $\hat{\mathcal{U}}(t, t')$ in Fock space

$$|\Psi(t)\rangle = \hat{\mathcal{U}}(t, t')|\Psi(t')\rangle \tag{6.2}$$

The many-particle propagator $\hat{\mathcal{U}}$ differs from one-particle propagator $\hat{U}$, used earlier. $\hat{\mathcal{U}}$ acts in the Fock space, while $\hat{U}$ acts on the one-particle Hilbert space.

The many-particle propagator is defined by the differential equation

$$\Big[i\hbar\partial_t - \hat{H}(t)\Big]\,\hat{\mathcal{U}}(t,t') = 0 \tag{6.3}$$

and the boundary condition is (with the unit operator $\hat{1}$ in Fock space)

$$\hat{\mathcal{U}}(t,t) = \hat{1}\ . \tag{6.4}$$

Closed expression: The propagator has the form

$$\hat{\mathcal{U}}(t,t') = \sum_{m,n} \big|\Phi_m(t)\big\rangle \Big(\big\langle\Phi_m(t')\big|\Phi_n(t')\big\rangle\Big)^{-1}_{m,n} \big\langle\Phi_n(t')\big| \tag{6.5}$$

where the many-particle wave functions $|\Phi_n(t')\rangle$ form a complete basisset in Fock space. Each such state obeys the time-dependent Schrödinger equation

$$\Big[i\hbar\partial_t - \hat{H}(t)\Big]|\Phi_n(t)\rangle = 0 \tag{6.6}$$

The many-particle propagator obeys the same rules as those specified in section 4.3.1 on p. 175 for the propagator in the one-particle Hamiltonian.

Alternatively, we can also use the ordered exponential with Dyson's time-ordering operator $\mathcal{T}_D$.

$$\hat{\mathcal{U}}(t,t') = \mathcal{T}_D \exp\left(-\frac{i}{\hbar}\int_{t'}^{t} dt''\ \hat{H}(t'')\right) \tag{6.7}$$

Propagator for time-independent systems: For a stationary system, the propagator has the form

$$\hat{\mathcal{U}}(t,t') = \sum_n |\Phi_n\rangle \mathrm{e}^{-\frac{i}{\hbar}E_n(t-t')}\langle\Phi_n| \tag{6.8}$$

where the $|\Phi_n\rangle$ are the orthonormal eigenstates of the time-independent Schrödinger equation in Fock space.

$$\hat{H}|\Phi_n\rangle = |\Phi_n\rangle E_n \tag{6.9}$$

For a time-independent Hamiltonian $\hat{H}$, the propagator $\hat{\mathcal{U}}(t,t')$ from Eq. 6.8 can be expressed in the compact form

$$\hat{\mathcal{U}}(t,t') = \mathrm{e}^{-\frac{i}{\hbar}\hat{H}(t-t')} \tag{6.10}$$

which is verified by insertion into the Schrödinger equation:

$$i\hbar\partial_t \underbrace{\hat{\mathcal{U}}(t,t')|\psi(t')\rangle}_{|\psi(t)\rangle} = \hat{H}\,\underbrace{\hat{\mathcal{U}}(t,t')|\psi(t')\rangle}_{|\psi(t)\rangle} \tag{6.11}$$

Propagator for time-independent systems without interaction: For a non-interacting and time-independent Hamiltonian $\hat{H} = \hat{h}$, the propagator is, in occupation-number representation,

$$\hat{\mathcal{U}}(t,t') = \sum_{\vec{\sigma}} |\vec{\sigma}\rangle \mathrm{e}^{-\frac{i}{\hbar}(\sum_j \sigma_j\epsilon_j)(t-t')}\langle\vec{\sigma}| \tag{6.12}$$

Because the system is non-interacting, the eigenstates are Slater-determinants expressed in the one-particle basis with states $|\varphi_j\rangle$, that obey[1]

$$\hat{h}|\varphi_j\rangle = |\varphi_j\rangle\epsilon_j \tag{6.13}$$

We use the occupation-number representation. (See also section 1.4.1 on p. 23)

The Hamilton eigenstates for this non-interacting Hamiltonian $\hat{H} = \hat{h}$ obey the eigenvalue equation

$$\hat{h}|\vec{\sigma}\rangle = |\vec{\sigma}\rangle E_{\vec{\sigma}} \tag{6.14}$$

with energies

$$E_{\vec{\sigma}} = \sum_{j=1}^{\infty} \sigma_j \epsilon_j \tag{6.15}$$

6.2 Time as complex variable

6.2.1 Motivation

By allowing arbitrary time contours in the complex plane, the Green's-function formalism can be introduced in a unified way[71] rather than considering several distinct theories for zero-temperature time-dependent problems, finite-temperature static problems and non-equilibrium problems.

This section, 6.2.1, aims at providing a motivation, before I describe what needs to be considered in connection with complex time contours.

Allowing the time to vary along a contour in the complex plane is related to a mathematical trick used in connection with finite temperature. The gist of this trick is that both propagator $\hat{\mathcal{U}}(t, t')$ and thermal von-Neumann density matrix $\hat{\rho}^{vN}_{T,\mu}$ are both expressed in terms of exponentials of the Hamiltonian. I will also use the term **state operator** for the von-Neumann density matrix. By allowing complex time arguments, the von-Neumann density matrix can be expressed, partly, by a propagator.

$$\hat{\rho}_{T,\mu} = \frac{\mathrm{e}^{-\beta(\hat{H}-\mu\hat{N})}}{\mathrm{Tr}[\mathrm{e}^{-\beta(\hat{H}-\mu\hat{N})}]} = \frac{\mathrm{e}^{\beta\mu\hat{N}}\hat{\mathcal{U}}(-i\hbar\beta, 0)}{\mathrm{Tr}[\mathrm{e}^{\beta\mu\hat{N}}\hat{\mathcal{U}}(-i\hbar\beta), 0]} \tag{6.16}$$

where I used the propagator (with frozen $\hat{H}$)

$$\hat{\mathcal{U}}(-i\hbar\beta, 0) = \exp\Big(-\frac{i}{\hbar}\hat{H}\cdot\underbrace{(-i\hbar\beta)}_{(t-0)}\Big) = \mathrm{e}^{-\beta\hat{H}} \tag{6.17}$$

A time-dependent expectation value is obtained by propagating the states of the ensemble to the desired time. This allows us to start with a specific ensemble at $t = 0$ and propagate with a time-dependent Hamiltonian to the desired time.

$$\big\langle A(t)\big\rangle_{T,\mu} = \frac{\mathrm{Tr}\left\{\mathrm{e}^{\beta\mu\hat{N}}\hat{\mathcal{U}}(-i\hbar\beta, 0)\hat{\mathcal{U}}(0, t)\hat{A}\hat{\mathcal{U}}(t, 0)\right\}}{\mathrm{Tr}\left\{\mathrm{e}^{\beta\mu\hat{N}}\hat{\mathcal{U}}(-i\hbar\beta, 0)\hat{\mathcal{U}}(0, t)\hat{\mathcal{U}}(t, 0)\right\}} = \frac{\mathrm{Tr}\Big[\mathrm{e}^{\beta\mu\hat{N}}\mathcal{T}_{\mathcal{C}}\Big\{\hat{A}_S(t)\mathrm{e}^{-\frac{i}{\hbar}\int_{\mathcal{C}} dt'\ \hat{H}(t')}\Big\}\Big]}{\mathrm{Tr}\Big[\mathrm{e}^{\beta\mu\hat{N}}\mathcal{T}_{\mathcal{C}}\Big\{\mathrm{e}^{-\frac{i}{\hbar}\int_{\mathcal{C}} dt'\ \hat{H}(t')}\Big\}\Big]} \tag{6.18}$$

The propagation proceeds along the contour $\mathcal{C}$ leading along $0 \to t \to 0 \to -i\hbar\beta$ in the complex-time plane. The time argument $\hat{A}_S(t) = \hat{A}$ is only present to guide the time-ordering operator $\mathcal{T}_{\mathcal{C}}$, which orders the operators now along a one-dimensional time contour in the complex plane. A proper definition of this time-ordering operator will follow in Eq. 6.36 on p. 245. The Schrödinger operator $\hat{A}_S(t)$ must not confused with a Heisenberg operator $\hat{A}_H(t)$.

[1] Using $\hat{h}$ both in the Fock space and the one-particle Hilbert space may be irritating. In this special case, it is allowed considering that the one-particle Hilbert space is a sub-space of the Fock space.

This example shall demonstrate the general principle, rather than providing a working technique. The ensemble propagated here is, admittedly, weird. At this point this shall not disturb us. The complex time contour will later be put into more reasonable use. The goal is to make it plausible that thermal properties can be described with time arguments on the imaginary axis. For the time being, this shall suffice as motivation. Details will be made clear later.

While I will not exploit the complex time contour for quite some time, introducing it here allows me to define quantities already in its final generality.

6.2.2 Definitions and working rules

Complex time contour: Consider time to proceed along a one-dimensional contour $\mathcal{C}$ in the complex plane. Thus, time $t(s) \in \mathbb{C}$ is a complex-valued function of a one-dimensional real-valued parameter $s \in \mathbb{R}$.

$$t(s) : \mathbb{R} \to \mathbb{C} \tag{6.19}$$

An example of such complex time contour is shown in the box containing Eq. 10.22 on p. 315.

Let me write down some definitions that are required to describe the dynamics along a complex contour.

- a **contour integral** of a function $f(t)$, along a contour $\mathcal{C}$ in the complex plane has the form

$$\int_{\mathcal{C};t_a\in\mathcal{C}}^{t_b\in\mathcal{C}} dt\; f(t) \stackrel{\text{def}}{=} \int_{s_a}^{s_b} ds\; \frac{dt(s)}{ds} f(t(s)) \tag{6.20}$$

  where $t_a = t(s_a)$ and $t_b = t(s_b)$.

- Similarly, the **contour derivative** is

$$\frac{df}{dt} \stackrel{\text{def}}{=} \frac{df(t(s))}{ds} \left(\frac{dt}{ds}\right)^{-1} = \lim_{\Delta\to 0} \frac{f(t(s+\Delta)) - f(t(s))}{t(s+\Delta) - t(s)} \tag{6.21}$$

  The contour derivative is not to be confused with the Wirtinger derivatives (see appendix A.4 on p. 502)

$$df = \frac{df}{dt} dt + \frac{df}{dt^*} dt^* \tag{6.22}$$

- The **contour step function** for time arguments on the contour will be generalized so that it refers to the parameter s.

$$\theta_{\mathcal{C}}(t_1 - t_2) \stackrel{\text{def}}{=} \theta(s_1 - s_2) \qquad \text{where } t_1 = t(s_1) \text{ and } t_2 = t(s_2) \tag{6.23}$$

- the **contour delta function** is defined as the derivative of the contour step function. Thus, we can use

$$\delta(s) = \frac{d\theta(s)}{ds} = \frac{d\theta(t)}{dt}\frac{dt}{ds} = \delta(t)\frac{dt}{ds} \tag{6.24}$$

  Thus,

$$\delta_{\mathcal{C}}(t - t') \stackrel{\text{def}}{=} \left(\frac{dt}{ds}\right)^{-1} \delta(s - s') \tag{6.25}$$

- The **contour Schrödinger equation** translates into

$$\left[i\hbar\partial_t - \hat{H}(t)\right]|\psi(t)\rangle = \left[i\hbar\left(\frac{dt}{ds}\right)^{-1}\partial_s - \hat{H}(s)\right]|\psi(s)\rangle = 0 \tag{6.26}$$

  This converts the Schrödinger equation into a differential equation with respect to the real one-dimensional parameter s.

- The propagator $\hat{U}(t,t')$ of the one-particle states has been introduced previously in section 4.3.1 on p. 174. The **contour propagator** has the same form, which also holds for complex-valued time arguments.

$$\hat{U}(t,t') = \sum_{m,n} |\varphi_m(t)\rangle O^{-1}_{m,n}(t') \langle\varphi_n(t')| \tag{6.27}$$

The time-dependent one-particle states $\{|\varphi_n(t)\rangle\}$ form a complete set of wave functions that satisfy the contour Schrödinger equation. With

$$O_{m,n}(t) = \langle\varphi_m(t)|\varphi_n(t)\rangle \;, \tag{6.28}$$

we denote the time-dependent overlap matrix. The orthonormality of wave functions is conserved along the real time axis, but not away from it. Notice that the time argument of the inverse overlap matrix in Eq. 6.27 is connected to the second time argument of the propagator, which makes the expression asymmetric.

As a side remark, let me alert the you to an aspect that may easily be overlooked: The propagator for a time-independent Hamiltonian has a surprisingly simple form, despite being valid in the complex-time plane. Let me consider the solutions $|\varphi_n(t)\rangle$ of the contour Schrödinger equation for a *time-independent* Hamiltonian. The states shall be orthonormal at $t = 0$ and eigenstates of the Hamiltonian with eigenvalues ϵ_n

$$\begin{aligned}
& |\varphi_n(t)\rangle = |\varphi_n(0)\rangle \mathrm{e}^{-\frac{i}{\hbar}\epsilon_n t} \\
\Rightarrow \quad & \langle\varphi_n(t)| = \mathrm{e}^{+\frac{i}{\hbar}\epsilon_n t^*} \langle\varphi_n(0)| \\
\Rightarrow \quad & O_{m,n}(t) = \langle\varphi_m(t)|\varphi_n(t)\rangle = \mathrm{e}^{+\frac{i}{\hbar}\epsilon_n t^*} \underbrace{\langle\varphi_m(0)|\varphi_n(0)\rangle}_{\delta_{m,n}} \mathrm{e}^{-\frac{i}{\hbar}\epsilon_n t} = \delta_{m,n} \mathrm{e}^{+\frac{i}{\hbar}\epsilon_n (t^*-t)}
\end{aligned}$$

$$\Rightarrow \quad \sum_n O^{-1}_{m,n}(t) \langle\varphi_n(t)| = \sum_n \underbrace{\delta_{m,n} \mathrm{e}^{-\frac{i}{\hbar}\epsilon_n (t^*-t)}}_{O^{-1}_{m,n}(t)} \underbrace{\mathrm{e}^{+\frac{i}{\hbar}\epsilon_n t^*} \langle\varphi_n(0)|}_{\langle\varphi_n(t)|} = \mathrm{e}^{+\frac{i}{\hbar}\epsilon_m t} \langle\varphi_m(0)| \tag{6.29}$$

The propagator for a time-independent Hamiltonian $\hat{h}$ is

$$\begin{aligned}
\hat{U}(t,t') &= \sum_{m,n} \underbrace{|\varphi_m(0)\rangle \mathrm{e}^{-\frac{i}{\hbar}\epsilon_m t}}_{|\varphi_m(t)\rangle} \underbrace{\delta_{m,n} \mathrm{e}^{-\frac{i}{\hbar}\epsilon_n ((t')^*-t')}}_{O^{-1}_{m,n}(t')} \underbrace{\mathrm{e}^{+\frac{i}{\hbar}\epsilon_n (t')^*} \langle\varphi_n(0)|}_{\langle\varphi_n(t')|} \\
&= \sum_n |\varphi_n(0)\rangle \mathrm{e}^{-\frac{i}{\hbar}\epsilon_n (t-t')} \langle\varphi_n(0)| = \mathrm{e}^{-\frac{i}{\hbar}\hat{h}(t-t')}
\end{aligned} \tag{6.30}$$

The result is simple in a non-trivial way. The complications related to the complex-conjugate time and the inverse overlap matrix disappear.

For later reference, table 6.1 summarizes the rules for symbols on a complex contour. The subscript $\mathcal{C}$ will not be carried through consistently.

6.2.3 Memory hook

In this section, I make an attempt to make the choices for the contour derivatives, contour integrations etc. plausible using a minimal problem, namely one with a one-dimensional Hilbert space. A one-dimensional Hilbert space is spanned by a single orbital.

Consider the propagator in this one-dimensional Hilbert space, which is a simple complex function in the complex time plane. To simplify the discussion, we only consider the relative time argument, rather than the arguments of initial and final time.

$$u(t) = \mathrm{e}^{-\frac{i}{\hbar}\epsilon t} \tag{6.31}$$

in the complex plane. This function is a cartoon of a propagator described below.

∂_t	$\left(\frac{dt}{ds}\right)^{-1}\partial_s$	contour derivative
$\int_{t(s_a)}^{t(s_b)} dt$	$\int_{s_a}^{s_b} ds \frac{dt}{ds}$	contour integral
$\theta_{\mathcal{C}}(t-t')$	$\theta(s-s')$	step function
$\delta_{\mathcal{C}}(t-t')$	$\left(\frac{dt}{ds}\right)^{-1}\delta(s-s')$	delta function

Table 6.1: Translation rules of quantities defined on a complex-time contour $t(s)$ onto the real-valued contour parameter s.

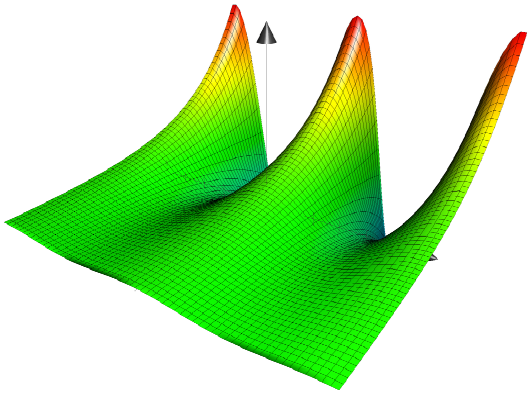


Fig. 6.1: Real part of the propagator $u(t)$ in a one-dimensional Hilbert space in the complex time plane. The propagator is a plane wave in the direction of the real time axis (towards right-front) and an exponential along the imaginary time axis. (towards right-back)

Contour derivative: $u(t) = \mathrm{e}^{-\frac{i}{\hbar}\epsilon t}$ obeys the differential equation

$$\Big(i\hbar\partial_t - \epsilon\Big)u(t) = 0 \tag{6.32}$$

when t proceeds along the real axis. This differential equation is analogous to the Schrödinger equation.

Consider now a path along the imaginary time axis,i.e. $t(s) = is$. The variable

$$\tau \stackrel{\text{def}}{=} -it \tag{6.33}$$

is called the **imaginary time**. Expressed in imaginary time, the propagator obeys the differential equation

$$\Big(\hbar\partial_\tau - \epsilon\Big)u(t(\tau)) = 0 \tag{6.34}$$

This is the Schrödinger equation in **imaginary time**. Its solution $u(t(\tau)) = \mathrm{e}^{\frac{1}{\hbar}\epsilon\tau}$ is an exponential, rather than a plane wave $u(t(\tau)) = \mathrm{e}^{-\frac{i}{\hbar}\epsilon\tau}$ obtained from the equation in real-valued time.

Both equations, Eq. 6.32 and Eq. 6.34, can be translated into each other using the replacement rule

$$\partial_t = \underbrace{\left(\frac{dt}{d\tau}\right)^{-1}}_{-i}\partial_\tau \tag{6.35}$$

Both differential equations, Eq. 6.32 and Eq. 6.34, can be considered as differential equations along one-dimensional contours $\mathcal{C}$ in the complex plane. In one case, the contour is defined by $t(s) = s$ and proceeds along the real time axis. In the other case, the contour is defined by $t(s) = is$ and proceeds along the imaginary-time axis.

6.2.4 Contour time-ordering operator

In section 4.3.3 on p. 176, the propagator has been represented as time-ordered exponential. In order to correct for the misordering of operators, Dyson's time-ordering operator Eq. 4.43 has been introduced.

In order to use this expression in connection with Heisenberg-type creation and annihilation operators, we need to introduce Wick's time-ordering operator. Wick's time-ordering operator introduces a sign change for every interchange of fermionic creation and annihilation operators.

Wick's time-ordering operator can be considered as a generalization of Dyson's time-ordering operator. Dyson's time-ordering operator has been introduced for observables, for which the fermionic operators occur in pairs. In this case, the sign changes introduced by Wick's time-ordering operator compensate.

Wick's time-ordering operator on the complex time contour is what we call the **contour time-ordering operator**.

CONTOUR TIME-ORDERING OPERATOR

The time-ordering operator acts on a product of operators $\hat{A}(t)$, which depend on the time-point $t(s)$ on a contour $\mathcal{C}$ in the complex plane. The time contour $\mathcal{C} : s \to t(s)$ is parameterized by a one-dimensional real-valued argument s.
The time-ordering operator rearranges the operators in the product such that the argument s increases from right to left. The time-ordering operators are no operators in the conventional sense: Namely, they do not act on states in the Hilbert or Fock space to map them onto other states. Rather, it is a prescription in which order the operators in a product shall be arranged.
Wick's time-ordering operator[64] or **contour time-ordering operator**. In his seminal paper[64] laying the foundation for the diagrammatic expansion of the Green's function, Wick introduced his time-ordering operator. This object is generalized to the contour time-ordering operator $\mathcal{T}_{\mathcal{C}}$.

$$\mathcal{T}_{\mathcal{C}}\hat{A}(t(s))\hat{B}(t(s')) = \begin{cases} \hat{A}(t(s))\hat{B}(t(s')) & \text{for } s \geq s' \\ \hat{B}(t(s'))\hat{A}(t(s)) & \text{for } s < s' \text{ and either } \hat{A} \text{ or } \hat{B} \text{ or both bosonic} \\ -\hat{B}(t(s'))\hat{A}(t(s)) & \text{for } s < s' \text{ and } \hat{A} \text{ and } \hat{B} \text{ fermionic} \end{cases} \quad (6.36)$$

Creation and annihilation operators of identical fermions are called fermionic operators. Odd-numbered products of such operators are themselves fermionic. Creation and annihilation operators of identical bosons are called bosonic operators. Even numbered products are of bosonic type. Thus, a Hamilton operator, which conserves the particle number is necessarily of bosonic type in the present context. This is confusing because this Hamiltonian still describes fermions).
The special rule for fermionic operators is due to Wick's theorem derived later. (In the expression for the time-ordered exponential, the special rule would actually be incorrect. We use the same object because Hamiltonians with fermionic operators are usually particle-number conserving, so that fermionic operators occur in pairs. Pairs of fermionic operators are again bosonic so that only the bosonic rule applies.) Editor: This should be explained better.

Time-ordered exponential on the contour

The propagator in Fock space with a time-dependent Hamiltonian $\hat{H}(t)$ has the form

$$\hat{\mathcal{U}}(t_2, t_1) = \mathcal{T}_{\mathcal{C}} \mathrm{e}^{-\frac{i}{\hbar}\int_{\mathcal{C},t_1}^{t_2} dt'\, \hat{H}(t)} \tag{6.37}$$

In the future, the contour will be implied in the time integral.

Expressed in the mapping $t(s)$ the time-ordered exponential is more explicitly given as.

$$\hat{\mathcal{U}}\big(t(s_2), t(s_1)\big) = \mathcal{T}_{\mathcal{C}} \mathrm{e}^{-\frac{i}{\hbar}\int_{\mathcal{C},s_1}^{s_2} ds\, \frac{dt(s)}{ds} \hat{H}\left(t(s)\right)} \tag{6.38}$$

It will be important that the propagator is not unitary for time arguments away from the real time axis. Transitivity still holds.

$$\hat{\mathcal{U}}\big(t_1, t_2\big)\hat{\mathcal{U}}\big(t_2, t_1\big) = \hat{1} \qquad \text{but} \qquad \hat{\mathcal{U}}\big(t_1, t_2\big) \neq \hat{\mathcal{U}}^{\dagger}\big(t_2, t_1\big) \tag{6.39}$$

6.2.5 Heisenberg operators

Special care is required with the generalization of Heisenberg operators to the complex time contour, because the propagator is unitary only when the contour lies on the real axis. We define the Heisenberg operators as follows:

HEISENBERG OPERATORS

A Heisenberg operator $\hat{A}_H(t)$ is obtained from a Schrödinger operator $\hat{A}_S(t)$ with the propagator $\hat{\mathcal{U}}(t, t') = \mathcal{T}_D \mathrm{e}^{-\frac{i}{\hbar}\int_{\mathcal{C}} dt' \hat{H}(t')}$ as

$$\hat{A}_H(t) \stackrel{\text{def}}{=} \hat{\mathcal{U}}(0, t)\hat{A}_S(t)\hat{\mathcal{U}}(t, 0) \tag{6.40}$$

In the Heisenberg picture, the creation and annihilation operators are no more complex conjugates of each other, unless the time lies on the real axis. Therefore, I introduce an alternate symbol $+$ to denote the creation operator in the Heisenberg picture, which is distinct from the one $\dagger$ used to denote the hermitian conjugate.

$$\begin{aligned} \hat{\psi}_H(\vec{x}, t) &\stackrel{\text{def}}{=} \hat{\mathcal{U}}(0, t)\hat{\psi}_S(\vec{x})\hat{\mathcal{U}}(t, 0) \\ \hat{\psi}^{+}_H(\vec{x}, t) &\stackrel{\text{def}}{=} \hat{\mathcal{U}}(0, t)\hat{\psi}^{\dagger}_S(\vec{x})\hat{\mathcal{U}}(t, 0) \end{aligned} \tag{6.41}$$

The creation and annihilation operators are not in general hermitian conjugates of each other.

$$\hat{\psi}^{+}_H(\vec{x}, t) \neq \big(\hat{\psi}_H(\vec{x}, t)\big)^{\dagger} \quad \text{unless for } t \in \mathbb{R} \tag{6.42}$$

The field operators in the Heisenberg picture obey the commutator relations known from the Schrödinger picture only for equal times.

$$\begin{aligned} \Big[\psi^{+}_H(\vec{x}, t), \psi_H(\vec{x'}, t')\Big]_+ &= \delta(\vec{x} - \vec{x'}) \qquad \text{only for } t = t' \\ \Big[\psi^{+}_H(\vec{x}, t), \psi^{+}_H(\vec{x'}, t')\Big]_+ &= 0 \qquad \text{only for } t = t' \\ \Big[\psi_H(\vec{x}, t), \psi_H(\vec{x'}, t')\Big]_+ &= 0 \qquad \text{only for } t = t' \end{aligned} \tag{6.43}$$

With this definition, the differential equation for the Heisenberg operators has the usual form[2]

$$\begin{aligned} i\hbar\partial_t A_H(t) &= \left(i\hbar\partial_t \hat{\mathcal{U}}(0,t)\right)\hat{A}_S(t)\hat{\mathcal{U}}(t,0) + \hat{\mathcal{U}}(0,t)\left(i\hbar\partial_t \hat{A}_S(t)\right)\hat{\mathcal{U}}(t,0) + \hat{\mathcal{U}}(0,t)\hat{A}_S(t)\left(i\hbar\partial_t \hat{\mathcal{U}}(t,0)\right) \\ &= \left[\hat{A}_H(t), \hat{H}_H(t)\right]_- + i\hbar\left(\frac{\partial \hat{A}}{\partial t}\right)_H \end{aligned} \tag{6.45}$$

However, the time-dependent expectation value is obtained only for times on the real axis.

$$\langle A(t)\rangle \overset{\text{def}}{=} \frac{\langle\psi_S(t)|\hat{A}_S|\psi_S(t)\rangle}{\langle\psi_S(t)|\psi_S(t)\rangle} \overset{t\in\mathbb{R}}{=} \frac{\langle\psi_H|\hat{A}_H(t)|\psi_H\rangle}{\langle\psi_H|\psi_H\rangle} \qquad \text{for } t\in\mathbb{R} \tag{6.46}$$

6.3 Home study and practice

[2]We use the differential equation $[i\hbar\partial_t - \hat{H}_S(t)]\hat{\mathcal{U}}(t,0) = 0$ and $\hat{\mathcal{U}}(0,t)\hat{\mathcal{U}}(t,0) = \hat{1}$. Specifically,

$$\begin{aligned} &\hat{\mathcal{U}}(0,t)\left[\left(i\hbar\partial_t\hat{\mathcal{U}}(t,0)\right) - \hat{H}_S\hat{\mathcal{U}}(t,0)\right]\hat{\mathcal{U}}(0,t) = 0 \\ \Rightarrow\quad &\hat{\mathcal{U}}(0,t)\underbrace{i\hbar\partial_t\hat{\mathcal{U}}(t,0)\hat{\mathcal{U}}(0,t)}_{=\hat{0}} - \underbrace{\hat{\mathcal{U}}(0,t)\hat{\mathcal{U}}(t,0)}_{\hat{1}}i\hbar\partial_t\hat{\mathcal{U}}(0,t) - \hat{\mathcal{U}}(0,t)\hat{H}_S\underbrace{\hat{\mathcal{U}}(t,0)\hat{\mathcal{U}}(0,t)}_{=\hat{1}} = 0 \end{aligned} \tag{6.44}$$

From the latter, we obtain $i\hbar\partial_t\hat{\mathcal{U}}(0,t) = -\hat{\mathcal{U}}(0,t)\hat{H}_S(t)$, respectively $i\hbar\partial_t\hat{\mathcal{U}}(0,t) = -\hat{H}_H\hat{\mathcal{U}}(0,t)$.

Chapter 7

Green's functions in many-particle physics

The transition of the Green's-function formalism from one-particle systems to a many-particle problems is conceptually non-trivial. There are a number of equations that remain the same, but the Green's function in many-particle physics is a generalization of the one-particle case, which has a different mathematical foundation. Often, I find that the Green's function is defined as mathematical expression, and the motivation becomes evident only a posteriori. In this chapter, I will try to motivate the choices that lead to the many-particle Green's function beforehand.

7.1 One-particle Green's functions in second quantization

The first step on the route from the Green's function for one-particle systems to that for many particles is to reformulate the one-particle Green's function in the language of second quantization.

The Green's function is obtained from the propagator $\hat{U}(t_2, t_1)$ via Eq. 4.40. In order to extend our definitions to the Fock space, I represent this propagator in terms of creation and annihilation operators. Note, however, that we still work with a one-particle problem. Let me choose a basisset of Hamilton eigenstates $|\varphi_m\rangle$ and the corresponding creation and annihilation operators $\hat{a}_m^\dagger$ and $\hat{a}_m$. The basis functions can be expressed by the vacuum state $|\mathcal{O}\rangle$ and the creation operator as

$$|\varphi_m\rangle \overset{\text{Eq. } 3.22}{=} \hat{a}_m^\dagger |\mathcal{O}\rangle \; . \tag{7.1}$$

Because the basis $\{|\varphi_m\rangle\}$ is orthonormal and complete, we obtain

$$\begin{aligned}
\hat{U}(t_2, t_1) &= \sum_{m,n} |\varphi_m\rangle\langle\varphi_m|\hat{U}(t_2, t_1)|\varphi_n\rangle\langle\varphi_n| \\
&\overset{\text{Eqs. } 3.22,\ 6.2}{=} \sum_{m,n} |\varphi_m\rangle\langle\mathcal{O}|\hat{a}_m \hat{\mathcal{U}}(t_2, t_1)\hat{a}_n^\dagger|\mathcal{O}\rangle\langle\varphi_n| \\
&\overset{\hat{\mathcal{U}}(t,0)|\mathcal{O}\rangle=|\mathcal{O}\rangle}{=} \sum_{m,n} |\varphi_m\rangle \underbrace{\langle\mathcal{O}|\hat{\mathcal{U}}(0, t_2)}_{\langle\mathcal{O}|} \hat{a}_m \hat{\mathcal{U}}(t_2, t_1)\hat{a}_n^\dagger \underbrace{\hat{\mathcal{U}}(t_1, 0)|\mathcal{O}\rangle}_{=|\mathcal{O}\rangle}\langle\varphi_n| \\
&\overset{\text{Eq. } 6.41}{=} \sum_{m,n} |\varphi_m\rangle\langle\mathcal{O}|\hat{a}_{H,m}(t_2)\hat{a}_{H,n}^+(t_1)|\mathcal{O}\rangle\langle\varphi_n|
\end{aligned} \tag{7.2}$$

where I used the many-particle propagator $\hat{\mathcal{U}}(t, t')$ in Fock space. In the last, line I introduced the Heisenberg operators as indicated by the additional subscript "H" defined in Eq. 6.41. I changed the $\dagger$ into $+$ to allow for complex valued time variables, for which the creator in the Heisenberg picture is no more the hermitean conjugate of the annihilation operator.

We arrive at the general notion that the Green's function is the probability and the phase for the process of adding a particle into one one-particle orbital and removing it from another orbital at a later time.

The propagators from $t = 0$ to t_1 and from t_2 back to $t = 0$ have been included to make the final result independent of a **global energy shift** Δ. This global shift can be identified with the energy of the vacuum state, i.e. $\hat{H}|\mathcal{O}\rangle = |\mathcal{O}\rangle\Delta$. Usually, and in the derivation above, this shift Δ is set to zero. If, instead, it is given a nonzero value, Δ introduces a phase factor $\mathrm{e}^{-\frac{i}{\hbar}\Delta(t_2-t_1)}$ into the propagator Eq. 6.7. The propagation back to the initial state ensures that a global shift, which is the energy of the vacuum state, does not affect the result.

The one-particle Green's function is therefore

$$\hat{G}(t_2,t_1) \overset{\text{Eq. 4.40}}{=} \frac{1}{i\hbar}\theta_{\mathcal{C}}(t_2-t_1)\sum_{m,n}|\varphi_m\rangle\langle\mathcal{O}|\hat{\mathcal{U}}(0,t_2)\hat{a}_m\hat{\mathcal{U}}(t_2,t_1)\hat{a}_n^\dagger\hat{\mathcal{U}}(t_1,0)|\mathcal{O}\rangle\langle\varphi_n| \tag{7.3}$$

Even though they describe only a single particle, the many-particle states in the matrix element live in Fock space and are propagated by the many-particle propagator $\hat{\mathcal{U}}(t,t')$ rather than the one-particle propagator $\hat{U}(t,t')$. The Green's function itself is still an operator in the one-particle Hilbert space.

Eq. 7.3 suggests an interpretation of the Green's function

$$\begin{aligned} G(\vec{x}_2,t_2,\vec{x}_1,t_1) &= \langle\vec{x}_2|\hat{G}(t_2,t_1)|\vec{x}_1\rangle \\ &= \frac{1}{i\hbar}\theta_{\mathcal{C}}(t_2-t_1)\langle\mathcal{O}|\hat{\mathcal{U}}(0,t_2)\hat{\psi}(\vec{x}_2)\hat{\mathcal{U}}(t_2,t_1)\hat{\psi}^\dagger(\vec{x}_1)\hat{\mathcal{U}}(t_1,0)|\mathcal{O}\rangle \end{aligned} \tag{7.4}$$

as probability amplitude for finding a particle at time t_2 in position $\vec{x}_2$, which has been added to the system at time t_1 in position $\vec{x}_1$. This will be a guiding principle in the definition of the Green's function for many-particle systems.

7.2 Propagate electrons in a non-interacting electron gas

While Eq. 7.3 describes an electron added to empty space, let us now study an electron added to a non-interacting many-electron system. To keep things simple, I limit the discussion to time-independent problems.

To generalize Eq. 7.3, I replace the vacuum state $|\mathcal{O}\rangle$ in Eq. 7.2 by an eigenstate $|\vec{\sigma}\rangle$ of a non-interacting Hamiltonian $\hat{h}$. I use the occupation-number representation for the eigenstates $|\vec{\sigma}\rangle$ of $\hat{h}$ with energies $E_{\vec{\sigma}} = \sum_{n=1}^{\infty}\sigma_n\epsilon_n$. In this way, Eq. 7.2 generalizes to

$$\begin{aligned} \hat{U}^{(e)}(t_2,t_1) &\overset{\text{Eq. 7.2}}{=} \sum_{n,m}|\varphi_m\rangle\left[\langle\vec{\sigma}|\hat{a}_{H,m}(t_2)\hat{a}^+_{H,n}(t_1)|\vec{\sigma}\rangle\right]\langle\varphi_n| \\ &= \sum_{n,m}|\varphi_m\rangle\Bigg[\langle\vec{\sigma}|\quad\underbrace{\underbrace{\hat{\mathcal{U}}(0,t_2)\,\hat{a}_m\hat{\mathcal{U}}(t_2,t_1)}_{\hat{a}_m\hat{a}_n^\dagger|\vec{\sigma}\rangle\mathrm{e}^{-\frac{i}{\hbar}(E_{\vec{\sigma}}+\epsilon_n-\epsilon_m)(0-t_2)}\mathrm{e}^{-\frac{i}{\hbar}(E_{\vec{\sigma}}+\epsilon_n)(t_2-t_1)}\mathrm{e}^{-\frac{i}{\hbar}E_{\vec{\sigma}}t_1}}\,\underbrace{\hat{a}_n^\dagger\hat{\mathcal{U}}(t_1,0)|\vec{\sigma}\rangle}_{\hat{a}_n^\dagger|\vec{\sigma}\rangle\mathrm{e}^{-\frac{i}{\hbar}E_{\vec{\sigma}}t_1}}}_{\hat{a}_m\hat{a}_n^\dagger|\vec{\sigma}\rangle\mathrm{e}^{-\frac{i}{\hbar}(E_{\vec{\sigma}}+\epsilon_n)(t_2-t_1)}\mathrm{e}^{-\frac{i}{\hbar}E_{\vec{\sigma}}t_1}}\Bigg]\langle\varphi_n| \\ &\overset{\text{Eq. 6.12}}{=} \sum_{n,m}|\varphi_m\rangle\left[\underbrace{\delta_{m,n}(1-\sigma_n)}_{\langle\vec{\sigma}|\hat{a}_m\hat{a}_n^\dagger|\vec{\sigma}\rangle}\mathrm{e}^{-\frac{i}{\hbar}\epsilon_n(t_2-t_1)}\right]\langle\varphi_n| \\ &= \sum_n(1-\sigma_n)\,|\varphi_n\rangle\mathrm{e}^{-\frac{i}{\hbar}\epsilon_n(t_2-t_1)}\langle\varphi_n| \end{aligned} \tag{7.5}$$

Except for the factor $(1-\sigma_n)$, this is identical to the propagator for a one-particle system Eq. 6.12. The factor $(1-\sigma_n)$ filters away all occupied states in the Slater determinant $|\vec{\sigma}\rangle$. This reflects that an electron can not be added to a filled orbital.

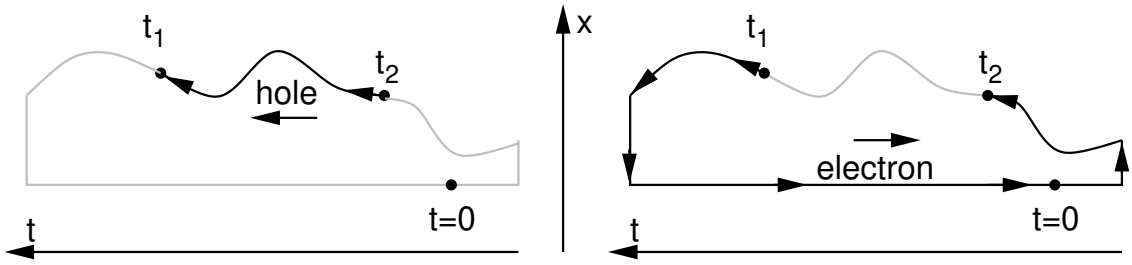


Fig. 7.1: Comparison of a hole propagation forward in time with that of an electron backward in time.

Let me construct a similar propagator $\hat{U}^{(h)}$ for the occupied states. The occupied states are selected by first (at t_2) applying the annihilator and later (at t_1) the creator. For reasons, that become clear below, I interchanged the indices of the time arguments compared to the electron propagator.

$$\begin{aligned}
\hat{U}^{(h)}(t_1,t_2) &= \sum_{n,m}|\varphi_m\rangle\Big[\langle\vec{\sigma}|\hat{a}^+_{H,n}(t_1)\hat{a}_{H,m}(t_2)|\vec{\sigma}\rangle\Big]\langle\varphi_n| \\
&= \sum_{n,m}|\varphi_m\rangle\Big[\langle\vec{\sigma}|\quad \hat{\mathcal{U}}(0,t_1)\,\hat{a}^\dagger_n\hat{\mathcal{U}}(t_1,t_2)\,\underbrace{\hat{a}_m\hat{\mathcal{U}}(t_2,0)|\vec{\sigma}\rangle}_{\hat{a}_m|\vec{\sigma}\rangle e^{-\frac{i}{\hbar}E_{\vec{\sigma}}t_2}}\Big]\langle\varphi_n| \\
&\qquad\qquad \underbrace{\underbrace{\hat{a}^\dagger_n\hat{a}_m|\vec{\sigma}\rangle e^{-\frac{i}{\hbar}(E_{\vec{\sigma}}-\epsilon_m)(t_1-t_2)}e^{-\frac{i}{\hbar}E_{\vec{\sigma}}t_2}}_{\hat{a}^\dagger_n\hat{a}_m|\vec{\sigma}\rangle e^{-\frac{i}{\hbar}(E_{\vec{\sigma}}-\epsilon_m+\epsilon_n)(0-t_1)}e^{-\frac{i}{\hbar}(E_{\vec{\sigma}}-\epsilon_m)(t_1-t_2)}e^{-\frac{i}{\hbar}E_{\vec{\sigma}}t_2}}}_{} \\
&\overset{\text{Eq. 6.12}}{=} \sum_{n,m}|\varphi_m\rangle\Big[\underbrace{\delta_{m,n}\sigma_n}_{\langle\vec{\sigma}|\hat{a}^\dagger_n\hat{a}_m|\vec{\sigma}\rangle}\ e^{-\frac{i}{\hbar}(-\epsilon_m)(t_1-t_2)}\Big]\langle\varphi_n| \\
&= \sum_n \sigma_n\,|\varphi_n\rangle e^{+\frac{i}{\hbar}\epsilon_n(t_1-t_2)}\langle\varphi_n| \qquad (7.6)
\end{aligned}$$

The factor σ_n filters away the empty states, so that this term projects exactly onto the occupied states, that have been missing in the electron propagator. However, because we removed an electron, rather than adding one, the energy ϵ_n enters with a minus sign.

Combining the electron and hole propagators reproduces the one-particle propagator.

$$\begin{aligned}
\hat{U}(t_2,t_1) &= \sum_n |\varphi_n\rangle e^{-\frac{i}{\hbar}(t_2-t_1)}\langle\varphi_n| \\
&= \hat{U}^{(e)}(t_2,t_1) + \hat{U}^{(h)}(t_1,t_2) \\
&= \sum_{m,n}|\varphi_m\rangle\langle\vec{\sigma}|\Big(\hat{\mathcal{U}}(0,t_2)\hat{a}_{S,m}\hat{\mathcal{U}}(t_2,t_1)\hat{a}^+_{S,n}\hat{\mathcal{U}}(t_1,0) + \hat{\mathcal{U}}(0,t_1)\hat{a}^+_{S,n}\hat{\mathcal{U}}(t_1,t_2)\hat{a}_{S,m}\hat{\mathcal{U}}(t_2,0)\Big)|\vec{\sigma}\rangle\langle\varphi_n| \\
&= \sum_{m,n}|\varphi_m\rangle\langle\vec{\sigma}|\Big[\hat{a}_{H,m}(t_2),\hat{a}^+_{H,n}(t_1)\Big]_+|\vec{\sigma}\rangle\langle\varphi_n| \qquad (7.7)
\end{aligned}$$

The time arguments for the hole propagator enter in the reversed order. This can loosely be explained by considering a hole as an electron moving backwards in time: (see also Fig,7.1)

- A hole propagates from t_2 to t_1 with $t_1 > t_2$. At time t_2 a positive charge appears and, at time t_1 it disappears. Rather than letting the positive charge disappear at t_1 one could also have created a negative charge, which compensates the positive charge created earlier.

- An electron propagates from a later time t_1 to an earlier time t_2 with $t_1 > t_2$: At the later time t_1 an electron is added and propagates into the future, returns to time $t = 0$ and from there to t_2, where it is removed from the system.

In both cases, the system becomes more positive at t_2 and it becomes more negative at t_1, indicating that the process is the same, albeit expressed in different words.

7.3 From the propagator of non-interacting electrons to the Green's function

So far, we generalized the propagator of an isolated electron to a propagator Eq. 7.2 of an electron, respectively a hole that has been added to a non-interacting many-electron system.

In order to obtain the Green's function, let us inspect the relation Eq. 4.40 from one-particle quantum mechanics, which links the Green's function to the propagator.

$$\begin{aligned}\hat{G}(t_2, t_1) &= \frac{1}{i\hbar}\theta(t_2 - t_1)\hat{U}(t_2, t_1) - \frac{C}{i\hbar}\hat{U}(t_2, t_1) \\ &= (1 - C)\frac{1}{i\hbar}\theta(t_2 - t_1)\hat{U}(t_2, t_1) - \frac{C}{i\hbar}\theta(t_1 - t_2)\hat{U}(t_2, t_1)\end{aligned} \tag{7.8}$$

I extended Eq. 4.40 by adding the propagator scaled by a real-valued constant C. For the one-particle case, the additional term is, up to a constant, the propagator, which obeys the Schrödinger equation. Therefore, the Green's function $\hat{G}(t, t')$ satisfies the defining differential equation for the Green's function for any finite C. For $C \neq 0$, however, it violates the initial condition $\hat{G}(t, t') = \hat{0}$ for $t = -\infty$.

In the many-particle case, the propagator has two terms: one for electrons and one for holes. Each term solves the one-particle Schrödinger equation independently. I am free to convert the propagator into Green's functions for electrons and for holes independently.

I am using $C = 0$ for the electrons and $C = 1$ for the holes and I add the electron and hole contributions together. In this way, the contour-ordered Green's function is obtained.

$$\begin{aligned}\hat{G}^{\mathcal{C}}(t_2, t_1) &= \frac{1}{i\hbar}\theta_{\mathcal{C}}(t_2 - t_1)\hat{U}^e(t_2, t_1) - \frac{1}{i\hbar}\theta_{\mathcal{C}}(t_1 - t_2)\hat{U}^h(t_1, t_2) \\ &= \sum_{m,n} |\varphi_m\rangle \Bigg\{ \frac{1}{i\hbar}\theta_{\mathcal{C}}(t_2 - t_1) \underbrace{\langle\vec{\sigma}|\hat{\mathcal{U}}(0, t_2)\hat{a}_n\hat{\mathcal{U}}(t_2, t_1)\hat{a}_m^\dagger\hat{\mathcal{U}}(t_1, 0)|\vec{\sigma}\rangle}_{\text{electrons from } (m, t_1) \text{ to } (n, t_2)} \\ &\qquad - \frac{1}{i\hbar}\theta_{\mathcal{C}}(t_1 - t_2) \underbrace{\langle\vec{\sigma}|\hat{\mathcal{U}}(0, t_1)\hat{a}_m^\dagger\hat{\mathcal{U}}(t_1, t_2)\hat{a}_n\hat{\mathcal{U}}(t_2, 0)|\vec{\sigma}\rangle}_{\text{holes from } (n, t_2) \text{ to } (m, t_1)} \Bigg\} \langle\varphi_n|\end{aligned} \tag{7.9}$$

The order of the time arguments of the Green's function does not specify, whether the system is propagated forward or backward in time, but whether electrons or holes are propagated. For $t_2 > t_1$, this Green's function describes the propagator for electrons (but not holes) from the earlier time t_1 to the later time t_2. For $t_1 > t_2$, the Green's function describes the propagator for holes (but not electrons) from the earlier time t_2 to the later time t_1.

Other choices for the Green's function are possible. For example, I could have used $C = 1$ for both, the electron and the hole channel, which would lead again to a Green's function, albeit another one. It would produce the one-particle propagator for a non-interacting system, and it would solve the differential for the Green's function. What would change, is the boundary condition at $t_2 = -\infty$. However, we make a different choice.

Why did we make this particular choice? From the background we have so far, we cannot motivate it. We will see later, that this choice is required for Wick's theorem, which again is the basis of the diagrammatic expansion of the Green's function. Other Green's function are typically obtained from the contour-ordered Green's function. The reason will become clear in the derivation of Wick's theorem in appendix L on p. 703, and it will be discussed on p. p. 725

Make things compact: The contour-ordered Green's function can be economically represented using operators in the Heisenberg picture Eq. 6.40. Furthermore, we can make use of the contour time-ordering operator $\mathcal{T}_\mathcal{C}$ from Eq. 6.36. (Remember, that an interchange of two fermionic operators by $\mathcal{T}_\mathcal{C}$ produces a sign flip.) Combining the propagators with the creation and annihilation operators, we obtain

$$\begin{aligned}\hat{G}^\mathcal{C}(t_2,t_1) &\overset{\text{Eq. 6.40}}{=} \sum_{m,n}|\varphi_m\rangle\Big\{\frac{1}{i\hbar}\theta_\mathcal{C}(t_2-t_1)\langle\vec{\sigma}|\hat{a}_{H,m}(t_2)\hat{a}^+_{H,n}(t_1)|\vec{\sigma}\rangle \\ &\qquad -\frac{1}{i\hbar}\theta_\mathcal{C}(t_1-t_2)\langle\vec{\sigma}|\hat{a}^+_{H,n}(t_1)\hat{a}_{H,m}(t_2)|\vec{\sigma}\rangle\Big\}\langle\varphi_n| \\ &\overset{\text{Eq. 6.36}}{=} \sum_{m,n}|\varphi_m\rangle\frac{1}{i\hbar}\langle\vec{\sigma}|\mathcal{T}_\mathcal{C}\hat{a}_{H,m}(t_2)\hat{a}^+_{H,n}(t_1)|\vec{\sigma}\rangle\langle\varphi_n| \end{aligned} \tag{7.10}$$

Some thought is required regarding the contour $\mathcal{C}$ chosen. Here, the contour starts at zero, passes to $t=-\infty$, proceeds along the real axis to $t=+\infty$, before it returns back to $t=0$. The contour can be modified by clipping closed loops. One exploits $\hat{\mathcal{U}}(t_2,t_1)\hat{\mathcal{U}}(t_1,t_2)=\hat{1}$. Therefore, it is not necessary to move all the way to $-\infty$ or $+\infty$.

7.4 Propagate interacting electrons at finite temperature

From the choices done so far, the remaining steps are straightforward.

General (potentially interacting) electron systems: For the generalization from non-interacting electrons to a general interacting electron system, we choose firstly the appropriate many-particle propagator for interacting electrons. Secondly, we determine the expectation value with a specified many-particle state $|\Phi\rangle$, which is not necessarily a Slater determinant. If one is interested in zero-temperature results, one would choose the ground state of the interacting electron system.

$$\hat{G}^\mathcal{C}(t_2,t_1)=\sum_{m,n}|\varphi_m\rangle\frac{1}{i\hbar}\langle\Phi|\mathcal{T}_\mathcal{C}\hat{a}_{H,m}(t_2)\hat{a}^+_{H,n}(t_1)|\Phi\rangle\langle\varphi_n| \tag{7.11}$$

Finite temperature: In order to obtain results at finite temperature, we need to generalize the Green's function to general ensembles $\{|\Phi_q\rangle,P_q\}$, which can be described by the von-Neumann density matrix $\hat{\rho}=\sum_q|\Phi_q\rangle P_q\langle\Phi_q|$.

$$\begin{aligned}\hat{G}^\mathcal{C}(t_2,t_1) &= \sum_{m,n}|\varphi_m\rangle\frac{1}{i\hbar}\sum_q P_q\langle\Phi_q|\mathcal{T}_\mathcal{C}\hat{a}_{H,m}(t_2)\hat{a}^+_{H,n}(t_1)|\Phi_q\rangle\langle\varphi_n| \\ &= \sum_{m,n}|\varphi_m\rangle\frac{1}{i\hbar}\mathrm{Tr}\Big\{\hat{\rho}\,\mathcal{T}_\mathcal{C}\hat{a}_{H,m}(t_2)\hat{a}^+_{H,n}(t_1)\Big\}\langle\varphi_n| \end{aligned} \tag{7.12}$$

This is the most general expression for the contour-ordered Green's function. It is convenient to specialize this expression somewhat. Namely, we introduce thermal ensembles instead of the most general ensemble. The limitation to thermal ensembles leads to considerable simplifications. Nevertheless, I will show in section 7.6 below, that this is not a restriction. Namely, for an arbitrary ensemble, one can construct a Hamiltonian that produces exactly that desired ensemble in thermal equilibrium.

For a grand-canonical ensemble, the (von-Neumann) density matrix is ($\beta=1/(k_BT)$)

$$\hat{\rho}_{T,\mu}\overset{\text{Eq. 2.57}}{=}\frac{1}{Z_{T,\mu}}\mathrm{e}^{-\beta(\hat{H}-\mu\hat{N})} \tag{7.13}$$

with the **partition function**

$$Z_{T,\mu} \overset{\text{Eq. 2.58}}{=} \mathrm{Tr}\Big\{ \mathrm{e}^{-\beta(\hat{H}-\mu\hat{N})} \Big\} . \tag{7.14}$$

With the thermal density matrix Eq. 7.13, we obtain the propagator in the form

$$\hat{G}^{\mathcal{C}}(t_2,t_1) = \sum_{m,n} |\varphi_m\rangle \frac{1}{i\hbar} \mathrm{Tr}\Big\{ \hat{\rho}_{T,\mu}\, \mathcal{T}_{\mathcal{C}}\, \hat{a}_{H,m}(t_2) \hat{a}^{+}_{H,n}(t_1) \Big\} \langle\varphi_n| \tag{7.15}$$

This is now our final definition for the contour-ordered Green's function. Let us now switch to a representation of general orbitals $|\chi_\alpha\rangle$, for which the creation and annihilation operators are $\hat{c}^\dagger_\alpha$ and $\hat{c}_\alpha$ ($\hat{c}^\dagger_\alpha|\mathcal{O}\rangle \overset{\text{Eq. 3.77}}{=} |\pi_\alpha\rangle$ with $\langle\pi_\alpha|\chi_\beta\rangle = \delta_{\alpha,\beta}$).

CONTOUR-ORDERED GREEN'S FUNCTION FOR COMPLEX TIME ARGUMENTS

The contour-ordered Green's function in complex time and orbital basis has the form

$$G^{\mathcal{C}}_{\alpha,\beta}(t,t') = \frac{1}{i\hbar} \mathrm{Tr}\Big\{ \hat{\rho}^{(W)}_{T,\mu} \mathcal{T}_{\mathcal{C}}\, \hat{c}_{H,\alpha}(t) \hat{c}^{+}_{H,\beta}(t') \Big\} \tag{7.16}$$

where $\hat{\rho}_{T,\mu} = \frac{1}{Z_{T,\mu}} \mathrm{e}^{-\beta(\hat{H}-\mu\hat{N})}$ is the many-particle density matrix and $\hat{H}$ is the Hamiltonian with interaction.[a] [b]
The operators

$$\begin{aligned} \hat{c}_{H,\alpha}(t) &= \hat{\mathcal{U}}(0,t) \hat{c}_{S,\alpha} \hat{\mathcal{U}}(t,0) \\ \hat{c}^{+}_{H,\alpha}(t) &= \hat{\mathcal{U}}(0,t) \hat{c}^\dagger_{S,\alpha} \hat{\mathcal{U}}(t,0) \end{aligned} \tag{7.17}$$

are Heisenberg operators defined with the many-particle propagator $\hat{\mathcal{U}}(t,t')$ along the complex time contour $\mathcal{C}$
Below, I will tend to omit the superscript $\mathcal{C}$ of the Green's function. The superscript will be made explicit, when is required to separate the contour-ordered Green's function from another type of Green's function. Editor: The reader should nevertheless be cautious, because the convention may not be carried through everywhere.

[a] I have attached the subscript (W) to the density operator to emphasize the difference to that for non-interacting electrons, which will be used later.
[b] This definition matches Eq.17.1 of Abrikosov, Gorkov, Dzyaloshinski[7] from 1965.

7.5 Contour-ordered Green's function of non-interacting particles

We will frequently use the Green's function for non-interacting particles: Firstly, the non-interacting system is the reference for a perturbation expansion in the interaction. Secondly, the non-interacting system is used to explore the underlying physics for a particularly simple system.

Let me consider a non-interacting, time-dependent Hamiltonian $\hat{h}(t)$. The time argument is considered as complex-valued, but the Hamiltonian $\hat{h}(t)$ depends only on the real-part of the time argument.

Below we will need to relation creation and annihilation operators in the interaction picture and the Schrödinger picture. The complete derivation is, unfortunately, quite involved. It is provided the

appendix p. 704 as Eq. L.1 and Eq. L.2.

$$\hat{c}^{+}_{I,\alpha}(t) \overset{\text{Eq. } L.1}{=} \sum_{\beta} \hat{c}^{\dagger}_{S,\beta} \langle \chi_\beta | \hat{U}(0,t) | \pi_\alpha \rangle \tag{7.18}$$

$$\hat{c}_{I,\alpha}(t) \overset{\text{Eq. } L.2}{=} \sum_{\beta} \langle \pi_\alpha | \hat{U}(t,0) | \chi_\beta \rangle \hat{c}_{S,\beta} \tag{7.19}$$

The operators with subscript I are in the interaction picture, while the subscript S denotes the common Schrödinger operators. For a non-interacting Hamiltonian considered here, the interaction picture is identical to the Heisenberg picture.

The propagator $\hat{U}(t,t')$, Eqs. 4.32, 6.27, is the propagator for the one-particle wave functions with the one-particle Hamiltonian $\hat{h}(t)$.

Simple (limited) derivation: The derivation of Eqs. 7.18, 7.19 given above is involved, because the equations are fairly general: They consider a time-dependent Hamiltonian and completely general non-orthonormal basissets. The underlying physics is better understood using a time-independent Hamiltonian and its (orthonormal) eigenstates, i.e. $\hat{h}|\varphi_n\rangle = |\varphi_n\rangle \bar{\epsilon}_n$. With these orbitals ($|\chi_\alpha\rangle \rightsquigarrow$)$|\varphi_n\rangle$ and projector functions ($\langle \pi_\alpha| \rightsquigarrow$)$\langle \varphi_n|$ and their creation and annihilation operators ($\hat{c}^{+}_{\alpha} \rightsquigarrow$)$\hat{a}^{+}_{n}$ and ($\hat{c}_{\alpha} \rightsquigarrow$)$\hat{a}_{n}$ we obtain instead

$$\hat{a}^{+}_{I,n}(t) \overset{\text{Eq. } L.1}{=} \sum_{m} \hat{a}^{\dagger}_{S,m} \langle \varphi_m | \hat{U}(0,t) | \varphi_n \rangle = \hat{a}^{\dagger}_{S,n} \mathrm{e}^{\frac{i}{\hbar}\bar{\epsilon}_n t} \tag{7.20}$$

$$\hat{a}_{I,n}(t) \overset{\text{Eq. } L.2}{=} \sum_{m} \langle \varphi_m | \hat{U}(t,0) | \varphi_n \rangle \hat{a}_{S,m} = \hat{a}_{S,n} \mathrm{e}^{-\frac{i}{\hbar}\bar{\epsilon}_n t} \tag{7.21}$$

For this special case, the derivation is straightforward, as shown for the creation operator and a complete set of eigenstates $|\vec{\sigma}\rangle$ of the non-interacting Hamiltonian $\hat{h}$ with eigenvalues $E_{\vec{\sigma}}$.

$$\begin{aligned} \forall_{\vec{\sigma}}: \quad \hat{a}^{+}_{I,n}(t)|\vec{\sigma}\rangle &= \underbrace{\hat{\mathcal{U}}^{(0)}(0,t)\hat{a}^{\dagger}_{S,n}}_{\hat{a}^{\dagger}_{S,n}|\vec{\sigma}\rangle \mathrm{e}^{+\frac{i}{\hbar}(E_{\vec{\sigma}}+\bar{\epsilon}_n)t}\mathrm{e}^{-\frac{i}{\hbar}E_{\vec{\sigma}}t}} \underbrace{\hat{\mathcal{U}}^{(0)}(t,n)|\vec{\sigma}\rangle}_{|\vec{\sigma}\rangle \mathrm{e}^{-\frac{i}{\hbar}E_{\vec{\sigma}}t}} = \hat{a}^{\dagger}_{S,n}\mathrm{e}^{\frac{i}{\hbar}\bar{\epsilon}_n t}|\vec{\sigma}\rangle \\ \Rightarrow \quad \hat{a}^{+}_{I,n}(t) &= \hat{a}^{\dagger}_{S,n}\mathrm{e}^{\frac{i}{\hbar}\bar{\epsilon}_n t} \end{aligned} \tag{7.22}$$

Back to the general case: The creation and annihilation operators refer to a one-particle basisset $\{|\chi_\alpha\rangle\}$, which may be non-orthonormal. Each orbital has a projector function $\langle \pi_\alpha| = \sum_\beta S^{-1}_{\alpha,\beta}\langle \chi_\beta|$.

Editor: Caution: The two symbols $\hat{\rho}^{\nu N(0)}_{T,\mu} = \hat{\rho}^{(0)}_{T,\mu}$ for the von-Neumann density matrix are used interchangeably. I am in the processes of changing to the more explicit

notation.

$$
\begin{aligned}
G^{\mathcal{C},(0)}_{\alpha,\beta}(t,t') &\overset{\text{Eq. 7.16}}{=} \frac{1}{i\hbar}\mathrm{Tr}\Big\{\hat{\rho}^{vN(0)}_{T,\mu}\mathcal{T}_{\mathcal{C}}\hat{c}_{H,\alpha}(t)\hat{c}^{+}_{H,\beta}(t')\Big\} \\
&\overset{\text{Eqs. L.1, L.2}}{=} \frac{\theta_{\mathcal{C}}(t-t')}{i\hbar}\mathrm{Tr}\Big\{\hat{\rho}^{vN(0)}_{T,\mu}\overbrace{\sum_{\gamma}\langle\pi_\alpha|\hat{U}(t,0)|\chi_\gamma\rangle\hat{c}_{S,\gamma}}^{\hat{c}_{H,\alpha}(t)}\overbrace{\sum_{\delta}\hat{c}^{\dagger}_{S,\delta}\langle\chi_\delta|\hat{U}(0,t')|\pi_\beta\rangle}^{\hat{c}^{+}_{H,\beta}(t')}\Big\} \\
&\quad - \frac{\theta_{\mathcal{C}}(t'-t)}{i\hbar}\mathrm{Tr}\Big\{\hat{\rho}^{vN(0)}_{T,\mu}\overbrace{\sum_{\delta}\hat{c}^{\dagger}_{S,\delta}\langle\chi_\delta|\hat{U}(0,t')|\pi_\beta\rangle}^{\hat{c}^{+}_{H,\beta}(t')}\overbrace{\sum_{\gamma}\langle\pi_\alpha|\hat{U}(t,0)|\chi_\gamma\rangle\hat{c}_{S,\gamma}}^{\hat{c}_{H,\alpha}(t)}\Big\} \\
&= \frac{\theta_{\mathcal{C}}(t-t')}{i\hbar}\sum_{\gamma,\delta}\langle\pi_\alpha|\hat{U}(t,0)|\chi_\gamma\rangle\underbrace{\mathrm{Tr}\Big\{\hat{\rho}^{vN(0)}_{T,\mu}\hat{c}_{S,\gamma}\hat{c}^{\dagger}_{S,\delta}\Big\}}_{\delta_{\gamma,\delta}-\rho^{(1)(0)}_{\gamma,\delta}\quad\text{Eq. 3.56}}\langle\chi_\delta|\hat{U}(0,t')|\pi_\beta\rangle \\
&\quad - \frac{\theta_{\mathcal{C}}(t'-t)}{i\hbar}\sum_{j,k}\langle\pi_\alpha|\hat{U}(t,0)|\chi_\gamma\rangle\underbrace{\mathrm{Tr}\Big\{\hat{\rho}^{vN(0)}_{T,\mu}\hat{c}^{\dagger}_{S,\delta}\hat{c}_{S,\gamma}\Big\}}_{\rho^{(1)(0)}_{\gamma,\delta}\quad\text{Eq. 3.56}}\langle\chi_\delta|\hat{U}(0,t')|\pi_\beta\rangle \\
&\overset{\text{Eq. 3.57}}{=} \frac{1}{i\hbar}\langle\pi_\alpha|\hat{U}(t,0)\Big(\underbrace{\theta_{\mathcal{C}}(t-t')\Big(\hat{1}-\hat{\rho}^{(1),(0)}_{T,\mu}\Big)}_{\text{empty}} - \underbrace{\theta_{\mathcal{C}}(t'-t)\hat{\rho}^{(1),(0)}_{T,\mu}}_{\text{filled}}\Big)\hat{U}(0,t')|\pi_\beta\rangle
\end{aligned}
\tag{7.23}
$$

The Green's function is conveniently expressed as an operator in the one-particle Hilbert space as

$$
\begin{aligned}
\hat{G}^{\mathcal{C},(0)}(t,t') &= \sum_{\alpha,\beta}|\chi_\alpha\rangle G^{\mathcal{C},(0)}_{\alpha,\beta}(t,t')\langle\chi_\beta| \\
&= \frac{1}{i\hbar}\hat{U}(t,0)\Big(\underbrace{\theta_{\mathcal{C}}(t-t')\Big(\hat{1}-\hat{\rho}^{(1),(0)}_{T,\mu}\Big)}_{\text{empty}} - \underbrace{\theta_{\mathcal{C}}(t'-t)\hat{\rho}^{(1),(0)}_{T,\mu}}_{\text{filled}}\Big)\hat{U}(0,t')
\end{aligned}
\tag{7.24}
$$

Unlike the von-Neumann density matrix $\hat{\rho}^{vN(0)}_{T,\mu}$, the one-particle-reduced density matrix $\hat{\rho}^{(1)(0)}_{T,\mu} = \sum_{\gamma,\delta}|\chi_\gamma\rangle\rho^{(1)}_{T,\mu,\gamma,\delta}\langle\chi_\delta|$ is an operator in the one-particle Hilbert space. The subscripts T,μ for temperature and chemical potential indicate that it is, like the von-Neumann density matrix $\hat{\rho}^{vN(0)}_{T,\mu}$, a thermal density matrix in the grand canonical ensemble.

For the non-interacting system, the one-particle-reduced density matrix can be expressed in terms of the Fermi distribution $f_{T,\mu}(\epsilon) \overset{\text{def}}{=} (1+\mathrm{e}^{\beta(\epsilon-\mu)})^{-1}$ as

$$
\hat{\rho}^{(1),(0)}_{T,\mu} = \sum_n |\varphi_n\rangle f_{T,\mu}(\epsilon_n)\langle\varphi_n| \tag{7.25}
$$

by the eigenvalues ϵ_n and eigenstates $|\varphi_n\rangle$ of the one-particle Hamiltonian $\hat{h}(0)$ at the time origin.

Let me consider now some common special cases

- If the creation and annihilation operators are formulated in terms of natural orbitals (the eigenstates of the $\hat{\rho}^{(1)}$), i.e. $\hat{\rho}^{(1)}|\varphi_n\rangle = |\varphi_n\rangle f_n$, the Green's function has the form

$$
\hat{G}^{\mathcal{C},(0)}(t,t') = \frac{1}{i\hbar}\sum_n \underbrace{\hat{U}(t,0)|\varphi_n\rangle}_{|\varphi_n(t)\rangle}\Big(\theta_{\mathcal{C}}(t-t')(1-f_n) - \theta_{\mathcal{C}}(t'-t)f_n\Big)\underbrace{\langle\varphi_n|\hat{U}(0,t')}_{\sum_j O^{-1}_{n,j}(t')\langle\varphi_j(t')|} \tag{7.26}
$$

Here, I also introduced the time-dependent orbitals $|\varphi_n(t)\rangle = \hat{U}(t,0)|\varphi_n\rangle$.

- For a time-independent Hamiltonian $\hat{h}$, the contour propagator for the one-particle states is given by Eq. 6.30

$$\hat{U}(t,t') = \mathrm{e}^{-\frac{i}{\hbar}\hat{h}(t-t')} \tag{7.27}$$

so that

$$\hat{G}^{\mathcal{C},(0)}_{m,n}(t,t') = \frac{1}{i\hbar}\sum_n |\varphi_n\rangle \Big(\theta_{\mathcal{C}}(t-t')(1-f_n) - \theta_{\mathcal{C}}(t'-t)f_n\Big)\mathrm{e}^{-\frac{i}{\hbar}\epsilon_n(t-t')}\langle\varphi_n| \tag{7.28}$$

where $\hat{h}|\varphi_n\rangle = |\varphi_n\rangle\epsilon_n$ and where the occupations are given by the Fermi-distribution $f_n = (1+\mathrm{e}^{-\beta(\epsilon_n-\mu)})^{-1}$.

- The bare contour Green's function for a time-independent and translation-invariant system, speak, of the **homogeneous electron gas** is the topic of the exercise 7.7.2 on p. 262. The result is provided in Eq. 7.57 below.

Green's function as function of energy

For a time-independent Hamiltonian, we can also evaluate the Fourier transform of the Green's function in terms of the time difference $t-t'$. Note that we consider here only the branch of the contour running along the real time axis in the positive direction.

$$\begin{aligned}
\hat{G}^{\mathcal{C},(0)}_{m,n}(\epsilon) &\stackrel{\text{def}}{=} \lim_{\eta\to 0^+}\int_{-\infty}^{\infty} d\tau\; \hat{G}^{\mathcal{C},(0)}_{m,n}(t+\tau,t)\mathrm{e}^{\frac{i}{\hbar}\epsilon\tau-\eta|\tau|} \\
&= \frac{1}{i\hbar}\sum_n |\varphi_n\rangle \int_{-\infty}^{\infty} d\tau\; \Big(\theta(\tau)(1-f_n) - \theta_{\mathcal{C}}(-\tau)f_n\Big)\mathrm{e}^{-\frac{1}{i\hbar}\left[(\epsilon-\epsilon_n)\tau+i\hbar\eta|\tau|\right]}\langle\varphi_n| \\
&= \frac{1}{i\hbar}\sum_n |\varphi_n\rangle \Big(\frac{1-f_n}{\frac{1}{i\hbar}(\epsilon-\epsilon_n+i\eta)} + \frac{f_n}{\frac{1}{i\hbar}(\epsilon-\epsilon_n-i\eta)}\Big)\langle\varphi_n| \\
&= \sum_n |\varphi_n\rangle \Big(\frac{1-f_n}{\epsilon-\epsilon_n+i\eta} + \frac{f_n}{\epsilon-\epsilon_n-i\eta}\Big)\langle\varphi_n|
\end{aligned} \tag{7.29}$$

The infinitesimal parameter η has been introduced to make the Fourier transform of the Green's function defined. This is a kind of **regularization**. The limit $\eta \to 0^+$ has been made explicit only in the first appearance, which is common practice. If η is sufficiently small, it does not affect the emerging physical picture. The parameter mimics a physical effect that is not part of the mathematical formulation, namely the environment: An environment introduces a finite coherence time and, consequently, a finite life-time broadening of the spectral features. Introducing the small parameter η is analogous to my trick of considering a "finite Universe" to avoid continuous spectra by limiting the wave functions to a very large, albeit finite region.

The poles of the Green's function of the empty states lie in below the real energy axis, while the poles of the filled states lie in above the real energy axis. Editor: Interesting are partially filled states, for which there are two poles, one on each side of the real energy axis.

Let me summarize this result in an orbital representation:

NON-INTERACTING GREEN'S FUNCTIONS FOR COMPLEX TIME ARGUMENTS

The contour-ordered Green's function for a non-interacting many-particle system which initially, at time $t = 0$, is in thermal equilibrium with a heat bath and a particle reservoir is

$$\begin{aligned}\hat{G}^{\mathcal{C},(0)}(t,t') &= \frac{1}{i\hbar}\hat{U}(t,0)\Big\{\underbrace{\theta_{\mathcal{C}}(t-t')\big(\hat{1}-\hat{\rho}^{(1),(0)}_{T,\mu}\big)}_{\text{electrons}} - \underbrace{\theta_{\mathcal{C}}(t'-t)\hat{\rho}^{(1)}_{T,\mu}}_{\text{holes}}\Big\}\hat{U}(0,t') \\ &= \frac{1}{i\hbar}\sum_n \underbrace{\hat{U}(t,0)|\varphi_n\rangle}_{|\varphi_n(t)\rangle}\Big\{\underbrace{\theta_{\mathcal{C}}(t-t')(1-f_n)}_{\text{electrons}} - \underbrace{\theta_{\mathcal{C}}(t'-t)f_n}_{\text{holes}}\Big\}\underbrace{\langle\varphi_n|\hat{U}(0,t')}_{\sum_j O^{-1}_{n,j}(t')\langle\varphi_j(t')|}\end{aligned} \tag{7.30}$$

where $\hat{\rho}^{(1)}_{T,\mu}$ is the one-particle-reduced density matrix, which is in thermal equilibrium with the initial Hamiltonian $\hat{h}(0)$. $\hat{U}(t,t')$ is the (non-interacting) propagator in the one-particle Hilbert space. The backward propagator $\hat{U}(0,t) = \hat{U}^{-1}(t,0)$ is the inverse of the forward propagator, but not necessarily its hermitian conjugate.[a]
$|\varphi_n\rangle$ are the natural orbitals and the $f_n = f_{T,\mu}(\epsilon_n)$ are the thermal occupations[b] of the initial Hamiltonian $\hat{h}(0)$. The energies ϵ_n are the eigenvalues of the initial Hamiltonian $\hat{h}(0)$. $|\varphi_n(t)\rangle = \hat{U}(t,0)|\varphi_n\rangle$ are the natural orbitals propagated in time. $O_{m,n}(t) = \langle\varphi_m(t)|\varphi_n(t)\rangle$ are the overlap matrix elements of the time-dependent orbitals.
For a time-independent Hamiltonian with eigenstates $|\varphi_n\rangle$ and eigenvalues ϵ_n, the Green's function is

$$\hat{G}^{\mathcal{C},(0)}(t,t') \overset{\text{Eq. 7.30}}{=} \frac{1}{i\hbar}\sum_n |\varphi_n\rangle\Big\{\underbrace{\frac{\theta_{\mathcal{C}}(t-t')}{1+\mathrm{e}^{-\beta(\epsilon_n-\mu)}}}_{\text{empty, }\sim(1-f_n)} - \underbrace{\frac{\theta_{\mathcal{C}}(t'-t)}{1+\mathrm{e}^{+\beta(\epsilon_n-\mu)}}}_{\text{filled, }\sim f_n}\Big\}\,\mathrm{e}^{-\frac{i}{\hbar}\epsilon_n(t-t')}\langle\varphi_n| \tag{7.31}$$

The energy-dependent Green's function for a time-independent non-interacting Hamiltonian is obtained as Fourier transform of the retardation $t - t'$.

$$\begin{aligned}\hat{G}^{\mathcal{C},(0)}(\epsilon) &\overset{\text{def}}{=} \int_{-\infty}^{\infty} d\tau\; \hat{G}^{\mathcal{C},(0)}(t+\tau,t)\mathrm{e}^{\frac{i}{\hbar}\epsilon\tau-\eta|\tau|} \\ &= \sum_n |\varphi_n\rangle\Big(\frac{1-f_n}{\epsilon-\epsilon_n+i\eta} + \frac{f_n}{\epsilon-\epsilon_n-i\eta}\Big)\langle\varphi_n|\end{aligned} \tag{7.32}$$

For the position of the poles, see also figure 9.1 on p. 290. In that figure $\hbar\omega$ translates into ϵ.
The matrix elements of the Green's function for (potentially non-orthonormal) orbitals $|\chi_\alpha\rangle$ with projector functions $\langle\pi_\alpha|$, respectively the Green's for the real-space-and-spin basis are

$$\begin{aligned}G^{\mathcal{C},(0)}_{\alpha,\beta}(t,t') &= \langle\pi_\alpha|\hat{G}^{\mathcal{C},(0)}(t,t')|\pi_\beta\rangle \\ G^{\mathcal{C},(0)}(\vec{x},t,\vec{x'},t') &= \langle\vec{x}|\hat{G}^{\mathcal{C},(0)}(t,t')|\vec{x'}\rangle\end{aligned} \tag{7.33}$$

[a] The difference is because we allow for complex-valued time arguments, so that the propagator is no more strictly unitary.

$$\hat{U}(t,0) = \sum_{m,n}|\varphi_n(t)\rangle\underbrace{O^{-1}_{m,n}(0)}_{\delta_{m,n}}\langle\varphi_n(0)|$$

$$\hat{U}(0,t) = \hat{U}^{-1}(t,0) = \sum_{m,n}|\varphi_n(0)\rangle O^{-1}_{m,n}(t)\langle\varphi_n(t)| \qquad \text{while} \qquad \hat{U}^\dagger(t,0) = \sum_n |\varphi_n(0)\rangle\langle\varphi_n(t)|$$

[b] $f_{T,\mu}(\epsilon) = (\mathrm{e}^{\beta(\epsilon-\mu)}+1)^{-1}$ is the Fermi distribution function.

If the reader gets confused by the complex time arguments, he may simply follow the arguments in the first run having a time contour on the real axis in mind. In a second reading, she may verify that the arguments also hold for complex time arguments.

7.6 Generality of the problem

7.6.1 Initial state:

The Green's functions, and thus all quantities derived from it, are thermal expectation values in a grand canonical ensemble. Many of the relations derived in the following apply to thermal (equilibrium) ensembles rather than arbitrary ensembles specified by many-particle states and their probabilities. I was wondering, whether this is a severe restriction of the theory, and whether the theory can be generalized to arbitrary non-equilibrium ensembles. Here, I show, that the generalization should be possible, because for any ensemble, there is a specific Hamiltonian, for which this ensemble is a thermal ensemble. Unfortunately, this Hamiltonian is much more complicated that the physical Hamiltonians we are used to.

Here, I will show that the form of a grand canonical ensemble can be used to describe an arbitrary ensemble without any reference to thermal equilibrium.[72]

Let us start with an arbitrary ensemble, which is characterized by its many-particle density matrix $\hat{\rho}$. Our goal is to construct a many-particle Hamiltonian $\hat{H}^{ini}$ which produces this, specified, von-Neumann density matrix $\hat{\rho}$ in thermal equilibrium.

$$\hat{\rho} \stackrel{!}{=} \frac{1}{Z^{ini}_{T,\mu}} \mathrm{e}^{-\beta(\hat{H}^{ini}-\mu\hat{N})} \qquad \text{with } Z^{ini}_{T,\mu} = \mathrm{Tr}\left[\mathrm{e}^{-\beta(\hat{H}^{ini}-\mu\hat{N})}\right] \tag{7.34}$$

Firstly, let us first determine the eigenvalues and eigenstates of the density operator.

$$\hat{\rho}|\Phi_q\rangle = |\Phi_q\rangle P_q \tag{7.35}$$

Because the density matrix $\hat{\rho}$ is hermitian, the eigenstates $|\Phi_q\rangle$ are orthonormal and the eigenvalues P_q are real. The condition $\mathrm{Tr}[\hat{\rho}] = 1$ reflects in $\sum_q P_q = 1$.

By taking the logarithm of Eq. 7.34

$$\begin{aligned} -k_B T \ln(\hat{\rho}) &= \hat{H}^{ini} - \mu\hat{N} + k_B T \ln(Z_{T,\mu}) \\ \Leftrightarrow \hat{H}^{ini} &= -k_B T \ln(\hat{\rho}) + \mu\hat{N} \underbrace{-k_B T \ln(Z_{T,\mu})}_{\Omega_{T,\mu}} \\ &= \mu\hat{N} + \sum_q |\Phi_q\rangle \Big(-k_B T \ln(P_q)\Big) \langle\Phi_q| + \Omega_{T,\mu}\hat{1} \end{aligned} \tag{7.36}$$

The last term, the grand potential, is a global energy shift, which does not have physical consequences: When the probabilities are calculated from the Boltzmann factors, they are normalized with the help of the partition function.

The density matrix, specified initially, can thus be written in the form of a grand canonical ensemble for a Hamiltonian

$$\underbrace{\hat{H}^{ini,\prime}}_{\hat{H}^{ini}-\Omega_{T,\mu}\hat{1}} = \mu\hat{N} + \sum_q |\Phi_q\rangle \Big(-k_B T \ln(P_q)\Big) \langle\Phi_q| \tag{7.37}$$

The Hamiltonian H^{ini} used here is not necessarily related to a physical Hamiltonian of the system. It merely describes the initial ensemble.

7.7 Home study and practice

7.7.1 Non-interacting contour Green's function for the non-interacting hydrogen molecule

Introduction

The goal of this exercise is to provide hand-s on contact to a simple, but real Green's function.

Problem

The hydrogen molecule without interaction has the Hamiltonian

$$\hat{h} = \sum_{R\in\{l,r\}} \sum_{\sigma\in\{\uparrow,\downarrow\}} \bar{\epsilon}\hat{c}^\dagger_{S,R,\sigma}\hat{c}_{S,R,\sigma} - t \sum_{\sigma\in\{\uparrow,\downarrow\}} \left(\hat{c}^\dagger_{S,l,\sigma}\hat{c}^\dagger_{S,r,\sigma} + \hat{c}^\dagger_{S,r,\sigma}\hat{c}^\dagger_{S,l,\sigma}\right) \tag{7.38}$$

1 Calculate the contour-ordered Green's function for the non-interacting hydrogen molecule. Provide the Green's function in terms of a basis of local orbitals, which is determined by a site index and a spin index.

2 Extract the one-particle-reduced density matrix from the Green's function from the previous problem. Determine the natural orbitals and occupations.

Solution

1 Calculate the contour-ordered Green's function for the non-interacting hydrogen molecule.

We use the expression Eq. 7.30 for the Green's function of a non-interacting electron system.

$$G^{\mathcal{C},(0)}_{\alpha,\beta}(t,t') \overset{\text{Eq. 7.30}}{=} \frac{1}{i\hbar}\sum_n \langle\pi_\alpha|\psi_n\rangle\Big\{\underbrace{\theta_{\mathcal{C}}(t-t')(1-f_n)}_{\text{electrons}} - \underbrace{\theta_{\mathcal{C}}(t'-t)f_n}_{\text{holes}}\Big\}\, \mathrm{e}^{-\frac{i}{\hbar}\epsilon_n(t-t')}\langle\psi_n|\pi_\beta\rangle \tag{7.39}$$

First, we determine the eigenvalues and eigenstates of the one-particle Hamiltonian. The non-interacting Hamiltonian in second quantization is

$$\hat{h} = \sum_{j\in\{1,2\}} \sum_{\sigma\in\{\uparrow,\downarrow\}} \bar{\epsilon}\hat{c}^\dagger_{j,\sigma}\hat{c}_{j,\sigma} - \bar{t} \sum_{\sigma\in\{\uparrow,\downarrow\}} \left(\hat{c}^\dagger_{1,\sigma}\hat{c}_{2,\sigma} + \hat{c}^\dagger_{2,\sigma}\hat{c}_{1,\sigma}\right) \tag{7.40}$$

This Hamilton operator is translated in one-particle quantum mechanics Editor: Is it clear how this is done?

$$\hat{h} = \sum_{j\in\{1,2\}} \sum_{\sigma\in\{\uparrow,\downarrow\}} |\pi_{j,\sigma}\rangle\bar{\epsilon}\langle\pi_{j,\sigma}| - \sum_{\sigma\in\{\uparrow,\downarrow\}} \left(|\pi_{1,\sigma}\rangle\bar{t}\langle\pi_{2,\sigma}| + |\pi_{2,\sigma}\rangle\bar{t}\langle\pi_{1,\sigma}|\right) \tag{7.41}$$

The eigenstates are (see section 1.5.1 on p. 26)

$$|\varphi_{\pm,\sigma}\rangle = \frac{1}{\sqrt{2}}\left(|\chi_{1,\sigma}\rangle \mp |\chi_{2,\sigma}\rangle\right) \tag{7.42}$$

with energies

$$\epsilon_{\pm,\sigma} = \bar{\epsilon} \pm \bar{t} \tag{7.43}$$

We had made the assumption that the orbitals $|\chi_\alpha\rangle$ are orthonormal.

In insert the eigenstates and eigenvalues. I use $\langle \pi_\alpha | \chi_\beta \rangle = \delta_{\alpha,\beta}$.

$$
\begin{aligned}
G^{\mathcal{C},(0)}_{j,\sigma;j',\sigma'}(t,t') = \frac{1}{i\hbar} \sum_{n\in\{+,-\}} \sum_{\sigma''\in\{\uparrow,\downarrow\}} & \underbrace{\langle \pi_{j,\sigma} | \varphi_{n,\sigma''} \rangle}_{=\delta_{\sigma,\sigma''}\frac{1}{\sqrt{2}}\left(\delta_{j,1}\mp\delta_{j,2}\right) \text{ for } n=\pm} \times \underbrace{\langle \varphi_{n,\sigma''} | \pi_{j',\sigma'} \rangle}_{=\delta_{\sigma'',\sigma'}\frac{1}{\sqrt{2}}\left(\delta_{j',1}\mp\delta_{j',2}\right) \text{ for } n=\pm} \\
& \times \left\{ \theta_{\mathcal{C}}(t-t') \underbrace{\left(1 - \frac{1}{1+\mathrm{e}^{\beta(\epsilon_{n,\sigma''}-\mu)}} \right)}_{\frac{1}{1+\mathrm{e}^{-\beta(\epsilon_{n,\sigma''}-\mu)}}} - \theta_{\mathcal{C}}(t'-t) \frac{1}{1+\mathrm{e}^{\beta(\epsilon_{n,\sigma''}-\mu)}} \right\} \mathrm{e}^{-\frac{i}{\hbar}\epsilon_{n,\sigma}(t-t')} \\
= \frac{1}{i\hbar}\delta_{\sigma,\sigma'} \Bigg\{ & \frac{1}{2}\Big(\delta_{j,1}+\delta_{j,2}\Big)\Big(\delta_{j',1}+\delta_{j',2}\Big) \left[\frac{\theta_{\mathcal{C}}(t-t')}{1+\mathrm{e}^{-\beta(\bar{\epsilon}-\bar{t}-\mu)}} - \frac{\theta_{\mathcal{C}}(t'-t)}{1+\mathrm{e}^{+\beta(\bar{\epsilon}-\bar{t}-\mu)}} \right] \mathrm{e}^{-\frac{i}{\hbar}(\bar{\epsilon}-\bar{t})(t-t')} \\
& + \frac{1}{2}\Big(\delta_{j,1}-\delta_{j,2}\Big)\Big(\delta_{j',1}-\delta_{j',2}\Big) \left[\frac{\theta_{\mathcal{C}}(t-t')}{1+\mathrm{e}^{-\beta(\bar{\epsilon}+\bar{t}-\mu)}} - \frac{\theta_{\mathcal{C}}(t'-t)}{1+\mathrm{e}^{+\beta(\bar{\epsilon}+\bar{t}-\mu)}} \right] \mathrm{e}^{-\frac{i}{\hbar}(\bar{\epsilon}+\bar{t})(t-t')} \Bigg\} \\
= \frac{1}{i\hbar}\delta_{\sigma,\sigma'} & \mathrm{e}^{-\frac{i}{\hbar}\bar{\epsilon}(t-t')} \\
& \times \Bigg\{ \frac{1}{2}\Big(\delta_{j,1}+\delta_{j,2}\Big)\Big(\delta_{j',1}+\delta_{j',2}\Big) \left[\frac{\theta_{\mathcal{C}}(t-t')\mathrm{e}^{+\frac{i}{\hbar}\bar{t}(t-t')}}{1+\mathrm{e}^{-\beta(\bar{\epsilon}-\bar{t}-\mu)}} - \frac{\theta_{\mathcal{C}}(t'-t)\mathrm{e}^{+\frac{i}{\hbar}\bar{t}(t-t')}}{1+\mathrm{e}^{+\beta(\bar{\epsilon}-\bar{t}-\mu)}} \right] \\
& + \frac{1}{2}\Big(\delta_{j,1}-\delta_{j,2}\Big)\Big(\delta_{j',1}-\delta_{j',2}\Big) \left[\frac{\theta_{\mathcal{C}}(t-t')\mathrm{e}^{-\frac{i}{\hbar}\bar{t}(t-t')}}{1+\mathrm{e}^{-\beta(\bar{\epsilon}+\bar{t}-\mu)}} - \frac{\theta_{\mathcal{C}}(t'-t)\mathrm{e}^{-\frac{i}{\hbar}\bar{t}(t-t')}}{1+\mathrm{e}^{+\beta(\bar{\epsilon}+\bar{t}-\mu)}} \right] \Bigg\} \qquad (7.44)
\end{aligned}
$$

$$
\begin{aligned}
\begin{pmatrix} G^{\mathcal{C},(0)}_{1,\sigma;1,\sigma'} & G^{\mathcal{C},(0)}_{1,\sigma;2,\sigma'} \\ G^{\mathcal{C},(0)}_{2,\sigma;1,\sigma'} & G^{\mathcal{C},(0)}_{2,\sigma;2,\sigma'} \end{pmatrix} = & \frac{1}{2i\hbar}\delta_{\sigma,\sigma'}\mathrm{e}^{-\frac{i}{\hbar}\bar{\epsilon}(t-t')} \\
& \times \Bigg\{ \begin{pmatrix} +1 & +1 \\ +1 & +1 \end{pmatrix} \left[\frac{\theta_{\mathcal{C}}(t-t')\mathrm{e}^{+\frac{i}{\hbar}\bar{t}(t-t')}}{1+\mathrm{e}^{-\beta(\bar{\epsilon}-\bar{t}-\mu)}} - \frac{\theta_{\mathcal{C}}(t'-t)\mathrm{e}^{+\frac{i}{\hbar}\bar{t}(t-t')}}{1+\mathrm{e}^{+\beta(\bar{\epsilon}-\bar{t}-\mu)}} \right] \\
& + \begin{pmatrix} +1 & -1 \\ -1 & +1 \end{pmatrix} \left[\frac{\theta_{\mathcal{C}}(t-t')\mathrm{e}^{-\frac{i}{\hbar}\bar{t}(t-t')}}{1+\mathrm{e}^{-\beta(\bar{\epsilon}+\bar{t}-\mu)}} - \frac{\theta_{\mathcal{C}}(t'-t)\mathrm{e}^{-\frac{i}{\hbar}\bar{t}(t-t')}}{1+\mathrm{e}^{+\beta(\bar{\epsilon}+\bar{t}-\mu)}} \right] \Bigg\} \qquad (7.45)
\end{aligned}
$$

This is the desired result.

Let me consider some limiting cases

- In the high-temperature limit $\beta \to 0$ the Fermi function contributes a factor $1/2$.

$$
\begin{aligned}
\begin{pmatrix} G^{\mathcal{C},(0)}_{1,\sigma;1,\sigma'} & G^{\mathcal{C},(0)}_{1,\sigma;2,\sigma'} \\ G^{\mathcal{C},(0)}_{2,\sigma;1,\sigma'} & G^{\mathcal{C},(0)}_{2,\sigma;2,\sigma'} \end{pmatrix} = & \frac{1}{i\hbar}\delta_{\sigma,\sigma'}\mathrm{e}^{-\frac{i}{\hbar}\bar{\epsilon}(t-t')} \underbrace{\Big(\theta_{\mathcal{C}}(t-t') - \theta_{\mathcal{C}}(t'-t)\Big)}_{\mathrm{sgn}(t-t')} \\
& \times \begin{pmatrix} \cos\left(\frac{1}{\hbar}\bar{t}(t-t')\right) & i\sin\left(\frac{1}{\hbar}\bar{t}(t-t')\right) \\ i\sin\left(\frac{1}{\hbar}\bar{t}(t-t')\right) & \cos\left(\frac{1}{\hbar}\bar{t}(t-t')\right) \end{pmatrix} \qquad (7.46)
\end{aligned}
$$

  One sees that the Green's function is not hermitian.

- For $\mu = \bar{\epsilon}$, we obtain the system with two particles. In the low-temperature limit, $\beta \to \infty$ only the bonding states contribute for $t < t'$ and the antibonding states contribute for $t > t'$.

$$
\begin{aligned}
\begin{pmatrix} G^{\mathcal{C},(0)}_{1,\sigma;1,\sigma'} & G^{\mathcal{C},(0)}_{1,\sigma;2,\sigma'} \\ G^{\mathcal{C},(0)}_{2,\sigma;1,\sigma'} & G^{\mathcal{C},(0)}_{2,\sigma;2,\sigma'} \end{pmatrix} = & \frac{1}{2i\hbar}\delta_{\sigma,\sigma'}\mathrm{e}^{-\frac{i}{\hbar}\bar{\epsilon}(t-t')} \\
\times \Bigg\{ & \begin{pmatrix} +1 & +1 \\ +1 & +1 \end{pmatrix} \left[-\theta_{\mathcal{C}}(t'-t)\mathrm{e}^{+\frac{i}{\hbar}\bar{t}(t-t')} \right] + \begin{pmatrix} +1 & -1 \\ -1 & +1 \end{pmatrix} \left[\theta_{\mathcal{C}}(t-t')\mathrm{e}^{-\frac{i}{\hbar}\bar{t}(t-t')} \right] \Bigg\} \qquad (7.47)
\end{aligned}
$$

2 Extract the one-particle-reduced density matrix from the Green's function from the previous problem. Determine the natural orbitals and occupations.

7.7.2 Bare contour Green's function of the homogeneous electron gas

Introduction

The homogeneous electron gas is a common model system. Therefore, the it is corresponding Green's function will be handy in many occasions.

The current exercise is special because (1) it determines the contour Green's function for arbitrary complex-valued time arguments, (2) it allows for arbitrary dispersion relations $\epsilon_{\vec{k},\sigma}$, (3) it works with a one-particle basisset with periodic boundary conditions in a finite unit cell.

The use of an arbitrary dispersion relation provides access also to band-structures which experience a self-energy shift from the interaction, such as the Hartree-Fock approximation or the screened Hartree-Fock approximation. Furthermore it is possible to introduce band gaps into the band structure and study insulators. This aspect may be of interest to investigate the implications of Fermi-liquid theory on insulators.

Problem

Consider a non-interacting system, which is translation invariant in space an time, with a Hamiltonian

$$\hat{h} = \sum_{\vec{k}} \sum_{\sigma\in\{\uparrow,\downarrow\}} |\vec{k},\sigma\rangle \epsilon_{\vec{k},\sigma} \langle \vec{k},\sigma| \tag{7.48}$$

The band structure $\epsilon_{\vec{k},\sigma}$ is not determined any further.

1 determine the bare Green's function for the above-mentioned system. Use Eq. 7.30.

Discussion

1 determine the bare Green's function for the above-mentioned system. Use Eq. 7.30.

We start out from the expression Eq. 7.30 from p. 258 for the non-interacting Greens' function.

$$\begin{aligned}\hat{G}^{\mathcal{C},(0)}(t,t') &= \frac{1}{i\hbar}\hat{U}(t,0)\Big\{\underbrace{\theta_{\mathcal{C}}(t-t')\big(\hat{1}-\hat{\rho}^{(1),(0)}_{T,\mu}\big)}_{\text{electrons}} - \underbrace{\theta_{\mathcal{C}}(t'-t)\hat{\rho}^{(1)}_{T,\mu}}_{\text{holes}}\Big\}\hat{U}(0,t') \\ &= \frac{1}{i\hbar}\sum_n \underbrace{\hat{U}(t,0)|\varphi_n\rangle}_{|\varphi_n(t)\rangle}\Big\{\underbrace{\theta_{\mathcal{C}}(t-t')(1-f_n)}_{\text{electrons}} - \underbrace{\theta_{\mathcal{C}}(t'-t)f_n}_{\text{holes}}\Big\}\underbrace{\langle\varphi_n|\hat{U}(0,t')}_{\sum_j O^{-1}_{n,j}(t')\langle\varphi_j(t')|}\end{aligned} \tag{7.49}$$

Let me use a plane wave basisset as the orbital set.

$$\langle \vec{r},\sigma'|\vec{k},\sigma\rangle = \delta_{\sigma,\sigma'}\frac{1}{\sqrt{L^3}}\mathrm{e}^{i\vec{k}\vec{r}} \tag{7.50}$$

I use periodic boundary conditions in a cubic box of side-length L, which ultimately shall approach

infinity.

$$k_j L = 2\pi j \Rightarrow k_j = \frac{2\pi}{L} j$$
$$\underbrace{(\Delta k)^3}_{\Rightarrow d^3k} = \frac{(2\pi)^3}{L^3} \tag{7.51}$$

The orbitals are normalized within the corresponding box:

$$\int_{L^3} d^3r \sum_{\sigma''} \left|\langle \vec{k}, \sigma | \vec{r}, \sigma'' \rangle\right|^2 = 1 \tag{7.52}$$

The wave functions $|\varphi_{\vec{k},\sigma}(t)\rangle$, which satisfy the time-dependent Schrödinger equation

$$\Big(i\hbar\partial_t - \sum_{\vec{k}',\sigma'} |\vec{k}', \sigma'\rangle \epsilon_{\vec{k}',\sigma'} \langle \vec{k}', \sigma'|\Big) |\varphi_{\vec{k},\sigma}(t)\rangle = 0 \tag{7.53}$$

along the time contour are

$$|\varphi_{\vec{k},\sigma}(t)\rangle = |\vec{k}, \sigma\rangle \mathrm{e}^{-\frac{i}{\hbar}\epsilon_{\vec{k},\sigma} t} \tag{7.54}$$

The wave functions are orthonormal on the real time axis, but not away from it in the complex time plane. The time-dependent overlap matrix is.

$$O_{\vec{k},\sigma,\vec{k}',\sigma'}(t) = \langle \varphi_{\vec{k},\sigma}(t) | \varphi_{\vec{k}',\sigma'}(t)\rangle = \delta_{\vec{k},\vec{k}'}\delta_{\sigma,\sigma'} \mathrm{e}^{+\frac{i}{\hbar}\epsilon\left(t^*-t\right)} = \delta_{\vec{k},\vec{k}'}\delta_{\sigma,\sigma'} \mathrm{e}^{+\frac{2}{\hbar}\epsilon_{\vec{k},\sigma}\mathrm{Im}[t]} \tag{7.55}$$

The Green's function in the complex-time plane is

$$\begin{aligned}
G^{\mathcal{C},(0)}_{\vec{k},\sigma,\vec{k}',\sigma'}(t,t') &= \langle \vec{k}, \sigma | \hat{G}^{\mathcal{C},(0)}(t,t') | \vec{k}', \sigma' \rangle \\
&= \frac{1}{i\hbar} \sum_{\vec{k}'',\sigma''} \underbrace{\langle \vec{k}, \sigma | \varphi_{\vec{k}'',\sigma''}(t)\rangle}_{\delta_{\vec{k},\vec{k}''}\delta_{\sigma,\sigma''} \mathrm{e}^{-\frac{i}{\hbar}\epsilon_{\vec{k},\sigma} t}} \left\{ \frac{\theta_{\mathcal{C}}(t-t')}{1+\mathrm{e}^{-\beta(\epsilon_{\vec{k}'',\sigma''}-\mu)}} - \frac{\theta_{\mathcal{C}}(t'-t)}{1+\mathrm{e}^{+\beta(\epsilon_{\vec{k}'',\sigma''}-\mu)}} \right\} \\
&\qquad \times \underbrace{\mathrm{e}^{-\frac{2}{\hbar}\epsilon_{\vec{k}'',\sigma''}\mathrm{Im}[t']}}_{O^{-1}(t')\rightsquigarrow} \underbrace{\langle \varphi_{\vec{k}'',\sigma''}(t') | \vec{k}', \sigma' \rangle}_{\delta_{\vec{k}',\vec{k}''}\delta_{\sigma',\sigma''} \mathrm{e}^{+\frac{i}{\hbar}\epsilon_{\vec{k}',\sigma'}(t')^*}} \\
&= \frac{1}{i\hbar}\delta_{\vec{k},\vec{k}'}\delta_{\sigma,\sigma'} \mathrm{e}^{-\frac{i}{\hbar}\epsilon_{\vec{k},\sigma} t} \left\{ \frac{\theta_{\mathcal{C}}(t-t')}{1+\mathrm{e}^{-\beta(\epsilon_{\vec{k},\sigma}-\mu)}} - \frac{\theta_{\mathcal{C}}(t'-t)}{1+\mathrm{e}^{+\beta(\epsilon_{\vec{k},\sigma}-\mu)}} \right\} \underbrace{\mathrm{e}^{+\frac{i}{\hbar}\epsilon_{\vec{k},\sigma}(t'-(t')^*)}}_{O^{-1}(t')\rightsquigarrow} \mathrm{e}^{\frac{i}{\hbar}\epsilon_{\vec{k},\sigma}(t')^*} \\
&= \frac{1}{i\hbar}\delta_{\vec{k},\vec{k}'}\delta_{\sigma,\sigma'} \left\{ \frac{\theta_{\mathcal{C}}(t-t')}{1+\mathrm{e}^{-\beta(\epsilon_{\vec{k},\sigma}-\mu)}} - \frac{\theta_{\mathcal{C}}(t'-t)}{1+\mathrm{e}^{+\beta(\epsilon_{\vec{k},\sigma}-\mu)}} \right\} \mathrm{e}^{-\frac{i}{\hbar}\epsilon_{\vec{k},\sigma}(t-t')} \\
&= \frac{1}{i\hbar}\delta_{\vec{k},\vec{k}'}\delta_{\sigma,\sigma'} \Big\{ \theta_{\mathcal{C}}(t-t')\Big(1 - f_{T,\mu}(\epsilon_{\vec{k},\sigma})\Big) - \theta_{\mathcal{C}}(t'-t) f_{T,\mu}(\epsilon_{\vec{k},\sigma}) \Big\} \mathrm{e}^{-\frac{1}{\hbar}\epsilon_{\vec{k},\sigma}(t-t')}
\end{aligned} \tag{7.56}$$

where $f_{T,\mu}(\epsilon)$ is the Fermi function.

BARE CONTOUR GREEN'S FUNCTION OF THE HOMOGENEOUS ELECTRON GAS

The bare contour Green's function of a homogeneous electron gas with a dispersion relation $\epsilon_{\vec{k},\sigma}$ is

$$\hat{G}^{\mathcal{C},(0)}(t,t') \overset{\text{Eq. 7.56}}{=} \frac{1}{i\hbar}\sum_{\vec{k}}\sum_{\sigma\in\{\uparrow,\downarrow\}} |\vec{k},\sigma\rangle\Big\{\theta_{\mathcal{C}}(t-t')\Big(1-f_{T,\mu}(\epsilon_{\vec{k},\sigma})\Big)-\theta_{\mathcal{C}}(t'-t)f_{T,\mu}(\epsilon_{\vec{k},\sigma})\Big\} \times \mathrm{e}^{-\frac{i}{\hbar}\epsilon_{\vec{k},\sigma}(t-t')}\langle\vec{k},\sigma| \tag{7.57}$$

where $f_{T,\mu}(\epsilon) = \left(1+\mathrm{e}^{\beta(\epsilon-\mu)}\right)^{-1}$ is the Fermi function. The one-particle basis states are plane waves $\langle\vec{r},\sigma|\vec{k},\sigma'\rangle = \delta_{\sigma,\sigma'}\frac{1}{\sqrt{L^3}}\mathrm{e}^{i\vec{k}\vec{r}}$ with periodic boundary conditions in simple cubic unit cell with side length L, which also determines the normalization volume. That is $\vec{k}_{i,j,k} = \frac{2\pi}{L}(i,j,k)$ with integer i,j,k.

Chapter 8

Exact properties of the many-particle Green's function

The typical approach towards many-body Green's functions is many-body perturbation theory (MBPT), which expands the Green's function about that of a (quasi) non-interacting case. Many-body perturbation theory is widely known through its elegant formulation in terms of Feynman diagrams. However, MBPT is also plagued by the often limited convergence radius of the perturbation expansion. Therefore, I find it important to know the few exact statements about Green's functions of many-particle systems.

In this chapter, I will introduce the equation of motion for the Green's function and the self energy as the second most important quantity. The self energy acts like a potential acting on the electrons, which however is non-local in time. It is retarded like an echo. An electron disturbs the surrounding electron gas and, later, this perturbation of the electron gas acts back on the dynamics of the traveling electron. We will see, how the self energy can be expressed in terms of a well-defined expectation value of the many-electron wave functions.

The Green's function contains all information on the dynamics of single electrons in contact with an electron gas. Thus, it is no surprise that the Green's function provides the one-particle-reduced density matrix. As the only two-particle expectation value, the interaction energy can be extracted from the Green's function. Thus, we obtain access to the total energy of the system.

8.1 Equation of motion for the many-particle Green's function

The Green's function of a many-particle system is not a Green's function in the mathematical sense. In mathematics, a Green's function is the inverse of a differential operator. This applies only to the Green function of one-particle systems. In solid-state physics, only the physical meaning of the Green's function has been kept, namely as probability amplitude between two events.

When we try to set up a differential equation analogous to the one-particle case, we are lead to higher Green's functions involving more and more particles. Nevertheless, we can define a retarded one-particle potential that replaces the action of the many-particle system. This potential is the **self energy**. If the self-energy is included, the Green's function obeys a differential equation as in the one-particle case.

In the following, I derive a differential equation for the interacting many-body Green's function.

The first step is to find a differential equation for a Heisenberg operator $\hat{c}_{H,\zeta}(t)$, because the time derivative will act on this operator within the expression for the Green's function

$$i\hbar\partial_t \hat{c}_{H,\zeta}(t) = \hat{\mathcal{U}}(0,t)\left[\hat{c}_{S,\zeta}, \hat{H}(t)\right]_- \hat{\mathcal{U}}(t,0) \tag{8.1}$$

In the remainder of the derivation, I will drop the time argument of the Hamiltonian, while I consider the Hamilton matrix elements to depend on the current time.

In order to continue, we need the commutator of the annihilation operator in the Schrödinger picture with the Hamiltonian. For the sake of simplicity, we drop the explicit subscript S denoting the Schrodinger picture. It is implicitly assumed.

$$\hat{H}(t) = \sum_{\alpha,\beta} h_{\alpha,\beta}(t)\hat{c}^\dagger_\alpha \hat{c}_\beta + \frac{1}{2}\sum_{\alpha,\beta,\gamma,\delta} W_{\alpha,\beta,\delta,\gamma}(t)\hat{c}^\dagger_\alpha \hat{c}^\dagger_\beta \hat{c}_\gamma \hat{c}_\delta \tag{8.2}$$

We begin with the one-particle operator

$$\left[\hat{c}_\zeta, \sum_{\alpha,\beta} h_{\alpha,\beta}\hat{c}^\dagger_\alpha \hat{c}_\beta\right]_- = \sum_{\alpha,\beta} h_{\alpha,\beta}\Bigg(\underbrace{\hat{c}_\zeta \hat{c}^\dagger_\alpha}_{\delta_{\zeta,\alpha}-\hat{c}^\dagger_\alpha\hat{c}_\zeta}\hat{c}_\beta - \hat{c}^\dagger_\alpha \underbrace{\hat{c}_\beta \hat{c}_\zeta}_{-\hat{c}_\zeta\hat{c}_\beta}\Bigg) = \sum_{\alpha,\beta} h_{\alpha,\beta}\delta_{\zeta,\alpha}\hat{c}_\beta = \sum_\beta h_{\zeta,\beta}\hat{c}_\beta \tag{8.3}$$

and continue with the interaction

$$\begin{aligned}
\left[\hat{c}_\zeta, \frac{1}{2}\sum_{\alpha,\beta,\gamma,\delta} W_{\alpha,\beta,\delta,\gamma}\hat{c}^\dagger_\alpha \hat{c}^\dagger_\beta \hat{c}_\gamma \hat{c}_\delta\right]_- &= \frac{1}{2}\sum_{\alpha,\beta,\gamma,\delta} W_{\alpha,\beta,\delta,\gamma}\Big(\hat{c}_\zeta \hat{c}^\dagger_\alpha \hat{c}^\dagger_\beta \hat{c}_\gamma \hat{c}_\delta - \hat{c}^\dagger_\alpha \hat{c}^\dagger_\beta \underbrace{\hat{c}_\gamma \hat{c}_\delta \hat{c}_\zeta}_{\hat{c}_\zeta\hat{c}_\gamma\hat{c}_\delta}\Big) \\
&= \frac{1}{2}\sum_{\alpha,\beta,\gamma,\delta} W_{\alpha,\beta,\delta,\gamma}\Bigg(\underbrace{\hat{c}_\zeta \hat{c}^\dagger_\alpha}_{\delta_{\zeta,\alpha}-\hat{c}^\dagger_\alpha\hat{c}_\zeta}\hat{c}^\dagger_\beta - \hat{c}^\dagger_\alpha \underbrace{\hat{c}^\dagger_\beta \hat{c}_\zeta}_{\delta_{\beta,\zeta}-\hat{c}_\zeta\hat{c}^\dagger_\beta}\Bigg)\hat{c}_\gamma \hat{c}_\delta \\
&= \frac{1}{2}\sum_{\alpha,\beta,\gamma,\delta} W_{\alpha,\beta,\delta,\gamma}\Big(\delta_{\zeta,\alpha}\hat{c}^\dagger_\beta - \hat{c}^\dagger_\alpha \delta_{\beta,\zeta}\Big)\hat{c}_\gamma \hat{c}_\delta \\
&= \frac{1}{2}\sum_{\beta,\gamma,\delta} W_{\zeta,\beta,\delta,\gamma}\hat{c}^\dagger_\beta \hat{c}_\gamma \hat{c}_\delta - \frac{1}{2}\sum_{\alpha,\gamma,\delta} \underbrace{W_{\alpha,\zeta,\delta,\gamma}}_{W_{\zeta,\alpha,\gamma,\delta}}\hat{c}^\dagger_\alpha \underbrace{\hat{c}_\gamma \hat{c}_\delta}_{-\hat{c}_\delta\hat{c}_\gamma} \\
&= \frac{1}{2}\sum_{\beta,\gamma,\delta} W_{\zeta,\beta,\delta,\gamma}\hat{c}^\dagger_\beta \hat{c}_\gamma \hat{c}_\delta + \frac{1}{2}\sum_{\beta,\gamma,\delta} W_{\zeta,\beta,\gamma,\delta}\hat{c}^\dagger_\beta \hat{c}_\delta \hat{c}_\gamma \\
&= \frac{1}{2}\sum_{\beta,\gamma,\delta} W_{\zeta,\beta,\delta,\gamma}\hat{c}^\dagger_\beta \hat{c}_\gamma \hat{c}_\delta + \overbrace{\frac{1}{2}\sum_{\beta,\gamma,\delta} W_{\zeta,\beta,\delta,\gamma}\hat{c}^\dagger_\beta \hat{c}_\gamma \hat{c}_\delta}^{\gamma\leftrightarrow\delta} \\
&= \sum_{\beta,\gamma,\delta} W_{\zeta,\beta,\delta,\gamma}\hat{c}^\dagger_\beta \hat{c}_\gamma \hat{c}_\delta
\end{aligned} \tag{8.4}$$

We exploited that a simultaneous interchange of the first two and, at the same time, the last two arguments leaves the value of the interaction matrix elements unchanged, i.e. $W_{\alpha,\beta,\gamma,\delta} = W_{\beta,\alpha,\delta,\gamma}$. This symmetry follows from the form of the interaction matrix elements defined in Eq. 3.51 on p. 141. Editor: This argument refers to the Coulomb interaction. What about the most general definition as $W(t) = \hat{H}(t) - \hat{h}$?

With the results Eqs. 8.3,8.4, we can return to Eq. 8.1 and evaluate the time derivative of the annihilator in the Heisenberg picture as

$$\begin{aligned}
i\hbar\partial_t \hat{c}_{H,\zeta}(t) &= \hat{\mathcal{U}}(0,t)\left[\hat{c}_{S,\zeta}, \hat{H}\right]_- \hat{\mathcal{U}}(t,0) \\
&\overset{Eqs.\ 8.3,8.4}{=} \hat{\mathcal{U}}(0,t)\Bigg(\sum_\beta h_{\zeta,\beta}\hat{c}_{S,\beta} + \sum_{\beta,\gamma,\delta} W_{\zeta,\beta,\delta,\gamma}\hat{c}^\dagger_{S,\beta}\hat{c}_{S,\gamma}\hat{c}_{S,\delta}\Bigg)\hat{\mathcal{U}}(t,0) \\
&= \sum_\beta h_{\zeta,\beta}\hat{c}_{H,\beta}(t) + \sum_{\beta,\gamma,\delta} W_{\zeta,\beta,\delta,\gamma}\hat{c}^+_{H,\beta}(t)\hat{c}_{H,\gamma}(t)\hat{c}_{H,\delta}(t)
\end{aligned} \tag{8.5}$$

Now, we can evaluate the time derivative of the Green's function Eq. 7.16. We use the short-hand notation $\left\langle \dots \right\rangle_{T,\mu} \overset{\text{def}}{=} \mathrm{Tr}\{\hat{\rho}^{(W)}_{T,\mu} \dots\}$. Note below that the time derivative acts only on t, but not on

the second time argument t'.

$$
\begin{aligned}
& i\hbar\partial_t G^{\mathcal{C}}_{\alpha,\beta}(t,t') \\
\overset{\text{Eq. 7.16}}{=}\ & i\hbar\partial_t\left[\frac{\theta(t-t')}{i\hbar}\left\langle \hat{c}_{H,\alpha}(t)\hat{c}^+_{H,\beta}(t')\right\rangle_{T,\mu} - \frac{\theta(t'-t)}{i\hbar}\left\langle \hat{c}^+_{H,\beta}(t')\hat{c}_{H,\alpha}(t)\right\rangle_{T,\mu}\right] \\
=\ & \delta(t-t')\left\langle \hat{c}_{H,\alpha}(t)\hat{c}^+_{H,\beta}(t')\right\rangle_{T,\mu} + \delta(t'-t)\left\langle \hat{c}^+_{H,\beta}(t')\hat{c}_{H,\alpha}(t)\right\rangle_{T,\mu} \\
+\ & \frac{\theta(t-t')}{i\hbar}\left\langle \left(i\hbar\partial_t\hat{c}_{H,\alpha}(t)\right)\hat{c}^+_{H,\beta}(t')\right\rangle_{T,\mu} - \frac{\theta(t'-t)}{i\hbar}\left\langle \hat{c}^+_{H,\beta}(t')\left(i\hbar\partial_t\hat{c}_{H,\alpha}(t)\right)\right\rangle_{T,\mu} \\
\overset{\text{Eq. 8.5}}{=}\ & \delta(t-t')\left\langle \left[\hat{c}_{H,\alpha}(t),\hat{c}^+_{H,\beta}(t')\right]_+\right\rangle_{T,\mu} \\
+\ & \frac{\theta(t-t')}{i\hbar}\left\langle \left(\sum_b h_{\alpha,b}\hat{c}_{H,b}(t) + \sum_{b,c,d} W_{\alpha,b,d,c}\hat{c}^+_{H,b}(t)\hat{c}_{H,c}(t)\hat{c}_{H,d}(t)\right)\hat{c}^+_{H,\beta}(t')\right\rangle_{T,\mu} \\
-\ & \frac{\theta(t'-t)}{i\hbar}\left\langle \hat{c}^+_{H,\beta}(t')\left(\sum_b h_{\alpha,b}\hat{c}_{H,b}(t) + \sum_{b,c,d} W_{\alpha,b,d,c}\hat{c}^+_{H,b}(t)\hat{c}_{H,c}(t)\hat{c}_{H,d}(t)\right)\right\rangle_{T,\mu} \\
=\ & \delta(t-t')\left\langle \left[\hat{c}_{H,\alpha}(t),\hat{c}^+_{H,\beta}(t')\right]_+\right\rangle_{T,\mu} \\
+\ & \sum_b h_{\alpha,b}\left(\frac{\theta(t-t')}{i\hbar}\left\langle \hat{c}_{H,b}(t)\hat{c}^+_{H,\beta}(t')\right\rangle_{T,\mu} - \frac{\theta(t'-t)}{i\hbar}\left\langle \hat{c}^+_{H,\beta}(t')\hat{c}_{H,b}(t)\right\rangle_{T,\mu}\right) \\
+\ & \sum_{b,c,d} W_{\alpha,b,d,c}\left(\frac{\theta(t-t')}{i\hbar}\left\langle \hat{c}^+_{H,b}(t)\hat{c}_{H,c}(t)\hat{c}_{H,d}(t)\hat{c}^+_{H,\beta}(t')\right\rangle_{T,\mu} - \frac{\theta(t'-t)}{i\hbar}\left\langle \hat{c}^+_{H,\beta}(t')\hat{c}^+_{H,b}(t)\hat{c}_{H,c}(t)\hat{c}_{H,d}(t)\right\rangle_{T,\mu}\right) \\
\overset{\text{Eq. 8.7}}{=}\ & \delta(t-t')\delta_{\alpha,\beta} + \sum_b h_{\alpha,b}G_{b,\beta}(t,t') \\
+\ & \sum_{b,c,d} W_{\alpha,b,d,c}\underbrace{\left(\frac{\theta(t-t')}{i\hbar}\left\langle \overbrace{\hat{c}^+_{H,b}(t)\hat{c}_{H,c}(t)\hat{c}_{H,d}(t)}^{A}\,\hat{c}^+_{H,\beta}(t')\right\rangle_{T,\mu} - \frac{\theta(t'-t)}{i\hbar}\left\langle \hat{c}^+_{H,\beta}(t')\,\overbrace{\hat{c}^+_{H,b}(t)\hat{c}_{H,c}(t)\hat{c}_{H,d}(t)}^{A}\right\rangle_{T,\mu}\right)}_{\frac{1}{i\hbar}\left\langle \mathcal{T}_{\mathcal{C}}\hat{c}^+_{H,b}(t)\hat{c}_{H,c}(t)\hat{c}_{H,d}(t)\hat{c}^+_{H,\beta}(t')\right\rangle_{T,\mu}}
\end{aligned}
\tag{8.6}
$$

The anticommutator relations for the Schrödinger operators do not hold for Heisenberg operators. Nevertheless, we have made use of the fact that the anticommutator is only required for equal times

$$
\left[\hat{c}^+_{H,\beta}(t),\hat{c}_{H,\alpha}(t)\right]_+ = \hat{\mathcal{U}}(0,t)\left[\hat{c}^\dagger_{S,\beta},\hat{c}_{S,\alpha}\right]_+\hat{\mathcal{U}}(t,0) = \hat{\mathcal{U}}(0,t)\delta_{\alpha,\beta}\hat{\mathcal{U}}(t,0) = \delta_{\alpha,\beta} \tag{8.7}
$$

Eq. 8.6 can be brought into a form similar to the defining equation Eq. 4.13 of the Green's function for non-interacting systems.

EQUATION OF MOTION FOR THE INTERACTING GREEN'S FUNCTION

$$\sum_\gamma \Big(\delta_{\alpha,\gamma} i\hbar\partial_t - h_{\alpha,\gamma}(t)\Big) G^{\mathcal{C}}_{\gamma,\beta}(t,t') =$$

$$= \delta_{\mathcal{C}}(t-t')\delta_{\alpha,\beta} + \sum_\gamma \sum_{b,c} W_{\alpha,b,\gamma,c}(t) \overbrace{\frac{1}{i\hbar}\mathrm{Tr}\Big\{\hat\rho^{(W)}_{T,\mu}\mathcal{T}_{\mathcal{C}}\, \underbrace{\hat c^+_{H,b}(t)\hat c_{H,c}(t)}_{\sim\text{density operator}}\, \hat c_{H,\gamma}(t)\hat c^+_{H,\beta}(t')\Big\}}^{G^{(2)}_{c,\gamma,b,\beta}(t,t,t^+,t')\quad \text{Eq. 8.14}} \tag{8.8}$$

$$= \delta_{\mathcal{C}}(t-t')\delta_{\alpha,\beta} + \sum_\gamma \frac{1}{i\hbar}\mathrm{Tr}\Big\{\hat\rho^{(W)}_{T,\mu}\mathcal{T}_{\mathcal{C}} \underbrace{\Big(\sum_{b,c} W_{\alpha,b,\gamma,c}(t)\, \underbrace{\hat c^+_{H,b}(t)\hat c_{H,c}(t)}_{\sim\text{density operator}}\Big)}_{\hat V_{ee}(t)} \hat c_{H,\gamma}(t)\hat c^+_{H,\beta}(t')\Big\} \tag{8.9}$$

$\hat V_{ee}$ is the operator describing the Coulomb potential from the (other) electrons. The two versions on the right-hand side are identical, but emphasize certain groupings of the terms.[a] The time argument t^+ is a short hand for a

[a] Eq. 8.8 is analogous to Eq. 10.11 in the book of Abrikosov, Gorkov, Dzyaloshinski[7].

Physical meaning of the interaction term: To get closer to the physical meaning interaction term of Eq. 8.8, let me do a rather crude approximation, which is equivalent to the Hartree approximation.[1][2]

$$\begin{aligned}
&\frac{1}{i\hbar}\mathrm{Tr}\Big\{\hat\rho^{(W)}_{T,\mu}\mathcal{T}_{\mathcal{C}}\hat c^+_{H,b}(t)\hat c_{H,c}(t)\hat c_{H,\gamma}(t)\hat c^+_{H,\beta}(t')\Big\} \\
&\approx \underbrace{\mathrm{Tr}\Big\{\hat\rho^{(W)}_{T,\mu}\mathcal{T}_{\mathcal{C}}\hat c^+_{H,b}(t)\hat c_{H,c}(t)\Big\}}_{\rho^{(1)}_{c,b}(t)\quad\text{from Eq. 3.56}} \underbrace{\frac{1}{i\hbar}\mathrm{Tr}\Big\{\hat\rho^{(W)}_{T,\mu}\mathcal{T}_{\mathcal{C}}\hat c_{H,\gamma}(t)\hat c^+_{H,\beta}(t')\Big\}}_{G^{\mathcal{C}}_{\gamma,\beta}(t,t')\quad\text{from Eq. 7.16}} \\
&= \rho^{(1)}_{c,b}(t) G^{\mathcal{C}}_{\gamma,\beta}(t,t')
\end{aligned} \tag{8.10}$$

In this approximation, the interaction simply replaces the interaction term in Eq. 8.8 by the Hartree potential

$$\Delta\hat h_{\alpha,\beta}(t) = \sum_{b,c} W_{\alpha,b,\beta,c}\rho^{(1)}_{c,b}(t) \tag{8.11}$$

which is added to $\hat h$.

Interaction term and two-particle Green's function: Eq. 8.8 allows a recipe to determine the Green's function, however, only if the interaction term on the right-hand side is known. The evaluation of this term is even more complicated than the direct calculation of the Green's function. It requires the knowledge of the two-particle Green's function

$$G^{(2)}(\vec x_1,t_1,\vec x_2,t_2;\vec x'_1,t'_1,\vec x'_2,t'_2) \overset{\text{def}}{=} \frac{1}{i\hbar}\mathrm{Tr}\Big\{\hat\rho^{(W)}_{T,\mu}\mathcal{T}_{\mathcal{C}}\hat\psi_H(\vec x_1,t_1)\hat\psi_H(\vec x_2,t_2)\hat\psi^+_H(\vec x'_1,t'_1)\hat\psi^+_H(\vec x'_2,t'_2)\Big\} \tag{8.12}$$

respectively, in an orbital representation,

$$G^{(2)}_{\alpha,\beta;\gamma,\delta}(t_1,,t_2;t'_1,t'_2) \overset{\text{def}}{=} \frac{1}{i\hbar}\mathrm{Tr}\Big\{\hat\rho^{(W)}_{T,\mu}\mathcal{T}_{\mathcal{C}}\hat c_{H,\alpha}(t_1)\hat c_{H,\beta}(t_2)\hat c^+_{H,\gamma}(t'_1)\hat c^+_{H,\delta}(t'_2)\Big\} \tag{8.13}$$

[1] Note that $\mathrm{Tr}[\hat\rho_{T,\mu}\cdots] = \langle\ldots\rangle_{T,\mu}$ is the thermal expectation value.
[2] we replace the product of the two operators marked in blue by their thermal expectation value

The interaction term in the equation of motion, Eq. 8.8, can be expressed in terms of the two-particle Green's function as

$$\begin{aligned}&\sum_{\gamma}\sum_{b,c} W_{\alpha,b,\gamma,c}\frac{1}{i\hbar}\mathrm{Tr}\left\{\hat{\rho}^{(W)}_{T,\mu}\mathcal{T}_{\mathcal{C}}\underbrace{\hat{c}^{+}_{H,b}(t^{+})\hat{c}_{H,c}(t)}_{\sim\text{density operator}}\hat{c}_{H,\gamma}(t)\hat{c}^{+}_{H,\beta}(t')\right\}\\ &=\sum_{\gamma}\sum_{b,c} W_{\alpha,b,\gamma,c}G^{(2)}_{c,\gamma,b,\beta}(t,t,t^{+},t') \qquad (8.14)\end{aligned}$$

Thus, the equation of motion for the one-particle Green's function $G^{\mathcal{C}}$ has an additional inhomogeneity, which depends on the two-particle Green's function.

One could proceed to determine an equation of motion for the two-particle Green's function, which however would introduce a term containing a three particle Green's function. In order to determine the latter we obtain a differential equation, where even higher-order Green's functions enter. We end up with an infinite sequence of increasingly more complicated differential equations, the so-called **Martin-Schwinger hierarchy**[73](see also [71]). One can hope that the terms will become smaller with each step in the hierarchy, so that it can be truncated.

8.2 Self energy

Eq. 8.8 shows that the Green's function of an interacting systems does not obey the same differential equation as the Green's function of non-interacting electrons.

DEFINITION OF THE SELF ENERGY

In order to recover a form more closely related to the defining equation of a Green's function we define a **self energy** $\Sigma_{\alpha,\beta}(t,t')$ via

$$\sum_{\gamma}\int_{\mathcal{C}} dt''\,\Sigma_{\alpha,\gamma}(t,t'')G_{\gamma,\beta}(t'',t') = \sum_{b,c,d} W_{\alpha,b,d,c}\frac{1}{i\hbar}\mathrm{Tr}\left\{\hat{\rho}^{(W)}_{T,\mu}\mathcal{T}_{\mathcal{C}}\hat{c}^{+}_{H,b}(t)\hat{c}_{H,c}(t)\hat{c}_{H,d}(t)\hat{c}^{+}_{H,\beta}(t')\right\} \qquad (8.15)$$

so that the equation of motion Eq. 8.8 assumes the form

$$\sum_{\gamma}\int dt''\left[\delta(t-t'')\Big(\delta_{\alpha,\gamma}i\hbar\partial_{t''}-h_{\alpha,\gamma}\Big)-\Sigma_{\alpha,\gamma}(t,t'')\right]G_{\gamma,\beta}(t'',t')=\delta(t-t')\delta_{\alpha,\beta} \qquad (8.16)$$

The self energy captures the Coulomb potential of the other electrons in the form of a retarded potential. Eq. 8.16 is analogous to Eq. 5.49 on p. 197 for a Green's function, which describes a one-particle system that experiences a retarded potential due to coupling to a bath.

Editor: Shall I mention that the self energy is also non-local in space?

Eqs. 8.15 and 8.16 have exactly the same information content as Eq. 8.8. They merely introduce the self energy as a quantity with an accessible physical interpretation. Furthermore, they introduce an equation of motion for the many-particle Green's function that is analogous to that in one-particle quantum mechanics.

Relation to the Hartree-Fock method: The self energy of the Hartree-Fock approximation is the sum of Hartree and exchange potential

$$\Sigma_{\alpha,\beta}(t,t') = \langle\chi_\alpha|\hat{V}_H+\hat{V}_X|\chi_\beta\rangle\delta(t,t') \qquad (8.17)$$

With this choice, the equation of motion turns into the Schrödinger equation with the Fock operator $\hat{h}+\hat{V}_H+\hat{V}_X$ (times $\delta(t-t')$) in place of $\hat{h}+\hat{\Sigma}$.

Dyson's equation: Editor: This is not suitable for the lecture. Introduce the concept of the inverse in the $\{\alpha, t\}$ space properly and make the section optional. Can Dyson's equation also be obtained conventionally?

Editor: Generalized multiplication and inverse

$$\langle(\boldsymbol{A}\circ\boldsymbol{B}\rangle)_{(\alpha,t),(\beta,t')} = \sum_\gamma \int dt'' A_{(\alpha,t),(\gamma,t'')} B_{(\gamma,t''),(\beta,t')}$$
$$\langle(\boldsymbol{A}^{\circ,-1}\circ\boldsymbol{A}\rangle)_{(\alpha,t),(\beta,t')} = \delta_{\alpha,\beta}\delta(t-t') \tag{8.18}$$

Eq. 8.16 is a **Dyson equation**, which has the form $(G_0^{-1} - \Sigma)G = 1$. In order to make the connection evident, let me introduce the non-interacting Green's function $G^{(0)}_{\gamma,\beta}(t,t')$, which obeys

$$\sum_\gamma \Big(\delta_{\alpha,\gamma} i\hbar\partial_t - h_{\alpha,\gamma}\Big) G^{(0)}_{\gamma,\beta}(t,t') = \delta_{\alpha,\beta}\delta(t-t') \tag{8.19}$$

We define a new inverse of the non-interacting Green's function with respect to matrix elements **and** time arguments as

$$\sum_\gamma \int dt''\; G^{(0),\circ,-1}_{\alpha,\gamma}(t,t'') G^{(0)}_{\gamma,\beta}(t'',t') = \delta(t-t')\delta_{\alpha,\beta} \tag{8.20}$$

Note, that this is not the simple matrix inversion. Rather it is a generalized matrix inversion that considers the time arguments on the same level as the orbital indices.

Comparison of Eq. 8.20 with Eq. 8.19, provides us with the identification

$$G^{(0),\circ,-1}_{\alpha,\beta}(t,t') = \delta(t-t')\Big(\delta_{\alpha,\gamma} i\hbar\partial_{t'} - h_{\alpha,\gamma}\Big) \tag{8.21}$$

With this definition, we can use Eq. 8.21 to rewrite Eq. 8.16 in the form of a Dyson's equation

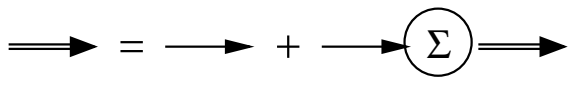
$$\sum_\gamma \int dt'' \left[G^{(0),\circ,-1}_{\alpha,\gamma}(t,t'') - \Sigma_{\alpha,\gamma}(t,t'')\right] G_{\gamma,\beta}(t'',t') = \delta(t-t')\delta_{\alpha,\beta} \tag{8.22}$$

or after multiplication of a non-interacting Green's function from the left and after moving the self-energy term to the right-hand side, we obtain the better known form of the Dyson's equation.

DYSON'S EQUATION

$$G_{\alpha,\beta}(t,t') = G^{(0)}_{\alpha,\beta}(t,t') + \sum_{\gamma,\delta}\int dt'' \int dt'''\; G^{(0)}_{\alpha,\gamma}(t,t'')\Sigma_{\gamma,\delta}(t'',t''')G_{\delta,\beta}(t''',t')\;. \tag{8.23}$$

It can be represented by the following diagram



where a double arrow represents the full Green's function $\boldsymbol{G}$, a single arrow represents a non-interacting (bare) Green's function $\boldsymbol{G}^{(0)}$ and the circle represents the self energy $\boldsymbol{\Sigma}$.
Dyson's equation is the equation of motion Eq. 8.8 for the Green's function expressed in terms of the self energy Eq. 8.15.

Editor: Check the following and make it more precise! It is a bit puzzling that the inverse of a matrix function is a differential operator, but this is a consequence to using the generalized inversion which includes the time argument. Most of the time, one will work in an energy representation with respect to the relative argument $t-t'$ instead of a time representation. The time convolution will turn into a simple product in the energy representation. As a result this generalized inversion will turn into a simple matrix inversion.

8.3 Expectation value of one-particle operators

Consider a one-particle operator, which can always be expressed as

$$\hat{A}_S(t) = \sum_{\alpha,\beta} \overbrace{A_{\alpha,\beta}(t)}^{\langle\chi_\alpha|\hat{A}(t)|\chi_\beta\rangle} \hat{c}^\dagger_{S,\alpha}\hat{c}_{S,\beta} = \int d^4x \int d^4x' \overbrace{A(\vec{x},\vec{x}',t)}^{\langle\vec{x}|\hat{A}(t)|\vec{x}'\rangle} \hat{\psi}^\dagger_S(x)\hat{\psi}_S(\vec{x}') \tag{8.24}$$

To keep things general, I allow for a time dependence of the operator $\hat{A}_S(t)$.

For most practical purposes, one would like to obtain the stationary expectation value. We can, however, easily deal with a more complex problem. Consider a thermal ensemble of many-particle states at time[3] $t = 0$. The Hamiltonian may, however, be time dependent and the wave functions $|\Phi_n(t)\rangle$ will change in time. As a consequence, one obtains a time-dependent expectation value $\langle A(t)\rangle_{T,\mu}$, even if the operator $\hat{A}_S$ itself does not depend on time.

The thermal expectation value at time t is obtained from the ensemble at time $t = 0$ and the propagator from $t = 0$ to the time of the "measurement".

$$\begin{aligned}
\Big\langle A(t)\Big\rangle_{T,\mu} &\overset{\text{def}}{=} \frac{\overbrace{\mathrm{Tr}\Big\{\hat{\rho}_{T,\mu}\hat{A}_H(t)\Big\}}}{\mathrm{Tr}\Big\{\hat{\rho}_{T,\mu}\hat{\mathcal{U}}(0,t)\hat{A}_S(t)\hat{\mathcal{U}}(t,0)\Big\}} \\
&\overset{\text{Eq. 8.24}}{=} \sum_{\alpha,\beta} A_{\alpha,\beta}(t)\mathrm{Tr}\Big\{\hat{\rho}_{T,\mu}\hat{\mathcal{U}}(0,t)\hat{c}^\dagger_{S,\alpha}\underbrace{\hat{\mathcal{U}}(t,0)\hat{\mathcal{U}}(0,t)}_{\hat{1}}\hat{c}_{S,\beta}\hat{\mathcal{U}}(t,0)\Big\} \\
&= \sum_{\alpha,\beta} A_{\alpha,\beta}(t)(-1)\lim_{t'\to t^+}\mathrm{Tr}\Big\{\hat{\rho}_{T,\mu}\mathcal{T}_\mathcal{C}\hat{c}_{H,\beta}(t)\hat{c}^+_{H,\alpha}(t')\Big\} \qquad (8.25) \\
&\overset{\text{Eq. 7.16}}{=} -i\hbar\lim_{t'\to t^+}\sum_{\alpha,\beta} A_{\alpha,\beta}(t)G_{\beta,\alpha}(t,t') \qquad (8.26)
\end{aligned}$$

EXPECTATION VALUES OF ONE-PARTICLE OPERATORS FROM GREEN'S FUNCTIONS

The thermal expectation value at time t of an operator $\hat{A}_S(t) = \sum_{\alpha,\beta} A_{\alpha,\beta}(t)\hat{c}^\dagger_\alpha\hat{c}_\beta$ is

$$\Big\langle A(t)\Big\rangle_{T,\mu} = -i\hbar\lim_{t'\to t^+}\sum_{\alpha,\beta} A_{\alpha,\beta}(t)G_{\beta,\alpha}(t,t') \tag{8.27}$$

One-particle expectation values can be expressed by the one-particle-reduced density matrix $\boldsymbol{\rho}^{(1)}$ as $\mathrm{Tr}\{\boldsymbol{\rho}^{(1)}\boldsymbol{A}\}$. Thus, we indirectly obtain the **one-particle-reduced density matrix** of the many-particle system as

ONE-PARTICLE-REDUCED DENSITY MATRIX FROM GREEN'S FUNCTION

$$\rho^{(1)}_{\alpha,\beta}(t) = -i\hbar\lim_{t'\to t^+} G_{\alpha,\beta}(t,t') \tag{8.28}$$

[3] This is not a restriction because the zero of the time axis can be placed arbitrarily.

8.4 Migdal-Galitskii-Koltun (MGK) sum rule and total energy

The equation of motion for the Green's function, Eq. 8.8, leads to the **Migdal-Galitskii-Koltun sum rule**[74], which gives the total energy in terms of the Green function.

In the previous section, we learned how to evaluate the thermal expectation value of a one-particle operator. The expectation value of two-particle operators, however, cannot be extracted from a one-particle Green's function. There is one exception, namely the interaction energy. The reason is that the equation of motion links an expectation value of the two-particle Green's function to the one-particle Green's function.

The interaction energy is

$$\begin{aligned}\left\langle \hat{W}(t)\right\rangle_{T,\mu} &= \frac{1}{2}\sum_{\alpha,b,c,d} W_{\alpha,b,d,c}\left\langle \hat{\mathcal{U}}(0,t)\hat{c}^{\dagger}_{S,\alpha}\hat{c}^{\dagger}_{S,b}\hat{c}_{S,c}\hat{c}_{S,d}\hat{\mathcal{U}}(t,0)\right\rangle_{T,\mu} \\ &= \frac{1}{2}\sum_{\alpha,b,c,d} W_{\alpha,b,d,c}\left\langle \hat{c}^{+}_{H,\alpha}(t)\hat{c}^{+}_{H,b}(t)\hat{c}_{H,c}(t)\hat{c}_{H,d}(t)\right\rangle_{T,\mu} \end{aligned} \tag{8.29}$$

The time dependence is understood as in the previous section. The interaction operator is time independent. At time $t = 0$, the system is prepared in a thermal ensemble. The dynamics may however, drive the system away from equilibrium, resulting in a time-dependent expectation value of the interaction energy.

The right-hand side of the equation of motion Eq. 8.8 for the Green's function is

$$Y_{\alpha,\beta}(t,t') \stackrel{\text{def}}{=} \delta_{\alpha,\beta}\delta(t-t') + \sum_{b,c,d} W_{\alpha,b,d,c}\frac{1}{i\hbar}\left\langle \mathcal{T}_C \hat{c}^{+}_{H,b}(t)\hat{c}_{H,c}(t)\hat{c}_{H,d}(t)\hat{c}^{+}_{H,\beta}(t')\right\rangle_{T,\mu} \tag{8.30}$$

In order to get the second creation operator to the front as in the interaction energy Eq. 8.29, we choose the time argument t' infinitesimally later than t. Then, the time-ordering operator places $\hat{c}^{+}_{H,\beta}(t')$ to the very left, while switching the sign for any permutation of two fermionic operators.

Shifting the time argument forward along the contour by an infinitesimal amount will be required frequently, so that a symbol[4] t^+ has been introduced. It denotes $t^+ \stackrel{\text{def}}{=} t(s+\delta)$, where δ is an infinitesimally small, positive number. $t(s)$ is the mapping onto the time contour. An example is

$$F(t,t^+) = \lim_{s'\to s^+} F(t,t(s')) = \lim_{\delta\to 0^+} F(t,t(s+\delta)) \tag{8.31}$$

Any time argument can be displaced in this manner. It would be OK to write "2^+ seconds". The notation t^+ under the limit has a similar but still different meaning than using t^+ as argument. It specifies that the limit is taken from the positive side. In contrast, using t^+ as argument implies implicitly that a limit is to be taken.

With this notation, we obtain

$$Y_{\alpha,\beta}(t,t^+) = -\sum_{b,c,d} W_{\alpha,b,d,c}\frac{1}{i\hbar}\left\langle \hat{c}^{+}_{H,\beta}(t^+)\hat{c}^{+}_{H,b}(t)\hat{c}_{H,c}(t)\hat{c}_{H,d}(t)\right\rangle_{T,\mu} \tag{8.32}$$

Comparison with Eq. 8.29 shows

$$\left\langle \hat{W}(t)\right\rangle_{T,\mu} = -\frac{i\hbar}{2}\sum_{\alpha} Y_{\alpha,\alpha}(t,t^+) \tag{8.33}$$

$Y(t,t')$ is the right-hand side of the equation of motion Eq. 8.8 for the Green's function, which

[4] see e.g. Fetter and Walecka[3] p.66 Eq.7.8

can be replaced by the left-hand side of the equation of Eq. 8.8.

$$\begin{aligned}\left\langle \hat{W}(t)\right\rangle_{T,\mu} &\overset{\text{Eq. 8.8}}{=} -\frac{i\hbar}{2}\sum_{\alpha}\underbrace{\sum_{\gamma}\Big(\delta_{\alpha,\gamma}i\hbar\partial_t - h_{\alpha,\gamma}\Big)G_{\gamma,\alpha}(t,t^+)}_{Y_{\alpha,\alpha}(t,t^+)} \\ &= \frac{1}{2}\sum_{\alpha,\gamma}\Big(\delta_{\alpha,\gamma}i\hbar\partial_t - h_{\alpha,\gamma}\Big)\Big(-i\hbar G_{\gamma,\alpha}(t,t^+)\Big) \end{aligned} \tag{8.34}$$

Thus, we obtain an expression for the interaction energy. This is probably the only two-particle expectation value that can be obtained directly from the one-particle Green's function.

We may now add the expectation value of the non-interacting Hamiltonian to obtain the expectation value of the total energy.

$$\left\langle \hat{h}(t)\right\rangle_{T,\mu} \overset{\text{Eq. 8.27}}{=} -i\hbar\lim_{t'\to t^+}\sum_{\alpha,\beta}h_{\alpha,\beta}(t)G_{\beta,\alpha}(t,t') \tag{8.35}$$

Because of the factor one-half in Eq. 8.34, adding the non-interacting Hamiltonian only changes the sign of the corresponding term.

MIGDAL-GALITSKII-KOLTUN SUM RULE

The thermal expectation value of $\hat{h}+\hat{W}$, the total energy at time t is

$$\left\langle E_{\text{tot}}(t)\right\rangle_{T,\mu} = \frac{1}{2}\lim_{t'\to t^+}\sum_{\alpha,\beta}\Big(\delta_{\alpha,\beta}i\hbar\partial_t \overset{!}{+} h_{\alpha,\beta}(t)\Big)\Big(-i\hbar G_{\beta,\alpha}(t,t')\Big) \tag{8.36}$$

The positive sign in front of $h_{\alpha,\beta}$ is correct! (see above). The time derivative acts only on the first argument of the Green's function.

The equation Eq. 8.36 for the total energy differs only by the sign in front of the non-interacting Hamilton matrix elements $h_{\alpha,\gamma}$ from that of the interaction energy Eq. 8.34. Remember, that Migdal-Galtskii sum rule relies on that the interaction term is a two-particle interaction such as the Coulomb interaction. A generalization may be possible, but needs to be done.

Energy is not grand potential: The total energy given by Eq. 8.36 is the thermal expectation value of non-interacting Hamiltonian and the interaction energy. Except for zero temperature, the quantity obtained is not a thermodynamic potential, from which the complete thermodynamic information can be extracted. In order to obtain the grand potential, which is the thermodynamic potential for a system in contact with a heat bath and a particle reservoir, i.e. a (T,μ)-ensemble, we would need to add the entropy. The entropy, however, cannot be extracted from the Green's function alone. At zero temperature $T=0$ the entropy vanishes, so that the expectation value of the total energy becomes identical with the internal energy.

A consequence of this is that there is no minimum principle for the total energy at finite temperature.

Use the self energy to obtain the total energy: The Migdal-Galitsky sum rule can be used to obtain the total energy, if the self energy is known. For this purpose, we use Dyson's equation

Eq. 8.16 to replace the time derivative in Eq. 8.36. This yields

$$\begin{aligned}\left\langle E_{\text{tot}}(t)\right\rangle_{T,\mu} &\overset{\text{Eq. 8.36}}{=} \frac{1}{2}\lim_{t'\to t^+}\sum_{\alpha,\beta}\Big(\delta_{\alpha,\beta}i\hbar\partial_t + h_{\alpha,\beta}(t)\Big)\Big(-i\hbar G_{\beta,\alpha}(t,t')\Big)\\ &\overset{\text{Eq. 8.16}}{=} -i\hbar\Big\{\sum_{\alpha,\beta}h_{\alpha,\beta}G_{\beta,\alpha}(t,t^+) + \frac{1}{2}\int dt''\sum_{\alpha,\beta}\Sigma_{\alpha,\beta}(t,t'')G_{\beta,\alpha}(t'',t^+)\Big\}\end{aligned} \tag{8.37}$$

In this expression the division into non-interacting Hamiltonian and interaction is again intact. The term containing the self energy is the expectation value of the interaction.

8.5 Home study and practice

8.5.1 Self-energy and contour Green's function of the Hubbard atom

Editor: needs to be done

Editor: See [75] on the Hubbard atom

The Hamiltonian for the Hubbard atom is

$$\begin{aligned}\hat{H} &= \underbrace{\sum_{\sigma\in\{\uparrow,\downarrow\}}\bar{\epsilon}\hat{c}^\dagger_{S,\sigma}\hat{c}_{S,\sigma}}_{\hat{h}} + \underbrace{\frac{1}{2}\sum_{\sigma,\sigma'\in\{\uparrow,\downarrow\}}U\hat{c}^\dagger_{S,\sigma}\hat{c}^\dagger_{S,\sigma'}\hat{c}_{S,\sigma'}\hat{c}_{S,\sigma}}_{\hat{W}}\\ &= \sum_{\sigma\in\{\uparrow,\downarrow\}}\bar{\epsilon}\hat{c}^\dagger_{S,\sigma}\hat{c}_{S,\sigma} + U\hat{c}^\dagger_{S,\uparrow}\hat{c}_{S,\uparrow}\hat{c}^\dagger_{S,\downarrow}\hat{c}_{S,\downarrow}\end{aligned} \tag{8.38}$$

The eigenstates of the many-particle Hamiltonian are

$$\begin{aligned}|\Phi_0\rangle &= |\mathcal{O}\rangle\\ |\Phi_\uparrow\rangle &= \hat{c}^\dagger_{S,\uparrow}|\mathcal{O}\rangle\\ |\Phi_\downarrow\rangle &= \hat{c}^\dagger_{S,\downarrow}|\mathcal{O}\rangle\\ |\Phi_{\uparrow,\downarrow}\rangle &= \hat{c}^\dagger_{S,\uparrow}\hat{c}^\dagger_{S,\downarrow}|\mathcal{O}\rangle\end{aligned} \tag{8.39}$$

and the corresponding energies are

$$\begin{aligned}E_0 &= 0\\ E_\uparrow &= \bar{\epsilon}\\ E_\downarrow &= \bar{\epsilon}\\ E_{\uparrow,\downarrow} &= 2\bar{\epsilon} + U\end{aligned} \tag{8.40}$$

The contour Green's function is defined as

$$
\begin{aligned}
G^{\mathcal{C}}_{\sigma,\sigma'}(t,t') &\overset{\text{Eq. 7.16}}{=} \frac{1}{i\hbar}\frac{\mathrm{Tr}\left\{\mathrm{e}^{-\beta(\hat{H}-\mu\hat{N})}\mathcal{T}_{\mathcal{C}}\hat{c}_{H\sigma}(t)\hat{c}^{+}_{H\sigma}(t')\right\}}{\mathrm{Tr}\left\{\mathrm{e}^{-\beta(\hat{H}-\mu\hat{N})}\right\}} \\
&= \frac{1}{i\hbar}\underbrace{\frac{1}{1+2\mathrm{e}^{-\beta(\bar{\epsilon}-\mu)}+\mathrm{e}^{-\beta(2\bar{\epsilon}+U-2\mu)}}}_{1/Z_{T,\mu}}\Bigg\{1\langle\mathcal{O}|\theta(t-t')\hat{c}_{H\sigma}(t)\hat{c}^{+}_{H\sigma'}(t')|\mathcal{O}\rangle \\
&+ \sum_{\bar{\sigma}\in\{\uparrow,\downarrow\}}\mathrm{e}^{-\beta(\bar{\epsilon}-\mu)}\langle\mathcal{O}|\hat{c}_{S,\bar{\sigma}}\Big(\theta(t-t')\hat{c}_{H\sigma}(t)\hat{c}^{+}_{H\sigma'}(t')-\theta(t'-t)\hat{c}^{+}_{H\sigma'}(t')\hat{c}_{H\sigma}(t)\Big)\hat{c}_{S,\bar{\sigma}}|\mathcal{O}\rangle \\
&+ \mathrm{e}^{-\beta(2\bar{\epsilon}+U-2\mu)}\langle\mathcal{O}|\hat{c}_{S,\downarrow}\hat{c}_{S,\uparrow}\Big(-\theta(t'-t)\hat{c}^{+}_{H\sigma'}(t')\hat{c}_{H\sigma}(t)\Big)\hat{c}^{+}_{S,\uparrow}\hat{c}^{+}_{S,\downarrow}|\mathcal{O}\rangle\Bigg\} \\
&= \frac{1}{i\hbar}\frac{1}{1+2\mathrm{e}^{-\beta(\bar{\epsilon}-\mu}+\mathrm{e}^{-\beta(2(\bar{\epsilon}-\mu)+U)}}\Bigg\{\delta_{\sigma,\sigma'}\theta(t-t')\mathrm{e}^{-\frac{i}{\hbar}\bar{\epsilon}(t-t')} \\
&+ \sum_{\bar{\sigma}\in\{\uparrow,\downarrow\}}\delta_{\sigma,\sigma'}\mathrm{e}^{-\beta(\bar{\epsilon}-\mu)}\Big(\theta(t-t')\delta_{\bar{\sigma},-\sigma}\mathrm{e}^{-\frac{i}{\hbar}(\bar{\epsilon}+U)(t-t')}-\theta(t'-t)\delta_{\bar{\sigma},\sigma}\mathrm{e}^{-\frac{i}{\hbar}(-\bar{\epsilon})(t'-t)}\Big) \\
&+ \mathrm{e}^{-\beta(2\bar{\epsilon}+U-2\mu)}\delta_{\sigma,\sigma'}\Big(-\theta(t'-t)\mathrm{e}^{-\frac{i}{\hbar}(-\bar{\epsilon}-U+\mu)(t'-t)}\Big)\Bigg\} \\
&= \frac{1}{i\hbar}\frac{\delta_{\sigma,\sigma'}}{1+2\mathrm{e}^{-\beta(\bar{\epsilon}-\mu)}+\mathrm{e}^{-\beta(2(\bar{\epsilon}-\mu)+U)}}\Bigg\{\theta(t-t')\Big(\mathrm{e}^{-\frac{i}{\hbar}\bar{\epsilon}(t-t')}+\mathrm{e}^{-\beta(\bar{\epsilon}-\mu)}\mathrm{e}^{-\frac{i}{\hbar}(\bar{\epsilon}+U)(t-t')}\Big) \\
&- \theta(t'-t)\Big(\mathrm{e}^{-\beta(\bar{\epsilon}-\mu)}\mathrm{e}^{+\frac{i}{\hbar}\bar{\epsilon}(t'-t)}+\mathrm{e}^{-\beta(2\bar{\epsilon}+U-2\mu)}\mathrm{e}^{+\frac{i}{\hbar}(\bar{\epsilon}+U)(t'-t)}\Big)\Bigg\} \\
&= \frac{\delta_{\sigma,\sigma'}}{i\hbar}\Bigg\{\theta(t-t')\frac{\mathrm{e}^{-\frac{i}{\hbar}\bar{\epsilon}(t-t')}\Big(1+\mathrm{e}^{-\beta(\bar{\epsilon}-\mu)}\mathrm{e}^{-\frac{i}{\hbar}U(t-t')}\Big)}{1+2\mathrm{e}^{-\beta(\bar{\epsilon}-\mu)}+\mathrm{e}^{-\beta(2(\bar{\epsilon}-\mu)+U)}} \\
&\quad -\theta(t'-t)\frac{\mathrm{e}^{-\beta(\bar{\epsilon}-\mu)}\mathrm{e}^{+\frac{i}{\hbar}\bar{\epsilon}(t'-t)}\Big(1+\mathrm{e}^{-\beta(\bar{\epsilon}-\mu+U)}\mathrm{e}^{+\frac{i}{\hbar}U(t'-t)}\Big)}{1+2\mathrm{e}^{-\beta(\bar{\epsilon}-\mu)}+\mathrm{e}^{-\beta(2(\bar{\epsilon}-\mu)+U)}}\Bigg\}
\end{aligned}
\tag{8.41}
$$

Special cases:

- $\mu \ll \bar{\epsilon}$

$$G^{\mathcal{C}}_{\sigma,\sigma'}(t,t') = \frac{\delta_{\sigma,\sigma'}}{i\hbar}\theta(t-t')\mathrm{e}^{-\frac{i}{\hbar}\bar{\epsilon}(t-t')} \tag{8.42}$$

  This Green's function describes the propagation of a single electron in an empty Hubbard atom.

- $\mu \gg \bar{\epsilon}+U$

$$G^{\mathcal{C}}_{\sigma,\sigma'}(t,t') = -\frac{\delta_{\sigma,\sigma'}}{i\hbar}\theta(t'-t)\mathrm{e}^{+\frac{i}{\hbar}(\bar{\epsilon}+U)(t'-t)} \tag{8.43}$$

  This Green's function describes the propagation of a hole in a doubly occupied Hubbard atom.

- $\mu = \bar{\epsilon}+\frac{1}{2}U$

$$
\begin{aligned}
G^{\mathcal{C}}_{\sigma,\sigma'}(t,t') = \frac{\delta_{\sigma,\sigma'}}{i\hbar}\Bigg\{&\theta(t-t')\frac{\mathrm{e}^{-\frac{i}{\hbar}\bar{\epsilon}(t-t')}\Big(1+\mathrm{e}^{\frac{1}{2}\beta U}\mathrm{e}^{-\frac{i}{\hbar}U(t-t')}\Big)}{2+2\mathrm{e}^{\frac{1}{2}\beta U}} \\
&-\theta(t'-t)\frac{\mathrm{e}^{+\frac{i}{\hbar}\bar{\epsilon}(t'-t)}\Big(1+\mathrm{e}^{-\frac{1}{2}\beta U}\mathrm{e}^{+\frac{i}{\hbar}U(t'-t)}\Big)}{2+2\mathrm{e}^{-\frac{1}{2}\beta U}}\Bigg\}
\end{aligned}
\tag{8.44}
$$

– For the non-interacting limit, i.e. $\beta U = 0$, I obtain

$$G^{\mathcal{C}}_{\sigma,\sigma'}(t,t') = \frac{\delta_{\sigma,\sigma'}}{i\hbar}\frac{\theta(t-t')-\theta(t'-t)}{2}\mathrm{e}^{-\frac{i}{\hbar}\bar{\epsilon}(t-t')} \tag{8.45}$$

The non-interacting limit is identical to the high-temperature limit.

– for strongly interacting limit, i.e. $\beta U \gg 1$, I obtain

$$G^{\mathcal{C}}_{\sigma,\sigma'}(t,t') = \frac{\delta_{\sigma,\sigma'}}{i\hbar}\frac{\theta(t-t')-\theta(t'-t)}{2}\mathrm{e}^{-\frac{i}{\hbar}(\bar{\epsilon}+U)(t-t')} \tag{8.46}$$

The strongly interacting limit is identical to the low-temperature limit, unless U vanishes precisely.

– in the intermediate regime, I obtain a superposition of two oscillations, one with $\bar{\epsilon}$ and the other with $\bar{\epsilon}+U$.

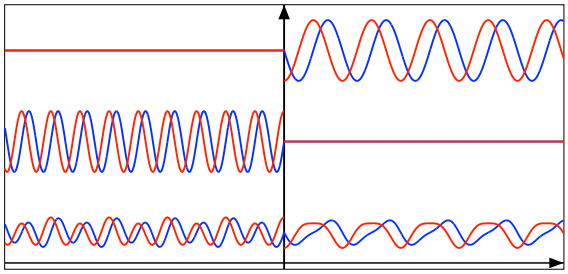


Fig. 8.1: Green's function $G(t,t')$ of the H^+ Hubbard ion, of the H^- Hubbard ion (middle), and of a half-filled Hubbard atom H^0 at finite temperature as function of the relative time argument $t-t'$. Real parts are shown in blue and imaginary parts are shown in red. Greens functions are displaced vertically for better visibility. The parameters are $\mathrm{e}^{\frac{1}{2}\beta U} = 1/4$ and $U = \bar{\epsilon}$.

Chapter 9

Spectral properties

Spectral functions are one of the three main purposes of many-particle calculations, which are

- thermodynamic properties, such as stability, phase transitions, etc.
- response of the material to external perturbations. The central element are response functions obtained via the **Green-Kubo formula**[76], Eqs. 16.9,16.10.
- spectral properties describe excitations of a material. The central quantity is the **spectral function** .

The spectral function describes one-particle excitations such as electron addition or electron removal in a general many-particle system. Thus, it provides the link to spectroscopy.

Spectral functions have been discussed earlier in section 2.6 in the context of the Hartree-Fock approximation. The reader may revisit that chapter. An early review on the spectral function of interacting electrons can be found by Hedin et al.[77].

In this section, the spectral function is introduced in its full generality. Specifically, we begin with the time-dependent spectral function and show later, how it relates to well known quantities such as the density of states.

Besides the spectral function, this chapter will introduce the concept of Lehmann amplitudes, or quasi-particle wave functions.

Finally, it will be shown, how the spectral function is obtained from the contour-ordered Green's function and vice versa.

9.1 Lehmann amplitudes

Before we approach spectral properties, let me introduce the concept of Lehmann amplitudes. Lehmann amplitudes are one-particle states, that generalize the one-particle wave functions used in the context of non-interacting particles, the Hartree-Fock approximation, or the average-phase approximation (APA) introduced earlier. In contrast to those, Lehmann amplitudes are a rigorous concept that is not linked to any approximation.

9.1.1 Motivation: Green's function in terms of Lehmann amplitudes

Let me start by showing how the Green's function of an interacting many-particle system can be written in terms of one-particle wave functions. I will use the expression for a general ensemble

expressed by probabilities P_q and microstates $|\Phi_q\rangle$.

$$\begin{aligned}
G^{\mathcal{C}}(\vec{x},t,\vec{x'},t') &\overset{\text{Eq. 7.16}}{=} \frac{1}{i\hbar}\mathrm{Tr}\Big\{\hat{\rho}^{(W)}_{T,\mu}\mathcal{T}_{\mathcal{C}}\hat{\psi}_H(\vec{x},t)\hat{\psi}^{+}_H(\vec{x'},t')\Big\} \\
&= \frac{1}{i\hbar}\mathrm{Tr}\Big\{\underbrace{\hat{\rho}^{(W)}_{T,\mu}}_{\sum_q |\Phi_q\rangle P_q\langle\Phi_q|}\Big(\theta_{\mathcal{C}}(t-t')\hat{\psi}_H(\vec{x},t)\underbrace{\hat{1}}_{\sum_{q'}|\Phi_{q'}\rangle\langle\Phi_{q'}|}\hat{\psi}^{+}_H(\vec{x'},t') - \theta_{\mathcal{C}}(t'-t)\hat{\psi}^{+}_H(\vec{x'},t')\underbrace{\hat{1}}_{\sum_{q'}|\Phi_{q'}\rangle\langle\Phi_{q'}|}\hat{\psi}_H(\vec{x},t)\Big)\Big\} \\
&= \frac{1}{i\hbar}\Big\{\theta_{\mathcal{C}}(t-t')\sum_{q,q'}P_q\underbrace{\langle\Phi_q|\hat{\psi}_H(\vec{x},t)|\Phi_{q'}\rangle}_{\psi^{\mathcal{L}a}_{q,q'}(\vec{x},t)}\underbrace{\langle\Phi_{q'}|\hat{\psi}^{+}_H(\vec{x'},t')|\Phi_q\rangle}_{\psi^{\mathcal{L}a,*}_{q,q'}(\vec{x'},t')} \\
&\qquad -\theta_{\mathcal{C}}(t'-t)\sum_{q,q'}P_q\underbrace{\langle\Phi_q|\hat{\psi}^{+}_H(\vec{x'},t')|\Phi_{q'}\rangle}_{\psi^{\mathcal{L}a,*}_{q',q}(\vec{x'},t')}\underbrace{\langle\Phi_{q'}|\hat{\psi}_H(\vec{x},t)|\Phi_q\rangle}_{\psi^{\mathcal{L}a}_{q',q}(\vec{x},t)}\Big\} \\
&\overset{t'\in\mathbb{R}}{=} \frac{1}{i\hbar}\sum_{q,q'}\Big(\theta_{\mathcal{C}}(t-t')P_q - \theta_{\mathcal{C}}(t'-t)P_{q'}\Big)\psi^{\mathcal{L}a}_{q,q'}(\vec{x},t)\psi^{\mathcal{L}a,*}_{q,q'}(\vec{x'},t') \\
&= \frac{1}{i\hbar}\sum_{q,q'}\Big(P_q+P_{q'}\Big)\psi^{\mathcal{L}a}_{q,q'}(\vec{x},t)\Big(\theta_{\mathcal{C}}(t-t')\underbrace{\big(1-f^{\mathcal{L}a}_{q,q'}\big)}_{\frac{P_q}{P_q+P_{q'}}} - \theta_{\mathcal{C}}(t'-t)\underbrace{f^{\mathcal{L}a}_{q,q'}}_{\frac{P_{q'}}{P_q+P_{q'}}}\Big)\psi^{\mathcal{L}a,*}_{q,q'}(\vec{x'},t') \qquad (9.1)
\end{aligned}$$

During this derivation I introduced new symbols, namely the **Lehmann amplitudes** $\psi^{\mathcal{L}a}_{q,q'}(\vec{x},t)$ and the **Lehmann occupations** defined below:

GREEN'S FUNCTION IN TERMS OF LEHMANN AMPLITUDES

$$\hat{G}^{\mathcal{C}}(t,t') \overset{t'\in\mathbb{R}}{=} \frac{1}{i\hbar}\sum_{q,q'}\Big(P_q+P_{q'}\Big)\Big|\psi^{\mathcal{L}a}_{q,q'}(t)\Big\rangle\Big\{\theta_{\mathcal{C}}(t-t')\big(1-f^{\mathcal{L}a}_{q,q'}\big) - \theta_{\mathcal{C}}(t'-t)f^{\mathcal{L}a}_{q,q'}\Big\}\Big\langle\psi^{\mathcal{L}a}_{q,q'}(t')\Big| \qquad (9.2)$$

The Green's function is expressed in terms of one-particle wave functions, the **Lehmann amplitudes**

$$\big|\psi^{\mathcal{L}a}_{q,q'}(t)\big\rangle \overset{\text{def}}{=} \int d^4x\,|\vec{x}\rangle\underbrace{\langle\Phi_q|\hat{\psi}_H(\vec{x},t)|\Phi_{q'}\rangle}_{\psi^{\mathcal{L}a}_{q,q'}(\vec{x},t)} \qquad (9.3)$$

and **Lehmann occupations**

$$f^{\mathcal{L}a}_{q,q'} \overset{\text{def}}{=} \frac{P_{q'}}{P_q+P_{q'}}\,. \qquad (9.4)$$

For a thermal ensemble with probabilities $P_q = \frac{1}{Z_{T,\mu}}\mathrm{e}^{-\beta(E_q-\mu N_q)}$, the Lehmann occupations are given by the familiar Fermi distribution $f_{T,\mu}(\epsilon)$

$$f^{\mathcal{L}a}_{q,q'} = \frac{1}{1+\mathrm{e}^{+\beta\left((E_{q'}-E_q)-\mu(N_{q'}-N_q)\right)}} = \frac{1}{1+\mathrm{e}^{+\beta(\epsilon^{\mathcal{L}a}_{q,q'}-\mu)}} = f_{T,\mu}(\epsilon^{\mathcal{L}a}_{q,q'}) \qquad (9.5)$$

with the **Lehmann energies**

$$\epsilon^{\mathcal{L}a}_{q,q'} \overset{\text{def}}{=} \frac{E_{q'}-E_q}{N_{q'}-N_q} \qquad (9.6)$$

Actually, this is the conceptual origin of the **Fermi distribution function**.

The derivation of Eq. 9.1 has been limited to the real-valued time axis, so that I can use $\big\langle\Phi_q\big|\hat{\psi}^{+}_H(\vec{x'},t')\big|\Phi_{q'}\big\rangle \overset{t'\in\mathbb{R}}{=} \big\langle\Phi_{q'}\big|\hat{\psi}_H(\vec{x'},t')\big|\Phi_q\big\rangle^*$.

What has been gained? First, the Green's function is expressed in terms of one-particle wave functions, rather than by many-particle wave functions. The Lehmann amplitudes are much simpler objects than the many-particle wave function and still capture (nearly) all information that is relevant for the Green's function.

Very convenient is that the expressions with Lehman amplitudes are very similar to the corresponding expression for non-interacting systems. The Green's function for non-interacting electrons Eq. 7.30 from p. 258 is

$$\hat{G}^{\mathcal{C},(0)}(t,t') \overset{\text{Eq. 7.30}}{=} \frac{1}{i\hbar} \sum_n \underbrace{|\varphi_n(t)\rangle}_{\hat{U}(t,0)|\varphi_n\rangle} \Big\{ \underbrace{\theta_{\mathcal{C}}(t-t')(1-f_n)}_{\text{electrons}} - \underbrace{\theta_{\mathcal{C}}(t'-t) f_n}_{\text{holes}} \Big\} \underbrace{\sum_j O^{-1}_{n,j}(t') \langle \varphi_j(t')|}_{\langle \varphi_n | \hat{U}(0,t')} \quad (9.7)$$

which can be compared to Eq. 9.2 above.

FROM LEHMANN AMPLITUDES TO NON-INTERACTING PARTICLES

There seems to be a simple translation from the Lehmann representation of interacting systems to the description of non-interacting electrons with one-particle wace functions.

sum over Lehmann amplitudes	$\sum_{q,q'}(P_q + P_{q'})$	$\rightsquigarrow$	$\sum_n$	sum over one-particle orbitals
Lehmann amplitude	$\|\psi^{\mathcal{L}a}_{q,q'}(t)\rangle$	$\rightsquigarrow$	$\|\varphi_n(t)\rangle$	one-particle orbital
Lehmann energy	$\epsilon^{\mathcal{L}a}_{q,q'}$	$\rightsquigarrow$	ϵ_n	energy level
Lehmann occupations	$f^{\mathcal{L}a}_{q,q'}$	$\rightsquigarrow$	f_n	occupation

With some caution, this correspondence in reverse may serve as memory aid to generalize the expressions from non-interacting to interacting electrons.

The comparison shows that the Lehmann amplitudes and Lehmann occupations are natural generalizations of the one-particle orbitals of non-interacting electrons and their occupations to interacting many-particle systems.

9.1.2 What are Lehmann amplitudes?

TIME-DEPENDENT LEHMANN AMPLITUDES

The **time-dependent Lehmann amplitudes** are the matrix elements of the annihilation operator in the Heisenberg picture.

$$\psi^{\mathcal{L}a}_{q,q'}(\vec{x},t) \overset{\text{def}}{=} \langle \Phi_q | \hat{\psi}_H(\vec{x},t) | \Phi_{q'} \rangle \overset{\text{Eq. 6.40}}{=} \langle \Phi_q(t) | \hat{\psi}_S(\vec{x}) | \Phi_{q'}(t) \rangle \quad (9.8)$$

The time-dependent many-particle wave functions $|\Phi_q(t)\rangle \overset{\text{def}}{=} \hat{\mathcal{U}}(t,0)|\Phi_q\rangle$ are obtained by propagating the the microstates $|\Phi_q\rangle$ of the ensemble. The time dependent many-particle wave functions $|\Phi_q(t)\rangle = \hat{\mathcal{U}}(t,0)|\Phi_q(0)\rangle$ are propagated with the Hamiltonian.

STATIONARY LEHMANN AMPLITUDES

More common than the time-dependent Lehmann amplitudes are the **stationary Lehmann amplitudes**. The stationary Lehmann amplitudes are useful, when the Hamiltonian is time independent and when the microstates are eigenstates of the Hamiltonian, i.e. $\hat{H}|\Phi_q\rangle = |\Phi_q\rangle E_q$. For the stationary Lehmann amplitudes I will make this choice.

$$\underbrace{\psi^{\mathcal{L}a}_{q,q'}(\vec{x})}_{\psi^{\mathcal{L}a}_{q,q'}(\vec{x},0)} \stackrel{\text{def}}{=} \big\langle \Phi_q \big| \hat{\psi}_S(\vec{x}) \big| \Phi_{q'} \big\rangle \tag{9.9}$$

with their **Lehmann energies** Eq. 9.6

$$\epsilon^{\mathcal{L}a}_{q,q'} \stackrel{\text{def}}{=} \frac{E_q - E_{q'}}{N_q - N_{q'}} \tag{9.10}$$

Time-dependent and stationary Lehmann amplitudes are related to each other like the solutions of the time-dependent or the time-independent Schrödinger equation.
For a time-independent Hamiltonian $\hat{h} + \hat{W}$, the time-dependent Lehmann amplitudes are

$$\underbrace{\psi^{\mathcal{L}a}_{q,q'}(\vec{x},t)}_{\langle\Phi_q|\hat{\psi}_H(\vec{x},t)|\Phi_{q'}\rangle} = \underbrace{\psi^{\mathcal{L}a}_{q,q'}(\vec{x})}_{\langle\Phi_q|\hat{\psi}_S(\vec{x})|\Phi_{q'}\rangle} \; \mathrm{e}^{-\frac{i}{\hbar}\epsilon^{\mathcal{L}a}_{q,q'}t} \tag{9.11}$$

[a]

[a] Compare Stefanucci and van Leeuwen[2] Stefanucci-Eq. 6.84.

Representations: To familiarize you with different representations of Lehmann amplitudes, let me list the examples for real-space-and-spin representation, for orthonormal orbitals, and non-orthonormal orbitals.

$$\begin{aligned}
\big|\psi^{\mathcal{L}a}_{q,q'}(t)\big\rangle &= \int d^4x\, |\vec{x}\rangle \underbrace{\langle\Phi_q|\hat{\psi}_H(\vec{x},t)|\Phi_{q'}\rangle}_{\psi^{\mathcal{L}a}_{q,q'}(\vec{x},t)} \\
&= \sum_n |\varphi_n\rangle \underbrace{\langle\Phi_q|\hat{a}_{H,n}(t)|\Phi_{q'}\rangle}_{\langle\varphi_n|\psi^{\mathcal{L}a}_{q,q'}(t)\rangle} \qquad \text{for } \langle\varphi_m|\varphi_n\rangle = \delta_{m,n} \\
&= \sum_\alpha |\chi_\alpha\rangle \underbrace{\langle\Phi_q|\hat{c}_{H,\alpha}(t)|\Phi_{q'}\rangle}_{\langle\pi_\alpha|\psi^{\mathcal{L}a}_{q,q'}(,t)\rangle} \qquad \text{for } \langle\pi_\alpha|\chi_\beta\rangle = \delta_{\alpha,\beta}
\end{aligned} \tag{9.12}$$

Most Lehmann amplitudes are zero: The Lehmann amplitudes are one-particle wave functions. On the one hand, there is an enormous number of Lehmann amplitudes, namely one for each pair of many-particle wave functions. On the other hand, most of them are zero. If the Hamiltonian conserves the particle number, the matrix elements are zero, unless the state $|\Phi_q\rangle$ on the left side has one particle less than the state $|\Phi_{q'}\rangle$ on the right side, that is, when $N_q = N_{q'} - 1$.

Nevertheless, the number of Lehmann amplitudes is much larger than that of one-particle wave functions used in the Hartree-Fock approximation (HFA) or the average-phase approximation (APA). In the Hartree-Fock approximation and the average-phase approximation, the eigenstates of the Hamiltonian are Slater determinants built from a common set of one-particle states. Therefore, only these one-particle states can occur as stationary Lehmann amplitudes.

For such a given one-particle state, there is a huge number of many-particle excitations, all of which add or remove an electron in that specific one-particle state. This number of such transitions equals that of many-particle wave functions in the Fock space!

In the mean-field approximation–often attributed to the Hartree-Fock approximation–, all excitation energies for a given one-particle state are degenerate! In the average phase approximation, each such transition has a different excitation energy, because the electron experiences the potential produced by the other electrons in the state $|\vec{\sigma}\rangle$. In the mean-field approximation this $|\vec{\sigma}\rangle$-dependent potential is replaced by the mean potential, so that all these excitations have the same excitation energy.

Completeness and one-particle-reduced density matrix

The Lehmann amplitudes satisfy a kind of completeness condition in the one-particle Hilbert space. Furthermore, the Lehmann amplitudes provide a simple equation for the one-particle-reduced density matrix.

COMPLETENESS OF LEHMANN AMPLITUDES AND ONE-PARTICLE-REDUCED DENSITY MATRIX

$$\hat{1} = \sum_{q,q'} (P_q + P_{q'}) \left|\psi^{\mathcal{L}a}_{q,q'}(t)\right\rangle\left\langle\psi^{\mathcal{L}a}_{q,q'}(t)\right| \tag{9.13}$$

$$\hat{\rho}^{(1)}(t) = \sum_{q,q'} (P_q + P_{q'}) \left|\psi^{\mathcal{L}a}_{q,q'}(t)\right\rangle f^{\mathcal{L}a}_{q,q'}\left\langle\psi^{\mathcal{L}a}_{q,q'}(t)\right| \tag{9.14}$$

Proof of the completeness relation Eq. 9.13 (Self study)

$$\begin{aligned}
&\langle\vec{x}| \left(\sum_{q,q'} (P_q + P_{q'}) \left|\psi^{\mathcal{L}a}_{q,q'}(t)\right\rangle\left\langle\psi^{\mathcal{L}a}_{q,q'}(t)\right| \right) |\vec{x'}\rangle \\
&= \sum_{q,q'} (P_q + P_{q'}) \psi^{\mathcal{L}a}_{q,q'}(\vec{x}, t) \psi^{\mathcal{L}a,*}_{q,q'}(\vec{x'}, t') \\
&= \sum_{q,q'} (P_q + P_{q'}) \left\langle\Phi_q\right|\hat{\psi}_H(\vec{x}, t)\left|\Phi_{q'}\right\rangle\left\langle\Phi_q\right|\hat{\psi}_H(\vec{x'}, t)\left|\Phi_{q'}\right\rangle^* \\
&\overset{t\in\mathbb{R}}{=} \sum_{q,q'} (P_q + P_{q'}) \left\langle\Phi_q\right|\hat{\psi}_H(\vec{x}, t)\left|\Phi_{q'}\right\rangle\left\langle\Phi_{q'}\right|\hat{\psi}^\dagger_H(\vec{x'}, t)\left|\Phi_q\right\rangle \\
&= \sum_q P_q \left\langle\Phi_q\right| \Big(\underbrace{\hat{\psi}_H(\vec{x}, t)\hat{\psi}^\dagger_H(\vec{x'}, t) + \hat{\psi}^\dagger_H(\vec{x'}, t)\hat{\psi}_H(\vec{x}, t)}_{=[\hat{\psi}_H(\vec{x},t),\hat{\psi}^\dagger_H(\vec{x'},t)]_+ = \delta(\vec{x}-\vec{x'})} \Big) \left|\Phi_q\right\rangle \\
&= \delta(\vec{x} - \vec{x'}) \sum_q P_q = \langle\vec{x}|\hat{1}|\vec{x'}\rangle \qquad q.e.d
\end{aligned} \tag{9.15}$$

Proof of Eq. 9.14 for the one-particle-reduced density matrix (Self study)

$$\begin{aligned}
\hat{\rho}^{(1)}(t) &\overset{\text{Eq. 3.57}}{=} \int d^4x \int d^4x' \; |\vec{x}\rangle \Big\{ \sum_q P_q \langle \Phi_q(t)|\hat{\psi}_S^\dagger(\vec{x'})\hat{\psi}_S(\vec{x})|\Phi_q(t)\rangle \Big\} \langle \vec{x'}| \\
&= \int d^4x \int d^4x' \; |\vec{x}\rangle \Big\{ \sum_{q,q'} P_q \underbrace{\langle \Phi_q|\hat{\psi}_H^\dagger(\vec{x'},t)|\Phi_{q'}\rangle}_{\langle \vec{x'}|\psi^{\mathcal{L}a}_{q',q}(t)\rangle^*} \underbrace{\langle \Phi_{q'}|\hat{\psi}_H(\vec{x},t)|\Phi_q\rangle}_{\langle \vec{x}|\psi^{\mathcal{L}a}_{q',q}(t)\rangle} \Big\} \langle \vec{x'}| \\
&= \sum_{q,q'} \Big(P_q + P_{q'}\Big) \Big|\psi^{\mathcal{L}a}_{q',q}(t)\Big\rangle \underbrace{f^{\mathcal{L}a}_{q',q}}_{P_q/(P_q+P_{q'})} \Big\langle \psi^{\mathcal{L}a}_{q',q}(t)\Big| \\
&= \sum_{q,q'} \Big(P_q + P_{q'}\Big) \Big|\psi^{\mathcal{L}a}_{q,q'}(t)\Big\rangle \underbrace{f^{\mathcal{L}a}_{q,q'}}_{P_{q'}/(P_q+P_{q'})} \Big\langle \psi^{\mathcal{L}a}_{q,q'}(t)\Big| \qquad (9.16)
\end{aligned}$$

Caution is required regarding the indices of the Lehmann occupations, because $f^{\mathcal{L}a}_{q,q'} = 1 - f^{\mathcal{L}a}_{q',q}$.

9.1.3 Lehmann amplitudes for ensembles of Slater determinants

If the eigenstates of the Hamiltonian are Slater-determinants $|\vec{\sigma}\rangle$ for a common basis of one-particle orbitals $|\varphi_j\rangle = \hat{a}_j^\dagger|\mathcal{O}\rangle$, the Lehmann amplitudes have a particularly simple form. This applies, for example, to the **average-phase approximation** (APA) described in section 2.6.1 on p. 78.

Let us consider a time-independent[1] Hamiltonian in the APA, which is diagonal in a basis of Slater determinants $|\vec{\sigma}\rangle$

$$\hat{H} = |\vec{\sigma}\rangle E_{\vec{\sigma}} \langle\vec{\sigma}| \qquad \text{where} \qquad |\vec{\sigma}\rangle = \prod_{j=1}^{\infty} \left(\hat{a}_j^\dagger\right)^{\sigma_j} |\mathcal{O}\rangle \; . \qquad (9.17)$$

For each state $|\Phi_q\rangle = |\vec{\sigma}\rangle$, there is at most one other state with a non-zero matrix element with the annihilator $\hat{a}_j$.

$$\langle\vec{\sigma}|\hat{a}_j|\vec{\sigma'}\rangle = \prod_k \delta_{\sigma_k,\sigma'_k-\delta_{k,j}} \qquad (9.18)$$

Thus, the corresponding Lehmann amplitudes are

$$\psi^{\mathcal{L}a}_{q,q'}(\vec{x},t) \overset{\text{def}}{=} \big\langle \Phi_q\big|\hat{\psi}_H(\vec{x},t)\big|\Phi_{q'}\big\rangle \overset{\text{Eq. 6.40}}{=} \big\langle \Phi_q(t)\big|\hat{\psi}_S(\vec{x})\big|\Phi_{q'}(t)\big\rangle \qquad (9.19)$$

$$\begin{aligned}
\overbrace{\psi^{\mathcal{L}a}_{\vec{\sigma},\vec{\sigma'}}(\vec{x},t)}^{\psi^{\mathcal{L}a}_{q,q'}(\vec{x},t)} &\overset{\text{Eq. 9.11}}{=} \underbrace{\overbrace{\langle\vec{\sigma}|}^{\langle\Phi_q|} \overbrace{\sum_{j'} \varphi_{j'}(\vec{x})\hat{a}_{S,j'}}^{\hat{\psi}_S(\vec{x})} \overbrace{|\vec{\sigma'}\rangle}^{|\Phi_{q'}\rangle}}_{\sum_{j'}\varphi_{j'}(\vec{x})\langle\vec{\sigma}|\hat{a}_{S,j'}|\vec{\sigma'}\rangle} \overbrace{\mathrm{e}^{-\frac{i}{\hbar}\epsilon^{\mathcal{L}a}_{q,q'}t}}^{\mathrm{e}^{-\frac{i}{\hbar}\epsilon^{(\vec{\sigma'})}_j t}} = \varphi_j(\vec{x})\mathrm{e}^{-\frac{i}{\hbar}\epsilon^{(\vec{\sigma'})}_j t} \prod_k \delta_{\sigma_k,\sigma'_k-\delta_{k,j}} \\
\ldots\ldots \quad \ldots \quad &\text{Caution! indices interchanged } \ldots \\
\big|\psi^{\mathcal{L}a}_{\vec{\sigma'},\vec{\sigma}}(t)\big\rangle &= \begin{cases} |\varphi_j\rangle \mathrm{e}^{-\frac{i}{\hbar}\epsilon^{(\vec{\sigma})}_j t} & \text{if } |\vec{\sigma'}\rangle = \hat{a}_j|\vec{\sigma}\rangle \\ |\varnothing\rangle & \text{else} \end{cases} . \qquad (9.20)
\end{aligned}$$

I introduced a new symbol, which is hopefully intuitive: $\epsilon^{(\vec{\sigma})}_j \overset{\text{def}}{=} \epsilon^{\mathcal{L}a}_{\vec{\sigma},\vec{\sigma'}}$ is the electron-removal energy for the one-particle state $|\varphi_j\rangle$ in the electron distribution of the many-particle state $\vec{\sigma}$. In the mean-field approximation the electron experiences the mean-field potential, which is independent of the many-particle state $|\vec{\sigma}\rangle$.

[1] The generalization to time-dependent APA Hamiltonians is straightforward.

The non-vanishing Lehmann amplitudes are identical to the one-particle orbitals $|\varphi_j\rangle$. For each such one-particle orbital, there are many Lehmann orbitals with the same shape, e.g. $|\varphi_j\rangle$, but with different energies $\epsilon^{\mathcal{L}a}_{\vec{\sigma},\vec{\sigma'}} = \epsilon_j^{(\vec{\sigma'})}$. The Lehmann amplitude is non-zero only, when $|\vec{\sigma'}\rangle = \hat{a}_j|\vec{\sigma}\rangle$ for one of the orbitals $|\varphi_j\rangle$.

The number of distinct Lehmann wave functions $|\varphi_j\rangle$ equals the number of states in the one-particle Hilbert space, while the number of Lehmann energies $\epsilon_j^{(\vec{\sigma})}$ is much larger by a factor equal to the number of states in the Fock space.

In the APA, most of the Lehmann amplitudes are identical and the Lehmann amplitudes can be identified with the natural orbitals $|\varphi_j\rangle$. Still, the quasi-particle energies depend on the individual Slater determinant. Every Slater determinant has its own electron distribution, which produces a distinct electrostatic potential for the electron to be removed, even if the electron is removed from the same one-particle orbital $|\varphi_j\rangle$.

In a mean-field theory such as the (thermal) Hartree-Fock approximation, this potential is averaged over all contributing Slater determinants, so that also the electron removal energy only depends on the orbital index but not on the Slater determinant at hand.

9.1.4 Lehmann amplitudes vs. quasi-particles vs. Dyson's orbitals

There are a few related concepts to Lehmann amplitudes and a number of names for them. Among them are **quasi-particle wave functions**[2] and **Dyson orbitals**[3]. It is my impression that the naming is not always uniform. One problem is that the difference between the concepts vanishes in many simpler, but common situations.

In order to avoid mixing up concepts, I introduced new terms, namely Lehmann occupations, Lehmann energies and I give them a unique definition. To my knowlegde, these terms have no other meaning, yet. Often these terms are called quasiparticle occupations, quasiparticle energies etc., but these latter terms may be mixed up with the quasi-particle concept of Landau's Fermi-liquid theory.

9.2 Spectral function

In section 2.6 on spectral properties of weakly-interacting systems, we discussed the spectral function for an ensemble of Slater determinants and for time-independent Hamiltonians.

Here, this definition is extended to ensembles of general many-particle states. Furthermore, the restriction to time-independent systems is relaxed. The spectral function is introduced as time-dependent object, from which the commonly used energy-dependent spectral function is obtained by a Fourier transform. This opens the way to true non-equilibrium situations.

9.2.1 Definition

Let me investigate the injection of an electron at space-spin-time $(\vec{x'}, t')$ and its removal at space-spin-time $(\vec{x}, t)$. The goal is to study a physical process so that we choose the time arguments on the real-valued time axis, i.e. $t, t' \in \mathbb{R}$. Nevertheless, we may also use the spectral function with complex-valued time arguments.

[2] Editor: Check the following reference, whether it refers to quasi-particle wave functions. I am not sure it is appropriate. *"A proper way of calculating quasiparticle energies is provided by the Green function theory.[78, 79]"* . Citation taken from Aryasetiawan[80] (p.2)in Anisimov's Book "Strong Coulomb correlations in electronic-structue calculations".

[3] For the definition of Dyson orbitals see e.g. the perspective article by Ortiz[81] or the book of Fulde[5] (Fulde-Eq. 9.2.61 and 9.2.62). See *Introduction to many-body Green-function theory*, J. Toulouse, 2015 https://www.lct.jussieu.fr/pagesperso/toulouse/enseignement/introduction_green.pdf retrieved June 3, 2020. Editor: Here, the Dyson orbitals are defined as eigenstates of the Dyson equation $[\hat{h} + \hat{\Sigma}(\epsilon) - \epsilon]|\psi\rangle = 0$ evaluated at the pole of the Green's function.

The spectral function for a general ensemble, characterized by the von-Neumann density matrix $\hat{\rho}^{vN} = \sum_q |\Phi_q\rangle P_q \langle\Phi_q|$, is determined as sum of two objects

$$\mathcal{A}(\vec{x}, t, \vec{x'}, t') \stackrel{\text{def}}{=} \mathcal{A}^{(h)}(\vec{x}, t, \vec{x'}, t') + \mathcal{A}^{(e)}(\vec{x}, t, \vec{x'}, t') \,, \tag{9.21}$$

an electron spectral function

$$\mathcal{A}^{(e)}(\vec{x}, t, \vec{x'}, t') \stackrel{\text{def}}{=} \frac{1}{2\pi\hbar} \mathrm{Tr}\Big\{ \underbrace{\hat{\rho}^{vN}}_{\sum_q |\Phi_q\rangle P_q \langle\Phi_q|} \hat{\psi}_H(\vec{x}, t) \hat{\psi}_H^+(\vec{x'}, t') \Big\} \tag{9.22}$$

and a hole spectral function

$$\mathcal{A}^{(h)}(\vec{x}, t, \vec{x'}, t') \stackrel{\text{def}}{=} \frac{1}{2\pi\hbar} \mathrm{Tr}\Big\{ \hat{\rho}^{vN} \hat{\psi}_H^+(\vec{x'}, t') \hat{\psi}_H(\vec{x}, t) \Big\} \,. \tag{9.23}$$

The electron spectral function describes the electron injection, which therefore probes the empty orbitals, while the hole spectral function describes hole injection and probes the filled orbitals.

For thermal ensembles, the electron and hole spectral functions can be recovered from the total spectral function. However, this is not the case for a general non-equilibrium ensemble.

SPECTRAL FUNCTION

$$\mathcal{A}(\vec{x}, t, \vec{x'}, t') \stackrel{\text{def}}{=} \frac{1}{2\pi\hbar} \mathrm{Tr}\Big\{ \hat{\rho}^{(W)}_{T,\mu} \big[\hat{\psi}_H(\vec{x}, t), \hat{\psi}_H^+(\vec{x'}, t') \big]_+ \Big\} \tag{9.24}$$

The right-standing arguments $(\vec{x'}, t')$ refer to the injection of an electron (or hole removal) and the left-standing $(\vec{x}, t)$ arguments refer to electron removal (or hole injection).
The energy-dependent spectral function is obtained by a Fourier transform.

$$\hat{\mathcal{A}}(\hbar\omega, t) = \lim_{\eta \to 0^+} \int d\tau \; \mathrm{e}^{-i\omega\tau - \eta|\tau|} \hat{\mathcal{A}}(t + \tau, t) \tag{9.25}$$

Remark: there are variants of the Fourier transform with different centering of the two time arguments $(t + \tau/2, t - \tau/2)$ or $(t, t - \tau)$ instead of $(t + \tau, t)$.

A word of caution: The spectral function can be defined for complex-valued time arguments on a time contour or as function of the real-valued physical time. These are two different physical objects, which are, however, identical on the real-valued time axis. Whenever the distinction is relevant, it must either be clear from the context at hand or it must be stated explicitely.

9.2.2 Spectral function in Lehmann amplitudes:

Let me convert the spectral function into the Lehmann representation

$$\begin{aligned}
\mathcal{A}(\vec{x}, t, \vec{x'}, t') &\stackrel{\text{Eq. 9.24}}{=} \frac{1}{2\pi\hbar} \mathrm{Tr}\Big\{ \hat{\rho}^{(W)}_{T,\mu} \big[\hat{\psi}_H(\vec{x}, t), \hat{\psi}_H^+(\vec{x'}, t') \big]_+ \Big\} \\
&= \frac{1}{2\pi\hbar} \sum_{q,q'} P_q \Big\{ \underbrace{\langle \Phi_q | \hat{\psi}_H(\vec{x}, t) | \Phi_{q'} \rangle}_{\langle \vec{x} | \psi^{\mathcal{L}a}_{q,q'}(t) \rangle} \underbrace{\langle \Phi_{q'} | \hat{\psi}_H^+(\vec{x'}, t') | \Phi_q \rangle}_{\langle \vec{x'} | \psi^{\mathcal{L}a}_{q,q'}(t') \rangle^*} \\
&\qquad + \underbrace{\langle \Phi_q | \hat{\psi}_H^+(\vec{x'}, t') | \Phi_{q'} \rangle}_{\langle \vec{x'} | \psi^{\mathcal{L}a}_{q',q}(t') \rangle^*} \underbrace{\langle \Phi_{q'} | \hat{\psi}_H(\vec{x}, t) | \Phi_q \rangle}_{\langle \vec{x} | \psi^{\mathcal{L}a}_{q',q}(t) \rangle} \Big\} \\
&= \frac{1}{2\pi\hbar} \sum_{q,q'} (P_q + P_{q'}) \langle \vec{x} | \psi^{\mathcal{L}a}_{q,q'}(t) \rangle \langle \psi^{\mathcal{L}a}_{q,q'}(t') | \vec{x'} \rangle
\end{aligned} \tag{9.26}$$

SPECTRAL FUNCTION IN LEHMANN AMPLITUDES

$$\hat{\mathcal{A}}(t,t') = \frac{1}{2\pi\hbar}\sum_{q,q'}(P_q + P_{q'})\big|\psi^{\mathcal{L}a}_{q,q'}(t)\big\rangle\big\langle\psi^{\mathcal{L}a}_{q,q'}(t')\big| \tag{9.27}$$

With the help of the Lehmann occupations $f^{\mathcal{L}a}_{q,q'} = P_{q'}/(P_q + P_{q'})$, the spectral function can be decomposed into one $\hat{\mathcal{A}}^e(t,t')$, for the electrons and one $\hat{\mathcal{A}}^h(t,t')$ for the holes.

$$\hat{\mathcal{A}}^e(t,t') = \frac{1}{2\pi\hbar}\sum_{q,q'}(P_q + P_{q'})\big|\psi^{\mathcal{L}a}_{q,q'}(t)\big\rangle(1 - f^{\mathcal{L}a}_{q,q'})\big\langle\psi^{\mathcal{L}a}_{q,q'}(t')\big| \tag{9.28}$$

$$\hat{\mathcal{A}}^h(t,t') = \frac{1}{2\pi\hbar}\sum_{q,q'}(P_q + P_{q'})\big|\psi^{\mathcal{L}a}_{q,q'}(t)\big\rangle f^{\mathcal{L}a}_{q,q'}\big\langle\psi^{\mathcal{L}a}_{q,q'}(t')\big|. \tag{9.29}$$

9.2.3 From the spectral function to the Green's function and back

Later, we will investigate many-body perturbation theory (MBPT) as one method to obtain the contour-ordered Green's function. In fact, the sole reason for concentrating on the contour-ordered Green's function is, that it is the most natural quantity in MBPT. As such they are the basic ingredient of Feynman diagrams. Once the Green's function has been obtained, we need to extract quantities that are closer to experiment, respectively that provide the physical content in a more intuitive manner. One of these quantities is the spectral function, which makes direct contact with spectral experiments.

We will see that the electron spectral function and the hole spectral function contain all the information contained in the contour-ordered Green's function. It is therefore possible to convert the two spectral functions $\hat{\mathcal{A}}^{(e)}(t,t)$ and $\hat{\mathcal{A}}^{(h)}(t,t)$ into the countour-ordered Green's function $\hat{G}^{\mathcal{C}}(t,t')$ and vice versa. Thus, the Green's function is a unique functional of the spectral function, which forms the basis of the spectral-density functional approach (SDFT)[82].

The conversions are given here, while the derivation will be given later.

GREEN'S FUNCTION AND SPECTRAL FUNCTION ON THE REAL-VALUED TIME AXIS

$$\hat{G}^{\mathcal{C}}(t,t') \overset{\text{Eq. 9.33}}{=} \frac{2\pi\hbar}{i\hbar}\Big\{\hat{\mathcal{A}}^{(e)}(t,t')\theta_{\mathcal{C}}(t-t') - \hat{\mathcal{A}}^{(h)}(t,t')\theta_{\mathcal{C}}(t'-t)\Big\} \tag{9.30}$$

$$\begin{aligned}
\hat{\mathcal{A}}^{(e)}(t,t') &= \frac{i}{2\pi}\Big\{\theta_{\mathcal{C}}(t-t')\hat{G}^{\mathcal{C}}(t,t') - \theta_{\mathcal{C}}(t'-t)\Big(\hat{G}^{\mathcal{C}}(t',t)\Big)^\dagger\Big\}\\
\hat{\mathcal{A}}^{(h)}(t,t') &= \frac{-i}{2\pi}\Big\{\theta_{\mathcal{C}}(t'-t)\hat{G}^{\mathcal{C}}(t,t') - \theta_{\mathcal{C}}(t-t')\Big(\hat{G}^{\mathcal{C}}(t',t)\Big)^\dagger\Big\}\\
\hat{\mathcal{A}}^{\text{tot}}(t,t') &= \frac{i}{2\pi}\text{sgn}_{\mathcal{C}}(t-t')\Big\{\hat{G}^{\mathcal{C}}(t,t') + \Big(\hat{G}^{\mathcal{C}}(t',t)\Big)^\dagger\Big\}
\end{aligned} \tag{9.31}$$

Contour-ordered Green's function from the spectral function

Once the Green's function has been obtained, we need to extract the spectral function. I approach the problem from the opposite end: Firstly, the Green's function is expressed in terms of electron

and hole spectral functions. Then, the inverse relation is determined.

The conversion is done best using Lehmann amplitudes: For the electron and hole spectral function we obtained

$$\begin{aligned}\hat{\mathcal{A}}^{(e)}(t,t') &\overset{\text{Eq. 9.27}}{=} \frac{1}{2\pi\hbar}\sum_{q,q'}(P_q+P_{q'})\big|\psi^{\mathcal{L}a}_{q,q'}(t)\big\rangle(1-f^{\mathcal{L}a}_{q,q'})\big\langle\psi^{\mathcal{L}a}_{q,q'}(t')\big| \\ \hat{\mathcal{A}}^{(h)}(t,t') &\overset{\text{Eq. 9.27}}{=} \frac{1}{2\pi\hbar}\sum_{q,q'}(P_q+P_{q'})\big|\psi^{\mathcal{L}a}_{q,q'}(t)\big\rangle f^{\mathcal{L}a}_{q,q'}\big\langle\psi^{\mathcal{L}a}_{q,q'}(t')\big| \end{aligned} \tag{9.32}$$

The contour-ordered Green's function (on the real-valued time axis) can be expressed in terms of the spectral functions.

$$\begin{aligned}\hat{G}^{\mathcal{C}}(t,t') &\overset{\text{Eq. 9.2}}{=} \frac{1}{i\hbar}\sum_{q,q'}\Big(P_q+P_{q'}\Big)\Big|\psi^{\mathcal{L}a}_{q,q'}(t)\Big\rangle\Big\{\theta_{\mathcal{C}}(t-t')(1-f^{\mathcal{L}a}_{q,q'})-\theta_{\mathcal{C}}(t'-t)f^{\mathcal{L}a}_{q,q'}\Big\}\Big\langle\psi^{\mathcal{L}a}_{q,q'}(t')\Big| \\ &= \frac{2\pi\hbar}{i\hbar}\Big\{\hat{\mathcal{A}}^{(e)}(t,t')\theta_{\mathcal{C}}(t-t')-\hat{\mathcal{A}}^{(h)}(t,t')\theta_{\mathcal{C}}(t'-t)\Big\}\end{aligned} \tag{9.33}$$

This prooves Eq. 9.30 given above.

Spectral function from the contour-ordered Green's function

Next, we extract the electron spectral function from the known Green's function and thus establish Eq. 9.29 and Eq. 9.28 above.

I exploit that, for a stationary Hamiltonian, the spectral function transforms under time inversion as

$$\hat{\mathcal{A}}^{(e)}(t,t') \overset{t,t'\in\mathbb{R}}{=} \Big(\hat{\mathcal{A}}^{(e)}(t',t)\Big)^\dagger \tag{9.34}$$

$$\hat{\mathcal{A}}^{(h)}(t,t') \overset{t,t'\in\mathbb{R}}{=} \Big(\hat{\mathcal{A}}^{(h)}(t',t)\Big)^\dagger \tag{9.35}$$

The relation can be verified using the Lehmann representation Eq. 9.28 and Eq. 9.29.

$$\begin{aligned}\hat{G}^{\mathcal{C}}(t,t') &\overset{\text{Eq. 9.33}}{=} \frac{2\pi\hbar}{i\hbar}\Big\{\hat{\mathcal{A}}^{(e)}(t,t')\theta_{\mathcal{C}}(t-t')-\hat{\mathcal{A}}^{(h)}(t,t')\theta_{\mathcal{C}}(t'-t)\Big\} \\ \Rightarrow\quad \Big(\hat{G}^{\mathcal{C}}(t',t)\Big)^\dagger &= \frac{-2\pi\hbar}{i\hbar}\Big\{\hat{\mathcal{A}}^{(e)}(t',t)\theta_{\mathcal{C}}(t'-t)-\hat{\mathcal{A}}^{(h)}(t',t)\theta_{\mathcal{C}}(t-t')\Big\}^\dagger \\ &\overset{\text{Eqs. 9.34 9.35}}{=} \frac{-2\pi\hbar}{i\hbar}\Big\{\hat{\mathcal{A}}^{(e)}(t,t')\theta_{\mathcal{C}}(t'-t)-\hat{\mathcal{A}}^{(h)}(t,t')\theta_{\mathcal{C}}(t-t')\Big\}\end{aligned} \tag{9.36}$$

The two equations Eq. 9.33 and Eq. 9.36 can be combined into

$$\begin{aligned}\hat{\mathcal{A}}^{(e)}(t,t') &= \frac{i}{2\pi}\Big\{\theta_{\mathcal{C}}(t-t')\hat{G}^{\mathcal{C}}(t,t')-\theta_{\mathcal{C}}(t'-t)\Big(\hat{G}^{\mathcal{C}}(t',t)\Big)^\dagger\Big\} \\ \hat{\mathcal{A}}^{(h)}(t,t') &= \frac{-i}{2\pi}\Big\{\theta_{\mathcal{C}}(t'-t)\hat{G}^{\mathcal{C}}(t,t')-\theta_{\mathcal{C}}(t-t')\Big(\hat{G}^{\mathcal{C}}(t',t)\Big)^\dagger\Big\} \\ \hat{\mathcal{A}}^{\text{tot}}(t,t') &= \hat{\mathcal{A}}^{(e)}(t,t')+\hat{\mathcal{A}}^{(h)}(t,t') \\ &= \frac{i}{2\pi}\text{sgn}_{\mathcal{C}}(t-t')\Big\{\hat{G}^{\mathcal{C}}(t,t')+\Big(\hat{G}^{\mathcal{C}}(t',t)\Big)^\dagger\Big\}\end{aligned} \tag{9.37}$$

9.3 Energy representation for thermal ensembles

Above, we defined the Lehmann amplitudes and spectral functions in its most general form, and we have shown how Green's function can be converted into spectral functions and vice versa.

Now, we return to the most common use cases, namely to energy-independent Hamiltonians and thermal ensembles.

9.3.1 Lehmann amplitudes

Let me return to Lehmann amplitudes introduced earlier. The time-dependent Lehmann amplitudes have been related to the stationary Lehmann amplitudes via

$$\underbrace{\psi^{\mathcal{L}a}_{q,q'}(\vec{x},t)}_{\langle\Phi_q|\hat{\psi}_H(\vec{x},t)|\Phi_{q'}\rangle} \overset{\text{Eq. 9.11}}{=} \underbrace{\psi^{\mathcal{L}a}_{q,q'}(\vec{x})}_{\langle\Phi_q|\hat{\psi}_S(\vec{x})|\Phi_{q'}\rangle} \mathrm{e}^{-\frac{i}{\hbar}\epsilon^{\mathcal{L}a}_{q,q'}t} \tag{9.38}$$

with the Lehmann energies

$$\epsilon^{\mathcal{L}a}_{q,q'} \overset{\text{Eq. 9.10}}{=} \frac{E_q - E_{q'}}{N_q - N_{q'}} \tag{9.39}$$

Fermi function as Lehmann occupation for thermal ensembles

For a thermal ensemble, the Lehmann occupations can be expressed via the Fermi distribution function $f_{T,\mu}(\epsilon) = 1/(\mathrm{e}^{\beta(\epsilon-\mu)}+1)$ and the Lehmann energies.

$$\begin{aligned} f^{\mathcal{L}a}_{q,q'} &\overset{\text{Eq. 9.4}}{=} \frac{P_{q'}}{P_q + P'_q} = \frac{Z^{-1}_{T,\mu}\mathrm{e}^{-\beta(E_{q'}-\mu N_{q'})}}{Z^{-1}_{T,\mu}\mathrm{e}^{-\beta(E_{q'}-\mu N_{q'})} + Z^{-1}_{T,\mu}\mathrm{e}^{-\beta(E_q-\mu N_q)}} = \frac{1}{1+\mathrm{e}^{\beta[(E_{q'}-E_q)-\mu(N_{q'}-N_q)]}} \\ &\overset{N_q=N'_q-1}{=} \frac{1}{\mathrm{e}^{\beta(\epsilon^{\mathcal{L}a}_{q,q'}-\mu)}+1} = f_{T,\mu}\big(\epsilon^{\mathcal{L}a}_{q,q'}\big) \end{aligned} \tag{9.40}$$

I find it interesting that the Fermi function occurs here in the context of a general many-body problem, while it had been introduced in the context of non-interacting electrons.

9.3.2 Spectral function

For a time-independent Hamiltonian, I can make use of the stationary Lehmann amplitudes and their Lehmannn energies, which yields.

$$\begin{aligned} \hat{\mathcal{A}}(t,t') &\overset{\text{Eqs. 9.27 ,9.38}}{=} \frac{1}{2\pi\hbar}\sum_{q,q'}(P_q+P_{q'})|\psi^{\mathcal{L}a}_{q,q'}(0)\rangle\mathrm{e}^{-\frac{i}{\hbar}\epsilon^{\mathcal{L}a}_{q,q'}(t-t')}\langle\psi^{\mathcal{L}a}_{q,q'}(0)| \\ &= \int\frac{d\hbar\omega}{2\pi\hbar}\,\mathrm{e}^{i\omega t}\underbrace{\sum_{q,q'}(P_q+P_{q'})|\psi^{\mathcal{L}a}_{q,q'}(0)\rangle\delta(\hbar\omega-\epsilon^{\mathcal{L}a}_{q,q'})\langle\psi^{\mathcal{L}a}_{q,q'}(0)|}_{\hat{\mathcal{A}}(\hbar\omega)} \end{aligned} \tag{9.41}$$

This yields the

FREQUENCY-DEPENDENT SPECTRAL FUNCTION

The frequency-dependent (energy-dependent) spectral function in terms of stationary Lehmann amplitudes is

$$\hat{\mathcal{A}}^{\text{tot}}(\hbar\omega) = \sum_{q,q'} (P_q + P_{q'}) \left|\psi^{\mathcal{L}a}_{q,q'}\right\rangle \delta\big(\hbar\omega - \epsilon^{\mathcal{L}a}_{q,q'}\big) \left\langle\psi^{\mathcal{L}a}_{q,q'}\right| \tag{9.42}$$

which can be divided with the help of the thermal Lehmann occupations Eq. 9.40 into the electron and hole spectral functions

$$\hat{\mathcal{A}}^{(e)}(\hbar\omega) = \Big(1 - f_{T,\mu}(\hbar\omega)\Big)\hat{\mathcal{A}}^{\text{tot}}(\hbar\omega) \tag{9.43}$$

$$\hat{\mathcal{A}}^{(h)}(\hbar\omega) = f_{T,\mu}(\hbar\omega)\hat{\mathcal{A}}^{\text{tot}}(\hbar\omega) \tag{9.44}$$

Properties: Let me summarize some properties of the spectral functions.

- the spectral function $\hat{\mathcal{A}}(\epsilon)$ is an operator in the one-particle Hilbert space. One can also construct spectral functions for two-particle excitations, which would be operators in the two-particle Hilbert space. However, these spectral functions differ from the spectral functions for one-particle excitations discussed here.
- The energy-dependent spectral functions are hermitian, which is seen from the defining equations Eq. 9.42 as well as Eq. 9.43 and Eq. 9.44.
- The total spectral function $\hat{\mathcal{A}}^{(tot)}(\epsilon)$ satisfies the sum rule

$$\int d\epsilon\, \hat{\mathcal{A}}^{(tot)}(\epsilon) \overset{\text{Eqs. } 9.42,9.13}{=} \hat{1} \tag{9.45}$$

- The integral of the hole spectral function $\hat{A}^{(h)}$ is the one-particle-reduced density matrix.

$$\int d\epsilon\, f_{T,\mu}(\epsilon)\hat{\mathcal{A}}^{(tot)}(\epsilon) \overset{\text{Eqs. } 9.42,9.14}{=} \hat{\rho}^{(1)} \tag{9.46}$$

- The peak positions of the spectral function are determined by the Hamiltonian $\hat{h} + \hat{W}$, respectively the differences $E_m - E_n$ of its eigenvalues. They do not depend on temperature or chemical potential. The quantities, that change with the thermodynamic state, are the intensities of the spectral peaks. The intensities are governed by the probabilities $\{P_n\}$.

  This is analogous to the spectrum in the average-phase approximation and it differs from the mean-field approximation on the Hartree-Fock level. As discussed in section G.7.2 on p. 654, the peak positions shift in the mean-field approximation, due to the change of the Fock operator, while the intensities of the bands remain unchanged. However, see also Fig. G.4 on p. 655, which shows how the true spectral function can produce an apparent behavior of the mean-field spectral function.

Spectral function in the APA: In the APA, the Lehmann amplitudes have a particular simple form

$$\begin{aligned}\hat{\mathcal{A}}(\hbar\omega) &\overset{\text{Eq. } 9.42}{=} \sum_{q,q'} (P_q + P_{q'}) |\psi^{\mathcal{L}a}_{q,q'}(0)\rangle \delta(\hbar\omega - \epsilon^{\mathcal{L}a}_{q,q'}) \langle\psi^{\mathcal{L}a}_{q,q'}(0)| \\ &\overset{\text{APA, Eq. } 9.20}{=} \sum_j |\varphi_j\rangle \left\{ \sum_{\vec{\sigma}} (P_{|\vec{\sigma}\rangle} + P_{\hat{a}_j|\vec{\sigma}\rangle})\, \delta\big(\hbar\omega - \epsilon_j^{(\vec{\sigma})}\big) \right\} \langle\varphi_j| \end{aligned} \tag{9.47}$$

The spectral function is diagonal in the basis of one-particle orbitals, which are, furthermore, the natural orbitals. Thus, we can assign a spectral function $\langle\varphi_n|\mathcal{A}(\hbar\omega)|\varphi_n\rangle$ to each natural orbital $|\varphi_n\rangle$, and, in the APA, these diagonal matrix elements contain the complete information of the spectral function.

9.3.3 Green's function

In order to transform the Green's function into the energy representation we use the relations Eq. A.15 derived in Appendix A.3.2 (p. 501)

$$\int_{-\infty}^{\infty} dt\ \theta(t)\mathrm{e}^{\frac{i}{\hbar}(\epsilon+i\eta)t} = \frac{i\hbar}{\epsilon+i\eta} \qquad \text{and} \qquad \int_{-\infty}^{\infty} dt\ \theta(-t)\mathrm{e}^{\frac{i}{\hbar}(\epsilon-i\eta)t} = \frac{-i\hbar}{\epsilon-i\eta} \tag{9.48}$$

The time integration is a contour integration along the entire real time axis in the positive direction.

$$\begin{aligned}
\hat{G}^{\mathcal{C}}(\hbar\omega) &\overset{\text{def}}{=} \int_{-\infty}^{\infty} dt\ \mathrm{e}^{i\omega t-\frac{1}{\hbar}\eta|t|}\hat{G}^{\mathcal{C}}(t,0) \\
&\overset{\text{Eq. 9.2}}{=} \int_{-\infty}^{\infty} dt\ \mathrm{e}^{i\omega t-\frac{1}{\hbar}\eta|t|)} \underbrace{\frac{1}{i\hbar}\sum_{q,q'}(P_q+P_{q'})\ \mathrm{e}^{-\frac{1}{\hbar}\epsilon^{\mathcal{L}a}_{q,q'}t}}_{\hat{G}^{\mathcal{C}}(t,0)\text{ cont'd...}} \\
&\quad \times \underbrace{\left|\psi^{\mathcal{L}a}_{q,q'}\right\rangle\left(\theta_{\mathcal{C}}(t)\left(1-f_{T,\mu}\left(\epsilon^{\mathcal{L}a}_{q,q'}\right)\right)-\theta_{\mathcal{C}}(-t)f_{T,\mu}\left(\epsilon^{\mathcal{L}a}_{q,q'}\right)\right)\left\langle\psi^{\mathcal{L}a}_{q,q'}\right|}_{\text{...cont'd }\hat{G}^{\mathcal{C}}(t,0)} \\
&= \sum_{q,q'}(P_q+P_{q'})\left|\psi^{\mathcal{L}a}_{q,q'}\right\rangle\left[\frac{1-f_{T,\mu}\left(\epsilon^{\mathcal{L}a}_{q,q'}\right)}{\hbar\omega-\epsilon^{\mathcal{L}a}_{q,q'}+i\eta}+\frac{f_{T,\mu}\left(\epsilon^{\mathcal{L}a}_{q,q'}\right)}{\hbar\omega-\epsilon^{\mathcal{L}a}_{q,q'}-i\eta}\right]\left\langle\psi^{\mathcal{L}a}_{q,q'}\right|
\end{aligned} \tag{9.49}$$

The energy-dependent Green's function can furthermore be expressed in terms if the spectral function.

$$\hat{G}^{\mathcal{C}}(\hbar\omega) \overset{\text{Eq. 9.42}}{=} \int d\epsilon\left[\frac{1-f_{T,\mu}(\epsilon)}{\hbar\omega-\epsilon+i\eta}+\frac{f_{T,\mu}(\epsilon)}{\hbar\omega-\epsilon-i\eta}\right]\underbrace{\sum_{q,q'}(P_q+P_{q'})\left|\psi^{\mathcal{L}a}_{q,q'}\right\rangle\delta\left(\epsilon-\epsilon^{\mathcal{L}a}_{q,q'}\right)\left\langle\psi^{\mathcal{L}a}_{q,q'}\right|}_{\hat{\mathcal{A}}(t,t')} \tag{9.50}$$

This yields the

LEHMANN REPRESENTATION OF THE GREEN'S FUNCTION

$$\begin{aligned}
G^{\mathcal{C}}_{\alpha,\beta}(\hbar\omega) &\overset{\text{def}}{=} \int_{-\infty}^{\infty} dt\ \mathrm{e}^{\frac{i}{\hbar}(\hbar\omega t+i\eta|t|)}G^{\mathcal{C}}_{\alpha,\beta}(t,0) \\
&= \sum_{q,q'}(P_q+P_{q'})\left|\psi^{\mathcal{L}a}_{q,q'}\right\rangle\left[\frac{1-f_{T,\mu}\left(\epsilon^{\mathcal{L}a}_{q,q'}\right)}{\hbar\omega-\epsilon^{\mathcal{L}a}_{q,q'}+i\eta}+\frac{f_{T,\mu}\left(\epsilon^{\mathcal{L}a}_{q,q'}\right)}{\hbar\omega-\epsilon^{\mathcal{L}a}_{q,q'}-i\eta}\right]\left\langle\psi^{\mathcal{L}a}_{q,q'}\right| \qquad (9.51) \\
&\overset{\text{Eq. 9.42}}{=} \int d\epsilon\ \hat{\mathcal{A}}^{\text{tot}}(\epsilon)\left[\frac{1-f_{T,\mu}(\epsilon)}{\hbar\omega-\epsilon+i\eta}+\frac{f_{T,\mu}(\epsilon)}{\hbar\omega-\epsilon-i\eta}\right] \\
&= \int d\epsilon\left[\frac{\hat{\mathcal{A}}^{(e)}(\epsilon)}{\hbar\omega-\epsilon+i\eta}+\frac{\hat{\mathcal{A}}^{(h)}(\epsilon)}{\hbar\omega-\epsilon-i\eta}\right] \qquad (9.52)
\end{aligned}$$

The time integration proceeds along the real-time axis in the positive direction. η is an infinitesimally small, positive number.

This expression makes the structure of the Green's function evident. It is shown in Fig.9.1 The Green's functions has poles at the one-particle excitation energies.[4] For the electron excitations, i.e. above the Fermi level, the poles are infinitesimally below the real frequency axis and for hole excitation, i.e. below the Fermi level they lie above the real axis. For infinitely large systems, the excitations may form a continuous spectrum. As a result, the discrete poles usually merge into a **branch cut**.

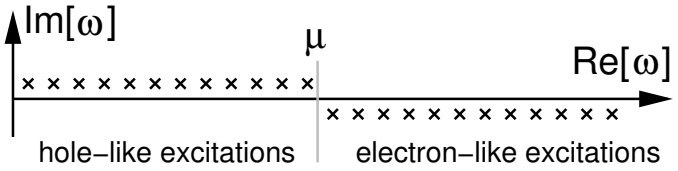


Fig. 9.1: Position of the poles of the Green's function for non-interacting electrons. The poles are located in the complex ω plane at the positions given by the excitation energy (real part) and $\pm\eta$ (imaginary part). For an interacting system the excitations may move a finite distance away from the real axis, which corresponds to a finite life time of the corresponding quasi particles.

$$\begin{aligned}
\hat{G}^{\mathcal{C}}_{\alpha,\beta}(\hbar\omega) - \left(\hat{G}^{\mathcal{C}}_{\alpha,\beta}(\hbar\omega)\right)^{\dagger} &\overset{\text{Eq. 9.52}}{=} \int d\epsilon\, \hat{\mathcal{A}}^{\text{tot}}(\epsilon)\left[\frac{1-f_{T,\mu}(\epsilon)}{\hbar\omega-\epsilon+i\eta}+\frac{f_{T,\mu}(\epsilon)}{\hbar\omega-\epsilon-i\eta}\right] \\
&\quad -\left(\hat{\mathcal{A}}^{\text{tot}}(\epsilon)\right)^{\dagger}\left[\frac{1-f_{T,\mu}(\epsilon)}{\hbar\omega-\epsilon-i\eta}+\frac{f_{T,\mu}(\epsilon)}{\hbar\omega-\epsilon+i\eta}\right] \\
&= \int d\epsilon\, \hat{\mathcal{A}}^{\text{tot}}(\epsilon)\left[\frac{1-2f_{T,\mu}(\epsilon)}{\hbar\omega-\epsilon+i\eta}-\frac{1-2f_{T,\mu}(\epsilon)}{\hbar\omega-\epsilon-i\eta}\right] \\
&= \int d\epsilon\, \hat{\mathcal{A}}^{\text{tot}}(\epsilon)\underbrace{\frac{-2i\eta}{(\hbar\omega-\epsilon)^2+\eta^2}}_{-2\pi i\delta(\hbar\omega-\epsilon)}\Big(1-2f_{T,\mu}(\epsilon)\Big) \\
\Rightarrow & \qquad (9.53)
\end{aligned}$$

ENERGY-DEPENDENT SPECTRAL FUNCTION FROM THE GREEN'S FUNCTION

$$\hat{\mathcal{A}}^{\text{tot}}(\epsilon) = \frac{i}{2\pi}\frac{\hat{G}^{\mathcal{C}}_{\alpha,\beta}(\epsilon) - \left(\hat{G}^{\mathcal{C}}_{\alpha,\beta}(\epsilon)\right)^{\dagger}}{1-2f_{T,\mu}(\epsilon)} \qquad (9.54)$$

Compare this result with the density of states Eq. 4.53 on p. 179 for non-interacting electrons.

$$\hat{D}(\epsilon) \overset{\text{Eq. 4.53}}{=} \frac{-1}{2\pi i}\Big(\hat{G}(\epsilon+i\eta) - \hat{G}^{\dagger}(\epsilon+i\eta)\Big) \qquad (9.55)$$

Editor: The restriction to real-valued time arguments came in when I expressed the matrix elements of the creation operator by those of the annihilation operator.

$$\langle\Phi_q|\hat{\psi}^{+}(\vec{x},t)|\Phi_{q'}\rangle = \langle\Phi_{q'}|\Big(\hat{\psi}^{+}(\vec{x},t)\Big)^{\dagger}|\Phi_q\rangle^{*} \overset{t\in\mathbb{R}}{=} \langle\Phi_{q'}|\hat{\psi}(\vec{x},t)|\Phi_q\rangle^{*} \qquad (9.56)$$

Editor: Look into https://arxiv.org/pdf/1912.08474

[4] Excitations with more than one particle have vanishing amplitudes $\langle\Phi_m|\hat{c}_{S,\alpha}|\Phi_n$.

9.4 Home-study and practice

9.4.1 Satellites in the spectral function

Introduction

In addition to the features in the spectral function that can be compared to the density of states of non-interacting electrons, one often observes so-called **satellites**, namely small peaks of the spectral function, which lie several eV below or above the main features. These satellites are due to the combination of a one-particle excitation, such as electron addition or electron removal, with a particle-number-conserving excitation. Such a particle-number-conserving excitation could be the creation of an electron-hole pair, a plasmon, spin waves, phonons or something else.

Editor: Include a figure with an experimental spectrum exhibiting a satellite.

A theory such as the Hartree-Fock approximation, that describes the ground state by a single Slater determinant, can not describe satellites. When the ground state or the final state of the excitation is a superposition of several Slater determinants, the "transition" to or from these Slater determinants contributes additional features in the spectral function. The reason for the admixture is the interaction $\hat{W}$. The transition can take these Slater determinants to eigenstates of the Hamiltonian that have not been accessible before. These eigenstates can be described in terms of particle-conserving excitations of those eigenstates contributing in the absence of the admixture. This excitation adds to the energy of the original transition. If the excitation energies are small, they lead to the **life-time broadening** of the quasi-particle peaks. If they are large, they produce separate replica of the quasi-particle peaks, which are then called **satellites**.

In this exercise, we will study a minimal model for a one-particle level that couples to a particle-number-conserving excitation.

The model consists of a one-particle state $|a\rangle$, to which we will add and remove a particle, and an electron-hole excitation from state $|b\rangle$ to $|c\rangle$. The one-particle level has energy $\bar{\epsilon}_a$. The excitation raises an electron from the energy level $\bar{\epsilon}_b$ to level $\bar{\epsilon}_c$. Let me consider the case $\bar{\epsilon}_b \ll \mu$ and $\mu \ll \bar{\epsilon}_c$.

The non-interacting Hamiltonian has the form

$$\hat{h} = \bar{\epsilon}_a \hat{a}^\dagger \hat{a} + \bar{\epsilon}_b \hat{b}^\dagger \hat{b} + \bar{\epsilon}_c \hat{c}^\dagger \hat{c} \tag{9.57}$$

where $\hat{a}, \hat{a}^\dagger$, $\hat{b}, \hat{b}^\dagger$, $\hat{c}, \hat{c}^\dagger$ are the annihilation and creation operators for the three one-particle orbitals.

The spectral function of this non-interacting model

$$\hat{\mathcal{A}}(\epsilon) = |a\rangle\delta\big(\epsilon - \bar{\epsilon}_a\big)\langle a| + |b\rangle\delta\big(\epsilon - \bar{\epsilon}_b\big)\langle b| + |c\rangle\delta\big(\epsilon - \bar{\epsilon}_c\big)\langle c| \tag{9.58}$$

has delta-peaks at the one-particle levels $\bar{\epsilon}_a$, $\bar{\epsilon}_b$, $\bar{\epsilon}_c$. The spectral function projected on orbital $|a\rangle$ has only one delta function at $\bar{\epsilon}_a$

Let me now add the interaction. I will consider specifically one contribution, that allows me to demonstrate satellites without adding other complications.

$$\hat{h} = \bar{\epsilon}_a \hat{a}^\dagger \hat{a} + \bar{\epsilon}_b \hat{b}^\dagger \hat{b} + \bar{\epsilon}_c \hat{c}^\dagger \hat{c} + V \hat{a}^\dagger \hat{a}\Big(\hat{b}^\dagger \hat{c} + \hat{c}^\dagger \hat{b}\Big) \tag{9.59}$$

The interaction term describes the Coulomb interaction of an electron in $|a\rangle$ with the charge density of the electron-hole pair. When the electron is present in a, the many-particle eigenstates have an admixture of the electron-hole pair. In other words the wave functions are superpositions of $|1,1,0\rangle$ and $|1,0,1\rangle$, so that both can be accessed by adding an electron to $|0,1,0\rangle$ in orbital $|a\rangle$.

Let me now simplify the Hamiltonian, while maintaining the features, which are required to describe the physical effect of interest, the satellites: I introduce the symbol $\Delta \stackrel{\text{def}}{=} \bar{\epsilon}_c - \bar{\epsilon}_b$ for the excitation energy of the electron-hole excitation. The Hamiltonian above preserves the number $n_b + n_v$ of electrons in the orbitals $|b\rangle$ and $|c\rangle$. For our purpose, only the case $n_B + n_C = 1$ with one electron in the orbitals $|b\rangle$ and $|c\rangle$ is of interest. The energy $n_b\bar{\epsilon}_b + n_c\bar{\epsilon}_c$ is a constant in the relevant subspace. Therefore, I simplify the Hamiltonian by setting $\bar{\epsilon}_B + \bar{\epsilon}_C = -\frac{\Delta}{2}$. Finally, I drop the subscript from $\bar{\epsilon}_a$.

The resulting, simplified model Hamiltonian is

$$\hat{H} = \bar{\epsilon}\hat{a}^\dagger\hat{a} + \Delta\hat{c}^\dagger\hat{c} + V\hat{a}^\dagger\hat{a}\left(\hat{b}^\dagger\hat{c} + \hat{c}^\dagger\hat{b}\right) \tag{9.60}$$

For our purposes we can exclude states with zero or two particles in $|b\rangle$ and $|c\rangle$. The relevant Fock space is spanned by four Slater determinants

$$\begin{aligned} |0,\downarrow\rangle &\stackrel{\text{def}}{=} |0,1,0\rangle \\ |0,\uparrow\rangle &\stackrel{\text{def}}{=} |0,0,1\rangle \\ |1,\downarrow\rangle &\stackrel{\text{def}}{=} |1,1,0\rangle \\ |1,\uparrow\rangle &\stackrel{\text{def}}{=} |1,0,1\rangle \end{aligned} \tag{9.61}$$

I have introduced a notation which makes explicit that one two states are allowed for the excitation. Either the electron is in the lower level $\downarrow\rangle$ or it is in the upper level $|\uparrow\rangle$.

Problem

Consider the model with a Hamiltonian

$$\hat{H} = \bar{\epsilon}\hat{a}^\dagger\hat{a} + \Delta\hat{c}^\dagger\hat{c} + V\left(\hat{b}^\dagger\hat{a}^\dagger\hat{a}\hat{c} + \hat{c}^\dagger\hat{a}^\dagger\hat{a}\hat{b}\right) \tag{9.62}$$

with three one-particle levels $|a\rangle$, $|b\rangle$ and $|c\rangle$. The model describes an electron acceptor $|a\rangle$, which is coupled to an excitation of an electron from state $|b\rangle$ to state $|c\rangle$.

1 Determine the many-particle eigenvalues and the eigenstates of the model with $n_b + n_c = 1$.

2 Determine the ground-state ensemble as function of the particle number N in the acceptor orbital. That is: Plot the probabilities P_m and the energy expectation value as function of the number N in the acceptor molecule in the limit $T \to 0$. Plot probabilities and ensemble energy as function of the chemical potential, while considering smalll but finite temperatures. A qualitative sketch is sufficient. Use calculations to the extent necessary to extract the qualitative features.

3 Construct the spectral function for the electron accepting orbital for particle numbers ranging from one to two.

Solution

1 Determine the many-particle eigenvalues and the eigenstates of the model with $n_b + n_c = 1$.

The Hamiltonian is

$$\hat{H} = \begin{pmatrix} |0,\downarrow\rangle \\ |0,\uparrow\rangle \\ |1,\downarrow\rangle \\ |1,\uparrow\rangle \end{pmatrix} \begin{pmatrix} 0 & 0 & 0 & 0 \\ 0 & \Delta & 0 & 0 \\ 0 & 0 & \bar{\epsilon} & V \\ 0 & 0 & V & \bar{\epsilon}+\Delta \end{pmatrix} \begin{pmatrix} \langle 0,\downarrow| \\ \langle 0,\uparrow| \\ \langle 1,\downarrow| \\ \langle 1,\uparrow| \end{pmatrix} \tag{9.63}$$

where the notation of Eq. 9.61 has been used for the basisstates. States with $n_b + n_c \neq 1$ have been excluded.

The energy eigenvalues are

$$\begin{aligned}
&E_{0,\downarrow} = 0 \qquad \text{with } |\Psi_{0,\downarrow}\rangle = |0,\downarrow\rangle \\
&E_{0,\uparrow} = \Delta \qquad \text{with } |\Psi_{0,\uparrow}\rangle = |0,\uparrow\rangle \\
&E_{1,\pm} = \bar{\epsilon} + \frac{\Delta}{2} \pm \sqrt{\left(\frac{\Delta}{2}\right)^2 + V^2} = \bar{\epsilon} + \frac{\Delta}{2}\left[1 \pm \underbrace{\sqrt{1+\left(\frac{2V}{\Delta}\right)^2}}_{=:1+2q/\Delta}\right] \approx \begin{cases} \bar{\epsilon} - \frac{V^2}{\Delta} \\ \bar{\epsilon} + \Delta + \frac{V^2}{\Delta} \end{cases}
\end{aligned} \tag{9.64}$$

The eigenstates are

$$\begin{aligned}
|\Psi_{1,-}\rangle &= |1,\downarrow\rangle\cos(\gamma) + |1,\uparrow\rangle\sin(\gamma) \\
|\Psi_{1,+}\rangle &= |1,\uparrow\rangle\cos(\gamma) - |1,\downarrow\rangle\sin(\gamma)
\end{aligned} \tag{9.65}$$

with the mixing angle γ defined by the eigenvalue equation of the Hamiltonian Eq. 9.63.

$$\begin{aligned}
\left\{\bar{\epsilon} - \bar{\epsilon} - \frac{\Delta}{2}\left(1 \pm \sqrt{1+\left(\frac{2V}{\Delta}\right)^2}\right)\right\}\cos(\gamma) + V\sin(\gamma) &= 0 \\
\left\{1 \pm \sqrt{1+\left(\frac{2V}{\Delta}\right)^2}\right\}\cos(\gamma) - \frac{2V}{\Delta}\sin(\gamma) &= 0 \\
\tan(\gamma) &= \frac{\Delta}{2V}\left[1 \pm \sqrt{1+\left(\frac{2V}{\Delta}\right)^2}\right]
\end{aligned} \tag{9.66}$$

$$\begin{aligned}
\cos(\gamma) &\overset{x=\tan(\gamma)}{=} \cos(\arctan(x)) = \frac{1}{\sqrt{1+x^2}} = \frac{1}{\sqrt{1+\tan^2(\gamma)}} \\
&= \left(1 + \left[\frac{\Delta}{2V}\left(1 \pm \sqrt{1+\left(\frac{2V}{\Delta}\right)^2}\right)\right]^2\right)^{-\frac{1}{2}} \\
&= \frac{2V}{\Delta}\left(\left(\frac{2V}{\Delta}\right)^2 + \left[1 \pm \sqrt{1+\left(\frac{2V}{\Delta}\right)^2}\right]^2\right)^{-\frac{1}{2}} \\
&= \frac{2V}{\Delta}\left(\left(\frac{2V}{\Delta}\right)^2 + 1 \pm 2\sqrt{1+\left(\frac{2V}{\Delta}\right)^2} + 1 + \left(\frac{2V}{\Delta}\right)^2\right)^{-\frac{1}{2}} \\
&= \frac{2V}{\Delta}\frac{1}{\sqrt{2}}\left(1 + \left(\frac{2V}{\Delta}\right)^2 \pm \sqrt{1+\left(\frac{2V}{\Delta}\right)^2}\right)^{-\frac{1}{2}} \\
&\approx \begin{cases} \frac{1}{2}\frac{2V}{\Delta} & \text{for } |V| \ll |\Delta| \text{ and } \pm = + \\ \frac{1}{\sqrt{2}}\mathrm{sgn}\left(\frac{2V}{\Delta}\right) & \text{for } |V| \gg |\Delta| \text{ and } \pm = + \\ \left[1 - \frac{1}{2}\left(\frac{V}{\Delta}\right)^2\right]\mathrm{sgn}\left(\frac{2V}{\Delta}\right) & \text{for } |V| \ll |\Delta| \text{ and } \pm = - \\ \frac{1}{\sqrt{2}}\mathrm{sgn}\left(\frac{2V}{\Delta}\right) & \text{for } |V| \gg |\Delta| \text{ and } \pm = - \end{cases}
\end{aligned} \tag{9.67}$$

The solution that is relevant for us is the one with $V \ll \Delta$ and $\pm = -$, because this connects $|1,-\rangle$ with $|1,\downarrow\rangle$ in the absence of V.

The many-particle states and their energies are

j	E_j	$\|\Psi_j\rangle$
1	0	$\|0,\downarrow\rangle$
2	Δ	$\|0,\uparrow\rangle$
3	$\bar{\epsilon}-q$	$\|1,\downarrow\rangle\cos(\gamma)+\|1,\uparrow\rangle\sin(\gamma)$
4	$\bar{\epsilon}+\Delta+q$	$\|1,\uparrow\rangle\cos(\gamma)-\|1,\downarrow\rangle\sin(\gamma)$

The parameter q has been defined in Eq. 9.64 as

$$q=\frac{\Delta}{2}\left(\sqrt{1+\left(\frac{2V}{\Delta}\right)^2}-1\right)\approx\frac{V^2}{\Delta}\quad\text{for } V\ll\Delta \tag{9.68}$$

2 Determine the ground-state ensemble as function of the particle number N in the acceptor orbital. That is: Plot the probabilities P_m and the energy expectation value as function of the number N in the acceptor molecule in the limit $T\to 0$. Plot probabilities and ensemble energy as function of the chemical potential, while considering smalll but finite temperatures. A qualitative sketch is sufficient. Use calculations to the extent necessary to extract the qualitative features.

Editor: This is not yet a muster solution but a collection of useful material related to it.

The purpose of this problem is a to clarify some basis question related to thermodynamics as opposed to "pure-state quantum mechanics".

For the ground state (ensemble) with a given (non-integer) particle number, at least two wave functions need to be considered. There is no eigenstate of the Hamiltonian with fractional particle number N (on the acceptor molecule). The particle number for an ensemble always implies the corresponding ensemble expectation value. For $T\to 0$, the ensemble with lowest grand potential consists of two wave functions, namely the wave function with lowest energy for $N=0$ and that for $N=1$.

When we consider the total number of particles for a general system, the construction would be as follows: First determine the lowest energy $E(N)=min_{q:\bar{N}_q=N}\bar{E}_q$ for each integer particle number. Plot those into graph $E(N)$ and then find the lower envelope, which defines $E(N)$ also for fractional particle number. The lower envelope consists of straight-line segments with kinks at the integer particle number. The slope of this graph is the chemical potential $\mu(N)$. For fractional N the ensemble consists of two eigenstates of the Hamiltonian with different particle numbers.

Another useful construction is to plot the energy as function of chemical potential. Take the energies $\bar{E}_q$ and particle numbers $\bar{N}_q$ of all many-particle eigenstates of the Hamiltonian. (The bar ontop of the symbols has no physical meaning and is only there to distinguish the symbol from those without a bar.) Include also the excited states. Then draw for every many particle state line $E_q(\mu)=\bar{E}_q-\mu\bar{N}_q$. In the low-temperature limit, we only need to determine the lowest $E_q(\mu)$ for each chemical potential. The slope of the resulting lower envelope determines the particle number $N(\mu)=-\partial_\mu \min_q(E_q-\mu N_q)$. At $T\to 0$ is envelope has straight-line segments and kinks. At the kinks the particle number changes abruptly from one integer number to another. At these points chemical potentials, the ground state ensemble consists of at least two wave functions with the same $E_q(\mu)$.

Editor: Mention a negative U system such as the vacancy in silicon.

3 Construct the spectral function projected on site a for T=0 of the system for particle numbers ranging from one to two.

Let me consider the spectral function of the accepting orbital as function of the number of electrons. The electron acceptor can accept between zero and one electrons. This number is denoted by x. The probabilities for the states are $P_1=1-x$ and $P_3=x$, while $P_2=P_4=0$ at zero temperature.

The spectral function is

$$\mathcal{A}^{\text{tot}}_{\alpha,\beta}(\epsilon) \overset{\text{Eq. ??}}{=} \sum_{m,n}(P_n + P_m)\langle\Phi_n|\hat{c}_{S,\alpha}|\Phi_m\rangle\langle\Phi_m|\hat{c}^\dagger_{S,\beta}|\Phi_n\rangle\delta\Big(\epsilon - (E_m - E_n)\Big)$$

$$\begin{aligned}
\mathcal{A}^{\text{tot}}_{a,a}(\epsilon) &= \underbrace{|\langle\Phi_2|\hat{c}^\dagger_{S,a}|\Phi_1\rangle|^2}_{0}\,\delta\Big(\epsilon - \underbrace{(E_2 - E_1)}_{\Delta}\Big)\,\underbrace{(1-x)}_{P_1+P_2} \\
&+ \underbrace{|\langle\Phi_3|\hat{c}^\dagger_{S,a}|\Phi_1\rangle|^2}_{\cos^2(\gamma)}\,\delta\Big(\epsilon - \underbrace{(E_3 - E_1)}_{\bar{\epsilon}-q}\Big)\,\underbrace{1}_{P_1+P_3} \\
&+ \underbrace{|\langle\Phi_4|\hat{c}^\dagger_{S,a}|\Phi_1\rangle|^2}_{\sin^2(\gamma)}\,\delta\Big(\epsilon - \underbrace{(E_4 - E_1)}_{\bar{\epsilon}+\Delta+q}\Big)\,\underbrace{1-x}_{P_1+P_4} \\
&+ \underbrace{|\langle\Phi_3|\hat{c}^\dagger_{S,a}|\Phi_2\rangle|^2}_{\sin^2(\gamma)}\,\delta\Big(\epsilon - \underbrace{(E_3 - E_2)}_{\bar{\epsilon}-q-\Delta}\Big)\,\underbrace{x}_{P_2+P_3} \\
&= \underbrace{\overbrace{\cos^2(\gamma)}^{Z}\,\delta\Big(\epsilon - (\bar{\epsilon} - q)\Big)}_{\text{quasi-particle peak}} \\
&+ \underbrace{\overbrace{\sin^2(\gamma)}^{1-Z}\Big[(1-x)\delta\Big(\epsilon - (\bar{\epsilon} + \Delta + q)\Big) + x\delta\Big(\epsilon - (\bar{\epsilon} - \Delta - q)\Big)\Big]}_{\text{satellites}}
\end{aligned} \tag{9.69}$$

The spectral function is sketched in figure 9.2.

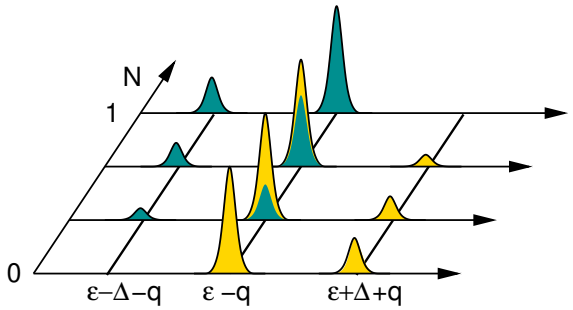


Fig. 9.2: Spectral function on the electron acceptor exhibiting satellites for different number of electrons (on the electron acceptor). In contrast to a mean-field spectrum, the energies do not shift with changing number of electrons, but the intensity of the satellites changes, while the excitation energies remain the same. The green shaded region denotes the occupied part of the spectral function, while the yellow shaded region denotes the unoccupied part.

Discussion

For the non-interacting system with $V = 0$, the spectral function has one spectral peak with energy $\epsilon = \bar{\epsilon}$. This feature is independent of the particle number on the electron acceptor level a.

When the interaction is taken into account, the main peak at $\bar{\epsilon}$ loses weight, and this weight is transferred to two satellites, which occur in the spectrum. One satellite is located Δ below the main peak and the other is located Δ above the main peak. If the acceptor level is empty, the satellite occurs above the main peak. As the electron number is increased, the weight is transferred continuously from the upper to the lower satellite. Editor: Note that the spectral function integrates to

one, as required. Derive the charge sum rule for interacting many-particle systems. So-far we derived it for non-interacting systems as intrinsic property of a matrix diagonalization

The satellites describe that an excitation can occur in parallel with the electron addition or removal. The one-electron excitation is coupled to the particle-number-conserving excitation by the interaction.

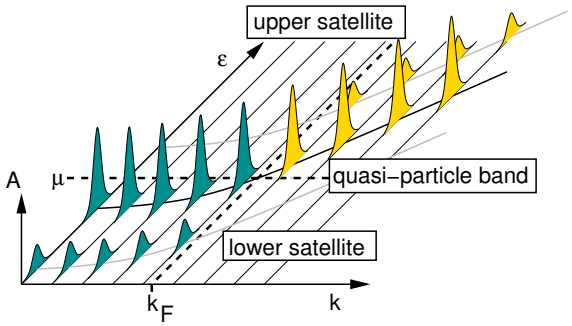


Fig. 9.3: Spectral function $A(\epsilon, k)$ of the free-electron gas with a single particle-conserving excitation with energy Δ and zero momentum producing satellite bands. The green shaded region denotes the occupied part of the spectral function, while the yellow shaded region denotes the unoccupied part.

The main peak at $\approx \bar{\epsilon}$ is the so-called **quasi-particle peak**. Its weight is the **quasi-particle weight** Z The quasi-particle weight is less than unity, because some of the weight is transferred to the satellites. The total weight on the orbital a is one.

In the mean-field approximation, the energy levels shift with increasing electron number, because the effective potential depends on the charge distribution. In the full calculation, the level positions are fixed, but the weights rearrange with the particle number.

The one-particle excitation is shifted from $\bar{\epsilon}$ in the non-interacting case to $\bar{\epsilon} - q$ in the presence of the interaction. The parameter q defined in Eq. 9.68 is the **quasi-particle shift**. The quasi-particle shift is due to **screening**. The Coulomb potential of the additional electron on the acceptor level induces a dipole on the bond. This dipole produces a favorable Coulomb potential stabilizing on the electron on the acceptor level. The formation of the induced electrostatic dipole is the origin of the **polarization** known from electrostatics.

The model is closely related to two famous approximations in many-particle physics, the random-phase approximation and, related, the GW method. In these methods the screening occurs through plasmons, which are cooperative charge oscillations the electron gas in a material. Satellites due to plasmon excitations have been calculated by Lundqvist[83**?** , 84] (see figure 2 of [84]). At that time one attributed the satellite peak to a quasi-particle called **plasmaron** made from and electron and a plasmon. The spectral function of the free-electron gas exhibiting the satellite structure has been calculated by Caruso and Giustino[53]. For the satellite structure in the spectral function of sodium, see [85].

9.4.2 Model for strongly retarded Green's function

Introduction

In an earlier exercise, section 4.6.2 on p. 182, we learned that a Lorentzian peak in the density of states, can be described by a Green's function having a pole in the complex plane. At that time we have still been studying one-particle systems.

The exercise at hand is related, but works the other way round. We show how a spectral function is obtained from the contour-ordered Green's function in real-valued time.

Problem

The non-interacting Green's function is changed upon a weak interaction by a shift of the poles of the Greens function into the complex plane. A minimal problem consists of only a single orbital with the Green's function having one orbital with a pole in the complex plane.

$$G(t_2,t_1) = \frac{1}{i\hbar}\left[(1-f_{T,\mu})\theta(t_2-t_1)\mathrm{e}^{-\frac{i}{\hbar}(\epsilon_0-i\Gamma)(t_2-t_1)} - f_{T,\mu}\theta(t_1-t_2)\mathrm{e}^{-\frac{i}{\hbar}(\epsilon_0+i\Gamma)(t_2-t_1)}\right] \quad (9.70)$$

1. Determine the spectral function $\mathcal{A}^{\mathrm{tot}}(\epsilon)$.
2. Determine the electron and hole Green's function separately.

Discussion

1. Determine the spectral function $\mathcal{A}^{\mathrm{tot}}(\epsilon)$.

The spectral function is obtained from Eq. **??**. Because Γ is finite, the pole is already displaced away from the real axis. Thus, we need not include the infinitesimal displacement $\eta \to 0$ of the energy away from the real axis

We begin with Eq. **??**. Because we consider only one orbital, we can treat the Green's function as a matrix element, which is a complex-valued number[5] rather than an operator. Therefore

$$\mathcal{A}(\epsilon) \overset{\text{Eq. ??}}{=} \frac{1}{1-2f_{T,\mu}(\epsilon)}\left(-\frac{1}{2\pi i}\left[G^{\mathcal{C}}(\epsilon) - G^{\mathcal{C},*}(\epsilon)\right]\right) = -\frac{1}{\pi}\frac{\mathrm{Im}[G^{\mathcal{C}}(\epsilon)]}{1-2f_{T,\mu}(\epsilon)} \quad (9.71)$$

We need to transform the Green's function into the energy representation, i.e. we need to Fourier transform it in the relative argument $t_2 - t_1$. In this case, the integration proceeds only along the real axis, not the contour $\mathcal{C}$.

$$\begin{aligned}
G^{\mathcal{C}}(\epsilon) &= \int_{-\infty}^{\infty} dt\; G^{\mathcal{C}}(t,0)\mathrm{e}^{\frac{i}{\hbar}\epsilon t} \\
&\overset{\text{Eq. 9.70}}{=} \frac{1-f}{i\hbar}\int_0^{\infty} dt\; \mathrm{e}^{\frac{i}{\hbar}(\epsilon-\epsilon_0+i\Gamma)t} - \frac{f}{i\hbar}\int_{-\infty}^{0} dt\; \mathrm{e}^{\frac{i}{\hbar}(\epsilon-\epsilon_0-i\Gamma)t} \\
&= \frac{1-f}{i\hbar}\left[\frac{\mathrm{e}^{\frac{i}{\hbar}(\epsilon-\epsilon_0+i\Gamma)t}}{\frac{i}{\hbar}(\epsilon-\epsilon_0+i\Gamma)}\right]_0^{\infty} - \frac{f}{i\hbar}\left[\frac{\mathrm{e}^{\frac{i}{\hbar}(\epsilon-\epsilon_0-i\Gamma)t}}{\frac{i}{\hbar}(\epsilon-\epsilon_0-i\Gamma)}\right]_{-\infty}^{0} \\
&= \frac{1-f}{i\hbar}\frac{-1}{\frac{i}{\hbar}(\epsilon-\epsilon_0+i\Gamma)} - \frac{f}{i\hbar}\frac{1}{\frac{i}{\hbar}(\epsilon-\epsilon_0-i\Gamma)} \\
&= \frac{(1-f)}{\epsilon-\epsilon_0+i\Gamma} + \frac{f}{\epsilon-\epsilon_0-i\Gamma} \\
&= \frac{(1-f)(\epsilon-\epsilon_0-i\Gamma)+f(\epsilon-\epsilon_0+i\Gamma)}{(\epsilon-\epsilon_0)^2+\Gamma^2} \\
&= \frac{\epsilon-\epsilon_0}{(\epsilon-\epsilon_0)^2+\Gamma^2} - i\frac{(1-2f)\Gamma}{(\epsilon-\epsilon_0)^2+\Gamma^2}
\end{aligned} \quad (9.72)$$

$$\mathcal{A}(\epsilon) = -\frac{1}{\pi}\frac{\mathrm{Im}[G^{\mathcal{C}}(\epsilon)]}{1-2f_{T,\mu}(\epsilon)} = -\frac{1}{\pi}\frac{-\Gamma}{(\epsilon-\epsilon_0)^2+\Gamma^2} = \frac{1}{\pi}\frac{\Gamma}{(\epsilon-\epsilon_0)^2+\Gamma^2} \quad (9.73)$$

[5] $z = \mathrm{Re}[z] + i\mathrm{Im}[z] \Rightarrow \mathrm{Im}[z] = \frac{z-z^*}{2i}$

Thus, we obtained a Lorentzian spectral function from this model Green's function, which is the desired result.

The model Green's function can be generalized to the form

$$G_{\alpha,\beta}(t_2,t_1) = \frac{1}{i\hbar}\sum_n \langle \pi_\alpha|\varphi_n\rangle \Big[(1-f_n)\theta(t_2-t_1)\mathrm{e}^{-\frac{i}{\hbar}(\epsilon_{0,n}-i\Gamma_n)(t_2-t_1)} - f_n\theta(t_1-t_2)\mathrm{e}^{-\frac{i}{\hbar}(\epsilon_{0,n}+i\Gamma_n)(t_2-t_1)}\Big]\langle\varphi_n|\pi_\beta\rangle \tag{9.74}$$

where the φ_n are a set of orthonormal one-particle functions. This model Green's function is defined by the parameters $\langle\pi_\alpha|\varphi_n\rangle, \epsilon_{0,n}, \Gamma_n$ and f_n.

The corresponding spectral function is

$$\mathcal{A}_{\alpha,\beta}(\epsilon) = \frac{1}{\pi}\sum_n \langle\pi_\alpha|\varphi_n\rangle \frac{\Gamma_n}{(\epsilon-\epsilon_{0,n})^2+\Gamma_n^2}\langle\varphi_n|\pi_\beta\rangle \tag{9.75}$$

The value of Γ indicates that this Green's function corresponds to a macroscopic system, which has a continuous spectrum. The delta-function peak of the spectral function in a non-interacting system is now smeared out into a Lorentzian peak. For a band structure, this implies that the bands are no more sharp but that they are a little smeared out, due to the life time of the quasi-particle described by $|\varphi_n\rangle$.

A strongly correlated system would differ in that the single peak would split into several distinct peaks or another a broad distribution. In that case the quasi-particles can no more considered as almost independent particles, albeit with a finite life time, but the correlations are a fundamental property of the system.

1. Determine the electron and hole Green's function separately.

$$\begin{aligned}\mathcal{A}^e_{T,\mu}(\epsilon) &= \mathcal{A}^{\mathrm{tot}}(\epsilon)(1-f_{T,\mu}(\epsilon)) = \frac{1}{\pi}\frac{\Gamma_n}{(\epsilon-\epsilon_{0,n})^2+\Gamma_n^2}\frac{1}{1+\mathrm{e}^{-\beta(\epsilon-\mu)}}\\ \mathcal{A}^h_{T,\mu}(\epsilon) &= \mathcal{A}^{\mathrm{tot}}(\epsilon)f_{T,\mu}(\epsilon) = \frac{1}{\pi}\frac{\Gamma_n}{(\epsilon-\epsilon_{0,n})^2+\Gamma_n^2}\frac{1}{1+\mathrm{e}^{+\beta(\epsilon-\mu)}}\end{aligned} \tag{9.76}$$

In contrast to the total spectral function, the electron and hole contributions depend on temperature and chemical ensemble.

9.4.3 One-particle spectrum of the Hubbard dimer

Exercise: Let us evaluate the spectral function for an interacting electron system, the Hubbard dimer. The Hubbard dimer, respectively the Hydrogen atom has been investigated previously in section 1.5.1 and 3.11.1.
The Hamiltonian of the Hubbard dimer is

$$\hat{H} = \sum_{j=1}^{2} \sum_{\sigma\in\{\uparrow,\downarrow\}} \bar{\epsilon}\hat{c}^\dagger_{j,\sigma}\hat{c}_{j,\sigma} - |t| \sum_{\sigma\in\{\uparrow,\downarrow\}} \left(\hat{c}^\dagger_{1,\sigma}\hat{c}_{2,\sigma} + \hat{c}^\dagger_{2,\sigma}\hat{c}_{1,\sigma}\right) + U\sum_{j=1}^{2} \sum_{\sigma,\sigma'\in\{\uparrow,\downarrow\}} \hat{c}^\dagger_{l,\sigma}\hat{c}^\dagger_{j,\sigma'}\hat{c}_{j,\sigma'}\hat{c}_{j,\sigma} \quad (9.77)$$

1. Rewrite the Hamiltonian in terms of occupation-number operators as much as possible to simplify the Hamiltonian. As we start with a basisset of Slater determinants, which are eigenstates of the occupation-number operator, this makes the calculation efficient.
2. Set up a complete basis of Slater determinants for the Hubbard dimer
3. Construct the joint eigenstates of $\hat{N}, \hat{S}_z, \hat{S}^2$ and $\hat{P}$, where $\hat{P}$ is the point-inversion about the bond center.
4. determine the eigenstates of the Hamiltonian and their energies
5. determine the peak positions of the spectral function
6. determine the quasi-particle wave functions
7. construct the spectral function as energy-dependent matrix
8. extract the projected density of states

Solution

The solution is given in the appendix D on p. 527. Section D.1 on p. 527 covers the general aspects, while section D.2 covers the specifically the Hubbard dimer.

Hamiltonian in terms of occupation-number operators The Hamiltonian of the Hubbard dimer is provided in Eq. D.15.

Complete basis of Slater determinants The Slater determinants that serve as basisset for our limited Fock space is given in table D.1

Eigenstates of $\hat{N}, \hat{S}_z, \hat{S}^2$ and $\hat{P}$, where $\hat{P}$ is the point-inversion about the bond center: The symmetry-adapted states of the Hubbard dimer are given in table D.4.

Eigenstates and their energies Except for one 2×2-block, all symmetry-adapted states are also eigenstates of the Hamiltonian. Their energy expectation values are are also their energy eigenvalues.

The 2×2-block can be diagonalized and yields the ground state Eq. D.22 with energy Eq. D.23.

peak positions of the spectral function The spectral function consists of delta functions centered at the energy differences of states, which differ by $\Delta N = \pm 1$.

$\bar{\epsilon} - \lvert t\rvert$	$\bar{\epsilon} + \lvert t\rvert$	(0/1),(1/2) lower Hubbard band
$\bar{\epsilon} + U - \lvert t\rvert$	$\bar{\epsilon} + U + \lvert t\rvert$	(1/2),(3/4) upper Hubbard band
$\bar{\epsilon} - \lvert t\rvert - \Delta_{st}$	$\bar{\epsilon} + \lvert t\rvert - \Delta_{st}$	(1/2)
$\bar{\epsilon} + U - \lvert t\rvert + \Delta_{st}$	$\bar{\epsilon} + U + \lvert t\rvert + \Delta_{st}$	(1/2)

quasi-particle wave functions

Spectral function

Projected density of states In Eq. 3.118, we obtained the ground state of the half-filled Hubbard dimer as

$$\begin{aligned} |\Psi_-\rangle &\overset{\text{Eq. } 3.118}{=} \\ &= \left[\frac{\cos\gamma_-}{\sqrt{2}}\left(\hat{c}^\dagger_{1\uparrow}\hat{c}^\dagger_{1\downarrow} + \hat{c}^\dagger_{2\uparrow}\hat{c}^\dagger_{2\downarrow}\right) + \frac{\sin(\gamma_-)}{\sqrt{2}}\left(\hat{c}^\dagger_{1\uparrow}\hat{c}^\dagger_{2\downarrow} - \hat{c}^\dagger_{1\downarrow}\hat{c}^\dagger_{2\uparrow}\right)\right]|\mathcal{O}\rangle \end{aligned} \tag{9.78}$$

with energy Eq. 3.119

$$\begin{aligned} E_- &\overset{\text{Eq. } 3.119}{=} 2\bar{\epsilon} + \frac{U+V}{2} - \sqrt{\left(\frac{U-V}{2}\right)^2 + 4|t|^2} \\ &= 2\bar{\epsilon} + U - 2|t|\tan(\gamma_-) \end{aligned} \tag{9.79}$$

γ_- changes from $\pi/8 = 45°$ for the non-interacting system to $\pi/4 = 90°$ in the strongly correlated limit.

Solution: At temperature much smaller than the singlet-triplet splitting, we only need to consider the singlet wave function.

We start from Eq. **??** for the spectral function

$$\mathcal{A}^{(tot)}_{\alpha,\beta}(\epsilon) \overset{\text{Eq. } ??}{=} -\frac{1}{\pi}\lim_{\zeta\to 0}\mathrm{Im}\left\{\int_{-\infty}^{\infty} dt\; G^{\mathcal{C}}_{\alpha,\beta}(t,0)\mathrm{sgn}(t)\mathrm{e}^{-\zeta|t|}\mathrm{e}^{\frac{i}{\hbar}\epsilon t}\right\} \tag{9.80}$$

At zero temperature and the appropriate chemical potential for half-filling, the probability for the state $|\Psi_-\rangle$ is one and the other probabilities vanish.

$$|\Psi\rangle \overset{\text{Eq. } 3.118}{=} \frac{1}{\sqrt{2}}\left(\hat{c}^\dagger_{1,\uparrow}\hat{c}^\dagger_{2,\downarrow} - \hat{c}^\dagger_{1,\downarrow}\hat{c}^\dagger_{2,\uparrow}\right)|\mathcal{O}\rangle \tag{9.81}$$

with energy

$$E \overset{\text{Eq. } 3.132}{=} 2\bar{\epsilon} + V + 2|t|\left(\frac{U-V}{4|t|} - \sqrt{1 + \left(\frac{U-V}{4|t|}\right)^2}\right) \tag{9.82}$$

The triplet states Eq. 3.122, 3.124, and 3.125 have the energy

$$E_d \overset{\text{Eq. } 3.133}{=} \left(2\bar{\epsilon} + V\right) \tag{9.83}$$

In order to obtain the spectral function with the Lehmann representation starting from the two-particle channel, we need to evaluate the many-particle states in the one-particle channel and the three-particle channel.

one-particle states: The one-particle states are obtained from section 1.5.1 by translating the bonding and antibonding orbitals into second quantization. We obtain four one-particle states

$$\begin{aligned}\Psi^{1p}_{b,\sigma} &= \frac{1}{\sqrt{2}}\left(\hat{c}^\dagger_{1,\sigma} + \hat{c}^\dagger_{1,\sigma}\right)|\mathcal{O}\rangle \\ \Psi^{1p}_{a,\sigma} &= \frac{1}{\sqrt{2}}\left(\hat{c}^\dagger_{1,\sigma} - \hat{c}^\dagger_{1,\sigma}\right)|\mathcal{O}\rangle\end{aligned} \tag{9.84}$$

with energies

$$\begin{aligned}E^{1p}_{b,\sigma} &= \bar{\epsilon} - 2|t| \\ E^{1p}_{a,\sigma} &= \bar{\epsilon} + 2|t|\end{aligned} \tag{9.85}$$

Obviously the interaction terms are not present in the case of a one-particle system.

three-particle states: The three-particle states can be obtained by exploiting **particle-hole symmetry**Editor: Demonstrate particle-hole symmetry.

I construct the four-particle state and then create a hole. The bonding state has the hole in the antibonding state, and vice versa.

$$\begin{aligned}\Psi^{3p}_{b,\sigma} &= \frac{1}{\sqrt{2}}\left(\hat{c}_{1,\sigma} - \hat{c}_{1,\sigma}\right) \prod_{R\in\{1,2\},\sigma'\in\{\uparrow,\downarrow\}} \hat{c}^\dagger_{R,\sigma'}|\mathcal{O}\rangle \\ \Psi^{3p}_{a,\sigma} &= \frac{1}{\sqrt{2}}\left(\hat{c}_{1,\sigma} - \hat{c}_{1,\sigma}\right)|\mathcal{O}\rangle \prod_{R\in\{1,2\},\sigma'\in\{\uparrow,\downarrow\}} \hat{c}^\dagger_{R,\sigma'}\end{aligned} \tag{9.86}$$

The energies are Editor: Caution! this is guessed!

$$E^{3p}_{b,\sigma} = 3\bar{\epsilon} + 3V + U - 2|t| \tag{9.87}$$

Spectral function for one site and spin:

$$\mathcal{A}_{\alpha,\beta}(\epsilon) = \tag{9.88}$$

9.4.4 Anderson impurity model

Editor: To be done

The **Anderson impurity model** [67] is a standard model for strongly correlated systems. It models on impurity having a strongly correlated orbital in contact with a bath of non-interacting conduction electrons. The conduction electrons are modeled by a one-dimensional chain of hydrogen atoms, which is characterized by a vanishing orbital energy and a nearest-neighbor hopping parameter. This chain is described with periodic boundary conditions. The impurity is coupled to one of the atoms in the chain with a hopping parameter V. The spatial Coulomb integral on the impurity defines the U-parameter.

1. Set up the many-particle Hamiltonian for the isolated impurity and bring it into the form that it can be expressed by the occupation-number operators. Once the Hamiltonian is obtained in second quantization, express the many-particle Hamiltonian as matrix.

2. Evaluate the finite-temperature Green's function of the isolated impurity in contact with a particle reservoir.

3. Evaluate the Green's function of the conduction electrons at finite temperature in contact with a particle reservoir.

4. determine the Green's function of the Anderson impurity in contact with the conduction electrons.

5. plot the spectral function using the equation for the density of states, which has been derived for non-interacting electrons for different temperatures and chemical potentials.

6. calculate the particle number on the impurity as function of temperature and chemical potential.

7. Discuss the results in the light of the characteristic energy scales of the problem $k_B T$, the band width of the bath t, the position of the empty impurity orbital ϵ_A, the coupling between impurity and bath V, and the Coulomb interaction U. Discuss the isolated limit, the strongly correlated limit, the high-temperature limit.

8. Read the original paper of Anderson[67]

9.4.5 Spectral function and momentum density of a 1d chain

Editor: This exercise is not finished yet!

Introduction

One of the puzzling findings in the early days of studying the interacting free-electron gas was that the momentum density does not resemble a step function as in the non-interacting free-electron gas.[84] Rather, one finds tails that emerge from the step function, which are interpreted as electron-hole pairs that screen the interaction.

The **momentum density** $\rho(\vec{p})$ of electrons is (See for example [86])

$$\rho(\vec{p}) \stackrel{\text{def}}{=} \sum_n f_n |\langle p|\varphi_n\rangle|^2 = \langle \vec{p}|\hat{\rho}^{(1)}|\vec{p}\rangle \tag{9.89}$$

where $|\varphi_n\rangle$ are the natural orbitals and f_n are their occupations. $|\vec{p}\rangle$ are the momentum eigenstates. $\hat{\rho}^{(1)}$ is the one-particle-reduced density matrix. The momentum density is thus related to the Fourier transform of the natural orbitals.

The momentum distribution is easily mistaken by the Fermi distribution. This misunderstanding is resolved by carefully distinguishing the expectation values of the momentum $\langle \varphi_{n,\vec{k}}|\hat{p}|\varphi_{n,\vec{k}}\rangle$ from the crystal momentum $\hbar\vec{k}$.

Secondly, at the origin of the Fermi distribution are non-interacting electrons. However, it also occurs rigorously in the division of the spectral function of an interacting system into the occupied and the empty contribution. At first, this seems to contradict the result for the momentum distribution.

$$f_{T,\mu}(\epsilon_n(\vec{k})) \neq \sum_n \int d\epsilon \; f_{T,\mu}(\epsilon_n(\vec{k}))\langle \vec{p}|\hat{\mathcal{A}}(\epsilon)|\vec{p}\rangle \tag{9.90}$$

In this exercise, an analogous effect will be investigated, but instead of the interaction we use a lattice potential.

For the spectral function and the momentum distribution in the RPA, see Lundqvist[84] Editor: Lundqvists work contains the explicit expressions, which shall be used to construct the relevant graphs. For a measurement of the momentum density in Al see Metz et al.[86].

Editor: Add a remark regarding Compton profiles.

Problem

Consider a one-dimensional, one-band Hubbard model with non-interacting, spin-less electrons.

1 Calculate the one-particle eigenstates $|\varphi_n(k)\rangle$ and energies $\epsilon(k)$ for a one-dimensional linear chain.

2 Calculate momentum density of the one-dimensional linear chain. Assume that the spatial Fourier transform of one of the local orbitals of the Hubbard chain is known.

3 Introduce a cos-like potential, which doubles the lattice constant. Calculate the new eigenstates and energies.

4 Calculate the momentum density of the perturbed system

Discussion

1 Calculate the one-particle eigenstates $|\varphi_n(k)\rangle$ and energies $\epsilon(k)$ for a one-dimensional linear chain.

The wave functions of the linear chain are

$$|\varphi_k^{(0)}\rangle = \sum_{j=1}^{N} |\chi_j\rangle \frac{1}{\sqrt{N}} e^{ika_{\text{lat}}j} \tag{9.91}$$

$$\epsilon^{(0)}(k) = \bar{\epsilon} - 2t\cos(ka_{\text{lat}}) \tag{9.92}$$

The variable N is the supercell for the periodic boundary conditions, which determines the normalization and the quantization of the wave vectors.

The quantization condition for the k-points is $k_n a_{\text{lat}} N = 2\pi n$, that is

$$k_n = \frac{2\pi}{N a_{\text{lat}}} n \quad \text{with } -\frac{N}{2} < n \leq \frac{N}{2} \text{ and } n \in \mathbb{I} \tag{9.93}$$

The orbitals $|\chi_j\rangle$ are related to each other by a translation

$$|\chi_j\rangle = \underbrace{\int d^3r' \, |\vec{r'} + \vec{R}_j\rangle\langle\vec{r'}| \, |\chi_0\rangle}_{\text{translation by } \vec{R}_j} \quad \Leftrightarrow \quad \langle\vec{r}|\chi_j\rangle = \langle\vec{r} - \vec{R}_j|\chi_0\rangle \tag{9.94}$$

2 Calculate momentum density of the one-dimensional linear chain. Assume that the spatial Fourier transform of one of the local orbitals of the Hubbard chain is known.

Editor: The formulation of the integration region is probably not concise. Editor: I am using vectors $\vec{k}, \vec{p}$ and switch to scalars. This needs more attention.

The momentum eigenstates are normalized to be unity within the supercell with N beads, which also restricts our set of k-points.

$$\langle x|\vec{p}\rangle = \frac{1}{\sqrt{N a_{\text{lat}}}} e^{\frac{i}{\hbar}px} \tag{9.95}$$

We can proceed now in two different directions:

- either we impose the same periodic boundary conditions also on the momentum eigenstates.
- or we consider the momentum as continuous and perform the matrix elements by integration over infinite space, albeit using wave functions of the chain which is strictly periodic with the supercell.

We will make the first choice.

Nevertheless, let me sketch the approach for the second one. The reader may skip this detour without harm.
Consider the overlap matrix element of an arbitrary momentum eigenstate with wave function $\psi(x)$, which is strictly periodic with the supercell of size $L = Na_{\text{lat}}$, i.e. $\langle x|\psi\rangle = \langle x-L|\psi\rangle$. The momentum eigenstate has the form $\langle x|p\rangle = \frac{1}{\sqrt{L}} e^{\frac{i}{\hbar}px}$.

$$\langle p|\psi\rangle = \int_{-\infty}^{\infty} dx\ \langle p|x\rangle\langle x|\psi\rangle = \sum_{j=-\infty}^{\infty} \int_{(j-1)L}^{jL} dx\ \langle p|x\rangle\langle x|\psi\rangle = \sum_{j=-\infty}^{\infty} \int_{0}^{L} dx\ \underbrace{\langle p|x+jL\rangle}_{=\langle p|x\rangle e^{+\frac{i}{\hbar}pLj}} \underbrace{\langle x+jL|\psi\rangle}_{=\langle x|\psi\rangle}$$

$$= \int_{0}^{L} dx\ \langle p|x\rangle\langle x|\psi\rangle \sum_{j=-\infty}^{\infty} \left(e^{-\frac{i}{\hbar}pL}\right)^{j} \tag{9.96}$$

Let me now study only the geometric sum:

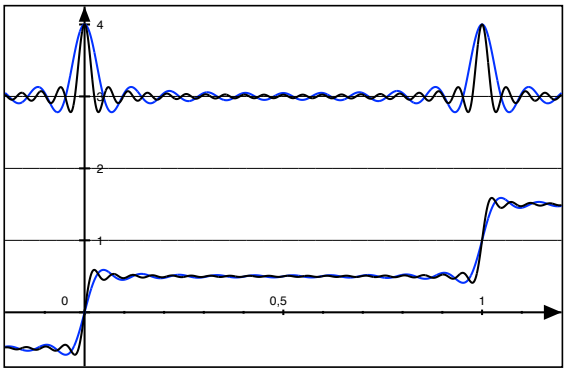
$$\sum_{j=-M}^{M} \left(e^{-\frac{i}{\hbar}pL}\right)^{j} = \frac{e^{+\frac{i}{\hbar}pL(M+\frac{1}{2})} - e^{-\frac{i}{\hbar}pL(M+\frac{1}{2})}}{e^{+\frac{i}{\hbar}pL\frac{1}{2}} - e^{-\frac{i}{\hbar}pL\frac{1}{2}}} = \frac{\sin(\frac{1}{\hbar}pL(M+\frac{1}{2})}{\sin(\frac{1}{2}\frac{1}{\hbar}pL)} \overset{M\to\infty}{=} \delta\Big(\frac{pL}{2\pi\hbar} - j\Big) \tag{9.97}$$

The last step towards the delta function is demonstrated by the graph below, which shows that the integral approaches a sequence of step functions, so the function, the derivative of the integral, approaches a sequence of delta functions.
In the graph below, I show the functions

$$\lim_{N\to\infty} \int_0^x dx' \frac{\sin\big((2N+1)\pi x'\big)}{\sin\big(\pi x'\big)} = C + \sum_{j=-\infty}^{\infty} \theta(x-j)$$

$$\lim_{N\to\infty} \frac{\sin\big((2N+1)\pi x\big)}{\sin\big(\pi x\big)} = \sum_{j=-\infty}^{\infty} \delta(x-j) \tag{9.98}$$

for $N = 10$ (blue) and $N = 20$ (black)where the second is scaled with $\frac{1}{2N+1}$ and shifted up by $+3$. C is an irrelevant constant that ensures that the function passed through the origin.



$$\int_{-\infty}^{\infty} dx\ \langle p|x\rangle\langle x|\psi\rangle = \int_{0}^{L} dx\ \langle p|x\rangle\langle x|\psi\rangle \sum_j \delta\Big(\frac{pL}{2\pi\hbar} - j\Big) \tag{9.99}$$

so that

$$\int \frac{dp}{2\pi\hbar L} \langle p|\psi\rangle = \sum_j \langle p_j|\psi\rangle \qquad \text{with } p_j = \frac{2\pi\hbar}{L}\cdot j \text{ and } L = Na_{\text{lat}} \tag{9.100}$$

$$\begin{aligned}
\langle \vec{p}|\varphi^{(0)}_{\vec{k}}\rangle &= \int_{0\le x<Na_{\text{lat}}} d^3r\ \mathrm{e}^{-\frac{i}{\hbar}\vec{p}\vec{r}}\langle\vec{r}|\varphi^{(0)}_k\rangle \quad \text{with } \vec{p}\in\left\{\frac{2\pi\hbar}{Na_{\text{lat}}}j; j\in\mathbb{I}\right\} \\
&\overset{\text{Eq. 9.91}}{=} \sum_{j=0}^{N-1}\int d^3r\ \mathrm{e}^{-\frac{i}{\hbar}\vec{p}\vec{r}}\langle\vec{r}|\chi_j\rangle\frac{1}{\sqrt{N}}\mathrm{e}^{ika_{\text{lat}}j} \\
&\overset{\text{Eq. 9.94}}{=} \sum_{j=0}^{N-1}\frac{1}{\sqrt{N}}\mathrm{e}^{ika_{\text{lat}}j}\ \mathrm{e}^{-\frac{i}{\hbar}\vec{p}\vec{R}_j}\underbrace{\int d^3r\ \mathrm{e}^{-\frac{i}{\hbar}\vec{p}(\vec{r}-\vec{R}_j)}\langle\vec{r}-\vec{R}_j|\chi_0\rangle}_{\langle\vec{p}|\chi_0\rangle} \\
&\overset{\vec{R}_j=\vec{e}_x a_{\text{lat}}j}{=} \langle\vec{p}|\chi_0\rangle\frac{1}{\sqrt{N}}\underbrace{\sum_{j=0}^{N-1}\mathrm{e}^{i(k-\frac{1}{\hbar}p)a_{\text{lat}}j}}_{=N\delta_{\hbar k,p}} = \langle\vec{p}|\chi_0\rangle\sqrt{N}\delta_{\hbar k,p}
\end{aligned} \tag{9.101}$$

I used that a the discrete average of a plane wave over an equi-spaced grid for a full period vanishes, except when it is a constant.[6] That is

$$\begin{aligned}
\rho(p) &= \sum_k f_{T,\mu}(\epsilon_k)\left|\langle\vec{p}|\varphi^{(0)}_k\rangle\right|^2 \\
&= |\langle\vec{p}|\chi_0\rangle|^2\sum_k f_{T,\mu}(\epsilon_k)N\delta_{p,\hbar k} \\
&= N\,|\langle\vec{p}|\chi_0\rangle|^2\, f_{T,\mu}\Big(\epsilon\left(\frac{1}{\hbar}p\right)\Big)
\end{aligned} \tag{9.102}$$

I selected the momenta on the discrete grid of k-points $p=\frac{2\pi}{Na_{a_{\text{lat}}}}j$ with $j\in\mathbb{I}$.

We notice that the momentum density reproduces the Fermi distribution function, with an additional modulation from the shape of the local orbitals. This result holds for zero and for finite temperatures.

3 Introduce a cos-like potential, which doubles the lattice constant. Calculate the new eigenstates and energies.

- The potential, which doubles the unit cell is

$$\hat{V} = \sum_j |\pi_j\rangle\bar{V}\cos\Big(\underbrace{\frac{\pi}{a_{\text{lat}}}}_{q}\cdot\underbrace{a_{\text{lat}}j}_{R_j}\Big)\langle\pi_j| = \sum_j |\pi_j\rangle\bar{V}(-1)^j\langle\pi_j| \tag{9.103}$$

- For each k-point, the new wave functions are superpositions of the ones from k and $k+q$, where $q=\pi/a_{\text{lat}}$. The Brillouin zone of the perturbed system is half as large as that of the unperturbed one. The k-points for the perturbed system are from the interval

$$k_n \in]-\frac{\pi}{2a_{\text{lat}}},\frac{\pi}{2a_{\text{lat}}}] \tag{9.104}$$

$$|\varphi^V_k\rangle = |\varphi^0_k\rangle c_{1,k} + |\varphi^0_{k+q}\rangle c_{2,k} \tag{9.105}$$

[6] This can be worked out by considering the sum as finite geometric series.

- The Hamiltonian for the perturbed Hamiltonian is

$$\begin{aligned}\hat{H} &= \sum_k \begin{pmatrix} |\varphi_k^{(0)}\rangle \\ |\varphi_{k+q}^{(0)}\rangle \end{pmatrix} \begin{pmatrix} \epsilon^{(0)}(k) & \bar{V} \\ \bar{V} & \epsilon^{(0)}(k+\frac{\pi}{a}) \end{pmatrix} \begin{pmatrix} \langle\varphi_k^{(0)}| \\ \langle\varphi_{k+q}^{(0)}| \end{pmatrix} \\ &= \sum_k \begin{pmatrix} |\varphi_k^{(0)}\rangle \\ |\varphi_{k+q}^{(0)}\rangle \end{pmatrix} \begin{pmatrix} \bar{\epsilon} - 2t\cos(ka) & \bar{V} \\ \bar{V} & \bar{\epsilon} + 2t\cos(ka) \end{pmatrix} \begin{pmatrix} \langle\varphi_k^{(0)}| \\ \langle\varphi_{k+q}^{(0)}| \end{pmatrix} \end{aligned} \tag{9.106}$$

- The eigenvalues are

$$\begin{aligned}\Big(\bar{\epsilon} - 2t\cos(ka) - \epsilon\Big)\Big(\bar{\epsilon} + 2t\cos(ka) - \epsilon\Big) - \bar{V}^2 &= 0 \\ \epsilon_\pm^V(k) = \bar{\epsilon} \pm \sqrt{V^2 + 4t^2\cos^2(ka)}&\end{aligned} \tag{9.107}$$

- The eigenvectors obey $\vec{c}_\pm(k) = (\cos(\gamma_\pm(k), \sin(\gamma_\pm(k)))$ are

$$\begin{aligned}\Big(-2t\cos(ka) \mp \sqrt{V^2 + 4t^2\cos^2(ka)}\Big)\cos(\gamma_\pm(k)) + V\sin(\gamma_\pm(k)) &= 0 \\ \gamma_\pm(k) = \operatorname{atan}\left(\frac{1}{V}\Big(2t\cos(ka) \pm \sqrt{V^2 + 4t^2\cos^2(ka)}\Big)\right)&\end{aligned} \tag{9.108}$$

  The wave functions are

$$|\varphi_\pm^V(k)\rangle = |\varphi_k^{(0)}\rangle\cos(\gamma_\pm(k)) + |\varphi_{k+q}^{(0)}\rangle\sin_\pm(k) \tag{9.109}$$

  The momentum matrix element is

$$\begin{aligned}\langle p|\varphi_{\pm,k}^V\rangle &= \langle p|\varphi_k^{(0)}\rangle\cos(\gamma_\pm(k)) + \langle p|\varphi_{k+q}^{(0)}\rangle\sin_\pm(k) \\ &= \langle\vec{p}|\chi_0\rangle\sqrt{N}\delta_{\hbar k,p}\cos(\gamma_\pm(k)) + \langle\vec{p}|\chi_0\rangle\sqrt{N}\delta_{\hbar k,p+\hbar q}\sin(\gamma_\pm(k)) \\ &= \langle\vec{p}|\chi_0\rangle\sqrt{N}\Big(\delta_{\hbar k,p}\cos(\gamma_\pm(k)) + \delta_{\hbar k,p+\hbar q}\sin(\gamma_\pm(k))\Big)\end{aligned} \tag{9.110}$$

  In the half-filled case, the states are filled for Bloch vectors $-\pi/(2a) < k < \pi/(2a)$ in the extended zone scheme. Each filled state contributes, two plane waves. A large contribution $\cos^2(\gamma_-(k))$ to the momentum density has a smaller momentum $|p| < \hbar\pi/(2a)$ while the second plane wave contributes with $\sin^2(\gamma_-(k))$ at a momentum $\hbar\pi/(2a) < |p|\hbar\pi/a$.

Editor: This is probably still incorrect!!!

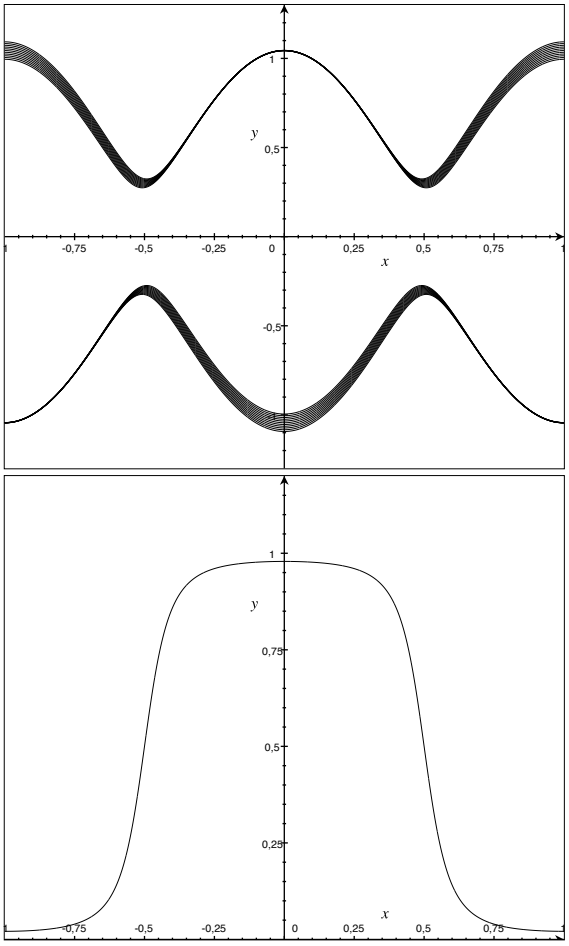
4 Calculate the momentum density of the perturbed system

For zero temperature and a half-filled band, we obtain the momentum density

$$\begin{aligned}\rho(\vec{p}) &= \sum_{n\in\{+,-\}}\sum_{k\in\left]-\frac{\pi}{2a_{\text{lat}}},\frac{\pi}{2a_{\text{lat}}}\right]} f_{T,\mu}(\epsilon_{\pm,k})\Big|\langle\vec{p}|\varphi_{n,k}^{(V)}\rangle\Big|^2 \\ &\overset{T=0,\mu=\bar{\epsilon}}{=} \sum_{k\in\left]-\frac{\pi}{2a_{\text{lat}}},\frac{\pi}{2a_{\text{lat}}}\right]} \Big|\langle\vec{p}|\varphi_{-,k}^{(V)}\rangle\Big|^2 \\ &= \sum_{k\in\left]-\frac{\pi}{2a_{\text{lat}}},\frac{\pi}{2a_{\text{lat}}}\right]} \Big|\langle\vec{p}|\chi_0\rangle\Big|^2 N\Big(\delta_{\hbar k,p}\cos(\gamma_-(k)) + \delta_{\hbar k,p+\hbar q}\sin(\gamma_-(k))\Big)^2 \\ &= \sum_{k\in\left]-\frac{\pi}{2a_{\text{lat}}},\frac{\pi}{2a_{\text{lat}}}\right]} \Big|\langle\vec{p}|\chi_0\rangle\Big|^2 N\Big(\delta_{\hbar k,p}\cos^2(\gamma_-(k)) + \delta_{\hbar(k-q),p}\sin^2(\gamma_-(k))\Big)\end{aligned} \tag{9.111}$$

Grapher-image: Draw fat bands with $100\Delta \in \{-5,-1,\ldots,5\}$, $V = 0.3$, $t = 1$ as function of $x = ka/\pi$.

$$y(x) = \begin{cases} -\sqrt{V^2 + t^2\cos^2(x\pi)} + \Delta\cos^2(\gamma_-(x\pi)) \\ +\sqrt{V^2 + t^2\cos^2(x\pi)} + \Delta\sin^2(\gamma_-(x\pi)) \end{cases}$$
$$\gamma_-(ka) = \operatorname{atan}\left(\frac{1}{V}\left(t\cos(ka) - \sqrt{V^2 + t^2\cos^2(ka)}\right)\right) \tag{9.112}$$



In the case of an external potential discussed here, we obtain a momentum distribution, which does not stop abruptly at the Fermi momentum as anticipated for a free-electron gas or the unperturbed linear chain. We can discuss this effect, in analogy with the RPA, as the formation of electron-hole pairs by the external potential. The electron-hole pairs mentioned here are those of the unperturbed system. Here, the electron-hole pairs are not created by the Coulomb interaction between the electrons but by an external potential. The momentum density has a smooth transition despite the presence of a band gap.

Editor: Idea: Plot the band structure in the extended zone scheme using

$$\pm = s(k) = \begin{cases} -1 & \text{for } |k| < \pi/(2a) \\ +1 & \text{for } \pi/(2a) < |ka| < \pi/a \end{cases} \tag{9.113}$$

Chapter 10

Diagrammatic expansion of the Green's function

So far, we defined the Green's function and we have shown what it is good for. Here, we explore one of the most common ways to evaluate the Green's functions, namely the perturbation expansion in orders of the interaction. This expansion rests on Wick's theorem. This expansion is often called **many-body perturbation theory (MBPT)** .

Several ways for this diagrammatic expansions are around. (1) Feynman's zero-temperature formalism for time-dependent phenomena, (2) Matsubara's finite-temperature formalism for equilibrium properties[87], (3) Keldysh's non-equilibrium formalism. As shown by Wagner in 1991[72], all these approaches can be merged in the (4) non-equilibrium formalism using contour integrations. The paper of Wagner is very recommendable and can be used alongside these lecture notes.

10.1 Interacting Green's function expressed by non-interacting ground states

Let me state the problem discussed in this chapter: the goal is to determine the Green's function

$$G^{\mathcal{C}}(x,t,x',t') \overset{\text{Eq. 7.16}}{=} \frac{1}{i\hbar}\mathrm{Tr}\Big\{\hat{\rho}^{(W)}_{T,\mu}\mathcal{T}_{\mathcal{C}}\left(\hat{\psi}_H(\vec{x},t)\hat{\psi}^{+}_H(\vec{x'},t')\right)\Big\}\,, \tag{10.1}$$

where the von-Neumann density matrix $\hat{\rho}^{(W)}_{T,\mu}$ of the grand canonical ensemble with $\hat{H}^{(W)} = \hat{h} + \hat{W}$ is

$$\hat{\rho}^{(W)}_{T,\mu} \overset{\text{Eq. 2.57}}{=} \frac{1}{Z_{T,\mu}} \mathrm{e}^{-\beta(\hat{H}^{(W)}-\mu\hat{N})} \tag{10.2}$$

and the partition function is

$$Z_{T,\mu} \overset{\text{Eq. 2.58}}{=} \mathrm{Tr}\Big\{\mathrm{e}^{-\beta(\hat{H}^{(W)}-\mu\hat{N})}\Big\}\,. \tag{10.3}$$

10.1.1 From Heisenberg to interaction picture:

Due to the presence of the Heisenberg operators in Eq. 10.1 and because of the statistical operator, we need to deal with exponentials of the interacting Hamiltonian $\hat{H}^{(W)}$. For this problem, it is convenient to switch from the Heisenberg picture to the interaction picture.

The interaction picture, which will be introduced below, limits the time-evolution of operators to the non-interacting Hamiltonian $\hat{h}$. The interaction $\hat{W}$ is moved into the propagator for the states.

The diagrammatic expansion of this propagator will then express it in terms of non-interacting Green's functions and the interaction matrix elements.

INTERACTION PICTURE

With the operators $\hat{A}_I$ and the states $|\psi_I\rangle$ in the interaction picture

$$\hat{A}_I(t) = \hat{\mathcal{U}}_S^{(0)}(0,t)\hat{A}_S(t)\ \underbrace{\hat{\mathcal{U}}_S^{(0)}(t,0)}_{\mathcal{T}_\mathcal{C}\mathrm{e}^{-\frac{i}{\hbar}\int_0^t dt'\ \hat{h}(t')}} \tag{10.4}$$

$$|\Psi_I(t)\rangle = \hat{\mathcal{U}}_S^{(0)}(0,t)|\Psi_S(t)\rangle \tag{10.5}$$

the equations of motion are

$$\begin{aligned} i\hbar\partial_t\hat{A}_I(t) &= \Big[\hat{A}_I(t),\hat{h}_I(t)\Big]_- + i\hbar\Big(\partial_t\hat{A}_S\Big)_I \\ i\hbar\partial_t|\Psi_I(t)\rangle &= \hat{W}_I(t)|\Psi_I(t)\rangle \end{aligned} \tag{10.6}$$

$\hat{\mathcal{U}}_S^{(0)}(t',t)$ propagates the wave function under the action of the non-interacting Hamiltonian $\hat{h}(t)$, i.e. $|\Psi_S(t')\rangle = \hat{\mathcal{U}}_S^{(0)}(t',t)|\Psi_S(t)\rangle$, when $i\hbar\partial_t|\Psi_S(t)\rangle = \hat{h}(t)|\Psi_S(t)\rangle$.

The Heisenberg picture has been introduced earlier in Eq. 6.40 on p. 246. It is shown here for comparison

HEISENBERG PICTURE

With the operators $\hat{A}_H$ and the states $|\psi_H\rangle$ in the interaction picture

$$\hat{A}_H(t) = \hat{\mathcal{U}}_S^{(W)}(0,t)\hat{A}_S(t)\quad \underbrace{\hat{\mathcal{U}}_S^{(W)}(t,0)}_{\mathcal{T}_\mathcal{C}\mathrm{e}^{-\frac{i}{\hbar}\int_0^t dt'\ \left(\hat{h}(t')+\hat{W}(t')\right)}} \tag{10.7}$$

$$|\Psi_H(t)\rangle = |\Psi_S(0)\rangle \tag{10.8}$$

the equations of motion are

$$\begin{aligned} i\hbar\partial_t\hat{A}_H(t) &= \Big[\hat{A}_H(t),\hat{H}_S(t)\Big]_- + i\hbar\Big(\partial_t\hat{A}_S\Big)_H \\ i\hbar\partial_t|\Psi_H(t)\rangle &= 0 \end{aligned} \tag{10.9}$$

$\hat{\mathcal{U}}_S^{(W)}(t',t)$ propagates the wave function under the action of the interacting Hamiltonian $\hat{H}(t) = \hat{h}(t) + \hat{W}(t)$, i.e. $|\Psi_S(t')\rangle = \hat{\mathcal{U}}_S^{(W)}(t',t)|\Psi_S(t)\rangle$, when $i\hbar\partial_t|\Psi_S(t)\rangle = \hat{H}(t)|\Psi_S(t)\rangle$.

Let me translate a general Heisenberg operator $\hat{A}_H(t)$ into the interaction picture, where $\hat{A}_S(t)$ is the corresponding operator in the Schrödinger picture and $\hat{A}_I(t)$ is the **operator in the interaction picture**.

$$\begin{aligned} \hat{A}_H(t) &= \hat{\mathcal{U}}_S^{(W)}(0,t)\hat{A}_S(t)\hat{\mathcal{U}}_S^{(W)}(t,0) \\ &= \overbrace{\hat{\mathcal{U}}_S^{(0)}(0,0)}^{\hat{1}}\ \underbrace{\hat{\mathcal{U}}_S^{(W)}(0,t)\hat{\mathcal{U}}_S^{(0)}(t,0)}_{\hat{\mathcal{U}}_I^{(W)}(0,t)}\ \underbrace{\hat{\mathcal{U}}_S^{(0)}(0,t)\hat{A}_S(t)\hat{\mathcal{U}}_S^{(0)}(t,0)}_{\hat{A}_I(t)}\ \underbrace{\hat{\mathcal{U}}_S^{(0)}(0,t)\hat{\mathcal{U}}_S^{(W)}(t,0)}_{\hat{\mathcal{U}}_I^{(W)}(t,0)}\ \overbrace{\hat{\mathcal{U}}_S^{(0)}(0,0)}^{\hat{1}} \\ &= \hat{\mathcal{U}}_I^{(W)}(0,t)\hat{A}_I(t)\hat{\mathcal{U}}_I^{(W)}(t,0) \end{aligned} \tag{10.10}$$

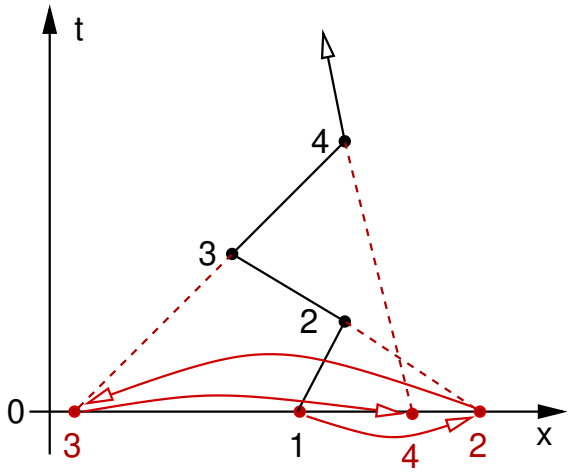


Fig. 10.1: Cartoon as memory hook for the interaction picture. A particle (here classical) propagates while repeatedly scattering at scattering centers, which may be due to the interaction with other particles. Each scattering event can be replaced by a change of the initial state by propagating the scattered trajectory backward in time without scattering. Thus, at each time, the state is replaced by the initial condition, which produces the same state without scattering.

We have introduced the **propagator in the interaction picture** as

$$\hat{\mathcal{U}}_I^{(W)}(t,t') \stackrel{\text{def}}{=} \hat{\mathcal{U}}_S^{(0)}(0,t)\hat{\mathcal{U}}_S^{(W)}(t,t')\hat{\mathcal{U}}_S^{(0)}(t',0) \tag{10.11}$$

10.1.2 S-matrix

Let me now rewrite the Green's function in terms of operators in the interaction picture.

$$\begin{aligned} G^{\mathcal{C}}(\vec{x},t,\vec{x'},t') &\stackrel{\text{Eq. 10.1}}{=} \frac{1}{i\hbar}\mathrm{Tr}\left\{\hat{\rho}_{T,\mu}^{(W)}\mathcal{T}_{\mathcal{C}}\left(\hat{\psi}_H(\vec{x},t)\hat{\psi}_H^+(\vec{x'},t')\right)\right\} \\ &\stackrel{\text{Eq. 10.10}}{=} \frac{1}{i\hbar}\mathrm{Tr}\left\{\hat{\rho}_{T,\mu}^{(W)}\mathcal{T}_{\mathcal{C}}\hat{\mathcal{U}}_I^{(W)}(0,t)\hat{\psi}_I(\vec{x},t)\underbrace{\hat{\mathcal{U}}_I^{(W)}(t,t')}_{\hat{\mathcal{U}}_I^{(W)}(t,0)\hat{\mathcal{U}}_I^{(W)}(0,t')}\hat{\psi}_I^+(\vec{x'},t')\hat{\mathcal{U}}_I^{(W)}(t',0)\right\} \\ &= \frac{1}{i\hbar}\mathrm{Tr}\left\{\hat{\rho}_{T,\mu}^{(W)}\mathcal{T}_{\mathcal{C}}\overbrace{\hat{\mathcal{S}}_{I,\mathcal{C}}}^{\mathcal{U}_I^{(\hat{W})}(0,t)\mathcal{U}_I^{(\hat{W})}(t,t')\mathcal{U}_I^{(\hat{W})}(t',0)}\hat{\psi}_I(\vec{x},t)\hat{\psi}_I^+(\vec{x'},t')\right\} \end{aligned} \tag{10.12}$$

In the last step, I combined the propagators in a single operator, the S-matrix $\hat{\mathcal{S}}_{I,\mathcal{C}}$, which I will define below in more detail. The S-matrix[1] is the propagator in the interaction picture along the chosen contour $\mathcal{C}$. As a result of the particle-number conservation, the Hamiltonian contains only terms with an even number of fermionic operators. Therefore, sign-changes due to the interchanges of two Hamilton operators need not be considered.

S-matrix: The propagator in the interaction picture along the entire contour is the S-matrix $\hat{\mathcal{S}}_{I,\mathcal{C}}$. For a general time contour $\mathcal{C}$, the **S-matrix** is

$$\hat{\mathcal{S}}_{I,\mathcal{C}} \stackrel{\text{def}}{=} \lim_{N\to\infty}\prod_{j=1}^{N}\hat{\mathcal{U}}_I^{(W)}(t_j,t_{j-1}) \qquad \text{with } t_j = \tau\left(s_i + \frac{s_f - s_i}{N}\cdot j\right) \tag{10.13}$$

[1] My notation differs somewhat from the common definitions. The S matrix is often used as propagator with explicit time arguments.

where s_i and s_f mark the initial and final values of the time contour and where $\tau(s)$ defines the time contour.

The S-matrix can alternatively be expressed as time-ordered exponential

$$\mathcal{S}_{I,\mathcal{C}} \stackrel{\text{def}}{=} \mathcal{T}_{\mathcal{C}} \exp\left(-\frac{i}{\hbar}\int_{\mathcal{C}} dt\, \hat{W}_I(t)\right) \tag{10.14}$$

where the time integral proceeds along the time contour. This expression is analogous to Eq. 4.43 on p. 176.

With the help of the time-ordering operator, the exponential can be expanded as power-series expansion in the interaction

$$\begin{aligned}
\mathcal{S}_{I,\mathcal{C}} &\stackrel{\text{Eq. 10.14}}{=} \mathcal{T}_{\mathcal{C}} \exp\left(-\frac{i}{\hbar}\int_{\mathcal{C}} dt\, \hat{W}_I(t)\right) \\
&= \mathcal{T}_{\mathcal{C}} \sum_{n=0}^{\infty} \frac{1}{n!}\left(-\frac{i}{\hbar}\int_{\mathcal{C}} dt\, \hat{W}_I(t)\right)^n \\
&= \sum_{n=0}^{\infty} \frac{1}{n!}\left(\frac{1}{i\hbar}\right)^n \int_{\mathcal{C}} dt_1 \cdots \int_{\mathcal{C}} dt_n\, \mathcal{T}_{\mathcal{C}} \hat{W}_I(t_1)\cdots\hat{W}_I(t_n)
\end{aligned} \tag{10.15}$$

The S-matrix should be considered as a sum of products of many creation and annihilation operators, each having its own time argument. This is required so that the time-ordering operator can place every operator into the correct position along the contour. It is a bit misleading that these time arguments are implicit and do not show up in the expression of the S-matrix.

The S-matrix for the specific time contour $\mathcal{C}$ is

$$\hat{\mathcal{S}}_{I,\mathcal{C}} = \hat{\mathcal{U}}_I^{(W)}(0,\infty)\hat{\mathcal{U}}_I^{(W)}(\infty,-\infty)\hat{\mathcal{U}}_I^{(W)}(-\infty,0) \tag{10.16}$$

The observant reader will notice that this S-matrix is just the unit operator. The S-matrix becomes useful in the context of a time-ordered product with other operators. Then, the S-matrix is split up into individual propagators in between the other operators. In case of doubt one should always refer to the definition Eq. 10.13, which divides the S-matrix into propagators along infinitesimally short time steps.[2]

With the help of the time contour and the S-matrix defined on it, the Green's function Eq. 10.12 obtains the simpler form of Eq. 10.17.

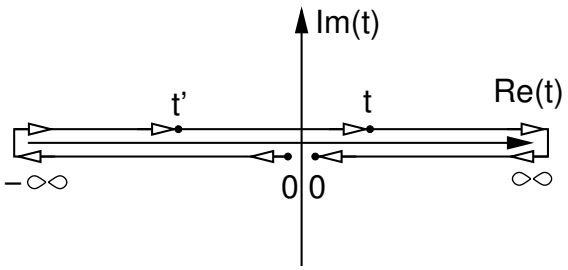
[2] This is one of the origins of the path-integral formulation of quantum physics.

GREEN'S FUNCTION WITH TIME CONTOUR

$$\hat{G}^{\mathcal{C}}(t,t') \overset{\text{Eq. } 10.12}{=} \int d^4x \int d^4x' \, |\vec{x}\rangle \underbrace{\frac{1}{i\hbar}\mathrm{Tr}\Big\{\hat{\rho}^{(W)}_{T,\mu}\mathcal{T}_{\mathcal{C}}\hat{S}_{I,\mathcal{C}}\hat{\psi}_I(\vec{x},t)\hat{\psi}^{+}_I(\vec{x'},t')\Big\}}_{G^{\mathcal{C}}(\vec{x},t,\vec{x'},t')} \langle\vec{x'}| \tag{10.17}$$

where the time contour $\mathcal{C}$ in the complex-time plane proceeds along the points

$$0 \to -\infty \to \min(t,t') \to \max(t,t') \to \infty \to 0 \tag{10.18}$$



The drawing does not imply that the time is displaced from the real time axis into the complex plane.

Uniqueness of initial time: The ensemble is defined such that it is in thermal equilibrium at time $t = 0$. The Hamiltonian usually drives the system out of thermal equilibrium as it propagates along the time contour. Choosing the time, at which the ensemble is in equilibrium, at time $t = 0$ is not a restriction, because a global time translation can shift it to any other time without changing the physical processes.

10.1.3 Interacting from non-interacting ensemble: complex-time contour

The Green's function in the form of Eq. 10.12 requires not only the propagator $\hat{S}_{I,\mathcal{C}}$ of the interacting system but also the von-Neumann density matrix $\hat{\rho}^{(W)}_{T,\mu}$ for the interacting system. Below, I will show how the interaction contained in the thermal von-Neumann density matrix $\hat{\rho}^{(W)}_{T,\mu}$ can be incorporated into the S-matrix by adjusting the time contour. The resulting contour will leave the real-time axis and extend into the complex plane. This justifies, why I introduced the propagator for arbitrary contours in the complex-time plane.

I exploit [3] the similarity between the statistical operator $\hat{\rho}^{(W)}_{T,\mu} = \frac{1}{Z^{(W)}_{T,\mu}}\mathrm{e}^{-\beta(\hat{H}^{(W)}-\mu\hat{N})}$ in the grand ensemble and the propagator $\hat{\mathcal{U}}(t,t') = \mathrm{e}^{\frac{1}{i\hbar}\hat{H}^{(W)}(t-t')}$ for a time-independent Hamiltonian.

The von-Neumann density matrix $\hat{\rho}^{(W)}_{T,\mu}$ of the interacting system is related to the exponential of the Hamiltonian and the partition function $Z^{(W)}_{T,\mu} = \mathrm{Tr}\left(\exp[-\beta(\hat{H}^{(W)} - \mu\hat{N})]\right)$. With the help of the propagator in imaginary time, it can be related to the density matrix $\hat{\rho}^{(0)}_{T,\mu}$ of the non-interacting system and its partition function $Z^{(0)}_{T,\mu} = \mathrm{Tr}\left(\exp[-\beta(\hat{h} - \mu\hat{N})]\right)$. The following steps rely on particle-number

[3] Literature:

- Joseph Maciejko, *An introduction to Nonequilibrium Many-Body Theory*, Lecture notes (2007) (`http://www.physics.arizona.edu/~stafford/Courses/560A/nonequilibrium.pdf`, retrieved July 2, 2016)
- Robert van Leeuwen and Nils Erik Dahlen, *An Introduction to Nonequilibrium Green Functions* (2005) (`http://theochem.chem.rug.nl/research/vanleeuwen/literature/NGF.pdf` retrieved July,2 2016); Lecture Notes Collection FreeScience.info ID1576 (`https://archive.org/details/R_van_Leeuwen_and_N_E_Dahlen__An_Introduction_to_Nonequilibrium_Green_Functions`)

conservation, i.e. that the particle-number operator commutates with the Hamiltonian independent of the interaction strength.

$$\begin{aligned}
\hat{\rho}_{T,\mu}^{(W)} &= \frac{1}{Z_{T,\mu}^{(W)}} \mathrm{e}^{-\beta(\hat{H}^{(W)}-\mu\hat{N})} \\
&= \frac{1}{Z_{T,\mu}^{(W)}} \mathrm{e}^{\beta\mu\hat{N}}\, \mathrm{e}^{-\frac{i}{\hbar}\hat{H}^{(W)}(-i\hbar\beta-0)} \\
&\overset{[\hat{H},\hat{N}]_-=0}{=} \frac{1}{Z_{T,\mu}^{(W)}} \underbrace{\frac{Z_{T,\mu}^{(0)}}{Z_{T,\mu}^{(0)}}}_{=1} \underbrace{\mathrm{e}^{-\beta(\hat{h}-\mu\hat{N})} \mathrm{e}^{\frac{i}{\hbar}\hat{h}(-i\hbar\beta)}}_{=\mathrm{e}^{\beta\mu\hat{N}}} \mathrm{e}^{-\frac{i}{\hbar}\hat{H}^{(W)}(-i\hbar\beta-0)} \underbrace{\mathrm{e}^{-\frac{i}{\hbar}\hat{h}(0)}}_{=\hat{1}} \\
&\overset{[\hat{h},\hat{N}]_-=0}{=} \frac{Z_{T,\mu}^{(0)}}{Z_{T,\mu}^{(W)}} \underbrace{\frac{1}{Z_{T,\mu}^{(0)}} \mathrm{e}^{-\beta(\hat{h}-\mu\hat{N})}}_{\hat{\rho}_{T,\mu}^{(0)}} \underbrace{\mathrm{e}^{\frac{i}{\hbar}\hat{h}(-i\hbar\beta)} \mathrm{e}^{-\frac{i}{\hbar}\hat{H}^{(W)}(-i\hbar\beta-0)} \mathrm{e}^{-\frac{i}{\hbar}\hat{h}(0)}}_{\hat{\mathcal{U}}_I^{(W)}(-i\hbar\beta,0) \quad \text{Eq. 10.11}} \\
&= \frac{Z_{T,\mu}^{(0)}}{Z_{T,\mu}^{(W)}} \hat{\rho}_{T,\mu}^{(0)} \hat{\mathcal{U}}_I^{(W)}(-i\hbar\beta,0)
\end{aligned} \tag{10.19}$$

The interesting point is that the interaction can be absorbed in a propagator along the imaginary axis of the complex-time plane.

The factor $Z_{T,\mu}^{(0)}/Z_{T,\mu}^{(W)}$ can be rewritten using the normalization condition of the von-Neumann density matrix $\hat{\rho}_{T,\mu}^{(W)}$

$$\begin{aligned}
1 = \mathrm{Tr}\left\{\hat{\rho}_{T,\mu}^{(W)}\right\} &\overset{\text{Eq. 10.19}}{=} \frac{Z_{T,\mu}^{(0)}}{Z_{T,\mu}^{(W)}} \mathrm{Tr}\left\{\hat{\rho}_{T,\mu}^{(0)} \hat{\mathcal{U}}_I^{(W)}(-i\hbar\beta,0)\right\} \\
\Rightarrow \qquad \frac{Z_{T,\mu}^{(0)}}{Z_{T,\mu}^{(W)}} &= \frac{1}{\mathrm{Tr}\left\{\hat{\rho}_{T,\mu}^{(0)} \hat{\mathcal{U}}_I^{(W)}(-i\hbar\beta,0)\right\}} = \frac{1}{\mathrm{Tr}\left\{\hat{\rho}_{T,\mu}^{(0)} \mathcal{T}_\mathcal{C} \hat{\mathcal{S}}_{I,\mathcal{C}}\right\}}
\end{aligned} \tag{10.20}$$

The contour is now the one from $t = 0$ along the imaginary time axis towards $-i\hbar\beta$. Furthermore, I extended the propagator by a closed contour around the real axis. This closed circle is a unit operator and thus does not change the result.

Remember, that the S-matrix should be considered as a product of short-time propagators between infinitesimally spaced points along the time contour, so that the time-ordering operator can divide it into the proper pieces and insert it between any other operators that occur in the time-ordered product.

Insertion of Eq. 10.20 into Eq. 10.19 for the density matrix of the interacting system yields

$$\hat{\rho}_{T,\mu}^{(W)} = \frac{\hat{\rho}_{T,\mu}^{(0)} \hat{\mathcal{U}}_I^{(W)}(-i\hbar\beta,0)}{\mathrm{Tr}\left\{\hat{\rho}_{T,\mu}^{(0)} \mathcal{T}_\mathcal{C} \hat{\mathcal{S}}_{I,\mathcal{C}}\right\}} \tag{10.21}$$

where the S-matrix is evaluated for the new contour $0 \to -\infty \to +\infty \to 0 \to -i\hbar\beta$.

Insertion of this density matrix for the grand potential into the Green's function Eq. 10.17 yields our result, which provides the Green's function as an expectation value of the density operator of the non-interacting system. The interaction appears only in one object, the S-matrix.

GREEN'S FUNCTION AS EXPECTATION VALUE OF THE NON-INTERACTING SYSTEM

$$\hat{G}^{\mathcal{C}}(t,t') \overset{\text{Eq. } 10.17}{=} \int d^4x \int d^4x' \, |\vec{x}\rangle \underbrace{\frac{1}{i\hbar} \frac{\mathrm{Tr}\Big\{\hat{\rho}^{(0)}_{T,\mu} \mathcal{T}_{\mathcal{C}} \hat{S}_{I,\mathcal{C}} \hat{\psi}_I(\vec{x},t) \hat{\psi}^+_I(\vec{x'},t')\Big\}}{\mathrm{Tr}\Big\{\hat{\rho}^{(0)}_{T,\mu} \mathcal{T}_{\mathcal{C}} \hat{S}_{I,\mathcal{C}}\Big\}}}_{G^{\mathcal{C}}(\vec{x},t,\vec{x'},t')} \langle \vec{x'}|$$

$$= \sum_{\alpha,\beta} |\chi_\alpha\rangle \underbrace{\frac{1}{i\hbar} \frac{\mathrm{Tr}\Big\{\hat{\rho}^{(0)}_{T,\mu} \mathcal{T}_{\mathcal{C}} \hat{S}_{I,\mathcal{C}} \hat{c}_{I,\alpha}(t) \hat{c}^+_{I,\beta}(t')\Big\}}{\mathrm{Tr}\Big\{\hat{\rho}^{(0)}_{T,\mu} \mathcal{T}_{\mathcal{C}} \hat{S}_{I,\mathcal{C}}\Big\}}}_{G^{\mathcal{C}}_{\alpha,\beta}(t,t')} \langle \chi_\beta| \tag{10.22}$$

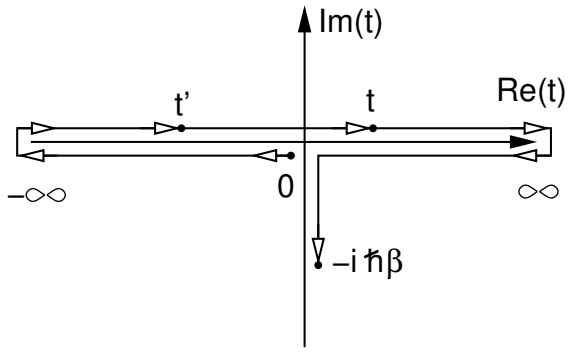
where the time contour $\mathcal{C}$ in the complex-time plane proceeds along the points

$$0 \to -\infty \to \min(t,t') \to \max(t,t') \to \infty \to 0 \to -i\hbar\beta \tag{10.23}$$

and the S-matrix

$$\hat{S}_{I,\mathcal{C}} = \mathcal{T}_{\mathcal{C}} \exp\Big(-\frac{i}{\hbar} \int_{\mathcal{C}} dt \, \hat{W}_I(t)\Big) \tag{10.24}$$

is the propagator along the same contour in the interaction picture.



In practice, other contours are in use, which may be obtained by deforming the one given here.

The big advantage is that we work now with the density operator of the non-interacting system, which is converted into that of the interacting system by a propagation along the imaginary-time axis towards the real-time axis. Inspection of the expression for the Green's function shows that the interaction is now entirely contained in the propagator. Wick's theorem shows how the perturbation expansion in terms of interaction strength can be accomplished.

Grand potential:

The partition function will establish an important link to the grand potential: We begin with the normalization condition Eq. 10.20 obtained earlier.

$$\frac{Z^{(0)}_{T,\mu}}{Z^{(W)}_{T,\mu}} \overset{\text{Eq. } 10.20}{=} \frac{1}{\mathrm{Tr}\Big\{\hat{\rho}^{(0)}_{T,\mu} \mathcal{T}_{\mathcal{C}} \hat{\mathcal{S}}_{I,\mathcal{C}}\Big\}}$$

$$\Rightarrow \quad \underbrace{+k_B T \ln\Big(Z^{(0)}_{T,\mu}\Big)}_{-\Omega^{(0)}_{T,\mu} \text{ Eq. } 2.61} \underbrace{-k_B T \ln\Big(Z^{(W)}_{T,\mu}\Big)}_{\Omega^{(W)}_{T,\mu} \text{ Eq. } 2.61} = -k_B T \ln \mathrm{Tr}\Big\{\hat{\rho}^{(0)}_{T,\mu} \mathcal{T}_{\mathcal{C}} \hat{\mathcal{S}}_{I,\mathcal{C}}\Big\} \tag{10.25}$$

Thus, we obtain the grand potential $\Omega^{(W)}_{T,\mu}$ of the interacting system as that, $\Omega^{(0)}_{T,\mu}$, of the non-interacting system plus an interaction part.

GRAND-POTENTIAL FROM THE S-MATRIX

$$\Omega^{(W)}_{T,\mu} = \Omega^{(0)}_{T,\mu} - k_B T \ln \mathrm{Tr}\Big\{\hat{\rho}^{(0)}_{T,\mu}\mathcal{T}_{\mathcal{C}}\hat{\mathcal{S}}_{I,\mathcal{C}}\Big\} \tag{10.26}$$

This equation of the grand potential, respectively its interaction part, will be converted below, Eq. 10.77 on p. 334, into a functional of the interaction matrix elements and the Green's function. In this form, the grand potential will become the key quantity for the diagrammatic expansion of the Green's function.

The grand potential $\Omega^{(0)}_{T,\mu}$ of a non-interacting electron gas in a Hamiltonian $\hat{h}$ has been worked out in Eq. L.104 on p. 726, as

$$\Omega^{(0)}_{T,\mu} = -k_B T \ln\left(Z^{(0)}_{T,\mu}\right) \overset{\text{Eq. } L.104}{=} -k_B T \ \mathrm{Tr}\Big\{\ln\Big(\underbrace{1+\mathrm{e}^{-\beta(\hat{h}-\mu\hat{1})}}_{\left(\hat{1}-f_{T,\mu}(\hat{h})\right)^{-1}}\Big)\Big\} \tag{10.27}$$

Also the non-interacting grand potential can be expressed as a functional of the non-interacting Green's function, as shown in appendix L.5.3.

10.2 Wick's theorem

We can obtain the Green's function using Eq. 10.22 as the ratio of two expectation values in the ensemble of non-interacting states. The interaction is completely contained in the S-matrix. The interaction is a product of creation and annihilation operators in the interaction picture. Thus, a perturbation expansion of the S-matrix in terms of the interaction strength

$$\begin{aligned}\mathrm{Tr}\Big\{\hat{\rho}^{(0)}_{T,\mu}\mathcal{T}_{\mathcal{C}}\hat{\mathcal{S}}_{I,\mathcal{C}}\hat{c}_{I,\alpha}(t)\hat{c}^{+}_{I,\beta}(t')\Big\} &\overset{\text{Eq. } 10.14}{=} \sum_{n=0}^{\infty}\frac{1}{n!}\left(\frac{1}{i\hbar}\right)^n\int dt_1\cdots dt_n \\ &\times\mathrm{Tr}\Big\{\hat{\rho}^{(0)}_{T,\mu}\mathcal{T}_{\mathcal{C}}\hat{W}_I(t_n)\hat{W}_I(t_{n-1})\cdots\hat{W}_I(t_1)\hat{c}_{I,\alpha}(t)\hat{c}^{+}_{I,\beta}(t')\Big\}\end{aligned} \tag{10.28}$$

will decompose the numerator and the denominator separately into a sum of expectation values of products of creation and annihilation operators in the interaction picture of the form

$$\mathrm{Tr}\Big\{\hat{\rho}^{(0)}_{T,\mu}\mathcal{T}_{\mathcal{C}}\hat{A}_{I,1}(t_1)\hat{A}_{I,2}(t_2)\ldots\hat{A}_{I,n}(t_n)\Big\} \tag{10.29}$$

where each operator $\hat{A}_{I,j}(t_j) \in \{\hat{c}^{\dagger}_{I,\alpha_j}(t_j), \hat{c}_{I,\alpha_j}(t_j)\}$ is a creation or annihilation operator in the interaction picture. Creation and annihilation operators occur in equal numbers.

The purpose of **Wick's theorem** is to convert this expectation value Eq. 10.29 of time-ordered products of creation and annihilation operators into a sum over products of non-interacting Green's functions.

While the original version of Wick's theorem[64] has been developed in the 1950's, we present here what is also called the generalized Wick's theorem. The generalized Wick's theorem has been proved by Matsubara[87]. The central part of Wick's theorem for finite temperatures rests on the so-called[4] **trace theorem** proven by Gaudin[88]. The generalized Wick's theorem has also been presented in the book Fetter and Walecka (Section 24).[3]

Before we arrive at the central points of Wick's theorem, let me introduce a few notations, that will simplify the derivation.

[4]Naming and reference from "Wick's Theorem at Finite temperature", T.S. Evans and D.A. Steer, arxiv:hep-ph/9601268

10.2.1 Notation: incoming and outgoing indices

In the following, I will try to adhere to the following convention:

- I will label an annihilation operator with an index i, which stands for **"incoming"**.
- A creation operator will be labeled by o, which stands for **"outgoing"**.

The notation is inspired by Feynman diagrams, which will be introduced only later: A Feynman diagram consists of interaction lines (wriggly lines) and directional particle lines (arrows). A **vertex** is a (space-spin-time)-point, where interaction lines and particle lines meet. A particle line is translated into an Green's function $G^{\mathcal{C}}_{i,o}(t_i, t_o)$, which begins an outgoing vertex (o, t_o) and ends at an incoming vertex $(i, , t_i)$. Because the first argument of the Green's function is connected to the annihilator and the second to the creation operator, the creator is connected to the outgoing vertex, where the Green's function emerges and the annihilation operator is connected to the incoming vertex.

10.2.2 Time order inside the interaction

Special care is required when translating the interaction into the interaction picture, because the interaction contains four operators with the same time argument. As a result, the time order of these operators is ambiguous. This problem was not present, when we introduced the time ordering in the context of one-particle quantum mechanics.

Each interaction operator is composed of creation and annihilation operators.

$$\hat{W} = \frac{1}{2} \sum_{i_1,o_1,i_2,o_2} W_{o_1,o_2,i_1,i_2} \hat{c}^\dagger_{S,o_1} \hat{c}^\dagger_{S,o_2} \hat{c}_{S,i_2} \hat{c}_{S,i_1} \tag{10.30}$$

which are transformed into the interaction picture

$$\begin{aligned}
\hat{W}_I(t) &= \hat{U}^{(0)}(0,t) \hat{W}_S(t) \hat{U}^{(0)}(t,0) \\
&= \frac{1}{2} \sum_{i_1,o_1,i_2,o_2} W_{o_1,o_2,i_1,i_2} \hat{U}^{(0)}(0,t) \hat{c}^\dagger_{S,o_1} \hat{c}^\dagger_{S,o_2} \hat{c}_{S,i_2} \hat{c}_{S,i_1} \hat{U}^{(0)}(t,0) \\
&= \frac{1}{2} \sum_{i_1,o_1,i_2,o_2} W_{o_1,o_2,i_1,i_2} \\
&\times \underbrace{\hat{U}^{(0)}(0,t) \hat{c}^\dagger_{S,o_1}}_{\hat{c}^+_{I,o_1}(t^+)} \overbrace{\hat{U}^{(0)}(t,0) \hat{U}^{(0)}(0,t)}^{\hat{1}} \hat{c}^\dagger_{S,o_2} \overbrace{\hat{U}^{(0)}(t,0) \hat{U}^{(0)}(0,t)}^{\hat{1}} \hat{c}_{S,i_2} \overbrace{\hat{U}^{(0)}(t,0) \hat{U}^{(0)}(0,t)}^{\hat{1}} \hat{c}_{S,i_1} \hat{U}^{(0)}(t,0) \\
&= \frac{1}{2} \sum_{i_1,o_1,i_2,o_2} W_{o_1,o_2,i_1,i_2} \mathcal{T}_{\mathcal{C}} \left\{ \hat{c}^+_{I,o_1}(t^+) \hat{c}^+_{I,o_2}(t^+) \hat{c}_{I,i_2}(t) \hat{c}_{I,i_1}(t) \right\}
\end{aligned} \tag{10.31}$$

In the last step, I introduced the contour time-ordering operator $\mathcal{T}_{\mathcal{C}}$. The time argument for the creation operators has been shifted forward by an infinitesimal amount[5] δ to the new time $t^+ = t(s + \delta)$. This is required, because the time-ordered product would otherwise be undefined: If creation and annihilation operators have the same time argument, the time-ordered product can produce two different values, depending on which time argument is considered later than the other.

$$\begin{aligned}
\mathcal{T}_{\mathcal{C}} \hat{c}^+_\alpha(t^+) \hat{c}_\beta(t) &= \hat{c}^+_\alpha(t^+) \hat{c}_\beta(t) = [\hat{c}^+_\alpha(t^+), \hat{c}_\beta(t)]_+ - \hat{c}_\beta(t) \hat{c}^+_\alpha(t^+) \\
\mathcal{T}_{\mathcal{C}} \hat{c}^+_\alpha(t) \hat{c}_\beta(t^+) &= -\hat{c}_\beta(t^+) \hat{c}^+_\alpha(t)
\end{aligned} \tag{10.32}$$

The two results differ by an anticommutator. This ambiguity does not exist for the product of either two annihilation operators or of two creation operators, because their anticommutator vanishes. The

[5] For the notation see Eq. 8.31 on p. 272

ambiguity is lifted by ensuring that the time arguments of creation and annihilation operators are different, i.e. by distinguishing t and t^+. By increasing the time of the creation operators they are brought into the order they occur in the interaction.

This feature, namely the distinction of t and t^+, has important consequences for the evaluation of Feynman diagrams lateron.

10.2.3 Alternating order inside the interaction

With the time-ordering in place we can rearrange the field operators further so that the operators of one **vertex** stand side-by-side. This is done for convenience.

$$\begin{aligned}\hat{W}_I(t) &\overset{\text{Eq. } L.97}{=} \frac{1}{2}\sum_{i_1,o_1,i_2,o_2} W_{o_1,o_2,i_1,i_2}\mathcal{T}_\mathcal{C}\left\{\hat{c}^+_{I,o_1}(t^+)\hat{c}^+_{I,o_2}(t^+)\hat{c}_{I,i_2}(t)\hat{c}_{I,i_1}(t)\right\} \\ &= \frac{1}{2}\sum_{i_1,o_1,i_2,o_2} W_{o_1,o_2,i_1,i_2}\mathcal{T}_\mathcal{C}\Big\{\underbrace{\hat{c}_{I,i_1}(t)\hat{c}^+_{I,o_1}(t^+)}_{\text{vertex 1}}\underbrace{\hat{c}_{I,i_2}(t)\hat{c}^+_{I,o_2}(t^+)}_{\text{vertex 2}}\Big\} \qquad (10.33)\end{aligned}$$

10.2.4 Single step of Wick's theorem

Here, I will present the derivation of Wick's theorem for time-independent Hamiltonians $\hat{h}$. The proof of generalized Wick's theorem for time-dependent Hamiltonians is a bit involved and and is provided in the appendix.

The goal of the generalized Wick's theorem is to express the expectation value

$$Y = \mathrm{Tr}\Big\{\hat{A}_1\hat{A}_2\cdots\hat{A}_{2M}\hat{\rho}^{(0)}_{T,\mu}\Big\} \tag{10.34}$$

of a product of creation and annihilation operators $A_j \in \{\hat{a}^+_{l,n_j}(t_j), \hat{a}_{l,n_j}(t_j)\}$ in terms of Green's functions of the non-interacting system.

We choose the eigenstates $|\varphi_n\rangle$ of the non-interacting Hamiltonian $\hat{h}$ as basisset for the creation and annihilation operators $\hat{a}^\dagger_{S,n}$, $\hat{a}_{S,n}$. Hence

$$|\varphi_n\rangle = \hat{a}^\dagger_{S,n}|\mathcal{O}\rangle \tag{10.35}$$

with

$$\hat{h}|\varphi_n\rangle = |\varphi_n\rangle\epsilon_n \qquad \text{and} \qquad \langle\varphi_m|\varphi_n\rangle = \delta_{m,n} \tag{10.36}$$

The eigenstates of the non-interacting one-particle-at-a-time Hamiltonian are Slater determinants $|\vec{\sigma}\rangle$ that satisfy the eigenvalue equation for the Hamiltonian $\hat{h}$ and the particle-number operator $\hat{N}$.

$$\hat{h}|\vec{\sigma}\rangle = |\vec{\sigma}\rangle\sum_j \sigma_j\epsilon_j \qquad \text{and} \qquad \hat{N}|\vec{\sigma}\rangle = |\vec{\sigma}\rangle\sum_j \sigma_j\ . \tag{10.37}$$

Furthermore, we assume

- The creation and annihilation operators are fermionic.
- The operator product in Y is ordered so that $t_1 \geq t_2 \geq \ldots$.
- The numbers of creation and annihilation operators are equal.

Some of these limitations will be relaxed as we proceed with the proof.

Single step of Wick's theorem

$$\begin{aligned}
Y &\overset{\text{Eq. 10.34}}{=} \mathrm{Tr}\Big\{\hat{A}_1\hat{A}_2\ldots\hat{A}_{2M}\hat{\rho}^{(0)}_{T,\mu}\Big\} \\
&= \mathrm{Tr}\Big\{[\hat{A}_1,\hat{A}_2]_+\ldots\hat{A}_{2M}\hat{\rho}^{(0)}_{T,\mu}\Big\} - \mathrm{Tr}\Big\{\hat{A}_2\hat{A}_1\ldots\hat{A}_{2M}\hat{\rho}^{(0)}_{T,\mu}\Big\} \\
&= \mathrm{Tr}\Big\{[\hat{A}_1,\hat{A}_2]_+\ldots\hat{A}_{2M}\hat{\rho}^{(0)}_{T,\mu}\Big\} - \mathrm{Tr}\Big\{\hat{A}_2[\hat{A}_1,\hat{A}_3]_+\ldots\hat{A}_{2M}\hat{\rho}^{(0)}_{T,\mu}\Big\} \\
&\quad + \mathrm{Tr}\Big\{\hat{A}_2\hat{A}_3\hat{A}_1\hat{A}_4\ldots\hat{A}_{2M}\hat{\rho}^{(0)}_{T,\mu}\Big\} \\
&= \underbrace{\sum_{j=2}^{2M}(-1)^j\mathrm{Tr}\Big\{(\hat{A}_2\cdots\hat{A}_{j-1})[\hat{A}_1,\hat{A}_j]_+(\hat{A}_{j+1}\cdots\hat{A}_{2M})\hat{\rho}^{(0)}_{T,\mu}\Big\}}_{X} \\
&\quad - \underbrace{(-1)^{2M}}_{=+1}\mathrm{Tr}\Big\{\hat{A}_2\cdots\hat{A}_{2M}\Big(\hat{A}_1\hat{\rho}^{(0)}_{T,\mu}\Big)\Big\}
\end{aligned} \tag{10.38}$$

Let us deal with the term denoted by X later.

We bring the last term of the previous equation to the left side.

$$\underbrace{\overbrace{\mathrm{Tr}\Big\{\hat{A}_2\dots\hat{A}_{2M}\hat{\rho}^{(0)}_{T,\mu}\hat{A}_1\Big\}}^{Y\quad\text{Eq. 10.34 and cycl.perm}}+\mathrm{Tr}\Big\{\hat{A}_2\cdots\hat{A}_{2M}\Big(\hat{A}_1\hat{\rho}^{(0)}_{T,\mu}\Big)\Big\}}_{\mathrm{Tr}\Big\{\hat{A}_2\dots\hat{A}_{2M}\big[\hat{\rho}^{(0)}_{T,\mu},\hat{A}_1\big]_+\Big\}}\overset{\text{Eq. }10.38}{=}X$$

$$\Rightarrow\qquad \mathrm{Tr}\Big\{\hat{A}_2\dots\hat{A}_{2M}\big[\hat{\rho}^{(0)}_{T,\mu},\hat{A}_1\big]_+\Big\}=X \tag{10.39}$$

X has been defined above in Eq. 10.38 as

$$X\overset{\text{def}}{=}\sum_{j=2}^{2M}(-1)^j\mathrm{Tr}\Big\{(\hat{A}_2\cdots\hat{A}_{j-1})[\hat{A}_1,\hat{A}_j]_+(\hat{A}_{j+1}\cdots\hat{A}_{2M})\hat{\rho}^{(0)}_{T,\mu}\Big\} \tag{10.40}$$

For the time being, Y got out of sight. It will turn up again below.

First commutator: Let us work out the anticommutator $\big[\hat{\rho}^{(0)}_{T,\mu},\hat{A}_1\big]_+$ for the annihilator $\hat{A}_1=\hat{a}_{I,n_1}(t_1)$. The derivation for the creator will proceed analogously. To demonstrate the operator identity, we use the complete basis of eigenstates of the non-interacting Hamiltonian $\hat{h}$, which are Slater determinants $|\vec{\sigma}\rangle$ with energy $E_{\vec{\sigma}}=\sum_j\sigma_j\epsilon_j$ and particle number $N_{\vec{\sigma}}=\sum_j\sigma_j$. I exploit that the Hamiltonian $\hat{h}$ commutates with itself and with the particle-number operator $\hat{N}$.

I start with the anticommutator in the Schrödinger picture:

$$\begin{aligned}\hat{a}_{S,n}\mathrm{e}^{-\beta(\hat{h}-\mu\hat{N})}|\vec{\sigma}\rangle=\hat{a}_{S,n}|\vec{\sigma}\rangle\mathrm{e}^{-\beta\sum_j\sigma_j(\epsilon_j-\mu)}\qquad&\text{and}\\ \mathrm{e}^{-\beta(\hat{h}-\mu\hat{N})}\hat{a}_{S,n}|\vec{\sigma}\rangle\mathrm{e}^{-\beta(\epsilon_n-\mu)}=\hat{a}_{S,n}|\vec{\sigma}\rangle\mathrm{e}^{-\beta\sum_j\sigma_j(\epsilon_j-\mu)}&\end{aligned} \tag{10.41}$$

Because the right-hand sides are equal, we conclude

$$\begin{aligned}&\hat{a}_{S,n}\mathrm{e}^{-\beta(\hat{h}-\mu\hat{N})}=\mathrm{e}^{-\beta(\hat{h}-\mu\hat{N})}\hat{a}_{S,n}\mathrm{e}^{-\beta(\epsilon_n-\mu)}\\
\Rightarrow\qquad&\mathrm{e}^{\frac{i}{\hbar}\hat{h}t}\frac{1}{Z^{(0)}_{T,\mu}}\Big(\hat{a}_{S,n}\mathrm{e}^{-\beta(\hat{h}-\mu\hat{N})}\Big)\mathrm{e}^{-\frac{i}{\hbar}\hat{h}t}=\mathrm{e}^{\frac{i}{\hbar}\hat{h}t}\frac{1}{Z^{(0)}_{T,\mu}}\Big(\mathrm{e}^{-\beta(\hat{h}-\mu\hat{N})}\hat{a}_{S,n}\mathrm{e}^{-\beta(\epsilon_n-\mu)}\Big)\mathrm{e}^{-\frac{i}{\hbar}\hat{h}t}\\
\Rightarrow\qquad&\overbrace{\mathrm{e}^{\frac{i}{\hbar}\hat{h}t}\hat{a}_{S,n}(t)\mathrm{e}^{-\frac{i}{\hbar}\hat{h}t}}^{\hat{a}_{I,n}(t)}\hat{\rho}^{(0)}_{T,\mu}=\hat{\rho}^{(0)}_{T,\mu}\overbrace{\mathrm{e}^{\frac{i}{\hbar}\hat{h}t}\hat{a}_{S,n}(t)\mathrm{e}^{-\frac{i}{\hbar}\hat{h}t}}^{\hat{a}_{I,n}(t)}\mathrm{e}^{-\beta(\epsilon_n-\mu)}\\
\Rightarrow\qquad&\big[\hat{\rho}^{(0)}_{T,\mu},\hat{a}_{I,n}(t)\big]_+=\hat{\rho}^{(0)}_{T,\mu}\hat{a}_{I,n}(t)\Big(1+\mathrm{e}^{-\beta(\epsilon_n-\mu)}\Big)=\hat{\rho}^{(0)}_{T,\mu}\hat{a}_{I,n}(t)\frac{1}{1-f_{T,\mu}(\epsilon_n)}\\
\text{analogous}\Rightarrow\qquad&\big[\hat{\rho}^{(0)}_{T,\mu},\hat{a}^+_{I,n}(t)\big]_+=\hat{\rho}^{(0)}_{T,\mu}\hat{a}^+_{I,n}(t)\Big(1+\mathrm{e}^{+\beta(\epsilon_n-\mu)}\Big)=\hat{\rho}^{(0)}_{T,\mu}\hat{a}^+_{I,n}(t)\frac{1}{f_{T,\mu}(\epsilon_n)}\end{aligned} \tag{10.42}$$

where $f_{T,\mu}(\epsilon)$ is the Fermi distribution function.

In the following, we need to distinguish two cases depending on the nature of the operator A_1. I use a superscript $+$ when $A_1=\hat{a}^+_{I,n_1}(t_1)$ is a creation operator and a superscript $-$ when $A_1=\hat{a}_{I,n_1}(t_1)$ is an annihilator.

$$Y=\begin{cases}Y^+_n & \text{for }\hat{A}_1=\hat{a}^+_{I,n}\\ Y^-_n & \text{for }\hat{A}_1=\hat{a}_{I,n}\end{cases}\qquad\text{and}\qquad X=\begin{cases}X^+_n & \text{for }\hat{A}_1=\hat{a}^+_{I,n}\\ X^-_n & \text{for }\hat{A}_1=\hat{a}_{I,n}\end{cases} \tag{10.43}$$

As long as the derivation is analogous, I will provide the explicit derivation only for the annihilator.

Let me now continue with Eq. 10.39.

$$\mathrm{Tr}\Big\{\hat{A}_2\ldots\hat{A}_{2M}\big[\hat{\rho}^{(0)}_{T,\mu},\underbrace{\hat{a}_{I,n}(t_1)}_{\hat{A}_1}\big]_+\Big\}\overset{\text{Eq. }10.42}{=}\underbrace{\mathrm{Tr}\Big\{\hat{A}_2\ldots\hat{A}_{2M}\hat{\rho}^{(0)}_{T,\mu}\underbrace{\hat{a}_{I,n}(t_1)}_{\hat{A}_1}\Big\}}_{Y_n^-\qquad\text{Eq. 10.34 + cycl.perm}}\frac{1}{1-f_{T,\mu}(\epsilon_n)}\overset{\text{Eq. }10.39}{=}X_n^-$$

$$\Rightarrow Y_n^- = \Big(1-f_{T,\mu}(\epsilon_n)\Big)X_n^- \tag{10.44}$$

$$\text{analogous}\Rightarrow Y_n^+ = f_{T,\mu}(\epsilon_n)X_n^+ \tag{10.45}$$

Second commutator: Let me now turn to X defined in Eq. 10.40:

$$X=\sum_{j=2}^{2M}(-1)^j\mathrm{Tr}\Big\{(\hat{A}_2\cdots\hat{A}_{j-1})[\hat{A}_1,\hat{A}_j]_+(\hat{A}_{j+1}\cdots\hat{A}_{2M})\hat{\rho}^{(0)}_{T,\mu}\Big\} \tag{10.46}$$

which requires the anticommutator $[\hat{A}_1,\hat{A}_j]_+$ between two field operators in the interaction picture. I use $\hat{a}_{I,n}(t)=\hat{a}_{S,n}\mathrm{e}^{-\frac{i}{\hbar}\epsilon_n t}$ and $\hat{a}^+_{I,m}(t')=\hat{a}^\dagger_{S,n}\mathrm{e}^{+\frac{i}{\hbar}\epsilon_m t'}$.

$$\begin{aligned}[\hat{a}_{I,n}(t),\hat{a}^+_{I,m}(t')]_+ &= \underbrace{\mathrm{e}^{+\frac{i}{\hbar}\hat{h}t}\hat{a}_{S,n}\mathrm{e}^{-\frac{i}{\hbar}\hat{h}t}}_{\hat{a}_{I,n}(t)}\underbrace{\mathrm{e}^{+\frac{i}{\hbar}\hat{h}t'}\hat{a}^\dagger_{S,m}\mathrm{e}^{-\frac{i}{\hbar}\hat{h}t'}}_{\hat{a}^+_{I,m}(t')}+\underbrace{\mathrm{e}^{+\frac{i}{\hbar}\hat{h}t'}\hat{a}^\dagger_{S,m}\mathrm{e}^{-\frac{i}{\hbar}\hat{h}t'}}_{\hat{a}^+_{I,m}(t')}\underbrace{\mathrm{e}^{+\frac{i}{\hbar}\hat{h}t}\hat{a}_{S,n}\mathrm{e}^{-\frac{i}{\hbar}\hat{h}t}}_{\hat{a}_{I,n}(t)}\\ &= \underbrace{\mathrm{e}^{-\frac{i}{\hbar}\epsilon_n t}\hat{a}_{S,n}}_{\hat{a}_{I,n}(t)}\underbrace{\hat{a}^\dagger_{S,m}\mathrm{e}^{+\frac{i}{\hbar}\epsilon_m t'}}_{\hat{a}^+_{I,m}(t')}+\underbrace{\hat{a}^\dagger_{S,m}\mathrm{e}^{+\frac{i}{\hbar}\epsilon_m t'}}_{\hat{a}^+_{I,m}(t')}\underbrace{\mathrm{e}^{-\frac{i}{\hbar}\epsilon_n t}\hat{a}_{S,n}}_{\hat{a}_{I,n}(t)}\\ &= \Big[\hat{a}_{S,n},\hat{a}^\dagger_{S,m}\Big]_+\mathrm{e}^{-\frac{i}{\hbar}(\epsilon_n t-\epsilon_m t')}\\ &= \delta_{m,n}\mathrm{e}^{-\frac{i}{\hbar}\epsilon_n(t-t')}\end{aligned} \tag{10.47}$$

The anticommutator of two annihilators, as well as that of two creators, vanishes. The anticommutator of annihilators and creators can be expressed by the Green's function as shown in the following.

The non-interacting Green's function of a time-independent Hamiltonian has been presented in Eq. 7.30 on p. 258.

$$\hat{G}^{(\mathcal{C})(0)}(t,t')\overset{\text{Eq. }7.30}{=}\frac{1}{i\hbar}\sum_n|\varphi_n\rangle\Big\{\theta_{\mathcal{C}}(t-t')\Big(1-f_{T,\mu}(\epsilon_n)\Big)-\theta_{\mathcal{C}}(t'-t)f_{T,\mu}(\epsilon_n)\Big\}\mathrm{e}^{-\frac{i}{\hbar}\epsilon_n(t-t')}\langle\varphi_n| \tag{10.48}$$

so that for $t_1>t_j$ in the contour-sense[6]

$$\begin{aligned}i\hbar G^{\mathcal{C},0}_{n_1,n_j}(t_1,t_j) &= \Big(1-f_{T,\mu}(\epsilon_{n_1})\Big)\delta_{n_1,n_j}\mathrm{e}^{-\frac{i}{\hbar}\epsilon_{n_1}(t_1-t_j)}\\ &\overset{\text{Eq. }10.47}{=}\Big(1-f_{T,\mu}(\epsilon_{n_1})\Big)\Big[\hat{a}_{I,n_1}(t_1),\hat{a}^+_{I,n_j}(t_j)\Big]_+\end{aligned} \tag{10.49}$$

$$\begin{aligned}-i\hbar G^{\mathcal{C},0}_{n_j,n_1}(t_j,t_1) &= f_{T,\mu}(\epsilon_{n_1})\delta_{n_1,n_j}\mathrm{e}^{+\frac{i}{\hbar}\epsilon_{n_1}(t_1-t_j)}\\ &\overset{\text{Eq. }10.47}{=}f_{T,\mu}(\epsilon_{n_1})\Big[\hat{a}^+_{I,n_1}(t_1),\hat{a}_{I,n_j}(t_j)\Big]_+\end{aligned} \tag{10.50}$$

Important is that the anticommutators are numbers, which can be moved out of the trace.

Let us insert the result into

$$X\overset{\text{Eq. }10.40}{=}\sum_{j=2}^{2M}(-1)^j\mathrm{Tr}\Big\{(\hat{A}_2\cdots\hat{A}_{j-1})[\hat{A}_1,\hat{A}_j]_+(\hat{A}_{j+1}\cdots\hat{A}_{2M})\hat{\rho}^{(0)}_{T,\mu}\Big\} \tag{10.51}$$

[6] $t_1>t_j$ in the contour sense meand $t_1=t(s_1)$, $t_j=t(s_j)$ and $s_1>s_2$.

- if $\hat{A}_1$ is an annihilator, the result is nonzero only when $\hat{A}_j$ is a creation operator. This yields

$$
\begin{aligned}
Y^- &\overset{\text{Eq. } 10.44}{=} \big(1 - f_{T,\mu}(\epsilon_{n_1})\big) X_1^- \\
&\overset{\text{Eq. } 10.51}{=} \sum_{\substack{j=2 \\ \hat{A}_j \text{ creator}}}^{2M} (-1)^j \underbrace{\Big(1 - f_{T,\mu}(\epsilon_{n_1})\Big) \big[\overbrace{\hat{a}_{l,n_1}(t_1)}^{\hat{A}_1}, \overbrace{\hat{a}^+_{l,n_j}(t_j)}^{\hat{A}_j}\big]_+}_{i\hbar G^{\mathcal{C}(0)}_{n_1,n_j}(t_1,t_j)} \operatorname{Tr}\Big\{(\hat{A}_2 \cdots \hat{A}_{j-1})(\hat{A}_{j+1} \cdots \hat{A}_{2M})\hat{\rho}^{(0)}_{T,\mu}\Big\} \\
&\overset{\text{Eq. } 10.49}{=} \sum_{\substack{j=2 \\ \hat{A}_j \text{ creator}}}^{2M} \underbrace{\overbrace{\epsilon_{1,j,\dots j-1,j+1,\dots,2M}}^{(-1)^j}}_{\text{Levi-Civita Symbol}} i\hbar G^{\mathcal{C}(0)}_{n_1,n_j}(t_1, t_j) \operatorname{Tr}\Big\{(\hat{A}_2 \cdots \hat{A}_{j-1})(\hat{A}_{j+1} \cdots \hat{A}_{2M})\hat{\rho}^{(0)}_{T,\mu}\Big\} \qquad (10.52)
\end{aligned}
$$

- if $\hat{A}_1$ is an creation operator, the result is nonzero only when $\hat{A}_j$ is a annihilator. This yields

$$
\begin{aligned}
Y^+ &\overset{\text{Eq. } 10.45}{=} f_{T,\mu}(\epsilon_{n_1}) X_1^+ \\
&\overset{\text{Eq. } 10.51}{=} \sum_{\substack{j=2 \\ \hat{A}_j \text{ annihilator}}}^{2M} (-1)^j \underbrace{f_{T,\mu}(\epsilon_{n_1}) \big[\overbrace{\hat{a}^+_{l,n_1}(t_1)}^{\hat{A}_1}, \overbrace{\hat{a}_{l,n_j}(t_j)}^{\hat{A}_j}\big]_+}_{-i\hbar G^{\mathcal{C}(0)}_{n_j,n_1}(t_j,t_1)} \operatorname{Tr}\Big\{(\hat{A}_2 \cdots \hat{A}_{j-1})(\hat{A}_{j+1} \cdots \hat{A}_{2M})\hat{\rho}^{(0)}_{T,\mu}\Big\} \\
&\overset{\text{Eq. } 10.50}{=} \sum_{\substack{j=2 \\ \hat{A}_j \text{ annihilator}}}^{2M} \underbrace{\overbrace{\epsilon_{j,1,2,\dots j-1,j+1,\dots,2M}}^{(-1)^j(-1)}}_{\text{Levi-Civita Symbol}} i\hbar G^{\mathcal{C}(0)}_{n_j,n_1}(t_j, t_1) \operatorname{Tr}\Big\{(\hat{A}_2 \cdots \hat{A}_{j-1})(\hat{A}_{j+1} \cdots \hat{A}_{2M})\hat{\rho}^{(0)}_{T,\mu}\Big\}
\end{aligned}
\qquad (10.53)
$$

The order of the indices of the Levi-Civita symbol reflects the order of the operators and introduces a sign change for each interchange of neighboring field operators.

This is one step of Wick's theorem. The product in the expectation values has become shorter, as two field operators have been moved out in the form of a Green's function. The price to pay is a large sum with M terms.

10.2.5 Sequence of Wick's iterations:

From here on we proceed analogous to appendix L.4.2, *"Sequence of Wick's iterations"* on p. 722.

After applying Wicks theorem M times, we arrive at a sum with $M!$ terms, where each term

- has a prefactor $(i\hbar)^M$ and
- a Levi-Civita symbol tracking the order of the indices in the Green's functions and
- a product of M Green's functions.

$$
\begin{aligned}
Y &\overset{\text{Eq. } 10.34}{=} \operatorname{Tr}\big[\hat{\rho}^{(0)}_{T,\mu} \mathcal{T}_{\mathcal{C}} \prod_{k=1}^{2M} \hat{A}_k\big] \\
&\overset{\text{Eqs. } 10.52,10.53}{=} (i\hbar)^M \sum_{\vec{\mathcal{P}}} \underbrace{\overbrace{\epsilon_{\mathcal{P}_1,\mathcal{P}_2,\dots\mathcal{P}_M}}^{\epsilon_{\vec{\mathcal{P}}}}}_{\text{Levi-Civita Symbol}} \left(\prod_{j=1}^{M} G^{\mathcal{C}(0)}_{i_{\mathcal{P}_j},o_j}(t_{\mathcal{P}_j}, t'_j)\right) \underbrace{\operatorname{Tr}\Big\{\hat{\rho}^{(0)}_{T,\mu}\Big\}}_{=1}
\end{aligned}
\qquad (10.54)
$$

The time-ordering operator $\mathcal{T}_{\mathcal{C}}$ does not have an effect yet, because the operator product is already time ordered per requirement.

The set of vectors $\{\vec{\mathcal{P}}\}$ contains all $M!$ permutations of the sequence $(1, 2, \dots, M)$.

The indices $(n_k, \bar{t}_k)$ of the operator $\hat{A}_k$ need to be translated into the indices (i_j, t_j) and (o_j, t'_j). (See Eq. 10.33)

- For the arguments (o_j, t'_j), we collect the subsequence of creation operators in $(\hat{A}_1, \ldots, \hat{A}_{2M})$ and identify $(o_j, t'_j) = (n_k, \bar{t}_k)$, where j refers to the position of the subsequence of creation operators, while k refers to the position in the original operator sequence.
- Similarly, we assign $(i_j, t_j) = (n_k, \bar{t}_k)$, where j refers to the position of the subsequence of annihilation operators, while k refers to the position in the original operator sequence.

Example:

$\hat{A}_1$	$\hat{A}_2$	$\hat{A}_3$	$\hat{A}_4$
$\hat{a}_{l,n_1}(\bar{t}_1)$	$\hat{a}_{l,n_2}(\bar{t}_2)$	$\hat{a}^+_{l,n_3}(\bar{t}_3)$	$\hat{a}^+_{l,n_4}(\bar{t}_4)$
$\hat{a}_{l,i_1}(t_1)$	$\hat{a}_{l,i_2}(t_2)$	$\hat{a}^+_{l,o_1}(t'_1)$	$\hat{a}^+_{l,o2}(t'_2)$
$(i_1, t_1) = (n_1, \bar{t}_1)$	$(i_2, t_2) = (n_2, \bar{t}_2)$	$(o_1, t'_1) = (n_3, \bar{t}_3)$	$(o_2, t'_2) = (n_4, \bar{t}_4)$

In the final result, an interchange of two Green's function does not affect the result, because it corresponds to moving indices in pairs. Let me therefore arrange the Green's functions such that the time of the right (outgoing) index of the Green's functions, the one connected to the creation operator, decreases from left to right. The left (incoming) indices, occur in all possible permutations, which I denote by permutation vectors $\vec{\mathcal{P}}$ with M components. There are $M!$ such permutation vectors. (as many as there are Green's functions).

Time order: Every interchange of two neighboring field operators in the operator product of Y introduces a sign change. Such a sign change is balanced by the Levi-Civita symbol on the right-hand side. Editor: Caution! the following is not yet clear

- An interchange of two neighboring creation operators translates in an interchange of two neighboring entries of the permutation vector $\mathcal{P}$, which causes a sign-change of the Levi-Civita symbol.
- An interchange of two neighboring creation operators translates in an interchange of two values of the permutation vector $\mathcal{P}$.
- an interchange of an annihilation operator with a neighboring creation operator changes the order of the arguments in the Green's function its preceeding sign. This is balanced by a sign change of the Levi-Civita symbol.

Thus, after introducing the time-ordering operator on the left-hand side, we may relax the requirement that the operator is time ordered, before applying the time ordering operator.

Alternating order of annihilation and creation operators: It is often convenient to bring the creation and annihilation operators under the time-ordering operator into a specific order, so that the annihilation operators alternate with creation operators.

$$\begin{aligned}\mathcal{T}_\mathcal{C}\hat{W}_I(t) &\overset{\text{Eq. L.97}}{=} \frac{1}{2}\sum_{i_1,o_1,i_2,o_2} W_{o_1,o_2,i_1,i_2}\mathcal{T}_\mathcal{C}\Big\{\hat{a}^+_{l,o_1}(t^+)\hat{a}^+_{l,o_2}(t^+)\hat{a}_{l,i_2}(t)\hat{a}_{l,i_1}(t)\Big\} \\ &= \frac{1}{2}\sum_{i_1,o_1,i_2,o_2} W_{o_1,o_2,i_1,i_2}\mathcal{T}_\mathcal{C}\Big\{\hat{a}_{l,i_1}(t)\hat{a}^+_{l,o_1}(t^+)\hat{a}_{l,i_2}(t)\hat{a}^+_{l,o_2}(t^+)\Big\} \qquad (10.55)\end{aligned}$$

There are no sign changes.

Inspection of the Green's function in Eq. 10.22 shows that this alternating order is consistent with the order of the operators in definition of the Green's function.

With this choice, the result Eq. L.98 obtains the form

$$\mathrm{Tr}\Big\{\hat{\rho}^{(0)}_{T,\mu}\mathcal{T}_\mathcal{C}\prod_{j=1}^{M}\hat{a}_{l,i_j}(t'_j)\hat{a}^\dagger_{l,o_j}(t^+_j)\Big\} \overset{\text{Eq. L.98}}{=} (i\hbar)^M\sum_{\vec{\mathcal{P}}}\epsilon_{\mathcal{P}_1,\ldots,\mathcal{P}_M}\prod_{j=1}^{M}G^{\mathcal{C}(0)}_{i_{\mathcal{P}_j},o_j}(t'_{\mathcal{P}_j}, t^+_j) \qquad (10.56)$$

10.2.6 Generalized Wick's theorem: Summary

Thus, we obtain the central message of Wick's theorem

WICK'S THEOREM

Wick's theorem maps the thermal expectation value of a time-ordered product of creation and annihilation operators in the interaction picture $\hat{A}_j \in \{\hat{c}^+_{l,\alpha}(t), \hat{c}_{l,\alpha}(t), \alpha \in \ldots\}$, onto a sum of products of non-interacting contour-ordered Green's functions. The ensemble is determined by thermal equilibrium with the initial ($t = 0$), non-interacting Hamiltonian $\hat{h}(0)$. The corresponding von-Neumann density matrix is $\hat{\rho}^{vN,(0)}_{T,\mu} = \frac{1}{Z^{(0)}_{T,\mu}} \mathrm{e}^{-\beta(\hat{h}(0)-\mu\hat{N})}$. $\mathcal{T}_\mathcal{C}$ is the time-ordering operator along the contour $\mathcal{C}$ in the complex-time plane.

$$\mathrm{Tr}\Big\{\hat{\rho}^{vN,(0)}_{T,\mu}\mathcal{T}_\mathcal{C}\prod_{j=1}^{L}\hat{c}_{l,i_j}(t'_j)\hat{c}^+_{l,o_j}(t_j)\Big\} \overset{\text{Eq. } L.102}{=} \sum_{\vec{\mathcal{P}}}\epsilon_{\mathcal{P}_1,\ldots,\mathcal{P}_L}(i\hbar)^L\prod_{j=1}^{L}G^{\mathcal{C},(0)}_{i_{\mathcal{P}_j},o_j}(t'_{\mathcal{P}_j},t_j)\,. \tag{10.57}$$

$\epsilon_{\mathcal{P}_1,\ldots,\mathcal{P}_L}$ is the fully antisymmetric tensor and the sum includes all integer vectors with elements $\mathcal{P}_j \in \{1,\ldots,L\}$. The fully antisymmetric tensor $\epsilon_{\mathcal{P}_1,\mathcal{P}_2,\ldots,\mathcal{P}_M}$ selects the permutation vectors with $\mathcal{P}_j \neq \mathcal{P}_k$.
The one-particle basisset $\{|\chi_\alpha\rangle\}$ defining the creation and annihilation operators may be non-orthonormal. The overlap matrix is $S_{\alpha,\beta} = \langle\chi_\alpha|\chi_\beta\rangle$. Each orbital $|\chi_\alpha\rangle$ has a projector function $\langle\pi_\alpha| = \sum_\beta S^{-1}_{\alpha,\beta}\langle\chi_\beta|$. The anticommutator relation of annihilation and creation operators in the Schrödinger picture is $\left[\hat{c}_\alpha, \hat{c}^\dagger_\beta\right]_+ = \langle\pi_\alpha|\pi_\beta\rangle$.
The non-interacting contour-ordered Green's function $G^{\mathcal{C}(0)}_{i,o}(t',t)$ has been defined in Eq. 7.30 (p.258) as

$$G^{\mathcal{C},(0)}_{i,o}(t',t) \overset{\text{Eq. } 7.30}{=} \frac{1}{i\hbar}\Big\langle\pi_i\Big|\hat{U}(t',0)\Big\{\underbrace{\theta_\mathcal{C}(t-t')\big(\hat{1}-\hat{\rho}^{(1)(0)}_{T,\mu}\big)}_{\text{electrons}} - \underbrace{\theta_\mathcal{C}(t'-t)\hat{\rho}^{(1)(0)}_{T,\mu}}_{\text{holes}}\Big\}\hat{U}(0,t)\Big|\pi_o\Big\rangle$$

The time-ordering operator $\mathcal{T}_\mathcal{C}$ rearranges the product in increasing order along some directed contour in the complex plane. The step function $\theta_\mathcal{C}(t-t')$ refers to the time ordering along the time contour consistent with the definition of the time-ordering operator.
Wick's theorem can also be expressed by a determinant

$$\mathrm{Tr}\Big\{\hat{\rho}^{(0)}_{T,\mu}\mathcal{T}_\mathcal{C}\prod_{j=1}^{L}\hat{c}_{l,\alpha_j}(t_j)\hat{c}^+_{l,\beta_j}(t'_j)\Big\} = (i\hbar)^L\det\begin{vmatrix} G^{\mathcal{C},(0)}_{\alpha_1,\beta_1}(t_1,t'_1)\; G^{\mathcal{C},(0)}_{\alpha_1,\beta_2}(t_1,t'_2)\;\ldots \\ G^{\mathcal{C},(0)}_{\alpha_2,\beta_1}(t_2,t'_1)\; G^{\mathcal{C},(0)}_{\alpha_2,\beta_2}(t_2,t'_2)\;\ldots \\ \vdots \qquad\qquad \vdots \qquad\quad \ddots \end{vmatrix} \tag{10.58}$$

10.3 Perturbation expansion of the Green's function

Let us use Wick's theorem to evaluate the Green's function.

$$G_{\alpha,\beta}(t,t') \overset{\text{Eq. } 10.22}{=} \frac{1}{i\hbar} \frac{\mathrm{Tr}\left\{\hat{\rho}^{(0)}_{T,\mu}\mathcal{T}_{\mathcal{C}}\hat{S}_{I,\mathcal{C}}\hat{c}_{I,\alpha}(t)\hat{c}^{+}_{I,\beta}(t')\right\}}{\mathrm{Tr}\left\{\hat{\rho}^{(0)}\mathcal{T}_{\mathcal{C}}\hat{S}_{I,\mathcal{C}}\right\}} \tag{10.59}$$

10.3.1 Outline

In the following sections, we will go through several theorems to set up a diagrammatic expansion of the Green's function and to simplify this expansion.

The steps, we will go through are

1. Enumerate and evaluate diagrams in the denominator of Eq. 10.59: closed diagrams
2. Obtain diagrams of the numerator of Eq. 10.59 from those in the denominator.
3. Green's function from "grand potential functional"
4. sign theorem (section 11.3)
5. linked-cluster theorem (section 11.4)
6. topologically inequivalent diagrams and symmetry factors (section 11.5)

When we are done, we arrived at an expression for the diagrammatic expansion of a grand potential $\mathcal{Q}_{T,\mu}[\boldsymbol{G}^{(0)}]$, which is a functional of the non-interacting Green's function. Each diagram has a value, Eq. 11.39, respectively Eq. 11.54, which itself is a functional of the non-interacting Green's function.

The derivative of the grand potential with the Green's function provides the **reducible self energy**, from which the interacting Green's function is obtained via Dyson's equation Eq. 10.78. I will call the reducible self energy also the **total self energy**.

10.3.2 Expansion of the S-matrix

The S-matrix can be expanded into a Taylor expansion

$$\begin{aligned}
\hat{S}_{I,\mathcal{C}} &\overset{\text{Eq. } 10.14}{=} \mathcal{T}_{\mathcal{C}} \exp\left(-\frac{i}{\hbar}\int_{\mathcal{C}} dt\, \hat{W}_I(t)\right) \\
&\overset{\text{Eq. } 10.15}{=} \sum_{n=0}^{\infty}\frac{1}{n!}\left(\frac{1}{i\hbar}\right)^n \int_{\mathcal{C}} dt_1 \cdots \int_{\mathcal{C}} dt_n\, \mathcal{T}_{\mathcal{C}}\hat{W}_I(t_1)\cdots\hat{W}_I(t_n) \\
&\overset{\text{Eq. } L.97}{=} \sum_{n=0}^{\infty}\frac{1}{n!}\left(\frac{1}{i\hbar}\right)^n \int_{\mathcal{C}} dt_1 \cdots \int_{\mathcal{C}} dt_n \sum_{o_1,i_1,\ldots,o_{2n},i_{2n}} \left[\frac{1}{2^n}\prod_{j=1}^{n} W_{o_{2j-1},o_{2j},i_{2j-1},i_{2j}}(t_j)\right] \\
&\quad \times \mathcal{T}_{\mathcal{C}}\Big[\underbrace{\hat{c}_{I,i_1}(t_1)\hat{c}^{+}_{I,o_1}(t_1^{+})\hat{c}_{I,i_2}(t_1)\hat{c}^{+}_{I,o_2}(t_1^{+})}_{\text{from } \hat{W}_I(t_1)} \cdots \underbrace{\hat{c}_{I,i_{2n-1}}(t_n)\hat{c}^{+}_{I,o_{2n-1}}(t_n^{+})\hat{c}_{I,i_{2n}}(t_n)\hat{c}^{+}_{I,o_{2n}}(t_n^{+})}_{\text{from } \hat{W}_I(t_n)}\Big]
\end{aligned} \tag{10.60}$$

The creation and annihilation operators have been brought into the and the time argument of the creation operators in each interaction term has been shifted according to Eq. L.97 on p. 724. The time dependence in the interaction matrix elements is present for the adiabatical switching factor in the zero-temperature theory.

The matrix elements are

$$W_{o_1,o_2,i_1,i_2} \overset{\text{Eq. 3.51}}{=} \int d^4x \int d^4x' \, \frac{e^2 \chi^*_{o_1}(\vec{x}) \chi^*_{o_2}(\vec{x}') \chi_{i_1}(\vec{x}) \chi_{i_2}(\vec{x}')}{4\pi\epsilon_0 |\vec{r} - \vec{r}'|} \tag{10.61}$$

It will be convenient to **double the number of time variables**.

$$\begin{aligned}\hat{S}_{I,\mathcal{C}} \overset{\text{Eq. 10.60}}{=} \sum_{n=0}^{\infty} \frac{1}{n!} \left(\frac{1}{i\hbar}\right)^n \int_{\mathcal{C}} dt_1 \cdots \int_{\mathcal{C}} dt_{2n} \sum_{o_1,i_1,\ldots,o_{2n},i_{2n}} \left[\frac{1}{2^n} \prod_{j=1}^{n} W_{o_{2j-1},o_{2j},i_{2j-1},i_{2j}} \delta_{\mathcal{C}}(t_{2j-1} - t_{2j})\right] \\ \times \mathcal{T}_{\mathcal{C}} \Big[\underbrace{\hat{c}_{I,i_1}(t_1)\hat{c}^+_{I,o_1}(t_1^+)\hat{c}_{I,i_2}(t_2)\hat{c}^+_{I,o_2}(t_2^+)}_{\text{from } \hat{W}_I(t_1,\,t_2)} \cdots \underbrace{\hat{c}_{I,i_{2n-1}}(t_{2n-1})\hat{c}^+_{I,o_{2n-1}}(t_{2n-1}^+)\hat{c}_{I,i_{2n}}(t_{2n})\hat{c}^+_{I,o_{2n}}(t_{2n}^+)}_{\text{from } \hat{W}_I(t_{2n-1},\,t_{2n})} \Big]\end{aligned} \tag{10.62}$$

While it appears at first as an unnecessary complication, this choice has a number of advantages

- it will simplify the expression for a Feynman diagram introduced later by treating time and orbital arguments in an analogous manner.
- Renormalization will later introduce a screened interaction, which will replace the bare Coulomb interaction in some of the expressions. The screened interaction is retarded and has naturally two time arguments.

10.3.3 Expansion of the denominator of the Green's function

The expansion Eq. 10.62 of the S-matrix is inserted into denominator and numerator of the Green's function Eq. 10.59.

Let me investigate the denominator first. Firstly, it is simpler. Secondly, the terms of the numerator can be derived from those of the denominator. This will be shown below.

In the denominator of the Green's function Eq. 10.59, we insert the expansion of the S-matrix Eq. 10.62, which turns it into a large sum of operator products. The contour time-ordered operator products in the sum are resolved via Wick's theorem Eq. 10.57 on p. 324. This turns the denominator of the Green's function into a sum of products of the non-interacting Green's function.

$$\begin{aligned}\mathrm{Tr}\Big\{\hat{\rho}^{(0)}_{T,\mu} \mathcal{T}_{\mathcal{C}} \hat{S}_{I,\mathcal{C}}\Big\} &\overset{\text{Eq. 10.62}}{=} \sum_{n=0}^{\infty} \frac{1}{n!} \left(\frac{1}{i\hbar}\right)^n \int_{\mathcal{C}} dt_1 \cdots \int_{\mathcal{C}} dt_{2n} \sum_{o_1,i_1,\ldots,o_{2n},i_{2n}} \left[\frac{1}{2^n} \prod_{j=1}^{n} W_{o_{2j-1},o_{2j},i_{2j-1},i_{2j}} \delta_{\mathcal{C}}(t_{2j-1} - t_{2j})\right] \\ &\times \mathrm{Tr}\Big\{\hat{\rho}^{(0)}_{T,\mu} \mathcal{T}_{\mathcal{C}} \Big[\underbrace{\hat{c}_{I,i_1}(t_1)\hat{c}^+_{I,o_1}(t_1^+)\hat{c}_{I,i_2}(t_2)\hat{c}^+_{I,o_2}(t_2^+)}_{\text{from } W_I(t_1,\,t_2))} \cdots \underbrace{\hat{c}_{I,i_{2n-1}}(t_{2n-1})\hat{c}^+_{I,o_{2n-1}}(t_{2n-1}^+)\hat{c}_{I,i_{2n}}(t_{2n})\hat{c}^+_{I,o_{2n}}(t_{2n}^+)}_{\text{from } W(t_n)} \Big]\Big\} \\ &\overset{\text{Eq. 10.57}}{=} \sum_{n=0}^{\infty} \frac{1}{n!} \left(\frac{1}{i\hbar}\right)^n \int_{\mathcal{C}} dt_1 \cdots \int_{\mathcal{C}} dt_{2n} \sum_{o_1,i_1,\ldots,o_{2n},i_{2n}} \left[\frac{1}{2^n} \prod_{j=1}^{n} W_{o_{2j-1},o_{2j},i_{2j-1},i_{2j}} \delta_{\mathcal{C}}(t_{2j-1} - t_{2j})\right] \\ &\times \; (i\hbar)^{2n} \sum_{\vec{\mathcal{P}}} \epsilon_{\mathcal{P}_1,\ldots,\mathcal{P}_{2n}} G^{(0)}_{i_{\mathcal{P}_1},o_1}\left(t_{\mathcal{P}_1}, t_1^+\right) \cdots G^{(0)}_{i_{\mathcal{P}_{2n}},o_{2n}}\left(t_{\mathcal{P}\mathcal{P}_{2n}}, t_{2n}^+\right) \qquad (10.63) \\ &= \; \sum_{n=0}^{\infty} \frac{1}{n! 2^n} \sum_{\vec{\mathcal{P}} \in \mathbb{A}_n} V(\vec{\mathcal{P}}) \qquad (10.64)\end{aligned}$$

The sum over the permutation vectors $\vec{\mathcal{P}} \in \mathbb{A}_n$ includes all $2n$-dimensional vectors with values $\mathcal{P}_j \in \{1, 2, \ldots, 2n\}$. The nonzero terms are related to permutation vectors $\vec{\mathcal{P}}$ that are obtained as permutation of the components of the vector $(1, \ldots, 2n)$. This selection is enforced by the fully antisymmetric tensor $\epsilon_{\mathcal{P}_1,\ldots,\mathcal{P}_{2n}}$, which also includes the proper sign.

The time argument t_j^+ of the creation operators is infinitesimally displaced forward in time relative to t_j.

10.3.4 Diagrams of the denominator

It will be useful to represent the terms in the denominator as follows

SUM AND VALUES OF CLOSED DIAGRAMS

$$\mathrm{Tr}\left\{\hat{\rho}^{(0)}_{T,\mu}\mathcal{T}_{\mathcal{C}}\hat{S}_{I,\mathcal{C}}\right\} \overset{\text{Eq. 10.63}}{=} \sum_{n=0}^{\infty}\sum_{\vec{\mathcal{P}}\in\mathbb{A}_n}\frac{\mathcal{V}(\vec{\mathcal{P}})}{n!2^n} \tag{10.65}$$

where

$$\mathcal{V}(\vec{\mathcal{P}}) = \epsilon_{\mathcal{P}_1,\ldots,\mathcal{P}_{2n}}(i\hbar)^n\int_{\mathcal{C}}dt_1\cdots\int_{\mathcal{C}}dt_{2n}\sum_{o_1,i_1,\ldots,o_{2n},i_{2n}}\left(\prod_{j=1}^{n}W_{o_{2j-1},o_{2j},i_{2j-1},i_{2j}}\delta_{\mathcal{C}}(t_{2j-1}-t_{2j})\right)$$
$$\times G^{\mathcal{C},(0)}_{i_{\mathcal{P}_1},o_1}(t_{\mathcal{P}_1},t_1^+)\cdots G^{\mathcal{C},(0)}_{i_{\mathcal{P}_{2n}},o_{2n}}(t_{\mathcal{P}_{2n}},t_{2n}^+) \tag{10.66}$$

The value of zeroth order diagrams is defined to be equal to 1. The reason is that $\mathrm{Tr}\left\{\hat{\rho}^{(0)}_{T,\mu}\right\}=1$, which is the normalization of the density operator.

The **value** $\mathcal{V}(\vec{\mathcal{P}})$ of a diagram should be considered as a **functional** $\mathcal{V}_{\vec{\mathcal{P}}}\left[\hat{G}^{(0)}(t,t')\right]$ of the non-interacting Green's function.

When the interaction tensor W and the non-interacting Green's function are known, each term is completely characterized by the permutation vector $\vec{\mathcal{P}}$. The dimension of $\vec{\mathcal{P}}$ determines the order n of the diagram. For example, the permutation vector $\vec{\mathcal{P}}$ in Eq. 10.66 has the dimension $2n$.

The value $\mathcal{V}(\vec{\mathcal{P}})$ of each term is dimension-less.[7]

10.3.5 Feynman diagrams

Editor: include here two graphs: one of a single interaction line with two vertices and at each vertex one incoming and one outgoing stump. The second graph shall be a non-interacting Green's function line with one outgoing and one incoming index. Also show the vertex.

Fig. 10.2: Elementary ingredients of a Feynman diagram for electrons with a Coulomb interaction. An arrow (a), called particle line, represents a bare (non-interacting) Green's function. A wriggly line, called an interaction line represents an interaction matrix element. The point where particle and interaction lines meet, is called a vertex. The vertex connects an incoming and an outgoing particle line with one end of an interaction line.

Each term $\mathcal{V}(\mathcal{P})$ can be represented by a graph, which is called a **diagram**. The basic elements of a diagram are **interaction lines**, represented by wriggly lines, and **particle lines**, represented by arrows. The particle lines correspond to non-interacting Green's functions, while the interaction lines correspond the interaction matrix elements. Interaction and particle lines are joined at so-called **vertices**. A vertex is the junction of an interaction line, an incoming particle line and an outgoing particle line. The outgoing particle line is connected to the vertex with the right index and the right time argument, while the incoming index, the arrow, is connected to the vertex with the left index and the left time argument.

The graphical representation of the diagram proceeds as follows:

[7] This is the reason for leaving the factor $(i\hbar)^n$ with the diagram.

- Draw n wriggly lines. Each wriggly line represents an interaction. The interaction has two ends, which are called **vertices**. Each vertex has an incoming index i and an outgoing index o.

  For the j-th interaction, one vertex has the outgoing index o_{2j-1} and the incoming index i_{2j-1}. the other vertex has the indices o_{2j} and i_{2j}

- Now draw $2n$ arrows representing Green's functions. The k-th Green's function ($k \in \{1, \ldots, 2n\}$) starts at the k-th vertex and is connected to the outgoing index o_k. It stops at vertex $\mathcal{P}_k$ and is connected to the incoming index $i_{\mathcal{P}_k}$.

Example: Let us draw the diagram for the specified permutation vector $\vec{\mathcal{P}} = (3, 4, 1, 6, 2, 5)$.

- We draw three wriggly lines and number the vertices. (Each interaction has one vertex with an odd number and one with the next higher even number.)
- We look up the permutation vector and form the ordered index pairs representing the Green's functions

$$(1 \to \underbrace{3}_{\mathcal{P}_1}); (2 \to \underbrace{4}_{\mathcal{P}_2}); (3 \to \underbrace{1}_{\mathcal{P}_3}); (4 \to \underbrace{6}_{\mathcal{P}_4}); (5 \to \underbrace{2}_{\mathcal{P}_5}); (6 \to \underbrace{5}_{\mathcal{P}_6}); \qquad (10.67)$$

  Now we connect the vertices according to this mapping.

- finally we rearrange the graph so that all connections remain intact but such that it is not all mixed up.

The result is shown in Fig. 10.3.

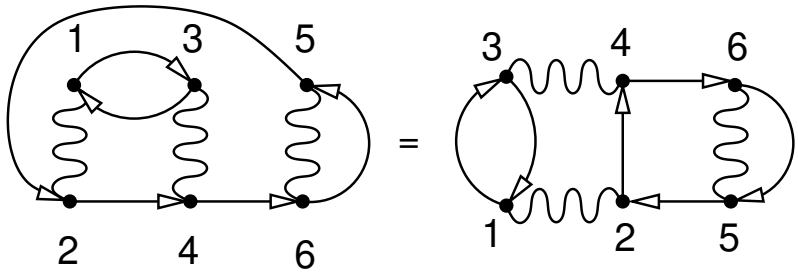


Fig. 10.3: Example for a labeled Feynman diagram corresponding to the permutation vector $\vec{\mathcal{P}} = (3, 4, 1, 6, 2, 5)$. Labels are the vertex numbers. Later, in section 11.5, we will encounter unlabeled diagrams, which are commonly used.

Example:

Let me work out the value of the diagram shown in Fig. 10.3 using Eq. 10.66.

Permutation vector: First we determine the permutation vector. For that purpose, we number the vertices such that vertices $(1, 2)$, $(3, 4)$, etc are related to one interaction. There are many ways of doing this, but each will give the same result. In the example shown in Fig. 10.3, the vertices are already numbered.

Now we can read off the end point of the Green's function starting at a given vertex. This gives the following mapping

outgoing vertex	1	2	3	4	5	6
incoming vertex	3	4	1	6	2	5

The array of incoming indices is the permutation vector $\vec{\mathcal{P}} = (3, 4, 1, 6, 2, 5)$.

Sign: The sign is obtained by enumerating the pair-wise permutations that bring the sequence $\mathcal{P}$ into increasing order. We start out with a given permutation vector $\vec{\mathcal{P}} = (3,4,1,6,2,5)$ and interchange its elements step by step as follows:

341625	+
3**14**625	-
134625	+
134**26**5	-
13**24**65	+
1**23**465	-
1234**56**	+

Each permutation causes a sign change shown in the second column. Thus, $\epsilon_{3,4,1,6,2,5} = +1$.

In section 11.3 below, we will learn how the sign can be determined in a simple manner using the so-called sign theorem.

All together: Let us put the result for the value of the diagram together

$$\mathcal{V}(\vec{\mathcal{P}}) \overset{\text{Eq. } 10.66}{=} \underbrace{+1}_{\text{sign}} (i\hbar)^3 \int_{\mathcal{C}} dt_1 \int_{\mathcal{C}} dt_2 \int_{\mathcal{C}} dt_3 \sum_{o_1,i_1,o_2,i_2\ldots,o_6,i_6} W_{o_1,o_2,i_1,i_2}(t_1) W_{o_3,o_4,i_3,i_4}(t_2) W_{o_5,o_6,i_5,i_6}(t_3)$$
$$\times G^{(0)}_{i_3,o_1}(t_2,t_1^+) G^{(0)}_{i_4,o_2}(t_2,t_1^+) G^{(0)}_{i_1,o_3}(t_1,t_2^+) G^{(0)}_{i_6,o_4}(t_3,t_2^+) G^{(0)}_{i_2,o_5}(t_1,t_3^+) G^{(0)}_{i_5,o_6}(t_3,t_3^+) \quad (10.68)$$

10.4 Diagrams of the numerator of the Green's function

10.4.1 Numerator from Wick's theorem

The decomposition Eq. 10.65 of the denominator of the Green's function Eq. 10.59 into Feynman diagrams helps us to determine the diagrammatic expansion of the numerator

$$\mathrm{Tr}\Big\{\hat{\rho}^{(0)}_{T,\mu} \mathcal{T}_{\mathcal{C}} \hat{S}_{I,\mathcal{C}} \hat{c}_{I,\alpha}(t) \hat{c}^+_{I,\beta}(t')\Big\} \quad (10.69)$$

Using $2n+1$ dimensional permutation vector: Following the recipe developed for Wick's theorem, Eq. 10.57, the diagrams in the numerator of the Green's function Eq. 10.59 can be constructed using permutation vectors. Compared to the diagrams of order n in the denominator, there is one additional pair of operators in the numerator. The diagrams of order n in the numerator can then be described by a $2n+1$ dimensional permutation vector. The additional creation operator $\hat{c}^+_{I,\beta}(t')$ is treated together with the outgoing indices, that is $(\beta, t') = o_{2n+1}$. The annihilation operator $\hat{c}_{I,\alpha}(t)$ with index α, is treated together with the incoming indices, that is (α, t).

The two operators $\hat{c}^+_{I,\beta}(t')$ and $\hat{c}_{I,\alpha}(t)$, , which are not connected to the interaction, are described as **external vertices**. Unlike the vertices connected to the interaction, only one Green's function is connected to an external vertex. We may describe the external indices of the Green's function also **half vertex** in the sense that each half of a vertex is connected to one end of a Green's function.

The table connecting outgoing and incoming indices is

o_j	1	2	...	$2n$	$2n+1$
i_j	$\mathcal{P}_1$	$\mathcal{P}_2$	...	$\mathcal{P}_{2n}$	$\mathcal{P}_{2n+1}$

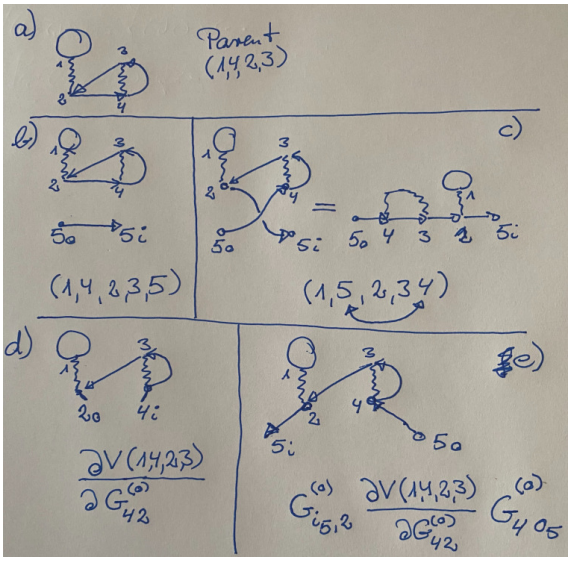


Fig. 10.4: Sketches to demonstrate the construction of diagrams in the numerator from those in the denominator.

Use the permutation vector of the denominator: Instead of constructing the $2n+1$ dimensional permutation vectors from scratch, they can be constructed from the $2n$ dimensional permutation vectors used for the denominator.

We pick one diagram from the expansion of the denominator as parent diagram for a subset of diagrams for the numerator. The parent diagram is identified by a $2n$-dimensional permutation vector $\vec{\mathcal{P}}_{\text{parent}}$. An example is given in figure 10.4.a for $\mathcal{P} = (1, 4, 2, 3)$.

- We begin with one diagram for the numerator, which consists of the parent diagram and a non-interacting Green's function line pointing directly from $o_{2n+1} = (\beta, t')$ to $i_{2n+1} = (\alpha, t)$. It is described by

o_j	1	2	...	$2n$	$2n+1$
i_j	$\mathcal{P}_1$	$\mathcal{P}_2$	...	$\mathcal{P}_{2n}$	$2n+1$

  For our example with parent $\mathcal{P} = (1, 4, 2, 3)$, this diagram is sketched in figure 10.4.b.

- The remaining $2n$ diagrams derived from the selected parent diagram are obtained by removing one Green's function line from the parent diagram, as shown in figure 10.4.d. This leaves one unconnected outgoing vertex o_j and one unconnected incoming index $i_{\mathcal{P}_j}$. Now, we attach one Green's function line connecting the unconnected outgoing index o_j with to the external vertex $\alpha = i_{n+1}$. Then, the we attach a further Green's function line connecting the external index $\beta = o_{n+1}$ to the unconnected incoming index $i_{\mathcal{P}_j}$. This is sketched in figure 10.4.c and e.

  Translated into the language of permutation vectors $\vec{\mathcal{P}}$, the last incoming index i_{2n+1} is exchanged with any of the other incoming indices. For each $j \in \{1, \ldots, 2n\}$, we obtain a permutation vector of the type

o_j	1	⋯	j	⋯	$2n$	$2n+1$
i_j	$\mathcal{P}_1$	⋯	$2n+1$	⋯	$\mathcal{P}_{2n}$	$\mathcal{P}_j$

This procedure produces $2n+1$ diagrams for the numerator out of each diagram in the denominator. This is exactly the number of terms we obtain by increasing the dimension of the permutation vector

by 1, confirming that all diagrams are considered. For our example, the resulting diagrams are shown, together with the corresponding parent diagram, in figure 10.5.

We need to ensure that (1) this procedure constructs all $2n+1$ dimensional permutation vectors from the $2n$ dimensional permutation vectors and that (2) no diagram is constructed twice.

- The proof that no diagram is constructed twice needs to show that none of the $2n+1$ dimensional permutation vectors is obtained from two different $2n$ dimensional permutation vectors. This is shown by giving a recipe to reconstruct the corresponding parent permutation vector. The recipe is to exchange the component with the highest value $\mathcal{P}_j = 2n+1$ with the value $\mathcal{P}_{2n+1}$ in the last position. This unique procedure produces the parent permutation vector on the first $2n$ components.
- The permutation vectors resulting from one parent diagram are distinguishable by the position of the index j of the component with $\mathcal{P}_j = 2n+1$.
- given that no two diagrams are constructed twice, we can show that all diagrams are constructed by counting the number $(2n+1)$ of additional diagrams.

Example: Let me demonstrate the construction using one second-order diagram of the denominator as example.

The permutation vector of the parent diagram is $\vec{\mathcal{P}} = (1,4,2,3)$

o_j	1	2	3	4
i_j	1	4	2	3

The first diagram derived from the diagram above is characterized by the permutation vector $\vec{\mathcal{P}} = (1,4,2,3,5)$. As described above the last entry connects the two external vertices. Thus, this diagram simply adds a **bare Green's-function line** [8] connecting the two external indices to the diagram of the denominator.

The other $2n$ permutation vectors are obtained by exchanging any of the $2n$ outgoing indices with the last one. In total, we obtain the permutation vectors

$$\begin{aligned}
\vec{\mathcal{P}} &= (\mathbf{5},4,2,3,\mathbf{1}) \\
\vec{\mathcal{P}} &= (1,\mathbf{5},2,3,\mathbf{4}) \\
\vec{\mathcal{P}} &= (1,4,\mathbf{5},3,\mathbf{2}) \\
\vec{\mathcal{P}} &= (1,4,2,\mathbf{5},\mathbf{3}) \\
\vec{\mathcal{P}} &= (1,4,2,3,\mathbf{5})
\end{aligned} \tag{10.70}$$

The j-th permutation vector has the incoming vertex on the j-th position.

10.4.2 Numerator from functional derivative of denominator

Editor: Show first, how the procedure is related to the graphical construction. Then show how the graphical construction translates step by step into the expression below.

The procedure just outlined can be related to an equation using functional derivatives of the parent diagram.

- We begin from specific parent diagram from the denominator such as the one shown in the upper left of Fig. 10.5. The diagram is specified by the permutation vector $\vec{\mathcal{P}}_{\text{parent}}$. For our example, the permutation vector of the parent diagram is $\vec{\mathcal{P}}_{\text{parent}} = (1,4,2,3)$. The diagram is considered as a functional of the bare (non-interacting) Green's function.

[8] A non-interacting Green's function is also called a bare Green's function.

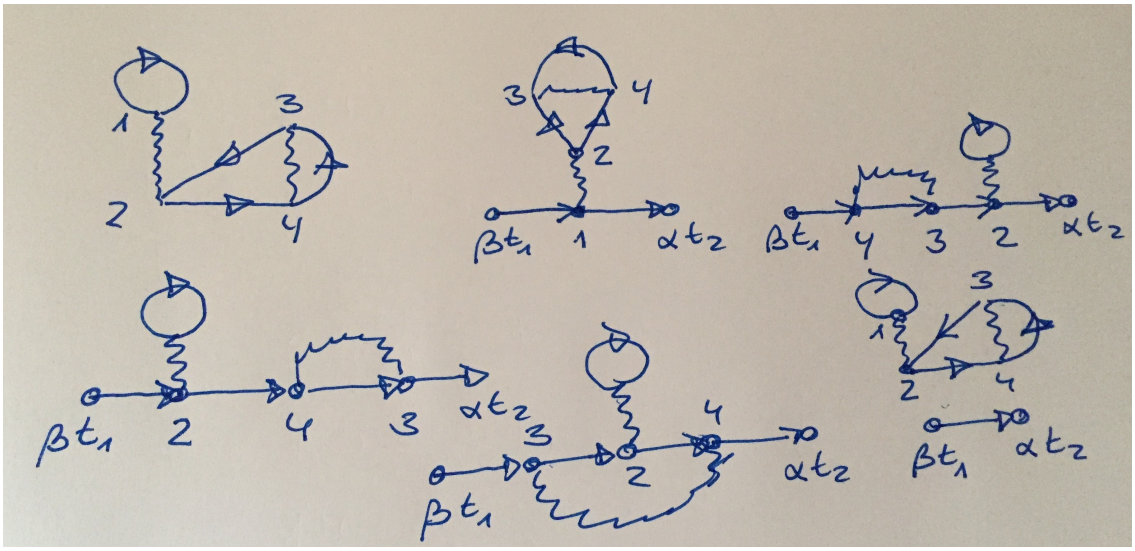


Fig. 10.5: Example for the construction of the diagrams in the numerator of the Green's function from those in the denominator. The diagram in the upper left shows a second-order diagram of the denominator, which is described by the permutation vector $\vec{\mathcal{P}} = (1, 4, 2, 3)$. The other diagrams are obtained by connecting one of the internal indices with the outgoing external index and by connecting the incoming external index to the no open vertex position. In the last diagram the two external vertices are directly connected.

- one of the derived diagrams is the parent diagram combined with a bare Green's function connecting the external vertices. The value of this diagram Eq. 10.66[9] There is no sign change, because all permutation are those of the parent diagram, while the last Green's function is simply attached to the end of its permutation vector.

- the removal of bare Green's functions $G^{(0)}_{\alpha,\beta}(t, t')$ from the parent diagram can be expressed by a functional derivative of the value $\mathcal{V}(\vec{\mathcal{P}})$ of the parent diagram

$$d\mathcal{V}[\vec{\mathcal{P}}] = \sum_{\delta,\gamma} \int_{\mathcal{C}} dt' \int_{\mathcal{C}} dt'' \, \frac{\delta \mathcal{V}(\vec{\mathcal{P}})}{\delta G^{(0)}_{\delta,\gamma}(t', t'')} dG^{(0)}_{\delta,\gamma}(t', t'') \tag{10.71}$$

  For each parent diagram of order n, this expression leads to a sum of $2n$ diagrams. Each is obtained by replacing one bare Green's functions at a time by its variation $dG^{(0)}$.

- Connecting the external indices (α, t) and (β, t') implies to replace

$$dG^{(0)}_{\delta,\gamma}(t', t'') \qquad \text{by} \qquad G^{(0)}_{\alpha,\gamma}(t_2, t'') G^{(0)}_{\delta,\beta}(t', t_1) \tag{10.72}$$

- Combining all $2n+1$ diagrams derived from the same parent diagram $\mathcal{V}(\vec{\mathcal{P}})$ yields

$$\underbrace{\mathcal{V}(\vec{\mathcal{P}})}_{\text{parent}} \rightsquigarrow \underbrace{i\hbar G^{(0)}_{\alpha,\beta}(t_2, t_1)\mathcal{V}(\vec{\mathcal{P}})}_{\text{"first term"}} \underbrace{-i\hbar \sum_{\gamma,\delta} \int dt' \int dt'' \, G^{(0)}_{\alpha,\gamma}(t_2, t'') \frac{\delta \mathcal{V}(\vec{\mathcal{P}})}{\delta G^{(0)}_{\delta,\gamma}(t', t'')} G^{(0)}_{\delta,\beta}(t', t_1)}_{\text{"second term"}} \tag{10.73}$$

[9] We use the same expression Eq. 10.66 for value of closed diagrams also for the **open diagrams**[10] This choice is consistent with Eq. 10.57.

The right-hand side is the sum of the values of all diagrams derived from the corresponding parent diagram on the left-hand side.

The minus sign results from the fact that each diagram in the second term is obtained from the diagram in the first term by one permutation of two elements of the permutation vector. (see Eq. 10.57.)

This implies that the diagrams for the numerator are obtained as derivative of the diagrams in the denominator with respect to a non-interacting Green's function.

$$\mathrm{Tr}\Big\{\hat{\rho}^{(0)}_{T,\mu}\mathcal{T}_{\mathcal{C}}\hat{S}_{I,\mathcal{C}}\Big\} = \sum_{n=0}^{\infty}\sum_{\vec{\mathcal{P}}\in\mathbb{A}_n}\frac{1}{n!2^n}\mathcal{V}(\vec{\mathcal{P}}) \tag{10.74}$$

$$\begin{aligned}
&\rightsquigarrow \quad \mathrm{Tr}\Big\{\hat{\rho}^{(0)}_{T,\mu}\mathcal{T}_{\mathcal{C}}\hat{S}_{I,\mathcal{C}}\hat{c}_{I,\alpha}(t_2)\hat{c}^{+}_{I,\beta}(t_1)\Big\}\\
&\overset{\text{Eq. }10.73}{=} \sum_{n=0}^{\infty}\sum_{\vec{\mathcal{P}}\in\mathbb{A}_n}\frac{1}{n!2^n}\, i\hbar\left[G^{(0)}_{\alpha,\beta}(t_2,t_1)\mathcal{V}(\vec{\mathcal{P}}) - \sum_{\gamma,\delta}\int dt'\int dt''\, G^{(0)}_{\alpha,\gamma}(t_2,t'')\frac{\partial\mathcal{V}(\vec{\mathcal{P}})}{\partial G^{(0)}_{\delta,\gamma}(t',t'')}G^{(0)}_{\delta,\beta}(t',t_1)\right]\\
&= \quad i\hbar\left[G^{(0)}_{\alpha,\beta}(t_2,t_1)\mathrm{Tr}\Big\{\hat{\rho}^{(0)}_{T,\mu}\mathcal{T}_{\mathcal{C}}\hat{S}_{I,\mathcal{C}}\Big\} - \sum_{\gamma,\delta}\int dt'\int dt''\, G^{(0)}_{\alpha,\gamma}(t_2,t'')\frac{\partial\mathrm{Tr}\Big\{\hat{\rho}^{(0)}_{T,\mu}\mathcal{T}_{\mathcal{C}}\hat{S}_{I,\mathcal{C}}\Big\}}{\partial G^{(0)}_{\delta,\gamma}(t',t'')}G^{(0)}_{\delta,\beta}(t',t_1)\right]
\end{aligned} \tag{10.75}$$

Insertion into the expression for the Green's function Eq. 10.59, yields[11]

$$\begin{aligned}
G_{\alpha,\beta}(t,t') &\overset{\text{Eq. }10.59}{=} \frac{1}{i\hbar}\frac{\mathrm{Tr}\Big\{\hat{\rho}^{(0)}_{T,\mu}\mathcal{T}_{\mathcal{C}}\hat{S}_{I,\mathcal{C}}\hat{c}_{I,\alpha}(t)\hat{c}^{+}_{I,\beta}(t')\Big\}}{\mathrm{Tr}\Big\{\hat{\rho}^{(0)}\mathcal{T}_{\mathcal{C}}\hat{S}_{I,\mathcal{C}}\Big\}}\\
&\overset{\text{Eq. }10.75}{=} G^{(0)}_{\alpha,\beta}(t_2,t_1) + \sum_{\gamma,\delta}\int dt'\int dt''\, G^{(0)}_{\alpha,\gamma}(t_2,t'')\frac{\partial\left(-\ln\mathrm{Tr}\Big\{\hat{\rho}^{(0)}_{T,\mu}\mathcal{T}_{\mathcal{C}}\hat{S}_{I,\mathcal{C}}\Big\}\right)}{\partial G^{(0)}_{\delta,\gamma}(t',t'')}G^{(0)}_{\delta,\beta}(t',t_1)
\end{aligned} \tag{10.76}$$

Eq. 10.76 is an important result: There is one functional of the bare Green's function, namely $\mathcal{Q}_{T,\mu}$ which provides the interacting Green's function.

[11] $\frac{1}{x}\frac{dy}{dx} = \frac{d\ln(y(x))}{dx}$.

GREEN'S FUNCTION FROM A FUNCTIONAL

The one-particle Green's function is completely defined by a functional[a] $\mathcal{Q}$ of the non-interacting Green's function

$$\mathcal{Q}_{T,\mu}[\boldsymbol{G}^{(0)}] \stackrel{\text{def}}{=} -k_B T \ln \mathrm{Tr}\left\{\hat{\rho}^{(0)}_{T,\mu}\mathcal{T}_{\mathcal{C}}\hat{S}_{I,\mathcal{C}}\right\} \stackrel{\text{Eq. } 10.65}{=} -\frac{1}{\beta}\ln\left[\sum_{n=0}^{\infty}\frac{1}{n!}\sum_{\vec{\mathcal{P}}\in\mathbb{A}_n}\frac{1}{2^n}\mathcal{V}(\vec{\mathcal{P}})\right] \tag{10.77}$$

where $\beta = 1/(k_B T)$. With $\vec{\mathcal{P}} \in \mathbb{A}_n$, I denote all permutation vectors of length $2n$, with components that are permutations of $(1, 2, \ldots, 2n)$.
The non-interacting Green's function is specified on a time-contour $\mathcal{C}$. The functional furthermore depends on the interaction matrix elements, which can be time dependent along the contour.
The functional derivative specifies the Green's function via Dyson's equation

$$\begin{aligned} G_{\alpha,\beta}(t_2,t_1) &\stackrel{\text{Eq. } 10.76}{=} G^{(0)}_{\alpha,\beta}(t_2,t_1) + \sum_{\gamma,\delta}\int_{\mathcal{C}} dt_4 \int_{\mathcal{C}} dt_3\, G^{(0)}_{\alpha,\gamma}(t_2,t_4)\underbrace{\frac{1}{k_B T}\frac{\delta \mathcal{Q}_{T,\mu}[G^{(0)},W]}{\delta G^{(0)}_{\delta,\gamma}(t_3,t_4)}}_{=:\Sigma^{\text{red}}_{\gamma,\delta}(t_4,t_3)} G^{(0)}_{\delta,\beta}(t_3,t_1) \\ &\stackrel{\text{Eq. } 10.79}{=} G^{(0)}_{\alpha,\beta}(t_2,t_1) + \sum_{\gamma,\delta}\int_{\mathcal{C}} dt_4 \int_{\mathcal{C}} dt_3\, G^{(0)}_{\alpha,\gamma}(t_2,t_4)\Sigma^{\text{red}}_{\gamma,\delta}(t_4,t_3)G^{(0)}_{\delta,\beta}(t_3,t_1) \end{aligned} \tag{10.78}$$

The self energy

$$\hat{\Sigma}^{red}(t,t') \stackrel{\text{def}}{=} \sum_{\alpha,\beta}|\pi_\alpha\rangle \frac{1}{k_B T}\frac{\delta \mathcal{Q}_{T,\mu}[G^{(0)},W]}{\delta G^{(0)}_{\beta,\alpha}(t',t)}\langle\pi_\beta| \tag{10.79}$$

is the so-called **reducible self energy** , which differs from the self energy used earlier.
With $\langle\pi_\alpha|$, I denote the projector function corresponding to the local basis function $\langle\chi_\alpha|$. The Green's function has the form $\hat{G}(t,t') = \sum_{\alpha,\beta}|\chi_\alpha\rangle G_{\alpha,\beta}(t,t')\langle\chi_\beta|$. The biorthogonality $\langle\pi_\alpha|\chi_\beta\rangle = \delta_{\alpha,\beta}$ holds.

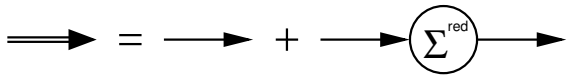
[a] This functional is identical to $\Phi_r[G]$ Stefanucci and van Leeuwen[2]. See their Eqs. 11.12-11.13

Table 10.1: Terminology for Green's functions and self energies. *"Irreducible"* stands here for **one-particle irreducible (1PI)**, which means that the corresponding diagram does not fall apart by removing any single particle line (Green's function). The reducible self energy Σ^{red} contains also irreducible diagrams and should actually be named *"reducible and irreducible"*, which I have not heard so-far. However, I encountered the naming *"proper and improper diagrams"*.

Terminology	
$\hat{G}(t,t')$	**full** Green's function, **dressed** G.f., **interacting** G.f.
$\hat{G}^{(0)}(t,t')$	**bare** Green's function, **non-interacting** G.f.
$\hat{\Sigma}^{\text{red}}(t,t')$	**reducible** self energy, (proper and) **improper** s.e.
$\hat{\Sigma}(t,t')$	**proper** self energy, **irreducible** s.e., **1PI** s.e.

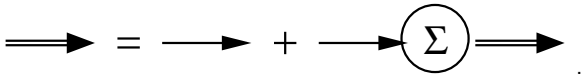
Reducible (improper) and irreducible (proper) self energy: The reducible self energy Eq. 10.79 differs from the self energy defined earlier in Eq. 8.15 on p. 269 (and in Eq. 5.34 on p. 195).

Eq. 10.78, which has the diagrammatic form



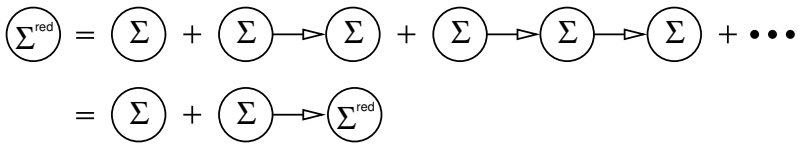
$$\hat{G}(t_2,t_1) = \hat{G}^{(0)}(t_2,t_1) + \int dt' \int dt''\, \hat{G}^{(0)}(t_2,t'')\hat{\Sigma}^{\text{red}}(t'',t')\hat{G}^{(0)}(t',t_1) \tag{10.80}$$

reminds of Dyson's equation Eq. 8.23 on p. 270.



$$\hat{G}(t_2,t_1) \overset{\text{Eq. 8.23}}{=} \hat{G}^{(0)}(t_2,t_1) + \int dt' \int dt''\, \hat{G}^{(0)}(t_2,t'')\hat{\Sigma}(t'',t')\hat{G}(t',t_1) \tag{10.81}$$

When we iterate Dyson's equation by repeatedly inserting Dyson's equation for the full Green's function on the right hand side [12], it becomes identical to the equation above, when we identify the reducible self energy with



Expressed with explicit time arguments, the self energies obey

$$\hat{\Sigma}^{\text{red}}(t_2,t_1) = \hat{\Sigma}(t_2,t_1) + \int dt \int dt'\, \hat{\Sigma}(t_2,t)\hat{G}^{(0)}(t,t')\hat{\Sigma}^{red}(t',t_1) \tag{10.83}$$

Proper self energy from the generating functional It may be tempting to obtain the proper self energy by removing all one-particle-reducible self-energy diagrams from the reducible self energy. This is a valid procedure for the exact generating functional, but it is not allowed for approximate ones.[13] This is unfortunate, because the generating functional is often used to arrive at consistent approximations.

[12] Let me work out the relation between proper and total self energy by comparing Dyson's equation with Eq. 10.78. I write the Green's function and self energies here as operators in one-particle Hilbert space and I suppress the time arguments. As shown below, each product also implies an integration of the common time argument.

$$\begin{aligned}
\boldsymbol{G} &\overset{\text{Eq. 8.23}}{=} \boldsymbol{G}^{(0)} + \boldsymbol{G}^{(0)}\boldsymbol{\Sigma}\boldsymbol{G} \\
&= \boldsymbol{G}^{(0)} + \boldsymbol{G}^{(0)}\boldsymbol{\Sigma}\underbrace{\left(\boldsymbol{G}^{(0)} + \boldsymbol{G}^{(0)}\boldsymbol{\Sigma}\boldsymbol{G}\right)}_{\boldsymbol{G}} \\
&= \boldsymbol{G}^{(0)} + \boldsymbol{G}^{(0)}\boldsymbol{\Sigma}\boldsymbol{G}^{(0)} + \boldsymbol{G}^{(0)}\boldsymbol{\Sigma}\boldsymbol{G}^{(0)}\boldsymbol{\Sigma}\underbrace{\left(\boldsymbol{G}^{(0)} + \boldsymbol{G}^{(0)}\boldsymbol{\Sigma}\boldsymbol{G}\right)}_{\boldsymbol{G}} \\
&= \boldsymbol{G}^{(0)} + \boldsymbol{G}^{(0)}\underbrace{\left(\boldsymbol{\Sigma} + \boldsymbol{\Sigma}\boldsymbol{G}^{(0)}\boldsymbol{\Sigma} + \boldsymbol{\Sigma}\boldsymbol{G}^{(0)}\boldsymbol{\Sigma}\boldsymbol{G}^{(0)}\boldsymbol{\Sigma} + \ldots\right)}_{\boldsymbol{\Sigma}^{\text{red}}}\boldsymbol{G}^{(0)} \\
&\overset{!}{=} \boldsymbol{G}^{(0)} + \boldsymbol{G}^{(0)}\boldsymbol{\Sigma}^{\text{red}}\boldsymbol{G}^{(0)} \qquad \text{compare with Eq. 10.78}
\end{aligned} \tag{10.82}$$

[13] When we collect all 1PI diagrams from a given approximate reducible self energy to form an approximate proper self energy, it is not guaranteed that the original reducible self energy can be regenerated from the resulting proper self energy by Dyson's equation.

$$\Sigma^{red} = \Sigma + \Sigma G^{\mathcal{C},(0)}\Sigma^{red} \tag{10.84}$$

Thus, the proper self energy constructed by removing reducible diagrams is not necessarily consistent with the generating functional, which defined the approximation in the first place. As a possible remedy, one may use Dyson's equation with the proper self energy just obtained to define (another) reducible energy and its corresponding generating functional This is a valid but different approximation.

Rather than by selecting 1PI diagrams from the reducible self energy, the proper self energy must be obtained from the reducible self energy using Dyson's equation. In a short-hand notation[14], this implies

$$\begin{aligned} \Sigma^{red} &\overset{\text{Eq. } 10.83}{=} \Sigma + \Sigma G^{\mathcal{C},(0)} \Sigma^{red} = \Sigma \Big(1 + G^{\mathcal{C},(0)} \Sigma^{red} \Big) \\ \Rightarrow \qquad \Sigma \quad &= \quad \Sigma^{red} \Big(1 + G^{\mathcal{C},(0)} \Sigma^{red} \Big)^{-1} = \Sigma^{red} \sum_{n=0}^{\infty} \Big(-G^{\mathcal{C},(0)} \Sigma^{red} \Big)^n \end{aligned} \tag{10.85}$$

This is itself a Dyson's equation for the proper self energy Σ, which must be solved iteratively. It produces an infinite number of terms, even if the generating functional is approximated by a few terms. Truncating this Dyson's equation will lead to yet another approximation, which has a complicated generating functional, reducible self energy and Green's function.

The construction of a generating functional for the proper self energy rather than the reducible self energy is the topic of chapter 12 on the **Luttinger-Ward functional**.

Generating functional $\mathcal{Q}_{T,\mu}$ from the reducible self energy: We just learned that the reducible self energy can be obtained from the generating functional $\mathcal{Q}_{T,\mu}[G^{\mathcal{C},(0)}]$. The reverse is also true, albeit with an additional complication: We need to know the self energy divided into individual orders of the interaction.

If we close a diagram of the reducible self energy with a non-interacting Green's function, we obtain a closed diagram, namely the parent diagram from which the specific self-energy diagram has been obtained. However, a diagram of the generating functional produces $2n$ self-energy diagrams, because the diagram is a product of $2n$ Green's functions. Thus, we overcount diagrams when we add up all self-energy diagrams after closing them.

Let me divide the self energy into powers of the interaction

$$\hat{\Sigma}^{red} = \sum_{n=1}^{\infty} \hat{\Sigma}^{red,(n)} \tag{10.86}$$

where $\hat{\Sigma}^{red,(n)}$ is the contribution of n-th order in the interaction.

With the reducible self energy available in individual orders of the interaction allows one to reconstruct the generating functional as

$$\mathcal{Q}_{T,\mu}[G^{\mathcal{C},(0)}] = \sum_{n=1}^{\infty} \frac{1}{2n} \int_{\mathcal{C}} dt \int_{\mathcal{C}} dt' \; \Sigma^{red,(n)}_{\alpha,\beta}(t,t') G^{\mathcal{C},(0)}_{\beta,\alpha}(t',t) \tag{10.87}$$

If the approximation is defined via a proper self energy, the corresponding reducible self energy need to be constructed first via Dyson's equation, before the generating functional $\mathcal{Q}[\boldsymbol{G}^{(0)}]$ can be obtained.

The reconstruction of the generating functional may be useful in order to arrive at a consistent theory from an approximate reducible self energy.

Relation to the grand potential: This functional $\mathcal{Q}[\boldsymbol{G}^{(0)}]$, is closely related to the **grand potential**. It is the interaction part of the grand potential, namely $\mathcal{Q}_{T,\mu} = \Omega^{(W)}_{T,\mu} - \Omega^{(0)}_{T,\mu}$. The close relation of $\mathcal{Q}[\boldsymbol{G}^{(0)}]$ with the grand potential has been the reason for adding the factor $k_B T$ in the definition of the grand potential $\mathcal{Q}_{T,\mu}$.

The grand potential of the interacting system is given in Eq. 10.26 on p. 316.

$$\Omega^{(W)}_{T,\mu} \overset{\text{Eq. } 10.26}{=} \Omega^{(0)}_{T,\mu} \underbrace{-k_B T \ln \Big(\mathrm{Tr} \Big\{ \hat{\rho}^{(0)}_{T,\mu} \mathcal{T}_{\mathcal{C}} \hat{\mathcal{S}}_{I,\mathcal{C}} \Big\} \Big)}_{\mathcal{Q}_{T,\mu} \quad \text{Eq. } 10.77} \tag{10.88}$$

[14] In this notation, a product involves a sum over orbital indices and a time integral.

The grand potential of the non-interacting electron gas has been expressed as functional of the non-interacting Green's function in Eq. L.120 from p. 728.

$$\Omega^{(W)}_{T,\mu} \overset{\text{Eq. } 10.26}{=} \underbrace{+k_B T \,\mathrm{Tr}\left\{\ln\left[i\hbar \lim_{t'\to t^+} \hat{G}^{(0)}(t',t)\right]\right\}}_{\Omega^{(0)}_{T,\mu}[\boldsymbol{G}^{(0)}]} \underbrace{-k_B T \ln\left(\mathrm{Tr}\left\{\hat{\rho}^{(0)}_{T,\mu}\mathcal{T}_{\mathcal{C}}\hat{\mathcal{S}}_{I,\mathcal{C}}\right\}\right)}_{\mathcal{Q}_{T,\mu} \quad \text{Eq. } 10.77} \tag{10.89}$$

In the remainder of this chapter, we will concentrate entirely on how to determine the functional $\mathcal{Q}(\boldsymbol{G}^{(0)})$.

Editor: In this section, we could also show that

$$G^W = \frac{\delta\Omega}{\delta(G^{(0)})^{-1}} \tag{10.90}$$

. However, this grand potential contains also the one without interaction.

10.5 Home study and practice

10.5.1 Green's function from generating functional

Introduction

Editor: The term generating functional needs to be properly explained. It must be clear that this generates the reducible self energy and not the correlation functions.

In this problem, we practice the calculation of the Green's function from the generating functional. To simplify matters, only a single diagram is considered in the generating functional. An expression for the generating functional used here, will emerge only in the following chapter through the linked-cluster theorem.

The linked-cluster theorem provides the generating functional in terms of linked diagrams $D \in \mathbb{L}$ as

$$\mathcal{Q}_{T,\mu}[G^{(0)}] \overset{\text{Eq. } 11.17}{=} -\frac{1}{\beta}\sum_{n=1}^{\infty}\sum_{D\in\mathbb{L}_n}\frac{\mathcal{V}(D)}{n!2^n} \tag{10.91}$$

where the logarithm is absent.

Problem

Calculate the Green's function from a specific generating functional $\bar{\mathcal{Q}}_{T,\mu}[G^{(0)}]$, namely

$$\bar{\mathcal{Q}}_{T,\mu}[G^{\mathcal{C}(0)}] = -\frac{1}{\beta}\frac{\mathcal{V}(D)}{n!2^n} \tag{10.92}$$

To simplify the task, only a single diagram D contributes to this generating functional, which is specified by the permutation vector $\vec{\mathcal{P}} = (1,4,2,3)$. I use the bar on-top of the symbol for the generating functional to distinguish it from the correct, general functional.
Caution: Using one diagram in the expression obtained so far, i.e. in Eq. 10.77, is much more difficult and it leads to a different result than using the form obtained after the linked-cluster theorem Eq. 11.17.

1 Write down the value of the diagram D with $\mathcal{P} = (1,4,2,3)$ as functional of the bare Green's function and the interaction tensor.

2 Use the result to write down $\bar{\mathcal{Q}}_{T,\mu}[G^{\mathcal{C},(0)}]$

3 extract the reducible self energy from $\bar{\mathcal{Q}}_{T,\mu}[G^{\mathcal{C},(0)}]$. It is advisable to identify the expressions for Hartree and exchange potential in order to make the expressions more compact.

4 construct the Green's function from $\bar{\mathcal{Q}}_{T,\mu}[G^{\mathcal{C},(0)}]$.

5 Draw the Feynman diagrams for

- the generating functional $\bar{\mathcal{Q}}_{T,\mu}[G^{\mathcal{C},(0)}]$
- the reducible self energy Σ^{red}
- the Green's function $G^{\mathcal{C}}$

Discussion

1 Write down the value of the diagram D with $\mathcal{P} = (1,4,2,3)$ as functional of the bare Green's function and the interaction tensor.

Let me work out the Green's function from a generating functional, which consists out of only a single Feynman diagram, namely the closed diagram in figure 10.5. The diagram belongs to the permutation vector $\mathcal{P} = (1,4,2,3)$.

First, we need to write out the value of the diagram itself

$$\begin{aligned}
\mathcal{V}(\vec{\mathcal{P}}) &\overset{\text{Eq. 10.66}}{=} \epsilon_{\mathcal{P}_1,\ldots,\mathcal{P}_{2n}}(i\hbar)^n \int_{\mathcal{C}} dt_1 \cdots \int_{\mathcal{C}} dt_{2n} \sum_{o_1,i_1,\ldots,o_{2n},i_{2n}} \left(\prod_{j=1}^{n} W_{o_{2j-1},o_{2j},i_{2j-1},i_{2j}} \delta_{\mathcal{C}}(t_{2j-1}-t_{2j})\right) \\
&\quad \times G^{\mathcal{C},(0)}_{i_{\mathcal{P}_1},o_1}(t_{\mathcal{P}_1},t_1^+)\cdots G^{\mathcal{C},(0)}_{i_{\mathcal{P}_{2n}},o_{2n}}(t_{\mathcal{P}_{2n}},t_{2n}^+) \\
&\overset{\vec{\mathcal{P}}=(1423)}{=} \underbrace{\epsilon_{1,4,2,3}}_{=+1}\underbrace{(i\hbar)^2}_{-\hbar^2}\int_{\mathcal{C}} dt_1 \cdots \int_{\mathcal{C}} dt_4 \sum_{o_1,i_1,\ldots,o_4,i_4} W_{o_1,o_2,i_1,i_2}\delta_{\mathcal{C}}(t_1-t_2) W_{o_3,o_4,i_3,i_4}\delta_{\mathcal{C}}(t_3-t_4) \\
&\quad \times G^{\mathcal{C},(0)}_{i_1,o_1}(t_1,t_1^+) G^{\mathcal{C},(0)}_{i_4,o_2}(t_4,t_2^+) G^{\mathcal{C},(0)}_{i_2,o_3}(t_2,t_3^+) G^{\mathcal{C},(0)}_{i_3,o_4}(t_3,t_4^+) \\
&= -\hbar^2 \sum_{o_1,i_1,\ldots,o_4,i_4} W_{o_1,o_2,i_1,i_2} W_{o_3,o_4,i_3,i_4} \\
&\quad \times \int_{\mathcal{C}} dt_1 \int_{\mathcal{C}} dt_3\, G^{\mathcal{C},(0)}_{i_1,o_1}(t_1,t_1^+) G^{\mathcal{C},(0)}_{i_4,o_2}(t_3,t_1^+) G^{\mathcal{C},(0)}_{i_2,o_3}(t_1,t_3^+) G^{\mathcal{C},(0)}_{i_3,o_4}(t_3,t_3^+)
\end{aligned} \tag{10.93}$$

2 Use the result to write down $\bar{\mathcal{Q}}_{T,\mu}[G^{\mathcal{C},(0)}]$

For our specific example we use just one diagram so that

$$\begin{aligned}\bar{\mathcal{Q}}_{T,\mu}[G^{(0)}] &= -\frac{1}{\beta}\frac{\mathcal{V}(\overbrace{\vec{\mathcal{P}}}^{(1,4,2,3)})}{8} \\ &\overset{\text{Eq. 10.93}}{=} \frac{\hbar^2}{8\beta}\sum_{o_1,i_1,\ldots,o_4,i_4} W_{o_1,o_2,i_1,i_2}W_{o_3,o_4,i_3,i_4} \\ &\quad\times\int_{\mathcal{C}} dt_1\int_{\mathcal{C}} dt_3\; G^{\mathcal{C},(0)}_{i_1,o_1}(t_1,t_1^+)G^{\mathcal{C},(0)}_{i_4,o_2}(t_3,t_1^+)G^{\mathcal{C},(0)}_{i_2,o_3}(t_1,t_3^+)G^{\mathcal{C},(0)}_{i_3,o_4}(t_3,t_3^+)\end{aligned} \tag{10.94}$$

3 extract the reducible self energy from $\bar{\mathcal{Q}}_{T,\mu}[G^{\mathcal{C},(0)}]$. It is advisable to identify the expressions for Hartree and exchange potential in order to make the expressions more compact.

Let me first work out the corresponding reducible self energy. I start with the first variation of the functional $\mathcal{Q}_{T,\mu}$ with respect to changes of the non-interacting Green's function.

$$\begin{aligned}d\bar{\mathcal{Q}}_{T,\mu} &= \frac{1}{8}k_BT\hbar^2\sum_{o_1,i_1,\ldots,o_4,i_4} W_{o_1,o_2,i_1,i_2}W_{o_3,o_4,i_3,i_4}\int_{\mathcal{C}} dt_1\int_{\mathcal{C}} dt_3 \\ &\quad\times\Big\{dG^{\mathcal{C},(0)}_{i_1,o_1}(t_1,t_1^+)G^{\mathcal{C},(0)}_{i_4,o_2}(t_3,t_1^+)G^{\mathcal{C},(0)}_{i_2,o_3}(t_1,t_3^+)G^{\mathcal{C},(0)}_{i_3,o_4}(t_3,t_3^+) \\ &\quad+G^{\mathcal{C},(0)}_{i_1,o_1}(t_1,t_1^+)dG^{\mathcal{C},(0)}_{i_4,o_2}(t_3,t_1^+)G^{\mathcal{C},(0)}_{i_2,o_3}(t_1,t_3^+)G^{\mathcal{C},(0)}_{i_3,o_4}(t_3,t_3^+) \\ &\quad+G^{\mathcal{C},(0)}_{i_1,o_1}(t_1,t_1^+)G^{\mathcal{C},(0)}_{i_4,o_2}(t_3,t_1^+)dG^{\mathcal{C},(0)}_{i_2,o_3}(t_1,t_3^+)G^{\mathcal{C},(0)}_{i_3,o_4}(t_3,t_3^+) \\ &\quad+G^{\mathcal{C},(0)}_{i_1,o_1}(t_1,t_1^+)G^{\mathcal{C},(0)}_{i_4,o_2}(t_3,t_1^+)G^{\mathcal{C},(0)}_{i_2,o_3}(t_1,t_3^+)dG^{\mathcal{C},(0)}_{i_3,o_4}(t_3,t_3^+)\Big\} \\ &= \frac{1}{8}k_BT\hbar^2\sum_{\delta,\gamma}\sum_{o_1,i_1,\ldots,o_4,i_4} W_{o_1,o_2,i_1,i_2}W_{o_3,o_4,i_3,i_4}\int_{\mathcal{C}} dt_1\int_{\mathcal{C}} dt_3 \\ &\quad\times\Big\{\delta_{i_1,\delta}\delta_{o_1,\gamma}\delta(t_1-t_a)\delta(t_1^+-t_b)G^{\mathcal{C},(0)}_{i_4,o_2}(t_3,t_1^+)G^{\mathcal{C},(0)}_{i_2,o_3}(t_1,t_3^+)G^{\mathcal{C},(0)}_{i_3,o_4}(t_3,t_3^+) \\ &\quad+G^{\mathcal{C},(0)}_{i_1,o_1}(t_1,t_1^+)\delta_{i_4,\delta}\delta_{o_2,\gamma}\delta(t_3-t_a)\delta(t_1^+-t_b)G^{\mathcal{C},(0)}_{i_2,o_3}(t_1,t_3^+)G^{\mathcal{C},(0)}_{i_3,o_4}(t_3,t_3^+) \\ &\quad+G^{\mathcal{C},(0)}_{i_1,o_1}(t_1,t_1^+)G^{\mathcal{C},(0)}_{i_4,o_2}(t_3,t_1^+)\delta_{i_2,\delta}\delta_{o_3,\gamma}\delta(t_1-t_a)\delta(t_3^+-t_b)G^{\mathcal{C},(0)}_{i_3,o_4}(t_3,t_3^+) \\ &\quad+G^{\mathcal{C},(0)}_{i_1,o_1}(t_1,t_1^+)G^{\mathcal{C},(0)}_{i_4,o_2}(t_3,t_1^+)G^{\mathcal{C},(0)}_{i_2,o_3}(t_1,t_3^+)\delta_{i_3,\delta}\delta_{o_4,\gamma}\delta(t_3-t_a)\delta(t_3^+-t_b)\Big\}dG^{\mathcal{C},(0)}_{\delta,\gamma}(t_a,t_b) \\ &\overset{!}{=} \int_{\mathcal{C}} dt_a\int_{\mathcal{C}} dt_b\sum_{\delta,\gamma}\underbrace{\frac{\delta\mathcal{Q}_{T,\mu}[G^{(0)},W]}{\delta G^{\mathcal{C},(0)}_{\delta,\gamma}(t_a,t_b)}}_{k_BT\Sigma^{\text{red}}_{\gamma,\delta}(t_b,t_a)}dG^{\mathcal{C},(0)}_{\delta,\gamma}(t_a,t_b)\end{aligned} \tag{10.95}$$

The reducible self energy Σ^{red} is

$$
\begin{aligned}
\Sigma^{\text{red}}_{\gamma,\delta}(t_b,t_a) &= \frac{1}{k_B T}\frac{\delta \mathcal{Q}_{T,\mu}[G^{(0)},W]}{\delta G^{\mathcal{C},(0)}_{\delta,\gamma}(t_a,t_b)} \\
&= \frac{\hbar^2}{8}\sum_{o_1,i_1,\ldots,o_4,i_4} W_{o_1,o_2,i_1,i_2}W_{o_3,o_4,i_3,i_4}\int_{\mathcal{C}} dt_1 \int_{\mathcal{C}} dt_3 \\
&\times \Big\{ \delta_{i_1,\delta}\delta_{o_1,\gamma}\delta(t_1-t_a)\delta(t_1^+-t_b)G^{\mathcal{C},(0)}_{i_4,o_2}(t_3,t_1^+)G^{\mathcal{C},(0)}_{i_2,o_3}(t_1,t_3^+)G^{\mathcal{C},(0)}_{i_3,o_4}(t_3,t_3^+) \\
&\quad + G^{\mathcal{C},(0)}_{i_1,o_1}(t_1,t_1^+)\delta_{i_4,\delta}\delta_{o_2,\gamma}\delta(t_3-t_a)\delta(t_1^+-t_b)G^{\mathcal{C},(0)}_{i_2,o_3}(t_1,t_3^+)G^{\mathcal{C},(0)}_{i_3,o_4}(t_3,t_3^+) \\
&\quad + G^{\mathcal{C},(0)}_{i_1,o_1}(t_1,t_1^+)G^{\mathcal{C},(0)}_{i_4,o_2}(t_3,t_1^+)\delta_{i_2,\delta}\delta_{o_3,\gamma}\delta(t_1-t_a)\delta(t_3^+-t_b)G^{\mathcal{C},(0)}_{i_3,o_4}(t_2,t_3^+) \\
&\quad + G^{\mathcal{C},(0)}_{i_1,o_1}(t_1,t_1^+)G^{\mathcal{C},(0)}_{i_4,o_2}(t_3,t_1^+)G^{\mathcal{C},(0)}_{i_2,o_3}(t_1,t_3^+)\delta_{i_3,\delta}\delta_{o_4,\gamma}\delta(t_3-t_a)\delta(t_3^+-t_b)\Big\} \\
&= \frac{\hbar^2}{8}\sum_{o_2,i_2,o_3,o_3,o_4,i_4} W_{\gamma,o_2,\delta,i_2}W_{o_3,o_4,i_3,i_4}\delta(t_a-t_b)\int_{\mathcal{C}} dt_3\; G^{\mathcal{C},(0)}_{i_4,o_2}(t_3,t_a^+)G^{\mathcal{C},(0)}_{i_2,o_3}(t_a,t_3^+)G^{\mathcal{C},(0)}_{i_3,o_4}(t_3,t_3^+) \\
&\quad + \frac{\hbar^2}{8}\sum_{o_1,i_1,i_2,o_3,i_3,o_4} W_{o_1,\gamma,i_1,i_2}W_{o_3,o_4,i_3,\delta}G^{\mathcal{C},(0)}_{i_1,o_1}(t_b,t_b^+)G^{\mathcal{C},(0)}_{i_2,o_3}(t_b,t_a^+)G^{\mathcal{C},(0)}_{i_3,o_4}(t_a,t_a^+) \\
&\quad + \frac{\hbar^2}{8}\sum_{o_1,i_1,o_2,i_3,o_4,i_4} W_{o_1,o_2,i_1,\delta}W_{\gamma,o_4,i_3,i_4}G^{\mathcal{C},(0)}_{i_1,o_1}(t_a,t_a^+)G^{\mathcal{C},(0)}_{i_4,o_2}(t_b,t_a^+)G^{\mathcal{C},(0)}_{i_3,o_4}(t_b,t_b^+) \\
&\quad + \frac{\hbar^2}{8}\sum_{o_1,i_1,o_2,i_2,o_3,o_4,i_4} W_{o_1,o_2,i_1,i_2}W_{o_3,\gamma,\delta,i_4}\delta(t_a-t_b)\int_{\mathcal{C}} dt_1\; G^{\mathcal{C},(0)}_{i_1,o_1}(t_1,t_1^+)G^{\mathcal{C},(0)}_{i_4,o_2}(t_a,t_1^+)G^{\mathcal{C},(0)}_{i_2,o_3}(t_1,t_a^+) \\
&= \frac{\hbar^2}{8}\delta(t_a-t_b)\sum_{o_2,i_2}W_{\gamma,o_2,\delta,i_2}\int_{\mathcal{C}} dt_3 \sum_{o_3,i_4} G^{\mathcal{C},(0)}_{i_2,o_3}(t_a,t_3^+)\underbrace{\Big(\sum_{i_3,o_4} W_{o_3,o_4,i_3,i_4}G^{\mathcal{C},(0)}_{i_3,o_4}(t_3,t_3^+)\Big)}_{\text{open oyster: } \frac{1}{i\hbar}v^{(0)}_{X,o_3,i_4}(t_3)} G^{\mathcal{C},(0)}_{i_4,o_2}(t_3,t_a^+) \\
&\quad + \frac{\hbar^2}{8}\sum_{i_2}\underbrace{\Big(\sum_{o_1,i_1} W_{o_1,\gamma,i_1,i_2}G^{\mathcal{C},(0)}_{i_1,o_1}(t_b,t_b^+)\Big)}_{\text{tadpole: } -\frac{1}{i\hbar}v^{(0)}_{H,\gamma,i_2}(t_b)}\sum_{o_3} G^{\mathcal{C},(0)}_{i_2,o_3}(t_b,t_a^+)\underbrace{\Big(\sum_{i_3,o_4} G^{\mathcal{C},(0)}_{i_3,o_4}(t_a,t_a^+)W_{o_3,o_4,i_3,\delta}\Big)}_{\text{open oyster: } \frac{1}{i\hbar}v^{(0)}_{X,o_3,\delta}(t_a)} \\
&\quad + \frac{\hbar^2}{8}\sum_{o_2,i_4}\underbrace{\Big(\sum_{i_3,o_4} W_{\gamma,o_4,i_3,i_4}G^{\mathcal{C},(0)}_{i_3,o_4}(t_b,t_b^+)\Big)}_{\text{open oyster: } \frac{1}{i\hbar}v^{(0)}_{X,\gamma,o4}(t_b)} G^{\mathcal{C},(0)}_{i_4,o_2}(t_b,t_a^+)\underbrace{\Big(\sum_{o_1,i_1} W_{o_1,o_2,i_1,\delta}G^{\mathcal{C},(0)}_{i_1,o_1}(t_a,t_a^+)\Big)}_{\text{tadpole: } -\frac{1}{i\hbar}v^{(0)}_{H,o_2,\delta}(t_a)} \\
&\quad + \frac{\hbar^2}{8}\delta(t_3-t_4)\sum_{o_2,i_2}\sum_{o_3,o_4,i_4} W_{o_3,\gamma,\delta,i_4}\int_{\mathcal{C}} dt_1\; G^{\mathcal{C},(0)}_{i_4,o_2}(t_a,t_1^+)\underbrace{\Big(\sum_{o_1,i_1} W_{o_1,o_2,i_1,i_2}G^{\mathcal{C},(0)}_{i_1,o_1}(t_1,t_1^+)\Big)}_{\text{tadpole: } -\frac{1}{i\hbar}v^{(0)}_{H,o_2,i_2}(t_1)} G^{\mathcal{C},(0)}_{i_2,o_3}(t_1,t_a^+)
\end{aligned}
\tag{10.96}
$$

In the last step, I grouped the terms in a sensible way. In that process I identified the Hartree potential

$$
v^{(0)}_{H,o,i}(t) = \sum_{o',i'} W_{o,o',i,i'}\underbrace{\Big(-i\hbar G^{\mathcal{C},(0)}_{i',o'}(t,t^+)\Big)}_{\rho^{(1),(0)}_{i',o'}(t)} \tag{10.97}
$$

and the exchange potential

$$
v^{(0)}_{X,o,i}(t) = -\sum_{o',i'} W_{o,o',i',i}\underbrace{\Big(-i\hbar G^{\mathcal{C},(0)}_{i',o'}(t)\Big)}_{\rho^{(1),(0)}_{i',o'}(t)} \tag{10.98}
$$

where $\rho^{(1),(0)}_{i,o}(t)$, is the one-particle-reduced density matrix Eq. 8.28 of the non-interacting electrons. The names *"tadpole"* and *"open oyster"* refer to the descriptive names of certain units of Feynman diagrams. (see p. 345 and p. 346.)

4 construct the Green's function from $\bar{\mathcal{Q}}_{T,\mu}[G^{\mathcal{C},(0)}]$.

Finally, we obtain the Greens function from

$$
\begin{aligned}
G^{\mathcal{C}}_{\alpha,\beta}(t_2,t_1) &\overset{\text{Eq. } 10.78}{=} G^{\mathcal{C},(0)}_{\alpha,\beta}(t_2,t_1) + \sum_{\gamma,\delta}\int_{\mathcal{C}} dt_4 \int_{\mathcal{C}} dt_3\; G^{\mathcal{C},(0)}_{\alpha,\gamma}(t_2,t_4) \underbrace{\frac{1}{k_B T}\frac{\delta \mathcal{Q}_{T,\mu}[G^{\mathcal{C},(0)},W]}{\delta G^{\mathcal{C},(0)}_{\delta,\gamma}(t_3,t_4)}}_{=:\Sigma^{\text{red}}_{\gamma,\delta}(t_4,t_3)} G^{\mathcal{C},(0)}_{\delta,\beta}(t_3,t_1) \\
&= G^{\mathcal{C},(0)}_{\alpha,\beta}(t_2,t_1) + \sum_{\gamma,\delta}\int_{\mathcal{C}} dt_4 \int_{\mathcal{C}} dt_3\; G^{\mathcal{C},(0)}_{\alpha,\gamma}(t_2,t_4) G^{\mathcal{C},(0)}_{\delta,\beta}(t_3,t_1) \\
\times\frac{\hbar^2}{8} &\Bigg\{ \delta(t_3-t_4)\sum_{o_2,i_2} W_{\gamma,o_2,\delta,i_2}(t_3)\int_{\mathcal{C}} dt_2 \sum_{o_3,i_4} G^{\mathcal{C},(0)}_{i_2,o_3}(t_3,t_2^+)\frac{-1}{i\hbar} v^{(0)}_{X,o_3,i_4}(t_2) G^{\mathcal{C},(0)}_{i_4,o_2}(t_2,t_3^+) \\
&+ \sum_{i_2,o_3} \frac{-v^{(0)}_{H,\gamma,i_2}(t_4)}{i\hbar} G^{\mathcal{C},(0)}_{i_2,o_3}(t_4,t_3^+)\frac{-v^{(0)}_{X,o_3,\delta}(t_3)}{i\hbar} \\
&+ \sum_{o_2,i_4} \frac{-1}{i\hbar} v^{(0)}_{X,\gamma,i_4} G^{\mathcal{C},(0)}_{i_4,o_2}(t_4,t_3^+)\frac{-v^{(0)}_{H,o_2,\delta}(t_3)}{i\hbar} \\
&+ \delta(t_3-t_4)\sum_{o_3,i_4} W_{o_3,\gamma,\delta,i_4}(t_3)\sum_{o_2,i_2}\int_{\mathcal{C}} dt_1 G^{\mathcal{C},(0)}_{i_4,o_2}(t_3,t_1^+)\frac{-v^{(1)}_{H,o_2,i_2}(t_1)}{i\hbar} G^{\mathcal{C},(0)}_{i_2,o_3}(t_1,t_3^+)\Bigg\}
\end{aligned}
\tag{10.99}
$$

5 Draw the Feynman diagrams for

- the generating functional $\bar{\mathcal{Q}}_{T,\mu}[G^{\mathcal{C},(0)}]$
- the reducible self energy Σ^{red}
- the Green's function $G^{\mathcal{C}}$

The graphical representation is provided in figure 10.6 below.

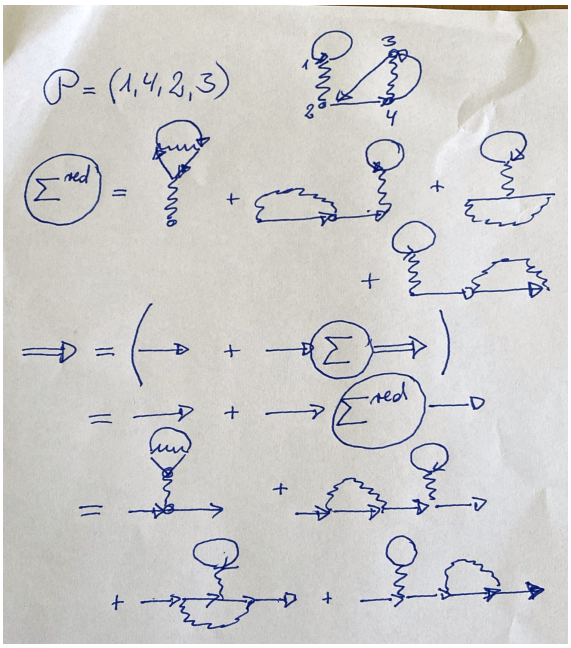


Fig. 10.6: Second part of the solution for the problem in section 10.5.1, demonstrating graphically the construction of the Green's function from a generating functional. Editor: The diagrams for the generating functional and the Green's function has been shown already in figure 10.5. The self energy graphs are not shown there.

Chapter 11

Diagrammatics of the generating functional

11.1 Classes of diagrams

In this section, I will present some terminology and names for diagrams, respectively for building blocks of them. By doing so, we will identify recurring patterns within the diagrams, that can be understood as one unit.

The elementary building blocks of a Feynman diagram are the particle line, the interaction line, and the vertex.

- The **particle line** represents a Green's function. The arrow with a single line represents a bare Green's function and the arrow with a double represents a full Green's function.

- The **interaction line** represents an interaction. It is represented by a wriggly line. When the wriggly line is drawn with a single line, the interaction line represents the bare Coulomb interaction. When it is drawn with a double line it represents the full or screened interaction.

- The point, which joins particle lines and interaction lines is the **vertex**. For the Coulomb interaction each vertex connects one incoming particle line, one outgoing particle line and one interaction line. The topology of the vertex was the reason for the naming incoming and outgoing indices of a particle line.

11.1.1 Green's function diagram

A general **Green's-function diagram** has two external *"half"*-vertices. One of the external half-vertices can accept an incoming particle line and an interaction line. The other can accept an outgoing particle line and an interaction line.

The most simple Green's function diagrams are the particle lines.

11.1.2 Interaction diagram

An **interaction diagram** has two external vertices, each of which can accept one incoming and one outgoing particle line.

11.1.3 Self-energy diagrams

A **self-energy diagram** has two external vertices. One of the external indices can accept an incoming particle line and the other can accept an outgoing particle line.

A self-energy diagram can be inserted into a self-energy diagram.

Examples are the tadpole on p. 345, the open-oyster diagram on p. 346 and the ring diagram on p. 347.

11.1.4 Polarization diagram

A **polarization diagram** has two external vertices, each of which can be connected to an interaction line.

A polarization diagram can be inserted into an interaction line.

A diagram with two external vertices, to which one can attach exactly one interaction lines each, is called a **polarization diagram** .

An example for a polarization diagram is the ring diagram on p. 347.

11.1.5 Vertex diagram

A diagram with three vertices, to which one can attach exactly one interaction line, one incoming and one outgoing Greens functions function line is called a **vertex diagram**.

11.1.6 Closed diagrams

The diagrams of the denominator of the Green's function are the so-called **closed diagrams**. They are called closed as opposed to the diagrams in the numerator of the Green's function, which have external indices. The closed diagrams with n interactions form the set of $\mathbb{A}_n$. This set of diagrams is easily constructed from all permutation vectors of dimension $2n$.

Editor: Note that the value of open diagrams has not been defined. Thus, their value should be taken with a grain of salt. I first have to supply a formula for the value.

A diagram that is not closed, is called **open diagram**. Open diagrams have an **external vertex**. An external vertex is one that is not fully connected by one interaction line, one incoming and one outgoing particle line.

11.1.7 Linked diagrams

A **linked diagram** or **linked cluster** is a diagram without disconnected parts, that are connected neither by a Green's function nor an interaction with the rest of the diagram.

The linked diagrams form a subset $\mathbb{L}_n$ of the set $\mathbb{A}_n$ of all closed, linked diagrams of order n.

From the second-order diagrams shown in figure 11.2, all diagrams but four are linked. The four exceptions are the two-by-two block in the upper-left corner. The unlinked diagrams consist of combinations of the closed diagrams of lower order.

11.1.8 One-particle-irreducible (1PI) diagrams

A diagram is **one-particle-irreducible (1PI)** if it does not fall apart when one Green's function is removed. Because Green's functions in closed diagrams form Fermi-loops, linked closed diagrams are one-particle irreducible.

11.1.9 Two-particle irreducible (2PI) diagrams

A diagram is **two-particle irreducible (2PI)** if it does not fall apart when two Green's function are removed. A diagram which is not two-particle irreducible, is called two-particle reducible. Closed, two-particle irreducible diagrams are also called **skeleton diagrams**. The set $\mathbb{S}_n$ of skeleton diagrams of order n is obtained from $\mathbb{L}_n$ by removing all two-particle reducible diagrams.

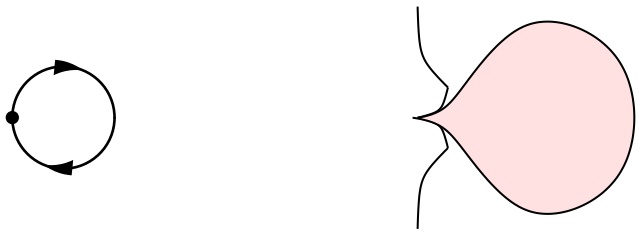
11.1.10 Named diagrams

There are patterns of diagrams that are easily recognized and interpreted. These structures shall be selected and discussed. In order to identify their values we refer to Eq. 10.66 on p. 327.

$$\begin{aligned}\mathcal{V}(\vec{\mathcal{P}}) \overset{\text{Eq. } 10.66}{=} \epsilon_{\mathcal{P}_1,\ldots,\mathcal{P}_{2n}} (i\hbar)^n \int_{\mathcal{C}} dt_1 \cdots \int_{\mathcal{C}} dt_n \sum_{o_1,i_1,\ldots,o_{2n},i_{2n}} \prod_{j=1}^{n} W_{o_{2j-1},o_{2j},i_{2j-1},i_{2j}}(t_j) \\ \times G^{(0)}_{i_{\mathcal{P}_1},o_1}\big(t(\mathcal{P}_1), t^+(1)\big) \cdots G^{(0)}_{i_{\mathcal{P}_{2n}},o_{2n}}\big(t(\mathcal{P}_{2n}), t^+(2n)\big) \end{aligned} \tag{11.1}$$

Many diagram names are taken from Mattuck[4]. (bubble p.18, ladder p.18, oyster p18, ring p.18., open oyster p.66.). The tadpole diagram has been used by Abdus Salam[89].

- **bubble diagram**: density matrix



The bubble diagram can be identified with the density matrix of the non-interacting system at a given time.

$$-G^{(0)}_{i,o}(t, t^+) \overset{\text{Eq. } 8.28}{=} \frac{1}{i\hbar}\rho^{(1)(0)}_{i,o}(t) \tag{11.2}$$

In a real-space representation, the one-particle-reduced density matrix would reduce to the density at a given point in space and time. A bubble diagram with a double-lined arrow indicating a full Green's function would yield the one-particle-reduced density matrix of the interacting system.

- **tadpole diagram**: Hartree potential



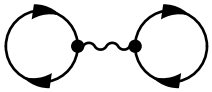
The tadpole diagram can be attributed to the Hartree potential

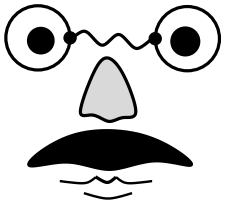
$$-i\hbar \sum_{i_2,o_2} W_{o_1,o_2,i_1,i_2}(t) G^{(0)}_{i2,o2}(t, t^+) \overset{\text{Eq. } 8.28}{=} \sum_{i_2,o_2} W_{o_1,o_2,i_1,i_2}(t) \hat{\rho}^{(1)(0)}_{i2,o2}(t) \overset{\text{Eq. } 2.34}{=} v^{(0)}_{H,o_1,i_1}(t) \tag{11.3}$$

The tadpole diagram describes the Hartree potential of the non-interacting or the interacting density, depending on whether a non-interacting or an interacting Green's function is present.

The order (o, i) of the orbital indices of the potential is opposite to that (i, o) in the one-particle-reduced density matrix. One rationale is that the trace of potential and one-particle-reduced density matrix $2E_H = \sum_{i,o} \rho^{(1)}_{i,o} v_{H,o,i}$ is (twice) the Hartree energy. Editor: Think of something more convincing, e.g. working it out brute force.

- **eyeglass diagram** or **double-bubble diagram**: Hartree term



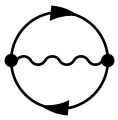


The eyeglass diagram can be attributed to the Hartree energy of the non-interacting electrons.

$$\begin{aligned}\mathcal{V}(\text{eyeglass diagram}) &= i\hbar \int_{\mathcal{C}} dt \sum_{i_1,o_1 i_2,o_2} W_{o_1,o_2,i_1,i_2}(t) G^{(0)}_{i1,o1}(t,t^+) G^{(0)}_{i2,o2}(t,t^+) \\ &= \frac{1}{i\hbar} \int_{\mathcal{C}} dt \sum_{i_1,o_1 i_2,o_2} W_{o_1,o_2,i_1,i_2}(t) \rho^{(1)(0)}_{i1,o1}(t) \rho^{(1)(0)}_{i2,o2}(t) \end{aligned} \tag{11.4}$$

The Hartree energy of interacting electrons is obtained by replacing the bare Green's function by the full one.

- **oyster diagram**: exchange term

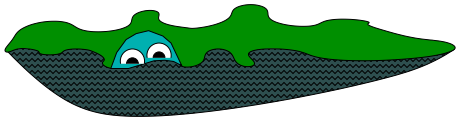


The oyster diagram can be attributed to the exchange energy

$$\begin{aligned}\mathcal{V}(\text{oyster diagram}) &= i\hbar \int_{\mathcal{C}} dt \sum_{i_1,o_1,i_2,o_2} W_{o_1,o_2,i_1,i_2}(t) G^{(0)}_{i1,o2}(t,t^+) G^{(0)}_{i2,o1}(t,t^+) \\ &\overset{\text{Eq. 8.28}}{=} \frac{1}{i\hbar} \int_{\mathcal{C}} dt \sum_{i_1,o_1,i_2,o_2} W_{o_1,o_2,i_1,i_2}(t) \rho^{(1)(0)}_{i1,o2}(t) \rho^{(1)(0)}_{i2,o1}(t) \end{aligned} \tag{11.5}$$

- **open-oyster diagram** : exchange potential

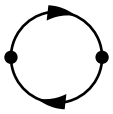




The open-oyster diagram can be attributed to the exchange potential

$$i\hbar \sum_{i_2,o_1} W_{o_1,o_2,i_1,i_2}(t) G^{(0)}_{i2,o1}(t,t^+) \overset{\text{Eq. 8.28}}{=} -\sum_{i_2,o_1} W_{o_1,o_2,i_1,i_2}(t) \rho^{(1)(0)}_{i2,o1}(t) \overset{\text{Eq. 2.37}}{=} v^{(0)}_{X,o_2,i_1}(t) \tag{11.6}$$

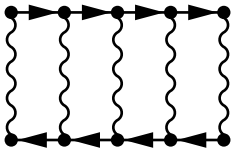
- **ring diagram**: virtual electron-hole pair. The electron-hole pair is induced by an electric field. I creates a dipole which screens the interaction. The screened interaction in a free-electron gas has an exponential tail, rather than the long-ranged $1/|\vec{r}|$ Coulomb tail.



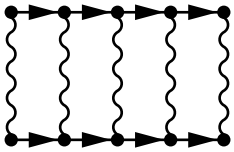
$$\Pi^{(ring)}_{i_1,o_1,i_2,o_2}(t,t') = -G^{(0)}_{i_2,o_1}(t',t)G^{(0)}_{i_1,o_2}(t,t') \tag{11.7}$$

Editor: Make the link to the bare polarization and electric susceptibility. Look up Mattuck-Eq.10.3.6. $\epsilon_{RPA}(\vec{q},\omega) = 1 + V_q\Pi(\vec{q},\omega)$.

- particle-hole ladder: Coulomb attraction between an electron and a hole. Responsible for exciton formation?



- particle-particle ladder: short-range Coulomb repulsion between two electrons or two holes.



11.2 Systematic construction of closed diagrams

The diagrams can be constructed systematically by forming all permutation vectors of length n.

11.2.1 Construct all permutation vectors

The guiding principle is that we construct the permutation vectors $\vec{\mathcal{P}}$ in a specific order.

In order to keep track of this order, we construct for each vector $\vec{\mathcal{P}}$ of length $2n$ a unique integer number

$$Z(\vec{\mathcal{P}}) \stackrel{\text{def}}{=} \sum_{j=1}^{2n} \mathcal{P}_j \cdot (2n)^{2n-j} \tag{11.8}$$

The number has no physical meaning. Its only purpose is to place all permutation vectors into a well-defined order. By working through an ordered list, we ensure that none of the permutation vectors is missed or considered twice. Z gives a value to any sequence of $2n$ numbers in the given range $0 < \mathcal{P}_j < 2n$, not only true permutations: This is not problematic because the purpose is not to enumerate permutations, but arrange them in a unique order.

Next, we set up a construction scheme for the permutation vectors $\mathcal{P}$ such that $Z(\vec{\mathcal{P}})$ increases from step to step.

1. start with all $2n$ indices in ascending order, that is $\vec{\mathcal{P}} = (1, 2, \ldots, 2n)$.

2. for a given permutation vector $\vec{\mathcal{P}}$ find the longest rightmost subsequence in descending order. If the rightmost sequence is ascending, consider the last element as the descending sequence.

   Examples:

   - for the sequence $(2, 3, 4, 1)$, the rightmost descending sequence is $(4, 1)$
   - for the sequence $(1, 2, 3, 4)$, the rightmost descending sequence is (4)

3. If the sequence with descending indices starts at position m, i.e.

$$\mathcal{P}_{m-1} < \mathcal{P}_m > \mathcal{P}_{m+1} > \ldots > \mathcal{P}_{2n} ,$$

   the preceding number $\mathcal{P}_{m-1}$ needs to be increased by the smallest possible amount. We pick from the decreasing sequence $\{\mathcal{P}_m, \ldots, \mathcal{P}_{2n}\}$ the smallest number, which, however, still is larger than $\mathcal{P}_{m-1}$. This number, let us denote it as $\mathcal{P}_q$, is placed on position $m-1$, and the other numbers from $\{\mathcal{P}_{m-1}, \ldots, \mathcal{P}_{q-1}, \mathcal{P}_{q+1} \ldots, \mathcal{P}_{2n}\}$ are arranged in increasing order and placed into positions $m, \ldots, 2n$.

   The resulting permutation vector $\vec{\mathcal{P}}'$ is equal to the original vector $\vec{\mathcal{P}}$ for the first $m-1$ elements. On the position m, $\mathcal{P}'_m = \mathcal{P}_q$. The components of the new permutation vector $\mathcal{P}'_j$ with $j > m$ consists of the components of the old vector with $j > m-1$ with the exception of $\mathcal{P}_q$. These components are arranged in ascending order.

   Examples:

   - for the permutation vector $\vec{\mathcal{P}} = (2, 3, 4, 1)$, the rightmost descending sequence is $(4, 1)$. That is, $m = 3$. We need to increase the value of $\mathcal{P}_{m-1} = 3$. The next higher number in the descending sequence $(4, 1)$ is 4. That is, $q = 3$. We place $\mathcal{P}_q = 4$ into $\mathcal{P}'_{m-1} = 4$ and remove it from the sequence $(3, 4, 1)$. The remaining numbers $\{3, 1\}$ are arranged in ascending order $(1, 3)$ and placed behind $\mathcal{P}'_{m-1} = 4$. Thus, one obtains as next permutation $\vec{\mathcal{P}}' = (2, 4, 1, 3)$.
   - for the permutation vector $\vec{\mathcal{P}} = (1, 2, 3, 4)$, the rightmost descending sequence is (4). This is the fourth component so that $m = 4$. The preceding component $\mathcal{P}_{m-1} = 3$ needs to be increased in value by picking the next higher number in the decreasing sequence, namely $\mathcal{P}_q = 4$, where $q = 4$. The remaining number from the sequence $(3, 4)$, namely 3 is placed into the last position. Thus, one obtains as next permutation $\vec{\mathcal{P}}' = (1, 2, 4, 3)$.

4. this step is repeated until all indices are in decreasing order.

5. One should count the number of permutations constructed in this way to verify that all $(2n)!$ diagrams have been formed.

11.2.2 First-order diagrams

The order in the interaction is one. We start constructing the permutation vectors $2n = 2$ dimensions.

Nr	$\vec{\mathcal{P}}$	
1	1	2
2	2	1

Thus, we obtain two diagrams which can be expressed by the column-wise mappings of the vertices by Green's functions.

- The first diagram with $\vec{\mathcal{P}} = (1, 2)$ has the mapping

1	2	3	4	5	**6**
1	2	3	4	5	**6**
			4	**6**	**5**
			5	4	**6**
			5	**6**	**4**
			6	4	**5**
		3	**6**	**5**	**4**
		4	3	5	**6**
			3	**6**	**5**
			5	3	**6**
			5	**6**	**3**
			6	3	**5**
		4	**6**	**5**	**3**
		5	3	4	**6**
			3	**6**	**4**
			4	3	**6**
			4	**6**	**3**
			6	3	**4**
		5	**6**	**4**	**3**

1	2	5	**6**	**4**	**3**
		6	3	4	**5**
			3	**5**	**4**
			4	3	**5**
			4	**5**	**3**
			5	3	**4**
	2	**6**	**5**	**4**	**3**
	3	2	4	5	**6**
			4	**6**	**5**
			5	4	**6**
			5	**6**	**4**
			6	4	**5**
		2	**6**	**5**	**4**
		4	2	5	**6**
			2	**6**	**5**
			5	2	**6**
			5	**6**	**2**
			6	2	**5**
		4	**6**	**5**	**2**

1	3	4	**6**	**5**	**2**
		5	2	4	**6**
			2	**6**	**4**
			4	2	**6**
			4	**6**	**2**
			6	2	**4**
		5	**6**	**4**	**2**
		6	2	4	**5**
			2	**5**	**4**
			4	2	**5**
			4	5	**2**
			5	2	**4**
	3	**6**	**5**	**4**	**2**
	4	2	3	5	**6**
			3	**6**	**5**
			5	3	**6**
			5	**6**	**3**
			6	3	**5**
		2	**6**	**5**	**3**

Table 11.1: Example for building up permutation vectors of length 6 using the technique of section 11.2.1. Only the first 54 permutation vectors from 720 in total are shown. The trailing descending sequence is marked as bold faced. The preceding element, which is to be increased in value, is marked in red. Elements that do not change are omitted. The top line in each column is the reference for starting the sequence below. It is a repetition of the last entry of the previous column.

o	1	2
i	1	2

This will produce Hartree diagram, which is also called **eyeglass diagram**. It is shown on the left of figure 11.1.

- The second diagram with $\vec{\mathcal{P}} = (2, 1)$ has the mapping

o	1	2
i	2	1

This will produce exchange diagram, which is also called **oyster diagram**. It is shown on the right of figure 11.1.

11.2.3 Second-order diagrams

The order in the interaction is two. We start constructing the $(2n)! = 24$ permutation vectors $2n = 4$ dimensions.

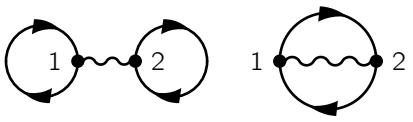


Fig. 11.1: First-order Feynman diagrams in the interaction. The left diagram is the Hartree diagram and the diagram to the right is the exchange diagram. The two diagrams describe the non-self-consistent Hartree-Fock approximation.

Nr	$\vec{\mathcal{P}}$			
1	1	2	3	4
2	1	2	4	3
3	1	3	2	4
4	1	3	4	2
5	1	4	2	3
6	1	4	3	2

Nr	$\vec{\mathcal{P}}$			
7	2	1	3	4
8	2	1	4	3
9	2	3	1	4
10	2	3	4	1
11	2	4	1	3
12	2	4	3	1

Nr	$\vec{\mathcal{P}}$			
13	3	1	2	4
14	3	1	4	2
15	3	2	1	4
16	3	2	4	1
17	3	4	1	2
18	3	4	2	1

Nr	$\vec{\mathcal{P}}$			
19	4	1	2	3
20	4	1	3	2
21	4	2	1	3
22	4	2	3	1
23	4	3	1	2
24	4	3	2	1

The diagrams are shown in figure 11.2. The diagrams are arranged line-by-line, as opposed to the column wise arrangement of the permutations given above.

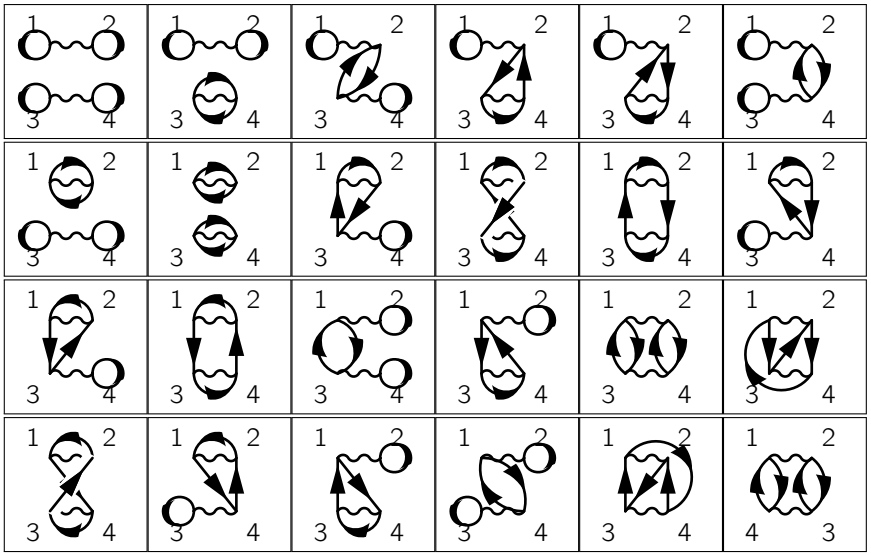


Fig. 11.2: Second-order Feynman diagrams in the interaction. Referring to the order of the pairings developed above the orderings run in rows rather than columns.

11.3 Sign theorem

The value $\mathcal{V}(D)$ of a diagram D specified by a permutation vector $\vec{\mathcal{P}}$ is given by Eq. 10.66 on p. 327. It contains a **sign factor**, namely the fully antisymmetric tensor $\epsilon_{\mathcal{P}_1,\mathcal{P}_2,\ldots}$ of the permutation vector $\vec{\mathcal{P}}$ specifying the diagram. Evaluating the sign factor can be rather cumbersome. The **sign theorem** simplifies this task so that the sign can be trivially read off from a Feynman diagram.

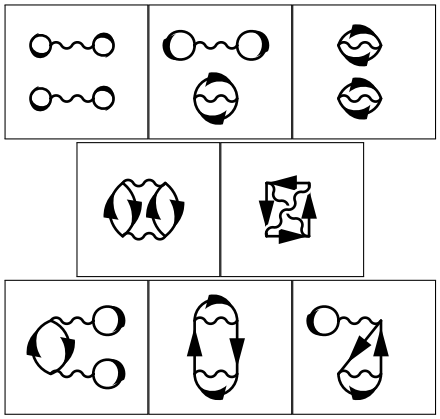


Fig. 11.3: Topologically distinct diagrams of second order grouped according to disconnected diagrams (top row), skeleton diagrams (middle row) and non-skeleton connected diagrams (bottom row). The number of Fermi loops L, the symmetry factor S, the multiplicities M and participating diagrams in parenthesis are: top-left: L=4, S=8, M=1, (1); top-middle: L=3,S=4, M=2, (2,7), top-right: L=2, S=8, M=1, (8), middle-left: L=2, S=4, M=2, (17,24), middle-right: L=1, S=4, M=2, (18,23); bottom-left: L=3, S=2, M=4, (3,6,22,15); bottom-middle: L=1, S=2, M=4, (10,11,14,19) bottom-right: L=2, S=1, M=8, (4,5,9,12,13,16,20,21). The graph numbers refer to the order in Fig. 11.2.

What is a Fermi loop?

Let me first introduce the concept of a **Fermi loop**: Consider any closed diagram: Let me pick out any Green's function in that diagram. The Green's function points to a vertex, which connects this Green's function to exactly one other (or the same) Green's function. When we proceed repeatedly from one Greens function to the next, we arrive at some point at the vertex where the first Green's function emerged from, because the diagram is closed. This ring of Green's function is called a Fermi loop. A closed diagram may have one or more such Fermi loops. A Fermi loop may only contain a single Green's function, which closes on itself, as in the tadpole diagram.

Identify Fermi-loops in a permutation vector $\vec{\mathcal{P}}$: Fermi loops can be identified from the permutation vector without drawing the diagram. The permutation vector is considered as a mapping between vertices, which allows to follow the Green's functions until they close a Fermi loop. Let me demonstrate the procedure at the following example:

$\vec{\mathcal{P}}_{tot} = \big($ 7, 1, 4, 3, 10, 5, 8, 2, 9 6 $\big)$

o	1	2	3	4	5	6	7	8	9	10
i	7	1	4	3	10	5	8	2	9	6

We start at the first outgoing vertex ($o = 1$) and follow the permutation vector to the corresponding incoming vertex $i = \mathcal{P}_1 = 7$. We denote this step by $(1 \to 7)$. Next, we choose the resulting vertex as outgoing vertex $o = 7$ and pass on to $i = \mathcal{P}_7 = 8$. We proceed until we arrive at the first vertex in the loop, namely 1, which implies that the first Fermi loop is closed. The Fermi loop consists of the hops

$$(1 \to 7), (7 \to 8), (8 \to 2), (2 \to 1) \tag{11.9}$$

and the vertices visited by the Fermi loop are

$$[1, 7, 8, 2] \tag{11.10}$$

The next Fermi loop starts at the first outgoing vertex that has not yet been visited, namely vertex 3. From here we identify the next Fermi loop.

$$(3 \to 4), (4 \to 3) \tag{11.11}$$

The vertices visited by the first two Fermi loops are

$$[1, 7, 8, 2][3, 4] \tag{11.12}$$

We proceed analogously to the third Fermi loop

$$(5 \to 10), (10 \to 6), (6 \to 5) \tag{11.13}$$

and the fourth Fermi loop

$$(9 \to 9)\ . \tag{11.14}$$

The grouping of the vertices into Fermi loops is therefore

$$\rightsquigarrow [1, 7, 8, 2][3, 4][5, 10, 6][9] \tag{11.15}$$

Now all vertices have been visited once. Thus, there are four Fermi loops in the corresponding diagram.

Sign theorem

With the concept of a Fermi loop, we can state the **sign theorem**:

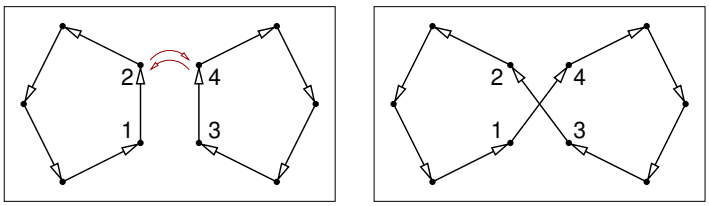
SIGN THEOREM

The sign $\epsilon_{\vec{\mathcal{P}}}$ due to the permutations of field operators is obtained from the number L of Fermi loops in a diagram as $\epsilon_{\mathcal{P}_1,\mathcal{P}_2,\mathcal{P}_3,\ldots} = (-1)^L$.
A **Fermi loop** is a closed chain of Green's functions.
The sign theorem in the form presented here is applicable only to closed diagrams.

Proof of the sign theorem

Let me verify the sign theorem.

- Let me start with a diagram specified by the permutation vector $\vec{\mathcal{P}} = (1, 2, 3, \ldots)$. Because the elements of the permutation are in ascending order, the sign factor is $+1$. The corresponding diagram consists of a product of so-called **eyeglass diagrams**, one for each interaction. An eyeglass diagram has two Fermi loops. Hence, the number of Fermi loops is even, and the sign theorem predicts, correctly, a positive sign factor.
- A sign change due to $\epsilon_{\mathcal{P}_1,\mathcal{P}_2,\ldots}$ is related to a permutation of two components of the permutation vector. Each permutation changes the number of Fermi loops by ± 1.
  - Consider the interchange of two components of the permutation vector $\vec{\mathcal{P}}$, which refer to vertices of **distinct Fermi loops**. As shown below, this will merge the two Fermi loops into one big Fermi loop.



  - Consider the interchange of two components of the permutation vector, which refer to vertices in the **same Fermi loop**. Each of the two Greens function, which are reattached closes a Fermi loop, so that the Fermi loop is divided into two Fermi loops. Because this step is related to a permutation of two indices, it is related to a sign change.

This shows that an even number of Fermi loops is related to a positive sign and an odd number of Fermi loops is related to a negative sign. This proves the sign theorem.

Exercise: Verify the sign theorem by evaluating the sign for eye-glass and oyster diagram, once with the Levi-Civita symbol and using the sign theorem.

11.4 Linked-cluster theorem

The **linked-cluster theorem**[90] [1] allows one to get rid of the logarithm in the generating functional $\mathcal{Q}_{T,\mu}$ defined in Eq. 10.77.

$$\mathcal{Q}_{T,\mu} \overset{\text{Eq. 10.77}}{=} -k_B T \ln \mathrm{Tr}\Big\{\hat{\rho}^{(0)}_{T,\mu}\mathcal{T}_{\mathcal{C}}\hat{S}_{I,\mathcal{C}}\Big\} \overset{\text{Eq. 10.77}}{=} -\frac{1}{\beta}\ln\Big\{\sum_{n=0}^{\infty}\frac{1}{n!}\frac{1}{2^n}\sum_{D\in\mathbb{A}_n}\mathcal{V}(D)\Big\} \tag{11.16}$$

Furthermore, the set $\mathbb{A}$ of general closed diagrams is reduced to a smaller set $\mathbb{L}$ of so-called linked diagrams.

[1] For the proof of the **linked-cluster theorem**, Luttinger points to Bloch and de Dominicis[91].

What is a linked diagram?

A **linked diagram** or **linked cluster** is a diagram without disconnected parts. Two parts of a diagram are disconnected, when they are neither connected by a Green's function nor by an interaction line.

Disconnected diagrams can easily be identified by inspection of the diagram. To identify disconnected diagrams on the computer or for formal derivations, a criterion based on the permutation vector $\vec{\mathcal{P}}$ is preferable. Let me develop such a criterion:

- The permutation vector maps a subset $\mathbb{B}$ of vertices onto another set $\mathbb{B}'$. When the permutation vector maps $\mathbb{B}$ onto itself, i.e. $\mathbb{B}' = \mathbb{B}$, this subset is not connected by Green's functions to the rest of the diagram. (It may still be connected by an interaction line.)
- Our rule to translate a permutation vector into a diagram enforces that an odd-numbered vertex j and the next higher even-numbered vertex $j+1$ are connected by an interaction line. This implies that all vertex pairs with subsequent odd-even-numbered labels are connected by interaction lines.

This implies that a sub diagram is disconnected from the rest, if it consists of a subset $\mathbb{B}$ of vertices , which, firstly, consists of odd-even numbered vertex pairs, and which, secondly, is mapped onto itself by the permutation vector. A procedure to identify disconnected diagrams from a set of permutation vectors is described in the appendix M.1 on p. 731.

Linked-cluster theorem

Let me now state the linked-cluster theorem, which I will prove below.

LINKED-CLUSTER THEOREM

The linked-cluster theorem removes the logarithm and reduces the sums over closed diagrams to the sum over linked diagrams, i.e.

$$\mathcal{Q}_{T,\mu}[G^{(0)}] \overset{\text{Eq. } 10.77}{=} -\frac{1}{\beta}\ln\Big\{\sum_{n=0}^{\infty}\sum_{D\in\mathbb{A}_n}\frac{\mathcal{V}(D)}{n!2^n}\Big\} = -\frac{1}{\beta}\sum_{n=1}^{\infty}\sum_{D\in\mathbb{L}_n}\frac{\mathcal{V}(D)}{n!2^n} \tag{11.17}$$

where $\mathbb{L}_n$ is the subset of linked diagrams in $\mathbb{A}_n$, the set of all closed diagrams of order n.
Note, that the sum on the right-hand side starts with element $n=1$ and not with $n=0$ as on the left-hand side.

The linked-cluster theorem represents the generating functional $\mathcal{Q}_{T,\mu}$, and thus the Green's function, as a power-series expansion in the interaction. Without the linked-cluster theorem, the Green's function is a fraction of two terms, each of which is a power series expansion of the interaction. A single power-series expansion is important to preserve symmetries with their conservation laws and sum rules. Truncating a Taylor expansion at any given order preserves all sum rules that are valid independent of the interaction strength. Truncating the sum inside the logarithm would violate these sum rules.

A pleasent side effect is a considerable reduction in the number of diagrams to be considered. Nevertheless, there still is an infinite number of them.

Proof of the linked-cluster theorem

We start taking the exponential function of both sides of the linked-cluster theorem Eq. 11.17.

$$\sum_{n=0}^{\infty}\sum_{D\in\mathbb{A}_n}\frac{\mathcal{V}(D)}{n!2^n} \overset{\text{Eq. } 11.17}{=} \exp\left(\sum_{n=1}^{\infty}\sum_{D\in\mathbb{L}_n}\frac{\mathcal{V}(D)}{2^n(n!)}\right) \tag{11.18}$$

The proof of the linked-cluster theorem Eq. 11.17 needs to verify Eq. 11.18.

Multiplicity vectors: The gist of the proof is to convert the sum over diagrams $D \in \mathbb{A}$ into a sum over what I call multiplicity vectors $\vec{m}$. The multiplicity vector describes how many linked clusters of each type are part of the composite diagram.

To prepare things, let me arrange all linked clusters $D_j \in \mathbb{L}$ in an arbitrary but well-defined sequence $(D_1, D_2, \ldots)$. The diagram D_j shall have n_j interaction lines.

Each composite diagram $D \in \mathbb{A}$ can be written as a combination of all linked diagrams $D_j \in \mathbb{L}$ with multiplicities m_j. The multiplicity vector $\vec{m}$ of a diagram D then tells that the composite diagram D in question consists of m_1 copies of the linked diagram D_1, and m_2 copies of the linked diagram D_2, and so on. The multiplicity m_j of the linked cluster D_j in the composite diagram D may be zero or any positive integer.

Hence,

- the composite diagram D in question with the multiplicity vector $\vec{m}$ consists of $\sum_{j=1}^{\infty} m_j$ mutually disconnected parts clusters.

- The value of the composite diagram D is the product of the values of its disconnected parts.

$$\mathcal{V}(D) = \prod_{j=1}^{\infty} \Big(\mathcal{V}(D_j) \Big)^{m_j} \tag{11.19}$$

- The composite diagram D has $n = \sum_{j=1}^{\infty} m_j n_j$ interaction lines, if n_j is the number of interaction lines in the linked diagram D_j.

There are many diagrams with the same multiplicity vector. However, each diagram with a given multiplicity vector has the same value $\mathcal{V}(D)$. Let us count the number $\mathcal{N}(\vec{m})$ of diagrams with the same multiplicity vector and then replace the sum over all diagrams $D \in \mathbb{A}$ by a sum over multiplicity vectors, i.e.

$$\sum_{D \in \mathbb{A}} \frac{\mathcal{V}(D)}{n! 2^n} = \sum_{\vec{m}} \mathcal{N}(\vec{m}) \frac{\prod_{j=1}^{\infty} \Big(\mathcal{V}(D_j) \Big)^{m_j}}{\big(\sum_j m_j n_j \big)! 2^{\sum_j m_j n_j}} \tag{11.20}$$

$\mathcal{N}(\vec{m})$ will be worked out below in Eq. 11.27.

Example An example for a disconnected diagram in $\mathbb{A}$ is

$\vec{\mathcal{P}}_{tot} = \big($ 7, 1,	4, 3,	10, 5,	8, 2,	9, 6 $\big)$					
o	1	2	3	4	5	6	7	8	9	10
i	7	1	4	3	10	5	8	2	9	6

I have colored the sections of the permutation vector $\vec{\mathcal{P}}_{tot}$ belonging to disconnected sub-clusters. The table specifies the pairs of vertex labels corresponding to the outgoing (right) (o) and incoming (left) (i) indices of a Green's function.
The diagram above consists of the following three subdiagrams, which are linked clusters and disconnected from each other. The arrows indicate the remapping of the vertex labels from the combined diagram $\mathcal{P}_{tot}$ to that of an isolated linked cluster $\vec{\mathcal{P}}_j$.

$\vec{\mathcal{P}}_1 = \big($ 3, 1, 4, 2 $\big)$									
o	1	2	-	-	-	-	$7 \to 3$	$8 \to 4$	-	-
i	$7 \to 3$	1	-	-	-	-	$8 \to 4$	2	-	-

$\vec{\mathcal{P}}_2 = \big($ 2, 1 $\big)$									
o	-	-	$3 \to 1$	$4 \to 2$	-	-	-	-	-	-
i	-	-	$4 \to 2$	$3 \to 1$	-	-	-	-	-	-

$\vec{\mathcal{P}}_3 = \big($ 4, 1, 3, 2 $\big)$									
o	-	-	-	-	$5 \to 1$	$6 \to 2$	-	-	$9 \to 3$	$10 \to 4$
i	-	-	-	-	$10 \to 4$	$5 \to 1$	-	-	$9 \to 3$	$6 \to 2$

This last diagram $\mathcal{P}_3$ consists of two Fermi loops with vertices $[1, 4, 2]$ and $[3]$, which are connected by an interaction between vertices 3 and 2.

Number $\mathcal{N}(\vec{m})$ of diagrams with a given multiplicity vector $\vec{m}$: Before I start, let me remind you of the rule that two diagrams are considered distinct, when their permutation vectors $\vec{P}$ differ. (I another context, the equivalence may be defined differently.)

I need to find out in how many ways one can map the permutation vectors of the linked diagrams onto a permutation vector of length $n_{tot} = \sum_j m_j n_j$ so, that the network of particle lines and interaction lines of each linked cluster remains intact.

According to our recipy,

- an interaction line connects an odd-numbered vertex with the next higher even numbered vertex.
- Once a subset of interaction lines of the composite diagram have been reserved for a specific linked diagram, the Green's functions can be inserted ina straightforward manner. This may be accomplished by mapping the vertex numbers of a permutation vector of the linked cluster to the corresponding vertex numbers of the composite diagram.

Let me now count the number of distinct ways one can assign the interaction lines of the linked cluster to those of the composite diagram, without changing the internal order of interactions inside the linked diagram.

I will first assign the interactions disregarding their internal order and then correct the overcounting due to the different internal orders by dividing by the number of permuorders is then corrected by dividing by the number $n_j!$ of the interactions inside the linked diagram.

1. The first interaction of the first linked diagram can be mapped onto any of the n_{tot} interactions of the composite diagram. The second interaction can be mapped onto $n_{tot} - 1$ interactions

and so on. There are

$$\frac{n_{tot}(n_{tot}-1)\dots(n_{tot}-n_1+1)}{n_1!} = \frac{n_{tot}!}{n_1!(n_{tot}-n_1)!} \tag{11.21}$$

possibilities to assign the n_1 interactions of D_1 to those of the combined diagram, while maintaining the internal order of the vertices in D_1. The factor $1/n_1!$ corrects the overcounting due to the different internal orders of the interactions.

2. If the cluster D_1 has a multiplicity larger than one, the interactions of the second copy can be placed in

$$\frac{(n_{tot}-n_1)\cdots(n_{tot}-n_1-n_1+1)}{n_1!} = \frac{(n_{tot}-n_1)!}{n_1!(n_{tot}-2n_1)!} \tag{11.22}$$

ways onto those of the composite diagram.

3. Combining Eq. 11.21 and Eq. 11.22 yields the number of ways to place two identical clusters onto the diagram. Because we place the two copies in both possible orders, each composite diagram occurs twice. This is corrected by an additional factor 1/2!, the number of permutations of the two copies.

$$\underbrace{\frac{1}{2!}}_{\text{correct double counting}} \underbrace{\frac{n_{tot}!}{n_1!(n_{tot}-n_1)!}}_{\text{Eq. 11.21}} \cdot \underbrace{\frac{(n_{tot}-n_1)!}{n_1!(n_{tot}-2n_1)!}}_{\text{Eq. 11.22}} = \frac{1}{2!}\cdot\frac{n_{tot}!}{(n_1!)^2(n_{tot}-2n_1)!} \tag{11.23}$$

4. Let us generalize this result to an arbitrary multiplicity of the linked diagram D_1

$$\frac{1}{m_1!}\cdot\frac{n_{tot}!}{(n_1!)^{m_1}(n_{tot}-m_1n_1)!} \tag{11.24}$$

The prefactor 1/2! has been changed to $1/m_1!$, which is the number of permutations of the copies of the linked cluster D_1.

5. We proceed with the second linked cluster D_2. The ways of adding the set of linked clusters D_2 is ontained by adjusting n_{tot} of the previous expression. We obtain

$$\frac{1}{m_2!}\cdot\frac{(n_{tot}-m_1n_1)!}{(n_2!)^{m_2}(n_{tot}-m_1n_1-m_2n_2)!} \tag{11.25}$$

Multiplication with the factor from the first diagram yields

$$\begin{aligned}&\frac{1}{m_1!}\cdot\frac{n_{tot}!}{(n_1!)^{m_1}(n_{tot}-m_1n_1)!}\times\frac{1}{m_2!}\cdot\frac{(n_{tot}-m_1n_1)!}{(n_2!)^{m_2}(n_{tot}-m_1n_1-m_2n_2)!}\\ &=\left(\frac{1}{m_1!(n_1!)^{m_1}}\right)\left(\frac{1}{m_2!(n_2!)^{m_2}}\right)\cdot\frac{n_{tot}!}{(n_{tot}-m_1n_1-m_2n_2)!}\end{aligned} \tag{11.26}$$

ways to map the interactions of the first two linked diagrams with their multiplicities onto the composite diagram.

6. Similarly, we proceed with the other linked clusters, which yields

$$\mathcal{N}(\vec{m}) = \frac{n_{tot}!}{\underbrace{(n_{tot}-\sum_{j=1}^{\infty}m_jn_j)!}_{n_{tot}}}\cdot\prod_{j=1}^{\infty}\left(\frac{1}{m_j!(n_j!)^{m_j}}\right) = n_{tot}!\prod_{j=1}^{\infty}\left(\frac{1}{m_j!}\frac{1}{(n_j!)^{m_j}}\right) \tag{11.27}$$

ways to map the interactions of all linked diagrams with their multiplicities onto the composite diagram. Eq. 11.27 is the number of distinct diagrams in $\mathbb{A}$, which fall apart into the linked clusters with the multiplicities specified by the multiplicity vector $\vec{m}$.

Putting things together Now, we can rewrite the sum over all diagrams in $\mathbb{A}$ on the left-hand side of Eq. 11.18 as a sum over all multiplicity vectors $\vec{m}$. Below, I will use that the number n_{tot} of interaction lines in the composite diagram is equal to the sum $n_{tot} = \sum_{j=1}^{\infty} m_j n_j$ of interaction lines of the contributing linked clusters. Furthermore, I exploit that the value $\mathcal{V}(D)$ of the composite diagram D is the product of the values $\mathcal{V}(D_j)$ of its constituent linked clusters.

$$\begin{aligned}
\sum_{n_{tot}=0}^{\infty} \sum_{D\in\mathbb{A}_{n_{tot}}} \frac{\mathcal{V}(D)}{n_{tot}!2^{n_{tot}}} &\overset{\text{Eq. 11.20}}{=} \sum_{\vec{m}} \overbrace{\left\{ n_{tot}! \prod_{j=1}^{\infty} \frac{1}{m_j!} \frac{1}{(n_j!)^{m_j}} \right\}}^{\mathcal{N}(\vec{m})\ \text{Eq. 11.27}} \left\{ \frac{1}{n_{tot}!2^{n_{tot}}} \overbrace{\prod_{j=1}^{\infty} \Big(\mathcal{V}(D_j)\Big)^{m_j}}^{\mathcal{V}(D)} \right\} \\
&= \sum_{\vec{m}} \prod_{j=1}^{\infty} \frac{1}{m_j!} \left(\frac{\mathcal{V}(D_j)}{n_j!2^{n_j}} \right)^{m_j} \\
&= \prod_{j=1}^{\infty} \underbrace{\left\{ \sum_{m_j=0}^{\infty} \frac{1}{m_j!} \left(\frac{\mathcal{V}(D_j)}{n_j!2^{n_j}} \right)^{m_j} \right\}}_{\exp\left(\frac{\mathcal{V}(D_j)}{n_j!2^{n_j}}\right)} \\
&= \exp\left\{ \sum_{j=1}^{\infty} \frac{\mathcal{V}(D_j)}{n_j!2^{n_j}} \right\} = \exp\left(\sum_{n=1}^{\infty} \sum_{D\in\mathbb{L}_n} \frac{\mathcal{V}(D)}{2^n(n!)} \right)
\end{aligned} \tag{11.28}$$

The sum over j is the sum over linked diagrams $\mathbb{L}$.

This proves Eq. 11.18. After taking the logarithm on both sides of Eq. 11.18 we arrive at the linked-cluster theorem Eq. 11.17.

11.5 Topologically-equivalent diagrams and symmetry factors

In this section, I will show that the set $\mathbb{L}$ of linked diagrams of the generating functional can be reduced to a much smaller set $\mathbb{T}$ of so-called **topologically distinct**, linked diagrams. The vertex labels, used so far, become irrelevant for this new set. The reduction in the number of terms is compensated with the help of a so-called **symmetry factor** $S(D)$.

The result of this section can be summarized in the following box:

SUM OVER TOPOLOGICALLY DISTINCT DIAGRAMS

The generating functional $\mathcal{Q}_{T,\mu}\big[G^{(0)}\big]$ of Eq. 11.16 can be expressed in terms of topologically distinct diagrams and their symmetry factor $S(D)$ as

$$\mathcal{Q}_{T,\mu}\big[G^{(0)}\big] \overset{\text{Eq. 11.35}}{=} -\frac{1}{\beta} \sum_{n=1}^{\infty} \sum_{D\in\mathbb{T}_n} \frac{\mathcal{V}(D)}{S(D)} \tag{11.29}$$

$\mathbb{T}_n$ is the set of all topologically distinct, linked, closed diagrams of order n. The value $\mathcal{V}(D)$ of the diagram is defined in Eq. 10.66. $S(D)$ is the symmetry factor of the diagram, which is obtained as the number of so-called "mere deformations" constructed by topology-preserving transformations among vertex labels.

What are topologically equivalent diagrams?

The topology of a diagram refers to its network of particle lines and interaction lines.

Many diagrams of the generating functional $\mathcal{Q}_{T,\mu}$ Eq. 11.17, have the same value $\mathcal{V}(D)$. Their values are equivalent, because the integrals in the expressions for $\mathcal{V}(D)$, Eq. 10.66, are related by

a mere renaming of integration variables. In the diagram, a renaming of the integration variables is equivalent to changing the vertex labels, while preserving the connectivity, the topology, of the diagram.

Relabeling vertices: Up to now, we have used so-called **labeled diagrams**, meaning that every vertex has a specific label (number). The labels allowed us to represent diagrams in terms of permutation vectors $\vec{\mathcal{P}}$.

Renaming (relabeling) the vertices can be done by a vector $\vec{M}$, which maps every vertex label j uniquely onto a new vertex label M_j. Mapping vectors $\vec{M}$ have much in common with permutation vectors $\vec{\mathcal{P}}$, because both are a unique mappings of the vertices in a diagram onto each other.

A Green's function that points from vertex j to vertex $\mathcal{P}_j$ turns, after remapping, into a Green's function from M_j to $M_{\mathcal{P}_j}$. The new permutation vector satisfies therefore[2]

$$\mathcal{P}'_{M_j} = M_{\mathcal{P}_j} \tag{11.30}$$

Considering both vectors $\vec{\mathcal{P}}$ and $\vec{M}$ as transformation operators acting on the vertex labels, this can also be written in the form[3]

$$\mathcal{P}' \circ M \overset{\text{Eq. 11.30}}{=} M \circ \mathcal{P} \qquad \Rightarrow \qquad \mathcal{P}' = M \circ \mathcal{P} \circ M^{-1} \tag{11.31}$$

Example for relabeling a diagram:

o	1	2	3	4
i	$\mathcal{P}_1$	$\mathcal{P}_2$	$\mathcal{P}_3$	$\mathcal{P}_4$

$\overset{\text{remap}}{\rightarrow}$

o	M_1	M_2	M_3	M_4
i	$M_{\mathcal{P}_1}$	$M_{\mathcal{P}_2}$	$M_{\mathcal{P}_3}$	$M_{\mathcal{P}_4}$

$\overset{\text{order}}{\rightarrow}$

o	1	2	3	4
i	$\mathcal{P}'_1$	$\mathcal{P}'_2$	$\mathcal{P}'_3$	$\mathcal{P}'_4$

In the first step "remap", all vertex labels, incoming and outgoing, are relabeled so that the vertex with label j receives the new label M_j. In the second step "order", the columns (outgoing-incoming pairs) are rearranged such that the outgoing vertex labels are in ascending order. The resulting sequence of incoming vertex labels form the new permutation vector $\vec{\mathcal{P}}'$.
Let me consider a specific example with $\vec{\mathcal{P}} = (3,1,4,2)$ and $\vec{M} = (2,1,3,4)$, which yields the new permutation vector $\vec{\mathcal{P}}' = (2,3,4,1)$.

o	1	2	3	4
i	3	1	4	2

$\overset{\text{remap}}{\rightarrow}$

o	2	1	3	4
i	3	2	4	1

$\overset{\text{order}}{\rightarrow}$

o	1	2	3	4
i	2	3	4	1

Topology-preserving transformations: Relabeling vertices in an arbitrary manner [4] preserves the network of Green's functions, but it could change the network of interactions lines. In order to also preserve the network of interaction lines, the following transformations are allowed:

- $n!$ interchanges of vertex-label pairs between interactions, while maintaining the internal odd-even-order of the vertex labels on each interaction.

[2] Consider a Green's function that points from vertex j to vertex $\mathcal{P}_j$. After renaming the vertices, the vertex j obtains a new vertex number M_j, and the vertex $\mathcal{P}_j$ obtains the new vertex number $M_{\mathcal{P}_j}$. Thus, the same Green's function points from M_j to $M_{\mathcal{P}_j}$. That is, $M_{\mathcal{P}_j}$ is the value of the new permutation vector $\vec{\mathcal{P}}'$ for the component M_j. Hence, $\mathcal{P}'_{M_j} = M_{\mathcal{P}_j}$.

[3] The inverse of the mapping M is obtained by, first, interchanging the sequences of outgoing and incoming vertices, and secondly reordering the (o,i) vertex pairs so that the new outgoing vertices are in ascending order.

o	1	2	3	4
i	2	1	3	4

$\overset{i \leftrightarrow o}{\rightarrow}$

o	2	1	3	4
i	1	2	3	4

$\overset{\text{order}}{\rightarrow}$

o	1	2	3	4
i	2	1	3	4

The inverse mapping $\vec{M}^{-1} = (2,1,3,4)$ is, in this case, identical to the forward mapping $\vec{M} = (2,1,3,4)$.

[4] Also an arbitrary mapping vector must be unique mapping of the vertex labels onto each other.

- 2^n interchanges of the vertex labels within interactions.

These $n!2^n$ operations form a group G_n of transformations of vertex labels, which maintain the same network of particle lines and interaction lines and therefore leave the value of the diagram unchanged.[5] The mapping vectors $\vec{M}$ for the second-order terms in the interaction , i.e. $n = 2$, are given as an example in table 11.2.

Table 11.2: The $2^n n!$ mappings of the vertices for order $n = 2$ in the interaction, which leave the topology of a diagram unchanged. Required is that all interactions connect an odd numbered vertex with the next higher even-numbered vertex. There are $n!2^n = 8$ such mappings.

V_i	1	2	3	4	
$M_1 = I$	1	2	3	4	identity
M_2	2	1	3	4	flips vertices of 1st interaction
$M_3 = M_5 \circ M_2 \circ M_5$	1	2	4	3	flips vertices of 2st interaction
$M_4 = (M_2 \circ M_5)^2$	2	1	4	3	flips vertices of both interactions
M_5	3	4	1	2	interchanges two interactions
$M_6 = M_5 \circ M_2$	3	4	2	1	inverts 1st interaction and interchanges interactions
$M_7 = M_2 \circ M_5$	4	3	1	2	inverts 2st interaction and interchanges interactions
$M_8 = M_2 \circ M_5 \circ M_2$	4	3	2	1	inverts both interactions and interchanges interactions

Mere deformations: Some of the topology-preserving transformations turn a diagram into itself, rather than into a different diagram with the same topology. More precisely, the resulting permutation vector is identical to the original one, i.e. $\vec{\mathcal{P}}' = \vec{\mathcal{P}}$. Such a transformation is called a **mere deformation**. Whether a transformation is a mere deformation depends on the diagram at hand. Following Eq. 11.30, a mere deformation satisfies

$$\mathcal{P}_{M_j} = M_{\mathcal{P}_j} \ . \tag{11.32}$$

When we consider permutation vector and mapping vector as transformations, Eq. 11.32 implies that these two transformations commutate.

[5] The generators of the group are (1) the interchange of the vertex labels on the first interaction and (2) the interchange of the vertex labels of every interaction, except the first, with the first. In total, the symmetry group for a diagram of order n has n generators. All other transformation of the symmetry group are obtained as products of these generators.

Example for a mere deformation: Let us pick the same permutation vector $\vec{\mathcal{P}} = (3, 1, 4, 2)$ as in the example above, but transform it with another re-mapping, namely $\vec{M} = (4, 3, 2, 1)$. In that case we obtain

o	1	2	3	4
i	3	1	4	2

$\xrightarrow{\text{remap}}$

o	4	3	2	1
i	2	4	1	3

$\xrightarrow{\text{order}}$

o	1	2	3	4
i	3	1	4	2

This remapping produces the same permutation vector $\vec{\mathcal{P}}' = \vec{\mathcal{P}}$ as the original one. Thus, we have not produced a new diagram, but a mere deformation of the original diagram.
Let me now implement the criterion Eq. 11.32 for a mere deformation given above

$$\begin{aligned}
\left(1 \xrightarrow{\mathcal{P}} 3 \xrightarrow{M} 2\right) &= \left(1 \xrightarrow{M} 4 \xrightarrow{\mathcal{P}} 2\right) \\
\left(2 \xrightarrow{\mathcal{P}} 1 \xrightarrow{M} 4\right) &= \left(2 \xrightarrow{M} 3 \xrightarrow{\mathcal{P}} 4\right) \\
\left(3 \xrightarrow{\mathcal{P}} 4 \xrightarrow{M} 1\right) &= \left(3 \xrightarrow{M} 2 \xrightarrow{\mathcal{P}} 1\right) \\
\left(4 \xrightarrow{\mathcal{P}} 2 \xrightarrow{M} 3\right) &= \left(4 \xrightarrow{M} 1 \xrightarrow{\mathcal{P}} 3\right)
\end{aligned}$$

We observe, that the mapping commutates with the permutation, which identifies this mapping as a mere deformation of the diagram specified by the permutation.

Set $\mathbb{T}$ of the topologically inequivalent (linked) diagrams: The goal is to pick only one diagram out of a set of topologically equivalent diagrams. This can be done, diagram by diagram: First, the set of all diagrams $\{\vec{\mathcal{P}}'\}$ that are topologically equivalent to $\vec{\mathcal{P}}$ is constructed by applying all topology-preserving transformations to a specific diagram $\vec{\mathcal{P}}$. Then, we define a criterion to select exactly one specific diagram from this set. If the current diagram satisfies the criterion, it is kept. Otherwise the diagram is discarded.

The criterion is that the number[6] $Z(\vec{\mathcal{P}})$ assigned to its permutation vector

$$Z(\vec{\mathcal{P}}) \overset{\text{Eq. 11.8}}{=} \sum_{j=1}^{2n} \mathcal{P}_j \cdot (2n)^{2n-j} \tag{11.33}$$

is the smallest in the set of topologically equivalent diagrams. The comparison of $Z(\vec{\mathcal{P}})$ of two diagrams $\vec{\mathcal{P}}$ and $\vec{\mathcal{P}}'$ is straightforward: We only need to compare the first distinct component of the permutation vectors from the left: If that component of $\vec{\mathcal{P}}$ is smaller than that of $\vec{\mathcal{P}}'$, this also holds for Z, i.e. $Z(\vec{\mathcal{P}}) < Z(\vec{\mathcal{P}}')$. That is

$$\mathcal{P}_j < \mathcal{P}'_j \quad \text{and} \quad \mathcal{P}_k = \mathcal{P}'_k \quad \text{for } k < j \qquad \Rightarrow Z(\vec{\mathcal{P}}) < Z(\vec{\mathcal{P}}') \tag{11.34}$$

Once the topologically equivalent diagrams have been removed from the set $\mathbb{L}$, the vertex labels are redundant. Any labeling of vertices that satisfies the odd-even rule[7] is as good as any other one.

Thus, we switch from a set $\mathbb{L}$ of **labeled** linked **diagrams** to the much smaller set $\mathbb{T}$ of **unlabeled** linked **diagrams**.

As shown in appendix M, there are 592 closed, linked diagrams of third order, while there are only 20 such topologically distinct diagrams (about 3 %). In the fourth order, the number of topologically distinct diagrams (107) is about 3 permille of the number of linked diagrams (33888).

Counting diagrams and symmetry factor: The weight of each diagram in the set $\mathbb{T}$ must account for topologically equivalent diagrams, that have been omitted.

[6] Eq. 11.8, has been introduced in order to systematically construct all permutation vectors in section 11.2.1.

[7] With odd-even rule I mean that an interaction always contains a vertex with an odd-numbered vertex and the vertex with the next higher even number.

The value $\mathcal{V}(D)$ of a diagram has been defined so that each diagram in $\mathbb{L}$ (or $\mathbb{A}$) contributes with a weight $\frac{1}{n!2^n}$ to the generating functional $\mathcal{Q}_{T,\mu}$ as given in Eq. 11.17. There are exactly $n!2^n$ transformations of vertex labels that lead to either distinct, topologically equivalent diagrams or mere deformations. If there were no mere deformations, each diagram in $\mathbb{T}$ would contribute with its value $\mathcal{V}(D)$: in this special case, there are $n!2^n$ topologically equivalent diagrams which would cancel the prefactor $\frac{1}{n!2^n}$. If the relabeling produces also mere deformations, the number of distinct, topologically equivalent diagrams is smaller than $n!2^n$ by a factor $S(D)$, which is called the **symmetry factor**.

Below, I will show that the symmetry factor is given as follows:

SYMMETRY FACTOR

The symmetry factor $S(D)$ is the number of mere deformations among the results of the topology-preserving transformations (including the identity) acted on the (labeled) diagram D.

Let me follow in spirit the argument given in section 2.3 of the textbook of Negele and Orland[8]: The topology-preserving transformations form a group G_n. [8] The transformations that produces mere deformations of a given diagram D form a subgroup F_D of the topology-preserving diagrams.

The sub-group F_D of transformations that produce mere deformations of a diagram D is constructed by applying all topology-preserving transformations of G_n to one diagram. If the permutation vector of a resulting diagram is identical to that of the original diagram, this specific transformation produces mere deformations. If a transformation produces a mere deformation for one diagram D it does so also for all other topologically equivalent diagrams. As an alternative to producing all topologically equivalent diagrams, one can use the test Eq. 11.32 to identify transformations in F_D. The number of elements of F_D will later be the symmetry factor.

The number of elements in the subgroup F_D must be a divisor of $n!2^n$: For any two distinct, but topologically equivalent diagrams, the transformations of the subgroup F_D produce two non-overlapping sets of mere deformations. Thus, the set of diagrams produced by the topology preserving transformations G_n falls apart into an integer number of non-overlapping subsets, each of which holds only mere deformations of each other. The diagrams of two different subsets are distinct. If F_D has $S(D)$ elements, the number of subsets of diagrams is therefore $n!2^n/S(D)$. In other words there are $n!2^n/S(D)$ distinct topologically equivalent diagrams in $\mathbb{L}$, which are combined into one diagram in the set $\mathbb{T}$ of topologically distinct diagrams.

$$\mathcal{Q}_{T,\mu} \overset{\text{Eq. 11.16}}{=} -\frac{1}{\beta}\sum_{n=1}^{\infty}\sum_{D\in\mathbb{L}_n}\frac{\mathcal{V}(D)}{n!2^n} = -\frac{1}{\beta}\sum_{n=1}^{\infty}\sum_{D\in\mathbb{T}_n}\frac{n!2^n}{S(D)}\frac{\mathcal{V}(D)}{n!2^n} = -\frac{1}{\beta}\sum_{n=1}^{\infty}\sum_{D\in\mathbb{T}_n}\frac{\mathcal{V}(D)}{S(D)} \quad (11.35)$$

Exercise 11.10.3 on p. 377 is strongly recommended to understand how to determine symmetry factors in practice.

Graphical approach to determine the symmetry factor

As an alternative, one can relabel the vertices in the graphical diagram according to the topology-preserving transformations. Each relabeled diagram is then deformed so that the vertex labels fall on-top of those of the original diagram. The remapped diagram is a **deformation** of the original one, if the Green's function lines, *including their orientation*, can be superimposed to those of the original diagram, while they remain attached to the vertices of the transformed diagram. A mere deformation is simply the same diagram as the original one.

The example for the diagram Eq. 11.78 is given in Fig. 11.4. There are two mere deformations, (upper left and lower right) which are mere deformations of the original diagram. This the symmetry factor is $S(D) = 2$. Because the identity is always included, the symmetry factor is never zero.

[8] A group is a set of elements with a binary operation $\circ$, which is (1) associative $A\circ(B\circ C) = (A\circ B)\circ C$, has (2) an identity $A\circ 1 = A$ and an (3) inverse of each element $A^{-1}\circ A = 1$.

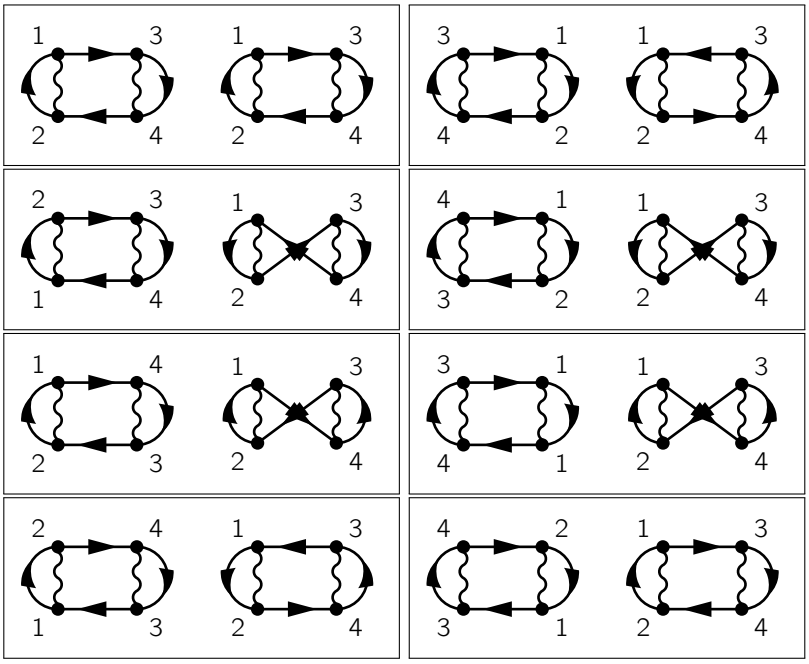


Fig. 11.4: Example for the graphical determination of the symmetry factor. Each box corresponds to one of the $n!2^n$ diagrams obtained by appropriate relabeling of the indices. In each box, the left diagram shows the same diagram after relabeling the indices. The right diagram in each box is obtained by deforming the diagram so that the vertices fall Ont of the original ones. If the diagrams on the right of two boxes look equivalent, considering also the directions of the Green's functions, the two boxes describe mere deformations of each other. The top-left and the bottom-right diagrams are mere deformations of the original diagram. Hence, the symmetry factor is $S(D) = 2$.

Note, that the upper right diagram changes the orientation of the Green's functions, which makes it a distinct diagram.

The set of topologically equivalent diagrams in Fig. 11.4 is divided into four subsets, each of which contains two diagrams, which are mere deformations of each other.

11.5.1 Hand's-on for the evaluation of symmetry factors

In this section, the sum over all closed, linked diagrams for a given order $\mathbb{L}_n$ has been replaced by a sum over only the topologically inequivalent, closed, linked diagrams $\mathbb{T}_n$. This reduction in the number of diagrams has to be accounted for by a symmetry factor $S(D)$.

What does this mean? Let us consider the contribution from the second-order diagrams

$$\sum_{D\in\mathbb{L}_2} \frac{\mathcal{V}(D)}{2!2^2} = \sum_{D\in\mathbb{L}_2} \frac{\mathcal{V}(D)}{8} \tag{11.36}$$

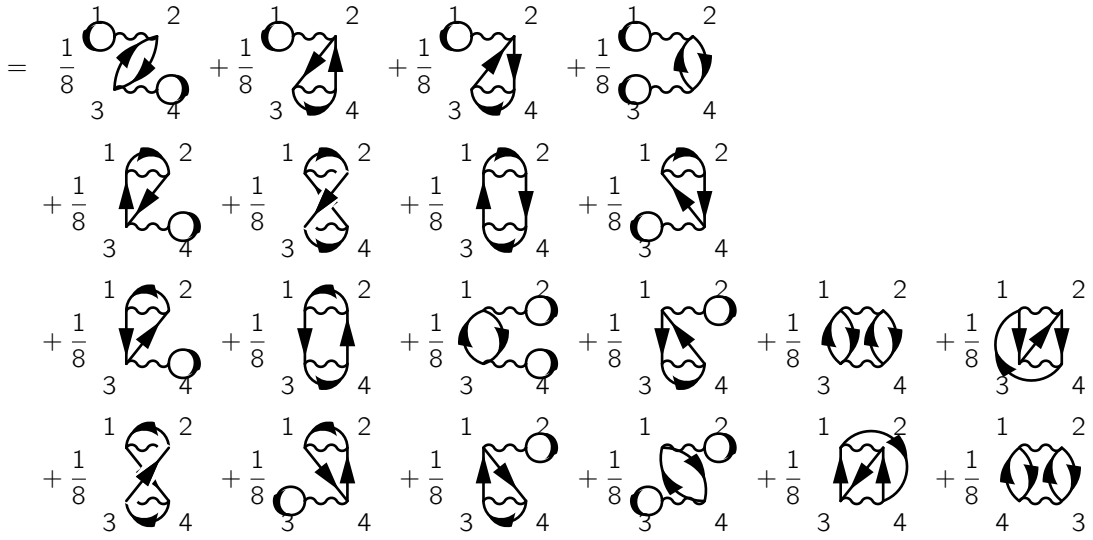
where all diagrams $D \in \mathbb{A}_2$ are listed in Fig. 11.2 on p. 350.

Before we start, we need to exclude the four diagrams from Fig. 11.2, which are not linked. Unlinked diagrams are part of $\mathbb{A}_2$ but not part of $\mathbb{L}_2$. They have been excluded by the linked-cluster theorem, which removed the logarithm in front of the sum over diagrams and the unlinked diagrams.

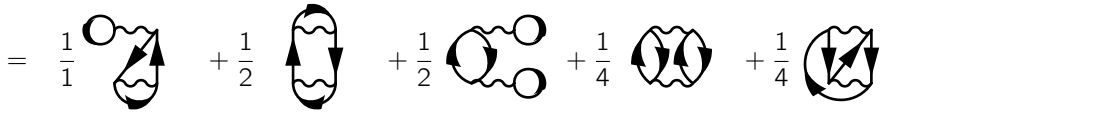
Many of the remaining 20 diagrams are topologically equivalent, that is, they correspond to the same integral, only with some integration variables renamed. In other words, they differ only by the vertex labels and irrelevant deformations, that do not affect the connectivity of the vertices.

In figure 11.5, the diagrams are grouped into sets of topologically equivalent diagrams. Each set contributes one diagram to the set of topologically distinct diagrams. This diagram receives the entire weight of the set.

$$\sum_{D\in L_2} \frac{\mathcal{V}(D)}{8}$$



$$= \frac{8}{8} \quad + \frac{4}{8} \quad + \frac{4}{8} \quad + \frac{2}{8} \quad + \frac{2}{8}$$



$$= \frac{1}{1} \quad + \frac{1}{2} \quad + \frac{1}{2} \quad + \frac{1}{4} \quad + \frac{1}{4}$$

$$= \sum_{D\in \mathbb{T}_2} \frac{\mathcal{V}(D)}{S(D)} \tag{11.37}$$

Fig. 11.5: Distribution of the second-order diagrams into sets of topologically equivalent diagrams, one for each topologically distinct diagram in $\mathbb{T}$. The weights are collected. The resulting prefactor $1/S(D)$ provides the symmetry factor S(D).

Confirm the result of figure 11.5 by yourself! The same scheme applies to all the other orders n in $\mathcal{Q}_{T,\mu}$. Therefore, you should be able to check this for $n = 1$. And if you really want to have fun, you might also like to check it for $n = 3$, by taking all 720 diagrams for $n = 3$, rejecting all unlinked diagrams and identifying all topologically equivalent ones.

11.6 Systematic rule to construct all topologically distinct, linked, closed diagrams

Determine all closed diagrams of order n as follows:

1. construct all permutation vectors of length $2n$. as described in section 11.2.1 on p. 347.

2. remove all permutation vectors that produce disconnected (un-linked) diagrams. This can be done by inspection after drawing the diagram, or by a procedure on the elements of the permutation vector as described in section 11.4 on p. 353.

3. For each diagram construct the topologically equivalent diagrams using the topology-preserving transformations. These transformations are the (1) vertex exchanges on one interaction and (2) the interchange of vertex pairs between interactions.

   Discard the current diagram if there is a topologically equivalent diagram with a value $Z(\vec{\mathcal{P}}')$ defined in Eq. 11.8 smaller than that of the current diagram.

   Determine the symmetry factor for the current diagram as the number of mere deformations as described in section 11.5 on p. 358.

11.7 Systematic rule to evaluate Feynman diagrams

11.7.1 Contour time and orbital basisset

GENERATING FUNCTIONAL

$$\mathcal{Q}_{T,\mu}[G^{(0)}] \overset{\text{Eq. } 10.77}{=} -\frac{1}{\beta}\mathrm{Tr}\left\{\hat{\rho}^{(0)}_{T,\mu}\mathcal{T}_{\mathcal{C}}\hat{S}_{I,\mathcal{C}}\right\} \overset{\text{Eq. } 11.17}{=} -\frac{1}{\beta}\sum_{n=1}^{\infty}\sum_{D\in\mathbb{L}_n}\frac{\mathcal{V}(D)}{n!2^n} \overset{\text{Eq. } 11.29}{=} -\frac{1}{\beta}\sum_{n=1}^{\infty}\sum_{D\in\mathbb{T}_n}\frac{\mathcal{V}(D)}{S(D)} \tag{11.38}$$

$\mathbb{L}_n$ is set of all linked, closed diagrams of order n in the interaction. $\mathbb{T}_n$ is set of all topologically distinct, linked, closed diagrams of order n in the interaction. $S(D)$ is the symmetry factor of the diagram D.
$\mathcal{V}(D)$ is the value of the diagram given below. Each diagram of order n can be represented by a $2n$ dimensional permutation vector $\vec{\mathcal{P}}$

$$\begin{aligned}\mathcal{V}(D) \overset{\text{Eq. } 10.66}{=} \epsilon_{\mathcal{P}_1,\ldots,\mathcal{P}_{2n}}(i\hbar)^n\int_{\mathcal{C}}dt_1\cdots\int_{\mathcal{C}}dt_{2n}\sum_{o_1,i_1,\ldots,o_{2n},i_{2n}}\left(\prod_{j=1}^{n}W_{o_{2j-1},o_{2j},i_{2j-1},i_{2j}}\delta_{\mathcal{C}}(t_{2j-1}-t_{2j})\right)\\ \times G^{\mathcal{C},(0)}_{i_{\mathcal{P}_1},o_1}\left(t_{\mathcal{P}_1},t_1^+\right)\cdots G^{\mathcal{C},(0)}_{i_{\mathcal{P}_{2n}},o_{2n}}\left(t_{\mathcal{P}_{2n}},t_{2n}^+\right)\end{aligned} \tag{11.39}$$

The interaction matrix elements are

$$W_{o_1,o_2,i_1,i_2} \overset{\text{Eq. } 3.48}{=} \int d^4x\int d^4x'\,\frac{e^2\chi^*_{o_1}(\vec{x})\chi^*_{o_2}(\vec{x'})\chi_{i_1}(\vec{x})\chi_{i_2}(\vec{x'})}{4\pi\epsilon_0|\vec{r}-\vec{r'}|} \tag{11.40}$$

and the non-interacting Green's function is

$$G^{\mathcal{C},(0)}_{i,o}(t,t') \overset{\text{Eq. } 7.30}{=} \frac{1}{i\hbar}\langle\pi_i|\hat{U}(t,0)\Big\{\underbrace{\theta_{\mathcal{C}}(t-t')\big(\hat{1}-\hat{\rho}^{(1),(0)}_{T,\mu}\big)}_{\text{electrons}}-\underbrace{\theta_{\mathcal{C}}(t'-t)\hat{\rho}^{(1)}_{T,\mu}}_{\text{holes}}\Big\}\hat{U}(0,t')|\pi_o\rangle \tag{11.41}$$

The full Green's function is obtained from the generating functional with Eq. 10.78 on p. 334 and the irreducible self energy is obtained by Eq. 10.79.

Draw a diagram from a permutation vector:

Determine the value of a drawn diagram

1. **Labels:** Label the vertices with numbers from 1 to $2n$ such that an odd-numbered vertex and the following even-numbered vertex on the same interaction line.

2. **Permutation vector:** The Green's function starting at vertex j points to vertex $\mathcal{P}_j$. While passing through the vertices in ascending order, note down the sequence of target vertices.

3. **Vertices:** For each vertex j include a time integral and a sum over all orbital indices for incoming and outgoing Green's functions.

$$\sum_{o_j,i_j} \int_{\mathcal{C}} dt_j \tag{11.42}$$

4. **Interaction lines:** For the interaction line with number j introduce a factor

$$i\hbar W_{o_{2j-1},o_{2j},i_{2j-1},i_{2j}} \delta_{\mathcal{C}}(t_{2j-1} - t_{2j}) \tag{11.43}$$

5. **Particle lines:**

   - For each particle line[9] introduce a factor

$$G^{\mathcal{C},(0)}_{i_{\mathcal{P}_j},o_j}(t_{\mathcal{P}_j}, t_j^+) \tag{11.44}$$

     j is the label of the vertex from which the Green's function emerges and $\mathcal{P}_j$ is the label of the vertex, where the Green's function arrives.

     The infinitesimal displacement Δ of the second time argument t_o of a Green's function to $t_o^+ = t_o + \Delta$ is only relevant for **non-propagating particle lines** , which otherwise have equal time arguments $t_i = t_o$. A **non-propagating Green's function**

$$G^{\mathcal{C},(0)}_{i,o}(t, t^+) \overset{\text{Eq. 8.28}}{=} \frac{1}{i\hbar} \hat{\rho}^{(1),(0)}_{i,o}(t) \tag{11.45}$$

     starts and ends at the same interaction line. Non-propagating Green's function lines are present only in bubbles, oysters and open-oysters. This infinitesimal shift has been introduced in section 10.2.2 to ensure the proper order of creation and annihilation operators of one interaction.

     For **propagating** Green's function lines the infinitesimal shift is without consequence and can be disregarded.

6. **Sign factor**: count the number of Fermi loops, including all bubbles (tadpoles), and introduce a sign change for each.

7. **Symmetry factor:**

   - When only topologically distinct diagrams are considered, introduce a factor $\frac{1}{S(D)}$ where $S(D)$ is the symmetry factor of the diagram.
   - when all linked diagrams are considered, irrespective of whether they are topologically equivalent or not, introduce a factor $\frac{1}{n!2^n}$

[9] In this context, one does not discriminate between particle lines and hole lines.

Comparison with Stefanucci-vanLeeuwen

As a sanity check, let me compare our result with that of Stefanucci and van Leeuwen[2].

The generating functional Eq. 11.38 is identical to $-k_B T \ln \frac{Z}{Z_0} = \mathcal{Q}_{T,\mu}(G^{(0)}, W)$ of Stefanucci-vanLeeuwen-Eq. 11.3.[10] [11]

Each diagram D of order n is represented by a permutation vector $\mathcal{P}$ of length $2n$. The sum over permutation vectors can be cast in the expression of a determinant, e.g.

$$\begin{aligned}
&\sum_{\vec{\mathcal{P}}} \epsilon_{\mathcal{P}_1,\ldots,\mathcal{P}_{2n}} G^{(0)}_{o_1,i_{\mathcal{P}_1}}(t_{i_{\mathcal{P}_1}}, t^+_{o_1}) G^{(0)}_{o_2,i_{\mathcal{P}_2}}(t_{i_{\mathcal{P}_2}}, t^+_{o_2}) G^{(0)}_{o_3,i_{\mathcal{P}_3}}(t_{i_{\mathcal{P}_3}}, t^+_{o_3}) \ldots G^{(0)}_{o_{2n},i_{\mathcal{P}_{2n}}}(t_{\mathcal{P}_{2n}}, t^+_{o_{2n}}) \\
&= \det \begin{vmatrix}
G^{(0)}_{o_1,i_1}(t_{i_1}, t^+_{o_1}) & G^{(0)}_{o_1,i_2}(t_{i_2}, t^+_{o_1}) & G^{(0)}_{o_1,i_3}(t_{i_3}, t^+_{o_1}) & \ldots & G^{(0)}_{o_1,i_{2n}}(t_{i_{2n}}, t^+_{o_1}) \\
G^{(0)}_{o_2,i_1}(t_{i_1}, t^+_{o_2}) & G^{(0)}_{o_2,i_2}(t_{i_2}, t^+_{o_2}) & G^{(0)}_{o_2,i_3}(t_{i_3}, t^+_{o_2}) & \ldots & G^{(0)}_{o_2,i_{2n}}(t_{i_{2n}}, t^+_{o_2}) \\
\vdots & \vdots & \vdots & & \vdots \\
G^{(0)}_{o_{2n},i_1}(t_{i_1}, t^+_{o_{2n}}) & G^{(0)}_{o_{2n},i_2}(t_{i_2}, t^+_{o_{2n}}) & G^{(0)}_{o_{2n},i_3}(t_{i_3}, t^+_{o_{2n}}) & \ldots & G^{(0)}_{o_{2n},i_{2n}}(t_{i_{2n}}, t^+_{o_{2n}})
\end{vmatrix}
\end{aligned} \tag{11.46}$$

The determinant of Stefanucci-vanLeeuwen is limited to the terms representing connected (=linked) diagrams, just as the sum over linked diagrams $D \in \mathbb{L}_n$ in Eq. 11.38

The diagram Eq. 10.66 translates into $D_{c,i} \stackrel{\text{def}}{=} \frac{1}{n!2^n}\mathcal{V}(\vec{\mathcal{P}})$ of Stefanucci-vanLeeuwen-Eq. 11.3.

In Stefanucci-vanLeeuwen-Eq. 11.12 the functional $\Phi_r[G^{(0)}, W]$ is introduced as

$$\Omega_{T,\mu} = -k_B T \ln[Z_{T,\mu}] = -k_B T \ln[Z^{(0)}_{T,\mu}] + k_B T \Phi_r[G^{(0)}, W] \tag{11.47}$$

In Stefanucci-vanLeeuwen-Eq. 11.13 it is shown how the reducible (improper) self energy is obtained as functional derivative of $\Phi_r[G^{(0)}, W]$ with respect to the bare Green's function $\hat{G}^{(0)}$.

11.7.2 Contour time and real-space-and-spin representation

It may be helpful to see Eq. 11.38 in various representations, other than discrete orbitals and time. In order to change the representation, one usually simply reinterprets the orbital indices in another basisset.

Even though this will require a few more steps, I choose to do the basis-transformation more explicit.

Non-interacting Green's function

In the first step, I express the non-interacting Green's function with orbital indices by the one with real-space-and-spin coordinates. The one-particle operator with the non-interacting Hamiltonian $\hat{h}(t)$ is $\hat{U}(t,0)$, which can be written as time ordered exponential $\hat{U}(t,0) = \mathcal{T}_{\mathcal{C}} \mathrm{e}^{-\frac{i}{\hbar}\int_{\mathcal{C},0}^{t} dt'\, h(t')}$. For a time-independent non-interacting Hamiltonian, this propagator simplifies to $\hat{U}(t,0) \rightsquigarrow \sum_n |\varphi_n\rangle \mathrm{e}^{-\frac{i}{\hbar}\epsilon_n t}\langle\varphi_n|$. I begin with the general representation of the non-interacting contour Green's function in terms of

[10] Stefanucci-vanLeeuwen include the zero'th order term, which is absent in my equation. I consider that a omission on their side, because there is no zero-order term except $ln(Z_0)$ in Stefanucci-vanLeeuwenFig. 11.1.

[11] Stefanucci-vanLeeuwen do not explicitly write "det" and they set $\hbar = 1$

non-orthonormal orbitals $|\chi_j\rangle$ and their projector functions $\langle\pi_j|$ given in Eq. 7.30 on p. 258.

$$
\begin{aligned}
G^{\mathcal{C},(0)}_{i,o}(t_i,t_o) &\overset{\text{Eq. 7.30}}{=} \frac{1}{i\hbar}\sum_n \underbrace{\langle\pi_i|\hat{U}(t_i,0)|\varphi_n\rangle}_{\rightsquigarrow\langle\pi_i|\varphi_n\rangle \mathrm{e}^{-\frac{i}{\hbar}\epsilon_n t_i}} \Big\{ \underbrace{\theta_{\mathcal{C}}(t_i-t_o)(1-f_n)}_{\text{electrons}} - \underbrace{\theta_{\mathcal{C}}(t_o-t_i)f_n}_{\text{holes}} \Big\} \underbrace{\langle\varphi_n|\hat{U}(0,t_o)|\pi_o\rangle}_{\rightsquigarrow \mathrm{e}^{\frac{i}{\hbar}\epsilon_n t_o}\langle\varphi_n|\pi_o\rangle} \\
&= \frac{1}{i\hbar}\sum_n \langle\pi_i| \underbrace{\int d^4x_i\, |\vec{x}_i\rangle\langle\vec{x}_i|}_{=\hat{1}} \underbrace{\hat{U}(t_i,0)|\varphi_n\rangle}_{\rightsquigarrow|\varphi_n\rangle \mathrm{e}^{-\frac{i}{\hbar}\epsilon_n t_i}} \Big\{ \underbrace{\theta_{\mathcal{C}}(t_i-t_o)(1-f_n)}_{\text{electrons}} - \underbrace{\theta_{\mathcal{C}}(t_o-t_i)f_n}_{\text{holes}} \Big\} \\
&\quad \times \underbrace{\langle\varphi_n|\hat{U}(0,t_o)}_{\rightsquigarrow \mathrm{e}^{+\frac{i}{\hbar}\epsilon_n t_o}\langle\varphi_n|} \underbrace{\int d^4x_o\, |\vec{x}_o\rangle\langle\vec{x}_o|}_{=\hat{1}}\, \pi_\beta\rangle \\
&= \int d^4x_i \int d^4x_o\, \langle\pi_i|\vec{x}_i\rangle\langle\vec{x}_o|\pi_o\rangle \\
&\quad \times \underbrace{\frac{1}{i\hbar}\sum_n \underbrace{\langle\vec{x}_i|\hat{U}(t_i,0)|\varphi_n\rangle}_{\rightsquigarrow\langle\vec{x}_i|\varphi_n\rangle \mathrm{e}^{-\frac{i}{\hbar}\epsilon_n t_o}} \Big\{ \underbrace{\theta_{\mathcal{C}}(t_i-t_o)(1-f_n)}_{\text{electrons}} - \underbrace{\theta_{\mathcal{C}}(t_o-t_i)f_n}_{\text{holes}} \Big\} \underbrace{\langle\varphi_n|\hat{U}(0,t_i)|\vec{x}_o\rangle}_{\rightsquigarrow \mathrm{e}^{+\frac{i}{\hbar}\epsilon_n t_i}\langle\varphi_n|\vec{x}_o\rangle}}_{G^{\mathcal{C},(0)}(\vec{x}_i,t_i,\vec{x}_o,t_o)} \\
&= \int d^4x_i \int d^4x_o\, \langle\pi_i|\vec{x}_i\rangle\, G^{\mathcal{C},(0)}(\vec{x}_i,t_i,\vec{x}_o,t_o)\, \langle\vec{x}_o|\pi_o\rangle \qquad (11.48)
\end{aligned}
$$

For each argument of the Green's function, I obtain one space-spin "integration" and one projector function $\langle\pi|\vec{x}\rangle$.

NON-INTERACTING GREEN'S FUNCTION IN REAL-SPACE-AND-SPIN REPRESENTATION

The non-interacting Green's function in real-space-and-spin representation is

$$
\begin{aligned}
G^{\mathcal{C},(0)}(\vec{x}_i,t_i,\vec{x}_o,t_o) &\overset{\text{Eq. 11.48}}{=} \frac{1}{i\hbar}\sum_n \underbrace{\langle\vec{x}_i|\hat{U}(t_i,0)|\varphi_n\rangle}_{\rightsquigarrow\langle\vec{x}_i|\varphi_n\rangle \mathrm{e}^{-\frac{i}{\hbar}\epsilon_n t_o}} \\
&\quad \times \Big\{ \underbrace{\theta_{\mathcal{C}}(t_i-t_o)(1-f_n)}_{\text{electrons}} - \underbrace{\theta_{\mathcal{C}}(t_o-t_i)f_n}_{\text{holes}} \Big\} \underbrace{\langle\varphi_n|\hat{U}(0,t_i)|\vec{x}_o\rangle}_{\rightsquigarrow \mathrm{e}^{+\frac{i}{\hbar}\epsilon_n t_i}\langle\varphi_n|\vec{x}_o\rangle} \qquad (11.49)
\end{aligned}
$$

Interaction matrix elements

In the second step, the projector functions from Eq. 11.48 $\langle\pi_\alpha|\vec{x}\rangle$ are combined with the corresponding orbitals $\langle\vec{x}|\chi_\beta\rangle$ from the interaction matrix elements

$$
W_{o_1,o_2,i_1,i_2} \overset{\text{Eq. 3.48}}{=} \int d^4x \int d^4x'\, \frac{e^2\chi^*_{o_1}(\vec{x})\chi^*_{o_2}(\vec{x'})\chi_{i_1}(\vec{x})\chi_{i_2}(\vec{x'})}{4\pi\epsilon_0|\vec{r}-\vec{r'}|}\,, \qquad (11.50)
$$

Then, one can exploit the completeness of the local orbitals

$$
\sum_\alpha \langle\vec{x}|\chi_\alpha\rangle\langle\pi_\alpha|\vec{x'}\rangle = \langle\vec{x}|\vec{x'}\rangle = \delta(\vec{x}-\vec{x'}) \qquad (11.51)
$$

to remove the orbital summations.

The Coulomb interaction

$$
v(\vec{x},t,\vec{x'},t') = \frac{e^2}{4\pi\epsilon_0|\vec{r}-\vec{r'}|}\delta(t-t') \qquad (11.52)
$$

can be replaced by any other pair-wise interaction.

I combine, firstly, the interaction matrix elements with the corresponding orbital summations and, secondly, the integrations and projector functions resulting from the Green's function. Rather than the product of Green's function I use some arbitrary function $Y(\vec{x}_{i_1}, \vec{x}_{i_2}, \vec{x}_{o_1}, \vec{x}_{o_2})$ of the coordinates, so that I can limit the discussion to only four arguments.

$$\begin{aligned}
&\sum_{i_1,o_1,i_2,o_2} \int d^4x_{o_1} \int d^4x_{i_1} \int d^4x_{o_2} \int d^4x_{i_2} \langle \pi_{i_1}|\vec{x}_{i_1}\rangle\langle \vec{x}_{o_1}|\pi_{o_1}\rangle\langle \pi_{i_2}|\vec{x}_{i_2}\rangle\langle \vec{x}_{o_2}|\pi_{o_2}\rangle \\
&\times W_{o_1,o_2,i_1,i_2} Y(\vec{x}_{i_1}, \vec{x}_{i_2}, \vec{x}_{o_1}, \vec{x}_{o_2}) \\
\overset{\text{Eq. 3.48}}{=}& \int d^4x \int d^4x' \int d^4x_{o_1} \int d^4x_{i_1} \int d^4x_{o_2} \int d^4x_{i_2} \frac{e^2}{4\pi\epsilon_0|\vec{r}-\vec{r}'|} Y(\vec{x}_{i_1}, \vec{x}_{i_2}, \vec{x}_{o_1}, \vec{x}_{o_2}) \\
&\times \underbrace{\sum_{i_1} \langle \vec{x}|\chi_{i_1}\rangle\langle \pi_{i_1}|\vec{x}_{i_1}\rangle}_{\delta(\vec{x}-\vec{x}_{i_1})} \underbrace{\sum_{o_1} \langle \vec{x}_{o_1}|\pi_{o_1}\rangle\langle \chi_{o_1}|\vec{x}\rangle}_{\delta(\vec{x}-\vec{x}_{o_1})} \underbrace{\sum_{i_2} \langle \vec{x}'|\chi_{i_2}\rangle\langle \pi_{i_2}|\vec{x}_{i_2}\rangle}_{\delta(\vec{x}'-\vec{x}_{i_2})} \underbrace{\sum_{o_2} \langle \vec{x}_{o_2}|\pi_{o_2}\rangle\langle \chi_{o_2}|\vec{x}'\rangle}_{\delta(\vec{x}'-\vec{x}_{o_2})} \\
=& \int d^4x \int d^4x' \frac{e^2}{4\pi\epsilon_0|\vec{r}-\vec{r}'|} Y(\vec{x}, \vec{x}', \vec{x}, \vec{x}')
\end{aligned} \tag{11.53}$$

By combining the terms from all interaction lines, and by replacing Y by the corresponding product of Green's functions I obtain the rule for the functional $\mathcal{Q}_{T,\mu}$.

SUM AND VALUES OF LINKED DIAGRAMS

$$\mathcal{Q}_{T,\mu}[G^{(0)}] = -\frac{1}{\beta}\mathrm{Tr}\left\{\hat{\rho}^{(0)}_{T,\mu}\mathcal{T}_{\mathcal{C}}\hat{S}_{I,\mathcal{C}}\right\} = -\frac{1}{\beta}\sum_{n=1}^{\infty}\sum_{D\in\mathbb{T}_n}\frac{\mathcal{V}(D)}{S(D)} \tag{11.54}$$

$\mathbb{T}_n$ is set of all topologically distinct, linked, closed diagrams of order n in the interaction. $S(D)$ is the symmetry factor of the diagram D and $\mathcal{V}(D)$ is the value of the diagram given below. Each diagram of order n can be represented by a $2n$ dimensional permutation vector $\vec{\mathcal{P}}$

$$\begin{aligned}
\mathcal{V}(D) \overset{\text{Eq. 10.66}}{=}& \epsilon_{\mathcal{P}_1,\ldots,\mathcal{P}_{2n}} (i\hbar)^n \int_{\mathcal{C}} dt_1 \cdots \int_{\mathcal{C}} dt_{2n} \int d^4x_1 \ldots \int d^4x_{2n} \left(\prod_{j=1}^{n} v(\vec{x}_{2j-1}, t_{2j-1}, \vec{x'}_{2j}, t_{2j})\right) \\
&\times G^{\mathcal{C},(0)}\left(\vec{x}_{\mathcal{P}_1}, t_{\mathcal{P}_1}, \vec{x}_1, t_1^+\right) \cdots G^{\mathcal{C},(0)}\left(\vec{x}_{\mathcal{P}_{2n}}, t_{\mathcal{P}_{2n}}, \vec{x}_{2n}, t_{2n}^+\right)
\end{aligned} \tag{11.55}$$

[a]

[a] I added a time dependence to the interaction matrix elements to allow for adiabatic switching-on.

11.8 Exploit the symmetry of the problem

11.8.1 Exploit time-translation symmetry

Editor: to be done: (Energy representation $t \rightsquigarrow \epsilon$. Try to do the energy representation first without time translation symmetry to include inelastic scattering terms.

Time-translation symmetry is the condition for energy conservation. For the diagrammatic expansion of the generating functional it implies that the interaction matrix elements does not have an explicit time dependence. Furthermore, the Green's function depends only on the relative time

argument.[12]

$$G^{\mathcal{C}(0)}_{i,o}(t,t') = \sum_m G^{\mathcal{C}(0)}_{i,o}(\epsilon_m) \mathrm{e}^{-\frac{i}{\hbar}\epsilon_m(t-t') - \frac{1}{\hbar}\eta|t-t'|} \tag{11.56}$$

$$\begin{aligned}
\mathcal{V}(D) &\overset{\text{Eq. 11.39}}{=} \epsilon_{\mathcal{P}_1,\ldots,\mathcal{P}_{2n}} (i\hbar)^n \int_{\mathcal{C}} dt_1 \cdots \int_{\mathcal{C}} dt_{2n} \sum_{o_1,i_1,\ldots,o_{2n},i_{2n}} \left(\prod_{j=1}^{n} W_{o_{2j-1},o_{2j},i_{2j-1},i_{2j}}(t_{2j-1},t_{2j}) \right) \\
&\quad \times G^{\mathcal{C},(0)}_{i_{\mathcal{P}_1},o_1}\left(t_{\mathcal{P}_1}, t_1^+\right) \cdots G^{\mathcal{C},(0)}_{i_{\mathcal{P}_{2n}},o_{2n}}\left(t_{\mathcal{P}_{2n}}, t_{2n}^+\right) \\
&\overset{\text{Eq. 7.30}}{=} \epsilon_{\mathcal{P}_1,\ldots,\mathcal{P}_{2n}} (i\hbar)^n \sum_{o_1,i_1,\ldots,o_{2n},i_{2n}} \left(\prod_{j=1}^{n} W_{o_{2j-1},o_{2j},i_{2j-1},i_{2j}}(0) \right) \int_{\mathcal{C}} dt_1 \cdots \int_{\mathcal{C}} dt_n \\
&\quad \times \underbrace{\sum_{m_1} G^{\mathcal{C}(0)}_{i_{\mathcal{P}_1},o_1}(\epsilon_{m_1}) \mathrm{e}^{-\frac{i}{\hbar}\epsilon_{m_1}\left(t_{\mathcal{P}_1}-t_1^+\right) - \frac{1}{\hbar}\eta\left|t_{\mathcal{P}_1}-t_1^+\right|} \ldots}_{G^{\mathcal{C},(0)}_{i_{\mathcal{P}_1},o_1}\left(t_{\mathcal{P}_1},t_1^+\right)} \\
&\quad \times \underbrace{\sum_{m_1} G^{\mathcal{C}(0)}_{i_{\mathcal{P}_{2n}},o_{2n}}(\epsilon_{m_{2n}}) \mathrm{e}^{-\frac{i}{\hbar}\epsilon_{m_{2n}}\left(t_{\mathcal{P}_{2n}}-t_{2n}^+\right) - \frac{1}{\hbar}\eta\left|t_{\mathcal{P}_{2n}}-t_{2n}^+\right|}}_{G^{\mathcal{C},(0)}_{i_{\mathcal{P}_{2n}},o_{2n}}\left(t_{\mathcal{P}_{2n}},t_{2n}^+\right)} \\
&=
\end{aligned} \tag{11.57}$$

Note here that the generating functional is a functional of the non-interacting Green's function. Therefore, it is not sensible to resolve the non-interacting Green's function Eq. 7.30 by the eigenvalues and eigenstates of the non-interacting system.

11.8.2 Exploit spatial translation symmetry

Editor: to be done: momentum representation (plane waves) $\vec{x} \rightsquigarrow (\vec{p}, \sigma)$.

11.8.3 Exploit spin-inversion symmetry

So-far we worked with general two-component spinor functions. However, often it is convenient to specialize the expressions to a basis set of $\hat{S}_z$ eigenstates.

In that case, the index of an creation or annihilation operator must be considered as a combined index $o = (\alpha(o), \sigma(o))$ describing the orbital index $\alpha(o)$ and the spin quantum number $\sigma(o)$ of the orbital.

$$W_{o_1,o_2,i_1,i_2} = W_{(\alpha_{o_1},\sigma_{o_1}),(\alpha_{o_2},\sigma_{o_2}),(\alpha_{i_1},\sigma_{i_1}),(\alpha_{i_2},\sigma_{i_2})} \delta_{\sigma_{o_1},\sigma_{i_1}} \delta_{\sigma_{o_2},\sigma_{i_2}} \tag{11.58}$$

Thus, the integration over all indices can be mapped onto an integration over all spatial indices, while the sum over spins is attributed to each vertex. The delta functions adds a sum rule, saying that the spin of the incoming Green's function is equal to that of the outgoing Green's function.

[12] The non-interacting Hamiltonian is time independent, as precondition for Wick's theorem. Therefore, the non-interacting Green's function should automatically only depend on the relative time argument. However, later we will use the generating functional also with the full Green's function as arguments. Time translation symmetry implies that we may restrict the domain for the functional to Green's functions that only depend on the relative time argument.

11.8.4 Exploit Bloch theorem

If the one-particle Hamiltonian is periodic, we may choose a basisset of Bloch states. In that case the orbital index is a combined index referring to a Bloch-vector $\vec{k}$, a band index n and a spin index σ.

We can make use that the Green's function of the non-interacting system is block diagonal in a basis of the Bloch states, i.e.

$$G^{(0)}_{i,o}(t,t') = \delta\Big(\vec{k}_i - \vec{k}_o\Big) G^{(0)}_{(\vec{k}_i,n_i,\sigma_i),(\vec{k}_o,n_o,\sigma_o)}(t,t') \tag{11.59}$$

Because the Coulomb interaction is isotropic and translation invariant under a shift of both spatial coordinates of the Green's function, the interaction conserves the momentum and thus has the form

$$W_{o_1,o_2,i_1,i_2} = \delta\Big((\vec{k}_{o_1} - \vec{k}_{i_1}) - (\vec{k}_{o_2} - \vec{k}_{i_2})\Big) W_{(\vec{k}_{o_1},n_{o_1},\sigma_{o_1}),(\vec{k}_{o_2},n_{o_2},\sigma_{o_2}),(\vec{k}_{i_1},n_{i_1},\sigma_{i_1}),(\vec{k}_{i_2},n_{i_2},\sigma_{i_2})} \tag{11.60}$$

This results in the rule that we can attribute the interaction matrix elements to a momentum $\vec{q}$, that is transferred from one vertex of the interaction to the other. Thus, we have momentum conservation at each vertex between the incoming and outgoing Green's function and the interaction.

11.9 Zoo of diagrams

In this section, I will mention a few common diagrams in order to provide some familiarity. Many expansions used in practice are related to the Skeleton expansion of the Luttinger ward functional discussed in the following chapter. In that chapter, I will also provide in section 14 an overview of the most common diagrams.

In this present section, I will not go into depth because much of the material is duplicated in section 14, where I will provide additional information.

The diagrams up to second order in the interaction and their self-energy diagrams are shown in figure 11.6 on p. 372

Editor: Interestingly the prefactor given by the symmetry factor is exactly canceled by the multiplicity of the self-energy diagrams.

There are classes of diagrams that can be summed up to infinite order, because they form a geometric series. The most simple ones, those for which the repeating unit is formed by one interaction and two particle lines are shown in figure 11.7.

11.9.1 First-order Hartree Fock

The diagrams A and B in figure 11.6 on p. 372, are the Hartree diagram (eyeglass) and exchange diagram (oyster).

The term Hartree-Fock approximation is used in many sometimes different context. Here, we refer to the first-order expansion in the interaction. The self-consistent Hartree-Fock approximation includes also higher order diagrams.

11.9.2 Random-phase approximation (RPA)

The sequence of diagrams denoted H in figure 11.7 defines the random-phase approximation.

Note, that the first-order term of this sequence is the exchange term denoted B in figure 11.6 and the second order term is the one denoted D. It is important to avoid double counting of these terms, when combining the RPA terms with the low-order diagrams.

As an introduction to the random-phase approximation, I recommend chapter 10 of Mattuck's textbook[4].

The polarization insertion for the free-electron gas has been evaluated in appendix E.4 on p. 575.

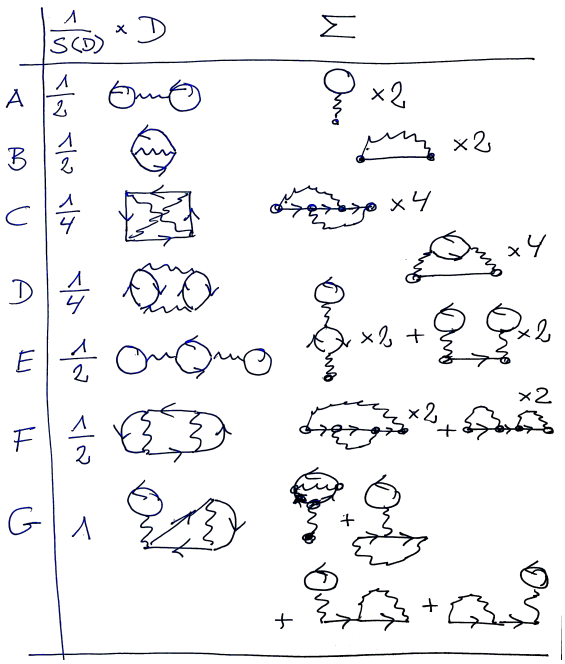


Fig. 11.6: Diagrams in $\mathbb{T}$ and their self-energy contributions up to second order in the interaction. The closed diagrams, which are part of the generating functional $\mathcal{Q}_{T,\mu}$ also carry the prefactor $1/S(D)$, where $S(D)$ is the symmetry factor. On the right, the self-energy diagrams resulting from the closed diagram on the left are shown including their multiplicity. See text for explanation.

11.9.3 Ladder- or T-matrix approximation

The sequence of diagrams denoted I and J in figure 11.7 defines the ladder approximation.

Note, that the first-order term of this sequence is the Hartree term denoted A in figure 11.6 and the second order term is the one denoted D. It is important to avoid double counting of these terms, when combining the ladder terms with the low-order diagrams. Note furthermore that some low-order diagrams of the particle-particle ladder and of the particle-hole ladder and those of the random-phase approximation are identical.

As an introduction to the ladder approximation, I recommend chapter 10 of Mattuck's textbook[4].

11.9.4 Fluctuation-exchange (FLEX) approximation

The fluctuating-exchange approximation combined the diagrams of the random-phase approximation and the ladder approximation with the sequence of diagrams denoted K in figure 11.7.

See the review of Bickers and Scalapino[92] on the fluctuating exchange approximation. The generalization to general lattice Hamiltonians has been done Esirgen and Bickers.[**?**]

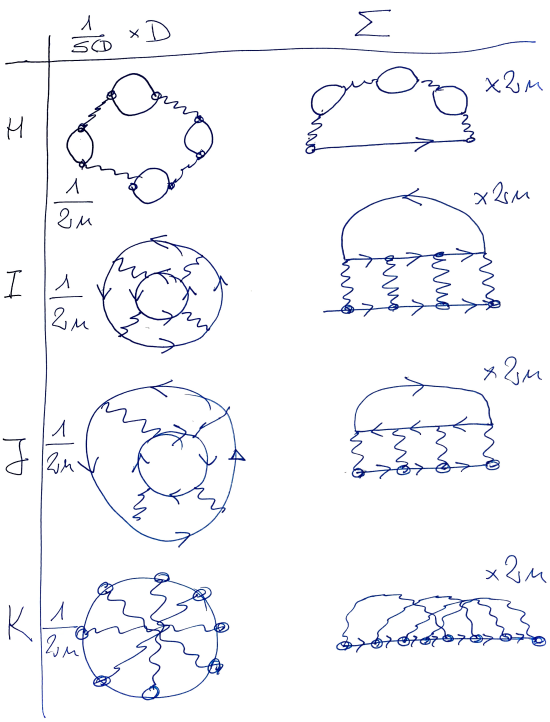


Fig. 11.7: Diagrams in $\mathbb{T}$ and their self-energy contributions in the interaction. The closed diagrams, which are part of the generating functional $\mathcal{Q}_{T,\mu}$ also carry the prefactor $1/S(D)$, where $S(D)$ is the symmetry factor. On the right, the self-energy diagrams resulting from the closed diagram on the left are shown including their multiplicity. See text for explanation.



Fig. 11.8: Diagrams for the generating functional $\mathcal{Q}[G^{(0)}]$ in the non-self-consistent Hartree-Fock approximation. The first diagram, the eyeglass, is the Hartree diagram, while the second diagram, the oyster, describes exchange.

11.10 Home study and practice

11.10.1 Enumerate permutations

Introduction

In section 11.2.1, a method has been presented to enumerate all permutations of a sequence of numbers. This is a useful method not only in the context of Feynman diagrams. It can be used to calculate a determinant of a matrix, even though I do not claim that it is the most efficient method.

The method can also be coded up easily as shown in appendix M. Therefore, it is useful to get familiar with it.

Problem

- Enumerate all permutations of the sequence numbers (1,2,3,4). Check that there are 4! = 24 such permutations.
- assign the sign to each diagram in this sequence (Use the sign theorem.)

Discussion

- Enumerate all permutations of the sequence numbers (1,2,3,4). Check that there are 4! = 24 such permutations.
- assign the sign to each diagram in this sequence (Use the sign theorem.)

The permutation vectors are listed in section 11.2.3 on p. 349. The diagrams are shown in figure 11.2 arranged row-wise. Using sign-theorem described in section 11.3, the signs are obtained by counting Fermi loops.

Nr	$\vec{\mathcal{P}}$	sign	Nr	$\vec{\mathcal{P}}$	sign
1	(1,2,3,4)	+	13	(3,1,2,4)	+
2	(1,2,4,3)	-	14	(3,1,4,2)	-
3	(1,3,2,4)	-	15	(3,2,1,4)	-
4	(1,3,4,2)	+	16	(3,2,4,1)	+
5	(1,4,2,3)	+	17	(3,4,1,2)	+
6	(1,4,3,2)	-	18	(3,4,2,1)	-
7	(2,1,3,4)	-	19	(4,1,2,3)	-
8	(2,1,4,3)	+	20	(4,1,3,2)	+
9	(2,3,1,4)	+	21	(4,2,1,3)	+
10	(2,3,4,1)	-	22	(4,2,3,1)	-
11	(2,4,1,3)	-	23	(4,3,1,2)	-
12	(2,4,3,1)	+	24	(4,3,2,1)	+

One sanity check is to ensure that half of the diagrams have positive and the other half have negative sign.

The number of diagrams if 4! = 24.

11.10.2 Feynman diagrams from permutation vectors

The recipe to construct Feynman diagrams depends on the strict enforcement of a consistent set of rules. (There are different sets of rules in the literature.) Therefore, this exercise is to practice the set of rules provided in this text.

Problem

1 Draw the Feynman diagrams related to the permutation vectors

$$\vec{\mathcal{P}} = (1, 3, 5, 6, 2, 4) \tag{11.61}$$
$$\vec{\mathcal{P}} = (1, 3, 5, 6, 4, 2) \tag{11.62}$$
$$\vec{\mathcal{P}} = (2, 3, 1, 5, 6, 4) \tag{11.63}$$
$$\vec{\mathcal{P}} = (2, 3, 4, 5, 6, 1) \tag{11.64}$$
$$\vec{\mathcal{P}} = (2, 3, 5, 1, 6, 4) \tag{11.65}$$
$$\vec{\mathcal{P}} = (2, 3, 5, 6, 1, 4) \tag{11.66}$$

and

- count the number of Fermi loops,
- determine the sign of the diagrams,
- identify the 2-particle reducible diagrams,
- identify the 1-particle reducible diagrams,

2 determine the diagrams for the Green's function resulting from the closed diagram $\vec{\mathcal{P}} = (2, 3, 4, 5, 6, 1)$.

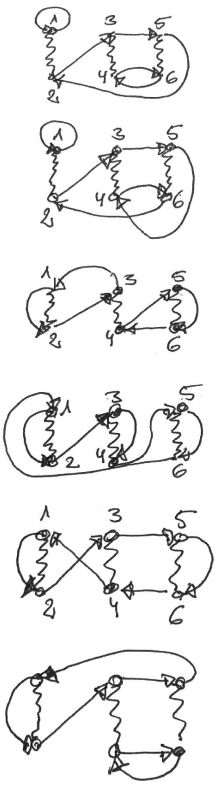
Discussion

1 Draw the Feynman diagrams related to the permutation vectors

$$\vec{\mathcal{P}} = (1, 3, 5, 6, 2, 4) \tag{11.67}$$
$$\vec{\mathcal{P}} = (1, 3, 5, 6, 4, 2) \tag{11.68}$$
$$\vec{\mathcal{P}} = (2, 3, 1, 5, 6, 4) \tag{11.69}$$
$$\vec{\mathcal{P}} = (2, 3, 4, 5, 6, 1) \tag{11.70}$$
$$\vec{\mathcal{P}} = (2, 3, 5, 1, 6, 4) \tag{11.71}$$
$$\vec{\mathcal{P}} = (2, 3, 5, 6, 1, 4) \tag{11.72}$$

and

- count the number of Fermi loops,
- determine the sign of the diagrams,
- identify the 2-particle reducible diagrams,
- identify the 1-particle reducible diagrams,



1. $\vec{\mathcal{P}} = (1, 3, 5, 6, 2, 4)$; 3 Fermi loops, sign= $-$, 2-particle reducible, 1-particle irreducible

2. $\vec{\mathcal{P}} = (1, 3, 5, 6, 4, 2)$ 2 Fermi loops, sign= $+$, 2-particle reducible, 1-particle irreducible

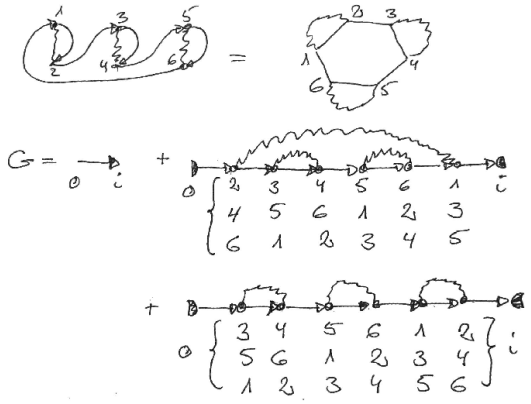
3. $\vec{\mathcal{P}} = (2, 3, 1, 5, 6, 4)$ 2 Fermi loops, sign= $+$, 2-particle reducible, 1-particle irreducible

4. $\vec{\mathcal{P}} = (2, 3, 4, 5, 6, 1)$ 1 Fermi loops, sign= $-$, 2-particle reducible, 1-particle irreducible

5. $\vec{\mathcal{P}} = (2, 3, 5, 1, 6, 4)$ 1 Fermi loops, sign= $-$, 2-particle reducible, 1-particle irreducible

6. $\vec{\mathcal{P}} = (2, 3, 5, 6, 1, 4)$ 2 Fermi loops, sign= $+$, 2-particle reducible, 1-particle irreducible

2 determine the diagrams for the Green's function resulting from the closed diagram $\vec{\mathcal{P}} = (2, 3, 4, 5, 6, 1)$.



11.10.3 Evaluate symmetry factors

Introduction

The reduction to topologically inequivalent diagrams results in a tremendous saving in the number of terms to be evaluated. Nevertheless it requires to evaluate the symmetry factor. While the operations are not very complicated, one needs to practice them to learn the technique properly.

In this exercise we exercise the technique for two examples, namely one that has been used as example in the main text, and another one which is new.

Problem

1 Determine the topology-preserving transformations of diagrams for the second order of the interaction. Describe them in words and provide the mapping vectors.

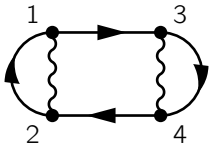
2 Construct the permutation vectors of all diagrams which are topologically equivalent (distinct or mere deformation) to the diagram.

$$\vec{\mathcal{P}} = (3, 1, 4, 2) \tag{11.73}$$

3 Use the criterion that permutation and relabeling commutate to determine the symmetry factor for the same diagram.

$$\vec{\mathcal{P}} = (3, 1, 4, 2) \tag{11.74}$$

4 Construct graphically the diagrams which are topologically equivalent to



(11.75)

determine mere deformations and the symmetry factor.

5 Work out the symmetry factor for the following second-order diagrams

$$\vec{\mathcal{P}} = (1, 3, 2, 4) \tag{11.76}$$

using the method of your choice.

Do not use the trivial approach of constructing all linked diagrams of a given order and search for topologically equivalent ones. This would not be feasible for diagrams of higher order.

Solution

The final solution can be read off from Fig. 11.5 on p. 364, which keeps all second-order diagrams and their symmetry factor.

1 Determine the topology-preserving transformations of diagrams for the second order of the interaction. Describe them in words and provide the mapping vectors.

The topologically equivalent diagrams are obtained by

- 2^n interchanges of the two vertices of the same interaction line, and
- $n!$ permutations of the interaction lines, that is of their indices, while preserving the *"orientation"* of the interaction, that is odd indices are mapped again onto odd indices and the even indices are mapped onto even indices.

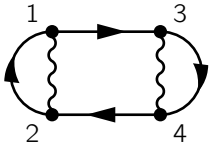
These vertex-mappings are given in table 11.2 on p. 360. The mappings for the second-order diagrams are

$\vec{M}_1 = (1234)$	$\vec{M}_5 = (3412)$
$\vec{M}_2 = (2134)$	$\vec{M}_6 = (4312)$
$\vec{M}_3 = (1243)$	$\vec{M}_7 = (3421)$
$\vec{M}_4 = (2143)$	$\vec{M}_8 = (4321)$

2 Construct the permutation vectors of all diagrams which are topologically equivalent (distinct or mere deformation) to the diagram.

$$\vec{\mathcal{P}} = (3,1,4,2) \tag{11.77}$$

The diagram represented by the permutation vector $\vec{\mathcal{P}} = (3,1,4,2)$ has the following appearance



(11.78)

This diagram can be represented by the mapping from the indices o to the indices i.

o	1	2	3	4
i	3	1	4	2

(11.79)

The permutation vector defining this diagram is given by the second line, i.e. $\vec{\mathcal{P}} = (3,1,2,4)$. The Green's functions can be described as mappings between vertices, $G^{(0)}_{i_3,o_1} \hat{=} (1 \to 3)$, $G^{(0)}_{i_1,o_2} \hat{=} (2 \to 1)$, $G^{(0)}_{i_4,o_3} \hat{=} (3 \to 4)$, and $G^{(0)}_{i_2,o_4} \hat{=} (4 \to 2)$.

Let me now construct all topologically equivalent diagrams using the mappings

1. $\vec{M}_1 = (1234)$, $\vec{\mathcal{P}}' = (1234)$

o	1	2	3	4	remap $\to$	o	1	2	3	4	order $\to$	o	1	2	3	4
i	3	1	4	2		i	3	1	4	2		i	3	1	4	2

2. $\vec{M}_2 = (2134)$, $\vec{\mathcal{P}}' = (2341)$

o	1	2	3	4	remap $\to$	o	2	1	3	4	order $\to$	o	1	2	3	4
i	3	1	4	2		i	3	2	4	1		i	2	3	4	1

3. $\vec{M}_3 = (1243)$, $\vec{\mathcal{P}}' = (4123)$

o	1	2	3	4	remap $\to$	o	1	2	4	3	order $\to$	o	1	2	3	4
i	3	1	4	2		i	4	1	3	2		i	4	1	2	3

4. $\vec{M}_4 = (2143)$, $\vec{\mathcal{P}}' = (2413)$

o	1	2	3	4	remap $\to$	o	2	1	4	3	order $\to$	o	1	2	3	4
i	3	1	4	2		i	4	2	3	1		i	2	4	1	3

5. $\vec{M}_5 = (3412)$, $\vec{\mathcal{P}}' = (2413)$

o	1	2	3	4	remap $\to$	o	3	4	1	2	order $\to$	o	1	2	3	4
i	3	1	4	2		i	1	3	2	4		i	2	4	1	3

At this point we already encounter two diagrams that are mere deformation of each other, namely the last two above. Thus, we can identify one operation that produces mere deformations of this diagram. It is the inverse of the fourth mapping leading $\vec{M}_4 = (2143)$ followed by the fifth mapping $\vec{M}_5 = (3412)$. The fourth mapping interchanges the vertices of the first interaction and of the second interaction. Its inverse does the same. $\vec{M}_5 = (3412)$ interchanges the two interactions. The combined operation is $M_5 \circ M_4^{-1} = (4321) = M_8$. This transformation produces a mere deformation rather than a topologically equivalent but distinct diagram.

We can actually stop here, because the same operation will produce a mere deformation of any diagram of the four distinct diagrams obtained $\vec{M}_1$ to $\vec{M}_4$. Thus, there are four mere deformations and four distinct diagrams. We obtain $r_D = \frac{4}{8} = \frac{1}{2}$ and $S(D) = \frac{1}{1-r_D} = 2$.

For the sake of completeness let me work through the remaining three mappings.

6 $\vec{M}_6 = (4312)$, $\vec{\mathcal{P}}' = (2341)$

o	1	2	3	4	remap $\to$	o	4	3	1	2	order $\to$	o	1	2	3	4
i	3	1	4	2		i	1	4	2	3		i	2	3	4	1

7 $\vec{M}_7 = (3421)$
$\vec{\mathcal{P}}' = (4123)$

o	1	2	3	4
i	3	1	4	2

remap →

o	3	4	2	1
i	2	3	1	4

order →

o	1	2	3	4
i	4	1	2	3

8 $\vec{M}_8 = (4321)$
$\vec{\mathcal{P}}' = (1234)$

o	1	2	3	4
i	3	1	4	2

remap →

o	4	3	2	1
i	2	4	1	3

order →

o	1	2	3	4
i	3	1	4	2

3 Use the criterion that permutation and relabeling commutate to determine the symmetry factor for the same diagram

$$\vec{\mathcal{P}} = (3, 1, 4, 2) \tag{11.80}$$

used in the previous problem

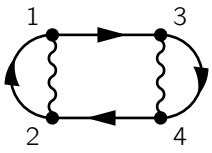
$M_1 \circ \mathcal{P}$	3142	M_1	1234	$\mathcal{P} \circ M_1$	3142
$M_2 \circ \mathcal{P}$	3241	M_2	2134	$\mathcal{P} \circ M_2$	1342
$M_3 \circ \mathcal{P}$	4132	M_3	1243	$\mathcal{P} \circ M_3$	3124
$M_4 \circ \mathcal{P}$	4231	M_4	2143	$\mathcal{P} \circ M_4$	1324
$M_5 \circ \mathcal{P}$	1324	M_5	3412	$\mathcal{P} \circ M_5$	3412
$M_6 \circ \mathcal{P}$	1423	M_6	4312	$\mathcal{P} \circ M_6$	2431
$M_7 \circ \mathcal{P}$	2314	M_7	3421	$\mathcal{P} \circ M_7$	4213
$M_8 \circ \mathcal{P}$	2413	M_8	4321	$\mathcal{P} \circ M_8$	2413

To set up the table above, I proceeded as follows

- I fill the first column with the permutation vector $\vec{\mathcal{P}}$, the second one with 1234 and the third column again with $\vec{\mathcal{P}}$
- now I perform, line-by-line, the transformations on the sequences of the second and the third column. This will construct the vectors $\vec{M}$ in the second column and $\mathcal{P} \circ M$ in the third.
- Finally I transform the sequences of the first column, which currently holds $\vec{\mathcal{P}}$ in each line, by the corresponding transformation M from the middle column. Starting with the first component, I look up $\mathcal{P}_j$, which tells me at which position of $\vec{M}$ I find the new value $M_{\mathcal{P}_j}$ for the j-th component of the vector in the first column. For each component j, this step is efficiently on all lines simultaneously.

From the table above, we find that mere deformations are the identity M_1 and M_8. The identity is trivial and is discarded. Thus, there is one mere deformation, except for the identity M_1, among the eight transformations in the group.

4 Construct graphically the diagrams which are topologically equivalent to



(11.81)

determine mere deformations and the symmetry factor.

The solution is given in figure 11.4 on p. 363.

5 Work out the symmetry factor for the following second-order diagram

$$\vec{\mathcal{P}} = (1, 3, 2, 4) \tag{11.82}$$

using the method of your choice.

This diagram is a ring diagram with a tadpole attached to either side.

$M_1 \circ \mathcal{P}$	1324	M_1	1234	$\mathcal{P} \circ M_1$	1324
$M_2 \circ \mathcal{P}$	2314	M_2	2134	$\mathcal{P} \circ M_2$	3124
$M_3 \circ \mathcal{P}$	1423	M_3	1243	$\mathcal{P} \circ M_3$	1342
$M_4 \circ \mathcal{P}$	2413	M_4	2143	$\mathcal{P} \circ M_4$	3142
$M_5 \circ \mathcal{P}$	3142	M_5	3412	$\mathcal{P} \circ M_5$	2413
$M_6 \circ \mathcal{P}$	4132	M_6	4312	$\mathcal{P} \circ M_6$	4213
$M_7 \circ \mathcal{P}$	3241	M_7	3421	$\mathcal{P} \circ M_7$	2431
$M_8 \circ \mathcal{P}$	4231	M_8	4321	$\mathcal{P} \circ M_8$	4231

There are two transformations including the identity that produce mere deformations of the given diagram, namely M_1 and M_8. Thus, the symmetry factor is $S(D) = 2$.

11.10.4 Value of a given Feynman diagrams

Editor: This exercise needs to be completed.

For the shown $\vec{\mathcal{P}} = (1, 4, 3, 2)$. Show the

$$P = (1432)$$

$$\mathcal{V}(1,4,3,2) = \epsilon_{1,4,3,2}(i\hbar)^2 \sum_{i_1,o_1,i_2,o_2,i_3,o_3,i_4,o_4} \int_{\mathcal{C}} dt_1 \int_{\mathcal{C}} dt_2$$

$$\times W_{o_1,o_2,i_1,i_2}(t) W_{o_3,o_4,i_3,i_4}(t') \tag{11.83}$$

$$G_{i_1,o_1}(t_1, t_1^+) G_{i_4,o_2}(t_2, t_1) G_{i_3,o_3}(t_2, t_2^+) G_{i_2,o_4}(t_1, t_2) \tag{11.84}$$

Feynman diagram

- extract a permutation vector
- work out value of the Feynman diagram in terms of non-interacting Green's function and the interaction matrix

Solution: place numbers onto the vertices. Read of vertex the green's function points to.

11.10.5 Example: Evaluate the Green's function for a specific example

Editor: This exercise needs to be completed.

So-far we manipulated expressions given in terms of Green's functions and interaction matrix elements. We did not practice to work out the Green's function for a specific system. In this section, we will work out the Green's function for the Hartree-Fock approximation for the Hubbard dimer.

11.11 Summary

A sequence of theorems have been required to set up the diagrammatic expansion of the Green's function

1. interaction picture and introduction of the S-matrix
2. replacement of the thermal von-Neumann density matrix by that of the non-interacting system. Description of the conversion by propagation along the imaginary time axis.
3. Wick's theorem
4. linked-cluster theorem
5. sign theorem
6. symmetry factors
7. conversion of $\mathcal{Q}_{T,\mu}$ into Green's functions

We learned how to enumerate all diagrams using permutation vectors.

Permutation vectors, Feynman diagrams and the expression for the value $\mathcal{V}(D)$ of a diagram can be translated into each other.

Part II

Additional topics

Chapter 12

Luttinger-Ward functional

Truncating the diagrammatic expansion can lead to Green's functions that violate conservation laws such as particle-number conservation, energy conservation, momentum conservation, angular momentum conservation.

Kadanoff and Baym[93, 94] have shown that these conservation laws can be enforced when the equations for the Green's function are derived from the so-called Luttinger-Ward functional[95].

The Luttinger-Ward functional paves the way to renormalization. Rather than summing up the Green's function term by term, we will obtain a set of equations, that need to be solved simultaneously, i.e. self-consistently. The number of diagrams to be considered is substantially smaller than for the expansion of our generating functional, but each particle line contains implicitely a large number of terms.

12.1 Compact notation: Generalized matrix algebra

The derivation of the Luttinger-Ward functional leads to expressions, in which the multitude of indices and arguments obscures the underlying principles. Therefore, I will use in this chapter a very compact notation. Later, I will explicitely go through some examples.

In the compact notation used here, a product is a matrix product, which involves a sum over orbital indices and a time integration over the contour chosen. Similarly the trace includes a sum over orbital indices and a time integration.

Time argument and orbital index is treated as one combined matrix index.

$$A_{\alpha,\beta}(t,t') \rightsquigarrow A_{(\alpha,t);(\beta,t')} \tag{12.1}$$

The time argument shall be considered discretized. The product is

$$C = AB \qquad \Leftrightarrow \qquad C_{\alpha,\beta}(t,t') = \sum_{\gamma} \int dt''\, A_{\alpha,\gamma}(t,t'') B_{\gamma,\beta}(t'',t') \tag{12.2}$$

We will also need derivatives in this compact notation. To define the derivative we start from the first variation. Consider the trace of two matrices

$$\begin{aligned} F[B] = \mathrm{Tr}[AB] \qquad &\Leftrightarrow \qquad F[B] = \int dt \int dt' \sum_{j,k} A_{j,k}(t,t') B_{k,j}(t',t) \\ dF = \mathrm{Tr}[A\,dB] \qquad &\Leftrightarrow \qquad dF = \int dt \int dt' \sum_{j,k} A_{j,k}(t,t') dB_{k,j}(t',t) \\ A = \frac{dF}{dB} \qquad &\Leftrightarrow \qquad A_{j,k}(t,t') = \frac{dF}{dB_{k,j}(t',t)} \end{aligned} \tag{12.3}$$

Important is to note the order of the arguments and indices in the derivative.

12.2 From our generating functional $\mathcal{Q}_{T,\mu}[G^{(0)}]$ to the Luttinger-Ward functional

From the reducible to the proper self energy

Let me rearrange Dyson's equation Eq. 8.23 to allow the comparison with Eq. 10.78.

$$\begin{aligned} G &\overset{\text{Eq. 8.23}}{=} G^{(0)} + G^{(0)}\Sigma G \\ &= G^{(0)} + G^{(0)}\Sigma G^{(0)} + G^{(0)}\Sigma G^{(0)}\Sigma G^{(0)} + \dots \\ &= G^{(0)} + G^{(0)} \underbrace{\left(\Sigma + \Sigma G^{(0)}\Sigma + \dots\right)}_{=\Sigma^{red},\ \text{see Eq. 10.78}} G^{(0)} \end{aligned} \tag{12.4}$$

By comparing Eq. 12.4 with Eq. 10.78, we obtain the reducible self energy Σ^{red} in terms of the bare Green's function $G^{(0)}$ and the proper self energy Σ, namely

$$\begin{aligned} \Sigma^{red} &= \Sigma + \Sigma G^{(0)}\Sigma + \Sigma G^{(0)}\Sigma G^{(0)}\Sigma + \dots \\ &= \sum_{n=0}^{\infty} \left(\Sigma G^{(0)}\right)^n \Sigma \\ &= \sum_{n=0}^{\infty} \frac{1}{n+1} \frac{\partial}{\partial G^{(0)}}\Big|_{\Sigma} \mathrm{Tr}\left[\left(\Sigma G^{(0)}\right)^{n+1}\right] \\ &\overset{n+1\to n}{=} \frac{\partial}{\partial G^{(0)}}\Big|_{\Sigma} \sum_{n=1}^{\infty} \frac{1}{n} \mathrm{Tr}\left[\left(\Sigma G^{(0)}\right)^{n}\right] \\ &\overset{\ln(1-x)=-\sum_{n=1}^{\infty}\frac{1}{n}x^n}{=} -\frac{\partial}{\partial G^{0}}\Big|_{\Sigma} \mathrm{Tr}\left[\ln\left(1-\Sigma G^{(0)}\right)\right] \end{aligned} \tag{12.5}$$

The logarithm and the inverse shall be understood as their Taylor expansions $(1-x)^{-1} = \sum_{n=0}^{\infty} x^n$ for $|x| < 1$ and $\ln(1-x) = -\sum_{n=1}^{\infty} \frac{1}{n} x^n$ for $|x| < 1$. The limited convergence radius implies that the expression is not defined when $\Sigma G^{(0)}$ has any eigenvalue with an absolute value equal or larger than 1.

This allows one to rewrite the identity Eq. 10.79

$$\beta \frac{\partial \mathcal{Q}}{\partial G^{(0)}} \overset{\text{Eq. 10.79}}{=} \Sigma^{red} \overset{\text{Eq. 12.5}}{=} -\frac{\partial}{\partial G^{0}}\Big|_{\Sigma} \underbrace{\mathrm{Tr}\left[\ln\left(1-\Sigma G^{(0)}\right)\right]}_{\text{functional of } \Sigma \text{ and } G^{(0)}} \tag{12.6}$$

in the form of a stationary condition for a function that depends on the bare Green's function and the proper self energy.

$$0 = \frac{\partial}{\partial G^{(0)}}\Big|_{\Sigma} \left\{ \mathcal{Q}\left[G^{(0)}\right] + k_B T\ \mathrm{Tr}\left[\ln\left(1-\Sigma G^{(0)}\right)\right] \right\} \tag{12.7}$$

This suggests to define a functional of the proper self energy Σ.

A functional of the proper self energy

Let me define a **self-energy functional** [96, 97] [1] [2] $F(\Sigma)$ by a generalized Legendre transform[3].

$$F[\Sigma] \overset{\text{def}}{=} \underset{G^{(0)}}{\mathrm{stat}} \left\{ \mathcal{Q}[G^{(0)}] + k_B T\ \mathrm{Tr} \ln\left(1-\Sigma G^{(0)}\right) \right\} \tag{12.8}$$

[1] Hofmann et al. [97] show the generalization of the self-energy functional to non-equilibrium Green's functions.

[2] Editor: The bare Green's function can be parameterized by an effective potential, which may be useful.

[3] In order to brush up on Legendre transforms you may consult section 3.2 of ΦSX:Statistical Physics[38].

What we just did is a generalized Legendre transform, which does not work with straight lines like a normal Legendre transform but with another family of functions. To explain, what I mean with generalized Legendre transform let me quickly review the ordinary Legendre transform in the following box.

Legendre transform in thermodynamics: Let me consider a normal Legendre transform in thermodynamics. Start from an internal energy $U(S)$ as function of the entropy S. The derivative of the internal energy defines a physical quantity, namely the temperature T:

$$T = \frac{dU}{dS} \tag{12.9}$$

Let me consider the problem of finding the entropy for a given temperature: I define a Legendre transform of the internal energy, namely the free energy[a] $F(T)$ by

$$F(T) = \operatorname*{stat}_S \Big\{ U(S) - TS \Big\} \tag{12.10}$$

The stationary condition[b] encapsulates the definition Eq. 12.9 of the temperature. The derivative of the free energy, in turn, is the (negative) entropy

$$\frac{dF}{dT} = \underbrace{\frac{\partial (U(S) - TS)}{\partial S}}_{=0} \frac{\partial S}{\partial T} + \underbrace{\frac{\partial (U(S) - TS)}{\partial T}}_{=-S} = -S \tag{12.11}$$

This is the desired result, namely the entropy as function of the temperature. The Legendre transform describes a function $U(S)$ not by values $U(S)$ for a given argument S, but by values $F(T)$ for given slope T of the original function $U(S)$. $F(T)$ describes the vertical (along the U-axis) displacement of a tangent $y_T(S) = F(T) + TS$. to the function $U(S)$.
Some caution is necessary, because a Legendre transform does not guarantee that the back transform is identical to the original function. The Legendre transform is bijective only, if the original function is purely convex or purely concave. Otherwise, several tangents with the same slope may exist, so that the Legendre transformed function $F(T)$ would be double valued. If the other branches of the Legendre transform are omitted, one obtains the outer envelope of the original function. This route is taken in the Legendre-Fenchel transform.
The arguments, given here for one-dimensional functions are not meant to be exhaustive, but they should raise the attention to problems that have been an issue[98] related to the existence of the Luttinger-Ward functional.

[a] The free energy has nothing to do with our self-energy functional, despite using the same symbol.
[b] I invented the symbol stat as generalization of min and max to any point with vanishing gradient. That is, saddle points are explicitly considered as well.

Let us now turn from the reminder of the regular Legendre-Fenchel transform to the generalized Legendre transform at hand. Rather than describing a function $U(S)$ by a family of tangential straight lines $y_T(S) = U(S) - TS$, we can also use other functions, in this case $y_\Sigma(G^{(0)}) = -k_B T \ \ln(1 - \Sigma G^{(0)})$. The parameter Σ is determined such that the slope of the original function $\mathcal{Q}(G^{(0)})$ is identical to that of $y_\Sigma(G^{(0)})$ at the point, where the two functions touch.

The stationary condition of the self-energy functional Eq. 12.8 with respect to the bare Green's function encapsulates the expression Eq. 12.7 for the proper self energy via the reducible self energy expressed as functional derivative of the generating functional $\mathcal{Q}[G^{(0)}]$.

The functional derivative of the self-energy functional is, up to the sign, the full Green's function

$$\beta \frac{\partial F[\Sigma]}{\partial \Sigma} \overset{\text{Eq. } 12.8}{=} -G^{(0)} \Big(1 - \Sigma G^{(0)} \Big)^{-1} \overset{\text{Eq. } 14.17}{=} -G \tag{12.12}$$

Thus, the self-energy functional $F(\Sigma)$ is a generating functional of the full Green's function.

The expression Eq. 12.12 for the functional derivative can be rewritten as a stationary condition.

$$0 = \frac{\partial}{\partial \Sigma}\bigg|_G \Big\{ F[\Sigma] + k_B T \ \mathrm{Tr}\big[G\Sigma\big] \Big\} \tag{12.13}$$

Luttinger-Ward functional

Let me now define a new functional $\Phi_T^{LW}[G]$, the so-called **Luttinger-Ward functional** [4][95]. of the full Green's function by a second Legendre transform

$$\begin{aligned} \Phi_T^{LW}(G) &\overset{\text{def}}{=} \operatorname*{stat}_{\Sigma} \Big\{ F[\Sigma] + \frac{1}{\beta}\mathrm{Tr}\big[\Sigma G\big] \Big\} \\ &\overset{\text{Eq. 12.8}}{=} \operatorname*{stat}_{\Sigma, G^{(0)}} \Big\{ \mathcal{Q}[G^{(0)}] + \frac{1}{\beta}\ \mathrm{Tr}\Big[\ln\Big(1 - \Sigma G^{(0)}\Big) + \Sigma G\Big] \Big\} \end{aligned} \tag{12.14}$$

The stationary conditions of the functional in curly brackets in Eq. 12.14 are,

- for the derivative with respect to the bare Green's function $G^{(0)}$,

$$\begin{aligned} 0 &\overset{!}{=} \underbrace{\frac{\delta \mathcal{Q}[G^{(0)}]}{\delta G^{(0)}}}_{=\frac{1}{\beta}\Sigma^{red} \quad \text{(Eq. 10.79)}} + \frac{1}{\beta}\Big[- \underbrace{\big(1 - \Sigma G^{(0)}\big)^{-1}}_{\sum_{j=0}^{\infty}(\Sigma G^{(0)})^j} \Sigma \Big] \\ &\Rightarrow \Sigma(G^{(0)}) = \frac{\delta \mathcal{Q}[G^{(0)}]}{\delta G^{(0)}} \left(1 + G^{(0)} \frac{\delta \mathcal{Q}[G^{(0)}]}{\delta G^{(0)}}\right)^{-1} \end{aligned} \tag{12.15}$$

- and for the derivative with respect to the self energy Σ, we obtain Dyson's equation

$$\begin{aligned} 0 &\overset{!}{=} \frac{1}{\beta}\Big[-G^{(0)} \underbrace{\Big(1 - \Sigma G^{(0)}\Big)^{-1}}_{\sum_{j=0}^{\infty}(\Sigma G^{(0)})^j} + G \Big] \qquad \Rightarrow \qquad \underbrace{G = G^{(0)} + G^{(0)}\Sigma G}_{\text{Dyson's equation}} \\ &\Rightarrow G(\Sigma, G^{(0)}) = \Big(1 - G^{(0)}\Sigma\Big)^{-1} G^{(0)} \end{aligned} \tag{12.16}$$

The stationary conditions provide the full Green's function G and the self energy as function of a non-interacting Green's function $G^{(0)}$.

To evaluate the Luttinger-Ward functional for a given argument G, this $G[G^{(0)}]$ dependency needs to be inverted to obtain $G^{(0)}[G]$. In other words, the non-interacting Green's function must be varied to obtain the desired full Green's function G as $G[G^{(0)}]$. Scanning through the non-interacting Green's function implies scanning over non-interacting Hamiltonians, i.e over all hermitean operators in the one-particle Hilbert space. If the desired Green's function G cannot be constructed from such a non-interacting Green's function, the Green's function G is not a valid argument for the Luttinger-Ward functional. Insertion of Σ and $G^{(0)}$ into Eq. 12.14 yields the value for the Luttinger-Ward functional.

When we exploit the stationary conditions, the functional derivative of the Luttinger-Ward functional is readily obtained as proper self energy

$$\beta \frac{\delta \Phi_T^{LW}(G)}{\delta G} \overset{\text{Eq. 12.14}}{=} \Sigma \tag{12.17}$$

Given a Luttinger-Ward functional obtained with a certain approximation scheme, the typical use case is to start from a non-interacting Hamiltonian, which defines the bare Green's function

[4] You will find different expressions for the Luttinger-Ward functional. Using Dyson's equation $G = G^{(0)} + G^{(0)}\Sigma G = G^{(0)} + G\Sigma G^{(0)}$, we obtain $G(1 - \Sigma G^{(0)}) = G^{(0)}$ and thus $(1 - \Sigma G^{(0)}) = G^{(0)} G^{-1}$.

$\hat{G}^{(0)}(t,t')$. The interacting Green's function is then obtained self-consistently via Dyson's equation and the proper self energy obtained from the Luttinger-Ward functional, that is

$$\hat{G} = G^{(0)} + G^{(0)}\Sigma G \qquad \text{and} \qquad \Sigma = \beta \frac{\delta \Phi_T^{LW}(G)}{\delta G} \tag{12.18}$$

LUTTINGER-WARD FUNCTIONAL

The **Luttinger-Ward functional** $\Phi_T^{LW}(G)$ is defined via the generating functional $\mathcal{Q}$ as

$$\Phi_T^{LW}(G) \overset{\text{Eq. } 12.14}{=} \underset{\Sigma, G^{(0)}}{\text{stat}} \left\{ \mathcal{Q}[G^{(0)}] + \frac{1}{\beta} \operatorname{Tr}\Big[\underbrace{\ln\Big(1 - \Sigma G^{(0)}\Big)}_{-\sum_{n=1}^{\infty} \frac{1}{n}\left(\Sigma G^{(0)}\right)^n} + \Sigma G \Big] \right\} \tag{12.19}$$

The domain of the Luttinger-Ward functional is discussed in section 12.2.1 below.
See explanations for Eq. 12.36 below for translating this short-hand notation into contour integrations.

Defining properties: The Luttinger-Ward functional has the following properties:[99]

- The derivative

$$\frac{\beta \delta \Phi_T^{LW}[\boldsymbol{G}, \hat{W}]}{\delta G_{b,a}(t',t)} \overset{\text{Eq. } 12.17}{=} \Sigma_{a,b}(t,t') \,. \tag{12.20}$$

  of the Luttinger-Ward functional evaluated at a physical Green's function defined by Eq. 7.15 yields a self energy that obeys Eq. 8.15.

- It is universal, that is it depends only on the interaction and the temperature, but not on the non-interacting Hamiltonian $\hat{h}$.

- It vanishes in the non-interacting case.

The Luttinger-Ward functional $\Phi_T^{LW}(G)$ has substantially fewer Feynman diagrams than $\mathcal{Q}(G_{T,\mu}^{(0)})$, because the full Green's functon contains itself of many diagrams of the bare Green's function.

The stationary principles encapsulate a set of equations, which need to be solved self-consistently. The self-consistent equations provide the proper self energy and the full Green's function.

Approximations which are done to the Luttinger-Ward functional are **conserving approximations**. [93, 94] This means that conservation laws are obeyed and the resulting theory is **thermodynamically consistent**.

12.2.1 Domain of the Luttinger-Ward functional

Which mathematical objects may be used as argument $\hat{G}$ for the Luttinger-Ward functional? This question is far from trivial.

The route presented in this book starts from a non-interacting Green's function and an interaction to obtain the generating functional $\mathcal{Q}(\hat{G}^0, \hat{W})$. The functional derivative of this generating functional $\mathcal{Q}$ provides the reducible self energy, from which the interacting Green's function is obtained. The Luttinger-Ward functional defined as Eq. 12.14 encodes exactly these steps.

Hence, only those Green's function, which are obtained from the stationary conditions in Eq. 12.14 with respect to non-interacting Green's functions $\hat{G}^{(0)}$ are "legal" arguments for the Luttinger-Ward functional.

What is a legal non-interacting Green's function? A non-interacting Green's function has the form of Eq. 7.30 on p. 258. It is defined by a one-particle-reduced density matrix and a propagator in

the one-particle Hilbert space. These, in turn, can be translated into a time-dependent Hamiltonian in one-particle Hilbert space.

The resulting interacting Green's function G must follow from the sequence

$$\hat{h}(t) \to \hat{G}^{(0)}(t,t') \overset{\hat{W}}{\to} \mathcal{Q} \to \hat{\Sigma}^{red}(t,t') \to \hat{G}(t,t') \tag{12.21}$$

In words, a non-interacting Hamiltonian leads via Eq. 7.30 to a non-interacting Green's function. The interaction defines a functional $\mathcal{Q}$ for non-interacting Green's functions. The variational principle results in a reducible self energy $\hat{\Sigma}^{red}(t,t')$, which in turn produces the interacting Green's function $\hat{G}(t,t')$. The latter is only meaningfull if it can be related to a non-interacting Hamiltonian via the sequence above.

The trouble is that there seem to be more objects $\hat{G}(t,t')$ that appear like physical Green's function, than there are non-interacting Green's functions. Tracing back from an unphysical Green's function $\hat{G}(t,t')$ may lead back to a an object $\hat{G}^{(0)}(t,t')$, which is not a physical non-interacting Green's function of some sort. The results obtained for such an unphysical Green's function are meaningless!

This point has been discussed under the heading "Existence of the Luttinger-Ward functional". See `https://www.pnas.org/content/pnas/115/10/2282.full.pdf` for a recent paper summarizing the state about the existence or non-existence of the Luttinger-Ward functions. Tarantino et al.[75] explore the problem using the Hubbard atom as example.

Kadanoff-Baym functional

Performing the Legendre transformations backwards will express our generating functional Eq. 10.77, respectively Eq. 11.38, in terms of the Luttinger-Ward functional.

GENERATING FUNCTIONAL FROM LUTTINGER-WARD FUNCTIONAL

$$\mathcal{Q}[G^0] \overset{\text{Eq. } 12.14}{=} \underset{\Sigma,G}{\text{stat}} \left\{ \Phi_T^{LW}(G) - \frac{1}{\beta} \text{Tr} \Big[\underbrace{\ln\Big(1 - \Sigma G^{(0)}\Big)}_{-\sum_{n=1}^{\infty} \frac{1}{n} \left(\Sigma G^{(0)}\right)^n} + \Sigma G \Big] \right\} \tag{12.22}$$

Each product involves a sum over the one-particle basis and an integration over the complex-valued time contour. The logarithm is expanded by its power series expansion. See explanations for Eq. 12.36 below for translating this short-hand notation into contour integrations.

This expression

1. provides the grand potential $\Omega_{T,\mu}^W$ by adding the grand potential $\Omega_{T,\mu}^0$ of the non-interacting system and
2. it allows to construct an approximate generating functional $\mathcal{Q}_{T,\mu}(G^{(0)})$ from an approximation of the Luttinger-Ward functional $\Phi_T^{LW}(G)$.

The so-called[5] Kadanoff-Baym functional $\Psi_{T,\mu}^{KB}$ provides the grand potential

$$\Omega_{T,\mu}(\hat{h} + \hat{W}) = \underset{G,\Sigma}{\text{stat}} \, \Psi_{T,\mu}^{KB}[\boldsymbol{G}, \boldsymbol{\Sigma}, \boldsymbol{h}, \hat{W}] \,, \tag{12.23}$$

where

$$\Psi_{T,\mu}^{KB}[\boldsymbol{G}, \boldsymbol{\Sigma}, \boldsymbol{h}, \hat{W}] = \underbrace{\Omega_{T,\mu}^{(0)}[\boldsymbol{h}]}_{-\frac{1}{\beta}\text{Tr}\ln(-i\hbar G^{(0)})} + \Phi_T^{LW}[\boldsymbol{G}, \hat{W}] - \frac{1}{\beta} \text{Tr} \Big\{ \ln\Big[\underbrace{\Big(\mathbf{1} - \boldsymbol{G}^{(0)}\boldsymbol{\Sigma}\Big)}_{[-i\hbar G]^{-1}[-i\hbar G^{(0)}]} \Big] + \boldsymbol{\Sigma}\boldsymbol{G} \Big\} \,. \tag{12.24}$$

[5] We adopt this naming of Luttinger-Ward and Kadanoff-Baym functional from Chitra and Kotliar [100].

The terms shown below the underbraces are often found in the literature, and the bare Green's functions in the two logarithm terms are often canceled against each other. Some caution is required because the expressions I found in the literature are expressed in the Matsubara formalism.Editor: Check whether this replacement is permitted. I am concerned because the Green's function may have units attached and must not stand alone in a logarithm. Secondly, $\mathrm{Tr}[AB] \neq Tr[A]Tr[B]$

Sanity check

The reader may skip this section. As a sanity check, let me compare Eq. 12.24 with the literature.

A few precautions are necessary: While my lecture notes work with a complex time contour, the results are often compared with the Matsubara formalism.

- Caution is required because many expressions are given in the Matsubara formalism. The Matsubara Green's function $\mathcal{G}(\tau_2, \tau_1) = -iG^{\mathcal{C}}(-i\tau_2, -i\tau_1)e^{\mu(\tau_2-\tau_1)/\hbar}$, Eq. **??** Editor: Chapter us hidden is defined different from the Matsubara part of the non-equilibrium Green's function used here.
- Secondly, the stationary condition for the self energy is usually resolved, so that $\Sigma = G^{(0),-1} - G^{-1}$ is eliminated. I do not do this step, because it is not yet clear to me, whether the required expressions are permitted on the complete complex-time contour.
- The non-interacting grand potential is often expressed as $\Omega^{(0)}_{T,\mu} = -\frac{1}{\beta}\mathrm{Tr}[\ln(-i\hbar G^{(0)})]$.Editor: caution check whether this holds on a general complex time contour. Once written in this form, it is canceled against another similar term in the other logarithm $\ln(1-\Sigma G^{(0)}) = \ln[G^{(0)}G^{-1}] = \ln(-i\hbar G^{(0)}) - \ln(-i\hbar G)$

with these remarks we can now compare to individual authors:

- Potthoff's equation[96]:

$$\Omega_{T,\mu}[G] = \Phi^{LW}_T[G] + \mathrm{Tr}\ln[-i\hbar G] - \mathrm{Tr}\Big[\underbrace{\big(G^{(0),-1} - G^{-1}\big)}_{\Sigma[G]} G\Big] \tag{12.25}$$

  can be compared with our Eq. 12.24. I have included a factor $i\hbar$, which is not present in Potthoff's expression.

- Luttinger and Ward [95] provide the connection between the grand potential (Y) and the Luttinger-Ward functional (Y') in their Eq. 47,

$$\Omega_{T,\mu} = -\frac{1}{\beta}\mathrm{Tr}\big[\ln(-G^{-1}) + G\Sigma\big] + \Phi^{LW}_T(G) \tag{12.26}$$

  Luttinger and Ward use the symbol G_r for the proper self energy, S_r for the full Green's function, while the bare Green's function is $1/(\zeta_l - \epsilon_r)$. As in the comparison with Pothoff given above, there is an additional factor $i\hbar$ in the comparison of Green's functions.

12.3 Skeleton expansion: diagrams of the Luttinger-Ward functional

The Luttinger-Ward functional has a diagrammatic expansion very similar to that of our generating functional $\mathcal{Q}_{T,\mu}$. The diagrammatic expansion of the Luttinger-Ward functional is obtained by removing all two-particle reducible diagrams from the diagrammatic expansion of $\mathcal{Q}$. Secondly, the bare Green's functions $G^{(0)}$ are replaced by the full Green's functions G.[95, 7] Each bare particle

line $G^{(0)}$ in the diagram is replaced by a double particle line G representing the full Green's function. This is shown as follows:

The definition of the Luttinger-Ward functional can be expressed by a coupled system of equations

$$\beta\Phi_T^{LW}[G] \overset{\text{Eq. } 12.19}{=} \beta\mathcal{Q}[G^{(0)}]) + \mathrm{Tr}\Big[\overbrace{-\sum_{j=1}^{\infty}\frac{1}{j}\Big(\Sigma G^{(0)}\Big)^j}^{\ln[1-\Sigma G^{(0)}]} + \Sigma G\Big] \tag{12.27}$$

$$\Sigma^{red} \overset{\text{Eq. } 12.15}{=} \Sigma\sum_{j=0}^{\infty}\Big(G^{(0)}\Sigma\Big)^j \qquad \rightsquigarrow \Sigma \tag{12.28}$$

$$G \overset{\text{Eq. } 12.16}{=} \sum_{j=0}^{\infty}\Big(G^{(0)}\Sigma\Big)^j G^{(0)} \tag{12.29}$$

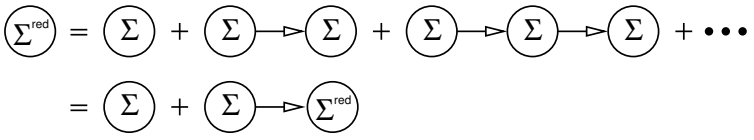
where

$$\mathcal{Q}_{T,\mu}[G^{(0)}] \overset{\text{Eq. } 11.38}{=} \frac{1}{\beta}\sum_{n=1}^{\infty}\sum_{D\in\mathbb{T}_n}\frac{\mathcal{V}(D)}{S(D)} \qquad \text{and} \tag{12.30}$$

$$\Sigma^{red} \overset{\text{Eq. } 10.79}{=} \beta\frac{d\mathcal{Q}[G^{(0)}]}{\partial G^{(0)}}\ . \tag{12.31}$$

The diagrammatic expansion of $\mathcal{Q}_{T,\mu}$ contains all linked, closed, and topologically distinct diagrams D. $\mathcal{V}(D,[G^{(0)}])$ is the value of the diagram and $S(D)$ is the symmetry factor. Remember, that the value of a diagram is in fact a functional of the bare Green's function, which I indicate here by adding the argument $[G^{(0)}]$.[6]

1. Let me start with the Dyson's equation for the reducible self energy $\Sigma^{\text{red}}[G^{(0)}]$.



   The proper self energy Σ can be extracted from the diagrams for the reducible self energy Σ^{red} by removing all one-particle-reducible self-energy diagrams.

   The diagrammatic expansion of the reducible self energy is obtained from the generating functional $\mathcal{Q}[G^{(0)}]$ by differentiating with respect to the bare Green's function. This process removes particle lines, one at a time, resulting in 2n self-energy diagrams from a n-th order diagram of the generating functional. Ignoring one-particle-reducible self-energy diagrams, one is left with the diagrammatic expansion of the proper self energy in terms of the non-interacting Green's function.

   The reducible self energy can be recovered by the Dyson's equation for the self energy $\Sigma^{red} = \Sigma + \Sigma G^{(0)}\Sigma^{red}$.

2. Let me take the proper self-energy diagrams, expressed in terms of the non-interacting Green's function, and remove all self-energy insertions. A **self-energy insertion** is a part of a diagram which is connected to exactly one incoming and one outgoing Green's function. By removing all self-energy insertions, a self-energy diagram is converted into a so-called **skeleton self energy diagram**.

   Editor: Insert a sketch of a self energy diagram with a self energy insertion.

[6] The value of a diagram can be considered, in addition, as a functional of the interaction and a function of temperature. Here, they are considered as fixed parameters and they are suppressed as arguments.

The conversion of a self-energy diagram into its corresponding skeleton diagram is a many-to-one relation. Each self-energy diagram is converted uniquely into a skeleton diagram. Many (proper) self-energy diagrams will be converted to the same **skeleton self-energy diagram**. Thus, one can classify the self-energy diagrams by the skeleton diagram they are converted into.

All diagrams of each class can be reconstructed from the corresponding skeleton diagram by inserting all possible self-energy insertions. Insertion of all possible self energy insertions into a single non-interacting Green's function is the same as replacing $G^{(0)}$ by the expansion $G^{(0)} + G^{(0)}\Sigma G^{(0)} + G^{(0)}\Sigma G^{(0)}\Sigma G^{(0)} + \ldots$, which is nothing but the full Green's function. Editor: Can it be shown that each diagram is only constructed once by expandin a skeleton diagram?

Hence, the inclusion of self-energy insertions into a skeleton diagram is the same as replacing every bare Green's function $G^{(0)}$ in the skeleton diagram by the full Green's function G.

The sum of all skeleton self-energy diagrams defines a new functional $K[G]$ of the full Green's function. Evaluated for the full Green's function, as defined by Dyson's equation with a given self energy, yields the proper self energy itself.

$$\Sigma[G^{(0)}] = K\Big[\underbrace{G^{(0)}\left(1 - \Sigma G^{(0)}\right)^{-1}}_{=G[G^{(0)}]}\Big] \tag{12.32}$$

This is a complete definition of the functional $K[G]$ for a given proper self-energy functional $\Sigma[G^{(0)}]$: For each $G^{(0)}$, one constructs the argument $G[G^{(0)}]$ using Dyson's equation and the functional value $K = \Sigma[G^{(0)}]$. This procedure provides all possible $(K[G], G)$-pairs, and hence the functional $K[G]$. This procedure also defines the domain of $K[G]$, the set of objects that may be used as argument for $K[G]$.

3. Our next goal ist to construct the Luttinger-Ward functional. The derivative of the Luttinger-Ward functional with respect to the full Green's function is the proper self energy.

$$\frac{\beta\partial\Phi_T^{LW}[G]}{\partial G} \overset{\text{Eq. } 12.20}{=} \Sigma = K[G] \tag{12.33}$$

Let me arrange the skeleton expansion into orders of the interaction-lines. $K^{\text{n-order}}[G]$ are all proper self-energy skeleton diagrams with n interaction lines and, correspondingly, $2n-1$ particle lines. The interactions contained in the Green's function are not considered.

This allows one to express the Luttinger-Ward functional as[7]

$$\beta\Phi_T^{LW}[G] = \sum_n \frac{1}{2n} G K^{\text{n-order}}[G] \tag{12.34}$$

I exploited that any function $f(x) = ax^n$, which is a pure power of its argument x, satisfies $\partial_x f(x) = \frac{n}{x} f(x)$ and therefore $f(x) = \frac{1}{n} x \partial_x f(x)$.

The diagrams $GK^{\text{n-order}}[G]$ have the form of closed skeleton diagrams. Closed skeleton diagrams are diagrams without self energy insertions. In other words, a skeleton diagram is **two-particle irreducible (2PI)**, which means that the diagram cannot be divided into two separate pieces when two particle lines are removed.

Each closed skeleton diagram of order n of the Luttinger-Ward functional produces exactly $2n$ self-energy diagrams in K. Closing those diagrams with a particle line, leads back to the same diagram in the Luttinger-Ward functional. Thus, the parent of a given self-energy skeleton diagram occurs $2n$ times in the Luttinger-Ward functional. This exactly compensates the factor $1/(2n)$.

[7] Compare to Eq. 11.18 of Stefanucci and van Leeuwen[2].

Thus, the Luttinger-Ward functional can be written as sum over all linked, closed, topologically distinct Skeleton diagrams weighted with the symmetry factor.

$$\Phi_T^{LW}[G] = \frac{1}{\beta}\sum_{n=1}^{\infty}\sum_{D\in\mathbb{S}_n}\frac{\mathcal{V}(D)}{S(D)} \tag{12.35}$$

We will refer to the functional $K[G]$ in future as $\Sigma[G]$. This is dangerous as it can be mixed up with $\Sigma[G^{(0)}]$, which has a altogether different functional form. They carry the same symbol because $\Sigma[G^{(0)}] = \Sigma\Big[G[G^{(0)}]\Big]$. i.e. they describe the same physical object, expressed in terms of two different physical objects as arguments.

The explanation above made a detour via the self-energy diagrams, which seems unnecessarily complicated. However, the direct route does not seem feasable. One of the problems is that the removal of self-energy insertions is not unique for closed diagrams, while it is unique for self-energy diagrams.

12.4 Summary on the Luttinger-Ward functional

GENERATING FUNCTIONAL FROM LUTTINGER-WARD FUNCTIONAL

Thus we are lead to again another form for the generating functional Eq. 10.77, respectively Eq. 11.38, now in terms of a sum of skeleton diagrams.

$$\mathcal{Q}[G^0] \overset{\text{Eq. } 12.22}{=} \underset{\Sigma,G}{\text{stat}}\left\{\underbrace{-\frac{1}{\beta}\sum_{D\in\mathbb{S}}\frac{\mathcal{V}(D,[G])}{S(D)}}_{\Phi_T^{LW}(G)} - \frac{1}{\beta}\text{Tr}\Big[\underbrace{\ln\Big(1-\Sigma G^{(0)}\Big)}_{-\sum_{n=1}^{\infty}\frac{1}{n}\left(\Sigma G^{(0)}\right)^n} + \Sigma G\Big]\right\} \tag{12.36}$$

With $\mathbb{S}$, we denote the subset of skeleton diagrams in the set of closed, topologically inequivalent, linked, diagrams. They are considered as functional of the full Green's function G, rather than as functional of the bare Green's function.
Each product involves a sum over the one-particle basis and an integration over the complex-valued time contour. The logarithm is expanded by its power-series expansion.

$$\begin{aligned}\text{Tr}\Big[\ln\Big(1-\Sigma G^{(0)}\Big)\Big] &\hat{=} -\sum_{n=1}^{\infty}\frac{1}{n}\int_{\mathcal{C}}dt_1\int_{\mathcal{C}}dt_1'\ldots\int_{\mathcal{C}}dt_n\int_{\mathcal{C}}dt_n' \\ &\quad\times\text{Tr}\Big[\hat{\Sigma}(t_1,t_1')\hat{G}^{(0)}(t_1',t_2)\ldots\hat{\Sigma}(t_n,t_n')\hat{G}^{(0)}(t_n',t_1)\Big] \\ \text{Tr}\Big[\Sigma G\Big] &\hat{=} \int_{\mathcal{C}}dt\int_{\mathcal{C}}dt'\;\text{Tr}\Big[\hat{\Sigma}(t,t')\hat{G}(t',t)\Big]\end{aligned}$$

The hat ontop of the equal sign indicates that we change the notation from the left to the right-hand side. On the right-hand side, the Green's functions and self energy are considered as operators in the one-particle Hilbert space. They depend on two time arguments on the complex-valued time contour $\mathcal{C}$.

The function of the Luttinger-Ward functional is to define a set of self-consistent equations via the stationary conditions or Eq. 12.36. This set of equations defines the physical Green's function of the system

$$\begin{aligned}G &\overset{\text{Eq. } 8.23}{=} G^{(0)}\Big(1-\Sigma G^{(0)}\Big)^{-1} = G^{(0)} + G^{(0)}\Sigma G^{(0)} + G^{(0)}\Sigma G^{(0)}\Sigma G^{(0)} + \ldots \\ \Sigma &\overset{\text{Eq. } 12.20}{=} \frac{1}{\beta}\Phi_T^{LW}(G)\end{aligned} \tag{12.37}$$

The reducible self energy is obtained as derivative with respect to the bare Green's function.

$$\Sigma^{red} \overset{\text{Eq. } 10.79}{=} \frac{\partial \mathcal{Q}}{\partial G^{(0)}} = -\frac{1}{\beta} \frac{1}{1 - \Sigma G^{(0)}} \Sigma = \Sigma + \Sigma G^{(0)} \Sigma + \Sigma G^{(0)} \Sigma G^{(0)} \Sigma + \dots \tag{12.38}$$

The reducible self energy, in turn, provides the full Green's function via Eq. 10.78.

One remark:

Consider that one starts from a full Green's function, and uses the Luttinger-Ward functional to generate the proper self energy. One could then calculate the bare Green's function from Dyson's equation. Such a procedure would guarantee that the stationary conditions are satisfied. However, it is not guaranteed that the bare Green's function $G^{(0)}$ has the analytical properties of a bare Greens function. Thus, the Green's function chosen initially is not a physical Green's function.

The argument above shows that there the Luttinger-Ward functional establishes a mapping from a bare Green's function to a physical full Green's function. However, many Green's functions G are not physical for any non-interacting Hamiltonian $\hat{h}$.

Is this mapping unique? It is not excluded that one bare Green's function is connected to several stationary points (Σ, G). If there are multiple stationary points for one bare Green's function, this implies that one Hamiltonian, characterized though a non-interacting Hamiltonian h and an interaction $\hat{W}$, has several possible physical states[8]. In turn this would be a hint for a quantum phase transition.

[8] A state in this sense is an ensemble of many-partucle states characterized by a von Neumann density matrix

Chapter 13

Shift the reference

One consequence of the Luttinger-Ward functional is that the Hartree energy[1] can be attributed to a specific diagram of the Luttinger-Ward functional. This allows one to remove it from the self energy and combine it with the non-interacting Green's function. As a result, the "new" non-interacting Green's function contains already the dominant part of the electron interaction. This may imply, that we start the Taylor expansion closer to the real system.[2]

13.1 Separating out the Hartree term

We can return to the equation of motion. The equation of motion, expressed in terms of the (proper) self energy is equivalent to Dyson's equation.

$$\left(\hat{1} i\hbar\partial_t - \hat{h}(t)\right)\hat{G}(t,t') - \int_{\mathcal{C}} dt''\, \hat{\Sigma}(t,t'')\hat{G}(t'',t') \overset{\text{Eq. } 8.16}{=} \hat{1}\delta(t-t') \tag{13.1}$$

The self energy $\hat{\Sigma}(t,t') = \sum_{o,i} |\pi_o\rangle \Sigma_{o,i}(t,t') \langle\pi_i|$ is the derivative of the Luttinger-Ward functional.

$$\hat{\Sigma}(t,t') \overset{\text{Eq. } 12.20}{=} \sum_{o,i} |\pi_o\rangle \frac{\beta \Phi_T^{LW}[G]}{\partial G_{i,o}(t',t)} \langle\pi_i| \tag{13.2}$$

These two equations, Eq. 13.1 and Eq. 13.2, must be solved self-consistently.

We may single out the eyeglass diagram from the Luttinger-Ward functional $\Phi_T^{LW}[G]$, which is responsible for the Hartree potential $\hat{V}_H$. The remainder $\hat{\Sigma}_{xc}$ is the **self energy due to exchange and correlation** .

$$\hat{\Sigma}(t,t') = \hat{V}_H(t)\delta(t-t') + \hat{\Sigma}_{xc}(t,t') \tag{13.3}$$

The Hartree potential depends itself on the Green's function.

The system of equations attains a slightly different form

$$\left(\hat{1} i\hbar\partial_t - \hat{h}(t) - \hat{V}_H(t)\right)\hat{G}(t,t') - \int_{\mathcal{C}} dt''\, \hat{\Sigma}_{xc}(t,t'')\hat{G}(t'',t') = \hat{1}\delta(t-t') \tag{13.4}$$

The self energy for exchange and correlation is the derivative of the Luttinger-Ward functional with the largest term, the Hartree potential, subtracted.

$$\hat{\Sigma}_{xc}(t,t') = \sum_{o,i} |\pi_o\rangle \frac{\beta \Phi_T^{LW}[G]}{\partial G_{i,o}(t',t)} \langle\pi_i| - \hat{V}_H(t)\delta(t-t')\,. \tag{13.5}$$

[1] The same is true for the exchange term.

[2] This statement must be taken with a grain of salt, because the finite convergence radius of the original expansion may already have left its traces in the Luttinger-Ward functional, we use as underlying theory for this step.

Often, the distinction between the proper self energy with and without the Hartree potential is not made explicit.

One may ask why one does not remove also the exchange term from the self energy and treat it, like the Hartree potential, alongside the non-interacting Hamiltonian. There is a physical reason for this. The exchange potential has a long-range tail, which is screened away by the interaction. Thus there are long-range contribution, both in the exchange and the correlation potential, which cancel each other. Therefore it is better to keep them together.

Outlook: One may also separate out any instantaneous (non-retarded) approximation of the self energy and treat it together with the Hartree potential. One such possibility is described in the next section about Density-Functional Theory (DFT).

13.2 Density-functional theory as reference

Density-functional theory (DFT)[33, 34][3] is a theoretical framework used for the majority of quantitative first-principles electronic-structure calculations. It provides properties of interacting electrons in thermal equilibrium such as electron densities, atomic structures, reaction energies and thermodynamic stability. While it provides some excitation spectra and while these are often compared to experiment, the theory does not justify the use of spectral functions from density-functional theory. In order to gain access to spectra, one needs to make contact to Green's functions, which is discussed here. Here, I will only summarize density-functional theory to the extent necessary for the purpose at hand. More details are given in appendix H.

Density-functional theory (DFT) provides the grand potential for a given one-particle hamiltonian $\hat{h}$ and an interaction $\hat{W}$ by a minimization over electron densities or one-particle-reduced density matrices.[4]

$$\Omega_{T,\mu}[\hat{h}] = \min_{\hat{\rho}^{(1)}} \Big\{ \mathrm{Tr}\Big[\hat{\rho}^{(1)}\hat{h}\Big] + \underbrace{E_H\Big[n\big[\hat{\rho}^{(1)}\big]\Big]}_{\text{Hartree energy, Eq. 2.33}} + \underbrace{E_{xc,T}\Big[n\big[\hat{\rho}^{(1)}\big]\Big]}_{\text{exchange and correlation, Eq. 13.8}} + \underbrace{k_B T\ \mathrm{Tr}\Big[\hat{\rho}^{(1)} \ln\Big(\hat{\rho}^{(1)}\Big) + \Big(\hat{1}-\hat{\rho}^{(1)}\Big)\ln\Big(\hat{1}-\hat{\rho}^{(1)}\Big)\Big]}_{= -TS^B \text{ with Boltzmann entropy } S^B[\hat{\rho}^{(1)}], \text{ Eq. 2.69}} - \mu \underbrace{\mathrm{Tr}\Big[\hat{\rho}^{(1)}\Big]}_{\text{particle number}} \Big\} \tag{13.6}$$

This expression looks very similar to the grand potential Eq. 2.74 of the thermal Hartree-Fock approximation. However, there are a few subtle but important differences.

1. Firstly, unlike thermal Hartree-Fock approximation, the grand potential Eq. 13.6 is exact. All the complexities of the many-particle problem are still present. They are not evident directly from Eq. 13.6, but hidden away in the **exchange and correlation energy** $E_{xc,T}[n]$ defined below in Eq. 13.8.

2. Secondly, the one-particle-reduced density matrix, which minimizes the functional, is not that of the physical system, but that of the so-called **Kohn-Sham system**. The Kohn-Sham system does not differ from the real system by mistake, but by construction. The Kohn-Sham system consists of non-interacting electrons in an effective potential[5] $v_{eff}(\vec{r})$. Only its electron density is that of the real system.[6]

[3] Walter Kohn received the 1998 Nobel Price for the "development of the density-functional theory"[101].

[4] Here, I use a formulation that uses one-particle-reduced density matrices, because it fits more natural into the notations used during this lecture. I am **not** describing a reduced density-matrix functional theory (rDMFT), which is similar to, but still different from DFT.

[5] It is not obvious that the effective potential is local in space.

[6] This is where density-functional theory gets its name.

Let me now walk through Eq. 13.6: I write the electron density $n(\vec{r})$ from a specified one-particle-reduced density matrix as

$$n\big(\big[\hat{\rho}^{(1)}\big],\vec{r}\big) = \sum_{\sigma\in\{\uparrow,\downarrow\}} \langle\vec{r},\sigma|\hat{\rho}^{(1)}|\vec{r},\sigma\rangle \tag{13.7}$$

With $E_H[n]$, I denote the Hartree energy Eq. 2.33 and S^B is the fermionic **Boltzmann entropy** Eq. 2.69, which is a functional of the one-particle-reduced density matrix. The minimization is done over all N-representable one-particle-reduced density matrices, i.e. hermitean matrices with eigenvalues between zero and one.

All the complications of the many-electron system are rigorously encapsulated in the **exchange and correlation functional** $E_{xc,T}[n]$ given below in Eq. 13.8. The sole purpose of showing this expression here is to point out, (1) that there is a well defined expression and (2) that this expression does not introduce any approximations.[7] It is not difficult to show by inserting Eq. 13.8 for the exchange-and-correlation energy that Eq. 13.6 is the correct grand potential. Like for any other theory, approximations ontop of the underlying theory are necessary to evaluate the resulting expressions in practice.

$$\begin{aligned}
&E_{xc,T}[n] \stackrel{\text{def}}{=} F_T^W[n] - F_T^0[n] - E_H[n] \\
&= \underbrace{\min_{\hat{\rho}^{vN}} \operatorname*{stat}_{\gamma}\Big\{-TS^{vN}[\hat{\rho}^{vN}] + \mathrm{Tr}\big[\hat{\rho}^{vN}\big(\hat{h}+\hat{W}\big)\big] + \overbrace{\int d^3r\,\gamma(\vec{r})\Big(\sum_{\sigma}\mathrm{Tr}\Big[\hat{\rho}^{vN}\hat{\psi}^\dagger(\vec{r},\sigma)\hat{\psi}(\vec{r},\sigma)\Big] - n(\vec{r})\Big)}^{\text{density constraint}}\Big\}}_{\text{universal density functional } F_T^W \text{ of the interacting system plus potential energy } \int d^3r\, n(\vec{r})v_{ext}(\vec{r})} \\
&\underbrace{- \min_{\hat{\rho}^{(1)}} \operatorname*{stat}_{\bar{\gamma}}\Big\{-TS^{B}\big[\hat{\rho}^{(1)}\big] + \mathrm{Tr}\Big[\hat{\rho}^{(1)}\hat{h}\Big] + \overbrace{\int d^3r\,\bar{\gamma}(\vec{r})\Big(\sum_{\sigma\in\{\uparrow,\downarrow\}}\langle\vec{r},\sigma|\hat{\rho}^{(1)}|\vec{r},\sigma\rangle - n(\vec{r})\Big)}^{\text{density constraint}}\Big\}}_{\text{universal density functional } F_T^0 \text{ of the non-interacting system plus potential energy } \int d^3r\, n(\vec{r})v_{ext}(\vec{r})} - E_H\big[n\big]
\end{aligned} \tag{13.8}$$

The exchange-correlation energy is a functional of the electron density distribution $n(\vec{r})$.[8] The von-Neumann density matrix of the first term of Eq. 13.8 is not consistent (in the sense of Eq. 3.57) with the one-particle-reduced density matrix in the second term: The former describes the physical, interacting system, while the latter is that of the corresponding Kohn-Sham system.

The exchange-correlation functional is **universal** in the sense that it does not depend on the external potential $v_{ext}(\vec{r})$. The external potential is $v_{ext}(\vec{r})$ contained in the one-particle Hamiltonian $\hat{h}$. Because both terms in Eq. 13.8 have the same density, and because the density remains constant during the minimization, the energy of the external potential v_{ext} cancels exactly. Therefore, the exchange-correlation functional depends only on intrinsic properties of the interacting electron gas, namely kinetic energy, interaction energy and entropy.

The one-particle-reduced density matrix of the Kohn-Sham system is obtained from the equilibrium condition of the grand potential Eq. 13.6, i.e. the gradient of the functional with respect to the one-

[7] Often, it is incorrectly assumed that the mean-field approximation is underlying the density-functional theory. The origin of this misunderstanding is a confusion of the effective Hamiltonian in density-functional theory with the Fock operator of the Hartree-Fock approximation.

[8] The minimization over the von-Neumann density matrices $\hat{\rho}^{vN} = \sum_q |\Phi_q\rangle P_q \langle\Phi_q|$ is performed over ensembles of normalized fermionic many-particle wave functions $|\Phi_q\rangle$ in Fock space and positive probabilities P_q that add up to one. The minimization over the one-particle-reduced density matrices $\hat{\rho}^{(1)} = \sum_n |\varphi_n\rangle f_n \langle\varphi_n|$ is performed over orthonormal sets of one-particle wave functions $|\varphi_n\rangle$ and occupations f_n, which take values between zero and one, i.e. $0 \le f_n \le 1$. The von-Neumann entropy is $S^{vN}[\hat{\rho}^{vN}] = -k_B \mathrm{Tr}\big[\hat{\rho}^{vN}\ln\hat{\rho}^{vN}\big]$ as defined in Eq. 2.49. The **Boltzmann entropy** $S^B\big[\hat{\rho}^{(1)}\big] = -k_B T\ \mathrm{Tr}\big[\hat{\rho}^{(1)}\ln\big(\hat{\rho}^{(1)}\big) + \big(\hat{1}-\hat{\rho}^{(1)}\big)\ln\big(\hat{1}-\hat{\rho}^{(1)}\big)\big]$, Eq. 2.69, is the maximum entropy for a specific one-particle-reduced density matrix.

particle-reduced density matrix is set to zero.

$$\hat{h} + \hat{V}_H + \hat{V}_{xc} + k_B T \ln \frac{\hat{\rho}^{(1)}}{\hat{1} - \hat{\rho}^{(1)}} - \mu \hat{1} \stackrel{!}{=} 0 \qquad \Rightarrow \quad \hat{\rho}^{(1)}_{T,\mu} = \left(\hat{1} + \mathrm{e}^{+\beta(\hat{h}+\hat{V}_H+\hat{V}_{xc}-\mu\hat{1})} \right)^{-1} \tag{13.9}$$

where

$$\hat{V}_{xc} = \int d^3 r \sum_{\sigma \in \{\uparrow,\downarrow\}} |\vec{r},\sigma\rangle \frac{dE_{xc,T}[n(r)]}{dn(r)} \langle \vec{r},\sigma| \tag{13.10}$$

The potentials can be combined into an **effective potential** for the Kohn-Sham system

$$\hat{V}_{eff} \stackrel{\text{def}}{=} \hat{V}_{\text{ext}} + \hat{V}_H + \hat{V}_{xc}. \tag{13.11}$$

13.2.1 DFT Green's function

Editor: Can we make a link to time-dependent DFT?

Once the Kohn-Sham equations Eq. 13.9 are solved, we can build the Green's function of the Kohn-Sham system, the **Kohn-Sham Green's function**

$$\Big(\hat{1} i\hbar\partial_t \underbrace{- \hat{h}(t) - \hat{V}_H(t) - \hat{V}_{xc}(t)}_{-\left(\frac{\hat{p}^2}{2m_e} + \hat{V}_{eff}\right)} \Big) G^{\mathcal{C},0}(t,t') = \hat{1}\delta_{\mathcal{C}}(t-t') \tag{13.12}$$

and use it as the zeroth-order Green's function in an expansion of the self energy.

We insert the Kohn-Sham Green's function into the equation of motion Eq. 8.16 for the full Green's function

$$\begin{aligned} &\Big(\hat{1} i\hbar\partial_t - \hat{h}(t) - \hat{V}_H(t) - \hat{V}_{xc}(t) \Big) G^{\mathcal{C}}(t,t') \\ &- \int_{\mathcal{C}} dt'' \Big(\underbrace{\hat{\Sigma}_{xc}(t,t'')}_{\hat{\Sigma}(t,t'') - \hat{V}_H(t)\delta(t-t'')} \underbrace{- \hat{V}_{xc}(t)\delta(t-t'')}_{\hat{\Sigma}_{dc}(t,t')} \Big) \hat{G}^{\mathcal{C}}(t'',t') = \hat{1}\delta_{\mathcal{C}}(t-t') \end{aligned} \tag{13.13}$$

to obtain Dyson's equation

$$\hat{G}^{\mathcal{C}}(t,t') = \hat{G}^{\mathcal{C},0}(t,t') + \int_{\mathcal{C}} dt'' \int_{\mathcal{C}} dt''' \, \hat{G}^{\mathcal{C},0}(t,t'') \Big(\Sigma_{xc}(t'',t''') - \hat{V}_{xc}\delta(t''-t''') \Big) \hat{G}^{\mathcal{C}}(t''',t') \tag{13.14}$$

The term Σ_{dc} is the **double-counting correction** of the self energy. It corrects for the interaction terms already present in the Kohn-Sham Green's function and, then again, in the self energy.

The electron density at $t = 0$ obtained from $\hat{G}^{\mathcal{C}}$ for is the same as that obtained from the Kohn-Sham Green's function $\hat{G}^{\mathcal{C},0}$, because both correspond to the physical density of the interacting electron system in thermal equilibrium.

The Hartree and exchange-and-correlation potentials are functionals of the Green's function of the physical system via the density $n(\vec{r},t) = -i\hbar \lim_{t' \to t^+} \sum_{\sigma\in\{\uparrow,\downarrow\}} \langle \vec{r},\sigma|\hat{G}^{\mathcal{C}}(t,t')|\vec{r},\sigma\rangle$, from Eq. 8.28. They inherit the time dependence from the Green's function.[9]

Editor: I have no proof yet that the initial density obtained from the full Green's function $\hat{G}^{\mathcal{C}}$ is identical to that obtained from the Kohn-Sham Green's function $\hat{G}^{\mathcal{C},0}$,

[9] The Hartree potential is, formally, time dependent, because it stems from the time-dependent self energy. To be consistent, the time-dependent instantaneous effective potential $\hat{V}_{eff} = \hat{V}_{ext} + \hat{V}_H + \hat{V}_{xc}$ needs to be used for the definition of the Kohn-Sham system. Per requirement of density-functional theory, the system is in thermal equilibrium and therefore time-independent. The physical relevance of the time-dependent effective potential is secondary, because we only shuffle terms between the terms of the equation of motion.

other that both produce the density of the physical system. Interesting would be to know the criteria on the Dyson's equation for leaving the density unchanged.

Editor: Is the following correct? The effective potential is constructed such that the bare Green's function produces already the physical density for $t = 0$, when the system is in thermal equilibrium. Therefore, the self energy term with Hartree and exchange terms subtracted, does not affect the electron density, nor the total energy, at t=0, but it does affect the spectral function.

Editor: The self-energy term can be expressed by the difference of the Luttinger-Ward functional and the universal density functional. The derivative of this difference is the self-energy correction ontop of the effective potential of the density-functional theory.

Editor: This is related to our paper *"Density-matrix functionals from Green's functions"* from 2013. [102]

Chapter 14

Common approximations

Here, I will discuss the most common diagrams

1. Hartree-Fock (HF) approximation
2. Second-order Born approximation
3. Random-Phase Approximation (RPA)
4. T-matrix approximation
5. Fluctuating EXchange (FLEX) approximation

The diagrams that constitued the approximations discussed here have been discussed in section 14. Because I used a very abstract notation for the derivation of the Luttinger-Ward functional, I will now try to be fairly explicit in the following.

14.1 Hartree-Fock approximation

The Luttinger-Ward functional with the two first-order skeleton diagrams define the Thermal Hartree-Fock approximation discussed earlier in section 2.5.7. The purpose of this section is to show how the thermal Hartree-Fock approximation connects to the Green's function formalism.

14.1.1 First-order skeleton diagrams

In first order of the interaction, the Luttinger-Ward functional consists of the eyeglass and the oyster diagram shown in figure 14.1. These two diagrams define the Hartree-Fock approximation. The eyeglass diagram represents the Hartree energy and the oyster represents the exchange energy.



Fig. 14.1: The two diagrams in the Luttinger-Ward functional of the self-consistent Hartree-Fock approximation. The first is the Hartree diagram, while the second describes exchange.

- The eyeglass diagram provides the Hartree term and is characterized by the permutation vector $\vec{\mathcal{P}} = (1, 2)$.

position	1	2
$\vec{\mathcal{P}}$	1	2

- The oyster diagram provides the exchange term and is characterized by the permutation vector $\vec{\mathcal{P}} = (2, 1)$.

position	1	2
$\vec{\mathcal{P}}$	2	1

14.1.2 Luttinger-Ward functional in the Hartree-Fock approximation

Let me work out the Luttinger-Ward functional in the Hartree-Fock approximation

$$\begin{aligned}
\Phi_T^{LW}[G] &\overset{\text{Eq. ??}}{=} -\frac{1}{\beta}\sum_{D\in\mathbb{S}}\frac{\mathcal{V}(D,[G])}{S(D)} \\
&\overset{\text{Eq. 11.39}}{=} -\frac{1}{\beta}\cdot i\hbar\int_{\mathcal{C}}dt_1\int_{\mathcal{C}}dt_2\sum_{o_1,i_1,o_2,i_2}W_{o_1,o_2,i_1,i_2}\delta_{\mathcal{C}}(t_1-t_2) \\
&\quad\times\Big(\underbrace{\epsilon_{1,2}}_{+1}\underbrace{\frac{1}{2}}_{1/S(D)}G^{\mathcal{C}}_{i_1,o_1}(t_1,t_1^+)G^{\mathcal{C}}_{i_2,o_2}(t_2,t_2^+)+\underbrace{\epsilon_{2,1}}_{-1}\underbrace{\frac{1}{2}}_{1/S(D)}G^{\mathcal{C}}_{i_2,o_1}(t_2,t_1^+)G^{\mathcal{C}}_{i_1,o_2}(t_1,t_2^+)\Big) \\
&\overset{\text{Eq. 11.39}}{=} -\frac{i\hbar}{\beta}\int_{\mathcal{C}}dt\sum_{o_1,i_1,o_2,i_2}W_{o_1,o_2,i_1,i_2}\frac{1}{2}\Big(G^{\mathcal{C}}_{i_1,o_1}(t,t^+)G^{\mathcal{C}}_{i_2,o_2}(t,t^+)-G^{\mathcal{C}}_{i_2,o_1}(t,t^+)G^{\mathcal{C}}_{i_1,o_2}(t,t^+)\Big) \\
&= -\frac{i\hbar}{2\beta}\int_{\mathcal{C}}dt\sum_{o_1,i_1,o_2,i_2}\Big(W_{o_1,o_2,i_1,i_2}-W_{o_1,o_2,i_2,i_1}\Big)G^{\mathcal{C}}_{i_1,o_1}(t,t^+)G^{\mathcal{C}}_{i_2,o_2}(t,t^+) \qquad (14.1)
\end{aligned}$$

In order to obtain the Green's function, we need to solve a set of equations Eq. 12.37

$$G = G^{(0)}\Big(1-\Sigma G^{(0)}\Big) \quad \text{and} \quad \Sigma = \beta\frac{d\Phi_T^{LW}(G)}{dG} \qquad (14.2)$$

To obtain the self energy, I form the first variation of the Luttinger-Ward functional

$$d\Phi_T^{LW} \overset{\text{Eq. 14.1}}{=} \frac{1}{\beta}\int_{\mathcal{C}}dt\int_{\mathcal{C}}dt'\underbrace{\sum_{o_2,i_2}\Big(-\frac{i\hbar}{2}\sum_{o_1,i_1}\Big(W_{o_1,o_2,i_1,i_2}-W_{o_1,o_2,i_2,i_1}\Big)2G^{\mathcal{C}}_{i_1,o_1}(t,t^+)\Big)\delta(t'-t^+)}_{\Sigma_{o_2,i_2}(t',t)}dG^{\mathcal{C}}_{i_2,o_2}(t,t')$$

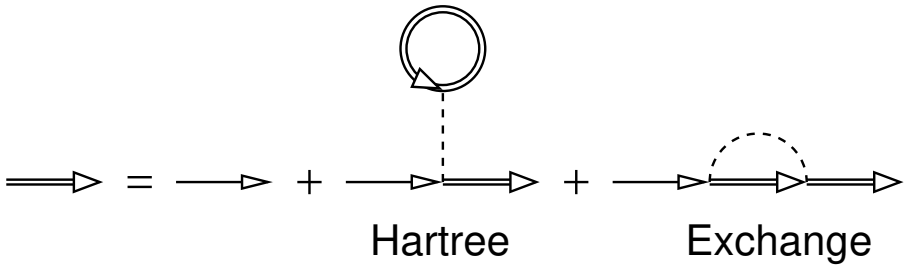
$$\begin{aligned}
\Sigma_{a,b}(t,t') &\overset{\text{Eq. 12.20}}{=} \frac{\beta\delta\Phi_T^{LW}[\boldsymbol{G},\hat{W}]}{\delta G_{b,a}(t',t)} \\
\Rightarrow \Sigma_{o_2,i_2}(t,t') &\overset{\text{Eq. 12.20}}{=} \sum_{o_1,i_1}\Big(W_{o_1,o_2,i_1,i_2}-W_{o_1,o_2,i_2,i_1}\Big)\underbrace{\Big(-i\hbar G^{\mathcal{C}}_{i_1,o_1}(t,t^+)\Big)}_{=\rho^{(1)}_{i_1,o_1}(t)\ \text{Eq. 8.28}}\delta(t'-t^+) \\
&= \langle\chi_{o_2}|\hat{V}_H(t)+\hat{V}_X(t)|\chi_{i_2}\rangle\delta(t'-t^+) \qquad (14.3)
\end{aligned}$$

with

$$\begin{aligned}
\hat{V}_H &= \sum_{o_2,i_2}|\pi_{o_2}\rangle\Big(\sum_{o_1,i_1}W_{o_1,o_2,i_1,i_2}\rho^{(1)}_{i_1,o_1}(t)\Big)\langle\pi_{i_2}| \\
\hat{V}_X &= \sum_{o_2,i_2}|\pi_{o_2}\rangle\Big(\sum_{o_1,i_1}W_{o_1,o_2,i_2,i_1}\rho^{(1)}_{i_1,o_1}(t)\Big)\langle\pi_{i_2}|
\end{aligned} \qquad (14.4)$$

The resulting equation of motion for the Green's function is

$$\Big(i\hbar\partial_t - \hat{h} \underbrace{-\hat{V}_H(t) - \hat{V}_X(t)}_{-\Sigma}\Big)\hat{G}^{\mathcal{C}}(t,t') = \hat{1}\delta_{\mathcal{C}}(t-t') \tag{14.5}$$



Because the Hartree and exchange potentials are not retarded, they can be evaluated like a non-interacting Green's function , albeit with an effective potential that includes the interaction between electrons. The non-interacting Green's function is given in Eq. 7.30.

$$\hat{G}^{\mathcal{C}}(t,t') \overset{\text{Eq. 7.30}}{=} \frac{1}{i\hbar}\sum_n |\varphi_n(t)\rangle\Big(\theta_{\mathcal{C}}(t-t')\big(1-f_{T,\mu}(\epsilon_n)\big) - \theta_{\mathcal{C}}(t'-t)f_{T,\mu}(\epsilon_n)\Big)\langle\varphi_0(t')| \tag{14.6}$$

with the one-particle orbitals $\varphi_n(t) \overset{\text{def}}{=} \hat{U}(t,0)|\varphi_n(0)\rangle$, that satisfy the time-dependent Schrödinger equation in the effective potential

$$\Big(i\hbar\partial_t - \hat{h} - \hat{V}_H(t) - \hat{V}_X(t)\Big)|\varphi_n(t)\rangle = 0 \tag{14.7}$$

The initial values $|\varphi_n(0)\rangle$ are the eigenstates of the Fock operator at $t=0$, and the energies ϵ_n are its eigenvalues.

The one-particle-reduced density matrix can directly be evaluated from the time-dependent orbitals $|\varphi_n(t)\rangle$ combined with the time-independent occupations $f_n = f_{T,\mu}(\epsilon_n)$.

$$\hat{\rho}^{(1)}(t) = \sum_n \big|\varphi_n(t)\big\rangle f_n \big\langle\varphi_n(t)\big| \tag{14.8}$$

14.2 Second-order Born approximation

Only two further diagrams contribute to the second order of the Luttinger-Ward functional. They are shown in fig. 14.2. The skeleton diagrams to first and second order form the **second-order Born approximation**.

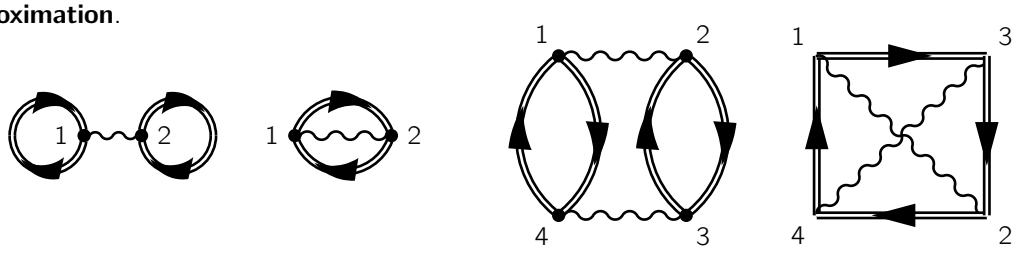


Fig. 14.2: The diagrams of the Luttinger-Ward functional of the second-order Born approximation. It includes the two first-order diagrams, eyeglass and oyster, of the Hartree-Fock approximation together with the double-ring and the double-exchange diagrams, which are the only two second order contributions to the Luttinger-Ward functional.

The second-order skeleton diagrams can be collected from all second-order diagrams shown in fig. 11.2 on p.350 by removing all non-skeleton diagrams. The various topologically distinct diagrams, disconnected, skeleton and connected non-skeleton, are shown in fig. 11.3.

Double ring diagram

position	1	2	3	4
$\vec{\mathcal{P}}$	4	3	2	1

Double-exchange diagram

position	1	2	3	4
$\vec{\mathcal{P}}$	3	4	2	1

14.3 Diagrammatic sequences that can be summed up analytically

There are sequences of Feynman diagrams that form a geometric series and can be summed up to infinite order.

While there are many of sequences of this kind, we concentrate on those with basic building blocks with four vertices of which two have an empty incoming and two have an empty outgoing index.

- **ring necklace** (RPA, GW)

position	1	2	3	4	5	...	2n-1	2n
$\vec{\mathcal{P}}$	2n	3	2	5	4	...	2n-2	1

Every even-numbered vertex is mapped onto the next higher index, while every odd-numbered index is mapped to the next lower one. By inspection of the diagrams in section M.8, I obtain a symmetry factor $2n$ for a n-th order ring necklace and a sign of $(-1)^n$.

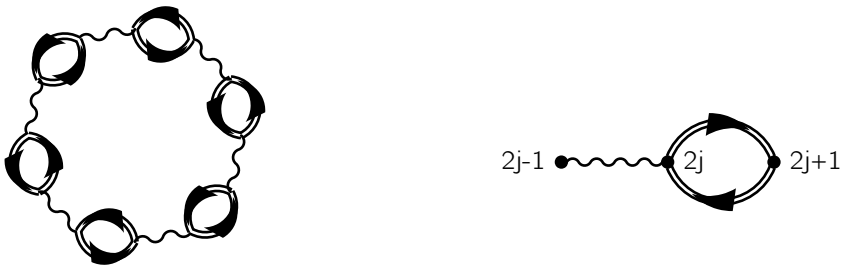


Fig. 14.3: The ring necklace and its elemental diagram.

The first-order ring necklace is the oyster, the exchange diagram. The second-order diagram is the double ring diagram in figure 14.2. It is important to ensure that diagrams are not considered several times, just because they are "hidden" in one or even several infinite sequences.

- The **particle-hole ladder diagram** (T-matrix approximation)

position	1	2	3	4	5	...	2n-1	2n
$\vec{\mathcal{P}}$	3	2n+1	5	2	7	...	1	2

Every odd-numbered vertex is mapped to the next-higher odd-numbered index. Every even-numbered vertex is mapped to the next lower even-numbered index. By inspection of the diagrams in section M.8, I obtain a symmetry factor $2n$ for a n-th order particle-hole ladders and a sign of $+1$.

The first-order particle-hole ladder is the eyeglass diagram responsible for the Hartree energy. The second-order particle-hole ladder is identical to the double-ring diagram in figure 14.2.

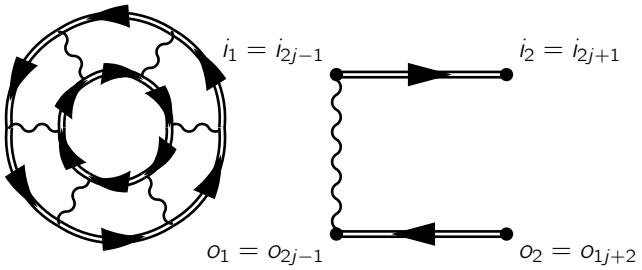


Fig. 14.4: Particle-hole ladder in the Luttinger-Ward functional. Ladders can also inserted into each ring diagram of the ring series.

Again, caution is needed to avoid double counting of diagrams. The double-ring diagram is part of the sequence of ring necklaces and of the second-order Born approximation. The first-order particle-hole diagram is the Hartree term, the eyeglas diagram.

The particle-hole ladders can also be drawn like the eyeglass diagram, for which the connecting interaction line is replaced by many parallel ones. The two particle lines must be oriented with opposite directions at the connection.

- The **particle-particle ladder diagram** are given by the permutation vectors.

position	1	2	3	4	5	...	2n-1	2n
$\vec{\mathcal{P}}$	3	4	5	6	7	...	1	2

All vertices are mapped to the next-higher index, i.e. $\mathcal{P}_j = j + 2$ with cyclic permutation. The diagram of lowest order is the eyeglass diagram of the Hartree approximation. The second diagram is the double-ring diagram of the second-order approximation. By inspection of the diagrams in section M.8, I obtain a symmetry factor $2n$ for a n-th order particle-particle ladders and a sign of $+1$.

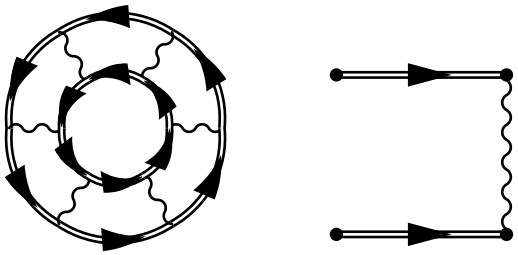


Fig. 14.5: The particle-particle ladder and its elemental diagram

The first-order particle-particle ladder is the eyeglass diagram responsible for the Hartree energy. This diagram is also contained in the particle particle ladder. The second-order particle-hole ladder is identical to the double ring-diagram in figure 14.2. The second-order terms of the ring-necklaces, the particle-hole diagram and the particle-particle diagram are identical.

- The **wheel** is given by the permutation vectors.

position	1	2	3	4	5	...	2n-1	2n
$\vec{\mathcal{P}}$	3	4	5	6	7	...	2	1

Any vertex, except the two last ones, is mapped to the second-next higher one. The last odd-numbered index, V_{2n-1} is mapped onto the first even-numbered vertex, V_2, and the last even-numbered vertex V_{2n} is mapped onto the first odd numbered index, V_1.

The diagram of lowest order is the oyster diagram of the Hartree-Fock approximation. The second-order wheel is second order exchange diagram of the second-order approximation.

By inspection of the diagrams in section M.8, I obtain a symmetry factor $2n$ for a n-th order wheel and a sign of -1.

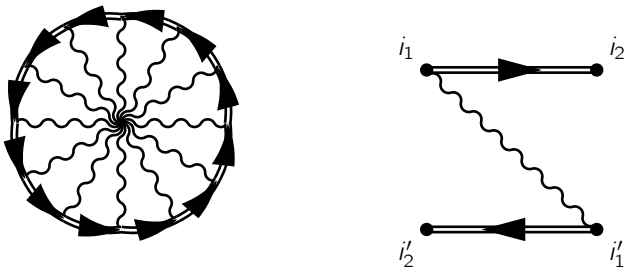


Fig. 14.6: The wheel and its elemental diagram

The wheel is obtained by introducing one exchange into particle-particle ladder as shown in figure 14.7.

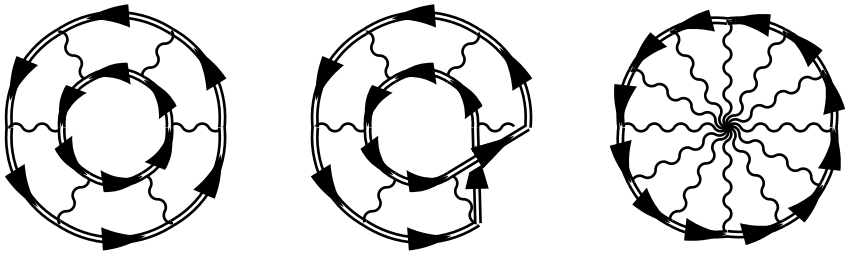


Fig. 14.7: The wheel diagram results from including exchanges into the particle-particle ladder. The diagram on the left is the particle-particle ladder. The diagram in the middle and on the right are equivalent: They contain one Fermi loop with $2n$ Green's functions, for which each interaction joins the Fermi loop after n Green's function again.

The first order wheel is the oyster, the exchange diagram. The second-order wheel is the double exchange in figure 14.2.

14.4 Random-Phase approximation

The so-called **random-phase approximation** (RPA)[50, 51, 52] has a very intuitive physical picture. One considers an effective one-particle picture on the Hartree-Fock level. However, instead of using the Coulomb interaction one uses an effective, so-called **screened interaction**. The Coulomb interaction becomes screened by the formation of electron-hole pairs, which themselves have a dipole, which orients opposite to the electric field. As a result, the Coulomb interaction is changed into a Yukawa potential

$$v_{\text{Yukawa}}(\vec{r},\vec{r'}) = \frac{e^2 \mathrm{e}^{-\lambda|\vec{r}-\vec{r'}|}}{4\pi\epsilon_0|\vec{r}-\vec{r'}|} \tag{14.9}$$

for which the long-ranged potential tail is damped out exponentially.

The **random-phase approximation**(**RPA**) [50, 51, 103] has been first introduced by Bohm and Pines[50] in a heuristic manner. The underlying idea is that the electrostatic interaction between electrons is largely absorbed by a plasma-mode of collective oscillation, while the remaining modes can be considered as weakly-interacting electrons with a screened interaction. Gell-Mann and Brueckner derived the random-phase approximation based on a partial sum of leading order ring necklaces and



Fig. 14.8: The diagrams of the Luttinger-Ward functional in the random-phase approximation (RPA) in terms of the screened interaction. The RPA differs from the Hartree-Fock approximation by the screened interaction W (double wriggly interaction line) replacing the bare interaction in the exchange diagram. The screened interaction converts the exchange diagram into an infinite sum of ring-necklaces, the latter using the bare interaction. Editor: This needs a second diagram with the Dyson's equation for the screened interaction. The polarization diagram in the dyson's equation is the ring diagram with the full Green's functions.

the second-order exchange[51]. A more systematic treatment than that of Bohm and Pines has been given by Nozieres and Pines[104](see [103]).

The GW-approximation has been invented by Lars Hedin in 1965[105]. The name GW is not an abbreviation of names as one may suspect, but the combination of the mathematical symbols G for Green's function and W for the interaction operator from the German word "Wechselwirkung".

The Luttinger-Ward functional in the random-phase approximation includes the eyeglass diagram and the complete sequence of the ring necklaces. The ring necklaces are shown in figure 14.3. The eyeglass diagram is responsible for the Hartree potential. The self-energy for exchange and correlation Σ_{xc} of the RPA is the derivative of the sum over all ring-necklaces as functional of the full Green's function. The exchange term represented by the oyster diagram is the first term in the series of ring-necklaces. The higher order terms screen the interaction between the electrons, but only in the exchange term. The Hartree-term (eyeglass diagram) is still calculated with the unscreened interaction. The ring diagram describes a virtual electron-hole pair, which creates a Coulomb potential that counteracts the bare Coulomb potential. Qualitatively, the screened interaction has the form of a Yukawa potential, which falls off exponentially with distance. This heals the common problems of the Hartree-Fock approximation, which are due to the long-ranged Coulomb interaction.

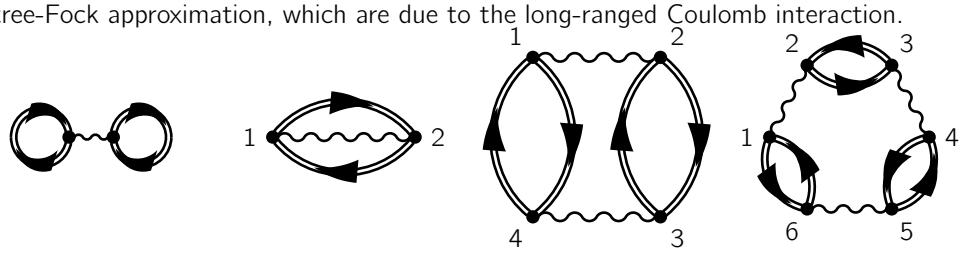


Fig. 14.9: The first four diagrams of the Luttinger-Ward functional in the random-phase approximation (RPA) expressed in terms of the bare interaction. The RPA contains the eyeglass diagram, which describes the Hartree energy, and the infinite sequence of ring-necklaces. The lowest-order ring-necklace is the exchange energy. These diagrams in sum are identical to the two diagrams shown in figure 14.8.

The screened interaction consists of an interaction with all possible ring-diagrams inserted. The random-phase approximation is obtained by a "small" modifications of the Hartree-Fock equations: The ring diagrams can be inserted into the Hartree-Fock equations, by replacing the bare interaction in the exchange diagram (the oyster) by the screened interaction. Important is that the Hartree term remains untouched and is evaluated with the bare (unscreened) interaction.

Each ring is represented as a **polarization term**

$$W = W^{(0)} + W^{(0)}\Pi^{(0)}W^{(0)} + W^{(0)}\Pi^{(0)}W^{(0)} + \ldots = W^{(0)} + W^{(0)}\Pi^{(0)}W \qquad (14.10)$$

This is a Dyson's equation for the interaction.

Hence we have four self-consisten equations, rather than two as in the Hartree-Fock approximation.

- the self energy as gradient of the Luttinger-Ward functional.
- the bare polarization $\Pi^{(0)}$ as the ring diagram.
- Dyson's equation for the interaction
- Dyson's equation for the Green's function

14.5 T-matrix approximation

The T-matrix approximation evolved out of nuclear physics. It is appropriate for very strong interactions, such as a hard core potential, which becomes infinitely repulsive below a given radius. This is the picture of the strong interaction between nucleons.

The particle-hole ladders are given by the permutation vectors.

position	1	2	3	4	5	...	2n-1	2n
$\vec{\mathcal{P}}$	3	2n+1	5	2	7	...	1	2

Any odd numbered vertex are mapped to the next-higher odd-numbered index. Any even-numbered vertex is mapped to the next lower even-numbered index.

14.6 Fluctuating-exchange approximation (FLEX)

Editor: FLEX has been invented by Bickers and Scalapino[92]. The generalization to general lattice Hamiltonians has been done Esirgen and Bickers.[?]. Sie also Katsnelson and Lichtenstein, J.Phys.Cond.Mat. 11, 2037 (1999).

The particle-particle ladders are given by the permutation vectors.

position	1	2	3	4	5	...	2n-1	2n
$\vec{\mathcal{P}}$	3	4	5	6	7	...	1	2

All odd-numbered vertices are mapped to the next-higher odd-numbered index. Any even-numbered vertex is mapped to the next higher even-numbered index.

The exchange wheel is given by the permutation vectors.

position	1	2	3	4	5	...	2n-1	2n
$\vec{\mathcal{P}}$	3	4	5	6	7	...	2	1

Any vertex, except the two last ones, is mapped to the second-next higher one. The last odd-numbered index, V_{2n-1} is mapped onto the first even-numbered vertex, V_2, and the last even-numbered vertex V_{2n} is mapped onto the first odd numbered index, V_1.

Introducing exchanges into the ring-necklace of the RPA will insert ladder insertions into rings.

14.7 Compact notations

14.7.1 Combined vertex indices

Often a short-hand notation is used:

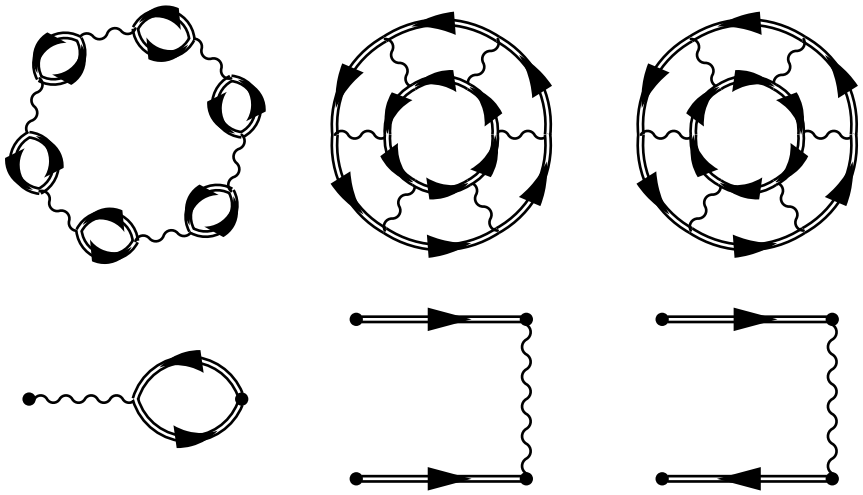


Fig. 14.10: The elemental diagrams of the FLEX approximation. There are two distinct ladder diagrams. The first-order Flex diagram is the Hartree diagram.

- rather than listing orbital indices o_j, i_j, and time arguments t_j connected to a vertex with label j, only a number is used.
  - $G^{(0)}(1,2)$ expands into $G^{\mathcal{C},(0)}_{o_1,i_2}(t_1, t_2^+)$
  - $G(1,2)$ expands into $G^{\mathcal{C}}_{o_1,i_2}(t_1, t_2^+)$
  - $W(1,2)$ expands into $i\hbar W_{o_1,o_2,i_1,i_2}\delta_{\mathcal{C}}(t_1 - t_2)$
  - $\int d1$ expands into $\sum_{o_1,i_1}\int_{\mathcal{C}} dt_1$
- Einstein notation is used. That is, if a vertex label occurs twice in a product, a sum over orbital indices and a time integration, i.e. $\int d1$ is implicitly assumed.

As an example, Dyson's equation has the form

$$G(1,2) \overset{\text{Eq. } 8.23}{=} G^{(0)}(1,2) + G^{(0)}(1,3)\Sigma(3,4)G(4,2) \tag{14.11}$$

The value of a closed diagram Eq. 10.66 in a short-hand notation reads as follows

$$\mathcal{V}(\vec{\mathcal{P}}) = \epsilon_{\mathcal{P}_1,\ldots,\mathcal{P}_{2n}}(i\hbar)^n \int d1 \cdots \int d2n \left(\prod_{j=1}^{n} W(2j-1, 2j)\right)\left(\prod_{k=1}^{2n} G^{\mathcal{C},(0)}(\mathcal{P}_k, k)\right) \tag{14.12}$$

From the generating functional $\mathcal{Q}[\boldsymbol{G}^{(0)}, \boldsymbol{W}]$, we obtain the Green's function via

$$G(2,1) \overset{\text{Eq. } 10.78}{=} G^{(0)}(2,1) + G^{(0)}(2,4)\Sigma^{red}(4,3)G^{(0)}(3,1) \tag{14.13}$$

which is a short-hand notation for

$$G_{i_2,o_1}(t_2,t_1) = G^{(0)}_{i_2,o_1}(t_2,t_1) + \int_{\mathcal{C}} dt_1 \int_{\mathcal{C}} dt_2 \sum_{i_3,o_4} G^{(0)}_{i_2,o_4}(t_2,t_4)\Sigma^{red}_{o_4,i_3}(t_4,t_3)G^{(0)}_{i_3,o_1}(t_3,t_1) \tag{14.14}$$

where the reducible self energy Σ^{red} is the functional derivative of the generating functional.

$$\Sigma^{red}_{o_2,i_1}(t_1,t_2) \overset{\text{Eq. } 10.79}{=} \beta \frac{\partial \mathcal{Q}[G^{(0)}]}{\partial G^{(0)}_{i_1,o_2}(t_2,t_1)} \tag{14.15}$$

or, in the short-hand notation,

$$\Sigma^{red}(2,1) \overset{\text{Eq. } 10.79}{=} \beta \frac{\partial \mathcal{Q}[G^{(0)}]}{\partial G^{(0)}(1,2)} \tag{14.16}$$

How is the reducible self energy Σ^{red} related to the proper self energy Σ, introduced earlier? The proper self energy is defined in Eq. 8.15 on 269, which converts the equation of motion Eq. 8.8 for the Green's function into Dyson's equation Eq. 8.23.

$$G(2,1) \overset{\text{Eq. } 8.23}{=} G^{(0)}(2,1) + \int_{3,4} G^{(0)}(2,4)\Sigma(4,3)G(3,1) \tag{14.17}$$

The full Green's function is given by the equation of motion.

Chapter 15

Functional of the Green's function and the screened interaction

Editor: This is under construction. It is in the process of collecting material.

The first result of the many-body perturbation theory was a functional $\mathcal{Q}[G^{(0)}, v]$ of the bare Green's function $G^{(0)}$ and the bare interaction v. Then, in chapter 12, we derived a self-energy functional and from that the Luttinger-Ward functional $\Phi^{LW}[G, v]$, which is a functional of the full Green's function and the bare interaction.

Here, we do an additional step, which will lead to a functional $\Psi[G, W]$ of the full Green's function and the screened interaction. As mentioned in [106], this functional has been investigated by Hedin[105] and Almbladh et al.[107, 108]. This functional has beenaaplied to the electron gas[107, 108] and atoms[109].

Editor: See also Giesbertz et al. **??**

The screened potential has been first introduced by Hubbard[110]. It is defined as[105]-Eq. 9.

$$W(1,2) = v(1,2) - \frac{i}{\hbar}\int d3 \int d4\; v(1,3)\big\langle \mathcal{T}\delta\rho(3)\delta\rho(4)\big\rangle v(4,2) \quad \text{where}$$
$$\delta\rho(1) = \hat{\psi}^\dagger(1)\hat{\psi}(1) - \big\langle \hat{\psi}^\dagger(1)\hat{\psi}(1)\big\rangle \tag{15.1}$$

Hedin[105]-Eq. 9. where

$$\begin{aligned}\Big\langle \mathcal{T}\delta\rho(3)\delta\rho(4)\Big\rangle &= \Big\langle \mathcal{T}\hat{\psi}^\dagger(3)\hat{\psi}(3)\hat{\psi}^\dagger(4)\hat{\psi}(4)\Big\rangle - \Big\langle \mathcal{T}\hat{\psi}^\dagger(3)\hat{\psi}(3)\big\langle\hat{\psi}^\dagger(4)\hat{\psi}(4)\big\rangle\Big\rangle \\ &\quad - \Big\langle \mathcal{T}\hat{\psi}^\dagger(4)\hat{\psi}(4)\big\langle\hat{\psi}^\dagger(3)\hat{\psi}(3)\big\rangle\Big\rangle + \Big\langle \mathcal{T}\big\langle\hat{\psi}^\dagger(3)\hat{\psi}(3)\big\rangle\big\langle\hat{\psi}^\dagger(4)\hat{\psi}(4)\big\rangle\Big\rangle \\ &= \underbrace{\Big\langle \mathcal{T}\hat{\psi}^\dagger(3)\hat{\psi}(3)\hat{\psi}^\dagger(4)\hat{\psi}(4)\Big\rangle}_{n^{(2)}(3,4)} - \underbrace{\big\langle\hat{\psi}^\dagger(3)\hat{\psi}(3)\big\rangle}_{n(3)}\underbrace{\big\langle\hat{\psi}^\dagger(4)\hat{\psi}(4)\big\rangle}_{n(4)}\end{aligned} \tag{15.2}$$

Polarization insertion (Stefanucci Sec.10.7): A **polarization insertion** is a part of a diagram that (1) can be cut away by removing two interaction lines, and that (2) does not fall apart by removing one interaction line. The **polarizability** P is the sum over all polarization insertions.

The **reducible polarizibility**. is defined by

$$P^{red}(1,2) = P(1,2) + \int d3 \int d4\; P(1,3)v_{3,4}P^{red}(4,2) \tag{15.3}$$

The **screened interaction** is defined by a Dyson equation

$$W(1,2) = v(1,2) + \int d3 \int d4\; v(1,3)P(3,4)W(3,2) \tag{15.4}$$

and hence, expressed in terms of the reducible polarizability,

$$W(1,2) = v(1,2) + \int d3 \int d4\ v(1,3) P^{red}(3,4) v(3,2) \tag{15.5}$$

A diagram is a W-**skeleton diagram**, if it does not contain polarization insertions.

Let me divide the self energy into a Hartree term and a exchange-correlation term.

$$\Sigma = \hat{V}_H + \hat{\Sigma}_{xc} \tag{15.6}$$

Let me begin with a by defining an general polarization diagram: Consider the skeleton expansion for the Luttinger-Ward diagram in terms of full Green's functions G and bare interaction lines v. Select one skeleton diagram and remove one of its interaction lines. What is left is a polarization diagram. A skeleton diagram of order n contributes n such polarization diagrams.

A polarization diagram is one, which can be inserted in between two bare interactions.

The reducible polarizibility is defined as

$$P^{red} = \frac{\partial \Phi^{LW}[G,v]}{\partial v} \tag{15.7}$$

Let me define the irreducible polarization P, with the property that is does not fall apart after removing two interaction lines.

$$P^{red} = P + PvP + PvPvP + \ldots \tag{15.8}$$

The screened interaction is

$$W = v + vPW \tag{15.9}$$

P is a polarization insertion. A polarization is a diagram which can be inserted in between two bare interactions. It must furthermore be 2-particle irreducible and 2-interaction-irreducible, after the polarization has been closed by an interaction line.

A closed diagram is two-interaction reducible, if it falls apart into two pieces after removing two interaction lines. Otherwise it is two-interaction irreducible.

Every skeleton diagram of the Luttinger-Ward functional can be divided into two-interaction-reducible and two-interaction irreducible diagrams.

The skeleton expansion may be simplified by removing all two-interaction reducible diagrams, if each remaining interaction line is replaced by a screened interaction W. The Luttinger-Ward functional is then recovered by inserting the expansion for the

$$P^{red} = P + PvP + PvPvP + \ldots = -\left.\frac{\partial}{\partial v}\right|_P \mathrm{Tr}\Big[\ln\Big(1 - Pv\Big)\Big] \tag{15.10}$$

$$\beta \frac{\partial \Phi^{LW}[G,v]}{\partial v} = P^{red} \tag{15.11}$$

This can be combined into a stationary condition

$$0 = \left.\frac{\partial}{\partial v}\right|_P \left\{ \Phi^{LW}[G,v] + k_B T \mathrm{Tr}\Big[\ln\Big(1 - Pv\Big)\Big] \right\} \tag{15.12}$$

Let me define a polarization functional

$$R[G,P] = \underset{v}{\mathrm{stat}} \big\{ \Phi^{LW}[G,v] + k_B T \mathrm{Tr}\Big[\ln\Big(1 - Pv\Big)\Big] \big\} \tag{15.13}$$

$$\beta\frac{\partial R[P]}{\partial P} = -v(1-Pv)^{-1} = -W \tag{15.14}$$

This expression can be rewritten as a stationary condition

$$\frac{\partial}{\partial P}\Big\{R[P] + k_B T\ \mathrm{Tr}\big[WP\big]\Big\} = 0 \tag{15.15}$$

Finally let me define a functional of the screened interaction W and the full Green's function.

$$\begin{aligned}\Psi[G,W] &= \underset{P}{\mathrm{stat}}\Big\{R[P] + k_B T\ \mathrm{Tr}\big[WP\big]\Big\} \\ &= \underset{P}{\mathrm{stat}}\,\underset{v}{\mathrm{stat}}\Big\{\Phi^{LW}[G,v] + k_B T\ \mathrm{Tr}\Big[\ln\Big(1-Pv\Big) + WP\Big]\Big\}\end{aligned} \tag{15.16}$$

Almbladh et al.[107, 108]: Eq. 2 of Almbladh

$$iE = \Phi - \mathrm{Tr}\Big[\Sigma G + \ln\Big(\Sigma - G_0^{-1}\Big)\Big] \qquad (Almbladh - Eq.2) \tag{15.17}$$

can be compared to our Eq. 10.89.

$$\begin{aligned}\Omega^W_{T,\mu} &\overset{\text{Eq. }10.89}{=} k_B T\ \mathrm{Tr}\big\{\ln\big[i\hbar\lim_{t'\to t^+}\hat{G}^{(0)}(t',t)\big]\big\} + \mathcal{Q}_{T,\mu}[G_0,v] \\ &\overset{\text{Eq. }12.36}{=} \frac{1}{\beta}\mathrm{Tr}\big\{\ln\big[i\hbar\lim_{t'\to t^+}\hat{G}^{(0)}(t',t)\big]\big\} + \underset{\Sigma,G}{\mathrm{stat}}\Big\{\Phi^{LW}_T[G,v] - \frac{1}{\beta}\mathrm{Tr}\Big[\ln\Big(1-\Sigma G^{(0)}\Big) + \Sigma G\Big]\Big\} \\ &= \quad + \underset{\Sigma,G}{\mathrm{stat}}\Big[\Phi^{LW}_T[G,v] - \frac{1}{\beta}\mathrm{Tr}\Big\{\ln\Big[\Big(\big(G^{(0)}\big)^{-1} - \Sigma\Big)G^{(0)}\Big] - \ln\Big[i\hbar\lim_{t'\to t^+}\hat{G}^{(0)}(t',t)\Big] + \Sigma G\Big\}\Big]\end{aligned} \tag{15.18}$$

The equations differ by factors $i\hbar$, which may be due to Almbladh's use of the Matsubara formalism.

I have not yet confirmed that the two logarithms can be combined as in Almbladh's case.

Almbladh 3

Dyson's equation results from the stationarity with respect to the selef energy

$$\begin{aligned}\frac{\beta\partial\Omega^W}{\partial\Sigma} &= -G^{(0)}\Big(1-\Sigma G^{(0)}\Big)^{-1} - G \overset{!}{=} 0 \\ &\Rightarrow -G^{(0)} = G - G\Sigma G^{(0)} \qquad \Rightarrow\end{aligned} \tag{15.19}$$

Almbladh Eq.11

$$Tr[\Sigma G] = -\mathrm{Tr}[PW] = -\mathrm{Tr}[v\chi] \tag{15.20}$$

$$W = v + vPW = v + v\chi v \tag{15.21}$$

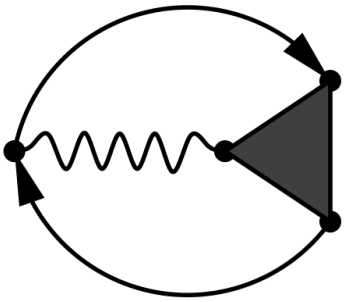
Screened interaction

Vertex corrections

Editor: Caution: do not read! This is not finished.

Consider an arbitrary skeleton diagram (except for the Hartree diagram). Let me single out one vertex, connected to one interaction as well as one incoming and one outgoing particle line. The opposite ends of these three items connect to an object, which can accept an incoming particle line, and outgoing particle line and one interaction. This object may be called a **renormalized vertex**.

The most simple diagram of a renormalized vertex is a bare vertex. The corresponding diagram is the oyster diagram, which describes the exchange energy. The other diagrams of the renormalized vertex are the **vertex corrections**.



The complete skeleton expansion can be represented by

- the Hartree energy, represented by the eyeglass diagram
- the exchange energy, represented by the oyster diagram
- the diagram with one bare vertex and the vertex corrections on the other side.

Chapter 16

Linear response and Kubo formula

Kubo's formula has been derived in section 13.4.2 of ΦSX: Quantum Theory[16] in the context of time-dependent perturbation theory. In this chapter, that derivation is revisited and expressed in terms of Green's functions.

Editor: Skip this! The Green's function part is missing. I am missing the piece to express the suceptibility by our contour-ordered Green's functions.

16.1 Linear-response theory

Consider a prototypical experiment of time-dependent phenomena: A system, or ensemble, is prepared at some time t_0. It is propagated under the influence of a time-dependent perturbation $\lambda(t)\hat{B}$, which is used to manipulate the system. The time-dependent Hamiltonian has the form

$$\hat{H}_\lambda(t) = \hat{H}_0 + \lambda(t)\hat{B} \tag{16.1}$$

where I consider, for the sake of simplicity[1], a time-independent unperturbed Hamiltonian $\hat{H}_0$. At some time, the observable $\hat{A}$ is measured, yielding the expectation value

$$A(t) = \langle\Psi(t)|\hat{A}|\Psi(t)\rangle \tag{16.2}$$

The goal of linear-response theory is to determine the change $\delta A(t)$ of an observable $\hat{A}$ due to a perturbation $\lambda(t)\hat{B}$ to first order in $\lambda(t)$.

The propagator of the unperturbed system is $\mathrm{e}^{-\frac{i}{\hbar}\hat{H}_0 t}$. Let me now determine the first-order change of the wave function due to the perturbation.

$$i\hbar\partial_t|\Psi_\lambda(t)\rangle = \left(\hat{H}_0 + \lambda(t)\hat{B}\right)|\Psi_\lambda(t)\rangle \tag{16.3}$$

Let me investigate the dynamics of a state $|\Psi_H(t)\rangle = \exp(\frac{i}{\hbar}H_0 t)|\Psi(t)\rangle \overset{\lambda=0}{=} |\Psi(0)\rangle$ in the Heisenberg picture.

$$i\hbar\partial_t \underbrace{\mathrm{e}^{\frac{i}{\hbar}\hat{H}_0 t}|\Psi_\lambda(t)\rangle}_{|\Psi_{H,\lambda}(t)\rangle} = \underbrace{-\hat{H}_0\mathrm{e}^{\frac{i}{\hbar}\hat{H}_0 t}}_{i\hbar\partial_t\mathrm{e}^{\frac{i}{\hbar}\hat{H}_0 t}}|\Psi_\lambda(t)\rangle + \mathrm{e}^{\frac{i}{\hbar}\hat{H}_0 t}\underbrace{\left(\hat{H}_0 + \lambda(t)\hat{B}\right)|\Psi_\lambda(t)\rangle}_{i\hbar\partial_t|\Psi_\lambda(t)\rangle} = \mathrm{e}^{\frac{i}{\hbar}\hat{H}_0 t}\lambda(t)\hat{B}|\Psi_\lambda(t)\rangle$$

$$\Rightarrow \quad \mathrm{e}^{\frac{i}{\hbar}\hat{H}_0 t}|\Psi_\lambda(t)\rangle = \mathrm{e}^{\frac{i}{\hbar}\hat{H}_0 t_0}|\Psi_\lambda(t_0)\rangle + \frac{1}{i\hbar}\int_{t_0}^{t} dt'\,\mathrm{e}^{\frac{i}{\hbar}\hat{H}_0 t'}\lambda(t')\hat{B}|\Psi_\lambda(t')\rangle$$

$$\Rightarrow \quad |\Psi_\lambda(t)\rangle = \mathrm{e}^{-\frac{i}{\hbar}\hat{H}_0(t-t_0)}|\Psi_\lambda(t_0)\rangle + \frac{1}{i\hbar}\int_{t_0}^{t} dt'\,\mathrm{e}^{-\frac{i}{\hbar}\hat{H}_0(t-t')}\lambda(t')\hat{B}|\Psi_\lambda(t')\rangle \tag{16.4}$$

[1] The generalization to time-dependent unperturbed Hamiltonians is possible by replacing the propagator $\mathrm{e}^{-\frac{i}{\hbar}\hat{H}_0(t-t')}$ by its general form $\hat{U}(t,t')$

I will use the Heisenberg operators $\hat{A}_H(t)$ and $\hat{B}_H(t)$ defined according to

$$\hat{A}_H = \mathrm{e}^{\frac{i}{\hbar}\hat{H}_0 t}\hat{A}\,\mathrm{e}^{-\frac{i}{\hbar}\hat{H}_0 t} \tag{16.5}$$

This definition is limited to time-independent Hamiltonians, and the distinction between Heisenberg picture and interaction picture is not clear cut. In section 6.2.5 below, I will provide a more general and concise definitions of Heisenberg operators.

Because we are interested in the linear response, I expand the wave function in powers of $\lambda(t)$ and ignore higher-order terms. That is, $|\Psi_\lambda\rangle = |\Psi_0\rangle + |\delta\Psi\rangle + O(\lambda^2)$. Let us assume that $\lambda(t) = 0$ for $t < t_0$.

$$\begin{aligned}
|\delta\Psi(t)\rangle &= \underbrace{|\delta\Psi(t_0)\rangle}_{=0} + \frac{1}{i\hbar}\int_{t_0}^{t} dt'\; \mathrm{e}^{-\frac{i}{\hbar}\hat{H}_0(t-t')}\lambda(t')\hat{B}|\Psi_0(t')\rangle \\
&= \frac{1}{i\hbar}\int_{t_0}^{t} dt'\; \mathrm{e}^{-\frac{i}{\hbar}\hat{H}_0(t-t')}\lambda(t')\hat{B}\mathrm{e}^{-\frac{i}{\hbar}\hat{H}_0(t'-t_0)}|\Psi_0(t_0)\rangle
\end{aligned} \tag{16.6}$$

The result is inserted into the first-order change of the expectation value

$$\begin{aligned}
\delta A(t) &= \Big\{\langle\Psi_0(t)|\hat{A}|\delta\Psi(t)\rangle + \langle\delta\Psi(t)|\hat{A}|\Psi_0(t)\rangle \\
&= \underbrace{\langle\Psi_0(t_0)|\mathrm{e}^{-\frac{i}{\hbar}\hat{H}_0(t_0-t)}}_{\langle\Psi_0(t)|}\underbrace{\frac{1}{i\hbar}\int_{t_0}^{t} dt'\; \hat{A}\,\mathrm{e}^{-\frac{i}{\hbar}H_0(t-t')}\hat{B}\mathrm{e}^{-\frac{i}{\hbar}H_0(t'-t_0)}|\Psi_0(t_0)\rangle}_{|\delta\Psi(t)\rangle}\lambda(t') \\
&\quad \underbrace{-\frac{1}{i\hbar}\int_{t_0}^{t} dt'\; \langle\Psi_0(t_0)|\mathrm{e}^{-\frac{i}{\hbar}\hat{H}_0(t_0-t')}\hat{B}\mathrm{e}^{-\frac{i}{\hbar}\hat{H}_0(t'-t)}\;\hat{A}}_{\langle\delta\psi(t)|}\underbrace{\mathrm{e}^{-\frac{i}{\hbar}H_0(t-t_0)}|\Psi_0(t_0)\rangle}_{|\Psi_0(t)\rangle}\lambda(t') \\
&= \frac{1}{i\hbar}\int_{t_0}^{t} dt'\; \underbrace{\langle\Psi_0(t_0)|\mathrm{e}^{-\frac{i}{\hbar}\hat{H}_0 t_0}}_{\langle\Psi_0(0)|}\Big[\underbrace{\mathrm{e}^{\frac{i}{\hbar}\hat{H}_0 t}\hat{A}\mathrm{e}^{-\frac{i}{\hbar}H_0 t}}_{\hat{A}_H(t)}, \underbrace{\mathrm{e}^{\frac{i}{\hbar}H_0 t'}B\mathrm{e}^{-\frac{i}{\hbar}H_0 t'}}_{\hat{B}_H(t')}\Big]_- \underbrace{\mathrm{e}^{\frac{i}{\hbar}H_0 t_0}|\Psi_0(t_0)\rangle}_{|\Psi_0(0)\rangle}\lambda(t') \\
&\overset{t_0\to-\infty}{=} \frac{1}{i\hbar}\int_{-\infty}^{\infty} dt'\; \theta(t-t')\langle\Psi_0(0)|\Big[\hat{A}_H(t), \hat{B}_H(t')\Big]_-|\Psi_0(0)\rangle\lambda(t')
\end{aligned} \tag{16.7}$$

Setting $t_0 = -\infty$ does not change the result as long as $\lambda(t) = 0$ for $t < t_0$, which implies that we "prepare the state" before we perturb it.

The result is easily generalized to ensembles: Instead of a single initial state, we perform an ensemble average over all states in the ensemble

$$\begin{aligned}
\delta A(t) &= \frac{1}{i\hbar}\int_{-\infty}^{\infty} dt'\; \theta(t-t')\sum_q P_q\langle\Phi_q|\Big[\hat{A}_H(t), \hat{B}_H(t')\Big]_-|\Phi_q\rangle\lambda(t') \\
&= \frac{1}{i\hbar}\int_{-\infty}^{\infty} dt'\; \theta(t-t')\mathrm{Tr}\left(\hat{\rho}^{vN}\Big[\hat{A}_H(t), \hat{B}_H(t')\Big]_-\right)\lambda(t')
\end{aligned} \tag{16.8}$$

The ensemble is the initial ensemble established at a time before the perturbation acts on the system.

This results in the well-known **Kubo formula**[76]

KUBO FORMULA

The linear response of an observable $\hat{A}$ at time t due to a perturbation $\lambda(t')\hat{B}$ at time t' is the susceptibility $\chi_{AB}(t,t')$. The linear response is[76]

$$\delta A(t) = \int_{-\infty}^{\infty} dt'\, \chi_{AB}(t,t')\lambda(t') \tag{16.9}$$

with the **susceptibility**

$$\chi_{AB}(t,t') = \theta(t-t')\frac{1}{i\hbar}\mathrm{Tr}\left\{\hat{\rho}^{vN}\left[\hat{A}_H(t),\hat{B}_H(t')\right]_-\right\}\theta(t-t') \tag{16.10}$$

One may wonder why there is a commutator rather than a simple product. An argument is that commutating variables do not affect each other.

Chapter 17

Models in many-particle theory

Editor: This chapter is not part of the regular course. I leave it here, because (1) it is a resource to look up certain effects and (2) because I want to extend it. Meaning that this chapter is UNDER CONSTRUCTION!

The physics of correlated materials is often studied using, what I call minimal models. Models that are just sufficiently complex to study a particular effect, but that avoid any other complication. The reason for using minimal models is not so much simplicity, but that they provide the focus onto what is truly relevant.

There is a large zoo of models, which is too large to be covered here. In this chapter, I focus on the most important models in the hope that the others can be accessed by their relation to the models described here.

The models chosen are given in table 17.1 Editor: This is the plan. Not all models in the list are described yet.

Table 17.1: Model systems in solid-state physics

Model	Effects
Jellium model	Fermi-liquid
Hubbard	Coulomb interaction, Mott insulator, metal-insulator transition, (Abrikosov-Suhl resonance?)
Heisenberg	ferromagnetism, antiferromagnetism, magnons
Anderson Kondo	Kondo effect, Abrikosov-Suhl resonance, heavy fermions
Holstein	e-phonon coupling, polaron, band vs. hopping transport
Bardeen-Cooper-Schrieffer (BCS)	superconductivity, Cooper pair
Su-Schrieffer-Heeger(SSH)	Peierls distortion, soliton, topological insulator
Jaynes-Cummings	light-matter interaction

17.1 Jellium model

The jellium model is the model for dense fermions with the highest possible symmetry, namely translation symmetry in space and time, isotropy in space and under spin rotation. Therefore, many calculations can be performed analytically for the free electron gas, which may be untractable for other systems.

17.1.1 The model

The free-electron gas has the highest possible symmetry, namely that of free space, i.e. translation symmetry in space and time and rotational symmetry in space and spin. This greatly simplifies many-particle calculations.

The Hamiltonian for the free-electron gas is

$$\begin{aligned}\hat{H} = &\int d^4x \underbrace{\hat{\psi}^\dagger(\vec{x})\frac{-\hbar^2}{2m_e}\vec{\nabla}^2\hat{\psi}(x)}_{\text{kinetic energy}} + \underbrace{\frac{1}{2}\int d^4x \int d^3x' \frac{e^2}{4\pi\epsilon_0|\vec{r}-\vec{r'}|}\hat{\psi}^\dagger(\vec{x})\hat{\psi}^\dagger(\vec{x'})\hat{\psi}(\vec{x'})\hat{\psi}(\vec{x})}_{\textbf{electron-electron repulsion}} \\ &\underbrace{-\int d^4x\, \hat{\psi}^\dagger(\vec{x})\hat{\psi}(\vec{x})\int d^3r' \frac{-e\rho_B}{4\pi\epsilon_0|\vec{r}-\vec{r'}|}}_{\textbf{electron interaction w. positive charge background}} + \underbrace{\frac{1}{2}\int d^3r \int d^3r' \frac{\rho_B^2}{4\pi\epsilon_0|\vec{r}-\vec{r'}|}}_{\text{self-energy of charge background}}\end{aligned} \tag{17.1}$$

The Hamiltonian is expressed in terms of field operators. The first term is the kinetic energy of the electrons. The second term is the Coulomb interaction between the electrons. These two terms would have an infinite energy density, because the Coulomb energy has infinite range. Therefore, a **neutralizing charge background** with positive charge density ρ_B is added, so that the average charge density is charge neutral. This charge-background density describes the atom cores (nuclei and core electrons), which are smeared out into a homogeneous positive charge density. The last two terms are the potential created by the charge background and the self energy of the charge background, respectively. If the integration is performed over the infinite space, the individual electrostatic terms are infinite, because each describes an infinite charge density. Once they are added together, however, these infinities cancel. In practice, the charge background does not show up itself, because it cancels the Hartree energy of the homogeneous electron density.

If the Fermi-level lies within the continuous spectrum, it is called a **degenerate Fermi gas**. The term "degenerate" has nothing to do with degenerate states, but it stands for "disfigured". A degenerate electron gas is a model for a metal. A "normal" electron gas, as opposed to a "degenerate" electron gas, has a Fermi level below the lower band edge. This situation describes the electrons in the conduction band of a semiconductor or insulator, where the electrons are due to thermal excitations or doping. In this case, the electron gas is dilute. In the dilute limit, the distinction between a Fermi-gas and a Boltzmann gas becomes negligible, because Fermi and Boltzmann distribution become similar for $\epsilon - \mu \gg k_B T$

For a non-interacting electron gas, the many-particle wave functions are Slater determinants formed from plane waves

$$\varphi_{\vec{k},\sigma}(\vec{r},\sigma') = \frac{1}{\sqrt{V}} e^{i\vec{k}\vec{r}}\delta_{\sigma,\sigma'} \tag{17.2}$$

The energies of the many-particle states are sums of the occupied one-particle energies. The one-particle energies are given by the energy dispersion

$$\epsilon_{\vec{k},\sigma} = \frac{\hbar\vec{k}^2}{2m_e} \tag{17.3}$$

The spectral function of the non-interacting electron gas can be represented as

$$\hat{\mathcal{A}}(\hbar\omega) \overset{\text{Eq. ??}}{=} \sum_{\sigma\in\{\uparrow,\downarrow\}} \frac{1}{V}\int \frac{d^3k}{(2\pi)^3} |\varphi_{k,\sigma}\rangle\, \delta\big(\hbar\omega - \epsilon(\vec{k},\sigma)\big)\, \langle\varphi_{\vec{k},\sigma}| \tag{17.4}$$

Editor: As a consequence of translational invariance, the natural orbitals of the free electron gas are plane waves. The natural orbitals of the free electron gas are, therefore, independent of the interaction strength. The one-particle-reduced density matrix of the free electron gas depends on the interaction only via the occupations, and so does the Fock operator. The total energy expression Eq. 2.140 can be used. When the entanglement entropy is neglected, the Hamiltonian may be approximated by Eq. 2.100 on p. 78. That Hamiltonian, i.e. the energies $E(\vec{\sigma})$, depends on the Fock operator, which, in turn depends parametrically on the occupations.

17.1.2 Fermi-liquid theory

Fermi-liquid theory goes back to a series of three papers[111, 112, 113] by Lev Landau.

A Fermi liquid is a system of fermions, which behaves qualitatively like a system of non-interacting particles, albeit with renormalized parameters. The underlying picture is that the one-particle states of non-interacting electrons evolve adiabatically into **quasi-particle states** with a defined dispersion relation $\epsilon_{\vec{k},\sigma}$ as the interaction is switched on. The defining property of a Fermi liquid is that the life-time broadening scales quadratically with the difference of the quasi-particle energy from the Fermi level.

$$\frac{1}{\tau} \approx (\epsilon - \mu)^2 + O\left((\epsilon - \mu)^2\right) \tag{17.5}$$

I feel that it is important to distinguish the thermodynamic and the dynamic aspects of Fermi-Liquid Theory. The so-called Landau expansion provides a solid framework on the thermodynamics of a Fermi liquid. In my current view, the quasi-particle concept developed from the Landau expansion, differs, however, from the quasi-particle concept from spectroscopy, which is used to study the dynamics of the Fermi liquid. The differences are subtle. They even vanish within certain approximations, such as the thermal Hartree-Fock approximation.

See section 5.10 of `http://eduardo.physics.illinois.edu/phys561/FL.pdf`

Abrikosov and Khalatnikov published a review in 1959[114]. In appendix A2 they describe amicroscopic theiry of a Fermi liquid at low temperatures.

17.1.3 Landau expansion

Editor: The section on the Landau expansion is probably ok, despite some open issues mentioned in the discussion.

In the first paper of his series of papers laying down the **Fermi-liquid theory**, "The Theory of a Fermi Liquid".[111] Landau makes a number of assumptions:

- *"as we gradually turn on the interaction,..., classification of the levels remains invariant"*
- *"The quasi-particle can, ..., be considered as a particle in the self-consistent field of surrounding particles."*
- *"... the energy of the whole system ... is a functional of the distribution function"*

Let me start from the third assumption, namely the existence of a functional of the distribution function. Such a distribution function can be defined rigorously as a universal density-matrix functional. $E[\hat{\rho}^{(1)}]$, where the one-particle-reduced density matrix $\hat{\rho}^{(1)} = \sum_n |\varphi_n\rangle f_n \langle\varphi_n|$ is given by the natural orbitals and the occupations f_n. The distribution function of Landau are the occupations.

The grand potential is given by

$$\Omega_{T,\mu} = \min_{\hat{\rho}^{(1)}} \left\{ \underbrace{E_T[\hat{\rho}^{(1)}]}_{\text{Eq. 17.8}} - TS^B[\hat{\rho}^{(1)}] - \mu N[\hat{\rho}^{(1)}] \right\} \tag{17.6}$$

where the minimization considers N-representable[1] one-center-reduced density matrices and

$$S^B[\hat{\rho}^{(1)}] = -k_B \mathrm{Tr}\left[\left(\hat{1}-\hat{\rho}^{(1)}\right)\ln\left(\hat{1}-\hat{\rho}^{(1)}\right)+\hat{\rho}^{(1)}\ln\left(\hat{\rho}^{(1)}\right)\right] \tag{17.7}$$

is the fermionic **Boltzmann entropy** Eq. 2.68 defined as maximum possible entropy for a specific one-particle-reduced density matrix.

The density-matrix functional $E_T[\hat{\rho}^{(1)}]$ for the energy in Eq. 17.6 can be defined rigorously as

$$E_T[\hat{\rho}^{(1)}] = k_B T S^B[\hat{\rho}^{(1)}] + \min_{\hat{\rho}^{vN},\{\lambda^{eff}_{\alpha,\beta}\}}\left\{\mathrm{Tr}\left[\hat{\rho}^{vN}\left(\hat{h}+\hat{W}\right)\right]\underbrace{+k_B T \mathrm{Tr}\left[\hat{\rho}^{vN}\ln\left(\hat{\rho}^{vN}\right)\right]}_{-TS^{vN}[\hat{\rho}^{vN}]}\right.$$
$$\left.-\sum_{\alpha,\beta}\lambda^{eff}_{\alpha,\beta}\Big(\underbrace{\mathrm{Tr}\left[\hat{\rho}^{vN}\hat{c}^\dagger_\alpha\hat{c}_\beta\right]-\left\langle\pi_\beta\middle|\hat{\rho}^{(1)}\middle|\pi_\alpha\right\rangle}_{\text{density-matrix constraint}}\Big)\right\} \tag{17.8}$$

where $\langle\pi_\alpha|$ are the projector functions for some complete basisset of one-particle states $|\chi_\alpha\rangle$, i.e $\langle\pi_\alpha|\chi_\beta\rangle = \delta_{\alpha,\beta}$. The energy functional $E_T[\hat{\rho}^{(1)}]$ depends on the temperature. This dependency is not discussed by Landau. With $\lambda_{\alpha,\beta}$ we denote the Lagrange multipliers for the constraint that the one-particle-reduced density matrix of the ensemble is the one specified in the argument.

An effective Hamiltonian $\hat{h}^{eff}$ can be defined[2] as derivative of the energy $E[\hat{\rho}^{(1)}]$

$$\delta E = \mathrm{Tr}\left[\left(\frac{\partial E}{\partial\hat{\rho}^{(1)}}\right)^\dagger\delta\hat{\rho}^{(1)}\right]+\ldots = \mathrm{Tr}\left[\hat{h}^{eff}\delta\hat{\rho}^{(1)}\right]+\ldots \tag{17.9}$$

The derivative defines an effective Hamiltonian

$$\hat{h}^{eff} = \left(\frac{\partial E}{\partial\hat{\rho}^{(1)}}\right)^\dagger \tag{17.10}$$

The eigenvalues of the effective Hamiltonian are the **quasi-particle energies**. [3]

$$\hat{h}^{eff}|\varphi_n\rangle = |\varphi_n\rangle\epsilon_n \tag{17.11}$$

The minimization of the grand potential with respect to N-representable one-particle-reduced density matrices yields the Fermi distribution.

$$\hat{\rho}^{(1)}_{T,\mu} = \left(e^{\beta(\hat{h}^{eff}-\mu)}+\hat{1}\right)^{-1} = \sum_n |\varphi_n\rangle f_{T,\mu}(\epsilon_n)\langle\varphi_n| \tag{17.12}$$

which is analogous to Eq. Landau-4.

In Eq. 6, Landau defines the second derivative of the energy functional, which leads to the so-called **Landau Expansion**.

$$E[\hat{\rho}^{(1)}] = E[\hat{\rho}^{(1)}_0]+\sum_{\alpha,\beta}\underbrace{\frac{\partial E}{\partial\rho^{(1)}_{\alpha,\beta}}}_{h^{eff}_{\beta,\alpha}[\hat{\rho}^{(1)}_0]}\delta\rho^{(1)}_{\alpha,\beta}+\frac{1}{2}\sum_{\alpha,\beta,\gamma,\delta}\underbrace{\frac{\partial^2 E}{\partial\rho^{(1)}_{\alpha,\beta}\partial\rho^{(1)}_{\gamma,\delta}}}_{Q_{\alpha,\beta,\gamma,\delta}}\delta\rho^{(1)}_{\alpha,\beta}\delta\rho^{(1)}_{\gamma,\delta}+\ldots \tag{17.13}$$

[1] The fermionic one-particle-reduced density matrix is N-representable, if it is hermitean and when its eigenvalues lie between zero and one.

[2] This is closely related to **Janak's theorem** which relates the energy levels in density-functional theory to the derivatives of the energy with respect to the occupations.

[3] The definition of the quasi-particle concept does not seem to be uniform. The quasi-particle concept used here differs from that used for spectroscopy. The effective Hamiltonian is the **self-consistent field** mentioned by Landau in one of the assumptions of Fermi-liquid theory. As far as I currently understand, Landau himself switched from the concept described here to the one used in spectroscopy.

which defines the **Landau parameters** $f_{\alpha,\beta,\gamma,\delta}$. To make the connection of the parameters Q with the Landau parameters f obvious we need to impose, like Landau, translational invariance.

While the foregoing considerations are general, let me now turn to the uniform systems: For a system with full translational and rotational symmetry, such as the uniform electron gas, the natural orbitals are momentum eigenstates, i.e. plane waves.

$$\varphi_n(\vec{r},\sigma) = \frac{1}{\sqrt{V}} e^{i\vec{k}_n\vec{r}} \delta_{\sigma,\sigma_n} \tag{17.14}$$

with the momentum $\vec{p}_n = \hbar\vec{k}_n$ and the spin quantum number $\sigma_n \in \{\uparrow,\downarrow\}$. V is the normalization volume. The physical one-particle-reduced density matrix of a uniform electron gas in a momentum-and-spin representation is therefore diagonal.

Because the natural orbitals of the uniform electron gas are independent of the interaction, the energy, and the grand potential, depend only on the occupations, so that

$$E[\{f_{\vec{k},\sigma}\}] = E[\{f_{T,\mu}(\epsilon_{\vec{k},\sigma})\}] + \sum_{\vec{k},\sigma} \underbrace{\epsilon_{\vec{k}}}_{\left.\frac{\partial E}{\partial f_{\vec{k},\sigma}}\right|_{T,\mu}} \delta f_{\vec{k},\sigma} + \frac{1}{2} \sum_{\vec{k},\sigma,\vec{k},\sigma'} \underbrace{Q_{\vec{k},\sigma,\vec{k}',\sigma'}}_{\left.\frac{\partial^2 E}{\partial f_{\vec{k},\sigma}\partial f_{\vec{k}',\sigma'}}\right|_{T,\mu}} \delta f_{\vec{k},\sigma}\delta f_{\vec{k}',\sigma'} \tag{17.15}$$

This explains why Landau uses a distribution which depends on only two rather than four momenta.

Even under spontaneous symmetry breaking, the thermal one-particle-reduced density matrix maintains its symmetry, because the thermal ensemble is an average over all equivalent broken-symmetry states.

A phase transition would become evident by a non-analytic behavior of the thermal occupations as function of interaction strength. When the behavior is analytic, the **adiabatic connection**[4], one of the requirements for a Fermi liquid, is satisfied.

When we move from the uniform electron gas to a general crystal, the natural orbitals can still be classified by the Bloch-vector $\vec{k}$, but there may be an additional band index. Furthermore, the natural orbitals are no more invariant under the interaction strength.

Discussion: Editor: Take the following discussion with a grain of salt: I need to study the microsopic picture [111] behind Fermi-liquid theory in more detail. So, take this as my current view on the topic.

My current understanding is that Fermi-Liquid theory uses concepts from two two distinct theories. Mixing up these concepts leads to inconsistencies. One of the theories is reduced-density-matrix-functional theory (rDMFT), which is closely related to Density-Functional Theory (DFT). The other is based on many-particle Green's functions. The former provides information about energetics and thermodynamics, while the latter provides information on spectral properties and dynamics, respectively transport.

The effective Hamiltonian h_{eff} describes an auxiliary non-interacting fermion system, which only has the one-particle-reduced density matrix in common with the interacting-electron system. This auxiliary non-interacting system is analogous the Kohn-Sham system in Density-Functional Theory. The difference between the Kohn-Sham Green's function and that of the physical interacting system is discussed in section 13.2.1 on p. 400.

This problem of Fermi-Liquid theory using concepts from distint theories is analogous to the difference between the excitation spectra of the non-interacting Kohn-Sham system in **density-functional theory** from that of the interacting electrons. This difference is why density-functional theory is limited to ground states, respectively equilibrium ensembles. The very same problem can already been seen on the level in the **thermal Hartree-Fock theory**, which has a similar discrepancy between the Fock operator Eq. 2.77 and the excitation spectra Eq. 2.100.

[4] Landau[111] says *"as we gradually turn on the interaction,..., classification of the levels remains invariant"*

Landau links the energy levels from the effective Hamiltonian to scattering and excitation levels, which is invalid for this type of definition. In his later papers[113], Landau makes contact to a microscopic description based on Green's functions. My current (certainly not final) view is that this later work relies on a comparison of excited state properties, which is not justified for a density-matrix functional theory.

In his first paper on Fermi-liquid theory[111], Landau proceeds to show that the specific heat grows linearly with temperature, Eqs. Landau-4 and Landau-5. Furthermore he links the speed of sound (Eq. Landau-18) to the Landau parameters and investigates the magnetic susceptibility Eq. Landau 27

Remarks on Landau's original paper[111] on Fermi-Liquid theory:

- Landau[111]-Eq. 5 seems to be in error.
- I believe, there is a typo in Landau[111]-Eq. 33 and Landau[111]-Eq. 35, where a ϵ is replaced by an s.

17.1.4 Long lifetime of low-energy quasi-particles

The basis of Fermi Liquid theory is the long life-time of quasi-particles. Landau says[111] *"... as is known, the collision probability for a given atom, which is in the diffuse Fermi zone, is proportional not only to the intensity of the interaction, but also to the square of the temperature."* (Landau envisages fermionic ^3He atoms rather than electrons.)

See Abrikosov[7] p. 59. *"In accordance with the phenomenological considerations described in §2, the condition $\gamma \ll (\epsilon(p)-\mu)$ only holds in the neighborhood $\epsilon(p) \sim \mu$. The validity of the assumption that $\gamma \ll (\epsilon(p) - \mu)$ as $\epsilon(p) \to \mu$ has been strictly prooved for numerous concrete examples (see e.g. §§21.22)."*

LONG LIFETIME OF QUASI-PARTICLES IN FERMI LIQUIDS

$$\frac{1}{\tau} \sim (p - p_F)^2 \tag{17.16}$$

Abrikosov, Gorkov, Dzyaloshinski, write on page 17 of their book[7]:
"The probability is best estimated by using the analogy with a Fermi gas. Let us consider the following process: a particle with momentum $\vec{p}_1(|\vec{p}_1| > p_F)$ interacts with a particle inside the Fermi sphere with momentum $\vec{p}_2(|\vec{p}_2| < p_F)$. As a result two particles are obtained, with ,momenta $\vec{p}_3$ and $\vec{p}_4 = \vec{p}_1 + \vec{p}_2 - \vec{p}_3$, where $|\vec{p}_3|, |\vec{p}_4| > p_F$. The particle with momentum $\vec{p}_1$ has thus "decomposed" into particles $\vec{p}_3$ and $\vec{p}_4$ and hole with momentum $\vec{p}_2$. The total probability of such process is proportional to

$$\int_{p_2<p_F} d^3p_2 \int_{p_3>p_F} d^3p_3 \, \delta(\epsilon_1 + \epsilon_2 - \epsilon_3 - \epsilon_4)\theta(|\vec{p}_1 + \vec{p}_2 - \vec{p}_3| - p_F) \tag{17.17}$$

It is easily seen that, for $|\vec{p}_1| - p_F \ll p_F$, the permissible domains of variation of the moduli of the vectors $\vec{p}_2$ and $\vec{p}_3$ are

$$p_F < |\vec{p}_3| < |\vec{p}_1 + \vec{p}_2| - p_F \qquad \text{and} \qquad 2p_F - |\vec{p}_1| < |\vec{p}_2| < p_F \tag{17.18}$$

The angle between $\vec{p}_1$ and $\vec{p}_2$ can be arbitrary. The angle between $\vec{p}_3$ and $\vec{p}_1 + \vec{p}_2$ is defined from the conservation of energy condition, whilst the integral over this angle makes the δ-function vanish. The remaining integral over $d^3p_2 d^3p_3$ is taken close to $p_2 \approx p_3 \approx p_F$ and gives the factor $(|\vec{p}|_1 - p_F)^2$."

... cont'd

... cont'd

Let me do the estimate in more detail: The energy is approximated by a linear dispersion $\epsilon(\vec{p}) = \epsilon_F + \vec{v}_F(|\vec{p}| - p_F)$. where $\epsilon_F = p_F^2/(2m_e) = \mu$ is the Fermi level, p_F is the Fermi momentum, and $v_F = p_F/m_e$ is the Fermi velocity.

A hole is created with momentum p_2. Because the traveling particle can only loose energy $\epsilon_1 - \mu$, the hole can only be kicked out from a state with energy $\mu - \epsilon_2 < \epsilon_1 - \mu$, that is $\epsilon_2 > 2\mu - \epsilon_1$.

$$\int_{2\mu-\epsilon_1<\epsilon_2<\mu} d^3p_2 \int_{\epsilon_3>\mu} d^3p_3 \underbrace{\int_{\epsilon_4>\mu} d^3p_4}_{\int d^3p_4\ \theta(\epsilon_4-\mu)} \underbrace{\delta(\vec{p}_3+\vec{p}_4-\vec{p}_2-\vec{p}_1)}_{\text{momentum conservation}} \underbrace{\overbrace{\delta\big(v_F(|\vec{p}_3|+|\vec{p}_4|-|\vec{p}_2|-|\vec{p}_1|)\big)}^{\epsilon_3+\epsilon_4-\epsilon_2-\epsilon_1}}_{\text{energy conservation}}$$

$$= \int_{\epsilon_2<\mu} d^3p_2 \int_{\epsilon_3>\mu} d^3p_3 \underbrace{\theta(\underbrace{|\vec{p}_1|+|\vec{p}_2|-|\vec{p}_3|}_{|\vec{p}_4|}-p_F)}_{\text{Heaviside step function}} \delta\big(v_F(|\vec{p}_3|+|\underbrace{\vec{p}_1+\vec{p}_2-\vec{p}_3}_{\vec{p}_4}|-|\vec{p}_2|-|\vec{p}_1|)$$

$$= \int_{2p_F-|\vec{p}_1|}^{p_F} dp_2\ p_2^2 \int_{p_F}^{|\vec{p}_1|+p_2-p_F} dp_3\ p_3^2 \underbrace{\int d\Omega_2 \int d\Omega_3}_{\text{angular integrations}}\ \delta\Big(v_F(|\vec{p}_3|+|\vec{p}_3-\vec{p}_2-\vec{p}_1|-|\vec{p}_2|-|\vec{p}_1|)\Big)$$

$$= \int_{2p_F-|\vec{p}_1|}^{p_F} dp_2\ p_2^2 \int_{p_F}^{|\vec{p}_1|+p_2-p_F} dp_3\ p_3^2$$
$$\times \int d\Omega_2 \int d\Omega_3\ \frac{1}{v_F}\delta\Big(|\vec{p}_3|-|\vec{p}_2|-|\vec{p}_1|+\sqrt{\vec{p}_3^2+\vec{p}_2^2+\vec{p}_1^2-2\vec{p}_2\vec{p}_3-2\vec{p}_1\vec{p}_3+2\vec{p}_1\vec{p}_2}\Big)$$

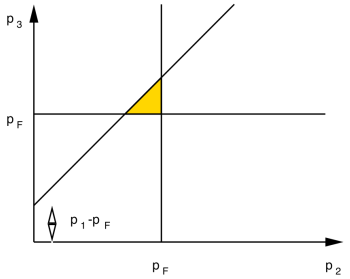
$$\approx \int_{2p_F-|\vec{p}_1|}^{p_F} dp_2\ \overbrace{p_2^2}^{\approx p_F^2} \int_{p_F}^{|\vec{p}_1|+p_2-p_F} dp_3\ \overbrace{p_3^2}^{\approx p_F^2}$$
$$\times \underbrace{\int d\Omega_2 \int d\Omega_3\ \frac{1}{v_F p_F}\delta\left(-1+\sqrt{3-2\frac{\vec{p}_2\vec{p}_3}{|\vec{p}_2||\vec{p}_3|}-2\frac{\vec{p}_1\vec{p}_3}{|\vec{p}_1||\vec{p}_3|}+2\frac{\vec{p}_1\vec{p}_2}{|\vec{p}_1||\vec{p}_2|}}\right)}_{=:\ C/(v_F p_F)\text{ independent of radial integrals. Use } |p_j|\approx p_F.}$$

$$= C\frac{p_F^3}{v_F}\int_{2p_F-|\vec{p}_1|}^{p_F} dp_2\ \Big(|\vec{p}_1|-p_F+p_2-p_F\Big) \overset{x=p_2-p_F}{=} C\frac{p_F^3}{v_F}\int_{p_F-|\vec{p}_1|}^{0} dx\ \Big(|\vec{p}_1|-p_F+x\Big)$$

$$= C\frac{p_F^3}{v_F}\left[(|\vec{p}_1|-p_F)x+\frac{1}{2}x^2\right]_{p_F-|\vec{p}_1|}^{0} = C\frac{p_F^3}{v_F}\left[(|\vec{p}_1|-p_F)^2-\frac{1}{2}(|\vec{p}_1|-p_F)^2\right] = C\frac{p_F^3}{2v_F}(|\vec{p}_1|-p_F)^2$$

$$\sim (|\vec{p}_1|-p_F)^2 \tag{17.19}$$

In the approximation, the lengths of all three vectors integrations are replaced by the Fermi momentum. The integration area for the radial integrations is indicated by the golden triangle in the image below.



Editor: For an accurate calculation of the spectral function of the free electron gas see Takada[115]. See his figure 5 for a k-resolved spectral function. See his Fig 10 for the Momentum distribution. See his Fig.14 or the dynamical structure factor $S(q,\omega)$. Interesting is their new exciton peak at $q = 2k_F$.

17.1.5 Spectral function of Fermi-liquid theory

Editor: This section on the spectral function is under construction!!!

Editor: Migdal's definition of the Green function differs from the one used here by a minus sign. In his Eq.1 of [116], he uses $G(\vec{r},t,\vec{r'},t') = +i\langle \mathcal{T}\hat{\psi}_H(\vec{r},t)\hat{\psi}^\dagger_H(\vec{r'},t')$. while we use in Eq. 7.16 a prefactor $\frac{1}{i\hbar}$ instead of $+i$.

Using the Lehmann representation, the Green's function can be expressed in the form

$$G_{\vec{k}}(\epsilon) \overset{\text{Eq. ??}}{=} \sum_{n,m} P_n \left[\underbrace{\frac{\langle\Phi_n|\hat{c}_{S,\alpha}|\Phi_m\rangle\langle\Phi_m|\hat{c}^\dagger_{S,\beta}|\Phi_n\rangle}{\hbar\omega - (E_m - E_n) + i\eta}}_{\text{electron like}} + \underbrace{\frac{\langle\Phi_n|\hat{c}^\dagger_{S,\beta}|\Phi_m\rangle\langle\Phi_m|\hat{c}_{S,\alpha}|\Phi_n\rangle}{\hbar\omega + (E_m - E_n) - i\eta}}_{\text{hole like}} \right] \tag{17.20}$$

Migdal mentions[116] *"It is easy to see that the quasi-particles have an attenuation proportional to* $(p-p_0)^2$*"*, where $p_0 = \hbar k_F$ is the Fermi momentum. The attenuation is the inverse life time. Editor: It is not clear to me where this comes from.

$$G(p,\epsilon) = \frac{Z}{\epsilon - \bar{\epsilon}_{\vec{k}} + i\Gamma_{\vec{k}}} + f_{\vec{k}}(\epsilon) \tag{17.21}$$

where f is regular at the pole at $\bar{\epsilon}_{\vec{k}} - i\Gamma_{\vec{k}}$. Γ changes sign at the Fermi momentum.

Let me consider the Green's function at a specific k-point $\vec{k}$. In order to describe the electronic structure next to the Fermi surface, let me expand the self energy Σ up to quadratic order in energy and momentum.

$$\Sigma(k,\epsilon) = \Sigma(k,\mu) + (\epsilon-\mu)\,\partial_\epsilon|_\mu \Sigma(k,\epsilon) + \frac{1}{2}(\epsilon-\mu)^2\,\partial^2_\epsilon|_\mu \Sigma(k,\epsilon) + O\Big((\epsilon-\mu)^3\Big) \tag{17.22}$$

The spectral function has the form of a Lorentzian Eq. A.27.

$$A_{\vec{k},\sigma}(\epsilon) = -\frac{1}{\pi}\mathrm{Im}\left[\frac{1}{\epsilon - \bar{\epsilon}(\vec{k}) + i\Gamma(\vec{k})}\right] \tag{17.23}$$

with $\Gamma(\vec{k}) \sim \left(\epsilon - \bar{\epsilon}(\vec{k})\right)^2$ and higher orders. The life time is $\hbar/\Gamma(\vec{k})$.

The resulting momentum distribution for zero temperature is

$$\begin{aligned} n(\vec{k}) &= \int_{-\infty}^{\mu} d\epsilon\, \frac{1}{\pi}\frac{\Gamma(\vec{k})}{(\epsilon - \bar{\epsilon}(\vec{k}))^2 + \Gamma^2(\vec{k})} \\ &= \frac{1}{\pi}\int_{-\infty}^{\mu} \frac{d\epsilon}{\Gamma} \underbrace{\frac{1}{1+\left(\frac{\epsilon-\bar{\epsilon}(\vec{k})}{\Gamma(\vec{k})}\right)^2}}_{\Gamma\partial_\epsilon \mathrm{atan}\left(\frac{\epsilon-\bar{\epsilon}}{\Gamma}\right)} = \frac{1}{\pi}\left[\mathrm{atan}\left(\frac{\epsilon-\bar{\epsilon}}{\Gamma}\right)\right]_{-\infty}^{\mu} \\ &= \frac{1}{2} + \frac{1}{\pi}\mathrm{atan}\left(\frac{\mu-\bar{\epsilon}}{\Gamma}\right) \end{aligned} \tag{17.24}$$

Fermi-liquid theory assumes $\Gamma = K(\bar{\epsilon}-\mu)^2$.

$$n(\vec{k}) = \frac{1}{2} - \frac{1}{\pi}\mathrm{atan}\left(\frac{1}{K(\epsilon-\mu)}\right) \tag{17.25}$$

which implies that $n(k)$ makes an step from one to zero as k crosses the Fermi surface.

The Green's function for the specified k-point is[5]

$$\begin{aligned} G(\epsilon) &= \frac{1}{\epsilon - \bar{\epsilon} - \Sigma(\epsilon)} \\ &= \frac{1}{\epsilon - \bar{\epsilon} - \mathrm{Re}[\Sigma(\epsilon)] - i\mathrm{Im}[\Sigma(\epsilon)]} \\ &= \frac{1}{\epsilon - \bar{\epsilon} - \mathrm{Re}[\Sigma(\epsilon)] - i\mathrm{Im}[\Sigma(\epsilon)]} \end{aligned} \tag{17.26}$$

The spectral function is obtained via Eq. **??** on p. **??**.

$$\begin{aligned} \mathcal{A}(\epsilon) &= \underbrace{\frac{1}{1-2f_{T,\mu}(\epsilon)}}_{\approx \mathrm{sgn}(\epsilon-\mu)} \left(\frac{-1}{2\pi i} \Big[\hat{G}(\epsilon) - \hat{G}^{\mathcal{C},\dagger}(\epsilon) \Big] \right) \\ &= \underbrace{\frac{1}{1-2f_{T,\mu}(\epsilon)}}_{\approx \mathrm{sgn}(\epsilon-\mu)} \left(\frac{-1}{2\pi i} \frac{-2i\mathrm{Im}[\Sigma(\epsilon)]}{\Big(\epsilon - \bar{\epsilon} - \mathrm{Re}[\Sigma(\epsilon)]\Big)^2 + \Big(\mathrm{Im}[\Sigma(\epsilon)]\Big)^2} \right) \\ &= \underbrace{\frac{1}{1-2f_{T,\mu}(\epsilon)}}_{\approx \mathrm{sgn}(\epsilon-\mu)} \left(\frac{1}{2\pi} \frac{2\mathrm{Im}[\Sigma(\epsilon)]}{\Big(\epsilon - \bar{\epsilon} - \mathrm{Re}[\Sigma(\epsilon)]\Big)^2 + \Big(\mathrm{Im}[\Sigma(\epsilon)]\Big)^2} \right) \end{aligned} \tag{17.27}$$

$$\begin{aligned} \hat{G}(\hbar\omega) &\overset{\text{Eq. ??}}{=} \int d\epsilon\, \hat{A}(\epsilon) \left[\frac{1 - f_{T,\mu}(\epsilon)}{\hbar\omega - \epsilon + i\eta} + \frac{f_{T,\mu}(\epsilon)}{\hbar\omega - \epsilon - i\eta} \right] \\ &= \int d\epsilon\, \hat{A}(\epsilon) \frac{\Big(1 - f_{T,\mu}(\epsilon)\Big)\Big(\hbar\omega - \epsilon - i\eta\Big) + f_{T,\mu}(\epsilon)\Big(\hbar\omega - \epsilon + i\eta\Big)}{(\hbar\omega - \epsilon)^2 + \eta^2} \\ &= \int d\epsilon\, \hat{A}(\epsilon) \frac{\Big(\hbar\omega - \epsilon\Big) - i\eta(1 - 2f_{T,\mu}(\epsilon))}{(\hbar\omega - \epsilon)^2 + \eta^2} \\ &= \int d\epsilon\, \hat{A}(\epsilon) \frac{\pi\delta(\hbar\omega - \epsilon)}{\eta} \Big(\Big(\hbar\omega - \epsilon\Big) - i\eta(1 - 2f_{T,\mu}(\epsilon)) \Big) \\ &= -i\pi \hat{A}(\hbar\omega) \Big(1 - 2f_{T,\mu}(\hbar\omega)\Big) \\ &= \frac{1}{\hbar\omega\hat{1} - \hat{h} - \hat{\Sigma}(\hbar\omega)} \end{aligned} \tag{17.28}$$

Furthermore, following the assumptions of Fermi-Liquid theory[6] let me set the imaginary part of the self energy at the Fermi level and its first derivative to zero, which reflects the infinite life time at the Fermi level

$$\mathrm{Im}\Big[\Sigma(k,\mu)\Big] = 0 \qquad \text{and} \qquad \partial_\epsilon\big|_\mu \,\mathrm{Im}[\Sigma(k,\epsilon)] = 0 \tag{17.29}$$

For the sake of simplicity, we ignore the second order of the Taylor expansion of the real part of the self energy,

$$\partial_\epsilon^2\big|_\mu \,\mathrm{Re}[\Sigma(k,\epsilon) = 0 \tag{17.30}$$

[5] The argument $\vec{k}$ is suppressed to avoid cluttering the equations.

[6] This assumption is not necessarily justified. When it is not, the system is, per definition, not a Fermi liquid.

while the second order of the imaginary part is maintained.

The Green's function for the specified k-point is[7]

$$
\begin{aligned}
G(\epsilon) &= \frac{1}{\epsilon - \bar{\epsilon} - \Sigma(\epsilon)} \\
&\approx \left[\overbrace{\epsilon - \mu - (\bar{\epsilon} - \mu)}^{\epsilon - \bar{\epsilon}} \overbrace{- \Sigma(\mu) - (\epsilon - \mu) \left.\frac{\partial \Sigma}{\partial \epsilon}\right|_\mu - \frac{1}{2}(\epsilon - \mu)^2 \left.\partial_\epsilon^2\right|_\mu \Sigma(k, \epsilon)}^{\approx -\Sigma(\epsilon)} \right]^{-1} \\
&\approx \left[\overbrace{\epsilon - \mu - (\bar{\epsilon} - \mu)}^{\epsilon - \bar{\epsilon}} \overbrace{- \Sigma(\mu) - (\epsilon - \mu) \left.\frac{\partial \mathrm{Re}[\Sigma]}{\partial \epsilon}\right|_\mu - i\frac{1}{2}(\epsilon - \mu)^2 \left.\frac{\partial^2 \mathrm{Im}[\Sigma]}{\partial \epsilon}\right|_\mu}^{\approx -\Sigma(\epsilon)} \right]^{-1} \\
&= \left[\left(1 - \left.\frac{\partial \mathrm{Re}[\Sigma]}{\partial \epsilon}\right|_\mu\right)(\epsilon - \mu) - \left(\bar{\epsilon} + \mathrm{Re}[\Sigma(\mu)] - \mu\right) - \frac{i}{2} \left.\frac{\partial^2 \mathrm{Im}\Sigma}{\partial \epsilon^2}\right|_\mu (\epsilon - \mu)^2 \right]^{-1} \\
&= \underbrace{\left(1 - \frac{\partial \mathrm{Re}[\Sigma]}{\partial \epsilon}\right)^{-1}}_{=:Z} \left[\epsilon - \mu - Z \cdot \left(\bar{\epsilon} + \mathrm{Re}[\Sigma(\mu)] - \mu\right) - i \left(\frac{1}{2} Z \left.\frac{\partial^2 \mathrm{Im}\Sigma}{\partial \epsilon^2}\right|_\mu (\epsilon - \mu)^2 \right) \right]^{-1} \\
&= Z \cdot \frac{\left[\epsilon - Z \cdot \left(\bar{\epsilon} + \mathrm{Re}[\Sigma(\mu)] - \mu\right] + i \left[\frac{1}{2} Z \left.\frac{\partial^2 \mathrm{Im}\Sigma}{\partial \epsilon^2}\right|_\mu (\epsilon - \mu)^2 \right]}{\left[\epsilon - \mu - Z \cdot \left(\bar{\epsilon} + \mathrm{Re}[\Sigma(\mu)] - \mu\right) \right]^2 + \left[\frac{1}{2} Z \left.\frac{\partial^2 \mathrm{Im}\Sigma}{\partial \epsilon^2}\right|_\mu (\epsilon - \mu)^2 \right]^2}
\end{aligned}
\tag{17.31}
$$

We introduced the so-called **quasi-particle weight**

$$
Z(\vec{k}) \stackrel{\mathrm{def}}{=} \left(1 - \left.\frac{\partial \mathrm{Re}[\Sigma(\vec{k}, \epsilon)]}{\partial \epsilon}\right|_\mu\right)^{-1} \tag{17.32}
$$

The Green's function exhibits a pole with a weight proportional to the quasi-particle weight.

The spectral function is obtained via Eq. **??** on p. **??**.

$$
\begin{aligned}
\mathcal{A}(\epsilon) &= \underbrace{\frac{1}{1 - 2 f_{T,\mu}(\epsilon)}}_{\approx \mathrm{sgn}(\epsilon - \mu)} \left(\frac{-1}{2\pi i} \left[\hat{G}(\epsilon) - \hat{G}^{\mathcal{C},\dagger}(\epsilon) \right] \right) \\
&= \frac{-Z}{2\pi} \frac{Z \left.\frac{\partial^2 \mathrm{Im}[\Sigma]}{\partial \epsilon^2}\right|_\mu \mathrm{sgn}(\epsilon - \mu)(\epsilon - \mu)^2}{\left[\epsilon - \mu - Z \cdot \left(\bar{\epsilon} + \mathrm{Re}[\Sigma(\mu)] - \mu\right) \right]^2 + \left(\frac{1}{2} Z \left.\frac{\partial^2 \mathrm{Im}[\Sigma]}{\partial \epsilon^2}\right|_\mu (\epsilon - \mu)^2 \right)^2} + \mathcal{A}^{\mathrm{incoh}}(\epsilon)
\end{aligned}
\tag{17.33}
$$

Editor: This cannot be correct because the spectral function must be positive.

The incoherent contribution $\mathcal{A}^{\mathrm{incoh}}$ will be discussed later.

The spectral function is a Lorentzian with weight Z positioned at the quasi-particle energy

$$
\bar{\epsilon}^* = \mu + Z \cdot \left(\bar{\epsilon} + \mathrm{Re}[\Sigma(\mu)] - \mu\right) \tag{17.34}
$$

and with a **life-time broadening**

$$
\Gamma = (\epsilon - \mu) Z \left.\frac{\partial \mathrm{Im}[\Sigma]}{\partial \epsilon}\right|_\mu . \tag{17.35}
$$

[7] The argument $\vec{k}$ is suppressed to avoid cluttering the equations.

A schematic graph of the k-dependent spectral function is shown in figure 3 of [49].

17.1.6 Some background material on Fermi liquid theory

Editor: Read footnote on p.17 of Abrikosov[7].

Editor: Read section 4.5.2 on p.85 of Gianmarchi[?].

Editor: Look up the section on Fermi-Liquid theory in *"Many-body quantum theory in condensed Matter physics"* by Henrik Bruus and Karsten Flensberg, (Oxford University Press ,2004) https://emineter.files.wordpress.com/2018/10/oxford-graduate-texts-henrik-bruus-kar pdf

Giamarchi on Fermi Liquids[117]

Editor: See Lundqvist[84] for the k-dependent spectral function of the free-electron gas in the random-phase approximation.

Editor: See Potorochin et al. Arxiv2112.00422 for a measurement of the quasiparticle spectrum of sodium

Editor: See if particles in a box with a hard-core repulsion can be solved exactly. This may be useful to demonstrate some fundamental properties such as the distinction of plane waves and quasi-particles. (Check if Galitskii has done the same[118]

Editor: for the connection of life time and position of Green function poles, as well as the relation to the kinetic equation, see Galitskii[74]

Editor: Reference to Nozieres and Pines[104]. Plasmons

17.1.7 A brief outlook to Fermi-Liquid theory

Landau and Peierls have introduced the so-called Fermi-liquid theory.[119]

For a (weakly) interacting system, the delta-peaks of the spectral functions broaden

$$\hat{\mathcal{A}}(\hbar\omega) = \sum_{\sigma\in\{\uparrow,\downarrow\}} \frac{1}{V}\int d^3k\, |\varphi_{k,\sigma}\rangle \frac{Z(\vec{k},\sigma)\cdot\Gamma(\vec{k},\sigma)}{\left(\epsilon-\bar{\epsilon}^*(\vec{k},\sigma)\right)^2+\Gamma^2(\vec{k},\sigma)}\langle\varphi_{\vec{k},\sigma}| + \mathcal{A}^{\text{incoh}}(\vec{k},\epsilon) \tag{17.36}$$

where Z is the **quasi-particle weight**, $\epsilon^*(\vec{k}),\sigma)$ is ther **quasi-particle energy** and Γ is the **life-time broadening**. $\mathcal{A}^{\text{incoh}}$ is "the rest". These meaning of these terms will be given below.

The width of the peaks corresponds to the life time of an electron in a particular state. The life time becomes finite, because electrons scatter at other electrons, phonons, plasmons etc. The term life time is chosen because scattering is described as a destruction of the electron and creation and the simultaneous creation of an electron with a different momentum or spin.

One of the central messages of Fermi-liquid theory is that the life time due to electron-electron scattering becomes very large near the Fermi surface. The reason is that the number of states available for scattering, i.e. those that conserve the total energy, total momentum and total spin of the scattering electrons become very small, if both particles are close to the Fermi surface.

A second effect is that the slope of $\epsilon_{\vec{k},\sigma}$ at the Fermi level changes (increases?[119]).

Long quasiparticle life time at the Fermi level

Editor: I am following section 4.5.2 on p.85 of Gianmarchi[?].

One of the defining properties of the Fermi-Liquid is that the life time $\tau(\vec{k})$ of the quasiparticles goes to infinity at the Fermi level like

$$\tau(\vec{k}) \sim (\epsilon(\vec{k})-\mu)^{-2}\,. \tag{17.37}$$

How can we understand that the life time at the Fermi level remains infinite in the presence of an interaction?

Consider a degenerate Fermi gas of electrons in the ground state having a Fermi level μ. To simplify the argument, let us ignore the interaction of the electrons in the Fermi sea.

Consider now an additional electron with energy ϵ_1 and momentum $\vec{p}_1$ in contact with this Fermi sea. Because the electron can only be placed into an empty orbital, its energy must lie above the Fermi level, i.e. $\epsilon_1 > \mu$.

The additional electron may interact with the Fermi sea and excite it from the ground state. While the electron creates an excitation in the Fermi sea with energy $\hbar\omega$ and momentum $\hbar\vec{q}$, it looses that amount of energy and momentum. The excitations of the Fermi sea are electron-hole pairs. That is, an electron in an occupied orbital is lifted into a formerly unoccupied orbital, thus leaving a hole below the Fermi level and an additional conduction electron above.

The number of excitations can be estimated, disregarding momenta and matrix elements, from the joint density of electrons and holes, which would form an electron-hole pair with an energy below $\hbar\omega < \epsilon_1 - \mu$

$$\int_0^{\epsilon_1} d(\hbar\omega) \int_\mu^{\mu+\hbar\omega} d\epsilon\; D(\epsilon)D(\epsilon-\hbar\omega) \approx D^2(\epsilon_F) \int_0^{\epsilon_1} d(\hbar\omega)\; \hbar\omega = D^2(\epsilon_F)\frac{1}{2}(\epsilon_1-\mu)^2 \quad (17.38)$$

When we identify the number of possible scattering events with the life time we arrive at the desired relation

$$\tau(\vec{k}) \sim (\epsilon(\vec{k}) - \mu)^{-2} \; . \quad (17.39)$$

Editor: It may be interesting to include the momentum conservation as well for a free-electron gas. This argument needs to be completed. Let the scattering electron have momentum $\vec{p}$. Its energy is $\epsilon = \frac{1}{2m_e}\vec{p}^2 > \mu$. Because the Fermi sea is in its ground state, the electron can only loose energy to it, but not gain energy The Pauli principle prohibits that the scattered electron ends up in a orbital that is already occupied. Hence:

$$\mu < \frac{1}{2m_e}(\vec{p}-\hbar\vec{q})^2 < \frac{1}{2m_e}\vec{p}^2 \quad (17.40)$$

Similarly the electron-hole pair formed by kicking out an electron with momentum $\vec{p}_h$ satisfies.

$$\frac{1}{2m_e}\vec{p}_h^2 < \mu < \frac{1}{2m_e}(\vec{p}_h+\hbar\vec{q})^2 \quad (17.41)$$

Editor: see also Luttinger 1961[120]

Incoherent contribution: In Eq. 17.33, I have added incoherent contribution $\mathcal{A}^{\text{incoh}}(\epsilon)$ to the self energy, which accounts for all the contributions of the self energy, which have been lost, when we linearized the self energy about the Fermi level. The incoherent part of the spectral function is due to the interaction with other electrons or other quasi-particles such as plasmons, phonons etc.

In order to understand this effect, consider again the asymmetric dimer-molecule. With a hybridization two orbitals repel each other. Both orbitals obtain some admixture from the other orbital. One orbital describes an electron, which may be in a plane wave state. The other orbital describes another quasi-particle, such as a plasmon, electron or phonon.

The level repulsion is responsible for the quasi-particle shift $\text{Re}[\Sigma]$. The quasi-particle weight Z is smaller than unity, because the electron has some weight from the other quasi-particles. Because this state is still normalized, the electron weight in this state is reduced. This weight is not completely lost, but it is transferred to the energy of the second eigenstate, which has the character of the other

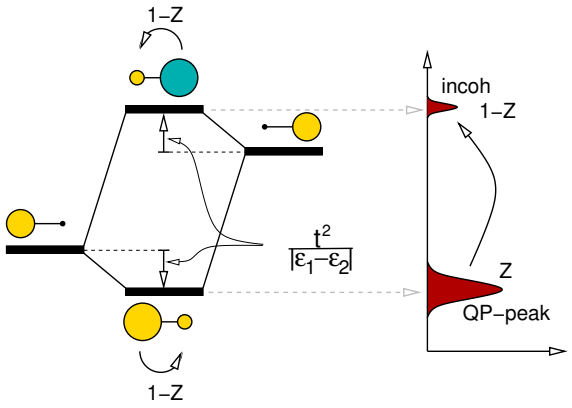


Fig. 17.1: Demonstration of the incoherent contribution of the spectral function on the example of a dimeric molecule. The left orbital represents the particle under investigation, while the right orbital describes another excitation of the Fermi gas. The graph on the right-hand side describes the spectral function projected onto the "left" orbital. It has two features, namely a quasi-particle peak and an incoherent contribution. Z is the quasi-particle weight.

quasi-particle. The electron admixture of this state contributes the incoherent part of the spectral function. Once the spectral function is integrated over all energies, each diagonal matrix element integrates up to unity (if that orbital is normalized).

Editor: The argument for the incoherent contribution of the spectral function is the general explanation for life-time broadening of absorption bands and of satellites. It should be placed into the section on spectral functions. Here, I can then only refer to that section.

Editor: The argument here is done on the basis of one-particle levels. It may be better to consider a system with consisting of one one-particle orbital, which may be filled or empty, coupled to a second system (such as a spin excitation) having one excitation energy. Then we can construct all many-particle eigenstates analytically. The spectral function will contain the one-particle level, but also the satellites, which are displaced by the excitation energy of the second system. One can extend this model to systems where the second system has its own, arbitrary spectral function before contact. Another extension is to use Slater determinants with three one-particle orbitals, where the spectral function of the first orbital is probed and the other two orbitals describe formation of an electron-hole pair.

k-dependence: Let me now build in also the k-dependence.

$$\mathcal{A}(k,\epsilon) = Z(k)\underbrace{\frac{(\epsilon-\mu)Z(k)\left.\frac{\partial \mathrm{Im}[\Sigma(k,\epsilon)]}{\partial\epsilon}\right|_\mu}{\left[\epsilon-\mu-Z(k)\Big(\bar{\epsilon}(k)+\mathrm{Re}[\Sigma(k,\mu)]-\mu\Big)\right]^2+\left[(\epsilon-\mu)Z(k)\left.\frac{\partial \mathrm{Im}[\Sigma(k,\epsilon)]}{\partial\epsilon}\right|_\mu\right]^2}}_{\text{Lorentzian}} + \mathcal{A}^{\text{incoh}}(k,\epsilon) \tag{17.42}$$

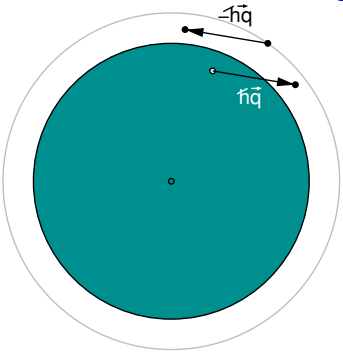
The Fermi velocity of the interacting Fermi liquid

$$v_F^* = \frac{1}{\hbar}\vec{\nabla}_k Z_k \cdot \big(\epsilon(k) + \mathrm{Re}[\Sigma(\vec{k},\mu)] \tag{17.43}$$

In addition to the gradient of the bare band structure $\vec{v} = \frac{1}{\hbar}\vec{\nabla}_k\bar{\epsilon}(\vec{k})$, the Fermi velocity has also a contribution from the self energy $\frac{1}{\hbar}\vec{\nabla}_k Z_k \cdot \mathrm{Re}[\Sigma]$. More important is the contribution $\frac{1}{\hbar}\vec{\nabla}_k(Z_k \cdot \epsilon(k))$

due to the quasi-particle weight. Because the Fermi velocity can be written as $v_F^* = \hbar k_F / m^*$, a reduction of the Fermi-velocity can be described as an increase of the effective mass m^* of the electrons. In other words, the electron gained mass by becoming dressed by other quasi-particles.

Editor: The following figure is not inserted at the correct place yet



Momentum distribution

Migdal has shown[116] that the momentum distribution $n(\vec{k}) = \sum_{\sigma\in\{\uparrow,\downarrow\}} \sum_q P_q \langle \Phi_q | \hat{a}^\dagger_{\vec{k},\sigma} \hat{a}_{\vec{k},\sigma} | \Phi_1 \rangle$. exhibits a finite step at the Fermi momentum for all strengths of the interaction. *"We shall prove that the momentum distribution of the particles in the ground state has a discontinuity at $p = p_0$, for any kind of interaction. This result refers to the distribution of particles and not of quasi-particles."*[116] The size of this step is the so-called **quasi-particle weight** or renormalization constant, as named by Migdal.

The momentum distribution is

$$n(\vec{p}) = \mathrm{Tr}\left[\hat{\rho}\hat{a}^\dagger_{\vec{p},\sigma}\hat{a}_{\vec{p},\sigma}\right] \tag{17.44}$$

where the $\hat{a}^\dagger_{\vec{p},\sigma}$ and $\hat{a}_{\vec{p},\sigma}$ are creation and annihilation operators for momentum eigenstates, that is plane waves. As Migdal emphasises, they are **not** related to quasi particles.

The exercise in section 9.4.5, demonstrates the difference between a momentum distribution from a quasi-particle distribution. It shows that quasi-particle a gapped system can be abrupt, while the momentum distribution exhibits a smooth transition from zero to one.

17.2 Hubbard model

The original Hubbard model was suggested in 1963 independently by Hubbard[18], Kanamori and Gutzwiller[20].

For a review, see Tasaki[121] (Recommendation by Stefanucci and van Leeuwen[2].)

Editor: The Falicov-Kimball model[122] describes a metal-insulator transition as function of temperature. It describes a lattice of localized orbitals, and band electrons, which act on each other with a (charge-charge) Coulomb interaction. Should that be mentioned?

Editor: Spectral functions of the 1d Hubbard model are shown in Pairault et al.[??]

Starting from a general Hamiltonian for interacting electrons formulated in spin orbitals $\alpha = (i, \sigma)$

$$\hat{H} = \sum_{\alpha,\beta} h_{\alpha,\beta} \left(\hat{c}^\dagger_\alpha \hat{c}_\beta + \hat{c}^\dagger_\beta \hat{c}_\alpha \right) + \frac{1}{2} \sum_{\alpha,\beta,\gamma,\delta} W_{\alpha,\beta,\delta,\gamma} \hat{c}^\dagger_\alpha \hat{c}^\dagger_\beta \hat{c}_\gamma \hat{c}_\delta \tag{17.45}$$

the following simplifications are made:

1. Only **onsite interaction** matrix elements are considered. The motivation is that not all electrons are described explicitly. The electrons described implicitly screen the interaction, which results in a short-ranged effective Coulomb interaction between the explicit electrons.
2. Only **nearest-neighbor hopping** matrix elements $h_{\alpha,\beta}$ are considered. A specific notation for nearest-neighbor sums has been introduced: $\sum_{\langle i,j \rangle}$ implies that the double sum includes only nearest-neighbor terms.
3. Only **one spatial orbital** (two spin orbitals) per site is considered. On speaks of a *"one-band Hubbard model"* to distinguish it from generalizations such as a *"two-band Hubbard model"*. This leads to the analogy of a crystal of hydrogen atoms.
4. All atoms are considered to be identical.

The resulting model Hamiltonian of the Hubbard model is

HUBBARD MODEL

$$\begin{aligned} \hat{H} &= \sum_j \sum_{\sigma \in \{\uparrow,\downarrow\}} \bar{\epsilon} \hat{c}^\dagger_{j,\sigma} \hat{c}_{j,\sigma} - \bar{t} \sum_{\langle i,j \rangle} \sum_{\sigma \in \{\uparrow,\downarrow\}} \left(\hat{c}^\dagger_{i,\sigma} \hat{c}_{j,\sigma} + \hat{c}^\dagger_{j,\sigma} \hat{c}_{i,\sigma} \right) + U \sum_j \sum_{\sigma,\sigma' \in \{\uparrow,\downarrow\}} \hat{c}^\dagger_{j,\sigma} \hat{c}^\dagger_{j,\sigma'} \hat{c}_{j,\sigma'} \hat{c}_{j,\sigma} \\ &= \sum_j \sum_{\sigma \in \{\uparrow,\downarrow\}} \bar{\epsilon} \hat{n}_{j,\sigma} - \bar{t} \sum_{\langle i,j \rangle} \sum_{\sigma \in \{\uparrow,\downarrow\}} \left(\hat{c}^\dagger_{i,\sigma} \hat{c}_{j,\sigma} + \hat{c}^\dagger_{j,\sigma} \hat{c}_{i,\sigma} \right) + U \sum_j \hat{n}_{j,\uparrow} \hat{n}_{j,\downarrow} \end{aligned} \tag{17.46}$$

The symbol $\langle i, j \rangle$ restricts the double sum to nearest-neighbor terms. The indices of the spin orbitals have been divided into a site index i and a spin index σ.

$\bar{t}$ is the hopping integral and U is the Coulomb parameter. Wrog[8], the zero of the energy axis is usually set equal to the onsite matrix elements $\bar{\epsilon}$, so that $\bar{\epsilon} = 0$.

17.2.1 Physics of the Hubbard model

The most striking effect described by the Hubbard model is the **metal-insulator transition** for the half-filled system: When the interaction between electrons is strong as in transition metals or rare-earth materials, systems that are expected to be metals become insulating, they become **Mott insulators**. Of interest is not only the existence of insulators, but the way this transition occurs, is truly puzzling.

[8] wrog without restriction of generality

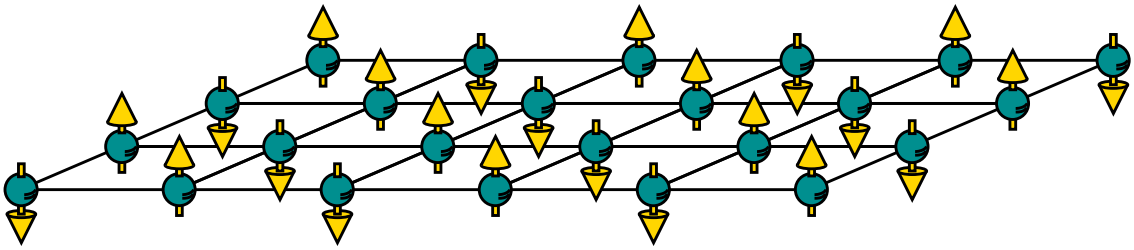


Fig. 17.2: Scheme for a two-dimensional Hubbard model at half filling. Every site has one electron. When an electron is added to this state, it must occupy an already occupied site, which costs a the Coulomb repulsion energy U. Therefore, the one-particle spectrum has a band gap between filled and empty states, explaining the Mott insulator. This band gap also reflect on the two-particle excitations, because the formation of an electron-hole pair requires to overcome the Coulomb repulsion U. Thus, charges are not mobile and the conductivity is low. The low-energy excitations are spin flips, which are described by the Heisenberg model. The figure is oversimplified as it describes the ground state as an Ising antiferromagnet, which neglects quantum fluctuations present in the true ground state.

The origin of the insulating behavior is not all that complicated: Imagine a lattice of atoms with one electron on each atom. In order to form a current, an electron has to be moved to a neighboring atom. This, however, comes at a cost because the Coulomb repulsion by the atom already there must be overcome. Thus, the lowest excitation energies are of order U and finite. In other words the half-filled Hubbard model with interaction is an insulator.

The valence band of this insulator is called the lower Hubbard band and the conduction band of this insulator is the upper Hubbard band. As the transition occurs, a third band emerges right at the Fermi level, the so-called **Abrikosov-Suhl** [123, 124] or **Kondo resonance**.

When choosing the parameters, it is important that the models are not obtained by simply ignoring terms. Rather, the parameters include implicitly a number of other terms of the real system. One of the many ways to arrive at such an effective model is down-folding discussed in Chapter 5.1.

The one-dimensional Hubbard model has been solved exactly by Lieb and Wu[125]. For half-filling the Hubbard model describes a Mott insulator. There is no metal-insulator transition for the half filled Hubbard model in one dimension.[125] The two-dimensional Hubbard model has been investigated with a variety of numerical methods[126].

Editor: On the Mott insulator, see the article by Laughlin https://arxiv.org/pdf/cond-mat/9709195.pdf; See the review by Mott[127].

Editor: Two papers on the true hydrogen chain as opposed to the Hubbard chain provide (1) an overview of many-particle methods[128] and on the physical properties of the hydrogen chain[129].

Editor: Zum Metall-Isolator Übergang: ‘‘In 3d Materialien tritt ein solcher Mott-Übergang auf, wenn Elektron-Loch Paare (Excitonen) dissoziieren, was zu einer dramatischen Abschirmung der langreichweitigen Coulomb-Wechselwirkung führt.’’ Dieter Vollhardt, *‘‘Das reiche Innenleben der Wasserstoffkette’’*, Physik Journal 11, 20, (2020)

17.2.2 Hubbard atom

The minimal model of interacting electrons is the **Hubbard atom**: there are only two spin orbitals.

The Hubbard atom has two orthonormal spin orbitals with index $\sigma \in \{\uparrow, \downarrow\}$. The Hamiltonian of the Hubbard atom has the simple form

$$\hat{H} = \bar{\epsilon}\left(\hat{n}_\uparrow + \hat{n}_\downarrow\right) + U\, \hat{n}_\uparrow \hat{n}_\downarrow \tag{17.47}$$

Interaction

Let me demonstrate here how the special form $\sum_i U\hat{n}_{i\uparrow}\hat{n}_{i,\downarrow}$ for the interaction in the one-band Hubbard model results from the most general form of a local interaction with two orbitals per site.

There are only few non-zero interaction matrix elements, because the product of a spin-up and a spin-down wave function vanishes $\sum_\sigma \chi_\uparrow(\vec{r},\sigma)\chi_\downarrow(\vec{r},\sigma) = 0$.

$$W_{\sigma_1,\sigma_2,\sigma_3,\sigma_4} = \int d^4x \int d^4x' \, \frac{e^2 \chi^*_{\sigma_1}(\vec{x})\chi^*_{\sigma_2}(\vec{x'})\chi_{\sigma_3}(\vec{x})\chi_{\sigma_4}(\vec{x'})}{4\pi\epsilon_0|\vec{r}-\vec{r'}|} = \delta_{\sigma_1,\sigma_3}\delta_{\sigma_2,\sigma_4}U \tag{17.48}$$

Because all the four orbitals have the same spatial dependence, all non-zero matrix elements can be described by a single Coulomb-repulsion parameter U.

The interaction has the form

$$\begin{aligned}\frac{1}{2}\sum_{\sigma,\sigma',\sigma'',\sigma'''} W_{\sigma,\sigma',\sigma''',\sigma''}\hat{c}^\dagger_\sigma \hat{c}^\dagger_{\sigma'}\hat{c}_{\sigma''}\hat{c}_{\sigma'''} &= \frac{1}{2}U\sum_{\sigma,\sigma'}\hat{c}^\dagger_\sigma\hat{c}^\dagger_{\sigma'}\hat{c}_{\sigma'}\hat{c}_\sigma = \frac{1}{2}U\sum_{\sigma,\sigma'}\Big(\hat{c}^\dagger_\sigma\hat{c}_\sigma\hat{c}^\dagger_{\sigma'}\hat{c}_{\sigma'} - \hat{c}^\dagger_\sigma\delta_{\sigma,\sigma'}\hat{c}_{\sigma'}\Big) \\ &= \frac{1}{2}U\sum_{\sigma,\sigma'}\Big(\underbrace{\hat{n}_\sigma\hat{n}_{\sigma'} - \delta_{\sigma,\sigma'}\hat{n}_\sigma}_{=0 \quad \text{for } \sigma=\sigma'}\Big) = U\,\hat{n}_\uparrow\hat{n}_\downarrow\end{aligned} \tag{17.49}$$

The Hamiltonian

In order to probe the Hubbard atom, let me vary the non-interacting Hamiltonian. The most general hermitian Hamiltonian with two orbitals can be obtained by introducing an explicit atomic level $\bar{\epsilon}$ and a magnetic field $\vec{B}$.[9]

The Hamiltonian can be written in the form

$$\hat{H} = \overbrace{\bar{\epsilon}\sum_{\sigma\in\{\uparrow,\downarrow\}}\hat{c}^\dagger_\sigma\hat{c}_\sigma - \gamma\sum_{j\in\{x,y,z\}}B_j\underbrace{\frac{\hbar}{2}\sum_{\sigma,\sigma'\in\{\uparrow,\downarrow\}}\sigma^{(j)}_{\sigma,\sigma'}\hat{c}^\dagger_\sigma\hat{c}_{\sigma'}}_{\hat{S}_j}}^{\hat{h}} + \overbrace{U\,\hat{n}_\uparrow\hat{n}_\downarrow}^{\hat{W}} \tag{17.50}$$

where γ is the gyromagnetic ratio of the electron. $\boldsymbol{\sigma}^{(j)}$ with $j \in \{x,y,z\}$ are the Pauli matrices.

Without restriction of generality, we choose the magnetic field along the z-direction and describe it by the **Zeeman splitting** $\Delta = 2\gamma|B_z|\frac{\hbar}{2}$. The Hamiltonian of the Hubbard atom in a magnetic field in z direction has the form

$$\hat{H} = \bar{\epsilon}(\hat{n}_\uparrow + \hat{n}_\downarrow) + \tfrac{1}{2}\Delta(\hat{n}_\uparrow - \hat{n}_\downarrow) + U\hat{n}_\uparrow\hat{n}_\downarrow \tag{17.51}$$

The parameter $\Delta \stackrel{\text{def}}{=} \epsilon_\uparrow - \epsilon_\downarrow$ is the **Zeeman splitting** of the energy levels.[10] The Coulomb repulsion of the two electrons is U. The occupation-number operator is $\hat{n}_\sigma = \hat{c}^\dagger_\sigma\hat{c}_\sigma$.

Many-particle states and energies

The Hubbard atom with the Hamiltonian Eq. 17.51 has only four many-particle states, which are listed in table 17.2.

Let me first investigate the dominating many-particle state depending on the position in the $\Delta-$ versus $-\mu$ phase diagram. For this purpose, I determine the state with maximum probability

$$P_j = \frac{1}{Z_{T,\mu}}\mathrm{e}^{-\beta(E_j-\mu N_j)} \tag{17.52}$$

[9] A hermitian (2×2) Hamiltonian has four degrees of freedom. A general hermitian (2×2) can be expressed as a superposition of the unit matrix and the three Pauli matrices. As a physical analogy, we describe their prefactors in terms of an electrostatic potential $\bar{\epsilon}$ and magnetic field $\vec{B}$.

[10] The Zeeman splitting is the splitting of two otherwise degenerate orbitals in a magnetic field.

many-p. state		energy
$\|\mathcal{O}\rangle$	$\|0\rangle$	0
$\hat{c}_\uparrow^\dagger\|\mathcal{O}\rangle$	$\|\uparrow\rangle$	$\bar{\epsilon}+\frac{1}{2}\Delta$
$\hat{c}_\downarrow^\dagger\|\mathcal{O}\rangle$	$\|\downarrow\rangle$	$\bar{\epsilon}-\frac{1}{2}\Delta$
$\hat{c}_\uparrow^\dagger\hat{c}_\downarrow^\dagger\|\mathcal{O}\rangle$	$\|\uparrow\downarrow\rangle$	$2\bar{\epsilon}+U$

Table 17.2: Many-particle states and energies of the Hubbard atom. Δ is the Zeeman splitting and U is the Coulomb parameter.

as function of the chemical potential μ and the Zeeman splitting Δ. The phase diagram as function of Zeeman splitting Δ and chemical potential μ is shown in figure 17.3. The regions indicated by different colors are characterized by a common ground state. For very low chemical potentials, the ground state is the vacuum or zero-particle state $|0\rangle$. For very large chemical potentials the two-particle state is filled.

In the absence of the magnetic field, i.e. $\Delta = 0$, the zero-particle state and the two-particle states are separated by a region, where the one-particle states are stable: It costs more energy to add the second electron compared to the first, because the two electrons repel each other. This region, however, shrinks to zero in the absence of an electron interaction.

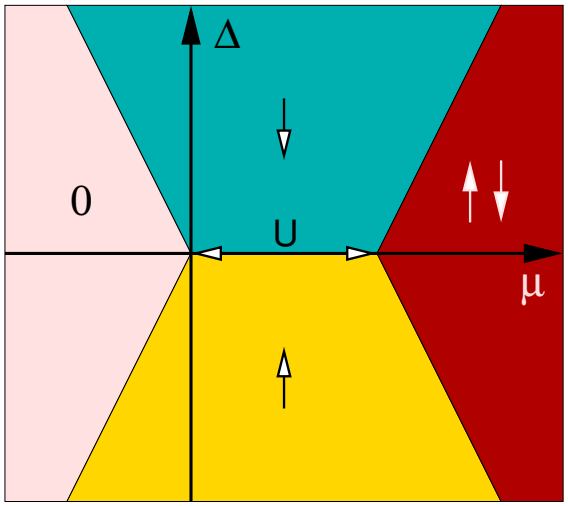


Fig. 17.3: Zero-temperature phase diagram of the Hubbard atom as function of chemical potential μ and magnetic field expressed as Zeeman splitting Δ.

Spectral function:

The spectral function is obtained from the definition Eq. **??** on p. **??**.

$$\mathcal{A}_{\alpha,\beta}(\epsilon) \overset{\text{Eq. ??}}{=} \sum_{m,n} (P_m + P_n)\, \langle\Phi_n|\hat{c}_\alpha|\Phi_m\rangle\langle\Phi_m|\hat{c}_\beta^\dagger|\Phi_n\rangle\, \delta\Big(\epsilon - (E_m - E_n)\Big) \tag{17.53}$$

In our case, the spectral function is diagonal and has the form

$$\begin{aligned}
\mathcal{A}_{\uparrow\uparrow}(\epsilon) &= \big(P_{|0\rangle} + P_{|\uparrow\rangle}\big) \underbrace{\langle 0|\hat{c}_\uparrow|\uparrow\rangle\langle\uparrow|\hat{c}_\uparrow^\dagger|0\rangle}_{=1} \delta\big(\epsilon - (E_{|\uparrow\rangle} - E_{|0\rangle}\big) \\
&\quad + \big(P_{|\downarrow\rangle} + P_{|\uparrow\downarrow\rangle}\big) \underbrace{\langle\downarrow|\hat{c}_\uparrow|\uparrow\downarrow\rangle\langle\uparrow\downarrow|\hat{c}_\uparrow^\dagger|\downarrow\rangle}_{=1} \delta\big(\epsilon - (E_{|\uparrow\downarrow\rangle} - E_{|\downarrow\rangle})\big) \\
&= \underbrace{\Big(P_{|0\rangle} + P_{|\uparrow\rangle}\Big)}_{\underbrace{P_{|0\rangle} + P_{|\uparrow\rangle} + P_{|\downarrow\rangle} + P_{|\uparrow\downarrow\rangle}}_{=1} - \underbrace{(P_{|\downarrow\rangle} + P_{|\uparrow\downarrow\rangle})}_{=f_\downarrow}} \delta\Big(\epsilon - \Big(\bar{\epsilon} + \frac{\Delta}{2}\Big)\Big) + \underbrace{\Big(P_{|\downarrow\rangle} + P_{|\uparrow\downarrow\rangle}\Big)}_{f_\downarrow} \delta\Big(\epsilon - \Big(\bar{\epsilon} + \frac{\Delta}{2} + U\Big)\Big) \\
&= \Big(1 - f_\downarrow\Big)\delta\big(\epsilon - \epsilon_\uparrow\big) + f_\downarrow \delta\big(\epsilon - (\epsilon_\uparrow + U)\big) \qquad (17.54) \\
\mathcal{A}_{\downarrow\downarrow}(\epsilon) &= \Big(1 - f_\uparrow\Big)\delta\big(\epsilon - \epsilon_\downarrow\big) + f_\uparrow \delta\big(\epsilon - (\epsilon_\downarrow + U)\big) \qquad (17.55)
\end{aligned}$$

Here, $f_\downarrow \overset{\text{Eq. } L.107}{=} P_{|\downarrow\rangle} + P_{|\uparrow,\downarrow\rangle}$ is the occupation of the $|\downarrow\rangle$ orbital, and $f_\uparrow \overset{\text{Eq. } L.107}{=} P_{|\uparrow\rangle} + P_{|\uparrow,\downarrow\rangle}$ is the occupation of the $|\uparrow\rangle$ orbital.

The spectral function of the Hubbard atom is shown in figure 17.4.

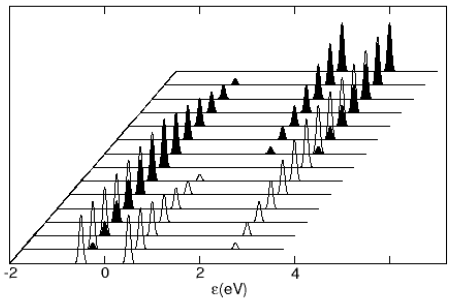


Fig. 17.4: Spectral function $\mathcal{A}(\epsilon) = \mathcal{A}_{\uparrow,\uparrow}(\epsilon) + \mathcal{A}_{\downarrow,\downarrow}(\epsilon)$, Eqs. 17.55, 17.55, of the Hubbard atom with $\bar{\epsilon} = 0$ in a magnetic field with Zeeman splitting $\Delta = 1$ and a Coulomb repulsion $U = 2$ for different numbers of electrons. The energy is shown on the horizontal axis, the spectral density is shown along the vertical axis and the number of electrons is shown by the third axis pointing into the paper (i.e. the graphs are shifted to the right and up to simulate a depth in the graph). The spectral functions are smeared out to Gaussians and displaced along the energy axis for better visibility. The filled area indicates the occupation of the states. That is, the filled area is the hole spectral function Eq. **??** and the white area is the electron spectral function Eq. **??**.

1. The first graph in the front of figure 17.4 exhibits two peaks, one at $\epsilon = \bar{\epsilon} - \frac{1}{2}\Delta$ and another one at $\epsilon = \bar{\epsilon} + \frac{1}{2}\Delta$. These are the atomic levels, which are split by the magnetic field into two Zeeman levels. Shown is the electron spectral function, which describes the electron-addition energies: electrons can be added to the lower and to the upper Zeeman level. The hole spectral function, describing electron-removal energies, vanishes, because there are no electrons to be removed.

2. As the electron number is raised, part of the lowest peak at $\bar{\epsilon} - \frac{1}{2}\Delta$ is painted black, indicating partial filling of this energy level with electrons. The filled part of the spectral function is the hole spectral function Eq. 9.29, i.e. the contribution for electron removal. The unpainted area of the spectral function is the electron spectral function Eq. 9.28.

For a grand canonical ensemble, the hole spectral function Eq. **??** is obtained from the total spectral function by multiplication with the Fermi distribution function. The electron spectral function is obtained by multiplication, Eq. **??**, with $1 - f_{T,\mu}(\epsilon)$.

From the observation that the lowest state is partially occupied at zero temperature, we can deduce that the Fermi level is pinned in the lowest band until there are one or more electrons on the Hubbard atom. At half filling, the Fermi level jumps from the lowest level $\mu = \bar{\epsilon} - \frac{1}{2}\Delta$ into the highest energy level at $\mu = \bar{\epsilon} + \frac{1}{2}\Delta + U$.

3. When the electron number is increased from zero, an additional level occurs at $\bar{\epsilon} + \frac{1}{2}\Delta + U$. This is the so-called upper Hubbard band, which is related to the empty orbital at $\bar{\epsilon} + \frac{1}{2}\Delta$. The weight of the upper Hubbard weight grows with increasing occupation of the lowest level. It describes the electron addition to a hydrogen atom, which already has one electron. If the lowest level holds a spin-up electron, the additional electron must be a spin-down electron. Due to the unfavorable spin-direction its addition has to overcome firstly the Zeeman splitting and secondly the Coulomb repulsion to the electron already present on the atom.

4. As the upper Hubbard band gains weight with increasing number of electrons, the lower Hubbard band at $\bar{\epsilon}+\frac{1}{2}\Delta$ looses weight. Mathematically, this reflects the sum rule $\int d\epsilon\, \mathcal{A}_{\downarrow,\downarrow}(\epsilon) = 1$ (see[11] Eq. 5.86 on p. 206). Physically, the spectral function is the superposition of the spectrum of two many-particle states, namely the vacuum state $|\mathcal{O}\rangle$ and the favorable one-particle state $|\uparrow\rangle$. As the electron number is increased, the probability $P_{|\mathcal{O}\rangle}$ of the vacuum state decreases and that, $P_{|\uparrow\rangle}$, of the one-particle state grows. At least in this case, the spectral function can be rationalized as an ensemble of spectral functions. In the case $0 < N < 1$, this implies $\mathcal{A}_N(\epsilon) = P_{|\mathcal{O}\rangle}\mathcal{A}^{(|\mathcal{O}\rangle)}(\epsilon) + P_{|\uparrow\rangle}\mathcal{A}^{(|\uparrow\rangle)}(\epsilon)$, where $N = P_{|\mathcal{O}\rangle}0 + P_{|\uparrow\rangle}1$.

   We make the striking observation, that the energy levels do not change with particle number, but their weights do.

5. When the Fermi level is pinned in one of the states, i.e. for $0 < N < 1$ at $\mu = \bar{\epsilon} - \frac{1}{2}\Delta$ and for $1 < N < 2$ at $\mu = \bar{\epsilon} + \frac{1}{2}\Delta + U$, the system is metallic in the sense of having no finite band gap between empty and filled states. Right at half filling however, the system is insulating with a band gap of $E_g = 2\Delta + U$. This is the so called **Mott-Hubbard gap** , It is one of the most puzzling phenomena for interaction electrons.

   A similar feature is also present in the extended Hubbard model. It leads to a so-called **metal-insulator transition** as the interaction is increased. This transition seems to contradict the notions of conventional band structures obtained from mean-field theory.

   This phenomenon is present in real materials such as some transition metal oxides with partially filled shells of d-electrons: Having a partially filled d shell one would expect them to be metallic. Experimentally, however they turn out as insulators. The d-states of transition metal atoms have a large Coulomb repulsion, which splits the d-states into an upper and a lower Hubbard band, which are separated by a band gap. The underlying physics is analogous to that observed in the Hubbard atom.

Mean-field energy and mean-field spectrum

In the mean-field approximation the energy was expressed in terms of the one-particle-reduced density matrix

$$\rho^{(1)}_{\sigma,\sigma'} = \sum_q P_q \langle \Psi_q | \hat{c}^\dagger_\sigma \hat{c}_{\sigma'} | \Psi_q \rangle \tag{17.56}$$

[11] The special form of the sum rule requires an orthonormal basis set, which is quietly assumed

The energy in the mean-field approximation is Eq. 2.66[12]

$$
\begin{aligned}
E^{mf}[\boldsymbol{\rho}^{(1)}] &\overset{\text{Eq. 2.66}}{=} \underbrace{\mathrm{Tr}\Big[\boldsymbol{\rho}^{(1)}\boldsymbol{h}\Big]}_{E_{1P}} + \underbrace{\frac{1}{2}\int d^3r \int d^3r' \, \frac{e^2 n(\vec{r}) n(\vec{r'})}{4\pi\epsilon_0|\vec{r}-\vec{r'}|}}_{E_H} \underbrace{-\frac{1}{2}\int d^4x \int d^4x' \, \frac{e^2 \rho^{(1)}(\vec{x},\vec{x'})\rho^{(1)}(\vec{x'},\vec{x})}{4\pi\epsilon_0|\vec{r}-\vec{r'}|}}_{E_X} \\
&= \sum_{\alpha,\beta} h_{\alpha,\beta}\rho^{(1)}_{\beta,\alpha} + \underbrace{\frac{1}{2}\sum_{\alpha,\beta,\gamma,\delta} W_{\alpha,\beta,\gamma,\delta}\rho^{(1)}_{\gamma,\alpha}\rho^{(1)}_{\delta,\beta}}_{\text{Hartree}} \underbrace{-\frac{1}{2}\sum_{\alpha,\beta,\gamma,\delta} W_{\alpha,\beta,\gamma,\delta}\rho^{(1)}_{\delta,\alpha}\rho^{(1)}_{\gamma,\beta}}_{\text{Exchange}} \\
&= \bar{\epsilon}\Big(n_\uparrow + n_\downarrow\Big) - \frac{\Delta}{2}\Big(n_\uparrow - n_\downarrow\Big) + \underbrace{\frac{1}{2}U\sum_{\sigma,\sigma'}\rho^{(1)}_{\sigma,\sigma}\rho^{(1)}_{\sigma',\sigma'}}_{\text{Hartree}} \underbrace{-\frac{1}{2}U\sum_{\sigma,\sigma'}\rho^{(1)}_{\sigma,\sigma'}\rho^{(1)}_{\sigma',\sigma}}_{\text{exchange}} \\
&\qquad \underbrace{\tfrac{1}{2}U\Big(\rho^{(1)}_{\uparrow,\uparrow}+\rho^{(1)}_{\downarrow,\downarrow}\Big)^2}_{} \quad \underbrace{-\tfrac{1}{2}U\Big[\Big(\rho^{(1)}_{\uparrow,\uparrow}\Big)^2+\Big(\rho^{(1)}_{\downarrow,\downarrow}\Big)^2+2\rho^{(1)}_{\uparrow,\downarrow}\rho^{(1)}_{\downarrow,\uparrow}\Big]}_{} \\
&= \bar{\epsilon}\Big(n_\uparrow + n_\downarrow\Big) - \frac{\Delta}{2}\Big(n_\uparrow - n_\downarrow\Big) + Un_\uparrow n_\downarrow - U\rho^{(1)}_{\uparrow,\downarrow}\rho^{(1)}_{\downarrow,\uparrow} \qquad (17.57)
\end{aligned}
$$

where $n_\sigma \overset{\text{def}}{=} \rho^{(1)}_{\sigma,\sigma}$

The energy expression looks very much like the Hamiltonian Eq. 17.51.

- One difference is in the last term $-U\rho^{(1)}_{\uparrow,\downarrow}\rho^{(1)}_{\downarrow,\uparrow}$, which describes deviations of the spin-direction from the z-axis. This term ensures that the interaction term of the mean-field energy is invariant under spin rotations.[13]
- The other, more important difference is that the interaction term is expressed by the product of two density matrices $\langle\hat{n}_\uparrow\rangle\langle\hat{n}_\downarrow\rangle$ rather than a product of to operators $\langle\hat{n}_\uparrow\hat{n}_\downarrow\rangle$. The difference is proportional to the **occupation-number fluctuations**.

$$
\langle\hat{n}_\uparrow\hat{n}_\downarrow\rangle - \langle\hat{n}_\uparrow\rangle\langle\hat{n}_\downarrow\rangle = \Big\langle\Big(\hat{n}_\uparrow - \langle\hat{n}_\uparrow\rangle\Big)\Big(\hat{n}_\downarrow - \langle\hat{n}_\downarrow\rangle\Big)\Big\rangle \qquad (17.61)
$$

The Fock operator is obtained as derivative of the energy with respect to the one-particle-reduced density matrix.

$$
F_{\alpha,\beta} = \frac{dE}{d\rho^{(1)}_{\beta,\alpha}} \quad \Rightarrow \quad \boldsymbol{F} = \begin{pmatrix} \bar{\epsilon} - \frac{\Delta}{2} + Un_\downarrow & -U\rho^{(1)}_{\downarrow,\uparrow} \\ -U\rho^{(1)}_{\uparrow,\downarrow} & \bar{\epsilon} + \frac{\Delta}{2} + Un_\uparrow \end{pmatrix} \qquad (17.62)
$$

[12] The mean field energy occurs in Eq. 2.74 as part of the grand potential $\Omega = E - TS - \mu N$ for ensembles of Slater determinants. In Eq. 2.140, the mean field energy is shown in the context of many-particle wave functions, together with the terms that go beyond the mean-field approximation.

[13] To demonstrate the spin-rotation invariance of the mean-field interaction, we exploit

$$
\begin{aligned}
\frac{1}{2}\Big(\mathrm{Tr}\Big[\boldsymbol{\rho}^{(1)}\vec{\boldsymbol{\sigma}}\Big]\Big)^2 &= \frac{1}{2}\sum_{j\in\{x,y,z\}}\Big(\mathrm{Tr}\Big[\boldsymbol{\rho}^{(1)}\boldsymbol{\sigma}^{(j)}\Big]\Big)^2 = \frac{1}{2}\Big(\underbrace{(\rho^{(1)}_{\uparrow,\downarrow}+\rho^{(1)}_{\downarrow,\uparrow})^2}_{j=x}\underbrace{-(\rho^{(1)}_{\uparrow,\downarrow}-\rho^{(1)}_{\downarrow,\uparrow})^2}_{j=y}+\underbrace{(\rho^{(1)}_{\uparrow,\uparrow}-\rho^{(1)}_{\downarrow,\downarrow})^2}_{j=z}\Big) \\
&= 2\rho^{(1)}_{\uparrow,\downarrow}\rho^{(1)}_{\downarrow,\uparrow} + \frac{1}{2}\Big(n_\uparrow - n_\downarrow\Big)^2 \qquad (17.58)
\end{aligned}
$$

and

$$
\Big(\rho^{(1)}_{\uparrow,\uparrow}\Big)^2 + \Big(\rho^{(1)}_{\downarrow,\downarrow}\Big)^2 = \frac{1}{2}\Big(n_\uparrow + n_\downarrow\Big)^2 + \frac{1}{2}\Big(n_\uparrow - n_\downarrow\Big)^2 \qquad (17.59)
$$

After a few manipulations we arrive at the mean-field energy

$$
E^{mf}[\boldsymbol{\rho}^{(1)}] = \bar{\epsilon}\Big(n_\uparrow + n_\downarrow\Big) - \frac{\Delta}{2}\Big(n_\uparrow - n_\downarrow\Big) + \frac{1}{4}U\Big(n_\uparrow + n_\downarrow\Big)^2 - \frac{1}{4}U\mathrm{Tr}\Big[\boldsymbol{\rho}^{(1)}\vec{\boldsymbol{\sigma}}\Big]^2 \qquad (17.60)
$$

The last term depends on the spin-polarization, but it is independent of the spin-orientation. Note, that the interaction term depending on the total density contains a contribution from the exchange term, which is evident from the factor $\frac{1}{4}$ as opposed to $\frac{1}{2}$.

The eigenvalues of the Fock matrix are the one-particle excitation energies, which occur in the spectral function. For the sake of simplicity, let me consider only diagonal density matrices. Then the electron numbers can be identified with the occupations, i.e. $f_\sigma = n_\sigma$.

- for the vacuum state the occupations are zero and the energies agree with the excitation energies of the many-particle states

$$\epsilon_\uparrow = \bar{\epsilon} - \frac{\Delta}{2} \qquad \text{and} \qquad \epsilon_\downarrow = \bar{\epsilon} + \frac{\Delta}{2} \tag{17.63}$$

- for an atom with an electron in the favorable $|\uparrow\rangle$-one-particle orbital

$$\epsilon_\uparrow = \bar{\epsilon} - \frac{\Delta}{2} \qquad \text{and} \qquad \epsilon_\downarrow = \bar{\epsilon} + \frac{\Delta}{2} + U \tag{17.64}$$

- for an atom with an electron in the unfavorable $|\downarrow\rangle$-one-particle orbital

$$\epsilon_\uparrow = \bar{\epsilon} - \frac{\Delta}{2} + U \qquad \text{and} \qquad \epsilon_\downarrow = \bar{\epsilon} + \frac{\Delta}{2} \tag{17.65}$$

- for two electrons

$$\epsilon_\uparrow = \bar{\epsilon} - \frac{\Delta}{2} + U \qquad \text{and} \qquad \epsilon_\downarrow = \bar{\epsilon} + \frac{\Delta}{2} + U \tag{17.66}$$

The spectral functions for states with integer occupations are identical to those of the Fock operator.

Interesting is the case with a fractional occupation such as $n_\uparrow = x$ and $n_\downarrow = 0$. The variable parameter x can vary from zero to one. Let us inspect this example closer:

- The eigenvalues of the Fock operator are

$$\epsilon_\uparrow = \bar{\epsilon} - \frac{\Delta}{2} \qquad \text{and} \qquad \epsilon_\downarrow = \bar{\epsilon} + \frac{\Delta}{2} + xU \tag{17.67}$$

  The mean-field approximation has its excitation energies at the eigenvalues of the Fock operator. The corresponding spectral function

$$\mathcal{A}^{mf}(\epsilon, x) = \delta\left(\bar{\epsilon} - \frac{\Delta}{2} - \epsilon\right) + \delta\left(\bar{\epsilon} + \frac{\Delta}{2} + xU - \epsilon\right) \tag{17.68}$$

  produces two peaks. The second peak shifts upward with increasing particle number $N = x$.

  The state with fractional particle number N is an ensemble with probabilities $P_{|0\rangle} = x$, $P_{|\uparrow\rangle} = (1-x)$, $P_{|\downarrow\rangle} = 0$, and $P_{|\uparrow\downarrow\rangle} = 0$. The true spectral function obtained from the many-particle states is

$$\mathcal{A}(\epsilon, x) = \delta\left(\bar{\epsilon} - \frac{\Delta}{2} - \epsilon\right) + (1-x)\delta\left(\bar{\epsilon} + \frac{\Delta}{2} - \epsilon\right) + x\delta\left(\bar{\epsilon} + \frac{\Delta}{2} + U - \epsilon\right) \tag{17.69}$$

  where the spectral function has three excitation energies instead of two in the mean-field approximation. The upper two excitation energies have partial weight. While the excitation levels do not change with x, the weights do.

The lesson from this analysis is that the mean-field approximation produces a good spectral function, when the occupations are integer, i.e. zero or one. When the occupations of the interacting many-particle system are truly integer, the corresponding many-particle wave function is a Slater determinant. This is the case for the example at hand, the Hubbard atom.

For fractional occupations, however, the mean-field approximation adjusts the energy levels rather than the weights of the absorption bands. Typically, the Fermi level is pinned at a state with fractional occupations, which reminds of metallic behavior.

Editor: Is there a precise equivalence between the spectra of Slater determinants?

Electron affinity and ionization potential: Editor: Here should be a section on energy as function of particle number. Electron affinity and ionization potential is related to $\partial E/\partial N$ respectively $E(N+1)-E(N)$

The two states at $\epsilon_\uparrow$ and $\epsilon_\uparrow+U$ can be related to the electron affinity and the ionization potential. The **electron affinity** is the electron-addition energy $A(N)=E(N+1)-E(N)$, while the **ionization potential** is the electron removal energy $I(N)=E(N)-E(N-1)$.

Let me investigate the electron affinity $A_\uparrow$ and the ionization potential $I_\uparrow$ of the $\uparrow$ orbital as function of particle number N on the two-state system. We consider that an electron can only be added to the $\uparrow$-orbital, when it is empty. An electron can only be removed if it is full. The following table is obtained from the exact total energies given above.

N	$A_\uparrow$	$I_\uparrow$
0	$\epsilon_\uparrow$	–
1	$\epsilon_\uparrow+U$	$\epsilon_\uparrow$
2	–	$\epsilon_\uparrow+U$

For the particle number $N=1$, for which electrons can be added and removed, we see that the upper orbital is the electron affinity and the lower orbital $\epsilon_\uparrow$.

In order to understand electron affinity and ionization potential in a thermodynamic sense, let me investigate the system in thermal equilibrium. For this purpose, let me plot in figure 17.5 the chemical potential $N(\mu)=-\frac{\partial\Omega(T,\mu)}{\partial\mu}$ as function of the chemical potential. $\Omega(T,\mu)$ is the grand potential.

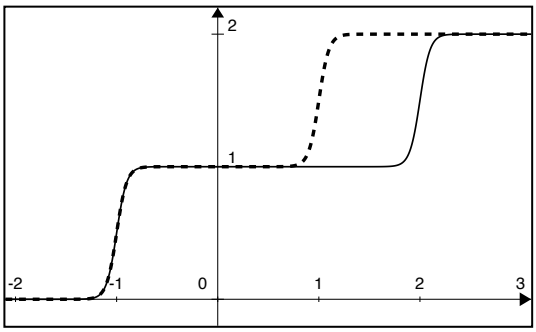


Fig. 17.5: Particle number N as function of chemical potential μ for a Hubbard atom with one-particle energies $\bar{\epsilon}_\uparrow=-1$ and $\bar{\epsilon}_\uparrow=+1$. The result is shown for an interaction $U=1$ (full line) and the non-interacting system $U=0$ (dashed line). The temperature has been chosen $k_BT=0.05$.

The **band gap** $E_g=A-I$, the difference between electron affinity and ionization potential. For integer occupations, it is $E_g=E(N+1)-2E(N)-E(N-1)$. We see how the particle number jumps quickly from one integer value to the next, as it is passing the energy level. The transition is smoothened at finite temperature.

The transitions occur at $\epsilon_\uparrow$ and $\epsilon_\downarrow+U$, when $\epsilon_\uparrow$ is the lower one-particle level. The band gap is therefore the band gap of the non-interacting system increased by the interaction energy. For a more general system, other than the Hubbard atom the increase will be smaller than U due to screening effects.

One striking observation is that, in the presence of an interaction, there is a band gap, even if it vanishes in the non-interacting system. This reflects that even atoms have an electron affinity, which differs from the ionization potential.

If the interaction is large, this atomic behavior, the splitting of energy levels, carries over into the

solid. The result is a so-called **Mott insulator**. If the Coulomb interaction grows larger than the bandwidth of the non-interacting system, a metallic system can turn abruptly into an insulator. In these cases one finds a **metal-insulator transition**, which is entirely due to the electron-electron interaction. The metal-insulator transition is the cause of, for example, the **colossal magnetoresistance effect** observed in manganites.

Editor: Demonstrate Hund's rule using the two-band Hubbard atom

Matsubara Green's function and self energy: Editor: Exercise: Calculate the time-dependent, finite-temperature Green's function from the spectral function of the Hubbard atom.

- calculate the Green's function for the half-filled Hubbard atom at zero temperature.
- determine the (proper) self energy, and plot it as function of time.
- Investigate the temperature dependence of the self energy by comparing $k_B T \ll U$, $k_B T = U$, $k_B T \gg U$.
- Consider the doped Hubbard atom, i.e. with $1+\delta$ electrons, where δ is a small number
- evaluate the first-order diagrams of the half-filled Hubbard monomer.

Caution! I did not do the calculations myself and may have overlooked difficulties.

Editor: Rewrite this in terms of time-dependent finite-temperature Green's function
We can use the spectral function to determine the Matsubara Green's function

$$\begin{aligned}
\mathcal{G}_{\uparrow,\uparrow}(i\omega_\nu) &= -\frac{1}{\hbar}\int d\epsilon\, \frac{\mathcal{A}_{\uparrow,\uparrow}(\epsilon)}{i\hbar\omega_\nu + \mu - \epsilon} \\
&= -\frac{1}{\hbar}\left\{ \frac{1-f_\downarrow}{i\hbar\omega_\nu + \mu - \epsilon_\uparrow} + \frac{f_\downarrow}{i\hbar\omega_\nu + \mu - \epsilon_\uparrow - U} \right\} \\
&= \mathcal{G}^{(0)}_{\uparrow,\uparrow}(i\omega_\nu)\left\{ 1 + f_\downarrow \left[\frac{i\hbar\omega_\nu + \mu - \epsilon_\uparrow}{i\hbar\omega_\nu + \mu - \epsilon_\uparrow - U} - 1 \right] \right\} \\
&= \mathcal{G}^{(0)}_{\uparrow,\uparrow}(i\omega_\nu)\left\{ 1 + f_\downarrow \left[\left(1 - \mathcal{G}^{(0)}_{\uparrow,\uparrow} U\right)^{-1} - 1 \right] \right\}
\end{aligned} \tag{17.70}$$

Thus, we obtain as self energy

$$\begin{aligned}
\Sigma_{\uparrow,\uparrow}(i\omega_\nu) &= \mathcal{G}^{(0),-1}_{\uparrow,\uparrow}(i\omega_\nu) - \mathcal{G}^{-1}_{\uparrow,\uparrow}(i\omega_\nu) \\
&= \mathcal{G}^{(0),-1}_{\uparrow,\uparrow}(i\omega_\nu)\left[1 - \left\{ 1 + f_\downarrow \left[\left(1 - \mathcal{G}^{(0)}_{\uparrow,\uparrow} U\right)^{-1} - 1 \right] \right\}^{-1} \right] \\
&= \frac{f_\downarrow U}{1 - (1-f_\downarrow)\mathcal{G}^{(0)}_{\uparrow,\uparrow} U} = \begin{cases} 0 & \text{for } f_\downarrow = 0 \\ U & \text{for } f_\downarrow = 1 \end{cases}
\end{aligned} \tag{17.71}$$

17.2.3 Hubbard dimer

Editor: See Vancini,Reining,Gatti[130] on the Hubbard dimer and the thesis of di Sabatino[131]

The Hubbard dimer is a model for a chemical bond. It describes a physical system that similar to the hydrogen molecule. The Hubbard dimer has a special correlation effect called **left-right correlation**. It describes that the covalent interaction is sacrificed to reduce the electron-electron interaction. For a large Coulomb interaction a singlet state with antiferromagnetic correlations is

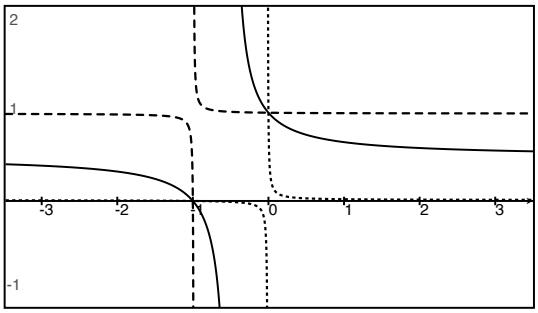


Fig. 17.6: Real part of the self energy $\Sigma_{\uparrow,\uparrow}(\hbar\omega)$ of the Hubbard atom for occupation $f_\downarrow = 0.01$ (short dashed), $f_\downarrow = 0.5$ (full line), $f_\downarrow = 0.99$ (long dashed), of the other state. The non-interacting orbital energy is $\epsilon_\uparrow = -1$ and the interaction is $U = 1$. Editor: Check this. I started from the Matsubara Green's functions and may have lost factors on the way. The high frequency value ($|\hbar\omega \to \infty$) of the self energy is $f_\downarrow U$

formed. Such a state cannot be described by a single Slater determinant. Therefore, Hartree-Fock approximation describes the system in the strongly interacting limit by an antiferromagnetic state.

The detailed calculations for many-particle energies and quasi-particle energies and wave functions for the Hubbard dimer can be found in appendix D.2 on p. 534.

The Hubbard dimer has also been discussed in the exercises section 1.5.1 and section 3.11.1.

Total energies

The many-particle energies of the 2-particle sector are shown as function of the Coulomb interaction in figure 17.7.

In the non-interacting limit, the wave functions are Slater determinants formed from bonding and antibonding orbitals. The total energies are obtained by adding up the orbital energies at $\bar{\epsilon} - |t|$ and $\bar{\epsilon} + |t|$.

Left-right correlation: Occupying the bonding and antibonding orbitals with two or more electrons results in a double occupancy of the atoms, and thus produces an energy penalty due to the Coulomb interaction. The two-particle Slater determinant of two bonding orbitals can be expressed as a sum of four Slater determinants in terms of local orbitals.

$$\frac{1}{2}\left(\hat{c}^\dagger_{1,\uparrow} + \hat{c}^\dagger_{2,\uparrow}\right)\left(\hat{c}^\dagger_{1,\downarrow} + \hat{c}^\dagger_{2,\downarrow}\right)|\mathcal{O}\rangle = \frac{1}{\sqrt{2}}\Bigg(\underbrace{\frac{1}{\sqrt{2}}}_{\cos(45^\circ)} \underbrace{\left(\hat{c}^\dagger_{1,\uparrow}\hat{c}^\dagger_{1,\downarrow} + \hat{c}^\dagger_{2,\uparrow}\hat{c}^\dagger_{2,\downarrow}\right)}_{\text{double occupancy}} + \underbrace{\frac{1}{\sqrt{2}}}_{\sin(45^\circ)} \underbrace{\left(\hat{c}^\dagger_{1,\uparrow}\hat{c}^\dagger_{2,\downarrow} \overbrace{+\hat{c}^\dagger_{2,\uparrow}\hat{c}^\dagger_{1,\downarrow}}^{-\hat{c}^\dagger_{1,\downarrow}\hat{c}^\dagger_{2,\uparrow}}\right)}_{\text{left-right correlated}} \Bigg)|\mathcal{O}\rangle \tag{17.72}$$

With increasing Coulomb interaction, the state with double occupancy is penalized and looses weight in the ground state, while the left-right correlated state dominates. This is achieved by increasing the angle from 45° to 90°. However, in both contributions, doubly occupied and left-right correlated states, the electrons are confined to one site only. Thus, they cannot profit from the delocalization due to the hopping term. The electrons can only delocalize, when both contributions are present. While the Coulomb energy can be lowered by suppressing the double-occupancy state, there is a loss of kinetic energy. Only in the limit of $U/|t| \to \infty$, the double-occupancy contribution is completely removed in favor of the left-right correlated state.

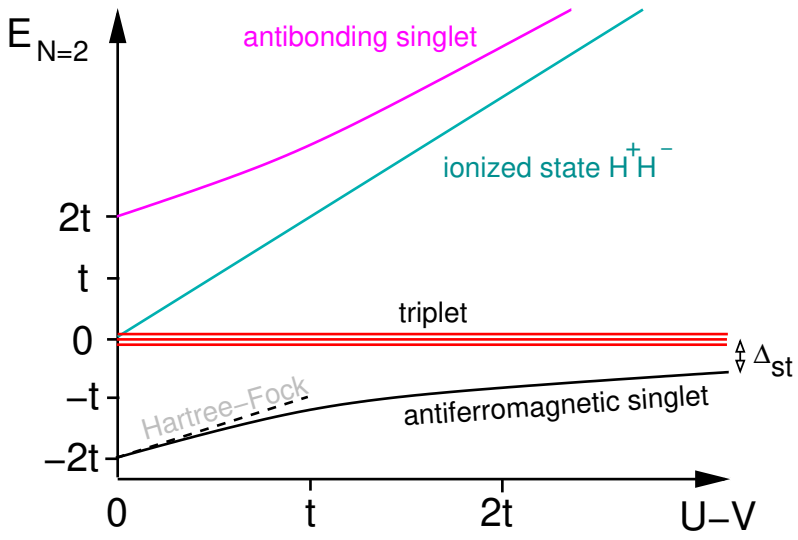


Fig. 17.7: Energies of the hydrogen molecule with two electrons are shown as function of $q = (U-V)/(4|t|)$ in units of the hopping $|t|$. The energies are shifted by $2|t| - 2\bar{\epsilon} - V$. The ground state, the antiferromagnetic singlet is shown in blue. The triplet states (artificially displaced are red. The double-occupancy state is shown in green and the state with two antibonding orbitals is shown in magenta. The black dashed line gives the spin-restricted Hartree-Fock energy with both electrons in the bonding orbital. Note that the Hartree-Fock ground state undergoes a transition to an antiferromagnetic broken-symmetry state for large q. Editor: A copy of this figure is figure 17.7 Editor: For the figure $V = 0$ has been used

Screening: Loosely speaking, one can say that the *"Coulomb interaction switches the chemical bond off"*. This is a common phenomenon. Without interaction, the ground state is obtained by optimizing the one-particle energies, loosely speaking, "the kinetic energy". With increasing interaction, electron-hole pairs are created, that screen the interaction. This can be demonstrated by representing the left-right correlated state as superposition of two Slater determinants, one of which describes two electrons in the bonding state and another one, which describes two electrons in the antibonding state.

$$\underbrace{\frac{1}{\sqrt{2}}\left(\hat{c}^\dagger_{1,\uparrow}\hat{c}^\dagger_{2,\downarrow} - \hat{c}^\dagger_{1,\downarrow}\hat{c}^\dagger_{2,\uparrow}\right)}_{\text{left-right correlated}}|\mathcal{O}\rangle = \frac{1}{\sqrt{2}}\Big(\underbrace{\frac{1}{2}\left(\hat{c}^\dagger_{1,\uparrow}+\hat{c}^\dagger_{2,\uparrow}\right)\left(\hat{c}^\dagger_{1,\downarrow}+\hat{c}^\dagger_{2,\downarrow}\right)}_{\text{2 electrons in bonding states}} - \underbrace{\frac{1}{2}\left(\hat{c}^\dagger_{1,\uparrow}-\hat{c}^\dagger_{2,\uparrow}\right)\left(\hat{c}^\dagger_{1,\downarrow}-\hat{c}^\dagger_{2,\downarrow}\right)}_{\text{2 electrons in anti-bonding states}}\Big)|\mathcal{O}\rangle$$
$$= \frac{1}{\sqrt{2}}\Big(\underbrace{\frac{1}{2}\left(\hat{c}^\dagger_{1,\uparrow}-\hat{c}^\dagger_{2,\uparrow}\right)\left(\hat{c}^\dagger_{1,\downarrow}+\hat{c}^\dagger_{2,\downarrow}\right)}_{\text{1 electron-hole pair}} - \underbrace{\frac{1}{2}\left(\hat{c}^\dagger_{1,\uparrow}+\hat{c}^\dagger_{2,\uparrow}\right)\left(\hat{c}^\dagger_{1,\downarrow}-\hat{c}^\dagger_{2,\downarrow}\right)}_{\text{1 electron-hole pair}}\Big)|\mathcal{O}\rangle \tag{17.73}$$

Thus, one-half of the electrons are promoted to the antibonding state, which compensates the energy gain from bond formation. In other words one electron-hole pair has been created *"to screen the Coulomb interaction"*.

Singlet-triplet splitting: The left-right-correlated contribution, can be described as a **singlet with antiferromagnetic correlations** . We will refer to it also as antiferromagnetic singlet.

The lowest excitation in the two-particle channel takes the system from the singlet with antiferromagnetic correlations to a triplet state[14]. With increasing interaction, the energy difference, the

[14] Other excitations are degenerate only in the non-interacting case

singlet-triplet splitting Δ_{st}, decreases.

Thus, we can describe the low-energy excitations in terms of a Heisenberg model.Editor: Describe Heisenberg model and magnons

If the singlet-triplet splitting is much smaller than k_BT, i.e. $\Delta_{st} \ll k_BT$ both, singlet and triplet, occur with about equal probability. Such an ensemble can be described by an ensemble of the particpating Slater determinants in local orbitals, i.e. $\hat{c}^\dagger_{1,\uparrow}\hat{c}^\dagger_{2,\uparrow}|\mathcal{O}\rangle$, $\hat{c}^\dagger_{1,\uparrow}\hat{c}^\dagger_{2,\downarrow}|\mathcal{O}\rangle$, $\hat{c}^\dagger_{1,\downarrow}\hat{c}^\dagger_{2,\uparrow}|\mathcal{O}\rangle$, and $\hat{c}^\dagger_{1,\downarrow}\hat{c}^\dagger_{2,\downarrow}|\mathcal{O}\rangle$. Therefore, the Hartree-Fock approximation, that is an ensemble of Slater determinants, will provide an accurate description of the thermal ensemble. This is another example, where quantum effects, in this case many-particle correlations, are limited to the low-temperature regime.

Loss of entanglement at high temperatures: Let me come back to the argument used above saying that the physics at high temperatures can be described by an ensemble of Slater determinants.

The density matrix at zero temperature describes only the ground state, which is the singlet state.

$$\hat{\rho}_{T=0} = \begin{pmatrix} \hat{c}^\dagger_{1,\uparrow}\hat{c}^\dagger_{2,\uparrow}|\mathcal{O}\rangle \\ \hat{c}^\dagger_{1,\uparrow}\hat{c}^\dagger_{2,\downarrow}|\mathcal{O}\rangle \\ \hat{c}^\dagger_{1,\downarrow}\hat{c}^\dagger_{2,\uparrow}|\mathcal{O}\rangle \\ \hat{c}^\dagger_{1,\downarrow}\hat{c}^\dagger_{2,\downarrow}|\mathcal{O}\rangle \end{pmatrix} \begin{pmatrix} 0 & 0 & 0 & 0 \\ 0 & \frac{1}{2} & -\frac{1}{2} & 0 \\ 0 & -\frac{1}{2} & \frac{1}{2} & 0 \\ 0 & 0 & 0 & 0 \end{pmatrix} \begin{pmatrix} \langle\mathcal{O}|\hat{c}_{2,\uparrow}\hat{c}_{1,\uparrow} \\ \langle\mathcal{O}|\hat{c}_{2,\downarrow}\hat{c}_{1,\uparrow} \\ \langle\mathcal{O}|\hat{c}_{2,\uparrow}\hat{c}_{1,\downarrow} \\ \langle\mathcal{O}|\hat{c}_{2,\downarrow}\hat{c}_{1,\downarrow} \end{pmatrix} \tag{17.74}$$

A high temperature, all four states, one singlet and three triplet states contribute equally with probability $\frac{1}{4}$

$$\hat{\rho}_{T=\infty} = \begin{pmatrix} \hat{c}^\dagger_{1,\uparrow}\hat{c}^\dagger_{2,\uparrow}|\mathcal{O}\rangle \\ \hat{c}^\dagger_{1,\uparrow}\hat{c}^\dagger_{2,\downarrow}|\mathcal{O}\rangle \\ \hat{c}^\dagger_{1,\downarrow}\hat{c}^\dagger_{2,\uparrow}|\mathcal{O}\rangle \\ \hat{c}^\dagger_{1,\downarrow}\hat{c}^\dagger_{2,\downarrow}|\mathcal{O}\rangle \end{pmatrix} \begin{pmatrix} \frac{1}{4} & 0 & 0 & 0 \\ 0 & \frac{1}{4} & 0 & 0 \\ 0 & 0 & \frac{1}{4} & 0 \\ 0 & 0 & 0 & \frac{1}{4} \end{pmatrix} \begin{pmatrix} \langle\mathcal{O}|\hat{c}_{2,\uparrow}\hat{c}_{1,\uparrow} \\ \langle\mathcal{O}|\hat{c}_{2,\downarrow}\hat{c}_{1,\uparrow} \\ \langle\mathcal{O}|\hat{c}_{2,\uparrow}\hat{c}_{1,\downarrow} \\ \langle\mathcal{O}|\hat{c}_{2,\downarrow}\hat{c}_{1,\downarrow} \end{pmatrix} \tag{17.75}$$

Thus, we may describe the system at high temperatures equally well by an ensemble of Slater determinants or by an ensemble of eigenstates of the Hamiltonian. The off-diagonal elements of the density matrix reflect the phase relationship of the Slater determinants, that is their entanglement. At sufficiently high temperature, also states with a phase relationship opposite to that of the ground state become occupied, which cancels the off-diagonal matrix elements in the von-Neumann density matrix. In other words, the entanglement vanishes at high temperatures.

Mott-Hubbard gap: For large U, all states with one electron per site have similar energy, while states with double occupancy are suppressed by the penalty of the Coulomb interaction. Moving an electron from a singly occupied site to a site that is already filled costs an energy U. This is evident from the particle-number conserving excitations.

The many-particle states in the 2-particle sector are given in table D.4 on p. 535. Later, we will also see this effect in the one-particle excitations.

The picture emerges that the Hubbard dimer has at low-temperatures an antiferromagnetic spin arrangement. At higher temperatures the spins fluctuate relative to each other. For an extended system this translates in the so-called[132] **Mott-Heisenberg insulator** state at low temperatures, while the ensemble with fluctuating spins is the so-called[132] **Mott-Hubbard insulator** .

Quasi-particles and spectral function

The quasi-particle wave functions and energies are calculated in appendix D.2.

1. We find excitations at $\bar{\epsilon} \pm |t|$ which corresponds to the non-interacting system. These states can be identified with the **lower Hubbard band**

2. A replica of this spectrum is shifted up in energy by U, which yields excitation energies at $\bar{\epsilon} + U \pm |t|$. These states can be identified with the **upper Hubbard band**

3. From these main peaks in the spectral function, smaller peaks are split off by $\pm\Delta_{st}$. In an extended model, the split-off peaks will show up as magnon-broadening of the upper and lower Hubbard bands.

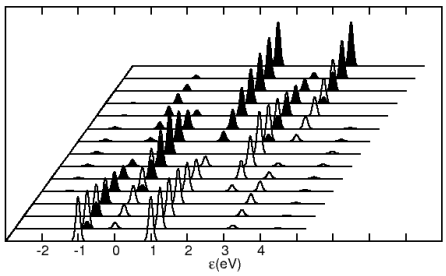


Fig. 17.8: Spectral function of the Hubbard dimer for different number of electrons. The energy is shown on the horizontal axis, the spectral density is shown along the vertical axis and the number of electrons is shown by the third axis pointing into the paper. The spectral functions are smeared out to Gaussians and displaced along the energy axis for better visibility. The filled area indicates the occupation of the states.

Satellites

In the spectrum we may observe small contributions to the spectral function that can not be attributed to the normal band structure respectively the upper or lower Hubbard band. These are called **satellites**. Satellites can be described as a combination of a one-particle excitation with another particle-number conserving, virtual excitation.

The notion of a virtual excitation describes that several Slater determinants contribute to a many-particle state. This is described by saying that there are virtual excitations from the dominant Slater determinant to the minor Slater determinants.

When we discuss excitations in terms of adding and removing electrons from one-particle orbitals, we are referring to transitions between Slater determinants. When we apply this language to a general many-particle wave function, we need to consider transitions to and from Slater determinants present, albeit with a smaller weight. Thus, we describe the transitions as those between the dominant Slater determinants with additional virtual excitations of the initial and/or final state. These virtual excitations describe the contribution of the minor Slater determinants in a multi-configuration state.

Editor: Does it make sense to discuss spectra in terms of density of states of Slater determinants?

Editor: Discuss the satellites at -2 eV and at +4 eV.

Editor: The state in the middle of a replica is not centered in the middle, but it is lower in the lower replica and higher in the upper replica.

17.2.4 Hubbard chain

The Hubbard chain is the minimal model for an extended interacting system. However, it should be noted that one-dimensional systems have special properties that are untypical for systems in higher dimensions. For example, phase transitions are more likely to occur.

There is a famous exact solution of the one-dimensional Hubbard model by Lieb and Wu[125].

In the non-interacting limit, the Hubbard chain is simply the linear chain discussed earlier in section 1.5.3.

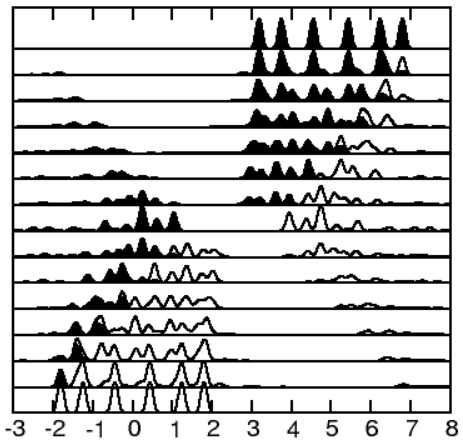


Fig. 17.9: Spectral function of the 6-membered Hubbard chain for different number of electrons. The energy is shown on the horizontal axis, the spectral density is shown along the vertical axis. The spectral functions for different number of electrons numbers are stacked vertically. The spectral functions are smeared out to Gaussians and displaced along the energy axis for better visibility. The filled area indicates the occupation of the states.

Editor: The spectral function of a 1-dimensional chain of hydrogen atoms has been investigated by Rusakov and Zgid [J. Chem. Phys. 144, 054106 (2016)<].[?]

17.3 Heisenberg model

The Heisenberg model is the minimal model for magnetic systems. It considers the interaction of spins on a lattice.

We will learn about two notions

- An antiferromagnet has a non-trivial ground state. The ground state contains quantum fluctuations of the spin system, which are an integral part of the ground state.
- A system of immobile spins exhibits excitations that can be identified with **quasi-particles**. These quasi-particles are called **magnons**. This is an example for a particle that emerges from a quantum field, analogous to elementary particles, which emerge as excitations of the vacuum.

17.3.1 The model

HEISENBERG MODEL

$$\hat{H} = -\sum_{\langle i,j\rangle} J\,\hat{\vec{S}}_i\hat{\vec{S}}_j = -\frac{1}{2}\sum_{i,j\in n.n.} J\,\hat{\vec{S}}_i\hat{\vec{S}}_j \tag{17.76}$$

The symbol $\langle i,j\rangle$ restricts the double sum to nearest-neighbor terms.[a] The parameter J is called **exchange parameter**. A positive exchange parameter J favors ferromagnetic alignment, while a negative exchange parameter favors antiferromagnetic spin alignment.

[a] I consider the common notation "$\langle i,j\rangle$" un-intuitive. Therefore, I often use the notation "$i,j \in$ n.n." instead and correct double countung by an factor 1/2. "n.n." stands for "nearest neighbors". The sum includes each pair twice, once as (i,j) and once as (j,i).

The Heisenberg model emerges from the half-filled Hubbard model in the limit of strong interaction.[133].[15] In the half-filled Hubbard model, there is one electron per site. The strong Coulomb interaction excludes fluctuations, where an electron moves to a site, which is already occupied. The only degrees of freedom left to the electrons are their spin orientations. These are described by the Heisenberg model.

The spin interaction, respectively the exchange parameter can already be deduced from the Hubbard dimer investigated earlier. The transition from the Hubbard model to the spin-$\frac{1}{2}$-Heisenberg model is demonstrated in section 3.11.1 on p. 148. These spin transitions are also described in section 17.2.3 on p. 444. In the Hubbard model, the ground state is antiferromagnetic and the exchange parameter is given in Eq. 3.127 as

$$J_{R,R'} \overset{\text{Eq. 3.127}}{=} -\frac{1}{2}\Delta_{st}\left(\frac{\hbar}{2}\right)^{-2} \approx -\frac{1}{2}\frac{(2t)^2}{U-V}\left(\frac{\hbar}{2}\right)^{-2} \text{ for } R, R' \text{ next neighbors} \tag{17.78}$$

where Δ_{st} is the singlet-triplet splitting of the hydrogen molecule, U is the onsite Coulomb repulsion, and V is the Coulomb interaction between electrons on different sites.

While I will limit myself to the spin-$\frac{1}{2}$ Heisenberg model, it can be formulated with spins of arbitrary size. The limit of infinite spin vectors is equivalent to the classical limit.

Editor: Literature: Auerbach[134], For spinons see Bethe[135] and Fadeev[136].

Editor: Caution! The Hamiltonian is used here with constant shifts, which are inconsistent. I need to make them consistent without a shift.

[15] Anderson [133] defines the spin interaction in his Eq. 17 as $V_{ex}^{in} = -\frac{1}{2}J(\frac{1}{2} + 2S_R S_{R'})$ which translates into

$$\hat{H} = \sum_{R,R'=n.n.} J_{R,R'}\left[\frac{1}{2}\left(\frac{\hbar}{2}\right)^2 - \hat{\vec{S}}_R\hat{\vec{S}}_{R'}\right] \tag{17.77}$$

and a positive exchange parameter. In Auerbach[134], I find the energy as $\frac{1}{2}J\vec{S}_R\vec{S}_{R'}$.,

17.3.2 Outlook on phenomena

For the Heisenberg model, I will demonstrate two physical phenomena, namely (1) the presence of quantum fluctuations in the ground state of an antiferromagnet and (2) a new type of quasi particles called magnons.

1. The nature of the ground state of an antiferromagnet is quite surprising. The first guess for the ground state is the Neél state with alternating spins

$$\ldots,\uparrow,\downarrow,\uparrow,\downarrow,\uparrow,\downarrow,\ldots \tag{17.79}$$

   However, application of the Hamiltonian Eq. 17.77 shows that this is not an eigenstate of the Heisenberg Hamiltonian. Rather, the Hamiltonian produces a superposition of all possible configurations with neighboring spins interchanged. One example is

$$\ldots,\uparrow,\downarrow,\underbrace{\downarrow,\uparrow}_{\leftrightarrow},\uparrow,\downarrow,\ldots \tag{17.80}$$

   The energy of such a configuration is higher in energy, because it contains also spin pairs with parallel spin. However, the **level repulsion** between the ground-state configuration $|G\rangle$ and this new state $\hat{H}|\hat{G}\rangle$ lowers the energy of the new ground state[16] $|G\rangle\cos(\phi)+\hat{H}|G\rangle\sin(\phi)$ below that of the Neél state. Also this state is only an approximation of the ground state, but it shows that the true ground state is characterized by (1) the Neél state but (2) also by **quantum fluctuations** for which neighboring sites can also have parallel spins.

2. Another physical phenomenon is the existence of **magnons**. Magnons are elementary excitations of a Heisenberg model which can be characterize by delocalized spin flips.[17] They are quasi-particles like electrons, phonons, etc. In a translationally invariant system, they are characterized by a quasi momentum $\hbar\vec{k}$ as quantum number and they have their own band structure.

I will limit myself first to the one-dimensional Heisenberg chain with spins $\frac{1}{2}\hbar$. To make the quantum fluctuations evident, I will present the analytic solution of a four-membered Heisenberg chain with periodic boundary conditions.

Bethe provided an exact solution for a one-dimensional spin $\frac{1}{2}$ chains[135], the so-called Bethe Ansatz.

Alois Loidl[137] reports on recent experiments by Wang[Z. Wang et al. Nature 554, 219 (2018)] on $SrCo_2V_2O_8$, which is a nearly ideal representation of an anisotropic one-dimensional Heisenberg chain. It forms chains of CoO_6 octahedra, of which each Co ion carries a spin-$\frac{1}{2}$.

17.3.3 Quantum fluctuations in the antiferromagnetic ground state

In this subsection, I will derive the ground state of a simple antiferromagnet. The result is provided in Eq. 17.110. One aspect of the derivation is that the reader can follow through every step analytically. Therefore, I have chosen very simple model system, for which one can work out all quantum states.

In the course of the derivation, I will introduce a number of elementary concepts.

- The relation of the Hamiltonian and spin interchanges
- The structure of the Hilbert states of a spin system. The analogy of spin configuration with Slater determinants.
- Ising model and Neél state
- The eigenstates of the four membered spin chaing are calculated analytically.

[16] The mixing angle ϕ is some parameter which needs to be calculated.

[17] Magnons are no spin waves. A spin wave would have zero net magnetization, while a magnon has a spin $\hbar$ like a local spin flip. The spin-density of a magnon is constant in space.

Spin operators for spin-$\frac{1}{2}$

Let me start with a reminder of the spin ladder-operators in a 2-dimensional Hilbert space spanned by $\{|\downarrow\rangle, |\uparrow\rangle\}$.

The spin operators are

$$\hat{S}_x = \frac{\hbar}{2}\begin{pmatrix} 0 & 1 \\ 1 & 0 \end{pmatrix} \qquad \text{and} \qquad \hat{S}_y = \frac{\hbar}{2}\begin{pmatrix} 0 & -i \\ i & 0 \end{pmatrix} \qquad \text{and} \qquad \hat{S}_z = \frac{\hbar}{2}\begin{pmatrix} 1 & 0 \\ 0 & -1 \end{pmatrix} \tag{17.81}$$

Let us introduce the ladder operators

$$\hat{S}_+ = \hat{S}_x + i\hat{S}_y = \hbar\begin{pmatrix} 0 & 1 \\ 0 & 0 \end{pmatrix} \qquad \text{and} \qquad \hat{S}_- = \hat{S}_x - i\hat{S}_y = \hbar\begin{pmatrix} 0 & 0 \\ 1 & 0 \end{pmatrix} \tag{17.82}$$

Usually, it is more convenient to work with $\hat{S}_+, \hat{S}_-$, and $\hat{S}_z$, rather than with $\hat{S}_x, \hat{S}_y$, and $\hat{S}_z$.

While the anti-commutator is

$$\left[\hat{S}_+, \hat{S}_-\right]_+ = \hat{1}\hbar \tag{17.83}$$

the spin-operators are not fermionic. They are of bosonic nature, because spin operators for different sites commutate, but do not anticommutate.

For a single spin-$\frac{1}{2}$ particle, we obtain from Eq. 17.82

$$\begin{aligned} &\hat{S}_+|\uparrow\rangle = |\varnothing\rangle \qquad \text{and} \qquad \hat{S}_-|\uparrow\rangle = |\downarrow\rangle\hbar \qquad \text{and} \qquad \hat{S}_z|\uparrow\rangle = |\uparrow\rangle\left(+\frac{1}{2}\hbar\right) \\ &\hat{S}_+|\downarrow\rangle = |\uparrow\rangle\hbar \qquad \text{and} \qquad \hat{S}_-|\downarrow\rangle = |\varnothing\rangle \qquad \text{and} \qquad \hat{S}_z|\downarrow\rangle = |\downarrow\rangle\left(-\frac{1}{2}\hbar\right) \end{aligned} \tag{17.84}$$

The squared spin is

$$\hat{\vec{S}}^2 = \frac{1}{2}\left(\hat{S}_+\hat{S}_- + \hat{S}_-\hat{S}_+\right) + \hat{S}_z\hat{S}_z \qquad \Rightarrow \qquad \begin{cases} \hat{\vec{S}}^2|\uparrow\rangle = |\uparrow\rangle\left(\frac{1}{2}\hbar^2 + \frac{1}{4}\hbar^2\right) = |\uparrow\rangle\frac{3}{4}\hbar^2 \\ \hat{\vec{S}}^2|\downarrow\rangle = |\downarrow\rangle\left(\frac{1}{2}\hbar^2 + \frac{1}{4}\hbar^2\right) = |\downarrow\rangle\frac{3}{4}\hbar^2 \end{cases} \tag{17.85}$$

The eigenvalue $\hbar\frac{3}{4} = \hbar\ell(\ell+1)$ is expected for a system with angular momentum $\ell = \frac{1}{2}$.

Spin coupling: Now, I investigate the spin coupling for a two-site problem

$$\begin{aligned} \hat{\vec{S}}_1\hat{\vec{S}}_2 &= \underbrace{\frac{1}{2}\left(\hat{S}_{1,+} + \hat{S}_{1,-}\right)}_{\hat{S}_{1,x}}\underbrace{\frac{1}{2}\left(\hat{S}_{2,+} + \hat{S}_{2,-}\right)}_{\hat{S}_{2,x}} + \underbrace{\frac{-i}{2}\left(\hat{S}_{1,+} - \hat{S}_{1,-}\right)}_{\hat{S}_{1,y}}\underbrace{\frac{-i}{2}\left(\hat{S}_{2,+} - \hat{S}_{2,-}\right)}_{\hat{S}_{2,y}} + \hat{S}_{1,z}\hat{S}_{2,z} \\ &= \frac{1}{2}\left(\hat{S}_{1,+}\hat{S}_{2,-} + \hat{S}_{1,-}\hat{S}_{2,+}\right) + \hat{S}_{1,z}\hat{S}_{2,z} \end{aligned} \tag{17.86}$$

The spin-coupling acts as follows

$$\begin{aligned} \hat{\vec{S}}_1\hat{\vec{S}}_2|\uparrow,\uparrow\rangle &= |\uparrow,\uparrow\rangle\frac{1}{4}\hbar^2 \\ \hat{\vec{S}}_1\hat{\vec{S}}_2|\uparrow,\downarrow\rangle &= |\downarrow,\uparrow\rangle\frac{1}{2}\hbar^2 - |\uparrow,\downarrow\rangle\frac{1}{4}\hbar^2 \\ \hat{\vec{S}}_1\hat{\vec{S}}_2|\downarrow,\uparrow\rangle &= |\uparrow,\downarrow\rangle\frac{1}{2}\hbar^2 - |\downarrow,\uparrow\rangle\frac{1}{4}\hbar^2 \\ \hat{\vec{S}}_1\hat{\vec{S}}_2|\downarrow,\downarrow\rangle &= |\downarrow,\downarrow\rangle\frac{1}{4}\hbar^2 \end{aligned} \tag{17.87}$$

which can be summarized in terms of a spin exchange between two sites

SPIN HAMILTONIAN AND SITE EXCHANGE

$$\Big(\hat{\vec{S}}_1\hat{\vec{S}}_2+\frac{\hbar^2}{4}\Big)|\sigma_1,\sigma_2\rangle=|\sigma_2,\sigma_1\rangle\frac{\hbar^2}{2}\quad\text{or}\quad\frac{1}{2}\Big(\hat{\vec{\sigma}}_1\hat{\vec{\sigma}}_2+1\Big)|\sigma_1,\sigma_2\rangle=|\sigma_2,\sigma_1\rangle \tag{17.88}$$

This simple rule will be very useful later on. It is convenient as it produces exactly one spin state from another one.

With this expression, we obtain the eigenstates of the spin coupling operator which are the singlet and triplet states.

$$\begin{aligned}
\Big(\hat{\vec{S}}_1\hat{\vec{S}}_2+\frac{\hbar^2}{4}\Big)\frac{1}{\sqrt{2}}\Big(|\uparrow,\downarrow\rangle-|\downarrow,\uparrow\rangle\Big)&=\frac{1}{\sqrt{2}}\Big(|\uparrow,\downarrow\rangle-|\downarrow,\uparrow\rangle\Big)\left(-\frac{\hbar^2}{2}\right)\qquad\text{singlet}\\
\Big(\hat{\vec{S}}_1\hat{\vec{S}}_2+\frac{\hbar^2}{4}\Big)\frac{1}{\sqrt{2}}\Big(|\uparrow,\downarrow\rangle+|\downarrow,\uparrow\rangle\Big)&=\frac{1}{\sqrt{2}}\Big(|\uparrow,\downarrow\rangle+|\downarrow,\uparrow\rangle\Big)\left(+\frac{\hbar^2}{2}\right)\qquad\text{triplet } S_{tot,z}=0\hbar\\
\Big(\hat{\vec{S}}_1\hat{\vec{S}}_2+\frac{\hbar^2}{4}\Big)|\uparrow,\uparrow\rangle&=|\uparrow,\uparrow\rangle\left(+\frac{\hbar^2}{2}\right)\qquad\text{triplet } S_{tot,z}=+1\hbar\\
\Big(\hat{\vec{S}}_1\hat{\vec{S}}_2+\frac{\hbar^2}{4}\Big)|\downarrow,\downarrow\rangle&=|\downarrow,\downarrow\rangle\left(+\frac{\hbar^2}{2}\right)\qquad\text{triplet } S_{tot,z}=-1\hbar
\end{aligned} \tag{17.89}$$

It is not surprising that we obtain the eigenstates of the squared total spin, because they are intimately related for spin-$\frac{1}{2}$ systems.

$$\hat{\vec{S}}_1\hat{\vec{S}}_2=\Big(\hat{\vec{S}}_1+\hat{\vec{S}}_2\Big)^2\underbrace{-\hat{\vec{S}}_1^2-\hat{\vec{S}}_2^2}_{-\frac{3}{2}\hbar^2}=\Big(\hat{\vec{S}}_1+\hat{\vec{S}}_2\Big)^2-\frac{3}{2}\hbar^2 \tag{17.90}$$

Basisset for spin-$\frac{1}{2}$ Heisenberg model

We assume here again, that each spin $\vec{S}_R$ acts on a spin-$\frac{1}{2}$. That is, the components $\hat{S}_{R,j}$ with $j\in\{x,y,z\}$ have eigenvalues $\pm\frac{\hbar}{2}$. In the single-site model, a single site of the Heisenberg model has a two-dimensional Hilbert space, that is, it has quantum numbers $\sigma_R\in\{\uparrow,\downarrow\}$. A general state of the single-site model is

$$|\Psi\rangle=\sum_{\sigma\in\{\uparrow,\downarrow\}}|\sigma\rangle c_\sigma \tag{17.91}$$

A general state in an extended Heisenberg model is

$$|\Psi\rangle=\sum_{\vec{\sigma}\in\{\uparrow,\downarrow\}^\infty}|\vec{\sigma}\rangle c_{\vec{\sigma}} \tag{17.92}$$

where every component of the vector $\vec{\sigma}$ can take one of two values $\sigma\in\{\uparrow,\downarrow\}$.

Notice the difference to the occupation-number representation, where the components of $\vec{\sigma}\in\{0,1\}$ determine whether an orbital is occupied or not. In the Heisenberg model, the number of electrons is the same for all states and is not even mentioned in the model. Rather, $\vec{\sigma}$ determines a certain spin state. A spin-flip from a $\downarrow$ spin to an $\uparrow$ spin in the Heisenberg model is performed by $\frac{2}{\hbar}S_{R,+}$, which is analogous to a creation operator. However, this is a creation operator of a spin-flip and not one of an electron. In the Hubbard model, the spin flip would be described by the operator $\hat{S}_+=\frac{\hbar}{2}\hat{c}^\dagger_{R,\uparrow}\hat{c}_{R,\downarrow}$, which is a two-particle excitation that conserves the electron number.

Ising model: When we calculate the energy expectation values between the basisstates $|\vec{\sigma}\rangle$ we obtain the energies of the **Ising model**.

$$\begin{aligned} E_{\vec{\sigma}} &\overset{\text{Eq. } 17.76}{=} \langle\vec{\sigma}|\left(-\sum_{i,j\in\text{n.n.}} J\hat{\vec{S}}_i\hat{\vec{S}}_j\right)|\vec{\sigma}\rangle \\ &\overset{\text{Eq. } 17.88}{=} \frac{J\hbar^2}{4}\sum_{i,j\in\text{n.n.}}\Bigg(1-2\underbrace{\langle\vec{\sigma}|\frac{1}{2}\left(\hat{\vec{\sigma}}_i\hat{\vec{\sigma}}_j+\hat{1}\right)|\vec{\sigma}\rangle}_{\text{spin interchange}\atop =1\text{ for }\sigma_i=\sigma_j;\ =0\text{ for }\sigma_i\neq\sigma_j}\Bigg) \\ &= \frac{J\hbar^2}{4}\Bigg(\sum_{i,j\in\text{n.n.}}1-2\underbrace{\frac{\sigma_i\sigma_j+1}{2}}_{=1\text{ for }\sigma_i=\sigma_j;\ =0\text{ for }\sigma_i\neq\sigma_j}\Bigg) \\ &= -\sum_{i,j\in\text{n.n.}}\frac{J\hbar^2}{4}\sigma_i\sigma_j \end{aligned} \tag{17.93}$$

$\sigma=+1$ for $|\uparrow\rangle$ and $\sigma=-1$ for $|\downarrow\rangle$. Note here, that σ_i and σ_j are numbers rather than operators $\hat{\sigma}_i$ and $\hat{\sigma}_j$.

Neél state: For $J>0$, the Slater determinant with the lowest energy is the so-called **Neél state** (See [138]), for which the spin directions alternate from site to site. For one dimension, this would be

$$|\cdots,\uparrow,\downarrow,\uparrow,\downarrow,\uparrow,\downarrow,\cdots\rangle \tag{17.94}$$

The Neél state is, however, not the true ground state of an antiferromagnet, which I will demonstrate in the following. Rather the ground state of an antiferromagnet is a superposition $\sum_{\vec{\sigma}}|\vec{\sigma}\rangle c_{\vec{\sigma}}$ of several spin configurations $|\vec{\sigma}\rangle$.

Antiferromagnetic ground state from second-order perturbation theory: Eq. 17.88 shows that each term of the Hamilton operator adds a copy with two neighboring spins interchanged.

$$\begin{aligned} \hat{H} &\overset{\text{Eq. } 17.76}{=} -\sum_{i,j\in\text{n.n.}}\Bigg[\underbrace{J\left(\hat{\vec{S}}_i\hat{\vec{S}}_j+\hat{1}\frac{\hbar^2}{4}\right)}_{\text{interchanges spins } i,j\atop\text{times } J\hbar^2/2}-\underbrace{\hat{1}J\frac{\hbar^2}{4}}_{\text{scaled}}\Bigg] \\ &\overset{\text{Eq. } 17.88}{=} J\frac{\hbar^2}{4}\sum_{i,j\in\text{n.n.}}\Bigg[\hat{1}-2\cdot\underbrace{\frac{1}{2}\left(\hat{\vec{\sigma}}_i\hat{\vec{\sigma}}_j+\hat{1}\right)}_{\text{interchanges spins } i,j}\Bigg] \end{aligned} \tag{17.95}$$

When this Hamiltonian is applied to the Neél state one obtains a superposition of many configurations. The Neél state is thus not the ground state and not even eigenstate of the Hamiltonian.

The ground state of the Heisenberg antiferromagnet is analytically only known for the one-dimensional Heisenberg chain.[135] In order to obtain an idea of the nature of the state let me demonstrate the case of a chain with periodic boundary conditions.

Let me apply one term of the Hamilton operator Eq. 17.95 to the Neél state

$$\begin{aligned} -J\vec{S}_i\vec{S}_j\underbrace{|\cdots,\uparrow,\downarrow,\uparrow,\overbrace{\downarrow}^{\text{pos } i},\overbrace{\uparrow}^{\text{pos } j},\downarrow,\uparrow,\downarrow,\cdots\rangle}_{\text{Neél state}} &= -|\cdots,\uparrow,\downarrow,\uparrow,\uparrow,\downarrow,\downarrow,\uparrow,\downarrow,\cdots\rangle\frac{J\hbar^2}{2} \\ &+\underbrace{|\cdots,\uparrow,\downarrow,\uparrow,\downarrow,\uparrow,\downarrow,\uparrow,\downarrow,\cdots\rangle}_{\text{Neél state}}\frac{J\hbar^2}{4} \end{aligned} \tag{17.96}$$

Because the Hamiltonian connects the Neél state to higher-lying states, the latter mix in and lower the energy of the new lowest state. This energy lowering is due to the common **level repulsion** that is a consequence of the matrix diagonalization.

Symmetry eigenstates

I can exploit translation symmetry and spin-inversion symmetry to block diagonalize the Hamiltonian. The details of exploiting symmetry in quantum physics are described in section 9 of ΦSX:Quantum Physics[16]. The **translation operator** $\hat{T}$ shifts the complete spin sequence by one bead to the right. Due to periodic boundary conditions the last bead is moved to the first position. Another symmetry is the **global spin inversion** $\hat{I}$.

For the four-membered ring, the operators are defined by

$$\begin{aligned}\hat{T}|\sigma_1,\sigma_2,\sigma_3,\sigma_4\rangle &= |\sigma_4,\sigma_1,\sigma_2,\sigma_3\rangle \\ \hat{I}|\sigma_1,\sigma_2,\sigma_3,\sigma_4\rangle &= |-\sigma_1,-\sigma_2,-\sigma_3,-\sigma_4\rangle\end{aligned} \tag{17.97}$$

where $(-\uparrow) = \downarrow$ and $(-\downarrow) = \uparrow$.

Because the total spin of the Neél state vanishes, $S_{\mathrm{tot},z} = 0$. The Hamiltonian introduces spin flips which conserves the total spin in z-direction $S_{\mathrm{tot},z}$. Let me therefore select all states with $S_{\mathrm{tot},z} = 0$. The states can be classified according to the positions of the $\uparrow$ spins as $(1,2)$, $(1,3)$, $(1,4)$, $(2,3)$, $(2,4)$, $(3,4)$.

Let me describe the result in terms of powers of translations $\hat{T}$ and the inversion $\hat{I}$.

$$\begin{aligned}(1,2) &\longrightarrow |\uparrow,\uparrow,\downarrow,\downarrow\rangle = \hat{T}^0|\uparrow,\uparrow,\downarrow,\downarrow\rangle = \hat{I}^0|\uparrow,\uparrow,\downarrow,\downarrow\rangle \\ (1,3) &\longrightarrow |\uparrow,\downarrow,\uparrow,\downarrow\rangle = \hat{T}^0|\uparrow,\downarrow,\uparrow,\downarrow\rangle = \hat{I}^0|\uparrow,\downarrow,\uparrow,\downarrow\rangle \\ (1,4) &\longrightarrow |\uparrow,\downarrow,\downarrow,\uparrow\rangle = \hat{T}^3|\uparrow,\uparrow,\downarrow,\downarrow\rangle = \hat{I}^0|\uparrow,\downarrow,\downarrow,\uparrow\rangle \\ (2,3) &\longrightarrow |\downarrow,\uparrow,\uparrow,\downarrow\rangle = \hat{T}^1|\uparrow,\uparrow,\downarrow,\downarrow\rangle = \hat{I}^1|\uparrow,\downarrow,\downarrow,\uparrow\rangle \\ (2,4) &\longrightarrow |\downarrow,\uparrow,\downarrow,\uparrow\rangle = \hat{T}^1|\uparrow,\downarrow,\uparrow,\downarrow\rangle = \hat{I}^1|\uparrow,\downarrow,\uparrow,\downarrow\rangle \\ (3,4) &\longrightarrow |\downarrow,\downarrow,\uparrow,\uparrow\rangle = \hat{T}^2|\uparrow,\uparrow,\downarrow,\downarrow\rangle = \hat{I}^1|\uparrow,\uparrow,\downarrow,\downarrow\rangle\end{aligned} \tag{17.98}$$

There are only two independent states, namely $|\uparrow,\downarrow,\uparrow,\downarrow\rangle$ and $|\uparrow,\uparrow,\downarrow,\downarrow\rangle$. All others can be constructed from the two by lattice translations. We exploit that the Hamilton operator commutates with the lattice translation. The lattice translation with periodic boundary conditions is a finite symmetry group with $\hat{T}^4 = \hat{1}$. Therefore, the eigenvalues of the translation operator are (see Eq. 9.5 of ΦSX:Quantum Physics[16])

$$s_\alpha = \mathrm{e}^{i\frac{2\pi}{4}\alpha} \qquad \text{with } \alpha = 0,1,2,3 \tag{17.99}$$

We can use the wave vectors $k_\alpha = \frac{2\pi}{a_{\mathrm{lat}}}\frac{\alpha}{4}$ as quantum numbers. a_{lat} is the lattice constant, i.e. the spacing of the spins.

An eigenstate is obtained via (Eq. 9.6 of ΦSX:Quantum Physics[16])

$$\sum_{j=0}^{N-1} \hat{T}^j|\chi\rangle s_\alpha^{-j} \tag{17.100}$$

Let me work out the eigenstates of the translation starting from the Neél state $|\chi\rangle = |\uparrow,\downarrow,\uparrow,\downarrow\rangle$. The eigenvalues are $s_\alpha = \exp(i\frac{2\pi}{4}\alpha) = i^\alpha$. I exploit that the translation $\hat{T}$ shifts the cyclic spin pattern by one bead to the right.

$$\begin{aligned}\sum_{j=0}^{3} \hat{T}^j|\uparrow,\downarrow,\uparrow,\downarrow\rangle(-i)^{j\alpha} &= |\uparrow,\downarrow,\uparrow,\downarrow\rangle + |\downarrow,\uparrow,\downarrow,\uparrow\rangle(-i)^\alpha + |\uparrow,\downarrow,\uparrow,\downarrow\rangle(-1)^\alpha + |\downarrow,\uparrow,\downarrow,\uparrow\rangle(+i)^\alpha \\ &= \begin{cases} 2\Big(|\uparrow,\downarrow,\uparrow,\downarrow\rangle + (-1)^{\alpha/2}|\downarrow,\uparrow,\downarrow,\uparrow\rangle\Big) & \text{for even } \alpha \\ |\varnothing\rangle & \text{for odd } \alpha \end{cases}\end{aligned} \tag{17.101}$$

I obtain four out of six states. The two missing two states require a different starting point. Therefore, I work out the eigenstates of the translation operator starting from the second independent state. Again, we shift the spin pattern successively to the right and multiply with the same factors as for the Neél state.

$$\sum_{j=0}^{3} \hat{T}^j |\uparrow,\uparrow,\downarrow,\downarrow\rangle (-i)^{j\alpha} = |\uparrow,\uparrow,\downarrow,\downarrow\rangle + |\downarrow,\uparrow,\uparrow,\downarrow\rangle (-i)^{\alpha} + |\downarrow,\downarrow,\uparrow,\uparrow\rangle (-1)^{\alpha} + |\uparrow,\downarrow,\downarrow,\uparrow\rangle (+i)^{\alpha} \tag{17.102}$$

Normalization of the two α-dependent eigenstates of the translation operator yields

$$\begin{aligned} |\Phi_1(\alpha)\rangle &\overset{\text{Eq. 17.101}}{=} \frac{1}{\sqrt{2}} \Big(|\uparrow,\downarrow,\uparrow,\downarrow\rangle + (-1)^{\alpha/2} |\downarrow,\uparrow,\downarrow,\uparrow\rangle \Big) \quad \text{for even } \alpha \\ |\Phi_2(\alpha)\rangle &\overset{\text{Eq. 17.102}}{=} \frac{1}{2} \Big(|\uparrow,\uparrow,\downarrow,\downarrow\rangle + |\downarrow,\uparrow,\uparrow,\downarrow\rangle (-i)^{\alpha} + |\downarrow,\downarrow,\uparrow,\uparrow\rangle (-1)^{\alpha} + |\uparrow,\downarrow,\downarrow,\uparrow\rangle (+i)^{\alpha} \Big) \end{aligned} \tag{17.103}$$

Energy eigenstates

With Eq. 17.88, the Hamilton operator has been written in the form Eq. 17.95, namely

$$\begin{aligned} \hat{H} &\overset{\text{Eq. 17.95}}{=} J\frac{\hbar^2}{4} \sum_{i,j \in \text{n.n.}} \Big[\hat{1} - 2 \cdot \underbrace{\frac{1}{2}\Big(\hat{\vec{\sigma}}_i \hat{\vec{\sigma}}_j + \hat{1} \Big)}_{\text{interchanges spins } i,j} \Big] \\ &= J\frac{\hbar^2}{4} \sum_{i=1}^{4} \Big[\hat{1} \cdot 2 - 4 \cdot \underbrace{\frac{1}{2}\Big(\hat{\vec{\sigma}}_i \hat{\vec{\sigma}}_{i+1} + \hat{1} \Big)}_{\text{interchanges spins } i,j} \Big] \\ &= 2J\hbar^2 \hat{1} - J\hbar^2 \sum_{i=1}^{4} \Big[\underbrace{\frac{1}{2}\Big(\hat{\vec{\sigma}}_i \hat{\vec{\sigma}}_j + \hat{1} \Big)}_{\text{interchanges spins } i,j} \Big] \end{aligned} \tag{17.104}$$

The energy expectation values of the two states are obtained using (1) the energy expectation values of the Ising model Eq. 17.93 and (2) the fact that a single exchange of a pair of spins does not produce any other of the contributions in the same symmetry eigenstate.

$$\langle \Phi_1(\alpha) | \hat{H} | \Phi_1(\alpha) \rangle = +2J\hbar^2 \qquad \text{and} \qquad \langle \Phi_2(\alpha) | \hat{H} | \Phi_2(\alpha) \rangle = 0 \tag{17.105}$$

The superposition $|\Phi_1(\alpha)\rangle$ of the two Neél states is lower in energy, because the exchange integral is negative for an antiferromagnet.

Specifically for even values of α, where $|\Phi_1(\alpha)\rangle$ exists, let me evaluate the Hamilton matrix element with $|\Phi_2(\alpha)\rangle$. We take the two contributions to $|\Phi_1(\alpha)\rangle$ and construct the new contributions by successively interchanging spins.

$$\begin{aligned} \hat{H}|\Phi_1(\alpha)\rangle &= |\Phi_1(\alpha)\rangle 2J\hbar^2 - \frac{1}{\sqrt{2}} \Bigg(\Big(|\downarrow,\uparrow,\uparrow,\downarrow\rangle + |\uparrow,\uparrow,\downarrow,\downarrow\rangle + |\uparrow,\downarrow,\downarrow,\uparrow\rangle + |\downarrow,\downarrow,\uparrow,\uparrow\rangle \Big) \\ &\qquad + (-1)^{\alpha/2} \Big(+ |\uparrow,\downarrow,\downarrow,\uparrow\rangle + |\downarrow,\downarrow,\uparrow,\uparrow\rangle + |\downarrow,\uparrow,\uparrow,\downarrow\rangle + |\uparrow,\uparrow,\downarrow,\downarrow\rangle \Big) \Bigg) J\hbar^2 \\ &= |\Phi_1(\alpha)\rangle 2J\hbar^2 - \frac{1}{\sqrt{2}} \Bigg(\underbrace{|\downarrow,\uparrow,\uparrow,\downarrow\rangle + |\uparrow,\uparrow,\downarrow,\downarrow\rangle + |\uparrow,\downarrow,\downarrow,\uparrow\rangle + |\downarrow,\downarrow,\uparrow,\uparrow\rangle}_{2|\Phi_2(\alpha)\rangle \text{ for } \alpha = 0} \Bigg) J\hbar^2 \underbrace{\Big(1 + (-1)^{\alpha/2} \Big)}_{=2\delta_{\alpha,0}} \\ &= |\Phi_1(\alpha)\rangle 2J\hbar^2 - |\Phi_2(\alpha)\rangle 2\sqrt{2} J\hbar^2 \delta_{\alpha,0} \end{aligned} \tag{17.106}$$

Thus, we obtain

$$\langle\Phi_2(\alpha)|\hat{H}|\Phi_1(\alpha)\rangle = -2\sqrt{2}J\hbar^2\delta_{\alpha,0} \tag{17.107}$$

For $\alpha = 0$ we need to diagonalize a 2×2-matrix

$$\begin{pmatrix} \langle\Phi_1(\alpha)|\hat{H}|\Phi_1(\alpha)\rangle & \langle\Phi_1(\alpha)|\hat{H}|\Phi_2(\alpha)\rangle \\ \langle\Phi_2(\alpha)|\hat{H}|\Phi_1(\alpha)\rangle & \langle\Phi_2(\alpha)|\hat{H}|\Phi_2(\alpha)\rangle \end{pmatrix} = 2J\hbar^2 \begin{pmatrix} 1 & -\sqrt{2}\delta_{\alpha,0} \\ -\sqrt{2}\delta_{\alpha,0} & 0 \end{pmatrix} \tag{17.108}$$

The eigenstates of this Hamiltonian is

$$\epsilon_\pm = \Big(\frac{1}{2} \pm \sqrt{\frac{9}{4}}\Big)2J\hbar^2 = J\hbar^2 \begin{cases} -2 & \text{for } \pm = + \\ 4 & \text{for } \pm = - \end{cases} \tag{17.109}$$

The energies for the $S_z = 0$ states of the Heisenberg chain with four beads and periodic boundary conditions are. (Note that J is negative for an antiferromagnet.)

$\epsilon/(J\hbar^2)$	4	2	0	0	0	-2
α	0	2	1	-1	2	0

GROUND STATE OF A LINEAR FOUR-SITE SPIN-$\frac{1}{2}$ ANTIFERROMAGNET

The ground state with energy $4J\hbar^2$ has the form

$$\begin{aligned} |\Psi_{\alpha=0,-}\rangle &= |\Phi_1(0)\rangle\sqrt{\frac{2}{3}} - |\Phi_2(0)\rangle\frac{1}{\sqrt{3}} \\ &= \Big(\underbrace{|\uparrow,\downarrow,\uparrow,\downarrow\rangle}_{\text{Neél state}} + \underbrace{|\downarrow,\uparrow,\downarrow,\uparrow\rangle}_{\text{Neél state}}\Big)\frac{1}{\sqrt{3}} \\ &\quad - \underbrace{\Big(|\uparrow,\uparrow,\downarrow,\downarrow\rangle + |\downarrow,\uparrow,\uparrow,\downarrow\rangle + |\downarrow,\downarrow,\uparrow,\uparrow\rangle + |\uparrow,\downarrow,\downarrow,\uparrow\rangle\Big)}_{\text{quantum fluctuations}}\frac{1}{2\sqrt{3}} \end{aligned} \tag{17.110}$$

This is the desired ground state.[a]

[a] This result matches the one given in van de Braak and Caspers[139]. Their Hamiltonian is $H = 2J\sum_{j=1}^{4}\vec{S}_j\vec{S}_{j+1}$. They obtain (their table 1) $\frac{E}{NJ} = -J$, where $N = 4$ is the number of sites.

The reason for doing this calculation was to demonstrate that the ground state differs considerably from the Neél state obtained from the Ising model. The ground state of the Heisenberg model actually obtains a considerable weight with parallel spins, which would seem unfavorable from the perspective of the Ising model.

From the perspective of the Hubbard model, the explanation is that electrons can delocalize onto the neighboring sites, if the electrons on those sites have opposite spin. In this way, the electrons can lower their kinetic energy at the cost of some loss of energy due to the Coulomb interaction. Interestingly, the admixture of the configurations with parallel spins does not depend on the size if the exchange parameter J, at least for the four-bead periodic Heisenberg chain.

17.3.4 Magnons

Ground state of a Ferromagnet

In contrast to the antiferromagnet, the ground state of a ferromagnet can be represented by a simple spin configuration, namely

$$\ldots,\uparrow,\uparrow,\uparrow,\uparrow,\uparrow,\ldots \tag{17.111}$$

The energy of the ferromagnetic state of a linear Heisenberg chain with N spin-$\frac{1}{2}$ beads is

$$\frac{1}{N}E \overset{\text{Eq. } 17.76}{=} J\frac{\hbar^2}{4} \tag{17.112}$$

A ferromagnet with N spin-$\frac{1}{2}$ beads has a total angular momentum of $\frac{N}{2}\hbar$. The spin in z-direction can therefore vary in steps of $\hbar$ from $-\frac{N}{2}\hbar$ to $+\frac{N}{2}\hbar$. Without changing the parallel alignment of spins, there are thus $2N+1$ distinct ferromagnetic states, which differ in the orientation of total spin.

Magnons, elementary excitations of a magnetic systems

I will be very brief on magnons. The main goal is to mention their existence. For the sake of simplicity, I will focus on a linear, ferromagnetic, spin-$\frac{1}{2}$ Heisenberg model. Magnons are not limited to ferromagnets and exist also for arbitrary spins.

Consider the excitations of the ferromagnet. The most elementary excitation seems to be the flip of a single spin. The resulting state $\hat{S}_{+,j}\big|\ldots,\downarrow,\downarrow,\downarrow,\ldots\big\rangle$ is not an eigenstate of a Hamiltonian.

In a translationally invariant system, we may use symmetry to block-diagonalize the Hamiltonian. In our simple example, this will suffice to produce eigenstates of the Hamiltonian. The eigenstates of the translation operator are Bloch states formed from spin-flips. For a cyclic chain with N beads, a state with a single magnon with wave vector $\vec{k}$ is

$$|\Phi_{\vec{k}}\rangle = \left(\frac{1}{\sqrt{N\hbar}}\sum_{j=1}^{N} \mathrm{e}^{i\vec{k}\vec{R}_j}\hat{S}_{+,j}\right) \underbrace{\big|\ldots,\downarrow,\downarrow,\downarrow,\ldots\big\rangle}_{\text{ferromagnetic ground state}} \tag{17.113}$$

$\big|\ldots,\downarrow,\downarrow,\downarrow,\ldots\big\rangle$ is the ferromagnetic state of down spins. The states in Eq. 17.113 are single-magnon states.

Beyond single-magnon states, we can also envisage states with several coexisting magnons. In order to describe those states, we may introduce a magnon-creation operator

$$\hat{m}^\dagger_{\vec{k}} = \frac{1}{\sqrt{N\hbar}}\sum_{j=1}^{N} \mathrm{e}^{i\vec{k}\vec{R}_j}\hat{S}_{+,j} \tag{17.114}$$

A magnon in a spin-$\frac{1}{2}$ system carries a spin of $\hbar$ corresponding to a flip of a spin-$\frac{1}{2}$. The spin density of a single magnon

$$\vec{S}(r_j) = \langle\ldots,\uparrow,\uparrow,\uparrow,\ldots|\hat{m}_{\vec{k}}\hat{\vec{S}}_j\hat{m}^\dagger_{\vec{k}}|\ldots,\uparrow,\uparrow,\uparrow,\ldots\rangle \tag{17.115}$$

is constant in space. [18] Magnons have a dispersion relation $\epsilon(\vec{k})$ just as electrons, phonons, photons etc. A magnon wave packet describes a spin density moving with velocity $\vec{v} = \frac{1}{\hbar}\vec{\nabla}_k\epsilon(\vec{k})$.

[18] Thus, magnons shall not be confused with spin waves.

Editor: The following equations need to be checked!

$$
\begin{aligned}
&\hat{H}\hat{m}_{\vec{k}}|\ldots,\uparrow,\uparrow,\uparrow,\ldots\rangle \\
&= -\sum_n J\hat{\vec{S}}_n\hat{\vec{S}}_{n+1}\left(\frac{1}{\sqrt{N\hbar}}\sum_{j=1}^{N}\mathrm{e}^{i\vec{k}\vec{R}_j}\hat{S}_{+j}\right)|\ldots,\uparrow,\uparrow,\uparrow,\ldots\rangle \\
&= -J\Bigg(\frac{1}{\sqrt{N\hbar}}\sum_{j=1}^{N}\mathrm{e}^{i\vec{k}\vec{R}_j}\underbrace{\left(\frac{1}{2}\left(\hat{S}_{n,+}\hat{S}_{n+1,-}+\hat{S}_{n,-}\hat{S}_{n+1,+}\right)+\hat{S}_{n,z}\hat{S}_{n+1,z}\right)}_{\hat{\vec{S}}_n\hat{\vec{S}}_{n+1}}\hat{S}_{+j}\Bigg)|\ldots,\uparrow,\uparrow,\uparrow,\ldots\rangle \\
&= -J\hbar^2\Bigg(\frac{1}{\sqrt{N\hbar}}\sum_{j=1}^{N}\mathrm{e}^{i\vec{k}\vec{R}_j}\Big[\frac{1}{2}\left(\hat{S}_{j-1,+}+\hat{S}_{j+1,+}\right)+\underbrace{\sum_n\frac{1}{4}(1-2\delta_{n,j}-2\delta_{n+1,j})}_{\frac{1}{4}(N-4)}\hat{S}_{+j}\Big]|\ldots,\uparrow,\uparrow,\uparrow,\ldots\rangle \\
&= \left(\frac{1}{\sqrt{N\hbar}}\sum_{j=1}^{N}\mathrm{e}^{i\vec{k}\vec{R}_j}\hat{S}_{+j}\right)|\ldots,\uparrow,\uparrow,\uparrow,\ldots\rangle\left(-\hbar^2J\left[\frac{1}{2}\left(\mathrm{e}^{-i\vec{k}a_{\mathrm{lat}}}+\mathrm{e}^{+i\vec{k}a_{\mathrm{lat}}}\right)+\frac{1}{4}(N-4)\right]\right) \qquad (17.116)
\end{aligned}
$$

Thus we obtain the dispersion relation.

$$\epsilon(k) = -\hbar^2 J\Big(\cos(k a_{\mathrm{lat}}) - 1\Big) \qquad (17.117)$$

Interestingly the dispersion relation is quadratic at the origin, which implies that magnons in a linear chain behave like particles having a mass.

For the difference between magnons and spinons, it may be useful to read *"Nature of spinons in the 1D spin chains"* by Teresa Kulka, Milosz Panfil, Mona Berciu, Krzysztof Wohlfeld arXiv:2303.02276, respectively `https://doi.org/10.48550/arXiv.2303.02276`

17.4 Anderson impurity model

Editor: See also https://ocw.mit.edu/courses/physics/8-512-theory-of-solids-ii-spring-2009/lecture-notes/

Editor: For the Abrikosov-Suhl resonance see the paper on the "asymmetric single impurioty andersen model" by Meyer, Wegner, Pothoff and Nolting.[140]. See also the article "Spectroscopic Properties of Mixed-Valence Compounds in the Impurity model" nby Kurt Schoenhammer, http://www.cond-mat.de/events/correl15.

The **single-impurity Anderson model (SIAM)**[67], named after its inventor P.W. Anderson[19], describes an impurity with a large onsite Coulomb repulsion, which is embedded in a normal (non-interacting) metal. This model explains the formation of a local magnetic moment on the impurity atom[67], the **Kondo effect** and **heavy fermions**.

The resistivity of normal metals falls off with lowering temperature proportional to T^5 because the phonons, which are the scattering centers for electrons, freeze out. In the 1930s, a different behavior has been observed in metals such as Cu, Ag, and Au, when they contain a very dilute concentration of magnetic impurities such as Mn, Co, Fe. In these materials, the resistivity passes through a minimum at about 10-20 K and then rises again with lower temperature.["Lecture note on Kondo Effect Solid-State Physics" by Masatsugu Sei Suzuki www.researchgate.net/publication/278020920] In 1964, Ju Kondo explained this by a many-particle effect, which couples the spin of the impurity to the conduction electrons.

The Anderson Hamiltonian has the form

$$\begin{aligned} H &= \underbrace{\sum_{\sigma\in\{\uparrow,\downarrow\}} \epsilon_d \hat{d}^\dagger_\sigma \hat{d}_\sigma + U \sum_{\sigma,\sigma'\in\{\uparrow,\downarrow\}} \hat{d}^\dagger_\sigma \hat{d}^\dagger_{\sigma'} \hat{d}_{\sigma'} \hat{d}_\sigma}_{\text{impurity}} + \underbrace{\sum_k \sum_{\sigma\in\{\uparrow,\downarrow\}} \epsilon_k \hat{c}^\dagger_{k,\sigma} \hat{c}_{k,\sigma}}_{\text{normal metal}} \underbrace{-\Delta \sum_k \sum_{\sigma\in\{\uparrow,\downarrow\}} \left(\hat{c}^\dagger_{k,\sigma} \hat{d}_\sigma + \hat{d}^\dagger_\sigma \hat{c}_{k,\sigma} \right)}_{\text{hybridization}} \\ &= \sum_{\sigma\in\{\uparrow,\downarrow\}} \epsilon_d \hat{n}_{d,\sigma} + U \hat{n}_{d,\uparrow} \hat{n}_{d,\downarrow} + \sum_k \sum_{\sigma\in\{\uparrow,\downarrow\}} \epsilon_k \hat{n}_{k,\sigma} - \Delta \sum_k \sum_{\sigma\in\{\uparrow,\downarrow\}} \left(\hat{c}^\dagger_{k,\sigma} \hat{d}_\sigma + \hat{d}^\dagger_\sigma \hat{c}_{k,\sigma} \right) \end{aligned} \tag{17.118}$$

1. The first term describes the local impurity with a large Coulomb interaction.[20] Here, we use the symbol $\hat{d}^\dagger$ and $\hat{d}$ for the creation and annihilation operators on the impurity. In other places the symbols $\hat{f}^\dagger$ and $\hat{f}$ are used in the same place. The letters derive from the d-electrons of transition metal atoms and the f-electrons of lanthanides and actinides.

2. The second term in Eq. 17.118 describes the normal metal in terms of the Bloch states and their creation and annihilators $\hat{c}^\dagger_k$ and $\hat{c}_k$.[21]

3. The third term describes the coupling between the impurity and the band states.

The Anderson model includes normal metal states also at the site of the impurity. This makes sense because also a transition metal has s- and p-electrons.

Editor: Read the report of Piers Coleman![141]. Schrieffer-Wolff transformation[142].

17.4.1 Anderson dimer

The key features of the Anderson impurity model are already present in the Anderson dimer, an asymmetric two-site molecule in which an electron with an onsite Coulomb interaction is coupled to an atom without a Coulomb interaction.

The detailed calculations have been performed in appendix D.3 on p. 540. The model has been presented earlier by Fulde and Zwicknagel[143, 144] (See also section 12.1 of [5]) See also Fig. 1 and

[19] P.W. Anderson, American physicist born 1923. Obtained the Nobel price in physics 1977.

[20] For the second form of the Coulomb interaction term see Eq. 17.49.

[21] Usually, I use the symbol $\hat{a}^\dagger$ and $\hat{a}$ for the natural orbitals $\hat{c}^\dagger_k$ and $\hat{c}_k$ for local orbitals. Here, the symbol "c" stands for "conduction electrons".

2 of Eva Pavarini chapter 11*"Dynamical Mean-Field Theory for Materials"* in *Many-Body Methods for Real materials* Schriftenreihe de Forschungszentrums Jülich, Reihe Modeling and Simulation, Vol. 9 (2019), `https://www.cond-mat.de/events/correl19/manuscripts/correl19.pdf`

The Anderson dimer is obtained by limiting the sum over the conduction states in Eq. 17.118 to a single spatial orbital. The Hamiltonian of the Anderson dimer is [22]

$$\begin{aligned}\hat{H} &= \underbrace{\sum_{\sigma\in\{\uparrow,\downarrow\}} \epsilon_f \hat{f}^\dagger_\sigma \hat{f}_\sigma + \frac{1}{2}U \sum_{\sigma,\sigma'\in\{\uparrow,\downarrow\}} \hat{f}^\dagger_\sigma \hat{f}^\dagger_{\sigma'} \hat{f}_{\sigma'} \hat{f}_\sigma}_{\text{impurity}} + \underbrace{\sum_{\sigma\in\{\uparrow,\downarrow\}} \epsilon_c \hat{c}^\dagger_\sigma \hat{c}_\sigma}_{\text{host}} \underbrace{-t \sum_{\sigma\in\{\uparrow,\downarrow\}} \left(\hat{f}^\dagger_\sigma \hat{c}_\sigma + \hat{c}^\dagger_\sigma \hat{f}_\sigma\right)}_{\text{hopping}} \\ &= \sum_{\sigma\in\{\uparrow,\downarrow\}} \epsilon_f \hat{f}^\dagger_\sigma \hat{f}_\sigma + \underbrace{\frac{1}{2}U \sum_{\sigma\in\{\uparrow,\downarrow\}} \hat{f}^\dagger_\sigma \hat{f}_\sigma \left(\hat{f}^\dagger_\sigma \hat{f}_\sigma - 1\right)}_{\text{self-interaction}} + \sum_\sigma \epsilon_c \hat{c}^\dagger_\sigma \hat{c}_\sigma - t \sum_\sigma \left(\hat{f}^\dagger_\sigma \hat{c}_\sigma + \hat{c}^\dagger_\sigma \hat{f}_\sigma\right) \\ &\quad + U \hat{f}^\dagger_\uparrow \hat{f}_\uparrow \hat{f}^\dagger_\downarrow \hat{f}_\downarrow \end{aligned} \tag{17.120}$$

In the following, I will ignore the self-interaction term, which is common practice.

The interesting case is $\epsilon_f < \epsilon_c$ and $\epsilon_f + U > \epsilon_c$ with $N = 2$ particles. We consider all states because the states $N = 1$ and $N = 3$ will be required to evaluate the spectral properties.

As in the Hubbard dimer, the ground state of the Anderson dimer is made from the four Slater determinants with one electron on the impurity and one in the bath. Three of these states, $\hat{f}^\dagger_\uparrow \hat{c}^\dagger_\uparrow |\mathcal{O}\rangle$, $\hat{f}^\dagger_\downarrow \hat{c}^\dagger_\downarrow |\mathcal{O}\rangle$ and $\frac{1}{\sqrt{2}}\left(\hat{f}^\dagger_\uparrow \hat{c}^\dagger_\downarrow - \hat{f}^\dagger_\downarrow \hat{c}^\dagger_\uparrow\right)|\mathcal{O}\rangle$, have parallel spin and form a triplet. The remaining singlet state with opposite spin is lower in energy because each electron can delocalize onto the neighboring site. This singlet state is the ground state for the Anderson dimer with two electrons.

The singlet-triplet splitting is related to the Kondo temperature. While the spins of impurity and the host are antiferromagnetically coupled, the spin pairs are broken up above the Kondo temperature.

In order to visualize these states it is helpful to inspect the quasi-particle states for one broken-symmetry state of the singlet state. These quasi-particle levels for the one-particle excitations out of the two-electron ground state are shown in fig. 17.10.Editor: These states have been derived using a `Figs/Codes/Kondo/src`

The lowest quasi-particle level describes the filled impurity orbital, analogous to the lower Hubbard band in the Hubbard model. Similarly the uppermost quasi-particle describes the empty impurity orbital, analogous to the upper Hubbard band of the Hubbard model. It is shifted up in energy because adding an electron $d^1 \to d^2$ into this orbital requires to overcome the Coulomb repulsion to the electron already residing on the impurity.

In between the two impurity states are the two states of the bath. As these states also have a contribution on the impurity, they result in a third peak in the density of states projected onto the impurity. These two states correspond to the so-called **Abrikosov-Suhl resonance** [123, 124] or **Kondo resonance**.

The quasi-particles are shown for only one of the two broken-symmetry state of the two-particle ground state. The other is obtained by reverting both spins.

Kondo effect: The lowest two-particle excitation lifts an electron within the **Abrikosov-Suhl resonance** [123, 124] from a filled to an empty quasi-particle level. The electron-hole interaction is neglected.) This turns the singlet into a triplet state. This is a very low-energy excitation, which can

[22]

$$\begin{aligned}\frac{1}{2}\sum_{\sigma,\sigma'\in\{\uparrow,\downarrow\}} \hat{f}^\dagger_\sigma \hat{f}^\dagger_{\sigma'} \hat{f}_{\sigma'} \hat{f}_\sigma &= -\frac{1}{2}\sum_{\sigma,\sigma'\in\{\uparrow,\downarrow\}} \hat{f}^\dagger_\sigma \hat{f}^\dagger_{\sigma'} \hat{f}_\sigma \hat{f}_{\sigma'} = -\frac{1}{2}\sum_{\sigma,\sigma'\in\{\uparrow,\downarrow\}} \left(\delta_{\sigma,\sigma'} \hat{f}^\dagger_\sigma \hat{f}_{\sigma'} - \hat{f}^\dagger_\sigma \hat{f}_\sigma \hat{f}^\dagger_{\sigma'} \hat{f}_{\sigma'}\right) = \frac{1}{2}\sum_{\sigma,\sigma'\in\{\uparrow,\downarrow\}} \hat{f}^\dagger_\sigma \hat{f}_\sigma \hat{f}^\dagger_{\sigma'} \hat{f}_{\sigma'} - \frac{1}{2}\sum_{\sigma\in\{\uparrow,\downarrow\}} \hat{f}^\dagger_\sigma \hat{f}_\sigma \\ &= \hat{n}_\uparrow \hat{n}_\downarrow + \sum_{\sigma\in\{\uparrow,\downarrow\}} \left(\hat{n}^2_\sigma - \hat{n}_\sigma\right)\end{aligned} \tag{17.119}$$

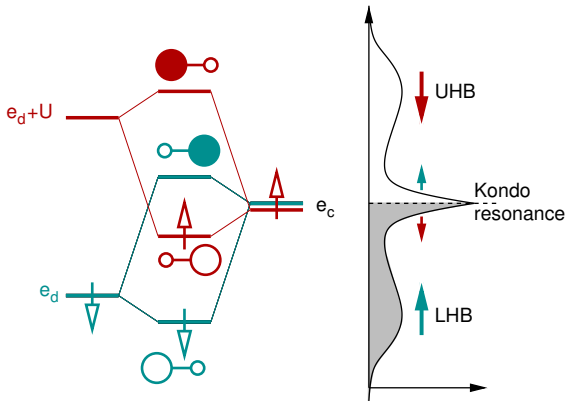


Fig. 17.10: Schematic diagrams of the spectral function of the Anderson dimer. The left graph indicates the quasi-particle states, while the right graph represents the spectral function in a solid. The Anderson impurity has an orbital energy ϵ_d and a Coulomb repulsion U. The orbital representing the conduction electrons of the host crystal is ϵ_c. The upper and lower Hubbard bands are denoted by UHB and LHB. The two states in the middle are responsible for the **Abrikosov-Suhl** [123, 124] (or Kondo resonance). Only one broken-symmetry state is shown. The ground state is the singlet formed from this broken-symmetry state and its partner obtained by reversing all spins.

be described by the **Kondo model**.

$$\begin{aligned}\hat{H} &= \sum_{k,\sigma} \epsilon_{k,\sigma} \hat{c}^\dagger_{k,\sigma} \hat{c}_{k,\sigma} + J \sum_k \begin{pmatrix} \hat{c}^\dagger_{k,\uparrow} \\ \hat{c}^\dagger_{k,\downarrow} \end{pmatrix} \begin{pmatrix} S_z & S_x - iS_y \\ S_x + iS_y & -S_z \end{pmatrix} \begin{pmatrix} \hat{c}_{k,\uparrow} \\ \hat{c}_{k,\downarrow} \end{pmatrix} \\ &= \sum_{k,\sigma} \epsilon_{k,\sigma} \hat{n}_{k,\sigma} + J \hat{\vec{s}}_{k,\sigma} \hat{\vec{S}} \end{aligned} \tag{17.121}$$

Here, $\hat{\vec{s}}$ describes the spin of the conduction electrons, while $\vec{S}$ is the spin on the impurity.

Just like the Heisenberg model describes the low-energy excitation of the Hubbard model for strong interactions, the Kondo model describes the low-energy physics of the Anderson impurity model.

Below the Kondo temperature $k_B T_K \sim \frac{\Delta^2}{(\epsilon_c - \epsilon_d)}$, only the singlet is present in the thermal ensemble, while the triplet states are absent.

Two-particle channel

Spectrum

When we investigate the spectra for adding and removing electrons, we can use Lehman representation. Let me use the ground singlet ground state which is a superposition of three Slater derminants with coefficients A, B, C.

$$|\Phi_s\rangle = \left[\hat{f}^\dagger_\uparrow \hat{f}^\dagger_\downarrow A + \hat{c}^\dagger_\uparrow \hat{c}^\dagger_\downarrow B + \frac{1}{\sqrt{2}} \left(\hat{f}^\dagger_\uparrow \hat{c}^\dagger_\downarrow + \hat{f}^\dagger_\downarrow \hat{c}^\dagger_\uparrow \right) C \right] |\mathcal{O}\rangle \tag{17.122}$$

with energy E_s.

For $\epsilon_c = 0$, $\epsilon_f = -1$, $U = 2$, $t = \frac{1}{2}$, I obtain (without full diagonalization of the $N = 2, S = 0$ channel)

ϵ	ψ_{qp}	
-1.048	$\|f,\sigma\rangle 0.68 + \|c,\sigma\rangle 0.06$	$f^1 \to f^0$
-0.029	$\|f,\sigma\rangle 0.20 + \|c,\sigma\rangle 0.70$	$f^1 \to f^0$
+0.029	$\|f,\sigma\rangle 0.20 - \|c,\sigma\rangle 0.70$	$f^0 \to f^1$
+1.048	$\|f,\sigma\rangle 0.68 - \|c,\sigma\rangle 0.06$	$f^0 \to f^1$

$$\begin{aligned}
\hat{f}^\dagger_\uparrow|\Psi_s\rangle &= \left[\hat{f}^\dagger_\uparrow\hat{c}^\dagger_\uparrow\hat{c}^\dagger_\downarrow b - \frac{1}{\sqrt{2}}\hat{f}^\dagger_\uparrow\hat{f}^\dagger_\downarrow\hat{c}^\dagger_\uparrow c\right]|\mathcal{O}\rangle \\
\hat{f}^\dagger_\downarrow|\Psi_s\rangle &= \left[\hat{f}^\dagger_\downarrow\hat{c}^\dagger_\uparrow\hat{c}^\dagger_\downarrow b - \frac{1}{\sqrt{2}}\hat{f}^\dagger_\uparrow\hat{f}^\dagger_\downarrow\hat{c}^\dagger_\downarrow c\right]|\mathcal{O}\rangle \\
\hat{c}^\dagger_\uparrow|\Phi_s\rangle &= \left[\hat{f}^\dagger_\uparrow\hat{f}^\dagger_\downarrow\hat{c}^\dagger_\uparrow a - \hat{f}^\dagger_\uparrow\hat{c}^\dagger_\uparrow\hat{c}^\dagger_\downarrow\frac{c}{\sqrt{2}}\right]|\mathcal{O}\rangle \\
\hat{c}^\dagger_\downarrow|\Psi_s\rangle &= \left[\hat{f}^\dagger_\uparrow\hat{f}^\dagger_\downarrow\hat{c}^\dagger_\uparrow a - \hat{f}^\dagger_\downarrow\hat{c}^\dagger_\uparrow\hat{c}^\dagger_\uparrow\frac{c}{\sqrt{2}}\right]|\mathcal{O}\rangle
\end{aligned} \tag{17.123}$$

Increasing the temperature reduces the singlet occupation which results in larger resistance.

Kondo Resonance=Abrikosov-Suhl resonance.

17.4.2 Weak-contact limit of the Anderson impurity model

In this section, I investigate a multi-orbital, interacting impurity in contact with a non-interacting metallic environment. The Hamiltonian does not include any coupling, but the two systems can exchange particles.

The origin of this model was our finding of impurity levels that are pinned at the Fermi level.

Editor: Note, that this is a mean-field model!!!

The model describes an atom with M degenerate, but strongly interacting orbitals, which is in weak contact with a metal. The metal is described by a featureless density of states with value D

Consider an atom with localized d-orbitals in contact with a metal. The total energy is

$$E[\vec{n}] = \underbrace{\int_0^{\epsilon_F(N_d)} d\epsilon\; D\;\epsilon}_{\text{energy } E_m \text{ of normal metal}} + \sum_{i=1}^{M}\epsilon_d n_i + \underbrace{\frac{1}{2}U\sum_{i,j=1}^{M} n_i n_j}_{\text{Hartree}} \underbrace{-\frac{1}{2}\alpha U\sum_{i=1}^{M} n_i^2}_{\text{Exchange}} \tag{17.124}$$

The energy $-\frac{N_{tot}}{2D}$ of the normal metal with the Fermi level at zero has been subtracted.

The density of states of the normal metal is $D(\epsilon) = D\theta(\epsilon - N_{\rm tot}/D)$, where $\theta(x)$ is the Heaviside step function. U is the Coulomb repulsion between the electrons on the atom and α is a screening factor for screened exchange. With $N_d = \sum_i n_i$, I denote the number of electrons in the d-shell, while n_i are orbital occupations. M is the degeneracy of the d-shell. ($M = 10$ for d-electrons and $M = 14$ for f-electrons.) With N_m I denote the number of electrons in the normal metal. Thus, the total number of electrons is $N_{\rm tot} = N_m + N_d$.

The Fermi level in the metal is determined by the global charge neutrality, i.e. $N_m + N_d = N_{\rm tot}$. Thus,

$$\begin{aligned}
N_m &= \int_{-N_{\rm tot}/D}^{\epsilon_F} d\epsilon\; D = D\cdot(\epsilon_F + N_{\rm tot}/D) \\
\Rightarrow \qquad \epsilon_F &= -\frac{N_{\rm tot}}{D} + \frac{N_m}{D} \quad \overset{N_d+N_m=N_{\rm tot}}{=} \quad -\frac{N_d}{D}
\end{aligned} \tag{17.125}$$

This says that the Fermi level is zero, when all atoms are in the normal metal. When electrons are transferred to the impurity the Fermi level shifts downward in energy.

The energy of the metal is

$$E_m = \int_0^{\epsilon_F(N_d)} d\epsilon \; D \; \epsilon = \frac{N_d^2}{2D} \tag{17.126}$$

The energy functional as function of the occupations of the impurity levels is

$$\begin{aligned} E[\vec{n}] &= \underbrace{\frac{N_d^2}{2D}}_{E_m} + \epsilon_d N_d + \frac{1}{2} U N_d^2 - \frac{1}{2}\alpha U \sum_i n_i^2 \\ &= \epsilon_d N_d + \frac{1}{2}\Big(U + D^{-1}\Big) N_d^2 - \frac{1}{2}\alpha U \sum_i n_i^2 \end{aligned} \tag{17.127}$$

Now we consider the case that at most one orbital has fractional occupation. We introduce the number N_d^{full} of completely filled states, and the occupation n_{frac} of the partially filled orbital, so that $N_d = N_d^{full} + n_{frac}$

$$\begin{aligned} E[N_d^{full}, n_{frac}] &= \epsilon_d\Big(N_d^{full} + n_{frac}\Big) + \frac{1}{2}\Big(U + \frac{1}{D}\Big)\Big(N_d^{full} + n_{frac}\Big)^2 - \frac{1}{2}\alpha U\Big(N_d^{full} + n_{frac}^2\Big) \\ &= \epsilon_d\Big(N_d^{full} + n_{frac}\Big) + \frac{1}{2}\Big(U + \frac{1}{D}\Big)\Big(N_d^{full} + n_{frac}\Big)^2 - \frac{1}{2}\alpha U\Big(N_d^{full} + n_{frac}\Big) - \frac{1}{2}\alpha U\Big(n_{frac}^2 - n_{frac}\Big) \\ &= \Big(\epsilon_d - \frac{1}{2}\alpha U\Big) N_d + \frac{1}{2}\Big(U + \frac{1}{D}\Big) N_d^2 - \frac{1}{2}\alpha U\Big(n_{frac}^2 - n_{frac}\Big) \end{aligned} \tag{17.128}$$

where $N_d = N_d^{full} + n_{frac}$.

The occupation n_{frac} is given by the equilibrium condition

$$\begin{aligned} 0 = \frac{\partial E}{\partial n_{frac}} &= \Big(\epsilon_d - \frac{1}{2}\alpha U\Big) + \Big(U + \frac{1}{D}\Big) N_d - \frac{1}{2}\alpha U\Big(2 n_{frac} - 1\Big) \\ &= \epsilon_d + \Big(U + \frac{1}{D}\Big) N_d - \alpha U n_{frac} \\ \Rightarrow \qquad n_{frac} &= \frac{\epsilon_d + \Big(U + \frac{1}{D}\Big) N_d}{\alpha U} \end{aligned} \tag{17.129}$$

The equilibrium condition implies that the Fermi level of the metal coincides with the partially filled d-level.

A partially filled d-level is present, when

$$\begin{aligned} 0 < n_{frac} &< 1 \\ \Rightarrow \qquad 0 < \epsilon_d + \left(U + \frac{1}{D}\right) N_d &< \alpha U \\ \Rightarrow \qquad -U N_d - \frac{N_d}{D} < \epsilon_d &< -U(N_d - \alpha) - \frac{N_d}{D} \end{aligned} \tag{17.130}$$

This implies that

- for $\alpha = 0$, which corresponds to DFT, there is no pinning at the Fermi level. The state crosses the Fermi level for one specific ϵ_d.
- for $\alpha = 1$, which corresponds to a Hartree-Fock calculation, there is always one level pinned at the Fermi level.
- For a partially screened exchange, i.e. for α between zero and one, there are energy regions for which pining occurs and other where it does not

The term $\Delta E = -\frac{1}{2}\alpha U\Big(n_{frac}^2 - n_{frac}\Big)$ vanishes for integer occupations, that is for $n_{frac} = 0$ and for $n_{frac} = 1$. I counteracts the curvature of $E(N_d)$ obtained from the mean-field expression ($\alpha = 0$), however the remaining curvature does not vanish. For each integer occupation, there is a kink in the $E(N_d)$ curve. This implies that as function of ϵ_d, there is a range of ϵ_d values for which the occupation is integer. However, there is also an intermediate range, where one orbital is fractional.

Thus, if ϵ_d falls accidentally into this intermediate range, we will find three orbital energies, one for the filled states, one for the empty states, and a third energy level, which is pinned at the Fermi level.

17.5 Holstein model for polarons

The **Holstein model** is a classical model for the investigation of polarons and in particular small polarons.[145, 146]

A polaron is a quasi-particle consisting of an electron and a lattice deformation, speak a phonon. The bound pair of an electron and a phonon can migrate throughout the crystal as a unit. Similar to any other bound pair it can be broken up by its excitations into its constituents.

When the lattice is only weakly deformed by the charge of the electron, a so-called **large polaron** is formed, also called a Fröhlich polaron. The other extreme is the **small polaron**, where the lattice distortion is very localized around the electron.

For the conversion of the Hamiltonian expressed in terms of atomic and electron positions into one given in electrons and phonons is given in Eq. **??** in chapter **??** of ΦSX: Introduction to Solid-State Theory.[1]

The Hamiltonian of electrons coupled coupled linearly to phonons is

$$\hat{H} = \underbrace{\sum_j \frac{\hat{p}_j^2}{2M_j} + \frac{1}{2}\sum_{i,j} \hat{u}_i C_{i,j} \hat{u}_j}_{\text{phonons}} + \underbrace{\sum_{\alpha,\beta} h_{\alpha,\beta} \hat{c}_\alpha^\dagger \hat{c}_\beta}_{\text{electrons}} - \underbrace{\sum_{j,\alpha,\beta} \gamma_{j,\alpha,\beta} \hat{x}_j \hat{c}_\alpha^\dagger \hat{c}_\beta}_{\text{e-ph coupling}} \tag{17.131}$$

$\hat{u}_j$ is the displacement vectors of the atom at positions $\vec{R}_j$ in direction $\nu_j \in \{x, y, z\}$. Thus, $j = (R_j, \nu_j)$ is a composite index of site and polarization. $\hat{p}_j$ is the canonical momenta of $\hat{u}_j$, i.e.

$$[\hat{p}_j, \hat{u}_{j'}]_- = \frac{\hbar}{i}\delta_{j,j'} \tag{17.132}$$

Both, $\hat{p}_j$ and $\hat{u}_j$ are operators in the Hilbert space of lattice displacements. With M_j, I denote the atomic masses and $C_{i,j}$ the force constants. The electrons are described in a one-particle basisset of spin-orbitals $|\chi_\alpha\rangle$ with the creation and annihilation operators $\hat{c}_\alpha^\dagger$ and $\hat{c}_\alpha$. $h_{\alpha,\beta}$ are the one-particle Hamilton matrix elements.

Note that the operators $\hat{u}_j, \hat{p}_j$ on the one side and $\hat{c}_\alpha^\dagger, \hat{c}_\alpha$ act on different Hilbert/Fock spaces.

In the Holstein model several simplifications are made.

- The phonons are local and only a single phonon mode is considered per site.
- The electron Hamiltonian is limited to nearest neighbor hopping with hopping parameter t. The atomic level $\bar{\epsilon}$ is set to zero
- All atoms are identical.

Using the local approximation is analogous in spirit to the Hubbard model.

The Holstein Hamiltonian has the form

$$\hat{H} = \underbrace{\sum_j \frac{\hat{p}_j^2}{2M} + \frac{1}{2}M\omega^2\hat{u}_j^2}_{\text{phonons}} + \underbrace{\sum_{(j,j')\in n.n}\sum_{\sigma\in\{\uparrow,\downarrow\}} t\left(\hat{c}_{j,\sigma}^\dagger \hat{c}_{j',\sigma} + \hat{c}_{j',\sigma}^\dagger \hat{c}_{j,\sigma}\right)}_{\text{electrons}} - \underbrace{\sum_j \gamma \hat{u}_j \hat{c}_{j,\sigma}^\dagger \hat{c}_{j,\sigma}}_{\text{e-ph coupling}} \tag{17.133}$$

Let me write down the same Hamiltonian in terms of phonon creation and annihilation operators (See Eq. 5.32 and Eq. 5.33 in section 5.6 of ΦSX: Quantum Physics[16])

$$\hat{b}_j \overset{\text{def}}{=} \frac{M\omega\hat{u}_j + i\hat{p}_j}{\sqrt{2M\hbar\omega}} \qquad \text{and} \qquad \hat{b}_j^\dagger \overset{\text{def}}{=} \frac{M\omega\hat{u}_j - i\hat{p}_j}{\sqrt{2M\hbar\omega}} \tag{17.134}$$

which yields

$$\hat{H} = \underbrace{\sum_j \hbar\omega\left(\hat{b}_j^\dagger\hat{b}_j + \frac{1}{2}\right)}_{\text{phonons}} + \underbrace{\sum_{\substack{(j,j')\in n.n \\ \sigma\in\{\uparrow,\downarrow\}}} t\left(\hat{c}_{j,\sigma}^\dagger \hat{c}_{j',\sigma} + \hat{c}_{j',\sigma}^\dagger \hat{c}_{j,\sigma}\right)}_{\text{electrons}} - \underbrace{\sum_j \hbar\omega\Gamma\left(\hat{b}_j^\dagger + \hat{b}_j\right)\hat{c}_{j,\sigma}^\dagger \hat{c}_{j,\sigma}}_{\text{e-ph coupling}} \tag{17.135}$$

where $\hbar\omega\Gamma \stackrel{\text{def}}{=} \frac{\hbar\gamma}{\sqrt{2M\hbar\omega}}$

17.5.1 Holstein monomer

A physical realization of a single Holstein monomer is a diatomic molecule with a variable bond length $d = d_0 + u$ as sketched in fig. 17.11. The Holstein model only considers the antibonding orbital of that molecule. If an electron is added to the antibond, the bond distance expands and the molecule vibrates around a new equilibrium distance.

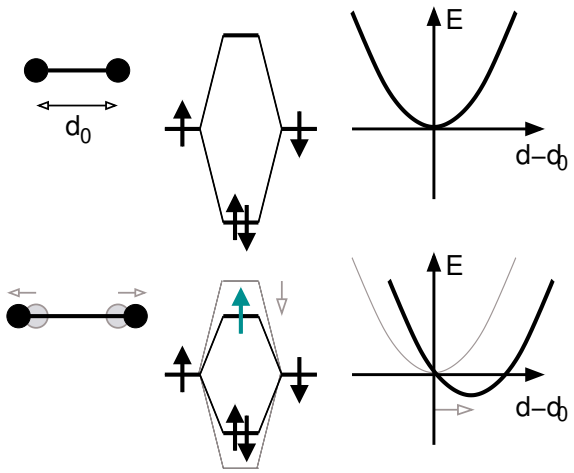


Fig. 17.11: The monomer of the Holstein model consists of a single electron orbital coupled to a single local harmonic oscillator. The electron orbital could be the antibonding state of a molecule and harmonic oscillator could be a molecular bond-length vibration. The excitations of the harmonic oscillator represent phonons. The electron-phonon coupling describes that the bond expands, when an electron is placed into the antibonding orbital.

The Hamiltonian has the form

$$\begin{aligned}\hat{H} &= \underbrace{\frac{\hat{p}^2}{2M} + \frac{1}{2}M\omega^2\hat{u}^2}_{\text{phonon}} \underbrace{- \gamma\hat{u}\sum_\sigma \hat{n}_\sigma}_{\text{e-ph coupling}} \\ &= \underbrace{\hbar\omega\left(\hat{b}^\dagger\hat{b} + \frac{1}{2}\right)}_{\text{phonons}} - \hbar\omega\Gamma\left(\hat{b}^\dagger + \hat{b}\right)\sum_\sigma \hat{n}_\sigma \end{aligned} \tag{17.136}$$

Firsov-Lang transformation: We can change from a representation of electrons and phonons to one of polarons and free phonons. The polarons replace the electrons. In contrast to the electrons, however, they receive an effective interaction, which is mediated via the phonons: One electron distorts the lattice, and the other profits from the distortion. This is the result of the so-called **Firsov-Lang transformation**[147].

The principle of the Firsov-Lang approximation can be demonstrated already on the level of the Holstein monomer. The Hamiltonian of the Holstein monomer can be transformed onto a new set of coordinates.

$$\begin{aligned}\hat{H} &= \hbar\omega\left(\hat{B}^\dagger\hat{B} + \frac{1}{2}\right) - \hbar\omega\Gamma^2\left(\sum_\sigma \hat{A}_\sigma^\dagger\hat{A}_\sigma\right)^2 \\ &= \hbar\omega\left(\hat{B}^\dagger\hat{B} + \frac{1}{2}\right) - \hbar\omega\Gamma^2\sum_\sigma \hat{A}_\sigma^\dagger\hat{A}_\sigma - 2\hbar\omega\Gamma^2\hat{A}_\uparrow^\dagger\hat{A}_\uparrow\hat{A}_\downarrow^\dagger\hat{A}_\downarrow \end{aligned} \tag{17.137}$$

The amplitudes $\hat{B}$ of the free phonons and the polaron creation operators $\hat{A}_\sigma$ are defined by

$$\begin{aligned} \hat{B}^\dagger &= \hat{b}^\dagger - \Gamma \sum_\sigma \hat{n}_\sigma \\ \hat{A}^\dagger_\sigma &= \hat{c}^\dagger_\sigma \mathrm{e}^{-\Gamma(\hat{b}^\dagger - \hat{b})} \end{aligned} \tag{17.138}$$

They are constructed so that they obey the same commutation, respectively anticommutation rules as phonons and electrons. The free phonon amplitudes $\hat{B}$ describe the vibration about the equilibrium position for a given electron occupation. Electrons and phonons seem to be decoupled, but an interaction between the polarons has emerged.

This is a first indication that the Holstein model can me mapped approximately onto a Hubbard model with an attractive interaction.

17.5.2 Holstein dimer

The Holstein dimer has been discussed in detail in section **??** and appendix **??** of ΦSX:Introduction to Solid State Theory[1].

For the spectral function of the Holstein dimer see also Gunnarsson et al. [148, 149].

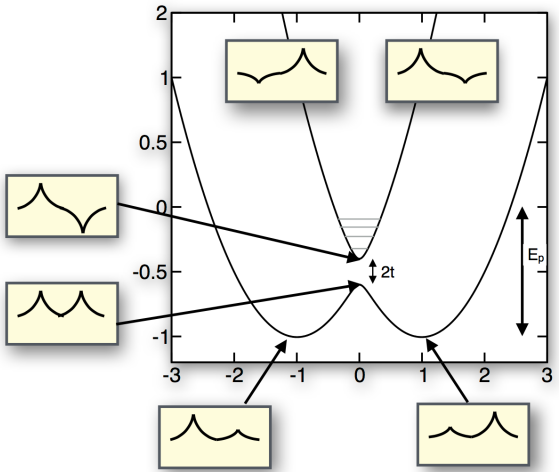


Fig. 17.12: The Born-Oppenheimer surfaces for ground and excited state of the Holstein dimer along the nuclear coordinate of the antisymmetric phonon amplitudes. The insets represent the filled electron wave function (one H-orbital per Holstein monomer).

- The **adiabaticity parameter** is defined[150] (see his Eq.25) as

$$\nu \stackrel{\text{def}}{=} \frac{t}{\hbar\omega_0} \tag{17.139}$$

  For $\nu \gg 1$, the spacing of the vibrational levels vanishes compared to the splitting of the Born-Oppenheimer surfaces. For $\nu \ll 1$ we have, what Firsov calls the **antiadiabatic limit**. In this case the hopping parameter is small compared to the level spacing of the phonons.

- The **polaron binding energy** or **polaron shift** E_b

$$E_b \stackrel{\text{def}}{=} \frac{\gamma^2}{c} \tag{17.140}$$

  The polaron binding energy is the energy in the electron-phonon coupling term.

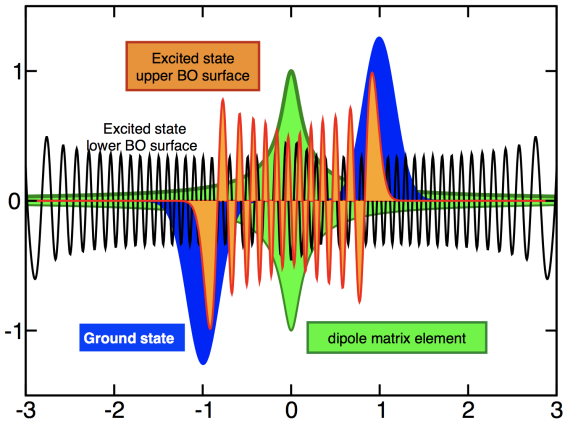


Fig. 17.13: Scheme describing an optical excitation in the Holstein dimer.

- The dimensionless parameter

$$\eta = \frac{t}{E_b} \tag{17.141}$$

separates the regime of **small polarons** $\eta < 1$ from that of **large polarons** $\eta > 1$.(See footnote 2 of Firsov [150]).

Editor: Spectral functions of the Holstein modelhttps://arxiv.org/pdf/1102.3716.pdf, https://qmlab.ubc.ca/ARPES/PUBLICATIONS/MSTheses/Christian_MSc.pdf and Green's function of the Holstein modelhttps://arxiv.org/pdf/cond-mat/0609597.pdf

<

17.5.3 Extended Holstein model

17.6 Bardeen-Cooper-Schrieffer model for superconductivity

Editor: Do not read!

Editor: Follow chapter 2.6 of Stefanucci and van Leeuwen[2].

Editor: For a BCS state in a two-site model, see chapter 2 *Many-electron states* by Eric Koch in E. Pavarini, E. Koch, and U. Schollwöck Emergent Phenomena in Correlated Matter Modeling and Simulation Vol. 3 Forschungszentrum Jülich, 2013, ISBN 978-3-89336-884-6 http://www.cond-mat.de/events/correl13

17.7 Su-Schrieffer-Heeger model for solitons and topological insulators

The **Su-Schrieffer-Heeger (SSH) model** [151, 152, 153] has been proposed in 1979 (Check erratum for [152] in Physical Review B 28, 1183 (1983)) to describe electron conduction in polyacetylene $(CH)_n$. The model allows to study a number of effects, such as Peierls distortion, polarons and solitons. Furthermore it is a classical model for topological insulators.

Alan Heeger received the Nobel price in chemistry 2000 "for the discovery and development of conductive polymers". Robert Schrieffer received the Nobel price in physics 1972 "for their jointly developed theory of superconductivity, usually called the BCS theory".

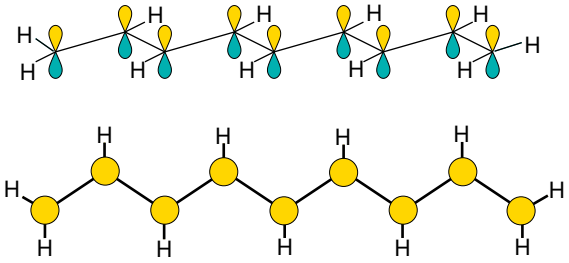


Fig. 17.14: Polyacetylene in the symmetric configuration. The relevant states, those responsible for the low-energy excitations, are p_z-orbitals perpendicular to the molecular plane. These orbitals can form π-bonds and antibonds. Viewed from the top one recognizes the analogy of the chain of p_z orbitals with a chain of hydrogen atoms.

The SSH model describes is a linear chain of atoms with non-interacting electrons and lattice vibrations, i.e. phonons. Electrons and phonons are coupled by the **electron-phonon coupling**. For the sake of simplicity, the electrons are considered as spin-less particles. The phonons are expressed by the displacements $\{u_j\}$ of the atoms from their ideal positions at $ja_{\text{lat}} + u_j(t)$. We will treat the displacements quantum mechanically.

The Hamiltonian of the SSH model is

$$\hat{H} = \underbrace{-t\sum_j \left(\hat{c}^\dagger_{j+1}\hat{c}_j + \hat{c}^\dagger_{j+1}\hat{c}_{j+1}\right)}_{\text{electrons}} + \underbrace{\frac{\hat{p}^2}{2M} + \frac{1}{2}K\sum_n (\hat{u}_{j+1} - \hat{u}_j)^2}_{\text{phonons}} + \underbrace{\sum_j \alpha(\hat{u}_{j+1} - \hat{u}_j)\left(\hat{c}^\dagger_{j+1}\hat{c}_j + \hat{c}^\dagger_j\hat{c}_{j+1}\right)}_{\text{electron-phonon coupling}} \tag{17.142}$$

t is the hopping parameter for the electrons, M is the mass of the CH unit, K is a spring constant. α is an electron-phonon coupling parameter.

While the Hamiltonian given above includes the kinetic energy of the atoms in terms of operators, the original SSH model has been proposed with classical nuclei.

Like the Holstein model, the SSH model describes local phonons, that couple to non-interacting electrons. However, in the SSH model the hopping parameters are modulated by the atomic displacement as opposed to the orbital levels in the Holstein model. This leads to a cooperativity of the phonon displacements, which are responsible for the SSH model being the most simple topological insulator.

The SSH model undergoes a so-called **Peierls distortion**. Peierls theorem says that one-dimensional metallic systems undergo a lattice distortion with a wave vector, which connects the two wave vectors of the Fermi surface. For a symmetric linear chain, $k_F = \pm\frac{\pi}{2a_{\text{lat}}}$ which results in a wave vector $q = \frac{\pi}{a_{\text{lat}}}$

of the lattice distortion. The wave length is $2a_{\text{lat}}$ which results in a doubling of the real space unit cell. As a consequence, a band gap opens and the distorted linear chain becomes an insulator. The Peierls theorem describes a form of **Fermi-surface nesting** , which is extreme in one-dimension. One can say that the Fermi surface of a 1-D system are planes perpendicular to the molecular axis.

The result of the Peierls instability is that the bond lengths alternate between two values, which reflects that there is an alternation of single and double bonds.

The pattern of bond alternation already shows many of the topological properties of the material. Mainly there are two distinct, even though symmetry-related arrangements of single and double bonds. If we arrange one side of the chain with one pattern and the other side with the other pattern, a **soliton** is formed. A soliton is an excitation (or perturbation), which can travel around in the system, but it can only anneal by recombination with another soliton or a surface. Editor: make this definition more precise.

The topological features are also evident, when we consider the surface. A the surface there may lone atom, which is not able to participate in double bond. Such a state lies energetically in the middle of the band gap. When the number of atoms is odd, there is always one such defect at the surface. If the number of atoms is even. there are either no defect states at the surface or two. The surface defect can, however, also convert itself into a soliton, which can travel throughout the chain.

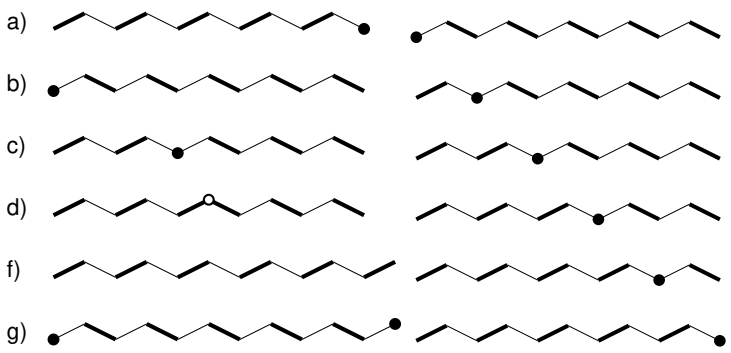


Fig. 17.15: Left: Bulk dimerization pattern, as well as surface and bulk defects in polyacetylene. a) even-numbered chain with surface defect on the right. b) even-numbered chain the opposite dimerization pattern and the surface defect on the left. c) Soliton defect with lone electron. d) soliton defect with lone hole. f) odd-numbered chain without defects. g) odd-numbered chain with two defects. Right: Time steps in the soliton motion from the left to the right end of a chain, which converts the two dimerization patterns into each other.

Editor: The dynamics in the ssh model has been studied by Su and Schrieffer[23]

17.7.1 Electronic structure with frozen displacements

Editor: See J. K. Asbóth, L. Oroszlány, A. Pályi, A Short Course on Topological Insulators; Band-structure topology and edge states in one and two dimensions https://arxiv.org/pdf/1509.02295.pdf, ibid, Lecture Notes in Physics 919, (Springer 2016) ISBN 978-3-319-25607-8

The band structure of the SSH model has been calculated earlier in exercise section 1.5.4 on p. 36. it is sketched in figure 17.17

The k-dependent Hamiltonian of the SH model is

$$\boldsymbol{h}(\vec{k}) \overset{\text{Eq. 1.123}}{=} \begin{pmatrix} \bar{\epsilon} & -t - t'\mathrm{e}^{-ika} \\ -t - t'\mathrm{e}^{ika} & \bar{\epsilon} \end{pmatrix} \tag{17.143}$$

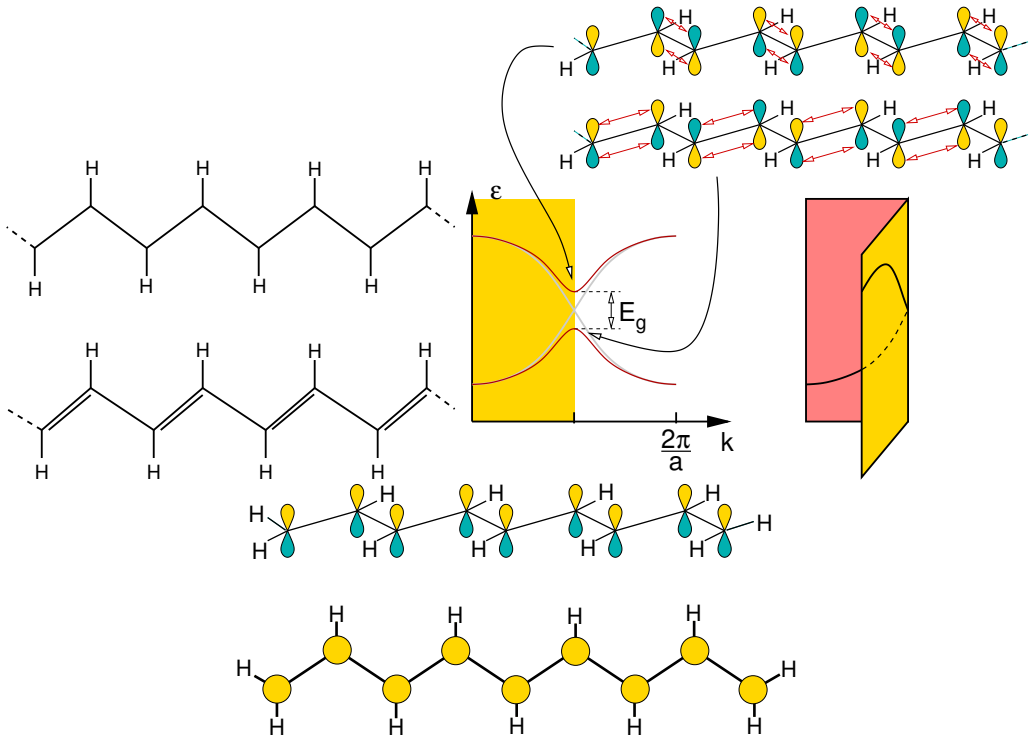


Fig. 17.16: Symmetry breaking in polyacetylene. When the bond distances alternate the reciprocal unit cell is cut into two and the bands are folded back into the unit cell. (Actually, they are not folded but translated into the other half of the reciprocal unit cell.) The alternating bond distances lift the degeneracy of states at the new zone boundary, creating a band gap.

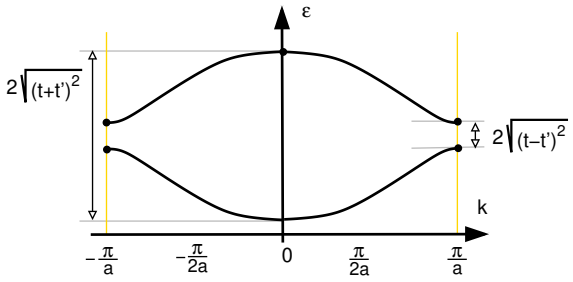


Fig. 17.17: Bandstructure of the alternating linear chain. See text for the definition of the symbols. The indices of the hopping parameters have been dropped. compare with figure 1.8

This produces the band structure

$$\epsilon_{\pm}(k) \overset{\text{Eq. } 1.124}{=} \bar{\epsilon} \pm \sqrt{(t-t')^2 + 4tt' \cos^2\left(\frac{1}{2} k a_{\text{lat}}\right)} \tag{17.144}$$

shown in figure 17.17.

$$
\begin{aligned}
0 &= (\bar{\epsilon} - \epsilon_-)\cos(\gamma_-(k)) - (t + t'\mathrm{e}^{-ika})\sin(\gamma_-(k))\mathrm{e}^{i\phi(k)} \\
\tan(\gamma) &= \left| \frac{\bar{\epsilon} - \epsilon_-}{t + t'\mathrm{e}^{-ika}} \right| \\
&= \frac{\sqrt{(t-t')^2 + 4tt'\cos^2\left(\frac{1}{2}ka_{\mathrm{lat}}\right)}}{t + t'\mathrm{e}^{-ika}} \\
&= \frac{\sqrt{(t-t')^2 + 4tt'\cos^2\left(\frac{1}{2}ka_{\mathrm{lat}}\right)}}{t + t'\cos(ka) - it'\sin(ka)} \\
&= \frac{\sqrt{(t-t')^2 + 4tt'\cos^2\left(\frac{1}{2}ka_{\mathrm{lat}}\right)}}{t + t'\cos(ka) - it'\sin(ka)} \\
&= \frac{\sqrt{(t-t')^2 + 4tt'\cos^2\left(\frac{1}{2}ka_{\mathrm{lat}}\right)}}{t + t'\cos(ka) - it'\sin(ka)}
\end{aligned}
\tag{17.145}
$$

17.8 Light-matter interaction

17.8.1 Introduction

The main puzzle of light-matter interaction is **spontaneous emission**: Experience tells that an excited state relaxes quickly into the ground state while emitting photons.[23] In order to emit electromagnetic radiation, moving charges are required. An eigenstate of an electronic system has a stationary charge density and, therefore, cannot emit light.

The puzzle is resolved by considering the electronic system in contact with the electromagnetic radiation. If the electronic system is coupled to the electromagnetic radiation, an excited electronic state without photons is not an eigenstate of the Hamiltonian. Rather, the eigenstates of the total Hamiltonian are superpositions of electronic states and photons. An excited electronic state without photons will evolve in time into the relaxed electronic state coexisting with emitted photons. This is consistent with the observation.

Spontaneous emission is demonstrated first by the minimalistic **Jaynes-Cummings model**, which describes a single electron and a single photon. **Wigner-Weisskopf theory** extends the Jaynes-Cummings model to all photons, rather than only one. This makes the description of light-matter interaction quantitative.

Below, I will also sketch the second quantization of Maxwell's equations. This will lead to explicit expressions for the parameters in the models obtained from first principles.

Apart of explaining spontaneous emission, the sections below also demonstrate further basic principles and techniques of **quantum optics**.

17.8.2 Jaynes-Cummings model

The **Jaynes-Cummings model**[154] is a minimal model for light-matter interaction. It considers a single optical mode interacting with an electronic two-state system. Considering a single optical mode transforms the problem into a two-state system coupled to quantum-mechanical harmonic oscillator.

- It describes **Rabi oscillations** as consequence of the hybridization of an atomic excitation with an optical mode. There are two eigenstates, a "bonding" and an "antibonding" state between the electronic excitation and the optical mode. The energy splitting defines the Rabi frequency. An eigenstate of the isolated atom is thus not an eigenstate of the combined system, but a superposition of "bonding" and "antibonding" combinations of electron and photon. The state is not stationary and thus exchanges energy between atom and optical field, the so-called **Rabi oscillations**.

- The model is able to describe **spontaneous emission** from the excited state of the atom.

Let me start with Hamiltonian for a system containing a two-state system coupled to an harmonic oscillator. This is equivalent to a system containing a fermion interacting with a single boson. The boson represents a single mode of an optical resonator.

$$\hat{H} = \underbrace{\underbrace{\sum_{j\in\{g,e\}} \epsilon_j \hat{a}_j^\dagger \hat{a}_j}_{\text{two-state}} + \underbrace{\hbar\omega\left(\hat{b}^\dagger\hat{b} + \frac{1}{2}\right)}_{\text{optic field}}}_{\hat{H}_0} + \underbrace{\underbrace{\hbar g(\hat{b}^\dagger + \hat{b})(\hat{a}_e^\dagger \hat{a}_g + \hat{a}_g^\dagger \hat{a}_e)}_{\text{coupling}}}_{\hat{W}} \tag{17.146}$$

The electronic system has a groundstate $|g\rangle$ and an excited state $|e\rangle$. The corresponding creation and annihilation operators are $\hat{a}_g^\dagger|\mathcal{O}\rangle = |g\rangle$ and $\hat{a}_e^\dagger|\mathcal{O}\rangle = |e\rangle$. The system contains exactly one electron

[23] There may also be competing relaxation channels.

in the two state system. This allows one to introduce creation and annihilation operators for the electronic **excitation**. $\hat{c}^\dagger|g\rangle = |e\rangle$ and $\hat{c}|e\rangle = |g\rangle$. Thus

$$\hat{c}^\dagger = \hat{a}_e^\dagger \hat{a}_g \qquad \text{and} \qquad \hat{c} = \hat{a}_g^\dagger \hat{a}_e \tag{17.147}$$

The Hamiltonian expressed in terms of excitation creation operators is

$$\hat{H} = \underbrace{\underbrace{\Delta \hat{c}^\dagger \hat{c}}_{\text{two-state}} + \underbrace{\hbar\omega \hat{b}^\dagger \hat{b}}_{\text{optic field}}}_{\hat{H}_0} + \underbrace{\underbrace{\hbar g(\hat{b}^\dagger + \hat{b})(\hat{c}^\dagger + \hat{c})}_{\text{coupling}}}_{\hat{W}} \tag{17.148}$$

where $\hat{c}^\dagger$ and $\hat{c}$ are fermionic creation and annihilation operators and $\hat{b}^\dagger$ and $\hat{b}$ are bosonic creation and annihilation operators [24]. The excitation energy of the electron is Δ and $\hbar\omega$ is the excitation energy of the photon. The zero-point energy $\frac{1}{2}\hbar\omega$ of the photon is omitted.

A general wave function can be expressed as superposition of product states of fermionic and bosonic degrees of freedom.

$$|\Psi\rangle = \sum_{\sigma=0}^{1} \sum_{n=0}^{\infty} \underbrace{\left(\hat{c}^\dagger\right)^\sigma \left(\hat{b}^\dagger\right)^n |\mathcal{O}\rangle \frac{1}{\sqrt{n!}}}_{|\sigma,n\rangle} a_{\sigma,n} = \sum_{\sigma,n} |\sigma, n\rangle a_{\sigma,n} \tag{17.150}$$

$\sigma \in \{0, 1\}$ specifies the excitation of the two state system and $n \in \{0, 1, 2, \ldots\}$ is the number of photons. $a_{\sigma,n}$ denotes the complex-valued coefficients.

The **rotating-wave approximation** reduces the Hamiltonian Eq. 17.148 to the final form of he Jaynes-Cummings model. The rotating-wave approximations limits the transitions to those that approximately satisfy energy conservation.

$$\hat{H} \approx \underbrace{\underbrace{\Delta \hat{c}^\dagger \hat{c}}_{\text{two-state}} + \underbrace{\hbar\omega \hat{b}^\dagger \hat{b}}_{\text{optic field}}}_{\hat{H}_0} + \underbrace{\underbrace{\hbar g(\hat{b}^\dagger \hat{c} + \hat{b}\hat{c}^\dagger)}_{\text{coupling}}}_{\hat{W}} \tag{17.151}$$

This Hamiltonian conserves the total number of electronic and bosonic excitations, i.e. of $\hat{c}^\dagger\hat{c} + \hat{b}^\dagger\hat{b}$.

After the rotating-wave approximation, the Hamiltonian is blocked into 2×2 sub-blocks, one for each n.

$$\hat{H} = \sum_{n=1}^{\infty} \begin{pmatrix} |0, n\rangle \\ |1, n-1\rangle \end{pmatrix} \begin{pmatrix} n\hbar\omega & \hbar g\sqrt{n} \\ \hbar g\sqrt{n} & (n-1)\hbar\omega + \Delta \end{pmatrix} \begin{pmatrix} \langle 0, n| \\ \langle 1, n-1| \end{pmatrix} \tag{17.152}$$

The state $|0, 0\rangle$, which describes the electron in the ground state without photons, has the energy zero, i.e. $\hat{H}|0, 0\rangle = 0$. This is why the sum starts with $n = 1$.

Let me specify the eigenstates with the quantum number $q \stackrel{\text{def}}{=} n + \sigma$ and a second index referring to two solutions for a given value of q. The energies and eigenstates of the Hamiltonian are

$$\begin{aligned} E_{\pm,q} &= q\hbar\omega + \frac{1}{2}\Delta \pm \sqrt{\left(\frac{\Delta}{2}\right)^2 + q\hbar^2 g^2} \\ |\psi_{-,q}\rangle &= |0, q\rangle \cos(\gamma_q) - |1, q-1\rangle \sin(\gamma_q) \\ |\psi_{+,q}\rangle &= |1, q-1\rangle \cos(\gamma_q) + |0, q\rangle \sin(\gamma_q) \end{aligned} \tag{17.153}$$

[24] Let me give a small reminder on bosonic creation and annihilation operators.

$$\begin{aligned} \hat{b}^\dagger|0, n\rangle &= |0, n+1\rangle\sqrt{n+1} \\ \hat{b}|0, n\rangle &= |0, n-1\rangle\sqrt{n} \\ \hat{b}^\dagger\hat{b}|0, n\rangle &= |0, n\rangle n \\ \hat{b}\hat{b}^\dagger|0, n\rangle &= |0, n\rangle(n+1) \end{aligned} \tag{17.149}$$

where I do not specify the mixing angles γ_q any further. For $q = n + \sigma = 0$, the energy vanishes, i.e. $E_{-,0} = 0$, and the (only) eigenstate is $|\psi_{-,0}\rangle = |0, 0\rangle$. This follows from the equations above for $q > 0$. when we set the state $|\sigma, -1\rangle = |\varnothing\rangle$ equal to the zero state.

With the eigenvalues $E_{\pm,q}$ and eigenstates $|\psi_{\pm,q}\rangle$ from Eq. 17.153, I can write down the time-dependent state

$$|\Phi(t)\rangle = \sum_{n=1}^{\infty} \sum_{\pm\in\{+,-\}} |\psi_{n,\pm}\rangle e^{-\frac{i}{\hbar} E_{n,\pm}\, t} \langle\psi_{n,\pm}|\Phi(0)\rangle \tag{17.154}$$

The Jaynes-Cummings model has been used to rationalize **spontaneous emission**: Spontaneous emission is related to the following puzzle: The charge density of an *isolated* atom in an excited eigenstate is time-independent. Therefore, the atom is not expected to emit electromagnetic radiation, but to remain in the excited state for ever. Reality is different: the atom falls into the ground state while emitting a photon. This puzzle is resolved by considering the coupling of electrons and photons. An excited electron alone is not in an eigenstate of the combined system and, therefore, it is not stationary.

The excited atom in the absence of any photons is described by a state $|\sigma, n\rangle = |1, 0\rangle$. The eigenstates of the combined system are superpositions of $|1, n\rangle$ and $|0, n+1\rangle$. Thus, if the system is prepared initially in the electronic excited state $|1, 0\rangle$, it will be in a superpositition of two eigenstates, namely $|\psi_{+,1}\rangle$ and $|\psi_{-,1}\rangle$. The energy difference $E_{+,1} - E_{-,1}$ between the two eigenstates determines an oscillation period which sets a time scale for the spontaneous emission of a photon.

Consider an atom with the electron in an excited state without any photons, i.e. $\sigma = 1$ and $n = 0$. This initial states is

$$|\Phi(0)\rangle = |1, 0\rangle \; . \tag{17.155}$$

This state is a superposition of two eigenstates with energies

$$E_{\pm,1} \overset{\text{Eq. } 17.153}{=} \hbar\omega + \frac{\Delta}{2} \pm \sqrt{\left(\frac{\Delta}{2}\right)^2 + (\hbar g)^2} \tag{17.156}$$

With Eq. 17.154, we can propagate this state to a later time

$$
\begin{aligned}
|\Phi(t)\rangle \overset{\text{Eq. 17.154}}{=} & \underbrace{\Big(|0,1\rangle\cos(\gamma_1) - |1,0\rangle\sin(\gamma_1)\Big)}_{|\psi_{1,-}\rangle} \mathrm{e}^{-\frac{i}{\hbar}E_{1,-}t} \underbrace{\big(-\sin(\gamma_1)\big)}_{\langle\psi_{1,-}|1,0\rangle} \\
& + \underbrace{\Big(|1,0\rangle\cos(\gamma_1) + |0,1\rangle\sin(\gamma_1)\Big)}_{|\psi_{1,+}\rangle} \mathrm{e}^{-\frac{i}{\hbar}E_{1,+}t} \underbrace{\cos(\gamma_1)}_{\langle\psi_{1,+}|1,0\rangle} \\
= & \quad |0,1\rangle\Big(-\mathrm{e}^{-\frac{i}{\hbar}E_{1,-}t} + \mathrm{e}^{-\frac{i}{\hbar}E_{1,+}t}\Big)\cos(\gamma_1)\sin(\gamma_1) + |1,0\rangle\Big(\cos^2(\gamma_1)\mathrm{e}^{-\frac{i}{\hbar}E_{1,+}t} + \sin^2(\gamma_1)\mathrm{e}^{-\frac{i}{\hbar}E_{1,-}t}\Big) \\
= & \quad \Bigg\{\underbrace{|0,1\rangle}_{\text{photon}} \underbrace{\Big(-\mathrm{e}^{+\frac{it}{\hbar}\sqrt{\left(\frac{\Delta}{2}\right)^2+(\hbar g)^2}} + \mathrm{e}^{-\frac{it}{\hbar}\sqrt{\left(\frac{\Delta}{2}\right)^2+(\hbar g)^2}}\Big)}_{-2i\sin\left(\frac{t}{\hbar}\sqrt{\left(\frac{\Delta}{2}\right)^2+(\hbar g)^2}\right)} \underbrace{\cos(\gamma_1)\sin(\gamma_1)}_{\frac{1}{2}\sin(2\gamma_1)} \\
& + \underbrace{|1,0\rangle}_{\text{excited electron}} \Big(\underbrace{\cos^2(\gamma_1)}_{\frac{1}{2}+\frac{1}{2}\cos(2\gamma_1)} \mathrm{e}^{-\frac{it}{\hbar}\sqrt{\left(\frac{\Delta}{2}\right)^2+(\hbar g)^2}} + \underbrace{\sin^2(\gamma_1)}_{\frac{1}{2}-\frac{1}{2}\cos(2\gamma_1)} \mathrm{e}^{+\frac{it}{\hbar}\sqrt{\left(\frac{\Delta}{2}\right)^2+(\hbar g)^2}}\Big)\Bigg\}\mathrm{e}^{-\frac{i}{\hbar}\left(\hbar\omega+\frac{1}{2}\Delta\right)t} \\
= & \quad \Bigg\{\underbrace{-|0,1\rangle}_{\text{photon}} i\sin\left(\frac{t}{\hbar}\sqrt{\left(\frac{\Delta}{2}\right)^2+(\hbar g)^2}\right)\sin(2\gamma_1) \\
& + \underbrace{|1,0\rangle}_{\text{excited electron}} \left[\cos\left(\frac{t}{\hbar}\sqrt{\left(\frac{\Delta}{2}\right)^2+(\hbar g)^2}\right) + i\cos(2\gamma_1)\sin\left(\frac{t}{\hbar}\sqrt{\left(\frac{\Delta}{2}\right)^2+(\hbar g)^2}\right)\right]\Bigg\}\mathrm{e}^{-\frac{i}{\hbar}\left(\hbar\omega+\frac{1}{2}\Delta\right)t}
\end{aligned}
\tag{17.157}
$$

We notice that the state is not stationary, but it is time dependent beyond the trivial time-dependent phase factor.

The resulting probability for being in the excited state is

$$
P_{|1,0\rangle}(t) = |\langle\Phi(t)|1,0\rangle|^2 = 1 - \sin^2(2\gamma_1)\sin^2\left(\frac{t}{\hbar}\sqrt{\left(\frac{\Delta}{2}\right)^2+(\hbar g)^2}\right) \tag{17.158}
$$

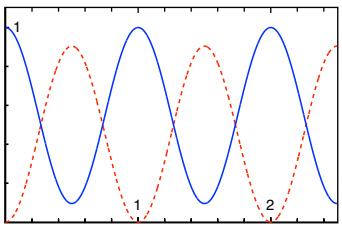


Fig. 17.18: Probability Eq. 17.158 for the excited state (blue) and that for a photon (red-dashed) in the Jaynes-Cummings model as function of time in units of the oxcillation period $T = 2\pi\hbar/\sqrt{\left(\frac{\Delta}{2}\right)^2+(\hbar g)^2}$. A value of $\gamma_1 = 0.2\pi$ has been chosen.

As shown in figure 17.18, the electron starts out in the excited state. Over time, the state converts into the ground state for the electron, while the energy is transferred to the photon. This is spontaneous emission. The emission is not complete, unless the resonance condition between the electronic excitation energy Δ and the energy $\hbar\omega$ of the photon is exactly satisfied, so that $\gamma_1 = \frac{1}{4}\pi$.

While the Jaynes-Cummings model is successful to capture the principle of spontaneous light emission, it has two artifacts:

- Firstly, the energy cannot be completely transferred to the light field, if $\hbar\omega \neq \Delta$, because only a single optical mode is available.
- The second artifact is that the photon is immediately reabsorbed. In the presence of photons with different frequencies, the amplitudes for the reabsorption interfere destructively, so that the probability for reabsorption goes to zero. This becomes evident in the Wigner-Weisskopf theory described below.

17.8.3 Wigner-Weisskopf theory

Weisskopf and Wigner[155][25] extended the Jaynes-Cummings model to a complete set of photons. The Wigner-Weisskopf theory cures the problem of the Jaynes-Cummings model that the photon from a spontaneous emission is immediately re-absorbed. Because the Wigner-Weisskopf theory considers many photons, the decay becomes irreversible.

As an additional approximation, Wigner and Weisskopf exclude memory effects. As a result, the excitation decays exponentially with a defined life time. The exponential decay is reflected in the corresponding **life-time broadening** of the spectral function.

The **Lamb shift**, the result of the level repulsion between photons and the excitation, is obtained as a side effect.

We start from the Hamiltonian of a two-state problem describing an electronic excitation coupled to photons in the rotating-wave approximation (See e.g. Eq. 17.151). In contrast to the Jaynes-Cummings model, many photons are introduced.

$$\hat{H} = \underbrace{\Delta \hat{c}^\dagger \hat{c}}_{\text{two-state}} + \underbrace{\sum_{j=1}^{\infty} \hbar\omega_j \hat{b}_j^\dagger \hat{b}_j}_{\text{optic field}} + \underbrace{\sum_{j=1}^{\infty} \hbar g_j \left(\hat{b}_j^\dagger \hat{c} + \hat{b}_j \hat{c}^\dagger\right)}_{\text{coupling}} \tag{17.159}$$

A single excitation with a specific orientation of the dipole is considered. This implies that the emission is non-isotropic and that it depends on the polarization of the light field. Potentially also a sum over spins is required.

Due to the rotating-wave approximation, the total number of photons and electronic excitations $\hat{c}^\dagger\hat{c} + \sum_{j=1} \hat{b}_j^\dagger \hat{b}_j$ is conserved. As in the Jaynes-Cummings model, the Fock space can therefore be limited[26] to the states with $\langle\Phi|\hat{c}^\dagger\hat{c} + \sum_{j=1} \hat{b}_j^\dagger \hat{b}_j|\Phi\rangle = 1$. The most general wave function with this property is

$$|\Phi(t)\rangle = \underbrace{\hat{c}^\dagger|\mathcal{O}\rangle}_{\text{electronic excitation}} \mathrm{e}^{-\frac{i}{\hbar}\Delta t} q_0(t) + \sum_{j=1} \underbrace{\hat{b}_j^\dagger|\mathcal{O}\rangle}_{\text{photon}} \mathrm{e}^{-i\omega_j t} q_j(t) \tag{17.160}$$

Note, that the sum over the photon states does not include the excitation of the two-state problem described by $q_0(t)$.

Insertion of the Ansatz 17.160 into the Schrödinger equation with the Hamiltonian Eq. 17.159 yields a coupled system of differential equations for the amplitudes $q_0(t)$ and $q_j(t)$.

$$\begin{aligned}
0 \quad &\stackrel{!}{=} \quad \left(i\hbar\partial_t - \hat{H}\right)|\Phi(t)\rangle \\
&\stackrel{\text{Eq. } 17.160}{=} \hat{c}^\dagger|\mathcal{O}\rangle \mathrm{e}^{-\frac{i}{\hbar}\Delta t}\left(\Delta \cdot q_0(t) + i\hbar\partial_t q_0(t) - \Delta \cdot q_0(t) - \sum_{j=1} \hbar g_j \mathrm{e}^{-\frac{i}{\hbar}(\hbar\omega_j - \Delta)t} q_j(t)\right) \\
&+ \quad \sum_{j=1} \hat{b}_j^\dagger|\mathcal{O}\rangle \mathrm{e}^{-i\omega_j t}\left(\hbar\omega_j q_j(t) + i\hbar\partial_t q_j(t) - \hbar g_j \mathrm{e}^{+\frac{i}{\hbar}(\hbar\omega_j - \Delta)t} q_0(t) - \hbar\omega_j q_j(t)\right)
\end{aligned} \tag{17.161}$$

[25] It may be interesting to see also the Thesis of Viktor Weisskopf *'Fundamental theory of the interactions of light with atoms'* at Gottingen University (1930)

[26] The problem can be expressed as an effective one-particle problem

The resulting coupled differential equations are

$$\Rightarrow i\hbar\partial_t q_0(t) = \sum_{j=1} \hbar g_j \mathrm{e}^{-\frac{i}{\hbar}(\hbar\omega_j-\Delta)t} q_j(t) \tag{17.162}$$

$$i\hbar\partial_t q_j(t) = \hbar g_j \mathrm{e}^{+\frac{i}{\hbar}(\hbar\omega_j-\Delta)t} q_0(t) \qquad \text{for } j \geq 1 \tag{17.163}$$

Initially, at $t = 0$, $q_0(t) = 1$ and $q_j(t) = 0$ for $j \geq 1$. I resolve the equation Eq. 17.163 for $q_j(t)$ with $j \geq 1$

$$q_j(t) \overset{\text{Eq. 17.163}}{=} \underbrace{q_j(0)}_{=0} - ig_j \int_0^t dt' \, \mathrm{e}^{+\frac{i}{\hbar}(\hbar\omega_j-\Delta)t'} q_0(t') \tag{17.164}$$

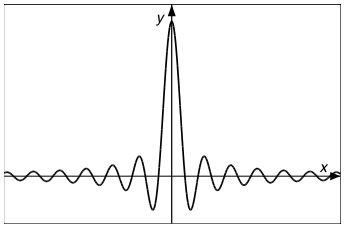
and insert it into the differential equation Eq. 17.162 for $q_0(t)$.

$$\begin{aligned} i\hbar\partial_t q_0(t) &\overset{\text{Eq. 17.162}}{=} \sum_{j=1} \hbar g_j \mathrm{e}^{-\frac{i}{\hbar}(\hbar\omega_j-\Delta)t} \overbrace{\left(-ig_j \int_0^t dt' \, \mathrm{e}^{+\frac{i}{\hbar}(\hbar\omega_j-\Delta)t'} q_0(t')\right)}^{q_j(t)} \\ &= -i\hbar \int_0^t dt' \underbrace{\left(\sum_{j=1} |g_j|^2 \mathrm{e}^{-\frac{i}{\hbar}(\hbar\omega_j-\Delta)(t-t')}\right)}_{K(t-t')} q_0(t') \end{aligned} \tag{17.165}$$

This is an integro-differential equation for the coefficient of the initial state with a **memory kernel** $K(t)$.

To obtain an impression of the memory kernel $K(t-t')$ let me consider a simple example with a constant spectral density within an energy window centered at $\bar{\epsilon}$ and of width w. The spectral density has been scaled so that the number of states is unity, independent of band width.

$$\frac{1}{\Delta} \int_{\bar{\epsilon}-\frac{1}{2}w}^{\bar{\epsilon}+\frac{1}{2}w} d\epsilon \, \mathrm{e}^{-\frac{i}{\hbar}\epsilon t} = \frac{1}{w} \left. \frac{\mathrm{e}^{-\frac{i}{\hbar}\epsilon t}}{-\frac{i}{\hbar}t} \right|_{\bar{\epsilon}-\frac{1}{2}w}^{\bar{\epsilon}+\frac{1}{2}w} = \mathrm{e}^{-\frac{i}{\hbar}\bar{\epsilon}t} \frac{1}{-\frac{w}{2\hbar}t} \frac{\mathrm{e}^{-\frac{iw}{2\hbar}t} - \mathrm{e}^{\frac{iw}{2\hbar}t}}{2i} = \mathrm{e}^{-\frac{i}{\hbar}\bar{\epsilon}t} \frac{\sin\left(\frac{w}{2\hbar}t\right)}{\frac{w}{2\hbar}t} \tag{17.166}$$



The reason for the decay is the destructive interference of the contributing plane waves at times different further away from zero. Hence, the memory kernel becomes short-ranged, if the contributing states are distributed over a wider energy region.
The model memory kernel (for $\bar{\epsilon} = 0$) is shown in the graph.[a]

[a] The function $\frac{\sin(x)}{x}$ equals unity at the origin, passes through zero at $\pm\pi$ and falls off in an oscillatory manner for larger arguments. With $\int_0^\infty dx \frac{\sin(x)}{x} = \frac{1}{2}\pi$, the model kernel (for $\bar{\epsilon} = 0$) satisfies expectation value $\int_{-\infty}^0 dt \, K(t) = \frac{\pi\hbar}{w}$. This integral is inversely proportional to the width of the spectral density. As we will see below, the resulting life time for this model is $\frac{1}{\Gamma} = \frac{w}{2\pi\hbar}$.

The memory kernel $K(t-t')$ is short-ranged in time, because it is a superposition of many plane waves. The **Wigner-Weisskopf approximation** [155] replaces it by a constant times a delta function.

$$K(t-t') \approx A \, \delta(t-t') \tag{17.167}$$

where

$$A \overset{\text{def}}{=} \int_{-\infty}^0 dt \, \sum_{j=1} |g_j|^2 \mathrm{e}^{-\frac{i}{\hbar}(\hbar\omega_j-\Delta)t} \tag{17.168}$$

This is the central approximation of the Wigner-Weisskopf theory besides the dipole approximation and the rotating-wave approximation. Replacing the memory kernel by a delta function [27] is a **Markov approximation**, that is, the complete neglect of memory effects for the dynamics of the excited state amplitude $q_0(t)$.

The value of A will be worked out below. Let me insert the Wigner-Weisskopf approximation into the equation of motion Eq. 17.165

$$\partial_t q_0(t) \overset{\text{Eq. 17.165}}{=} -\int_0^t dt' \underbrace{\sum_{j=1} |g_j|^2 \mathrm{e}^{-\frac{i}{\hbar}(\hbar\omega_j-\Delta)(t-t')}}_{K(t-t')\approx A\delta(t-t')} q_0(t') \overset{\text{Eq. 17.167}}{\approx} -Aq_0(t)$$

$$\Rightarrow q_0(t) = \mathrm{e}^{-At} q_0(0) \tag{17.170}$$

The wave-function amplitude of the excited two-state system falls off exponentially with time.[28] The real part of A determines the (inverse) life time. Note, however, that the imaginary part of A does not vanish.

Emission spectrum: Let me now turn to the emitted photons: We start from the equation of motion for the photon amplitudes and insert the amplitude Eq. 17.170 of the excited state

$$\begin{aligned}
i\hbar\partial_t q_j(t) &\overset{\text{Eq. 17.163}}{=} \hbar g_j \mathrm{e}^{+\frac{i}{\hbar}(\hbar\omega_j-\Delta)t} q_0(t) \\
&\overset{\text{Eq. 17.170}}{=} \hbar g_j \mathrm{e}^{+\frac{i}{\hbar}(\hbar\omega_j-\Delta)t} \mathrm{e}^{-At} q_0(0) \\
\Rightarrow \quad q_j(t) &= \underbrace{q_j(0)}_{=0} - ig_j \int_0^t dt' \, \mathrm{e}^{+\frac{i}{\hbar}(\hbar\omega_j-\Delta)t'} \mathrm{e}^{-At'} q_0(0) \\
&\overset{q_j(0)=0}{=} -ig_j \left[\frac{\mathrm{e}^{+\frac{i}{\hbar}(\hbar\omega_j-\Delta+i\hbar A)t}}{+\frac{i}{\hbar}(\hbar\omega_j-\Delta+i\hbar A)} \right]_0^t q_0(0) \\
&= -\hbar g_j \frac{\mathrm{e}^{+\frac{i}{\hbar}(\hbar\omega_j-\Delta+i\hbar A)t}-1}{(\hbar\omega_j-\Delta+i\hbar A)} q_0(0) \\
q_j(+\infty) &= \frac{\hbar g_j}{(\hbar\omega_j-\Delta+i\hbar A)} q_0(0) \\
\Rightarrow \quad \underbrace{\hbar\omega_j |q_j(\infty)|^2}_{\text{emitted energy}} &= \underbrace{\frac{\pi\hbar\omega_j|\hbar g_j|^2}{\Delta\hbar\mathrm{Re}[A]}}_{\text{should sum up to 1}} \underbrace{\frac{\frac{1}{\pi}\hbar\mathrm{Re}[A]}{\left(\hbar\omega_j-\Delta-\hbar\mathrm{Im}[A]\right)^2+\left(\hbar\mathrm{Re}[A]\right)^2}}_{\text{Lorentzian}} \underbrace{\Delta|q_0(0)|^2}_{\text{initial energy}}
\end{aligned} \tag{17.171}$$

Thus, the emitted photons have a Lorentzian distribution with a life-time broadening given by the real part of A. Editor: One should do some some massaging of the result to make clear that the energy of the initial excitation is conserved.

[27] The Markov approximation used above is the first term of an expansion

$$\int_{-\infty}^0 dt\, K(t) f(t) = \int_{-\infty}^0 dt\, K(t) \Big(\sum_{n=0}^\infty \frac{1}{n!} \frac{d^n f}{dt^n}\Big|_0 t^n \Big) = \sum_{n=0}^\infty \underbrace{\left[\frac{1}{n!}\int_{-\infty}^0 dt\, K(t) t^n\right]}_{R^{(n)}} \frac{d^n f}{dt^n}\Big|_0 = \sum_{n=0}^\infty R^{(n)}\, \partial_t^n|_{t=0}\, f(t)$$

$$\int_{-\infty}^t dt'\, K(t-t') f(t') = \sum_{n=0}^\infty R^{(n)} \partial_t^n f(t) \tag{17.169}$$

The Wigner-Weisskopf approximation truncates the expansion after the first term with $n = 0$.

[28] The exponential decay may seem unphysical because of a discontinuous slope of $q(t)$. Consider a thought-experiment in which the coupling constant is switched on at time zero. Initially, the system is in the excited electronic eigenstate. An exponential decay produces an amplitude $q_0(t)$ with a discontinuous slope at $t = 0$. This artifact is due to the Wigner-Weisskopf approximation. A remedy is to carry the expansion of the Kernel $K(t - t')$ in Wigner-Weisskopf approximation further to include higher time derivatives, as described in an earlier footnote. This produces an amplitude $q_0(t)$ with a discontinuity only in higher time derivatives.

Below, in Eq. 17.176, we will see that

$$\hbar \mathrm{Re}[A] \overset{\text{Eq. } 17.176}{=} \frac{\pi}{\hbar} \sum_{j=1} |\hbar g_j|^2 \delta(\hbar\omega_j - \Delta) \tag{17.172}$$

This expression contains a delta-function as opposed to the Lorentzian in Eq. 17.171. This discrepancy is due to the Wigner-Weisskopf approximation Eq. 17.167. As a consequence, the energy conservation is only approximately satisfied.[29]

Life time: Let me work out the life time from the parameter A defined in Eq. 17.168. Let me express A by two new parameters, the inverse life time[30] Γ and the Lamb shift δ_{Lamb}.

$$A = \frac{\Gamma}{2} + i\delta_{\mathrm{Lamb}} \overset{\text{Eq. } 17.168}{=} \int_{-\infty}^{0} dt \sum_{j=1}^{\infty} |g_j|^2 \mathrm{e}^{-\frac{i}{\hbar}(\hbar\omega_j - \Delta)t} \tag{17.173}$$

Let me do some math on a side, that will be required:

$$\begin{aligned} \lim_{\eta\to 0^+} \int_{-\infty}^{0} dt\, \mathrm{e}^{-\frac{i}{\hbar}(\epsilon+i\eta)t} &= \lim_{\eta\to 0^+} \Big[\frac{\mathrm{e}^{-\frac{i}{\hbar}(\epsilon+i\eta)t}}{-\frac{i}{\hbar}(\epsilon+i\eta)} \Big]_{-\infty}^{0} = \lim_{\eta\to 0^+} \frac{i\hbar}{\epsilon+i\eta} = \lim_{\eta\to 0^+} \frac{i\hbar(\epsilon - i\eta)}{\epsilon^2+\eta^2} \\ &= i\hbar\Big(\mathbb{P}\left(\frac{1}{\epsilon}\right) - i\pi\delta(\epsilon) \Big) = i\hbar\mathbb{P}\left(\frac{1}{\epsilon}\right) + \hbar\pi\delta(\epsilon) \end{aligned} \tag{17.174}$$

where $\mathbb{P}\left(\frac{1}{\epsilon}\right)$ is Cauchys principal part.

$$\begin{aligned} A &\overset{\text{Eq. } 17.173}{=} \sum_{j=1}^{\infty} |g_j|^2 \int_{-\infty}^{0} dt\, \mathrm{e}^{-\frac{i}{\hbar}(\hbar\omega_j - \Delta)t} \\ &\overset{\text{Eq. } 17.174}{=} \sum_{j=1} |g_j|^2 \left(i\hbar\mathbb{P}\left(\frac{1}{\hbar\omega_j - \Delta}\right) + \hbar\pi\delta(\hbar\omega_j - \Delta) \right) \\ &= i\hbar \sum_{j=1} |g_j|^2 \mathbb{P}\left(\frac{1}{\hbar\omega_j - \Delta}\right) + \hbar\pi \sum_j |g_j|^2 \delta(\hbar\omega_j - \Delta) \end{aligned} \tag{17.175}$$

Thus, I obtain

$$\begin{aligned} \mathrm{Re}[A] &= \frac{1}{2}\Gamma = \hbar\pi \sum_{j=1} |g_j|^2 \delta(\hbar\omega_j - \Delta) \qquad \text{and} \\ \mathrm{Im}[A] &= \delta_{\mathrm{Lamb}} = \hbar \sum_{j=1} |g_j|^2 \mathbb{P}\left(\frac{1}{\hbar\omega_j - \Delta}\right) \end{aligned} \tag{17.176}$$

This is the final result in terms of the model parameters. The imaginary part of A is responsible for the **Lamb shift** δ_{Lamb}, while the real part of A determines the life time of the electron level.

Photon modes: Let me insert the photon dispersion $\omega_\alpha(\vec{k}) = c|\vec{k}|$, and the integration over all phonon modes, where the polarizations are indicated by the subscript α.

$$\begin{aligned} \sum_{j=1} &\rightsquigarrow \sum_{\alpha} \frac{L^3}{(2\pi)^3} \int d^3k \\ \int d^3k &\overset{k=|\vec{k}|}{=} 4\pi \int_0^\infty dk k^2 \overset{\omega=c|\vec{k}|}{=} \frac{4\pi}{c^3} \int_0^\infty d\omega\, \omega^2 \end{aligned} \tag{17.177}$$

[29] This problem could be cured by rescaling all photon intensities by a common factor.

[30] The factor $\frac{1}{2}$ in front of the life time Γ in Eq. 17.173 has the following origin: The wave function amplitude of the excited state falls of as $\mathrm{e}^{-\frac{1}{2}\Gamma t}$. The resulting probability for the excited state falls off like $\mathrm{e}^{-\Gamma t}$. The life time of the excited state is therefore Γ.

First, we evaluate the photon density of states $D_{ph}(E)$

$$D_{ph}(E) \stackrel{\text{def}}{=} \sum_j \delta(\hbar\omega_j - E) = \sum_\alpha \frac{L^3}{(2\pi)^3}\frac{4\pi}{c^3}\int_0^\infty d\omega\, \omega^2 \delta(\hbar\omega - E) = \sum_\alpha \frac{L^3}{(2\pi)^3}\frac{4\pi}{c^3}E^2 \quad (17.178)$$

Secondly, we determine the averaged coupling

$$\bar{g}(E) \stackrel{\text{def}}{=} \sqrt{\frac{\sum_j |g_j|^2 \delta(\hbar\omega_j - E)}{\sum_j \delta(\hbar\omega_j - E)}} \quad (17.179)$$

so that

$$\begin{aligned} \mathrm{Re}[A] &\stackrel{\text{Eq. 17.176}}{=} \hbar\pi \sum_j |g_j|^2 \delta(\hbar\omega_j - \Delta) = \hbar\pi D_{ph}(\Delta)|\bar{g}(\Delta)|^2 = \hbar\pi \sum_\alpha \frac{L^3}{(2\pi)^3}\frac{4\pi}{c^3}\Delta^2|\bar{g}(\Delta)|^2 \\ &= \sum_\alpha \frac{L^3}{(2\pi)^3}\frac{4\pi^2\hbar\Delta^2}{c^3}|\bar{g}(\Delta)|^2 \end{aligned} \quad (17.180)$$

Editor: Check the result and work out $\bar{g}(\Delta)$

Editor: The life time of the hydrogen 2p state with an wavelength of $\lambda = 121.57$ nm is calculated $\tau = 1.595$ ns vs measured $\tau - 1.60$ ns.
Source: https://wp.optics.arizona.edu/opti544/wp-content/uploads/sites/54/2021/05/OPTI-544-Lecture-Posted-Monday-05032021.pdf. Retrieved Aug.8, 2023

Editor: See also: http://physics.unm.edu/Courses/Deutsch/Phys566F19/Lectures/Phys566_Lect14.pdf, respectively http://info.phys.unm.edu/~ideutsch/Classes/Phys566F15/Lectures/

17.8.4 Related models

The idea of spontaneous emission goes back to Einstein's investigation of Planck's black-body spectrum.

Closely related to the Jaynes-Cummings model is the Rabi model: The Rabi model treats the excitation of a two-state system by a classical light wave, while the Jaynes-Cummings model treats the light mode in second quantization. It has been investigated in appendix I.3 of ΦSX: Quantum Physics[16]

Editor: The author shall consult: Merlin[156] and Burt[157].

17.8.5 Quantization of photons

For my notation and background on gauge potentials, see ΦSX: Elektrodynamik [24], chapter 9.

Classical Electrodynamics

The electric and magnetic fields can be expressed by the **gauge potentials**, the electric potential $\Phi(\vec{r}, t)$ and the vector potential $\vec{A}(\vec{r}, t)$.

$$\begin{aligned} \vec{E} &= -\partial_t \vec{A} - \vec{\nabla}\Phi \\ \vec{B} &= \vec{\nabla} \times \vec{A} \end{aligned} \quad (17.181)$$

The gauge potentials satisfy

$$\begin{aligned} \left[\vec{\nabla}^2 - \frac{1}{c^2}\partial_t^2\right]\Phi + \partial_t\left[\vec{\nabla}\vec{A} + \frac{1}{c^2}\partial_t\Phi\right] &= -\frac{1}{\epsilon_0}\rho \\ \left[\vec{\nabla}^2 - \frac{1}{c^2}\partial_t^2\right]\vec{A} - \vec{\nabla}\left[\vec{\nabla}\vec{A} + \frac{1}{c^2}\partial_t\Phi\right] &= -\mu_0\vec{j} \end{aligned} \quad (17.182)$$

Let me fix the gauge to the **Coulomb gauge**, which requires

$$\vec{\nabla}\vec{A} = 0 \tag{17.183}$$

The resulting electric potential Φ is given by the instantaneous charge density $\rho(\vec{r}, t)$.

$$\Phi(\vec{r}, t) = \int d^3r \frac{\rho(\vec{r}, t)}{4\pi\epsilon_0 |\vec{r} - \vec{r'}|} \tag{17.184}$$

The vector potential satisfies, in addition to the gauge condition,

$$\left[\vec{\nabla}^2\vec{A} - \frac{1}{c^2}\partial_t^2\vec{A}\right] = -\mu_0\vec{j} + \frac{1}{c^2}\partial_t\vec{\nabla}\Phi \tag{17.185}$$

Editor: Let me consider the right hand side

$$\vec{\nabla}\left(\vec{j} + \partial_t\epsilon_0\vec{\nabla}\Phi\right) = \vec{\nabla}\vec{j} + \partial_t \underbrace{\epsilon_0\vec{\nabla}^2\Phi}_{\rho(\vec{r},t)} = \vec{\nabla}\vec{j} + \partial_t\rho \overset{\text{charge conservation}}{=} 0$$

$$\Rightarrow \vec{j} + \partial_t\epsilon_0\vec{\nabla}\Phi = \vec{\nabla} \times \vec{Q}(\vec{r}, t) \tag{17.186}$$

The divergence of the right-hand side vanishes. Therefore, it must be the rotation of a vector field, which I denote as $\vec{Q}$.

The energy of the electromagnetic field is ($c = 1/\sqrt{\epsilon_0\mu_0}$)

$$\begin{aligned} E &= \int d^3r \left(\frac{1}{2}\vec{E}\vec{D} + \frac{1}{2}\vec{B}\vec{H}\right) = \int d^3r \left(\frac{\epsilon_0}{2}\vec{E}^2 + \frac{1}{2\mu_0}\vec{B}^2\right) \\ &= \frac{1}{2\mu_0}\int d^3r \left[\frac{1}{c^2}\left(-\partial_t\vec{A} - \underbrace{\vec{\nabla}\vec{A}}_{=0}\right)^2 + \left(\vec{\nabla} \times \vec{A}\right)^2\right] \\ &= \frac{1}{2\mu_0}\int d^3r \left[\frac{1}{c^2}\left(\partial_t\vec{A}\right)^2 + \left(\vec{\nabla} \times \vec{A}\right)^2\right] \end{aligned} \tag{17.187}$$

Optic modes

For our purposes, we consider waves in free space

$$\vec{A}(\vec{r}, t) = \sum_\alpha \sum_{\vec{k}} \frac{1}{2}\left[A_{\alpha,\vec{k}}\vec{e}_{\alpha,\vec{k}}e^{i(\vec{k}\vec{r} - \omega_{\vec{k}}t)} + A^*_{\alpha,\vec{k}}\vec{e}^*_{\alpha,\vec{k}}e^{-i(\vec{k}\vec{r} - \omega_{\vec{k}}t)}\right] \tag{17.188}$$

with $\vec{e}_{\alpha,\vec{k}}\vec{k} = 0$ and $\omega_{\vec{k}} = c|\vec{k}|$. The index α denotes the two polarizations $\vec{e}_{\alpha,\vec{k}}$, i.e. the orientation of the vector potential $\vec{A}$, which is perpendicular to the wave vector. This vector satisfies $\vec{e}^*_{\alpha,\vec{k}}\vec{e}_{\alpha',\vec{k}} = \delta_{\alpha,\alpha'}$. Note that the polarization may be complex-valued to describe **circular polarization** with the angular momentum parallel or antiparallel to the wave vector. [31]

Let me introduce **periodic boundary conditions** in a cube with sidelength L. This discretizes the modes so that

$$\vec{k}_{\vec{j}} = \frac{2\pi}{L}\vec{j} \tag{17.189}$$

where the three-dimensional vector $\vec{j}$ has integer components. The mode with $\vec{k} = 0$ is not observable, because it is neither connected to the electric nor to the magnetic field. Therefore, it can be excluded from the sum.

[31] See Sakurai, Advances Quantum Mechanics. For the two linear polarization vectors $\vec{e}_1, \vec{e}_2$, forming a right-handed system with the wave vector $\vec{k}$, the circular polarizations are $\vec{e}_+ = \frac{-1}{\sqrt{2}}(\vec{e}_1 + i\vec{e}_2)$ for $m = +1$ and $\vec{e}_- = \frac{+1}{\sqrt{2}}(\vec{e}_1 - i\vec{e}_2)$ for $m = -1$. The angular momentum quantum numbers $m = \pm 1$ result from the rotation behavior of the polarization vectors about the wave vector.

$$\begin{aligned}E &= \frac{1}{2\mu_0}\int d^3r\,\Big[\frac{1}{c^2}\Big(\partial_t\vec{A}\Big)^2+\Big(\vec{\nabla}\times\vec{A}\Big)^2\Big]\\ &= \frac{1}{2\mu_0}\int d^3r\,\Big\{\Big(\frac{1}{2}\sum_{\vec{k}}\sum_{\alpha}\Big[-i\frac{\omega_{\vec{k}}}{c}A_{\alpha,\vec{k}}\vec{e}_{\alpha,\vec{k}}\mathrm{e}^{i(\vec{k}\vec{r}-\omega_{\vec{k}}t)}+i\frac{\omega_{\vec{k}}}{c}\vec{A}^*_{\alpha,\vec{k}}\vec{e}^*_{\alpha,\vec{k}}\mathrm{e}^{-i(\vec{k}\vec{r}-\omega_{\vec{k}}t)}\Big]\Big)^2\\ &\qquad+\Big(\frac{1}{2}\sum_{\vec{k}}\sum_{\alpha}\Big[i\vec{k}\times A_{\alpha,\vec{k}}\vec{e}_{\alpha,\vec{k}}\mathrm{e}^{i(\vec{k}\vec{r}-\omega_{\vec{k}}t)}-i\vec{k}\times A^*_{\alpha,\vec{k}}\vec{e}^*_{\alpha,\vec{k}}\mathrm{e}^{-i(\vec{k}\vec{r}-\omega_{\vec{k}}t)}\Big]\Big)^2\Big\}\end{aligned} \tag{17.190}$$

I exploit the orthonormality of the plane waves and the polarization directions.

$$\int_{L^3}d^3r\;\mathrm{e}^{i(\vec{k}-\vec{k}')\vec{r}}=L^3\delta_{\vec{k},\vec{k}'}\qquad\text{and}\qquad\vec{e}^*_{\alpha,\vec{k}}\vec{e}_{\alpha',\vec{k}}=\delta_{\alpha,\alpha'} \tag{17.191}$$

$$\begin{aligned}E &= \frac{L^3}{2\mu_0}\frac{1}{4}\sum_{\alpha}\sum_{\vec{k}}\Big\{\underbrace{\Big(-\frac{\omega_{\vec{k}}\omega_{-\vec{k}}}{c^2}+\vec{k}^2\Big)}_{=0}\vec{e}^2_{\alpha,\vec{k}}\mathrm{e}^{i(\omega_{\vec{k}}+\omega_{-\vec{k}})t}A_{\alpha,\vec{k}}A_{\alpha,-\vec{k}}+\underbrace{\Big(-\frac{\omega_{\vec{k}}\omega_{-\vec{k}}}{c^2}+\vec{k}^2\Big)}_{=0}\vec{e}^{*2}_{\alpha,\vec{k}}\mathrm{e}^{-i(\omega_{\vec{k}}+\omega_{-\vec{k}})t}A^*_{\alpha,\vec{k}}A^*_{\alpha,-\vec{k}}\\ &\quad+\underbrace{\Big(\frac{\omega^2_{\vec{k}}}{c^2}+\vec{k}^2\Big)}_{2\vec{k}^2}\Big(A_{\alpha,\vec{k}}A^*_{\alpha',\vec{k}}+A^*_{\alpha,\vec{k}}A_{\alpha,\vec{k}}\Big)\Big\}\\ &= \sum_{\alpha}\sum_{\vec{k}}\hbar\omega_{\vec{k}}\underbrace{\Big(\frac{4\pi\epsilon_0L^3\hbar\omega_{\vec{k}}}{8\pi\hbar^2}\Big)}_{\frac{1}{\hbar\omega}\frac{L^3}{2\mu_0}\frac{1}{4}2\frac{\omega^2}{c^2}2}\frac{1}{2}\Big(A_{\alpha,\vec{k}}A^*_{\alpha,\vec{k}}+A^*_{\alpha,\vec{k}}A_{\alpha,\vec{k}}\Big)\\ &= \sum_{\alpha}\sum_{\vec{k}}\hbar\omega_{\vec{k}}\frac{1}{2}\Big(b_{\alpha,\vec{k}}b^*_{\alpha,\vec{k}}+b^*_{\alpha,\vec{k}}b_{\alpha,\vec{k}}\Big)\end{aligned} \tag{17.192}$$

with

$$b_{\alpha,\vec{k}}=\sqrt{\frac{4\pi\epsilon_0L^3\hbar\omega_{\vec{k}}}{8\pi\hbar^2}}A_{\alpha,\vec{k}}\qquad\Leftrightarrow\qquad A_{\alpha,\vec{k}}=\sqrt{\frac{8\pi\hbar^2}{4\pi\epsilon_0L^3\hbar\omega_{\vec{k}}}}b_{\alpha,\vec{k}} \tag{17.193}$$

Expressed in terms of phonon amplitudes $b_{\alpha,\vec{k}}$ the vector potential is

$$\begin{aligned}\vec{A}(\vec{r},t) &\overset{\text{Eq. 17.188}}{=} \sum_{\alpha}\sum_{\vec{k}}\frac{1}{2}\Big[A_{\alpha,\vec{k}}\vec{e}_{\alpha,\vec{k}}\mathrm{e}^{i(\vec{k}\vec{r}-\omega_{\vec{k}}t)}+A^*_{\alpha,\vec{k}}\vec{e}^*_{\alpha,\vec{k}}\mathrm{e}^{-i(\vec{k}\vec{r}-\omega_{\vec{k}}t)}\Big]\\ &= \sum_{\alpha}\sum_{\vec{k}}\sqrt{\frac{8\pi\hbar^2}{4\pi\epsilon_0L^3\hbar\omega_{\vec{k}}}}\frac{1}{2}\Big[b_{\alpha,\vec{k}}\vec{e}_{\alpha,\vec{k}}\mathrm{e}^{i(\vec{k}\vec{r}-\omega_{\vec{k}}t)}+b^*_{\alpha,\vec{k}}\vec{e}^*_{\alpha,\vec{k}}\mathrm{e}^{-i(\vec{k}\vec{r}-\omega_{\vec{k}}t)}\Big]\end{aligned} \tag{17.194}$$

The electric field is

$$\vec{E}(\vec{r},t)=\sum_{\alpha}\sum_{\vec{k}}\sqrt{\frac{8\pi\hbar\omega_{\vec{k}}}{4\pi\epsilon_0L^3}}\frac{-i}{2}\Big[b_{\alpha,\vec{k}}\vec{e}_{\alpha,\vec{k}}\mathrm{e}^{i(\vec{k}\vec{r}-\omega_{\vec{k}}t)}-b^*_{\alpha,\vec{k}}\vec{e}^*_{\alpha,\vec{k}}\mathrm{e}^{-i(\vec{k}\vec{r}-\omega_{\vec{k}}t)}\Big] \tag{17.195}$$

and the magnetic field is

$$\vec{B}(\vec{r},t)=\sum_{\alpha}\sum_{\vec{k}}\sqrt{\frac{8\pi\hbar^2}{4\pi\epsilon_0L^3\hbar\omega_{\vec{k}}}}\frac{i}{2}\Big[b_{\alpha,\vec{k}}(\vec{k}\times\vec{e}_{\alpha,\vec{k}})\mathrm{e}^{i(\vec{k}\vec{r}-\omega_{\vec{k}}t)}-b^*_{\alpha,\vec{k}}(\vec{k}\times\vec{e}^*_{\alpha,\vec{k}})\mathrm{e}^{-i(\vec{k}\vec{r}-\omega_{\vec{k}}t)}\Big] \tag{17.196}$$

Quantization

The quantization of the vector potential is not done in all detail. The goal here is to verify the constants in the matrix elements.

This Hamiltonian corresponds to a harmonic oscillator for each real and imaginary part of the photon amplitude $b_{\alpha,\vec{k}}$.

Let me introduce the creation and annihilation operators

$$[\hat{b}_{\alpha,\vec{k}}, \hat{b}^\dagger_{\alpha,\vec{k}}]_- = \delta_{\alpha,\alpha'}\delta_{\vec{k},\vec{k}'} \qquad \text{and} \qquad [\hat{b}^\dagger_{\alpha,\vec{k}}, \hat{b}^\dagger_{\alpha,\vec{k}}]_- = 0 \qquad \text{and} \qquad [\hat{b}_{\alpha,\vec{k}}, \hat{b}_{\alpha,\vec{k}}]_- = 0 \tag{17.197}$$

The classical photon amplitudes translate into the annihilation operators in the Heisenberg picture: In the absence of an interaction, the photon amplitudes discussed above are time independent.

$$\begin{aligned} b_{\alpha,\vec{k}} e^{-i\omega_{\vec{k}}t} &\to \hat{b}_{S,\alpha,\vec{k}} = \hat{b}_{H,\alpha,\vec{k}} e^{-i\omega_{\vec{k}}t} \\ b^*_{\alpha,\vec{k}} e^{+i\omega_{\vec{k}}t} &\to \hat{b}^\dagger_{S,\alpha,\vec{k}} = \hat{b}^\dagger_{H,\alpha,\vec{k}} e^{+i\omega_{\vec{k}}t} \end{aligned} \tag{17.198}$$

Editor: check this equation!

The Hamiltonian is

$$\hat{H} = \sum_{\alpha,\vec{k}} \hbar\omega_{\vec{k}} \left(\hat{b}^\dagger_{\alpha,\vec{k}} \hat{b}_{\alpha,\vec{k}} + \frac{1}{2} \right) \tag{17.199}$$

The vector potential is correspondingly

$$\vec{A}(\vec{r},t) = \sum_\alpha \sum_{\vec{k}} \sqrt{\frac{8\pi\hbar^2}{4\pi\epsilon_0 L^3 \hbar\omega_{\vec{k}}}} \frac{1}{2} \left[\hat{b}_{S,\alpha,\vec{k}} \vec{e}_{\alpha,\vec{k}} e^{i\vec{k}\vec{r}} + \hat{b}^\dagger_{S,\alpha,\vec{k}} \vec{e}^*_{\alpha,\vec{k}} e^{-i\vec{k}\vec{r}} \right] \tag{17.200}$$

Editor: Why is the factor $e^{-i\omega t}$ present above but not below? Heisenberg vs. Schroedinger operators?

Coupling to the dipole oscillations

The Hamiltonian for electrons in an electromagnetic field is

$$\hat{H} = \frac{(\hat{\vec{p}} - q_e \vec{A}(\vec{r},t))^2}{2m_e} + q_e \Phi(\vec{r},t) \tag{17.201}$$

In the absence of the light field, the Hamiltonian is

$$\hat{H}_0 = \frac{\hat{\vec{p}}^2}{2m_e} + q_e \Phi(\vec{r},t) \tag{17.202}$$

The perturbation is

$$\hat{W} = \frac{q_e}{2m_e} \left(-\hat{\vec{p}}\vec{A}(\vec{r},t) - \vec{A}(\vec{r},t)\hat{\vec{p}} + q_e \vec{A}^2(\vec{r},t) \right) \tag{17.203}$$

In terms of creation and annihilation operators, we obtain

$$\begin{aligned} \hat{W} &= \int d^4x\, \hat{\psi}^\dagger(\vec{x}) \frac{q_e}{2m_e} \left(-\frac{\hbar}{i}\vec{\nabla}\vec{A}(\vec{r},t) - \vec{A}(\vec{r},t)\frac{\hbar}{i}\vec{\nabla} + q_e\vec{A}^2(\vec{r},t) \right) \hat{\psi}(\vec{x}) \\ &\overset{\text{Eq. 3.61}}{=} \sum_{i,j} \hat{c}^\dagger_i \underbrace{\left[\int d^4x\, \varphi^*_i(\vec{x}) \frac{q_e}{2m_e} \left(-\frac{\hbar}{i}\vec{\nabla}\vec{A}(\vec{r},t) - \vec{A}(\vec{r},t)\frac{\hbar}{i}\vec{\nabla} + q_e\vec{A}^2(\vec{r},t) \right) \varphi_j(\vec{x}) \right]}_{W_{i,j}} \hat{c}_j \\ &= \sum_{i,j} W_{i,j} \hat{c}^\dagger_i \hat{c}_j \end{aligned} \tag{17.204}$$

with the matrix elements

$$
\begin{aligned}
W_{i,j} &= \left\langle \varphi_i \middle| \frac{q_e}{2m_e}\left(-\hat{\vec{p}}\vec{A}(\vec{r},t) - \vec{A}(\vec{r},t)\hat{\vec{p}} + q_e\vec{A}^2(\vec{r},t)\right)\middle|\varphi_j\right\rangle \\
&= \Bigg\langle \varphi_i \Bigg| \frac{q_e}{2m_e}\Bigg\{ \underbrace{-\sum_\alpha\sum_{\vec{k}} \hbar\vec{k}\sqrt{\frac{8\pi\hbar^2}{4\pi\epsilon_0 L^3\hbar\omega_{\vec{k}}}}\frac{1}{2}\left[\hat{b}_{S,\alpha,\vec{k}}\vec{e}_{\alpha,\vec{k}}\mathrm{e}^{i\vec{k}\vec{r}} - \hat{b}^\dagger_{S,\alpha,\vec{k}}\vec{e}^*_{\alpha,\vec{k}}\mathrm{e}^{-i\vec{k}\vec{r}}\right]}_{=0 \text{ because } \vec{k}\vec{e}_{\alpha,\vec{k}}=0 \text{ (from } -\hat{\vec{p}}\vec{A})} \\
&\quad \underbrace{-2\sum_\alpha\sum_{\vec{k}}\sqrt{\frac{8\pi\hbar^2}{4\pi\epsilon_0 L^3\hbar\omega_{\vec{k}}}}\frac{1}{2}\left[\hat{b}_{S,\alpha,\vec{k}}\vec{e}_{\alpha,\vec{k}}\mathrm{e}^{i\vec{k}\vec{r}} + \hat{b}^\dagger_{S,\alpha,\vec{k}}\vec{e}^*_{\alpha,\vec{k}}\mathrm{e}^{-i\vec{k}\vec{r}}\right]\hat{\vec{p}}}_{(\text{from } -2\vec{A}\hat{\vec{p}})} \\
&\quad \underbrace{+ q_e\left(\sum_\alpha\sum_{\vec{k}}\sqrt{\frac{8\pi\hbar^2}{4\pi\epsilon_0 L^3\hbar\omega_{\vec{k}}}}\frac{1}{2}\left[\hat{b}_{S,\alpha,\vec{k}}\vec{e}_{\alpha,\vec{k}}\mathrm{e}^{i\vec{k}\vec{r}} + \hat{b}^\dagger_{S,\alpha,\vec{k}}\vec{e}^*_{\alpha,\vec{k}}\mathrm{e}^{-i\vec{k}\vec{r}}\right]\right)^2}_{\text{will be ignored below (from } q\vec{A}^2)}\Bigg\}\Bigg|\varphi_j\Bigg\rangle \\
&= -\frac{q_e}{2m_e}2\sum_\alpha\sum_{\vec{k}}\sqrt{\frac{8\pi\hbar^2}{4\pi\epsilon_0 L^3\hbar\omega_{\vec{k}}}}\frac{1}{2}\left\{\hat{b}_{S,\alpha,\vec{k}}\vec{e}_{\alpha,\vec{k}}\left\langle\varphi_i\middle|\mathrm{e}^{i\vec{k}\vec{r}}\hat{\vec{p}}\middle|\varphi_j\right\rangle + \hat{b}^\dagger_{S,\alpha,\vec{k}}\vec{e}^*_{\alpha,\vec{k}}\left\langle\varphi_i\middle|\mathrm{e}^{-i\vec{k}\vec{r}}\hat{\vec{p}}\middle|\varphi_j\right\rangle\right\}
\end{aligned}
\tag{17.205}
$$

We use

$$
\begin{aligned}
\vec{e}^*_{\alpha,\vec{k}}\left\langle\varphi_i\middle|\mathrm{e}^{-i\vec{k}\vec{r}}\hat{\vec{p}}\middle|\varphi_j\right\rangle &= \vec{e}^*_{\alpha,\vec{k}}\frac{\hbar}{i}\left\langle\varphi_i\middle|\mathrm{e}^{-i\vec{k}\vec{r}}\middle|\vec{\nabla}\varphi_j\right\rangle = \left(-\frac{\hbar}{i}\vec{e}_{\alpha,\vec{k}}\left\langle\vec{\nabla}\varphi_j\middle|\mathrm{e}^{+i\vec{k}\vec{r}}\middle|\varphi_i\right\rangle\right)^* \\
&= \left(\vec{e}_{\alpha,\vec{k}}\left\langle\varphi_j\middle|\frac{\hbar}{i}\vec{\nabla}\mathrm{e}^{+i\vec{k}\vec{r}}\middle|\varphi_i\right\rangle\right)^* = \Big(\underbrace{\vec{e}_{\alpha,\vec{k}}\hbar\vec{k}}_{=0}\left\langle\varphi_j\middle|\mathrm{e}^{+i\vec{k}\vec{r}}\middle|\varphi_i\right\rangle + \vec{e}_{\alpha,\vec{k}}\left\langle\varphi_j\middle|\mathrm{e}^{+i\vec{k}\vec{r}}\hat{p}\middle|\varphi_i\right\rangle\Big)^* \\
&= \left(\vec{e}_{\alpha,\vec{k}}\left\langle\varphi_j\middle|\mathrm{e}^{+i\vec{k}\vec{r}}\hat{p}\middle|\varphi_i\right\rangle\right)^*
\end{aligned}
\tag{17.206}
$$

Thus, we obtain for the electron-photon coupling

$$
\hat{W} = \sum_{i,j}\left(\sum_{\vec{k}}\sum_\alpha g^*_{j,i,\alpha,\vec{k}}\hat{b}^\dagger_{\alpha,\vec{k}} + g_{i,j,\alpha,\vec{k}}\hat{b}_{\alpha,\vec{k}}\right)\hat{c}^\dagger_i\hat{c}_j \tag{17.207}
$$

with

$$
g_{i,j,\alpha,\vec{k}} = -\frac{q_e}{2m_e}2\sum_\alpha\sum_{\vec{k}}\sqrt{\frac{8\pi\hbar^2}{4\pi\epsilon_0 L^3\hbar\omega_{\vec{k}}}}\frac{1}{2}\vec{e}_{\alpha,\vec{k}}\left\langle\varphi_i\middle|\mathrm{e}^{i\vec{k}\vec{r}}\hat{\vec{p}}\middle|\varphi_j\right\rangle \tag{17.208}
$$

Chapter 18

Organization and examination

18.1 Teaching goals

- Fock space, Slater determinants, occupation-number representation, Mazny-particle wave functions, ensembles.
- Hartree- and exchange energy, exchange-correlation hole. Hund's rule.
- mean-field approximation (Hartree Fock) and self-consistent equations, Fock operator
- creation and annihilation operators. Relation to Slater determinants. Calculations.
- Spectral function as electron addition and removal energies. quasi-particles and their interaction.
- downfolding, self energy, retarded potentials.
- one-particle Green's function of a many-particle system.
- many-body perturbation theory (MBPT). (limited to fermions interacting via the Coulomb interaction.)
  - Wick's theorem
  - enumerate diagrams
  - sign theorem
  - linked-cluster theorem
  - topologically inequivalent diagrams
  - symmetry factors
  - self energy (proper vs reducible)
- full Green's function from generating functional
- convert Feynman diagrams into formulas and vice versa

18.2 Examination

Here, I am collecting some material that could be relevant for the examination. When it is complete it should cover the main points conveyed in the lecture. `Editor: It is still far from complete!` The student can orient themself on this list while preparing for the lecture. I do not

recommend, however, to use this as the sole approach to prepare because this will accumulate ill-connected knowledge, which is of little practical value and which is thus easily forgotten. Rather the student is encouraged to consult this list during learning the material to remind themself and to gain confidence.

- know the concept of level repulsion, the “energy sum rule” and the ”charge sum rule”. (see asymmetric dimer.)
- know the Hartree and exchange energy. Derive the Fock operator.
- know the difference of the one-particle-reduced density matrix and the von-Neumann density matrix. Obtain the former from the latter.
- know the grand potential of the Thermal Hartree Fock approximation.
- know the Fock operator.
- describe the mean-field approximation. `Editor: This question should be more concrete`
- properties of the exchange hole. Relation of the exchange hole to the two-particle density.
- provide creation and annihilation operators in terms of Slater determinants, once as real-space- and spin wave functions, as well as using Slater determinants in occupation-number representation.
- explain the physical significance of the spectral function. (relation to photoemission, inverse photoemission and optical excitation) Why is the one-particle spectral function insufficient to describe optical spectra? What is missing?
- know the definition of natural orbitals and occupations.
- know the concept of a Boltzmann entropy (according to my definition!) and von-Neumann’s entropy. Know the functional form for fermions.
- Convert a one-particle Hamiltonian in Dirac notation into a one-particle-at-a-time operator with creation and annihilation operators.
- Slater-Condon rules and maximum coincidence.
- down-folding: example is the non-interacting Hubbard dimer
- conversion between: (1) Slater determinant (2) occupation-number representation (3) creation and annihilation operators applied to vacuum state
- transformation of one-particle basis set between: (1) orbital representation (2) eigenstates of the non-interacting Hamiltonian (3) real-space (4) reciprocal space
- translate a general operator into its representation with creation and annihilation operators.
- manipulate expressions with creation and annihilation operators
- Schrödinger-, Heisenberg- and interaction picture
- construct the Green’s function from the vacuum (closed) diagrams. (For example considering only a single diagram.)
- understand and work with retarded potentials
- derive the spectral function from a non-interacting Green’s function
- express the propagator in Fock space once using energy dependent wave functions and once as time-ordered exponential.

- Lehmann's representation of the Green function
- spectral function in terms of quasiparticle amplitudes.
- spectral function of the interacting Hubbard atom
- express the Green's function using the spectral function. (for a time-independent Hamiltonian.)
- know the definition of a quasi-particle.
- properties of the propagator (in complex time)
- time-ordered exponential
- Green's function
  - construct the bare (non-interacting) Green's function with a given Hamiltonian
  - contour-ordered GF in the Heisenberg picture
  - contour-ordered GF in the interaction picture using the trace with the non-interacting ensemble.
  - Explain contours: What is the Matsubara branch good for?
  - extract the full Green's function from a given generating functional of the bare Green's function.
- know the main formulas: eg. one-particle-reduced density matrix, many-particle Green's function, self energy, equation of motion of the many-particle Green's function, Dyson's equation, Lehmann representation, spectral density, Wick's theorem.
- understand the difference between contours in the interaction and the Heisenberg picture. Why are the contours different?
- diagrams:
  - conversion between: (1) Feynman diagram (2) permutation vector (3) formula
  - sign factor using sign theorem
  - symmetry factors
  - Define the meaning of "sum over all diagrams" in the generating functional. Each labeled diagram of order n corresponds to an $2n$-dimensional permutation vector. Unlinked diagrams need to be excluded. Eeach labeled diagram carries a factor $1/(n!2^n)$ and each unlabeled diagram has a factor $1/S(D)$ where S is the symmetry factor of diagram D.
- perform functional derivatives
- transform Green's function from time arguments into energy arguments.
- be able to determine the time-dependent wave function in the presence of an energy dependent self energy.

18.3 Summary

In this section, I will collect the expression of some physical quantities in different forms. I will not explain the symbols here, but I include the link to the equation in the text. For better comparison, I will give preference to the general operator form.

- one-particle-reduced density matrix (Watch the order of the indices/arguments!)

$$\begin{aligned}\hat{\rho}^{(1)}(t) &= \sum_{\alpha,\beta} |\chi_\alpha\rangle \underbrace{\left\{ \sum_q P_q \langle \Phi_q(t) | \hat{c}_\beta^\dagger \hat{c}_\alpha | \Phi_q(t)\rangle \right\}}_{\rho^{(1)}_{\alpha,\beta}(t)} \langle \chi_\beta| \\ &= \int dx \int d^4x' \, |\vec{x}\rangle \underbrace{\left\{ \sum_q P_q \left\langle \Phi_q(t) \middle| \hat{\psi}^\dagger(\vec{x}') \hat{\psi}(\vec{x}) \middle| \Phi_q(t) \right\rangle \right\}}_{\rho^{(1)}(\vec{x},\vec{x}',t)} \langle \vec{x}'| \\ &= \sum_n |\varphi_n\rangle f_n \langle \varphi_n| \\ &= -i\hbar \lim_{t' \to t^+} \hat{G}^{\mathcal{C}}(t,t') \end{aligned} \tag{18.1}$$

- Green's function

$$\begin{aligned}\hat{G}^{\mathcal{C}}(t,t') &= \sum_{\alpha,\beta} |\chi_\alpha\rangle G^{\mathcal{C}}_{\alpha,\beta}(t,t') \langle \chi_\beta| \\ &\overset{\text{Eq. 7.16}}{=} \sum_{\alpha,\beta} |\chi_\alpha\rangle \frac{1}{i\hbar} \mathrm{Tr}\left\{ \hat{\rho}^{(W)}_{T,\mu} \mathcal{T}_{\mathcal{C}} \hat{c}_{H,\alpha}(t) \hat{c}^+_{H,\beta}(t') \right\} \langle \chi_\beta| \\ &\overset{\text{Eq. 10.17}}{=} \sum_{\alpha,\beta} |\chi_\alpha\rangle \left[\frac{1}{i\hbar} \mathrm{Tr}\left\{ \hat{\rho}^{(W)}_{T,\mu} \mathcal{T}_{\mathcal{C}} \hat{S}_{I,\mathcal{C}} \hat{c}_{I,\alpha}(t) \hat{c}^+_{I,\beta}(t') \right\} \right] \langle \chi_\beta| \\ &\overset{\text{Eq. 10.17}}{=} \sum_{\alpha,\beta} |\chi_\alpha\rangle \left[\frac{1}{i\hbar} \frac{\mathrm{Tr}\left\{ \hat{\rho}^{(0)}_{T,\mu} \mathcal{T}_{\mathcal{C}} \hat{S}_{I,\mathcal{C}} \hat{c}_{I,\alpha}(t) \hat{c}^+_{I,\beta}(t') \right\}}{\mathrm{Tr}\left\{ \hat{\rho}^{(0)}_{T,\mu} \mathcal{T}_{\mathcal{C}} \hat{S}_{I,\mathcal{C}} \right\}} \right] \langle \chi_\beta| \\ &\overset{\text{Eq. ??}}{=} \frac{1}{i\hbar} \int_{-\infty}^{\infty} d\epsilon \, \hat{\mathcal{A}}^{(tot)}(\epsilon) \Big([1 - f_{T,\mu}(\epsilon)] \theta(t-t') - f_{T,\mu}(\epsilon) \theta(t'-t) \Big) \mathrm{e}^{-\frac{i}{\hbar}\epsilon(t-t')} \end{aligned} \tag{18.2}$$

$$\begin{aligned}\hat{G}^{\mathcal{C}}(\hbar\omega) &\overset{\text{Eq. ??}}{=} \lim_{\eta \to 0^+} \int_{-\infty}^{\infty} dt \, \mathrm{e}^{\frac{i}{\hbar}(\hbar\omega t + i\eta|t|)} \hat{G}^{\mathcal{C}}(t,0) \quad \text{for } \hbar\omega \in \mathbb{R} \\ &\overset{\text{Eq. ??}}{=} \lim_{\eta \to 0^+} \int_{-\infty}^{\infty} d\epsilon \, \hat{\mathcal{A}}^{(tot)}(\epsilon) \left[\frac{1 - f_{T,\mu}(\epsilon)}{\hbar\omega - \epsilon + i\eta} + \frac{f_{T,\mu}(\epsilon)}{\hbar\omega - \epsilon - i\eta} \right] \end{aligned} \tag{18.3}$$

- von-Neumann density matrix

$$\hat{\rho}^{vN} = \sum_q |\Phi_q\rangle P_q \langle \Phi_q| \qquad \text{with } \langle \Phi_q | \Phi_q \rangle = 1, \; P_q \geq 0, \; \sum_q P_q = 1 \tag{18.4}$$

- thermal von-Neumann density matrix (grand ensemble)

$$\begin{aligned}\hat{\rho}^{vN}_{T,\mu} &= \frac{1}{Z_{T,\mu}} \mathrm{e}^{-\beta(\hat{H} - \mu\hat{N})} \\ &= \sum_q |\Phi_q\rangle \frac{1}{Z_{T,\mu}} \mathrm{e}^{-\beta(E_q - N_q)} \langle \Phi_q| \qquad \text{with } \hat{H}|\Phi_q\rangle = |\Phi_q\rangle E_q \text{ and } \hat{N}|\Phi_q\rangle = |\Phi_q\rangle N_q \end{aligned} \tag{18.5}$$

- Slater determinant

$$
\begin{aligned}
|\vec{\sigma}\rangle &\overset{\text{Eq. 3.21}}{=} \prod_{j=1}^{\infty} \left(\hat{a}_j^\dagger\right)^{\sigma_j} |\mathcal{O}\rangle \qquad \text{watch the order!} \\
\langle \vec{x}_1, \vec{x}_2, \ldots, \vec{x}_N | \vec{\sigma}\rangle &\overset{\text{Eq. 1.88}}{=} \frac{1}{\sqrt{N!}} \sum_{i_1,\ldots,i_N} \epsilon_{i_1,\ldots,i_N} \varphi_{i_1}(\vec{x}_1) \cdots \varphi_{i_N}(\vec{x}_N) \\
&\overset{\text{Eq. 1.88}}{=} \frac{1}{\sqrt{N!}} \det \begin{vmatrix} \varphi_1(\vec{x}_1) & \varphi_1(\vec{x}_2) & \ldots & \varphi_1(\vec{x}_N) \\ \varphi_2(\vec{x}_1) & \varphi_2(\vec{x}_2) & \ldots & \varphi_2(\vec{x}_N) \\ \vdots & \vdots & & \vdots \\ \varphi_N(\vec{x}_1) & \varphi_N(\vec{x}_2) & \ldots & \varphi_N(\vec{x}_N) \end{vmatrix}
\end{aligned} \tag{18.6}
$$

18.4 Todo

This section collects suggestions from the students for improvements.

- make symbols uniform
- prepare a time plan for the material
- select one exercise per week. (The exercises are relatively extensive.) Also include smaller exercises in the spirit of examination questions as opposed to the "mini-projects".
- explain teaching goals for the exercises in their introduction and connect them with the material in the lecture.
- Specific: Introduce an exercise on functional derivatives before the derivation of the Fock operator.
- In the exercises add tasks such as "discuss the physics of the result just obtained"
- the von-Neumann density of states is still denoted as $\hat{\rho}$ without the superscript vN. The superscript shall be included consistently. Similarly the von-Neumann entropy shall be named consistently as S^{vN}.
- Check that the thermal density matrix have consistently the superscripts T, μ.
- the section on Wick's theorem shall demonstrate the derivation using a constant Hamiltonian, which simplifies the derivation dramatically. This derivation is currently in the appendix 10.2.4 on p. 319.

18.5 Distribution of the teaching load

Editor: Do not read this. It is in preparation.

The teaching period of semester has 14 weeks. The lecture aims at four academic hours of teaching and two academic hours of exercise classes. An academic hour consists of 45 min teaching.

Type refers to lecture "L" and exercises "E". Sections refer to the section number in these lecture notes. Note, however that the numbers may become asynchronous with the lecture notes and need to be updated.

Week	type	sections	topics
1	L	1.1-1.2	**One-particle QM and N-particle QM**
			Bra-ket notation, spin orbitals, extended states, non-orthonormal orbitals
			Slater determinants
1	L	1.3-1.4	**Many-particle states and thermodynamics**
			Fock space, occupation-number representation
			ensembles, entropy, grand potential, Fermi distribution
1	E	1.5	**Non-interacting electrons**
			hydrogen molecule, linear chain, free-electron gas, 2 1-d particles in a box
2	L	2.1-2.4	**Hartree-Fock total energy and selfconsistency**
			one and two-particle operators, Slater rules, HF total energy
			Hartree and exchange energy, 1-p reduced density matrix, Fock operator
2	L	2.5-2.9	**Spectral properties and exchange hole**
			Experiments, addition and removal energies, spectral function
			exciton binding energy
			exchange hole, Hund's rule, HF of the free-electron gas
2	E		
3	L	3.1-3.5	**Creation and annihilation operators**
3	L	2.5-2.9	**Field operators, change of representation**
3	E		**Conversion to and from field operators**
4	L	4	**Green's functions in one-particle QM**
4	L	5	**Open systems and down folding**
4	E		**Simple Green's function problems**
5	L	6	**Propagator, time-ordering operator**
5	L	7.1-7.7	**Green's function concept in many-particle physics**
5	E		
5	L		
5	L		
5	E		
6	L		
6	L		
6	E		
7	L		
7	L		
7	E		

Week	type	sections	topics
8	L		
8	L		
8	E		
9	L		
9	L		
9	E		
10	L		
10	L		
10	E		
11	L		
11	L		
11	E		
12	L		
12	L		
12	E		
13	L		
13	L		
13	E		
14	L		
14	L		
14	E		

18.6 List of exercises

1. Chapter 1: Non-interacting electrons
   (a) 1.6.1 Hydrogen molecule
   (b) 1.6.2 General diatomic molecule
   (c) 1.6.3 Linear chain of hydrogen atoms
   (d) 1.6.4 Insulating linear chain
   (e) 1.6.5 Free-electron gas or jellium model
   (f) ~~1.6.6 Thermodynamics of the hydrogen molecule~~
2. Chapter 2: Weakly interacting electrons
   (a) 2.9.1 The hydrogen atom in the Hartree-Fock approximation
   (b) 2.9.2 Two one-dimensional particles in a box
   (c) 2.9.3 Two fermions in a 1d-box
   (d) 2.9.4 Self-made density functional
3. Chapter 3: Second Quantization
   (a) ~~3.11.1 Hartree Fock at finite temperature~~
   (b) 3.11.2 Hydrogen molecule with interacting electrons !
   (c) 3.11.3 Spin eigenstates !
   (d) 3.11.4 Ground state of the linear chain in second quantization

4. Chapter 4: Green's functions in one-particle quantum mechanics
   (a) 4.6.1 ~~Role of boundary conditions~~
   (b) 4.6.2 Green's function for a Lorentzian-shaped density of states
5. Chapter 5: Composite and open systems: down-folding and retarded potentials
   (a) 5.4.1 Minimal model for a quantum system coupled to a bath
   (b) 5.4.2 System in contact with a bath having a finite life time
   (c) 5.4.3 Fano-Anderson model
   (d) 5.4.5 Surface Green's function of a one-dimensional linear chain
   (e) 5.4.6 ~~Interfaces and metal-induced gap states (sketch only)~~
   (f) 5.4.7 ~~Inelastic tunneling (Sketch only)~~
6. Chapter 6: Dynamics in Fock space and complex time
   No exercises yet
7. Chapter 7: Green's functions in many-particle physics
   (a) 7.6.1 Non-interacting contour Green's function for the non-interacting hy- drogen molecule
8. Chapter 8: Exact properties of the many-particle Green's function
   (a) 8.5.1 Self-energy and contour Green's function of the Hubbard atom
9. Chapter 9: Spectral properties
   (a) 9.6.1 Model for strongly retarded Green's function
   (b) ~~9.6.3 Exercise: Anderson impurity model~~
   (c) ~~9.6.4 Home study and practice: spectral function and momentum density of a 1d chain~~
10. Chapter 10: Diagrammatic expansion of the Green's function
    (a) 10.5.1 Green's function from generating functional
11. Chapter 11: Diagrammatics of the generating functional
    (a) 11.9.1 Enumerate permutations !
    (b) 11.9.2 Feynman diagrams from permutation vectors !
    (c) 11.9.3 Value of a Feynman diagrams ! Editor: complete
    (d) 11.9.4 Evaluate the symmetry factor ! Editor: complete
    (e) ~~11.9.5 Example: Evaluate the Green's function for a specific example~~

18.7 Timeline 2024

1	Tue 09.04	Ch.1 non-interacting electrons, Slater determinants
2	Thu 11.04	1p and 2p operators, 1p expectation values, 1p-reduced density matrix
3	Tue 16.04	2p expectation values, Hartree and Exchange
4	Thu 18.04	xc hole, ensemble, vN density matrix, vN entropy
5	Tue 23.04	Thermal Hartree Fock
6	Thu 25.04	Hartree-Fock equations
7	Tue 30.04	Spectral properties
8	Thu 02.05	Sick-leave
9	Tue 07.05	Holiday
10	Thu 09.05	Second Quantization up to Slater Condon rules
11	Tue 14.05	Second Quantization Representation, Field operators
12	Thu 16.05	Green's function
13	Tue 21.05	Green's function as propagator, Dyson operator
14	Thu 23.05	
15	Tue 28.05	
16	Thu 30.05	
17	Tue 04.06	
18	Thu 06.06	
19	Tue 11.06	
20	Thu 13.06	
21	Tue 18.06	
22	Thu 29.06	
23	Tue 25.06	
24	Thu 27.06	
25	Tue 02.07	
26	Thu 04.07	
27	Tue 09.07	
28	Thu 11.07	

18.8 Timeline 2026

1	We 15.04	Ch.1 non-interacting electrons, Slater determinants
2	Thu 16.04	1p and 2p operators, 1p expectation values, 1p-reduced density matrix
3	We 22.04	2p expectation values, Hartree and Exchange
4	Thu 23.04	xc hole, ensemble, vN density matrix, vN entropy
5	We 29.04	Thermal Hartree Fock
6	Thu 30.04	Hartree-Fock equations
7	We 06.04	Spectral properties
8	Thu 07.05	Sick-leave
9	We 13.05	Second Quantization up to Slater Condon rules
10	Thu 14.05	—- Holiday —— Christi Himmelfahrt
11	We 20.05	Second Quantization Representation, Field operators
12	Thu 21.05	Green's function
13	We 27.05	Green's function as propagator, Dyson operator
14	Thu 28.05	
15	We 03.06	
16	Thu 04.06	
17	We 10.06	
18	Thu 11.06	
19	We 17.06	
20	Thu 18.06	
21	We 24.06	
22	Thu 26.06	
23	We 01.07	
24	Thu 02.07	
25	We 08.07	
26	Thu 09.07	
27	We 15.07	
28	Thu 16.07	

Part III

Appendices

Appendix A

Mathematical expressions

A.1 Crazy idea: representation of the entropy

Editor: Crazy idea: This is a note for myself.

The following may be very useful for a numerical description, because the approximations avoid the infinite slope at the boundaries of the interval. The consequences of the finite slope on the physics needs to be understood.

Replace Shannon's entropy by an approximation that avoids the singularity at the origin.

$$-x\ln(x) = \lim_{N\to\infty} x\sum_{n=1}^{2N+1}\frac{1}{n}(1-x)^n \tag{A.1}$$

Approximations are obtained with a finite N. The highest power must be odd, so that the approximated function is bounded from above. The slope of the expansion at $x = 0$ is not infinity as in the original function. The expansion is a lower bound in the interval $x \in]0, 1[$. It is bounded from above for every N. The expansion vanishes for both $x = 0$ and $x = 1$.

For the Boltzmann entropy I can use

$$\begin{aligned} -x\ln(x) - (1-x)\ln(1-x) &= x\sum_{n=1}^{2N+1}\frac{1}{n}(1-x)^n + (1-x)\sum_{n=1}^{2N+1}\frac{1}{n}x^n \\ &= \sum_{n=1}^{2N+1}\frac{1}{n}\Big(x(1-x)^n + (1-x)x^n\Big) \end{aligned} \tag{A.2}$$

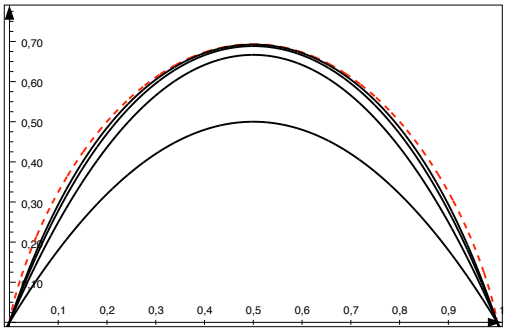


Fig. A.1: Approximate Boltzmann entropy Eq. A.2 for $N = \{0; 1; 2; 3\}$ (black) compared to the correct result (red dashed).

The result is shown in figure A.1.

One may ask what is the corresponding approximation of the Fermi distribution. The Fermi function can be obtained from the variational principle for a single-level Hamiltonian.

$$\begin{aligned} E &= -k_B T\Big(f\ln(f) + (1-f)\ln(1-f)\Big) + (\epsilon-\mu)f \\ 0 &\stackrel{!}{=} \frac{\partial E}{\partial f} - k_B T ln(f) + 1 - ln(1-f) - 1 + (\epsilon-\mu) \Rightarrow f = \Big(1+e^{\beta(\epsilon-\mu)}\Big)^{-1} \end{aligned} \tag{A.3}$$

With the approximate entropy term the result is as follows:

$$\begin{aligned} E' &= k_B T \sum_{n=1}^{2N+1} \frac{1}{n}\Big(f(1-f)^n + (1-f)f^n\Big) + (\epsilon-\mu)f \\ 0 &\stackrel{!}{=} \frac{\partial E'}{\partial f} = k_B T \sum_{n=1}^{2N+1} \frac{1}{n}\Big((1-f)^n - nf(1-f)^{n-1} - f^n + (1-f)nf^{n-1}\Big) + \epsilon - \mu \end{aligned} \tag{A.4}$$

I cannot resolve this for $f(\epsilon)$ but one can evaluate the inverse function $\epsilon(f)$

$$\epsilon(f) = \mu + k_B T \sum_{n=1}^{2N+1}\Big[(1-f)^n\Big(\frac{1}{n} - \frac{f}{1-f}\Big) - f^n\Big(\frac{1}{n} - \frac{1-f}{f}\Big)\Big] \tag{A.5}$$

The approximate Fermi function is not bounded in the interval $[0,1]$ and thus violates N-representability. Thus we need to freeze the occupations to zero or one, if the energy lies outside a specific energy window centered at the chemical potential.

- For $N = 15$, the approximate Fermi function leaves the interval $[0,1]$ for $|\epsilon - \mu| > 5.0272 k_B T$.
- For $N = 3$, the approximate Fermi function leaves the interval $[0,1]$ for $|\epsilon - \mu| > 3.5928 k_B T$.
- For $N = 2$, the approximate Fermi function leaves the interval $[0,1]$ for $|\epsilon - \mu| > 3.2925 k_B T$.

Remedy:

The occupations must be clamped to $f = 0$ or $f = 1$ if the energy leaves the interval for which the approximate occupations would leave the interval $[0,1]$. The corresponding entropy is zero.

A.2 Laplace expansion theorem (not needed)

Let D be the determinant of an $N \times N$ matrix $\boldsymbol{A}$, and let $D^{i,j}_{N-1}$ be the determinant of the matrix obtained from $\boldsymbol{A}$ by deleting the i-th line and the j-th column. Then

$$D = \sum_{i=1}^{N} (-1)^{i+j} A_{i,j} D^{i,j}_{N-1}$$

The Laplace expansion theorem can be applied twice, leading to

$$D = \sum_{i=1}^{N}\sum_{k=1}^{N} (-1)^{i+j+k+l} A_{i,j} A_{k,l} D^{ik,jl}_{N-2}$$

where $D^{ik,jl}$ is the determinant of the matrix $\boldsymbol{A}$ with the i-th and k-th line, and the j-th and l-th column deleted.

A.3 Fourier transforms

Here, I summarize only the main formulas used in this lecture. More on the Fourier transform can be found in ΦSX:Quantum physics[16].

A.3.1 Choices

Fourier transforms in time

$$F(\omega) = \int dt\ f(t) \mathrm{e}^{i\omega t} \tag{A.6}$$

$$f(t) = \int \frac{d\omega}{2\pi}\ F(\omega) \mathrm{e}^{-i\omega t} \tag{A.7}$$

$$F(\epsilon) = \int dt\ f(t) \mathrm{e}^{\frac{i}{\hbar}\epsilon t} \tag{A.8}$$

$$f(t) = \int \frac{d\epsilon}{2\pi\hbar}\ F(\omega) \mathrm{e}^{-\frac{i}{\hbar}\epsilon t} \tag{A.9}$$

$f(t)$	$F(\omega)$
$\delta(t)$	1
1	$2\pi\delta(\omega)$

Fourier transforms in space

$$F(\vec{k}) = \int d^3r\ f(\vec{r}) \mathrm{e}^{-i\vec{k}\vec{r}} \tag{A.10}$$

$$f(\vec{r}) = \int \frac{d^3k}{(2\pi)^3} F(\vec{k}) \mathrm{e}^{i\vec{k}\vec{r}} \tag{A.11}$$

$$F(\vec{p}) = \int d^3r\ f(\vec{r}) \mathrm{e}^{-\frac{i}{\hbar}\vec{p}\vec{r}} \tag{A.12}$$

$$f(\vec{p}) = \int \frac{d^3p}{(2\pi\hbar)^3} F(\vec{k}) \mathrm{e}^{i\vec{k}\vec{r}} \tag{A.13}$$

A.3.2 Fourier transform of the step function

Here, we derive the relation

$$\int_{-\infty}^{\infty} dt\ \theta(t) \mathrm{e}^{\frac{i}{\hbar}(\epsilon+i\eta)t} = \frac{i\hbar}{\epsilon+i\eta} \tag{A.14}$$

$$\int_{-\infty}^{\infty} dt\ \theta(-t) \mathrm{e}^{\frac{i}{\hbar}(\epsilon-i\eta)t} = \frac{-i\hbar}{\epsilon-i\eta} \tag{A.15}$$

where $\eta > 0$.

Derivation:

$$\int_{-\infty}^{\infty} dt\ \theta(t) \mathrm{e}^{\frac{i}{\hbar}(\epsilon+i\eta)t} = \int_{0}^{\infty} dt\ \mathrm{e}^{\frac{i}{\hbar}(\epsilon+i\eta)t} = \frac{1}{\frac{i}{\hbar}(\epsilon+i\eta)} \mathrm{e}^{\frac{i}{\hbar}(\epsilon+i\eta)t}\Big|_{0}^{\infty}$$
$$\overset{\eta>0}{=} \frac{-1}{\frac{i}{\hbar}(\epsilon+i\eta)} = \frac{i\hbar}{\epsilon+i\eta}$$

$$\int_{-\infty}^{0} dt\ \theta(-t) \mathrm{e}^{\frac{i}{\hbar}(\epsilon-i\eta)t} = \int_{-\infty}^{0} dt\ \mathrm{e}^{\frac{i}{\hbar}(\epsilon-i\eta)t} = \frac{1}{\frac{i}{\hbar}(\epsilon-i\eta)} \mathrm{e}^{\frac{i}{\hbar}(\epsilon-i\eta)t}\Big|_{-\infty}^{0}$$
$$\overset{\eta>0}{=} \frac{1}{\frac{i}{\hbar}(\epsilon-i\eta)} = \frac{-i\hbar}{\epsilon-i\eta}$$

The function is a simple pole at $\epsilon = -i\eta$ or $\epsilon = +i\eta$ respectively.

A.4 Wirtinger derivatives

In order to form the derivatives with respect to complex numbers, it is advantageous to be familiar with the **Wirtinger derivatives**, which are described briefly in ΦSX: Klassische Mechanik.

Wirtinger derivatives The essence of Wirtinger derivatives is that we can write the identity

$$\begin{aligned} df &= \frac{\partial f}{\partial \mathrm{Re}[z]} d\mathrm{Re}[z] + \frac{\partial f}{\partial \mathrm{Im}[z]} d\mathrm{Im}[z] \\ &= \underbrace{\frac{1}{2}\Big(\frac{\partial f}{\partial \mathrm{Re}[z]} - i\frac{\partial f}{\partial \mathrm{Im}[z]}\Big)}_{df/dz} \underbrace{\Big(d\mathrm{Re}[z] + i d\mathrm{Im}[z]\Big)}_{dz} + \underbrace{\frac{1}{2}\Big(\frac{\partial f}{\partial \mathrm{Re}[z]} + i\frac{\partial f}{\partial \mathrm{Im}[z]}\Big)}_{df/dz^*} \underbrace{\Big(d\mathrm{Re}[z] - i d\mathrm{Im}[z]\Big)}_{dz^*} \\ &= \frac{df}{dz} dz + \frac{df}{dz^*} dz^* \end{aligned} \tag{A.16}$$

for the first variation of f. Thus, we can form the variations of a function of complex arguments, as if the variable and its complex conjugate were completely independent variables.
The Wirtinger derivatives are defined as

$$\begin{aligned} \frac{\partial f}{\partial z} &= \frac{1}{2}\Big(\frac{\partial f}{\partial \mathrm{Re}[z]} - i\frac{\partial f}{\partial \mathrm{Im}[z]}\Big) \\ \frac{\partial f}{\partial z^*} &= \frac{1}{2}\Big(\frac{\partial f}{\partial \mathrm{Re}[z]} + i\frac{\partial f}{\partial \mathrm{Im}[z]}\Big). \end{aligned} \tag{A.17}$$

The Wirtinger derivatives obey the following rules:

- linearity

$$\begin{aligned} \frac{\partial\Big(af(z,z^*) + bg(z,z^*)\Big)}{\partial z} &= a\frac{\partial f(z,z^*)}{\partial z} + b\frac{\partial g(z,z^*)}{\partial z} \\ \frac{\partial\Big(af(z,z^*) + bg(z,z^*)\Big)}{\partial z^*} &= a\frac{\partial f(z,z^*)}{\partial z^*} + b\frac{\partial g(z,z^*)}{\partial z^*} \end{aligned} \tag{A.18}$$

- product rule

$$\begin{aligned} \frac{\partial\Big(f(z,z^*)g(z,z^*)\Big)}{\partial z} &= \frac{\partial f(z,z^*)}{\partial z} g(z,z^*) + f(z,z^*)\frac{\partial g(z,z^*)}{\partial z} \\ \frac{\partial\Big(f(z,z^*)g(z,z^*)\Big)}{\partial z^*} &= \frac{\partial f(z,z^*)}{\partial z^*} g(z,z^*) + f(z,z^*)\frac{\partial g(z,z^*)}{\partial z^*} \end{aligned} \tag{A.19}$$

- complex conjugation

$$\begin{aligned} \frac{\partial\,[f(z,z^*)]^*}{\partial z} &= \left(\frac{\partial f(z,z^*)}{\partial z^*}\right)^* \\ \frac{\partial\,[f(z,z^*)]^*}{\partial z^*} &= \left(\frac{\partial f(z,z^*)}{\partial z}\right)^* \end{aligned} \tag{A.20}$$

- chain rule

$$\begin{aligned} \frac{\partial\Big[f\left(g(z,z^*), g^*(z,z^*)\right)\Big]}{\partial z} &= \frac{\partial f(g,g^*)}{\partial g}\frac{\partial g(z,z^*)}{\partial z} + \frac{\partial f(g,g^*)}{\partial g^*}\left(\frac{\partial g^*(z,z^*)}{\partial z}\right) \\ \frac{\partial\Big[f\left(g(z,z^*), g^*(z,z^*)\right)\Big]}{\partial z^*} &= \frac{\partial f(g,g^*)}{\partial g}\frac{\partial g(z,z^*)}{\partial z^*} + \frac{\partial f(g,g^*)}{\partial g^*}\left(\frac{\partial g(z,z^*)}{\partial z}\right)^* \end{aligned} \tag{A.21}$$

A complex function is analytic, if $\frac{\partial f}{\partial z^*} = 0$.
My personal recommendation is to produce the rules from the first variation of the complex function in terms of dz and dz', rather than to memorize these equations.

For the derivatives, we use

$$\frac{d\Psi_n^*(\vec{r},\sigma)}{d\Psi_k^*(\vec{r}_0,\sigma_0)} = \delta(\vec{r}-\vec{r}_0)\delta_{\sigma,\sigma_0}\delta_{n,k} \qquad \text{and} \qquad \frac{d\Psi_n(\vec{r},\sigma)}{d\Psi_k^*(\vec{r}_0,\sigma_0)} = 0 \tag{A.22}$$

A.5 Cauchy relation

Editor: Relation to Kramers-Kronig relations

(Cauchy relation Eq.2.23 of Stefanucci.)

$$\lim_{\eta\to 0^+} \frac{1}{\epsilon-\epsilon_0 \pm i\eta} = P\frac{1}{\epsilon-\epsilon_0} \mp i\pi\delta(\epsilon-\epsilon_0) \tag{A.23}$$

where P denotes the principal part.

Cauchy principal value is[Bronstein and Semendyayev 1997, p. 283]

$$P\int_a^b dx\, f(x) = \lim_{\epsilon\to 0^+}\left[\int_a^{c-\epsilon} dx\, f(x) + \int_{c+\epsilon}^b dx\, f(x)\right] \tag{A.24}$$

A.6 Imaginary part of a pole and spectral density

In Eq. 4.54 on p. 4.54, we used the identity

IMAGINARY PART OF A POLE AND THE DELTA FUNCTION

$$-\frac{1}{\pi}\lim_{\eta\to 0}\mathrm{Im}\Big(\frac{1}{x+i\eta}\Big) = \delta(x) \tag{A.25}$$

It is used to extract the density of states respectively the spectral function from a Green's function.

First, we determine the imaginary part

$$\frac{1}{x+i\eta} = \frac{x-i\eta}{x^2+\eta^2} \qquad \Rightarrow \qquad \mathrm{Im}\Big(\frac{1}{x+i\eta}\Big) = \frac{-\eta}{x^2+\eta^2} \tag{A.26}$$

The imaginary part of an inverse pole in the complex plane is closely related to a **Lorentzian** $L_\eta(x)$.

LORENTZIAN

$$L_\eta(x) \stackrel{\text{def}}{=} \frac{1}{\pi}\frac{\eta}{x^2+\eta^2} = -\frac{1}{\pi}\mathrm{Im}\Big(\frac{1}{x+i\eta}\Big) \tag{A.27}$$

The Lorentzian is fairly pathological function because of its long ranged tails. While the integral is defined, its first and higher moments $M_n = \int_{-\infty}^{\infty} dx\, x^n L(x)$ with $n \geq 1$ are ill-defined.

Let me demonstrate that the Lorentzian integrates to one. [1]

$$\int_{-\infty}^{\infty} dx\ \frac{\eta}{x^2+\eta^2} = \int_{-\infty}^{\infty} \frac{dx}{\eta}\ \frac{1}{\left(1+\frac{x}{\eta}\right)^2} \overset{z\overset{\text{def}}{=}\frac{x}{\eta}}{=} \int_{-\infty}^{\infty} dz\ \frac{1}{1+z^2} \overset{z(q)=\tan(q)}{=} \int_{-\infty}^{\infty} dz\ \frac{dq}{dz} = \int_{-\frac{\pi}{2}}^{\frac{\pi}{2}} dq = \pi$$

$$\Rightarrow \qquad \int_{-\infty}^{\infty} dx\ L_\eta(x) = 1 \tag{A.30}$$

Next I will demonstrate, that the Lorentzians approach the delta function for $\eta \to 0$.

$$\lim_{\eta\to 0} L_\eta(x) = \lim_{\eta\to 0} \mathrm{Im}\Big[-\frac{1}{\pi}\frac{\eta}{x^2+\eta^2}\Big] = \delta(x) \tag{A.31}$$

In other words, when the position $x + i\eta$ of the pole approaches the real axis, its imaginary part approaches, up to a constant, a delta function.

A complete proof for the identity of $L_0(x)$ with the delta function would need to establish

$$\int dx\ L_0(x) g(x) = g(0) \tag{A.32}$$

for any function that is differentiable to arbitrary high order.

Here. we we will show that it is a series of functions, that (1) integrate to one, that (2) are positive and that (3) approach zero except for the origin.

- We have already shown above that the integral of the Lorentzian equals unity.
- From the defining equation Eq. A.27, it is easily seen that a Lorentzian is positive everywhere.
- In the limit $\eta \to 0$, the Lorentzian vanishes except at the origin.

$$\lim_{\eta\to 0} \frac{\eta}{x^2+\eta^2} \overset{x\neq 0}{=} \lim_{\eta\to 0} \frac{\eta}{x^2} = 0 \qquad \text{for} \qquad x \neq 0 \tag{A.33}$$

Thus, we have shown that Eq. A.25 is valid.

A.7 Padé approximation

Editor: In progress:

The Padé approximation[2] is used to perform an analytic continuation of the Matsubara Green's function or the self energy from the imaginary frequency axis to the real frequency axis. Its values on the real frequency axis is the spectral function.

In this section, I am following the article of Schött et al. [doi:10.1103/PhysRevB.93.075104].

The Padé approximation is an interpolation of a complex function by a rational polynomial.

$$P_{k,r}(z) = \frac{\sum_{i=1}^{k+1} a_i z^{i-1}}{\left[\sum_{i=1}^{r} b_i z^{i-1}\right] + z^r} \tag{A.34}$$

[1] In the derivation, we use the variable transform

$$q(z) \overset{\text{def}}{=} \mathrm{atan}(z) \qquad \Rightarrow \qquad q(z=\pm\infty) = \pm\frac{\pi}{2} \tag{A.28}$$

$$z(q) = \tan(q) \qquad \Rightarrow \qquad \frac{dz}{dq} = \frac{\sin^2(q)+\cos^2(q)}{\cos^2(q)} = \frac{\sin^2(q)}{\cos^2(q)} + 1 = 1 + \tan^2(q) = 1 + z^2 \tag{A.29}$$

[2] Named after the French Mathematician Henri Padé. Earlier work has been published by Georg Frobenius. (Source: Wikipeida: Padé approximation)

This polynomial has poles at the zeros of the denominator, while the numerator controls the weights of the poles.

For large $|z|$ the function approaches

$$P_{k,r}(z) \to a_{k+1}z^{k-r} + \Big(a_k - a_{k+1}b_r\Big)z^{k-r-1} + \dots \tag{A.35}$$

For Greens function which fall off as $\frac{1}{z}$ the case $k = r - 1$ is relevant. The self energy behaves similarly, once the static contribution is subtracted. Therefore, we will be concerned with

$$P_r(z) = \frac{\sum_{i=1}^{r} a_i z^{i-1}}{\left[\sum_{i=1}^{r} b_i z^{i-1}\right] + z^r} \tag{A.36}$$

A.7.1 Problems

It is often said that the analytic continuation using the Padé approximation is unreliable when using noisy data as those obtained from a Quantum Monte Carlo calculation.

I myself made a few observations:

1. The spectral function is obtained from the imaginary part of the Green's function on the real frequency axis. If the poles are still close to the real frequency axis, small numerical errors can create results that vary strongly.

   The reason is that the imaginary part of a complex function varies extremely rapidly along the imaginary direction.

   $$-\frac{1}{\pi}\mathrm{Im}\left(\frac{1}{x+iy}\right) = -\frac{1}{\pi}\frac{y}{x^2+y^2} \overset{x\to 0}{\to} -\frac{1}{\pi}\frac{1}{y} \tag{A.37}$$

   Thus, a small shift, which displaces the pole across the real axis, can even change the sign of the density of states. A negative spectral function is furthermore nonphysical and renders the description useless.

   A possible remedy of this problem is to determine the spectral function for several lines, which are displaced along the imaginary component. This allows to identify the position of the pole and to correct it such that is falls on the correct side of the real frequency axis.

2. Matsubara Green's function spreads the information unevenly along the imaginary frequency axis. The Laurent expansion coefficients of the Green's function contain the energy moments of the spectral function, while the behavior close to the origin determines the structure of the spectral function near the Fermi level. The details of the spectral function are probably exponentially damped out beyond a few times $k_B T$ away from the Fermi level

   Therefore, I suggest to take one point for the interpolation at $i\omega_x$, which is the outermost point on the grid. The next few points are chosen at $\omega_j = i\omega_x 2^{-j}$. This captures the first few moments of the density of states. For the remaining points one could take the Matsubara frequencies next to the origin. The attempt to improve the result by increasing the points to be interpolated may worsen the results because it may give too much weight to region, where the Matsubara Green's function does not carry significant information.

A.7.2 Least-square Padé

From the requirement that the function $f(z)$ to be interpolated is represented at a given point z by the rational polynomial, we obtain the conditions

$$f(z) = P_r(z) \overset{\text{Eq. A.36}}{=} \frac{\sum_{i=1}^{r} a_i z^{i-1}}{\left[\sum_{i=1}^{r} b_i z^{i-1}\right] + z^r} \tag{A.38}$$

we obtain

$$\sum_{i=1}^{r} \left(z^{i-1}\right) a_i + \sum_{i=1}^{r} \left(-f(z)z^{i-1}\right) b_i = f(z)z^r \tag{A.39}$$

Let us now require the identity $f(z) = P_r(z)$ for a set of M points z_j with $j = 1, \ldots, M$. We obtain an equation system with M equations and $2r$ unknowns, the coefficients a_i and b_i.

$$\sum_{i=1}^{r} \left(z_j^{i-1}\right) a_i + \sum_{i=1}^{r} \left(-f(z_j)z_j^{i-1}\right) b_i = f(z_j)z_j^r \quad \text{for } j = 1, M \tag{A.40}$$

This system of equations is overdetermined with $M > 2r$. Therefore, we solve it with singular-value decomposition, which amounts to a least-square fit. The singular-value decomposition is a standard linear algebra operation, which is for example implemented in the numerical library LAPACK.

The singular value decomposition rewrites a $M \times 2r$ matrix $\boldsymbol{A}$ as

$$\boldsymbol{A} = \boldsymbol{U}\boldsymbol{\Sigma}\boldsymbol{V}^\dagger \tag{A.41}$$

where $\boldsymbol{U}$ is a unitary $M \times M$ matrix, $\boldsymbol{\Sigma}$ is a diagonal $M \times 2r$ matrix holding the real-values singular values on the diagonal. $\boldsymbol{V}$ is a unitary $2r \times 2r$ matrix.

The equation system $\boldsymbol{A}\vec{x} = \vec{b}$ can be solves approximately by

$$\boldsymbol{A}\vec{x} = \boldsymbol{U}\boldsymbol{\Sigma}\boldsymbol{V}^\dagger\vec{x} = \vec{b} \quad \Rightarrow \quad \vec{x} = \boldsymbol{V}\Sigma^{-1}\boldsymbol{U}^\dagger\vec{b} \tag{A.42}$$

The inversion of the singular values is done such that the inverse of a zero singular value is set to zero. This implies that the corresponding contribution is projected out.

The resulting vector x contains the coefficients a_i and b_i. This defines the interpolating rational polynomial, which can be evaluated for the desired values.

Sum of poles: The rational polynomial can be transformed into a sum of poles

$$P_r(z) \overset{\text{Eq. A.36}}{=} \frac{\sum_{i=1}^{r} a_i z^{i-1}}{\left[\sum_{i=1}^{r} b_i z^{i-1}\right] + z^r} = \sum_{k=1}^{r} \frac{A_k}{z - \bar{z}_k} \tag{A.43}$$

The coefficients are obtained as follows. First, we determine the poles $\bar{z}_k$ of the rational polynomial. The pole positions are the zeros of the polynomial in the denominator of the rational polynomial. The zero's can be obtained using the method of Vieta.

$$\begin{aligned}
P_r(z) = \frac{\sum_{i=1}^{r} a_i z^{i-1}}{\prod_{j=1}^{r}(z - \bar{z}_j)} &= \sum_{k=1}^{r} \frac{A_k}{z - z_k} \\
\Leftrightarrow \quad \sum_{i=1}^{r} a_i z^{i-1} &= \sum_{k=1}^{r} A_k \prod_{j=1; j\neq k}^{r} (z - \bar{z}_j) \\
\Rightarrow \quad \sum_{i=1}^{r} a_i \bar{z}_\ell^{i-1} &= \sum_{k=1}^{r} A_k \prod_{j=1; j\neq k}^{r} (\bar{z}_\ell - \bar{z}_j) = A_\ell \prod_{j=1; j\neq \ell}^{r} (\bar{z}_\ell - \bar{z}_j) \\
\Rightarrow \quad A_\ell &= \frac{\sum_{i=1}^{r} a_i \bar{z}_\ell^{i-1}}{\prod_{j=1; j\neq \ell}^{r}(\bar{z}_\ell - \bar{z}_j)}
\end{aligned} \tag{A.44}$$

Thus, we obtain as interpolation

$$P(z) = \sum_{k=1}^{r} \frac{1}{z - \bar{z}_k} \frac{\sum_{i=1}^{r} a_i \bar{z}_k^{i-1}}{\prod_{j=1; j\neq k}^{r}(\bar{z}_k - \bar{z}_j)} \tag{A.45}$$

Sum of poles: If the poles are on the wrong side of the real frequency axis, it will contribute with the wrong sign to the spectral function. Therefore, we shift all poles with the wrong imaginary part onto the real frequency axis.

In order to smoothen the spectral function I evaluate the spectral function on the imaginary axis.

A.8 Baker-Hausdorff Theorem

The Baker-Hausdorff theorem [3][158, 159, 160, 161, 162, 163] provides a method to evaluate the product of two exponentials of non-commutating operators[164]. Specifically we look for the resulting operator $\hat{C}$ of

$$e^{\hat{A}}e^{\hat{B}} = e^{\hat{C}}$$

for two given operators A, B.

Here, we will only investigate a few special cases.

A.8.1 Baker-Hausdorff Theorem

Here, I show a specialization of the Baker-Haussdorf theorem, which applies if certain commutator relations hold.

BAKER-HAUSDORFF THEOREM

$$e^{\hat{A}+\hat{B}} = e^{\hat{A}}e^{\hat{B}}e^{-\frac{1}{2}[\hat{A},\hat{B}]_-} \tag{A.46}$$

if both operators commutate with their commutator, i.e.

$$[\hat{A},[\hat{A},\hat{B}]_-]_- = [\hat{B},[\hat{A},\hat{B}]_-]_- = 0 \tag{A.47}$$

Proof:[4]

$$\begin{aligned} F(\alpha) &\stackrel{\text{def}}{=} e^{\alpha\hat{A}+\beta\hat{B}} \\ \frac{dF}{d\alpha} &= \frac{d}{d\alpha}\sum_{n=0}^{\infty}\frac{1}{n!}(\alpha\hat{A}+\beta\hat{B})^n \\ &= \sum_{n=0}^{\infty}\frac{1}{n!}\sum_{j=0}^{n-1}(\alpha\hat{A}+\beta\hat{B})^j\hat{A}(\alpha\hat{A}+\beta\hat{B})^{n-j-1} \end{aligned}$$

Let us now analyze the individual terms:

$$\begin{aligned} (\alpha\hat{A}+\beta\hat{B})\hat{A} &= \hat{A}(\alpha\hat{A}+\beta\hat{B}) + \beta[\hat{B},\hat{A}]_- \\ (\alpha\hat{A}+\beta\hat{B})^k\hat{A} &= (\alpha\hat{A}+\beta\hat{B})^{k-1}\hat{A}(\alpha\hat{A}+\beta\hat{B}) + (\alpha\hat{A}+\beta\hat{B})^{k-1}\beta[\hat{B},\hat{A}]_- \\ &\stackrel{\text{Eq. A.47}}{=} (\alpha\hat{A}+\beta\hat{B})^{k-1}\hat{A}(\alpha\hat{A}+\beta\hat{B}) + \beta[\hat{B},\hat{A}]_-(\alpha\hat{A}+\beta\hat{B})^{k-1} \\ &= \hat{A}(\alpha\hat{A}+\beta\hat{B})^k + k\beta[\hat{B},\hat{A}]_-(\alpha\hat{A}+\beta\hat{B})^{k-1} \end{aligned}$$

[3] Felix Hausdorff, 1868-1942 German mathematician. Professor in Leipzig, Bonn, Greifswald, Bonn. Is considered as co-founder of the modern topology. He invented the Hausdorff dimension, which is used to characterize fractals. The corresponding work is the most cited original paper in mathematics between 1910 and 1920. The Jewish Hausdorff, his wife and her sister committed suicide as they about to be deported into a concentration camp under the NS Dictatorship.

[4] from *Cavity Quantum Electrodynamics: The Strange Theory of Light in a Box*, S.M. Dutra, (John Wiley, 2005)

$$\begin{aligned}
\frac{dF}{d\alpha} &= \sum_{n=0}^{\infty}\frac{1}{n!}\sum_{j=0}^{n-1}(\alpha\hat{A}+\beta\hat{B})^j\hat{A}(\alpha\hat{A}+\beta\hat{B})^{n-j-1} \\
&= \sum_{n=0}^{\infty}\frac{1}{n!}\sum_{j=0}^{n-1}\left(\hat{A}(\alpha\hat{A}+\beta\hat{B})^{n-1}+j\beta[\hat{B},\hat{A}]_-(\alpha\hat{A}+\beta\hat{B})^{n-2}\right) \\
&= \sum_{n=0}^{\infty}\frac{1}{n!}\left(n\hat{A}(\alpha\hat{A}+\beta\hat{B})^{n-1}+\frac{n(n-1)}{2}\beta[\hat{B},\hat{A}]_-(\alpha\hat{A}+\beta\hat{B})^{n-2}\right) \\
&= \hat{A}\sum_{n=1}^{\infty}\frac{1}{(n-1)!}(\alpha\hat{A}+\beta\hat{B})^{n-1}+\frac{1}{2}\beta[\hat{B},\hat{A}]_-\sum_{n=2}^{\infty}\frac{1}{(n-2)!}(\alpha\hat{A}+\beta\hat{B})^{n-2} \\
&= \left(\hat{A}+\frac{1}{2}\beta[\hat{B},\hat{A}]_-\right)F(\alpha)
\end{aligned}$$

This is a differential equation for $F(\alpha)$, which can be solved as if the operator were a number because only one operator, namely $\hat{A}+\frac{1}{2}\beta[\hat{B},\hat{A}]_-$ is involved.

We obtain

$$\begin{aligned}
F(\alpha) = F(0)\mathrm{e}^{\alpha\left(\hat{A}+\frac{1}{2}\beta[\hat{B},\hat{A}]_-\right)} &= \mathrm{e}^{\beta\hat{B}}\left(\mathrm{e}^{\alpha\hat{A}}\mathrm{e}^{\frac{1}{2}\alpha\beta[\hat{B},\hat{A}]_-}\right) \\
\Rightarrow \qquad \mathrm{e}^{\alpha\hat{A}+\beta\hat{B}} = \mathrm{e}^{\beta\hat{B}}\mathrm{e}^{\alpha\hat{A}}\mathrm{e}^{\frac{1}{2}\alpha\beta[\hat{B},\hat{A}]_-} &= \mathrm{e}^{\beta\hat{B}}\mathrm{e}^{\alpha\hat{A}}\mathrm{e}^{-\frac{1}{2}\alpha\beta[\hat{A},\hat{B}]_-} \qquad \text{q.e.d.}
\end{aligned}$$

In the last step, we exploited that $\hat{A}$ commutates with the commutator $[\hat{A},\hat{B}]_-$, so that we can disentangle the exponential as if the operators were numbers.

A.8.2 Hadamard Lemma

The Hadamard Lemma is a specialization of Zassenhaus formula[164], which again is a variant of the Baker-Campbell-Hausdorff theorem. It is useful to work out simple operators in the interaction picture.

HADAMARD' S LEMMA

$$\begin{aligned}
\mathrm{e}^{\lambda\hat{A}}\hat{B}\mathrm{e}^{-\lambda\hat{A}} &\overset{\text{Eq. A.52}}{=} \sum_{n=0}^{\infty}\hat{X}_n\lambda^n \\
\text{with} \qquad \hat{X}_{n+1} &= \frac{1}{n+1}[\hat{A},\hat{X}_n]_- \qquad \text{and} \qquad \hat{X}_0 = \hat{B}
\end{aligned} \tag{A.48}$$

$$\mathrm{e}^{\lambda\hat{A}}\hat{B}\mathrm{e}^{-\lambda\hat{A}} = \left(\sum_{i=0}^{\infty}\frac{1}{i!}(\lambda\hat{A})^i\right)\hat{B}\left(\sum_{j=0}^{\infty}\frac{1}{j!}(-\lambda\hat{A})^j\right) \tag{A.49}$$

$$= \sum_{n=0}^{\infty}\lambda^n\underbrace{\left(\sum_{j=0}^{n}\frac{(-1)^j}{(n-j)!j!}\hat{A}^{n-j}\hat{B}\hat{A}^j\right)}_{\hat{X}_n} \tag{A.50}$$

Let us now work out the expression denoted $\hat{X}_n$ in Eq. A.50. $\hat{X}_0 = \hat{B}$ can be determined directly. The higher $\hat{X}_n$ are obtained by recursion.

$$\begin{aligned}
[\hat{A}, \hat{X}_n]_- &= \sum_{j=0}^{n} \frac{(-1)^j}{(n-j)!j!} \hat{A}^{n+1-j} \hat{B} \hat{A}^j - \sum_{j=0}^{n} \frac{(-1)^j}{(n-j)!j!} \hat{A}^{n-j} \hat{B} \hat{A}^{j+1} \\
&= \sum_{j=0}^{n} \frac{(n+1-j)(-1)^j}{(n+1-j)!j!} \hat{A}^{n+1-j} \hat{B} \hat{A}^j + \sum_{j=0}^{n} \frac{(j+1)(-1)^{j+1}}{(n+1-(j+1))!(j+1)!} \hat{A}^{n+1-(j+1))} \hat{B} \hat{A}^{j+1} \\
&\overset{j+1 \to j}{=} \sum_{j=0}^{n} \frac{(n+1-j)(-1)^j}{(n+1-j)!j!} \hat{A}^{n+1-j} \hat{B} \hat{A}^j + \sum_{k=1}^{n+1} \frac{j(-1)^j}{(n+1-j)!j!} \hat{A}^{n+1-j))} \hat{B} \hat{A}^j \\
&= (n+1) \sum_{j=0}^{n+1} \left(\frac{(-1)^j}{(n+1-j)!j!} \hat{A}^{n+1-j} \hat{B} \hat{A}^j \right. \\
&= (n+1) \hat{X}_{n+1}
\end{aligned} \tag{A.51}$$

Thus, we obtain the Baker-Campbell-Hausdorff theorem saying

$$\begin{aligned}
& e^{\lambda \hat{A}} \hat{B} e^{-\lambda \hat{A}} \overset{\text{Eq. A.50}}{=} \sum_{n=0}^{\infty} \hat{X}_n \lambda^n \\
\text{with} \qquad & \hat{X}_{n+1} \overset{\text{Eq. A.51}}{=} \frac{1}{n+1} [\hat{A}, \hat{X}_n]_- \qquad \text{and} \qquad \hat{X}_0 = \hat{B}
\end{aligned} \tag{A.52}$$

A.9 Sum rules related to the f-sum rule

Source: W. Thomas, "Über die Zahl der Dispersionselectronen, die einem stationären Zustande zugeordnet sind. Vorläufige Mitteilung", Naturwiss. 13, 627 (1925); W. Kuhn, "Über die Gesamtstärke der von einem Zustande ausgehenden Absorptionslinien", Z. Phys. 33, 408-412 (1925); F. Reiche and W. Thomas, "Über die Zahl der Dispersionselektronen, die einem stationären Zustand zugeordnet sind", ibid. 34, 510-525 (1925)

A.9.1 General derivation by Wang

I follow here the very general derivation given by Wang[165], from which a number of other sum rules can be derived in a straightforward manner.

For a general operator $\hat{A}$ we obtain

$$\begin{aligned}
\sum_n (E_n - E_0) \left| \langle 0|\hat{A}|n\rangle \right|^2 &= \sum_n (E_n - E_0) \langle 0|\hat{A}|n\rangle \langle n|\hat{A}^\dagger|0\rangle \\
&= \sum_n \Big(-\langle 0|\hat{H}\hat{A}|n\rangle + \langle 0|\hat{A}\hat{H}|n\rangle \Big) \langle n|\hat{A}^\dagger|0\rangle \\
&= \sum_n \langle 0|[\hat{A}, \hat{H}]_-|n\rangle \langle n|\hat{A}^\dagger|0\rangle \\
&= \langle 0|[\hat{A}, \hat{H}]_- \hat{A}^\dagger|0\rangle
\end{aligned} \tag{A.53}$$

We proceed completely analogously but for the commutator with the second matrix element

$$\begin{aligned}\sum_n (E_n - E_0)\left|\langle 0|\hat{A}^\dagger|n\rangle\right|^2 &= \sum_n (E_n - E_0)\langle 0|\hat{A}^\dagger|n\rangle\langle n|\hat{A}|0\rangle \\ &= \sum_n \langle 0|\hat{A}^\dagger|n\rangle\Big(\langle n|\hat{H}\hat{A}|0\rangle - \langle n|\hat{A}\hat{H}|0\rangle\Big) \\ &= -\sum_n \langle 0|\hat{A}^\dagger|n\rangle\langle n|[\hat{A},\hat{H}]|0\rangle \\ &= -\langle 0|\hat{A}^\dagger[\hat{A},\hat{H}]|0\rangle \end{aligned} \tag{A.54}$$

Adding the two results, Eq. A.53 and Eq. A.54, yields

WANG'S SUM RULE

$$\sum_n (E_n - E_0)\left(\left|\langle 0|\hat{A}|n\rangle\right|^2 + \left|\langle 0|\hat{A}^\dagger|n\rangle\right|^2\right) = \langle 0|\left[\hat{A}^\dagger,\left[\hat{A},\hat{H}\right]_-\right]_-|0\rangle \tag{A.55}$$

This is a rather general result, from which the f-sum rule can be obtained by choosing $\hat{A} = \hat{x}$ and the one-dimensional Hamilton operator of the form $\hat{H} = \frac{\hat{p}^2}{2m} + V(\hat{x})$.

A.9.2 f-sum rule or Thomas-Reiche-Kuhn sum rule

The **f-sum rule** or **Thomas-Reiche-Kuhn sum rule** can be obtained from Eq. A.55 with $\hat{A} = \hat{\vec{r}}$ and the one-dimensional Hamilton operator of the form $\hat{H} = \frac{\hat{\vec{p}}^2}{2m} + V(\hat{\vec{r}})$. Here, we first calculate the one-dimensional case from which the three-dimensional can be obtained immediately.

Hence, we insert $\hat{A} = \hat{x}$ and the one-dimensional Hamilton operator of the form $\hat{H} = \frac{\hat{p}^2}{2m} + V(\hat{x})$ into Wang's sum rule Eq. A.55. We begin with the right-hand side of Eq. A.55.

$$\begin{aligned}\left[\hat{H},\hat{x}\right]_- &= \left[\frac{\hat{p}^2}{2m} + V(\hat{x}),\hat{x}\right]_- = \frac{1}{2m}\Big(\hat{p}^2\hat{x} \underbrace{-\hat{p}\hat{x}\hat{p} + \hat{p}\hat{x}\hat{p}}_{=0} - \hat{x}\hat{p}^2\Big) \\ &= \frac{1}{2m}\Big(\hat{p}\left[\hat{p},\hat{x}\right]_- + \left[\hat{p},\hat{x}\right]_-\hat{p}\Big) = \frac{1}{2m}\frac{\hbar}{i}\Big(\hat{p}+\hat{p}\Big) = \frac{-i\hbar}{m}\hat{p}\end{aligned} \tag{A.56}$$

$$\left[\hat{x}^\dagger,\left[\hat{H},\hat{x}\right]_-\right]_- \overset{\text{Eq. A.56}}{=} \left[\hat{x}^\dagger,\frac{-i\hbar}{m}\hat{p}\right]_- = \frac{-i\hbar}{m}\left[\hat{x}^\dagger,\hat{p}\right]_- = \frac{\hbar^2}{m} \tag{A.57}$$

Thus, we obtain with Eq. A.55

$$\sum_n (E_n - E_0)\left|\langle 0|\hat{x}|n\rangle\right|^2 = \frac{\hbar^2}{2m} \tag{A.58}$$

which is the one-dimensional version of the f-sum rule.

Now, we sum over the three coordinates and obtain the f- or Thomas-Reiche sum rule.

F-SUM RULE OR THOMAS-REICHE-KUHN SUM RULE

$$\sum_n (E_n - E_0)\left|\langle 0|\hat{\vec{r}}|n\rangle\right|^2 = \frac{3\hbar^2}{2m} \tag{A.59}$$

A.9.3 Bethe sum rule

The **Bethe sum rule** can be obtained from Eq. A.55 with $\hat{A} = e^{i\vec{q}\hat{r}}$ and the Hamiltonian $\hat{H} = \frac{\hat{p}^2}{2m} + V(\hat{r})$.

$$\begin{aligned}\left[\hat{H}, e^{i\vec{q}\hat{r}}\right]_- &= \left[\frac{\hat{p}^2}{2m} + V(\hat{r}), e^{i\vec{q}\hat{r}}\right]_- = \frac{1}{2m}\Big(\hat{p}^2 e^{i\vec{q}\hat{r}} \underbrace{-\hat{p}e^{i\vec{q}\hat{r}}\hat{p} + \hat{p}e^{i\vec{q}\hat{r}}\hat{p}}_{=0} - e^{i\vec{q}\hat{r}}\hat{p}^2\Big) \\ &= \frac{1}{2m}\Big(\hat{p}\left[\hat{p}, e^{i\vec{q}\hat{r}}\right]_- + \left[\hat{p}, e^{i\vec{q}\hat{r}}\right]_-\hat{p}\Big) = \frac{1}{2m}\Big(\hat{p}\hbar\vec{q}e^{i\vec{q}\hat{r}} + \hbar\vec{q}e^{i\vec{q}\hat{r}}\hat{p}\Big) \\ &= \frac{\hbar\vec{q}}{2m}\Big(\hat{p}e^{i\vec{q}\hat{r}} + e^{i\vec{q}\hat{r}}\hat{p}\Big) \end{aligned} \tag{A.60}$$

$$\begin{aligned}\left[\left(e^{i\vec{q}\hat{r}}\right)^\dagger, \left[\hat{H}, e^{i\vec{q}\hat{r}}\right]_-\right]_- &\overset{\text{Eq. A.60}}{=} \left[e^{-i\vec{q}\hat{r}}, \frac{\hbar\vec{q}}{2m}\Big(\hat{p}e^{i\vec{q}\hat{r}} + e^{i\vec{q}\hat{r}}\hat{p}\Big)\right]_- \\ &= \frac{\hbar\vec{q}}{2m}\Big(e^{-i\vec{q}\hat{r}}\underbrace{\hat{p}e^{i\vec{q}\hat{r}}}_{\hbar\vec{q}e^{i\vec{q}\hat{r}}+e^{i\vec{q}\hat{r}}\hat{p}}\underbrace{+\hat{p}-\hat{p}}_{=0} - e^{i\vec{q}\hat{r}}\underbrace{\hat{p}e^{-i\vec{q}\hat{r}}}_{-\hbar\vec{q}e^{-i\vec{q}\hat{r}}+e^{-i\vec{q}\hat{r}}\hat{p}}\Big) \\ &= \frac{\hbar\vec{q}}{2m}\Big((\hbar\vec{q}+\hat{p}) - (-\hbar\vec{q}+\hat{p})\Big) = \frac{(\hbar\vec{q})^2}{m} \end{aligned} \tag{A.61}$$

Insertion into Wang's sum rule Eq. A.55 results in **Bethe's sum rule**.

BETHE SUM RULE

$$\sum_n (E_n - E_0)\left|\langle 0|e^{i\vec{q}\hat{r}}|n\rangle\right|^2 = \frac{(\hbar\vec{q})^2}{2m} \tag{A.62}$$

A.10 Friedel sum rule

Editor: This section on the Friedel sum rule is preliminary. It is geared strongly towards the Anderson impurity model

Editor: For the Friedel sum rule, see also Jones and March *"Theoretical Solid State Physics"* Vol. 2 section 10.3.3, p.993.

Editor: I am following Antoine Georges[166], *" The beauty of impurities: Two revivals of Friedel's virtual bound-state concept"* C. R. Physique 17 (2016) 430-446. (C.R.Physique=Comptes Rendus Physique) http://dx.doi.org/10.1016/j.crhy.2015.12.005

Consider an impurity in an otherwise homogeneous material

$$\hat{H} = \sum_\sigma \epsilon_d \hat{d}^\dagger_\sigma \hat{d}_\sigma + \sum_k \sum_{\sigma\in\{\uparrow,\downarrow\}} \epsilon_{\vec{k}} \hat{c}^\dagger_{\vec{k},\sigma}\hat{c}_{\vec{k},\sigma} + \sum_{\sigma\in\{\uparrow,\downarrow\}}\sum_k V_{\vec{k},\sigma}\left(\hat{d}^\dagger_\sigma \hat{c}_{\vec{k},\sigma} + \hat{c}^\dagger_{\vec{k},\sigma}\hat{d}_\sigma\right) \tag{A.63}$$

For the sake of simplicity, I drop the spin index.

$$\hat{H} = \epsilon_d \hat{d}^\dagger\hat{d} + \sum_k \epsilon_{\vec{k}}\hat{c}^\dagger_{\vec{k}}\hat{c}_{\vec{k}} + \sum_k V_{\vec{k}}\left(\hat{d}^\dagger\hat{c}_{\vec{k}} + \hat{c}^\dagger_{\vec{k}}\hat{d}\right) \tag{A.64}$$

The resulting Hamiltonian describes **spin-less fermions**. The physics, however, is that of paired electrons, where the spin-up electrons behave exactly like the spin-down electrons. Other names would be that of a **spin-restricted** or **non-spin-polarized** calculation.

The bare Green's functions for the isolated impurity of the decoupled bath are

$$\begin{aligned}\bar{G}_d(\epsilon) &= \frac{1}{\epsilon - \bar{\epsilon}_d + i0^+} \\ \bar{G}^{(c)}_{\vec{k},\vec{k'}}(\epsilon) &= \delta_{\vec{k},\vec{k'}} \frac{1}{\epsilon - \bar{\epsilon}(\vec{k}) + i0^+}\end{aligned} \tag{A.65}$$

The full Green's function are then

$$\begin{aligned}G^{(d)}(\epsilon) &= \left(\left(\bar{G}^{(d)}(\epsilon) \right)^{-1} - \underbrace{\vec{V} \boldsymbol{\bar{G}}^{(c)}(\epsilon) \vec{V}}_{\Sigma^{(d)}(\epsilon)} \right)^{-1} = \left(\epsilon - \bar{\epsilon}_d - \Sigma^{(d)}(\epsilon) \right)^{-1} \\ G^{(d)}(\epsilon) &= \left(\epsilon - \bar{\epsilon}_d - \sum_{\vec{k},\vec{k'}} V_{\vec{k}} \bar{G}^{(c)}_{\vec{k},\vec{k'}}(\epsilon) V_{\vec{k'}} \right)^{-1} \\ \boldsymbol{G}^{(c)}(\epsilon) &= \left(\left(\bar{\boldsymbol{G}}^{(c)}(\epsilon) \right)^{-1} - \underbrace{\vec{V} \otimes \bar{G}^{(d)}(\epsilon) \otimes \vec{V}}_{\boldsymbol{\Sigma}^{(c)}(\epsilon)} \right)^{-1} \\ &= \sum_{n=0}^{\infty} \left(\bar{\boldsymbol{G}}^{(c)} \boldsymbol{\Sigma}^{(c)} \right)^n \bar{\boldsymbol{G}}^{(c)} \\ &= \bar{\boldsymbol{G}}^{(c)} + \bar{\boldsymbol{G}}^{(c)} \underbrace{\left[\sum_{n=0} \left(\boldsymbol{\Sigma}^{(c)} \bar{\boldsymbol{G}}^{(c)} \right)^n \boldsymbol{\Sigma}^{(c)} \right]}_{= \boldsymbol{T} \text{ reducible self energy}} \bar{\boldsymbol{G}}^{(c)} \\ &= \bar{\boldsymbol{G}}^{(c)}(\epsilon) + \bar{\boldsymbol{G}}^{(c)}(\epsilon) \boldsymbol{T}^{(c)} \bar{\boldsymbol{G}}^{(c)}(\epsilon) \\ G^{(c)}_{\vec{k},\vec{k'}}(\epsilon) &= \bar{G}^{(c)}_{\vec{k}}(\epsilon) \delta_{\vec{k},\vec{k'}} + \bar{G}^{(c)}_{\vec{k}}(\epsilon) T_{\vec{k},\vec{k'}}(\epsilon) G^{(c)}_{\vec{k'}}(\epsilon)\end{aligned} \tag{A.66}$$

where $\boldsymbol{T}$ is the **scattering T-matrix**. The T-matrix is the reducible self energy for the conduction electrons.

$$\boldsymbol{T} = \boldsymbol{\Sigma} + \boldsymbol{\Sigma} \bar{\boldsymbol{G}}^{(c)} \boldsymbol{\Sigma} + \ldots = \boldsymbol{\Sigma} + \boldsymbol{\Sigma} \bar{\boldsymbol{G}}^{(c)} \boldsymbol{T} \tag{A.67}$$

In the present case this yields

$$\begin{aligned}\boldsymbol{T} &= \boldsymbol{\Sigma} + \boldsymbol{\Sigma} \bar{\boldsymbol{G}}^{(c)} \boldsymbol{\Sigma} + \ldots \\ &= \underbrace{\vec{V} \left\{ \bar{G}^{(d)} + \bar{G}^{(d)} \underbrace{\vec{V} \bar{\boldsymbol{G}}^{(c)} \vec{V}}_{\Sigma^{(d)}} \bar{G}^{(d)} + \bar{G}^{(d)} \underbrace{\vec{V} \bar{\boldsymbol{G}}^{(c)} \vec{V}}_{\Sigma^{(d)}} \bar{G}^{(d)} \underbrace{\vec{V} \bar{\boldsymbol{G}}^{(c)} \vec{V}}_{\Sigma^{(d)}} \bar{G}^{(d)} + \ldots \right\} \vec{V}}_{G^{(d)}(\epsilon)} \\ &= \vec{V} G^{(d)}(\epsilon) \vec{V}\end{aligned} \tag{A.68}$$

I used the impurity Green's function

$$\begin{aligned}G^{(d)}(\epsilon) &= \frac{1}{\epsilon - \epsilon_d - \Sigma^d(\epsilon) + i\Gamma} = \frac{1}{\epsilon - \epsilon_d - \mathrm{Re}\left[\Sigma^d(\epsilon)\right] - i\left(\mathrm{Im}\left[\Sigma^d(\epsilon)\right] - \Gamma\right)} \\ &= \frac{\left(\epsilon - \epsilon_d - \mathrm{Re}[\Sigma^d]\right) + i\left(\mathrm{Im}[\Sigma^d] - \Gamma\right)}{\left(\epsilon - \epsilon_d - \mathrm{Re}[\Sigma^d]\right)^2 + \left(\mathrm{Im}[\Sigma^d] - \Gamma\right)^2}\end{aligned} \tag{A.69}$$

Scattering phase shift: The **scattering phase shift** $\delta(\omega)$ is defined by

$$T_{\vec{k},\vec{k'}}(\epsilon) = -|T_{\vec{k},\vec{k'}}(\epsilon)| e^{i\varphi_{\vec{k},\vec{k'}}(\epsilon)} \tag{A.70}$$

Under the simplification, that the coupling parameters $V_{\vec{k}}$ are all real-valued, the phase shifts $\varphi_{\vec{k},\vec{k}'}(\epsilon)$ are equal to that of the bare impurity Green's function, and thus they are equal for all scattering processes. Editor: Is this a harmless restriction, or is it central to the proof?

$$G^{(d)}(\epsilon) = -|G^{(d)}(\epsilon)|e^{i\varphi(\epsilon)} \tag{A.71}$$

Hence

$$\begin{aligned}\varphi(\epsilon) &= \arg(-G^{(d)}(\epsilon)) = \frac{\pi}{2} + n\pi - \arctan\left[\frac{\mathrm{Re}[G^{(d)}(\epsilon)]}{\mathrm{Im}[G^{(d)}(\epsilon)]}\right] \\ \tan\left(\varphi(\epsilon)\right) &= \frac{\mathrm{Im}[G^{(d)}(\epsilon)]}{\mathrm{Re}[G^{(d)}(\epsilon)]} = \frac{\mathrm{Im}\left[\Sigma^d(\epsilon)\right] - \Gamma}{\epsilon - \epsilon_d - \mathrm{Re}[\Sigma^d]}\end{aligned} \tag{A.72}$$

The factor $n\pi$ has been added, because n counts the number of states below the chosen energy. (Number of nodes)

Spectral function: The spectral function on the impurity is

$$\begin{aligned}\mathcal{A}^{(d)}(\epsilon) &= \frac{1}{\pi}\mathrm{Im}[G^{(d)}(\epsilon)] = \frac{1}{\pi}\frac{\left(\mathrm{Im}\left[\Sigma^d(\epsilon)\right] - \Gamma\right)}{\left(\epsilon - \epsilon_d - \mathrm{Re}\left[\Sigma^d(\epsilon)\right]\right)^2 + \left(\mathrm{Im}\left[\Sigma^d(\epsilon)\right] - \Gamma\right)^2} \\ &\overset{\text{Eq. A.72}}{=} \frac{1}{\pi}\frac{\left(\mathrm{Im}[\Sigma^d] - \Gamma\right)}{\left(\tan^{-2}\left(\varphi(\epsilon)\right) + 1\right)\left(\mathrm{Im}\left[\Sigma^d(\epsilon)\right] - \Gamma\right)^2} = \frac{1}{\pi\left(\mathrm{Im}\left[\Sigma^d(\epsilon)\right] - \Gamma\right)}\frac{1}{1 + \tan^{-2}\left(\varphi(\epsilon)\right)} \\ &= \frac{\sin^2(\varphi(\epsilon))}{\pi\left(\mathrm{Im}\left[\Sigma^d(\epsilon)\right] - \Gamma\right)}\end{aligned} \tag{A.73}$$

Occupation on the impurity: Let me integrate the bare Green's function of the impurity to obtain the number of d-electrons. **The bare Green's function is used as opposed to the full d-Green's function for the sake of simplicity.**

$$\begin{aligned}n_d &\approx \int_{-\infty}^{\mu} d\epsilon\, \bar{\mathcal{A}}_d(\epsilon) \\ &= \int_{-\infty}^{\mu} d\epsilon \left(-\frac{1}{\pi}\mathrm{Im}[\bar{G}_d(\epsilon)]\right) \\ &= \int_{-\infty}^{\mu} d\epsilon\, \frac{1}{\pi}\frac{\Gamma}{(\epsilon - \epsilon_d)^2 + \Gamma^2} \\ &= \frac{1}{\pi}\int_{-\infty}^{\mu} \frac{d\epsilon}{\Gamma}\, \frac{1}{1 + \left(\frac{\epsilon - \epsilon_d}{\Gamma}\right)^2} \\ &= \frac{1}{\pi}\int_{-\infty}^{(\mu-\epsilon_d)/\Gamma} dx\, \underbrace{\frac{1}{1+x^2}}_{\partial_x \arctan(x)} \\ &= \frac{1}{\pi}\arctan(\frac{\mu - \epsilon_d}{\Gamma}) + 1/2\end{aligned} \tag{A.74}$$

Attention! This result is for a spin-less model. In the spin-dependent model we need a factor two for the spin degeneracy.

Thus, we obtain including the spin degeneracy

$$n_d = 1 + \frac{2}{\pi}\arctan\left(\frac{\mu - \epsilon_d}{\Gamma}\right) \tag{A.75}$$

Friedel sum rule At the Fermi level we exploit the quasi-particle life time in a Fermi-liquid becomes infinite at the Fermi level. Hence also

$$\begin{aligned} \Sigma^{(d)}(\epsilon) &= \vec{V}\bar{\boldsymbol{G}}^{(c)}(\epsilon)\vec{V} \\ \Rightarrow \quad \mathrm{Im}[\Sigma^{(d)}(\mu)] &= \vec{V}\underbrace{\mathrm{Im}\left[\bar{\boldsymbol{G}}^{(c)}(\mu)\right]}_{=0}\vec{V} = 0 \end{aligned} \tag{A.76}$$

Thus,

$$\tan\left(\varphi(\mu)\right) \overset{\text{Eq. A.72}}{=} \frac{\mathrm{Im}\left[\Sigma^{d}(\mu)\right] - \Gamma}{\mu - \epsilon_d - \mathrm{Re}[\Sigma^{d}]} \overset{\mathrm{Im}[G^{(c)}(\mu)]=0}{=} \frac{\Gamma}{\epsilon_d + \mathrm{Re}[\Sigma^{d}(\mu)] - \mu} \tag{A.77}$$

$$n_d = 1 + \frac{2}{\pi}\arctan\left(\frac{\mu - \epsilon_d}{\Gamma}\right) = \frac{2}{\pi}\arctan\left(\frac{\Gamma}{\epsilon_d - \mu}\right) \approx \frac{2}{\pi}\varphi(\mu) \tag{A.78}$$

FRIEDEL SUM RULE

The occupation of an orbital is given by the scattering phase shift $\varphi(\epsilon)$ at the Fermi level.

$$n_d \approx \frac{2}{\pi}\varphi(\mu) \tag{A.79}$$

Caveat: The derivation is approximate, while Friedel sum rule is probably strictly valid.

Density of states at the Fermi level: Friedel's sum rule links the scattering phase shift firstly to the occupation of the orbital and secondly to the density of states

$$\mathcal{A}^{d}(\mu) \overset{\text{Eq. A.73}}{=} \frac{\sin^2\left(\varphi(\mu)\right)}{-\pi\Gamma} \overset{\text{Eq. A.79}}{=} -\frac{1}{\pi\Gamma}\sin^2\left(\frac{\pi}{2}n_d\right) \tag{A.80}$$

This result is of interest for the Kondo or **Abrikosov-Suhl resonance** [123, 124]. It shows that the density of states right at the Fermi level is linked to total d-occupation of the impurity. As the interaction is increased, which shift weight from the central quasi-particle peak to the Hubbard bands, the width of the Abrikosov-Suhl resonance shrinks, while the maximum value of the Dos at the Fermi level remains constant.

A.11 Sherman-Morrison Formula

The Sherman-Morrison Formula provides a simple way to update the inverse of a matrix upon adding an outer product to the original matrix. [Sherman, Jack; Morrison, Winifred J. (1949). "Adjustment of an Inverse Matrix Corresponding to Changes in the Elements of a Given Column or a Given Row of the Original Matrix (abstract)". Annals of Mathematical Statistics. 20: 621. doi:10.1214/aoms/1177729959.] (Source: `https://en.wikipedia.org/wiki/ShermanâĂŞMorrison_formula`)

The Sherman-Morrison Formula is a special case fo the Woodbury matrix identity. Here, the proof is shown for operators.

$$\left(\hat{A} + |u\rangle\langle v|\right)^{-1} = \hat{A}^{-1} - \frac{\hat{A}^{-1}|u\rangle\langle v|\hat{A}^{-1}}{1 + \langle v|\hat{A}^{-1}|u\rangle} \tag{A.81}$$

$$
\begin{aligned}
&\left(\hat{A}+|u\rangle\langle v|\right)\left(\hat{A}^{-1}-\frac{\hat{A}^{-1}|u\rangle\langle v|\hat{A}^{-1}}{1+\langle v|\hat{A}^{-1}|u\rangle}\right)\\
&=\hat{1}-\frac{|u\rangle\langle v|\hat{A}^{-1}}{1+\langle v|\hat{A}^{-1}|u\rangle}+|u\rangle\langle v|\hat{A}^{-1}-\frac{|u\rangle\langle v|\hat{A}^{-1}|u\rangle\langle v|\hat{A}^{-1}}{1+\langle v|\hat{A}^{-1}|u\rangle}\\
&=\hat{1}+|u\rangle\langle v|\hat{A}^{-1}-|u\rangle\underbrace{\left(\frac{1}{1+\langle v|\hat{A}^{-1}|u\rangle}+\frac{\langle v|\hat{A}^{-1}|u\rangle}{1+\langle v|\hat{A}^{-1}|u\rangle}\right)}_{=1}\langle v|\hat{A}^{-1}=\hat{1}
\end{aligned}
\tag{A.82}
$$

The proof for the opposite order is analogous.

Woodbury Matrix identity (Source:`https://en.wikipedia.org/wiki/Woodbury_matrix_identity`)

$$
\left(\hat{A}+\sum_{i,j}|u_i\rangle C_{i,j}\langle v_j|\right)^{-1}=\hat{A}^{-1}-\sum_{i,j}\hat{A}^{-1}|u_i\rangle\Big(\boldsymbol{C}^{-1}+\langle v|\hat{A}^{-1}|v\rangle\Big)_{i,j}\langle v_j|\hat{A}^{-1}
\tag{A.83}
$$

Appendix B

Non-orthonormal basissets

Quantum field theory is usually formulated in an orthonormal one-particle basisset. This is because of the enormous simplification of matrix elements in the form of the Slater-Condon rules. On the other hand, the interaction is most important at short distances and strongest between localized orbitals such as d- and f-orbitals. This suggests to use an atom-centered basisset.

Both properties, orthonormality and locality, can be satisfied by so-called **Wannier orbitals**.

However, in practical calculations, Wannier orbitals are still rather extended. In order to construct even more localized orbitals, we need to give up the orthonormality condition. It turns out that many-particle physics, at least on the basis of many-particle Green's functions, can be formulated in non-orthonormal basissets in a rather straight-forward way, without the exponential complexity of matrix elements between many-particle states.

In this appendix, I summarize the notation of non-orthonormal basissets using projector functions. Non-orthonormal basissets have been introduced in the main text in section 1.1.7 on p. 10.

B.1 Creation and annihilation operators for non-orthonormal orbitals

While it has been important to consider orthonormal orbitals for the evaluation of the Slater-Condon rules, the operators can easily be transformed into any non-orthonormal one-particle basis set.

Non-orthonormal basissets have been described in the introduction, namely in section 1.1.7 on p. 10.

Let us consider any non-orthonormal basisset of orbitals $|\chi_\alpha\rangle$ with the overlap matrix $S_{\alpha,\beta} = \langle\chi_\alpha|\chi_\beta\rangle$. For the basis functions, we define furthermore projector functions $|\pi_\alpha\rangle$, which obey the bi-orthogonality condition

$$\langle\pi_\alpha|\chi_\beta\rangle \overset{\text{Eq. 1.46}}{=} \delta_{\alpha,\beta} \tag{B.1}$$

If the orbitals $|\chi_\alpha\rangle$ and the projector functions $|\pi_\alpha\rangle$ are both complete, the unity can be expressed as

$$\hat{1} = \sum_\alpha |\chi_\alpha\rangle\langle\pi_\alpha| \tag{B.2}$$

or as

$$\hat{1} = \sum_\alpha |\pi_\alpha\rangle\langle\chi_\alpha| \ . \tag{B.3}$$

Let us now introduce creation and annihilation operators, analogously to Eq. 3.64, with the difference that the orbitals are no more orthonormal

$$\begin{aligned}\hat{c}_\alpha^\dagger &= \int d^4x\, \hat{\psi}^\dagger(\vec{x})\langle\vec{x}|\pi_\alpha\rangle \\ \hat{c}_\alpha &= \int d^4x\, \langle\pi_\alpha|\vec{x}\rangle\hat{\psi}(\vec{x})\end{aligned} \tag{B.4}$$

With this definition, the creation operator produces the projector function.

$$|\pi_\alpha\rangle = \hat{c}_\alpha^\dagger|\mathcal{O}\rangle \tag{B.5}$$

There is some arbitrariness regarding the choice of using the projector functions in Eq. B.4 rather than the orbitals.[1] This is analogous to co- and contra-variant vectors in geometry. Our choice gives up the relation $|\chi_\alpha\rangle = \hat{c}_\alpha^\dagger|\mathcal{O}\rangle$ in favor of the form of matrix elements of operators defined later in Eq. B.9 and Eq. B.10.

Back transform to real-space field operators: Let us work out the back transform as

$$\hat{\psi}^\dagger(\vec{x}) = \int d^4x'\, \hat{\psi}^\dagger(\vec{x'})\, \underbrace{\langle\vec{x'}|\underbrace{\sum_\alpha |\pi_\alpha\rangle\langle\chi_\alpha|}_{\hat{1}}\vec{x}\rangle}_{\delta(\vec{x'}-\vec{x})} = \sum_\alpha \underbrace{\int d^4x'\, \hat{\psi}^\dagger(\vec{x'})\langle\vec{x'}|\pi_\alpha\rangle}_{\hat{c}_\alpha^\dagger}\langle\chi_\alpha|\vec{x}\rangle = \sum_\alpha \hat{c}_\alpha^\dagger\langle\chi_\alpha|\vec{x}\rangle$$

The back transform is

$$\begin{aligned}\hat{\psi}^\dagger(\vec{x}) &= \sum_\alpha \hat{c}_\alpha^\dagger\langle\chi_\alpha|\vec{x}\rangle \\ \hat{\psi}(\vec{x}) &= \sum_\alpha \langle\vec{x}|\chi_\alpha\rangle\hat{c}_\alpha\end{aligned} \tag{B.6}$$

Anticommutator relations with non-orthonormal orbitals

Special care is required with the anticommutator relations which are non-trivial.

$$\left[\hat{c}_\alpha, \hat{c}_\beta^\dagger\right]_+ \overset{\text{Eq. B.4}}{=} \int d^4x \int d^4x'\, \langle\pi_\alpha|\vec{x}\rangle \underbrace{\left[\hat{\psi}(\vec{x}), \hat{\psi}^\dagger(\vec{x'})\right]_+}_{\delta(\vec{x}-\vec{x'})}\langle\vec{x'}|\pi_\beta\rangle = \int d^4x \langle\pi_\alpha|\vec{x}\rangle\langle\vec{x}|\pi_\beta\rangle = \langle\pi_\alpha|\pi_\beta\rangle \tag{B.7}$$

Thus, we obtain the anticommutator relations for non-orthonormal orbitals as

$$\begin{aligned}\left[\hat{c}_\alpha, \hat{c}_\beta^\dagger\right]_+ &= \langle\pi_\alpha|\pi_\beta\rangle = S^{-1}_{\alpha,\beta} \\ \left[\hat{c}_\alpha^\dagger, \hat{c}_\beta^\dagger\right]_+ &= 0 \\ \left[\hat{c}_\alpha, \hat{c}_\beta\right]_+ &= 0\end{aligned} \tag{B.8}$$

[1] Exchanging projector functions and orbitals leads again to a mathematically consistent formalism. As a result it is not always obvious how to choose the correct one.

B.1.1 Operators and matrix elements

In order to represent the operators by creation and annihilation operators in the non-orthonormal basisset, we need to work out their matrix elements.

The derivation of the Slater-Condon rules in a non-orthonormal basisset is awfully cumbersome, because each matrix element of a N-particle Slater determinant produces in general $(N!)^2$ matrix elements of product states. Therefore, it is more economical to take the matrix elements in a orthonormal basisset, which has been obtained with the help of the Slater-Condon rules and transform the result into a general basisset. We even have a later starting point, because we can start from the real-space representation.

For a one-particle operator $\hat{A}$ we obtain

$$\begin{aligned}
\hat{A} &\overset{\text{Eq. 3.66}}{=} \int d^4x \int d^4x' \; A(\vec{x},\vec{x'})\hat{\psi}^\dagger(\vec{x})\hat{\psi}(\vec{x'}) \\
&\overset{\text{Eq. B.6}}{=} \sum_{\alpha,\beta}\Big(\int d^4x \int d^4x' \; \langle\chi_\alpha|\vec{x}\rangle A(\vec{x},\vec{x'})\langle\vec{x'}|\chi_\beta\rangle\Big)\hat{c}_\alpha^\dagger\hat{c}_\beta \\
&= \sum_{\alpha,\beta} A_{\alpha,\beta}\hat{c}_\alpha^\dagger\hat{c}_\beta
\end{aligned} \tag{B.9}$$

with

$$A_{\alpha,\beta} = \int d^4x \int d^4x' \; \langle\chi_\alpha|\vec{x}\rangle A(\vec{x},\vec{x'})\langle\vec{x'}|\chi_\beta\rangle = \langle\chi_\alpha|\hat{A}|\chi_\beta\rangle \tag{B.10}$$

The derivation for the matrix elements of an interaction operator $\hat{W}$ is obtained analogously. Take note of the order of the two annihilators in the following expressions!

$$\begin{aligned}
\hat{W} &\overset{\text{Eq. 3.75}}{=} \frac{1}{2}\int d^4x \int d^4x' \; \hat{\psi}^\dagger(\vec{x})\hat{\psi}^\dagger(\vec{x'})\frac{e^2}{4\pi\epsilon_0|\vec{r}-\vec{r'}|}\hat{\psi}(\vec{x'})\hat{\psi}(\vec{x}) \\
&\overset{\text{Eq. B.6}}{=} \frac{1}{2}\int d^4x \int d^4x' \; \frac{e^2}{4\pi\epsilon_0|\vec{r}-\vec{r'}|}\underbrace{\Big(\sum_\alpha \hat{c}_\alpha^\dagger\langle\chi_\alpha|\vec{x}\rangle\Big)}_{\hat{\psi}^\dagger(\vec{x})}\underbrace{\Big(\sum_\beta \hat{c}_\beta^\dagger\langle\chi_\beta|\vec{x'}\rangle\Big)}_{\hat{\psi}^\dagger(\vec{x'})}\underbrace{\Big(\sum_\gamma \langle\vec{x'}|\chi_\gamma\rangle\hat{c}_\gamma\Big)}_{\hat{\psi}(\vec{x'})}\underbrace{\Big(\sum_\delta \langle\vec{x}|\chi_\delta\rangle\hat{c}_\delta\Big)}_{\hat{\psi}(\vec{x})} \\
&= \frac{1}{2}\sum_{\alpha,\beta,\gamma,\delta}\left(\int d^4x \int d^4x' \; \frac{e^2\chi_\alpha^*(\vec{x})\chi_\beta^*(\vec{x'})\chi_\delta(\vec{x})\chi_\gamma(\vec{x'})}{4\pi\epsilon_0|\vec{r}-\vec{r'}|}\right)\hat{c}_\alpha^\dagger\hat{c}_\beta^\dagger\hat{c}_\gamma\hat{c}_\delta \\
&= \frac{1}{2}\sum_{\alpha,\beta,\gamma,\delta} W_{\alpha,\beta,\delta,\gamma}\hat{c}_\alpha^\dagger\hat{c}_\beta^\dagger\hat{c}_\gamma\hat{c}_\delta
\end{aligned} \tag{B.11}$$

with[2]

$$W_{\alpha,\beta,\gamma,\delta} = \int d^4x \int d^4x' \; \frac{e^2\chi_\alpha^*(\vec{x})\chi_\beta^*(\vec{x'})\chi_\gamma(\vec{x})\chi_\delta(\vec{x'})}{4\pi\epsilon_0|\vec{r}-\vec{r'}|} \tag{B.12}$$

The expression for the matrix elements maintain their simple form also in a non-orthonormal basisset. The complication shows up again when evaluating matrix elements of operators expressed in creation and annihilation operators, because every permutation of creation and annihilation operators introduces an inverse overlap matrix instead of a unit matrix. A usual technique to evaluate matrix elements is to permute the annihilators to the very right or the very left, which then blows up the number of terms in an non-orthonormal basisset tremendously. This problem is usually avoided by an intermediate basis transformation to an orthonormal basisset.

[2]Note the interchange of γ and δ!

Summary

Let me summarize here the equations for non-orthonormal orbitals for future reference. Memorizing these equations may be advantageous over memorizing the ones for orthonormal orbitals, because the latter are readily derived from the more general equations.

CREATION AND ANNIHILATION OPERATORS IN NON-ORTHONORMAL ORBITALS

Consider a set of non-orthonormal orbitals $|\chi_\alpha\rangle$ having the overlap matrix

$$S_{\alpha,\beta} \stackrel{\text{def}}{=} \langle\chi_\alpha|\chi_\beta\rangle \tag{B.13}$$

A set of projector functions $\langle\pi_\alpha|$ is defined which obeys the bi-orthogonality condition

$$\langle\pi_\alpha|\chi_\beta\rangle = \delta_{\alpha,\beta} \tag{B.14}$$

Thus,

$$\langle\pi_\alpha|\pi_\beta\rangle = \Big(\boldsymbol{S}\Big)^{-1}_{\alpha,\beta} \tag{B.15}$$

The creation and annihilation operators $\hat{c}^\dagger_\alpha$ and $\hat{c}^\dagger$ and obey the anticommutator relations

$$\begin{aligned}
\Big[\hat{c}^\dagger_\alpha, \hat{c}^\dagger_\beta\Big]_+ &\stackrel{\text{Eq. ??}}{=} 0 \\
\Big[\hat{c}_\alpha, \hat{c}_\beta\Big]_+ &\stackrel{\text{Eq. ??}}{=} 0 \\
\Big[\hat{c}^\dagger_\alpha, \hat{c}_\beta\Big]_+ &\stackrel{\text{Eq. ??}}{=} \langle\pi_\alpha|\pi_\beta\rangle
\end{aligned} \tag{B.16}$$

The creation and annihilation operators $\hat{c}^\dagger_\alpha$ and $\hat{c}^\dagger$ are related to the real-space field operators by

$$\begin{aligned}
\hat{\psi}^\dagger(\vec{x}) &\stackrel{\text{Eq. B.6}}{=} \sum_\alpha \hat{c}^\dagger_\alpha \langle\chi_\alpha|\vec{x}\rangle \\
\hat{\psi}(\vec{x}) &\stackrel{\text{Eq. B.6}}{=} \sum_\alpha \langle\vec{x}|\chi_\alpha\rangle \hat{c}_\alpha
\end{aligned} \tag{B.17}$$

and

$$\begin{aligned}
\hat{c}^\dagger_\alpha &\stackrel{\text{Eq. B.4}}{=} \int d^4x\, \hat{\psi}^\dagger(\vec{x}) \langle\vec{x}|\pi_\alpha\rangle \\
\hat{c}_\alpha &\stackrel{\text{Eq. B.4}}{=} \int d^4x\, \langle\pi_\alpha|\vec{x}\rangle \hat{\psi}(\vec{x})
\end{aligned} \tag{B.18}$$

A creation operator creates the projector function $|\pi_\alpha\rangle$, rather than the local orbital.

$$|\pi_\alpha\rangle \stackrel{\text{Eq. B.5}}{=} \hat{c}^\dagger_\alpha |\mathcal{O}\rangle \tag{B.19}$$

The Hamiltonian has the form

$$\hat{H} = \sum_{\alpha,\beta} h_{\alpha,\beta} \hat{c}^\dagger_\alpha \hat{c}_\beta + \frac{1}{2} \sum_{\alpha,\beta,\gamma,\delta} W_{\alpha,\beta,\delta,\gamma} \hat{c}^\dagger_\alpha \hat{c}^\dagger_\beta \hat{c}_\delta \hat{c}_\gamma \tag{B.20}$$

with matrix elements

$$h_{\alpha,\beta} = \langle\chi_\alpha|\hat{H}_0|\chi_\beta\rangle \tag{B.21}$$

and

$$W_{\alpha,\beta,\gamma,\delta} = \langle\chi_\alpha\chi_\beta|\hat{W}|\chi_\gamma\chi_\delta\rangle = \int d^4x \int d^4x' \, \frac{e^2 \chi^*_\alpha(\vec{x}) \chi^*_\beta(\vec{x'}) \chi_\gamma(\vec{x}) \chi_\delta(\vec{x'})}{4\pi\epsilon_0 |\vec{r} - \vec{r'}|} \tag{B.22}$$

Appendix C

Fermions and bosons

Editor: This is under construction and needs to be verified

The focus of these lecture notes are fermions. In this chapter, I will present the relevant expressions for fermions and bosons side-by-side. The expressions for fermions and bosons differ by the position of a sign-factor *"eta"* η_{FB}.

$$\begin{aligned} \eta_{FB} &= +1 \qquad \text{for bosons} \\ \eta_{FB} &= -1 \qquad \text{for fermions} \end{aligned} \tag{C.1}$$

The subscript "FB" indicates that the sign distingishes fermions and bosons.

Particle permutations

$$\langle \vec{x}_1, \vec{x}_2 | \Psi \rangle = \eta_{FB} \langle \vec{x}_2, \vec{x}_1 | \Psi \rangle \tag{C.2}$$

Fermionic wave functions are antisymmetric under exchange of two particles, while bosons are symmetric under particle exchange.

Slater determinants and permanents

The antisymmetrized product states relevant for fermions are Slater determinants Eq. 1.88. The symmetrized product states relevant for bosons are permanents Eq. 1.89.

- Fermions: The occupation numbers of fermions are $\sigma_n \in \{0, 1\}$. That is, for a specified, ordered set of one-particle states, a Slater determinant can be specified by $|\vec{\sigma}\rangle$, where $\vec{\sigma}$ is a string of zeros and ones.

- bosons: The occupation numbers of bosons are non-negative integers $\sigma_n \in \{0, 1, 2, \ldots\}$. That is, for a specified, ordered set of one-particle states, a permanent can be specified by $|\vec{\sigma}\rangle$, where $\vec{\sigma}$ is a string of non-negative integers.

Grand potential of non-interacting particles

The grand potential of non-interacting particles for fermions is given in Eq. L.104.

$$\Omega^{(0)}_{T,\mu} \overset{\text{Eq. } L.104}{=} \eta_{FB} k_B T \ \mathrm{Tr}\Big\{ \ln\Big(1 - \eta_{FB} \mathrm{e}^{-\beta(\epsilon - \mu \hat{1})} \Big) \Big\} \tag{C.3}$$

Thermal occupations

The thermal occupations of non-interacting electrons are the Fermi- and Bose-distributions

$$f_{T,\mu}(\epsilon) = \frac{1}{\mathrm{e}^{+\beta(\epsilon-\mu)} - \eta_{FB}} \tag{C.4}$$

one-particle-reduced density matrix

$$\hat{\rho}^{(1)} = \sum_n |\varphi_n\rangle f_n \langle\varphi_n| \tag{C.5}$$

The occupations of fermions are $f_n \in [0,1]$. The occupations of bosons are non negative, real-valued numbers.

Two-particle interaction

Interaction

$$\langle\Phi|\hat{W}|\Phi\rangle = \frac{1}{2}\sum_{m,n} f_m f_n \left[\langle\varphi_m,\varphi_n|\hat{W}|\varphi_m,\varphi_n\rangle + \eta_{FB}\langle\varphi_m,\varphi_n|\hat{W}|\varphi_n,\varphi_m\rangle\right] \tag{C.6}$$

The Coulomb interaction is usually not relevant for bosons. Exchange enhances the interaction matrix elements for bosons, in contrast to fermions.

Creation and annihilation operators

The creation and annihilation operators for fermions have been defined in Eqs. 3.15, 3.17 on p. 133.

$$\begin{aligned}
\hat{a}_i^\dagger &= \sum_{\vec{\sigma}} \Big|\sigma_1,\sigma_2,\ldots,\sigma_i+1,\ldots\Big\rangle \left(\left[\eta_{FB}{}^{\sum_{j<i}\sigma_j}\right]\sqrt{1+\eta_{FB}\sigma_i}\right)\Big\langle\sigma_1,\sigma_2,\ldots,\sigma_i,\ldots\Big| \\
\hat{a}_i &= \sum_{\vec{\sigma}} \Big|\sigma_1,\sigma_2,\ldots,\sigma_i-1,\ldots\Big\rangle \left(\left[\eta_{FB}{}^{\sum_{j<i}\sigma_j}\right]\sqrt{\sigma_i}\right)\Big\langle\sigma_1,\sigma_2,\ldots,\sigma_i,\ldots\Big|
\end{aligned} \tag{C.7}$$

This yields $\hat{n}_i = \hat{a}_i^\dagger \hat{a}_i = \sum_\sigma |\vec{\sigma}\rangle\sigma_i\langle\vec{\sigma}|$

Commutator- and anti-commutator rules

For creation and annihilation operators for an orthonormal one-particle basisset, the commutator, respectively anticommutator rules are

$$\begin{aligned}
\left[\hat{a}_m, \hat{a}_n^\dagger\right]_{-\eta_{FB}} &= \delta_{m,n} \\
\left[\hat{a}_m^\dagger, \hat{a}_n^\dagger\right]_{-\eta_{FB}} &= 0 \\
\left[\hat{a}_m, \hat{a}_n\right]_{-\eta_{FB}} &= 0
\end{aligned} \tag{C.8}$$

For non-orthonormal basissets $\{|\chi_\alpha\rangle\}$ with projector functions $\{|\pi_\alpha\rangle\}$, the inverse overlap operator replaces the unit matrix

$$\left[\hat{c}_\alpha, \hat{c}_\beta^\dagger\right]_{-\eta_{FB}} = \langle\pi_\alpha|\pi_\beta\rangle \tag{C.9}$$

where $S_{\alpha,\beta} = \langle\chi_\alpha|\chi_\beta\rangle$ is the overlap matrix of the orbitals and where the overlap of the projector functions $\langle\pi_\alpha|\pi_\beta\rangle = S^{-1}_{\alpha,\beta}$ is the inverse overlap of the orbitals

Spectral function

$$\begin{aligned}\mathcal{A}^{tot}_{\alpha,\beta}(\epsilon) &= \sum_n P_n \langle \Phi_n | \left[\hat{c}_{S,\alpha}, \hat{c}^\dagger_{S,\beta}\right]_{-\eta_{FB}} | \Phi_n \rangle \delta\Big(\epsilon - (E_m - E_n)\Big) \\ &= \sum_{m,n} \Big(P_n - \eta_{FB} P_m\Big) \langle \Phi_n | \hat{c}_{S,\alpha} | \Phi_m \rangle \langle \Phi_m | \hat{c}^\dagger_{S,\beta} | \Phi_n \rangle \delta\Big(\epsilon - (E_m - E_n)\Big) \end{aligned} \tag{C.10}$$

Appendix D

Hubbard dimer and hydrogen molecule

In these lecture notes, I am relying on dimer molecules with 1s orbitals to demonstrate many of the concepts introduced. The dimer serves as minimal model for a wealth of many-particle effects. Despite its simplicity, some of the calculations are quite involved and this distracts from the physical effects. Therefore, I introduce here the derivations of expressions, which I will refer to in the text. Note, that there are some repetitions in the text: In this appendix, I am using also advanced concepts that are only introduced later in the text than its first reference.

In this chapter, I am describing first the asymmetric dimer having a basis of 1s orbitals. Later, I will work out the matrix elements for the hydrogen molecule using atomic orbitals.[1]

Editor: see also Giesbertz[167] on reduced density matrix functional theory from many-particle perturbation theory and their calculations on the hubbard dimer.

D.1 Asymmetric two-site model

The asymmetric dimer consists of two distinct sites. It prepares the ground, both, for the Hubbard-dimer with two identical sites, and the Anderson dimer[143, 144] which describes one strongly interacting site coupled to a non-interacting environment.

The naming of the two sites relates to the Anderson impurity model, where one site contains d- or f-electrons described by the creation and annihilation operators $\hat{f}_\sigma^\dagger$ and $\hat{f}_\sigma$, while the other site has electrons described by $\hat{c}_\sigma^\dagger \hat{c}_\sigma$.

The Hamiltonian for the asymmetric dimer is

$$\hat{H} = \underbrace{\sum_\sigma \bar{\epsilon}_f \hat{f}_\sigma^\dagger \hat{f}_\sigma + \frac{1}{2} U_f \sum_{\sigma,\sigma'} \hat{f}_\sigma^\dagger \hat{f}_{\sigma'}^\dagger \hat{f}_{\sigma'} \hat{f}_\sigma}_{\text{atom F}} + \underbrace{\sum_\sigma \bar{\epsilon}_c \hat{c}_\sigma^\dagger \hat{c}_\sigma + \frac{1}{2} U_c \sum_{\sigma,\sigma'} \hat{c}_\sigma^\dagger \hat{c}_{\sigma'}^\dagger \hat{c}_{\sigma'} \hat{c}_\sigma}_{\text{atom C}}$$
$$\underbrace{-t \sum_\sigma \left(\hat{f}_\sigma^\dagger \hat{c}_\sigma + \hat{c}_\sigma^\dagger \hat{f}_\sigma \right)}_{\text{hopping}} \tag{D.1}$$

For the calculations, it is convenient to combine the operators, wherever possible, to particle-

[1] A similar derivation has been done by Pavarini in the appendix of chapter 11 *"Dynamical Mean-Field Theory for Materials"* in *Many-Body Methods for Real materials* Schriftenreihe de Forschungszentrums Jülich, Reihe Modeling and Simulation, Vol. 9 (2019), https://www.cond-mat.de/events/correl19/manuscripts/correl19.pdf

number operators $\hat{n}_{f,\sigma} = \hat{f}_\sigma^\dagger \hat{f}_\sigma$ and $\hat{n}_{c,\sigma} = \hat{c}_\sigma^\dagger \hat{c}_\sigma$. [2]

$$\hat{H} = \overbrace{\sum_{\sigma\in\{\uparrow,\downarrow\}} \bar{\epsilon}_f \hat{n}_{f,\sigma} + U_f \hat{n}_{f,\uparrow}\hat{n}_{f,\downarrow} + \frac{1}{2}U_f \sum_{\sigma\in\{\uparrow,\downarrow\}} \underbrace{\hat{n}_{f,\sigma}\big(\hat{n}_{f,\sigma}-1\big)}_{=\hat{0}}}^{\text{atom F}}$$
$$+ \overbrace{\sum_{\sigma\in\{\uparrow,\downarrow\}} \bar{\epsilon}_c \hat{n}_{c,\sigma} + U_c \hat{n}_{c,\uparrow}\hat{n}_{c,\downarrow} + \frac{1}{2}U_c \sum_{\sigma\in\{\uparrow,\downarrow\}} \underbrace{\hat{n}_{c,\sigma}\big(\hat{n}_{c,\sigma}-1\big)}_{=\hat{0}}}^{\text{atom C}}$$
$$\underbrace{-t \sum_{\sigma\in\{\uparrow,\downarrow\}} \left(\hat{f}_\sigma^\dagger \hat{c}_\sigma + \hat{c}_\sigma^\dagger \hat{f}_\sigma\right)}_{\text{hopping}} \tag{D.3}$$

Each atom has two onsite Coulomb terms. The second shows up in the mean-field approximation, while it is exactly zero in the full description.[3]

D.1.1 Symmetry-adapted many-particle states

Before we determine the eigenstates for the Hamiltonian of the asymmetric dimer, I first construct symmetry eigenstates in order to block diagonalize the Hamiltonian.

I start with setting up the basis set of Slater determinants in the local basis. These states are given in table D.1.

[2]

$$\frac{1}{2}\sum_{\sigma,\sigma'\in\{\uparrow,\downarrow\}} \hat{f}_\sigma^\dagger \hat{f}_{\sigma'}^\dagger \hat{f}_{\sigma'}\hat{f}_\sigma = -\frac{1}{2}\sum_{\sigma,\sigma'} \hat{f}_\sigma^\dagger \hat{f}_{\sigma'}^\dagger \hat{f}_\sigma \hat{f}_{\sigma'} = -\frac{1}{2}\sum_{\sigma,\sigma'}\Big(\delta_{\sigma,\sigma'}\hat{f}_\sigma^\dagger \hat{f}_{\sigma'} - \hat{f}_\sigma^\dagger \hat{f}_\sigma \hat{f}_{\sigma'}^\dagger \hat{f}_{\sigma'}\Big) = \frac{1}{2}\sum_{\sigma,\sigma'} \hat{f}_\sigma^\dagger \hat{f}_\sigma \hat{f}_{\sigma'}^\dagger \hat{f}_{\sigma'} - \frac{1}{2}\sum_\sigma \hat{f}_\sigma^\dagger \hat{f}_\sigma$$
$$= \hat{n}_{f,\uparrow}\hat{n}_{f,\downarrow} + \frac{1}{2}\sum_\sigma \underbrace{\left(\hat{n}_{f,\sigma}^2 - \hat{n}_{f,\sigma}\right)}_{=0} \tag{D.2}$$

[3] $\hat{n}_{f,\sigma}(\hat{n}_{f,\sigma}-1)$ vanishes, because the occupation-number operator for fermions has eigenvalues zero and one, so that the eigenvalues of $\hat{n}_{f,\sigma}(\hat{n}_{f,\sigma}-1)$ vanish. Hence, is the zero operator $\hat{n}_{f,\sigma}(\hat{n}_{f,\sigma}-1)$.

Table D.1: Slater determinants, which form a basis set of many-particle wave functions for the asymmetric dimer.

Nr.	$\lvert f_\uparrow, f_\downarrow, c_\uparrow, c_\downarrow\rangle$	Basisstate	N	$S_z/\hbar$
1	$\lvert 0,0,0,0\rangle$	$\lvert\mathcal{O}\rangle$	$N=0$	$S_z=0$
2	$\lvert 1,0,0,0\rangle$	$f_\uparrow^\dagger\lvert\mathcal{O}\rangle$	$N=1$	$S_z=+\frac{1}{2}$
3	$\lvert 0,1,0,0\rangle$	$f_\downarrow^\dagger\lvert\mathcal{O}\rangle$	$N=1$	$S_z=-\frac{1}{2}$
4	$\lvert 1,1,0,0\rangle$	$f_\uparrow^\dagger f_\downarrow^\dagger\lvert\mathcal{O}\rangle$	$N=2$	$S_z=0$
5	$\lvert 0,0,1,0\rangle$	$c_\uparrow^\dagger\lvert\mathcal{O}\rangle$	$N=1$	$S_z=\frac{1}{2}$
6	$\lvert 1,0,1,0\rangle$	$f_\uparrow^\dagger c_\uparrow^\dagger\lvert\mathcal{O}\rangle$	$N=2$	$S_z=+1$
7	$\lvert 0,1,1,0\rangle$	$f_\downarrow^\dagger c_\uparrow^\dagger\lvert\mathcal{O}\rangle$	$N=2$	$S_z=0$
8	$\lvert 1,1,1,0\rangle$	$f_\uparrow^\dagger f_\downarrow^\dagger c_\uparrow^\dagger\lvert\mathcal{O}\rangle$	$N=3$	$S_z=+\frac{1}{2}$
9	$\lvert 0,0,0,1\rangle$	$c_\downarrow^\dagger\lvert\mathcal{O}\rangle$	$N=1$	$S_z=-\frac{1}{2}$
10	$\lvert 1,0,0,1\rangle$	$f_\uparrow^\dagger c_\downarrow^\dagger\lvert\mathcal{O}\rangle$	$N=2$	$S_z=0$
11	$\lvert 0,1,0,1\rangle$	$f_\downarrow^\dagger c_\downarrow^\dagger\lvert\mathcal{O}\rangle$	$N=2$	$S_z=-1$
12	$\lvert 1,1,0,1\rangle$	$f_\uparrow^\dagger f_\downarrow^\dagger c_\downarrow^\dagger\lvert\mathcal{O}\rangle$	$N=3$	$S_z=-\frac{1}{2}$
13	$\lvert 0,0,1,1\rangle$	$c_\uparrow^\dagger c_\downarrow^\dagger\lvert\mathcal{O}\rangle$	$N=2$	$S_z=0$
14	$\lvert 1,0,1,1\rangle$	$f_\uparrow^\dagger c_\uparrow^\dagger c_\downarrow^\dagger\lvert\mathcal{O}\rangle$	$N=3$	$S_z=+\frac{1}{2}$
15	$\lvert 0,1,1,1\rangle$	$f_\downarrow^\dagger c_\uparrow^\dagger c_\downarrow^\dagger\lvert\mathcal{O}\rangle$	$N=3$	$S_z=-\frac{1}{2}$
16	$\lvert 1,1,1,1\rangle$	$f_\uparrow^\dagger f_\downarrow^\dagger c_\uparrow^\dagger c_\downarrow^\dagger\lvert\mathcal{O}\rangle$	$N=4$	$S_z=0$

Before diagonalizing the Hamiltonian, I select common eigenstates of a set of symmetry operators of the Hamiltonian. In the basis of symmetry eigenstates, the Hamiltonian will become block diagonal, which simplifies the diagonalization. Alongside with the symmetry operators, I include also the particle number into the set of operators that commutate with the Hamiltonian and the other symmetry operators.

First, I classify the states in table D.1 according to their particle number and $\hat{S}_Z$ eigenvalues. Then, I will break up the blocks according to the $\vec{S}^2$ eigenvalues. The states in the individual blocks are given in table D.2.

One-particle channel

The Hamiltonian projected onto the one-particle sector ($N=1$) and the eigenstates with $S_z=\frac{\hbar}{2}\sigma$ is

$$\hat{P}_{1,\sigma}\hat{H}\hat{P}_{1,\sigma}=\begin{pmatrix}\hat{f}_\sigma^\dagger|\mathcal{O}\rangle\\ \hat{c}_\sigma^\dagger|\mathcal{O}\rangle\end{pmatrix}\begin{pmatrix}\bar{\epsilon}_f & -|t|\\ -|t| & \bar{\epsilon}_c\end{pmatrix}\begin{pmatrix}\langle\mathcal{O}|\hat{f}_\sigma\\ \langle\mathcal{O}|\hat{c}_\sigma\end{pmatrix} \tag{D.4}$$

where $\hat{P}_{1,\sigma}$ is the corresponding projection operator onto states with $N=1$ and $S_z=\frac{\hbar}{2}\sigma$.

The eigenvalues are

$$\epsilon_\pm=\frac{\bar{\epsilon}_f+\bar{\epsilon}_c}{2}\pm\sqrt{\left(\frac{\bar{\epsilon}_f-\bar{\epsilon}_c}{2}\right)^2+|t|^2} \tag{D.5}$$

Table D.2: Symmetry eigenstates states constructed from the Slater determinants in table D.1. The Slater determinants can be grouped according to their eigenvalues with respect to particle number N and S_z. Using the total spin, i.e. $\hat{\vec{S}}^2$, the block with $N = 2$ and $S_z = 0$ can be divided further into one triplet state with $S = 1$ and a block with three states with $S = 0$ as decribed in section D.1.1

N	$S_z/\hbar$	S		
0	0	0	$\|1\rangle$	$\|\mathcal{O}\rangle$
1	$-\frac{1}{2}$	$\frac{1}{2}$	$\|3\rangle, \|9\rangle$	$\hat{f}_\downarrow^\dagger\|\mathcal{O}\rangle$, $\hat{c}_\downarrow^\dagger\|\mathcal{O}\rangle$
1	$+\frac{1}{2}$	$\frac{1}{2}$	$\|2\rangle, \|5\rangle$	$\hat{f}_\uparrow^\dagger\|\mathcal{O}\rangle$, $\hat{c}_\uparrow^\dagger\|\mathcal{O}\rangle$
2	-1	1	$\|11\rangle$	$\hat{f}_\downarrow^\dagger\hat{c}_\downarrow^\dagger\|\mathcal{O}\rangle$
2	0	1	$\frac{1}{\sqrt{2}}\big(\|7\rangle + \|10\rangle\big)$	$\frac{1}{\sqrt{2}}\big(\hat{f}_\downarrow^\dagger\hat{c}_\uparrow^\dagger + \hat{f}_\uparrow^\dagger\hat{c}_\downarrow^\dagger\big)\|\mathcal{O}\rangle$
2	0	0	$\|4\rangle$,$\|13\rangle$, $\frac{1}{\sqrt{2}}\Big(\|7\rangle - \|10\rangle\Big)$	$\hat{f}_\uparrow^\dagger\hat{f}_\downarrow^\dagger\|\mathcal{O}\rangle$, $\hat{c}_\uparrow^\dagger\hat{c}_\downarrow^\dagger\|\mathcal{O}\rangle$, $\frac{1}{\sqrt{2}}\big(\hat{f}_\downarrow^\dagger\hat{c}_\uparrow^\dagger - \hat{f}_\uparrow^\dagger\hat{c}_\downarrow^\dagger\big)\|\mathcal{O}\rangle$
2	$+1$	1	$\|6\rangle$	$\hat{f}_\uparrow^\dagger\hat{c}_\uparrow^\dagger$
3	$-\frac{1}{2}$	$\frac{1}{2}$	$\|12\rangle, \|15\rangle$	$\hat{f}_\uparrow^\dagger\hat{f}_\downarrow^\dagger\hat{c}_\downarrow^\dagger\|\mathcal{O}\rangle$, $\hat{f}_\downarrow^\dagger\hat{c}_\uparrow^\dagger\hat{c}_\downarrow^\dagger\|\mathcal{O}\rangle$
3	$+\frac{1}{2}$	$\frac{1}{2}$	$\|8\rangle, \|14\rangle$	$\hat{f}_\uparrow^\dagger\hat{f}_\downarrow^\dagger\hat{c}_\uparrow^\dagger\|\mathcal{O}\rangle$, $\hat{f}_\uparrow^\dagger\hat{c}_\uparrow^\dagger\hat{c}_\downarrow^\dagger\|\mathcal{O}\rangle$
4	0	0	$\|16\rangle$	$\hat{f}_\uparrow^\dagger\hat{f}_\downarrow^\dagger\hat{c}_\uparrow^\dagger\hat{c}_\downarrow^\dagger\|\mathcal{O}\rangle$

The eigenstates $\psi_\pm$ are

$$\begin{aligned}|\psi_-\rangle &= \Big(\hat{f}_\sigma^\dagger\cos(\alpha_1) + \hat{c}_\sigma^\dagger\sin(\alpha_1)\Big)|\mathcal{O}\rangle \\ |\psi_+\rangle &= \Big(\hat{f}_\sigma^\dagger\sin(\alpha_1) - \hat{c}_\sigma^\dagger\cos(\alpha_1)\Big)|\mathcal{O}\rangle\end{aligned} \tag{D.6}$$

This Ansatz guarantees that the states are orthonormal.

The angle α_1 is obtained by inserting the Ansatz Eq. D.6 of $|\psi_-\rangle$ into the eigenvector equation with Eq. D.4

$$\begin{aligned}&(\bar{\epsilon}_f - \epsilon_-)\cos(\alpha_1) - |t|\sin(\alpha_1) = 0 \\ \Rightarrow \tan(\alpha_1) &= \frac{1}{|t|}\Big(\bar{\epsilon}_f - \epsilon_-\Big) \\ &= \frac{1}{|t|}\left(\frac{\bar{\epsilon}_f - \bar{\epsilon}_c}{2} + \sqrt{\left(\frac{\bar{\epsilon}_f - \bar{\epsilon}_c}{2}\right)^2 + |t|^2}\right) \\ &= \frac{\bar{\epsilon}_f - \bar{\epsilon}_c}{2|t|} + \sqrt{1 + \left(\frac{\bar{\epsilon}_f - \bar{\epsilon}_c}{2|t|}\right)^2} \\ \alpha_1 &= \operatorname{atan}\Big(q + \sqrt{1+q}\Big) \qquad \text{with } q = \frac{\bar{\epsilon}_f - \bar{\epsilon}_c}{2|t|}\end{aligned} \tag{D.7}$$

- For the symmetric case, $\bar{\epsilon}_f = \bar{\epsilon}_c$ we obtain $\tan(\alpha_1) = 1$ and $\alpha_1 = 45° = \pi/4$. This describes the bonding and antibonding orbitals.
- For the asymmetric limit $|\bar{\epsilon}_f - \bar{\epsilon}_c| \gg |t|$, I obtain $\tan(\alpha_1) = \infty$ or $\alpha_1 = 90° = \pi/2$. In this case each wave function is localized either on one or the other site.

Three-particle channel

The three-particle channel can be worked out analogous to the one-particle channel.

The Hamiltonian projected onto the three-particle sector and the eigenstates with $S_z = \frac{\hbar}{2}\sigma$ is

$$\hat{P}_{3,\sigma}\hat{H}\hat{P}_{3,\sigma} = \begin{pmatrix} \hat{f}_{\bar{\sigma}}^\dagger \hat{f}_\sigma^\dagger \hat{c}_\sigma^\dagger |\mathcal{O}\rangle \\ \hat{c}_{\bar{\sigma}}^\dagger \hat{f}_\sigma^\dagger \hat{c}_\sigma^\dagger |\mathcal{O}\rangle \end{pmatrix} \begin{pmatrix} 2\bar{\epsilon}_f + U_f + \bar{\epsilon}_c & -|t| \\ -|t| & \bar{\epsilon}_f + 2\bar{\epsilon}_c + U_c \end{pmatrix} \begin{pmatrix} \langle\mathcal{O}|\hat{c}_\sigma \hat{f}_\sigma \hat{f}_{\bar{\sigma}} \\ \langle\mathcal{O}|\hat{c}_\sigma \hat{f}_\sigma \hat{c}_{\bar{\sigma}} \end{pmatrix} \tag{D.8}$$

where $\hat{P}_{3,\sigma}$ is the projection operator on the three-particle states with $S_z = \frac{\hbar}{2}\sigma$. **With $\bar{\sigma}$, I denote the spin direction opposite to σ, i.e. $\bar{\sigma} = \downarrow$ for $\sigma = \uparrow$ and vice versa.**

The Slater determinants used here differ from the ones used initially by the order of the operators. Note, that $\hat{c}_{\bar{\sigma}}\hat{f}_\sigma\hat{c}_\sigma = +\hat{f}_\sigma\hat{c}_\sigma\hat{c}_{\bar{\sigma}}$. The order of the spin indices on the doubly occupied orbital is reversed in both orbitals. This changes the sign of one orbital with respect to the other.

The eigenvalues are

$$\epsilon_\pm = \frac{3\bar{\epsilon}_f + U_f + 3\bar{\epsilon}_c + U_c}{2} \pm \sqrt{\left(\frac{\bar{\epsilon}_f + U_f - \bar{\epsilon}_c - U_c}{2}\right)^2 + |t|^2} \tag{D.9}$$

The eigenstates $\psi_\pm$ are

$$\begin{aligned} |\psi_-\rangle &= \left(\hat{f}_{\bar{\sigma}}^\dagger \cos(\alpha_2) + \hat{f}_{\bar{\sigma}}^\dagger \sin(\alpha_2)\right) \hat{f}_\sigma^\dagger \hat{c}_\sigma^\dagger |\mathcal{O}\rangle \\ |\psi_+\rangle &= \left(\hat{f}_{\bar{\sigma}}^\dagger \sin(\alpha_2) - \hat{f}_{\bar{\sigma}}^\dagger \cos(\alpha_2)\right) \hat{f}_\sigma^\dagger \hat{c}_\sigma^\dagger |\mathcal{O}\rangle \end{aligned} \tag{D.10}$$

This Ansatz guarantees that the states are orthonormal.

The angle α_1 is obtained by inserting the Ansatz of $|\psi_-\rangle$ into the eigenvector equation

$$\begin{aligned} & (2\bar{\epsilon}_f + U_f + \bar{\epsilon}_c - \epsilon_-)\cos(\alpha_2) - |t|\sin(\alpha_2) = 0 \\ \Rightarrow \tan(\alpha_2) &= \frac{1}{|t|}\left(2\bar{\epsilon}_f + U_f + \bar{\epsilon}_c - \epsilon_-\right) \\ &= \frac{1}{|t|}\left(\frac{\bar{\epsilon}_f + U_f - \bar{\epsilon}_c - U_c}{2} + \sqrt{\left(\frac{\bar{\epsilon}_f + U_f - \bar{\epsilon}_c - U_c}{2}\right)^2 + |t|^2}\right) \\ &= \frac{\bar{\epsilon}_f + U_f - \bar{\epsilon}_c - U_c}{2|t|} + \sqrt{1 + \left(\frac{\bar{\epsilon}_f + U_f - \bar{\epsilon}_c - U_c}{2|t|}\right)^2} \\ \alpha_2 &= \operatorname{atan}\left(q + \sqrt{1+q}\right) \qquad \text{with } q = \frac{\bar{\epsilon}_f + U_f - \bar{\epsilon}_c - U_c}{2|t|} \end{aligned} \tag{D.11}$$

- For the symmetric case, $\bar{\epsilon}_f + U_f = \bar{\epsilon}_c + U_c$, I obtain $\tan(\alpha_2) = 1$ and $\alpha_2 = 45° = \pi/4$. This describes the bonding and antibonding orbitals for the minority-spin direction and a completely filled majority-spin direction.
- For the asymmetric limit $|\bar{\epsilon}_f + U_f - \bar{\epsilon}_c - U_c| \gg |t|$, I obtain $\tan(\alpha_2) = \infty$ or $\alpha_2 = 90° = \pi/2$. In this case one site has two electrons, while other has an occupied orbital in the majority-spin direction.
- The three-particle case is very similar to the one-particle sector, when the atomic orbital levels of the one-particle case are shifted up by the corresponding U-term.

Two-particle channel

In the basisset given in table D.1, the largest block of the Hamiltonian is the one with $N = 2$ and $S_z = 0$, which contains four states. In order to break down this block further, let us exploit the symmetry under spin rotation. $\hat{\vec{S}}^2$ commutates with the Hamiltonian and with the particle number and S_z. Thus, we can break down the blocks of the Hamiltonian into subblocks which are eigenstates of N, S_z and S^2.

This calculation is done in exercise 3.11.2 on p. 160. The eigenstates of $\hat{\vec{S}}^2$ in the two-particle channel are given in Eq. 3.153 and Eq. 3.152: We obtained three states with spin quantum number $S = 1$, namely

$$\begin{aligned} |6\rangle &\overset{\text{Eq. 3.152}}{=} \hat{f}_\uparrow^\dagger \hat{c}_\uparrow^\dagger |\mathcal{O}\rangle \qquad S_z = +1 \\ |11\rangle &\overset{\text{Eq. 3.152}}{=} \hat{f}_\downarrow^\dagger \hat{c}_\downarrow^\dagger |\mathcal{O}\rangle \\ \frac{1}{\sqrt{2}}\Big(|7\rangle + |10\rangle\Big) &\overset{\text{Eq. 3.152}}{=} \frac{1}{\sqrt{2}}\Big(\hat{f}_\downarrow^\dagger \hat{c}_\uparrow^\dagger + \hat{f}_\uparrow^\dagger \hat{c}_\downarrow^\dagger\Big)|\mathcal{O}\rangle \end{aligned} \tag{D.12}$$

and three states with $S = 0$, namely

$$\begin{aligned} |4\rangle &\overset{\text{Eq. 3.153}}{=} \hat{f}_\uparrow^\dagger \hat{f}_\downarrow^\dagger |\mathcal{O}\rangle \\ |13\rangle &\overset{\text{Eq. 3.153}}{=} \hat{c}_\uparrow^\dagger \hat{c}_\downarrow^\dagger |\mathcal{O}\rangle \\ \frac{1}{\sqrt{2}}\Big(|7\rangle - |10\rangle\Big) &\overset{\text{Eq. 3.153}}{=} \frac{1}{\sqrt{2}}\Big(\hat{f}_\downarrow^\dagger \hat{c}_\uparrow^\dagger - \hat{f}_\uparrow^\dagger \hat{c}_\downarrow^\dagger\Big)|\mathcal{O}\rangle \end{aligned} \tag{D.13}$$

This splits the subblock of the Hamiltonian with the four Slater determinants $\{|4\rangle, |7\rangle, |10\rangle, |13\rangle\}$ with $N = 2$ and $S_z = 0$ into one state with $S = 1$ and a block of three singlet states with $S = 0$. (The eigenvalues of $\hat{S}^2$ are $\hbar^2 S(S+1)$.)

The Hamiltonian projected onto the two-particle sector and the eigenstates with $S = 0$ is

$$\hat{P}_{2,0}\hat{H}\hat{P}_{2,0} = \begin{pmatrix} \hat{f}_\uparrow^\dagger \hat{f}_\downarrow^\dagger |\mathcal{O}\rangle \\ \hat{c}_\uparrow^\dagger \hat{c}_\downarrow^\dagger |\mathcal{O}\rangle \\ \frac{1}{\sqrt{2}}\big(\hat{f}_\uparrow^\dagger \hat{c}_\downarrow^\dagger - \hat{f}_\downarrow^\dagger \hat{c}_\uparrow^\dagger\big)|\mathcal{O}\rangle \end{pmatrix} \begin{pmatrix} 2\bar{\epsilon}_f + U_f & 0 & -\sqrt{2}|t| \\ 0 & 2\bar{\epsilon}_c + U_c & -\sqrt{2}|t| \\ -\sqrt{2}|t| & -\sqrt{2}|t| & \bar{\epsilon}_c + \bar{\epsilon}_f \end{pmatrix} \begin{pmatrix} \langle\mathcal{O}|\hat{f}_\downarrow \hat{f}_\uparrow \\ \langle\mathcal{O}|\hat{c}_\downarrow \hat{c}_\uparrow \\ \langle\mathcal{O}|\frac{1}{\sqrt{2}}\big(\hat{c}_\downarrow \hat{f}_\uparrow - \hat{c}_\uparrow \hat{f}_\downarrow\big) \end{pmatrix} \tag{D.14}$$

where $\hat{P}_{2,0}$ is the projection operator onto the two-particle states ($N = 2$) with $S_z = 0\hbar$.

Table D.3: Hamilton eigenstates of the asymmetric dimer.

N	S	$S_z/\hbar$	$\lvert\Phi\rangle$	$\langle\Phi\lvert\hat{H}\rvert\Phi\rangle$
$N=0$	$S=0$	$S_z=0$	$\lvert\mathcal{O}\rangle$	$E=0$
$N=1$	$S=\frac{1}{2}$	$S_z=+\frac{1}{2}$	$\Big(\hat{f}_\uparrow^\dagger\cos(\alpha_1)+\hat{c}_\uparrow^\dagger\sin(\alpha_1)\Big)\lvert\mathcal{O}\rangle$	$\frac{\bar{\epsilon}_c+\bar{\epsilon}_f}{2}-\sqrt{\left(\frac{\bar{\epsilon}_c-\bar{\epsilon}_f}{2}\right)^2+t^2}$
$N=1$	$S=\frac{1}{2}$	$S_z=+\frac{1}{2}$	$\Big(\hat{f}_\uparrow^\dagger\sin(\alpha_1)-\hat{c}_\uparrow^\dagger\cos(\alpha_1)\Big)\lvert\mathcal{O}\rangle$	$\frac{\bar{\epsilon}_c+\bar{\epsilon}_f}{2}+\sqrt{\left(\frac{\bar{\epsilon}_c-\bar{\epsilon}_f}{2}\right)^2+t^2}$
$N=1$	$S=\frac{1}{2}$	$S_z=-\frac{1}{2}$	$\Big(\hat{f}_\downarrow^\dagger\cos(\alpha_1)+\hat{c}_\downarrow^\dagger\sin(\alpha_1)\Big)\lvert\mathcal{O}\rangle$	$\frac{\bar{\epsilon}_c+\bar{\epsilon}_f}{2}-\sqrt{\left(\frac{\bar{\epsilon}_c-\bar{\epsilon}_f}{2}\right)^2+t^2}$
$N=1$	$S=\frac{1}{2}$	$S_z=-\frac{1}{2}$	$\Big(\hat{f}_\downarrow^\dagger\sin(\alpha_1)+\hat{c}_\downarrow^\dagger\cos(\alpha_1)\Big)\lvert\mathcal{O}\rangle$	$\frac{\bar{\epsilon}_c+\bar{\epsilon}_f}{2}+\sqrt{\left(\frac{\bar{\epsilon}_c-\bar{\epsilon}_f}{2}\right)^2+t^2}$
$N=2$	$S=0$	$S_z=0$	$\approx\hat{f}_\uparrow^\dagger\hat{f}_\downarrow^\dagger\lvert\mathcal{O}\rangle$	$\approx 2\bar{\epsilon}_f+U_f+O(t,1/U)$
$N=2$	$S=0$	$S_z=0$	$\approx\hat{c}_\uparrow^\dagger\hat{c}_\downarrow^\dagger\lvert\mathcal{O}\rangle$	$\approx 2\bar{\epsilon}_c+U_c+O(t,1/U)$
$N=2$	$S=0$	$S_z=0$	$\approx\frac{1}{\sqrt{2}}\big(\hat{f}_\uparrow^\dagger\hat{c}_\downarrow^\dagger-\hat{f}_\downarrow^\dagger\hat{c}_\uparrow^\dagger\big)\lvert\mathcal{O}\rangle$	$\approx\bar{\epsilon}_f+\bar{\epsilon}_c+O(t,1/U)$
$N=2$	$S=1$	$S_z=1$	$\hat{f}_\uparrow^\dagger\hat{c}_\uparrow^\dagger\lvert\mathcal{O}\rangle$	$E=\bar{\epsilon}_f+\bar{\epsilon}_c$
$N=2$	$S=1$	$S_z=0$	$\frac{1}{\sqrt{2}}\big(\hat{f}_\uparrow^\dagger\hat{c}_\downarrow^\dagger+\hat{f}_\downarrow^\dagger\hat{c}_\uparrow^\dagger\big)\lvert\mathcal{O}\rangle$	$E=\bar{\epsilon}_f+\bar{\epsilon}_c$
$N=2$	$S=1$	$S_z=-1$	$\hat{f}_\downarrow^\dagger\hat{c}_\downarrow^\dagger\lvert\mathcal{O}\rangle$	$E=\bar{\epsilon}_f+\bar{\epsilon}_c$
$N=3$	$S=\frac{1}{2}$	$S_z=+\frac{1}{2}$	$\hat{f}_\uparrow^\dagger\hat{c}_\uparrow^\dagger\Big(\hat{f}_\downarrow^\dagger\cos(\alpha_2)+\hat{c}_\downarrow^\dagger\sin(\alpha_2)\Big)\lvert\mathcal{O}\rangle$	$\frac{3\bar{\epsilon}_c+U_c+3\bar{\epsilon}_f+U_f}{2}-\sqrt{\left(\frac{\bar{\epsilon}_f+U_f-\bar{\epsilon}_c-U_c}{2}\right)^2+t^2}$
$N=3$	$S=\frac{1}{2}$	$S_z=+\frac{1}{2}$	$\hat{f}_\uparrow^\dagger\hat{c}_\uparrow^\dagger\Big(\hat{f}_\downarrow^\dagger\sin(\alpha_2)-\hat{c}_\downarrow^\dagger\cos(\alpha_2)\Big)\lvert\mathcal{O}\rangle$	$\frac{3\bar{\epsilon}_c+U_c+3\bar{\epsilon}_f+U_f}{2}+\sqrt{\left(\frac{\bar{\epsilon}_f+U-\bar{\epsilon}_c-U_c}{2}\right)^2+t^2}$
$N=3$	$S=\frac{1}{2}$	$S_z=-\frac{1}{2}$	$\hat{f}_\downarrow^\dagger\hat{c}_\downarrow^\dagger\Big(\hat{f}_\uparrow^\dagger\cos(\alpha_2)+\hat{c}_\uparrow^\dagger\sin(\alpha_2)\Big)\lvert\mathcal{O}\rangle$	$\frac{3\bar{\epsilon}_c+U_c+3\bar{\epsilon}_f+U_f}{2}-\sqrt{\left(\frac{\bar{\epsilon}_f+U_f-\bar{\epsilon}_c-U_c}{2}\right)^2+t^2}$
$N=3$	$S=\frac{1}{2}$	$S_z=-\frac{1}{2}$	$\hat{f}_\downarrow^\dagger\hat{c}_\downarrow^\dagger\Big(\hat{f}_\uparrow^\dagger\sin(\alpha_2)-\hat{c}_\uparrow^\dagger\cos(\alpha_2)\Big)\lvert\mathcal{O}\rangle$	$\frac{3\bar{\epsilon}_c+U_c+3\bar{\epsilon}_f+U_f}{2}+\sqrt{\left(\frac{\bar{\epsilon}_f+U_f-\bar{\epsilon}_c-U_c}{2}\right)^2+t^2}$
$N=4$	$S=0$	$S_z=0$	$\hat{f}_\uparrow^\dagger\hat{f}_\downarrow^\dagger\hat{c}_\uparrow^\dagger\hat{c}_\downarrow^\dagger\lvert\mathcal{O}\rangle$	$E=2\bar{\epsilon}_c+2\bar{\epsilon}_f+U_f+U_c$

D.2 Hubbard dimer

Let me now study the Hubbard dimer, which is the symmetric case of the asymmetric dimer studied in the previous section D.1.

The physics of the Hubbard dimer is described in section 17.2.3 on p. 444.

The difference to the asymmetric dimer is that the atomic orbital energies, named $\bar{\epsilon}$, are equal, i.e. $\bar{\epsilon}_c = \bar{\epsilon}_f = \bar{\epsilon}$, and that the Coulomb repulsion parameters, named U, are equal too, i.e. $U_c = U_f$. We adhere to the notation naming the atoms F and C and their creators $\hat{f}_\sigma^\dagger$ and $\hat{c}_\sigma^\dagger$. The letters simply stand for left and right atom.

$$\begin{aligned}\hat{H} &= \underbrace{\sum_\sigma \bar{\epsilon}\hat{f}_\sigma^\dagger \hat{f}_\sigma + \frac{1}{2}U\sum_{\sigma,\sigma'}\hat{f}_\sigma^\dagger \hat{f}_{\sigma'}^\dagger \hat{f}_{\sigma'}\hat{f}_\sigma}_{\text{atom F}} + \underbrace{\sum_\sigma \bar{\epsilon}\hat{c}_\sigma^\dagger \hat{c}_\sigma + \frac{1}{2}U\sum_{\sigma,\sigma'}\hat{c}_\sigma^\dagger \hat{c}_{\sigma'}^\dagger \hat{c}_{\sigma'}\hat{c}_\sigma}_{\text{atom C}} \underbrace{-|t|\sum_\sigma\Big(\hat{f}_\sigma^\dagger \hat{c}_\sigma + \hat{c}_\sigma^\dagger \hat{f}_\sigma\Big)}_{\text{hopping}} \\ &= \overbrace{\sum_\sigma \bar{\epsilon}\hat{n}_{f,\sigma} + U\hat{n}_{f,\uparrow}\hat{n}_{f,\downarrow} + \underbrace{U\sum_\sigma \hat{n}_{f,\sigma}\big(\hat{n}_{f,\sigma}-1\big)}_{=0}}^{\text{atom F}} + \overbrace{\sum_\sigma \bar{\epsilon}\hat{n}_{c,\sigma} + U\hat{n}_{c,\uparrow}\hat{n}_{c,\downarrow} + \underbrace{U\sum_\sigma \hat{n}_{c,\sigma}\big(\hat{n}_{c,\sigma}-1\big)}_{=0}}^{\text{atom C}} \\ &\quad \underbrace{-|t|\sum_\sigma\Big(\hat{f}_\sigma^\dagger \hat{c}_\sigma + \hat{c}_\sigma^\dagger \hat{f}_\sigma\Big)}_{\text{hopping}}\end{aligned} \tag{D.15}$$

Table D.4: Symmetry-adapted orbitals for the Hubbard dimer. The states are classified according to particle number, spin quantum numbers S and S_z and spatial inversion with eigenvalue $P = \pm 1$. The total spin eigenvalues are $\hbar^2 s(s+1)$. The spin in z-direction is $\hbar s_z$. The energies are the **energy expectation values** of the symmetry-adapted states rather than the eigenvalues of the Hamiltonian. For the 2×2 block with $N = 2$, $S = 0$ and $P = +1$, they are not eigenstates of the Hamiltonian.

N	S	S_z	P	$\|\Phi\rangle$	$\langle\Phi\|\hat{H}\|\Phi\rangle$
$N=0$	$S=0$	$S_z=0$	$P=1$	$\|\mathcal{O}\rangle$	0
$N=1$	$S=\frac{1}{2}$	$S_z=+\frac{1}{2}$	$P=+1$	$\frac{1}{\sqrt{2}}\left(\hat{f}_\uparrow^\dagger + \hat{c}_\uparrow^\dagger\right)\|\mathcal{O}\rangle$	$\bar{\epsilon} - \|t\|$
$N=1$	$S=\frac{1}{2}$	$S_z=+\frac{1}{2}$	$P=-1$	$\frac{1}{\sqrt{2}}\left(\hat{f}_\uparrow^\dagger - \hat{c}_\uparrow^\dagger\right)\|\mathcal{O}\rangle$	$\bar{\epsilon} + \|t\|$
$N=1$	$S=\frac{1}{2}$	$S_z=-\frac{1}{2}$	$P=+1$	$\frac{1}{\sqrt{2}}\left(\hat{f}_\downarrow^\dagger + \hat{c}_\downarrow^\dagger\right)\|\mathcal{O}\rangle$	$\bar{\epsilon} - \|t\|$
$N=1$	$S=\frac{1}{2}$	$S_z=-\frac{1}{2}$	$P=-1$	$\frac{1}{\sqrt{2}}\left(\hat{f}_\downarrow^\dagger - \hat{c}_\downarrow^\dagger\right)\|\mathcal{O}\rangle$	$\bar{\epsilon} + \|t\|$
$N=2$	$S=0$	$S_z=0$	$P=-1$	$\frac{1}{\sqrt{2}}\left(\hat{f}_\uparrow^\dagger \hat{f}_\downarrow^\dagger - \hat{c}_\uparrow^\dagger \hat{c}_\downarrow^\dagger\right)\|\mathcal{O}\rangle$	$2\bar{\epsilon} + U$
$N=2$	$S=0$	$S_z=0$	$P=+1$	$\frac{1}{\sqrt{2}}\left(\hat{f}_\uparrow^\dagger \hat{f}_\downarrow^\dagger + \hat{c}_\uparrow^\dagger \hat{c}_\downarrow^\dagger\right)\|\mathcal{O}\rangle$	$2\bar{\epsilon} + U$
$N=2$	$S=0$	$S_z=0$	$P=+1$	$\frac{1}{\sqrt{2}}\left(\hat{f}_\uparrow^\dagger \hat{c}_\downarrow^\dagger - \hat{f}_\downarrow^\dagger \hat{c}_\uparrow^\dagger\right)\|\mathcal{O}\rangle$	$2\bar{\epsilon}$
$N=2$	$S=1$	$S_z=1$	$P=-1$	$\hat{f}_\uparrow^\dagger \hat{c}_\uparrow^\dagger\|\mathcal{O}\rangle$	$2\bar{\epsilon}$
$N=2$	$S=1$	$S_z=0$	$P=-1$	$\frac{1}{\sqrt{2}}\left(\hat{f}_\uparrow^\dagger \hat{c}_\downarrow^\dagger + \hat{f}_\downarrow^\dagger \hat{c}_\uparrow^\dagger\right)\|\mathcal{O}\rangle$	$2\bar{\epsilon}$
$N=2$	$S=1$	$S_z=-1$	$P=-1$	$\hat{f}_\downarrow^\dagger \hat{c}_\downarrow^\dagger\|\mathcal{O}\rangle$	$2\bar{\epsilon}$
$N=3$	$S=\frac{1}{2}$	$S_z=+\frac{1}{2}$	$P=-1$	$\hat{f}_\uparrow^\dagger \hat{c}_\uparrow^\dagger \frac{1}{\sqrt{2}}\left(\hat{f}_\downarrow^\dagger + \hat{c}_\downarrow^\dagger\right)\|\mathcal{O}\rangle$	$3\bar{\epsilon} + U - \|t\|$
$N=3$	$S=\frac{1}{2}$	$S_z=+\frac{1}{2}$	$P=+1$	$\hat{f}_\uparrow^\dagger \hat{c}_\uparrow^\dagger \frac{1}{\sqrt{2}}\left(\hat{f}_\downarrow^\dagger - \hat{c}_\downarrow^\dagger\right)\|\mathcal{O}\rangle$	$3\bar{\epsilon} + U + \|t\|$
$N=3$	$S=\frac{1}{2}$	$S_z=-\frac{1}{2}$	$P=-1$	$\hat{f}_\downarrow^\dagger \hat{c}_\downarrow^\dagger \frac{1}{\sqrt{2}}\left(\hat{f}_\uparrow^\dagger + \hat{c}_\uparrow^\dagger\right)\|\mathcal{O}\rangle$	$3\bar{\epsilon} + U - \|t\|$
$N=3$	$S=\frac{1}{2}$	$S_z=-\frac{1}{2}$	$P=+1$	$\hat{f}_\downarrow^\dagger \hat{c}_\downarrow^\dagger \frac{1}{\sqrt{2}}\left(\hat{f}_\uparrow^\dagger - \hat{c}_\uparrow^\dagger\right)\|\mathcal{O}\rangle$	$3\bar{\epsilon} + U + \|t\|$
$N=4$	$S=0$	$S_z=0$	$P=+1$	$\hat{f}_\uparrow^\dagger \hat{f}_\downarrow^\dagger \hat{c}_\uparrow^\dagger \hat{c}_\downarrow^\dagger\|\mathcal{O}\rangle$	$4\bar{\epsilon} + 2U$

D.2.1 Symmetry-adapted many-particle states

We start from the symmetry-adapted states of the asymmetric dimer and include the spatial inversion with eigenvalue $P \in \{+, -\}$ as additional symmetry.

The symmetry-adapted many-particle states are given in table D.4. All states are eigenstates except for the 2×2 block in the 2-particle channel.

For a non-interacting system, the two states combine into a Slater determinant formed by two bonding orbitals or one with two antibonding orbitals.

$$\begin{aligned}
\frac{1}{\sqrt{2}}\left[\frac{1}{\sqrt{2}}\left(\hat{f}_\uparrow^\dagger \hat{f}_\downarrow^\dagger + \hat{c}_\uparrow^\dagger \hat{c}_\downarrow^\dagger\right) + \frac{1}{\sqrt{2}}\left(\hat{f}_\uparrow^\dagger \hat{c}_\downarrow^\dagger - \hat{f}_\downarrow^\dagger \hat{c}_\uparrow^\dagger\right)\right]|\mathcal{O}\rangle &= \frac{1}{2}\left(\hat{f}_\uparrow^\dagger + \hat{c}_\uparrow^\dagger\right)\left(\hat{f}_\downarrow^\dagger + \hat{c}_\downarrow^\dagger\right)|\mathcal{O}\rangle \\
\frac{1}{\sqrt{2}}\left[\frac{1}{\sqrt{2}}\left(\hat{f}_\uparrow^\dagger \hat{f}_\downarrow^\dagger + \hat{c}_\uparrow^\dagger \hat{c}_\downarrow^\dagger\right) - \frac{1}{\sqrt{2}}\left(\hat{f}_\uparrow^\dagger \hat{c}_\downarrow^\dagger - \hat{f}_\downarrow^\dagger \hat{c}_\uparrow^\dagger\right)\right]|\mathcal{O}\rangle &= \frac{1}{2}\left(\hat{f}_\uparrow^\dagger - \hat{c}_\uparrow^\dagger\right)\left(\hat{f}_\downarrow^\dagger - \hat{c}_\downarrow^\dagger\right)|\mathcal{O}\rangle
\end{aligned} \qquad \text{(D.16)}$$

2-particle channel

The Hamiltonian in the 2×2 sub-block with $N = 2$, $S = 0$, $P = 1$ is

$$\hat{P}_{N=2,S=0,P=1}\hat{H}\hat{P}_{N=2,S=0,P=1} = \begin{pmatrix} \frac{1}{\sqrt{2}}(\hat{f}_\uparrow^\dagger \hat{f}_\downarrow^\dagger + \hat{c}_\uparrow^\dagger \hat{c}_\downarrow^\dagger)|\mathcal{O}\rangle \\ \frac{1}{\sqrt{2}}(\hat{f}_\uparrow^\dagger \hat{c}_\downarrow^\dagger - \hat{f}_\downarrow^\dagger \hat{c}_\uparrow^\dagger)|\mathcal{O}\rangle \end{pmatrix} \begin{pmatrix} 2\bar{\epsilon} + U & -2|t| \\ -2|t| & 2\bar{\epsilon} \end{pmatrix} \begin{pmatrix} \langle\mathcal{O}|\frac{1}{\sqrt{2}}(\hat{f}_\downarrow \hat{f}_\uparrow + \hat{c}_\downarrow \hat{c}_\uparrow) \\ \langle\mathcal{O}|\frac{1}{\sqrt{2}}(\hat{c}_\downarrow \hat{f}_\uparrow - \hat{c}_\uparrow \hat{f}_\downarrow) \end{pmatrix} \tag{D.17}$$

The energy eigenvalues are

$$\begin{aligned} E_\pm &= 2\bar{\epsilon} + \frac{1}{2}U \pm \sqrt{\left(\frac{1}{2}U\right)^2 + 4t^2} \\ &= 2\bar{\epsilon} + 2|t| \left(\frac{U}{4|t|} \pm \sqrt{1 + \left(\frac{U}{4|t|}\right)^2} \right) \\ &= \begin{cases} 2\bar{\epsilon} - \Delta_{st} & \text{for } \pm = - \\ 2\bar{\epsilon} + U + \Delta_{st} & \text{for } \pm = + \end{cases} \end{aligned} \tag{D.18}$$

with the singlet-triplet splitting

$$\Delta_{st} = 2|t| \left(\sqrt{1 + q^2} - q \right) \qquad \text{with } q = \frac{U}{4|t|} \tag{D.19}$$

The eigenstates are

$$\begin{aligned} |\Psi_-\rangle &= \frac{\cos(\gamma)}{\sqrt{2}} \underbrace{(\hat{f}_\uparrow^\dagger \hat{f}_\downarrow^\dagger + \hat{c}_\uparrow^\dagger \hat{c}_\downarrow^\dagger)|\mathcal{O}\rangle}_{\text{double occupancy}} + \frac{\sin(\gamma)}{\sqrt{2}} \underbrace{(\hat{f}_\uparrow^\dagger \hat{c}_\downarrow^\dagger - \hat{f}_\downarrow^\dagger \hat{c}_\uparrow^\dagger)|\mathcal{O}\rangle}_{\text{left-right correlated}} \\ |\Psi_+\rangle &= \frac{\sin(\gamma)}{\sqrt{2}}(\hat{f}_\uparrow^\dagger \hat{f}_\downarrow^\dagger + \hat{c}_\uparrow^\dagger \hat{c}_\downarrow^\dagger)|\mathcal{O}\rangle - \frac{\cos(\gamma)}{\sqrt{2}}(\hat{f}_\uparrow^\dagger \hat{c}_\downarrow^\dagger - \hat{f}_\downarrow^\dagger \hat{c}_\uparrow^\dagger)|\mathcal{O}\rangle \end{aligned} \tag{D.20}$$

The ansatz with cosine and sine of an angle for the eigenstates guarantee that the two states are orthonormal.

The angle is obtained by inserting the Ansatz for $|\Psi_-\rangle$ into the Schrödinger equation.

$$\begin{aligned} 0 &= (2\bar{\epsilon} + U - E_-)\cos(\gamma) - 2|t|\sin(\gamma) \\ \Rightarrow \qquad \tan(\gamma) &= \frac{1}{2|t|}(2\bar{\epsilon} + U - E_-) \\ &= \frac{1}{2|t|}\left(2\bar{\epsilon} + U - 2\bar{\epsilon} - \frac{1}{2}U + \sqrt{(\frac{1}{2}U)^2 + 4t^2}\right) \\ &= \frac{1}{2|t|}\left(\frac{1}{2}U + \sqrt{U^2 + 4t^2}\right) \\ &= \frac{U}{4|t|} + \sqrt{1 + \left(\frac{U}{4|t|}\right)^2} \\ \gamma &= \operatorname{atan}\left(q + \sqrt{1 + q^2}\right) \qquad \text{with } q = \frac{U}{4|t|} \end{aligned} \tag{D.21}$$

2-PARTICLE GROUND STATE OF THE HUBBARD DIMER

The ground state energy of the Hubbard dimer in the two-particle sector

$$|\Psi_-\rangle = \frac{\cos(\gamma)}{\sqrt{2}} \underbrace{(\hat{f}_\uparrow^\dagger \hat{f}_\downarrow^\dagger + \hat{c}_\uparrow^\dagger \hat{c}_\downarrow^\dagger)|\mathcal{O}\rangle}_{\text{double occupancy}} + \frac{\sin(\gamma)}{\sqrt{2}} \underbrace{(\hat{f}_\uparrow^\dagger \hat{c}_\downarrow^\dagger - \hat{f}_\downarrow^\dagger \hat{c}_\uparrow^\dagger)|\mathcal{O}\rangle}_{\text{left-right correlated}} \tag{D.22}$$

and has the energy

$$E_- = 2\bar{\epsilon} - \underbrace{2|t|\left(\sqrt{1+q^2} - q\right)}_{=:\Delta_{st}} = 2\bar{\epsilon} - \Delta_{st} \tag{D.23}$$

with

$$\gamma = \text{atan}\left(q + \sqrt{1+q^2}\right) \qquad \text{and } q \stackrel{\text{def}}{=} \frac{U}{4|t|} \tag{D.24}$$

- In the non-interacting limit, $q = 0$, we obtain $\gamma = \pi/4 = 45°$, for which $\cos(\gamma) = \sin(\gamma) = \frac{1}{\sqrt{2}}$. The single-triplet splitting is $\Delta_{st} = 2|t|$, which corresponds to the energy to transfer one-electron from the bonding to the antibonding orbital. In order to flip the spin of one of the two electrons, it must be lifted into the antibonding state.

- In the strongly interacting limit, $q \to \infty$, we can approximate $\gamma \approx \text{atan}(2q) \to \pi/2 = 90°$. In this limit, we obtain a lower, exactly left-right-correlated state $|\Psi_-\rangle$ with energy $E_- = 2\bar{\epsilon} - \Delta_{st}$ and an upper state $|\Psi_+\rangle$ with double occupancy with energy $E_+ = 2\bar{\epsilon} + U + \Delta_{st}$. The singlet-triplet splitting is

$$\begin{aligned}\Delta_{st} &= 2|t|\Big(\sqrt{1+q^2} - q\Big) = 2|t|q\Big(\sqrt{1+(1/q)^2} - 1\Big) = 2|t|q\Big(1 + \frac{1}{2q^2} + O(q^{-4}) - 1\Big) \\ &= \frac{|t|}{q} + |t|O(q^{-4}\Big) = \frac{4|t|^2}{U} + |t|O\left(\left(\frac{4|t|}{U}\right)^4\right)\end{aligned} \tag{D.25}$$

Table D.5: One-particle excitations of the Hubbard dimer between 0-particle, 1-particle and 2-particle states. Note that the symbol $\hat{c}$ is overloaded and used once as a generic field operator $\hat{c}_\alpha \in \{\hat{c}_\uparrow, \hat{c}_\downarrow, \hat{f}_\uparrow, \hat{f}_\downarrow\}$ and once as the field operator at one of the sites $\hat{c}_\sigma$. The quasi-particle wave function is $|\psi^{\text{Dyson}}_{f,i}\rangle = \sum_\alpha \hat{c}^\dagger_\alpha q_\alpha |\mathcal{O}\rangle$ with $q_\alpha = \langle\Psi_i|\hat{c}_\alpha|\Psi_f\rangle$.

$\|\Psi_i\rangle$	$\|\Psi_f\rangle$	$\hat{c}^\dagger_\alpha$	$\langle\Psi_i\|\hat{c}_\alpha\|\Psi_f\rangle$	$\Delta E - \bar{\epsilon}$
$0 \to 1$ with final $S_z = -\hbar/2$				
$\|\mathcal{O}\rangle$	$\frac{1}{\sqrt{2}}\left(\hat{f}^\dagger_\downarrow + \hat{c}^\dagger_\downarrow\right)\|\mathcal{O}\rangle$	$\hat{f}^\dagger_\downarrow$	$\frac{1}{\sqrt{2}}$	$-\|t\|$
$\|\mathcal{O}\rangle$	$\frac{1}{\sqrt{2}}\left(\hat{f}^\dagger_\downarrow + \hat{c}^\dagger_\downarrow\right)\|\mathcal{O}\rangle$	$\hat{c}^\dagger_\downarrow$	$\frac{1}{\sqrt{2}}$	$-\|t\|$
$\|\mathcal{O}\rangle$	$\frac{1}{\sqrt{2}}\left(\hat{f}^\dagger_\downarrow - \hat{c}^\dagger_\downarrow\right)\|\mathcal{O}\rangle$	$\hat{f}^\dagger_\downarrow$	$\frac{1}{\sqrt{2}}$	$+\|t\|$
$\|\mathcal{O}\rangle$	$\frac{1}{\sqrt{2}}\left(\hat{f}^\dagger_\downarrow - \hat{c}^\dagger_\downarrow\right)\|\mathcal{O}\rangle$	$\hat{c}^\dagger_\downarrow$	$-\frac{1}{\sqrt{2}}$	$+\|t\|$
$1 \to 2$ with initial $S_z = -\hbar/2$				
$\frac{1}{\sqrt{2}}\left(\hat{f}^\dagger_\downarrow + \hat{c}^\dagger_\downarrow\right)\|\mathcal{O}\rangle$	$\hat{f}^\dagger_\downarrow\hat{c}^\dagger_\downarrow\|\mathcal{O}\rangle$	$\hat{f}^\dagger_\downarrow$	$\frac{1}{\sqrt{2}}$	$+\|t\|$
$\frac{1}{\sqrt{2}}\left(\hat{f}^\dagger_\downarrow + \hat{c}^\dagger_\downarrow\right)\|\mathcal{O}\rangle$	$\hat{f}^\dagger_\downarrow\hat{c}^\dagger_\downarrow\|\mathcal{O}\rangle$	$\hat{c}^\dagger_\downarrow$	$-\frac{1}{\sqrt{2}}$	$+\|t\|$
$\frac{1}{\sqrt{2}}\left(\hat{f}^\dagger_\downarrow + \hat{c}^\dagger_\downarrow\right)\|\mathcal{O}\rangle$	$\frac{1}{\sqrt{2}}\left(\hat{f}^\dagger_\uparrow\hat{f}^\dagger_\downarrow - \hat{c}^\dagger_\uparrow\hat{c}^\dagger_\downarrow\right)\|\mathcal{O}\rangle$	$\hat{f}^\dagger_\uparrow$	$\frac{1}{2}$	$+\|t\| + U$
$\frac{1}{\sqrt{2}}\left(\hat{f}^\dagger_\downarrow + \hat{c}^\dagger_\downarrow\right)\|\mathcal{O}\rangle$	$\frac{1}{\sqrt{2}}\left(\hat{f}^\dagger_\uparrow\hat{f}^\dagger_\downarrow - \hat{c}^\dagger_\uparrow\hat{c}^\dagger_\downarrow\right)\|\mathcal{O}\rangle$	$\hat{c}^\dagger_\uparrow$	$-\frac{1}{2}$	$+\|t\| + U$
$\frac{1}{\sqrt{2}}\left(\hat{f}^\dagger_\downarrow + \hat{c}^\dagger_\downarrow\right)\|\mathcal{O}\rangle$	$\frac{\cos(\gamma)}{\sqrt{2}}\left(\hat{f}^\dagger_\uparrow\hat{f}^\dagger_\downarrow + \hat{c}^\dagger_\uparrow\hat{c}^\dagger_\downarrow\right) + \frac{\sin(\gamma)}{\sqrt{2}}\left(\hat{f}^\dagger_\uparrow\hat{c}^\dagger_\downarrow - \hat{f}^\dagger_\downarrow\hat{c}^\dagger_\uparrow\right)\|\mathcal{O}\rangle$	$\hat{f}^\dagger_\uparrow$	$\frac{\cos(\gamma)+\sin(\gamma)}{2}$	$+\|t\| - \Delta_{st}$
$\frac{1}{\sqrt{2}}\left(\hat{f}^\dagger_\downarrow + \hat{c}^\dagger_\downarrow\right)\|\mathcal{O}\rangle$	$\frac{\cos(\gamma)}{\sqrt{2}}\left(\hat{f}^\dagger_\uparrow\hat{f}^\dagger_\downarrow + \hat{c}^\dagger_\uparrow\hat{c}^\dagger_\downarrow\right) + \frac{\sin(\gamma)}{\sqrt{2}}\left(\hat{f}^\dagger_\uparrow\hat{c}^\dagger_\downarrow - \hat{f}^\dagger_\downarrow\hat{c}^\dagger_\uparrow\right)\|\mathcal{O}\rangle$	$\hat{c}^\dagger_\uparrow$	$\frac{\sin(\gamma)+\cos(\gamma)}{2}$	$+\|t\| - \Delta_{st}$
$\frac{1}{\sqrt{2}}\left(\hat{f}^\dagger_\downarrow + \hat{c}^\dagger_\downarrow\right)\|\mathcal{O}\rangle$	$\frac{\sin(\gamma)}{\sqrt{2}}\left(\hat{f}^\dagger_\uparrow\hat{f}^\dagger_\downarrow + \hat{c}^\dagger_\uparrow\hat{c}^\dagger_\downarrow\right) - \frac{\cos(\gamma)}{\sqrt{2}}\left(\hat{f}^\dagger_\uparrow\hat{c}^\dagger_\downarrow - \hat{f}^\dagger_\downarrow\hat{c}^\dagger_\uparrow\right)\|\mathcal{O}\rangle$	$\hat{f}^\dagger_\uparrow$	$\frac{\sin(\gamma)-\cos(\gamma)}{2}$	$+\|t\| + U + \Delta_{st}$
$\frac{1}{\sqrt{2}}\left(\hat{f}^\dagger_\downarrow + \hat{c}^\dagger_\downarrow\right)\|\mathcal{O}\rangle$	$\frac{\sin(\gamma)}{\sqrt{2}}\left(\hat{f}^\dagger_\uparrow\hat{f}^\dagger_\downarrow + \hat{c}^\dagger_\uparrow\hat{c}^\dagger_\downarrow\right) - \frac{\cos(\gamma)}{\sqrt{2}}\left(\hat{f}^\dagger_\uparrow\hat{c}^\dagger_\downarrow - \hat{f}^\dagger_\downarrow\hat{c}^\dagger_\uparrow\right)\|\mathcal{O}\rangle$	$\hat{c}^\dagger_\uparrow$	$\frac{\sin(\gamma)-\cos(\gamma)}{2}$	$+\|t\| + U + \Delta_{st}$
$\frac{1}{\sqrt{2}}\left(\hat{f}^\dagger_\downarrow - \hat{c}^\dagger_\downarrow\right)\|\mathcal{O}\rangle$	$\hat{f}^\dagger_\downarrow\hat{c}^\dagger_\downarrow\|\mathcal{O}\rangle$	$\hat{f}^\dagger_\downarrow$	$-\frac{1}{\sqrt{2}}$	$-\|t\|$
$\frac{1}{\sqrt{2}}\left(\hat{f}^\dagger_\downarrow - \hat{c}^\dagger_\downarrow\right)\|\mathcal{O}\rangle$	$\hat{f}^\dagger_\downarrow\hat{c}^\dagger_\downarrow\|\mathcal{O}\rangle$	$\hat{c}^\dagger_\downarrow$	$-\frac{1}{\sqrt{2}}$	$-\|t\|$
$\frac{1}{\sqrt{2}}\left(\hat{f}^\dagger_\downarrow - \hat{c}^\dagger_\downarrow\right)\|\mathcal{O}\rangle$	$\frac{1}{\sqrt{2}}\left(\hat{f}^\dagger_\uparrow\hat{f}^\dagger_\downarrow - \hat{c}^\dagger_\uparrow\hat{c}^\dagger_\downarrow\right)\|\mathcal{O}\rangle$	$\hat{f}^\dagger_\uparrow$	$\frac{1}{2}$	$-\|t\| + U$
$\frac{1}{\sqrt{2}}\left(\hat{f}^\dagger_\downarrow - \hat{c}^\dagger_\downarrow\right)\|\mathcal{O}\rangle$	$\frac{1}{\sqrt{2}}\left(\hat{f}^\dagger_\uparrow\hat{f}^\dagger_\downarrow - \hat{c}^\dagger_\uparrow\hat{c}^\dagger_\downarrow\right)\|\mathcal{O}\rangle$	$\hat{c}^\dagger_\uparrow$	$\frac{1}{2}$	$-\|t\| + U$
$\frac{1}{\sqrt{2}}\left(\hat{f}^\dagger_\downarrow - \hat{c}^\dagger_\downarrow\right)\|\mathcal{O}\rangle$	$\frac{\cos(\gamma)}{\sqrt{2}}\left(\hat{f}^\dagger_\uparrow\hat{f}^\dagger_\downarrow + \hat{c}^\dagger_\uparrow\hat{c}^\dagger_\downarrow\right) + \frac{\sin(\gamma)}{\sqrt{2}}\left(\hat{f}^\dagger_\uparrow\hat{c}^\dagger_\downarrow - \hat{f}^\dagger_\downarrow\hat{c}^\dagger_\uparrow\right)\|\mathcal{O}\rangle$	$\hat{f}^\dagger_\uparrow$	$\frac{\cos(\gamma)-\sin(\gamma)}{2}$	$-\|t\| - \Delta_{st}$
$\frac{1}{\sqrt{2}}\left(\hat{f}^\dagger_\downarrow - \hat{c}^\dagger_\downarrow\right)\|\mathcal{O}\rangle$	$\frac{\cos(\gamma)}{\sqrt{2}}\left(\hat{f}^\dagger_\uparrow\hat{f}^\dagger_\downarrow + \hat{c}^\dagger_\uparrow\hat{c}^\dagger_\downarrow\right) + \frac{\sin(\gamma)}{\sqrt{2}}\left(\hat{f}^\dagger_\uparrow\hat{c}^\dagger_\downarrow - \hat{f}^\dagger_\downarrow\hat{c}^\dagger_\uparrow\right)\|\mathcal{O}\rangle$	$\hat{c}^\dagger_\uparrow$	$\frac{\sin(\gamma)-\cos(\gamma)}{2}$	$-\|t\| - \Delta_{st}$
$\frac{1}{\sqrt{2}}\left(\hat{f}^\dagger_\downarrow - \hat{c}^\dagger_\downarrow\right)\|\mathcal{O}\rangle$	$\frac{\sin(\gamma)}{\sqrt{2}}\left(\hat{f}^\dagger_\uparrow\hat{f}^\dagger_\downarrow + \hat{c}^\dagger_\uparrow\hat{c}^\dagger_\downarrow\right) - \frac{\cos(\gamma)}{\sqrt{2}}\left(\hat{f}^\dagger_\uparrow\hat{c}^\dagger_\downarrow - \hat{f}^\dagger_\downarrow\hat{c}^\dagger_\uparrow\right)\|\mathcal{O}\rangle$	$\hat{f}^\dagger_\uparrow$	$\frac{\sin(\gamma)+\cos(\gamma)}{2}$	$-\|t\| + U + \Delta_{st}$
$\frac{1}{\sqrt{2}}\left(\hat{f}^\dagger_\downarrow - \hat{c}^\dagger_\downarrow\right)\|\mathcal{O}\rangle$	$\frac{\sin(\gamma)}{\sqrt{2}}\left(\hat{f}^\dagger_\uparrow\hat{f}^\dagger_\downarrow + \hat{c}^\dagger_\uparrow\hat{c}^\dagger_\downarrow\right) - \frac{\cos(\gamma)}{\sqrt{2}}\left(\hat{f}^\dagger_\uparrow\hat{c}^\dagger_\downarrow - \hat{f}^\dagger_\downarrow\hat{c}^\dagger_\uparrow\right)\|\mathcal{O}\rangle$	$\hat{c}^\dagger_\uparrow$	$\frac{\sin(\gamma)+\cos(\gamma)}{2}$	$-\|t\| + U + \Delta_{st}$

D.2.2 Spectral function of the Hubbard dimer

The quasi-particle states and energies are obtained within the Lehman representation.

We use the many-particle energies and states from table D.4 and Eq. D.20 Eq. D.18

The one-particle excitations of the Hubbard dimer are listed in table D.5 and table D.6

Table D.6: One-particle excitations of the Hubbard dimer between 2-particle, 3-particle and 4-particle states. For additional details see caption of table D.5

$\lvert\Psi_i\rangle$	$\lvert\Psi_f\rangle$	$\hat{c}_\alpha^\dagger$	$\langle\Psi_i\lvert\hat{c}_\alpha\rvert\Psi_f\rangle$	$\Delta E - \bar{\epsilon}$
$2 \to 3$ with final $S_z = \hbar/2$				
$\hat{f}_\uparrow^\dagger \hat{c}_\uparrow^\dagger \lvert\mathcal{O}\rangle$	$\hat{f}_\uparrow^\dagger \hat{c}_\uparrow^\dagger \frac{1}{\sqrt{2}}\left(\hat{f}_\downarrow^\dagger + \hat{c}_\downarrow^\dagger\right)\lvert\mathcal{O}\rangle$	$\hat{f}_\uparrow^\dagger$	$\frac{1}{\sqrt{2}}$	$U - \lvert t\rvert$
$\hat{f}_\uparrow^\dagger \hat{c}_\uparrow^\dagger \lvert\mathcal{O}\rangle$	$\hat{f}_\uparrow^\dagger \hat{c}_\uparrow^\dagger \frac{1}{\sqrt{2}}\left(\hat{f}_\downarrow^\dagger + \hat{c}_\downarrow^\dagger\right)\lvert\mathcal{O}\rangle$	$\hat{c}_\uparrow^\dagger$	$\frac{1}{\sqrt{2}}$	$U - \lvert t\rvert$
$\hat{f}_\uparrow^\dagger \hat{c}_\uparrow^\dagger \lvert\mathcal{O}\rangle$	$\hat{f}_\uparrow^\dagger \hat{c}_\uparrow^\dagger \frac{1}{\sqrt{2}}\left(\hat{f}_\downarrow^\dagger - \hat{c}_\downarrow^\dagger\right)\lvert\mathcal{O}\rangle$	$\hat{f}_\uparrow^\dagger$	$\frac{1}{\sqrt{2}}$	$U + \lvert t\rvert$
$\hat{f}_\uparrow^\dagger \hat{c}_\uparrow^\dagger \lvert\mathcal{O}\rangle$	$\hat{f}_\uparrow^\dagger \hat{c}_\uparrow^\dagger \frac{1}{\sqrt{2}}\left(\hat{f}_\downarrow^\dagger - \hat{c}_\downarrow^\dagger\right)\lvert\mathcal{O}\rangle$	$\hat{c}_\uparrow^\dagger$	$-\frac{1}{\sqrt{2}}$	$U + \lvert t\rvert$
$\frac{\cos(\gamma)}{\sqrt{2}}\left(\hat{f}_\uparrow^\dagger \hat{f}_\downarrow^\dagger + \hat{c}_\uparrow^\dagger \hat{c}_\downarrow^\dagger\right) + \frac{\sin(\gamma)}{\sqrt{2}}\left(\hat{f}_\uparrow^\dagger \hat{c}_\downarrow^\dagger - \hat{f}_\downarrow^\dagger \hat{c}_\uparrow^\dagger\right)\lvert\mathcal{O}\rangle$	$\hat{f}_\uparrow^\dagger \hat{c}_\uparrow^\dagger \frac{1}{\sqrt{2}}\left(\hat{f}_\downarrow^\dagger + \hat{c}_\downarrow^\dagger\right)\lvert\mathcal{O}\rangle$	$\hat{f}_\uparrow^\dagger$	$\frac{\cos(\gamma)+\sin(\gamma)}{2}$	$U - \lvert t\rvert + \Delta_{st}$
$\frac{\cos(\gamma)}{\sqrt{2}}\left(\hat{f}_\uparrow^\dagger \hat{f}_\downarrow^\dagger + \hat{c}_\uparrow^\dagger \hat{c}_\downarrow^\dagger\right) + \frac{\sin(\gamma)}{\sqrt{2}}\left(\hat{f}_\uparrow^\dagger \hat{c}_\downarrow^\dagger - \hat{f}_\downarrow^\dagger \hat{c}_\uparrow^\dagger\right)\lvert\mathcal{O}\rangle$	$\hat{f}_\uparrow^\dagger \hat{c}_\uparrow^\dagger \frac{1}{\sqrt{2}}\left(\hat{f}_\downarrow^\dagger + \hat{c}_\downarrow^\dagger\right)\lvert\mathcal{O}\rangle$	$\hat{c}_\uparrow^\dagger$	$\frac{-\cos(\gamma)+\sin(\gamma)}{2}$	$U - \lvert t\rvert + \Delta_{st}$
$\frac{\cos(\gamma)}{\sqrt{2}}\left(\hat{f}_\uparrow^\dagger \hat{f}_\downarrow^\dagger + \hat{c}_\uparrow^\dagger \hat{c}_\downarrow^\dagger\right) + \frac{\sin(\gamma)}{\sqrt{2}}\left(\hat{f}_\uparrow^\dagger \hat{c}_\downarrow^\dagger - \hat{f}_\downarrow^\dagger \hat{c}_\uparrow^\dagger\right)\lvert\mathcal{O}\rangle$	$\hat{f}_\uparrow^\dagger \hat{c}_\uparrow^\dagger \frac{1}{\sqrt{2}}\left(\hat{f}_\downarrow^\dagger - \hat{c}_\downarrow^\dagger\right)\lvert\mathcal{O}\rangle$	$\hat{f}_\uparrow^\dagger$	$\frac{\cos(\gamma)+\sin(\gamma)}{2}$	$U + \lvert t\rvert + \Delta_{st}$
$\frac{\cos(\gamma)}{\sqrt{2}}\left(\hat{f}_\uparrow^\dagger \hat{f}_\downarrow^\dagger + \hat{c}_\uparrow^\dagger \hat{c}_\downarrow^\dagger\right) + \frac{\sin(\gamma)}{\sqrt{2}}\left(\hat{f}_\uparrow^\dagger \hat{c}_\downarrow^\dagger - \hat{f}_\downarrow^\dagger \hat{c}_\uparrow^\dagger\right)\lvert\mathcal{O}\rangle$	$\hat{f}_\uparrow^\dagger \hat{c}_\uparrow^\dagger \frac{1}{\sqrt{2}}\left(\hat{f}_\downarrow^\dagger - \hat{c}_\downarrow^\dagger\right)\lvert\mathcal{O}\rangle$	$\hat{c}_\uparrow^\dagger$	$\frac{-\cos(\gamma)+\sin(\gamma)}{2}$	$U + \lvert t\rvert + \Delta_{st}$
$3 \to 4$ with initial $S_z = \hbar/2$				
$\hat{f}_\uparrow^\dagger \hat{c}_\uparrow^\dagger \frac{1}{\sqrt{2}}\left(\hat{f}_\downarrow^\dagger + \hat{c}_\downarrow^\dagger\right)\lvert\mathcal{O}\rangle$	$\hat{f}_\uparrow^\dagger \hat{f}_\downarrow^\dagger \hat{c}_\uparrow^\dagger \hat{c}_\downarrow^\dagger \lvert\mathcal{O}\rangle$	$\hat{f}_\downarrow^\dagger$	$-\frac{1}{\sqrt{2}}$	$U + \lvert t\rvert$
$\hat{f}_\uparrow^\dagger \hat{c}_\uparrow^\dagger \frac{1}{\sqrt{2}}\left(\hat{f}_\downarrow^\dagger + \hat{c}_\downarrow^\dagger\right)\lvert\mathcal{O}\rangle$	$\hat{f}_\uparrow^\dagger \hat{f}_\downarrow^\dagger \hat{c}_\uparrow^\dagger \hat{c}_\downarrow^\dagger \lvert\mathcal{O}\rangle$	$\hat{c}_\downarrow^\dagger$	$\frac{1}{\sqrt{2}}$	$U + \lvert t\rvert$
$\hat{f}_\uparrow^\dagger \hat{c}_\uparrow^\dagger \frac{1}{\sqrt{2}}\left(\hat{f}_\downarrow^\dagger - \hat{c}_\downarrow^\dagger\right)\lvert\mathcal{O}\rangle$	$\hat{f}_\uparrow^\dagger \hat{f}_\downarrow^\dagger \hat{c}_\uparrow^\dagger \hat{c}_\downarrow^\dagger \lvert\mathcal{O}\rangle$	$\hat{f}_\downarrow^\dagger$	$\frac{1}{\sqrt{2}}$	$U - \lvert t\rvert$
$\hat{f}_\uparrow^\dagger \hat{c}_\uparrow^\dagger \frac{1}{\sqrt{2}}\left(\hat{f}_\downarrow^\dagger - \hat{c}_\downarrow^\dagger\right)\lvert\mathcal{O}\rangle$	$\hat{f}_\uparrow^\dagger \hat{f}_\downarrow^\dagger \hat{c}_\uparrow^\dagger \hat{c}_\downarrow^\dagger \lvert\mathcal{O}\rangle$	$\hat{c}_\downarrow^\dagger$	$\frac{1}{\sqrt{2}}$	$U - \lvert t\rvert$

D.3 Anderson dimer

The Anderson dimer is the dimer version for the Anderson model. The Anderson model describes a single site with strong interaction in contact with a metal. In the Anderson dimer the metal environment is replaced by a single site. Thus, there are two distinct atoms, of which only one has an Coulomb repulsion.

The Andersen dimer has been studied previously by Fulde et al.[143, 144].

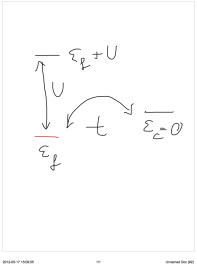
The physics of the Anderson model is discussed in section 17.4.1 on p. 460. This chapter describes the analytical calculations of the Anderson dimer.

This is not finished. It only contains notes after a talk.

This section is inspired by section 12.1 of Fulde's book *"Electron Correlation in Molecules and Solids"*, Springer 1995.

Editor: Check `Figs/Codes/src`

The model for the Kondo effect is a two-site model, where one represents an impurity orbital with strong Coulomb interaction and the second orbital represents the bath.



The Hamiltonian is [4]

$$\begin{aligned}\hat{H} &= \underbrace{\sum_\sigma \epsilon_f \hat{f}_\sigma^\dagger \hat{f}_\sigma + \frac{1}{2}U\sum_{\sigma,\sigma'} \hat{f}_\sigma^\dagger \hat{f}_{\sigma'}^\dagger \hat{f}_{\sigma'}\hat{f}_\sigma}_{\text{Anderson impurity}} + \underbrace{\sum_\sigma \epsilon_c \hat{c}_\sigma^\dagger \hat{c}_\sigma}_{\text{bath}} \underbrace{-|t|\sum_\sigma \left(\hat{f}_\sigma^\dagger \hat{c}_\sigma + \hat{c}_\sigma^\dagger \hat{f}_\sigma\right)}_{\text{hopping}} \\ &= \sum_\sigma \epsilon_f \hat{f}_\sigma^\dagger \hat{f}_\sigma + U\hat{f}_\uparrow^\dagger \hat{f}_\uparrow \hat{f}_\downarrow^\dagger \hat{f}_\downarrow + \underbrace{\frac{1}{2}U\sum_\sigma \hat{f}_\sigma^\dagger \hat{f}_\sigma \left(\hat{f}_\sigma^\dagger \hat{f}_\sigma - 1\right)}_{\text{self-interaction}} + \sum_\sigma \epsilon_c \hat{c}_\sigma^\dagger \hat{c}_\sigma - t\sum_\sigma \left(\hat{f}_\sigma^\dagger \hat{c}_\sigma + \hat{c}_\sigma^\dagger \hat{f}_\sigma\right) \\ &= \sum_\sigma \epsilon_f \hat{n}_{f,\sigma} + U\hat{n}_{f,\uparrow}\hat{n}_{f,\downarrow} + \underbrace{\frac{1}{2}U\sum_\sigma \hat{n}_{f,\sigma}\left(\hat{n}_{f,\sigma} - 1\right)}_{\text{self-interaction}} + \sum_\sigma \epsilon_c \hat{n}_{c,\sigma} - t\sum_\sigma \left(\hat{f}_\sigma^\dagger \hat{c}_\sigma + \hat{c}_\sigma^\dagger \hat{f}_\sigma\right) \quad \text{(D.27)}\end{aligned}$$

The self-interaction term is often ignored, because it contributes nothing when applied to a Slater determinant. Therefore, it is also no more mentioned in the following discussion. Nevertheless, it gives a non-vanishing contribution in the mean-field approximation.

The interesting case is $\epsilon_f < \epsilon_c$ and $\epsilon_f + U > \epsilon_c$ with $N = 2$ particles. We consider all states because the states $N = 1$ and $N = 3$ will be required to evaluate the spectral properties.

---

[4]

$$\begin{aligned}\frac{1}{2}\sum_{\sigma,\sigma'} \hat{f}_\sigma^\dagger \hat{f}_{\sigma'}^\dagger \hat{f}_{\sigma'}\hat{f}_\sigma &= -\frac{1}{2}\sum_{\sigma,\sigma'} \hat{f}_\sigma^\dagger \hat{f}_{\sigma'}^\dagger \hat{f}_\sigma \hat{f}_{\sigma'} = -\frac{1}{2}\sum_{\sigma,\sigma'}\left(\delta_{\sigma,\sigma'}\hat{f}_\sigma^\dagger \hat{f}_{\sigma'} - \hat{f}_\sigma^\dagger \hat{f}_\sigma \hat{f}_{\sigma'}^\dagger \hat{f}_{\sigma'}\right) = \frac{1}{2}\sum_{\sigma,\sigma'} \hat{f}_\sigma^\dagger \hat{f}_\sigma \hat{f}_{\sigma'}^\dagger \hat{f}_{\sigma'} - \frac{1}{2}\sum_\sigma \hat{f}_\sigma^\dagger \hat{f}_\sigma \\ &= \hat{n}_\uparrow \hat{n}_\downarrow + \sum_\sigma\left(\hat{n}_\sigma^2 - \hat{n}_\sigma\right) \quad \text{(D.26)}\end{aligned}$$

D.3.1 Many-particle eigenstates

The symmetry-adapted many-particle states, which I will use as a basisset are provided in table D.1 on p. 529. From the symmetry-adapted wave functions, the eigenstates of the Hamiltonian are constructed. They are listed in table D.3.

Table D.7: Energy eigenstates of the Andersen dimer.

N	S	S_z	eigenstate	energy
$N=0$	$S=0$	$S_z=0$	$\|\mathcal{O}\rangle$	$E=0$
$N=1$	$S=\frac{1}{2}$	$S_z=+\frac{1}{2}$	$\left(\hat{f}_\uparrow^\dagger\cos(\alpha_1)+\hat{c}_\uparrow^\dagger\sin(\alpha_1)\right)\|\mathcal{O}\rangle$	$\frac{\epsilon_c+\epsilon_f}{2}-\sqrt{\left(\frac{\epsilon_c-\epsilon_f}{2}\right)^2+t^2}$
$N=1$	$S=\frac{1}{2}$	$S_z=+\frac{1}{2}$	$\left(\hat{f}_\uparrow^\dagger\sin(\alpha_1)-\hat{c}_\uparrow^\dagger\cos(\alpha_1)\right)\|\mathcal{O}\rangle$	$\frac{\epsilon_c+\epsilon_f}{2}+\sqrt{\left(\frac{\epsilon_c-\epsilon_f}{2}\right)^2+t^2}$
$N=1$	$S=\frac{1}{2}$	$S_z=-\frac{1}{2}$	$\left(\hat{f}_\downarrow^\dagger\cos(\alpha_1)+\hat{c}_\downarrow^\dagger\sin(\alpha_1)\right)\|\mathcal{O}\rangle$	$\frac{\epsilon_c+\epsilon_f}{2}-\sqrt{\left(\frac{\epsilon_c-\epsilon_f}{2}\right)^2+t^2}$
$N=1$	$S=\frac{1}{2}$	$S_z=-\frac{1}{2}$	$\left(\hat{f}_\downarrow^\dagger\sin(\alpha_1)+\hat{c}_\downarrow^\dagger\cos(\alpha_1)\right)\|\mathcal{O}\rangle$	$\frac{\epsilon_c+\epsilon_f}{2}+\sqrt{\left(\frac{\epsilon_c-\epsilon_f}{2}\right)^2+t^2}$
$N=2$	$S=0$	$S_z=0$	$\approx\hat{f}_\uparrow^\dagger\hat{f}_\downarrow^\dagger\|\mathcal{O}\rangle$	$\approx 2\epsilon_f+U+O(t,1/U)$
$N=2$	$S=0$	$S_z=0$	$\approx\hat{c}_\uparrow^\dagger\hat{c}_\downarrow^\dagger\|\mathcal{O}\rangle$	$\approx 2\epsilon_c+O(t,1/U)$
$N=2$	$S=0$	$S_z=0$	$\approx\frac{1}{\sqrt{2}}(\hat{f}_\uparrow^\dagger\hat{c}_\downarrow^\dagger-\hat{f}_\downarrow^\dagger\hat{c}_\uparrow^\dagger)\|\mathcal{O}\rangle$	$\approx\epsilon_f+\epsilon_c+O(t,1/U)$
$N=2$	$S=1$	$S_z=1$	$\hat{f}_\uparrow^\dagger\hat{c}_\uparrow^\dagger\|\mathcal{O}\rangle$	$E=\epsilon_f+\epsilon_c$
$N=2$	$S=1$	$S_z=0$	$\frac{1}{\sqrt{2}}(\hat{f}_\uparrow^\dagger\hat{c}_\downarrow^\dagger+\hat{f}_\downarrow^\dagger\hat{c}_\uparrow^\dagger)\|\mathcal{O}\rangle$	$E=\epsilon_f+\epsilon_c$
$N=2$	$S=1$	$S_z=-1$	$\hat{f}_\downarrow^\dagger\hat{c}_\downarrow^\dagger\|\mathcal{O}\rangle$	$E=\epsilon_f+\epsilon_c$
$N=3$	$S=\frac{1}{2}$	$S_z=+\frac{1}{2}$	$\hat{f}_\uparrow^\dagger\hat{c}_\uparrow^\dagger\left(\hat{f}_\downarrow^\dagger\cos(\alpha_2)+\hat{c}_\downarrow^\dagger\sin(\alpha_2)\right)\|\mathcal{O}\rangle$	$\frac{3\epsilon_c+3\epsilon_f+U}{2}-\sqrt{\left(\frac{\epsilon_f+U-\epsilon_c}{2}\right)^2+t^2}$
$N=3$	$S=\frac{1}{2}$	$S_z=+\frac{1}{2}$	$\hat{f}_\uparrow^\dagger\hat{c}_\uparrow^\dagger\left(\hat{f}_\downarrow^\dagger\sin(\alpha_2)-\hat{c}_\downarrow^\dagger\cos(\alpha_2)\right)\|\mathcal{O}\rangle$	$\frac{3\epsilon_c+3\epsilon_f+U}{2}+\sqrt{\left(\frac{\epsilon_f+U-\epsilon_c}{2}\right)^2+t^2}$
$N=3$	$S=\frac{1}{2}$	$S_z=-\frac{1}{2}$	$\hat{f}_\downarrow^\dagger\hat{c}_\downarrow^\dagger\left(\hat{f}_\uparrow^\dagger\cos(\alpha_2)+\hat{c}_\uparrow^\dagger\sin(\alpha_2)\right)\|\mathcal{O}\rangle$	$\frac{3\epsilon_c+3\epsilon_f+U}{2}-\sqrt{\left(\frac{\epsilon_f+U-\epsilon_c}{2}\right)^2+t^2}$
$N=3$	$S=\frac{1}{2}$	$S_z=-\frac{1}{2}$	$\hat{f}_\downarrow^\dagger\hat{c}_\downarrow^\dagger\left(\hat{f}_\uparrow^\dagger\sin(\alpha_2)-\hat{c}_\uparrow^\dagger\cos(\alpha_2)\right)\|\mathcal{O}\rangle$	$\frac{3\epsilon_c+3\epsilon_f+U}{2}+\sqrt{\left(\frac{\epsilon_f+U-\epsilon_c}{2}\right)^2+t^2}$
$N=4$	$S=0$	$S_z=0$	$\hat{f}_\uparrow^\dagger\hat{f}_\downarrow^\dagger\hat{c}_\uparrow^\dagger\hat{c}_\downarrow^\dagger\|\mathcal{O}\rangle$	$E=2\epsilon_c+2\epsilon_f+U$

The singlet states in the two-particle sector require special attention. From Eq. D.14 on p. 532, we obtain

$$\hat{P}_{2,0}\hat{H}\hat{P}_{2,0}=\begin{pmatrix}\hat{f}_\uparrow^\dagger\hat{f}_\downarrow^\dagger|\mathcal{O}\rangle\\ \hat{c}_\uparrow^\dagger\hat{c}_\downarrow^\dagger|\mathcal{O}\rangle\\ \frac{1}{\sqrt{2}}(\hat{f}_\uparrow^\dagger\hat{c}_\downarrow^\dagger-\hat{f}_\downarrow^\dagger\hat{c}_\uparrow^\dagger)|\mathcal{O}\rangle\end{pmatrix}\begin{pmatrix}2\epsilon_f+U_f & 0 & -\sqrt{2}|t|\\ 0 & 2\epsilon_c & -\sqrt{2}|t|\\ -\sqrt{2}|t| & -\sqrt{2}|t| & \epsilon_c+\epsilon_f\end{pmatrix}\begin{pmatrix}\langle\mathcal{O}|\hat{f}_\downarrow\hat{f}_\uparrow\\ \langle\mathcal{O}|\hat{c}_\downarrow\hat{c}_\uparrow\\ \langle\mathcal{O}|\frac{1}{\sqrt{2}}(\hat{c}_\downarrow\hat{f}_\uparrow-\hat{c}_\uparrow\hat{f}_\downarrow)\end{pmatrix} \tag{D.28}$$

Of interest is the case where $\epsilon_f<\epsilon_c<\epsilon_f+U$, which is the case with one electron on the impurity. In that case the ground state has one electron in the impurity and a spin-paired state in the bath-site. The spin coupling is determined by the singlet-triplet splitting. The singlet-triplet splitting defines the **Kondo temperature**.

In the limit of large U and small t, the Hamiltonian is diagonal and we obtain (1) a state with two electrons in the bath site, and another one (2), with energy $\epsilon_c+\epsilon_f$, which is equally distributed

over the bath and the impurity. The third state lies at high energies and has two electrons on the impurity.

We can diagonalize the Hamiltonian approximately using **down-folding** as described in chapter 5.1 and specifically in Eq. 5.23 on p. 193.

In order to obtain an accurate description in the limit of large interaction, we down-fold the wave function with a doubly occupied impurity. The self energy due to the down-folded orbital is[5]

$$\mathbf{\Sigma}(E) \overset{\text{Eq. 5.12}}{=} \frac{2|t|^2}{E-2\epsilon_f-U_f}\begin{pmatrix}0&0\\0&1\end{pmatrix} \tag{D.29}$$

The self energy is added to the subblock of the two other orbitals

$$\begin{aligned}
\boldsymbol{M}(E) &= \begin{pmatrix} 2\epsilon_c - E & -t\sqrt{2} \\ -t\sqrt{2} & \epsilon_c+\epsilon_f+\frac{2|t|^2}{E-2\epsilon_f-U} - E \end{pmatrix} \\
&= \begin{pmatrix} 2\epsilon_c - E_\nu & -t\sqrt{2} \\ -t\sqrt{2} & \epsilon_c+\epsilon_f-\frac{2t^2}{2\epsilon_f+U-E_\nu} - E_\nu \end{pmatrix} - \begin{pmatrix} 1 & 0 \\ 0 & 1+\frac{2t^2}{(2\epsilon_f+U-E_\nu)^2} \end{pmatrix}(E-E_\nu) + O\left((E-E_\nu)^2\right) \\
&= \underbrace{\begin{pmatrix} 2\epsilon_c & -t\sqrt{2} \\ -t\sqrt{2} & \epsilon_c+\epsilon_f-\frac{2t^2}{2\epsilon_f+U-E_\nu}+\frac{2t^2E_\nu}{(2\epsilon_f+U-E_\nu)^2} \end{pmatrix}}_{\tilde{H}(E_\nu)} - \underbrace{\begin{pmatrix} 1 & 0 \\ 0 & 1+\frac{2t^2}{(2\epsilon_f+U-E_\nu)^2} \end{pmatrix}}_{\tilde{O}(E_\nu)} E + O\left((E-E_\nu)^2\right)
\end{aligned} \tag{D.30}$$

We can orthonormalize the states and obtain a new Hamiltonian

$$\begin{aligned}
\tilde{\boldsymbol{O}}^{-\frac{1}{2}}\tilde{\boldsymbol{H}}\tilde{\boldsymbol{O}}^{-\frac{1}{2}} &= \begin{pmatrix} 2\epsilon_c & -t\sqrt{2} \\ -t\sqrt{2} & \bar{E} \end{pmatrix} \\
\text{with}\quad \bar{E} &= \left(\epsilon_c+\epsilon_f-\frac{2t^2}{2\epsilon_f+U-E_\nu}+\frac{2t^2E_\nu}{(2\epsilon_f+U-E_\nu)^2}\right)\left(1+\frac{2t^2}{(2\epsilon_f+U-E_\nu)^2}\right)^{-1}
\end{aligned} \tag{D.31}$$

This yields the energies

$$E_\pm = \frac{2\epsilon_c+\bar{E}}{2} \pm \sqrt{\left(\frac{2\epsilon_c-\bar{E}}{2}\right)^2+2t^2} \tag{D.32}$$

For the state near $\epsilon_f+\epsilon_c$, one chooses $E_\nu = \epsilon_f+\epsilon_c$.

$$\begin{aligned}
\bar{E} &= \left(\epsilon_c+\epsilon_f-\frac{2t^2}{\epsilon_f+U-\epsilon_c}+\frac{2t^2(\epsilon_c+\epsilon_f)}{(\epsilon_f+U-\epsilon_c)^2}\right)\left(1+\frac{2t^2}{(\epsilon_f+U-\epsilon_c)^2}\right)^{-1} \\
&= \left(\epsilon_c+\epsilon_f-\frac{2t^2}{\epsilon_f+U-\epsilon_c}+\frac{4t^4}{(\epsilon_f+U-\epsilon_c)^3}\right)+O\left(\left(\frac{2t^2}{(\epsilon_f+U-\epsilon_c)^2}\right)^2\right)
\end{aligned} \tag{D.33}$$

In the limit of large U, we obtain a bonding and an antibonding state. For the bonding state the energy is below $\epsilon_c+\min(\epsilon_f,\epsilon_c)$ for the antibonding state it is at $\epsilon_c+\max(\epsilon_f,\epsilon_c)$

For large U, there lowest state with $N=2$ is a singlet state, for which one electron is in the non-interacting orbital, and the other is delocalized over both sites. This state is lower than the triplet state, irrespective of $\epsilon_f-\epsilon_c$.

We see that the singlet two-particle state lies below the triplet state, because only the singlet state can hybridize with higher lying states, when t is switched on. A simplification the infinite-U limit, in which case we may exclude any states with two electrons on the impurity. The stabilization is mainly due to the delocalization of the electron in one spin direction between impurity and bath. The Coulomb repulsion is a secondary effect.

[5] We use the symbol E for the many-particle energies, rather than the symbol ϵ which is used for one-particle energies.

D.3.2 Spectrum

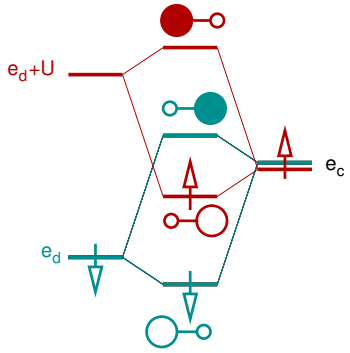


Fig. D.1: Schematic diagrams of the spectral function of the Kondo dimer. Scheme of the one-particle orbitals of the Kondo singlet. It represents only one of the two Slater determinants contributing to the two-particle ground state.

When we investigate the spectra for adding and removing electrons, we can use Lehman representation. Let me use the ground singlet ground state

$$|\Phi_s\rangle = \left[\hat{f}^\dagger_\uparrow \hat{f}^\dagger_\downarrow A + \hat{c}^\dagger_\uparrow \hat{c}^\dagger_\downarrow B + \frac{1}{\sqrt{2}}\left(\hat{f}^\dagger_\uparrow \hat{c}^\dagger_\downarrow - \hat{f}^\dagger_\downarrow \hat{c}^\dagger_\uparrow\right) C\right]|\mathcal{O}\rangle \tag{D.34}$$

with energy E_s.

For $\epsilon_c = 0$, $\epsilon_f = -1$, $U = 2$, $t = \frac{1}{2}$, I obtain (without full diagonalization of the $N = 2, S = 0$ channel)

ϵ	ψ_{qp}	
-1.048	$\|f,\sigma\rangle 0.68 + \|c,\sigma\rangle 0.06$	$f^1 \to f^0$
-0.029	$\|f,\sigma\rangle 0.20 + \|c,\sigma\rangle 0.70$	$f^1 \to f^0$
+0.029	$\|f,\sigma\rangle 0.20 - \|c,\sigma\rangle 0.70$	$f^0 \to f^1$
+1.048	$\|f,\sigma\rangle 0.68 - \|c,\sigma\rangle 0.06$	$f^0 \to f^1$

$$\begin{aligned}
\hat{f}^\dagger_\uparrow|\Psi_s\rangle &= \left[\hat{f}^\dagger_\uparrow \hat{c}^\dagger_\uparrow \hat{c}^\dagger_\downarrow b - \frac{1}{\sqrt{2}}\hat{f}^\dagger_\uparrow \hat{f}^\dagger_\downarrow \hat{c}^\dagger_\uparrow c\right]|\mathcal{O}\rangle \\
\hat{f}^\dagger_\downarrow|\Psi_s\rangle &= \left[\hat{f}^\dagger_\downarrow \hat{c}^\dagger_\uparrow \hat{c}^\dagger_\downarrow b - \frac{1}{\sqrt{2}}\hat{f}^\dagger_\uparrow \hat{f}^\dagger_\downarrow \hat{c}^\dagger_\downarrow c\right]|\mathcal{O}\rangle \\
\hat{c}^\dagger_\uparrow|\Phi_s\rangle &= \left[\hat{f}^\dagger_\uparrow \hat{f}^\dagger_\downarrow \hat{c}^\dagger_\uparrow a - \hat{f}^\dagger_\uparrow \hat{c}^\dagger_\uparrow \hat{c}^\dagger_\downarrow \frac{c}{\sqrt{2}}\right]|\mathcal{O}\rangle \\
\hat{c}^\dagger_\downarrow|\Psi_s\rangle &= \left[\hat{f}^\dagger_\uparrow \hat{f}^\dagger_\downarrow \hat{c}^\dagger_\uparrow a - \hat{f}^\dagger_\downarrow \hat{c}^\dagger_\uparrow \hat{c}^\dagger_\uparrow \frac{c}{\sqrt{2}}\right]|\mathcal{O}\rangle
\end{aligned} \tag{D.35}$$

Increasing the temperature reduces the singlet occupation which results in larger resistance.

Kondo Resonance=Abrikosov-Suhl resonance.

D.3.3 Andersen dimer and the Hartree-Fock method

In this section I want to explore how well the broken symmetry states obtained with a single Slater determinant are able to capture the Kondo physics. This is of relevance to understand the limitations

of conventional density-functional calculations. The Anderson dimer is a system where exact and Hartree-Fock calculations should be, firstly, feasible and, secondly, intelligible.

The following is an attempt to describe the two-particle state in terms of two Slater determinants. The singlet state is $|\Psi_s\rangle$ and the triplet state is $|\Psi_t\rangle$. In the singlet state, we can use the bonding state with the filled majority-spin f-orbital and the bonding state with the empty minority-spin f orbital. In contrast, the triplet state has to use bonding and antibonding states with the majority spin orbital. This is the origin of the singlet-triplet splitting.

$$\begin{aligned}
|\Psi_s\rangle &= \frac{1}{2}\Big[\Big(\hat{f}^\dagger_\uparrow\cos(\alpha)+\hat{c}^\dagger_\uparrow\sin(\alpha)\Big)\Big(\hat{f}^\dagger_\downarrow\sin(\beta)+\hat{c}^\dagger_\downarrow\cos(\beta)\Big)+\Big(\hat{f}^\dagger_\uparrow\sin(\beta)+\hat{c}^\dagger_\uparrow\cos(\beta)\Big)\Big(\hat{f}^\dagger_\downarrow\cos(\alpha)+\hat{c}^\dagger_\downarrow\sin(\alpha)\Big)\Big]|\mathcal{O}\rangle \\
&= \Big[\hat{f}^\dagger_\uparrow\hat{f}^\dagger_\downarrow\cos(\alpha)\sin(\beta)+\hat{c}^\dagger_\uparrow\hat{c}^\dagger_\downarrow\sin(\alpha)\cos(\beta) \\
&\quad +\hat{f}^\dagger_\uparrow\hat{c}^\dagger_\downarrow\frac{\cos(\alpha)\cos(\beta)+\sin(\alpha)\sin(\beta)}{2}+\hat{c}^\dagger_\uparrow\hat{f}^\dagger_\downarrow\frac{\sin(\alpha)\sin(\beta)+\cos(\alpha)\cos(\beta)}{2}\Big]|\mathcal{O}\rangle \\
&= \Big[\hat{f}^\dagger_\uparrow\hat{f}^\dagger_\downarrow\cos(\alpha)\sin(\beta)+\hat{c}^\dagger_\uparrow\hat{c}^\dagger_\downarrow\sin(\alpha)\cos(\beta)+\Big(\hat{f}^\dagger_\uparrow\hat{c}^\dagger_\downarrow-\hat{f}^\dagger_\downarrow\hat{c}^\dagger_\uparrow\Big)\frac{\cos(\alpha)\cos(\beta)+\sin(\alpha)\sin(\beta)}{2}\Big]|\mathcal{O}\rangle \\
|\Psi_t\rangle &= \Big(\hat{f}^\dagger_\uparrow\cos(\alpha)+\hat{c}^\dagger_\uparrow\sin(\alpha)\Big)\Big(\hat{f}^\dagger_\uparrow\sin(\alpha)-\hat{c}^\dagger_\uparrow\cos(\alpha)\Big)|\mathcal{O}\rangle \\
&= \Big[-\hat{f}^\dagger_\uparrow\hat{c}^\dagger_\uparrow\cos^2(\alpha)+\hat{c}^\dagger_\uparrow\hat{f}^\dagger_\uparrow\sin^2(\alpha)\Big]|\mathcal{O}\rangle \\
&= -\hat{f}^\dagger_\uparrow\hat{c}^\dagger_\uparrow|\mathcal{O}\rangle
\end{aligned} \tag{D.36}$$

Without coupling to the environment, one obtains the solution with $\alpha=\beta=0$. We find, that all the three Slater determinants contributing to the $S=0, N=2$ ground state contribute with independent parameters. (The three coefficients are constrained by the norm to two parameters, which can be expressed in terms of α and β.) This tells us that the Ansatz given above is able to capture the ground state wave function.

Broken-symmetry Slater determinants

Here, I want to explore the limits of the Hartree-Fock method.[6] I consider two broken-symmetry Slater-determinants, which are related by a global spin inversion. The two Slater determinants have $S_z=0$, so that we may recover singlet and triplet state, when both Slater determinants are superimposed. We use two one-particle orbitals that are polarized individually along the dimer axis.

$$\begin{aligned}
|\Phi_1\rangle &= \Big(\hat{f}^\dagger_\uparrow\cos(\alpha)+\hat{c}^\dagger_\uparrow\sin(\alpha)\Big)\Big(\hat{f}^\dagger_\downarrow\sin(\beta)+\hat{c}^\dagger_\downarrow\cos(\beta)\Big)|\mathcal{O}\rangle \\
|\Phi_2\rangle &= \Big(\hat{f}^\dagger_\uparrow\sin(\beta)+\hat{c}^\dagger_\uparrow\cos(\beta)\Big)\Big(\hat{f}^\dagger_\downarrow\cos(\alpha)+\hat{c}^\dagger_\downarrow\sin(\alpha)\Big)|\mathcal{O}\rangle
\end{aligned} \tag{D.37}$$

Now we work out Hamilton and overlap matrices in this two-dimensional sub-space $\{|\Phi_1(\alpha,\beta)\rangle, |\Phi_2(\alpha,\beta)\rangle\}$ of the Fock space. The one-particle orbitals of the two states can be varied in a two-dimensional space.

Overlap matrix elements of the broken-symmetry Slater determinants: The wave functions $|\Phi_1\rangle$, $|\Phi_2\rangle$ are, per construction, normalized, i.e.

$$\langle\Phi_j|\Phi_j\rangle = 1 \qquad \text{for } j\in\{1,2\} \tag{D.38}$$

The overlap is obtained as follows

$$\begin{aligned}
\langle\Phi_1|\Phi_2\rangle &= \cos^2(\alpha)\sin^2(\beta)+2\cos(\alpha)\sin(\alpha)\cos(\beta)\sin(\beta)+\sin^2(\alpha)\cos^2(\beta) \\
&= \Big(\cos(\alpha)\sin(\beta)+\sin(\alpha)\cos(\beta)\Big)^2 \\
&= \sin^2(\alpha+\beta)
\end{aligned} \tag{D.39}$$

[6] A similar analysis has been performed by Kamil et al.[168] for the symmetric dimer.

Note, that orthonormality between the two Slater determinants is not required.

Hamilton matrix elements of the Slater determinants:

$$
\begin{aligned}
\hat{H}|\Phi_1\rangle &= \hat{H}\Big[\hat{f}_\uparrow^\dagger \hat{f}_\downarrow^\dagger \cos(\alpha)\sin(\beta) + \hat{f}_\uparrow^\dagger \hat{c}_\downarrow^\dagger \cos(\alpha)\cos(\beta) + \hat{c}_\uparrow^\dagger \hat{f}_\downarrow^\dagger \sin(\alpha)\sin(\beta) + \hat{c}_\uparrow^\dagger \hat{c}_\downarrow^\dagger \sin(\alpha)\cos(\beta)\Big]\mathcal{O}\rangle \\
&= \Bigg[\Big((2\epsilon_f + U)\hat{f}_\uparrow^\dagger \hat{f}_\downarrow^\dagger - 2t\Big(\hat{c}_\uparrow^\dagger \hat{f}_\downarrow^\dagger + \hat{f}_\uparrow^\dagger \hat{c}_\downarrow^\dagger\Big)\Big)\cos(\alpha)\sin(\beta) \\
&\quad + \Big((\epsilon_f + \epsilon_c)\hat{f}_\uparrow^\dagger \hat{c}_\downarrow^\dagger - 2t\Big(\hat{f}_\uparrow^\dagger \hat{f}_\downarrow^\dagger + \hat{c}_\uparrow^\dagger \hat{c}_\downarrow^\dagger\Big)\Big)\cos(\alpha)\cos(\beta) \\
&\quad + \Big((\epsilon_f + \epsilon_c)\hat{c}_\uparrow^\dagger \hat{f}_\downarrow^\dagger - 2t\Big(\hat{f}_\uparrow^\dagger \hat{f}_\downarrow^\dagger + \hat{c}_\uparrow^\dagger \hat{c}_\downarrow^\dagger\Big)\Big)\sin(\alpha)\sin(\beta) \\
&\quad + \Big(2\epsilon_c \hat{c}_\uparrow^\dagger \hat{c}_\downarrow^\dagger - 2t\Big(\hat{f}_\uparrow^\dagger \hat{c}_\downarrow^\dagger + \hat{c}_\uparrow^\dagger \hat{f}_\downarrow^\dagger\Big)\Big)\sin(\alpha)\cos(\beta)\Bigg]|\mathcal{O}\rangle \\
&= \Bigg[\hat{f}_\uparrow^\dagger \hat{f}_\downarrow^\dagger \Big((2\epsilon_f + U)\cos(\alpha)\sin(\beta) - 2t\Big(\cos(\alpha)\cos(\beta) + \sin(\alpha)\sin(\beta)\Big)\Big) \\
&\quad + \hat{f}_\uparrow^\dagger \hat{c}_\downarrow^\dagger \Big((\epsilon_f + \epsilon_c)\cos(\alpha)\cos(\beta) - 2t\Big(\cos(\alpha)\sin(\beta) + \sin(\alpha)\cos(\beta)\Big)\Big) \\
&\quad + \hat{c}_\uparrow^\dagger \hat{f}_\downarrow^\dagger \Big((\epsilon_f + \epsilon_c)\sin(\alpha)\sin(\beta) - 2t\Big(\cos(\alpha)\sin(\beta) + \sin(\alpha)\cos(\beta)\Big)\Big) \\
&\quad + \hat{c}_\uparrow^\dagger \hat{c}_\downarrow^\dagger \Big(2\epsilon_c \sin(\alpha)\cos(\beta) - 2t\Big(\cos(\alpha)\cos(\beta) + \sin(\alpha)\sin(\beta)\Big)\Big)\Bigg]|\mathcal{O}\rangle
\end{aligned}
\tag{D.40}
$$

$$
\begin{aligned}
\langle\Phi_1|\hat{H}|\Phi_1\rangle = &\Big[\cos(\alpha)\sin(\beta)\Big((2\epsilon_f+U)\cos(\alpha)\sin(\beta)-2t\Big(\cos(\alpha)\cos(\beta)+\sin(\alpha)\sin(\beta)\Big)\Big)\\
&+\cos(\alpha)\cos(\beta)\Big((\epsilon_f+\epsilon_c)\cos(\alpha)\cos(\beta)-2t\Big(\cos(\alpha)\sin(\beta)+\sin(\alpha)\cos(\beta)\Big)\Big)\\
&+\sin(\alpha)\sin)\beta)\Big((\epsilon_f+\epsilon_c)\sin(\alpha)\sin(\beta)-2t\Big(\cos(\alpha)\sin(\beta)+\sin(\alpha)\cos(\beta)\Big)\Big)\\
&+\sin(\alpha)\cos(\beta)\Big(2\epsilon_c\sin(\alpha)\cos(\beta)-2t\Big(\cos(\alpha)\cos(\beta)+\sin(\alpha)\sin(\beta)\Big)\Big)\Big]\\
=&\cos^2(\alpha)\sin^2(\beta)\Big(2\epsilon_f+U\Big)+\sin^2(\alpha)\cos^2(\beta)2\epsilon_c\\
&+(\epsilon_f+\epsilon_c)\Big(\cos^2(\alpha)\sin^2(\beta)+\sin^2(\alpha)\cos^2(\beta)\Big)\\
&-2t\underbrace{\Big(2\cos(\beta)\sin(\beta)+2\cos(\alpha)\sin(\alpha)\Big)}_{2\cos^2(\alpha)\cos(\beta)\sin(\beta)+2\cos(\alpha)\sin(\alpha)\sin^2(\beta)+2\cos(\alpha)\sin(\alpha)\cos^2(\beta)+2\sin^2(\alpha)\cos(\beta)\sin(\beta)}\\
=&\cos^2(\alpha)\sin^2(\beta)\Big(\epsilon_f+U-\epsilon_c\Big)+\sin^2(\alpha)\cos^2(\beta)\Big(\epsilon_c-\epsilon_f\Big)\\
&+(\epsilon_f+\epsilon_c)\underbrace{\Big((\cos^2(\alpha)+\sin^2(\alpha))(\cos^2(\beta)+\sin^2(\beta))\Big)}_{=1}\\
&-2t\Big(2\cos(\beta)\sin(\beta)+2\cos(\alpha)\sin(\alpha)\Big)\\
=&(\epsilon_f+\epsilon_c)+\overbrace{\frac{1}{2}\Big(\cos(2\beta)-\cos(2\alpha)\Big)}^{\sin^2(\alpha)\cos^2(\beta)-\cos^2(\alpha)\sin^2(\beta)}\Big(\epsilon_c-\epsilon_f\Big)+\cos^2(\alpha)\sin^2(\beta)U\\
&-2t\Big(\sin(2\alpha)+\sin(2\beta)\Big)
\end{aligned}
\tag{D.41}
$$

$$
\begin{aligned}
\cos^2(x)\sin^2(y)+\sin^2(x)\cos^2(y)&=\frac{1}{4}\Big(2-\cos(2(x+y))-2\cos(2(x-y))\Big)\\
2\sin(x)\cos(x)&=\sin(2x)
\end{aligned}
\tag{D.42}
$$

$$
\begin{aligned}
\langle\Phi_2|\hat{H}|\Phi_1\rangle = \Bigg[&\cos(\alpha)\sin(\beta)\Big((2\epsilon_f+U)\cos(\alpha)\sin(\beta)-2t\Big(\cos(\alpha)\cos(\beta)+\sin(\alpha)\sin(\beta)\Big)\Big)\\
&+\sin(\alpha)\sin(\beta)\Big((\epsilon_f+\epsilon_c)\cos(\alpha)\cos(\beta)-2t\Big(\cos(\alpha)\sin(\beta)+\sin(\alpha)\cos(\beta)\Big)\Big)\\
&+\cos(\alpha)\cos(\beta)\Big((\epsilon_f+\epsilon_c)\sin(\alpha)\sin(\beta)-2t\Big(\cos(\alpha)\sin(\beta)+\sin(\alpha)\cos(\beta)\Big)\Big)\\
&+\sin(\alpha)\cos(\beta)\Big(2\epsilon_c\sin(\alpha)\cos(\beta)-2t\Big(\cos(\alpha)\cos(\beta)+\sin(\alpha)\sin(\beta)\Big)\Big)\Bigg]\\
=\Big((&2\epsilon_f+U)\cos^2(\alpha)\sin^2(\beta)+2(\epsilon_f+\epsilon_c)\cos(\alpha)\sin(\alpha)\cos(\beta)\sin(\beta)\\
&+2\epsilon_c\sin^2(\alpha)\cos^2(\beta)\\
&-2t\Big(\sin(2\beta)+\sin(2\alpha)\Big)
\end{aligned}
\tag{D.43}
$$

Minimum for the broken-symmetry Slater determinants

$$
\begin{aligned}
\langle\Phi_j|\hat{H}|\Phi_j\rangle &= (\epsilon_f+\epsilon_c)+\frac{1}{2}\Big(\cos(2\beta)-\cos(2\alpha)\Big)\Big(\epsilon_c-\epsilon_f\Big)+\cos^2(\alpha)\sin^2(\beta)U\\
&\quad -2t\Big(\sin(2\alpha)+\sin(2\beta)\Big)\\
\frac{\partial\langle\Phi_j|\hat{H}|\Phi_j\rangle}{\partial\alpha} &= +\sin(2\alpha)\Big(\epsilon_c-\epsilon_f\Big)-\overbrace{\sin(2\alpha)}^{2\cos(\alpha)\sin(\alpha)}\overbrace{\Big(\frac{1}{2}-\frac{1}{2}\cos(2\beta)\Big)}^{\sin^2(\beta)}U-4t\cos(2\alpha)\\
&= +\sin(2\alpha)\Big(\epsilon_c-\epsilon_f-\Big[\frac{1}{2}-\frac{1}{2}\cos(2\beta)\Big]U\Big)-4t\cos(2\alpha)\stackrel{!}{=}0\\
4t\cot(2\alpha) &= \Big(\epsilon_c-\epsilon_f-\Big[\frac{1}{2}-\frac{1}{2}\cos(2\beta)\Big]U\Big)\\
\frac{\partial\langle\Phi_j|\hat{H}|\Phi_j\rangle}{\partial\beta} &= -\sin(2\beta)\Big(\epsilon_c-\epsilon_f\Big)+\overbrace{\Big(\frac{1}{2}+\frac{1}{2}\cos(2\alpha)\Big)}^{\cos^2(\alpha)}\overbrace{\sin(2\beta)}^{2\sin(\beta)\cos(\beta)}U-4t\cos(2\beta)\\
&= -\sin(2\beta)\Big(\epsilon_c-\epsilon_f-\Big[\frac{1}{2}+\frac{1}{2}\cos(2\alpha)\Big]U\Big)-4t\cos(2\beta)\stackrel{!}{=}0\\
4t\cot(2\beta) &= -\Big(\epsilon_c-\epsilon_f-\Big[\frac{1}{2}+\frac{1}{2}\cos(2\alpha)\Big]U\Big)
\end{aligned}
\tag{D.44}
$$

Δ/t	U/t	α/π	β/π
0	0	1/4	1/4
0	∞	$\frac{1}{4}$	0
0	∞	$\frac{1}{2}$	0
0	∞	$\frac{1}{2}$	$\frac{1}{4}$
0	0	$\frac{1}{2}-\frac{1}{4}$	$\frac{1}{4}$
4	0	$\frac{1}{2}-\frac{1}{8}$	$\frac{1}{8}$
9	0	$\frac{1}{2}-\frac{1}{15}$	$\frac{1}{15}$
25	0	$\frac{1}{2}-\frac{1}{40}$	$\frac{1}{40}$
100	0	$(8/100)^2$	$\frac{1}{2}-\left(\frac{8}{100}\right)^2$
∞	0	$\frac{1}{2}$	0
10	100	$\frac{1}{2}-\frac{1}{20}$	$\frac{1}{20}$

Symmetric solution: There is one series of solutions with $\alpha+\beta=\frac{\pi}{2}$. With $\beta=\frac{\pi}{2}-\alpha$ the two Slater determinants $|\Phi_1\rangle$ and $|\Phi_2\rangle$ are identical and equal to

$$|\Phi_1\rangle = |\Phi_2\rangle = \Big(\hat{f}_\uparrow^\dagger \cos(\alpha) + \hat{c}_\uparrow^\dagger \sin(\alpha)\Big)\Big(\hat{f}_\downarrow^\dagger \cos(\alpha) + \hat{c}_\downarrow^\dagger \sin(\alpha)\Big)|\mathcal{O}\rangle \tag{D.45}$$

For this series of solutions both one-particle orbitals polarize in one direction to account for the asymmetry of the two sites. The strength of the polarization is described by $\gamma = \alpha - \frac{\pi}{4}$

$$\begin{aligned}
4t\cot(2\alpha) &= \left(\epsilon_c - \epsilon_f - \left[\frac{1}{2} - \frac{1}{2}\cos(\pi - 2\alpha)\right] U\right) \\
&= \left(\epsilon_c - \epsilon_f - \left[\frac{1}{2} + \frac{1}{2}\cos(2\alpha)\right] U\right) \\
4t\frac{\cos(\frac{\pi}{2} + 2\gamma)}{\sin(\frac{\pi}{2} - 2\gamma)} &= -\left(\epsilon_c - \epsilon_f - \left[\frac{1}{2} + \frac{1}{2}\cos(\frac{\pi}{2} + 2\gamma)\right] U\right) \\
-4t\frac{\sin(2\gamma)}{\cos(2\gamma)} &= -\left(\epsilon_c - \epsilon_f - \left[\frac{1}{2} - \frac{1}{2}\sin(2\gamma)\right] U\right) \\
4\sin(2\gamma) &= -\left(\frac{\epsilon_f - \epsilon_c}{t} + \frac{U}{2t}\right)\cos(2\gamma) + \sin(2\gamma)\cos(2\gamma)\frac{U}{2t} \\
\left(4 - \cos(2\gamma)\frac{U}{2t}\right)\sin(2\gamma) &= -\left(\frac{\epsilon_f - \epsilon_c}{t} + \frac{U}{2t}\right)\cos(2\gamma) \\
4\sin(2\gamma) &= -\left(\frac{\epsilon_f - \epsilon_c}{t} + \frac{U}{2t}\right)\cos(2\gamma) + \sin(2\gamma)\cos(2\gamma)\frac{U}{2t} \\
\overbrace{1 - \cos^2(2\gamma)}^{\sin^2(2\gamma)} &= \left(\frac{-\left(\frac{\epsilon_f - \epsilon_c}{t} + \frac{U}{2t}\right)\cos(2\gamma)}{4 - \cos(2\gamma)\frac{U}{2t}}\right)^2 \\
\overset{x=\cos(2\gamma)}{\Rightarrow} 1 - x^2 &= \left(\frac{-\left(\frac{\epsilon_f - \epsilon_c}{t} + \frac{U}{2t}\right)x}{4 - x\frac{U}{2t}}\right)^2 \\
0 &= 4 - 8x\frac{U}{2t} + x^2\left(\frac{U}{2t}\right)^2 - 4x^2 + 8x^3\frac{U}{2t} - x^4\left(\frac{U}{2t}\right)^2 - \left(\frac{\epsilon_f - \epsilon_c}{t} + \frac{U}{2t}\right)^2 x^2 \\
&= 4 - 8\frac{U}{2t}x + \left[\left(\frac{U}{2t}\right)^2 - 4 - \left(\frac{\epsilon_f - \epsilon_c}{t} + \frac{U}{2t}\right)^2\right] x^2 + 8x^3\frac{U}{2t} - x^4\left(\frac{U}{2t}\right)^2 \\
&= 4 - 8\frac{U}{2t}x - \left[4 + \left(\frac{\epsilon_f - \epsilon_c}{t}\right)^2 + 2\left(\frac{\epsilon_f - \epsilon_c}{t}\right)\frac{U}{2t}\right] x^2 + 8x^3\frac{U}{2t} - x^4\left(\frac{U}{2t}\right)^2 \\
&= 4 - 8\frac{U}{2t}(1 - x^2)x - \left[4 + \left(\frac{\epsilon_f - \epsilon_c}{t}\right)^2 + 2\left(\frac{\epsilon_f - \epsilon_c}{t}\right)\frac{U}{2t}\right] x^2 - x^4\left(\frac{U}{2t}\right)^2
\end{aligned} \tag{D.46}$$

This is a polynomial of fourth order.

Broken symmetry states: When the interaction is increased, this solution splits into three. For the symmetric case this is probably the transition into the antiferromagnetic broken-symmetry state. The solution with $\alpha + \beta = \frac{\pi}{2}$ becomes the unstable solution, while the two other states are stable solutions. For the symmetric solution we obtain

D.4 Hydrogen atom

This appendix shall provide the matrix elements for the hydrogen molecule using atomic orbitals as basis set. Many matrix elements can be evaluated analytically, which makes this a convenient system for

benchmarks.Editor: This is taken from the paw_lmto report of the PAW code on May 11, 2020. The text is thus duplicated. The PAW data have been removed in this version.

The Hartree-Fock energy of the hydrogen atom is

$$E_{\text{tot}} = \underbrace{\langle\psi|\frac{\hat{\vec{p}}^2}{2m_e}|\psi\rangle}_{E_{\text{kin}}} \underbrace{- \int d^3r \frac{e^2 n(\vec{r})}{4\pi\epsilon_0|\vec{r}-\vec{R}|}}_{E_{ne}} + \underbrace{\frac{1}{2}\int d^3r \int d^3r' \frac{e^2 n(\vec{r})n(\vec{r'})}{4\pi\epsilon_0|\vec{r}-\vec{r'}|}}_{E_H} \underbrace{-\frac{1}{2}\int d^4x \int d^4x' \frac{e^2\rho^{(1)}(\vec{x},\vec{x'})\rho^{(1)}(\vec{x'},\vec{x})}{4\pi\epsilon_0|\vec{r}-\vec{r'}|}}_{E_X} \tag{D.47}$$

The expression serves to define the energy terms evaluated below.

The exact energies of the hydrogen atom derived below are listed in table D.8.

Table D.8: Exact energies of the hydrogen atom. E_{self} is the electrostatic self energy of the electron density. $E_{\text{self}}+E_{\text{pot}}$ is the Hartree energy including electron-electron and electron-proton interactions. The energies in eV are approximate.

E_{tot}	E_{kin}	E_{pot}	ϵ_{1s}
$-\frac{1}{2}$ H -13.606 eV	$\frac{1}{2}$ H 13.606 eV	-1 H -27.211 eV	$-\frac{1}{2}$ H -13.606 eV
$\epsilon_{2s}-\epsilon_{1s}$	$E_{\text{self}}+E_{\text{pot}}$	E_{self}	E_X
$\frac{3}{8}$ H 10.204 eV	-11/16 H=-0.6875 H -18.707 eV	5/16 H=+0.3125 H 8.503 eV	-5/16 H=-0.3125 H -8.503 eV

Wave function and density of the H-atom

The wave functions $\psi(\vec{r})$ of the hydrogen atom and its electron density $n(\vec{r})$ are[7]

$$\psi(\vec{r}) = \frac{1}{\sqrt{\pi a_0^3}} e^{-|\vec{r}|/a_0} \tag{D.50}$$

$$n(\vec{r}) = \frac{1}{\pi a_0^3} e^{-2|\vec{r}|/a_0} \tag{D.51}$$

[7]The wave functions of the hydrogen atom are taken from ΦSX: Quantum Physics. The Coulomb potential of the charge density is obtained with the help of Eq. 5.42 of PhiSX:Elektrodynamik. Furthermore, the following equations from Bronstein are used:

$$\int_0^x dx\, x e^{ax} = e^{ax}\left(\frac{x}{a}-\frac{1}{a^2}\right) \qquad \text{Bronstein p.61 Sec. 1.1.3.3 Eq.448}$$

$$\int_0^x dx\, x^2 e^{ax} = e^{ax}\left(\frac{x^2}{a}-\frac{2x}{a^2}+\frac{2}{a^3}\right) \qquad \text{Bronstein p.61 Sec. 1.1.3.3 Eq.449} \tag{D.48}$$

$$\int_0^\infty dx x^n e^{-ax} = \frac{n!}{a^{n+1}} \qquad \text{Bronstein p65 Sec. 1.1.3.4 Eq.1} \tag{D.49}$$

Kinetic energy of the H-atom

$$
\begin{aligned}
E_{\text{kin}} &= \int d^3r\ \psi^*(\vec{r})\frac{-\hbar^2\vec{\nabla}^2}{2m_e}\psi(\vec{r}) \\
&= \frac{-\hbar^2}{2m_e}4\pi\int dr\ r^2\ \underbrace{\frac{1}{\sqrt{\pi a_0^3}}\mathrm{e}^{-|\vec{r}|/a_0}}_{=\psi^*(r)}\ \frac{1}{r}\partial_r^2 r\ \underbrace{\frac{1}{\sqrt{\pi a_0^3}}\mathrm{e}^{-|\vec{r}|/a_0}}_{=\psi(r)} \\
&= \frac{-\hbar^2}{2m_e}\frac{1}{\pi a_0^3}4\pi\int dr\ r^2\mathrm{e}^{-r/a_0}\quad \underbrace{\frac{1}{r}\partial_r^2 r\mathrm{e}^{-|\vec{r}|/a_0}}_{\underbrace{\frac{1}{r}\partial_r\left(\mathrm{e}^{-r/a_0}-\frac{r}{a_0}\mathrm{e}^{-r/a_0}\right)}_{-\frac{2}{ra_0}\mathrm{e}^{-r/a_0}+\frac{1}{a_0^2}\mathrm{e}^{-r/a_0}}} \\
&= \frac{-\hbar^2}{2m_e}\frac{1}{\pi a_0^3}\frac{2}{a_0^2}4\pi\int dr\ r^2\mathrm{e}^{-2r/a_0}\left(-\frac{a_0}{r}+\frac{1}{2}\right) \\
&= \frac{-\hbar^2}{2m_e}\frac{2}{a_0^2}\left(\frac{a_0 4\pi\epsilon_0}{e^2}\underbrace{\int d^3r\ \frac{1}{\pi a_0^3}\mathrm{e}^{-2r/a_0}\frac{-e^2}{4\pi\epsilon_0 r}}_{E_{ne}=-1\ H}+\frac{1}{2}\underbrace{\int d^3r\ \frac{1}{\pi a_0^3}\mathrm{e}^{-2r/a_0}}_{=1}\right) \\
&= +\frac{1}{2}\ H
\end{aligned}
\tag{D.52}
$$

Coulomb potential of the electrons of the H-atom

The Coulomb potential $v_e(\vec{r})$ of the electronic charge density $n(\vec{r})$ Eq. D.51 of the H-atom can be evaluated using the radial Green's function of the Poisson equation. (see ΦSX: Elektrodynamik.)

$$
\begin{aligned}
v_e(\vec{r}) &= \int d^3r'\ \frac{e^2 n(\vec{r'})}{4\pi\epsilon|\vec{r}-\vec{r'}|} \\
&= \frac{e^2}{4\pi\epsilon_0}4\pi\left[\frac{1}{|\vec{r}|}\int_0^{|\vec{r}|}dr'\ (r')^2 n(r') + \int_{|\vec{r}|}^{\infty}dr'\ r' n(r')\right] \\
&= \frac{e^2}{4\pi\epsilon_0}4\pi\frac{1}{\pi a_0^3}\left[\frac{1}{|\vec{r}|}\int_0^{|\vec{r}|}dr'\ (r')^2\mathrm{e}^{-2r'/a_0} + \int_{|\vec{r}|}^{\infty}dr'\ r'\mathrm{e}^{-2r'/a_0}\right] \\
&= \frac{e^2}{4\pi\epsilon_0}4\pi\frac{1}{\pi a_0^3}\left\{\frac{1}{|\vec{r}|}\frac{a_0^3}{4}\left[1-\left(2\left(\frac{r}{a_0}\right)^2+2\left(\frac{r}{a_0}\right)+1\right)\mathrm{e}^{-2r/a_0}\right]+\frac{a_0^3}{4}\frac{1}{a_0}\left(2\frac{r}{a_0}+1\right)\mathrm{e}^{-2r/a_0}\right\} \\
&= \frac{e^2}{4\pi\epsilon_0}\left\{\frac{1}{|\vec{r}|}\left[1-\left(2\left(\frac{r}{a_0}\right)^2+2\left(\frac{r}{a_0}\right)+1\right)\mathrm{e}^{-2r/a_0}\right]+\frac{1}{r}\left(2\left(\frac{r}{a_0}\right)^2+\left(\frac{r}{a_0}\right)\right)\mathrm{e}^{-2r/a_0}\right\} \\
&= \frac{e^2}{4\pi\epsilon_0|\vec{r}|}\left\{\left[1-\left(\left(\frac{r}{a_0}\right)+1\right)\mathrm{e}^{-2r/a_0}\right]\right\}
\end{aligned}
\tag{D.53}
$$

Electron-proton interaction energy

The Coulomb interaction E_{ne} between the electron and the proton is evaluated using the Coulomb potential v_e of the electronic density

$$
E_{ne} = \int d^3r\frac{-e^2 n(\vec{r})}{4\pi\epsilon_0|\vec{r}-\vec{R}|} = -v_e(\vec{R}) \overset{\text{Eq. D.53}}{=} -\frac{e^2}{4\pi\epsilon_0 a_0} = -1\ \mathrm{H} \tag{D.54}
$$

Electronic Hartree energy

The electronic Hartree energy is the Coulomb self energy of the electronic charge density.

$$E_{\text{self}} = \frac{1}{2}\int d^3r \int d^3r' \frac{e^2 n(\vec{r}) n(\vec{r'})}{4\pi\epsilon_0 |\vec{r}-\vec{r'}|} \tag{D.55}$$

The self energy is the Coulomb interaction energy of the electron density with itself. This energy is canceled by the exchange energy. Thus, the self energy can be used to obtain, independently, the Hartree energy and the exchange energy.

$$\begin{aligned}
E_{\text{self}} &= \frac{1}{2}\int d^3r\; n(\vec{r}) v(\vec{r}) \\
&= \frac{1}{2}\left(\frac{1}{\pi a_0^3}\right)\left(\frac{e^2}{4\pi\epsilon_0}\right) 4\pi \int_0^\infty dr\; r^2 \mathrm{e}^{-2r/a_0} \frac{1}{r}\left[1-\left(\left(\frac{r}{a_0}\right)+1\right)\mathrm{e}^{-2r/a_0}\right] \\
&= \frac{1}{2}\left(\frac{1}{\pi a_0^3}\right)\left(\frac{e^2}{4\pi\epsilon_0}\right) 4\pi a_0^2 \int_0^\infty dx\; x\mathrm{e}^{-2x}\left[1-(x+1)\,\mathrm{e}^{-2x}\right] \\
&= \frac{1}{2}\frac{1}{\pi a_0^3}\frac{e^2}{4\pi\epsilon_0 a_0} 4\pi a_0^3 \int_0^\infty dx\; \left[x\mathrm{e}^{-2x} - x^2\mathrm{e}^{-4x} - x\mathrm{e}^{-4x}\right] \\
&= 2\underbrace{\frac{e^2}{4\pi\epsilon_0 a_0}}_{1H} \underbrace{\left[\frac{1!}{2^2}-\frac{2!}{4^3}-\frac{1!}{4^2}\right]}_{1/4-1/32-1/16=(8-1-2)/32=5/32} \\
&= \frac{5}{16}\frac{e^2}{4\pi\epsilon_0 a_0} = 0.3125\; H \qquad \textit{(exact)}
\end{aligned} \tag{D.56}$$

Exchange energy of the H-atom

The exchange energy of a one-electron system cancels the electronic Hartree energy precisely. Thus, the exchange energy is

$$E_X = -E_H = -\frac{5}{16}\frac{e^2}{4\pi\epsilon_0 a_0} = -0.3125\; H \qquad \textit{(exact)} \tag{D.57}$$

U-tensor of the H-atom

The U-tensor is twice the self energy, Eq. D.56, i.e.

$$U = 2E_{\text{self}} = 2E_X = \frac{5}{8}\frac{e^2}{4\pi\epsilon_0 a_0} \tag{D.58}$$

The energy E_{e-nuc} is the complete electrostatic energy including Hartree energy $E_{\text{pot}} + E_{\text{self}}$ and exchange energy E_X. This tells us that $E_X = -E_{\text{self}}$ This result for the exchange energy $E_X = -0.3125$ is also given in [P.M.W. Gill and J.A. Pople, Phys Rev. A 47, 2383 (1993)][169].

D.5 Hydrogen molecule

$$\begin{aligned}
E_{\text{tot}} = &\underbrace{\sum_{\sigma\in\{\uparrow,\downarrow\}} f_{b,\sigma}\langle\psi_{b,\sigma}|\frac{\hat{\vec{p}}^2}{2m_e}|\psi_{b,\sigma}\rangle}_{E_{\text{kin}}} \underbrace{- \sum_{R\in\{R_1,R_2\}}\int d^3r \frac{e^2\Big(n(\vec{r})+Z(\vec{r})\Big)\Big(n(\vec{r'})+Z(\vec{r'})\Big)}{4\pi\epsilon_0|\vec{r}-\vec{R}|}}_{E_H+E_{ne}+E_{nn}} \\
&\underbrace{-\frac{1}{2}\int d^4x \int d^4x'\; \frac{e^2\rho^{(1)}(\vec{x},\vec{x'})\rho^{(1)}(\vec{x'},\vec{x})}{4\pi\epsilon_0|\vec{r}-\vec{r'}|}}_{E_X}
\end{aligned} \tag{D.59}$$

All matrix elements are evaluated using atomic orbitals

$$\langle \vec{r}, \sigma | \chi_{j,\sigma'} \rangle = \frac{1}{\sqrt{\pi a_0^3}} \mathrm{e}^{-|\vec{r}-\vec{R}_j|/a_0} \delta_{\sigma,\sigma'} \tag{D.60}$$

The bound state wave function $|\psi_{b,\sigma}\rangle$ expressed in normalized atomic orbitals $|\chi_{j,\sigma}\rangle$ is

$$|\psi_{b,\sigma}\rangle = \Big(|\chi_{1,\sigma}\rangle + |\chi_{2,\sigma}\rangle \Big) \frac{1}{\sqrt{2(1+S)}} \tag{D.61}$$

with the off-site overlap matrix elements

$$S = \langle \chi_{1,\sigma} | \chi_{2,\sigma} \rangle \tag{D.62}$$

which are obtained below in Eq. D.68.

Editor: continue here!

The matrix elements of the hydrogen atom have been worked out by van Leeuwen[167].

D.5.1 Two-center integral of spherical functions

The integrations of interest are of the form of a two-center integral of two spherical functions with centers that are separated by the distance d.

$$\begin{aligned}
\langle f | g \rangle &= \int d^3r \; f(|\vec{r}|) g(|\vec{e}_z d - \vec{r}|) \\
&= \int_0^\infty dr \; r^2 \int_0^{2\pi} d\phi \int_0^\pi d\theta \sin(\theta) f(r) g(\sqrt{(d - r\cos(\theta))^2 + (r\sin(\theta))^2}) \\
&= 2\pi \int_0^\infty dr \; r^2 f(r) \int_0^\pi d\theta \sin(\theta) g(\sqrt{d^2 - 2dr\cos(\theta)) + r^2}) \\
&= 2\pi \int_0^\infty dr \; r^2 f(r) \frac{1}{dr} \int_{|d-r|}^{|d+r|} dy \; y g(y) \\
&= \frac{2\pi}{d} \int_0^\infty dr \; r f(r) \int_{|d-r|}^{|d+r|} dy \; y g(y) \\
&= \frac{2\pi}{d} \left[\int_0^d dr \; r f(r) \int_{d-r}^{r+d} dy \; y g(y) + \int_d^\infty dr \; r f(r) \int_{r-d}^{r+d} dy \; y g(y) \right]
\end{aligned} \tag{D.63}$$

We used

$$\begin{aligned}
y(\theta) = \sqrt{d^2 - 2dr\cos(\theta) + r^2} \qquad &\Rightarrow \qquad dy = \frac{1}{2y} 2dr \sin(\theta) d\theta \\
y(\theta = 0) = |d - r| \qquad &\text{and} \qquad y(\theta = \pi) = d + r
\end{aligned} \tag{D.64}$$

D.5.2 Overlap

Let me evaluate the overlap of two hydrogen orbitals $S(d)$ at centers separated by the distance d.

$$S(d) = \frac{1}{\pi a_0^3} \int d^3r \; \mathrm{e}^{-|\vec{r}|/a_0} \mathrm{e}^{-|\vec{r}-\vec{e}_z d|/a_0} \tag{D.65}$$

In the following, I will use the undetermined integrals from Bronstein,

$$\begin{aligned}
\int dx\, \mathrm{e}^{-ax} &= -\frac{1}{a}\mathrm{e}^{-ax} \\
\int dx\, x\mathrm{e}^{-ax} &= -\frac{ax+1}{a^2}\mathrm{e}^{-ax} \\
\int dx\, x^2\mathrm{e}^{-ax} &= -\frac{(ax)^2+2ax+2}{a^3}\mathrm{e}^{-ax} \\
\int dx\, x^n\mathrm{e}^{-ax} &= \frac{-n!}{a^{n+1}}\mathrm{e}^{-ax}\sum_{j=0}^{n}\frac{1}{j!}(ax)^j
\end{aligned} \tag{D.66}$$

The parameter a is unrelated to the Bohr radius a_0.

Let be introduce a dimensionless parameter $\vec{x} = \frac{\vec{r}}{a_0}$ and $z = \frac{d}{a_0}$. With $\vec{e}_z$, I denote the unit vector pointing along the z-axis. Caution: Here, the symbol $\vec{x}$ is unrelated to the combined position-and-spin variable $\vec{x} = (\vec{r}, \sigma)$.

$$\begin{aligned}
S(d = za_0) &= \frac{1}{\pi}\int d^3x\, \mathrm{e}^{-|\vec{x}|}\mathrm{e}^{-|\vec{x}-z\vec{e}_z|} \\
&\overset{\text{Eq. } D.63}{=} \frac{2}{z}\left[\int_0^z dx\, x\mathrm{e}^{-x}\int_{z-x}^{x+z} dy\, y\mathrm{e}^{-y} + \int_z^\infty dx\, x\mathrm{e}^{-x}\int_{x-z}^{x+z} dy\, y\mathrm{e}^{-y}\right] \\
&= \frac{2}{z}\left\{\int_0^z dx\, x\mathrm{e}^{-x}\Big[-(1+y)\mathrm{e}^{-y}\Big]_{z-x}^{x+z} + \int_z^\infty dx\, x\mathrm{e}^{-x}\Big[-(1+y)\mathrm{e}^{-y}\Big]_{x-z}^{x+z}\right\} \\
&= \frac{2}{z}\left\{\int_0^z dx\, x\mathrm{e}^{-x}\Big[-(1+x+z)\,\mathrm{e}^{-(x+z)} + (1+z-x)\,\mathrm{e}^{-(z-x)}\Big]\right. \\
&\quad \left. + \int_z^\infty dx\, x\mathrm{e}^{-x}\Big[-(1+x+z)\,\mathrm{e}^{-(x+z)} + (1+x-z)\,\mathrm{e}^{-(x-z)}\Big]\right\} \\
&= \frac{2}{z}\left\{\mathrm{e}^{-z}\int_0^z dx\, \Big[-(1+z)\,x\mathrm{e}^{-2x} - x^2\mathrm{e}^{-2x} + (1-z)\,x + x^2\Big]\right. \\
&\quad \left. + \int_z^\infty dx\, \Big[\Big(\mathrm{e}^{+z}(1-z) - \mathrm{e}^{-z}(1+z)\Big)x\mathrm{e}^{-2x} + \Big(\mathrm{e}^{+z} - \mathrm{e}^{-z}\Big)x^2\mathrm{e}^{-2x}\Big]\right\} \\
&= \frac{2}{z}\left\{\mathrm{e}^{-z}\left[-(1+z)\,\frac{-2x-1}{4}\mathrm{e}^{-2x} - \frac{(-2x)^2-2(-2x)+2}{-8}\mathrm{e}^{-2x} + \frac{1+z}{2}x^2 - \frac{1}{3}x^3\right]_0^z\right. \\
&\quad \left. + \left[\Big(\mathrm{e}^{+z}(1-z) - \mathrm{e}^{-z}(1+z)\Big)\frac{-2x-1}{4}\mathrm{e}^{-2x} + \Big(\mathrm{e}^{+z} - \mathrm{e}^{-z}\Big)\frac{(-2x)^2-2(-2x)+2}{-8}\mathrm{e}^{-2x}\right]_z^\infty\right\} \\
&= \frac{2}{z}\left\{\mathrm{e}^{-z}\left[(1+z)\,\frac{2z+1}{4}\mathrm{e}^{-2z} - \frac{2z^2+2z+1}{4}\mathrm{e}^{-2z} + \frac{1+z}{2}z^2 - \frac{1}{3}z^3 + (1+z)\,\frac{-1}{4} - \frac{1}{4}\right]\right. \\
&\quad \left. - \left[\Big(\mathrm{e}^{+z}(1-z) - \mathrm{e}^{-z}(1+z)\Big)\frac{-2z-1}{4}\mathrm{e}^{-2z} + \Big(\mathrm{e}^{+z} - \mathrm{e}^{-z}\Big)\frac{2z^2+2z+1}{-4}\mathrm{e}^{-2z}\right]\right\} \\
&= \Big(\frac{1}{3}z^2 + z + 1\Big)\mathrm{e}^{-z}
\end{aligned} \tag{D.67}$$

Thus, the overlap matrix element of two hydrogen 1s-orbitals is

OVERLAP OF TWO HYDROGEN 1S ORBITALS

$$S(d) = \left[\frac{1}{3}\left(\frac{d}{a_0}\right)^2 + \left(\frac{d}{a_0}\right) + 1\right]\mathrm{e}^{-\frac{d}{a_0}} \tag{D.68}$$

D.5.3 Coulomb repulsion between the protons

$$E_{nn}(d) = \frac{e^2}{4\pi\epsilon_0 d} \tag{D.69}$$

D.5.4 Electron-proton interaction matrix elements

The electrostatic energy between electron density on one site with a proton on the other side is obtained from the electrostatic potential $v_w(\vec{r})$ of the atomic density at the distance of the nucleus

$$\begin{aligned} E_{xx} &= -\int d^3r \frac{e^2 n_1(\vec{r})}{4\pi\epsilon_0|\vec{r}-\vec{R}_2|} = -v_e(d\vec{e}_z) \\ &\overset{\text{Eq. } D.53}{=} -\frac{e^2}{4\pi\epsilon_0 a_0}\left\{\left(\frac{d}{a_0}\right)^{-1}\left[1-\left(\left(\frac{d}{a_0}\right)+1\right)\mathrm{e}^{-2d/a_0}\right]\right\} \end{aligned} \tag{D.70}$$

D.5.5 Electron-nucleus Coulomb matrix elements

The matrix elements from this subsection are copied from the internet and they are not verified. `http://www.pci.tu-bs.de/aggericke/PC4e/Kap_II/H2-Ion.htm`

The **Coulomb integral** J is the Coulomb interaction of one atom with the nucleus of the other atom.

$$J = \frac{e^2}{4\pi\epsilon_0 d} - \int d^3r\, \psi_{1s}(\vec{r})\psi_{1s}(\vec{r})\frac{e^2}{4\pi\epsilon_0|\vec{r}-\vec{e}_z d|} = \left(1+\frac{1}{d}\right)\mathrm{e}^{-2d/a_0} \tag{D.71}$$

The **resonance integral** K describes the overlap density of two orbitals on different sites with the nucleus of one site

$$K = \frac{e^2 S(d)}{4\pi\epsilon_0 d} - \int d^3r\, \frac{e^2\psi_{1s}(\vec{r}-\vec{e}_z d)\psi_{1s}(\vec{r})}{4\pi\epsilon_0|\vec{r}-\vec{e}_z d|} = \frac{e^2}{4\pi\epsilon_0}\left(\frac{a_0}{d}-\frac{2}{3}\frac{d}{a_0}\right)\mathrm{e}^{-d/a_0} \tag{D.72}$$

D.5.6 U-tensor

The 31 matrix elements are those with three orbitals on one site and one on the other. The 22 matrix elements are those with one density on one site and another density on the other.

The U-tensor can be constructed from the following basic matrix elements. For the sake of simplicity we refer here only to the spatial part of the wave functions and ignore the spin part. The matrix elements $W_{\alpha,\beta,\gamma,\delta}$, which also account of the spin indices, can be calculated from these matrix elements U. The indices refer to the two sites of the H_2-molecule.

$$\begin{aligned} U_{1111} &= \int d^3r \int d^3r' \frac{e^2\chi_1^*(\vec{r})\chi_1^*(\vec{r'})\chi_1(\vec{r})\chi_1(\vec{r'})}{4\pi\epsilon_0|\vec{r}-\vec{r'}|} \\ U_{1112} &= \int d^3r \int d^3r' \frac{e^2\chi_1^*(\vec{r})\chi_1^*(\vec{r'})\chi_1(\vec{r})\chi_2(\vec{r'})}{4\pi\epsilon_0|\vec{r}-\vec{r'}|} = \int d^3r \left(v_e(\vec{r})\chi(\vec{r})\right)\chi(\vec{r}-\vec{e}_z d) \\ U_{1212} &= \int d^3r \int d^3r' \frac{e^2\chi_1^*(\vec{r})\chi_2^*(\vec{r'})\chi_1(\vec{r})\chi_2(\vec{r'})}{4\pi\epsilon_0|\vec{r}-\vec{r'}|} = \int d^3r \left(v_e(\vec{r})\right)\chi^2(\vec{r}-\vec{e}_z d) \\ U_{1221} &= \int d^3r \int d^3r' \frac{e^2\chi_1^*(\vec{r})\chi_2^*(\vec{r'})\chi_2(\vec{r})\chi_1(\vec{r'})}{4\pi\epsilon_0|\vec{r}-\vec{r'}|} \end{aligned} \tag{D.73}$$

The Coulomb potential v_e from the electrons of one hydrogen atom is Eq. D.53

$$v_e(\vec{r}) = \frac{e^2}{4\pi\epsilon_0|\vec{r}|}\left[1-\left(1+\frac{r}{a_0}\right)\mathrm{e}^{-2r/a_0}\right] \tag{D.74}$$

1. The element U_{1111} has four orbitals on one site, and can be identified with the U-parameter Eq. D.58 of the hydrogen atom.

2. The element U_{1112} describes the interaction of the electrons on one site with a bond charge density, i.e. the density from the overlap of orbitals from both sites.

3. The matrix element U_{1212} is the Coulomb interaction of the electronic charge density from one atom with that of the other.

4. The matrix element U_{1221} is the Coulomb interaction of the bond charge density with itself.Editor: I do not have an analytical expression for this matrix element yet.

Editor: Caution! The following derivation is not carried through to the end and need to be tested. At the end a Maple result is introduced! See Appendix A of [167].

The integrations for two matrix elements are of a similar form, namely $U_{1112} = I(3,1)$ and $U_{1212} = I(2,2)$ with

$$\begin{aligned}\frac{e^2}{4\pi\epsilon_0 a_0} I_{2+m,n}(d = z a_0) &\stackrel{\text{def}}{=} \int d^3r\; v_e(\vec{r})\psi_{1s}^n(\vec{r})\psi_{1s}^m(\vec{r} - \vec{e}_z d) \\ &= \frac{e^2}{4\pi\epsilon_0 a_0}\frac{1}{\pi a_0^3}\int d^3r\; \frac{a_0}{|\vec{r}|}\left[1 - \left(1 + \frac{|\vec{r}|}{a_0}\right)\mathrm{e}^{-2\frac{|\vec{r}|}{a_0}}\right]\mathrm{e}^{-m\frac{|\vec{r}|}{a_0}}\mathrm{e}^{-n\frac{|\vec{r}-\vec{e}_z d|}{a_0}} \\ &= \frac{e^2}{4\pi\epsilon_0 a_0}\frac{1}{\pi}\int d^3r\; \frac{1}{|\vec{x}|}\left[1 - (1 + |\vec{x}|)\,\mathrm{e}^{-2|\vec{x}|}\right]\mathrm{e}^{-m|\vec{r}|}\mathrm{e}^{-n|\vec{x}-\vec{e}_z z|} \qquad \text{(D.75)}\end{aligned}$$

with $z = d/a_0$.

$$
\begin{aligned}
I_{4-n,n}(z) &= \frac{1}{\pi}\int d^3r\,\frac{1}{|\vec{X}|}\left[1-(1+|\vec{X}|)\,\mathrm{e}^{-2|\vec{X}|}\right]\mathrm{e}^{-(2-n)|\vec{r}|}\mathrm{e}^{-n|\vec{X}-\vec{e}_z z|}\\
&= \frac{1}{\pi}\frac{2\pi}{z}\left\{\int_0^z dx\,x\underbrace{\frac{1}{x}\left[1-(1+x)\,\mathrm{e}^{-2x}\right]\mathrm{e}^{-(2-n)x}}_{f(x)}\int_{z-x}^{x+z}dy\,y\underbrace{\mathrm{e}^{-ny}}_{g(y)}\right.\\
&\quad\left.+\int_z^\infty dx\,x\underbrace{\frac{1}{x}\left[1-(1+x)\,\mathrm{e}^{-2x}\right]\mathrm{e}^{-(2-n)x}}_{f(x)}\int_{x-z}^{x+z}dy\,y\underbrace{\mathrm{e}^{-ny}}_{g(y)}\right\}\\
&= \frac{2}{z}\left\{\int_0^z dx\;\left[1-(1+x)\,\mathrm{e}^{-2x}\right]\mathrm{e}^{-(2-n)x}\left[\frac{-ny-1}{n^2}\mathrm{e}^{-ny}\right]_{z-x}^{x+z}\right.\\
&\quad\left.+\int_z^\infty dx\;\left[1-(1+x)\,\mathrm{e}^{-2x}\right]\mathrm{e}^{-(2-n)x}\left[\frac{-ny-1}{n^2}\mathrm{e}^{-ny}\right]_{x-z}^{x+z}\right\}\\
&= \frac{-2}{n^2 z}\left\{\int_0^z dx\;\left[1-(1+x)\,\mathrm{e}^{-2x}\right]\mathrm{e}^{-(2-n)x}\right.\\
&\qquad\qquad\left.\times\left[(1+n(z+x))\mathrm{e}^{-nz}\mathrm{e}^{-nx}-(1+nz-nx)\mathrm{e}^{-nz}\mathrm{e}^{+nx}\right]\right.\\
&\quad\left.+\int_z^\infty dx\;\left[1-(1+x)\,\mathrm{e}^{-2x}\right]\mathrm{e}^{-(2-n)x}\right.\\
&\qquad\qquad\left.\times\left[(1+nz+nx)\mathrm{e}^{-nz}-(1-nz+nx)\mathrm{e}^{+nz}\right]\mathrm{e}^{-nx}\right\}\\
&= \frac{-2}{n^2 z}\left\{\int_0^z dx\;\left[1-(1+x)\,\mathrm{e}^{-2x}\right]\right.\\
&\qquad\qquad\left.\times\mathrm{e}^{-nz}\left[(1+nz+nx)\mathrm{e}^{-2x}-(1+nz-nx)\mathrm{e}^{-(2-2n)x}\right]\right.\\
&\quad\left.+\int_z^\infty dx\;\left[1-(1+x)\,\mathrm{e}^{-2x}\right]\right.\\
&\qquad\qquad\left.\times\left[\Big((1+nz+nx)\mathrm{e}^{-nz}-(1-nz+nx)\mathrm{e}^{+nz}\Big)\right]\mathrm{e}^{-2x}\right\}
\end{aligned}
\tag{D.76}
$$

$$
\begin{aligned}
I_{22} = \frac{-2}{4z}\Bigg\{ & \int_0^z dx\ \left[1-(1+x)\,\mathrm{e}^{-2x}\right] \\
& \qquad \times \mathrm{e}^{-2z}\Big[(1+2z+2x)\mathrm{e}^{-2x}-(1+2z-2x)\mathrm{e}^{+2x}\Big] \\
& + \int_z^\infty dx\ \left[1-(1+x)\,\mathrm{e}^{-2x}\right] \\
& \qquad \times \Big[\Big((1+2z+2x)\mathrm{e}^{-2z}-(1-2z+2x)\mathrm{e}^{+2z}\Big)\Big]\mathrm{e}^{-2x}\Bigg\} \\
= \frac{-1}{2z}\Bigg\{ & \int_0^z dx\ \mathrm{e}^{-2z}\Big[(1+2z+2x)\mathrm{e}^{-2x}-(1+2z-2x)\mathrm{e}^{+2x}\Big] \\
& + \int_z^\infty dx\ \Big[\Big((1+2z+2x)\mathrm{e}^{-2z}-(1-2z+2x)\mathrm{e}^{+2z}\Big)\Big]\mathrm{e}^{-2x} \\
& - \int_0^z dx\ \mathrm{e}^{-2z}\Big[(1+2z+2x)\mathrm{e}^{-4x}-(1+2z-2x)\Big] \\
& - \int_z^\infty dx\ \Big[\Big((1+2z+2x)\mathrm{e}^{-2z}-(1-2z+2x)\mathrm{e}^{+2z}\Big)\Big]\mathrm{e}^{-4x} \\
& - \int_0^z dx\ \mathrm{e}^{-2z}\Big[(1+2z+2x)\mathrm{e}^{-4x}-(1+2z-2x)\Big]x \\
& - \int_z^\infty dx\ \Big[\Big((1+2z+2x)\mathrm{e}^{-2z}-(1-2z+2x)\mathrm{e}^{+2z}\Big)\Big]x\mathrm{e}^{-4x}\Bigg\} \\
= \frac{-1}{2z}\Bigg\{ & \left[\left(\frac{1+2z}{-2}-2\frac{1+2x}{4}\right)\mathrm{e}^{-2(x+z)}-\left(\frac{1+2z}{+2}+2\frac{1-2x}{4}\right)\mathrm{e}^{+2(x-z)}\right]_0^z \\
& + \left[\left(\frac{1+2z}{-2}-2\frac{2x+1}{4}\right)\mathrm{e}^{-2(x+z)}-\left(\frac{1-2z}{2}+2\frac{1-2x}{4}\right)\mathrm{e}^{+2(z-x)}\right)\Big]_z^\infty \\
& - \left[\left(\frac{1+2z}{-4}-2\frac{1+4x}{16}\right)\mathrm{e}^{-4x-2z}-\left(x+2xz-x^2\right)\mathrm{e}^{-2z}\right]_0^z \\
& - \left[\left(\frac{1+2z}{-4}-2\frac{1+4x}{16}\right)\mathrm{e}^{-2z-4x}-\left(\frac{1-2z}{-4}-2\frac{1+4x}{16}\right)\mathrm{e}^{+2z-4x}\right]_z^\infty \\
& - \left[\left(\frac{(1+2z)(1+4z)}{16}+2\frac{16x^2+8x+2}{(-4)^3}\right)\mathrm{e}^{-4x-2z}-\left(\frac{1+2z}{2}x^2-\frac{2}{3}x^3\right)\mathrm{e}^{-2z}\right]_0^z \\
& - \Bigg[\left(-\frac{(1+2z)(1+4x)}{16}+2\frac{16x^2+8x+2}{-4^3}\right)\mathrm{e}^{-2z-4x} \\
& \qquad - \left(-\frac{(1-2z)(1+4x)}{16}+2\frac{16x^2+8x+2}{-4^3}\right)\mathrm{e}^{+2z-4x}\Bigg]_z^\infty\Bigg\}
\end{aligned}
\tag{D.77}
$$

This calculation is not finished. I am continuing with the Result from Maple.

Maple:

$$
\begin{aligned}
I_{31}(z) &= \left(z^2+\frac{1}{8}z+\frac{5}{16}\right)\frac{1}{z}\mathrm{e}^{-z}-\left(\frac{1}{8}z+\frac{5}{16}\right)\frac{1}{z}\mathrm{e}^{-3z} \\
&= z\mathrm{e}^{-z}+\left(\frac{1}{8}z+\frac{5}{16}\right)\frac{1}{z}\left(\mathrm{e}^{-z}-\mathrm{e}^{-3z}\right) \\
I_{22} &= \frac{1}{z}-\left(\frac{1}{6}z^3+\frac{3}{4}z^2+\frac{11}{8}z+1\right)\frac{1}{z}\mathrm{e}^{-2z}
\end{aligned}
\tag{D.78}
$$

OFFSITE U-TENSOR MATRIX ELEMENTS

The offsite U-tensor matrix elements $U_{31} = W_{1,1,1,2}$ and $U_{22} = W_{1,2,1,2}$ are

$$U_{31}(d = za_0) = \frac{e^2}{4\pi\epsilon_0 a_0} I_{31} = \frac{e^2}{4\pi\epsilon_0 a_0}\left[z\mathrm{e}^{-z} + \left(\frac{1}{8}z + \frac{5}{16}\right)\frac{1}{z}\left(\mathrm{e}^{-z} - \mathrm{e}^{-3z}\right)\right]$$
$$U_{22}(d = za_0) = \frac{e^2}{4\pi\epsilon_0 a_0} I_{22} = \frac{e^2}{4\pi\epsilon_0 a_0}\left[\frac{1}{z} - \left(\frac{1}{6}z^3 + \frac{3}{4}z^2 + \frac{11}{8}z + 1\right)\frac{1}{z}\mathrm{e}^{-2z}\right] \quad \text{(D.79)}$$

- Both terms approach at short distances

$$I_{33}(z) = \frac{5}{8} + O(x^2)$$
$$I_{22}(z) = \frac{5}{8} + O(x^2) \quad \text{(D.80)}$$

  The limit $x \to 0$ is equal to the onsite U-tensor, because in this limit, all four orbitals are centered on a single site. The electrostatic self energy E_{self} of the hydrogen atom calculated above is 5/16, which is $\frac{1}{2}U$.

- at long distances the integrals approach

$$I_{22}(z) \overset{z\to\infty}{\to} \frac{1}{z}$$
$$I_{33}(z) \overset{z\to\infty}{\to} ze^{-z} \quad \text{(D.81)}$$

In order to remove the long-ranged part, I subtracted the multipole expansion of the 22 term. This, however, introduces singularities of the remaining term at the origin. A better strategy would be to replace 1/r by

$$\frac{1}{z} \to \frac{1}{z} - \left(1 - \frac{1}{2}(\lambda z)^2\right)\frac{\mathrm{e}^{-\lambda z}}{z} \cdot$$
$$\frac{1}{z^2} \to \frac{1}{z^2} - \left(1 + (\lambda z) - \frac{1}{3}(\lambda z)^3\right)\frac{\mathrm{e}^{-\lambda z}}{z^2}$$
$$\frac{1}{z^3} \to \frac{1}{z^3} - \left(1 + (\lambda z) + \frac{1}{2}(\lambda z)^2 - \frac{1}{8}(\lambda z)^4\right)\frac{\mathrm{e}^{-\lambda z}}{z^3}$$
$$\mathrm{e}^{-\lambda z} \to (1 + \lambda z)\mathrm{e}^{-\lambda z} \quad \text{(D.82)}$$

For a finite screening we need to multiply the right hand side with $(1+\gamma z)\mathrm{e}^{-\gamma z}$, so that the slope at the origin remains zero.

$$\frac{1}{z}\mathrm{e}^{-\gamma z} \to \left(\frac{1}{z} - \left(1 - \frac{1}{2}((\lambda + \gamma)z)^2\right)\frac{\mathrm{e}^{-\lambda z}}{z}\cdot\right)\mathrm{e}^{-\gamma z}$$
$$\frac{1}{z^2} \to \frac{1}{z^2} - \left(1 + (\lambda z) - \frac{1}{3}\lambda^2\right)\frac{\mathrm{e}^{-\lambda z}}{z^2}$$
$$\frac{1}{z^3} \to \frac{1}{z^3} - \left(1 + (\lambda z) + \frac{1}{2}\lambda^2 - \frac{1}{8}(\lambda x)^4\right)\frac{\mathrm{e}^{-\lambda z}}{z^3}$$
$$\mathrm{e}^{-\lambda z} \to (1 + \lambda z)\mathrm{e}^{-\lambda z} \quad \text{(D.83)}$$

D.6 Dihydrogen cation

The H_2^+ ion is another one-electron system. It will not be treated exactly, but rather in the basisset of the wave functions of atomic hydrogen. The goal of this is to benchmark the matrix elements for the off-site exchange.

With the knowledge of the matrix elements the individual contributions of the dihydrogen cation can be calculated in the basis of atomic orbitals.

Data are in `Testsimplelmto/Calc/H2cation`

The wave function is

$$|\psi\rangle = |\chi_1\rangle c_1 + |\chi_1\rangle c_2 = (|\chi_1\rangle + |\chi_1\rangle)\,\frac{1}{\sqrt{2+2S}} \tag{D.84}$$

where $S = \langle\chi_1|\chi_2\rangle$ is the offsite overlap matrix element.

Thus, the density matrix elements all have the same value

$$\rho_{\alpha,\beta} = c_\alpha c_\beta = \frac{1}{2+2S} \tag{D.85}$$

The number of electrons on a single site $N_{on,i}$ and that N_{off} in the off-site terms is thus

$$\begin{aligned} N_{on,i} &= c_\alpha^2 = \frac{1}{2+2S} \\ N_{off} &= c_1 S c_2 S + c_2 S c_1 = \frac{2S}{2+2S} \\ 1 &= N_{on,1} + N_{on,1} + N_{off} \end{aligned} \tag{D.86}$$

The onsite Hartree and the onsite exchange energy is

$$\begin{aligned} E_{H,on,i} &= \frac{1}{2} U_{1111}\rho_{11}\rho_{11} \overset{\text{Eq. } D.58}{=} \frac{1}{2}\frac{5}{8}\frac{1}{(2+2S)^2} = \frac{5}{16}\frac{1}{(2+2S)^2} \\ E_{X,on,i} &= -E_{H,on,i} \end{aligned} \tag{D.87}$$

The energy related to the offsite exchange terms are

$$\begin{aligned} E_{X,22} &= -\frac{1}{2}\sum_{R\neq R'}\sum_{\alpha,\gamma\in R}\sum_{\beta,\delta\in R} W_{\alpha,\beta,\gamma,\delta}\rho_{\delta,\alpha}\rho_{\gamma,\beta} \\ &= -\frac{1}{2}\Big(W_{1,2,1,2}\rho_{2,1}\rho_{1,2} + W_{2,1,2,1}\rho_{2,1}\rho_{1,2}\Big) = -\frac{U_{22}}{(2+2S)^2} \\ E_{X,31} &= -\frac{1}{2}\sum_{R\neq R'} 4 \sum_{\alpha,\beta,\gamma\in R}\sum_{\delta\in R'} W_{\alpha,\beta,\gamma,\delta}\rho_{\delta,\alpha}\rho_{\gamma,\beta} \\ &= -\frac{1}{2}4\Big(W_{1,1,1,2}\rho_{2,1}\rho_{1,1} + W_{2,2,2,1}\rho_{1,2}\rho_{2,2}\Big) = -\frac{4U_{31}}{(2+2S)^2} \end{aligned} \tag{D.88}$$

Appendix E

Homogeneous electron gas

In this chapter, I am including material on the homogeneous electron gas, which does not fit into the main text.

E.1 Energy contributions of the homogeneous electron gas

In figure E.1, the individual energy contributions per electron are shown as function of the density.

One observes that the Coulomb energy dominates in the low-density region. This is the region where one can expect the electron interaction to be dominant. In the ultra-low density region, the electrons even undergo a phase transition to a Wigner crystal.

In the low-density region, the simple box model provides a fairly good description of the exchange-correlation energy. This is anticipated because the exchange hole with a box-like shape minimizes the Coulomb repulsion between the electrons. Thus, it is best suited in strongly-interacting limit.

In the high-density region, the kinetic energy dominates over the Coulomb energy. As a consequence, the exchange-correlation hole is similar to that of a non-interacting electron gas, which is obtained in the Hartree-Fock approximation.

Both models, the Hartree-Fock approximation of the homogeneous electron gas and the box model, use a fixed shape of the exchange-correlation hole. The hole for different densities is only scaled in value and distance. As a result, the corresponding exchange-correlation energy per electron scales like $n^{\frac{1}{3}}$. The corresponding prefactor of the exchange-correlation energy of is determined by the different shapes. The exchange-correlation hole of interacting electron gas changes from the compact hole in the low-density region to a more dilute hole in the high-density region.

E.2 Non-interacting homogeneous electron gas

On p. 45, we calculated the kinetic energy of a non-interacting homogeneous electron gas with a specified total density and spin density. The result is

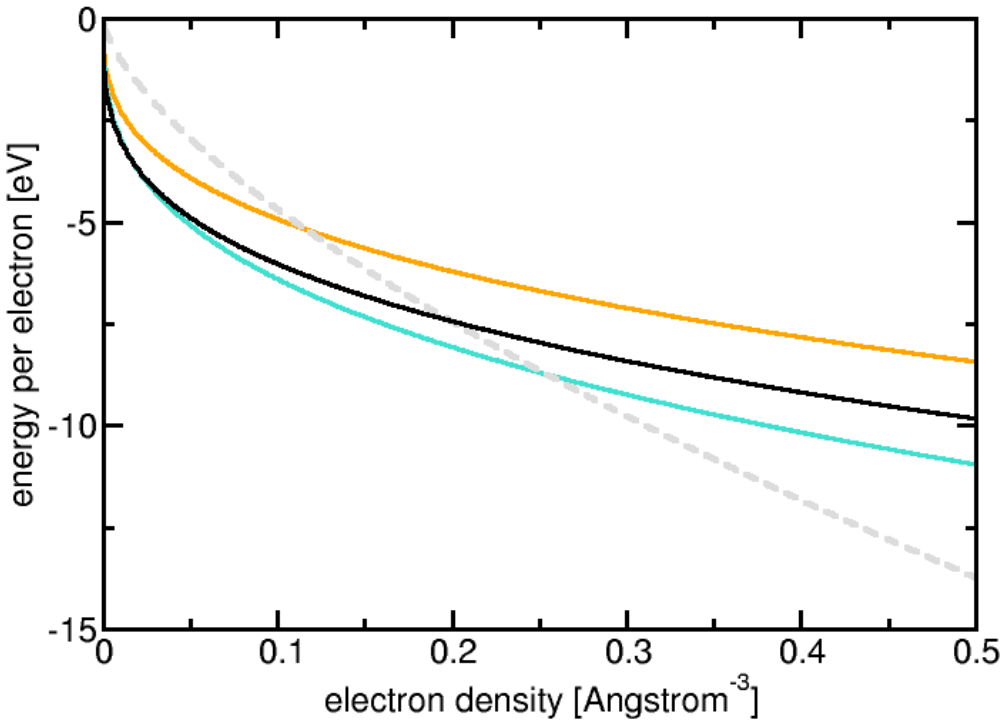


Fig. E.1: Energies of the free electron gas as function of the density. The grey dashed line is, up to a sign change, the kinetic energy per electron. The black line is the exchange-correlation energy per electron of the interacting electron gas[55, 170], the orange line is from the Hartree-Fock approximation and the green line is from the box model discussed in section 2.11.5 on p. 121. The box model replaces the exchange-correlation hole for each spin direction by a homogeneously charged sphere. The valence-electron density of bulk aluminium is 0.18 Å^{-3}.

KINETIC ENERGY OF THE NON-INTERACTING FREE ELECTRON GAS

This is the Thomas-Fermi expression for the kinetic energy of a non-interacting homogeneous electron gas at zero Kelvin. (See Eq. 1.149.)

$$\frac{1}{L^3}E_{\text{kin}}(n_t, n_s) \overset{\text{Eq. 1.149}}{=} \underbrace{\frac{3}{10}\left(3\pi^2\right)^{\frac{2}{3}}\frac{\hbar^2}{m_e}n_t^{\frac{5}{3}}}_{E(n_t,0)/L^3} \cdot \underbrace{\frac{1}{2}\left[\left(1+\frac{n_s}{n_t}\right)^{\frac{5}{3}}+\left(1-\frac{n_s}{n_t}\right)^{\frac{5}{3}}\right]}_{\approx 1+(2^{\frac{2}{3}}-1)\left(\frac{n_s}{n_t}\right)^2} \tag{E.1}$$

where $n_t \overset{\text{def}}{=} \frac{1}{L^3}\mathcal{N}(\mu) = n_\uparrow + n_\downarrow$ is the **total electron density** (both spin directions)and $n_s = n_\uparrow - n_\downarrow$ is the **spin density** .
The spin dependence of the kinetic energy is shown in Fig. 1.11. The dependence of the spin polarization can fairly well be approximated by a simple parabola.

E.2.1 Gradient correction of the kinetic energy

Von Weizsäcker[171] contributed a gradient correction to the kinetic energy [1]

GRADIENT CORRECTION FOR THE KINETIC ENERGY

The kinetic energy of a homogeneous electron gas can be be improved further by a gradient correction developed by von Weizsäcker.[171]

$$\frac{1}{\Omega}T_W \overset{\text{Eq. } E.16}{=} \frac{\hbar^2}{m}\frac{1}{8}\frac{|\vec{\nabla}n_t|^2}{n_t} \tag{E.3}$$

where Ω is the probe volume and n_t is the total electron density.
As shown below in Eq. E.16, the gradient correction is independent of the spin polarization factor $\zeta = \frac{n_s}{n_t}$, if ζ is a constant. (See also `https://en.wikipedia.org/wiki/Thomas-Fermi_model`)

The von-Weizsäcker formula for the kinetic energy is important for **orbital-free density-functional theory** . Historically, it also played a role to improve on the Thomas-Fermi approximation, which is a predecessor of **Density-Functional Theory**.

Derivation of v. Weizsäcker

In the following, I reproduce the derivation of Weizsäcker in order generalize the result to spin-polarized electron densities. While I follow the original proof closely in spirit, I hope that I could streamline it a bit.

I start with the density, the density gradient and the kinetic-energy density e_{kin}. I only consider a specific spin direction $\sigma \in \{\uparrow,\downarrow\}$. The spin index is omitted until the results for the two spin directions are combined.

$$\begin{aligned}
n(\vec{r}) &= \sum_n f_n \psi_n^*(\vec{r})\psi_n(\vec{r}) \\
\vec{\nabla}n(\vec{r}) &= \sum_n f_n 2\mathrm{Re}\Big(\psi_n^*(\vec{r})\vec{\nabla}\psi_n(\vec{r})\Big) = \sum_n f_n\psi_n^*(\vec{r})\psi_n(\vec{r})\cdot 2\mathrm{Re}\Big(\frac{\vec{\nabla}\psi_n(\vec{r})}{\psi_n(\vec{r})}\Big) \\
E_{kin} &= \int d^3r\; e_{kin} \quad \text{with} \qquad e_{kin} = \sum_n f_n \frac{\hbar^2}{2m}\left|\vec{\nabla}\psi_n(\vec{r})\right|^2
\end{aligned} \tag{E.4}$$

Note, that we used the kinetic-energy expression using the product of wave function gradients rather than the expression with the Laplacian. The form used here produces the kinetic-energy density locally, while the other form requires the Gauss theorem, which relies on a global property, the boundary conditions.

Von Weizsäcker introduces an amplitude variation[2] in the wave functions of the free electron gas,

[1] See Weizsäcker[171]-Gl.9 for the energy per unit volume. Weizsäcker denotes this energy with E_{kin}, in contrast to our $\frac{1}{\Omega}E_{kin}$.

$$\frac{1}{\Omega}E_{kin} = \frac{4\pi(\overbrace{2\pi\hbar}^{h})^2}{5m}\left(\frac{3\rho}{8\pi}\right)^{\frac{5}{3}} + \frac{(\overbrace{2\pi\hbar}^{h})^2}{32\pi^2 m}\frac{|\vec{\nabla}\rho|^2}{\rho} = \frac{\hbar^2}{m}\frac{3}{10}\left(3\pi^2\right)^{\frac{2}{3}}\rho^{\frac{5}{3}} + \underbrace{\frac{\hbar^2}{m}\frac{1}{8}\frac{|\vec{\nabla}\rho|^2}{\rho}}_{\frac{1}{\Omega}T_W} \tag{E.2}$$

[2] The form used by von Weizsäcker differs slightly from the one used here, namely

$$\psi_n(\vec{r}) = \frac{1}{\sqrt{\Omega}}\Big(1+\vec{a}_n\vec{r}\Big)\mathrm{e}^{i\vec{k}_n\vec{r}} \tag{E.5}$$

which is governed by a state-dependent, real-valued vector $\vec{a}_n$.

$$\psi_n(\vec{r}) = \frac{1}{\sqrt{\Omega}} \mathrm{e}^{(\vec{a}_n + i\vec{k}_n)\vec{r}} \tag{E.6}$$

so that

$$\vec{\nabla}\psi_n(\vec{r}) = (\vec{a}_n + i\vec{k}_n)\psi_n(\vec{r}) \tag{E.7}$$

These wave functions correspond to damped plane waves that fall off exponentially. Note, that these functions are not normalized nor normalizable. For $\vec{a}_n = \vec{0}$, the wave functions of the homogeneous electron gas are recovered.

The kinetic-energy density is

$$\begin{aligned} e_{kin} &= \sum_n f_n \frac{\hbar^2}{2m} \left|\vec{\nabla}\psi_n(\vec{r})\right|^2 \overset{\text{Eq. } E.6}{=} \sum_n f_n \frac{\hbar^2}{2m} \psi_n^*(\vec{r})\psi_n(\vec{r}) \left(\vec{a}_n^2 + \vec{k}_n^2\right) \\ &= \underbrace{\sum_n f_n \frac{\hbar^2 \vec{k}_n^2}{2m} \psi_n^*(\vec{r})\psi_n(\vec{r})}_{E_{kin}/\Omega \text{ of the homogenous electron gas}} + \underbrace{\frac{\hbar^2}{2m} \sum_n f_n \psi_n^*(\vec{r})\psi_n(\vec{r}) \cdot \vec{a}_n^2}_{\rightsquigarrow T_W/\Omega} \end{aligned} \tag{E.8}$$

which has two terms. One term is the kinetic-energy density for $\vec{a} = \vec{0}$, which is the kinetic energy for a homogeneous electron gas. The other will result in the correction T_W of v. Weizsäcker.

The density gradient is related to the vectors $\vec{a}_n$

$$\vec{\nabla} n \overset{\text{Eq. } E.6}{=} \sum_n f_n \psi_n^*(\vec{r})\psi_n(\vec{r}) 2\vec{a}_n \tag{E.9}$$

Now comes an ingenious[3] trick: v. Weizsäcker imposes Eq. E.9 for a specified density gradient as constraint on the values for $\vec{a}_n$. Then he minimizes the kinetic-energy density Eq. E.8 under that constraint.

$$\begin{aligned} e_{kin} = \sum_n f_n \frac{\hbar^2 \vec{k}_n^2}{2m} \psi_n^*(\vec{r})\psi_n(\vec{r}) + \min_{\vec{a}_n} \operatorname{stat}_{\lambda} \Bigg\{ & \frac{\hbar^2}{2m} \sum_n f_n \psi_n^*(\vec{r})\psi_n(\vec{r}) \cdot \vec{a}_n^2 \\ & - \frac{\hbar^2}{2m} \vec{\lambda} \Big(\sum_n f_n \psi_n^*(\vec{r})\psi_n(\vec{r}) 2\vec{a}_n - \vec{\nabla} n(\vec{r}) \Big) \Bigg\} \end{aligned} \tag{E.10}$$

The minimum condition for the variation of $\vec{a}_n$ yields

$$\vec{a}_n = \vec{\lambda} \tag{E.11}$$

which implies that the optimum set of vectors a_n is state independent.

The value of λ is determined so that the constraint is satisfied.

$$\vec{\nabla} n \overset{\vec{a}_n = \vec{\lambda}}{=} \underbrace{\sum_n f_n \psi_n^*(\vec{r})\psi_n(\vec{r})}_{n} 2 \underbrace{\vec{a}_n}_{\vec{\lambda} \text{ Eq. E.11}} \qquad \Rightarrow \qquad \lambda = \vec{a}_n = \frac{\vec{\nabla} n}{2n} \tag{E.12}$$

Finally, we insert this expression for $\vec{a}_n$ into the expression for the kinetic energy Eq. E.8 obtained

[3] I am not yet sure, whether this is physics or number-magic. Given the local ansatz for the wave function, I have some doubts whether such a variational principle for the local density is justified. It serves the purpose to remove the freedom of choice of the Ansatz.

earlier

$$e_{kin} \overset{\text{Eq. } E.8}{=} \underbrace{\sum_n f_n \frac{\hbar^2 \vec{k}_n^2}{2m} \psi_n^*(\vec{r})\psi_n(\vec{r})}_{E_{kin}/\Omega \text{ of the homogenous electron gas}} + \frac{\hbar^2}{2m} \underbrace{\sum_n f_n \psi_n^*(\vec{r})\psi_n(\vec{r})}_{n} \cdot \underbrace{\left(\frac{\vec{\nabla} n}{2n}\right)^2}_{\vec{a}_n^2}$$

$$= \underbrace{\sum_n f_n \frac{\hbar^2 \vec{k}^2}{2m} \psi_n^*(\vec{r})\psi_n(\vec{r})}_{E_{kin}/\Omega \text{ of the homogenous electron gas}} + \underbrace{\frac{\hbar^2}{8m} \frac{\left(\vec{\nabla} n\right)^2}{n}}_{T_W/\Omega} \tag{E.13}$$

So far, the derivation has been for spin-less electrons. When we include both spin contributions, we obtain for the gradient correction of Weizsäcker

$$T_W = \frac{\hbar^2}{8m} \sum_{\sigma \in \{\uparrow,\downarrow\}} \frac{\left(\vec{\nabla} n_\sigma\right)^2}{n_\sigma} \tag{E.14}$$

For electrons with a fixed spin-polarization factor ζ

$$\zeta \overset{\text{def}}{=} \frac{n_s}{n_t} \qquad \Rightarrow \qquad n_\uparrow = \frac{1+\zeta}{2} n_t \qquad \text{and} \qquad n_\downarrow = \frac{1-\zeta}{2} n_t \tag{E.15}$$

the result depends only on the total density and not on the spin-polarization factor ζ.

$$T_W = \frac{\hbar^2}{8m} \sum_{\sigma \in \{\uparrow,\downarrow\}} \frac{\left(\vec{\nabla} n_\sigma\right)^2}{n_\sigma} = \frac{\hbar^2}{8m} \frac{\left(\vec{\nabla} n_t\right)^2}{n_t} \left(\frac{\left(\frac{1+\zeta}{2}\right)^2}{\frac{1+\zeta}{2}} + \frac{\left(\frac{1-\zeta}{2}\right)^2}{\frac{1-\zeta}{2}} \right) = \frac{\hbar^2}{8m} \frac{\left(\vec{\nabla} n_t\right)^2}{n_t} \tag{E.16}$$

This confirms the gradient correction Eq. E.3 for the kinetic energy.

E.3 Hartree-Fock description of the free-electron gas

Here, we derive the changes in the dispersion relation $\epsilon(\vec{k})$ of the free-electron gas due to the exchange potential discussed in section 2.6.6 on p. 87.

Because of the translation symmetry, we can assume that the charge density is spatially constant.[4] Since the problem is translation invariant, we can furthermore deduce that the eigenstates are plane waves.

E.3.1 Exchange potential as non-local potential

Let us evaluate the non-local exchange potential Eq. 2.37 using plane waves

$$\varphi_{\vec{k},\sigma}(\vec{r},\sigma') = \langle \vec{r},\sigma' | \varphi_{\vec{k},\sigma} \rangle = \frac{1}{\sqrt{\Omega}} e^{i\vec{k}\vec{r}} \delta_{\sigma,\sigma'} \tag{E.17}$$

as defined in Eq. 1.36 as basis functions.

The exchange potential $\hat{V}_X$ has been expressed in terms of the one-particle-reduced density matrix $\hat{\rho}^{(1)}$ as

$$V_X(\vec{x},\vec{x}') \overset{\text{Eq. } 2.37}{=} -\sum_{j=1}^{N} \frac{e^2 \rho^{(1)}(\vec{x},\vec{x}')}{4\pi\epsilon_0 |\vec{r} - \vec{r}'|} \tag{E.18}$$

[4] We assume that there is no symmetry breaking.

with the one-particle-reduced density matrix Eq. 2.15

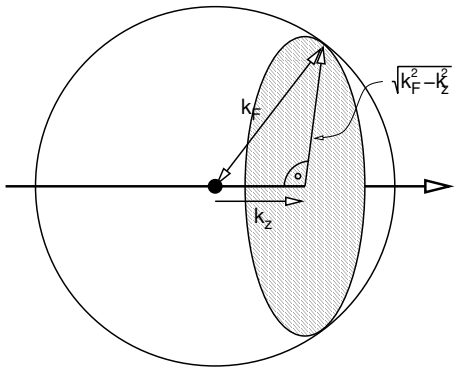
$$\begin{aligned}\rho^{(1)}(\vec{x},\vec{x'}) &\overset{\text{Eq. 2.15}}{=} \sum_{n=1}^{\infty}\langle\vec{x}|\varphi_n\rangle f_n\langle\varphi_n|\vec{x'}\rangle \\ &\overset{\text{Eq. 1.36}}{=} \sum_{\vec{k}}\theta(k_F-|\vec{k}|)\underbrace{\frac{\overbrace{(2\pi)^3}^{1}}{\Omega}}_{\to d^3k}\frac{\Omega}{(2\pi)^3}\frac{\delta_{\sigma,\sigma'}}{\Omega}e^{i\vec{k}(\vec{r'}-\vec{r})} \\ &= \frac{\delta_{\sigma,\sigma'}}{(2\pi)^3}\int d^3k\;\theta(k_F-|\vec{k}|)e^{i\vec{k}(\vec{r'}-\vec{r})} \end{aligned} \tag{E.19}$$

where $\theta(x)$ is the Heaviside step function and k_F is the Fermi momentum. The **Fermi momentum** is defined for a free-electron gas and specifies the maximum wave vector of all occupied states. In other words, it is the radius of the so-called Fermi sphere. The electron density n is obtained as

$$n(\vec{r}) = \sum_{\sigma\in\{\uparrow,\downarrow}\rho^{(1)}(\vec{r},\sigma,\vec{r},\sigma) \overset{\text{Eq. E.19}}{=} \frac{2}{(2\pi)^3}\frac{4\pi}{3}k_F^3 \qquad with \qquad k_F = 2\pi\sqrt[3]{\frac{1}{2}\frac{3n}{4\pi}} \tag{E.20}$$

This relation[5] is used to obtain the Fermi momentum from a given electron density.

The integral in Eq. E.19 is isotropic in $\vec{r'}-\vec{r}$. Thus, we can assume, without loss of generality, that the distance vector $\vec{r'}-\vec{r}$ points in z-direction, that is $\vec{r'}-\vec{r}=\vec{e}_z s$ with $s=|\vec{r'}-\vec{r}|$. $\vec{e}_z$ is the unit vector pointing in z-direction.



[5] The factor 1/2 stems from the spin degeneracy for a paramagnetic free-electron gas.

Let us resolve the integral without the factors.

$$\begin{aligned}
\int d^3k\ \theta(k_F - |\vec{k}|)\mathrm{e}^{i\vec{k}\vec{e}_z s} &= \int_{\vec{k}\leq k_F} d^3k\ \mathrm{e}^{ik_z s} = \int_{-k_F}^{k_F} dk_z\ \mathrm{e}^{ik_z s} \underbrace{\int_{k_x^2+k_y^2<k_F^2-k_z^2} dk_x dk_y}_{\pi(k_F^2-k_z^2)} \\
&= \int_{-k_F}^{k_F} dk_z\ \pi(k_F^2 - k_z^2)\mathrm{e}^{ik_z s} \\
&= \pi k_F^2 \int_{-k_F}^{k_F} dk_z\ \mathrm{e}^{ik_z s} - \pi \int_{-k_F}^{k_F} dk_z\ k_z^2 \mathrm{e}^{ik_z s} \\
&= \pi k_F^2 \int_{-k_F}^{k_F} dk_z\ \mathrm{e}^{ik_z s} + \pi \frac{d^2}{ds^2} \int_{-k_F}^{k_F} dk_z\ \mathrm{e}^{ik_z s} \\
&= \pi \left[k_F^2 + \frac{d^2}{ds^2}\right] \left[\frac{1}{is}\mathrm{e}^{ik_z s}\right]_{-k_F}^{k_F} \\
&= \pi \left[k_F^2 + \frac{d^2}{ds^2}\right] \frac{\mathrm{e}^{ik_F s} - \mathrm{e}^{-ik_F s}}{is} \\
&= 2\pi k_F^3 \left[1 + \frac{d^2}{d(k_F s)^2}\right] \frac{\sin(k_F s)}{k_F s} \\
&= 2\pi k_F^3 \left[\left(1 + \frac{d^2}{dx^2}\right) \frac{\sin(x)}{x}\right]_{x=k_F s} \\
&= 2\pi k_F^3 \left[\frac{\sin(x)}{x} - \frac{\sin(x)}{x} - \frac{2\cos(x)}{x^2} + \frac{2\sin(x)}{x^3}\right]_{x=k_F s} \\
&= \frac{4\pi}{3} k_F^3 \left[-3\frac{\cos(k_F s)}{(k_F s)^2} + 3\frac{\sin(k_F s)}{(k_F s)^3}\right]
\end{aligned} \tag{E.21}$$

Now we insert the integral Eq. E.21 into the one-particle-reduced density matrix Eq. E.19

$$\begin{aligned}
\rho^{(1)}(\vec{x},\vec{x'}) &\overset{\text{Eq. E.19}}{=} \frac{\delta_{\sigma,\sigma'}}{(2\pi)^3} \int d^3k\ \theta(k_F - |\vec{k}|)\mathrm{e}^{i\vec{k}(\vec{r'}-\vec{r})} \\
&\overset{\text{Eq. E.21}}{=} \frac{\delta_{\sigma,\sigma'}}{(2\pi)^3} \frac{4\pi}{3} k_F^3 \left[-3\frac{\cos(k_F|\vec{r}-\vec{r'}|)}{(k_F|\vec{r}-\vec{r'}|)^2} + 3\frac{\sin(k_F|\vec{r}-\vec{r'}|)}{(k_F|\vec{r}-\vec{r'}|)^3}\right]
\end{aligned} \tag{E.22}$$

Finally, I insert the one-particle-reduced density matrix Eq. E.22 into the expression for the non-local potential. With $s \overset{\text{def}}{=} |\vec{r}-\vec{r'}|$, we obtain

$$\begin{aligned}
V_X(\vec{x},\vec{x'}) &\overset{Eqs.\ E.18, E.22}{=} \frac{-e^2\delta_{\sigma,\sigma'}}{4\pi\epsilon_0|\vec{r}-\vec{r'}|} \frac{1}{(2\pi)^3} \underbrace{4\pi k_F^3 \left[-\frac{\cos(k_F s)}{(k_F s)^2} + \frac{\sin(k_F s)}{(k_F s)^3}\right]}_{\int d^3k\ \theta(k_F-|\vec{k}|)\mathrm{e}^{i\vec{k}(\vec{r'}-\vec{r})}} \\
&= \frac{e^2\delta_{\sigma,\sigma'}}{4\pi\epsilon_0 s} \frac{1}{(2\pi)^3} \frac{4\pi}{3} k_F^3 \left[3\frac{(k_F s)\cos(k_F s) - \sin(k_F s)}{(k_F s)^3}\right]
\end{aligned} \tag{E.23}$$

The exchange potential acts only between electrons of the same spin. It is important to realize that this non-local potential is not an interaction potential between two electrons, but it is a one-particle potential acting on each electron individually.

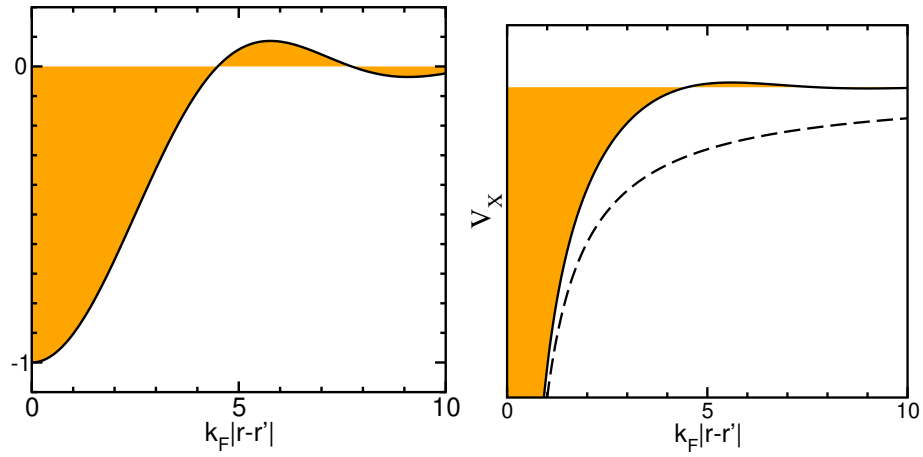


Fig. E.2: Non-local exchange potential $V_X(\vec{r},\sigma,\vec{r'},\sigma)$ Eq. E.23 as function of distance (right) for a free-electron gas as calculated in the Hartree-Fock method. The horizontal axis is $k_F|\vec{r}-\vec{r'}|$. The dashed line corresponds to a Coulomb interaction. On the left-hand side, the function $3\frac{x\cos(x)-\sin(x)}{x^3}$ is shown.

E.3.2 Exchange energy of the homogeneous electron gas

The exchange energy of the nonmagnetic homogeneous electron gas is obtained as

$$
\begin{aligned}
E_X^P &= -\frac{1}{2}\int d^4x \int d^4x' \, \frac{e^2\rho(\vec{x},\vec{x'})\rho(\vec{x'},\vec{x})}{4\pi\epsilon_0|\vec{r}-\vec{r'}|} \\
&\overset{\text{Eq. E.22}}{=} -\frac{1}{2}\int d^4x \int d^4x' \, \frac{e^2}{4\pi\epsilon_0|\vec{r}-\vec{r'}|}\left\{\frac{\delta_{\sigma,\sigma'}}{(2\pi)^3}\frac{4\pi}{3}k_F^3\left[-3\frac{\cos(k_F|\vec{r}-\vec{r'}|)}{(k_F|\vec{r}-\vec{r'}|)^2}+3\frac{\sin(k_F|\vec{r}-\vec{r'}|)}{(k_F|\vec{r}-\vec{r'}|)^3}\right]\right\}^2 \\
&= -\frac{1}{2}\int d^3r \sum_\sigma 4\pi\int_0^\infty ds\, s^2 \frac{e^2}{4\pi\epsilon_0 s}\left\{\frac{1}{(2\pi)^3}\frac{4\pi}{3}k_F^3\left[-3\frac{\cos(k_Fs)}{(k_Fs)^2}+3\frac{\sin(k_Fs)}{(k_Fs)^3}\right]\right\}^2 \\
&= -\frac{1}{2}\int d^3r \sum_\sigma \frac{e^2}{4\pi\epsilon_0}\frac{4\pi}{k_F^2}\left\{\frac{1}{(2\pi)^3}\frac{4\pi}{3}k_F^3\right\}^2\int_0^\infty d(k_Fs)\,(k_Fs)^2\frac{1}{k_Fs}\left\{\left[-3\frac{\cos(k_Fs)}{(k_Fs)^2}+3\frac{\sin(k_Fs)}{(k_Fs)^3}\right]\right\}^2 \\
&= -\frac{1}{2}\int d^3r \sum_\sigma \frac{e^2}{4\pi\epsilon_0}\underbrace{\frac{9\cdot 4\pi}{k_F^2}}_{\frac{9\cdot4\pi}{(3\pi^2 n_t)^{\frac{2}{3}}}}\underbrace{\left\{\frac{1}{(2\pi)^3}\frac{4\pi}{3}k_F^3\right\}^2}_{(\frac{1}{2}n_t)^2\quad\text{Eq. E.20}}\underbrace{\int_0^\infty dx\,\frac{\left(\sin(x)-x\cos(x)\right)^2}{x^5}}_{\frac{1}{4}} \\
&= -\left(\frac{1}{2}\sum_{\sigma\in\{\uparrow,\downarrow\}}\right)\frac{e^2}{4\pi\epsilon_0}\frac{9\cdot 4\pi\frac{1}{4}\frac{1}{4}}{(3\pi^2)^{\frac{2}{3}}}\int d^3r\, n_t^{\frac{4}{3}} = -\left(\frac{1}{2}\sum_{\sigma\in\{\uparrow,\downarrow\}}\right)\frac{e^2}{4\pi\epsilon_0}\frac{3}{4}\left(\frac{3^3\pi^3}{3^2\pi^4}\right)^{\frac{1}{3}}\int d^3r\, n_t^{\frac{4}{3}} \\
&= -\underbrace{\left(\frac{1}{2}\sum_{\sigma\in\{\uparrow,\downarrow\}}\right)}_{=1}\underbrace{\frac{e^2}{4\pi\epsilon_0}}_{1H}\frac{3}{4}\left(\frac{3}{\pi}\right)^{\frac{1}{3}}\int d^3r\, n_t^{\frac{4}{3}} \qquad \text{(E.24)}
\end{aligned}
$$

The integral over $x = k_F s$ is solved in the footnote.[6]

The spin polarization dependence can be included when we exploit that the exchange consists of two independent spin contributions.

$$\begin{aligned} E_X(n_\uparrow, n_\downarrow) &= \frac{1}{2} \sum_{\sigma \in \{\uparrow,\downarrow\}} E_X^P(2n_\sigma) \\ &= -\frac{3}{4}\left(\frac{3}{\pi}\right)^{\frac{1}{3}} \underbrace{\frac{e^2}{4\pi\epsilon_0}}_{1H} \int d^3r \, \frac{(2n_\uparrow)^{\frac{4}{3}} + (2n_\downarrow)^{\frac{4}{3}}}{2} \\ &= -\frac{3}{4}\left(\frac{3}{\pi}\right)^{\frac{1}{3}} \underbrace{\frac{e^2}{4\pi\epsilon_0}}_{1H} \int d^3r \, n_t^{\frac{4}{3}} \frac{(1+\zeta)^{\frac{4}{3}} + (1-\zeta)^{\frac{4}{3}}}{2} \qquad \text{with } n_t = n_\uparrow + n_\downarrow \text{ and } \zeta = \frac{n_\uparrow - n_\downarrow}{n_t} \end{aligned} \tag{E.27}$$

E.3.3 Energy-level shifts by the exchange potential

In order to obtain the change of the band structure by the interaction, we need to evaluate the expectation values of this potential.

$$\begin{aligned} d\epsilon_n &= \langle \varphi_n | \hat{V}_X | \varphi \rangle = \int d^4x \int d^4x' \, \varphi_n^*(\vec{x}) V_X(\vec{x}, \vec{x'}) \varphi(\vec{x'}) \\ d\epsilon_{\vec{k},\sigma} &\overset{\text{Eq. E.17}}{=} \frac{1}{\Omega} \int d^3r \int d^3r' \, V_X(\vec{r}, \sigma, \vec{r'}, \sigma) e^{i\vec{k}(\vec{r}-\vec{r'})} \\ &= \int d^3s \, V_X(s) e^{i\vec{k}\vec{s}} \end{aligned} \tag{E.28}$$

whee I introduced the short-hand notation $V_X(s)$ for Eq. E.23, which makes evident that the exchange potential of the free-electron gas depends only on the distance between the two electron coordinates (and the relative spin orientation).

Now, we decompose the plane wave into spherical harmonics(see appendix "Distributionen, d-

[6] Solve the integral

$$\begin{aligned} \int_a^b dx \, \frac{[\sin(x) - x\cos(x)]^2}{x^5} &= \int_a^b dx \left(\frac{\sin^2(x)}{x^5} - 2\frac{\sin(x)\cos(x)}{x^4} + \frac{\cos^2(x)}{x^3} \right) \\ &= \frac{1}{2} \int_a^b d(2x) \left(2^5 \frac{\frac{1}{2}(1-\cos^2(2x))}{(2x)^5} - 2^5 \frac{\frac{1}{2}\sin(2x)}{(2x)^4} + 2^3 \frac{\frac{1}{2}(1+\cos(2x))}{(2x)^3} \right) \\ &= 2 \int_{2a}^{2b} dy \left(4\frac{1-\cos(y)}{y^5} - 4\frac{\sin(y)}{y^4} + \frac{1+\cos(y)}{y^3} \right) \\ &= 2 \left[-\frac{1}{x^4} - \frac{1}{2x^2} + \frac{\cos(x)}{x^4} + \frac{\sin(x)}{x^3} \right]_{2a}^{2b} \\ \int_0^\infty dx \, \frac{[\sin(x) - x\cos(x)]^2}{x^5} &= \frac{1}{4} \end{aligned} \tag{E.25}$$

Let me now use

$$\begin{aligned} \partial_x x^{-4}\cos(x) &= -4x^{-5}\cos(x) - x^{-4}\sin(x) \\ \partial_x x^{-3}\sin(x) &= -3x^{-4}\sin(x) + x^{-3}\cos(x) \\ \partial_x \left(-\frac{\cos(x)}{x^4} - \frac{\sin(x)}{x^3} \right) &= 4\frac{\cos(x)}{x^5} + \frac{\sin(x)}{x^4} + 3\frac{\sin(x)}{x^4} - \frac{\cos(x)}{x^4} \\ \left. \frac{\cos(x)}{x^4} + \frac{\sin(x)}{x^3} \right|_{2a}^{2b} &= \int_{2a}^{2b} dx \left(-4\frac{\cos(x)}{x^5} - 4\frac{\sin(x)}{x^4} + \frac{\cos(x)}{x^4} \right) \end{aligned} \tag{E.26}$$

Funktionen und Fourier transformationen in the text book of Messiah[172])

$$e^{i\vec{k}\vec{r}} = 4\pi \sum_{\ell=1}^{\infty} \sum_{m=-\ell}^{\ell} i^{\ell} j_{\ell}(|\vec{k}||\vec{r}|) Y^*_{\ell,m}(\vec{k}) Y^*_{\ell,m}(\vec{r}) \tag{E.29}$$

Insertion yields

$$\begin{aligned} d\epsilon_{\vec{k},\sigma} &= \int d^3s\, V_x(s) 4\pi \sum_{\ell=1}^{\infty} \sum_{m=-\ell}^{\ell} i^{\ell} j_{\ell}(|\vec{k}||\vec{s}|) Y^*_{\ell,m}(\vec{k}) Y^*_{\ell,m}(\vec{s}) \\ &= 4\pi \sum_{\ell=1}^{\infty} \sum_{m=-\ell}^{\ell} i^{\ell} Y^*_{\ell,m}(\vec{k}) \int d^3s\, V_x(s) j_{\ell}(|\vec{k}||\vec{s}|) Y^*_{\ell,m}(\vec{s}) \end{aligned} \tag{E.30}$$

Because the non-local potential is isotropic, only the term with $\ell = 0$ contributes.

$$\begin{aligned} d\epsilon_{\vec{k},\sigma} &= 4\pi \underbrace{Y^*_{0,0}(\vec{k})}_{\frac{1}{\sqrt{4\pi}}} \int d^3s\, V_x(s) \underbrace{j_0(|\vec{k}||\vec{s}|)}_{j_0(x)=\frac{\sin(x)}{x}} \underbrace{Y^*_{0,0}(\vec{s})}_{\frac{1}{\sqrt{4\pi}}} \\ &= \int d^3s\, V_x(s) \frac{\sin(|\vec{k}||\vec{s}|)}{|\vec{k}||\vec{s}|} \\ &\overset{s \overset{\text{def}}{=} |\vec{s}|}{=} 4\pi \int_0^{\infty} ds\, s^2 V_x(s) \frac{\sin(|\vec{k}|s)}{|\vec{k}|s} \\ &= \frac{4\pi}{|\vec{k}|} \int_0^{\infty} ds\, V_X(s) s \sin(|\vec{k}|s) \\ &\overset{\text{Eq. } E.23}{=} \frac{4\pi}{|\vec{k}|} \int_0^{\infty} ds\, \frac{e^2}{4\pi\epsilon_0 s} \frac{1}{(2\pi)^3} \frac{4\pi}{3} k_F^3 \left[3\frac{k_F s \cos(k_F s) - \sin(k_F s)}{(k_F s)^3} \right] s\, \sin(|\vec{k}|s) \\ &= \frac{4\pi}{|\vec{k}|} \frac{e^2}{4\pi\epsilon_0} \frac{1}{(2\pi)^3} \frac{4\pi}{3} k_F^3 \int_0^{\infty} ds\, \left[3\frac{k_F s \cos(k_F s) - \sin(k_F s)}{(k_F s)^3} \right] \sin(|\vec{k}|s) \\ &\overset{x \overset{\text{def}}{=} k_F s}{=} \frac{4\pi}{k_F |\vec{k}|} \frac{e^2}{4\pi\epsilon_0} \frac{1}{(2\pi)^3} \frac{4\pi}{3} k_F^3 \int_0^{\infty} dx\, \left[3\frac{x\cos(x) - \sin(x)}{x^3} \right] \sin\left(\frac{|\vec{k}|}{k_F} x \right) \end{aligned} \tag{E.31}$$

Now we need to solve the integral

$$I = \int_0^{\infty} dx\, \left[3\frac{x\cos(x) - \sin(x)}{x^3} \right] \sin(ax) \tag{E.32}$$

where $a = |\vec{k}|/k_F$. The difficulty with this integral is that we cannot take the two terms apart, because the individual parts of the integrand diverge at the origin. Thus, during the derivation, we have to deal with divergent expressions.

$$\partial_x \frac{\sin(x)}{x^{n-1}} = -(n-1)\frac{\sin(x)}{x^n} + \frac{\cos(x)}{x^{n-1}}$$
$$\Rightarrow \frac{\sin(x)}{x^n} = \frac{1}{(n-1)}\left[\frac{\cos(x)}{x^{n-1}} - \partial_x \frac{\sin(x)}{x^{n-1}}\right] \tag{E.33}$$

$$\overset{\text{Eq. } E.33}{\Rightarrow} \int_0^\infty dx \frac{\sin(x)}{x^3}\sin(ax) = \frac{1}{2}\int_0^\infty dx\ \frac{\cos(x)}{x^2}\sin(ax) - \frac{1}{2}\int_0^\infty dx\ \sin(ax)\partial_x\frac{\sin(x)}{x^2}$$
$$= \frac{1}{2}\int_0^\infty dx \frac{\cos(x)}{x^2}\sin(ax)$$
$$-\frac{1}{2}\left[\sin(ax)\frac{\sin(x)}{x^2}\right]_0^\infty + \frac{a}{2}\int_0^\infty dx\ \frac{\sin(x)}{x^2}\cos(ax)$$
$$= \frac{a}{2} + \frac{1}{2}\int_0^\infty dx \frac{\cos(x)\sin(ax) + a\sin(x)\cos(ax)}{x^2} \tag{E.34}$$

$$\overset{\text{Eq. } E.33}{\Rightarrow} \int_0^\infty dx \frac{\sin(x)}{x^2}\cos(ax) = \int_0^\infty dx\ \frac{\cos(x)}{x}\cos(ax) - \int_0^\infty dx\ \cos(ax)\partial_x\frac{\sin(x)}{x}$$
$$= \int_0^\infty dx \frac{\cos(x)}{x}\cos(ax)$$
$$-\left[\cos(ax)\frac{\sin(x)}{x}\right]_0^\infty - a\int_0^\infty dx\ \frac{\sin(x)}{x}\sin(ax)$$
$$= 1 + \int_0^\infty dx \frac{\cos(x)\cos(ax) - a\sin(x)\sin(ax)}{x} \tag{E.35}$$

Thus, we obtain

$$\begin{aligned}
I &= 3\int_0^\infty dx\ \frac{x\cos(x) - \sin(x)}{x^3}\sin(ax) \\
&= 3\int_0^\infty dx\ \frac{\cos(x)\sin(ax)}{x^2} - 3\int_0^\infty dx\ \frac{\sin(x)\sin(ax)}{x^3} \\
&\overset{\text{Eq. } E.34}{=} 3\int_0^\infty dx\ \frac{\cos(x)\sin(ax)}{x^2} - \frac{3a}{2} - \frac{3}{2}\int_0^\infty dx\ \frac{\cos(x)\sin(ax) + a\sin(x)\cos(ax)}{x^2} \\
&= -\frac{3a}{2} + \frac{3}{2}\int_0^\infty dx\ \frac{\cos(x)\sin(ax)}{x^2} - \frac{3a}{2}\int_0^\infty dx\ \frac{\sin(x)\cos(ax)}{x^2} \\
&= -\frac{3a}{2} + \frac{3a}{2}\int_0^\infty dy\ \frac{\cos(\frac{1}{a}y)\sin(y)}{y^2} - \frac{3a}{2}\int_0^\infty dx\ \frac{\sin(x)\cos(ax)}{x^2} \\
&\overset{\text{Eq. } E.35}{=} -\frac{3a}{2} + \frac{3a}{2}\left[1 + \int_0^\infty dy\ \frac{\cos(\frac{1}{a}y)\cos(y) - \frac{1}{a}\sin(\frac{1}{a}y)\sin(y)}{y}\right] \\
&\quad -\frac{3a}{2}\left[1 + \int_0^\infty dx\ \frac{\cos(ax)\cos(x) - a\sin(ax)\sin(x)}{x}\right] \\
&= -\frac{3a}{2} + \frac{3a}{2}\left[\int_0^\infty dx\ \frac{\cos(x)\cos(ax) - \frac{1}{a}\sin(x)\sin(ax)}{x}\right] \\
&\quad -\frac{3a}{2}\left[\int_0^\infty dx\ \frac{\cos(ax)\cos(x) - a\sin(ax)\sin(x)}{x}\right] \\
&= -\frac{3a}{2} + \frac{3a}{2}(-\frac{1}{a} + a)\left[\int_0^\infty dx\ \frac{\sin(x)\sin(ax)}{x}\right] \\
&= -\frac{3a}{2} + \frac{3}{2}(a^2 - 1)\left[\int_0^\infty dx\ \frac{\sin(x)\sin(ax)}{x}\right]
\end{aligned}$$

We recognize that the integral is the Fourier transform of $\frac{\sin(x)}{x}$. From the Fourier transform tables

of Bronstein[69] we take

$$\sqrt{\frac{2}{\pi}}\int_0^\infty dx\ \sin(xy)\frac{\sin(ax)}{x} \overset{Bronstein}{=} \frac{1}{\sqrt{2\pi}}\ln\left|\frac{y+a}{y-a}\right|$$
$$\overset{a\to 1;y\to a}{\Rightarrow}\int_0^\infty dx\ \sin(ax)\frac{\sin(x)}{x} = \frac{1}{2}\ln\left|\frac{a+1}{a-1}\right| = \frac{1}{2}\ln\left|\frac{1+a}{1-a}\right|$$

Thus, we obtain

$$I = -\frac{3a}{2} + \frac{3}{4}(a^2-1)\ln\left|\frac{1+a}{1-a}\right|$$

with $a = |\vec{k}|/k_F$ as defined below Eq. E.32. We are done with the Integral.

We insert the result into the correction for the energy eigenvalues Eq. E.31

$$\begin{aligned} d\epsilon_{\vec{k},\sigma} &\overset{\text{Eq. } E.31}{=} \frac{4\pi}{k_F|\vec{k}|}\frac{e^2}{4\pi\epsilon_0}\frac{1}{(2\pi)^3}\frac{4\pi}{3}k_F^3\left[-\frac{3a}{2}+\frac{3(a^2-1)}{4}\ln\left|\frac{a+1}{a-1}\right|\right] \\ &= \frac{4\pi}{k_F^2}\frac{e^2}{4\pi\epsilon_0}\frac{1}{(2\pi)^3}\frac{4\pi}{3}k_F^3\left[-\frac{3}{2}+\frac{3(a^2-1)}{4a}\ln\left|\frac{a+1}{a-1}\right|\right] \\ &= -\frac{e^2}{4\pi\epsilon_0}\frac{2k_F}{\pi}\left[\frac{1}{2}+\frac{1-a^2}{4a}\ln\left|\frac{1+a}{1-a}\right|\right] \end{aligned} \tag{E.36}$$

The function in parenthesis is shown in Fig. E.3 and the resulting dispersion relation is discussed in section 2.6.6 on p. 87.

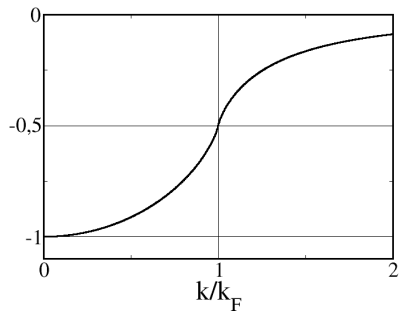


Fig. E.3: Lindhard function $f(a) = \left(\frac{1}{2} + \frac{1-a^2}{4a}\ln\left|\frac{1+a}{1-a}\right|\right)$ as function of $a = k/k_F$. The slope for $k = k_F$ is infinite. For $k \gg k_F$ the function approaches zero.

E.3.4 Density of states of the free-electron gas

The one-particle density of states of a non-interacting electrons has several physical meanings, which need to be differentiated when dealing with interacting electrons.

- The density of states is closely related to the thermodynamic properties of the system. Thus, the density of states can be obtained as the derivative of the number of electrons with respect to the Fermi level at zero temperature.

$$D(\epsilon) = \left.\frac{dN}{d\mu}\right|_{\mu=\epsilon} \tag{E.37}$$

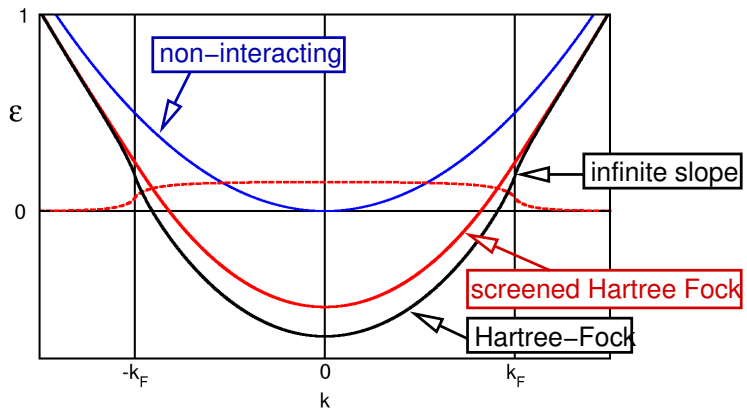


Fig. E.4: Dispersion relation $\epsilon(k)$ of the free-electron gas as calculated with Hartree-Fock (black), screened Hartree-Fock (red) and and without interactions (blue). The Fermi momentum has been chosen as $k_F = 1/a_0$ and the screening length for the screened Hartree-Fock calculation has been 6 a_0, where a_0 is the Bohr radius. The red, dashed line is the difference between the bands obtained with screened and unscreened Hartree-Fock. Only the bands of unscreened Hartree-Fock exhibit an infinite slope at the Fermi level. The Fermi level is at $\epsilon(k_F)$.

- The density of states summarizes the optical excitation spectrum. (It does not reflect matrix elements, though.) Thus, it reflects the **spectral function**.

The two definitions are different and need not produce the same result. Thus, we need to be careful when discussing the spectrum of the Hartree-Fock method or interacting systems in general.

Density of states of the free-electron gas from the energy levels of the Hartree-Fock approximation

In this section, I describe how the density of states for the Hartree-Fock spectrum in Fig. 2.6 on p. 89, respectively in Fig. E.5 below, has been evaluated.

Let me extract the density of states from the dispersion relation obtained from the Hartree-Fock approximation.

$$\epsilon_{\vec{k},\sigma} \overset{\text{Eq. ??}}{=} \frac{\hbar^2\vec{k}^2}{2m_e} - \frac{e^2}{4\pi\epsilon_0}\frac{2k_F}{\pi}\left[\frac{1}{2} + \frac{1-a^2}{4a}\ln\left|\frac{1+a}{1-a}\right|\right] \tag{E.38}$$

with $a = |\vec{k}|/k_F$ as defined below Eq. E.32

The number of states in a volume Ω for a given Fermi level μ at zero temperature is

$$N(\mu) = \Omega\int\frac{d^3k}{(2\pi)^3}\theta\big(\mu - \epsilon(\vec{k})\big) \tag{E.39}$$

The density of states is its derivative with respect to the Fermi level.

$$D(\epsilon) = \frac{dN(\epsilon)}{d\epsilon} \tag{E.40}$$

For the dispersion relation of the free-electron gas in the Hartree-Fock approximation, we obtain

$$N(\epsilon(k_F)) = \sum_{\sigma\in\uparrow,\downarrow}\frac{\frac{4\pi}{3}k_F^3}{(\frac{2\pi}{L})^3} = \Omega\sum_{\sigma\in\uparrow,\downarrow}\frac{k_F^3}{6\pi^2} \tag{E.41}$$

When doing the derivative we need to distinguish $k \stackrel{\text{def}}{=} |\vec{k}|$ and k_F. The band structure $\epsilon(k)$ depends on the Fermi momentum k_F. This is considered as a fixed parameter. The derivative is taken not with respect to k_F but with respect to k, which plays the role of the Fermi wave vector albeit in a rigid band structure.

Thus,

$$\begin{aligned} D(\epsilon(k)) &= \Omega \sum_{\sigma\in\uparrow,\downarrow} \frac{k^2}{2\pi^2} \left(\frac{d\epsilon}{dk}\right)^{-1} \\ &= \Omega \sum_{\sigma\in\uparrow,\downarrow} \frac{k^2}{2\pi^2} \left(\frac{\hbar^2\vec{k}}{m_e} - \frac{e^2}{4\pi\epsilon_0}\frac{2k_F}{\pi}\Big[\frac{-2a}{4a}\ln\left|\frac{1+a}{1-a}\right| - \frac{1-a^2}{4a^2}\ln\left|\frac{1+a}{1-a}\right| \right. \\ &\quad \left. + \frac{1-a^2}{4a}\left(\frac{1+a}{1-a}\right)^{-1}\Big(\frac{1}{1-a}+\frac{1+a}{(1-a)^2}\Big)\Big]\frac{1}{k_F}\right)^{-1} \\ &= \Omega \sum_{\sigma\in\uparrow,\downarrow} \frac{k^2}{2\pi^2} \left(\frac{\hbar^2\vec{k}}{m_e} - \frac{e^2}{4\pi\epsilon_0}\frac{2}{\pi}\Big[-\frac{1+a^2}{4a^2}\ln\left|\frac{1+a}{1-a}\right| + \frac{1}{2a}\Big]\right)^{-1} \end{aligned} \tag{E.42}$$

The density of states here is given as function of the wave vector. By plotting the energy as function of wave vector versus the density of state as function of wave vector, the density of states as function of energy is obtained.

We observe that the density of states of the free-electron gas vanishes at the Fermi level, i.e. for $a = 1$ due to the singularity of the logarithm. This behavior is nonphysical and it is healed by including electron correlation.

E.3.5 Exchange hole of the free-electron gas

The exchange hole can be expressed by the one-particle-reduced density matrix. The two-particle density can be extracted from the expression for the interaction energy of a Slater determinant.

$$n^{(2)}(\vec{r},\vec{r'}) = n(\vec{r})n(\vec{r'}) - \sum_{\sigma,\sigma'} \rho^{(1)}(\vec{x},\vec{x'})\rho^{(1)}(\vec{x'},\vec{x}) \tag{E.43}$$

$$\begin{aligned} h(\vec{r},\vec{r'}) &= \frac{n^{(2)}(\vec{r},\vec{r'}) - n^{(1)}(\vec{r})n^{(1)}(\vec{r'})}{n^{(1)}(\vec{r})} \\ &= -\frac{\sum_{\sigma,\sigma'}\left|\rho^{(1)}(\vec{r},\sigma,\vec{r'},\sigma')\right|^2}{\sum_{\sigma''}\rho^{(1)}(\vec{r},\sigma,\vec{r},\sigma'')} \\ &= \frac{1}{(2\pi)^3}\frac{4\pi}{3}k_F^3\left(-3\frac{\cos(k_F|\vec{r}-\vec{r'}|)}{(k_F|\vec{r}-\vec{r'}|)^2} + 3\frac{\sin(k_F|\vec{r}-\vec{r'}|)}{(k_F|\vec{r}-\vec{r'}|)^3}\right)^2 \end{aligned} \tag{E.44}$$

Because of the Coulomb singularity, the behavior of the exchange hole at the origin is important. To explore the behavior at the origin, I use the Taylor expansion

$$\begin{aligned} -3\frac{\cos(x)}{x^2} + 3\frac{\sin(x)}{x^3} &= -6\sum_{k=1}^{\infty}\frac{(-1)^k\cdot k}{(2k+1)!}x^{2k-2} \\ &= 1 - \frac{1}{10}x^2 + \frac{1}{280}x^4 + O(x^6) \end{aligned} \tag{E.45}$$

To approximate exchange-correlation hole, one could consider a Gaussian

$$h(\vec{r},\vec{r'}) \approx \frac{1}{(2\pi)^3}\frac{4\pi}{3}k_F^3\exp\left(-\frac{1}{5}\left(k_F|\vec{r}-\vec{r'}|\right)^2\right) \tag{E.46}$$

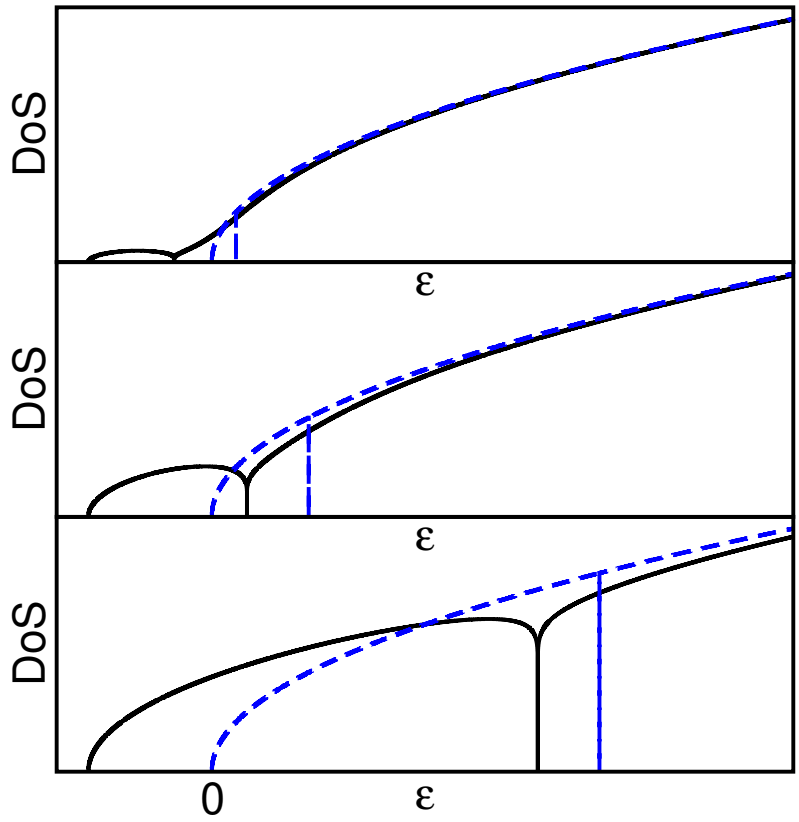


Fig. E.5: Density of states in the Hartree-Fock approximation (solid black) as compared to the free-electron gas (dashed blue) for different electron densities. The density of states is obtained from the energy dispersion of the Fock operator, and not from the thermodynamic properties, i.e. the total energies. The electron density increases from top to bottom. The density of states for the Hartree-Fock calculation drops to zero at the Fermi level. The energy of the bottom of the band is independent of the electron density and depends only on the strength of the interaction.

The approximate form reproduces the Taylor expansion near $\vec{r} = \vec{r'}$ up to third order in the distance, and it has a reasonable overall agreement.

As expected, the on-top value of the exchange hole is exactly one-half the electron density. The radius of the exchange hole is proportional to k_F, respectively $n^{\frac{1}{3}}$.

E.4 Polarization insertion

Editor: This section is under construction. Do not read!

In this section, I am evaluating the polarization insertion of the homogeneous electron gas in lowest order. A **polarization insertion** is a diagram with two external vertices that can be inserted into an interaction line. Specifically, I am limiting myself the most simple and therefore prototypical polarization integral, the **ring diagram**.

The polarization is at the origin of **screening** and of **life-time broadening**. It will provide an approximate expression for the momentum and frequency dependent dielectric constant. Furthermore, it underpins **Fermi-liquid theory** by demonstrating that the life-time broadening near the Fermi level is smaller than the quasi-particle energy $\epsilon - \mu$. Furthermore the polarization insertion is the starting point for **plasmons**.

Let me list a few statements taken from Mattuck[4].Editor: Caution regarding the units.

- The relative dielectric constant in the random-phase approximation is

$$\epsilon_r^{RPA}(q,\omega) = 1 + V_q \Pi_0(q,\omega) \tag{E.47}$$

  where V_q is the Fourier transform of the Coulomb interaction.

- The screened interaction is

$$V_{eff}^{RPA} = \frac{1}{\epsilon^{RPA}(q,\omega)} V_{\vec{q}} \tag{E.48}$$

  The screened interaction is frequency dependent. It describes that the system needs time to respond to a perturbation. Editor: This needs to be shown: the high-frequency limit of the dielectric constant approaches unity.

- the zeros of the dielectric constant provides a first estimate for the plasmon dispersion relation.

A derivation of the polarization insertion can be found in the textbook of Fetter and Walecka on p. 158, "Evaluation of Π^0".Editor: See also Caruso et al.[53]. Editor: Mattuck[4] refers to the p.93 of the textbook of T.D. Schultz, *"Quantum Field Theoryand the Many-Body problem"*Gordon Breach, 1964.

I redid the derivation myself in a slightly different manner and with a lot of detail in order to make the underlying principles evident and to understand, if and how the result can be carried beyond the free electron gas. Most importantly, I had to ensure that the result is compatible with a contour in the complex-time plane of the non-equilibrium Greens function. I will start from the fairly general expressions and I will become increasingly more specific as seems reasonable to keep the calculation managable. The reason is twofold. Once, the implications of the individual approximations shall become clear. Secondly, the more general equations may provide a suitable starting point for the implementation as computer code to obtain results for real materials.

The lowest order of the polarization insertion is the ring diagram, which is a product of two non-interacting Green's functions.

$$\Pi^{(0)}(\vec{r}_1,t_1,\vec{r}_2,t_2) \stackrel{\text{def}}{=} i\hbar \underbrace{(-1)}_{\text{Fermi loop}} \sum_{\sigma_1,\sigma_2\in\{\uparrow,\downarrow\}} G^{\mathcal{C},(0)}(\vec{x}_1,t_1,\vec{x}_2,t_2) G^{\mathcal{C},(0)}(\vec{x}_2,t_2,\vec{x}_1,t_1) \tag{E.49}$$

After considering the different normalization definitions.[7], this equation is equivalent to Eq.12.27 of Fetter-Walecka, The reason to connect the polarization insertion to two positions, rather than four orbitals, is that the interaction connects two, rather than four positions. Because the interaction is spin-independent, we perform the sum over spin degrees of freedom already inside the polarization insertion.

E.4.1 Polarisation insertion for homogeneous systems

The derivation is based on the contour Green's function for a time-independent Hamiltonian.

This derivation is limited to the homogeneous systems with plane waves as Hamilton eigenstates

$$\langle \vec{r},\sigma'|\vec{k},\sigma\rangle = \frac{1}{\sqrt{L^3}} e^{i\vec{k}\vec{r}} \delta_{\sigma,\sigma'} \tag{E.50}$$

I am considering a normalization volume L^3 and periodic boundary conditions for a cubic box with side-length L. This results in a discrete grid of k-points with spacing $\frac{2\pi}{L}$.

[7] The polarization insertion has been defined in FW-Eq.-9.39, where FW stands for the textbook of Fetter and Walecka.[3]. Eq. E.49 compares to FW-Eq. 12.27.[3]. The convention for the Green's function is obtained by the comparison in FW-Eq. 7.1, i.e. $G^{\Phi SX} = \frac{1}{\hbar} G^{FW}$. The factor 2 in the FW-Eq. 12.27 is absorbed in the sum over spin orbitals of our Eq. E.49

Initially, I do not limit the band structure $\epsilon_{\vec{k},\sigma}$ to the free-electron parabola, but allow for more general isotropic dispersion relations. Later, I will nevertheless introduce the free electron parabola to keep the derivation tractable.

While I will start from the finite-temperature formalism, the results will be worked out for zero temperature.

The zeroth-order polarization diagram requires only the non-interacting Green's function as input. The bare contour Green's function is given in Eq. 7.57 on p. 264, respectively from Eq. 7.31 on p. 258.

$$\hat{G}^{\mathcal{C},(0)}(t,t') \overset{\text{Eq. 7.57}}{=} \frac{1}{i\hbar}\sum_{\vec{k}}\sum_{\sigma\in\{\uparrow,\downarrow\}} |\vec{k},\sigma\rangle\Big\{\theta_{\mathcal{C}}(t-t')\Big(1-f_{T,\mu}(\epsilon_{\vec{k},\sigma})\Big)-\theta_{\mathcal{C}}(t'-t)f_{T,\mu}(\epsilon_{\vec{k},\sigma})\Big\} \times \mathrm{e}^{-\frac{i}{\hbar}\epsilon_{\vec{k},\sigma}(t-t')}\langle\vec{k},\sigma| \tag{E.51}$$

In position-and-spin representation this is

$$\overset{\text{Eq. E.50}}{\Rightarrow} G^{\mathcal{C},(0)}(\vec{x}_1,t_1,\vec{x}_2,t_2) = \frac{1}{i\hbar L^3}\sum_{\vec{k}}\sum_{\sigma\in\{\uparrow,\downarrow\}}\delta_{\sigma_1,\sigma}\delta_{\sigma_2,\sigma}\mathrm{e}^{i\vec{k}(\vec{r}_1-\vec{r}_2)}\mathrm{e}^{-\frac{i}{\hbar}\epsilon_{\vec{k},\sigma}(t_1-t_2)} \times\Big\{\theta_{\mathcal{C}}(t_1-t_2)\Big(1-f_{T,\mu}(\epsilon_{\vec{k},\sigma_1})\Big)-\theta_{\mathcal{C}}(t_2-t_1)f_{T,\mu}(\epsilon_{\vec{k},\sigma})\Big\} \tag{E.52}$$

The corresponding zeroth order polarization insertion Eq. E.49 is

$$\begin{aligned}
\Pi^{(0)}(\vec{r}_1,t_1,\vec{r}_2,t_2) &\overset{\text{Eq. E.49}}{=} i\hbar\underbrace{(-1)}_{\text{Fermi loop}}\sum_{\sigma_1,\sigma_2\in\{\uparrow,\downarrow\}} G^{\mathcal{C},(0)}(\vec{x}_1,t_1,\vec{x}_2,t_2)G^{\mathcal{C},(0)}(\vec{x}_2,t_2,\vec{x}_1,t_1)\\
&\overset{\text{Eq. E.52}}{=} i\hbar\underbrace{(-1)}_{\text{Fermi loop}}\sum_{\sigma_1,\sigma_2\in\{\uparrow,\downarrow\}}\\
&\times \underbrace{\frac{1}{i\hbar L^3}\sum_{\vec{k}}\sum_{\sigma\in\{\uparrow,\downarrow\}}\delta_{\sigma_1,\sigma}\delta_{\sigma_2,\sigma}\mathrm{e}^{i\vec{k}(\vec{r}_1-\vec{r}_2)}\mathrm{e}^{-\frac{i}{\hbar}\epsilon_{\vec{k},\sigma}(t_1-t_2)}\Big\{\theta_{\mathcal{C}}(t_1-t_2)\Big(1-f_{T,\mu}(\epsilon_{\vec{k},\sigma})\Big)-\theta_{\mathcal{C}}(t_2-t_1)f_{T,\mu}(\epsilon_{\vec{k},\sigma})\Big\}}_{G^{\mathcal{C},(0)}(\vec{x}_1,t_1,\vec{x}_2,t_2)}\\
&\times \underbrace{\frac{1}{i\hbar L^3}\sum_{\vec{k}'}\sum_{\sigma'\in\{\uparrow,\downarrow\}}\delta_{\sigma_1,\sigma'}\delta_{\sigma_2,\sigma'}\mathrm{e}^{i\vec{k}'(\vec{r}_2-\vec{r}_1)}\mathrm{e}^{-\frac{i}{\hbar}\epsilon_{\vec{k}',\sigma'}(t_2-t_1)}\Big\{\theta_{\mathcal{C}}(t_2-t_1)\Big(1-f_{T,\mu}(\epsilon_{\vec{k}',\sigma'})\Big)-\theta_{\mathcal{C}}(t_1-t_2)f_{T,\mu}(\epsilon_{\vec{k}',\sigma'})\Big\}}_{G^{\mathcal{C},(0)}(\vec{x}_2,t_2,\vec{x}_1,t_1)}\\
&= \frac{1}{i\hbar}\underbrace{(-1)}_{\text{Fermi loop}}\sum_{\sigma\in\{\uparrow,\downarrow\}}\overbrace{\frac{1}{L^6}\sum_{\vec{k},\vec{k}'}}^{\sim\int\frac{d^3k}{(2\pi)^3}\int\frac{d^3k'}{(2\pi)^3}}\mathrm{e}^{i(\vec{k}-\vec{k}')(\vec{r}_1-\vec{r}_2)}\mathrm{e}^{-\frac{i}{\hbar}\left(\epsilon_{\vec{k},\sigma}-\epsilon_{\vec{k}',\sigma}\right)(t_1-t_2)}\\
&\times \Big\{\theta_{\mathcal{C}}(t_1-t_2)\Big(1-f_{T,\mu}(\epsilon_{\vec{k},\sigma})\Big)-\theta_{\mathcal{C}}(t_2-t_1)f_{T,\mu}(\epsilon_{\vec{k},\sigma})\Big\}\\
&\times \Big\{\theta_{\mathcal{C}}(t_2-t_1)\Big(1-f_{T,\mu}(\epsilon_{\vec{k}',\sigma})\Big)-\theta_{\mathcal{C}}(t_1-t_2)f_{T,\mu}(\epsilon_{\vec{k}',\sigma})\Big\}\\
&= \frac{1}{i\hbar}\underbrace{(-1)}_{\text{Fermi loop}}\sum_{\sigma\in\{\uparrow,\downarrow\}}\frac{1}{L^6}\sum_{\vec{k},\vec{k}'}\mathrm{e}^{i(\vec{k}-\vec{k}')(\vec{r}_1-\vec{r}_2)}\mathrm{e}^{-\frac{i}{\hbar}\left(\epsilon_{\vec{k},\sigma}-\epsilon_{\vec{k}',\sigma}\right)(t_1-t_2)}\\
&\times \Big\{-\theta_{\mathcal{C}}(t_1-t_2)\Big(1-f_{T,\mu}(\epsilon_{\vec{k},\sigma})\Big)f_{T,\mu}(\epsilon_{\vec{k}',\sigma})-\theta_{\mathcal{C}}(t_2-t_1)f_{T,\mu}(\epsilon_{\vec{k},\sigma})\Big(1-f_{T,\mu}(\epsilon_{\vec{k}',\sigma})\Big)\Big\}\\
&= A(\vec{r}_2,t_2,\vec{r}_1,t_1)+A(\vec{r}_1,t_1,\vec{r}_2,t_2)
\end{aligned} \tag{E.53}$$

with

$$A(\vec{r}_1,t_1,\vec{r}_2,t_2) \stackrel{\text{def}}{=} \overbrace{\frac{i}{\hbar}\theta_{\mathcal{C}}(t_2-t_1)}^{-\theta_{\mathcal{C}}(t_2-t_1)\frac{1}{i\hbar}} \underbrace{(-1)}_{\text{Fermi loop}} \sum_{\sigma\in\{\uparrow,\downarrow\}} \overbrace{\frac{1}{L^6}\sum_{\vec{k},\vec{k}'}}^{\sim\int \frac{d^3k}{(2\pi)^3}\frac{d^3k'}{(2\pi)^3}} e^{i(\vec{k}-\vec{k}')(\vec{r}_1-\vec{r}_2)} e^{-\frac{i}{\hbar}\left(\epsilon_{\vec{k},\sigma}-\epsilon_{\vec{k}',\sigma}\right)(t_1-t_2)}$$
$$\times\ f_{T,\mu}(\epsilon_{\vec{k},\sigma})\Big(1-f_{T,\mu}(\epsilon_{\vec{k}',\sigma})\Big) \tag{E.54}$$

The function $A(x_1,t_1,x_2,t_2)$ contains the complete information of the polarization insertion. It is valid on the entire complex-valued-time contour.

Let me now work on $A(\vec{r}_1,t_1,\vec{r}_2,t_2)$: I introduce new variables $\vec{q}=\vec{k}'-\vec{k}$ and $\hbar\omega=\epsilon_{\vec{k}',\sigma}-\epsilon_{\vec{k},\sigma}=\epsilon_{\vec{k}+\vec{q},\sigma}-\epsilon_{\vec{k},\sigma}$.

$$\begin{aligned}
A(\vec{r}_1,t_1,\vec{r}_2,t_2) &= \theta_{\mathcal{C}}(t_2-t_1)\frac{i}{\hbar}\overbrace{(-1)}^{\text{Fermi loop}} \sum_{\sigma\in\{\uparrow,\downarrow\}} \overbrace{\frac{1}{L^3}\sum_{\vec{q}}}^{\sim\int\frac{d^3q}{(2\pi)^3}} e^{-i\vec{q}(\vec{r}_1-\vec{r}_2)} \overbrace{\frac{1}{L^3}\sum_{\vec{k}}}^{\sim\int\frac{d^3k}{(2\pi)^3}} f_{T,\mu}(\epsilon_{\vec{k},\sigma})\Big(1-f_{T,\mu}(\epsilon_{\vec{k}+\vec{q},\sigma}\Big) \\
&\quad\times \underbrace{\int_{-\infty}^{\infty} d\epsilon\ \delta(\epsilon-\epsilon_{\vec{k},\sigma})}_{=1} \underbrace{\int_{-\infty}^{\infty} d\epsilon'\ \delta(\epsilon'-\epsilon_{\vec{k}+\vec{q},\sigma})}_{=1} \underbrace{\int_{-\infty}^{\infty} d(\hbar\omega)\ \delta(\epsilon_{\vec{k}+\vec{q},\sigma}-\epsilon_{\vec{k},\sigma}-\hbar\omega)e^{i\omega(t_1-t_2)}}_{=e^{-\frac{i}{\hbar}(\epsilon_{\vec{k},\sigma}-\epsilon_{\vec{k}+\vec{q},\sigma})(t_1-t_2)}} \\
&= \theta_{\mathcal{C}}(t_2-t_1)\frac{i}{\hbar}\int_{-\infty}^{\infty} d(\hbar\omega)\ \overbrace{\frac{1}{L^3}\sum_{\vec{q}}}^{\sim\int\frac{d^3q}{(2\pi)^3}} e^{-i[\vec{q}(\vec{r}_1-\vec{r}_2)-\omega(t_1-t_2)]} \\
&\quad\times \underbrace{\overbrace{(-1)}^{\text{Fermi loop}} \sum_{\sigma\in\{\uparrow,\downarrow\}} \int d\epsilon \int d\epsilon'\ \delta(\epsilon'-\epsilon-\hbar\omega) f_{T,\mu}(\epsilon)\Big(1-f_{T,\mu}(\epsilon')\Big) \overbrace{\frac{1}{L^3}\sum_{\vec{k}}\ \delta(\epsilon-\epsilon_{\vec{k},\sigma})\ \delta(\epsilon'-\epsilon_{\vec{k}+\vec{q},\sigma})}^{K_{\vec{q},\sigma}(\epsilon,\epsilon')}}_{\bar{F}_{\vec{q}}(\hbar\omega)} \\
&= \theta_{\mathcal{C}}(t_2-t_1)\frac{i}{\hbar}\int_{-\infty}^{\infty} d(\hbar\omega)\ \overbrace{\frac{1}{L^3}\sum_{\vec{q}}}^{\sim\int\frac{d^3q}{(2\pi)^3}} e^{-i[\vec{q}(\vec{r}_1-\vec{r}_2)-\omega(t_1-t_2)]}\,\bar{F}_{\vec{q}}(\hbar\omega)
\end{aligned} \tag{E.55}$$

with

$$\begin{aligned}
\bar{F}_{\vec{q}}(\hbar\omega) &\stackrel{\text{def}}{=} \underbrace{(-1)}_{\text{Fermi loop}} \sum_{\sigma\in\{\uparrow,\downarrow\}} \int d\epsilon \int d\epsilon'\ \delta(\epsilon'-\epsilon-\hbar\omega) K_{\vec{q},\sigma}(\epsilon,\epsilon') f_{T,\mu}(\epsilon)\Big(1-f_{T,\mu}(\epsilon')\Big) \\
&= \underbrace{(-1)}_{\text{Fermi loop}} \sum_{\sigma\in\{\uparrow,\downarrow\}} \int d\epsilon\ f_{T,\mu}(\epsilon) K_{\vec{q},\sigma}(\epsilon,\epsilon+\hbar\omega)\Big(1-f_{T,\mu}(\epsilon+\hbar\omega)\Big)
\end{aligned} \tag{E.56}$$

and

$$K_{\vec{q},\sigma}(\epsilon,\epsilon') \stackrel{\text{def}}{=} \frac{1}{L^3}\sum_{\vec{k}} \delta(\epsilon-\epsilon_{\vec{k},\sigma})\delta(\epsilon'-\epsilon_{\vec{k}+\vec{q},\sigma}) \tag{E.57}$$

- Eq. E.53 for the polarization insertion is valid for complex-valued time arguments. It is limited to non-interacting systems that are translationally invariant in space and time. This enforces that the one-particle energies are time-independent and that the one-particle states are plane waves in real space. The dispersion relation $\epsilon_{\vec{k},\sigma}$, is given in the extended zone scheme but otherwiese not restricted.

- The function $\bar{F}_{\vec{q}}(\hbar\omega)$ is a real-valued quantity.
- For zero-temperature, the $\bar{F}_{\vec{q}}(\hbar\omega)$ vanishes for negative $\hbar\omega$.
- $K_{\vec{q},\sigma}(\epsilon,\epsilon')$ is the one-dimensional intersection of two energy iso-surfaces of the band structure $\epsilon_{\vec{k},\sigma}$. One of the iso-surfaces is displaced in k-space by $\vec{q}$.
- It must not be forgotten that $\bar{F}_{\vec{q}}(\hbar\omega)$ is not a Fourier transform of $A(\vec{r},t,\vec{r'},t')$, because we work on a complex time contour. Therefore, it cannot directly be compared to similar expressions in the literature. Thus, the Fourier transform must be recovered from "our" $\bar{F}(\vec{q},\hbar\omega')$ by a complicated frequency integration.
- In the expression above, the wave vectors are taken from a discrete grid. The discrete sum over k-points can be turned into into an integral using $\sum_{\vec{k}} \to L^3 \int \frac{d^3k}{(2\pi)^3}$. I exploit that the reciprocal-space volume per k-point is $(2\pi/L)^3$.

  The infinities resulting from the factor L^3 are balanced by the norm of the basisfunctions, which are themselfes normalized on a volume of size L^3.

  With the transition to continuous momenta, the Kronecker for the momentum transfer $\vec{q}$ must be converted into a delta-function $\delta_{\vec{q},\vec{q'}} = (2\pi/L)^3\delta(\vec{q}-\vec{q'}) = d^3q\ \delta(\vec{q}-\vec{q'})$. The volume element d^3q is used later to convert the integral for the discrete mesh of momentum transfers into a density of continous values.

E.4.2 Material-specific term $K_{\vec{q}}(\epsilon,\epsilon')$

The term $K_{\vec{q}}(\epsilon,\epsilon')$ defined in Eq. E.56 contains all material-specific information. It is the intersection of the iso-energy surfaces at ϵ,ϵ', which are displaced in k-space by the vector $\vec{q}$.

The expression for $K_{\vec{q}}(\epsilon,\epsilon')$ can be expressed in terms of derivatives of a volume integral by exploiting $\delta(x) = \partial_x\theta(x) = -\partial_x\theta(-x)$.

$$\begin{aligned} K_{\vec{q},\sigma}(\epsilon,\epsilon') &\overset{\text{Eq. E.57}}{=} \frac{1}{L^3}\sum_{\vec{k}} \delta(\epsilon-\epsilon_{\vec{k},\sigma})\delta(\epsilon'-\epsilon_{\vec{k}+\vec{q},\sigma}) \\ &= \frac{d}{d\epsilon}\frac{d}{d\epsilon'} \underbrace{\left\{ \overbrace{\frac{1}{L^3}\sum_{\vec{k}}}^{\sim\int\frac{d^3k}{(2\pi)^3}} \theta(\epsilon_{\vec{k},\sigma}-\epsilon)\theta(\epsilon_{\vec{k}+\vec{q},\sigma}-\epsilon') \right\}}_{=:(V+V')/(2\pi)^3} \end{aligned} \tag{E.58}$$

For isotropic systems the volume denoted above by $V+V'$ is the intersection of two spheres, to which we will return below.

Isotropic systems: I introduce the **assumption** that the system is isotropic. Isotropy implies that the energy levels $\epsilon_{\vec{k},\sigma}$ depend only on the length of the reciprocal lattice vector $|\vec{k}|$ but not on its direction. Instead of $\epsilon_\sigma(|\vec{k}|)$, I can use the inverse function $k_\sigma(\epsilon)$, which is the length of the wave vector as function of energy.

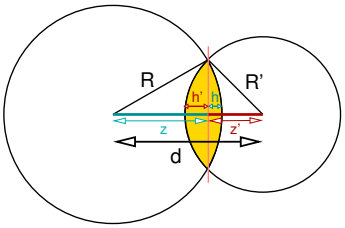
While I restrict the system by imposing isotropy, I leave the dispersion relation otherwise undetermined. The purpose is to explore also systems with a band gap.

With the isotropic dispersion relation, $K_{\vec{q},\sigma}(\epsilon,\epsilon')$ can be reduced to a geometric problem, namely to evaluate the common volume of two spheres, each with its own radius, which are displaced by a vector $\vec{q}$. The step functions in Eq. E.58 selects the overlap of two spheres in k-space. One sphere is centered at the origin $\vec{0}$ and has a radius $k_\sigma(\epsilon)$, and the other sphere is centered at $-\vec{q}$ and has

radius $k_\sigma(\epsilon')$. The integral for the sphere overlap is

$$\begin{aligned}\frac{V+V'}{(2\pi)^3} &= \int \frac{d^3k}{(2\pi)^3}\theta(\epsilon_{\vec{k},\sigma}-\epsilon)\theta(\epsilon_{\vec{k}+\vec{q},\sigma}-\epsilon') \\ &= \frac{1}{(2\pi)^3}\int d^3r\;\theta\big(R-|\vec{r}|\big)\theta\big(R'-|\vec{r}-d\vec{e}_z|\big)\end{aligned} \tag{E.59}$$

where I introduced more convenient symbols:



$$\begin{aligned} d &\stackrel{\text{def}}{=} |\vec{q}| \\ R(\epsilon) &\stackrel{\text{def}}{=} k_\sigma(\epsilon) \\ R'(\epsilon') &\stackrel{\text{def}}{=} k_\sigma(\epsilon') \end{aligned} \tag{E.60}$$

$\vec{e}_z$ is the unit vector in z-direction. (The choice of this direction is irrelevant.) The volume of the lens-shaped overlap of the two spheres is worked out below. Considering also the derivatives in Eq. E.58 yields Eq. E.67, which I will use below.

Thus, one obtains the material-specific term for an isotropic dispersion relation.

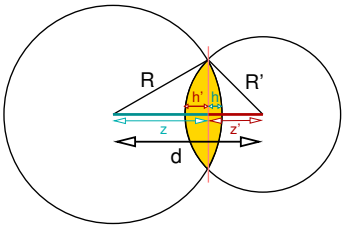
$$\begin{aligned} K_{\vec{q},\sigma}(\epsilon,\epsilon') &\stackrel{\text{Eq. }E.58}{=} \frac{d}{d\epsilon}\frac{d}{d\epsilon'}\left\{\int \frac{d^3k}{(2\pi)^3}\theta(\epsilon_{\vec{k},\sigma}-\epsilon)\theta(\epsilon_{\vec{k}+\vec{q},\sigma}-\epsilon')\right\} \\ &\stackrel{\text{Eq. }E.59}{=} \frac{1}{(2\pi)^3}\underbrace{\left(\frac{dR}{d\epsilon}\right)}_{\left(\frac{d\epsilon_\sigma(k)}{dk}\big|_{k_\sigma(\epsilon)}\right)^{-1}}\underbrace{\left(\frac{dR'}{d\epsilon'}\right)}_{\left(\frac{d\epsilon_\sigma(k)}{dk}\big|_{k_\sigma(\epsilon')}\right)^{-1}}\left\{\frac{d}{dR}\frac{d}{dR'}\int d^3r\;\theta\big(R-|\vec{r}|\big)\theta\big(R'-|\vec{r}-d\vec{e}_z|\big)\right\} \\ &\stackrel{\text{Eq. }E.67}{=} \frac{1}{(2\pi)^3}\underbrace{\left(\frac{dR}{d\epsilon}\right)}_{\left(\frac{d\epsilon_\sigma(k)}{dk}\big|_{k_\sigma(\epsilon)}\right)^{-1}}\underbrace{\left(\frac{dR'}{d\epsilon'}\right)}_{\left(\frac{d\epsilon_\sigma(k)}{dk}\big|_{k_\sigma(\epsilon')}\right)^{-1}}\left\{\frac{2\pi RR'}{d}\theta\Big(R'-|d-R|\Big)\;\theta\Big(d+R-R'\Big)\right\} \\ &= \frac{1}{(2\pi)^3}\left(\frac{d\epsilon_\sigma(k)}{dk}\bigg|_{k_\sigma(\epsilon)}\right)^{-1}\left(\frac{d\epsilon_\sigma(k)}{dk}\bigg|_{k_\sigma(\epsilon')}\right)^{-1} \\ &\quad\times\left\{\frac{2\pi k_\sigma(\epsilon)k_\sigma(\epsilon')}{|\vec{q}|}\theta\Big(k_\sigma(\epsilon')-\big||\vec{q}|-k_\sigma(\epsilon)\big|\Big)\;\theta\Big(|\vec{q}|+k_\sigma(\epsilon)-k_\sigma(\epsilon')\Big)\right\} \end{aligned} \tag{E.61}$$

The two step functions limit the result to regions with intersecting spheres, i.e. with

$$|k_\sigma(\epsilon)-|\vec{q}|| < k_\sigma(\epsilon') < k_\sigma(\epsilon)+|\vec{q}| \tag{E.62}$$

E.4.3 Geometric problem

Let me now work out the geometric problem of the overlap region $V+V'$ of two spheres, which leads to Eq. E.67 used above.



Volume of a spherical segment: Consider a spherical segment, i.e. the part of a sphere, which is cut off from the sphere by a plane. The radius of the sphere shall be R. The plane cuts through the sphere at distance z from the sphere center. The width of the spherical segment is $h = R - z$, $h \in [0, 2R]$.

$$\begin{aligned} V &= \underbrace{\frac{1}{2}\frac{4\pi R^3}{3}}_{\text{half sphere}} - \int_0^{R-h} dz\ \underbrace{\pi(R^2 - z^2)}_{\text{circle area}} \\ &= \frac{2\pi R^3}{3} - \pi\left[R^2 z - \frac{1}{3}z^3\right]_0^{R-h} \\ &= \frac{2\pi R^3}{3} - \pi\left(R^2(R-h) - \frac{1}{3}(R-h)^3\right) \\ &= \frac{2\pi R^3}{3} - \frac{\pi}{3}\left(3R^3 - 3R^2 h - R^3 + 3R^2 h - 3Rh^2 + h^3\right) \\ &= \frac{2\pi R^3}{3} - \frac{\pi}{3}\left(2R^3 - 3Rh^2 + h^3\right) \\ &= \frac{\pi}{3}\left(3Rh^2 - h^3\right) \qquad \text{for } h \in [0, 2R] \end{aligned} \tag{E.63}$$

For $h > 2R$, the formula above is meaningless and the volume is instead that of the sphere, namely $V = 4\pi R^3/3$. The radius must be positive.

Sphere overlap: The volume $V + V'$ in Eq. E.58 is the lens-shaped intersection of two sphere. For the lens-shaped object made from two spherical segments, the radius a of the intersection must be the same.

$$\begin{aligned} & z^2 + a^2 = R^2 \qquad \text{and} \qquad (d-z)^2 + a^2 = (R')^2 \\ \Rightarrow \quad & (d-z)^2 - z^2 = (R')^2 - R^2 \\ \Rightarrow \quad & d^2 - 2dz = (R')^2 - R^2 \\ \Rightarrow \quad & z = \frac{d}{2} - \frac{(R')^2 - R^2}{2d} \\ & h'(R, R', d) \overset{\text{def}}{=} R' - (d - z) = R' - \frac{1}{2}d - \frac{(R')^2 - R^2}{2d} = -\frac{(R'-d)^2 - R^2}{2d} \\ & h(R, R', d) \overset{\text{def}}{=} R - z = R - \frac{d}{2} + \frac{(R')^2 - R^2}{2d} = \frac{(R')^2 - (R-d)^2}{2d} \end{aligned} \tag{E.64}$$

Thus, we obtain the volume integral in Eq. E.59, namely the overlapping volume $V + V'$ of the two spheres, as

$$V + V' \overset{\text{Eq. } E.59}{=} \int d^3 r\ \theta\big(R - |\vec{r}|\big)\theta\big(R' - |\vec{r} - d\vec{e}_z|\big) \overset{\text{Eq. } E.63}{=} \underbrace{\frac{\pi}{3}\left(h^2(3R - h) + (h')^2(3R' - h')\right)}_{V+V'}$$
$$\text{for } R + R' > d, |R - R'| < d, \text{ and } R, R', d \geq 0 \tag{E.65}$$

with $h(R, R', d)$ and $h'(R, R', d)$ from Eq. E.64. I do not resolve h, h', because in Eq. E.58, we need the second derivatives of $V + V'$. The expression will become simpler, when the derivatives are taken.

Intersection of sphere surfaces: Let me now do the second derivative with respect to the radii R and R'

$$\frac{d^2(V + V')}{dR\,dR'} \overset{\text{Eq. } E.65}{=} \frac{d}{dR'}\frac{d}{dR}\frac{\pi}{3}\left(3Rh^2 - h^3 + 3R'(h')^2 - (h')^3\right) \tag{E.66}$$

where h and h' are themselfes functions of R, R', d given in Eq. E.64.

$$\begin{aligned}
\frac{d^2(V+V')}{dRdR'} &= \frac{d}{dR'}\frac{d}{dR}\frac{\pi}{3}\left[\left(3Rh^2-h^3\right)+\left(3R'(h')^2-(h')^3\right)\right] \\
&= \frac{\pi}{3}\left\{\frac{d}{dR'}\left[3h^2+\left(6Rh-3h^2\right)\frac{\partial h}{\partial R}\right]+\frac{d}{dR}\left[3(h')^2+\left(6R'(h')-3(h')^2\right)\frac{\partial h'}{\partial R'}\right]\right\} \\
&= \frac{\pi}{3}\left\{\left[\left(6h+(6R-6h)\underbrace{\frac{\partial h}{\partial R}}_{(d-R)/d}\right)\underbrace{\frac{\partial h}{\partial R'}}_{R'/d}+\left(6Rh-3h^2\right)\underbrace{\frac{\partial^2 h}{\partial R\partial R'}}_{=0}\right]\right. \\
&\qquad \left.+\left[\left(6h'+(6R'-6h')\underbrace{\frac{\partial h'}{\partial R'}}_{(d-R')/d}\right)\underbrace{\frac{\partial h'}{\partial R}}_{R/d}+\left(6R'(h')-3(h')^2\right)\underbrace{\frac{\partial^2 h'}{\partial R'\partial R}}_{=0}\right]\right\} \\
&= \frac{2\pi}{d^2}\left\{\left[\underbrace{\Big(hd+(R-h)(d-R)\Big)}_{R(d-R+h)}R'\right]+\underbrace{\Big(h'd+\big(R'-h'\big)(d-R')\Big)}_{R'(d-R'+h')}R\right]\right\} \\
&= \frac{2\pi}{d^2}\left\{RR'(d-R+h)+RR'(d-R'+h')\right\} \\
&= \frac{2\pi RR'}{d^2}\left\{\underbrace{2d-(R+R')+\overbrace{R+R'-d}^{h+h'}}_{=d}\right\} \\
&= \frac{2\pi RR'}{d}\underbrace{\theta(d^2-(R'-R)^2)\theta((R+R')^2-d^2)}_{\theta(R'-|d-R|)\theta(d+R-R')}
\end{aligned} \tag{E.67}$$

The step functions have been included to make the region of validity of the above expression explicit, namely $|R-R'| \le d \le |R+R'|$.

This result, Eq. E.67, will be used for the derivation of Eq. E.61 above.

E.4.4 Free electron gas at zero temperature

Let me now move away from a gemeral isotropic system to a free electron gas, which has a parabolic dispersion relation. This implies

$$\epsilon(\vec{k},\sigma) = \frac{\hbar^2 k^2}{2m} \qquad \text{and} \qquad \frac{1}{k}\frac{d\epsilon}{dk} = \frac{\hbar^2}{m} \qquad \text{and} \qquad k(\epsilon,\sigma) = \frac{1}{\hbar}\sqrt{2m\epsilon}\,. \tag{E.68}$$

$$\begin{aligned}
K_{\vec{q},\sigma}(\epsilon,\epsilon') &\overset{\text{Eq. E.61}}{=} \frac{1}{(2\pi)^3}\frac{2\pi}{|\vec{q}|}\underbrace{\left(\left.\frac{d\epsilon_\sigma(k)}{dk}\right|_{k_\sigma(\epsilon)}\right)^{-1}\left(\left.\frac{d\epsilon_\sigma(k)}{dk}\right|_{k_\sigma(\epsilon')}\right)^{-1}k_\sigma(\epsilon)k_\sigma(\epsilon')}_{=(m/\hbar^2)^2 \text{ for the free-electron gas}} \\
&\qquad \times\theta\Big(k_\sigma(\epsilon')-\big||\vec{q}|-k_\sigma(\epsilon)\big|\Big)\,\theta\Big(|\vec{q}|+k_\sigma(\epsilon)-k_\sigma(\epsilon')\Big) \\
&= \overbrace{\frac{1}{(2\pi)^3}\frac{2\pi}{|\vec{q}|}\left(\frac{m}{\hbar^2}\right)^2}^{\left(\frac{m}{2\pi\hbar^2}\right)^2\frac{1}{|\vec{q}|}}\theta\left(\epsilon'-\left(\sqrt{\epsilon}-\frac{\hbar|\vec{q}|}{\sqrt{2m}}\right)^2\right)\theta\left(\left(\sqrt{\epsilon}+\frac{\hbar|\vec{q}|}{\sqrt{2m}}\right)^2-\epsilon'\right)
\end{aligned} \tag{E.69}$$

The step functions single out the area within a diagonal parabola, which touches the ϵ- and the ϵ'-axis at $\frac{\hbar^2\vec{q}^2}{2m}$. This area in the $\epsilon-\epsilon'$ plane grows wider with increasing $|\vec{q}|$.

The fact that $\left(\frac{d\epsilon_\sigma(k)}{dk}\big|_{k_\sigma(\epsilon)}\right)^{-1} = \frac{m}{\hbar^2}$ is a constant is specific for the parabolic dispersion relation of the free electron gas.

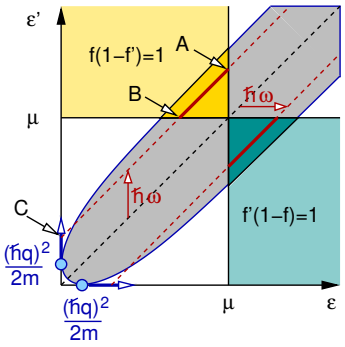


Fig. E.6: Integration region for the double energy integral in the ϵ, ϵ'-plane. The yellow and green regions select the electron-hole-pair excitations and are given by the occupations $f = f_{T,\mu}(\epsilon)$ and $f' = f_{T,\mu}(\epsilon')$. The straight red line implements the energy conservation $\hbar\omega = |\epsilon' - \epsilon|$. The grey region indicates the values for two quasi-particle energies, where the iso-energy surfaces intersect. Outside the grey region the contribution to the integral vanishes. In this graph the shape of grey region is taken from a free-electron-gas. It touches the axis at a point related to the momentum transfer. With increasing momentum transfer, the parabola grows wider, and its bottom shift upward along the main diagonal.

Let me insert the result for $K_{\vec{q},\sigma}(\epsilon, \epsilon')$ into $\bar{F}_{\vec{q}}(\hbar\omega)$ defined in Eq. E.56. Because the temperature

is set to zero, the Fermi functions can be replaced by step functions.

$$\bar{F}_{\vec{q}}(\hbar\omega) \overset{\text{Eq. } E.56}{=} \underbrace{(-1)}_{\text{Fermi loop}} \sum_{\sigma\in\{\uparrow,\downarrow\}} \int_0^\infty d\epsilon \; \underbrace{f_{T,\mu}(\epsilon)}_{\theta(\mu-\epsilon)} K_{\vec{q},\sigma}(\epsilon,\epsilon+\hbar\omega) \underbrace{\Big(1-f_{T,\mu}(\epsilon+\hbar\omega)\Big)}_{\theta(\epsilon+\hbar\omega-\mu)}$$

$$\overset{\text{Eq. } E.69}{=} \underbrace{(-1)}_{\text{Fermi loop}} \sum_{\sigma\in\{\uparrow,\downarrow\}} \underbrace{\int_0^\infty d\epsilon \quad \overbrace{\theta(\mu-\epsilon)\theta(\epsilon+\hbar\omega-\mu)}^{\text{yellow area with } f(1-f')=1 \text{ in Fig. E.6}}}_{\int_{\max(0,\mu-\hbar\omega)}^{\mu} d\epsilon}$$

$$\times \underbrace{\left(\frac{m}{2\pi\hbar^2}\right)^2 \frac{1}{|\vec{q}|} \theta\left(\overbrace{\epsilon+\hbar\omega}^{\epsilon'} - \left(\sqrt{\epsilon}-\frac{\hbar|\vec{q}|}{\sqrt{2m}}\right)^2\right) \theta\left(\left(\sqrt{\epsilon}+\frac{\hbar|\vec{q}|}{\sqrt{2m}}\right)^2 \overbrace{-\epsilon-\hbar\omega}^{-\epsilon'}\right)}_{K_{\vec{q},\sigma}(\epsilon,\epsilon+\hbar\omega)}$$

$$= \underbrace{(-1)}_{\text{Fermi loop}} \left(\frac{m}{2\pi\hbar^2}\right)^2 \frac{1}{|\vec{q}|} \sum_{\sigma\in\{\uparrow,\downarrow\}}$$

$$\times \int_{\mu-\hbar\omega}^{\mu} d\epsilon \; \underbrace{\overbrace{\theta\left(\epsilon+\hbar\omega-\left(\sqrt{\epsilon}-\frac{\hbar|\vec{q}|}{\sqrt{2m}}\right)^2\right)}^{\text{equals unity inside the grey parabola in Fig. E.6}}}_{\theta\left(\epsilon-\frac{1}{4}\frac{2m}{\hbar^2\vec{q}^2}\left(\frac{\hbar^2\vec{q}^2}{2m}-\hbar\omega\right)^2\right)} \underbrace{\theta\left(\left(\sqrt{\epsilon}+\frac{\hbar|\vec{q}|}{\sqrt{2m}}\right)^2-\epsilon-\hbar\omega\right)}_{\theta\left(\epsilon-\frac{1}{4}\frac{2m}{\hbar^2\vec{q}^2}\left(\frac{\hbar^2\vec{q}^2}{2m}-\hbar\omega\right)^2\right)}$$

$$= \underbrace{(-1)}_{\text{Fermi loop}} \left(\frac{m}{2\pi\hbar^2}\right)^2 \frac{1}{|\vec{q}|} \sum_{\sigma\in\{\uparrow,\downarrow\}} \underbrace{\int_{\mu-\hbar\omega}^{\mu} d\epsilon \; \theta\left[\epsilon-\frac{1}{4}\frac{2m}{\hbar^2\vec{q}^2}\left(\frac{\hbar^2\vec{q}^2}{2m}-\hbar\omega\right)^2\right]}_{\int_{\max(0,\mu-\hbar\omega,\frac{1}{4}\frac{2m}{\hbar^2q^2}(\frac{\hbar^2q^2}{2m}-\hbar\omega)^2)}^{\mu}} \tag{E.70}$$

$$= \underbrace{(-1)}_{\text{F.L.}} \left(\frac{m}{2\pi\hbar^2}\right)^2 \frac{1}{|\vec{q}|} \sum_{\sigma\in\{\uparrow,\downarrow\}} \max\Big[0, \underbrace{\min\left(\hbar\omega, \mu-\frac{1}{4}\frac{2m}{\hbar^2\vec{q}^2}\left(\hbar\omega-\frac{\hbar^2\vec{q}^2}{2m}\right)^2\right)}_{\left\{\mu-\max\left(\mu-\hbar\omega,\frac{1}{4}\frac{2m}{\hbar^2\vec{q}^2}\left(\hbar\omega-\frac{\hbar^2\vec{q}^2}{2m}\right)^2\right)\right\}}\Big] \tag{E.71}$$

Let me now introduce a more compact notation, which allows me to express the ω and the $\vec{q}$ dependence by a single, dimension-less function $X_{\hbar\omega}(\vec{q}) = \frac{2m\hbar\omega}{\hbar^2\vec{q}^2}$. To avoid cluttering the expressions, I suppress the $\vec{q}$ dependence

$$\bar{F}_{\vec{q}}(\hbar\omega) = \sum_{\sigma\in\{\uparrow,\downarrow\}} \underbrace{(-1)}_{\text{F.L.}} \left(\frac{m}{2\pi\hbar^2}\right)^2 \sqrt{\frac{\hbar^2\mu}{2m}} \frac{1}{\sqrt{X_\mu}} \max\left[0, \min\left(X_{\hbar\omega}, X_\mu - \frac{1}{4}\Big(X_{\hbar\omega}-1\Big)^2\right)\right]$$

$$\text{with } X_{\hbar\omega} \overset{\text{def}}{=} \frac{2m\hbar\omega}{\hbar^2\vec{q}^2} \text{ and } X_\mu \overset{\text{def}}{=} \frac{2m\mu}{\hbar^2\vec{q}^2} \tag{E.72}$$

Domains The function $\bar{F}_{\vec{q}}(\hbar\omega)$ consists of three distinct functional forms for distinct domains. The regions are limited by

$$\begin{aligned} 0 &= X_{\hbar\omega} \\ 0 &= X_\mu - \frac{1}{4}(X_{\hbar\omega}-1)^2 \qquad \Rightarrow X_{\hbar\omega} = 1 \pm 2\sqrt{X_\mu} = (\sqrt{X_\mu}\pm 1)^2 - X_\mu \\ X_{\hbar\omega} &= X_\mu - \frac{1}{4}(X_{\hbar\omega}-1)^2 \qquad \Rightarrow X_{\hbar\omega} = -1 \pm 2\sqrt{X_\mu} = -\Big((\sqrt{X_\mu}\pm 1)^2 - X_\mu\Big) \end{aligned} \tag{E.73}$$

Thus, we obtain

- the low-energy region

$$\bar{F}_{\vec{q}}(\hbar\omega) = \sum_{\sigma\in\{\uparrow,\downarrow\}} \underbrace{(-1)}_{\text{F.L.}} \left(\frac{m}{2\pi\hbar^2}\right)^2 \underbrace{\sqrt{\frac{\hbar^2\mu}{2m}} \frac{1}{\sqrt{X_\mu}} X_{\hbar\omega}}_{\frac{\hbar\omega}{|\vec{q}|}} \tag{E.74}$$

for

$$\begin{aligned} & 0 < X_{\hbar\omega} < \max\left\{0; \overbrace{X_\mu - \left(\sqrt{X_\mu} - 1\right)^2}^{-1-2\sqrt{X_\mu}}\right\} \\ \Leftrightarrow \qquad & 0 < \hbar\omega < \max\left\{0; \mu - \left(\sqrt{\frac{\hbar^2 q^2}{2m}} - \sqrt{\mu}\right)^2\right\} \end{aligned} \tag{E.75}$$

- and the high-energy region

$$\bar{F}_{\vec{q}}(\hbar\omega) = \sum_{\sigma\in\{\uparrow,\downarrow\}} \underbrace{(-1)}_{\text{F.L.}} \left(\frac{m}{2\pi\hbar^2}\right)^2 \underbrace{\sqrt{\frac{\hbar^2\mu}{2m}} \frac{1}{\sqrt{X_\mu}}}_{|\vec{q}|} \left(X_\mu - \frac{1}{4}\left(X_{\hbar\omega} - 1\right)^2\right) \tag{E.76}$$

for

$$\begin{aligned} & \max\left\{\overbrace{X_\mu - \left(\sqrt{X_\mu} - 1\right)^2}^{-1-2\sqrt{X_\mu}}; -X_\mu + \left(\sqrt{X}_\mu - 1\right)^2\right\} < X_{\hbar\omega} < -X_\mu + \left(\sqrt{X_\mu} + 1\right)^2 \\ \Leftrightarrow \qquad & \max\left\{\mu - \left(\sqrt{\frac{\hbar^2 q^2}{2m}} - \sqrt{\mu}\right)^2; -\mu + \left(\sqrt{\frac{\hbar^2 \vec{q}^2}{2m}} - \sqrt{\mu}\right)^2\right\} < \hbar\omega < -\mu + \left(\sqrt{\frac{\hbar^2 \vec{q}^2}{2m}} + \sqrt{\mu}\right)^2 \end{aligned} \tag{E.77}$$

The function $F_{\vec{q}}$ depends only on the absolute value of $\vec{q}$. The function X equals unity on the free electron parabola $\hbar\omega = \frac{\hbar^2 q^2}{2m}$,

The ϵ integral returns the length of the ϵ-interval, which makes all step function to unity.

I chose the maximum of zero and the calculated value to make the result defined, albeit zero, in the regions where the contribution vanishes.

The ϵ-integration in Eq. E.70 is limited to

$$\mu - \hbar\omega < \epsilon < \mu \qquad \text{and} \qquad \epsilon > \frac{1}{4}\frac{2m}{\hbar^2\vec{q}^2}\left(\hbar\omega - \frac{\hbar^2\vec{q}^2}{2m}\right)^2 \tag{E.78}$$

This results in different regions in the $|\vec{q}|, \omega$-plane that are treated differently. In the following, Let me determine the lines where the boundary of the gray region in figure E.6 touches the points indicated as A, B, C.

$$\begin{aligned} \mathrm{A} &= (\epsilon, \epsilon') = (\mu, \mu + \hbar\omega) \\ \mathrm{B} &= (\epsilon, \epsilon') = (\mu - \hbar\omega, \mu) \\ \mathrm{C} &= (\epsilon, \epsilon') = (0, \hbar\omega) \end{aligned} \tag{E.79}$$

A:

$$\underbrace{\mu + \hbar\omega}_{\epsilon'} = \left(\underbrace{\sqrt{\mu}}_{\sqrt{\epsilon}} \pm \frac{\hbar|\vec{q}|}{\sqrt{2m}}\right)^2 \qquad \Rightarrow \qquad \hbar|\vec{q}| = \mp\sqrt{2m\mu} + \sqrt{2m(\mu + \hbar\omega)} \tag{E.80}$$

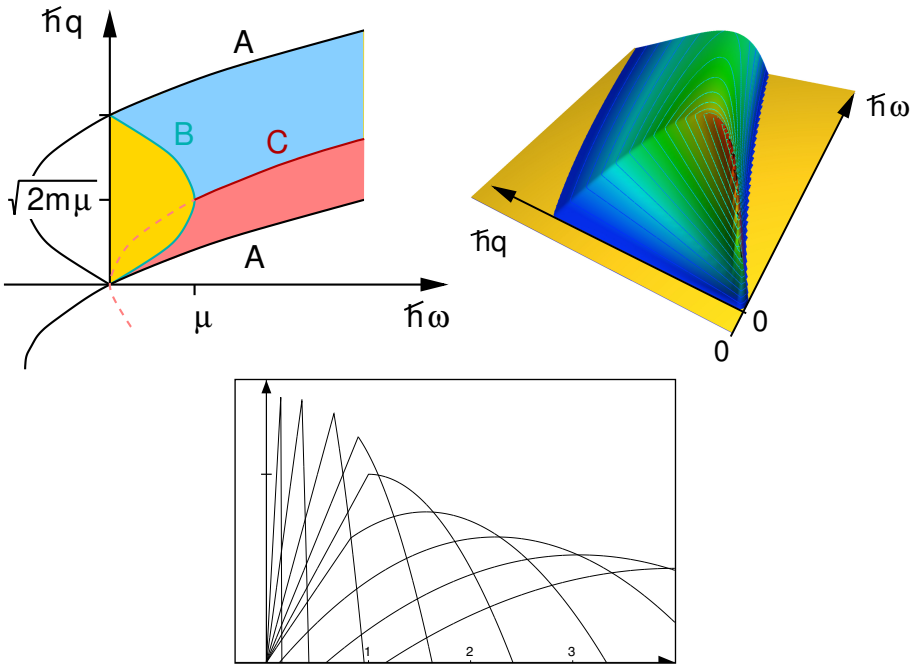


Fig. E.7: Region with finite polarization insertion **for non-interacting electrons** as function of momentum transfer $\hbar|\vec{q}|$ and energy transfer $\hbar\omega$. The contribution vanishes outside the colored regions. The lines denoted A, B, C indicate values where the boundary of the gray region in figure E.6 touches the points A, B, C. The bottom image shows $\bar{F}_{\vec{q}}(\hbar\omega)$ as function of the energy transfer $\hbar\omega$ for several values of $\hbar|\vec{q}|$

Only the solution with the positive square root $\sqrt{2m(\mu+\hbar\omega)}$ is related to positive $\hbar|\vec{q}|$ and positive $\hbar\omega$. Therefore, the branch with the negative square root is excluded. The two branches bounded by the point A denote the region of momenta and frequency with a non-vanishing contribution to the polarization diagram.

B:

$$\underbrace{\mu}_{\epsilon'} = \Big(\underbrace{\sqrt{\mu-\hbar\omega}}_{\sqrt{\epsilon}} \pm \frac{\hbar|\vec{q}|}{\sqrt{2m}}\Big)^2 \qquad \Rightarrow \qquad \hbar|\vec{q}| = \mp\sqrt{2m(\mu-\hbar\omega)} + \sqrt{2m\mu} \tag{E.81}$$

The region enclosed by the line B is the region where the line segment from A to B is not constrained by the theta functions.

C:

$$\underbrace{\hbar\omega}_{\epsilon'} = \Big(\underbrace{0}_{\sqrt{\epsilon}} \pm \frac{\hbar|\vec{q}|}{\sqrt{2m}}\Big)^2 \qquad \Rightarrow \qquad \hbar|\vec{q}| = \mp\sqrt{2m(\mu-\hbar\omega)} + \sqrt{2m\mu} \tag{E.82}$$

Summary

$$\Pi^{(0)}(\vec{r}_1,t_1,\vec{r}_2,t_2) \overset{\text{Eq. } E.49}{=} i\hbar \underbrace{(-1)}_{\text{Fermi loop}} \sum_{\sigma_1,\sigma_2\in\{\uparrow,\downarrow\}} G^{\mathcal{C},(0)}(\vec{x}_1,t_1,\vec{x}_2,t_2)G^{\mathcal{C},(0)}(\vec{x}_2,t_2,\vec{x}_1,t_1)$$

$$= \frac{i}{\hbar}\int_0^\infty d(\hbar\omega)\ \overbrace{\frac{1}{L^3}\sum_{\vec{q}}}^{\sim\int\frac{d^3q}{(2\pi)^3}}\left[\theta_{\mathcal{C}}(t_2-t_1)\mathrm{e}^{-i[\vec{q}(\vec{r}_1-\vec{r}_2)-\omega(t_1-t_2)]}+\theta_{\mathcal{C}}(t_1-t_2)\mathrm{e}^{+i[\vec{q}(\vec{r}_1-\vec{r}_2)-\omega(t_1-t_2)]}\right]\bar{F}_{\vec{q}}(\hbar\omega) \tag{E.83}$$

Because $\bar{F}_{\vec{q}}(\hbar\omega)$ is isotropic with respect to $\vec{q}$, and because the integral covers all $\vec{q}$, we may interchange in the prefactor$\vec{q}$ with $-\vec{q}$.

$$\Pi^{(0)}(\vec{r}_1,t_1,\vec{r}_2,t_2)$$

$$= \frac{i}{\hbar}\int_0^\infty d(\hbar\omega)\ \overbrace{\frac{1}{L^3}\sum_{\vec{q}}}^{\sim\int\frac{d^3q}{(2\pi)^3}}\mathrm{e}^{i\vec{q}(\vec{r}_1-\vec{r}_2)}\underbrace{\left[\theta_{\mathcal{C}}(t_2-t_1)\mathrm{e}^{+i\omega(t_1-t_2)]}+\theta_{\mathcal{C}}(t_1-t_2)\mathrm{e}^{-i\omega(t_1-t_2)]}\right]}_{\mathrm{e}^{i\omega|t_1-t_2|}}\bar{F}_{\vec{q}}(\hbar\omega)$$

$$= \frac{i}{\hbar}\overbrace{\frac{1}{L^3}\sum_{\vec{q}}}^{\sim\int\frac{d^3q}{(2\pi)^3}}\mathrm{e}^{i\vec{q}(\vec{r}_1-\vec{r}_2)}\int_0^\infty d(\hbar\omega)\ \mathrm{e}^{i\omega|t_1-t_2|}$$

$$\times\underbrace{\underbrace{(-1)}_{\text{F.L.}}\left(\frac{m}{2\pi\hbar^2}\right)^2\sqrt{\frac{\hbar^2\mu}{2m}}\sum_{\sigma\in\{\uparrow,\downarrow\}}\frac{1}{\sqrt{X_\mu}}\begin{cases}X_{\hbar\omega} & \text{for } 0<X_{\hbar\omega}<-1-2\sqrt{X_\mu}\\ X_\mu-\frac{1}{4}\left(X_{\hbar\omega}-1\right)^2 & \text{for } \pm1-2\sqrt{X_\mu}<X_{\hbar\omega}<1-2\sqrt{X_\mu}\end{cases}}_{\bar{F}_{\vec{q}}(\hbar\omega)\text{ from Eq. E.72}}$$

$$\text{with } X_{\hbar\omega}=\frac{2m\hbar\omega}{\hbar^2\vec{q}^2} \text{ and } X_\mu=\frac{2m\mu}{\hbar^2\vec{q}^2}$$

$$= \frac{i}{\hbar}\underbrace{(-1)}_{\text{F.L.}}\left(\frac{m}{2\pi\hbar^2}\right)^2\sqrt{\frac{\hbar^2\mu}{2m}}\sum_{\sigma\in\{\uparrow,\downarrow\}}\overbrace{\frac{1}{L^3}\sum_{\vec{q}}}^{\sim\int\frac{d^3q}{(2\pi)^3}}\mathrm{e}^{i\vec{q}(\vec{r}_1-\vec{r}_2)}\frac{1}{\sqrt{X_\mu}}\left(\frac{dX_{\hbar\omega}}{\hbar\omega}\right)^{-1}$$

$$\times\left\{\int_0^{-1-2\sqrt{X_\mu}}dX_{\hbar\omega}\ \mathrm{e}^{i\omega|t_1-t_2|}X_{\hbar\omega}+\int_{\max(\pm1-2\sqrt{X_\mu})}^{+1-2\sqrt{X_\mu}}dX_{\hbar\omega}\mathrm{e}^{i\omega|t_1-t_2|}\left(X_\mu-\frac{1}{4}\left(X_{\hbar\omega}-1\right)^2\right)\right\} \tag{E.84}$$

Let me now turn to the integration: I use

$$\omega|t_1-t_2| = X\mathcal{T} = \frac{2m\hbar\omega}{\hbar^2\vec{q}^2}\mathcal{T} \qquad \Rightarrow \qquad \mathcal{T}=\frac{\hbar^2\vec{q}^2}{2m\hbar}|t_1-t_2| \tag{E.85}$$

$$
\begin{aligned}
Y_n &\stackrel{\text{def}}{=} \int_{X_1}^{X_2} dX\, \mathrm{e}^{iX\mathcal{T}} X^n = \Big(-i\partial_{\mathcal{T}}\Big)^n \int_{X_1}^{X_2} dX\, \mathrm{e}^{iX\mathcal{T}} = \Big(-i\partial_{\mathcal{T}}\Big)^n \left[\frac{\mathrm{e}^{iX\mathcal{T}}}{i\mathcal{T}}\right]_{X_1}^{X_2} = (-i)^{n+1}\left[\Big(\partial_{\mathcal{T}}\Big)^n \frac{\mathrm{e}^{iX\mathcal{T}}}{\mathcal{T}}\right]_{X_1}^{X_2} \\
Y_0 &= \frac{-i}{\mathcal{T}}\left[\mathrm{e}^{iX\mathcal{T}}\right]_{X_1}^{X_2} \\
Y_1 &= (-i)^2\partial_{\mathcal{T}}\left[\frac{\mathrm{e}^{iX\mathcal{T}}}{\mathcal{T}}\right]_{X_1}^{X_2} = -\left[\frac{iX\mathrm{e}^{iX\mathcal{T}}}{\mathcal{T}} - \frac{\mathrm{e}^{iX\mathcal{T}}}{\mathcal{T}^2}\right]_{X_1}^{X_2} = \frac{1}{\mathcal{T}^2}\left[\Big(1+(-iX\mathcal{T})\Big)\mathrm{e}^{iX\mathcal{T}}\right]_{X_1}^{X_2} \\
Y_2 &= \underbrace{(-i)^3}_{i}\partial_{\mathcal{T}}^2\left[\frac{\mathrm{e}^{iX\mathcal{T}}}{\mathcal{T}}\right]_{X_1}^{X_2} = i\partial_{\mathcal{T}}\left[\frac{-1+iX\mathcal{T}}{\mathcal{T}^2}\mathrm{e}^{iX\mathcal{T}}\right]_{X_1}^{X_2} = i\left[\Big(\frac{2}{\mathcal{T}^3} - \frac{iX}{\mathcal{T}^2} + \Big(\frac{-1+iX\mathcal{T}}{\mathcal{T}^2}\Big)iX\Big)\mathrm{e}^{iX\mathcal{T}}\right]_{X_1}^{X_2} \\
&= \frac{2i}{\mathcal{T}^3}\left[\Big(1+(-iX\mathcal{T}) + \frac{1}{2}(-iX\mathcal{T})^2\Big)\mathrm{e}^{iX\mathcal{T}}\right]_{X_1}^{X_2}
\end{aligned}
\tag{E.86}
$$

$$
\begin{aligned}
\int_{X_1}^{X_2} dX \mathrm{e}^{iX\mathcal{T}}\Big(X-1\Big)^2 &= \underbrace{\frac{2i}{\mathcal{T}^3}\left[\Big(1+(-iX\mathcal{T}) + \frac{1}{2}(-iX\mathcal{T})^2\Big)\mathrm{e}^{iX\mathcal{T}}\right]_{X_1}^{X_2}}_{Y_2} \\
&\quad \underbrace{-2\,\frac{1}{\mathcal{T}^2}\left[\Big(1+(-iX\mathcal{T})\Big)\mathrm{e}^{iX\mathcal{T}}\right]_{X_1}^{X_2}}_{Y_1} + \underbrace{\frac{-i}{\mathcal{T}}\left[\mathrm{e}^{iX\mathcal{T}}\right]_{X_1}^{X_2}}_{Y_0} \\
&= \frac{2i}{\mathcal{T}^3}\left[\Big(1+(-iX\mathcal{T}) + \frac{1}{2}(-iX\mathcal{T})^2 + i\mathcal{T}\Big(1+\big(-iX\mathcal{T}\big)\Big) - \frac{1}{2}\mathcal{T}^2\Big)\mathrm{e}^{iX\mathcal{T}}\right]_{X_1}^{X_2} \\
&= \frac{2i}{\mathcal{T}^3}\left[\Big(\Big(1+i\mathcal{T}+\frac{1}{2}(i\mathcal{T})^2\Big) + (-iX\mathcal{T})\Big(1+i\mathcal{T}\Big) + \frac{1}{2}(-iX\mathcal{T})^2\Big)\mathrm{e}^{iX\mathcal{T}}\right]_{X_1}^{X_2}
\end{aligned}
\tag{E.87}
$$

$$
\begin{aligned}
\int_0^{-1-2\sqrt{X_\mu}} dX_{\hbar\omega}\, \mathrm{e}^{iX_{\hbar\omega}\mathcal{T}} X_{\hbar\omega} &= \frac{1}{\mathcal{T}^2}\left[\Big(1+(-iX\mathcal{T})\Big)\mathrm{e}^{iX_{\hbar\omega}\mathcal{T}}\right]_0^{-1-2\sqrt{X_\mu}} \\
&= \frac{1}{\mathcal{T}^2}\left[\Big(1+i(1+2\sqrt{X_\mu})\mathcal{T}\Big)\mathrm{e}^{-i(1+2\sqrt{X_\mu})\mathcal{T}} - 1\right] \\
&= \frac{1}{\mathcal{T}^2}\left[\Big(1+i\mathcal{T}+2i\sqrt{X_\mu}\mathcal{T}\Big)\mathrm{e}^{-i(1+2\sqrt{X_\mu})\mathcal{T}} - 1\right]
\end{aligned}
\tag{E.88}
$$

ZEROTH-ORDER POLARIZATION OF THE FREE ELECTRON GAS

$$\Pi^{(0)}(\vec{r}_1,t_1,\vec{r}_2,t_2) \overset{\text{Eq. } E.49}{=} i\hbar \underbrace{(-1)}_{\text{Fermi loop}} \sum_{\sigma_1,\sigma_2\in\{\uparrow,\downarrow\}} G^{\mathcal{C},(0)}(\vec{x}_1,t_1,\vec{x}_2,t_2)G^{\mathcal{C},(0)}(\vec{x}_2,t_2,\vec{x}_1,t_1)$$

$$\overset{\text{Eq. } E.55}{=} \frac{i}{\hbar}\int_0^\infty d(\hbar\omega)\ \overbrace{\frac{1}{L^3}\sum_{\vec{q}}}^{\sim\int\frac{d^3q}{(2\pi)^3}}\left[\theta_{\mathcal{C}}(t_2-t_1)\mathrm{e}^{-i[\vec{q}(\vec{r}_1-\vec{r}_2)-\omega(t_1-t_2)]}+\theta_{\mathcal{C}}(t_1-t_2)\mathrm{e}^{+i[\vec{q}(\vec{r}_1-\vec{r}_2)-\omega(t_1-t_2)]}\right]$$

$$\times \underbrace{\underbrace{(-1)}_{\text{F.L.}}\left(\frac{m}{2\pi\hbar^2}\right)^2\frac{1}{|\vec{q}|}\sum_{\sigma\in\{\uparrow,\downarrow\}}\max\left[0,\min\left(\hbar\omega,\mu-\frac{1}{4}\frac{2m}{\hbar^2\vec{q}^2}\left(\hbar\omega-\frac{\hbar^2\vec{q}^2}{2m}\right)^2\right)\right]}_{\bar{F}_{\vec{q}}(\hbar\omega)\ \text{Eq. E.72}}$$

$$\text{with } X(|\vec{q}|,\omega)=\frac{2m\hbar\omega}{\hbar^2\vec{q}^2}$$

$$\overset{\text{Eq. } E.55}{=} \frac{i}{\hbar}\underbrace{(-1)}_{\text{F.L.}}\left(\frac{m}{2\pi\hbar^2}\right)^2\frac{\hbar}{\sqrt{2m\mu}}$$

$$\times \overbrace{\frac{1}{L^3}\sum_{\vec{q}}}^{\sim\int\frac{d^3q}{(2\pi)^3}}\int_0^\infty d(\hbar\omega)\left[\theta_{\mathcal{C}}(t_2-t_1)\mathrm{e}^{-i[\vec{q}(\vec{r}_1-\vec{r}_2)-\omega(t_1-t_2)]}+\theta_{\mathcal{C}}(t_1-t_2)\mathrm{e}^{+i[\vec{q}(\vec{r}_1-\vec{r}_2)-\omega(t_1-t_2)]}\right]$$

$$\times\left(\frac{dX_{\hbar\omega}}{d\hbar\omega}\right)^{-1}\underbrace{\sqrt{X_\mu}}_{\frac{\sqrt{2m\mu}}{\hbar|\vec{q}|}}\sum_{\sigma\in\{\uparrow,\downarrow\}}\max\left[0,\min\left(X_{\hbar\omega},X_\mu-\frac{1}{4}\left(X_{\hbar\omega}-1\right)^2\right)\right]$$

$$\text{with } X_{\hbar\omega}=\frac{2m\hbar\omega}{\hbar^2\vec{q}^2} \text{ and } X_\mu=\frac{2m\mu}{\hbar^2\vec{q}^2} \tag{E.89}$$

This result for the polarization insertion is valid for a **free electron gas** at **zero temperature** $T=0$. The polarization insertion is defined for **complex-valued time** arguments on the contour $\mathcal{C}$ in the complex time plane. On the other hand, ω **is a real valued** quantity, because it is the difference of two energy eigenvalues. The limitation of the ω-integration to positive values is a consequence of $\bar{F}(q,\omega)$, which, in the zero-temperature limit, vanishes for negative ω. It reflects the absence of thermal electron-hole pairs at zero temperature, from which energy can be extracted.

Editor: This result needs to be verified by comparison with the literature. This requires a Fourier transform along the real time axis.

E.4.5 Frequency moments of the polarization

Let me determine the first ω-moments of

$$\begin{aligned}
\bar{F}_{\vec{q}}(\hbar\omega) &\overset{\text{Eq. E.72}}{=} \underbrace{(-1)}_{\text{F.L.}} \left(\frac{m}{2\pi\hbar^2}\right)^2 \frac{1}{|\vec{q}|} \sum_{\sigma\in\{\uparrow,\downarrow\}} \max\left[0, \min\left(\hbar\omega, \mu - \frac{1}{4}\frac{2m}{\hbar^2\vec{q}^2}\left(\hbar\omega - \frac{\hbar^2\vec{q}^2}{2m}\right)^2\right)\right] \\
&= \underbrace{(-1)}_{\text{F.L.}} \left(\frac{m}{2\pi\hbar^2}\right)^2 \frac{1}{|\vec{q}|} \sum_{\sigma\in\{\uparrow,\downarrow\}} \frac{\hbar^2\vec{q}^2}{2m} \max\left[0, \min\left(\frac{2m\hbar\omega}{\hbar^2\vec{q}^2}, \frac{2m\mu}{\hbar^2\vec{q}^2} - \frac{1}{4}\left(\frac{2m\hbar\omega}{\hbar^2\vec{q}^2} - 1\right)^2\right)\right] \\
&= \underbrace{(-1)}_{\text{F.L.}} \left(\frac{m}{2\pi\hbar^2}\right)^2 \frac{1}{|\vec{q}|} \left(\frac{dX(\vec{q},\omega)}{d\hbar\omega}\right)^{-1} \sum_{\sigma\in\{\uparrow,\downarrow\}} \max\left[0, \min\left(X(|\vec{q}|,\omega), X(|\vec{q}|,\mu) - \frac{1}{4}\Big(X(\vec{q},\omega) - 1\Big)^2\right)\right] \\
&\qquad \text{with } X(|\vec{q}|,\omega) = \frac{2m\hbar\omega}{\hbar^2\vec{q}^2}
\end{aligned} \tag{E.90}$$

For $\hbar|\vec{q}| < \sqrt{2m\mu}$, the moments are

$$\begin{aligned}
M_b &\overset{\text{def}}{=} \int_0^\infty d(\hbar\omega)\ (\hbar\omega)^b \bar{F}_{\vec{q}}(\hbar\omega) \\
&= \int_0^\infty \underbrace{dX \left(\frac{dX}{d\hbar\omega}\right)^{-1}}_{d\hbar\omega} \underbrace{\left(\frac{dX}{d\hbar\omega}\right)^{-b} X^b(\vec{q},\omega)}_{(\hbar\omega)^b} \bar{F}_{\vec{q}}(\hbar\omega(X)) \\
&= \left(\frac{dX}{d\hbar\omega}\right)^{-1-b} \int_0^\infty dX\ X^b(\vec{q},\omega) \bar{F}_{\vec{q}}(\hbar\omega(X)) \\
&= \underbrace{(-1)}_{\text{F.L.}} \left(\frac{m}{2\pi\hbar^2}\right)^2 \frac{1}{|\vec{q}|} \underbrace{\left(\frac{\hbar^2\vec{q}^2}{2m}\right)^{b+2}}_{\left(\frac{dX}{d\hbar\omega}\right)^{-2-b}} \sum_{\sigma\in\{\uparrow,\downarrow\}} \\
&\quad \times \int_0^\infty dX\ X^b \max\left[0, \min\left(X, X_\mu - \frac{1}{4}\Big(X-1\Big)^2\right)\right] \qquad \text{with } X_\mu = X(\vec{q},\mu)
\end{aligned} \tag{E.91}$$

Let me consider the case with $\hbar|q| \le 2\sqrt{2m\mu}$. This is the region in $\vec{q}$ space with electron-hole down to vanishing excitation energy. The integration can be divided into two regions.

- The two functions intersect at

$$\begin{aligned}
X &= X_\mu - \frac{1}{4}(X-1)^2 \\
X^2 - 2X + 1 + 4X &= 4X_\mu \\
(X+1)^2 &= 4X_\mu \\
X &= -1 + 2\sqrt{X_\mu}
\end{aligned} \tag{E.92}$$

- the maximum of the integral is given by

$$\begin{aligned}
0 &= X_\mu - \frac{1}{4}(X-1)^2 \\
X &= 1 + 2\sqrt{X_\mu}
\end{aligned} \tag{E.93}$$

Let me evaluate the integral

$$
\begin{aligned}
&\int_0^\infty dX\, X^b \max\Big[0, \min\Big(X, X_\mu - \frac{1}{4}\big(X-1\big)^2\Big)\Big] \\
&= \int_0^{-1+2\sqrt{X_\mu}} dX\, X^{b+1} + \int_{-1+2\sqrt{X_\mu}}^{1+2\sqrt{X_\mu}} dX\, X^b \Big(X_\mu - \frac{1}{4}\big(X-1\big)^2\Big)\Big] \\
&= \Big[\frac{X^{b+2}}{b+2}\Big]_0^{-1+2\sqrt{X_\mu}} + \Big[\underbrace{-\frac{1}{4}\Big(1-2\sqrt{X_\mu}\Big)\Big(1+2\sqrt{X_\mu}\Big)}_{X_\mu-\frac{1}{4}} \frac{X^{b+1}}{b+1} - \frac{X^{b+3}}{4(b+3)} + \frac{X^{b+2}}{2(b+2)}\Big]_{-1+2\sqrt{X_\mu}}^{1+2\sqrt{X_\mu}} \\
&= \frac{(-1+2\sqrt{X_\mu})^{b+2}}{b+2} + \Big[-\frac{1}{4}\Big(1-2\sqrt{X_\mu}\Big)\Big(1+2\sqrt{X_\mu}\Big)\frac{(1+2\sqrt{X_\mu})^{b+1}}{b+1} - \frac{(1+2\sqrt{X_\mu})^{b+3}}{4(b+3)} + \frac{(1+2\sqrt{X_\mu})^{b+2}}{2(b+2)}\Big] \\
&\quad - \Big[-\frac{1}{4}\Big(1-2\sqrt{X_\mu}\Big)\Big(1+2\sqrt{X_\mu}\Big)\frac{(-1+2\sqrt{X_\mu})^{b+1}}{b+1} - \frac{(-1+2\sqrt{X_\mu})^{b+3}}{4(b+3)} + \frac{(-1+2\sqrt{X_\mu})^{b+2}}{2(b+2)}\Big] \\
&\quad \text{...here with underbraces...} \\
&= \frac{(-1+2\sqrt{X_\mu})^{b+2}}{b+2} + \underbrace{\Big[-\frac{1}{4}\Big(1-2\sqrt{X_\mu}\Big)\frac{(1+2\sqrt{X_\mu})^{b+2}}{b+1} - \frac{(1+2\sqrt{X_\mu})^{b+3}}{4(b+3)} + \frac{(1+2\sqrt{X_\mu})^{b+2}}{2(b+2)}\Big]}_{\frac{1}{4}(1+2\sqrt{X_\mu})^{b+2}\Big(\underbrace{\frac{-1}{b+1} + \frac{2\sqrt{X_\mu}}{b+1} - \frac{1}{b+3} - \frac{2\sqrt{X_\mu}}{b+3} + \frac{2}{b+2}}_{-\frac{2b+4+2}{(b+1)(b+3)} + \frac{2+4\sqrt{X_\mu}}{(b+1)(b+3)} + \frac{2}{(b+2)} = -2\frac{1}{(b+1)(b+2)} + 2\frac{1+2\sqrt{X_\mu}}{(b+1)(b+3)}}\Big)} \\
&\quad - \underbrace{\Big[+\frac{1}{4}\Big(1+2\sqrt{X_\mu}\Big)\frac{(-1+2\sqrt{X_\mu})^{b+2}}{b+1} - \frac{(-1+2\sqrt{X_\mu})^{b+3}}{4(b+3)} + \frac{(-1+2\sqrt{X_\mu})^{b+2}}{2(b+2)}\Big]}_{\frac{1}{4}(-1+2\sqrt{X_\mu})^{b+2}\Big(\underbrace{\frac{1}{b+1} + \frac{2\sqrt{X_\mu}}{b+1} + \frac{1}{b+3} - \frac{2\sqrt{X_\mu}}{b+3} + \frac{2}{b+2}}_{\frac{2b+4+2}{(b+1)(b+3)} + \frac{-2+4\sqrt{X_\mu}}{(b+1)(b+3)} + \frac{2}{b+2} = 2\frac{2b+3}{(b+1)(b+2)} + 2\frac{-1+2\sqrt{X_\mu}}{(b+1)(b+3)}}\Big)} \\
&= \frac{1}{2}(1+2\sqrt{X_\mu})^{b+2}\Big(\frac{-1}{(b+1)(b+2)} + \frac{1+2\sqrt{X_\mu}}{(b+1)(b+3)}\Big) \\
&\quad - \frac{1}{2}(-1+2\sqrt{X_\mu})^{b+2}\Big(\frac{2b+3}{(b+1)(b+2)} + \frac{-1+2\sqrt{X_\mu}}{(b+1)(b+3)}\Big) + \frac{(-1+2\sqrt{X_\mu})^{b+2}}{b+2} \\
&= \frac{1}{2}(2\sqrt{X_\mu}+1)^{b+2}\Big(\frac{-1}{(b+1)(b+2)} + \frac{2\sqrt{X_\mu}+1}{(b+1)(b+3)}\Big) \\
&\quad - \frac{1}{2}(2\sqrt{X_\mu}-1)^{b+2}\Big(\frac{1}{(b+1)(b+2)} + \frac{2\sqrt{X_\mu}-1}{(b+1)(b+3)}\Big) \\
&= \frac{\Big(-(b+3)\frac{(2\sqrt{X_\mu}+1)^{b+2}+(2\sqrt{X_\mu}-1)^{b+2}}{2} + (b+2)\frac{(2\sqrt{X_\mu}+1)^{b+3}-(2\sqrt{X_\mu}-1)^{b+3}}{2}\Big)}{(b+1)(b+2)(b+3)}
\end{aligned}
\tag{E.94}
$$

Editor: This derivation is numerically verified with MacOS Grapher Remember that this expression for the integral is limited to $\hbar|q| < \sqrt{2m\mu}$.

Thus, I obtain the moments for $\hbar|q| < 2\sqrt{2m\mu}$. as

$$
\begin{aligned}
M_b &\stackrel{\text{def}}{=} \int_0^\infty d(\hbar\omega)\,(\hbar\omega)^b \bar{F}_{\vec{q}}(\hbar\omega) \\
&= \underbrace{(-1)}_{\text{F.L.}} \left(\frac{m}{2\pi\hbar^2}\right)^2 \frac{1}{|\vec{q}|} \left(\frac{\hbar^2\vec{q}^2}{2m}\right)^{b+2} \sum_{\sigma\in\{\uparrow,\downarrow\}} \\
&\quad \times \underbrace{\frac{\left(-(b+3)\frac{(2\sqrt{X_\mu}+1)^{b+2}+(2\sqrt{X_\mu}-1)^{b+2}}{2} + (b+2)\frac{(2\sqrt{X_\mu}+1)^{b+3}-(2\sqrt{X_\mu}-1)^{b+3}}{2}\right)}{(b+1)(b+2)(b+3)}}_{\int_0^\infty dX\, X^b \max\left[0,\min\left(X,X_\mu-\frac{1}{4}\left(X-1\right)^2\right)\right]} \\
&\qquad \text{with } X_\mu = X(\vec{q},\mu) = \frac{2m\mu}{\hbar^2\vec{q}^2} \geq \frac{1}{4} \\
&\qquad \ldots\text{Caution: the following has been estimated graphically...} \\
&= \underbrace{(-1)}_{\text{F.L.}} \left(\frac{m}{2\pi\hbar^2}\right)^2 \frac{1}{|\vec{q}|} \sum_{\sigma\in\{\uparrow,\downarrow\}} \begin{cases} \mu^2 \frac{1}{6} X_\mu^{-1}(12 - X_\mu^{-1}) & \text{for } b=0 \\ \mu^3 \frac{8}{3} X_\mu^{-\frac{3}{2}} & \text{for } b=1 \\ \mu^4 4 X_\mu^{-1}(1+O(X_\mu^{-1})) & \text{for } b=2 \end{cases} \\
&= \underbrace{(-1)}_{\text{F.L.}} \left(\frac{m\mu}{2\pi\hbar^2}\right)^2 \frac{1}{|\vec{q}|} \sum_{\sigma\in\{\uparrow,\downarrow\}} \begin{cases} \frac{1}{6}\frac{\hbar^2\vec{q}^2}{2m\mu}(12 - \frac{\hbar^2\vec{q}^2}{2m\mu}) & \text{for } b=0 \\ \mu \frac{8}{3}\left(\frac{\hbar^2\vec{q}^2}{2m\mu}\right)^{\frac{3}{2}} & \text{for } b=1 \\ \mu^2 4 \frac{\hbar^2\vec{q}^2}{2m\mu}(1+O(X_\mu^{-1})) & \text{for } b=2 \end{cases}
\end{aligned}
\tag{E.95}
$$

The mean frequency is M_1/M_0 and the variance is $(M_2/M_0 - (M_1/M_0)^2)$.

$$
\begin{aligned}
\frac{M_1}{M_0} &= \underbrace{\frac{\mu}{X_\mu}}_{\left(\frac{\hbar^2\vec{q}^2}{2m}\right)} \underbrace{\frac{1}{4}}_{\frac{1\cdot2\cdot3}{2\cdot3\cdot4}} \frac{\left(-4\frac{(2\sqrt{X_\mu}+1)^3+(2\sqrt{X_\mu}-1)^3}{2} + 3\frac{(2\sqrt{X_\mu}+1)^4-(2\sqrt{X_\mu}-1)^4}{2}\right)}{\left(-3\frac{(2\sqrt{X_\mu}+1)^2+(2\sqrt{X_\mu}-1)^2}{2} + 2\frac{(2\sqrt{X_\mu}+1)^3-(2\sqrt{X_\mu}-1)^3}{2}\right)} = \mu\frac{16\sqrt{\frac{\hbar^2\vec{q}^2}{2m\mu}}}{12-\frac{\hbar^2\vec{q}^2}{2m\mu}} \\
\frac{M_2}{M_0} &= \underbrace{\frac{\mu^2}{X_\mu^2}}_{\left(\frac{\hbar^2\vec{q}^2}{2m}\right)} \underbrace{\frac{1}{10}}_{\frac{1\cdot2\cdot3}{3\cdot4\cdot5}} \frac{\left(-5\frac{(2\sqrt{X_\mu}+1)^4+(2\sqrt{X_\mu}-1)^4}{2} + 4\frac{(2\sqrt{X_\mu}+1)^5-(2\sqrt{X_\mu}-1)^5}{2}\right)}{\left(-3\frac{(2\sqrt{X_\mu}+1)^2+(2\sqrt{X_\mu}-1)^2}{2} + 2\frac{(2\sqrt{X_\mu}+1)^3-(2\sqrt{X_\mu}-1)^3}{2}\right)} \approx
\end{aligned}
\tag{E.96}
$$

Grapher code: The trailing simplifications have been obtained by trial an error!

$$
\begin{aligned}
M(b,Y) &= \frac{1}{(b+1)(b+2)(b+3)} \frac{1}{Y^{b+2}} \left[-(b+3)\frac{(2\sqrt{Y}+1)^{b+2}+(2\sqrt{Y}-1)^{b+2}}{2}\right. \\
&\qquad \left. +(b+2)\frac{(2\sqrt{Y}+1)^{b+3}-(2\sqrt{Y}-1)^{b+3}}{2}\right] \\
\text{weight} &= M(0,x^{-2}) \stackrel{?}{=} \left(2x^2 - \frac{1}{6}x^4\right) \quad \text{appears exact} \\
\text{1st moment} &= M(1,x^{-2}) \stackrel{?}{=} \frac{8}{3}\theta(x)x^3 \quad \text{appears exact} \\
\text{2nd moment} &= M(2,x^{-2}) \stackrel{?}{=} 4x^4 + \frac{2}{3}x^6 - \frac{1}{60}x^8 \quad \text{appears exact} \\
\text{mean value} &= \frac{M(1,x^{-2})}{M(0,x^{-2})} \stackrel{?}{=} \frac{16x}{12-x^2} \quad \text{appears exact} \\
\text{variance} &= \frac{M(2,x^{-2})M(0,x^{-2}) - M^2(1,x^{-2})}{M^2(0,x^{-2})}
\end{aligned}
\tag{E.97}
$$

Editor: With the grapher code I played with parameters until the results appear visually identical. This is not a proof that the results are analytically correct. They may just be very good approximations.

We can now make an approximation

$$F_{\vec{q}}(\hbar\omega) = M_0(\vec{q})\frac{1}{\pi}\frac{\frac{1}{2}\Gamma}{\Big(\hbar\omega - M_1(\vec{q})/M_0(\vec{q})\Big)^2 + \left(\frac{1}{2}\Gamma\right)^2} \tag{E.98}$$

E.4.6 Fourier transform of the Coulomb potential

$$\int \frac{d^3q}{(2\pi)^3}\, e^{i\vec{q}\vec{r}}\frac{1}{\vec{q}^2 + a^2} = \frac{1}{4\pi|\vec{r}|}e^{-a|\vec{r}|} \tag{E.99}$$

Let me choose spherical coordinates

$$\begin{aligned} q_x &= q\cos(\phi)\sin(\theta) \\ q_y &= q\sin(\phi)\sin(\theta) \\ q_z &= q\cos(\theta) \\ d^3q &= dq q^2 d\phi d\theta \sin(\theta) \end{aligned} \tag{E.100}$$

with $r \in [0, \infty[$, $\theta \in [0, \pi]$ and $\phi \in [0, 2\pi[$.

Let me choose the $\vec{r}$ vector in z-direction, so that $\vec{r} = z\vec{e}_z$

$$\begin{aligned} \int \frac{d^3q}{(2\pi)^3}\, e^{i\vec{q}\vec{r}}\frac{1}{q^2 + a^2} &= \frac{1}{(2\pi)^3}\int_0^{2\pi} d\phi \int_0^{\pi} d\theta \sin(\theta) \int dq \frac{q^2}{q^2 + a^2} e^{iq\cos(\theta)z} \\ &\overset{z\cos(\theta)=y}{=} \frac{1}{(2\pi)^2}\underbrace{\frac{1}{z}\int_{-z}^{z} dy}_{\int_0^\pi d\theta \sin(\theta)} \int_0^{\infty} dq\, \frac{q^2}{q^2 + a^2} e^{iqy} \\ &= \frac{1}{(2\pi)^2}\frac{1}{z}\int_0^{\infty} dq\, \frac{q^2}{q^2 + a^2}\underbrace{\frac{1}{iq}(e^{iqz} - e^{-iqz})}_{\int_{-z}^{z} dy e^{iqy}} \\ &= \frac{1}{(2\pi)^2}\frac{1}{z}\underbrace{2\int_0^{\infty} dq}_{\int_{-\infty}^{\infty} dq}\, \frac{\overbrace{q\sin(qz)}^{\mathrm{Im}(e^{iqz})}}{q^2 + a^2} \\ &= \frac{1}{(2\pi)^2}\frac{1}{z}\mathrm{Im}\left\{\int_{-\infty}^{\infty} dq\, \frac{qe^{iqz}}{q^2 + a^2}\right\} \\ &\quad \text{...Residue theorem...} \\ &= \frac{1}{(2\pi)^2}\frac{1}{z}\mathrm{Im}\left\{2\pi i\left[\frac{qe^{iqz}}{q + ia}\right]_{q=ia}\right\} \\ &= \frac{1}{(2\pi)^2}\frac{1}{z}\mathrm{Im}\left\{2\pi i\frac{iae^{-az}}{2ia}\right\} \\ &= \frac{1}{4\pi}\frac{e^{-az}}{z} \end{aligned} \tag{E.101}$$

Finally we let a approach zero.

$$\int \frac{d^3q}{(2\pi)^3}\, e^{i\vec{q}\vec{r}}\frac{1}{q^2} = \frac{1}{4\pi}\frac{1}{z} \tag{E.102}$$

Polarization insertion in the momentum representation

Because $F_{\vec{q}}(\hbar\omega)$ depends only on the absolute value of $\vec{q}$, we can flip the sign of the momentum in the second term.

$$\Pi^{(0)}(\vec{r}_1,t_1,\vec{r}_2,t_2) = \overbrace{\frac{1}{L^3}\sum_{\vec{q}}}^{\sim\int\frac{d^3q}{(2\pi)^3}} \mathrm{e}^{-i\vec{q}(\vec{r}_1-\vec{r}_2)}\Pi^{(0)}(\vec{q},t_1,t_2) \tag{E.103}$$

with

$$\begin{aligned}\Pi^{(0)}(\vec{q},t_1,t_2) &\overset{\text{Eq. E.89}}{=} \frac{i}{\hbar}\int_0^\infty d(\hbar\omega)\left[\theta_{\mathcal{C}}(t_2-t_1)\mathrm{e}^{i\omega(t_1-t_2)}+\theta_{\mathcal{C}}(t_1-t_2)\mathrm{e}^{-i\omega(t_1-t_2)}\right]\\ &\times\underbrace{\underbrace{(-1)}_{\text{F.L.}}\left(\frac{m}{2\pi\hbar^2}\right)^2\frac{1}{|\vec{q}|}\sum_{\sigma\in\{\uparrow,\downarrow\}}\max\left[0,\min\left(\hbar\omega,\mu-\frac{1}{4}\frac{2m}{\hbar^2\vec{q}^2}\left(\hbar\omega-\frac{\hbar^2\vec{q}^2}{2m}\right)^2\right)\right]}_{\bar{F}_{\vec{q}}(\hbar\omega)\text{ Eq. E.72}}\end{aligned} \tag{E.104}$$

This is the polarization insertion of a free electron gas at zero temperature for complex-valued time arguments in the momentum representation.

Polarization insertion in momentum and frequency representation In order to obtain the polarization insertion in momentum and frequency representation, an explicit Fourier transform need to be done.

$$\begin{aligned}\Pi^{(0)}(\vec{q},\omega) &= \int_{-\infty}^{\infty} d\tau\ \mathrm{e}^{-i\omega\tau-\eta|\tau|}\ \Pi^{(0)}(\vec{q},\tau,0)\\ \Leftrightarrow\qquad \Pi^{(0)}(\vec{q},t_1,t_2) &= \int_{-\infty}^{\infty}\frac{d\omega}{2\pi}\ \mathrm{e}^{i\omega(t_1-t_2)}\ \Pi^{(0)}(\vec{q},\omega)\end{aligned} \tag{E.105}$$

where the time integration proceeds along the real-valued time axis. I introduce an infinitesimal parameter η, which regularizes the integrations. In the end, I will let this parameter approach zero.

Let me consider first the time dependence alone:

$$\begin{aligned}&\int dt\ \mathrm{e}^{-i\omega t-\eta|t|}\left\{\theta(t)\mathrm{e}^{-i\bar{\omega}t}+\theta(-t)\mathrm{e}^{+i\bar{\omega}t}\right\}\\ &=\int dt\left\{\theta(t)\mathrm{e}^{-i(\omega+\bar{\omega}+i\eta)t}+\theta(-t)\mathrm{e}^{-i(\omega-\bar{\omega}-i\eta)t}\right\}\\ &=\left[\frac{\mathrm{e}^{-i(\omega+\bar{\omega}-i\eta)t}}{-i(\omega+\bar{\omega}-i\eta)}\right]_0^\infty+\left[\frac{\mathrm{e}^{-i(\omega-\bar{\omega}+i\eta)t}}{-i(\omega-\bar{\omega}+i\eta)}\right]_{-\infty}^0\\ &=\frac{-1}{-i(\omega+\bar{\omega}-i\eta)}+\frac{+1}{-i(\omega-\bar{\omega}+i\eta)}\\ &=\frac{i}{\omega+\bar{\omega}-i\eta}+\frac{-i}{\omega-\bar{\omega}+i\eta}\\ &=\frac{i(\omega+\bar{\omega})+\eta}{(\omega+\bar{\omega})^2+\eta^2}+\frac{-i(\omega-\bar{\omega})+\eta}{(\omega-\bar{\omega})^2+\eta^2}\\ &=\pi\Big(\delta(\omega+\bar{\omega})+\delta(\omega-\bar{\omega})\Big)+i\left(\frac{1}{\omega+\bar{\omega}}-\frac{1}{\omega-\bar{\omega}}\right)\end{aligned} \tag{E.106}$$

$$\Pi^{(0)}(\vec{q},\omega) = \frac{i\pi}{\hbar} \underbrace{(-1)}_{\text{F.L.}} \left(\frac{m}{2\pi\hbar^2}\right)^2 \frac{1}{|\vec{q}|} \sum_{\sigma\in\{\uparrow,\downarrow\}} \underbrace{\max\left[0, \min\left(\hbar|\omega|, \mu - \frac{1}{4}\frac{2m}{\hbar^2\vec{q}^2}\left(\hbar|\omega| - \frac{\hbar^2\vec{q}^2}{2m}\right)^2\right)\right]}_{\bar{F}_{\vec{q}}(\hbar\omega) \text{ Eq. E.72}}$$
$$- \frac{1}{\hbar}\int_0^\infty d(\hbar\bar{\omega}) \left(\frac{1}{\omega+\bar{\omega}} - \frac{1}{\omega-\bar{\omega}}\right)$$
$$\times \underbrace{(-1)}_{\text{F.L.}} \left(\frac{m}{2\pi\hbar^2}\right)^2 \frac{1}{|\vec{q}|} \sum_{\sigma\in\{\uparrow,\downarrow\}} \underbrace{\max\left[0, \min\left(\hbar\bar{\omega}, \mu - \frac{1}{4}\frac{2m}{\hbar^2\vec{q}^2}\left(\hbar\bar{\omega} - \frac{\hbar^2\vec{q}^2}{2m}\right)^2\right)\right]}_{\bar{F}_{\vec{q}}(\hbar\omega) \text{ Eq. E.72}} \quad \text{(E.107)}$$

Editor: Caution regarding negative $\bar{\omega}$!! This equation needs to be carefully checked. It is only a sketch.

Comparison with Negele Orland My derivation is quite different from previous ones, that work directly in frequency-momentum space where the frequency results from a fourier transform along the real-valued time axis. Hence, I avoid the complex time integrations in the complex ω-plane and the use of the residual theorem. I have done so to avoid the limitation to real-valued time axis.

Comparison with Eq. 5.109b of Negele and Orland[8]. Caution! There seem to be some typos. $\tilde{q} \overset{\text{def}}{=} q/k_F$ and $\tilde{\omega} \overset{\text{def}}{=} \omega m/k_F^2$. $\mu = \hbar^2 k_F^2/(2m)$ and $\sum_\sigma \frac{1}{(2\pi)^3}\frac{4\pi}{3}k_F^3 = N/V$ and hence $k_F = \sqrt[3]{3\pi^2 N/V}$

$$\begin{aligned}
\mathrm{Im}D_0(q,\omega) &= \frac{-mk_F}{4\pi q}\begin{cases} 1-\left(\frac{\tilde{\omega}}{\tilde{q}}-\frac{\tilde{q}}{2}\right)^2 & \text{for } \frac{\tilde{q}}{2}-\tilde{q} < \tilde{\omega} \le \frac{\tilde{q}}{2}+\tilde{q} \\ 2\tilde{\omega} & \text{for } 0 \le \tilde{\omega} \le \tilde{q}-\frac{\tilde{q}^2}{2} \end{cases} \\
&= \frac{-mk_F}{4\pi q}\begin{cases} 1-\frac{k_F^2}{q^2}\left(\frac{\omega m}{k_F^2}-\frac{1}{2}\frac{q^2}{k_F^2}\right)^2 & \text{for } \frac{\tilde{q}}{2}-\tilde{q} < \tilde{\omega} \le \frac{\tilde{q}}{2}+\tilde{q} \\ 2\frac{\omega m}{k_F^2} & \text{for } 0 \le \tilde{\omega} \le \tilde{q}-\frac{\tilde{q}^2}{2} \end{cases} \\
&= \frac{-mk_F}{4\pi q}\frac{2m}{k_F^2}\begin{cases} \frac{k_F^2}{2m}-\frac{1}{4}\frac{2m}{q^2}\left(\omega-\frac{q^2}{2m}\right)^2 & \text{for } \frac{\tilde{q}}{2}-\tilde{q} < \tilde{\omega} \le \frac{\tilde{q}}{2}+\tilde{q} \\ \omega & \text{for } 0 \le \tilde{\omega} \le \tilde{q}-\frac{\tilde{q}^2}{2} \end{cases} \\
&= \underbrace{(-1)\left(\frac{m}{2\pi\hbar^2}\right)^2 \frac{1}{q}\sum_\sigma \begin{cases} \mu-\frac{1}{4}\frac{2m}{\hbar^2q^2}\left(\hbar\omega-\frac{\hbar^2q^2}{2m}\right)^2 & \text{for } \frac{\tilde{q}}{2}-\tilde{q} < \tilde{\omega} \le \frac{\tilde{q}}{2}+\tilde{q} \\ \hbar\omega & \text{for } 0 \le \tilde{\omega} \le \tilde{q}-\frac{\tilde{q}^2}{2} \end{cases}}_{\bar{F}_{\vec{q}}} \\
&\quad \times \underbrace{\pi}_{\text{from Fourier transform of } t_2-t_1} \times \underbrace{\frac{1}{k_F}}_{\text{discrepancy}} \qquad \text{(E.108)}
\end{aligned}$$

The factor π is not contained in $\bar{F}$, but results from the Fourier transform of the relative time.

Editor: There is different prefactor!

Comparison with Fetter Walecka Fetter Walecka Eq.12.41, 12.43, 12.45.

$$\mathrm{Im}\Pi^0(\vec{q},\nu) = -\frac{mk_F}{\hbar^2}\frac{1}{4\pi q}\begin{cases} \left[1-\left(\frac{\nu}{q}-\frac{1}{2}q\right)^2\right] & \text{for } q-\frac{1}{2}q^2 \mathit{Ie}\nu \le +\frac{1}{2}q^2 \\ 2\nu & \text{for } 0 \le \nu \le q-\frac{1}{2}q^2 \text{ and } q<2 \end{cases} \qquad \text{(E.109)}$$

with Eq. Walecke 12.35: $\nu = \hbar q_0 \frac{m}{\hbar^2 k_F^2}$. I did not find the definition of q_0. (I believe, it is my ω, the time component of the four-momentum.) (Furthermore, I believe that Fetter's q is my $|\vec{q}|/k_F$.)

Discussion of the lowest-order polarization insertion Editor: The following is a set of personal notes for the author. They have not been verified!

The polarization insertion in lowest order is shown in figure E.7. If the polarization insertion is renormalized by considering all chains of ring diagrams connected by interactions, a **plasmon branch** splits off from the continuum.

In lowest order we find a pronounced ridge for small energy- and momentum-transfer. It reminds of the dispersion relation of a boson with velocity equal to the Fermi velocity. Editor: Will this feature turn into the plasmon band, when interaction is switched on? When this feature is considered as a spectral function of bosons, they move marginally slower (line B in figure E.7) than the electrons (line A). (check this!) Hence an interacting system will transfer kinetic energy to this boson. This may be one possible explanation for the finite life time of the electrons.

At $\hbar\omega = \mu$, this ridge disappears in the continuum of electron-hole excitations. Editor: What is special at the Fermi energy? Is it that the excitation energy can reach the (flat) bottom of the free-electron band?

E.4.7 Screened interaction and dielectric constant

Editor: Sketch: do not read!!!

$$\begin{aligned}\Pi^{RPA} &= \Pi^{(0)} + \Pi^{(0)}V\Pi^{(0)} + \Pi^{(0)}V\Pi^{(0)}V\Pi^{(0)} + \dots \\ &= \Pi^{(0)} + \Pi^{(0)}V\Pi^{RPA} \\ \Pi^{RPA} &= \left(1 - \Pi^{(0)}V\right)^{-1}\Pi^{(0)}\end{aligned} \tag{E.110}$$

$$\begin{aligned}V^{scr,RPA} &= V^{(0)} + V^{(0)}\Pi^{(0)}V^{(0)} + V^{(0)}\Pi^{(0)}V^{(0)}\Pi^{(0)}V^{(0)} + \dots \\ &= V^{(0)} + V^{(0)}\Pi^{(0)}V^{(scr,RPA)} \\ &= \underbrace{\left(1 - V^{(0)}\Pi^{(0)}\right)^{-1}}_{\frac{1}{\epsilon_r^{RPA}}} V^{(0)}\end{aligned} \tag{E.111}$$

$$\epsilon_r^{RPA} = 1 - V^{(0)}\Pi^{(0)} \tag{E.112}$$

Of particular interest are the zeros of the dielectric constant. For those momenta $\hbar\vec{q}$ and energies $\hbar\omega$, the screened potential does not become smaller than the bare potential, but it becomes infinite. A charge fluctuation with these momenta and frequencies can occur spontaneously. It can be considered a quasi-particle, which is called a **plasmon**.

Four-center integrals in a plane-wave basis:

When the interaction matrix elements for the interaction are expressed in terms of plane waves, there are selection rules which require certain matric elements to be zero. Let me therefore analyze these four center integrals.

For our basisset the four-center integrals are

$$\begin{aligned} W_{\vec{k}_1,\sigma_1,\vec{k}_2,\sigma_2,\vec{k}_3,\sigma_3,\vec{k}_4,\sigma_4} &= \frac{e^2}{4\pi\epsilon_0}\delta_{\sigma_1,\sigma_3}\delta_{\sigma_2,\sigma_4}\int d^3r\int d^3r'\;\frac{1}{L^6}\frac{\mathrm{e}^{i(\vec{k}_3-\vec{k}_1)\vec{r}}\mathrm{e}^{i(\vec{k}_4-\vec{k}_2)\vec{r}'}}{|\vec{r}-\vec{r}'|} \\ &= \frac{e^2}{4\pi\epsilon_0}\delta_{\sigma_1,\sigma_3}\delta_{\sigma_2,\sigma_4}\underbrace{\int d^3r\;\frac{1}{L^3}\mathrm{e}^{i(\vec{k}_3-\vec{k}_1+\vec{k}_4-\vec{k}_2)\vec{r}}}_{\delta_{\vec{k}_3-\vec{k}_1+\vec{k}_4-\vec{k}_2,0}}\frac{1}{L^3}\int d^3r'\;\frac{\mathrm{e}^{i(\vec{k}_4-\vec{k}_2)\left(\vec{r}'-\vec{r}\right)}}{|\vec{r}-\vec{r}'|} \\ &= \frac{e^2}{4\pi\epsilon_0}\delta_{\sigma_1,\sigma_3}\delta_{\sigma_2,\sigma_4}\delta_{\vec{k}_3-\vec{k}_1+\vec{k}_4-\vec{k}_2,\vec{0}}\frac{4\pi}{|\vec{k}_4-\vec{k}_2|^2} \end{aligned} \tag{E.113}$$

I introduce $\vec{q}\stackrel{\text{def}}{=}\vec{k}_4-\vec{k}_2$ and $\vec{q}'\stackrel{\text{def}}{=}\vec{k}_1-\vec{k}_3$. The four-center matrix elements are

$$W_{\vec{k}_1,\sigma_1,\vec{k}_2,\sigma_2,\vec{k}_1-\vec{q}',\sigma_3,\vec{k}_2+\vec{q},\sigma_4} = \frac{4\pi e^2}{4\pi\epsilon_0|\vec{q}|^2}\delta_{\sigma_1,\sigma_3}\delta_{\sigma_2,\sigma_4}\delta_{\vec{q},\vec{q}'} \tag{E.114}$$

The four-center matrix elements do not depend on $\vec{k}_1$ nor on $\vec{k}_2$. More importantly it only depends on the difference of the two wave vectors and spins on each of the two vertices.

Appendix F

Additional topics on Downfolding

F.1 Embedding in the time domain

Here we return to section 5.1 on p. 187 and investigate coupled systems in the time representation rather than the energy representation.

I begin with the time-dependent Schrodinger equation for a composite system, which consists of two subsystems A and B. The wave function of the systen is

$$|\psi(t)\rangle = \sum_\alpha |\chi^A_\alpha\rangle c^A_\alpha(t) + \sum_\beta |\chi^B_\beta\rangle c^B_\beta(t) \tag{F.1}$$

where the $\{|\chi^A_\alpha\rangle\} \cup \{|\chi^B_\beta\rangle\}$ are orthonormal.

$$\begin{pmatrix} \mathbf{1}^{AA} i\hbar\partial_t - \boldsymbol{H}^{AA}(t) & -\boldsymbol{V}^{AB}(t) \\ -\boldsymbol{V}^{BA}(t) & \mathbf{1}^{BB} i\hbar\partial_t - \boldsymbol{H}^{BB}(t) \end{pmatrix} \begin{pmatrix} \vec{c}^A(t) \\ \vec{c}^B(t) \end{pmatrix} = 0 \tag{F.2}$$

which can be broken up into two equations

$$-\boldsymbol{V}^{BA}(t)\vec{c}^A(t) + \Big(\mathbf{1}^{BB} i\hbar\partial_t - \boldsymbol{H}^{BB}(t)\Big)\vec{c}^B(t) = 0 \tag{F.3}$$

$$\Big(\mathbf{1}^{AA} i\hbar\partial_t - \boldsymbol{H}^{AA}(t)\Big)\vec{c}^A(t) - \boldsymbol{V}^{AB}(t)\vec{c}^B(t) = 0 \tag{F.4}$$

Let me define an auxiliary quantity $\vec{q}^B(t)$, such that

$$\vec{c}^B(t) = \int dt'\, \bar{\boldsymbol{G}}^{BB}(t,t')\vec{q}^B(t') \tag{F.5}$$

where

$$\Big(\mathbf{1}^{BB} i\hbar\partial_t - \boldsymbol{H}^{BB}(t)\Big)\bar{\boldsymbol{G}}^{BB}(t,t') = \mathbf{1}^{BB}\delta(t-t') \quad \text{and } \bar{\boldsymbol{G}}^{BB}(t,t') = 0 \text{ for } t \le t' \tag{F.6}$$

The object $\bar{\boldsymbol{G}}^{BB}(t,t')$ is the Green's function of the isolated system B. The bar ontop of the symbol distinguishes it from the projection of the Green's function of the composite system onto the subsystem A.

Now, I begin with the first (lower) Schrödinger equation Eq. F.3 to express $\vec{q}^A$ by $\vec{c}^A$.

$$\begin{aligned}
\text{Eq. F.3} &\overset{\text{Eq. F.5}}{\Rightarrow} -\boldsymbol{V}^{BA}(t)\vec{c}^A(t) + \underbrace{\Big(\mathbf{1}^{BB} i\hbar\partial_t - \boldsymbol{H}^{BB}(t)\Big) \overbrace{\int dt'\, \bar{\boldsymbol{G}}^{BB}(t,t')\vec{q}^B(t')}^{\vec{c}^B(t)}}_{\vec{q}^B(t)} = 0 \\
&\Rightarrow \quad \vec{q}^B(t) = \boldsymbol{V}^{BA}(t)\vec{c}^A(t) \\
&\Rightarrow \quad \vec{c}^B(t) \overset{\text{Eq. F.5}}{=} \int dt'\, \bar{\boldsymbol{G}}^{BB}(t,t') \overbrace{\boldsymbol{V}^{BA}(t')\vec{c}^A(t')}^{\vec{q}^B(t')}
\end{aligned} \tag{F.7}$$

With the relation Eq. F.7 between $\vec{c}^A(t)$ and $\vec{c}^B(t)$, we turn to the 2nd, upper Schrödinger equation Eq. F.4

$$\begin{aligned}
\text{Eq. F.4} &\Rightarrow \Big(\mathbf{1}^{AA} i\hbar\partial_t - \boldsymbol{H}^{AA}(t)\Big)\vec{c}^A(t) - \boldsymbol{V}^{AB}(t) \overbrace{\int dt'\, \bar{\boldsymbol{G}}^{BB}(t,t') \underbrace{\boldsymbol{V}^{BA}(t')\vec{c}^A(t')}_{\vec{q}^B(t')}}^{\vec{c}^B(t)} = 0 \\
&\Rightarrow \quad \Big(\mathbf{1}^{AA} i\hbar\partial_t - \boldsymbol{H}^{AA}(t)\Big)\vec{c}^A(t) - \int_{-\infty}^{t} dt'\, \underbrace{\boldsymbol{V}^{AB}(t)\bar{\boldsymbol{G}}^{BB}(t,t')\boldsymbol{V}^{BA}(t')}_{\boldsymbol{\Sigma}^{AA}(t,t')}\vec{c}^A(t') = 0 \\
&\Rightarrow \quad \int_{-\infty}^{t} dt' \left[\Big(\mathbf{1}^{AA} i\hbar\partial_t - \boldsymbol{H}^{AA}(t)\Big)\delta(t-t') - \boldsymbol{\Sigma}^{AA}(t,t')\right]\vec{c}^A(t') = 0
\end{aligned} \tag{F.8}$$

where the **self energy** is

$$\boldsymbol{\Sigma}^{AA}(t,t') \overset{\text{def}}{=} \boldsymbol{V}^{AB}(t)\bar{\boldsymbol{G}}^{BB}(t,t')\boldsymbol{V}^{BA}(t') \tag{F.9}$$

The self energy $\Sigma^{AA}(\vec{x},t,\vec{x}',t') = \sum_{\alpha,\beta\in A}\langle\vec{x}|\pi_\alpha\rangle\Sigma^{AA}_{\alpha,\beta}(t,t')\langle\pi_\beta|\vec{x}'\rangle$ is non-local in space and time. In the many-body Green's function approach, the self energy is the second-most important quantity after the Green's function.

Thus, with Eq. F.8 we arrive at an integro-differential equation for the orbital coefficients $\vec{c}^A(t)$ of subsystem A. The bounds for the time integration stem from the properties of the (retarded) Green's function $\bar{\boldsymbol{G}}^{BB}(t,t')$ which is non-zero only for $t > t'$.

On the one hand, an integro-differential equation is usually more complicated to solve than a differential equation. On the other hand, the subsystem A may be a substantially smaller problem than the composite system.

The wave function can be described as

$$\begin{aligned}
|\psi(t)\rangle &\overset{\text{Eq. F.7}}{=} \sum_{\alpha\in A}|\chi^A_\alpha\rangle c^A_\alpha(t) + \sum_{\alpha\in A,\beta\in B}|\chi^B_\beta\rangle \int dt' \left(\bar{\boldsymbol{G}}^{BB}(t,t')\boldsymbol{V}^{BA}(t')\right)_{\beta,\alpha} c^A_\alpha(t') \\
&= \int dt'\, |\tilde{\chi}^A(t,t')\rangle\vec{c}^A(t')
\end{aligned} \tag{F.10}$$

with a retarded basisset

$$|\tilde{\chi}^A(t,t')\rangle = |\chi^A\rangle\delta(t-t') + |\chi^B\rangle\bar{\boldsymbol{G}}^{BB}(t,t')\boldsymbol{V}^{BA}(t') \tag{F.11}$$

These retarded orbitals $|\tilde{\chi}^A(t,t')\rangle$ are explicitely time dependent. They extend over system A, but also cover system B. It describes exactly that part of system B that can be influenced by system A.

Let me sumarize the result

TIME-DEPENDENT EMBEDDING

$$|\psi(t)\rangle \overset{\text{Eq. F.7}}{=} \int dt' \left\{ \underbrace{|\vec{\chi}^A\rangle\delta(t-t') + |\vec{\chi}^B\rangle \bar{\boldsymbol{G}}^{BB}(t,t')\boldsymbol{V}^{BA}(t')}_{|\tilde{\chi}^A(t,t')\rangle} \right\} \underbrace{\langle \vec{\chi}^A|\psi(t')\rangle}_{\vec{c}^A(t')}$$

plus stuff only in B

$$= \int dt' \sum_\alpha \underbrace{\left\{ |\chi^A_\alpha\rangle\delta(t-t') + \sum_{\beta,\beta'\in B} |\chi^B_\beta\rangle \bar{G}^{BB}_{\beta,\beta'}(t,t')V^{BA}_{\beta',\alpha}(t') \right\}}_{|\tilde{\chi}^A_\alpha(t,t')\rangle} \underbrace{\langle \chi^A_\alpha|\psi(t')\rangle}_{c^A_\alpha(t')} \quad \text{(F.12)}$$

In order to determine the wave function in subsysten A, I need to know the complete history of $\psi(t)$ in A.

Transformation into the energy representation

Editor: From here on it is construction. The question, I want to address is whether/why the Hamilton-matrix elements for complex-valued energies are $\langle\chi_\alpha(\epsilon^*)|\hat{H}|\chi_\beta(\epsilon)\rangle$, with a complex conjugate energy in the bra.

For a time-independent Hamiltonian, the orbitals depend only on the retardation $\tau = t - t'$, and the orbital can be Fourier transformed in τ.

$$|\tilde{\chi}^A(t,t')\rangle = \int d\epsilon\, |\tilde{\chi}^A(\epsilon)\rangle e^{-\frac{i}{\hbar}\epsilon(t-t')} \quad \text{(F.13)}$$

Just to prepare the ground let me repeat the normal transformation from the time-dependent to the time-independent Schrödinger equation.

$$\begin{aligned} 0 \overset{!}{=} \left(i\hbar\partial_t - \hat{H}\right)|\psi(t)\rangle &= \left(i\hbar\partial_t - \hat{H}\right)\sum_\epsilon |\psi(\epsilon)\rangle e^{-\frac{i}{\hbar}\epsilon t} \\ &= \sum_\epsilon (\epsilon - \hat{H})|\psi(\epsilon)\rangle e^{-\frac{i}{\hbar}\epsilon t} \\ \Rightarrow \qquad (\epsilon - \hat{H})|\psi(\epsilon)\rangle &= 0 \end{aligned} \quad \text{(F.14)}$$

Appendix G

Hartree-Fock approximation

G.1 Boltzmann entropy

In section 2.5.6 on p. 70, I refer to Boltzmann entropy. Here, I present the relevant derivations, and I provide results for, both, fermions and bosons, as well as the dilute limit.

The Boltzmann entropy (as I choose to call it) is the maximum entropy for a given-one-particle-reduced density matrix. Therefore, it plays a role whenever the one-particle-reduced density matrix plays a central role. This is the case for non-interacting systems, but also for the thermal Hartree-Fock approximation, density-functional theory, reduced-density-matrix functional theory. Similarly, it is an important ingredient for the Boltzmann equation.

Here, I will derive

- the functional form of the Boltzmann entropy as functional of the density matrix and
- the von-Neumann density matrix Eq. 2.71, that maximizes the entropy for a specified one-particle-reduced density matrix in terms of occupations and natural orbitals.

G.1.1 Definition

As specified in Eq. 2.68, the Boltzmann entropy S^B is defined as the maximum entropy which can be obtained for a given one-particle-reduced density matrix

$$\begin{aligned} S^B[\hat{\rho}^{(1)}] &\overset{\text{Eq. 2.68}}{=} \max_{\hat{\rho}^{vN}} \operatorname{stat}_{\boldsymbol{B},\lambda} \Bigg\{ \underbrace{-k_B \mathrm{Tr}\left[\hat{\rho}^{vN} \ln\left(\hat{\rho}^{vN}\right)\right]}_{\text{von-Neumann entropy}} - \sum_{\alpha,\beta} k_B B_{\alpha,\beta} \underbrace{\left(\mathrm{Tr}\left[\hat{\rho}^{vN} \hat{c}_\alpha^\dagger \hat{c}_\beta\right] - \langle \pi_\beta | \hat{\rho}^{(1)} | \pi_\alpha \rangle\right)}_{\text{density-matrix constraint}} \\ &\qquad - k_B(\lambda - 1) \underbrace{\left(\mathrm{Tr}\left[\hat{\rho}^{vN}\right] - 1\right)}_{\text{norm constraint}} \Bigg\} \qquad \text{(G.1)} \\ &= \max_{\hat{\rho}^{vN}} \operatorname{stat}_{\boldsymbol{B},\lambda} \mathcal{S}^B[\hat{\rho}^{(1)}, \hat{\rho}^{vN}, \boldsymbol{B}, \lambda] \end{aligned}$$

The matrix $\boldsymbol{B}$ and λ are Lagrange multipliers, which enforce the constraints for the one-particle-reduced density matrix and the norm.

G.1.2 Maximum-entropy ensemble for a one-particle-reduced density matrix

At the constrained maximum, the variation of $\mathcal{S}^B$ vanishes. The variation is

$$\delta\mathcal{S}^B \overset{\text{Eq. } G.1}{=} -k_B \mathrm{Tr}\left[\delta\hat{\rho}^{vN}\left(\ln\left(\hat{\rho}^{vN}\right) + \hat{1}\lambda + \sum_{\alpha,\beta} B_{\alpha,\beta}\hat{c}_\alpha^\dagger \hat{c}_\beta\right)\right] \tag{G.2}$$

$$-k_B \sum_{\alpha,\beta} \delta B_{\alpha,\beta}\left(\mathrm{Tr}\left[\hat{\rho}^{vN}\hat{c}_\alpha^\dagger \hat{c}_\beta\right] - \langle\pi_\beta|\hat{\rho}^{(1)}|\pi_\alpha\rangle\right) \tag{G.3}$$

$$+k_B \mathrm{Tr}_{1P}\left[\delta\hat{\rho}^{(1)}\left(\sum_{\alpha,\beta}|\pi_\alpha\rangle B_{\alpha,\beta}\langle\pi_\beta|\right)\right] - k_B\delta\lambda\left(\mathrm{Tr}\left[\hat{\rho}^{vN}\right] - 1\right) \tag{G.4}$$

The subscript at Tr_{1P} emphasises that the trace is performed over the one-particle Hilbert space, rather than the many-particle Fock space.

The maximum and the stationary conditions $\delta\mathcal{S}^B = 0$ require

$$\hat{0} = \ln\left(\hat{\rho}^{vN}\right) + \hat{1}\lambda + \sum_{\alpha,\beta} B_{\alpha,\beta}\hat{c}_\alpha^\dagger \hat{c}_\beta \qquad \text{equilibrium condition} \tag{G.5}$$

$$0 = \mathrm{Tr}\left[\hat{\rho}^{vN}\hat{c}_\alpha^\dagger \hat{c}_\beta\right] - \langle\pi_\beta|\hat{\rho}^{(1)}|\pi_\alpha\rangle \qquad \text{density-matrix constraint} \tag{G.6}$$

$$0 = \mathrm{Tr}\left[\hat{\rho}^{vN}\right] - 1 \qquad \text{norm constraint} \tag{G.7}$$

The equilibrium condition $\delta\mathcal{S}^B/\delta\hat{\rho}^{vN} = \hat{0}$, together with the norm condition $\delta\mathcal{S}^B/\delta\lambda = 0$, yields

$$\hat{\rho}^{vN}[\hat{\rho}^{(1)}] \overset{\text{Eq. } G.5}{=} \exp\left(-\lambda\hat{1} - \sum_{\alpha,\beta}^{\infty} B_{\alpha,\beta}\hat{c}_\alpha^\dagger \hat{c}_\beta\right) \overset{\text{Eq. } G.7}{=} \frac{\exp\left(-\sum_{\alpha,\beta} B_{\alpha,\beta}\hat{c}_\alpha^\dagger \hat{c}_\beta\right)}{\mathrm{Tr}\left[\exp\left(-\sum_{\alpha',\beta'} B_{\alpha',\beta'}\hat{c}_{\alpha'}^\dagger \hat{c}_{\beta'}\right)\right]} \tag{G.8}$$

This links the von-Neumann density matrix to the exponential of an one-particle-at-a-time operator $\hat{B} = \sum_{\alpha,\beta} B_{\alpha,\beta}\hat{c}_\alpha^\dagger \hat{c}_\beta$ expressed by the Lagrange multipliers $\boldsymbol{B}$.

With the eigenstates $|\varphi_n\rangle$ and the eigenvalues b_n of $\hat{B} = \sum_{\alpha,\beta}|\pi_\alpha\rangle B_{\alpha,\beta}\langle\pi_\beta|$ defined by $\hat{B}|\varphi_n\rangle = |\varphi_n\rangle b_n$, the following eigenvalue equation holds for the Slater determinants (or permanents in the case of bosons) built over the basisset $\{|\varphi_n\rangle\}$.

$$\sum_{\alpha,\beta} B_{\alpha,\beta}\hat{c}_\alpha^\dagger \hat{c}_\beta|\vec{\sigma}\rangle = |\vec{\sigma}\rangle \sum_n \sigma_n b_n \tag{G.9}$$

For fermions, the components of the occupation-number vector $\vec{\sigma}$ can assume only two values $\sigma_n \in \{0, 1\}$, while the occupation numbers for bosons can be any non-negative integer $\sigma_n \in \{0, 1, 2, \ldots\}$. Therefore, also the sum over occupation-number vectors $\vec{\sigma}$ is much more extended for bosons. These summations have the form of geometric sums, which can be worked out analytically. The difference between fermions and bosons will become evident only later, when we perform the sums over occupation numbers.

With the help of Eq. G.9, Eq. G.8 obtains the form

$$\hat{\rho}^{vN}[\hat{\rho}^{(1)}] \overset{\text{Eq. } G.8}{=} \sum_{\vec{\sigma}} |\vec{\sigma}\rangle \underbrace{\frac{\mathrm{e}^{-\sum_n b_n\sigma_n}}{\sum_{\vec{\sigma}} \mathrm{e}^{-\sum_j b_j\sigma_j}}}_{P_{\vec{\sigma}}} \langle\vec{\sigma}| \tag{G.10}$$

The one-particle-reduced density matrix is obtained after imposing the density-matrix constraint

$$\mathrm{Tr}\left[\hat{\rho}^{vN}\hat{c}_\alpha^\dagger \hat{c}_\beta\right] \overset{\text{Eq. } G.6}{=} \langle\pi_\beta|\hat{\rho}^{(1)}|\pi_\alpha\rangle \qquad \Rightarrow \qquad \sum_{\alpha,\beta}|\chi_\beta\rangle \mathrm{Tr}\left[\hat{\rho}^{vN}\hat{c}_\alpha^\dagger \hat{c}_\beta\right]\langle\chi_\alpha| = \hat{\rho}^{(1)} \tag{G.11}$$

and

$$
\begin{aligned}
\Rightarrow \qquad \hat{\rho}^{(1)} &\overset{\text{Eq. G.10}}{=} \sum_{\alpha,\beta} |\chi_\beta\rangle \mathrm{Tr}\Bigg[\underbrace{\sum_{\vec{\sigma}} |\vec{\sigma}\rangle \frac{\mathrm{e}^{-\sum_n b_n \sigma_n}}{\sum_{\vec{\sigma}} \mathrm{e}^{-\sum_j b_j \sigma_j}} \langle\vec{\sigma}|}_{\hat{\rho}^{vN}} \hat{c}_\alpha^\dagger \hat{c}_\beta \Bigg] \langle\chi_\alpha| \\
&\overset{\text{cycl.perm.}}{=} \sum_{\alpha,\beta} |\chi_\beta\rangle \Bigg[\sum_{\vec{\sigma}} \frac{\mathrm{e}^{-\sum_n b_n \sigma_n}}{\sum_{\vec{\sigma}} \mathrm{e}^{-\sum_j b_j \sigma_j}} \underbrace{\langle\vec{\sigma}|\hat{c}_\alpha^\dagger \hat{c}_\beta|\vec{\sigma}\rangle}_{\sum_n \sigma_n \langle\varphi_n|\pi_\alpha\rangle\langle\pi_\beta|\varphi_n\rangle} \Bigg] \langle\chi_\alpha| \\
&= \underbrace{\Big(\sum_\beta |\chi_\beta\rangle\langle\pi_\beta|\Big)}_{\hat{1}} \sum_n |\varphi_n\rangle \underbrace{\left(\frac{\sum_{\vec{\sigma}} \mathrm{e}^{-\sum_n b_n \sigma_n} \sigma_n}{\sum_{\vec{\sigma}} \mathrm{e}^{-\sum_j b_j \sigma_j}} \right)}_{-\partial_{b_n} \ln \sum_{\vec{\sigma}} \mathrm{e}^{-\sum_j b_j \sigma_j}} \langle\varphi_n| \underbrace{\Big(\sum_\alpha |\pi_\alpha\rangle\langle\chi_\alpha|\Big)}_{\hat{1}} \\
&= \sum_n |\varphi_n\rangle \Big(-\partial_{b_n} \ln \sum_{\vec{\sigma}} \mathrm{e}^{-\sum_j b_j \sigma_j} \Big) \langle\varphi_n| \qquad \text{(G.12)}
\end{aligned}
$$

In the second line, I exploited Eq. 2.10 from p. 51 which says that the expectation value of any one-particle-at-a-time operator $\hat{A}$ with a Slater determinant is a sum over one-particle basis orbitals

$$
\begin{aligned}
& & \langle\vec{\sigma}|\hat{A}|\vec{\sigma}\rangle &\overset{\text{Eq. 2.10}}{=} \sum_n \sigma_n \langle\varphi_n|\hat{A}|\varphi_n\rangle \\
\Leftrightarrow \qquad & \langle\vec{\sigma}| \underbrace{\sum_{\alpha,\beta} A_{\alpha,\beta} \hat{c}_\alpha^\dagger \hat{c}_\beta}_{\hat{A}} |\vec{\sigma}\rangle &= \sum_n \sigma_n \langle\varphi_n| \underbrace{\sum_{\alpha,\beta} |\pi_\alpha\rangle A_{\alpha,\beta} \langle\pi_\beta|}_{\hat{A}} |\varphi_n\rangle \\
\Rightarrow \qquad & \langle\vec{\sigma}|\hat{c}_\alpha^\dagger \hat{c}_\beta|\vec{\sigma}\rangle &= \sum_n \sigma_n \langle\varphi_n|\pi_\alpha\rangle\langle\pi_\beta|\varphi_n\rangle \qquad \text{(G.13)}
\end{aligned}
$$

Because the right-hand side of Eq. G.12 is diagonal in the basis of the eigenstates of $\hat{B}$, the identity requires that its eigenstates $|\varphi_n\rangle$ are also the eigenstates of the one-particle-reduced density matrix, the natural orbitals. Furthermore, the matrix elements $-\partial_{b_n} \ln \sum_{\vec{\sigma}} \mathrm{e}^{-\sum_j b_j \sigma_j}$ must be identical to the eigenvalues of the one-particle-reduced density matrix, the occupations f_n.

Hence,

$$
\begin{aligned}
f_n &\overset{\text{Eq. G.12}}{=} -\partial_{b_n} \ln \sum_{\vec{\sigma}} \mathrm{e}^{-\sum_j b_j \sigma_j} = -\partial_{b_n} \ln \prod_j \sum_{\sigma_j} \mathrm{e}^{-b_j \sigma_j} = -\partial_{b_n} \sum_j \ln \sum_\sigma \mathrm{e}^{-b_j \sigma} = -\partial_{b_n} \ln \sum_\sigma \mathrm{e}^{-b_n \sigma} \\
&= \begin{cases} -\partial_{b_n} \ln\Big(1 + \mathrm{e}^{-b_n}\Big) = \frac{\mathrm{e}^{-b_n}}{1+\mathrm{e}^{-b_n}} & \text{for fermions} \\ -\partial_{b_n} \ln\Big(\frac{1}{1-\mathrm{e}^{-b_n}}\Big) = \frac{\mathrm{e}^{-b_n}}{1-\mathrm{e}^{-b_n}} & \text{for bosons} \end{cases} \\
&= \Big(\mathrm{e}^{+b_n} - \eta\Big)^{-1} \qquad \text{(G.14)}
\end{aligned}
$$

with $\eta = -1$ for fermions and $\eta = +1$ for bosons. We obtain

$$
\mathrm{e}^{-b_n} \overset{\text{Eq. G.14}}{=} \frac{f_n}{1 + \eta f_n} \qquad \text{(G.15)}
$$

Now we insert e^{-b_n} into the von-Neumann density matrix

$$\begin{aligned}
\hat{\rho}^{vN}[\hat{\rho}^{(1)}] &\overset{\text{Eq. } G.10}{=} \sum_{\vec{\sigma}} |\vec{\sigma}\rangle \underbrace{\frac{\mathrm{e}^{-\sum_n b_n \sigma_n}}{\sum_{\vec{\sigma}} \mathrm{e}^{-\sum_j b_j \sigma_j}}}_{P_{\vec{\sigma}}} \langle\vec{\sigma}| \overset{\text{Eq. } G.15}{=} \sum_{\vec{\sigma}} |\vec{\sigma}\rangle \prod_n \frac{\left(\frac{f_n}{1+\eta f_n}\right)^{\sigma_n}}{\sum_{\sigma'} \left(\frac{f_n}{1+\eta f_n}\right)^{\sigma'}} \langle\vec{\sigma}| \\
&= \sum_{\vec{\sigma}} |\vec{\sigma}\rangle \prod_n \frac{\left(\frac{f_n}{1+\eta f_n}\right)^{\sigma_n}}{\left(1-\eta\left(\frac{f_n}{1+\eta f_n}\right)\right)^{-\eta}} \langle\vec{\sigma}| \\
&= \sum_{\vec{\sigma}} |\vec{\sigma}\rangle \prod_n \Big(f_n\Big)^{\sigma_n} \Big(1+\eta f_n\Big)^{-\sigma_n} \Big(1+\eta f_n\Big)^{-\eta} \langle\vec{\sigma}| \\
&= \sum_{\vec{\sigma}} |\vec{\sigma}\rangle \underbrace{\prod_n f_n^{\sigma_n} \big(1+\eta f_n\big)^{-\sigma_n-\eta}}_{P_{\vec{\sigma}}} \langle\vec{\sigma}| \qquad \text{(G.16)}
\end{aligned}$$

Thus, we obtained the von-Neumann density matrix, which maximises the entropy for a specific one-particle-reduced density matrix given by $\hat{\rho}^{(1)} = \sum_n |\varphi_n\rangle f_n \langle\varphi_n|$.

No correlated occupation-number fluctuations

The maximum-entropy ensemble for a specified one-particle-reduced density matrix does not exhibit correlated occupation-number fluctuations. This implies that the energy in the thermal Hartree-Fock approximation is equal to the mean-field expression.

Thus,

$$\big\langle \sigma_m \sigma_n \big\rangle - \big\langle \sigma_m \big\rangle \big\langle \sigma_n \big\rangle = 0 \qquad \text{for } \hat{\rho}^{vN} \text{ from } \hat{\rho}^{vN}[\hat{\rho}^{(1)}] \text{ Eq. G.16} \qquad \text{(G.17)}$$

The correlated occupation-number fluctuations are

$$\begin{aligned}
\big\langle \sigma_m \sigma_n \big\rangle - \big\langle \sigma_m \big\rangle \big\langle \sigma_n \big\rangle &= \Big\langle \Big(\sigma_m - \big\langle \sigma_m \big\rangle\Big)\Big(\sigma_n - \big\langle \sigma_n \big\rangle\Big) \Big\rangle \\
&= \sum_{\vec{\sigma}} P_{\vec{\sigma}} \sigma_m \sigma_n - \underbrace{\Big(\sum_{\vec{\sigma}} P_{\vec{\sigma}} \sigma_m\Big)}_{f_m} \underbrace{\Big(\sum_{\vec{\sigma}} P_{\vec{\sigma}} \sigma_n\Big)}_{f_n} \\
&= \sum_{\vec{\sigma}} P_{\vec{\sigma}} \Big(\sigma_m - f_m\Big)\Big(\sigma_n - f_n\Big) \\
&\overset{\text{Eq. } G.16}{=} \sum_{\vec{\sigma}} \Big(\prod_j f_j^{\sigma_j} \big(1+\eta f_j\big)^{-\sigma_j-\eta}\Big) \Big(\sigma_m - f_m\Big)\Big(\sigma_n - f_n\Big) \\
&= \Big(\prod_{j \notin \{m,n\}} \sum_{\sigma_j} f_j^{\sigma_j} \big(1+\eta f_j\big)^{-\sigma_j-\eta}\Big) \\
&\quad \times \Big(\sum_{\sigma_m} f_m^{\sigma_m} \big(1+\eta f_m\big)^{-\sigma_m-\eta} \Big(\sigma_m - f_m\Big)\Big) \Big(\sum_{\sigma_n} f_n^{\sigma_n} \big(1+\eta f_n\big)^{-\sigma_n-\eta} \Big(\sigma_n - f_n\Big)\Big) \\
&= \Big(\prod_{j \notin \{m,n\}} \underbrace{\sum_{\sigma} f_j^{\sigma} \big(1+\eta f_j\big)^{-\sigma-\eta}}_{=1 \text{ Eq. G.19}}\Big) \\
&\quad \times \underbrace{\Big(\sum_{\sigma} f_m^{\sigma} \big(1+\eta f_m\big)^{-\sigma-\eta} \Big(\sigma - f_m\Big)\Big)}_{=0 \text{ Eq. G.19}} \underbrace{\Big(\sum_{\sigma} f_n^{\sigma} \big(1+\eta f_n\big)^{-\sigma-\eta} \Big(\sigma - f_n\Big)\Big)}_{=0 \text{ Eq. G.19}} \\
&= 0 \qquad \textit{...q.e.d.} \qquad \text{(G.18)}
\end{aligned}$$

In the last line, I exploited the two identities

$$\sum_\sigma f^\sigma \big(1+\eta f\big)^{-\sigma-\eta} = 1$$
$$\sum_\sigma f^\sigma \big(1+\eta f\big)^{-\sigma-\eta}\sigma = f \tag{G.19}$$

which follow from the derivation. I will nevertheless include independent derivations

- Fermions $\eta = -1$

$$\sum_{\sigma=0}^{1} f^\sigma \big(1-f\big)^{1-\sigma} = f^0(1-f)^1 + f^1(1-f)^0 = 1\cdot(1-f) + f\cdot 1 = 1$$
$$\sum_{\sigma=0}^{1} f^\sigma \big(1-f\big)^{1-\sigma}\sigma = f^0\big(1-f\big)\cdot 0 + f\big(1-f\big)^0\cdot 1 = f \tag{G.20}$$

- Bosons $\eta = 1$

$$\sum_{\sigma=0}^{\infty} f^\sigma \big(1+f\big)^{-\sigma-1} = \frac{1}{1+f}\underbrace{\sum_{\sigma=0}^{\infty}\Big(\frac{f}{1+f}\Big)^\sigma}_{\text{geometric series}} = \frac{1}{1+f}\frac{1}{1-\frac{f}{1+f}} = \frac{1}{1+f-f} = 1$$
$$\sum_{\sigma=0}^{\infty} f^\sigma \big(1+f\big)^{-\sigma-1}\sigma = \frac{1}{1+f}\sum_{\sigma=0}^{\infty}\Big(\frac{f}{1+f}\Big)^\sigma\sigma \overset{\text{Eq. G.22}}{=} \frac{1}{1+f}\frac{\frac{f}{1+f}}{\Big(1-\frac{f}{1+f}\Big)^2} = f \tag{G.21}$$

I used

$$\sum_{j=1}^{\infty} j q^j = q\frac{d}{dq}\sum_{j=1}^{\infty} q^j = q\frac{d}{dq}\frac{1}{1-q} = \frac{q}{(1-q)^2} \tag{G.22}$$

G.1.3 Functional form of the Boltzmann entropy

The Boltzmann entropy can be evaluated from the von-Neumann density matrix just obtained. I use the probabilities from Eq. G.16.

$$\begin{aligned}
S^B[\hat\rho^{(1)}] &= -k_B\sum_{\vec\sigma} P_{\vec\sigma}\ln\Big(P_{\vec\sigma}\Big)\\
&\overset{\text{Eq. G.16}}{=} -k_B\sum_{\vec\sigma} P_{\vec\sigma}\ln\Big(\prod_n f_n^{\sigma_n}\big(1+\eta f_n\big)^{-\sigma_n-\eta}\Big)\\
&= -k_B\sum_{\vec\sigma} P_{\vec\sigma}\sum_n\Big(\sigma_n\ln(f_n) - (\sigma_n+\eta)\ln\big(1+\eta f_n\big)\Big)\\
&\overset{\sum_{\vec\sigma}P_{\vec\sigma}\sigma_n = f_n}{=} -k_B\sum_n\Big(f_n\ln(f_n) - \overbrace{\eta(1+\eta f_n)}^{f_n+\eta}\ln\big(1+\eta f_n\big)\Big)\\
&= -k_B\mathrm{Tr}\Big[\hat\rho^{(1)}\ln(\hat\rho^{(1)}) - \eta(\hat 1+\eta\hat\rho^{(1)})\ln\big(\hat 1+\eta\hat\rho^{(1)}\big)\Big]
\end{aligned} \tag{G.23}$$

This is the functional form of the Boltzmann entropy in terms of the one-particle-reduced density matrix. It is valid for both, fermions and bosons, but not for distinguishable particles.

G.1.4 Fermi and Bose distribution

For a given non-interacting Hamiltonian, the one-particle-reduced density matrix can be obtained from the minimum principle of the grand potential

$$\Omega_{T,\mu} = \min_{\hat{\rho}^{(1)}} \left\{ \mathrm{Tr}\left[\hat{\rho}^{(1)}\hat{h}\right] - TS^B\left[\hat{\rho}^{(1)}\hat{h}\right] - \mu \mathrm{Tr}\left[\hat{\rho}^{(1)}\hat{h}\right] \right\} \tag{G.24}$$

The minimum condition yields

$$\begin{aligned} 0 &\overset{\text{Eq. G.23}}{=} \hat{h} + k_B T\Big(\ln\left(\hat{\rho}^{(1)}\right) - \ln\left(\hat{1} + \eta\hat{\rho}^{(1)}\right)\Big) - \mu\hat{1} \\ \Rightarrow \qquad \frac{\hat{\rho}^{(1)}}{\hat{1} + \eta\hat{\rho}^{(1)}} &= \exp\Big(-\frac{1}{k_B T}\left(\hat{h} - \mu\hat{1}\right)\Big) \\ \Rightarrow \qquad \hat{\rho}^{(1)} &= \Big(\mathrm{e}^{\frac{1}{k_B T}(\hat{h}-\mu\hat{1})} - \eta\Big)^{-1} \end{aligned} \tag{G.25}$$

This are the well-known Fermi- and Bose distributions.

Hamiltonian from one-particle-reduced density matrix: Even for interacting particles, one can exploit the relation between non-interacting Hamiltonian and one-particle-reduced density matrix to construct an effective Hamiltonian $\hat{h}^{eff}$ from the one-particle-reduced density matrix so that

$$\hat{\rho}^{(1)} = \Big(\mathrm{e}^{\frac{1}{k_B T}(\hat{h}_{eff}-\mu\hat{1})} - \eta\Big)^{-1} \tag{G.26}$$

which results in

$$\hat{h}^{eff} \overset{\text{Eq. G.25}}{=} \mu\hat{1} - k_B T\left[\ln\Big(\hat{\rho}^{(1)}\Big) - \ln\Big(1 + \eta\hat{\rho}^{(1)}\Big)\right] \tag{G.27}$$

I call it $\hat{h}^{eff}$ to avoid the confusion with the non-interacting part $\hat{h}$ of an interacting Hamiltonian $\hat{H} = \hat{h} + \hat{W}$.

This effective Hamiltonian plays an important role in many-particle physics. In the Hartree-Fock approximation, the effective Hamiltonian is the Fock operator. In density-functional theory, the effective Hamiltonian is the so-called Kohn-Sham Hamiltonian. The effective Hamiltonian is a well defined object, even for strongly correlated many-particle systems, and independent of any approximation. The effective Hamiltonian $\hat{h}_{eff}$ usually differs strongly from the interacting part of the Hamiltonian $\hat{h}$, while the distinction is often not made evident.

The thermal ensemble for non-interacting particles with the effective Hamiltonian is the same as the maximum-entropy ensemble Eq. G.16 for the specified one-particle-reduced density matrix

$$P_{\vec{\sigma}} \overset{\text{Eq. G.16}}{=} \prod_n f_n^{\sigma}\left(1 + \eta f_n\right)^{-\sigma-\eta} = \frac{\mathrm{e}^{-\beta\sum_n(\epsilon_n^{eff}-\mu)\sigma_n}}{\sum_{\vec{\sigma}}\mathrm{e}^{-\beta\sum_n(\epsilon_n^{eff}-\mu)\sigma_n}} \tag{G.28}$$

where $\hat{h}^{eff}|\varphi_n\rangle = |\varphi_n\rangle\epsilon_n^{eff}$ and where the Slater determinants are built from the eigenstates of the effective Hamiltonian .

G.1.5 Dilute limit (Boltzman distribution)

The Boltzmann distribution should be considered as the dilute limit of the Bose- and Fermi- distributions. Loosely speaking, the behavior under particle exchange becomes irrelevant for dilute systems, because of the large interparticle distance.

The Boltzmann entropy in the dilute limit is obtained from that that of fermions and bosons.

$$\begin{aligned} S^B[\vec{f}] &= -k_B \sum_n \Big(f_n \ln(f_n) - f_n\Big) + O\Big(\vec{f}^2\Big) \quad \text{respectively} \\ S^B[\hat{\rho}^{(1)}] &= -k_B \mathrm{Tr}\Big[\hat{\rho}^{(1)}\ln(\hat{\rho}^{(1)}) - \hat{\rho}^{(1)}\Big] + O\Big(\left(\hat{\rho}^{(1)}\right)^2\Big) \end{aligned} \tag{G.29}$$

The term quadratic or higher in the occupations differs between the Fermi and the Bose distribution.

As a sanity check let me derive the Boltzmann distribution.

$$\begin{aligned} \Omega_{T,\mu} &= \min_{\vec{f}} \sum_n f_n \epsilon_n + k_B T \sum_n \Big(f_n \ln(f_n) - f_n \Big) - \mu \sum_n f_n \\ \delta\Omega = 0 \quad \Rightarrow \quad 0 &= \epsilon_n + k_B T \ln(f_n) + 1 - 1 - \mu \\ \Rightarrow \quad f_n &= \exp\Big(-\frac{1}{k_B T} (\epsilon_n - \mu) \Big) \\ \Rightarrow \quad \hat{\rho}^{(1)} &= \exp\Big(-\frac{1}{k_B T} (\hat{h} - \mu \hat{1}) \Big) \end{aligned} \tag{G.30}$$

This is the well-known Boltzmann distribution.

G.1.6 Summary

BOLTZMANN ENTROPY

Boltzmann's entropy $S^B[\hat{\rho}^{(1)}]$ has been defined in Eq. 2.68 on p. 70 as the maximum von-Neumann entropy for a specified one-particle-reduced density matrix $\hat{\rho}^{(1)}$. The eigenstates of the one-particle-reduced density matrix are the natural orbitals $|\varphi_n\rangle$ and its eigenvalues are the occupations f_n. The Slater determinants, respectively the permanents for bosons, are characterized by the vector of occupation numbers $|\vec{\sigma}\rangle$. The occupation numbers σ range from zero to one for fermions $\sigma \in \{0, 1\}$ and $\sigma \in \{0, 1, 2, \ldots\}$ for bosons. The results are characterized by $\eta = -1$ for fermions, $\eta = +1$ for bosons and $\eta = 0$ for the dilute limit, the Boltzmann distribution.
The functional form of the Boltzmann entropy is

$$\begin{aligned} S^B[\hat{\rho}^{(1)}] &\overset{\text{Eq. } G.23}{=} -k_B \mathrm{Tr}\Big(\hat{\rho}^{(1)} \ln(\hat{\rho}^{(1)}) - \eta(1 + \eta\hat{\rho}^{(1)}) \ln(1 + \eta\hat{\rho}^{(1)}) + (\eta^2 - 1)\hat{\rho}^{(1)} \Big) \\ &= -k_B \sum_{n=1}^{\infty} \begin{cases} \mathrm{Tr}\Big[\hat{\rho}^{(1)} \ln(\hat{\rho}^{(1)}) + (\hat{1} - \hat{\rho}^{(1)}) \ln(\hat{1} - \hat{\rho}^{(1)}) \Big] & \text{for fermions } (\eta = -1) \\ \mathrm{Tr}\Big[\hat{\rho}^{(1)} \ln(\hat{\rho}^{(1)}) - (\hat{1} + \hat{\rho}^{(1)}) \ln(\hat{1} + \hat{\rho}^{(1)}) \Big] & \text{for bosons } (\eta = +1) \\ \mathrm{Tr}\Big[\hat{\rho}^{(1)} \ln(\hat{\rho}^{(1)}) - \hat{\rho}^{(1)} \Big] & \text{for the dilute limit } (\eta = 0) \end{cases} \end{aligned} \tag{G.31}$$

The maximum-entropy ensemble for a specific one-particle-reduced density matrix is characterized by the von-Neumann density matrix for bosons and fermions. (I am not yet sure whether the case $\eta = 0$ makes sense.)

$$\hat{\rho}^{vN}[\hat{\rho}^{(1)}] \overset{\text{Eq. } G.16}{=} \sum_{\vec{\sigma}} |\vec{\sigma}\rangle \underbrace{\prod_n f_n^{\sigma_n} \big(1 + \eta f_n\big)^{-\sigma_n - \eta}}_{P_{\vec{\sigma}}} \langle\vec{\sigma}| \tag{G.32}$$

where the micro states $|\vec{\sigma}\rangle$ are Slater-determinants, or permanents in the case of bosons, which are built from the natural orbitals $|\varphi_n\rangle$, the eigenstates of the one-particle-reduced density matrix. The σ_n are the occupation numbers of the Slater determinant $|\vec{\sigma}|rangle$ at hand, while the f_n are the occupations, the eigenvalues of the one-particle-reduced density matrix, respectively the mean occupation number $f_n = \sum_{\vec{\sigma}} P_{\vec{\sigma}} \sigma_n$.
For a non-interacting system in a one-particle Hamiltonian $\hat{h}$ the maximum-entropy state is characterized by the Fermidistribution ($\eta = -1$), respectively the Bose distribution ($\eta = +1$) or the Boltzmann distribution ($\eta = 0$)

$$\hat{\rho}^{(1)} \overset{\text{Eqs. G.25,G.30}}{=} \Big(\mathrm{e}^{\frac{1}{k_B T}(\hat{h} - \mu\hat{1})} - \eta \Big)^{-1} \tag{G.33}$$

G.2 Averaged-phase approximation

The **thermal Hartree-Fock approximation** (THFA) and the **thermal single-determinant approximation** (TSDA) have been defined by a constrained search for the maximum-entropy ensemble, which is restricted to ensembles of Slater determinants. In the thermal Hartree-Fock approximation (THFA) , this constrained search is further restricted to ensembles without **correlated occupation-number fluctuations** , i.e. so that $\langle\sigma_m\sigma_n\rangle - \langle\sigma_m\rangle\langle\sigma_n\rangle$.

The restriction of the constrained search to Slater determinants can also be expressed in terms of the average-phase approximation (APA), described here in detail. This approximation selectively removes the **entanglement energy** defined in Eq. 2.140 on p. 93 and can thus be used to define this energy term.

The first and second lines of Eq. 2.139 on p. 93 describe the interaction energy for an ensemble of Slater determinants $|\vec{\sigma}\rangle$ with probabilities $P_{\vec{\sigma}}$.

$$\langle W\rangle = \sum_{\vec{\sigma}} P_{\vec{\sigma}} \langle\vec{\sigma}|\hat{W}|\vec{\sigma}\rangle \tag{G.34}$$

The neglect of the entanglement energy (third term of Eq. 2.139 can be described as **Averaged-Phase Approximation**. Here, I will define the averaged-phase approximation and show, that it selectively discards the off-diagonal Hamilton matrix elements between Slater determinants.

The natural name for this approximation would be *"random-phase approximation"* rather than *"averaged-phase approximation"*. We use the latter term because the name *"random-phase approximation"* is already in use for a different approximation. To my knowledge the two approximations are unrelated.

In the averaged-phase approximation, the interaction energy $\langle\Psi|\hat{W}|\Psi\rangle$ is evaluated for a transformed many-particle wave function $\hat{R}(\vec{\gamma})|\Psi\rangle$, for which each Slater determinant $|\vec{\sigma}\rangle$ is multiplied with individual phase factor $e^{i\gamma_{\vec{\sigma}}}$. Then, the interaction energy is averaged over the phases $\gamma_{\vec{\sigma}} \in [0, 2\pi[$ of each Slater determinant independently.

Let me step through the individiual steps of the averaged-phase approximation:

First, we define a one-particle basisset $|\varphi_n\rangle$ from which a many-particle basisset of Slater determinants $|\vec{\sigma}\rangle$ is constructed. The choice of the one-particle basisset determines the quality of the approximation. To be concise let us choose the natural orbitals, the eigenstates of the one-particle-reduced density matrix.

Secondly, a transformation $\hat{R}(\vec{\gamma})$ of the many-particle wave functions is defined, which multiplies each Slater determinant with an individual phase factor $e^{i\gamma_{\vec{\sigma}}}$ for each Slater determinant.

$$\hat{R}(\vec{\gamma}) = \sum_{\vec{\sigma}} |\vec{\sigma}\rangle e^{i\gamma_{\vec{\sigma}}} \langle\vec{\sigma}| \tag{G.35}$$

There is one angle $\gamma_{\vec{\sigma}}$ for every Slater determinant in Fock space. That is, $\vec{\gamma}$ is a vector in Fock space, not in the one-particle Hilbert space.

The averaged-phase approximation implies an average over the phases $\vec{\gamma}$. This average yields

$$\begin{aligned}
\left\langle\Psi\middle|\hat{h}+\hat{W}\middle|\Psi\right\rangle \quad &\overset{APA}{\approx} \quad \left(\prod_{\vec{\sigma}}\int_0^{2\pi}\frac{d\gamma_{\vec{\sigma}}}{2\pi}\right)\langle\Psi|\hat{R}^\dagger(\vec{\gamma})\left(\hat{h}+\hat{W}\right)\hat{R}(\vec{\gamma})|\Psi\rangle \\
&\overset{|\Psi\rangle=\sum_{\vec{\sigma}}|\vec{\sigma}\rangle c_{\vec{\sigma}}}{=} \left(\prod_{\vec{\sigma}}\int_0^{2\pi}\frac{d\gamma_{\vec{\sigma}}}{2\pi}\right)\sum_{\vec{\sigma}',\vec{\sigma}''} c^*_{\vec{\sigma}'}\langle\vec{\sigma}'|\hat{h}+\hat{W}|\vec{\sigma}''\rangle c_{\vec{\sigma}''} e^{i(\gamma_{\vec{\sigma}''}-\gamma_{\vec{\sigma}'})} \\
&= \sum_{\vec{\sigma}',\vec{\sigma}''} c^*_{\vec{\sigma}'}\langle\vec{\sigma}'|\hat{h}+\hat{W}|\vec{\sigma}''\rangle c_{\vec{\sigma}''} \underbrace{\int_0^{2\pi}\frac{d\gamma_{\vec{\sigma}'}}{2\pi}\int_0^{2\pi}\frac{d\gamma_{\vec{\sigma}''}}{2\pi}e^{i(\gamma_{\vec{\sigma}''}-\gamma_{\vec{\sigma}'})}}_{\delta_{\vec{\sigma}',\vec{\sigma}''}} \\
&= \sum_{\vec{\sigma}} \underbrace{c^*_{\vec{\sigma}}c_{\vec{\sigma}}}_{P_{\vec{\sigma}}}\langle\vec{\sigma}|\hat{h}+\hat{W}|\vec{\sigma}\rangle
\end{aligned} \tag{G.36}$$

The averaged-phase approximation (APA) converts a correlated many-particle wave function $|\vec{\Psi}\rangle = \sum_{\vec{\sigma}} |\vec{\sigma}\rangle c_{\vec{\sigma}}$ into a statistical ensemble of Slater determinants $|\vec{\sigma}\rangle$ with probabilities $P_{\vec{\sigma}} = |c_{\vec{\sigma}}|^2$. In other words, it removes the entanglement term from Eq. 2.139 without affecting the other two energy terms.

The derivation can easily be generalized to ensembles $\{|\Psi_q\rangle, \bar{P}_q\}$ of many-particle wave functions $|\Psi_q\rangle = \sum_{\vec{\sigma}} |\vec{\sigma}\rangle c_{\vec{\sigma},q}$, rather than a single many-particle wave function used in this proof. In this case the probabilities of the Slater determinants are $P_{\vec{\sigma}} = \sum_q \bar{P}_q c^*_{\vec{\sigma},q} c_{\vec{\sigma},q}$.

Noteworthy is, that the averaged-phase approximation converts pure quantum states into ensembles. The averaged-phase approximation can, however, be applied to pure states and ensembles alike.

Let me alert you to a common mistake: It is important to understand, which phases are averaged. In the derivation above, we have first chosen a one-particle basisset. This choice defines the set of Slater determinants. It is the phases between the Slater determinants, rather than those of the one-particle orbitals that is averaged over.[1]

The choice of the one-particle basisset, which, in turn, determines the set of Slater determinants, and thus, whether the random (averaged)-phase approximation is a good or a poor approximation.

Approximate Hamiltonian The averaged-phase approximation defines an approximate Hamiltonian with eigenstates that are Slater determinants.

$$\hat{H}^{APA} = \left(\prod_{\vec{\sigma}} \int_0^{2\pi} \frac{d\gamma_{\vec{\sigma}}}{2\pi} \right) \hat{R}^\dagger(\vec{\gamma}) \left(\hat{h} + \hat{W} \right) \hat{R}(\vec{\gamma}) = \sum_{\vec{\sigma}} |\vec{\sigma}\rangle \underbrace{E_{\vec{\sigma}}}_{\langle\vec{\sigma}|\hat{h}+\hat{W}|\vec{\sigma}\rangle} \langle\vec{\sigma}| \tag{G.37}$$

If the natural orbitals of the thermal Hartree-Fock approximation are used to define the phases of the averaged-phase approximation, this approximate Hamiltonian reproduces the ensemble from thermal Hartree-Fock, if the search for the maximum-entropy ensemble excludes correlated occupation-number fluctuations.

G.3 Correlated occupation-number fluctuations

In Eq. 2.140 on p. 93 I investigated the terms of the interaction that are ignored in the mean-field approximation, respectively in the thermal Hartree-Fock approximation. The second term in this expression described an effect of **occupation-number fluctuations**. This term describes important correlation effects beyond the Hartree-Fock approximation. The correlations reduce the repulsion of electrons in strongly interacting orbitals.

It has been shown that the energy gain due to occupation-number fluctuations is related to the **double occupancy**. Electrons attempt to avoid a double occupancy of orbitals, which are connected by a strong Coulomb repulsion.

G.3.1 Two-orbital model

Let me investigate this effect in a minimal model of only two orbitals. Consider two natural orbitals and probabilities P_{σ_a,σ_b}. The model Hamiltonian is expressed by occupation numbers

$$\hat{H} = \bar{\epsilon}_1 \hat{c}_1^\dagger \hat{c}_1 + \bar{\epsilon}_2 \hat{c}_2^\dagger \hat{c}_2 + V \hat{c}_1^\dagger \hat{c}_1 \hat{c}_2^\dagger \hat{c}_2 \tag{G.38}$$

where $\bar{\epsilon}_\alpha \stackrel{\text{def}}{=} \langle\chi_\alpha|\hat{h}|\chi_\alpha\rangle$ and $V \stackrel{\text{def}}{=} \langle\chi_1\chi_2|\hat{W}|\chi_1,\chi_2\rangle - \langle\chi_1\chi_2|\hat{W}|\chi_2,\chi_1\rangle$

[1] A similar random (averaged)-phase approximation can be used to arrive at the Boltzmann equation. There, however, the phases of one-particle orbitals are averaged, which is a much more severe approximation than the one done here.

Let me define the **double occupancy**

$$d_{m,n} \stackrel{\text{def}}{=} \sum_{\vec{\sigma}} P_{\vec{\sigma}} \sigma_m \sigma_n \tag{G.39}$$

which, in the two-orbital model, equals $d = P_{11}$.

For a given set of occupations (f_1, f_2) and a specified double occupancy d, we obtain the probabilities as

$$\begin{aligned} P_{0,0} + P_{1,0} + P_{0,1} + P_{1,1} &= 1 \\ P_{1,0} + P_{1,1} &= f_1 \\ P_{0,1} + P_{1,1} &= f_2 \\ P_{1,1} &= d \end{aligned} \tag{G.40}$$

so that

$$P_{0,0} = 1 + d - f_1 - f_2; \qquad P_{1,0} = f_1 - d; \qquad P_{0,1} = f_2 - d \qquad \text{and} \qquad P_{1,1} = d \tag{G.41}$$

Range of the double occupancy: The double occupancy d cannot be chosen arbitrary. The requirement that all probabilities must be positive, leads to the following limitations.

$$\begin{aligned} 0 \le P_{00} = 1 + d - f_1 - f_2 \quad &\Rightarrow \quad f_1 + f_2 - 1 \le d \\ 0 \le P_{10} = f_1 - d \quad &\Rightarrow \quad d \le f_1 \\ 0 \le P_{01} = f_2 - d \quad &\Rightarrow \quad d \le f_2 \\ 0 \le P_{11} = d \quad &\Rightarrow \quad 0 \le d \end{aligned} \tag{G.42}$$

$$\begin{aligned} \Rightarrow \qquad & \max(0, f_1 + f_2 - 1) \le \quad d \quad \le \min(f_1, f_2) \\ \Rightarrow \qquad & -\min\Big(f_1 f_2, (1-f_1)(1-f_2)\Big) \le d - f_1 f_2 \le \min\Big(f_1(1-f_2), (1-f_1)f_2\Big) \end{aligned} \tag{G.43}$$

Energy correction: In the two-orbital model, the energy correction ΔE_{conf} due to correlated occupation-number fluctuations is[2]

$$\Delta E_{conf} = \Big(\underbrace{\sum_{\vec{\sigma}} P_{\vec{\sigma}} (\sigma_1 - f_1)(\sigma_2 - f_2)}_{d - f_1 f_2}\Big) V = \Big(d - f_1 f_2\Big) V \tag{G.45}$$

The energy ΔE_{conf} is to be added to the energy from the thermal Hartree Fock approximation. The second term, which is proportional to $f_1 f_2$, subtracts the mean-field interaction energy. For given occupations, the lowest energy is obtained by the smallest possible value for the double occupancy d, namely

$$d = \max(0, f_1 + f_2 - 1) \tag{G.46}$$

[2]

$$\begin{aligned} \frac{1}{V}\Delta E_{conf} = \sum_{\vec{\sigma}} P_{\vec{\sigma}} (\sigma_1 - f_1)(\sigma_2 - f_2) &= P_{0,0} f_1 f_2 + P_{1,0}(f_1 - 1) f_2 + P_{0,1} f_1 (f_2 - 1) + P_{1,1}(f_1 - 1)(f_2 - 1) \\ &= f_1 f_2 - P_{1,0} f_2 - P_{0,1} f_1 + P_{1,1}(1 - f_1 - f_2) \\ &= f_1 f_2 - (f_1 - d) f_2 - (f_2 - d) f_1 + d(1 - f_1 - f_2) \\ &= f_1 f_2 - f_1 f_2 - f_1 f_2 + d(f_2 + f_1 + 1 - f_1 - f_2) \\ &= d - f_1 f_2 \end{aligned} \tag{G.44}$$

When the occupation-number fluctuations are considered, the interaction energy of the two orbital model is determined by the double occupancy d as dV. The interaction energy of the two orbital model with the optimum double occupancy is therefore

$$E_{int} = V \max(0, f_1 + f_2 - 1) \tag{G.47}$$

In order to minimize the interaction energy, the system will place the electrons into one orbital, while keeping the other empty. In other words, the singly occupied Slater determinants $|0,1\rangle$ and $|1,0\rangle$ are used as long as there is less than one electron $f_1 + f_2 < 1$. This removes the repulsion between the electrons altogether. Only for $f_1 + f_2 > 1$, the doubly occupied Slater determinant enters the thermal ensemble.

The resulting energy is not smooth, but it consists of segments, which depend linearly on the occupations, and which merge with an abrupt change of the slope. This behavior is very problematic for numerical optimization routines. The behavior is absent in the thermal Hartree Fock approxiation. Finite temperatures also smoothen the abrupt behhavior.

Entropy term: Editor: Caution: There may be a mistake below

In the two orbital model, the correlated occupation-number fluctuations lower the interaction energy, but they also rise the entropy term $-TS$. The von-Neumann entropy of an ensemble is always equal or lower than the corresponding Boltzmann entropy.

The corrections are calculated for a fixed one-particle-reduced density matrix.

$$\begin{aligned} -TS^{vN} &= k_B T \Big(P_{00} \ln(P_{00}) + P_{10} \ln(P_{10}) + P_{01} \ln(P_{01}) + P_{11} \ln(P_{11}) \Big) \\ &\overset{\text{Eq. } G.41}{=} k_B T \Big[\Big(1 + d - f_1 - f_2\Big) \ln\Big(1 + d - f_1 - f_2\Big) + d \ln\Big(d\Big) \\ &\quad + \Big(f_1 - d\Big) \ln\Big(f_1 - d\Big) + \Big(f_2 - d\Big) \ln\Big(f_2 - d\Big) \Big] \end{aligned} \tag{G.48}$$

The Boltzmann entropy for a system with occupations f_a and f_b is

$$S^B = -k_B \Big[\sum_{n=1}^{2} \Big(f_n \ln\left(f_n\right) + (1 - f_n) \ln\left(1 - f_n\right) \Big] \tag{G.49}$$

The entropy correction is thus

$$\begin{aligned} -T\Delta S_{conf} &= -TS + TS^B \\ &= k_B T \Big[\Big(1 + d - f_1 - f_2\Big) \ln\Big(1 + d - f_1 - f_2\Big) + d \ln\Big(d\Big) \\ &\quad + \Big(f_1 - d\Big) \ln\Big(f_1 - d\Big) + \Big(f_2 - d\Big) \ln\Big(f_2 - d\Big) \Big] \\ &\quad - k_B T \Big[\sum_{n=1}^{2} \Big(f_n \ln\left(f_n\right) + (1 - f_n) \ln\left(1 - f_n\right) \Big) \Big] \end{aligned} \tag{G.50}$$

Optimum double occupancy For a given one-particle-reduced density matrix, the double occupancy is the only free parameter in the two orbital model. This parameter can be fixed by minimizing the grand potential. Because the mean-field energy is independent of the double occupancy, it is

sufficient to optimize the correction due to correlated occupation-number fluctuations.

$$\begin{aligned}\Delta\Omega^{conf} &= (d - f_1 f_2)V - k_B T \Delta S^{conf} \\ &= (d - f_1 f_2)V + k_B T \Big[\Big(1 + d - f_1 - f_2\Big) \ln\Big(1 + d - f_1 - f_2\Big) + d \ln\Big(d\Big) \\ &\quad + \Big(f_1 - d\Big) \ln\Big(f_1 - d\Big) + \Big(f_2 - d\Big) \ln\Big(f_2 - d\Big) \Big] \\ &\quad - k_B T \Big[\sum_{n=1}^{2} \Big(f_n \ln\left(f_n\right) + (1 - f_n) \ln\left(1 - f_n\right) \Big) \Big] \end{aligned} \tag{G.51}$$

The optimum double occupancy is obtained as follows

$$\begin{aligned}\frac{\partial \Delta\Omega^{conf}_{T,\mu}(f_1, f_2, d)}{\partial d} &= V + k_B T \Big\{ \ln\Big(1 + d - f_1 - f_2\Big) + 1 + \ln\Big(d\Big) + 1 \\ &\qquad - \ln\Big(f_1 - d\Big) - 1 - \ln\Big(f_2 - d\Big) - 1 \Big\} = 0 \\ \Rightarrow \ln\Big(\frac{d(1 + d - f_1 - f_2)}{(f_1 - d)(f_2 - d)}\Big) &= -\frac{V}{k_B T} \\ \Rightarrow \frac{d(1 + d - f_1 - f_2)}{(f_1 - d)(f_2 - d)} &= \underbrace{\exp\Big(-\frac{V}{k_B T}\Big)}_{=:q} \\ \Rightarrow \underbrace{d(1 + d - f_1 - f_1)}_{d^2 + d - d(f_1 + f_2)} &= \underbrace{q(f_1 - d)(f_2 - d)}_{q f_1 f_2 - 2qd(f_1 + f_2) + qd^2} \\ \Rightarrow 0 &= (1 - q)d^2 + d\Big[1 + (2q - 1)(f_1 + f_2)\Big] - q f_1 f_2 \\ 0 &= d^2 + d\frac{1 + (2q - 1)(f_1 + f_2)}{1 - q} - \frac{q}{1 - q} f_1 f_2 \\ 0 &= \left(d + \frac{1 + (2q - 1)(f_1 + f_2)}{2(1 - q)}\right)^2 - \left(\frac{1 + (2q - 1)(f_1 + f_2)}{2(1 - q)}\right)^2 - \frac{q}{1 - q} f_1 f_2 \\ d &= -\frac{1 + (2q - 1)(f_1 + f_2)}{2(1 - q)} \pm \sqrt{\left(\frac{1 + (2q - 1)(f_1 + f_2)}{2(1 - q)}\right)^2 + \frac{q}{1 - q} f_1 f_2} \end{aligned} \tag{G.52}$$

$q = \mathrm{e}^{-\beta V}$ can assume values between zero ($U \gg k_B T$) and one ($V \ll k_B T$). The double occupancy must be between $\max(0, f_1 + f_2 - 1)$ and $\min(f_1, f_2)$. This excludes the negative root, so that the double occupancy yields

Editor: Caution: the double occupancy for $f_1 = f_2 = 1$ must be equal to $d = 1$. The result of the expression abovel produces instead $d = \frac{1}{3}$.

$$\begin{aligned} d &= \frac{1 + (2q - 1)(f_1 + f_2)}{2(1 - q)} \left(-1 + \sqrt{1 + \left(\frac{2(1 - q)}{1 + (2q - 1)(f_1 + f_2)}\right)^2 \frac{q}{1 - q} f_1 f_2} \right) \\ &\to \begin{cases} \max(0, f_1 + f_2 - 1) & \text{for } V \gg k_B T \\ \frac{f_1 f_2}{1 + f_1 + f_2} & \text{for } 0 \le V \ll k_B T \end{cases} \end{aligned} \tag{G.53}$$

The two limiting cases are obtained as follows:

- In the high-temperature limit $q \to 1 - \beta V$, I obtain

$$\begin{aligned} d &= -\frac{1+(1-2\beta V)(f_1+f_2)}{2\beta V} + \sqrt{\left(\frac{1+(1-2\beta V)(f_1+f_2)}{2\beta V}\right)^2 + \frac{1-\beta V}{\beta V} f_1 f_2} \\ &\approx \frac{1}{2\beta V}\left[-\Big(1+(1-2\beta U)(f_1+f_2)\Big) + \sqrt{\Big(1+(1-2\beta V)(f_1+f_2)\Big)^2 + 4\beta V f_1 f_2}\right] \\ &\approx \frac{f_1 f_2}{1+(f_1+f_2)} \end{aligned} \tag{G.54}$$

- In the low-temperature limit $q = 0$

$$d = -\frac{1-(f_1+f_2)}{2} + \sqrt{\left(\frac{1-(f_1+f_2)}{2}\right)^2} = \max(0, 1-f_1-f_2) \tag{G.55}$$

G.3.2 Attempt to construct a new density-matrix functional

Editor: The following is a collection of ideas, which are of limited use for the reader.

We can use the result as a pairwise correction for the density matrix functional. The result is still a density matrix functional, because only the occupations enter. The interaction energy $E_{int}^{(TSDA)}$ of the two-orbital model including the mean-field interaction energy and the energy correction due to correlated occupation-number fluctuations is

$$\begin{aligned} E_{int}^{(TSDA)} &= \underbrace{\frac{1}{2}\sum_{m,n} f_m f_n \Big(\langle\varphi_m,\varphi_n|\hat{W}|\varphi_m,\varphi_n\rangle - \langle\varphi_m,\varphi_n|\hat{W}|\varphi_n,\varphi_m\rangle\Big)}_{E_{int}^{mf}=E_H+E_X} \\ &\quad \underbrace{-\frac{1}{2}\sum_{m,n} \max\Big(f_m f_n, (1-f_m)(1-f_n)\Big)\Big(\langle\varphi_m,\varphi_n|\hat{W}|\varphi_m,\varphi_n\rangle - \langle\varphi_m,\varphi_n|\hat{W}|\varphi_n,\varphi_m\rangle\Big)}_{\text{correlated occupation-number fluctuations}} \\ &= \frac{1}{2}\sum_{m,n}\Big(\langle\varphi_m,\varphi_n|\hat{W}|\varphi_m,\varphi_n\rangle - \langle\varphi_m,\varphi_n|\hat{W}|\varphi_n,\varphi_m\rangle\Big) \times \begin{cases} 0 & \text{for } f_m+f_n \le 1 \\ f_1+f_2-1 & \text{for } f_m+f_n \ge 1 \end{cases} \end{aligned} \tag{G.56}$$

This equation expresses, that the electrons try to avoid the Coulomb repulsion by localizing in one orbital, while leaving the other as empty as possible.

The new energy functional has a piecewise linear dependence on the one-particle-reduced density matrix. This rules out using numerical optimization schemes, which are based on approximately quadratic behavior. It also implies that the minimum (at $T = 0$) will be an ensemble of several coexisting Slater determinants.

The energy of correlated occupation-number fluctuation is largest between states of opposite spin, because the exchange term $\langle\varphi_m,\varphi_n|\hat{W}|\varphi_n\varphi_m\rangle$ vanishes, for spin orbitals with opposite spin. Furthermore it is large for spatial orbitals that are localized in the same spatial region.

This suggests to apply the correction for correlated occupation-number fluctuations from the two orbital model for discussed above for pairs of spin orbitals with the same spatial wave function and opposite spin.

G.4 Hartree-Fock equations in the zero-temperature case

G.4.1 Prologue to this section

This section contains a chapter on the Hartree-Fock equations, which I lifted from the main course before I decided to get into finite temperature description right away. It may be used by the novice to get a direct entry to the Hartree-Fock method without the obstructions of the finite-temperature formalism. It has the advantage that the formulation is closer to the wave function notation used in first-principles electronic structure methods. The zero-temperature formalism suffers from conceptual problems related to degenerate ground states and symmetry breaking.

G.4.2 Hartree-Fock equations

To first-order perturbation theory in the interaction $\hat{W}$, we can use the many-particle eigenstates of the non-interacting Hamiltonian $\hat{h}$ to estimate the energies of the interacting system. The wave functions of a non-interacting Hamiltonian are Slater determinants. Slater determinants are much simpler to handle than general many-particle wave functions. However, the eigenstates of the non-interacting Hamiltonian $\hat{h}$ may not be the best choice. Instead, one could also search for the "best possible" non-interacting system.

What is the best non-interacting system? Because the ground state of the system is the minimum of the energy $\langle\Phi|\hat{h}+\hat{W}|\Phi\rangle$ for all fermionic many-particle wave functions, any restriction of the wave function to Slater determinants leads to an upper bound of the ground-state energy. We consider the Slater determinant with the lowest energy as the best approximation of the ground state wave function by a Slater determinant.

To obtain this "best" Slater determinant, we start with the total energy Eq. 2.39 and determine its minimum with respect to the permitted variations of the one-particle-reduced density matrix. The one-particle-reduced density matrix is expressed by its natural orbitals $|\varphi_n\rangle$ and occupations f_n. Therefore, we need to minimize the total energy with respect to the one-particle orbitals $|\varphi_n\rangle$ and the occupations f_n. The orbitals must be kept orthonormal and this constraint is enforced using the method of **Lagrange multipliers**. The occupations are kept in the allowed range by expressing it as the $f_n = \sin^2(\gamma_n)$, where γ_n can have any real value. [3]

[3] The careful reader may notice that for the problem at hand, we may set the occupations to either zero or one and keep them frozen. This implies a restriction of the search to Slater determinants. This is no problem, because we are only looking for solutions that are Slater determinants. Keeping general occupations, the results are readily generalized to finite temperatures and the search can be extended to arbitrary many-particle wave functions or their ensembles.

HARTREE-FOCK ENERGY FUNCTIONAL

In the Hartree-Fock approximation, the ground-state total energy for a given particle number N is the minimum of a functional of one-particle wave functions $|\varphi_n\rangle$ and occupations $f_n \in [0,1]$, which encode the one-particle-reduced density matrix

$$\hat{\rho}^{(1)} \overset{\text{Eq. 2.15}}{=} \sum_{n=0}^{\infty} |\varphi_n\rangle f_n \langle\varphi_n| \tag{G.57}$$

and the electron density $n(\vec{r}) = \sum_{\sigma\in\{\uparrow,\downarrow\}} \rho^{(1)}(\vec{x},\vec{x})$.

$$\begin{aligned} E_N^{GS-HF} \overset{\text{Eq. 2.39}}{=} \min_{\{|\varphi_n\rangle, f_n\in[0,1]\}} \operatorname*{stat}_{\mathbf{\Lambda},\mu} \Bigg\{ & \underbrace{\mathrm{Tr}\left[\hat{\rho}^{(1)}\hat{h}\right]}_{E_{1P}} \\ & + \underbrace{\frac{1}{2}\int d^3r \int d^3r' \, \frac{e^2 n(\vec{r}) n(\vec{r'})}{4\pi\epsilon_0 |\vec{r}-\vec{r'}|}}_{\text{Hartree energy } E_H} \underbrace{-\frac{1}{2}\int d^4x \int d^4x' \, \frac{e^2 \rho^{(1)}(\vec{x},\vec{x'})\rho^{(1)}(\vec{x'},\vec{x})}{4\pi\epsilon_0|\vec{r}-\vec{r'}|}}_{\text{exchange energy } E_X} \\ & - \sum_{i,j} \Lambda_{j,i} \underbrace{\left(\langle\varphi_i|\varphi_j\rangle - \delta_{i,j}\right)}_{\text{orthogonality constraint}} - \mu \underbrace{\left(\mathrm{Tr}\left[\hat{\rho}^{(1)}\right] - N\right)}_{\text{particle-number constraint}} \Bigg\} \end{aligned} \tag{G.58}$$

The N-representability constraint $0 \le f_n \le 1$ can, for example, be enforced by representing the occupation by $f_n = \sin^2(\gamma_n)$. Then the unrestricted variables γ_n are varied to scan the occupations in the permitted range.
Because the energy expression is valid only for single Slater determinants, the final occupations must be either zero or one. This implies, that the variation of the occupations should be suppressed. Allowing fractional occupations $f_n \notin \{0,1\}$ implies to impose an additional approximation, the mean-field approximation. This is a subtle point, that is discussed in section 2.5 below.

The matrix $\mathbf{\Lambda}$ are the Lagrange multipliers for the orthogonality constraint of the natural orbitals. We will see later that the eigenvalues of $\mathbf{\Lambda}$ are related to the one-particle energies.

The chemical potential μ is the Lagrange multiplier for the particle-number constraint. Note that $\mathrm{Tr}[\hat{\rho}^{(1)}] = \sum_n f_n$.

Minimum condition: Let me denote the term in the curly brackets of Eq. G.58 as $\mathcal{E}_N^{HF}[\{|\varphi_j\rangle, f_j\}]$. As elaborated below, the minimum condition of $\mathcal{E}_N^{HF}$. with respect to a variation of the one-particle orbitals $|\varphi_n\rangle$ is

$$0 \overset{!}{=} \frac{1}{f_n}\frac{\partial \mathcal{E}^{HF}}{\partial\langle\varphi_n|} = \underbrace{\left[\hat{h} + \hat{V}_H + \hat{V}_X\right]}_{\text{Fock operator } \hat{F}} |\varphi_n\rangle - |\varphi_n\rangle\mu - \sum_m |\varphi_m\rangle \Lambda_{m,n}\frac{1}{f_n} \tag{G.59}$$

where $\hat{F}$ is the **Fock operator**.

FOCK OPERATOR

$$\hat{F} \overset{\text{Eq. 2.77}}{=} \hat{h} + \hat{V}_H + \hat{V}_X$$
$$= \hat{h} + \overbrace{\int d^4x \left|\vec{x}\right\rangle \underbrace{\int d^3r' \frac{e^2 n(\vec{r})}{4\pi\epsilon_0|\vec{r}-\vec{r'}|}}_{v_H(\vec{r})} \left\langle\vec{x}\right|}^{\hat{V}_H} - \overbrace{\int d^4x \int d^4x' \left|\vec{x}\right\rangle \underbrace{\frac{e^2\rho^{(1)}(\vec{x},\vec{x'})}{4\pi\epsilon_0|\vec{r}-\vec{r'}|}}_{-v_X(\vec{x},\vec{x'})} \left\langle\vec{x'}\right|}^{\hat{V}_X} \quad \text{(G.60)}$$

The Fock operator is a one-particle operator, which depends on density and one-particle-reduced density matrix.

The Fock operator defines an **effective potential** $\hat{V}_{eff}$

$$\hat{F} = \hat{T} + \hat{V}_{ext} + \hat{V}_H + \hat{V}_X = \hat{T} + \hat{V}_{eff} \quad \text{(G.61)}$$

I used the symbol $\hat{T}$ to denote the kinetic-energy operator and $\hat{V}_{ext}$ to denote the external-potential operator, which typically is the Coulomb potential of the nuclei. Because of the exchange term, the effective potential is a non-local potential $\hat{V}_{eff} = \int d^4x \int d^4x' \, |\vec{x}\rangle v_{eff}(\vec{x},\vec{x'})\langle\vec{x}|$.

In order to arrive at Eq. G.59, let me work out the derivatives of the individual terms of the total energy functional Eq. G.58:

- The derivative of the energy E_{1P} from the non-interacting Hamiltonian $\hat{h}$ is[4] Eqs. 2.34,2.37

$$\frac{1}{f_n}\frac{\partial E_{1P}}{\partial\langle\varphi_n|} = \mathrm{Tr}\left[\underbrace{\frac{\partial E_{1P}}{\partial\hat{\rho}^{(1)}}}_{\hat{h}} \frac{1}{f_n}\frac{\partial\hat{\rho}^{(1)}}{\partial\langle\varphi_n|}\right] = \mathrm{Tr}\left[\hat{h}\,\frac{1}{f_n}\underbrace{\frac{\partial}{\partial\langle\varphi_n|}\overbrace{\sum_j |\varphi_j\rangle f_j\langle\varphi_j|}^{\hat{\rho}^{(1)}}}_{|\varphi_n\rangle f_n}\right] = \hat{h}|\varphi_n\rangle \quad \text{(G.64)}$$

- The derivative of the Hartree energy E_H is

$$\frac{1}{f_n}\frac{\partial E_H}{\partial\langle\varphi_n|} = \int d^3r \underbrace{\frac{dE_H}{dn(\vec{r})}}_{v_H(\vec{r})}\frac{1}{f_n}\frac{\partial n(\vec{r})}{\partial\langle\varphi_n|} \overset{\text{Eq. 2.34}}{=} \int d^3r \, v_H(\vec{r}) \frac{1}{f_n}\underbrace{\frac{\partial}{\partial\langle\varphi_n|}\overbrace{\sum_\sigma\sum_j \langle\vec{x}|\varphi_j\rangle f_j\langle\varphi_j|\vec{x}\rangle}^{n(\vec{r})}}_{\sum_\sigma |\vec{x}\rangle\langle\vec{x}|\varphi_n\rangle f_n}$$
$$= \underbrace{\sum_\sigma \int d^3r \, |\vec{x}\rangle v_H(\vec{r})\langle\vec{x}|\,\varphi_n\rangle}_{\hat{V}_H} = \hat{V}_H|\varphi_n\rangle \quad \text{(G.65)}$$

[4] The derivative with respect to a matrix is defined as follows:

$$dE = \sum_{i,j}\frac{\partial E(\boldsymbol{a})}{\partial a_{i,j}} da_{i,j} = \mathrm{Tr}\left[\frac{\partial E(\boldsymbol{a})}{\partial \boldsymbol{a}} d\boldsymbol{a}\right] \Rightarrow \left(\frac{\partial E}{\partial \boldsymbol{a}}\right)_{i,j} \overset{\text{def}}{=} \frac{\partial E}{\partial \boldsymbol{a}_{j,i}} \quad \text{(G.62)}$$

Notice, that the order of the indices in the definition is swapped. This corresponds to the so-called "numerator-layout notation".(see `https://en.wikipedia.org/wiki/Matrix_calculus`) There is also another notation called "denominator-layout notation", which will not be used here.

The derivative with respect to an operator is defined analogously to the matrix case, so that

$$dE = \mathrm{Tr}\left[\frac{\partial E(\hat{a})}{\partial \hat{a}} d\hat{a}\right] \quad \text{(G.63)}$$

- The derivative of the exchange energy E_X is

$$\begin{aligned}\frac{1}{f_n}\frac{\partial E_X}{\partial\langle\varphi_n|} &= \int d^4x \int d^4x' \underbrace{\frac{dE_X}{d\rho^{(1)}(\vec{x},\vec{x'})}}_{v_X(\vec{x'},\vec{x})} \frac{1}{f_n}\frac{\partial\rho^{(1)}(\vec{x},\vec{x'})}{\partial\langle\varphi_n|} \\ &\overset{\text{Eq. 2.37}}{=} \int d^4x \int d^4x' \; v_X(\vec{x'},\vec{x})\frac{1}{f_n}\underbrace{\frac{\partial}{\partial\langle\varphi_n|}\sum_j \langle\vec{x}|\varphi_j\rangle f_j\langle\varphi_j|\vec{x'}\rangle}_{\sum_\sigma |\vec{x'}\rangle\langle\vec{x}|\varphi_n\rangle f_n} \\ &= \underbrace{\int d^4x \int d^4x' \; |\vec{x'}\rangle v_X(\vec{x'},\vec{x})\langle\vec{x}\,|}_{\hat{V}_X}|\varphi_n\rangle = \hat{V}_X|\varphi_n\rangle \end{aligned} \tag{G.66}$$

  I recommend to carefully inspect the order of the indices in the derivative of the exchange energy with the density matrix $\rho^{(1)}(\vec{x},\vec{x'})$ and those in $v_X(\vec{x'},\vec{x})$.

- Derivative of the orthonormality constraint:

$$\frac{1}{f_n}\frac{\partial}{\partial\langle\varphi_n|}\Big(-\sum_{i,j}\Lambda_{j,i}\left[\langle\varphi_i|\varphi_j\rangle-\delta_{i,j}\right]\Big) = -\sum_j |\varphi_j\rangle\Lambda_{j,n}\frac{1}{f_n} \tag{G.67}$$

- Derivative of the particle-number constraint:

$$\frac{1}{f_n}\frac{\partial}{\partial\langle\varphi_n|}\Big[-\mu\Big(\mathrm{Tr}\big[\hat{\rho}^{(1)}\big]-N\Big)\Big] = \frac{1}{f_n}\frac{\partial}{\partial\langle\varphi_n|}\Big[-\mu\Big(\sum_j f_j\langle\varphi_j|\varphi_j\rangle-N\Big)\Big] = -|\varphi_n\rangle\mu \tag{G.68}$$

These five derivatives are then combined to yield Eq. G.59, which, in turn, determines the Fock operator $\hat{F}$ in Eq. G.60.

The derivatives with respect to the occupation variables γ_n are determined analogously.

Self-consistency: For a given Fock operator, the system of equations can be solved by matrix diagonalization

$$\hat{F}|\varphi_n\rangle = |\varphi_n\rangle\epsilon_n \tag{G.69}$$

which yields the eigenstates $|\varphi_n\rangle$ and the one-particle energies ϵ_n. The matrix of Lagrange multipliers has the simple form $\Lambda_{m,n}\frac{1}{f_n} = \epsilon_n\delta_{m,n}$.

The Fock operator changes with changing density and one-particle-reduced density matrix and, thus, with the orbitals.

This implies that one needs to solve the following system of equations

- The eigenvalue equation Eq. **??** with the Fock operator Eq. 2.77 expressed in terms of Hartree and exchange potentials $\hat{V}_H$ and $\hat{V}_X$,

- Eq. G.57, which provides the density matrix $\rho^{(1)}$ and the density n from the orbitals $|\varphi_n\rangle$ and their occupations.

- Eq. 2.34 and Eq. 2.37, which provide the Hartree potential $\hat{V}_H$ and the exchange potential $\hat{V}_X$ from the density n and the density matrix $\rho^{(1)}$.

Fock operator and total energy: As we will see below, the Fock operator describes the spectral properties, but it does not provide directly the total energy as its expectation value.

$$E_{\text{tot}} \neq \langle\Phi|\hat{F}|\Phi\rangle \tag{G.70}$$

However, comparing the expectation value of the Fock operator with the total energy expression Eq. 2.31 or Eq. 2.74, we find

$$E_{\text{tot}} = \langle\Phi|\frac{1}{2}\Big(\hat{h}+\hat{F}\Big)|\Phi\rangle = \sum_n f_n\langle\varphi_n|\frac{1}{2}\Big(\hat{h}+\hat{F}\Big)|\varphi_n\rangle \tag{G.71}$$

A similar expression, the **Migdal-Galitskii-Koltun sum rule** Eq. 8.36, is also valid for interactions of arbitrary strength. The Migdal-Galitskii-Koltun sum rule can be rewritten in the form Eq. 8.37, which is closer to the expression given above.

G.4.3 Zero-temperature Hartree Fock in second quantization

This is a sketch for a derivation of the Hartree Fock equations using creation and annihilation operators.

The energy functional is the total energy of a Slater determinant, which depends on a variable one-particle basiset $\{|\psi_n\rangle\}$. The variable states $|\psi_n\rangle$ are a superposition of the orthonormal basisstates $|\varphi_j\rangle = \hat{a}_j^\dagger|\mathcal{O}\rangle$, which define tyhe creation and annihilation operators.

$$|\psi_n\rangle = \sum_j |\varphi_j\rangle U_{j,n}|\mathcal{O}\rangle = \sum_j \hat{a}_j^\dagger U_{j,n}|\mathcal{O}\rangle \tag{G.72}$$

where $\boldsymbol{U}$ is a unitary matrix. The unitary property is a result of the orthonormality requirement for the variable one-particle states $|\psi_n\rangle$.

$$\langle\psi_m|\psi_n\rangle = \sum_{j,k} U_{m,j}^\dagger\langle\varphi_j|\varphi_k\rangle U_{k,n} = \sum_j U_{m,j}^\dagger U_{j,n} \stackrel{!}{=} \delta_{m,n} \tag{G.73}$$

The corresponding N-particleSlater determinant is

$$|\Phi\rangle = \prod_{n=1}^{N}\Big(\sum_j \hat{a}_j^\dagger U_{j,n}\Big)|\mathcal{O}\rangle \tag{G.74}$$

The energy functional $\mathcal{E}(\boldsymbol{U})$ is the energy of the Slater determinant with the Hamiltonian $\hat{H} = \hat{h}+\hat{W}$ with the constraint that $\boldsymbol{U}$ be unitary.

$$\begin{aligned}\mathcal{E}(\boldsymbol{U}) = \langle\mathcal{O}|\Big(\prod_{n=1}^{N}\Big(\sum_m \hat{a}_m^\dagger U_{m,n}\Big)\Big)^\dagger \hat{H}\Big(\prod_{n'=1}^{N}\Big(\sum_{m'} \hat{a}_{m'}^\dagger U_{m',n'}\Big)\Big)|\mathcal{O}\rangle \\ -\sum_{m,n} h_{n,m}\Big(\sum_k U_{m,k}^\dagger U_{k,n} - \delta_{m,n}\Big)\end{aligned} \tag{G.75}$$

For the ground state the first variation of the energy functional vanishes. Here we follow the Wirtinger derivatives in spirit and determine the zero of the first variation with respect to $\boldsymbol{U}^\dagger$, while

keeping $\boldsymbol{U}$ fixed.

$$\begin{aligned}
\delta\mathcal{E} = \sum_{q,p=1}^{N} \Bigg\{ & \langle\mathcal{O}| \Bigg(\prod_{N}^{n=1\neq q} \Big(\sum_{m} \hat{a}_m^\dagger U_{m,n} \Big) \Bigg)^\dagger \delta U_{q,p}^\dagger \hat{a}_p \\
& \times \hat{H} \Big(\sum_{m'} \hat{a}_{m'}^\dagger U_{m',q} \Big) \Bigg(\prod_{n'=1\neq q}^{N} \Big(\sum_{m''} \hat{a}_{m''}^\dagger U_{m'',n'} \Big) \Bigg) |\mathcal{O}\rangle \\
& - \sum_{n} h_{n,q} \delta U_{q,p}^\dagger U_{p,n} \Bigg\} \\
= \sum_{q,p=1}^{N} \Bigg\{ & \underbrace{\sum_{r} \underbrace{\sum_{j} U_{p,j} U_{j,r}^\dagger}_{\delta_{p,r}}}_{=1} \sum_{m'} \\
& \times \langle\mathcal{O}| \Bigg(\prod_{n=1\neq q}^{N} \Big(\sum_{m} \hat{a}_m^\dagger U_{m,n} \Big) \Bigg)^\dagger \hat{a}_p \hat{H} \hat{a}_{m'}^\dagger \Bigg(\prod_{n'=1\neq q}^{N} \Big(\sum_{m''} \hat{a}_{m''}^\dagger U_{m'',n'} \Big) \Bigg) |\mathcal{O}\rangle U_{m',q} \\
& - \sum_{n} U_{p,n} h_{n,q} \Bigg\} \delta U_{q,p}^\dagger \\
= \sum_{q,p,j=1}^{N} U_{p,j} \Bigg\{ & \sum_{r} U_{j,r}^\dagger \sum_{m'} \langle\mathcal{O}| \Bigg(\prod_{N}^{n=1\neq q} \Big(\sum_{m} \hat{a}_m^\dagger U_{m,n} \Big) \Bigg)^\dagger \\
& \times \hat{a}_r \hat{H} \hat{a}_{m'}^\dagger \Bigg(\prod_{n'=1\neq q}^{N} \Big(\sum_{m''} \hat{a}_{m''}^\dagger U_{m'',n'} \Big) \Bigg) |\mathcal{O}\rangle U_{m',q} - h_{j,q} \Bigg\} \delta U_{q,p}^\dagger \stackrel{!}{=} 0
\end{aligned} \tag{G.76}$$

This produces a definition of the effective Hamiltonian $\hat{h}$.

First we extract the one-particle hamilton matrix $\bar{h}$ defined as

$$\bar{h}_{r,m'} = \langle\mathcal{O}| \Bigg(\prod_{N}^{n=1\neq q} \Big(\sum_{m} \hat{a}_m^\dagger U_{m,n} \Big) \Bigg)^\dagger \hat{a}_r \hat{H} \hat{a}_{m'}^\dagger \Bigg(\prod_{n'=1\neq q}^{N} \Big(\sum_{m''} \hat{a}_{m''}^\dagger U_{m'',n'} \Big) \Bigg) |\mathcal{O}\rangle \tag{G.77}$$

The stationary condition is then

$$\sum_{r,m'} U_{j,r}^\dagger \bar{h}_{r,m'} U_{m',q} - h_{j,q} = 0 \tag{G.78}$$

On solution for $\boldsymbol{U}$ and $\boldsymbol{h}$ is obtained after diagionalizing $\bar{\boldsymbol{h}}$

$$\sum_{j} \big(\bar{h}_{i,j} - \epsilon_n \delta_{i,j} \big) U_{j,n} = 0 \tag{G.79}$$

The unitary matrix $\boldsymbol{U}$ satisfies the equation, if the Lagrange multipliers are $h_{i,j} = \epsilon_i \delta_{i,j}$. This identifies $\bar{\boldsymbol{h}}$ with the effective Hamiltonian, respectively the Fock operator.

G.5 Contributions to exchange

While the Hartree energy has a very transparent physical interpretation, the exchange term is less accessible. The exchange is not only important in the Hartree-Fock approximation. Also in an approximation of many-particle theory, the random-phase approximation, the potential acting on the electrons can be represented by an exchange term, albeit with a screened interaction instead of the bare Coulomb potential. Another use is in a class of density functionals, the hybrid functionals which represent part of the exchange-correlation energy by a Fock term.

G.5.1 Decompose the exchange term into local orbitals

Let me express the exchange term in local orbitals $|\chi_\alpha\rangle$. The occupied one-particle wave function are expanded in these local orbitals

$$|\varphi_n\rangle = \sum_\alpha |\chi_\alpha\rangle c_{\alpha,n} \tag{G.80}$$

and the one-particle-reduced density matrix has the form

$$\hat{\rho}^{(1)} = \sum_n |\varphi_n\rangle f_n \langle\varphi_n| = \sum_{\alpha,\beta} |\chi_\alpha\rangle \rho^{(1)}_{\alpha,\beta} \langle\chi_\beta| \tag{G.81}$$

The exchange energy can be expressed by the matrix elements of the density matrix and the Coulomb matrix elements in local orbitals, called the four-center integrals.

$$\begin{aligned}
E_X &\overset{\text{Eq. 2.36}}{=} -\frac{1}{2}\sum_{m,n} f_m f_n \int d^4x \int d^4x' \, \frac{e^2 \varphi^*_m(\vec{x})\varphi^*_n(\vec{x'})\varphi_n(\vec{x})\varphi_m(\vec{x'})}{4\pi\epsilon_0|\vec{r}-\vec{r'}|} \\
&= -\frac{1}{2}\sum_{\alpha,\beta,\gamma,\delta} \rho^{(1)}_{\alpha,\beta}\rho^{(1)}_{\gamma,\delta} \int d^4x \int d^4x' \, \frac{e^2 \chi^*_\beta(\vec{x})\chi^*_\delta(\vec{x'})\chi_\gamma(\vec{x})\chi_\alpha(\vec{x'})}{4\pi\epsilon_0|\vec{r}-\vec{r'}|} \\
&= -\frac{1}{2}\sum_{\alpha,\beta,\gamma,\delta} \rho^{(1)}_{\alpha,\beta}\rho^{(1)}_{\gamma,\delta} W_{\beta,\delta,\gamma,\alpha} \\
\text{with} \qquad W_{\beta,\delta,\gamma,\alpha} &= \int d^4x \int d^4x' \, \frac{e^2 \chi^*_\beta(\vec{x})\chi^*_\delta(\vec{x'})\chi_\gamma(\vec{x})\chi_\alpha(\vec{x'})}{4\pi\epsilon_0|\vec{r}-\vec{r'}|}
\end{aligned} \tag{G.82}$$

Compare the definition of the Coulomb matrix element given here with Eq. 3.51.

Two contributions will be of interest: The contribution E_X to the energy, and secondly to the one-particle spectrum of the electrons. The shift $\Delta\epsilon_n$ of the one-particle level ϵ_n due to exchange can be written as

$$\Delta\epsilon_n = \frac{\partial E_X}{\partial f_n} = -\sum_{\alpha,\beta} \langle\psi_n|\pi_\beta\rangle \Big(\sum_{\gamma,\delta} W_{\beta,\delta,\gamma,\alpha}\rho^{(1)}_{\gamma,\delta}\Big)\langle\pi_\alpha|\psi_n\rangle \tag{G.83}$$

where $|\pi_\alpha\rangle$ is the projector function for the local orbitl $|\chi_\alpha\rangle$.

G.5.2 Long-range exchange

Let me consider large distances, that is distances $|\vec{r}-\vec{r'}|$ so large hat the orbitals connected to different coordinates do not overlap.

For each orbital $|\chi_\alpha\rangle$, I define the position of the atom, on which it is centered as $\vec{R}_\alpha$. In order to approximate the position of the density of a product of two orbitals, let me furthermore define

$$\vec{R}_{\alpha,\beta} = \frac{1}{2}\Big(\vec{R}_\alpha + \vec{R}_\beta\Big) \tag{G.84}$$

$$\begin{aligned}
E_X &\approx -\frac{1}{2}\sum_{\alpha,\beta,\gamma,\delta} \rho^{(1)}_{\alpha,\beta}\rho^{(1)}_{\gamma,\delta} \frac{e^2}{4\pi\epsilon_0|\vec{R}_{\beta,\gamma}-\vec{R}_{\alpha,\delta}|} \underbrace{\Big(\int d^4x \, \chi^*_\beta(\vec{x})\chi_\gamma(\vec{x})\Big)}_{O_{\beta,\gamma}} \underbrace{\Big(\int d^4x' \, \chi^*_\delta(\vec{x'})\chi_\alpha(\vec{x'})\Big)}_{O_{\delta,\alpha}} \\
&= -\frac{1}{2}\sum_{\alpha,\beta,\gamma,\delta} \rho^{(1)}_{\alpha,\beta} O_{\beta,\gamma}\rho^{(1)}_{\gamma,\delta} O_{\delta,\alpha} \frac{e^2}{4\pi\epsilon_0|\vec{R}_{\beta,\gamma}-\vec{R}_{\alpha,\delta}|}
\end{aligned} \tag{G.85}$$

For an orthonormal basisset ($O_{\alpha,\beta} = \delta_{\alpha,\beta}$) this expression becomes even simpler, namely

$$E_X = -\frac{1}{2}\sum_{\alpha,\gamma}\frac{e^2\rho^{(1)}_{\alpha,\gamma}\rho^{(1)}_{\gamma,\alpha}}{4\pi\epsilon_0|\vec{R}_{\gamma,\gamma}-\vec{R}_{\alpha,\alpha}|} \qquad \text{for } O_{\alpha,\beta}=\delta_{\alpha,\beta} \tag{G.86}$$

Apparently the range of the exchange term is linked to the range of the density matrix. This range is itself connected to the **coherence length**.

In order to understand the concept of coherence length let me consider again the free-electron gas. The one-particle-reduced density matrix of a free-electron gas is Editor: up to some factors

$$\rho^{(1)}(\vec{r},\vec{r}') = C\int d^3k\;\theta(k_F-|\vec{k}|)e^{i\vec{k}(\vec{r}-\vec{r}')} \overset{\text{Eq. E.21}}{=} C\cdot\frac{4\pi}{3}k_F^3\left[-3\frac{\cos(k_Fs)}{(k_Fs)^2}+3\frac{\sin(k_Fs)}{(k_Fs)^3}\right] \tag{G.87}$$

where $s=|\vec{r}-\vec{r}'|$. The expression shows that the exchange term falls off with order $|\vec{R}-\vec{R}|^{-5}$. The number of terms increases proportional to $|\vec{R}-\vec{R}|^2$, so that the contribution from a given radius falls of like $|\vec{R}-\vec{R}|^{-3}$.

This implies that the decay of the exchange contributions is algebraic rather than exponential. This changes as soon as temperature is switched on. Let me do a dimensional argument: at finite temperature the temperature broadening is proportional to k_BT. This leads to a momentum broadening of $\Delta\epsilon = \frac{\partial\epsilon}{\partial|\vec{k}|}\Delta k_F = v_F\Delta k_F$, where v_F is the Fermi velocity. Let me estimate the coherence length ℓ_c as that distance where the thermally excited electrons and holes are out of phase, i.e. $(k_F+\frac{1}{2}\Delta k_F)\ell_c = (k_F-\frac{1}{2}\Delta k_F)\ell_c+\pi$. We obtain the estimate

$$\ell_c = \frac{\pi}{\Delta k_F} = \frac{v_F\pi}{k_BT} \tag{G.88}$$

Editor: work out values.

Not only temperature reduces the coherence length. While temperature creates electron-hole pairs, which destroy the coherence, also the interaction can induce electron-hole pairs which essentially have the same effect. However, here the term is described as screening the potential. Electron-hole pairs are formed which act against the interaction, so that the Coulomb potential in the exchange term is replaced by a Yukawa potential having an exponential decay.

For insulators the decay of the density matrix is more rapid. Editor: I need to find an intuitive argument.

G.5.3 On-site exchange

Evaluation of onsite Coulomb parameters

For pure angular momentum eigenstates the Coulomb matrix elements can be traced back to simple radial integrations.

We make the assumption that the orbitals are eigenstates of angular momentum and spin, i.e. they can be expressed in terms of radial functions $\mathcal{R}_\alpha(r)$, spherical harmonics $Y_{\ell,m}(\vec{r})$ and eigenstates of $\hat{S}_z$ as

$$\chi_\alpha(\vec{r},\sigma) = \delta_{\sigma,\sigma_\alpha}\mathcal{R}_\alpha(|\vec{r}|)Y_{\ell_\alpha,m_\alpha}(\vec{r}) \tag{G.89}$$

The angular momentum eigenstates are combined into one, i.e. $L=(\ell,m)$. The spherical harmonics are defined such that

$$\frac{1}{r^2}\int d^3r\;\delta(|\vec{r}|-r)Y^*_L(\vec{r})Y_{L'}(\vec{r}) = \delta_{L,L'} \tag{G.90}$$

We make use of the Gaunt coefficients $C_{L,L',L''}$ defined via

$$Y_L(\vec{r}) = \sum_{L',L''}C_{L,L',L''}Y_{L'}(\vec{r})Y_{L''}(\vec{r}) \tag{G.91}$$

Furthermore we use

$$Y_{-L}(\vec{r}) = Y_L^*(\vec{r}) \tag{G.92}$$

where $-L$ is a short hand for $\ell, -m$. Note that this relation differs for real spherical harmonics!

For a density in an angular momentum decomposition

$$\rho(\vec{r}) = \sum_{\ell,m} \rho_{\ell,m}(|\vec{r}|) Y_{\ell,m}(\vec{r}) \tag{G.93}$$

the electrostatic potential is(see Eq. 5.42 in ΦSX: Elektrodynamik[24])

$$\begin{aligned}\Phi(\vec{r} &= \int d^3r' \frac{\rho(\vec{r'})}{4\pi\epsilon_0|\vec{r}-\vec{r'}|} \\ &= \frac{1}{4\pi\epsilon_0}\sum_{\ell,m}\frac{4\pi}{2\ell+1}Y_{\ell,m}(\vec{r})\left\{r^\ell\int_r^\infty dr_0\ r_0^2 r_0^{-\ell-1}\rho_{\ell,m}(r_0) + r^{-\ell-1}\int_0^r dr_0\ r_0^2 r_0^\ell \rho_{\ell,m}(r_0)\right\}\end{aligned} \tag{G.94}$$

Now we can evaluate the Coulomb matrix element

$$\begin{aligned}U_{L,L',L'',L'''} &= \int d^3r \int d^3r' \ \frac{e^2\left(\mathcal{R}_\ell^*(r)Y_L^*(\vec{r})\right)\left(\mathcal{R}_{\ell'}^*(r')Y_{L'}^*(\vec{r'})\right)\left(\mathcal{R}_{\ell''}(r)Y_{L''}(\vec{r})\right)\left(\mathcal{R}_{\ell'''}(r')Y_{L'''}(\vec{r'})\right)}{4\pi\epsilon_0|\vec{r}-\vec{r'}|} \\ &= \sum_{\bar{L},\bar{L}'} C_{\bar{L},-L,L''}C_{\bar{L}',-L',L'''}\int d^3r\int d^3r'\ \frac{e^2\left(\mathcal{R}_\ell^*(r)\mathcal{R}_{\ell''}(r)Y_{\bar{L}}(\vec{r})\right)\left(\mathcal{R}_{\ell'}^*(r')\mathcal{R}_{\ell'''}(r')Y_{\bar{L}'}(\vec{r'})\right)}{4\pi\epsilon_0|\vec{r}-\vec{r'}|} \\ &= \sum_{\bar{L}}\frac{4\pi}{2\bar{\ell}+1}C_{\bar{L},L,L''}C_{\bar{L},L',L'''}F^L_{\ell,\ell',\ell'',l'''}\end{aligned} \tag{G.95}$$

with the so-called **Slater integrals** [5]

$$F^L_{\ell,\ell',\ell'',l'''} \stackrel{\text{def}}{=} \frac{e^2}{4\pi\epsilon_0}\int dr\ r^2\int dr'\ r'^2\ \mathcal{R}_\ell^*(r)\mathcal{R}_{\ell''}(r)\frac{[\min(r,r')]^\ell}{[\max(r,r')]^{\ell+1}}\mathcal{R}_{\ell'}^*(r')\mathcal{R}_{\ell'''}(r') \tag{G.96}$$

Kanamori parameters

Let me now consider the opposite limit, namely that all four orbitals contributing to a given exchange term are located on the same atom.

Kanamori parameters[19]

$$\begin{aligned}U &= \int d^4x\int d^4x'\ \frac{e^2\chi_m^*(\vec{x})\chi_m^*(\vec{x'})\chi_m(\vec{x})\chi_m(\vec{x'})}{4\pi\epsilon_0|\vec{r}-\vec{r'}|} \\ U' &= \int d^4x\int d^4x'\ \frac{e^2\chi_m^*(\vec{x})\chi_{m'}^*(\vec{x'})\chi_m(\vec{x})\chi_{m'}(\vec{x'})}{4\pi\epsilon_0|\vec{r}-\vec{r'}|} \\ J &= \int d^4x\int d^4x'\ \frac{e^2\chi_m^*(\vec{x})\chi_{m'}^*(\vec{x'})\chi_{m'}(\vec{x})\chi_m(\vec{x'})}{4\pi\epsilon_0|\vec{r}-\vec{r'}|} \\ J' &= \int d^4x\int d^4x'\ \frac{e^2\chi_m^*(\vec{x})\chi_m^*(\vec{x'})\chi_{m'}(\vec{x})\chi_{m'}(\vec{x'})}{4\pi\epsilon_0|\vec{r}-\vec{r'}|}\end{aligned} \tag{G.97}$$

- Terms that describe the interaction of spherical densities

[5] Compare the notation with Tran et al.[173]

- the largest term is the one with all four indices equal. This term favors that the electrons accumulate in few spatial and spin orbitals. It disfavors that the electrons distribute over many orbitals. If the electrons are in one spatial orbital, this term favors that the electrons have the same spin. This term is identified with the *intraband Coulomb parameter* U.
- The second largest term is $L_\alpha = -L_\delta$ and $L_\beta = -L_\delta$, but $L_\alpha \neq L_\beta$, because each pair produces a spherical contribution to the density. There is only a contribution if $\sigma_\alpha = \sigma_\delta$ and $\sigma_\beta = \sigma_\gamma$. This term is identified with the *interband Coulomb parameter* U'.

Model for an atom

Let us make a model, which describes a d- or f-shell of an atom with localized wave functions.

I begin with the approximate Hamiltonian Eq. 2.100 on p. 78.

$$\hat{H} \overset{\text{Eq. 2.100}}{\approx} \sum_{\vec{\sigma}} |\vec{\sigma}\rangle\, E\big(|\vec{\sigma}\rangle\big)\, \langle\vec{\sigma}| \tag{G.98}$$

with the many-electron energies

$$\underbrace{E\big(|\vec{\sigma}\rangle\big)}_{\langle\vec{\sigma}|\hat{h}+\hat{W}|\vec{\sigma}\rangle} \overset{\text{Eq. 2.101}}{=} \sum_{j=1}^{\infty} \sigma_j \langle\varphi_j|\hat{h}|\varphi_j\rangle + \frac{1}{2}\sum_{i,j=1}^{\infty} \sigma_i\sigma_j \Big(\langle\varphi_i\varphi_j|\hat{W}|\varphi_i\varphi_j\rangle - \langle\varphi_i\varphi_j|\hat{W}|\varphi_j\varphi_i\rangle\Big) \tag{G.99}$$

This Hamiltonian is obtained from the full many-electron Hamiltonian by neglecting the off-diagonal matrix elements in a basis of Slater determinants, i.e. we set $\langle\vec{\sigma}|\hat{H}|\vec{\sigma'}\rangle = 0$ for $|\vec{\sigma}\rangle \neq |\vec{\sigma'}\rangle$. The choice of this Hamiltonian is part of our model assumptions. I will therefore drop the approximate sign in the following.

The Hamiltonian Eq. 2.100 can be rewritten in terms of occupation-number operators[6] $\hat{n}_j = \hat{c}_j^\dagger \hat{c}_j$ in the form

$$\hat{H} = \sum_j \langle\varphi_j|\hat{h}|\varphi_j\rangle \hat{n}_j + \frac{1}{2}\sum_{i,j} \Big(\langle\varphi_i\varphi_j|\hat{W}|\varphi_i\varphi_j\rangle - \langle\varphi_i\varphi_j|\hat{W}|\varphi_i\varphi_j\rangle\Big)\hat{n}_i\hat{n}_j \tag{G.100}$$

Let me ignore the one-particle term, and let me furthermore consider the orbitals $|m,\sigma\rangle$ with $\sigma \in \{\uparrow,\downarrow\}$, where m is the magnetic angular momentum quantum number $-\ell \leq m \leq \ell$.

For the Coulomb integrals, I distinguish the Hartree integrals U, where the orbital densities $\varphi_m(\vec{r},\sigma)\varphi_m(\vec{r},\sigma)$ interact, from the exchange terms J, for which the overlap densities $\varphi_m(\vec{r},\sigma)\varphi_{m'}(\vec{r},\sigma)$ of two different ($m \neq m'$) orbitals interact with themselfes. Note, that I do not distinguish U and U' in the sense of Kanamori Eq. G.97.

$$\begin{aligned}
\hat{H} &= \frac{1}{2}\sum_{m,m'}\sum_{\sigma,\sigma'\in\{\uparrow,\downarrow\}} \Bigg(\underbrace{U}_{\langle\varphi_i\varphi_j|\hat{W}|\varphi_i\varphi_j\rangle} \underbrace{-\delta_{\sigma,\sigma'}\Big(U\delta_{m,m'} + J(1-\delta_{m,m'})\Big)}_{\langle\varphi_i\varphi_j|\hat{W}|\varphi_j\varphi_i\rangle}\Bigg)\hat{n}_{m,\sigma}\hat{n}_{m',\sigma'} \\
&= \frac{1}{2}\sum_{m,m'}\sum_{\sigma\in\{\uparrow,\downarrow\}} U\hat{n}_{m,\sigma}\hat{n}_{m',-\sigma} + \frac{1}{2}\sum_{m,m'}\sum_{\sigma\in\{\uparrow,\downarrow\}} \Big(U(1-\delta_{m,m'}) - J(1-\delta_{m,m'})\Big)\hat{n}_{m,\sigma}\hat{n}_{m',\sigma} \\
&= \frac{1}{2}\sum_{m,m'}\sum_{\sigma\in\{\uparrow,\downarrow\}} U\hat{n}_{m,\sigma}\hat{n}_{m',-\sigma} + \frac{1}{2}\sum_{m,m',m\neq m'}\sum_{\sigma\in\{\uparrow,\downarrow\}} (U-J)\hat{n}_{m,\sigma}\hat{n}_{m',\sigma}
\end{aligned} \tag{G.101}$$

[7] This Hamiltonian is consistent with Eq. 9 of [174].

[6] Remember, that Slater determinants are the eigenstates of the occupation-number operators in an orthormal one-particle basis.

[7] It assumes that the Coulomb energy between any pair of orbitals is identical, namely U. (U' in Eq. G.97.) This

Let me now bring this Hamiltonian into a form that is closer to the expressiuns used in density-functional theory.

$$\begin{aligned}\hat{H} &= \frac{1}{2}\sum_{m,m',\sigma} U\hat{n}_{m,\sigma}\hat{n}_{m',-\sigma} + \frac{1}{2}\sum_{m,m',\sigma;m\neq m'} (U-J)\hat{n}_{m,\sigma}\hat{n}_{m',\sigma} \\ &= \underbrace{\frac{1}{2}\sum_{m,m',\sigma,\sigma'} U\hat{n}_{m,\sigma}\hat{n}_{m',\sigma'}}_{\text{Hartree energy}} \underbrace{-\frac{1}{2}\sum_{m,\sigma} U\hat{n}_{m,\sigma}^2 - \frac{1}{2}\sum_{\sigma}\sum_{m,m'} J\hat{n}_{m,\sigma}\hat{n}_{m',\sigma} + \frac{1}{2}\sum_{m,\sigma} J\hat{n}_{m,\sigma}^2}_{\text{exchange energy}} \\ &= \frac{1}{2}U\Big(\sum_{m,\sigma}\hat{n}_{m,\sigma}\Big)^2 - \frac{1}{2}J\underbrace{\sum_{\sigma}\Big(\sum_{m}\hat{n}_{m,\sigma}\Big)^2}_{\frac{1}{2}(\hat{n}_\uparrow+\hat{n}_\downarrow)^2+\frac{1}{2}(\hat{n}_\uparrow-\hat{n}_\downarrow)^2} \underbrace{-\frac{1}{2}(U-J)\sum_{m,\sigma}\hat{n}_{m,\sigma}^2}_{\text{self-energy correction}} \\ &= \frac{1}{2}(U-\frac{1}{2}J)\hat{n}_t^2 - \frac{1}{4}J\hat{n}_s^2 \underbrace{-\frac{1}{2}(U-J)\sum_{m,\sigma}\hat{n}_{m,\sigma}^2}_{\text{self-energy correction}} \end{aligned} \tag{G.104}$$

where

$$\begin{aligned}\hat{n}_t &= \sum_{m,\sigma}\hat{n}_{m,\sigma} \\ \hat{n}_\sigma &= \sum_{m}\hat{n}_{m,\sigma} \\ \hat{n}_s &= \hat{n}_\uparrow - \hat{n}_\downarrow \end{aligned} \tag{G.105}$$

In order to arrive at the mean-field approximation, I express each operator by its expectation value and the fluctuation operator about the expectation value.

$$\begin{aligned}\hat{H} &= \frac{1}{2}\Big(U-\frac{1}{2}J\Big)\Big(\hat{n}_t - \langle n_t\rangle\Big)^2 - \frac{1}{4}J\Big(\hat{n}_s - \langle n_s\rangle\Big)^2 - \frac{1}{2}(U-J)\sum_{m,\sigma}\Big(\hat{n}_{m,\sigma} - \langle n_{m,\sigma}\rangle\Big)^2 \\ &+ \Big[\frac{1}{2}(U-\frac{1}{2}J)\langle n_t\rangle\Big]\Big(\hat{n}_t - \langle n_t\rangle\Big) - \Big[\frac{1}{2}J\langle n_s\rangle\Big]\Big(\hat{n}_s - \langle n_s\rangle\Big) - \sum_{m,\sigma}\Big[(U-J)\langle n_{m,\sigma}\rangle\Big]\Big(\hat{n}_{m,\sigma} - \langle n_{m,\sigma}\rangle\Big) \\ &+ \frac{1}{2}(U-\frac{1}{2}J)\langle n_t\rangle^2 - \frac{1}{4}J\langle n_s\rangle^2 - \frac{1}{2}(U-J)\sum_{m,\sigma}\langle n_{m,\sigma}\rangle^2 \end{aligned} \tag{G.106}$$

The Hartree-Fock approximation amounts to ignoring the quadratic terms in the fluctuations. The terms linear in the fluctuation define the band structure, but do not affect the total energy, because the expectation value of the fluctuations vanish, i.e.

$$\Big\langle \hat{n} - \langle n\rangle \Big\rangle = 0\ . \tag{G.107}$$

Thus, the total energy of the Hartree-Fock term is the last line

$$E^{HF} = \frac{1}{2}\Big(U-\frac{1}{2}J\Big)\langle n_t\rangle^2 - \frac{1}{4}J\langle n_s\rangle^2 - \frac{1}{2}\Big(U-J\Big)\sum_{m,\sigma}\langle n_{m,\sigma}\rangle^2 \tag{G.108}$$

---

energy can be divided into equal spin contributions and opposite spin contributions. Thus the Hartree energy is

$$\frac{1}{2}\sum_{m,\sigma,m',\sigma'} U\hat{n}_{m,\sigma}\hat{n}_{m',\sigma'} = \frac{1}{2}\sum_{m,m'} U\hat{n}_{m,\sigma}\hat{n}_{m',-\sigma} + \frac{1}{2}\sum_{m,\sigma,m',\sigma} U\hat{n}_{m,\sigma}\hat{n}_{m',\sigma} \tag{G.102}$$

The exchange energy acts only between states with equal spin.

$$-\frac{1}{2}\sum_{m,\sigma,m,\sigma} U\hat{n}_{m,\sigma}\hat{n}_{m,\sigma} - \frac{1}{2}\sum_{m,m';m\neq m'} J\hat{n}_{m,\sigma}\hat{n}_{m',\sigma} \tag{G.103}$$

The first term is the Self-interaction correction, which compensates the interaction of electrons with themselfes.

and the energy levels are obtained from the second line, the mean-field Hamiltonian

$$\begin{aligned}\hat{H}_{MF} &= \Big[(U-\frac{1}{2}J)\langle n_t\rangle\Big]\hat{n}_t - \Big[\frac{1}{2}J\langle n_s\rangle\Big]\hat{n}_s - \sum_{m,\sigma}\Big[(U-J)\langle n_{m,\sigma}\rangle\Big]\hat{n}_{m,\sigma} \\ &= \sum_{m,\sigma}\Big(U\langle n_t\rangle - J\langle n_\sigma\rangle - (U-J)\langle n_{m,\sigma}\rangle\Big)\hat{n}_{m,\sigma} \\ \epsilon_{m,\sigma} &= \Big(U\langle n_t\rangle - J\langle n_\sigma\rangle - (U-J)\langle n_{m,\sigma}\rangle\Big) \\ &= \sum_{m'(\neq m)}(U-J)\langle n_{m',\sigma}\rangle + \sum_{m'}U\langle n_{m',-\sigma}\rangle \end{aligned} \tag{G.109}$$

It can be shown that Janak's Theorem[175] holds, that is the one-particle energies are obtained as derivatives

$$\epsilon^{HF}_{m,\sigma} = \frac{\partial E^{HF}}{\partial n_{m,\sigma}} \tag{G.110}$$

of the mean-field total energy with respect to the corresponding average occupation.

The first term of $\epsilon_{m,\sigma}$, $U\langle n_t\rangle$, expresses that the one-particle energy levels shift as result of the Coulomb repulsion. The second term, $-J\langle n_\sigma\rangle$, describes Hund's rule, i.e. electrons are stabilized by other electrons with the same spin, because they avoid each other better than electrons with equal spin. The last term, $-(U-J)\langle n_{m,\sigma}\rangle$, describes that filled orbitals are stabilized with respect to unoccupied orbitals by $U-J$.

The last term, the self-interaction correction is the most important term of Hartree-Fock compared to the Kohn-Sham bandstructure of DFT. This term is responsible for ensuring Koopmanns' theorem[176, 177], which says that the energy difference can be calculated from energy levels. In other words it says that

$$\frac{\partial \epsilon^{HF}_{m,\sigma}}{\partial n_{m_\sigma}} = 0 \qquad \text{for } 0 < n_{m,\sigma} < 1 \tag{G.111}$$

Note, however, that this equation is only valid for the derivatives with respect to the occupation on the *same* orbital!

This property follows from the fact that for isolated systems a state with fractional occupation is a classical mixture of two states (ensembles) with different particle numbers.

The self energy correction term makes sure that energy differences for different occupations can be estimated from the energy level differences as seen in Figure G.2.

G.5.4 Bond-exchange

Let me consider a two-center bond. That is, the bonding orbital is polarized in one or the other bonding partner. The asymmetry is governed by the angle α. The bonding orbital $|\varphi_b\rangle$ and the antibonding orbital $|\varphi_a\rangle$ are

$$\begin{aligned}|\psi_b\rangle &= +|\chi_{1,\sigma}\rangle\cos(\alpha) + |\chi_{2,\sigma}\rangle\sin(\alpha) \quad \text{with occupation } f_b \\ |\psi_a\rangle &= -|\chi_{1,\sigma}\rangle\sin(\alpha) + |\chi_{2,\sigma}\rangle\cos(\alpha) \quad \text{with occupation } f_a \end{aligned} \tag{G.112}$$

$|\chi_1\rangle$ on the orbital on the left atom R_1 and $|\chi_2\rangle$ is the one on the right atom R_2.

A value of $\alpha = \pi/4 = 45°$ describes the symmetric case. In a half-filled system, i.e. $f_b = 1$ and $f_a = 0$,

- $\alpha = 0°$: the electron is localized on the left atom R_1
- $\alpha = 45°$: the electron is delocalized over both orbitals

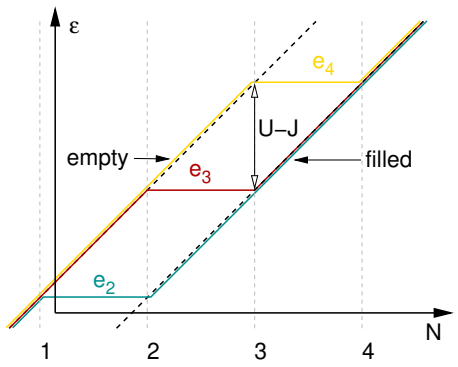


Fig. G.1: Energy level diagram of an atom with several degenerate atomic levels, that change only due to the Coulomb interaction. Occupied and unoccupied orbitals must be different, if the energy level, that receives an electron must not shift upon charging. The fact that the energy level remains constant upon charging reflects the fact that the energy is a sequence of piece-wise linear segments describing the coexistence of two ensembles with different particle numbers.

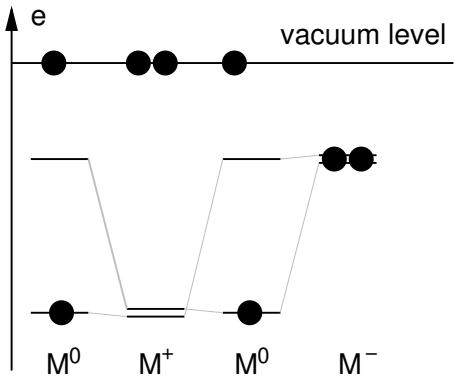


Fig. G.2: Schematic energy level of an atom in the Hartree-Fock approximation with two degenerate energy levels, that become different only via occupation. Note that the energy level, that changes its occupation remains fixed, while the other orbitals shift due to the coulomb interaction with the electron that is shifted around.

- $\alpha = 90°$: the electron is localized on the right atom R_2.

The corresponding density matrix is

$$\begin{aligned}\boldsymbol{\rho} &= \begin{pmatrix} \rho_{11} & \rho_{12} \\ \rho_{21} & \rho_{22} \end{pmatrix} = \begin{pmatrix} f_b \cos^2(\alpha) + f_a \sin^2(\alpha) & (f_b - f_a)\cos(\alpha)\sin(\alpha) \\ (f_b - f_a)\cos(\alpha)\sin(\alpha) & f_b \sin^2(\alpha) + f_a \cos^2(\alpha) \end{pmatrix} \\ &= \frac{f_a + f_b}{2} \begin{pmatrix} 1 & 0 \\ 0 & 1 \end{pmatrix} + \frac{f_b - f_a}{2} \begin{pmatrix} \cos(2\alpha) & \sin(2\alpha) \\ \sin(2\alpha) & -\cos(2\alpha) \end{pmatrix} \end{aligned} \tag{G.113}$$

The exchange energy is

$$\begin{aligned}
E_X &= -\frac{1}{2}\sum_{\alpha,\beta,\gamma,\delta}\rho^{(1)}_{\alpha,\beta}\rho^{(1)}_{\gamma,\delta}\int d^4x\int d^4x'\,\frac{e^2\chi^*_\beta(\vec{x})\chi^*_\delta(\vec{x'})\chi_\gamma(\vec{x})\chi_\alpha(\vec{x'})}{4\pi\epsilon_0|\vec{r}-\vec{r'}|}\\
&= -\frac{1}{2}\sum_{\alpha,\beta,\gamma,\delta}\rho^{(1)}_{\alpha,\beta}\rho^{(1)}_{\gamma,\delta}W_{\alpha,\beta,\gamma,\delta}\\
&= -\frac{1}{2}\sum_{\alpha=1}^{2}\underbrace{\rho^{(1)}_{\alpha,\alpha}\rho^{(1)}_{\alpha,\alpha}W_{\alpha,\alpha,\alpha,\alpha}}_{\text{onsite}}\\
&\quad -\frac{1}{2}\sum_{\alpha\neq\beta=1}^{2}\Big\{\underbrace{\rho^{(1)}_{\alpha,\beta}\rho^{(1)}_{\beta,\alpha}W_{\beta,\alpha,\beta,\alpha}}_{\text{NDDO}}+\underbrace{\rho^{(1)}_{\alpha,\beta}\rho^{(1)}_{\alpha,\beta}W_{\beta,\beta,\alpha,\alpha}+\rho^{(1)}_{\alpha,\alpha}\rho^{(1)}_{\beta,\beta}W_{\alpha,\beta,\beta,\alpha}}_{\text{bondx}}\\
&\quad +\underbrace{\rho^{(1)}_{\alpha,\beta}\rho^{(1)}_{\beta,\beta}W_{\beta,\beta,\beta,\alpha}+\rho^{(1)}_{\beta,\alpha}\rho^{(1)}_{\beta,\beta}W_{\alpha,\beta,\beta,\beta}+\rho^{(1)}_{\beta,\beta}\rho^{(1)}_{\alpha,\beta}W_{\beta,\beta,\alpha,\beta}+\rho^{(1)}_{\beta,\beta}\rho^{(1)}_{\beta,\alpha}W_{\beta,\alpha,\beta,\beta}}_{\text{31 terms}}\Big\}
\end{aligned}\tag{G.114}$$

Let me exploit the symmetry of the four-center integrals $W_{\alpha,\beta,\gamma,\delta}$:

$$W_{\alpha,\beta,\gamma,\delta}=W_{\beta,\alpha,\delta,\gamma}=W^*_{\gamma,\delta,\alpha,\beta}=W^*_{\delta,\gamma,\beta,\alpha}\tag{G.115}$$

For real-valued orbitals, where $\chi^*_\alpha(\vec{r})\chi_\beta(\vec{r})=\chi^*_\beta(\vec{r})\chi_\alpha(\vec{r})$, we can furthermore exploit

$$\begin{aligned}
W_{\alpha,\beta,\gamma,\delta} &= W_{\gamma,\beta,\alpha,\delta}=W_{\alpha,\delta,\gamma,\beta}\\
&= W_{\delta,\alpha,\beta,\gamma}=W_{\beta,\gamma,\delta,\delta}\\
&= W^*_{\alpha,\delta,\gamma,\beta}=W^*_{\gamma,\beta,\alpha,\delta}\\
&= W^*_{\beta,\gamma,\delta,\alpha}=W^*_{\delta,\alpha,\beta,\gamma}
\end{aligned}\tag{G.116}$$

With these simplifications, we arrive at

$$\begin{aligned}
E_X = &\underbrace{-\frac{1}{2}\rho^{(1)}_{1,1}\rho^{(1)}_{1,1}W_{1,1,1,1}-\frac{1}{2}\rho^{(1)}_{2,2}\rho^{(1)}_{2,2}W_{2,2,2,2}}_{\text{onsite}}\\
&-\underbrace{\rho^{(1)}_{1,2}\rho^{(1)}_{2,1}W_{1,2,1,2}}_{\text{NDDO}}-\underbrace{2\rho^{(1)}_{1,2}\rho^{(1)}_{1,2}W_{1,1,2,2}}_{\text{bondx}}-\underbrace{2\rho^{(1)}_{1,2}\rho^{(1)}_{2,2}W_{1,2,2,2}-2\rho^{(1)}_{1,2}\rho^{(1)}_{1,1}W_{2,1,1,1}}_{\text{31-terms}}
\end{aligned}\tag{G.117}$$

Let me now insert the density matrix Eq. G.113

$$\begin{aligned}
E_X = &\underbrace{-\frac{1}{8}\Big((f_b+f_a)+(f_b-f_a)\cos(2\alpha)\Big)^2W_{1,1,1,1}-\frac{1}{8}\Big((f_b+f_a)-(f_b-f_a)\cos(2\alpha)\Big)^2W_{2,2,2,2}}_{\text{onsite}}\\
&-\frac{1}{4}(f_b-f_a)^2\sin^2(2\alpha)\Big(\underbrace{W_{1,2,1,2}}_{\text{NDDO}}+\underbrace{2W_{1,1,2,2}}_{\text{bondx}}\Big)\\
&-\underbrace{\frac{1}{2}(f_b-f_a)\sin(2\alpha)\Big[\Big((f_b+f_a)-(f_b-f_a)\cos(2\alpha)\Big)W_{1,2,2,2}+\Big((f_b+f_a)+(f_b-f_a)\cos(2\alpha)\Big)W_{2,1,1,1}\Big)}_{\text{31-terms}}
\end{aligned}\tag{G.118}$$

Let me now calculate the shift of the band edges due to the exchange term for $f_b = 1$ and $f_a = 0$

$$\begin{aligned}\Delta\epsilon_a = &\underbrace{-\frac{1}{4}\overbrace{\Big(1-\cos^2(2\alpha)\Big)}^{\sin^2(2\alpha)} W_{1,1,1,1} - \frac{1}{4}\overbrace{\Big(1-\cos^2(2\alpha)\Big)}^{\sin^2(2\alpha)} W_{2,2,2,2}}_{\text{onsite}} \\ &+\frac{1}{2}\sin^2(2\alpha)\Big(\underbrace{W_{1,2,1,2}}_{\text{NDDO}} + \underbrace{2W_{1,1,2,2}}_{\text{bondx}}\Big) \underbrace{-\sin(2\alpha)\cos(2\alpha)\Big(W_{1,2,2,2} - W_{2,1,1,1}\Big)}_{\text{31-terms}} \qquad \text{(G.119)} \\ \Delta\epsilon_b = &\underbrace{-\frac{1}{8}\Big(1+\cos(2\alpha)\Big)^2 W_{1,1,1,1} - \frac{1}{8}\Big(1-\cos(2\alpha)\Big)^2 W_{2,2,2,2}}_{\text{onsite}} \\ &-\frac{1}{2}\sin^2(2\alpha)\Big(\underbrace{W_{1,2,1,2}}_{\text{NDDO}} + \underbrace{2W_{1,1,2,2}}_{\text{bondx}}\Big) \\ &\underbrace{-\sin(2\alpha)\Big(W_{1,2,2,2} + W_{1,2,2,2}\Big) + \sin(2\alpha)\cos(2\alpha)\Big(W_{1,2,2,2} - W_{1,2,2,2}\Big)}_{\text{31-terms}} \qquad \text{(G.120)}\end{aligned}$$

- Left-right correlation: Left-right correlation describes the tendency of electrons to localize on opposite sides of a bond, in order to reduce the energy cost of their Coulomb repulsion. Considering a symmetric bond, the onsite terms have the form

$$E_X = -\frac{W_{1111}}{4}\Big((f_a+f_b)^2 + (f_b-f_a)^2\cos^2(2\alpha)\Big) \qquad \text{(G.121)}$$

  This term favors the polarization of the bond to one or the other side.

  There is, however, a competition between the kinetic energy and this exchange term. The bond polarization destroys the delocalization of the electron over both bond partners and thus the chemical bond. A hydrogen molecule, the Hubbard dimer, undergoes a phase transition to an antiferromagnetic structure beyond a certain strength of the interaction. In the antiferromagnetic configuration, the spin-up electron is one atom and the spin-down electron is on the other atom. A weak delocalization to the other atom is still present. The spin-up electron can polarize in one or the other direction. Each of these two configurations can be described by a Slater determinant. The fully correlated state is a superposition of these two Slater determinants, resulting in a spin-singlet state with antiferromagnetic correlations.

- The term denoted NDDO describes the exchange term due to the intersite Coulomb interaction. The term favors $\alpha = 45°$, that is, it it favors a symmetric bond with delocalized electrons. This term is closely related to the kinetic energy $E_{\text{kin}} = -t(f_b - f_a)\sin(2\alpha)$. The terms (NDDO+BONDX) can be expressed as $E_X^{NDDO+BONDX} = -\frac{W_{1212}+2W_{1,1,22}}{4t^2}E_{\text{kin}}^2$.

  The term is sensitive to the phase shift of bonding and antibonding orbitals, and it tends to open up the band gaps which are due to covalent bond formation.

- The terms denoted *31-terms* open up the band gap for ionic bonds. The 31-terms do not shift the empty orbital in a symmetric bond. The empty orbital is shifted up when the bond is strongly polarized, while the effect vanishes for a completely polarized ?????.

  In a simple approximation (the density of the orbitals form a homogeneously charged sphere) the matrix elements can be related to the radius of the orbitals. $W_{1222} = \frac{Q_{12}}{r_2}$ $W_{2111} = \frac{Q_{12}}{r_1}$. Therefore, the level shift due to the 31 term is $\frac{1}{2}\sin(4\alpha)Q_{12}\left(\frac{1}{r_2} - \frac{1}{r_1}\right)$. Thus, the conduction band is shifted up if the bond is polarized towards the more extended orbital, which it is shifted down, if the orbital is polarized towards the more localized orbital.

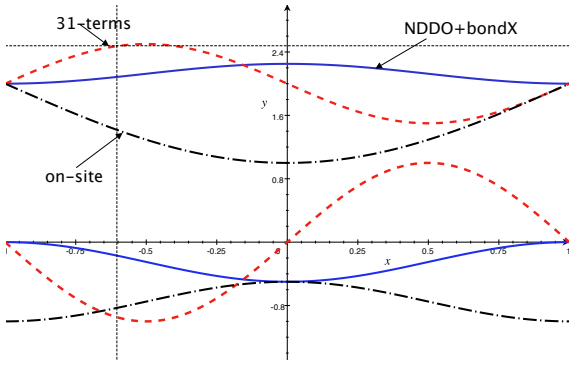


Fig. G.3: Shift of the band edges due to different exchange terms. full line in blue: NDDO+BONDX Red dash-dotted line: 31-terms and black dashed lines: symmetric onsite term. Empty states are shifted up for better visibility. Each term must be scaled by the respective matrix elements.

G.6 Self-consistent Hartree-Fock code for finite temperatures

Below, I discuss how the thermal Hartree-Fock approxmation can be implented in a code for a finite system. We start from an interacting Hamiltonian $\hat{H} = \hat{h} + \hat{W}$ with known matrix elements for the non-interacting Hamiltonian $\hat{h}$ and the interaction $\hat{W}$. The code is built for demonstration purposes. It is simple, but neither efficient nor robust.

The code rests on the grand potential Eq. 2.74 on p. 72 of the thermal Hartree-Fock approximation, as well as the selfconsistent equations in Eq. 2.81 on p. 74.

We are interested in an ensemble with fixed particle number N, rather than a system in contact with a particle reservoir. Remember though, that this particle number N is the thermal expectation value of the particle number rather than an ensemble with micro states that all have the same particle number N.

The thermodynamic potential for this ensemble is the **Helmholtz potential**.

$$A_{T,N} = \operatorname*{stat}_{\mu}\Big(\Omega_{T,\mu} + \mu N\Big) \tag{G.122}$$

Rather than using the conventional self-consistency cycle we use a dynamical scheme to find the thermal ensemble. This technique has been invented by Roberto Car and Michele Parrinello in 1985[178] and it was the advent of ab-initio molecular dynamics. One treats the wave function coefficients like classical variables. The forces are acting on these variables are calculated and a friction force is added. The resulting equations of motion are solved. The friction ensures that the system comes to rest at the minimum of the Helmholtz potential.

Editor: Notation changed:

- $h^{(0)} \to h$
- $h^{out} \to \hat{F}; h^{eff}$

.

G.6.1 Theoretical background

At finite temperature T, the grand potential is, expressed as functional of the one-particle-reduced density matrix $\boldsymbol{\rho}^{(1)}$,

$$\Omega^{HF}_{T,\mu}[\boldsymbol{\rho}^{(1)}] \overset{\text{Eq. 2.74}}{=} \underbrace{\sum_{\alpha,\beta} h^{(0)}_{\alpha,\beta}\rho^{(1)}_{\beta,\alpha} + \frac{1}{2}\sum_{\alpha,\beta,\gamma,\delta}\Big(W_{\alpha,\beta,\gamma,\delta} - W_{\alpha,\beta,\delta,\gamma}\Big)\rho^{(1)}_{\gamma,\alpha}\rho^{(1)}_{\delta,\beta}}_{E_{\text{tot}}}$$
$$+ \quad \underbrace{k_B T\ \mathrm{Tr}\left[\boldsymbol{\rho}^{(1)}\ln(\boldsymbol{\rho}^{(1)}) + (\mathbf{1}-\boldsymbol{\rho}^{(1)})\ln(\mathbf{1}-\boldsymbol{\rho}^{(1)})\right]}_{-TS}\underbrace{-\mu\mathrm{Tr}[\boldsymbol{\rho}^{(1)}]}_{-\mu N} \tag{G.123}$$

1. The first term describes the kinetic energy and the potential energy contribution from the interaction with the atom cores. The non-interacting Hamiltonian $\boldsymbol{h}^{(0)}$ contains the orbital energies on the diagonal and the hopping matrix elements on the off-diagonal elements.
2. The second term describes the electron-electron interaction with the interaction tensor $\boldsymbol{W}$. It is divided into the Hartree energy (first) and the exchange energy (second).
3. The third term describes the heat bath, which exchanges heat with the electrons. For a single Slater determinant, this term would vanish, because the occupations are all either zero or one. We use the entropy expression of non-interacting electrons. This heat bath extends Hartree-Fock theory to finite temperatures.[8]
4. The fourth and last term is the particle reservoir.

The domain[9] of this free-energy functional are all hermitian matrices $\boldsymbol{\rho}$ in the one-particle Hilbert space with eigenvalues between zero and one.[31].

The derivative of the grand potential is

$$\frac{\partial\Omega_{T,\mu}[\boldsymbol{\rho}^{(1)}]}{\partial\rho^{(1)}_{u,v}} = \underbrace{h^{(0)}_{v,u} + \sum_{\alpha,\gamma}\Big(W_{\alpha,v,\gamma,u} - W_{\alpha,v,u,\gamma}\Big)\rho^{(1)}_{\gamma,\alpha}}_{h^{out}} + k_B T\left\{\ln\left[\boldsymbol{\rho}^{(1)}(\mathbf{1}-\boldsymbol{\rho}^{(1)})^{-1}\right]\right\}_{v,u} - \mu\delta_{u,v} \tag{G.124}$$

$$\frac{\partial\Omega_{T,\mu}[\boldsymbol{\rho}^{(1)}]}{\partial\mu} = \underbrace{-\mathrm{Tr}[\boldsymbol{\rho}^{(1)}]}_{-N}\,. \tag{G.125}$$

$$\frac{\partial\Omega_{T,\mu}[\boldsymbol{\rho}^{(1)}]}{\partial T} = \underbrace{k_B\mathrm{Tr}\left[\boldsymbol{\rho}^{(1)}\ln(\boldsymbol{\rho}^{(1)}) + (\mathbf{1}-\boldsymbol{\rho}^{(1)})\ln(\mathbf{1}-\boldsymbol{\rho}^{(1)})\right]}_{-S} \tag{G.126}$$

A new one-particle Hamiltonian $\boldsymbol{h}^{out}$ has been introduced, which we call output Hamiltonian and which is defined by the density matrix via

$$h^{out}_{\alpha,\beta} \overset{\text{def}}{=} h^{(0)}_{\alpha,\beta} + \sum_{\gamma,\delta}\Big(W_{\delta,\alpha,\gamma,\beta} - W_{\delta,\alpha,\beta,\gamma}\Big)\rho^{(1)}_{\gamma,\delta}\,. \tag{G.127}$$

Effective Hamiltonian

Next, we express the density matrix as functional of an effective Hamiltonian $\boldsymbol{h}^{eff}$

$$\boldsymbol{\rho}^{(1)}[\boldsymbol{h}^{eff},\mu] \overset{\text{def}}{=} \left[1 + \mathrm{e}^{\beta(\boldsymbol{h}^{eff}-\mu\mathbf{1})}\right]^{-1}$$
$$\Leftrightarrow \quad \rho^{(1)}_{\alpha,\beta}[\boldsymbol{h}^{eff},\mu] = \sum_n \psi_{\alpha,n}\frac{1}{1+\mathrm{e}^{\beta(\epsilon_n-\mu)}}\psi^*_{\beta,n} \tag{G.128}$$

[8] The extension to an ensemble of a Slater determinant is questionable, because the electron-electron interaction is no more consistent with a model of an ensemble of Slater determinants.

[9] The domain of a functional is the set of arguments for which the functional is defined.

where the ϵ_n are the eigenvalues of the effective Hamiltonian $\boldsymbol{h}^{eff}$ and $\vec{\psi}_n$ are its eigenvectors.

This representation simplifies the derivatives of the reservoirs $-TS-\mu N$ considerably, because we can use

$$\boldsymbol{h}^{eff} \overset{\text{Eq. } G.128}{=} \mu\mathbf{1} - k_B T \ln\Big[\boldsymbol{\rho}^{(1)}(\mathbf{1}-\boldsymbol{\rho}^{(1)})^{-1}\Big] \tag{G.129}$$

which leads to

$$\frac{d\Omega_{T,\mu}[\boldsymbol{\rho}^{(1)}]}{d\rho^{(1)}_{u,v}} \overset{\text{Eq. } G.124}{=} \underbrace{h^{(0)}_{v,u} + \sum_{\alpha,\gamma}\Big(W_{\alpha,v,\gamma,u} - W_{\alpha,v,u,\gamma}\Big)\rho^{(1)}_{\gamma,\alpha}}_{h^{out}} - h^{eff}_{v,u} = h^{out}_{v,u} - h^{eff}_{v,u} \tag{G.130}$$

The condition, that this derivative vanishes, determines the minimum of the grand potential. Thus, for the physical density matrix, the output Hamiltonian is identical to the effective Hamiltonian. This is the so-called self-consistency condition of the Hartree-Fock method.

Derivative of the density matrix with respect to the effective Hamiltonian

Let me work out the derivative of the one-particle-reduced density matrix with respect to the effective Hamiltonian. We need to consider that the variation $d\boldsymbol{h}$ of the Hamiltonian does not commutate with the Hamiltonian $\boldsymbol{h}$. Therefore, let me calculate the changes $d\epsilon_n$ of eigenvalues and those, $d\vec{\psi}_n$, of the eigenvectors by perturbation theory.

Let me consider a Hamiltonian $\hat{h}$, which has eigenvalues ϵ_n and eigenstates $|\psi_n\rangle$. The response of the density matrix with respect to a change of the Hamiltonian is obtained as follows.

$$\begin{aligned}
\delta\epsilon_n &= \langle\psi_n|\delta\hat{h}|\psi_n\rangle \\
\delta|\psi_n\rangle &= \sum_{m,m\neq n}|\psi_m\rangle\frac{\langle\psi_m|\delta\hat{h}|\psi_n\rangle}{\epsilon_n-\epsilon_m} \qquad (G.131)\\
\delta\hat{\rho}^{(1)} &= \sum_n |\delta\psi_n\rangle f_n\langle\psi_n| + \sum_n |\psi_n\rangle f_n\langle\delta\psi_n| + \sum_n |\psi_n\rangle\delta f_n\langle\psi_n| \\
&\overset{\text{Eq. } G.131}{=} \sum_{n,m;m\neq n}|\psi_m\rangle\frac{\langle\psi_m|\delta\hat{h}|\psi_n\rangle}{\epsilon_n-\epsilon_m}f_n\langle\psi_n| + \sum_{n,m;m\neq n}|\psi_n\rangle f_n\frac{\langle\psi_m|\delta\hat{h}|\psi_n\rangle^*}{\epsilon_n-\epsilon_m}\langle\psi_m| \\
&\quad + \sum_n|\psi_n\rangle\underbrace{\left(-\Big[\frac{1}{1+e^{\beta(\epsilon_n-\mu)}}\Big]^{-2}\beta(\delta\epsilon_n-\delta\mu)e^{\beta(\epsilon_n-\mu)}\right)}_{=\delta f_n=\delta\left[1+e^{\beta(\epsilon_n-\mu)}\right]^{-1}=-\beta f_n(1-f_n)(\delta\epsilon_n-\delta\mu)}\langle\psi_n| \\
&= \sum_{n,m;m\neq n}|\psi_m\rangle\frac{\langle\psi_m|\delta\hat{h}|\psi_n\rangle}{\epsilon_n-\epsilon_m}f_n\langle\psi_n| + \sum_{n,m;m\neq n}|\psi_n\rangle\frac{\langle\psi_n|\delta\hat{h}|\psi_m\rangle}{\epsilon_n-\epsilon_m}f_n\langle\psi_m| \\
&\quad -\beta\sum_n|\psi_n\rangle f_n(1-f_n)\Big(\langle\psi_n|\delta\hat{h}|\psi_n\rangle-\delta\mu\Big)\langle\psi_n| \\
&= \sum_{n,m;m\neq n}|\psi_n\rangle\langle\psi_n|\delta\hat{h}|\psi_m\rangle\frac{f_n-f_m}{\epsilon_n-\epsilon_m}\langle\psi_m| - \beta\sum_n|\psi_n\rangle\langle\psi_n|\delta\hat{h}|\psi_n\rangle f_n(1-f_n)\langle\psi_n| \\
&\quad +\delta\mu\,\beta\sum_n|\psi_n\rangle f_n(1-f_n)\langle\psi_n|
\end{aligned}$$

$$\frac{\partial\rho^{(1)}_{\alpha,\beta}[\boldsymbol{h}^{eff},\mu]}{\partial h^{eff}_{\gamma,\delta}} = \sum_{m,n}\psi_{\alpha,n}\psi^*_{\beta,m}\psi^*_{\gamma,n}\psi_{\delta,m}\begin{cases}(f_n-f_m)/(\epsilon_n-\epsilon_m) & \text{for } \epsilon_n\neq\epsilon_m\\ -\beta f_n(1-f_n) & \text{for } \epsilon_n=\epsilon_m\end{cases} \tag{G.132}$$

$$\frac{\partial\rho^{(1)}_{\alpha,\beta}[\boldsymbol{h}^{eff},\mu]}{\partial\mu} = \beta\sum_n\psi_{\alpha,n}f_n(1-f_n)\psi^*_{\beta,n} = \beta\Big(\boldsymbol{\rho}^{(1)}(\mathbf{1}-\boldsymbol{\rho}^{(1)}\Big)_{\alpha,\beta} \tag{G.133}$$

For equal orbital indices, the quantity used, $-\beta f_n(1-f_n)$, is the limit of $(f_n - f_m)/(\epsilon_n - \epsilon_m)$ for $\epsilon_m - \epsilon_n \to 0$. Therefore, we use the same expression for equal diagonal terms also for any pair of degenerate eigenvalues.

The derivative has a symmetry, which we will exploit lateron.

$$\frac{\partial \rho^{(1)}_{\alpha,\beta}[\boldsymbol{h}^{eff},\mu]}{\partial h^{eff}_{\gamma,\delta}} \overset{\text{Eq. } G.132}{=} \frac{\partial \rho^{(1)}_{\delta,\gamma}[\boldsymbol{h}^{eff},\mu]}{\partial h^{eff}_{\beta,\alpha}} \tag{G.134}$$

Thus, we may replace the upper and lower index pairs, if we also revert the order in each index pair.

Let me derive the inverse of $d\boldsymbol{\rho}^{(1)}[h_{eff},\mu]/d\boldsymbol{h}^{eff}$, because it will be used later. The inverse is defined via

$$\sum_{\gamma,\delta} K_{\alpha',\beta',\gamma,\delta} \frac{\partial \rho^{(1)}_{\beta,\alpha}[\boldsymbol{h}^{eff},\mu]}{\partial h^{eff}_{\gamma,\delta}} = \delta_{\alpha,\alpha'}\delta_{\beta,\beta'} \tag{G.135}$$

The expression for the inverse,

$$K_{\alpha,\beta,\gamma,\delta} = \sum_{m,n} \psi^*_{\alpha,n}\psi_{\beta,m}\psi_{\gamma,n}\psi^*_{\delta,m} \begin{cases} (\epsilon_n - \epsilon_m)/(f_n - f_m) & \text{for } \epsilon_n \neq \epsilon_m \\ -[\beta f_n(1-f_n)]^{-1} & \text{for } \epsilon_n = \epsilon_m \end{cases} \tag{G.136}$$

can be verified by insertion of Eq. G.132 into the defining equation for the inverse Eq. G.136.

Derivative of the grand potential

Finally, we obtain the derivative of the energy with respect to the effective Hamiltonian in the form

$$\begin{aligned}
\delta\Omega_{T,\mu}\left[\boldsymbol{\rho}^{(1)}[\boldsymbol{h}^{eff},\mu]\right] &= \sum_{u,v} \frac{\partial \Omega_{T,\mu}[\boldsymbol{\rho}^{(1)}]}{\partial \rho^{(1)}_{u,v}} \delta\rho_{u,v} + \frac{\partial \Omega_{T,\mu}[\boldsymbol{\rho}^{(1)}]}{\partial \mu}\delta\mu \\
&= \sum_{u,v} \frac{\partial \Omega_{T,\mu}[\boldsymbol{\rho}^{(1)}]}{\partial \rho^{(1)}_{u,v}} \left(\sum_{x,y} \frac{\partial \rho^{(1)}_{u,v}[\boldsymbol{h}^{eff},\mu]}{\partial h^{eff}_{x,y}} \delta h^{eff}_{x,y} + \frac{\partial \rho^{(1)}_{u,v}[\boldsymbol{h}^{eff},\mu]}{\partial \mu}\delta\mu \right) + \frac{\partial \Omega_{T,\mu}[\boldsymbol{\rho}^{(1)}]}{\partial \mu}\delta\mu \\
&= \sum_{u,v} \frac{\partial \Omega_{T,\mu}[\boldsymbol{\rho}^{(1)}]}{\partial \rho^{(1)}_{u,v}} \sum_{x,y} \frac{\partial \rho^{(1)}_{u,v}[\boldsymbol{h}^{eff},\mu]}{\partial h^{eff}_{x,y}} \delta h^{eff}_{x,y} \\
&+ \left(\sum_{u,v} \frac{\partial \Omega_{T,\mu}[\boldsymbol{\rho}^{(1)}]}{\partial \rho^{(1)}_{u,v}} \frac{\partial \rho_{u,v}[\boldsymbol{h}^{eff},\mu]}{\partial \mu} + \frac{\partial \Omega_{T,\mu}[\boldsymbol{\rho}^{(1)}]}{\partial \mu} \right) \delta\mu \\
&= \sum_{u,v} \left(h^{out}_{v,u} - h^{eff}_{v,u} \right) \sum_{x,y} \frac{\partial \rho^{(1)}_{u,v}[\boldsymbol{h}^{eff},\mu]}{\partial h^{eff}_{x,y}} dh^{eff}_{x,y} \\
&+ \left(\sum_{u,v} \left(h^{out}_{v,u} - h^{eff}_{v,u} \right) \beta \left(\boldsymbol{\rho}^{(1)}(\mathbf{1} - \boldsymbol{\rho}^{(1)}) \right)_{u,v} - \mathrm{Tr}[\boldsymbol{\rho}^{(1)}] \right) d\mu
\end{aligned} \tag{G.137}$$

- For a variation at fixed chemical potential, we set $d\mu = 0$, which leaves us with the partial derivative with respect to the effective Hamiltonian.
- For a variation of the grand potential at fixed particle number we set

$$d\mu = \frac{\partial \mu[h^{eff},N]}{\partial h^{eff}_{x,y}} dh^{eff}_{x,y} \tag{G.138}$$

At this point, I switch from the grand potential to the Helmholtz potential, the thermodynamic potential for an ensemble with fixed temperature and particle number.

$$A_{T,N}[\boldsymbol{h}^{eff}] = \Omega_{T,\mu(N)} + \mu(N)\cdot N \tag{G.139}$$

$$\begin{aligned}\frac{dA_{T,N}[\boldsymbol{h}^{eff}]}{dh^{eff}_{x,y}} &= \frac{\partial\Omega_{T,\mu}[h^{eff}]}{\partial h^{eff}_{x,y}} + \left(\frac{\partial\Omega_{T,\mu}[h^{eff}]}{\partial\mu} + N\right)\frac{d\mu[h^{eff},N]}{dh^{eff}_{x,y}} \\ &= \sum_{u,v}\left(h^{out}_{v,u} - h^{eff}_{v,u}\right)\sum_{x,y}\left.\frac{d\rho^{(1)}_{u,v}[\boldsymbol{h}^{eff},\mu]}{\partial h^{eff}_{x,y}}\right|_{\mu[\boldsymbol{h}^{eff},N]} \\ &+ \left(\mathrm{Tr}\Big[\Big(\boldsymbol{h}^{out} - \boldsymbol{h}^{eff}\Big)\beta\boldsymbol{\rho}^{(1)}(\mathbf{1}-\boldsymbol{\rho}^{(1)})\Big]\underbrace{-\mathrm{Tr}[\boldsymbol{\rho}^{(1)}] + N}_{=0}\right)\frac{d\mu[h^{eff},N]}{dh^{eff}_{x,y}} \end{aligned} \quad \text{(G.140)}$$

The variation of the chemical potential at constant particle number is obtained from the constraint equation

$$\begin{aligned}\mathrm{Tr}[\boldsymbol{\rho}^{(1)}[h^{eff},\mu] &= N \\ \Rightarrow \mathrm{Tr}\left[\frac{\partial\boldsymbol{\rho}}{\partial h^{eff}_{x,y}}dh^{eff}_{x,y} + \frac{\partial\boldsymbol{\rho}^{(1)}}{\partial\mu}d\mu\right] &= 0 \\ \Rightarrow d\mu = -\left(\mathrm{Tr}\left[\frac{\partial\boldsymbol{\rho}^{(1)}}{\partial\mu}\right]\right)^{-1}\sum_{x,y}\frac{\partial\mathrm{Tr}[\boldsymbol{\rho}^{(1)}]}{\partial h^{eff}_{x,y}}dh^{eff}_{x,y} &= \sum_{u,v}\frac{-\delta_{u,v}}{\mathrm{Tr}\left[\beta\boldsymbol{\rho}^{(1)}(\mathbf{1}-\boldsymbol{\rho}^{(1)})\right]}\frac{d\rho_{u,v}}{dh^{eff}_{x,y}}dh^{eff}_{x,y}\end{aligned} \quad \text{(G.141)}$$

This provides us with the derivative of the grand potential at constant particle number

$$\begin{aligned}\frac{dA_{T,N}[h^{eff}]}{dh^{eff}_{x,y}} &= \sum_{u,v}\left(h^{out}_{v,u} - h^{eff}_{v,u}\right)\sum_{x,y}\frac{d\rho^{(1)}_{u,v}[\boldsymbol{h}^{eff},\mu]}{\partial h^{eff}_{x,y}} \\ &+ \mathrm{Tr}\Big[\Big(\boldsymbol{h}^{out} - \boldsymbol{h}^{eff}\Big)\beta\boldsymbol{\rho}^{(1)}(\mathbf{1}-\boldsymbol{\rho}^{(1)})\Big]\underbrace{\sum_{u,v}\frac{-\delta_{u,v}}{\mathrm{Tr}\left[\beta\boldsymbol{\rho}^{(1)}(\mathbf{1}-\boldsymbol{\rho}^{(1)})\right]}\frac{d\rho^{(1)}_{u,v}}{dh^{eff}_{x,y}}}_{d\mu/dh^{eff}} \\ &= \sum_{\alpha,\beta}\left[\left(h^{out}_{\beta,\alpha} - h^{eff}_{\beta,\alpha}\right) - \underbrace{\frac{\mathrm{Tr}\Big[\big(\boldsymbol{h}^{out} - \boldsymbol{h}^{eff}\big)\beta\boldsymbol{\rho}^{(1)}(\mathbf{1}-\boldsymbol{\rho}^{(1)})\Big]}{\mathrm{Tr}\left[\beta\boldsymbol{\rho}^{(1)}(\mathbf{1}-\boldsymbol{\rho}^{(1)})\right]}\delta_{\beta,\alpha}}_{\text{constraint}}\right] \\ &\times \underbrace{\sum_{m,n}\psi_{\alpha,n}\psi^*_{x,n}\psi_{y,m}\psi^*_{\beta,m}\begin{cases}(f_n - f_m)/(\epsilon_n - \epsilon_m) & \text{for } \epsilon_n \neq \epsilon_m \\ -\beta f_n(1-f_n) & \text{for } \epsilon_n = \epsilon_m\end{cases}}_{d\rho_{\alpha,\beta}/\partial h^{eff}_{x,y}}\end{aligned} \quad \text{(G.142)}$$

The term denoted *"constraint"* ensures that the gradient $dA_{T,N}/d\boldsymbol{h}$ is trace-less. This is due to a fact that a shift of the effective Hamiltonian by a constant energy does not affect the density matrix, because the chemical potential shifts along, if the particle-number constraint is enforced. This term could as well be implemented by simply removing the trace of the final expression for $dA_{T,N}/d\boldsymbol{h}^{eff}$.

The contribution of $d\rho_{\alpha,\beta}/\partial h^{eff}_{x,y}$ related to the terms diagonal in the band indices m, n describe the response of the Helmholtz potential to the eigenvalues of $\boldsymbol{h}^{eff}$. This means that only these diagonal terms are present if $\boldsymbol{h}^{out}$ is diagonal in the eigenstates of $\boldsymbol{h}^{eff}$.

Self-consistent cycle

1. The derivative of the free energy with respect to the effective Hamiltonian can used to set up a gradient-following scheme, which improves the effective Hamiltonian iteratively.

$$\boldsymbol{h}_{n+1} = \boldsymbol{h}_n - \alpha_f \left.\frac{dA_{T,N}}{d\boldsymbol{h}^{eff}}\right|_{\boldsymbol{h}_n} \quad \text{(G.143)}$$

α_f is a suitably chosen mixing factor α.

2. The simple mixing is not efficient. A better choice is a two-parameter mixing

$$\boldsymbol{h}_{n+1} = \frac{2}{1+a_f}\boldsymbol{h}_n - \frac{1-a_f}{1+a_f}\boldsymbol{h}_{n-1} - \left.\frac{dA_{T,N}}{d\boldsymbol{h}^{eff}}\right|_{\boldsymbol{h}_n} \frac{\Delta^2}{1+a_f} \tag{G.144}$$

The values of the two parameters can be chosen in the range $0 < a_f < 1$ and $0 < \Delta$. We call a_f **friction parameter** and Δ the **time step**.

This scheme is inspired by the **Car-Parrinello method** .[178]. Here, we start from a Lagrangian

$$\mathcal{L}[\boldsymbol{h}, \boldsymbol{v}] = \frac{1}{2} Tr\left[\boldsymbol{v}\boldsymbol{v}^\dagger\right] - A_{T,N}[\boldsymbol{h}] \tag{G.145}$$

together with the action

$$\mathcal{S}[\boldsymbol{h}(t)] = \int dt\, \mathcal{L}[\boldsymbol{h}, \dot{\boldsymbol{h}}] \tag{G.146}$$

The stationary principle of the action yields the Euler-Lagrange equation to which I added a friction term.

$$\ddot{\boldsymbol{h}}(t) = -\left.\frac{dA_{T,N}}{d\boldsymbol{h}^{eff}}\right|_{\boldsymbol{h}(t)} \underbrace{-\alpha_f \dot{\boldsymbol{h}}(t)}_{\text{friction}} \tag{G.147}$$

The differential equation is discretized using the Verlet algorithm. In the **Verlet algorithm**[179], the time derivatives are replaced by the differential quotients

$$\begin{aligned}
\dot{\boldsymbol{h}}(t) &\to \frac{1}{2\Delta}\Big(\boldsymbol{h}(t+\Delta) - \boldsymbol{h}(t-\Delta)\Big) \\
\ddot{\boldsymbol{h}}(t) &\to \frac{1}{\Delta^2}\Big(\boldsymbol{h}(t+\Delta) - 2\boldsymbol{h}(t) + \boldsymbol{h}(t-\Delta)\Big)
\end{aligned} \tag{G.148}$$

This turns the differential equation into an equation for the effective Hamiltonian at discrete times $t_n = \Delta \cdot n$. For a given time t_n it connects three successive Hamiltonians, $\boldsymbol{h}(t_n + \Delta)$, $\boldsymbol{h}(t_n)$ and $\boldsymbol{h}(t_n - \Delta)$. Resolving for $\boldsymbol{h}(t_n + \Delta)$ and identifying $\boldsymbol{h}_n^{eff} = \boldsymbol{h}(t_n)$ yields the iterative procedure suggested above. The parameter a_f in Eq. G.144 is related to α_f by $a_f = \alpha_f \Delta/2$.

3. Only those parts of the effective Hamiltonian, which affect the density matrix, experiences forces. Eigenstates of the effective Hamiltonian, which are sufficiently far from the Fermi level, will not be updated.

One solution is to discard the term $d\boldsymbol{\rho}/d\boldsymbol{h}^{eff}$ and simply proceed to a mixing scheme of Hamiltonians.

$$\boldsymbol{h}^{eff,n+1} = \boldsymbol{h}^{eff,n} + \alpha\Big(\boldsymbol{h}^{out} - \boldsymbol{h}^{eff} - \mathbf{1}\frac{\mathrm{Tr}\left[\boldsymbol{h}^{out} - \boldsymbol{h}^{eff}\right]}{\mathrm{Tr}[\mathbf{1}]}\Big) \tag{G.149}$$

4. The price to be paid is that we arrive again at a fairly inefficient iteration scheme. Therefore, we return to the fictitious Lagrangian method of Car and Parrinello, but we change the kinetic energy. The new Lagrangian

$$\mathcal{L}[\boldsymbol{h}, \boldsymbol{v}] = -\frac{1}{2}\underbrace{\Big[\sum_{\alpha,\beta,\gamma,\delta} v_{\beta,\alpha} \left.\frac{d\rho^{(1)}_{\alpha,\beta}}{dh^{eff}_{\gamma,\delta}}\right|_{\boldsymbol{h}} v_{\gamma,\delta}\Big]}_{\mathrm{Tr}\left[\dot{\boldsymbol{h}}\dot{\boldsymbol{\rho}}^{(1)}\right]} - A_{T,N}[\boldsymbol{h}] \tag{G.150}$$

has the Euler-Lagrange equation

$$-\left.\frac{d\rho^{(1)}_{\beta,\alpha}}{dh^{eff}_{\gamma,\delta}}\right|_{\boldsymbol{h}} \ddot{h}_{\alpha,\beta} - \left.\frac{d^2\rho^{(1)}_{\beta,\alpha}}{dh^{eff}_{\gamma,\delta}\,dh^{eff}_{\zeta,\eta}}\right|_{\boldsymbol{h}} \dot{h}_{\zeta,\eta}\dot{h}_{\alpha,\beta} = -\left.\frac{\partial A_{T,N}}{\partial h^{eff}_{\gamma,\delta}}\right|_{\boldsymbol{h}} = -\left.\frac{\partial A_{T,N}}{\partial \rho^{(1)}_{\beta,\alpha}}\right|_{\boldsymbol{\rho}[\boldsymbol{h},\mu[N]]} \left.\frac{\partial \rho^{(1)}_{\beta,\alpha}}{\partial h^{eff}_{\gamma,\delta}}\right|_{\boldsymbol{h}}$$

$$\Rightarrow \ddot{h}_{\alpha,\beta} = +\left.\frac{\partial A_{T,N}}{\partial \rho^{(1)}_{\beta,\alpha}}\right|_{\boldsymbol{\rho}[\boldsymbol{h},\mu[N]]} + \sum_{\gamma,\delta,\alpha',\beta'} K_{\alpha,\beta;\gamma,\delta} \left.\frac{d^2\rho^{(1)}_{\beta',\alpha'}}{dh^{eff}_{\gamma,\delta}\,dh^{eff}_{\zeta,\eta}}\right|_{\boldsymbol{h}} \dot{h}_{\zeta,\eta}\dot{h}_{\alpha',\beta'} \qquad \text{(G.151)}$$

with $K_{\alpha',\beta';\gamma,\delta}$ defined by

$$\sum_{\gamma,\delta} K_{\alpha',\beta';\gamma,\delta} \left.\frac{d\rho^{(1)}_{\beta,\alpha}}{dh^{eff}_{\gamma,\delta}}\right|_{\boldsymbol{h}} = \delta_{\alpha,\alpha'}\delta_{\beta,\beta'} \qquad \text{(G.152)}$$

The explicit form of $K_{\alpha',\beta';\gamma,\delta}$ is given in Eq. G.136.

We managed to get rid of $d\boldsymbol{\rho}^{(1)}/d\boldsymbol{h}^{eff}$ in the main terms, but we are left with a complicated velocity-dependent term. The latter term applies an effective friction if an eigenstate of the effective Hamiltonian approaches the chemical potential, and thus starts to contribute to the kinetic energy. Because this would break the energy conservation, the velocity is reduced to compensate its effect.

The remedy is to remove the velocity dependent term from the equation of motion, but to monitor the resulting energy change. When we add in addition a friction term we obtain

$$\ddot{h}_{\alpha,\beta} = \left.\frac{\partial A_{T,N}}{\partial \rho_{\beta,\alpha}}\right|_{\boldsymbol{\rho}^{(1)}[\boldsymbol{h},\mu[N]]} - \mathcal{C}\dot{h}_{\alpha,\delta} \qquad \text{(G.153)}$$

This yields our equation of motion

$$\ddot{h}_{\alpha,\beta} = \left[\left(h^{out}_{\alpha,\beta} - h^{eff}_{\alpha,\beta}\right) - \underbrace{\frac{\mathrm{Tr}\left[\left(\boldsymbol{h}^{out} - \boldsymbol{h}^{eff}\right)\beta\boldsymbol{\rho}^{(1)}(\mathbf{1}-\boldsymbol{\rho}^{(1)})\right]}{\mathrm{Tr}\left[\beta\boldsymbol{\rho}^{(1)}(\mathbf{1}-\boldsymbol{\rho}^{(1)})\right]}\delta_{\alpha,\beta}}_{\text{constraint}}\right] - \mathcal{C}\dot{h}_{\alpha,\delta} \qquad \text{(G.154)}$$

The result appears trivial because it integrates the product of equation of motion and $\dot{\boldsymbol{\rho}}^{(1)}$.

Monitor energy conservation

$$\begin{aligned} E &= \sum_i \frac{\partial \mathcal{L}}{\partial v_i} v_i - \mathcal{L}(\vec{x},\vec{v},t) \\ \dot{E} &= \left(\frac{d}{dt}\frac{\partial \mathcal{L}}{\partial v_i}\right) v_i + \underbrace{\frac{\partial \mathcal{L}}{\partial v_i}\dot{v}_i - \frac{\partial \mathcal{L}}{\partial v_i}\dot{v}_i}_{=0} - \frac{\partial \mathcal{L}}{\partial x_i}\dot{x}_i - \frac{\partial \mathcal{L}}{\partial t} \\ &\overset{v_i \equiv \dot{x}_i}{=} \sum_i v_i\left(\frac{d}{dt}\frac{\partial \mathcal{L}}{\partial v_i} - \frac{\partial \mathcal{L}}{\partial x_i}\right) - \frac{\partial \mathcal{L}}{\partial t} \end{aligned} \qquad \text{(G.155)}$$

Es expected, we obtain the energy conservation law. The energy is conserved if (1) the Euler Lagrange equations are satisfied, and (2) the Lagrangian is not explicitly time dependent.

Let me now specialize the Lagrangian to be closed to our problem at hand

$$\mathcal{L}(\vec{x},\vec{v},t) = \frac{1}{2}\sum_{i,j} v_i M_{i,j}(\vec{x}) v_j - A(\vec{x}) \qquad \text{(G.156)}$$

$$\dot{E} = \sum_i \dot{x}_i \Bigg(\underbrace{\sum_{j,k} \frac{dM_{i,j}(\vec{x})}{dx_k} \dot{x}_k \dot{x}_j + \sum_j M_{i,j}(\vec{x}) \ddot{x}_j}_{d/dt\, \partial \mathcal{L}/\partial v_i} \underbrace{- \frac{1}{2} \sum_{j,k} \frac{dM_{j,k}}{dx_i} \dot{x}_j \dot{x}_k + \frac{A(\vec{x})}{\partial x_i}}_{-\partial \mathcal{L}/\partial x_i} \Bigg) \tag{G.157}$$

Instead of the Euler-Lagrange equations, which would lead to a conserved energy, I use another equation of motion, which is analogous to

$$\sum_j M_{i,j}(\vec{x}) \ddot{x}_j + \frac{A(\vec{x})}{\partial x_i} + C \sum_i M_{i,j}(\vec{x}) \dot{x}_j = 0 \tag{G.158}$$

With this equation of motion, I obtain

$$\begin{aligned}
\dot{E} &= \sum_i \dot{x}_i \left(\sum_{j,k} \frac{dM_{i,j}(\vec{x})}{dx_k} \dot{x}_k \dot{x}_j - \frac{1}{2} \sum_{j,k} \frac{dM_{j,k}}{dx_i} \dot{x}_j \dot{x}_k - C \sum_j M_{i,j}(\vec{x}) \dot{x}_j \right) \\
&= \frac{1}{2} \sum_{i,j,k} \frac{dM_{i,j}(\vec{x})}{dx_k} \dot{x}_k \dot{x}_i \dot{x}_j - C \sum_{i,j} \dot{x}_i M_{i,j}(\vec{x}) \dot{x}_j \\
&= \frac{1}{2} \sum_{i,j} \dot{x}_i \dot{M}_{i,j} \dot{x}_j - C \sum_i \dot{x}_i M_{i,j} \dot{x}_j \\
&= \frac{d}{dt} \left(\frac{1}{2} \sum_{i,j} \dot{x}_i M_{i,j} \dot{x}_j \right) - \sum_{i,j} \dot{x}_i M_{i,j} \ddot{x}_j - C \sum_i \dot{x}_i M_{i,j} \dot{x}_j
\end{aligned} \tag{G.159}$$

In order to obtain a conserved energy, we need to compensate for this energy change

$$\begin{aligned}
\mathcal{E}_{cons} = \mathcal{L}(\vec{x}, \vec{v}, t) &= \sum_{i,j} \frac{1}{2} v_i M_{i,j}(\vec{x}) v_j + A(\vec{x}) - \dot{E} \\
&= \sum_{i,j} \frac{1}{2} v_i M_{i,j}(\vec{x}) v_j + A(\vec{x}) - \int dt \left(\frac{d}{dt} \Big(\frac{1}{2} \sum_{i,j} \dot{x}_i M_{i,j} \dot{x}_j \Big) - \sum_{i,j} \dot{x}_i M_{i,j} \ddot{x}_j - C \sum_i \dot{x}_i M_{i,j} \dot{x}_j \right) \\
&= A(\vec{x}) + \int dt \left(\sum_{i,j} \dot{x}_i M_{i,j} \ddot{x}_j + C \sum_i \dot{x}_i M_{i,j} \dot{x}_j \right)
\end{aligned} \tag{G.160}$$

Translating this into our equation, using $\boldsymbol{M} = -d\boldsymbol{\rho}^{(1)}/d\boldsymbol{h}$, we obtain an energy

$$\begin{aligned}
\mathcal{E}(t) &= A_{T,N}[\boldsymbol{h}] - \int dt \left\{ \sum_{\alpha,\beta,\gamma,\delta} \ddot{h}_{\alpha,\beta} \frac{\partial \rho^{(1)}_{\beta,\alpha}}{\partial h^{eff}_{\gamma,\delta}} \dot{h}_{\gamma,\delta} - C \sum_{\alpha,\beta,\gamma,\delta} \dot{h}_{\alpha,\beta} \frac{\partial \rho^{(1)}_{\beta,\alpha}}{\partial h^{eff}_{\gamma,\delta}} \dot{h}_{\gamma,\delta} \right\} \\
&= A_{T,N}[\boldsymbol{h}] - \int dt \left\{ \sum_{\alpha,\beta} \ddot{h}_{\alpha,\beta} \dot{\rho}^{(1)}_{\beta,\alpha} - C \sum_{\alpha,\beta} \dot{h}_{\alpha,\beta} \dot{\rho}^{(1)}_{\beta,\alpha} \right\} \\
&= A_{T,N}[\boldsymbol{h}] - \int dt \; \mathrm{Tr} \left[\ddot{\boldsymbol{h}} \dot{\boldsymbol{\rho}}^{(1)} + C \dot{\boldsymbol{h}} \dot{\boldsymbol{\rho}}^{(1)} \right]
\end{aligned} \tag{G.161}$$

G.6.2 Calculating one step of the HF loop

We start the iteration with the non-interacting Hamiltonian $\boldsymbol{h}^{eff,n} = \boldsymbol{h}^{(0)}$ and $\boldsymbol{h}^{eff,n-1} = \boldsymbol{h}^{(0)}$. The superscript n of the effective Hamiltonian identifies a particular iteration in the sequence leading to the converged result.

1. The effective Hamiltonian $\boldsymbol{h}^{eff}$ is diagonalized

$$\sum_\gamma \hat{h}^{eff}_{\alpha,\beta} \psi_{\beta,n} = \psi_{\alpha,n} \epsilon_n \tag{G.162}$$

2. The occupations f_n are obtained as Fermi function.

$$f_n = \left(1 + e^{\beta(\epsilon_n - \mu)}\right)^{-1} \qquad \text{with} \qquad \sum_n f_n = N \; . \tag{G.163}$$

   An internal loop adjusts the chemical potential consistent with the selected particle number N.

3. The one-particle-reduced density matrix is obtained as

$$\rho^{(1)}_{\alpha,\beta} = \sum_n \psi_{\alpha,n} f_n \psi^*_{\beta,n} \tag{G.164}$$

4. The Helmholtz potential is evaluated as

$$\begin{aligned} A_{T,N}[\boldsymbol{\rho}] = & \underbrace{\sum_{\alpha,\beta} h^{(0)}_{\alpha,\beta}\rho^{(1)}_{\beta,\alpha} + \frac{1}{2}\sum_{\alpha,\beta,\gamma,\delta}\Big(W_{\alpha,\beta,\gamma,\delta} - W_{\alpha,\beta,\delta,\gamma}\Big)\rho^{(1)}_{\gamma,\alpha}\rho^{(1)}_{\delta,\beta}}_{E_{\text{tot}}} \\ & + \underbrace{k_B T \; \text{Tr}\left[\boldsymbol{\rho}^{(1)}\ln(\boldsymbol{\rho}^{(1)}) + (\mathbf{1} - \boldsymbol{\rho}^{(1)})\ln(\mathbf{1} - \boldsymbol{\rho}^{(1)})\right]}_{-TS} \end{aligned} \tag{G.165}$$

5. The output potential is determined as

$$h^{out}_{\nu,u} = h^{(0)}_{\nu,u} + \sum_{\alpha,\gamma}\Big(W_{\alpha,\nu,\gamma,u} - W_{\alpha,\nu,u,\gamma}\Big)\rho^{(1)}_{\gamma,\alpha} \tag{G.166}$$

6. The derivative of the Helmholtz potential is

$$\begin{aligned} \frac{dA_{T,N}}{dh_{x,y}} = & \sum_{\alpha,\beta}\left[\left(h^{out}_{\beta,\alpha} - h^{eff}_{\beta,\alpha}\right) - \frac{\text{Tr}\Big[\big(\boldsymbol{h}^{out} - \boldsymbol{h}^{eff}\big)\beta\boldsymbol{\rho}^{(1)}(\mathbf{1} - \boldsymbol{\rho}^{(1)})\Big]}{\text{Tr}\left[\beta\boldsymbol{\rho}^{(1)}(\mathbf{1} - \boldsymbol{\rho}^{(1)})\right]}\delta_{\beta,\alpha}\right] \\ & \times \sum_{m,n}\psi_{\alpha,n}\psi^*_{x,n}\psi_{y,m}\psi^*_{\beta,m}\begin{cases}(f_n - f_m)/(\epsilon_n - \epsilon_m) & \text{for } \epsilon_n \neq \epsilon_m \\ -\beta f_n(1 - f_n) & \text{for } \epsilon_n = \epsilon_m\end{cases} \end{aligned} \tag{G.167}$$

7. The effective Hamiltonian is updated using the force and the effective Hamiltonians of the two previous iterations

$$\boldsymbol{h}^{eff,n+1} = \frac{1}{1+a}\boldsymbol{h}^{eff,n} - \frac{1-a}{1+a}\boldsymbol{h}^{eff,n-1} - \left.\frac{dA_{T,N}}{d\boldsymbol{h}^{eff}}\right|_{\boldsymbol{h}^{eff,n}}\frac{\Delta^2}{1+a} \tag{G.168}$$

8. In order to only store at most three effective Hamiltonians, the arrays are mapped $\boldsymbol{h}^{eff,n} \to \boldsymbol{h}^{eff,n-1}$ and then $\boldsymbol{h}^{eff,n+1} \to \boldsymbol{h}^{eff,n}$.

The sequence is repeated until the free energy $A(T, N)$ remains constant.

G.6.3 Source code

The source code uses the LAPACK library for the matrix diagonalization.

On my MacBook, I compile and run the code below with

```
gfortran -framework accellerate -o code.x code.f90
code.x
```

The input parameters are specified in the parameter section of the main code.

The code `hfscf.f90` can be downloaded from the ΦSX Website `phisx.org`. For the sake of completeness it is included below.

```
!
!     ...1.........2.........3.........4.........5.........6.........7.........8
      program main
!     ************************************************************************
!     ** hartree fock code for the hydrogen dimer.                           **
!     ** uses diagonalization of the effective hamiltonian and follows the    **
!     ** energy gradient                                                     **
!     **                                                                     **
!     ** caution: demonstration code:  simple rather than efficient          **
!     ** caution: do not choose the temperature too low                      **
!     **                                                                     **
!     ** for demonstration purposes only. use at own risk                    **
!     ****************************************Peter Bloechl, Goslar 2018*******
      implicit none
      integer(4),parameter :: norb=4        ! #(spin orbitals)
      real(8)   ,parameter :: kbt=1.d-3     ! k_B*T: T=temperature
      real(8)   ,parameter :: thop=1.d0     ! hopping parameter
      real(8)   ,parameter :: u=3.d0        ! interaction parameter
      real(8)   ,parameter :: nel=2.1d0     ! #(electrons)
      real(8)   ,parameter :: dt=5.d-2      ! time step (5.d-1 is still ok)
      real(8)   ,parameter :: anne=1.d-4    ! friction parameter
      logical(4),parameter :: tstopandgo=.false. ! accelerates optimization
      real(8)   ,parameter :: tol=1.d-6          ! scf convergence criterion
      real(8)   ,parameter :: ampran=1.d-1     ! size for initial randomization
      integer(4),parameter :: niter=10000      ! x#(iterations)
      integer(4),parameter :: nfilo=6
      integer(4),parameter :: nfiltra=1001
      complex(8),parameter :: cone=(1.d0,0.d0)  ! complex 1
      complex(8)           :: hni(norb,norb)    ! non-interacting hamiltonian
      complex(8)           :: w(norb,norb,norb,norb) !interaction tensor
      complex(8)           :: heff(norb,norb)   ! effective hamiltonian
      complex(8)           :: hm(norb,norb)
      complex(8)           :: hp(norb,norb)
      complex(8)           :: rhom(norb,norb)
      complex(8)           :: rhop(norb,norb)
      real(8)              :: etot
      real(8)              :: ekin
      real(8)              :: energyreservoir
      real(8)              :: efric
      real(8)              :: firstetot
      real(8)              :: etotlast
      real(8)              :: eig(norb)
      complex(8)           :: dedrho(norb,norb)
      complex(8)           :: psi(norb,norb)
      integer(4)           :: i,j,iter
      logical(4)           :: convg
!     ************************************************************************
      open(nfiltra,form='formatted',file='tra.dat')
      rewind nfiltra
!
```

```
!     ========================================================================
!     == set up hamiltonian
!     == (left,up)(left,dn),(right,up),(right,dn)
!     ========================================================================
      hni=(0.d0,0.d0)
      hni(1,3)=-cone*thop
      hni(2,4)=-cone*thop
      do i=1,norb
        do j=i+1,norb
          hni(j,i)=conjg(hni(i,j))
        enddo
      enddo
!
      w=(0.d0,0.d0)
      do i=1,2
        do j=1,2
          w(i,j,i,j)=cone*u
          w(i+2,j+2,i+2,j+2)=cone*u
        enddo
      enddo
!
!     ========================================================================
!     == scf loop
!     ========================================================================
!
!     == initial conditions ==================================================
      call randomham(norb,ampran,heff)
      heff=heff+hni
      hm=heff

      etotlast=huge(etotlast)
      energyreservoir=0.d0
      do iter=1,niter
!       == total energy and forces
        call hfetot(norb,kbt,nel,hni,w,heff,etot,dedrho)
!
!       == repeat previous step with zero velocity if energy goes up ===========
        if(tstopandgo.and.etot.gt.etotlast) then
          heff=hm
          efric=efric+energyreservoir
          energyreservoir=0.d0
          cycle
        end if
        etotlast=etot
!
!       == propagate ===========================================================
        hp=(heff*2.d0-hm*(1.d0-anne)+dedrho*dt**2)/(1.d0+anne)
!
!       == report ==============================================================
        call rhoofh(norb,kbt,nel,hm,rhom)
        call rhoofh(norb,kbt,nel,hp,rhop)

        ekin=-0.5d0*real(sum((hp-hm)*conjg(rhop-rhom)))/(2.d0*dt)**2
        energyreservoir=energyreservoir &
```

```
       &        -real(sum((hp-2.d0*heff+hm)*conjg(rhop-rhom)))/(2.d0*dt**2)
        efric=efric+4.d0*anne*ekin   ! dissipated energy
        write(*,fmt='(i10," ekin,etot,econs=",10f20.5)') &
      &                                iter,ekin,etot,etot+energyreservoir
        if(iter.eq.1)firstetot=etot
        write(nfiltra,fmt='(i10,10f20.5)')iter,ekin,etot-firstetot &
       &                                  ,ekin+etot-firstetot &
       &                                  ,etot-firstetot+energyreservoir
!
!       == check convergence and terminate loop ==============================
        convg=maxval(abs(dedrho)).lt.tol
        if(convg) exit
!
!       == switch ============================================================
        hm=heff
        heff=hp
      enddo
      if(convg) then
        write(*,fmt='("scf convergence ok")')
      else
        write(*,fmt='("scf loop not converged")')
      end if
!
!     ========================================================================
!     == write eigenvalues and eigenstates ===================================
!     ========================================================================
      write(*,*)
      call mydiag(norb,heff,eig,psi)
      do i=1,norb
        write(*,fmt='("ib=",i3," e=",f10.5," psi=",10(2f7.3,";  "))') &
     &               i,eig(i),psi(:,i)
      enddo
      stop
      end
!
!     ...1.........2.........3.........4.........5.........6.........7.........8
      subroutine randomham(norb,ampran,ranh)
!     **************************************************************************
!     ** produces a random hermitean matrix                                   **
!     ** the matrix elements are equally distributed in [-ampran,ampran]      **
!     ****************************************Peter Bloechl, Goslar 2018*******
      implicit none
      integer(4),intent(in) :: norb
      real(8)   ,intent(in) :: ampran            !
      complex(8),intent(out):: ranh(norb,norb)   !random matrix
      integer(4)            :: i,j
      real(8)               :: ran1,ran2
!     **************************************************************************
      do i=1,norb
        do j=1,norb
          call random_number(ran1)
          call random_number(ran2)
          ran1=(2.d0*ran1-1.d0)*ampran
          ran2=(2.d0*ran2-1.d0)*ampran
```

```
          ranh(i,j)=cmplx(ran1,ran2,kind=8)
          ranh(j,i)=cmplx(ran1,-ran2,kind=8)
        enddo
         ranh(i,i)=real(ranh(i,i),kind=8)
      enddo
      return
      end
!
!     ...1.........2.........3.........4.........5.........6.........7.........8
      subroutine hfetot(norb,kbt,nel,hni,w,heff,etot,dedrho)
!     ******************************************************************
!     ****************************************Peter Bloechl, Goslar 2018*******
      implicit none
      integer(4),intent(in) :: norb
      real(8)   ,intent(in) :: kbt
      real(8)   ,intent(in) :: nel
      complex(8),intent(in) :: hni(norb,norb)
      complex(8),intent(in) :: w(norb,norb,norb,norb)
      complex(8),intent(in) :: heff(norb,norb)
      real(8)   ,intent(out):: etot
      complex(8),intent(out):: dedrho(norb,norb)
      logical(4),parameter  :: tpr=.false.
      logical(4),parameter  :: ttest=.true.
      logical(4),parameter  :: tgrandpot=.false.
      complex(8),parameter  :: cnull=(0.d0,0.d0)
      complex(8),parameter  :: cone=(1.d0,0.d0)
      real(8)               :: eig(norb)
      complex(8)            :: psi(norb,norb)
      real(8)               :: occ(norb)
      complex(8)            :: rho(norb,norb)
      complex(8)            :: mat(norb,norb)
      real(8)               :: mu
      real(8)               :: nofmu
      real(8)               :: etot1
      real(8)               :: svar
      integer(4)            :: i,j,k
      real(8)               :: trdrhodmu,trdedrhodrhodmu
!     ******************************************************************
!
!     ================================================================
!     ==  diagonalize heff using lapack routine
!     ================================================================
      call mydiag(norb,heff,eig,psi)
!
!     ================================================================
!     ==  determine chemical potential and occupations
!     ================================================================
      call muofn(kbt,nel,norb,eig,mu,occ)
      nofmu=sum(occ)
!
!     ================================================================
!     ==  determine density matrix
!     ================================================================
      rho=cnull
```

```
      do i=1,norb
        do j=1,norb
          do k=1,norb
            rho(i,j)=rho(i,j)+psi(i,k)*occ(k)*conjg(psi(j,k))
          enddo
        enddo
      enddo
!
!     ================================================================
!     ==  grand potential and derivative
!     ================================================================
      call eofrho(norb,hni,w,rho,etot,dedrho)
      dedrho=dedrho-heff
!
!     == electron entropy ============================================
      etot1=0.d0
      do k=1,norb
        if(occ(k).ne.0.d0.and.occ(k).ne.1.d0) then
          etot1=etot1+kbt*(occ(k)*log(occ(k))+(1.d0-occ(k))*log(1.d0-occ(k)))
        end if
      enddo
      etot=etot+etot1
!
!     ================================================================
!     ==  constraint
!     ================================================================
      mat=cnull
      do i=1,norb
        mat(i,i)=cone
      enddo
      mat=matmul(rho,mat-rho)/kbt   !drhodmu
!
      trdrhodmu=0.d0
      trdedrhodrhodmu=0.d0
      do i=1,norb
        trdrhodmu=trdrhodmu+real(mat(i,i),kind=8)
        do j=1,norb
          trdedrhodrhodmu=trdedrhodrhodmu+real(dedrho(i,j)*mat(j,i),kind=8)
        enddo
      enddo
!
!     == dedrho=dedrho-(domega/dmu*dmu+mu*N)/drho ====================
      svar=-trdedrhodrhodmu/trdrhodmu
      do i=1,norb
        dedrho(i,i)=dedrho(i,i)+svar
      enddo
      return
      end
!
!     ...1.........2.........3.........4.........5.........6.........7.........8
      subroutine eofrho(norb,hni,w,rho,etot,detot)
!     ******************************************************************
!     **************************************Peter Bloechl, Goslar 2018*******
      implicit none
```

```
      integer(4),intent(in) :: norb
      complex(8),intent(in) :: hni(norb,norb)
      complex(8),intent(in) :: w(norb,norb,norb,norb)
      complex(8),intent(in) :: rho(norb,norb)
      real(8)   ,intent(out):: etot
      complex(8),intent(out):: detot(norb,norb)
      complex(8),parameter  :: cnull=(0.d0,0.d0)
      integer(4)            :: i,j,k,l
!     ****************************************Peter Bloechl, Goslar 2018*******
!
!     ==========================================================================
!     ==  total energy and output hamiltonian
!     ==========================================================================
      etot=0.d0
      detot(:,:)=cnull
!
      do i=1,norb
        do j=1,norb
          etot=etot+real(hni(i,j)*rho(j,i),kind=8)
          detot(i,j)=detot(i,j)+hni(i,j)
        enddo
      enddo
!
      do i=1,norb
        do j=1,norb
          do k=1,norb
            do l=1,norb
              etot=etot &
     &            +0.5d0*real((w(l,i,k,j)-w(l,i,j,k))*rho(k,l)*rho(j,i),kind=8)
              detot(i,j)=detot(i,j)+0.5d0*(w(l,i,k,j)-w(l,i,j,k))*rho(k,l)
              detot(l,k)=detot(l,k)+0.5d0*(w(l,i,k,j)-w(l,i,j,k))*rho(j,i)
            enddo
          enddo
        enddo
      enddo
!
      return
      end
!
!     ...1.........2.........3.........4.........5.........6.........7.........8
      subroutine rhoofh(norb,kbt,nel,heff,rho)
!     **************************************************************************
!     ****************************************Peter Bloechl, Goslar 2018*******
      implicit none
      integer(4),intent(in) :: norb
      real(8)   ,intent(in) :: kbt
      real(8)   ,intent(in) :: nel
      complex(8),intent(in) :: heff(norb,norb)
      complex(8),intent(out):: rho(norb,norb)
      complex(8),parameter  :: cnull=(0.d0,0.d0)
      real(8)               :: eig(norb)
      complex(8)            :: psi(norb,norb)
      real(8)               :: mu
      real(8)               :: occ(norb)
```

```
      integer(4)            :: i,j,k
!     ************************************************************************
!
!     ========================================================================
!     ==  diagonalize heff using lapack routine
!     ========================================================================
      call mydiag(norb,heff,eig,psi)
!
!     ========================================================================
!     ==  determine chemical potential and occupations
!     ========================================================================
      call muofn(kbt,nel,norb,eig,mu,occ)
!
!     ========================================================================
!     ==  determine density matrix
!     ========================================================================
      rho=cnull
      do i=1,norb
        do j=1,norb
          do k=1,norb
            rho(i,j)=rho(i,j)+psi(i,k)*occ(k)*conjg(psi(j,k))
          enddo
        enddo
      enddo
     return
     end
!
!     ...1.........2.........3.........4.........5.........6.........7.........8
      subroutine muofn(kbt,nel,norb,eig,mu,occ)
!     ************************************************************************
!     ****************************************Peter Bloechl, Goslar 2018*******
      implicit none
      real(8)   ,intent(in) :: kbt
      real(8)   ,intent(in) :: nel
      integer(4),intent(in) :: norb
      real(8)   ,intent(in) :: eig(norb)
      real(8)   ,intent(out):: mu
      real(8)   ,intent(out):: occ(norb)
      logical(4),parameter  :: ttest=.true.
      logical(4),parameter  :: tpr=.false.
      real(8)   ,parameter  :: neltol=1.d-12
      real(8)   ,parameter  :: mutol=1.d-12
      real(8)               :: mulo,muhi
      real(8)               :: nlo,nhi,nofmu
      integer(4)            :: i
!     ************************************************************************
      mulo=eig(1)   -30.d0*kbt
      muhi=eig(norb)+30.d0*kbt
      call occofmu(kbt,mulo,norb,eig,occ)
      nlo=sum(occ)
      call occofmu(kbt,muhi,norb,eig,occ)
      nhi=sum(occ)
      if((nlo-nel)*(nhi-nel).gt.0) then
        print*,'nlo,nhi=',nlo,nhi,' mulo,muhi=',mulo,muhi
```

```
        stop 'bisection error'
      end if
      do i=1,10000
        mu=0.5d0*(mulo+muhi)
        call occofmu(kbt,mu,norb,eig,occ)
        nofmu=sum(occ)
        if(abs(nofmu-nel).lt.neltol.and.(abs(muhi-mulo).lt.mutol)) then
          if(tpr) print*,'converged: iter=',i,' nofmu-n=',nofmu-nel &
     &                 ,'mulo muhi=',mulo,muhi
          exit
        end if
        if(nofmu.gt.nel) then
          muhi=mu
        else
          mulo=mu
        end if
      enddo

      if(ttest) then
        if(abs(nel-nofmu).gt.neltol) then
          print*,'abs(nel-nofmu) ',abs(nel-nofmu)
          stop 'test2 failed'
        end if
        if(abs(muhi-mulo).gt.mutol) then
          print*,'muhi-mulo ',muhi-mulo
          stop 'test3 failed'
        end if
      end if
      return
      end
!
!     ...1.........2.........3.........4.........5.........6.........7.........8
      subroutine occofmu(kbt,mu,norb,eig,occ)
!     ************************************************************************
!     ****************************************Peter Bloechl, Goslar 2018*******
      implicit none
      real(8)   ,intent(in) :: kbt
      real(8)   ,intent(in) :: mu
      integer(4),intent(in) :: norb
      real(8)   ,intent(in) :: eig(norb)
      real(8)   ,intent(out):: occ(norb)
      real(8)   ,parameter  :: xexparg=700.d0
      integer(4)            :: i
      real(8)               :: svar
!     ************************************************************************
      do i=1,norb
        svar=(eig(i)-mu)/kbt
        if(abs(svar).lt.xexparg) then
          occ(i)=1.d0/(1.d0+exp(svar))
        else
          occ(i)=0.d0
          if(svar.lt.0) occ(i)=1.d0
        end if
      enddo
```

```
      return
      end
!
!     ...1.........2.........3.........4.........5.........6.........7.........8
      subroutine mydiag(n,h,e,u)
!     ************************************************************************
!     ****************************************Peter Bloechl, Goslar 2018*******
      implicit none
      integer(4),intent(in) :: n
      complex(8),intent(in) :: h(n,n)
      real(8)   ,intent(out):: e(n)
      complex(8),intent(out):: u(n,n)
      logical(4),parameter  :: ttest=.true.
      real(8)               :: rwork(3*n)
      integer(4),parameter  :: lwork=100
      complex(8)            :: cwork(lwork)
      complex(8)            :: hout(n,n)
      integer(4)            :: info
      integer(4)            :: i,j
!     ************************************************************************
      u=h
      call zheev('v','u',n,u,n,e,cwork,lwork,rwork,info)
      if(info.lt.0) then
        write(*,fmt='("the ",i3,"-th argument had an illegal value")')-info
        stop 'error stop in mydiag'
      else if(info.gt.0) then
        write(*,fmt='("the algorithm failed to converge")')
        write(*,fmt='(i3," off-diagonal elements of an intermediate")')info
        write(*,fmt='("tridiagonal form did not converge to zero")')
        stop 'error stop in mydiag'
      end if

      if(ttest) then
        hout=-h
        do i=1,n
          do j=1,n
            hout(i,j)=hout(i,j)+sum(u(i,:)*e(:)*conjg(u(j,:)))
          enddo
        enddo
        if(maxval(abs(hout)).gt.1.d-6) then
          print*,'deviation ',maxval(abs(hout))
          stop 'test1 failed'
        end if
      end if

      return
      end
```

G.6.4 Generalization to periodic systems

Editor: This section is under construction!

The discussion of the previous sections did not consider the translation symmetry of a crystal. The generalization to a system with translation symmetry is, however, quite straightforward.

The key element is to replace indices as followsEditor: Is the $\vec{t}$ correct? Time is not a vector...

$$\begin{aligned} \alpha &\to \alpha, \vec{t} \\ n &\to n, \vec{k} \end{aligned} \tag{G.169}$$

We consider a supercell with $\mathcal{N}$ primitive unit cells. In this supercell, we consider the wave functions to be strictly periodic. This requirement determines a discrete grid of $\mathcal{N}$ k-points in the reciprocal unit cell.

The goal is to generalize the Helmholtz potential of Eq. G.123 to periodic systems. Because the energy of an infinite system is infinite, we determine the Helmholtz potential per unit cell.

We start with the energy from Eq. G.123. We skip the entropy contribution later for the time being and return to it later.

$$\begin{aligned} E = \frac{1}{\mathcal{N}} \Bigg\{ & \sum_{\alpha,\vec{t},\beta,\vec{t}'} h_{(\alpha,\vec{t}),(\beta,\vec{t}')} \rho_{(\beta,\vec{t}'),(\alpha,\vec{t})} + \frac{1}{2} \sum_{\alpha,\vec{t},\beta,\vec{t}',\gamma,\vec{t}'',\delta,\vec{t}'''} W_{(\alpha,\vec{t}),(\beta,\vec{t}'),(\gamma,\vec{t}''),(\delta,\vec{t}''')} \\ & \times \left(\rho_{(\gamma,\vec{t}''),(\alpha,\vec{t})} \rho_{(\delta,\vec{t}'''),(\beta,\vec{t}')} - \rho_{(\delta,\vec{t}'''),(\alpha,\vec{t})} \rho_{(\gamma,\vec{t}''),(\beta,\vec{t}')} \right) \Bigg\} \end{aligned} \tag{G.170}$$

Now we use Bloch theorem to block-diagonalize the density matrix. The natural orbitals, i.e. the eigenstates of the density matrix, are expressed as Bloch states.

$$\psi_{(\alpha,\vec{t}),(n,\vec{k})} = \psi_{(\alpha,\vec{0}),(n,\vec{k})} e^{i\vec{k}\vec{t}} \tag{G.171}$$

We normalize the wave function such that their contribution in one unit cell equals one.

$$\sum_{\alpha} \psi_{(\alpha,\vec{0}),(n,\vec{k})} \psi_{(\alpha,\vec{0}),(m,\vec{k})} = \delta_{n,m} \tag{G.172}$$

This differs from the discussion without lattice translation, where the norm is evaluated as a sum over the entire system.

Thus, the density matrix has the form

$$\begin{aligned} \rho_{(\alpha,\vec{t}),(\beta,\vec{t}')} &= \frac{1}{\mathcal{N}} \sum_{n,\vec{k}} \psi_{(\alpha,\vec{t}),(n,\vec{k})} f_{(n,\vec{k})} \psi^*_{(\beta,\vec{t}'),(n,\vec{k})} \\ &= \frac{1}{\mathcal{N}} \sum_{n,\vec{k}} \psi_{(\alpha,\vec{0}),(n,\vec{k})} f_{(n,\vec{k})} \psi^*_{(\beta,\vec{0}),(n,\vec{k})} e^{i\vec{k}(t-t')} \\ &= \frac{1}{\mathcal{N}} \sum_{\vec{k}} \rho_{\alpha,\beta}(\vec{k}) e^{i\vec{k}(t-t')} \end{aligned} \tag{G.173}$$

with the k-dependent density matrix

$$\rho_{\alpha,\beta}(\vec{k}) \stackrel{\text{def}}{=} \sum_{n} \psi_{(\alpha,\vec{0}),(n,\vec{k})} f_{(n,\vec{k})} \psi^*_{(\beta,\vec{0}),(n,\vec{k})} \tag{G.174}$$

The potential acting on the electrons due to the interaction can be calculated as

$$\begin{aligned} v_{(\alpha,\vec{t}),(\beta,\vec{t}')} &\stackrel{\text{def}}{=} \frac{1}{\mathcal{N}} \frac{\partial E_{int}}{\partial \rho_{(\beta,\vec{t}'),(\alpha,\vec{t})}} \\ &= \frac{1}{\mathcal{N}} \sum_{(\gamma,\vec{t}''),(\delta,\vec{t}''')} \left(W_{(\alpha,\vec{t}),(\delta,\vec{t}'''),(\beta,\vec{t}'),(\gamma,\vec{t}'')} - W_{(\alpha,\vec{t}),(\delta,\vec{t}'''),(\gamma,\vec{t}''),(\beta,\vec{t}')} \right) \rho_{(\gamma,\vec{t}''),(\delta,\vec{t}''')} \\ &= \frac{1}{\mathcal{N}} \sum_{\vec{k}} \sum_{\gamma,\delta} \left\{ \frac{1}{\mathcal{N}} \sum_{\vec{t}'',\vec{t}'''} \left(W_{(\alpha,\vec{t}),(\delta,\vec{t}'''),(\beta,\vec{t}'),(\gamma,\vec{t}'')} - W_{(\alpha,\vec{t}),(\delta,\vec{t}'''),(\gamma,\vec{t}''),(\beta,\vec{t}')} \right) e^{i\vec{k}(\vec{t}''-\vec{t}''')} \right\} \rho_{\gamma,\delta}(\vec{k}) \end{aligned} \tag{G.175}$$

Now we insert the density matrix, expressed in terms of the k-dependent density matrix into the energy expression. Before doing so, however, we eliminate one sum over unit cells by exploiting the periodicity of the material.

$$\begin{aligned} h_{(\alpha,\vec{t}),(\beta,\vec{t}')} &= h_{(\alpha,\vec{0}),(\beta,\vec{t}'-\vec{t})} \\ W_{(\alpha,\vec{t}),(\beta,\vec{t}'),(\gamma,\vec{t}''),(\delta,\vec{t}''')} &= W_{(\alpha,\vec{0}),(\beta,\vec{t}'-\vec{t}),(\gamma,\vec{t}''-\vec{t}),(\delta,\vec{t}'''-\vec{t})} \end{aligned} \tag{G.176}$$

$$\begin{aligned} E = \frac{1}{\mathcal{N}}\Bigg\{ & \sum_{\alpha,\beta}\sum_{\vec{t},\vec{t}'} h_{(\alpha,\vec{t}),(\beta,\vec{t}')} \underbrace{\frac{1}{\mathcal{N}}\sum_{\vec{k}} \rho_{\beta,\alpha}(\vec{k}) \mathrm{e}^{i\vec{k}(\vec{t}'-\vec{t})}}_{\rho_{(\beta,\vec{t}'),(\alpha,\vec{t})}} \\ & + \frac{1}{2}\sum_{\alpha,\beta,\gamma,\delta}\sum_{\vec{t},\vec{t}',\vec{t}'',\vec{t}'''} W_{(\alpha,\vec{t}),(\beta,\vec{t}'),(\gamma,\vec{t}''),(\delta,\vec{t}''')} \\ & \quad \times \Bigg(\underbrace{\frac{1}{\mathcal{N}}\sum_{\vec{k}} \rho_{\gamma,\alpha}(\vec{k}) \mathrm{e}^{i\vec{k}(\vec{t}''-\vec{t})}}_{\rho_{(\gamma,\vec{t}''),(\alpha,\vec{t})}} \underbrace{\frac{1}{\mathcal{N}}\sum_{\vec{k}'} \rho_{\delta,\beta}(\vec{k}') \mathrm{e}^{i\vec{k}'(\vec{t}'''-\vec{t}')}}_{\rho_{(\delta,\vec{t}'''),(\beta,\vec{t}')}} - \underbrace{\frac{1}{\mathcal{N}}\sum_{\vec{k}} \rho_{\delta,\alpha}(\vec{k}) \mathrm{e}^{i\vec{k}(\vec{t}'''-\vec{t})}}_{\rho_{(\delta,\vec{t}'''),(\alpha,\vec{t})}} \underbrace{\frac{1}{\mathcal{N}}\sum_{\vec{k}'} \rho_{\gamma,\beta}(\vec{k}') \mathrm{e}^{i\vec{k}'(\vec{t}''-\vec{t}')}}_{\rho_{(\gamma,\vec{t}''),(\beta,\vec{t}')}} \Bigg\} \\ & = \frac{1}{\mathcal{N}}\sum_{\vec{k}}\sum_{\alpha,\beta} \underbrace{\left(\frac{1}{\mathcal{N}}\sum_{\vec{t}\vec{t}'} h_{(\alpha,\vec{t}),(\beta,\vec{t}')} \mathrm{e}^{i\vec{k}(\vec{t}'-\vec{t})}\right)}_{h_{\alpha,\beta}(\vec{k})} \rho_{\beta,\alpha}(\vec{k}) \\ & + \frac{1}{2}\frac{1}{\mathcal{N}^2}\sum_{\vec{k},\vec{k}'}\sum_{\alpha,\beta,\gamma,\delta} \Bigg\{ \underbrace{\left(\frac{1}{\mathcal{N}}\sum_{\vec{t},\vec{t}',\vec{t}'',\vec{t}'''} W_{(\alpha,\vec{t}),(\beta,\vec{t}'),(\gamma,\vec{t}''),(\delta,\vec{t}''')} \mathrm{e}^{i\vec{k}(\vec{t}''-\vec{t})} \mathrm{e}^{i\vec{k}'(\vec{t}'''-\vec{t}')}\right)}_{W_{\alpha,\beta,\gamma,\delta}(\vec{k},\vec{k}';\vec{k},\vec{k}')} \rho_{\gamma,\alpha}(\vec{k})\rho_{\delta,\beta}(\vec{k}') \\ & \qquad - \underbrace{\left(\frac{1}{\mathcal{N}}\sum_{\vec{t},\vec{t}',\vec{t}'',\vec{t}'''} W_{(\alpha,\vec{t}),(\beta,\vec{t}'),(\gamma,\vec{t}''),(\delta,\vec{t}''')} \mathrm{e}^{i\vec{k}(\vec{t}'''-\vec{t})} \mathrm{e}^{i\vec{k}'(\vec{t}''-\vec{t}')}\right)}_{W_{\alpha,\beta,\gamma,\delta}(\vec{k},\vec{k}';\vec{k}',\vec{k})} \rho_{\delta,\alpha}(\vec{k})\rho_{\gamma,\beta}(\vec{k}') \Bigg\} \\ & = \frac{1}{\mathcal{N}}\sum_{\vec{k}}\sum_{\alpha,\beta} h_{\alpha,\beta}(\vec{k})\rho_{\beta,\alpha}(\vec{k}) \\ & + \frac{1}{2}\frac{1}{\mathcal{N}^2}\sum_{\vec{k},\vec{k}'}\sum_{\alpha,\beta,\gamma,\delta} \Big(W_{\alpha,\beta,\gamma,\delta}(\vec{k},\vec{k}',\vec{k},\vec{k}') - W_{\alpha,\beta,\delta,\gamma}(\vec{k},\vec{k}',\vec{k}',\vec{k}) \Big) \rho_{\gamma,\alpha}(\vec{k})\rho_{\delta,\beta}(\vec{k}') \end{aligned} \tag{G.177}$$

with

$$\begin{aligned} h_{\alpha,\beta}(\vec{k}) &\stackrel{\text{def}}{=} \sum_{\vec{t}'} h_{(\alpha,\vec{0}),(\beta,\vec{t})} \mathrm{e}^{i\vec{k}\vec{t}} \\ W_{\alpha,\beta,\gamma,\delta}(\vec{k},\vec{k}';\vec{k}'',\vec{k}''') &= \frac{1}{\mathcal{N}}\sum_{\vec{t},\vec{t}',\vec{t}'',\vec{t}'''} W_{(\alpha,\vec{t}),(\beta,\vec{t}'),(\gamma,\vec{t}''),(\delta,\vec{t}''')} \mathrm{e}^{-i\vec{k}\vec{t}} \mathrm{e}^{-i\vec{k}\vec{t}'} \mathrm{e}^{i\vec{k}'\vec{t}''} \mathrm{e}^{i\vec{k}''\vec{t}'''} \\ &= \sum_{\vec{t}',\vec{t}'',\vec{t}'''} W_{(\alpha,\vec{0}),(\beta,\vec{t}'),(\gamma,\vec{t}''),(\delta,\vec{t}''')} \mathrm{e}^{-i\vec{k}\vec{t}'} \mathrm{e}^{i\vec{k}'\vec{t}''} \mathrm{e}^{i\vec{k}''\vec{t}'''} \end{aligned} \tag{G.178}$$

Because of translation symmetry, many interaction matrix elements vanish

$$W_{\alpha,\beta,\gamma,\delta}(\vec{k},\vec{k}';\vec{k}'',\vec{k}''') = 0 \qquad \text{for } \vec{k}+\vec{k}' \neq \vec{k}''+\vec{k}''' \tag{G.179}$$

which is equivalent to momentum conservation during scattering.

Entropy contribution

We need to determine the entropy for the electrons in Eq. G.123. As for the energy, the entropy is calculated per unit cell.

$$S[\boldsymbol{\rho}] = \frac{1}{\mathcal{N}} \left\{ -k_B \, \mathrm{Tr} \left[\boldsymbol{\rho} \ln(\boldsymbol{\rho}) + (\mathbf{1} - \boldsymbol{\rho}) \ln(\mathbf{1} - \boldsymbol{\rho}) \right] \right\} \tag{G.180}$$

The density matrix of the entire system is already decomposed in eigenstates and eigenvalues of the density matrix.

$$\rho_{(\alpha,\vec{t}),(\beta,\vec{t}')} = \sum_{n,\vec{k}} \frac{1}{\sqrt{\mathcal{N}}} \psi_{(\alpha,\vec{t}),(n,\vec{k})} f_{(n,\vec{k})} \frac{1}{\sqrt{\mathcal{N}}} \psi^*_{(\beta,\vec{t}'),(n,\vec{k})} \tag{G.181}$$

The entropy can be written as

$$\begin{aligned} S[\boldsymbol{\rho}] &= -k_B \, \frac{1}{\mathcal{N}} \sum_{\vec{k}} \sum_{n} \left[f_{n,k} \ln(f_{n,k}) + (1 - f_{n,k}) \ln(1 - f_{n,k}) \right] \\ &= -k_B \, \frac{1}{\mathcal{N}} \sum_{\vec{k}} \mathrm{Tr} \left[\boldsymbol{\rho}(\vec{k}) \ln(\boldsymbol{\rho}(\vec{k})) + (\mathbf{1} - \boldsymbol{\rho}(\vec{k})) \ln(\mathbf{1} - \boldsymbol{\rho}(\vec{k})) \right] \end{aligned} \tag{G.182}$$

Helmholtz potential

Adding the energy Eq. G.177 and the entropy Eq. G.182, we arrive at the Helmholtz potential

$$\begin{aligned} A_{T,N}[\{\boldsymbol{\rho}(\vec{k})\}] = & \frac{1}{\mathcal{N}} \sum_{\vec{k}} \sum_{\alpha,\beta} h_{\alpha,\beta}(\vec{k}) \rho_{\beta,\alpha}(\vec{k}) \\ & + \frac{1}{2} \frac{1}{\mathcal{N}^2} \sum_{\vec{k},\vec{k}'} \sum_{\alpha,\beta,\gamma,\delta} \Big(W_{\alpha,\beta,\gamma,\delta}(\vec{k},\vec{k}',\vec{k},\vec{k}') - W_{\alpha,\beta,\delta,\gamma}(\vec{k},\vec{k}',\vec{k}',\vec{k}) \Big) \rho_{\gamma,\alpha}(\vec{k}) \rho_{\delta,\beta}(\vec{k}') \\ & + k_B T \frac{1}{\mathcal{N}} \sum_{\vec{k}} \mathrm{Tr} \left[\boldsymbol{\rho}(\vec{k}) \ln(\boldsymbol{\rho}(\vec{k})) + (\mathbf{1} - \boldsymbol{\rho}(\vec{k})) \ln(\mathbf{1} - \boldsymbol{\rho}(\vec{k})) \right] \end{aligned} \tag{G.183}$$

Effective one-particle Hamiltonian as independent variable

We introduce an effective Hamiltonian $h^{eff}_{\alpha,\beta}(\vec{k})$, which parameterizes the one-particle-reduced density matrix.

$$\boldsymbol{\rho}(\vec{k}) = \left[\mathbf{1} + \exp\Big(\beta(\hat{h}^{eff}(\vec{k}) - \mu \mathbf{1}) \Big) \right]^{-1} \tag{G.184}$$

The density matrix is evaluated by diagonalizing the effective potential

$$h^{eff}_{\alpha,\beta}(\vec{k}) \psi_{\alpha,0,n,\vec{k}} = \psi_{\alpha,0,n,\vec{k}} \epsilon_n(\vec{k}) \qquad \text{with} \qquad \sum_{\alpha} \psi_{\alpha,0,n,\vec{k}} \psi^*_{\alpha,0,m,\vec{k}} = \delta_{n,m} \tag{G.185}$$

which yields the density matrix as

$$\rho_{\alpha,\beta}(\vec{k}) = \sum_{n} \psi_{\alpha,0,n,\vec{k}} f_{n,\vec{k}} \psi^*_{\beta,0,n,\vec{k}} \tag{G.186}$$

with the occupations

$$f_{n,\vec{k}} = \frac{1}{1 + \exp\Big(\beta(\epsilon_n(\vec{k}) - \mu) \Big)} \tag{G.187}$$

The chemical potential is determined so that the particle number per unit cell is correct

$$N = \frac{1}{\mathcal{N}} \sum_{n,\vec{k}} f_{n,\vec{k}} \tag{G.188}$$

Thus, we obtain the k-dependent reduced density matrix as function of a k-dependent effective Hamiltonian. This in turn allows one to express the Helmholtz potential as functional of this Hamiltonian.

$$A_T[\{\boldsymbol{h}^{eff}(\vec{k})\}] = A_T\left[\left\{\boldsymbol{\rho}\left(\vec{k}, \left\{\boldsymbol{h}^{eff}(\vec{k})\right\}\right)\right\}\right] \tag{G.189}$$

With braces we denote that the contributions from all k-points contribute.

Minimum condition

At self consistency the effective Hamiltonian has the form

$$\begin{aligned}\mathcal{N}\frac{\partial \Omega_{T,\mu}}{\partial \rho_{\beta,\alpha}(\vec{k})} = h_{\alpha,\beta}(\vec{k}) + \frac{1}{\mathcal{N}} \sum_{\vec{k}'} \sum_{\alpha,\beta,\gamma,\delta} \Big(W_{\alpha,\gamma,\beta,\delta}(\vec{k},\vec{k}',\vec{k},\vec{k}') - W_{\alpha,\gamma,\delta,\beta}(\vec{k},\vec{k}',\vec{k}',\vec{k}) \Big) \rho_{\delta,\gamma}(\vec{k}') \\ - h^{eff}_{\alpha,\beta}(\vec{k}) \stackrel{!}{=} 0\end{aligned} \tag{G.190}$$

This yields an expression for the effective Hamiltonian

$$\begin{aligned}h^{eff}_{\alpha,\beta}(\vec{k}) = h_{\alpha,\beta}(\vec{k}) \\ + \frac{1}{\mathcal{N}} \sum_{\vec{k}'} \sum_{\alpha,\beta,\gamma,\delta} \Big(W_{\alpha,\gamma,\beta,\delta}(\vec{k},\vec{k}',\vec{k},\vec{k}') - W_{\alpha,\gamma,\delta,\beta}(\vec{k},\vec{k}',\vec{k}',\vec{k}) \Big) \rho_{\delta,\gamma}(\vec{k}')\end{aligned} \tag{G.191}$$

The derivative with respect to the Hamiltonian introduces a further term

$$\mathcal{N}\frac{\partial \Omega_{T,\mu}}{\partial h_{\alpha,\beta}(\vec{k})} = \mathcal{N} \sum_{\vec{k}} \sum_{\gamma,\delta} \frac{\partial \Omega_{T,\mu}}{\partial \rho_{\delta,\gamma}(\vec{k}')} \frac{\partial \rho_{\delta,\gamma}(\vec{k}')}{\partial h^{eff}_{\alpha,\beta}(\vec{k})} \tag{G.192}$$

where

$$\begin{aligned}\frac{\partial \rho_{\delta,\gamma}(\vec{k}')}{\partial (h^{eff}_{\alpha,\beta}(\vec{k}) - \mu\delta_{\alpha,\beta})} &\stackrel{\text{Eq. G.132}}{=} \delta_{\vec{k},\vec{k}'} \sum_{m,n} \psi_{\delta,\vec{0},m,\vec{k}} \psi^*_{\alpha,\vec{0},m,\vec{k}} \psi_{\beta,\vec{0},n,\vec{k}} \psi^*_{\gamma,\vec{0},n,\vec{k}} \\ &\quad \times \begin{cases} (f_{n,\vec{k}} - f_{m,\vec{k}})/(\epsilon_{n,\vec{k}} - \epsilon_{m,\vec{k}}) & \text{for } \epsilon_{n,\vec{k}} \neq \epsilon_{m,\vec{k}} \\ -\frac{1}{k_B T} f_{n,\vec{k}}(1 - f_{n,\vec{k}}) & \text{for } \epsilon_{n,\vec{k}} = \epsilon_{m,\vec{k}} \end{cases}\end{aligned} \tag{G.193}$$

We obtain at fixed chemical potential

$$\begin{aligned}\frac{\partial \rho_{\delta,\gamma}(\vec{k}')}{\partial h^{eff}_{\alpha,\beta}(\vec{k})} &= \sum_{u,v} \frac{\partial \rho_{\delta,\gamma}(\vec{k}')}{\partial (h^{eff}_{u,v}(\vec{k}) - \mu\delta_{u,v})} \frac{\partial h^{eff}_{u,v}(\vec{k})}{\partial h^{eff}_{\alpha,\beta}(\vec{k})} \\ &= \frac{\partial \rho_{\delta,\gamma}(\vec{k}')}{\partial (h^{eff}_{\alpha,\beta}(\vec{k}) - \mu\delta_{\alpha,\beta})}\end{aligned} \tag{G.194}$$

Thus, we obtain

$$\begin{aligned}\frac{\partial \Omega_{T,\mu}}{\partial h_{\alpha,\beta}(\vec{k})} &= \sum_{\vec{k}} \sum_{\gamma,\delta} \frac{\partial \Omega_{T,\mu}}{\partial \rho_{\delta,\gamma}(\vec{k}')} \frac{\partial \rho_{\delta,\gamma}(\vec{k}')}{\partial h^{eff}_{\alpha,\beta}(\vec{k})} \\ &= \frac{1}{\mathcal{N}} \sum_{\vec{k}} \sum_{m,n} \psi_{\beta,\vec{0},n,\vec{k}} \Big(\sum_{\gamma,\delta} \psi^*_{\gamma,\vec{0},n,\vec{k}} \Big(h^{out}_{\gamma,\delta}(\vec{k}) - h^{eff}_{\gamma,\delta}(\vec{k}) \Big) \psi_{\delta,\vec{0},m,\vec{k}} \Big) \psi^*_{\alpha,\vec{0},m,\vec{k}} \\ &\quad \times \begin{cases} (f_{n,\vec{k}} - f_{m,\vec{k}})/(\epsilon_{n,\vec{k}} - \epsilon_{m,\vec{k}}) & \text{for } \epsilon_{n,\vec{k}} \neq \epsilon_{m,\vec{k}} \\ -\frac{1}{k_B T} f_{n,\vec{k}}(1 - f_{n,\vec{k}}) & \text{for } \epsilon_{n,\vec{k}} = \epsilon_{m,\vec{k}} \end{cases}\end{aligned} \tag{G.195}$$

This term determines the forces acting on the effective Hamiltonian, which are required t=o steer the system towards self-consistency.

G.7 Spectral function in the Hartree-Fock approximation

G.7.1 Spectral function of Hartree-Fock at finite temperatures

In this section, I work out the exact spectral function for the thermal ensemble from the thermal Hartree-Fock approximation. For a single Slater determinant, the one-particle spectral function exhibits delta peaks at the eigenvalues of the Fock operator.

At finite temperatures, considered here, the excitations experience thermal fluctuations, which leads to a thermal broadening of the spectral bands.

Let me start with the expression for the one-particle spectral function from the Lehmann representation.

$$\hat{\mathcal{A}}(\epsilon) \overset{\text{Eq. ??}}{=} \sum_{m,n} |\varphi_m\rangle \Bigg(\sum_{\vec{\sigma},\vec{\sigma'}} \Big(P_{\vec{\sigma}} + P_{\vec{\sigma'}} \Big) \langle \vec{\sigma} | \hat{a}_m | \vec{\sigma'} \rangle \langle \vec{\sigma'} | \hat{a}_n^\dagger | \vec{\sigma} \rangle \delta(\epsilon - (E_{\vec{\sigma'}} - E_{\vec{\sigma}})) \Bigg) \langle \varphi_n | \tag{G.196}$$

We will use the micro states $|\vec{\sigma}\rangle$ and probabilities $P_{\vec{\sigma}} = \frac{1}{Z} \mathrm{e}^{-\beta \sum_n (\epsilon_n^{\text{eff}} - \mu)}$ from the thermal Hartree-Fock approximation, where ϵ_n^{eff} are the eigenvalues of the Fock operator for the ensemble.

The excitation energies are obtained from the total energies $E_{\vec{\sigma}}$ of the individual micro states.

$$\begin{aligned} E_{\vec{\sigma}} &= \langle \vec{\sigma} | \hat{h} + \hat{W} | \vec{\sigma} \rangle \\ &= \sum_n \sigma_n \langle \varphi_n | \hat{h} | \varphi_n \rangle + \frac{1}{2} \sum_{m,n=1}^{\infty} \sigma_m \sigma_n \Big(\langle \varphi_m, \varphi_n | \hat{W} | \varphi_m, \varphi_n \rangle - \langle \varphi_m, \varphi_n | \hat{W} | \varphi_n, \varphi_m \rangle \Big) \end{aligned} \tag{G.197}$$

The energy to add a particle in state $|\varphi_n\rangle$ to $|\vec{\sigma}\rangle$ is

$$\begin{aligned} \Delta E &= \langle \varphi_n | \hat{h} | \varphi_n \rangle + \sum_m^{\infty} \sigma_m \Big(\langle \varphi_m, \varphi_n | \hat{W} | \varphi_m, \varphi_n \rangle - \langle \varphi_m, \varphi_n | \hat{W} | \varphi_n, \varphi_m \rangle \Big) \\ &= \underbrace{\langle \varphi_n | \hat{h} + \hat{V}_H + \hat{V}_X | \varphi_n \rangle}_{\epsilon_n^{\text{eff}}} + \sum_m^{\infty} (\sigma_m - f_m) \Big(\langle \varphi_m, \varphi_n | \hat{W} | \varphi_m, \varphi_n \rangle - \langle \varphi_m, \varphi_n | \hat{W} | \varphi_n, \varphi_m \rangle \Big) \end{aligned} \tag{G.198}$$

It does not matter whether the sum over m includes n or not, because the corresponding matrix element for $m = n$ is zero. The energy ϵ_n^{eff} is the corresponding eigenstate of the Fock operator $\hat{h}^{\text{eff}} = \hat{h} + \hat{V}_H + \hat{V}_X$, which acts as an effective Hamiltonian.

While the first term ϵ_n^{eff} is the same for all micro states the ensemble, the second term describes thermal fluctuations, which differ from micro state to micro state. These fluctuations are low-energy excitations, which are thermally accessible.

The resulting spectral function is

$$\begin{aligned}
\mathcal{A}(\epsilon) &\overset{\text{Eq. ??}}{=} \sum_{m,n} |\varphi_n\rangle \Bigg\{ \sum_{\vec{\sigma},\vec{\sigma}'} \underbrace{\frac{\left(\mathrm{e}^{-\beta\sum_j \sigma_j(\epsilon_j-\mu)} + \mathrm{e}^{-\beta\sum_j \sigma'_j(\epsilon_j-\mu)}\right)}{\sum_{\vec{\sigma}''} \mathrm{e}^{-\beta\sum_j \sigma''_j(\epsilon_j-\mu)}}}_{P_{\vec{\sigma}}+P_{\vec{\sigma}'}} \underbrace{\delta_{\sigma_n,0}\delta_{\sigma'_n,1} \prod_{m;m\neq n} \delta_{\sigma_m,\sigma'_m}}_{\langle\vec{\sigma}|\hat{a}_m|\vec{\sigma}'\rangle\langle\vec{\sigma}'|\hat{a}_n^\dagger|\vec{\sigma}\rangle} \\
&\quad \times\delta\Bigg(\epsilon - \epsilon_n^{\text{eff}} - \sum_m^\infty (\sigma_m - f_m)\Big(\langle\varphi_m,\varphi_n|\hat{W}|\varphi_m,\varphi_n\rangle - \langle\varphi_m,\varphi_n|\hat{W}|\varphi_n,\varphi_m\rangle\Big)\Bigg)\Bigg\}\langle\varphi_n| \\
&= \sum_n |\varphi_n\rangle \Bigg\{ \frac{1}{\sum_{\vec{\sigma}'} \mathrm{e}^{-\beta\sum_j \sigma'_j(\epsilon_j-\mu)}} \sum_{\vec{\sigma}} \delta_{\sigma_n,0} \mathrm{e}^{-\beta\sum_j \sigma_j(\epsilon_j-\mu)} \Big(1 + \mathrm{e}^{-\beta(\epsilon_n^{eff}-\mu)}\Big) \\
&\quad \times\delta\Bigg(\epsilon - \epsilon_n^{\text{eff}} - \sum_m^\infty (\sigma_m - f_m)\Big(\langle\varphi_m,\varphi_n|\hat{W}|\varphi_m,\varphi_n\rangle - \langle\varphi_m,\varphi_n|\hat{W}|\varphi_n,\varphi_m\rangle\Big)\Bigg)\Bigg\}\langle\varphi_n| \\
&= \sum_n |\varphi_n\rangle \Bigg\{ \sum_{\vec{\sigma}} \delta_{\sigma_n,0} \frac{\mathrm{e}^{-\beta\sum_j \sigma_j(\epsilon_j-\mu)}}{\sum_{\vec{\sigma}'} \delta_{\sigma'_n,0} \mathrm{e}^{-\beta\sum_j \sigma'_j(\epsilon_j-\mu)}} \\
&\quad \times\delta\Bigg(\epsilon - \epsilon_n^{\text{eff}} - \sum_m^\infty (\sigma_m - f_m)\Big(\langle\varphi_m,\varphi_n|\hat{W}|\varphi_m,\varphi_n\rangle - \langle\varphi_m,\varphi_n|\hat{W}|\varphi_n,\varphi_m\rangle\Big)\Bigg)\Bigg\}\langle\varphi_n|
\end{aligned} \tag{G.199}$$

We see that each natural orbital contributes a large number of δ-peaks to the density of states. In other words, the density of states is broadened. The broadening is due to the potential fluctuations induced by the fluctuations of the occupation of other orbitals. These fluctuations are absent for orbitals with integer occupations $f_n = 0$ or $f_n = 1$.

If only one Slater determinant contributes to the ensemble (at $T = 0$) this thermal broadening is absent. If the ground state is, for example, doubly degenerate, the spectral function is the average of the two Slater determinants in the ground state ensemble.

Because the broadening is hard to calculate, the mean-field approximation is also done for the spectral function.

$$\hat{\mathcal{A}}^{mf}(\epsilon) = \sum_n |\varphi_n\rangle \delta\big(\epsilon - \epsilon_n^{\text{eff}}\big) \langle\varphi_n| \tag{G.200}$$

G.7.2 Spectral function beyond the mean-field spectral function

The discussion above rested on the mean-field approximation, where all particles experience the same potential.

In the spirit of section 2.6, we explore the spectrum of an ensemble of Slater determinants built from the natural orbitals. This goes beyond the mean-field approximation, and it is consistent with the random(averaged)-phase approximation.

The one-particle energies $\epsilon_{n,\vec{\sigma}} = \langle\varphi_n|\hat{h} + \hat{V}_{H,\vec{\sigma}} + \hat{V}_{X,\vec{\sigma}}|\varphi_n\rangle$ depend on the specific Slater determinant in the ensemble, because each Slater determinant produces its own Hartree and exchange potential. The spectral function of the ensemble is

$$\hat{\mathcal{A}}(\epsilon) = \sum_{\vec{\sigma}} P_{\vec{\sigma}} \sum_n |\varphi_n\rangle \delta(\epsilon - \epsilon_{n,\vec{\sigma}}) \langle\varphi_n| = \sum_n |\varphi_n\rangle \Big\{ \sum_{\vec{\sigma}} P_{\vec{\sigma}} \delta(\epsilon - \epsilon_{n,\vec{\sigma}}) \Big\} \langle\varphi_n| \tag{G.201}$$

For each natural orbital $|\varphi_n\rangle$, I obtain a multitude of contributions at different energies $\epsilon_{n,\vec{\sigma}}$ with different weights $P_{\vec{\sigma}}$.

In the mean-field approximation the contributions for one natural orbital collapse into a single, average energy level at

$$\epsilon_n^{mf} = \sum_{\vec{\sigma}} P_{\vec{\sigma}} \epsilon_{n,\vec{\sigma}} \tag{G.202}$$

that is, the spectral function in the mean-field approximation is

$$\hat{\mathcal{A}}^{mf}(\epsilon) = \sum_n |\varphi_n\rangle \delta(\epsilon - \epsilon_n^{mf}) \langle\varphi_n| \tag{G.203}$$

The total weight and the mean energy of each natural orbital remains unchanged

$$\begin{aligned} \int d\epsilon\, \langle\varphi_n|\hat{\mathcal{A}}(\epsilon)|\varphi_n\rangle &= \int d\epsilon\, \langle\varphi_n|\hat{\mathcal{A}}^{mf}(\epsilon)|\varphi_n\rangle = 1 \\ \int d\epsilon\, \langle\varphi_n|\hat{\mathcal{A}}(\epsilon)|\varphi_n\rangle\, \epsilon &= \int d\epsilon\, \langle\varphi_n|\hat{\mathcal{A}}^{mf}(\epsilon)|\varphi_n\rangle\, \epsilon = \sum_{\vec{\sigma}} P_{\vec{\sigma}} \epsilon_{n,\vec{\sigma}} = \epsilon_n^{mf} \end{aligned} \tag{G.204}$$

When we adjust the ensemble, keeping the natural orbitals unchanged for the sake of simplicity, we find that the energy levels in the mean-field approximation shift when electrons are added or removed. The weight of each excitation energy remains unchanged.

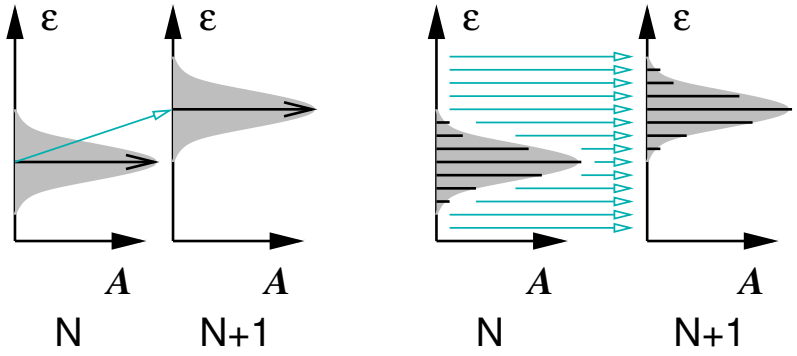


Fig. G.4: Scheme to demonstrate the a spectral function $\mathcal{A}_n(\epsilon, \vec{k})$ of a single band $\epsilon_n(\vec{k})$ for a specific k-point $\vec{k}$ in the mean-field approximation (left) in comparison to the spectral function obtained from a complete many-particle description (right). In the mean-field approximation the spectral function for a specific k-point and band index is a delta-function centered at the one-particle energy $\epsilon_n(\vec{k})$ as shown on the left. As a parameter such as the particle number N is changed, the delta function shifts with the one-particle energy, but it maintains its total weight. The true spectral function consists of a large, possibly continuous, set of peaks at the many-particle total-energy differences. For weak interactions they can be combined approximately into a Lorentzian of finite width. As the electron number N, or any other parameter, is changed, it is the weight of the individual peaks that change, while the positions of the many-particle energy differences remains fixed. Caution: The individual bands are not regular as in the graph, and the positions of the individual peaks are not strictly fixed.

Beyond the mean-field approximation, the energy levels $\epsilon_{n,\vec{\sigma}}$ remain unchanged, but the individual weights adjust with the changed ensemble as sketched in Fig. G.4. This consideration provides a first glimpse on the definition of the spectral function for general many-particle states and their ensemble in section **??**

G.8 Excitations in the thermal Hartree-Fock approximation

In section 2.6.1 on p. 78, I suggested an approximate interacting Hamiltonian to study the excitations in the thermal Hartree-Fock approximation.

$$\hat{H}^{THFA} \overset{\text{Eq. } 2.100}{=} \sum_{\vec{\sigma}} |\vec{\sigma}\rangle \underbrace{E_{\vec{\sigma}}}_{\langle\vec{\sigma}|\hat{h}+\hat{W}|\vec{\sigma}\rangle} \langle\vec{\sigma}| \tag{G.205}$$

The Slater determinants $|\vec{\sigma}\rangle$ are constructed from natural orbitals, respectively from the eigenstates of the Fock operator of the thermal Hartree-Fock approximation.

The eigenvalues of this approximate many-particle Hamiltonian are the expectation values $E_{\vec{\sigma}} = \langle\vec{\sigma}|\hat{h}+\hat{W}|\vec{\sigma}\rangle$ of the correct interacting Hamiltonian with the Slater determinants. Note that H^{THFA} is not the Fock operator!

G.8.1 Green's function in the thermal Hartree-Fock approximation

In this section the Green's function of the APA is derived in the energy representation. It is not the full non-equilibrium Green's function.

Editor: Discuss the relation between the APA and the THFA for Green's functions

Using the Lehmann representation, the Green's function can be expressed in the form

$$G_{\alpha,\beta}(\hbar\omega) \overset{\text{Eq. ??}}{=} \sum_{n,m} P_n \left[\underbrace{\frac{\langle\Phi_n|\hat{c}_{S,\alpha}|\Phi_m\rangle\langle\Phi_m|\hat{c}^\dagger_{S,\beta}|\Phi_n\rangle}{\hbar\omega-(E_m-E_n)+i\eta}}_{\text{electron like}} + \underbrace{\frac{\langle\Phi_n|\hat{c}^\dagger_{S,\beta}|\Phi_m\rangle\langle\Phi_m|\hat{c}_{S,\alpha}|\Phi_n\rangle}{\hbar\omega+(E_m-E_n)-i\eta}}_{\text{hole like}} \right] \tag{G.206}$$

In the **thermal Hartree-Fock approximation**, the ensemble is given by Slater determinants $|\vec{\sigma}\rangle$ formed from the eigenstates $|\varphi_n\rangle$ of the Fock operator, which is the effective Hamiltonian discussed here.

$$|\vec{\sigma}\rangle \overset{\text{Eq. 3.21}}{=} \prod_{j=1}^{\infty} \left(\hat{c}_j^\dagger\right)^{\sigma_j} |\mathcal{O}\rangle \tag{G.207}$$

The probabilities of the ensemble are

$$P_{\vec{\sigma}} \overset{\text{Eq. 2.71}}{=} \prod_{j=1}^{\infty} f_j^{\sigma_j}(1-f_j)^{1-\sigma_j} \tag{G.208}$$

For the thermal Hartree-Fock approximation, the occupations f_j are given by the Fermi function. The terms in the probabilities are

$$f_j^{\sigma_j}(1-f_j)^{1-\sigma_j} = \begin{cases} f_{T,\mu}(\epsilon_j) & \text{for } \sigma_j = 1 \\ 1-f_{T,\mu}(\epsilon_j) & \text{for } \sigma_j = 0 \end{cases} \tag{G.209}$$

The energies of the Slater determinants are

$$\underbrace{E(|\vec{\sigma}\rangle)}_{\langle\vec{\sigma}|\hat{h}+\hat{W}|\vec{\sigma}\rangle} \overset{\text{Eq. 2.31}}{=} \sum_{j=1}^{\infty} \sigma_j \langle\varphi_j|\hat{h}|\varphi_j\rangle + \frac{1}{2}\sum_{i,j=1}^{\infty} \sigma_i\sigma_j \Big(\langle\varphi_i\varphi_j|\hat{W}|\varphi_i\varphi_j\rangle - \langle\varphi_i\varphi_j|\hat{W}|\varphi_j\varphi_i\rangle \Big) \tag{G.210}$$

so that the energy differences are

- For $\sigma'_j = \sigma_j + \delta_{j,n}$, I obtain

$$\begin{aligned} E_{\vec{\sigma}+\vec{e}_n} - E_{\vec{\sigma}} &= \langle\varphi_n|\hat{h}|\varphi_n\rangle + \frac{1}{2}\sum_{i,j=1}^{\infty}\Big[\Big(\sigma_i+\delta_{n,i}\Big)\Big(\sigma_j+\delta_{n,j}\Big)-\sigma_i\sigma_j\Big]\Big(\langle\varphi_i\varphi_j|\hat{W}|\varphi_i\varphi_j\rangle - \langle\varphi_i\varphi_j|\hat{W}|\varphi_j\varphi_i\rangle\Big) \\ &= \langle\varphi_n|\hat{h}|\varphi_n\rangle + \sum_{j=1}^{\infty}\sigma_j\Big(\langle\varphi_n\varphi_j|\hat{W}|\varphi_n\varphi_j\rangle - \langle\varphi_n\varphi_j|\hat{W}|\varphi_j\varphi_n\rangle\Big) \\ &= \epsilon_n + \sum_{j=1}^{\infty}\Big(\sigma_j-f_j\Big)\Big(\langle\varphi_n\varphi_j|\hat{W}|\varphi_n\varphi_j\rangle - \langle\varphi_n\varphi_j|\hat{W}|\varphi_j\varphi_n\rangle\Big) \end{aligned} \tag{G.211}$$

where $\epsilon_n = \langle\varphi_n|\hat{h}+\hat{V}_H+\hat{V}_X|\varphi_n\rangle$ are the eigenstates of the Fock operator of the ensemble. $\hat{V}_H = \sum_n |\varphi_n\rangle\Big(\sum_j f_j\langle\varphi_n\varphi_j|\hat{W}|\varphi_n\varphi_j\rangle\Big)\langle\varphi_n|$ and $\hat{V}_X = \sum_n |\varphi_n\rangle\Big(-\sum_j f_j\langle\varphi_n\varphi_j|\hat{W}|\varphi_j\varphi_n\rangle\Big)\langle\varphi_n|$.

- For $\sigma'_j = \sigma_j - \delta_{j,n}$, I obtain

$$\begin{aligned} E_{\vec{\sigma}-\vec{e}_n} - E_{\vec{\sigma}} &= -\langle\varphi_n|\hat{h}|\varphi_n\rangle + \frac{1}{2}\sum_{i,j=1}^{\infty}\Big[\Big(\sigma_i - \delta_{n,i}\Big)\Big(\sigma_j - \delta_{n,j}\Big) - \sigma_i\sigma_j\Big]\Big(\langle\varphi_i\varphi_j|\hat{W}|\varphi_i\varphi_j\rangle - \langle\varphi_i\varphi_j|\hat{W}|\varphi_j\varphi_i\rangle\Big) \\ &= -\langle\varphi_n|\hat{h}|\varphi_n\rangle - \sum_{j=1}^{\infty}\sigma_j\Big(\langle\varphi_n\varphi_j|\hat{W}|\varphi_n\varphi_j\rangle - \langle\varphi_n\varphi_j|\hat{W}|\varphi_j\varphi_n\rangle\Big) \\ &= -\epsilon_n - \sum_{j=1}^{\infty}\Big(\sigma_j - f_j\Big)\Big(\langle\varphi_n\varphi_j|\hat{W}|\varphi_n\varphi_j\rangle - \langle\varphi_n\varphi_j|\hat{W}|\varphi_j\varphi_n\rangle\Big) \end{aligned} \tag{G.212}$$

The matrix elements have a simple form

$$\begin{aligned} \langle\vec{\sigma'}|\hat{c}^{\dagger}_{S,n}|\vec{\sigma}\rangle &= (1-\sigma_n)\prod_{j=1}^{\infty}\delta_{\sigma'_j,\sigma_j+\delta_{j,n}} \\ \langle\vec{\sigma'}|\hat{c}_{S,n}|\vec{\sigma}\rangle &= \sigma_n\prod_{j=1}^{\infty}\delta_{\sigma'_j,\sigma_j-\delta_{j,n}} \end{aligned} \tag{G.213}$$

The resulting Green's function is

$$\begin{aligned} G_{m,n}(\hbar\omega) = \delta_{m,n}\sum_{\vec{\sigma}} & \underbrace{P_{\vec{\sigma}}}_{\prod_{j=1}^{\infty}\left(f_{T,\mu}(\epsilon_j)\right)^{\sigma_j}\left(1-f_{T,\mu}(\epsilon_j)\right)^{1-\sigma_j}} \\ & \times\Bigg[\underbrace{\frac{1-\sigma_n}{\hbar\omega-\epsilon_n-\sum_{j=1}^{\infty}\Big(\sigma_j-f_j\Big)\Big(\langle\varphi_n\varphi_j|\hat{W}|\varphi_n\varphi_j\rangle-\langle\varphi_n\varphi_j|\hat{W}|\varphi_j\varphi_n\rangle\Big)+i\eta}}_{\text{electron like}} \\ & +\underbrace{\frac{\sigma_n}{\hbar\omega+\epsilon_n+\sum_{j=1}^{\infty}\Big(\sigma_j-f_j\Big)\Big(\langle\varphi_n\varphi_j|\hat{W}|\varphi_n\varphi_j\rangle-\langle\varphi_n\varphi_j|\hat{W}|\varphi_j\varphi_n\rangle\Big)-i\eta}}_{\text{hole like}}\Bigg] \end{aligned} \tag{G.214}$$

The energy levels ϵ_j, the natural orbitals $|\varphi_j\rangle$ and the occupations $f_j = f_{T,\mu}(\epsilon_j)$ depend on temperature, the chemical potential and the interaction.

The expression for the Green function implies that each Slater determinant in the ensemble contributes a pole for each eigenstate of the effective Hamiltonian. They add up to a thermal broadening of the quasi-particle peaks.

For an ensemble, which is a single Slater determinant, one obtains

$$G_{m,n}(\hbar\omega) \overset{f_j\in\{0,1\}}{=} \delta_{m,n}\Bigg[\underbrace{\frac{f_n}{\hbar\omega-\epsilon_n+i\eta}}_{\text{electron like}}+\underbrace{\frac{1-f_n}{\hbar\omega+\epsilon_n-i\eta}}_{\text{hole like}}\Bigg] \tag{G.215}$$

This looks like the non-interacting Green's function. However, the energies are the eigenstates of the Fock operator, here $\hat{h}^{eff}$, rather than those of the non-interacting Hamilonian.

There are situations, where few, but still several, Slater determinants coexist at zero temperature. Examples are symmetry-breaking transitions and systems with non-integral particle number. Examples for symmetry-breaking transitions are Peierls distortions or some magnetic order. In those cases, the thermal Hartree-Fock approximation yields the superposition of the spectra of the coexisting Slater determinants, rather than a spectrum of non-interacting electrons for a single, averaged, effective Hamiltonian.

Editor: This derivation shows that the quasi-particle energies obtained as energy derivative and that of the spectral function agree within the thermal Hartree-Fock approximation, if the ensemble consists of a single Slater determiant.

Editor: The derivation above may be of interest as exercise for the section on the spectral function. It does not describe the lifetime induced by the interaction, which was the original intention.

G.9 Post Hartree-Fock methods: Quantum chemistry

Editor: Sketch here the main ideas of post-Hartree-Fock methods of quantum chemistry. It may include configuration interaction (CI), complete active space (CAS) CI, Multireference, coupled cluster (CC) and possibly Møller-Plesset (MP) perturbation theory.

G.9.1 Coupled cluster:

Coupled-cluster theory is a quantum-chemical method, which overcomes the problem of **size inconsistency** in the configuration interaction methods. It has been invented in the context of nuclear physics by Fritz Coester and Herman Kümmel in the early 1960s.[10] [11]

Use a unitary transformation $\hat{U}$ in Fock space to represent a general many-particle wave function $|\Phi\rangle$ in terms of some reference wave function $|\bar{\Phi}\rangle$.

The Fock-space can be spanned either by variation of the reference wave function or by variation of the transformation operator. This allows one to restrict the reference wave functions, for example, to Slater determinants.

$$|\Phi_{\vec{\sigma}}\rangle = \hat{U}|\bar{\Phi}\rangle = \mathrm{e}^{\frac{i}{\hbar}\hat{A}}|\bar{\Phi}\rangle = \mathrm{e}^{\frac{i}{\hbar}\left(\sum_{\alpha,\beta} a_{\alpha,\beta}\hat{c}^\dagger_\alpha \hat{c}_\beta + \sum_{\alpha,\beta,\gamma,\delta} b_{\alpha,\beta,\gamma,\delta}\hat{c}^\dagger_\alpha \hat{c}^\dagger_\beta \hat{c}_\gamma \hat{c}_\delta + \ldots\right)}|\bar{\Phi}\rangle \tag{G.216}$$

A unitary operator can be expressed in terms of an exponential of a hermitean operator $\hat{A}$. It makes sense to choose the operator as particle-number conserving, which implies that each term in $\hat{A}$ has the same number of creation and annihilation operators.

The parameters $a_{\alpha,\beta}$, $b_{\alpha,\beta,\gamma,\delta}$ are considered as variational parameters for the total energy, alongside with some reference wave function.

The total energy can be obtained by minimizing

$$\begin{aligned} E &= \min_{|\Phi\rangle} \operatorname*{stat}_{\Lambda}\Big\{\langle\Phi|\hat{H}|\Phi\rangle - \Lambda\Big(\langle\Phi|\Phi\rangle - 1\Big)\Big\} \\ &= \min_{|\bar{\Phi}\rangle,\hat{A}} \operatorname*{stat}_{\Lambda}\Big\{\langle\bar{\Phi}|\mathrm{e}^{-i\hat{A}}\hat{H}\mathrm{e}^{i\hat{A}}|\bar{\Phi}\rangle - \Lambda\Big(\langle\bar{\Phi}|\underbrace{\mathrm{e}^{-i\hat{A}}\mathrm{e}^{i\hat{A}}}_{=\hat{1}\text{ if }\hat{A}=\hat{A}^\dagger}|\bar{\Phi}\rangle - 1\Big)\Big\} \\ &= \min_{|\bar{\Phi}\rangle,\hat{A}(\hat{A}=\hat{A}^\dagger)} \operatorname*{stat}_{\Lambda}\Big\{\langle\bar{\Phi}|\mathrm{e}^{-i\hat{A}}\hat{H}\mathrm{e}^{i\hat{A}}|\bar{\Phi}\rangle - \Lambda\Big(\langle\bar{\Phi}|\bar{\Phi}\rangle - 1\Big)\Big\} \end{aligned} \tag{G.217}$$

Rather than using the stationary condition with respect to the operator $\hat{A}$, the stationary condition with respect to the reference wave function is used

$$\mathrm{e}^{-i\hat{A}}\hat{H}\mathrm{e}^{i\hat{A}}|\bar{\Phi}\rangle = |\bar{\Phi}\rangle\Lambda \tag{G.218}$$

This strategy is permitted, as long as the same portion of Fock space is spanned by the variation of $\hat{A}$ and the variation of the reference wave function.

[10] see [180] and references

[11] See also Sinanoglu[181] who introduced a variational formulation which is considered a predecessor of coupled cluster theory. This may be close to what I am using here.

This equation is solved by introducing a basis of Slater determinants $|\vec{\sigma}\rangle$.

$$\langle\vec{\sigma}|\mathrm{e}^{-i\hat{A}}\hat{H}\mathrm{e}^{i\hat{A}}|\bar{\Phi}\rangle = \langle\vec{\sigma}|\bar{\Phi}\rangle\Lambda \tag{G.219}$$

where the basis of Slater determinants $\langle\vec{\sigma}|$ must be sufficienly large to determine all parameters of the transformation operator, respectively of $\hat{A}$. It is convenient to select the Slater determinants such that the reference wave function is one of them.

Appendix H

Density-functional theory

Density-functional theory[33, 34] is an extremely powerful technique. It is based on an exact theorem that the ground-state energy is determined solely by the density alone.

The theorem says

- that all ground-state properties are unique functionals of the electron density and
- that the electron density can be obtained from a one-particle Schrödinger equation in an effective potential.

Density-functional theory maps the interacting electron system onto a system of non-interacting electrons in an effective potential. The effective potential depends in turn on the electron distribution and describes the interacting between the electrons in an effective way.

H.1 Existence of a density functional for the energy

Density-functional theory says that all ground-state properties can be expressed, at least in principle, as functionals of the charge density alone.

This statement is nontrivial, because the wave function contains far more information than the density. The statement also provides a dramatic simplification as the density, in contrast to the wave function, can be handled on a computer: The density is a function in three dimensions, while the wave function is a function in 3^N dimensions.

The original proof of existence for density functionals goes back to Hohenberg and Kohn[182]. Later, Levy[183, 184] and Lieb[185] have given a recipe how the density functional can actually be constructed . This proof contains the proof of existence. For this reason, I will not present the original proof of Hohenberg and Kohn, but show the one by Levy.

H.1.1 The many-particle Hamiltonian

Let us start with a Hamilton operator

$$\hat{H}_\lambda = \hat{T} + \hat{V}_{ext} + \lambda \hat{W} \ , \tag{H.1}$$

where the kinetic energy is

$$\hat{T} = \int d^4x \ \hat{\psi}^\dagger(\vec{x}) \frac{-\hbar^2}{2m_e} \vec{\nabla}^2 \hat{\psi}(\vec{x}) = \sum_{\alpha,\beta} \underbrace{\langle \chi_\alpha | \frac{\hat{\vec{p}}^2}{2m_e} | \chi_\beta \rangle}_{t_{\alpha,\beta}} \hat{c}^\dagger_\alpha \hat{c}_\beta \tag{H.2}$$

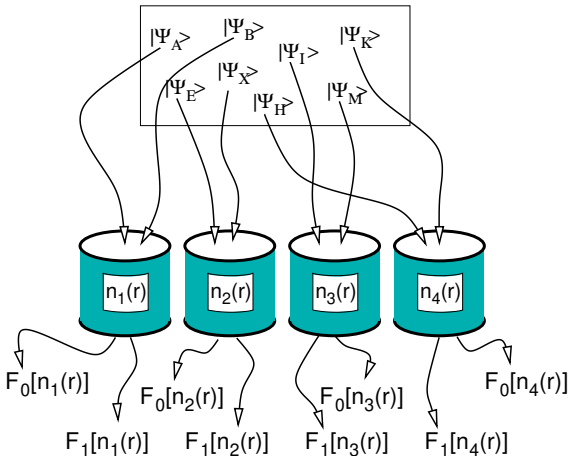


Fig. H.1: Sketch of Levy's derivation of a density functional.

The external potential operator describes the Coulomb potential of the nuclei

$$\hat{V} = \int d^4x \; v_{ext}(\vec{r}) \underbrace{\hat{\psi}^\dagger(\vec{x})\hat{\psi}(\vec{x})}_{\hat{n}(\vec{x})} = \sum_{\alpha,\beta} \underbrace{\langle \chi_\alpha | \hat{v}_{ext} | \chi_\beta \rangle}_{v_{\alpha,\beta}} \hat{c}^\dagger_\alpha \hat{c}_\beta \tag{H.3}$$

The interaction operator is

$$\begin{aligned} \hat{W} &\overset{\text{Eq. 3.75}}{=} \frac{1}{2} \int d^4x \int d^4x' \; \hat{\psi}^\dagger(\vec{x})\hat{\psi}^\dagger(\vec{x'}) \frac{e^2}{4\pi\epsilon_0 |\vec{r} - \vec{r'}|} \hat{\psi}(\vec{x'})\hat{\psi}(\vec{x}) \\ &= \frac{1}{2} \sum_{\alpha,\beta,\gamma,\delta} \underbrace{\int d^4x \int d^4x' \; \frac{e^2 \chi^*_\alpha(\vec{x})\chi^*_\beta(\vec{x'})\chi_\gamma(\vec{x'})\chi_\delta(\vec{x})}{4\pi\epsilon_0 |\vec{r} - \vec{r'}|}}_{U_{\alpha,\beta,\delta,\gamma}} \hat{c}^\dagger_\alpha \hat{c}^\dagger_\beta \hat{c}_\gamma \hat{c}_\delta \end{aligned} \tag{H.4}$$

The **U-tensor** is defined with the arguments $\vec{x}$ and $\vec{x'}$ in the same order for the product wave function and its complex conjugate.

$$U_{\alpha,\beta,\gamma,\delta} \overset{\text{def}}{=} \int d^4x \int d^4x' \; \frac{e^2 \chi^*_\alpha(\vec{x})\chi^*_\beta(\vec{x'})\chi_\gamma(\vec{x})\chi_\delta(\vec{x'})}{4\pi\epsilon_0 |\vec{r} - \vec{r'}|} \tag{H.5}$$

Editor: Caution! double use of the symbol $\mathbb{A}$. The other use is a set of Feynman diagrams.

We scaled the electron-electron interaction by a coupling parameter λ, which allows us later to switch the electron-electron interaction on an off. This is not required for the proof of Levy, but later-on, we will often refer also to Hamiltonians without or with scaled interaction.

H.1.2 The proof: constrained search

The idea of the proof is very simple:

1. Group all normalized, antisymmetric many-particle wave functions $\{|\Phi\rangle\}$ according to their density.[1] Each such subset $\mathbb{A}[n]$ contains all wave functions in the **Fock space** $\mathbb{F}$ with the same density distribution $n(r)$.

$$\mathbb{A}[n] \overset{\text{def}}{=} \{|\Phi\rangle \in \mathbb{F} : \forall_{\vec{r}} \; \langle \Phi | \hat{n}(\vec{r}) | \Phi \rangle = n(\vec{r})\} \tag{H.6}$$

[1] the density is considered as function not as value at a specific point in space.

2. For each subset $\mathbb{A}[n]$, that is for each density, we determine that wave function $\left|\Phi_\lambda^{(0)}[n]\right\rangle$ that provides the lowest energy $\langle\Phi|\hat{H}_\lambda|\Phi\rangle$. The minimum of the total energy defines the total energy functional $E_\lambda[n(\vec{r})]$ of the electron density.

$$E_\lambda[n] = \min_{|\Phi\rangle\in\mathbb{A}[n]} \left\langle \Phi \left| \hat{H}_\lambda \right| \Phi \right\rangle = \left\langle \Phi_\lambda^{(0)}[n] \left| \hat{H}_\lambda \right| \Phi_\lambda^{(0)}[n] \right\rangle \tag{H.7}$$

3. The energy can be divided into a **universal density functional** $F_\lambda[n(\vec{r})]$, which is a general property of the electron gas, and a system-specific term, that depends on the external potential.

$$E_\lambda[n] = \underbrace{F_\lambda[n]}_{\langle\Phi_\lambda^{(0)}[n]|\hat{T}+\lambda\hat{W}|\Phi_\lambda^{(0)}[n]\rangle} + \underbrace{\int d^3r\; n(\vec{r})v_{ext}(\vec{r})}_{\langle\Phi_\lambda^{(0)}[n]|\hat{V}|\Phi_\lambda^{(0)}[n]\rangle} \tag{H.8}$$

   Because the energy related to the external potential only depends on the density, it is a constant within each group $\mathbb{A}[n]$ of wave functions with a given density. Thus, we can directly determine the universal functional $F_\lambda[n]$ as minimum of $\langle\Phi|\hat{T}+\lambda\hat{W}|\Phi\rangle$ for all wave functions with the specified density. $\hat{T}$ is the kinetic-energy operator.

   UNIVERSAL DENSITY FUNCTIONAL

$$F_\lambda[n] \stackrel{\text{def}}{=} \min_{|\Phi\rangle\in\mathbb{A}[n]} \langle\Phi|\hat{T}+\lambda\hat{W}|\Phi\rangle \tag{H.9}$$

4. To find the ground-state energy $E_\lambda^{(0)}$ of an electron gas with N electrons in a given external potential, we minimize the total energy functional with respect to the density under the constraint of a specified total number of electrons.

$$E_\lambda^{(0)} = \min_{n(\vec{r}):\int d^3r\; n(\vec{r})=N} \left\{ F_\lambda[n] + \int d^3r\; n(\vec{r})v_{ext}(\vec{r}) \right\}$$

   This minimization with respect to the density provides us with the ground-state density and the ground-state energy. If we have remembered the wave function $\left|\Phi^0[n]\right\rangle$ that minimized the total energy within a group with given density distribution $n(\vec{r})$, we can, in principle work our way back to the ground-state wave function, which contains all information about the electronic ground state.

This concludes the proof by Levy on the existence of a universal functional of the density, that allows one to determine the ground-state energy and, in principle, all other properties of the electronic ground state.

H.2 More explicit proof at finite temperature

The previous section shows the principle of Levy's constrained-search algorithm with the minimum conceptual complication. In this section, we generalize the proof given above to finite temperature.

- This will make us familiar with a few thermodynamic relations, that will be used later again. Thus, it shows, that the limitation to ground states implies the generalization to ensembles in thermal equilibrium.
- The second motivation for repeating the proof is to make the steps for constrained minimization more explicit. These expression provide us then with the set of equations that specify the minimum.

H.2.1 Grand potential

Let us start with the grand potential for a system of electrons. The grand potential[2] $\Omega_{T,\mu}$ is the thermodynamic potential for a system in contact with a heat bath and a particle reservoir. The heat bath is characterized by the temperature T and the particle reservoir is characterized by the chemical potential μ.

The **grand potential** has the form

$$\Omega_{T,\mu} = \min_{\{|\Phi_q\rangle, P_q\}} \operatorname*{stat}_{\boldsymbol{\Lambda},\eta} \Bigg\{ \underbrace{k_B T \sum_q P_q \ln(P_q)}_{-TS} + \underbrace{\sum_q P_q \langle \Phi_q | \hat{H} - \mu \hat{N} | \Phi_q \rangle}_{E-\mu N} - \sum_{q,q'} \Lambda_{q,q'} \Big(\langle \Phi_{q'} | \Phi_q \rangle - \delta_{q',q} \Big) - \eta \Big(\sum_q P_q - 1 \Big) \Bigg\} \tag{H.10}$$

where $|\Phi_q\rangle$ are many-electron wave functions in the Fock space and the P_q are their probabilities. The set $\{P_q, |\Phi_q\rangle\}$ of many-particle wave functions and their probabilities describes a general **ensemble**. The ensemble is a **macro state**, while a single many-particle wave function describes a **micro state**. The symbol "stat" specifies a stationary point of the expression, which may be a minimum, a maximum or a saddle point, while the symbol "min" is reserved for true minima.

The minimum condition with respect to the probabilities can readily be worked out as

$$P_q = \frac{1}{Z_{T,\mu}} \mathrm{e}^{-\beta \langle \Phi_q | \hat{H} - \mu \hat{N} | \Phi_q \rangle} \tag{H.11}$$

with the **partition function**

$$Z_{T,\mu} = \sum_q \mathrm{e}^{-\beta \langle \Phi_q | \hat{H} - \mu \hat{N} | \Phi_q \rangle} \tag{H.12}$$

Inserting these probabilities into the expression for the grand potential, we obtain

$$\Omega_{T,\mu} = \min_{|\Phi_j\rangle} \operatorname*{stat}_{\boldsymbol{\Lambda}} \Bigg\{ -k_B T \ln \Bigg[\sum_q \mathrm{e}^{-\beta \langle \Phi_q | \hat{H} - \mu \hat{N} | \Phi_q \rangle} \Bigg] - \sum_{q,q'} \Lambda_{q,q'} \Big(\langle \Phi_{q'} | \Phi_q \rangle - \delta_{q',q} \Big) \Bigg\} \tag{H.13}$$

The minimization with respect to the many-particle wave functions $|\Phi_q\rangle$ can be performed by diagonalizing $\hat{H} - \mu \hat{N}$. When the wave functions $|\Phi_q\rangle$ obey

$$\hat{H} |\Phi_q\rangle = |\Phi_q\rangle E_q \qquad \text{and} \qquad \hat{N} |\Phi_q\rangle = |\Phi_q\rangle N_q \ , \tag{H.14}$$

the grand potential obtains the form

$$\Omega_{T,\mu} = -k_B T \ln \Bigg[\sum_q \langle \Phi_q | \mathrm{e}^{-\beta(\hat{H} - \mu \hat{N})} | \Phi_q \rangle \Bigg] = -k_B T \ln \operatorname{Tr} \Big[\mathrm{e}^{-\beta(\hat{H} - \mu \hat{N})} \Big] \tag{H.15}$$

H.2.2 Helmholtz potential

In many practical problems, the particle number is fixed rather than the chemical potential. An equilibrium ensemble with constant temperature and particle number is called the **canonical ensemble**. The thermodynamic potential for the canonical ensemble is the **Helmholtz potential** $A_{T,N}$. It describes a system in the presence of a heat-bath, but, in contrast to the grand potential, without a particle reservoir.

[2] The thermodynamic potential of a homogeneous system, that only depends on intrinsic variables does not exist, because it would either be eaten up or grow to infinity in the presence of the reservoirs. Here, the situation is different, because there are still the atoms, which are not affected by adding or removing energy or electrons.

The Helmholtz potential is obtained from the grand potential by a **Legendre-Fenchel transform**

$$A_{T,N} = \operatorname*{stat}_{\mu} \Big[\Omega_{T,\mu} + \mu N \Big] \tag{H.16}$$

If the expression Eq. H.10 for the grand potential is inserted, we recognize that the stationary condition is part of a constraint condition imposed by the method of Lagrange multipliers. We obtain

$$\begin{aligned} A_{T,N} = \min_{\{|\Phi_q\rangle, P_q\}} \operatorname*{stat}_{\boldsymbol{\Lambda},\eta,\mu} \Bigg\{ & \underbrace{k_B T \sum_q P_q \ln(P_q)}_{-TS} + \underbrace{\sum_q P_q \langle \Phi_q | \hat{H} | \Phi_q \rangle}_{E} \\ & - \mu \Big(\sum_q P_q \langle \Phi_q | \hat{N} | \Phi_q \rangle - N \Big) - \sum_{q,q'} \Lambda_{q,q'} \Big(\langle \Phi_{q'} | \Phi_q \rangle - \delta_{q',q} \Big) - \eta \Big(\sum_q P_q - 1 \Big) \Bigg\} \end{aligned} \tag{H.17}$$

The Helmholtz potential approaches the ground state energy in the low-temperature limit.

In the following discussion, I will often refer to the Helmholtz potential as the energy. I do this for pedagogical reasons. The rationale is that the Helmholtz potential is a generalization of the energy for finite temperatures.

H.2.3 Density as fundamental variable

The important observation is that the external potential only acts on the electron density

$$\sum_q P_q \langle \Phi_q | \hat{V}_{ext} | \Phi_q \rangle = \int d^3 r \; v_{ext}(\vec{r}) n(\vec{r}) \tag{H.18}$$

The electron density of an ensemble is defined as [3]

$$\begin{aligned} n(\vec{r}) &\stackrel{\text{def}}{=} \sum_{\sigma \in \{\uparrow,\downarrow\}} \sum_q P_q \langle \Phi_q | \underbrace{\hat{\psi}^\dagger(\vec{x})}_{\sum_\beta \hat{c}^\dagger_\beta \langle \chi_\beta | \vec{x} \rangle} \overbrace{\hat{\psi}(\vec{x})}^{\sum_\alpha \langle \vec{x} | \chi_\alpha \rangle \hat{c}_\alpha} | \Phi_q \rangle \\ &= \sum_{\sigma \in \{\uparrow,\downarrow\}} \sum_{\alpha,\beta} \underbrace{\sum_q P_q \langle \Phi_q | \hat{c}^\dagger_\beta \hat{c}_\alpha | \Phi_q \rangle}_{\rho^{(1)}_{\alpha,\beta} \quad \text{Eq. 3.56}} \chi^*_\beta(\vec{x}) \chi_\alpha(\vec{x}) = \sum_{\alpha,\beta} \rho^{(1)}_{\alpha,\beta} \sum_{\sigma \in \{\uparrow,\downarrow\}} \chi_\alpha(\vec{x}) \chi^*_\beta(\vec{x}) \end{aligned} \tag{H.19}$$

where

$$\rho^{(1)}_{\alpha,\beta} \stackrel{\text{Eq. 3.56}}{=} \sum_q P_q \langle \Phi_q | \hat{c}^\dagger_\beta \hat{c}_\alpha | \Phi_q \rangle \tag{H.20}$$

is the **one-particle-reduced density matrix**..

H.2.4 Constrained search

The fact that the external potential acts only on the density suggests that we divide the minimization into two steps: The first step identifies the minimum for a given density. The second step performs

[3] I use the representation of field operators Eq. B.6 on p. B.6 in terms of non-orthonormal orbitals $|\chi_\alpha\rangle\}$. For an orthonormal basis $\{|\varphi_j\rangle\}$, the transformation is given in Eq. 3.61 from p. 142.

the minimization of these density-specific minima over all densities.

$$\begin{aligned}
\Omega_{T,\mu} &\overset{\text{Eq. } H.10}{=} \min_{|\Phi_j\rangle,P_j} \operatorname*{stat}_{\boldsymbol{\Lambda},\eta} \Bigg\{ \underbrace{k_B T \sum_j P_j \ln(P_j)}_{-TS} + \underbrace{\sum_j P_j \langle\Phi_j|\hat{H}-\mu\hat{N}|\Phi_j\rangle}_{E-\mu N} \\
&- \sum_{j,k} \Lambda_{j,k}\Big(\langle\Phi_k|\Phi_j\rangle - \delta_{k,j}\Big) - \eta\Big(\sum_j P_j - 1\Big)\Bigg\} \\
&= \min_{n(\vec{r})}\Bigg\{ \min_{|\Phi_j\rangle,P_j} \operatorname*{stat}_{\boldsymbol{\Lambda},\eta,\gamma(\vec{r}}\Bigg\{ \underbrace{k_B T \sum_j P_j \ln(P_j)}_{-TS} + \underbrace{\sum_j P_j \langle\Phi_j|\hat{H}-\mu\hat{N}|\Phi_j\rangle}_{E-\mu N} \\
&+ \int d^3r\, \gamma(\vec{r})\Big(\Big(\sum_j P_j \sum_\sigma \langle\Phi_j|\hat{\psi}^\dagger(\vec{x})\hat{\psi}(\vec{x})|\Phi_j\rangle\Big) - n(\vec{r})\Big) \\
&- \sum_{j,k} \Lambda_{j,k}\Big(\langle\Phi_k|\Phi_j\rangle - \delta_{k,j}\Big) - \eta\Big(\sum_j P_j - 1\Big)\Bigg\}\Bigg\} \\
&= \min_{n(\vec{r})}\Bigg\{ \int d^3r\, n(\vec{r}) v_{ext}(\vec{r}) + F_T^W[n(\vec{r})] - \mu \int d^3r\, n(\vec{r})\Bigg\} \qquad \text{(H.21)}
\end{aligned}$$

with

UNIVERSAL DENSITY FUNCTIONAL

The quantity

$$\begin{aligned}
F_T^{\lambda\hat{W}}[n(\vec{r})] \overset{\text{def}}{=} \min_{|\Phi_j\rangle,P_j} \operatorname*{stat}_{\boldsymbol{\Lambda},\eta,\gamma(\vec{r}} \Bigg\{ & \underbrace{k_B T \sum_j P_j \ln(P_j)}_{-TS} + \sum_j P_j \langle\Phi_j|\hat{T}+\lambda\hat{W}|\Phi_j\rangle \\
&+ \int d^3r\, \gamma(\vec{r})\Big(\Big(\sum_j P_j \sum_\sigma \langle\Phi_j|\hat{\psi}^\dagger(\vec{x})\hat{\psi}(\vec{x})|\Phi_j\rangle\Big) - n(\vec{r})\Big) \\
&- \sum_{j,k} \Lambda_{j,k}\Big(\langle\Phi_k|\Phi_j\rangle - \delta_{k,j}\Big) - \eta\Big(\sum_j P_j - 1\Big)\Bigg\} \qquad \text{(H.22)}
\end{aligned}$$

is the **universal density functional** . It is called universal, because it is an intrinsic property of the electron gas and independent of the external potential. This implies that the universal density functional is independent of the particular system.
The universal density functional depends on the mass of the particles, the temperature, the interaction $\lambda\hat{W}$ and the property that they are fermions.

H.2.5 Exchange and correlation energy

It turns out that the universal functional as defined above is so complicated, that it is difficult to find good approximations for it. The difficulty is related to the kinetic energy, which is responsible for chemical binding. A way out is to separate out the kinetic energy of a non-interacting electron gas. For the sake of convenience, we also separate out the Hartree energy, which itself is a functional of the electron density.

$$F_T^{\lambda\hat{W}}[n] = F_T^0[n] + E_H[n] + \underbrace{E_{xc}[n]}_{F_T^{\lambda\hat{W}}[n]-F_T^0[n]-E_H[n]} \qquad \text{(H.23)}$$

This defines the exchange correlation functional

$$E_{xc,T}[n] = F_T^{\lambda\hat{W}}[n] - F_T^0[n] - E_H[n] \tag{H.24}$$

The universal density functional can be determined for any interaction $\hat{W}$. Setting the interaction to zero yields the kinetic energy functional

$$\begin{aligned} F_T^0[n(\vec{r})] \stackrel{\text{def}}{=} \min_{|\Phi_j\rangle, P_j} \operatorname*{stat}_{\mathbf{\Lambda},\eta,\gamma(\vec{r})} \Bigg\{ & \underbrace{k_B T \sum_j P_j \ln(P_j)}_{-TS} + \sum_j P_j \langle\Phi_j|\hat{T}|\Phi_j\rangle \\ & + \int d^3r\, \gamma(\vec{r}) \Bigg(\Big(\sum_j P_j \sum_\sigma \langle\Phi_j|\hat{\psi}^\dagger(\vec{x})\hat{\psi}(\vec{x})|\Phi_j\rangle \Big) - n(\vec{r}) \Bigg) \\ & - \sum_{j,k} \Lambda_{j,k} \Big(\langle\Phi_k|\Phi_j\rangle - \delta_{k,j} \Big) - \eta \Big(\sum_j P_j - 1 \Big) \Bigg\} \end{aligned} \tag{H.25}$$

For a given density, the minima for the interacting and the non-interacting functionals differ. That is, the many-particle wave functions differ. Nevertheless, we may rewrite the grand potential in the form

$$\begin{aligned} \Omega_{T,\mu} = \min_{n(\vec{r})} \Bigg\{ & F^0[n(\vec{r})] + \int d^3r\, n(\vec{r}) v_{ext}(\vec{r}) + E_H[n(\vec{r})] \\ & + \underbrace{\Big(F_T^W[n(\vec{r})] - F^0[n(\vec{r})] - E_H[n(\vec{r})] \Big)}_{E_{xc}[n(\vec{r})]} - \mu \int d^3r\, n(\vec{r}) \Bigg\} \end{aligned} \tag{H.26}$$

where E_H is the Hartree energy defined in Eq. 2.33 on p. 58.

EXCHANGE AND CORRELATION ENERGY

Thus, the grand potential is

$$\Omega_{T,\mu} = \min_{n(\vec{r})} \Bigg\{ F^0[n(\vec{r})] + \int d^3r\, n(\vec{r}) v_{ext}(\vec{r}) + E_H[n(\vec{r})] + E_{xc,T}[n(\vec{r})] - \mu \int d^3r\, n(\vec{r}) \Bigg\} \tag{H.27}$$

with the **exchange-correlation functional**

$$E_{xc,T}[n(\vec{r})] \stackrel{\text{def}}{=} F_T^W[n(\vec{r})] - F^0[n(\vec{r})] - E_H[n(\vec{r})] \tag{H.28}$$

It turns out that it is much simpler to find good approximations for the exchange-correlation functional than for the universal density functional. This is the underlying reason for the success of density-functional theory.

Remember, that F_T^0 is **not** the kinetic energy of interacting electrons, but that of non-interacting electrons. Notice, that this is not an approximation, as long as we include the kinetic-energy correction $F^W - F^{(0)}$ in the exchange-correlation energy.

H.2.6 Kinetic-energy functional

The kinetic-energy functional

$$\begin{aligned} F_T^0[n(\vec{r})] \overset{\text{Eq. } H.25}{=} \operatorname*{stat}_{\gamma(\vec{r})} \Bigg\{ & - \int d^3r\, \gamma(\vec{r}) n(\vec{r}) \\ & + \min_{|\Phi_j\rangle, P_j} \operatorname*{stat}_{\mathbf{\Lambda}, \eta} \Bigg\{ k_B T \sum_j P_j \ln(P_j) + \sum_j P_j \langle \Phi_j | \Big[\hat{T} + \int d^4x\, \gamma(\vec{r}) \hat{\psi}^\dagger(\vec{x}) \hat{\psi}(\vec{x}) \Big] | \Phi_j \rangle \\ & - \sum_{j,k} \Lambda_{j,k} \Big(\langle \Phi_k | \Phi_j \rangle - \delta_{k,j} \Big) - \eta \Big(\sum_j P_j - 1 \Big) \Bigg\} \end{aligned} \tag{H.29}$$

can be expressed in terms of one-particle wave functions $|\psi_n\rangle$, the so-called **natural orbitals**, and **occupations** f_n of a non-interacting electron gas in an external potential $\gamma(\vec{r})$. The concept of natural orbitals and occupations will be described below in more detail.

$$\begin{aligned} F_T^0[n(\vec{r})] = \operatorname*{stat}_{\gamma(\vec{r})} \Bigg\{ & - \int d^3r\, \gamma(\vec{r}) n(\vec{r}) \\ & + \min_{f_n \in [0,1], |\psi_n\rangle} \operatorname*{stat}_{\mathbf{\Lambda}} \Bigg\{ k_B T \sum_n \Big(f_n \ln(f_n) + (1-f_n) \ln(1-f_n) \Big) + \sum_n f_n \langle \psi_n | \frac{\hat{\vec{p}}^2}{2m_e} + \hat{\gamma} | \psi_n \rangle \\ & - \sum_{m,n} \Lambda_{n,m} \Big(\langle \psi_m | \psi_n \rangle - \delta_{m,n} \Big) \Bigg\} \Bigg\} \end{aligned} \tag{H.30}$$

The ground state of the non-interacting system is a statistical average over Slater determinants in a basis of eigenstates of the one-particle Hamiltonian

$$\hat{h} = \int d^4x |\vec{x}\rangle \left[\frac{-\hbar^2}{2m_e} \vec{\nabla}^2 + \gamma(\vec{r}) \right] \langle \vec{x}| \tag{H.31}$$

Because of this form the Lagrange multiplier in the kinetic energy functional is named effective potential $v_{eff}(\vec{r}) = \gamma(\vec{r})$.

Thus, we arrive at the final form for the grand potential as it is used in density-functional calculations

$$\begin{aligned} \Omega_{T,\mu} = \min_{n(\vec{r})} \Bigg\{ & \min_{f_n \in [0,1], |\psi_n\rangle} \operatorname*{stat}_{\mathbf{\Lambda}, \gamma(\vec{r})} \Bigg\{ \underbrace{\sum_n f_n \langle \psi_n | \frac{\hat{\vec{p}}^2}{2m_e} | \psi_n \rangle}_{\text{non-interacting } E_{\text{kin}}} + \int d^3r\, n(\vec{r}) v_{ext}(\vec{r}) \\ & + \underbrace{\frac{1}{2} \int d^3r \int d^3r'\, \frac{e^2 n(\vec{r}) n(\vec{r'})}{4\pi\epsilon_0 |\vec{r} - \vec{r'}|}}_{\text{Hartree energy}} + E_{xc}[n(\vec{r})] \\ & + \underbrace{k_B T \sum_n \Big(f_n \ln(f_n) + (1-f_n) \ln(1-f_n) \Big)}_{-TS;\ S = \text{entropy of non-interacting electrons}} \underbrace{-\mu \int d^3r\, n(\vec{r})}_{-\mu N} \Bigg\} \\ & + \int d^4x\, \gamma(\vec{r}) \Big(\sum_n f_n \psi_n^*(\vec{x}) \psi_n(\vec{x}) - n(\vec{r}) \Big) - \sum_{m,n} \Lambda_{n,m} \Big(\langle \psi_m | \psi_n \rangle - \delta_{m,n} \Big) \Bigg\} \end{aligned} \tag{H.32}$$

H.2.7 Self-consistent equations

The minimum and stationary conditions define a set of equations that need to be obeyed simultaneously. It is called the set of self-consistent equations. These self-consistent equations can be solved iteratively to find the ground state.

We start with the variation with respect to density $n(\vec{r})$, one-particle wave functions $|\psi_n\rangle$ and occupations f_n.

$$\begin{aligned}
\frac{\partial\Omega}{\partial n(\vec{r})} &= v_{ext}(\vec{r}) + \underbrace{\int d^3r' \, \frac{e^2 n(\vec{r'})}{4\pi\epsilon_0|\vec{r}-\vec{r'}|}}_{v_H(\vec{r})} + \frac{\partial E_{xc}}{\partial n(\vec{r})} - \mu - \gamma(\vec{r}) \stackrel{!}{=} 0 \\
\frac{1}{f_n}\frac{\partial\Omega}{\partial\langle\psi_n|} &= \Big[\frac{\hat{\vec{p}}^2}{2m_e} + \gamma(\vec{r})\Big]|\psi_n\rangle - \sum_m |\psi_m\rangle\Lambda_{m,n}\frac{1}{f_n} \stackrel{!}{=} 0 \\
\frac{\partial\Omega}{\partial f_n} &= \langle\psi_n|\Big[\frac{\hat{\vec{p}}^2}{2m_e} + \gamma(\vec{r})\Big]|\psi_n\rangle + k_B T\Big[\ln(f_n) - \ln(1-f_n)\Big] \stackrel{!}{=} 0
\end{aligned} \tag{H.33}$$

From the first equation we obtain a definition for the **effective potential** for the non-interacting electrons.

$$v_{eff}(\vec{r}) \stackrel{\text{def}}{=} \gamma(\vec{r}) + \mu = v_{ext}(\vec{r}) + \underbrace{\int d^3r' \, \frac{e^2 n(\vec{r'})}{4\pi\epsilon_0|\vec{r}-\vec{r'}|}}_{v_H(\vec{r})} + \frac{\partial E_{xc}}{\partial n(\vec{r})} \tag{H.34}$$

The middle equation, is kind of Schrödinger equation.

$$\Big[\frac{\hat{\vec{p}}^2}{2m_e} + v_{eff}(\vec{r})\Big]|\psi_n\rangle = \sum_m |\psi_m\rangle\Big(\Lambda_{m,n} - \mu\delta_{m,n}\Big) \tag{H.35}$$

The Lagrange multipliers is the Hamilton matrix shifted relative to the chemical potential

$$\Lambda_{m,n} = \langle\psi_m|\Big[\frac{\hat{\vec{p}}^2}{2m_e} + v_{eff}(\vec{r})\Big]|\psi_n\rangle - \mu\delta_{m,n} \tag{H.36}$$

From the last equation, we obtain the equilibrium occupations as the Fermi distribution function. The diagonal elements of $\Lambda_{m,n}$ act here as energies.

$$f_n = \frac{1}{1+e^{\beta(\Lambda_{n,n}-\mu)}} \tag{H.37}$$

The relation between the density and the wave functions and occupations is obtained from the constraint equation, i.e. the variation with respect to $\gamma(\vec{r})$

$$n(\vec{r}) = \sum_n f_n \psi_n^*(\vec{x})\psi_n(\vec{x}) \tag{H.38}$$

If all occupations differ, the wave functions must be furthermore eigenstates of the effective Hamiltonian.[4]

$$\Big[\frac{\hat{\vec{p}}^2}{2m_e} + v_{eff}(\vec{r})\Big]|\psi_n\rangle = |\psi_n\rangle\epsilon_n \tag{H.39}$$

The energy eigenvalues are called **Kohn-Sham energies**.

[4] Editor: This is not convincing yet! Show the energy variation under a unitary transform.

SELF-CONSISTENT EQUATIONS OF DFT

$$v_{eff}(\vec{r}) = v_{ext}(\vec{r}) + \int d^3r' \, \frac{e^2 n(\vec{r'})}{4\pi\epsilon_0 |\vec{r} - \vec{r'}|} + \frac{\partial E_{xc}}{\partial n(\vec{r})} \tag{H.40}$$

$$\Big[\frac{\hat{\vec{p}}^2}{2m_e} + v_{eff}(\vec{r})\Big]|\psi_n\rangle = |\psi_n\rangle\epsilon_n \tag{H.41}$$

$$n(\vec{r}) = \sum_n f_n \psi_n^*(\vec{x})\psi_n(\vec{x}) \tag{H.42}$$

$$f_n = \frac{1}{1 + e^{\beta(\epsilon_n - \mu)}} \tag{H.43}$$

H.3 One-particle density matrices and two-particle densities

In order to get used with the terminology, let me introduce a number of definitions related to density matrices[48].

H.3.1 Pair-correlation function and hole function

Another quantity that is useful is the **pair-correlation function**

PAIR-CORRELATION FUNCTION

$$g(\vec{r}, \vec{r}_0) = \frac{n^{(2)}(\vec{r}, \vec{r}_0)}{n(\vec{r}_0)}$$

The pair-correlation function describes the probability to find an electron at position $\vec{r}$, given that there is one at $\vec{r}_0$. The pair-correlation function is the electron density seen by one electron that is located at $\vec{r}_0$. Consider an N-electron system. Pick out one electron and determine the density of the remaining $N-1$ electrons.

Given that an electron will see at large distances nothing but the charge density itself, it makes sense to define a more short-ranged quantity, namely the **exchange-correlation hole function** $h(\vec{r}, \vec{r}_0)$

HOLE FUNCTION

$$g(\vec{r}, \vec{r}_0) = n(\vec{r}) + h(\vec{r}, \vec{r}_0)$$

The physical picture of the hole function is that each electron "sees" the total density $n(\vec{r})$ and the density $h(\vec{r}, \vec{r'})$ of "one missing electron". The density $h(\vec{r}, \vec{r'})$ is like a hole in the total charge density due to the fact that the remaining electrons do not come near to the electron in question. Thus, the Coulomb repulsion between the electrons is reduced relative to the Hartree energy by the attraction of the electron to its exchange-correlation hole.

The two-particle density can now be expressed by the density and the exchange-correlation hole function as

$$n^{(2)}(\vec{r}, \vec{r}_0) = n(\vec{r}_0)\,[n(\vec{r}) + h(\vec{r}, \vec{r}_0)]$$

Now, we can also rewrite the interaction energy in the form

$$E_{int} = \underbrace{\frac{1}{2}\int d^3r \int d^3r' \; \frac{e^2 n(\vec{r}) n(\vec{r'})}{4\pi\epsilon_0 |\vec{r} - \vec{r'}|}}_{E_H} + \underbrace{\int d^3r \; n(\vec{r}) \frac{1}{2} \int d^3r' \; \frac{e^2 h(\vec{r'}, \vec{r})}{4\pi\epsilon_0 |\vec{r} - \vec{r'}|}}_{U_{xc}} \tag{H.44}$$

U_{xc} is the **potential energy of exchange and correlation**. It differs from the exchange and correlation energy E_{xc}, because it does not contain the kinetic energy contribution to the correlation energy.

H.4 Adiabatic connection

We learned that one can reasonably estimate the exchange-correlation hole, and evaluate the potential energy of exchange and correlation. However, it is nearly hopeless to estimate the contribution of the kinetic energy to the correlation energy, needed to arrive at the exchange and correlation energy functional $E_{xc}[n(\vec{r})]$.

If there would be no cost to deform the exchange-correlation hole, the latter would simply adjust such that the electrostatic energy is optimized. One can easily estimate how the hole would look like: It would have the shape of a hard sphere centered at the reference electron. Its radius would be determined by the sum rule that says that there is exactly one positive charge in the exchange-correlation hole. The reason for this shape is that the electron would repel its neighbors as much as possible, in order to reduce its electrostatic interaction.

However as the exchange-correlation hole is deformed, there is a price to pay, namely that the kinetic energy goes up. In the extreme case of a hard-sphere like hole, the wave functions would have steps, that is infinite curvature. The kinetic energy is just a measure of the curvature of the wave function. Thus, the deformation of the hole costs kinetic energy. The final shape of the XC-hole is therefore a balance between electrostatic gain and kinetic energy cost.

The **adiabatic connection**[186, 187, 188] is a theorem that allows one to relate the net energy gain, including the kinetic energy cost, to the electrostatic energy gain only, but for variable strengths of the interaction energy. While this theorem looks like mystery, it cannot be applied directly. Nevertheless it provides an important route that allows important approximations to be made. The theorem is demonstrated in the following:

In order to simplify the derivation we consider only a single many-particle wave function instead of an ensemble. The generalization can be done without difficulties.

We consider a given electron density for which the non-interacting functional $F_0[n(\vec{r})]$ is exactly known.

$$\begin{aligned} F_\lambda[n(\vec{r})] = {} & \langle \Phi_\lambda | \hat{T} + \lambda \hat{W} | \Phi_\lambda \rangle \\ & + \int d^3r \; \mu_\lambda(\vec{r}) \Big(\langle \Phi_\lambda | \hat{n}(\vec{r}) | \Phi_\lambda \rangle - n(\vec{r}) \Big) - E_\lambda \Big(\langle \Phi_\lambda | \Phi_\lambda \rangle - 1 \Big) \end{aligned}$$

where $|\Phi_\lambda\rangle$ is the many-electron wave function that minimizes F_λ under the constraint that the density of the wave function is equal to $n(\vec{r})$. The function $\mu_\lambda(\vec{r})$ represents the Lagrange parameters. The operator

$$\hat{n}(\vec{r}) \stackrel{\text{def}}{=} \sum_\sigma \hat{\psi}^\dagger(\vec{x}) \hat{\psi}(\vec{x})$$

is the operator that extracts the electron density from the wave function.

The wave functions that minimize the functional obey the Schrödinger equation

$$\left[\hat{T} + \lambda \hat{W} + \int d^3r \; \mu_\lambda(\vec{r}) \hat{n}(\vec{r}) - E_\lambda \right] |\Phi_\lambda\rangle = 0 \tag{H.45}$$

This means that as the interaction strength is increased, a local potential, $\mu_\lambda(\vec{r})$, is switched on that ensures that the electron density remains unchanged.

If we know the derivatives of the functional with respect to the interaction strength λ, and if we know the functional for the non-interacting electron gas, we can determine the functional for the interacting electron gas as

$$\begin{aligned} F_1[n(\vec{r})] &= F_0[n(\vec{r})] + \int_0^1 d\lambda \, \frac{dF_\lambda[n(\vec{r})]}{d\lambda} \\ &= \langle\Phi_0|\hat{T}|\Phi_0\rangle + \int_0^1 d\lambda \, \frac{dF_\lambda[n(\vec{r})]}{d\lambda} \end{aligned}$$

The first term is simply the kinetic energy of the non-interacting electron gas with the same density as the interacting system.

Now we can show that the derivative of the functional with respect to the interaction strength can be determined from the interaction energy alone. The proof rests on the **Hellmann-Feynman theorem**.

$$\begin{aligned} \frac{dF_\lambda[n(\vec{r})]}{d\lambda} &= \frac{d}{d\lambda}\Big[\langle\Phi_\lambda|\hat{T}+\lambda\hat{W}|\Phi_\lambda\rangle \\ &\quad + \int d^3r\, \mu_\lambda(\vec{r})\Big(\langle\Phi_\lambda|\hat{n}(\vec{r})|\Phi_\lambda\rangle - n(\vec{r})\Big) - E_\lambda\Big(\langle\Phi_\lambda|\Phi_\lambda\rangle - 1\Big)\Big] \\ &= \Big\langle\frac{d\Phi_\lambda}{d\lambda}\Big|\hat{T}+\lambda\hat{W}\Big|\Phi_\lambda\Big\rangle + \Big\langle\Phi_\lambda\Big|\hat{W}\Big|\Phi_\lambda\Big\rangle + \Big\langle\Phi_\lambda\Big|\hat{T}+\lambda\hat{W}\Big|\frac{d\Phi_\lambda}{d\lambda}\Big\rangle \\ &\quad + \int d^3r\, \frac{d\mu_\lambda(\vec{r})}{d\lambda}\underbrace{\Big(\langle\Phi_\lambda|\hat{n}(\vec{r})|\Phi_\lambda\rangle - n(\vec{r})\Big)}_{=0} \\ &\quad + \int d^3r\, \mu_\lambda(\vec{r})\left(\Big\langle\frac{d\Phi_\lambda}{d\lambda}\Big|\hat{n}(\vec{r})\Big|\Phi_\lambda\Big\rangle + \Big\langle\Phi_\lambda\Big|\hat{n}(\vec{r})\Big|\frac{d\Phi_\lambda}{d\lambda}\Big\rangle\right) \\ &\quad - \frac{dE_\lambda}{d\lambda}\underbrace{\Big(\langle\Phi_\lambda|\Phi_\lambda\rangle - 1\Big)}_{=0} - E_\lambda\Big(\Big\langle\frac{d\Phi_\lambda}{d\lambda}\Big|\Phi_\lambda\Big\rangle + \Big\langle\Phi_\lambda\Big|\frac{d\Phi_\lambda}{d\lambda}\Big\rangle\Big) \\ &= \langle\Phi_\lambda|\hat{W}|\Phi_\lambda\rangle \\ &\quad + \Big\langle\frac{d\Phi_\lambda}{d\lambda}\Big|\underbrace{\Big[\hat{T}+\lambda\hat{W}+\int d^3r\,\mu_\lambda(\vec{r})\hat{n}(\vec{r}) - E_\lambda\Big]}_{=0}\Big|\Phi_\lambda\Big\rangle \\ &\quad + \underbrace{\Big\langle\Phi_\lambda\Big|\Big[\hat{T}+\lambda\hat{W}+\int d^3r\,\mu_\lambda(\vec{r})\hat{n}(\vec{r}) - E_\lambda\Big]}_{=0}\Big|\frac{d\Phi_\lambda}{d\lambda}\Big\rangle \\ &\overset{\text{Eq. } H.45}{=} \langle\Phi_\lambda|\hat{W}|\Phi_\lambda\rangle \end{aligned}$$

Thus, we can express the functional for the finite interaction strength as

$$F_1[n(\vec{r})] = \langle\Phi_0|\hat{T}|\Phi_0\rangle + \underbrace{\int_0^1 d\lambda\, \langle\Phi_\lambda|\hat{W}|\Phi_\lambda\rangle}_{E_H[n(\vec{r})]+E_{xc}[n(\vec{r})]}$$

Thus, we have obtained an explicit expression for the exchange-correlation energy, that does not directly refer to the kinetic energy.

$$E_{xc}[n(\vec{r})] = \int_0^1 d\lambda\, \langle\Phi_\lambda|\hat{W}|\Phi_\lambda\rangle - \underbrace{\frac{1}{2}\int d^3r \int d^3r' \, \frac{e^2 n(\vec{r})n(\vec{r'})}{4\pi\epsilon_0|\vec{r}-\vec{r'}|}}_{E_H}$$

This expression has the problem that we still need the wave functions $|\Phi_\lambda\rangle$ for all possible values for the interaction strength.

The interaction energy can further be expressed by the exchange-correlation hole for a given value of the interaction, namely

$$\langle\Phi_\lambda|\hat{W}|\Phi_\lambda\rangle = \frac{1}{2}\int d^3r \int d^3r' \, \frac{e^2 n(\vec{r}) n(\vec{r'})}{4\pi\epsilon_0|\vec{r}-\vec{r'}|} + \int d^3r \; n(\vec{r}) \frac{1}{2}\int d^3r' \, \frac{e^2 h_\lambda(\vec{r},\vec{r'})}{4\pi\epsilon_0|\vec{r}-\vec{r'}|}$$

so that

$$E_{xc} = \int d^3r \; n(\vec{r}) \underbrace{\int_0^1 d\lambda \; \frac{1}{2}\int d^3r' \, \frac{e^2 h_\lambda(\vec{r},\vec{r'})}{4\pi\epsilon_0|\vec{r}-\vec{r'}|}}_{=:\epsilon_{xc}} \tag{H.46}$$

The variable ϵ_{xc}, which itself is a functional of the density is the exchange-correlation energy per electron.

H.5 Ideas that guide the construction of density functionals

H.5.1 Screened interaction

It is possible[5] to reformulate the exchange-correlation energy by the exchange-only energy with a screened interaction. This is a form that reminds of the so-called **GW approximation**, where the self-energy is expressed by Green's-function times screened interaction.

$$\begin{aligned} E_{xc} &\overset{\text{Eq. H.46}}{=} \frac{1}{2}\int d^3r \int d^3r' \; n(r) h_0(r,r') \underbrace{\int d\lambda \frac{h_\lambda(\vec{r},\vec{r'})}{h_0(\vec{r},\vec{r'})} \frac{e^2}{4\pi\epsilon_0|\vec{r}-\vec{r'}|}}_{v_{scr}(\vec{r}-\vec{r'})} \\ &= \frac{1}{2}\sum_{ij}\int d^3r \int d^3r' \; \varphi_i^*(\vec{r})\varphi_j(\vec{r}) v_{scr}(\vec{r}-\vec{r'}) \varphi_j^*(\vec{r'})\varphi_i(\vec{r'}) \end{aligned}$$

where the screened interaction is defined as

$$v_{scr}(\vec{r}-\vec{r'}) \overset{\text{def}}{=} \int d\lambda \; \frac{h_\lambda(\vec{r},\vec{r'})}{h_0(\vec{r},\vec{r'})} \frac{e^2}{4\pi\epsilon_0|\vec{r}-\vec{r'}|}$$

Note that, in contrast to the GW approximation, our expression is exact, but, on the other hand, it is limited to the ground state.

Note also that the screened interaction in this formulation only enters the exchange term, but not the Hartree term. It also includes the kinetic energy correction.

The qualitative behavior can be understood easily:

- The hole function $h_\lambda(\vec{r},\vec{r'})$ for a finite interaction is generally more compact than the on obtained without interaction. Thus, the screened interaction v_{scr} is generally more short ranged than the unscreened interaction.
- The screened interaction for $\vec{r}=\vec{r'}$ is identical to the unscreened interaction, because the hole function cancels exactly the spin density, independent of the strength of the interaction.
- Due to the compression of the hole upon increasing interaction and because of the sum-rule that the hole integrates to exactly one positive charge, the interaction must be enhanced for intermediate distances.

[5] This is an idea from the author, that has not been crosschecked properly. Therefore, some caution is required.

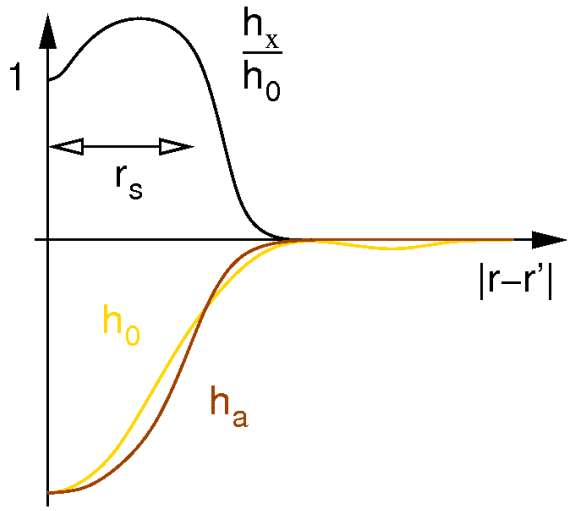


Fig. H.2: Schematic diagram of the effect of the screening of the interaction. The golden line h_0 is the hole function of the non-interacting reference system, while the red line h_λ is the hole function in presence of a scaled interaction. The ratio scales the Coulomb interaction in the exchange term. It suppresses the long-range tail of the interaction, and enhances the interaction for intermediate distances. r_s is the average electron radius $\frac{4\pi}{3} r_s^2 * n = 1$. ($h_a$ and h_x should be h_λ; Problem with the drawing program.)

- The screening will be more effective, if the price for the distortion of the wave function is low, that is for a low density. This implies that the unscreened interaction is a reasonable approximation in the high-density region around the atomic center, while the tail region of a molecule is better described by a more short-ranged interaction.

H.5.2 Hybrid functionals

The adiabatic connection scheme is exploited in the construction of so-called **hybrid functionals**. These density functionals describe the exchange-correlation energy as a mixture of the correct exchange, obtained as in the Hartree-Fock method and another local or gradient corrected functional.

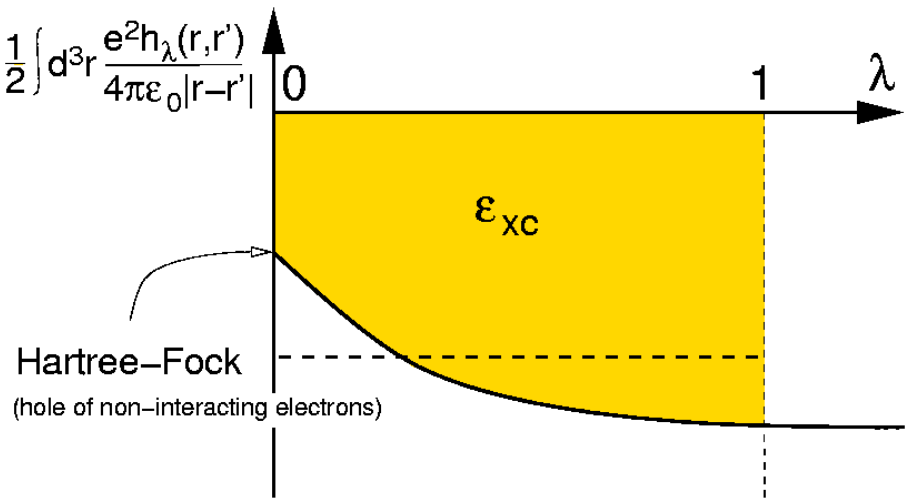
The performance of the hybrid functionals is probably among the best. They have the disadvantage that they require that the Hartree-Fock exchange must be evaluated, which is computationally more challenging than the evaluation of the regular density functionals.

The idea behind the hybrid functionals is that the local functionals are appropriate if the interaction energy is very large. However if the interaction energy is small, the exchange hole is given by Hartree-Fock exchange.

If for example the kinetic energy dominates, the shape of the exchange-correlation hole cannot adjust, and we can approximate $h_\lambda(\vec{r}, \vec{r'}) \approx h_0(\vec{r}, \vec{r'})$ by the hole of the non-interacting electron gas. Thus, we obtain

$$\epsilon_{xc} \approx \frac{1}{2} \int d^3r' \, \frac{e^2 h_0(\vec{r}, \vec{r'})}{4\pi\epsilon_0 |\vec{r} - \vec{r'}|}$$

If the electrostatic interaction dominates over the kinetic energy then $h_1(\vec{r}, \vec{r'})$ would be a hard sphere, and therefore fairly local. Therefore, the hybrid functionals try to approximate the integral by a superposition of HF-exchange and a local density functional.



H.6 Scaling of with a fixed shape of the XC-hole function

Even before the invention of density-functional theory per se, the so-called X_α method has been introduced. Today, the X_α method has mostly historical value. The X_α method uses the expression for the exchange of a homogeneous electron gas instead of the exchange-correlation energy. However, the exchange energy has been scaled with a parameter, namely X_α, that has been adjusted to Hartree-Fock calculations. The results are shown in Fig. H.3.

The rationale behind the X_α-method is a dimensional argument. Choose a given shape for the exchange-correlation hole, but scale it according to the density and the electron sum rule. Then the exchange-correlation energy per electron always scales like $n^{\frac{1}{3}}$. Each shape corresponds to a pre-factor.

Consider a given shape described by a function $f(\vec{r})$ with

$$f(\vec{0}) = 1$$
$$\int d^3r\, f(\vec{r}) = 1$$

Now, we express the hole function by the function f by scaling its magnitude at the origin such that the amplitude of the hole cancels the electron density. Secondly, we stretch the function in space so that the sum rule, which says that the hole must integrate to -1, is fulfilled. These conditions yield the model for the exchange-correlation hole.

$$h(\vec{r}_0, \vec{r}) = -n(\vec{r}_0) f(\frac{\vec{r} - \vec{r}_0}{n(\vec{r}_0)^{\frac{1}{3}}})$$

The corresponding exchange-correlation energy per electron is

$$\epsilon_{xc}(\vec{r}) = -\frac{1}{2} \int d^3r'\, \frac{e^2}{4\pi\epsilon_0 |\vec{r} - \vec{r'}|} f(\frac{\vec{r} - \vec{r'}}{n(\vec{r})^{\frac{1}{3}}})$$

If we introduce a variable transform

$$\vec{y} = \frac{\vec{r} - \vec{r'}}{n(\vec{r})^{\frac{1}{3}}}$$

we obtain

$$\epsilon_{xc}(\vec{r}) = -\frac{n(\vec{r})^{\frac{1}{3}}}{2} \int d^3y'\, \frac{e^2}{4\pi\epsilon_0 |\vec{y}|} f(\vec{y}) = -C n^{\frac{1}{3}}$$

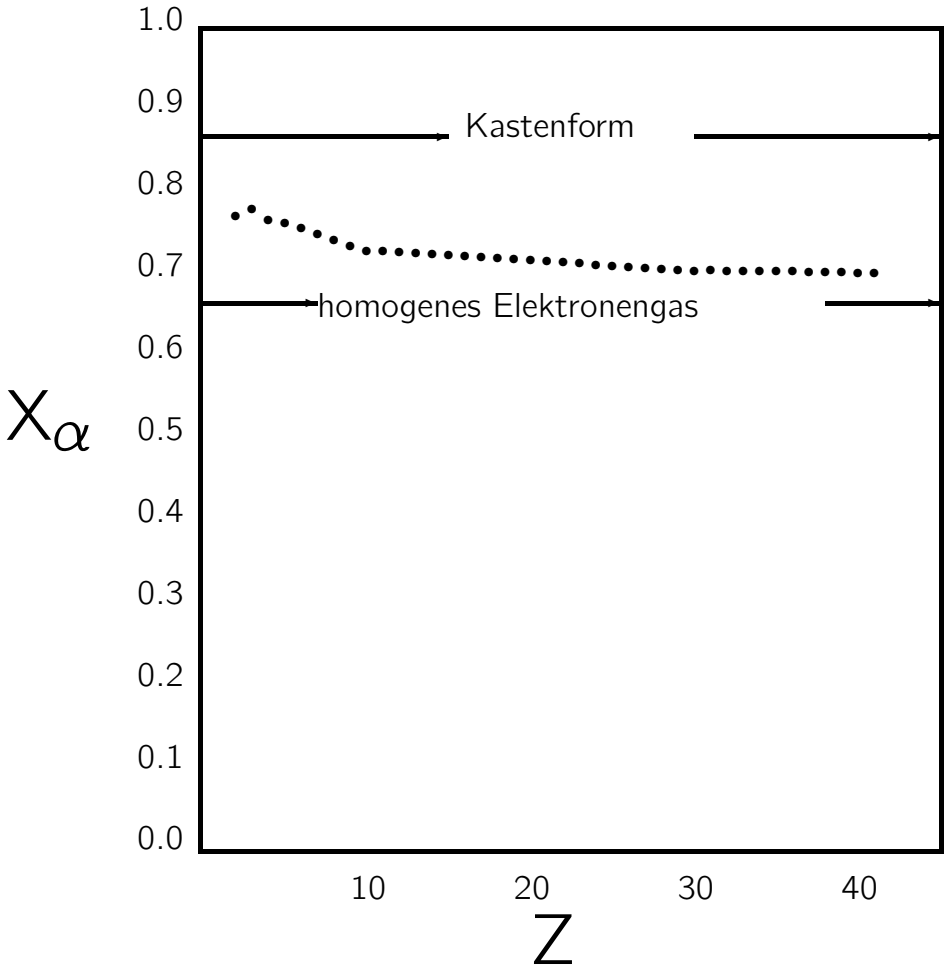


Fig. H.3: X_α value obtained by comparison of the atomic energy with exact Hartree-Fock calculations as function of atomic number of the atom.[189, 190]

where C is a constant that is entirely defined by the shape function $f(\vec{r})$.

In general, the X_α method yields larger band gaps than density-functional theory. The latter severely underestimates band gaps. This is in accord with the tendency of Hartree-Fock to overestimate band gaps. In contrast to Hartree-Fock, however, the X_α method is superior for the description of metals because it does not lead to a vanishing density of states at the Fermi level.

H.7 Local density functionals

The first true density functionals were constructed for the homogeneous electron gas, by extracting the exchange-correlation energy per electron ϵ_{xc} from a calculation of the interacting homogeneous electron gas.

A breakthrough came about when Ceperley and Alder[55] performed quantum Monte-Carlo calculations of the homogeneous electron gas as function of the density. Quantum Monte-Carlo calculations are computationally expensive, but provide the energy of an interacting electron gas in principle exactly, that is with the exceptions of numerical errors. These results have been parameterized by Perdew and Zunger[170] and combined with so-called RPA results for the high-density limit. **RPA** stands for **Random-Phase Approximation**[50], which is accurate in the high density limit.

These density functionals exhibit very good results for solids. Electron densities are nearly perfect.

Bond distances are typically underestimated by 1-3 % and bond angles agree with experiment within few degrees. Binding energies, on the other hand, are strongly overestimated. The errors are in the range of electron volts and thus comparable to bond energies. Thus, these functionals have been useless for studying chemical reactions. However, the results for solid-state processes such as diffusion have been very good. This has lead to a long-standing misunderstanding between solid-state physicists and chemists about the usefulness of density-functional theory. The density functionals worked find for solids, which was what the physicists are interested in, while they were a disaster for the binding energies of molecules, the major interest of chemists. This difficulty has been overcome by the gradient corrected density functionals discussed later.

The overestimate of the binding energies covers up the lack of Van der Waals interactions. For example, the binding energy and the bond distances of Nobel gases are in very good agreement with experiment. However, the agreement is good for the wrong reason. The weak van der Waals interaction is not described properly in local density functionals, but the overbinding compensates for this fact.

For a long time it was surprising that the approximate density functionals work at all. They have been derived from a completely homogeneous electron gas and are applied to an electron density of real materials, which are far from homogeneous. Jones and Gunnarsson gave one explanation, namely that density functionals observe an important sum rule, namely that the exchange-correlation hole integrates to minus one electron charge. Fig. H.4 compares the exchange hole of a free-electron gas with that of a nitrogen atom, demonstrating that despite their very different shape, their contributions to the exchange energy are similar.

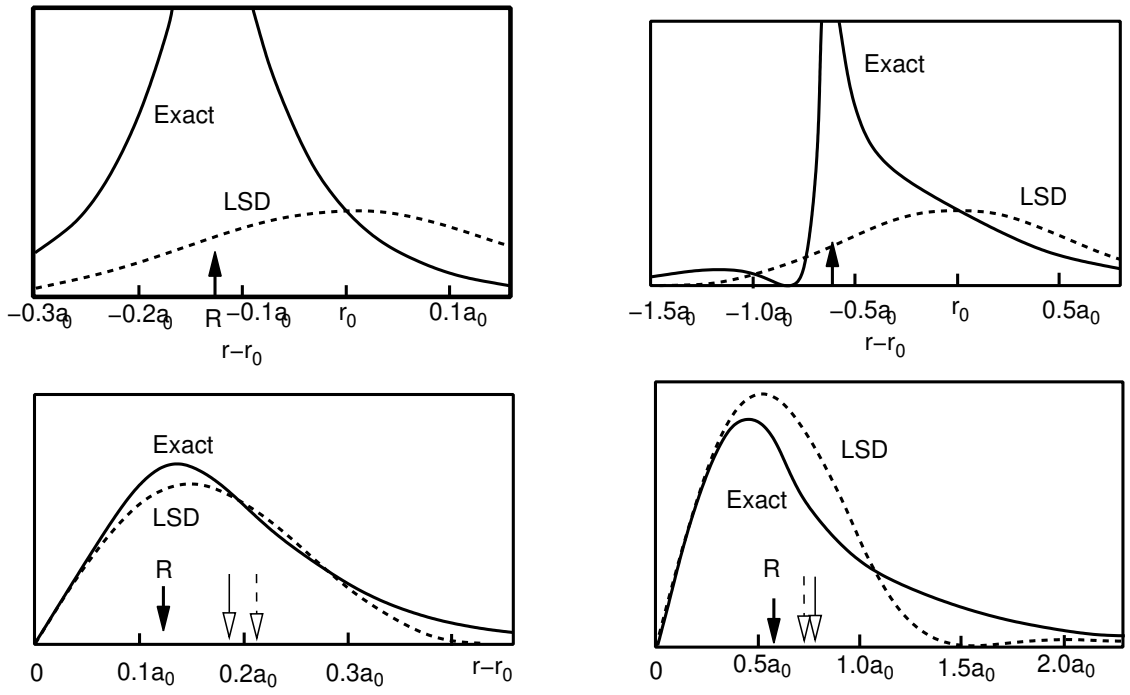


Fig. H.4: exchange-correlation hole of an electron in the nitrogen atom (full line) and in the local density-functional approximation (dashed) [191]. In the left row, the reference electron is located 0.13 a_0 from the nucleus and on the right it is located further, at 0.63 a_0. Even though the shape of the DFT-exchange hole deviates grossly from the correct exchange hole, the spherical averages shown in the bottom figures are similar, which is attributed to the particle sum rule, obeyed in the local density approximation (LDA). The arrows pointing down indicate the exact and the DFT result of $\left[\int d^3r \, \frac{|h(\vec{r},\vec{r}_0)|}{|\vec{r}-\vec{r}_0|}\right]^{-1}$. Similar results are available for neon[170].

H.8 Local spin-density approximation

In order to describe magnetic systems, or so-called open-shell molecules, one uses the local spin-density approximation, where the spin-dependent density $n(\vec{x}) = n(\vec{r}, \sigma)$ is used instead of the total density $n(\vec{r}) = \sum_\sigma n(\vec{x})$. As a result, we obtain one-particle wave functions with spin-up and spin-down character and one obtains two effective potentials, one for the spin-up electrons and another for the spin-down electrons.

The difference between the effective potentials acts like a magnetic field, even though its origin is purely electrostatic, namely exchange and correlation also called the **exchange interaction**.

H.8.1 Non-collinear local spin-density approximation

While the local spin-density formalism only allows one-particle wave function to have either purely spin-up or purely spin-down character, the non-collinear formulation allows the wave functions to have a mixed spin-up and spin-down character. As a result, the magnetization can not only vary in magnitude but also in direction.

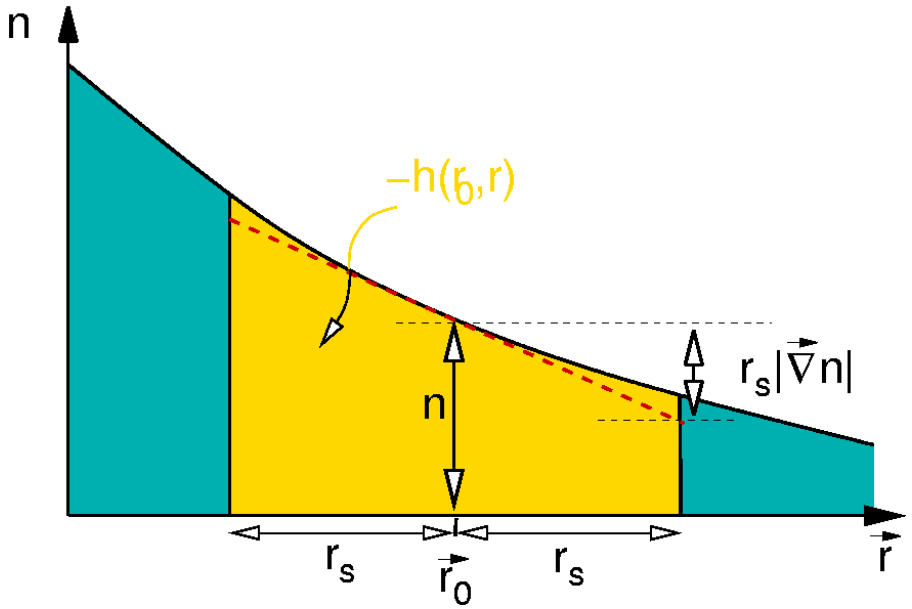
H.9 Generalized gradient functionals

For a long time one has hoped to obtain better functionals by including also a dependence on the gradient of the density. The first attempts started from a model with a weakly oscillating electron density. The resulting functionals however were worse than the local functionals.

The reason for this failure was that when the expansion for slowly varying densities are extrapolated to strongly oscillating densities, the density of the exchange-correlation hole was overcompensating the total density.

Later, one realized that one should introduce a dimension-less scaled gradient defined as

$$s = \frac{r_s|\vec{\nabla} n|}{n}$$



The scaled gradient allows one to switch off the gradient corrections in a physical sense, that is if the hole runs into the danger of producing a negative correlation function $g(\vec{x'}, \vec{x})$.

One way to construct the density is to use the results for slowly varying densities, which provides the parameter β.

$$\epsilon_{xc}(n,s) = \epsilon_{xc}^{hom}\Big[1+\beta(n)s^2\Big] \qquad \text{for} \qquad s << 1 \tag{H.47}$$

Surprisingly, the scaled gradient is largest in the tails of the wave functions, where the density falls off exponentially, that is

$$n(\vec{r}) \approx A\mathrm{e}^{-\lambda\vec{e}\vec{r}}$$

where $\vec{e}$ is the unit vector pointing into the direction in which the density falls off. Let us determine the scaled gradient for this density

$$s = \sqrt[3]{\frac{3}{4\pi}}\frac{A\lambda\exp(-\lambda\vec{e}\vec{r})}{A^{\frac{4}{3}}\lambda\exp(-\frac{4}{3}\lambda\vec{e}\vec{r})} = \sqrt[3]{\frac{3}{4\pi}}\lambda n^{-\frac{1}{3}} \to \infty$$

If we use only the gradient correction with the small-s expansion, the exchange-correlation energy per particle clearly becomes infinite.

However, in the tail region we can make use of other information. Consider an electron that is far outside of a molecule. It is clear that it "sees" a molecule with $N-1$ electrons. Thus, the hole is entirely localized on the molecule and the center of the hole is far from the reference electron. If the hole is at the molecule and the reference electron is far from it, we can estimate its interaction by

$$\epsilon_{xc} = \frac{1}{2r} \tag{H.48}$$

where r is the distance of the electron from the molecule.

Let me demonstrate the construction of such a gradient corrected functional using the example of Becke's gradient correction for exchange[192]. We make an ansatz for the exchange energy per electron as

$$\epsilon_{xc} = Cn^{\frac{1}{3}}F(s) \tag{H.49}$$

where C is the pre-factor for the exchange energy. The function $F(s)$ is determined such that small gradient expansion, Eq. H.47, is reproduced, and that the exchange energy per electron in the tail region is correct.

To consider the tail region we require

$$\epsilon_{xc} \overset{\text{Eq. H.49}}{=} Cn^{\frac{1}{3}}F(s) \overset{\text{Eq. H.48}}{=} \frac{1}{2r} \qquad \Rightarrow \qquad F(s) = \frac{1}{2Crn^{\frac{1}{3}}} \qquad \text{for} \quad s \to \infty$$

First we express the radius by the density and insert the result in Eq. H.50 to obtain an expression for $F(n(s))$.

$$n(r) = A\mathrm{e}^{-\lambda r} \qquad \Rightarrow \qquad r(n) = -\frac{1}{\lambda}\ln\Big[\frac{n}{A}\Big]$$
$$\Rightarrow F(s) = \frac{1}{2Crn^{\frac{1}{3}}} = \frac{-\lambda}{2Cn^{\frac{1}{3}}\left(\ln[n]-\ln[A]\right)}$$

Next we express the density by the scaled gradient and insert the result in the above equation to

obtain an expression for $F(s)$.

$$\begin{aligned} s(n) &= \sqrt[3]{\frac{3}{4\pi}}\lambda n^{-\frac{1}{3}} \qquad \Rightarrow \qquad n(s) = \frac{3\lambda^3}{4\pi}s^{-3} \\ \Rightarrow F(s) &= \frac{-\lambda}{2Cn^{\frac{1}{3}}\left(\ln[n] - \ln[A]\right)\right)} \\ &= \frac{-\lambda}{2C\sqrt[3]{\frac{3\lambda^3}{4\pi}}\frac{1}{s}\left(\ln[\frac{3\lambda^3}{4\pi}s^{-3}] - \ln[A]\right)} \\ &= \frac{-s}{2C\sqrt[3]{\frac{3}{4\pi}}\left(\ln[\frac{3\lambda^3}{4\pi A^3}s^{-3}] - 3\ln[s]\right)} \\ &\overset{s\to\infty}{\approx} \frac{1}{6C}\sqrt[3]{\frac{4\pi}{3}}\frac{s^2}{s\ln[s]} \end{aligned}$$

This equation gives us the large gradient limit of $F(s)$.

In order to connect the low gradient limit with the large gradient limit we choose

$$F(s) = 1 + \frac{\beta s^2}{1 + 6C\beta s \sinh^{-1}(s)}$$

The result is shown in Fig. H.5.

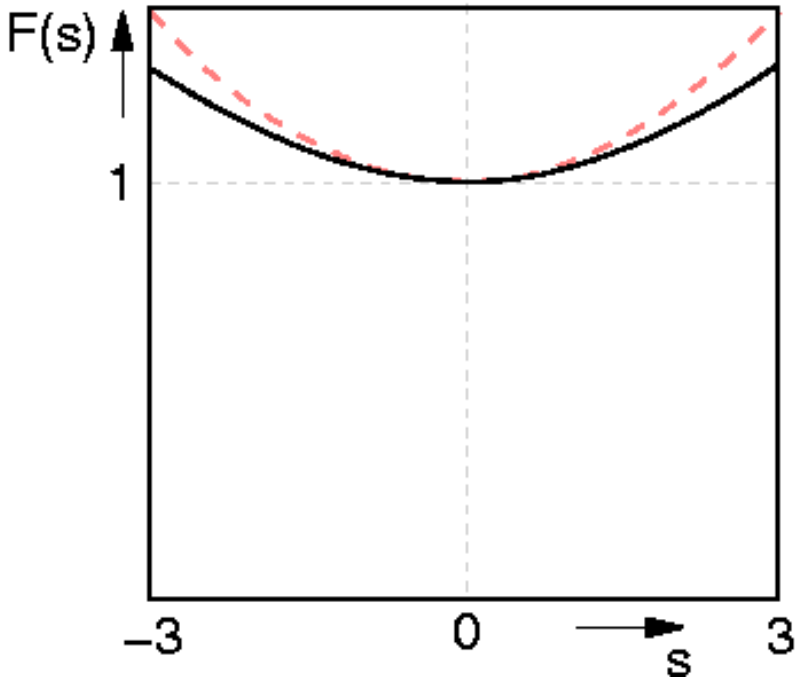


Fig. H.5: The function $F(s)$ from Becke's gradient corrected functional [192] for the exchange energy and from the small gradient expansion (dashed). Note that the gradient correction of Becke is smaller than the expansion for large gradients.

The gradient correction plays the role of a surface energy, as it contributes mostly in the tail region. While the exchange-correlation energy per electron falls off exponentially in the local functionals, it falls off as $\frac{1}{2r}$ in the gradient corrected functionals. This effect lowers the energy in the tail region of a molecule compared to the local functionals. If we break a bond, the surface area of a molecule

increases, because the bond is transformed into a tail region. Thus, the gradient correction favors the dissociation of the bonds. As a consequence, gradient corrected functionals avoid the artificial overbinding of the local functionals. This argument also explains that local functionals perform fairly well in solids: If an atom diffuses, there is no additional surface created so that the gradient correction is minor.

Up to know there is an entire suite of different gradient corrected functionals. They are called **Generalized Gradient Approximations (GGA)** to differentiate them from the gradient expansions. The most common functionals are the Perdew-Wang-91-GGA, which has been superseded by the simpler Perdew-Burke-Ernzerhof functional. Both yield nearly identical results.

As shown in Fig. H.6, the performance of gradient corrected functionals is extremely good also for binding energies, which were unsatisfactory in the local density functionals. This has drawn also the chemists into the field of density-functional calculations.

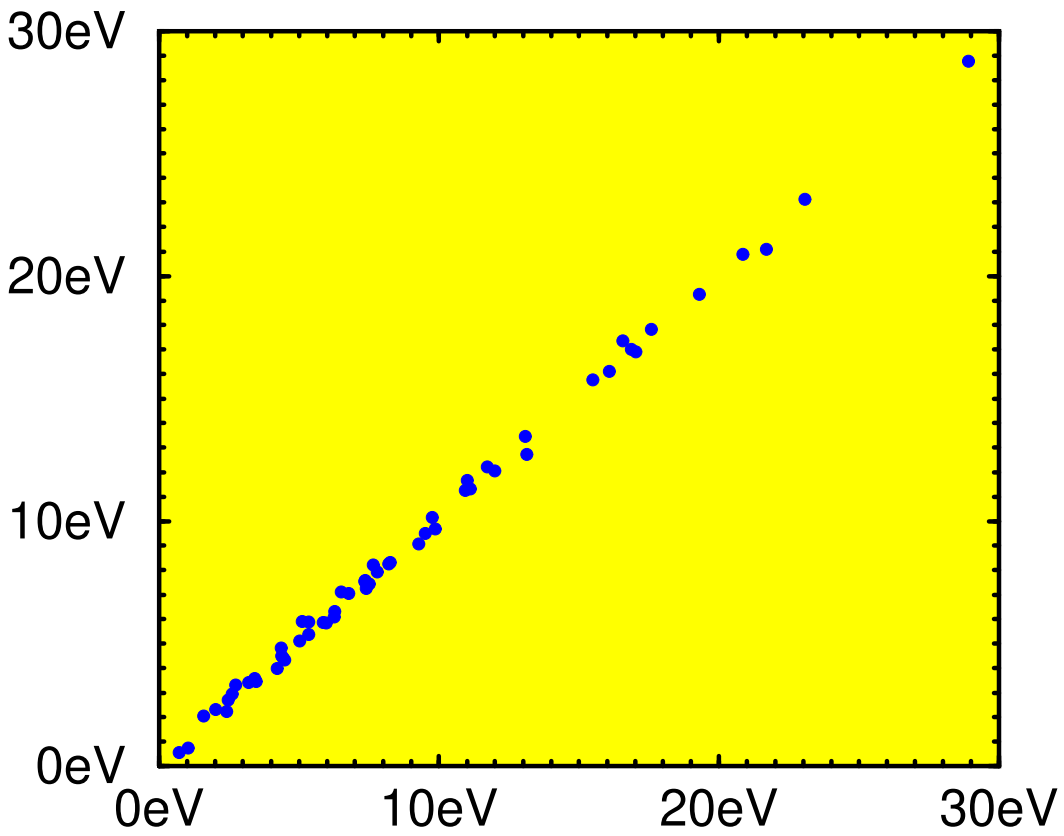


Fig. H.6: Accuracy of the atomization energies calculated with the Becke88-Perdew86 density functional compared to experiment.

H.10 Additional material

H.10.1 Relevance of the highest occupied Kohn-Sham orbital

According to Perdew[193, 194], the energy of the highest occupied Kohn Sham orbital is the ionization potential of the material.

This statement has been disputed by Kleinman[195].

H.10.2 Correlation inequality and lower bound of the exact density functional

H.11 Reliability of DFT

If we knew the exact density functional, we would be able to determine exactly

- the total energy
- the electron density and
- the energy of the highest occupied orbital

The argument that DFT predicts the highest occupied orbital, while the orbital energies of all other one-particle orbitals are, in principle, without physical meaning goes as follows: Far from the surface of a crystal the density of a one-particle orbital falls off as $e^{-\lambda z}$ where λ is related to the orbital energy by $\lambda = \frac{1}{\hbar}\sqrt{-2m_e\epsilon}$, where the orbital energy is measured relative to the vacuum level, that is $\lim_{z\to\infty} v_{eff}(\vec{r})$. For large distances the highest occupied orbital, which has the slowest decay, will dominate the electron density. Thus, if we would know the electron density very accurately far from a surface, we would be able to determine the dominant exponential decay constant and thus the energy of the highest occupied orbital.[6] Thus, the energy of the highest occupied orbital can be determined from the density, which is an exact prediction of DFT.

Of course, even though exact DFT predicts these quantities accurately, it remains to be seen in each case if that also holds for the approximate functionals used in practice.

- Bond energies: Local functionals overestimate binding by often more than 1 eV. Energies are fairly good as long as the effective surface area of the system is not changed. This poor result is dramatically improved by the GGA's.
- Structures: bond lengths are underestimated in LDA by 0-2 %. They are overestimated by GGA's by 0-2 %.
- Dipole moments standard deviation 0.1 Debye[196]

H.12 Deficiencies of DFT

Below, I collect some of the deficiencies of current density functionals. Some of these deficiency are related to spectral properties, and the stem from the illegal comparison of the Kohn-Sham spectra with spectral functions of real systems. Other deficiencies are related to the limitations of the various parameterizations of the density functional. Many of these deficiencies can be overcome with the appropriate choice of functionals.

- **Missing Van der Waals interaction:** The van-der-Waals interaction is not included in semi-local density functionals.

[6] There is a caveat in the argument. Consider an insulator which may have surface states in the band gap. In that case the density would probe the highest occupied surface state, which may lie above the highest occupied bulk state.

Surprisingly the description of van der Waals bonds is nearly perfect with truly local density functionals. This, however, is an artifact. Local density functionals tend to overbind on the one hand, and they lack the van der Waals interactions on the other. Since the overbinding of covalent bonds introduces errors in the range of 1 eV, it is generally not a good idea to use truly local density functionals instead of their gradient corrected counterparts.

A density functional for the van der Waals interaction has been developed by Dion et al.[197]. It is named vdWDF (van-der-Waals density functional).

- **Band-gap Problem:** If we compare the spectrum of Kohn Sham states with optical absorption spectra we observe that the band gaps are too small. This is not a deficiency of density-functional theory, but an over-interpretation of the Kohn Sham spectrum. The excited states should not be calculated from the same potential as the ground state.
- **Reduced band width:** Band width of alkaline metals.
- **Mott insulators:** A number of transition metal oxides are Mott insulators.
- **unstable negative ions:**
- **Broken symmetry spin states:** singlet O_2 Molecule[198].
- **Transition states:**
- **High-energy spectrum:** The high energy part if the Kohn-Sham spectrum is too low compared to the measured optical spectrum[199]. The reason is that the exchange-correlation hole cannot follow the very fast electrons, while in the functionals we assume that full relaxation is always possible. Editor: It seems that the descrepancy[199] starts to grow above the plasma frequency.

Appendix I

Derivation of Slater-Condon rules

In this section, I derive the Slater-Condon rules[25, 56] spelled out in section 3.5 on p. 138.

The expectation values of Slater determinants[25] have been motivated earlier in the chapter 2 on the Hartree-Fock approximation in section 2.2.2 on p. 50 and section 2.2.4 on p. 55.

I.1 Maximum coincidence and orthonormality

An important ingredient to make the derivation of the Slater-Condon rule feasible is the concept of maximum coincidence:

Two Slater determinants, expressed in the same one-particle basisset, are in **maximum coincidence**, if all one-particle orbitals, which are present in both Slater determinants, are in the same position in both Slater determinants.

For example:

- the following determinants are in maximum coincidence with $|abcd\rangle$: $|efcd\rangle$, $|abcd\rangle$,$|aecd\rangle$.
- The determinants $|bacd\rangle$, $|eacd\rangle$ are not in maximum coincidence with $|abcd\rangle$. They can be brought into maximum coincidence by permuting one-particle orbitals, where each permutation contributes a factor (-1).

When two Slater-determinants $|\Phi\rangle$ and $|\Psi\rangle$ are in maximum coincidence, the distinct one-particle orbitals can be moved to the front without changing the matrix elements $\langle\Phi|\hat{A}|\Psi\rangle$ between the Slater determinants. This special form simplifies the bookkeeping in the arguments following below:

The other requirement for the derivation is that the one-particle orbitals are **orthonormal**. For non-orthonormal one-particle orbitals the expressions are considerably more complicated. When the expressions for non-orthonormal basis functions are needed, they can be obtained by transforming the expressions obtained with an orthonormal basisset.

I.2 Matrix elements with identical Slater determinants

The expectation values with a Slater determinant[25] make up the first set Slater-Condon rule Eq. 3.41.

I.2.1 Expectation value of a one-particle operator

First, we evaluate only the matrix element of the one-particle operator $\hat{h}_1$, that acts only on the coordinates of only one particle, namely the first. This result is then generalized for the other

particles and then summed up. Thus, we obtain the expectation value of the non-interacting part of the Hamiltonian.

To be concise, we write here the detailed expressions for the matrix elements of the one-particle Hamilton operator. The generalization to any other one-particle operator is straightforward. The expectation value with a one-particle orbital $|\varphi\rangle$ is

$$\begin{aligned}\langle\varphi|\hat{h}|\varphi\rangle &= \int d^4x \int d^4x' \; \langle\varphi|\vec{x}\rangle \quad \overbrace{\underbrace{\langle\vec{x}|\hat{h}|\vec{x'}\rangle}_{\delta(\vec{r}-\vec{r'})\delta_{\sigma,\sigma'}\left(-\frac{\hbar^2}{2m_e}\vec{\nabla}^2+v_{ext}(\vec{r})\right)}} \quad \langle\vec{x'}|\varphi\rangle \\ &= \sum_\sigma \int d^3r \; \varphi^*(\vec{r},\sigma)\left[\frac{-\hbar^2}{2m_e}\vec{\nabla}^2+v_{ext}(\vec{r})\right]\varphi(\vec{r},\sigma) \end{aligned} \tag{I.1}$$

The one-particle Hamiltonian $\hat{h}_j$ acting on the j-th particle in a many-particle wave function $|\Psi\rangle$ yields the expectation value

$$\langle\Psi|\hat{h}_j|\Psi\rangle = \int d^4x_1 \cdots \int d^4x_N \; \Psi^*(\vec{x}_1,\ldots,\vec{x}_N)\left(\frac{-\hbar^2}{2m_e}\vec{\nabla}_j^2+v_{ext}(\vec{r}_j)\right)\Psi(\vec{x}_1,\ldots,\vec{x}_N) \tag{I.2}$$

so that the matrix element for two product wave functions $|\varphi_1,\ldots,\varphi_N\rangle$ and $|\psi_1,\ldots,\psi_N\rangle$ is

$$\langle\varphi_1,\ldots,\varphi_N|\hat{h}_j|\psi_1,\ldots,\psi_N\rangle = \langle\varphi_1|\psi_1\rangle\cdots\langle\varphi_j|\hat{h}|\psi_j\rangle\cdots\langle\varphi_N|\psi_N\rangle \tag{I.3}$$

A Slater determinant $|\Psi\rangle$ has the form

$$\langle\vec{x}_1,\ldots,\vec{x}_N|\Psi\rangle \overset{\text{Eq. 1.88}}{=} \frac{1}{\sqrt{N!}}\sum_{i_1,\ldots,i_N=1}^{N}\epsilon_{i_1,\ldots,i_N}\langle\vec{x}_1|\varphi_{i_1}\rangle\cdots\langle\vec{x}_N|\varphi_{i_N}\rangle \tag{I.4}$$

Thus, the matrix element of a one-particle operator Eq. 2.5 is

$$\begin{aligned}\langle\Psi|\sum_{i=1}^{N}\hat{h}_i|\Psi\rangle &= N\langle\Psi|\hat{h}_1|\Psi\rangle \\ &\overset{\text{Eq. I.4}}{=} N\cdot\frac{1}{N!}\sum_{i_1,i_2,\ldots,i_N}^{N}\sum_{j_1,j_2,\ldots,j_N}^{N}\epsilon_{i_1,i_2,\ldots,i_N}\langle\varphi_{i_1},\ldots,\varphi_{i_N}|\hat{h}_1|\varphi_{j_1},\ldots,\varphi_{j_N}\rangle\epsilon_{j_1,j_2,\ldots,j_N} \\ &\overset{\text{Eq. I.3}}{=} N\frac{1}{N!}\sum_{i_1,i_2,\ldots,i_N}^{N}\sum_{j_1,j_2,\ldots,j_N}^{N}\epsilon_{i_1,i_2,\ldots,i_N}\epsilon_{j_1,j_2,\ldots,j_N}\langle\varphi_{i_1}|\hat{h}_1|\varphi_{j_1}\rangle\underbrace{\langle\varphi_{i_2}|\varphi_{j_2}\rangle}_{\delta_{i_2,j_2}}\cdots\underbrace{\langle\varphi_{i_N}|\varphi_{j_N}\rangle}_{\delta_{i_N,j_N}} \\ &= N\frac{1}{N!}\sum_{i_1,j_1=1}^{N}\langle\varphi_{i_1}|\hat{h}_1|\varphi_{j_1}\rangle\underbrace{\sum_{i_2,\ldots,i_N}^{N}\epsilon_{i_1,i_2,\ldots,i_N}\epsilon_{j_1,i_2,\ldots,i_N}}_{\delta_{i_1,j_1}(N-1)!} \\ &= \sum_{j=1}^{N}\langle\varphi_j|\hat{h}_1|\varphi_j\rangle\end{aligned}$$

In the last step, we exploited, that the sum over j_1 only contributes when $j_1 = i_1$: There is only one orbital left if all the orbitals but the first are determined. Thus, the first orbital must be the same for both Levi-Civita Symbols.

Finally, we obtain the expectation value of the one-particle Hamiltonian for a Slater determinant $|\Psi\rangle$ as

EXPECTATION VALUE OF A ONE-PARTICLE OPERATOR WITH A SLATER DETERMINANT

$$\langle\Psi|\sum_{i=1}^{N}\hat{h}_i|\Psi\rangle = \sum_{i=1}^{N}\langle\varphi_i|\hat{h}|\varphi_i\rangle \tag{I.5}$$

Here, $|\Psi\rangle$ is a N-particle Slater determinant built from the one-particle orbitals $|\varphi_i\rangle$, and $\sum_{i=1}^{N}\hat{h}_i$ is a one-particle operator.

This is Eq. 2.10 provided on p. 51 and it is the first of the Slater-Condon rules Eq. 3.41 provided on p. 140.

I.2.2 Expectation value of a two-particle operator

We proceed as for the expectation value of a one-particle operator and relate the interaction energy between all particles to the interaction between the first two electrons. This is allowed because of the indistinguishability of the electrons: The interaction between any two electrons is identical to any other pair. There are $\frac{N(N-1)}{2}$ ordered pairs and therefore the interaction energy is

$$\begin{aligned}
E_W &= \langle\Psi|\frac{1}{2}\sum_{i\neq j}^{N}\hat{W}_{i,j}|\Psi\rangle = \frac{N(N-1)}{2}\langle\Psi|\hat{W}_{1,2}|\Psi\rangle \\
&\overset{\text{Eq. I.4}}{=} \frac{N(N-1)}{2}\frac{1}{N!}\sum_{i_1,i_2,\ldots,i_N}^{N}\sum_{j_1,j_2,\ldots,j_N}^{N}\epsilon_{i_1,i_2,\ldots,i_N}\epsilon_{j_1,j_2,\ldots,j_N}\langle\varphi_{i_1},\ldots,\varphi_{i_N}|\hat{W}_{12}|\varphi_{j_1},\ldots,\varphi_{j_N}\rangle \\
&= \frac{1}{2\cdot(N-2)!}\sum_{i_1,i_2,\ldots,i_N}^{N}\sum_{j_1,j_2,\ldots,j_N}^{N}\epsilon_{i_1,i_2,\ldots,i_N}\epsilon_{j_1,j_2,\ldots,j_N}\langle\varphi_{i_1},\varphi_{i_2}|\hat{W}_{12}|\varphi_{j_1},\varphi_{j_2}\rangle\underbrace{\langle\varphi_{i_3}|\varphi_{j_3}\rangle}_{\delta_{i_3,j_3}}\cdots\underbrace{\langle\varphi_{i_N}|\varphi_{j_N}\rangle}_{\delta_{i_N,j_N}} \\
&= \frac{1}{2\cdot(N-2)!}\sum_{i_1,i_2,j_1,j_2}^{N}\langle\varphi_{i_1},\varphi_{i_2}|\hat{W}_{12}|\varphi_{j_1},\varphi_{j_2}\rangle\underbrace{\sum_{i_3,\ldots,i_N}^{N}\epsilon_{i_1,i_2,i_3\ldots,i_N}\epsilon_{j_1,j_2,i_3\ldots,i_N}}_{=\begin{cases}(N-2)!\;\epsilon_{i_1,i_2}\epsilon_{j_1,j_2} & \text{for } i_1,i_2\in\{j_1,j_2\}\\ 0 & \text{else}\end{cases}} \\
&= \frac{1}{2}\sum_{i_1,i_2}^{N}\sum_{j_1,j_2\in\{i_1,i_2\}}\langle\varphi_{i_1},\varphi_{i_2}|\hat{W}_{12}|\varphi_{j_1},\varphi_{j_2}\rangle\underbrace{\epsilon_{i_1,i_2}\epsilon_{j_1,j_2}}_{\delta_{i_1,j_1}\delta_{i_2,j_2}-\delta_{i_1,j_2}\delta_{i_1,j_2}} \\
&= \frac{1}{2}\sum_{i_1,i_2}^{N}\Big(\langle\varphi_{i_1},\varphi_{i_2}|\hat{W}_{12}|\varphi_{i_1},\varphi_{i_2}\rangle - \langle\varphi_{i_1},\varphi_{i_2}|\hat{W}_{12}|\varphi_{i_2},\varphi_{i_1}\rangle\Big)
\end{aligned} \tag{I.6}$$

In the last step, I exploited that the two interaction terms cancel when the indices i_1 and i_2 are identical. Therefore, they need not be excluded from the sum. The expression with the terms $i_1 = i_2$ is more convenient to discuss the physical implications, while the former is commonly used in the quantum chemical literature.

Thus, we obtain the expectation value of the interaction energy of a Slater determinant as

EXPECTATION VALUE OF THE INTERACTION WITH A SLATER DETERMINANT

$$\langle\Psi|\frac{1}{2}\sum_{i\neq j}^{N}\hat{W}_{i,j}|\Psi\rangle = \frac{1}{2}\sum_{i,j=1}^{N}\Big[\langle\varphi_i,\varphi_j|\hat{W}|\varphi_i,\varphi_j\rangle - \langle\varphi_i,\varphi_j|\hat{W}|\varphi_j,\varphi_i\rangle\Big] \tag{I.7}$$

The matrix elements used in the above equation Eq. I.7 are

$$\langle\varphi_a,\varphi_b|\hat{W}|\varphi_c,\varphi_d\rangle \stackrel{\text{def}}{=} \sum_{\sigma,\sigma'}\int d^3r\int d^3r'\;\varphi_a^*(\vec{r},\sigma)\varphi_b^*(\vec{r'},\sigma')\frac{e^2}{4\pi\epsilon_0|\vec{r}-\vec{r'}|}\varphi_c(\vec{r},\sigma)\varphi_d(\vec{r'},\sigma') \tag{I.8}$$

I.3 Slater determinants differing by one orbital

I.3.1 One-particle operator

The matrix element of a one-particle operator with Slater determinants differing by one orbital is obtained as follows:

First, we consider Slater determinants

$$\langle\vec{x}_1,\ldots,\vec{x}_N|\Psi\rangle = \frac{1}{\sqrt{N!}}\sum_{i_1,\ldots,i_N=1}^{N}\epsilon_{i_1,\ldots,i_N}\langle\vec{x}_1|\psi_{i_1}\rangle\cdots\langle\vec{x}_N|\psi_{i_N}\rangle \tag{I.9}$$

$$\langle\vec{x}_1,\ldots,\vec{x}_N|\Phi\rangle = \frac{1}{\sqrt{N!}}\sum_{j_1,\ldots j_N=1}^{N}\epsilon_{j_1,\ldots j_N}\langle\vec{x}_1|\varphi_{j_1}\rangle\cdots\langle\vec{x}_N|\varphi_{j_N}\rangle \tag{I.10}$$

that differ by exactly one one-particle orbital. Due to the form of **maximum coincidence** defined in section 3.5, we can place these two orbitals in the first position. Hence, $|\psi_1\rangle \neq |\varphi_1\rangle$, but $|\psi_i\rangle = |\varphi_i\rangle$ for $i \neq 1$. Thus,

$$\langle\psi_i|\varphi_j\rangle = \delta_{i,j}(1-\delta_{i,1}) \tag{I.11}$$

Now, we can work out the matrix element for the one-particle operator $\hat{A}_1$ acting on the first particle coordinate.

$$\begin{aligned}\langle\Psi|\hat{A}_1|\Phi\rangle &= \frac{1}{N!}\sum_{i_1,\ldots,i_N=1}^{N}\sum_{j_1,\ldots j_N=1}^{N}\epsilon_{i_1,i_2,\ldots,i_N}\epsilon_{j_1,j_2,\ldots,j_N}\langle\psi_{i_1}|\hat{A}|\varphi_{j_1}\rangle\underbrace{\langle\psi_{i_2}|\varphi_{j_2}\rangle}_{\delta_{i_2,j_2}(1-\delta_{i_2,1})}\cdots\underbrace{\langle\psi_{i_N}|\varphi_{j_N}\rangle}_{\delta_{i_N,j_N}(1-\delta_{i_N,1})}\\ &\stackrel{\text{Eq. I.11}}{=} \frac{1}{N!}\sum_{i_2\ldots,i_N=1}^{N}\sum_{i_1,j_1=1}^{N}\underbrace{\epsilon_{i_1,i_2,\ldots,i_N}\epsilon_{j_1,i_2,\ldots,i_N}(1-\delta_{i_2,1})\ldots(1-\delta_{i_N,1})}_{(B)}\langle\psi_{i_1}|\hat{A}|\varphi_{j_1}\rangle\end{aligned} \tag{I.12}$$

The Levi-Civita symbol $\epsilon_{i_1,\ldots,i_N}$ is non-zero only, when all its indices differ. Thus, the term denoted as (B), is non-zero only,

- if the indices $i_2,\ldots,i_N$ are all different and
- if the indices are from $i_2,\ldots,i_N \in \{2,\ldots,N\}$.

Hence the Levi-Civita symbols are nonzero only when $i_1 = j_1 = 1$. When these conditions are fulfilled the term (B) equals $B = 1$.

Thus, we obtain

$$\langle\Psi|\hat{A}_1|\Phi\rangle = \frac{1}{N!}\sum_{i_2\ldots,i_N=2}^{N}(\epsilon_{1,i_2,\ldots,i_N})^2\,\langle\psi_1|\hat{A}|\varphi_1\rangle \tag{I.13}$$

The Levi-Civita symbols contribute, if all indices are different, This happens $(N-1)!$ times, which corresponds to the number of permutations of the indices $2,\ldots,N$. Thus, we obtain

$$\langle\Psi|\hat{A}_1|\Phi\rangle = \frac{1}{N}\langle\psi_1|\hat{A}|\varphi_1\rangle \tag{I.14}$$

Since the operator has the form $\hat{A} = \sum_{i=1}^{N}\hat{A}_i$, and since all operators $\hat{A}_i$ contribute the same result, we obtain

$$\langle\Psi|\hat{A}|\Phi\rangle = \langle\psi_1|\hat{A}|\varphi_1\rangle. \tag{I.15}$$

which corresponds to the first line in the second Slater-Condon rule Eq. 3.42.

I.3.2 Two-particle operator

The matrix element of a two-particle operator with Slater determinants differing by one orbital is obtained as follows:

We consider the matrix element between two Slater determinants

$$\langle\vec{x}_1,\ldots,\vec{x}_N|\Psi\rangle = \frac{1}{\sqrt{N!}}\sum_{i_1,\ldots,i_N=1}^{N}\epsilon_{i_1,\ldots,i_N}\langle\vec{x}_1|\psi_{i_1}\rangle\cdots\langle\vec{x}_N|\psi_{i_N}\rangle \tag{I.16}$$

$$\langle\vec{x}_1,\ldots,\vec{x}_N|\Phi\rangle = \frac{1}{\sqrt{N!}}\sum_{j_1,\ldots,j_N=1}^{N}\epsilon_{j_1,\ldots,j_N}\langle\vec{x}_1|\varphi_{j_1}\rangle\cdots\langle\vec{x}_N|\varphi_{j_N}\rangle \tag{I.17}$$

Because only the first orbital of the two Slater determinants $|\Psi\rangle$ and $|\Phi\rangle$ differ, the overlap between the one-particle orbitals has the result

$$\langle\psi_i|\varphi_j\rangle = \delta_{ij}(1-\delta_{i,1}) \tag{I.18}$$

we obtained already earlier in Eq. I.11

Note, that the Slater determinants are chosen in **maximum coincidence**, defined in section 3.5: the two orbitals that are present in only one of the two Slater determinants stand at the same position, namely the first and second. That is, $|\psi_1\rangle$ and $|\psi_2\rangle$ differ from all $|\phi_j\rangle$ for $j\in\{1,\ldots,N\}$, and $|\phi_1\rangle$ and $|\phi_2\rangle$ differ from all $|\psi_j\rangle$ for $j\in\{1,\ldots,N\}$. The orbitals which are identical for both Slater determinants are in the same position, i.e. $|\phi_j\rangle = |\psi_j\rangle$ for $j\in\{3,\ldots,N\}$.

Now, we can work out the matrix element of the interaction operator $\hat{W}_{1,2}$ that acts exclusively on the first two particle coordinates. If the interaction would act onto any other orbital, at least one of the orbitals in the first position would be connected with another one by an overlap matrix element. This overlap matrix element vanishes because the orbitals in the first position are orthogonal to all other orbitals involved.

Later, we will see that the result is the same for each pair of coordinates, so that the sum over

pairs is done easily at the end of the calculation.

$$\begin{aligned}
\langle\Psi|\hat{W}_{1,2}|\Phi\rangle &= \frac{1}{N!}\sum_{i_1,\ldots,i_N=1}^{N}\sum_{j_1,\ldots,j_N=1}^{N}\epsilon_{i_1,i_2,\ldots,i_N}\epsilon_{j_1,j_2,\ldots,j_N} \\
&\quad\cdot\langle\psi_{i_1}\psi_{i_2}|\hat{W}_{1,2}|\varphi_{j_1}\varphi_{j_2}\rangle\underbrace{\langle\psi_{i_3}|\varphi_{j_3}\rangle}_{\delta_{i_3,j_3}(1-\delta_{i_3,1})}\cdots\underbrace{\langle\psi_{i_N}|\varphi_{j_N}\rangle}_{\delta_{i_N,j_N}(1-\delta_{i_N,1})} \\
&= \frac{1}{N!}\sum_{i_3,\ldots,i_N=1}^{N}\sum_{i_1,i_2,j_1,j_2=1}^{N}\underbrace{\epsilon_{i_1,i_2,i_3,\ldots,i_N}\epsilon_{j_1,j_2,i_3,\ldots,i_N}(1-\delta_{i_3,1})\ldots(1-\delta_{i_N,1})}_{(B)}\langle\psi_{i_1}\psi_{i_2}|\hat{W}_{1,2}|\varphi_{j_1}\varphi_{j_2}\rangle \\
&= \frac{1}{N!}\sum_{i_3,\ldots,i_N=2}^{N}\sum_{n=2}^{N}\sum_{i_1,i_2,j_1,j_2\in\{1,n\}}\epsilon_{i_1,i_2,i_3,\ldots,i_N}\epsilon_{j_1,j_2,i_3,\ldots,i_N}\langle\psi_{i_1}\psi_{i_2}|\hat{W}_{1,2}|\varphi_{j_1}\varphi_{j_2}\rangle \\
&= \frac{1}{N!}\sum_{n=2}^{N}\sum_{i_1,i_2,j_1,j_2\in\{1,n\}}\langle\psi_{i_1}\psi_{i_2}|\hat{W}_{1,2}|\varphi_{j_1}\varphi_{j_2}\rangle\sum_{i_3,\ldots,i_N=2}^{N}\epsilon_{i_1,i_2,i_3,\ldots,i_N}\epsilon_{j_1,j_2,i_3,\ldots,i_N}
\end{aligned} \tag{I.19}$$

The factor (B) is nonzero, if the indices $i_3,\ldots,i_N$ are different from each other and if they are element of $\{2,\ldots,N\}$. We exploit that for each set $i_3,\ldots,i_N$ in the sum, there is one pair of numbers $\{1,\ldots,N\}$, which has not been used. One number is 1, and the other we call n. The second number n is selected by adding the sum, while we exploit that the only nozero term in that sum is the one from the elements not covered already, which differs from 1.

The only nonzero contributions for $i_1,i_2,j_1,j_2\in\{1,n\}$ with $n\in\{2,\ldots,N\}$ are

$$\begin{aligned}
\sum_{i_3,\ldots,i_N=2}^{N}\epsilon_{i_1,i_2,i_3,\ldots,i_N}\epsilon_{j_1,j_2,i_3,\ldots,i_N} &= (N-2)(N-3)\cdots 1\begin{cases}+1 & \text{for } i_1=j_1 \text{ and } i_2=j_2\\ -1 & \text{for } i_1=j_2 \text{ and } i_2=j_1\\ 0 & \text{else}\end{cases} \\
&= (N-2)!\left(\delta_{i_1,j_1}\delta_{i_2,j_2}-\delta_{i_1,j_2}\delta_{i_2,j_1}\right)
\end{aligned} \tag{I.20}$$

Thus, we obtain

$$\begin{aligned}
\langle\Psi|\hat{W}_{1,2}|\Phi\rangle &= \frac{(N-2)!}{N!}\sum_{n=2}^{N}\Big(\langle\psi_1\psi_n|\hat{W}|\varphi_1\varphi_n\rangle-\langle\psi_1\psi_n|\hat{W}|\varphi_n\varphi_1\rangle-\langle\psi_n\psi_1|\hat{W}|\varphi_1\varphi_n\rangle+\langle\psi_n\psi_1|\hat{W}|\varphi_n\varphi_1\rangle\Big) \\
&= \frac{2}{N(N-1)}\sum_{n=2}^{N}\Big(\langle\psi_1\psi_n|\hat{W}|\varphi_1\varphi_n\rangle-\langle\psi_1\psi_n|\hat{W}|\varphi_n\varphi_1\rangle\Big)
\end{aligned} \tag{I.21}$$

In the last line, we exploited that the simultaneous interchange of the two orbitals in the bra and those in the ket do not change the matrix element of the interaction.

Since the operator has the form $\hat{W}=\frac{1}{2}\sum_{i\neq j}^{N}\hat{W}_{i,j}$. Each pair contributes the same result. As there are $N(N-1)$ distinct pairs in the double-sum, we obtain

$$\langle\Psi|\hat{W}|\Phi\rangle=\sum_{n=1}^{N}\left(\langle\psi_1\psi_n|\hat{W}_{1,2}|\varphi_1\varphi_n\rangle-\langle\psi_1\psi_n|\hat{W}_{1,2}|\varphi_n\varphi_1\rangle\right) \tag{I.22}$$

This result corresponds to the Slater-Condon rule Eq. 3.43. The sum runs now over all terms because the element with $n=1$ cancels anyway.

I.4 Slater determinants differing by two orbitals

I.4.1 One-particle operator

The matrix element of a one-particle operator with Slater determinants differing by two orbitals is

$$\begin{aligned}\langle\Psi|\hat{A}_1|\Phi\rangle = \frac{1}{N!}\sum_{i_1,\ldots,i_N=1}^{N}\sum_{j_1,\ldots j_N=1}^{N}\epsilon_{i_1,i_2,\ldots,i_N}\epsilon_{j_1,j_2,\ldots j_N} \\ \cdot\langle\psi_{i_1}|\hat{A}|\varphi_{j_1}\rangle \underbrace{\langle\psi_{i_2}|\varphi_{j_2}\rangle}_{\delta_{i_2,j_2}(1-\delta_{i_2,1})(1-\delta_{i_2,2})} \cdots \underbrace{\langle\psi_{i_N}|\varphi_{j_N}\rangle}_{\delta_{i_N,j_N}(1-\delta_{i_N,1})(1-\delta_{i_N,2})} = 0\end{aligned} \tag{I.23}$$

It is evident that this matrix element vanishes, because in each term there is at least one scalar product between to orbitals that differ in the two Slater determinants.

This result corresponds to the first line in the third Slater-Condon rule Eq. 3.44.

I.4.2 Two-particle operator

The matrix element of a two-particle operator with Slater determinants differing by two orbitals is

$$\begin{aligned}\langle\Psi|\hat{W}_{x_1,x_2}|\Phi\rangle &= \frac{1}{N!}\sum_{i_1,\ldots,i_N}\sum_{j_1,\ldots j_N}\epsilon_{i_1,i_2,\ldots,i_N}\epsilon_{j_1,j_2,\ldots j_N} \\ &\quad\cdot\langle\psi_{i_1}\psi_{i_2}|\hat{W}|\varphi_{j_1}\varphi_{j_2}\rangle \underbrace{\langle\psi_{i_3}|\varphi_{j_3}\rangle}_{\delta_{i_3,j_3}(1-\delta_{i_3,1})(1-\delta_{i_3,2})} \cdots \underbrace{\langle\psi_{i_N}|\varphi_{j_N}\rangle}_{\delta_{i_N,j_N}(1-\delta_{i_N,1})(1-\delta_{i_N,2})} \\ &= \frac{1}{N!}\sum_{i_1,i_2=1}^{2}\sum_{j_1,j_2=1}^{2}\langle\psi_{i_1}\psi_{i_2}|\hat{W}|\varphi_{j_1}\varphi_{j_2}\rangle\sum_{i_3,\ldots,i_N}\epsilon_{i_1,i_2,i_3\ldots,i_N}\epsilon_{j_1,j_2,i_3\ldots,i_N} \\ &= \frac{1}{N!}\sum_{i_1,i_2=1}^{2}\sum_{j_1,j_2=1}^{2}\langle\psi_{i_1}\psi_{i_2}|\hat{W}|\varphi_{j_1}\varphi_{j_2}\rangle(N-2)!\,(\delta_{i_1,j_1}\delta_{i_2,j_2}-\delta_{i_1,j_2}\delta_{i_2,j_1}) \\ &= \frac{2}{N(N-1)}\left(\langle\psi_1\psi_2|\hat{W}|\varphi_1\varphi_2\rangle - \langle\psi_1\psi_2|\hat{W}|\varphi_2\varphi_1\rangle\right)\end{aligned} \tag{I.24}$$

With the interaction $\hat{W} = \frac{1}{2}\sum_{i\neq j}^{N}\hat{W}_{i,j}$ we obtain with $\langle\Psi|W_{i,j}|\Phi\rangle = \langle\Psi|W_{1,2}|\Phi\rangle$

$$\langle\Psi|\hat{W}|\Phi\rangle = \langle\psi_1\psi_2|\hat{W}|\varphi_1\varphi_2\rangle - \langle\psi_1\psi_2|\hat{W}|\varphi_2\varphi_1\rangle \tag{I.25}$$

This result corresponds to the second line in the third Slater-Condon rule Eq. 3.45.

I.5 Slater determinants differing by more than two orbitals

The matrix elements of one- and two-particle operators between two Slater determinants differing by more than two orbitals vanish. The argument is analogous to that about in Section I.4.1

Appendix J

One- and two-particle operators expressed by field operators

Here, we will explicitly derive the form of one- and two-particle operators by field operators as given by Eqs. 3.49 and 3.50 on p. 141.

OPERATORS EXPRESSED BY ANNIHILATION AND CREATION OPERATORS

A one-particle operator has the form

$$\hat{A} = \sum_{i,j} A_{i,j} \hat{c}_i^\dagger \hat{c}_j \tag{J.1}$$

and a two-particle operator has the form

$$\hat{W} = \frac{1}{2} \sum_{i,j,k,l} W_{i,j,k,l} \hat{c}_i^\dagger \hat{c}_j^\dagger \hat{c}_l \hat{c}_k \tag{J.2}$$

Note the reversed order of the annihilators relative to the indices!

Our approach will be to work out the matrix elements of a product of creation and annihilation operators between Slater determinants. Then the result will be compared with the Slater-Condon rules Eqs. 3.41 -3.44 on p. 140

Our argument is restricted to Slater determinants constructed from the zero state by a product of creation operators in a unique basis of one-particle orbitals. Thus, these states are eigenstates of the occupation-number operator

$$\hat{n}_k \stackrel{\text{def}}{=} \hat{c}_k^\dagger \hat{c}_k \tag{J.3}$$

That is, we consider here only states that obey

$$\hat{n}_k |\Phi\rangle = |\Phi\rangle n_k \tag{J.4}$$

As the occupation-number eigenstates for a complete orthonormal basis of one-particle eigenstates form a complete basis in the Fock space, we will obtain general matrix elements using the rules determined here.

J.1 Matrix elements between identical Slater determinants

One-particle operator

Let us determine the matrix element of a one-particle operator between two identical Slater determinants $|\Phi\rangle$.

In the first step, we use $\langle\Phi|\hat{c}_i^\dagger\hat{c}_j|\Phi\rangle = 0$ for $i \neq j$: Applied to a Slater determinant, $\hat{c}_i^\dagger\hat{c}_j$ with $i \neq j$ produces a different Slater determinant that is orthogonal to the original one. Thus, only the diagonal terms contribute.

$$\langle\Phi|\hat{c}_j^\dagger\hat{c}_k|\Phi\rangle = \delta_{j,k}\langle\Phi|\underbrace{\hat{n}_j}_{\hat{c}_j^\dagger\hat{c}_j}|\Phi\rangle \overset{\text{Eq. J.4}}{=} \delta_{j,k}n_j$$

$$\Rightarrow \langle\Phi|\sum_{j,k}A_{j,k}\hat{c}_j^\dagger\hat{c}_k|\Phi\rangle = \sum_{j=1}^{\infty}n_jA_{j,j} \overset{\text{Eq. 3.51}}{=} \sum_{j=1}^{\infty}n_j\langle\varphi_j|\hat{A}|\varphi_j\rangle \tag{J.5}$$

where $|\varphi_j\rangle = \hat{c}_j^\dagger|\mathcal{O}\rangle$ are the one-particle states related to the creation operators. $|\mathcal{O}\rangle$ is the vacuum state.

Eq. J.5 is identical to the first Slater-Condon rule for one-particle operators Eq. 3.41 on p.140. Thus,

$$\langle\Phi|\sum_{j,k}A_{j,k}\hat{c}_j^\dagger\hat{c}_k|\Phi\rangle \overset{\text{Eq. J.5}}{=} \sum_{j=1}^{\infty}n_j\langle\varphi_j|\hat{A}|\varphi_j\rangle \overset{\text{Eq. 3.41}}{=} \langle\Phi|\hat{A}|\Phi\rangle \tag{J.6}$$

In Eq. J.5, we sum over all one-particle basis functions and the occupation numbers n_i select those that are present in the Slater determinant. In Eq. 3.41, the sum goes directly over the one-orbitals in the determinant.

Thus, we have shown that the operator $\sum_{i,j}A_{i,j}\hat{c}_i^\dagger\hat{c}_j$ has the same matrix elements as the operator $\hat{A}$, if both wave functions are identical Slater determinants.

Two-particle operator

To work out the expressions for a two-particle operator, we use a similar argument. Unless the operator $\hat{c}_i^\dagger\hat{c}_j^\dagger\hat{c}_k\hat{c}_l$ creates all orbitals that it destroys, the resulting Slater determinant will differ from and be orthogonal to the original Slater determinant. There are just two possibilities that contribute to a nonzero value, namely

- case 1: $i = k$ and $j = l$.

$$\hat{c}_i^\dagger\hat{c}_j^\dagger\hat{c}_i\hat{c}_j \overset{[\hat{c}_i^\dagger,\hat{c}_j]_+=\delta_{i,j}}{=} \hat{c}_i^\dagger\delta_{i,j}\hat{c}_j - \hat{c}_i^\dagger\hat{c}_i\hat{c}_j^\dagger\hat{c}_j = \delta_{i,j}\hat{n}_i - \hat{n}_i\hat{n}_j$$

- case 2: $i = l$ and $j = k$

$$\hat{c}_i^\dagger\hat{c}_j^\dagger\hat{c}_j\hat{c}_i \overset{[\hat{c}_j,\hat{c}_j]_+=0}{=} -\hat{c}_i^\dagger\hat{c}_j^\dagger\hat{c}_i\hat{c}_j \overset{[\hat{c}_i^\dagger,\hat{c}_j]_+=\delta_{i,j}}{=} -\hat{c}_i^\dagger\delta_{i,j}\hat{c}_j + \hat{c}_i^\dagger\hat{c}_i\hat{c}_j^\dagger\hat{c}_j = -\delta_{i,j}\hat{n}_i + \hat{n}_i\hat{n}_j$$

- All other cases vanish because the creators and annihilators do not match.

Thus, we obtain

$$\begin{aligned}\langle\Phi|\hat{c}_i^\dagger\hat{c}_j^\dagger\hat{c}_k\hat{c}_l|\Phi\rangle &= \delta_{i,k}\delta_{j,l}\Big(\delta_{i,j}n_i - n_in_j\Big) + \delta_{i,l}\delta_{j,k}\Big(-\delta_{i,j}n_i + n_in_j\Big)\\ &= \underbrace{\delta_{i,k}\delta_{j,l}\delta_{i,j}n_i}_{a} - \underbrace{\delta_{i,k}\delta_{j,l}n_in_j}_{b} - \underbrace{\delta_{i,l}\delta_{j,k}\delta_{i,j}n_i}_{c} + \underbrace{\delta_{i,l}\delta_{j,k}n_in_j}_{d}\\ &\overset{a=c}{=} \underbrace{\delta_{i,l}\delta_{j,k}n_in_j}_{d} - \underbrace{\delta_{i,k}\delta_{j,l}n_in_j}_{b}\end{aligned}$$

which yields

$$\Rightarrow \langle\Phi| \sum_{i,j,k,l} W_{i,j,k,l} \hat{c}_i^\dagger \hat{c}_j^\dagger \hat{c}_l \hat{c}_k |\Phi\rangle = \sum_{i,j} n_i n_j \left[W_{i,j,i,j} - W_{i,j,j,i}\right]$$

Note, that we interchanged the two annihilators which changes the sign of the expression.

Let us compare this result again with that of the first Slater-Condon rule Eq. 3.41 on p. 140.

J.2 Matrix elements between Slater determinants differing by one orbital

We construct pairs of N-particle Slater determinants that differ by a single orbital from a common $(N-1)$-particle Slater determinant $|\Phi\rangle$ by creating two different one-particle orbitals (one for each). We obtain $\hat{c}_a^\dagger|\Phi\rangle$ and $\hat{c}_b^\dagger|\Phi\rangle$. They differ by exactly one one-particle orbital since $a \neq b$ and they are automatically in **maximum coincidence**. Remember, that the bra related to $\hat{c}_a^\dagger|\Phi\rangle$ is $\langle\hat{c}_a^\dagger\Phi| = \langle\Phi|\hat{c}_a$.

One-particle operators

Let us construct the matrix element of a one-particle operator $\hat{A} = \sum_{j,k} A_{j,k} \hat{c}_j^\dagger \hat{c}_k$ between two Slater determinants $|\Phi_a\rangle \stackrel{\text{def}}{=} \hat{c}_a^\dagger|\Phi\rangle$ and $|\Phi_b\rangle \stackrel{\text{def}}{=} \hat{c}_b^\dagger|\Phi\rangle$ differing by two distinct one-particle orbitals $|\psi_a\rangle$ and $|\psi_b\rangle$, i.e. $a \neq b$.

$$\langle\Phi|\hat{c}_a \hat{c}_j^\dagger \hat{c}_k \hat{c}_b^\dagger|\Phi\rangle \stackrel{a\neq b}{=} \delta_{a,j}(1-n_j)\delta_{k,b}(1-n_b)$$

$$\Rightarrow \langle\Phi|\hat{c}_a \left(\sum_{j,k} A_{j,k} \hat{c}_j^\dagger \hat{c}_k\right) \hat{c}_b^\dagger|\Phi\rangle = \sum_{j,k} A_{j,k}\delta_{a,i}(1-n_i)\delta_{j,b}(1-n_b) = A_{a,b}(1-n_a)(1-n_b)$$

where $n_j = \langle\Phi|\hat{c}_j^\dagger \hat{c}_j|\Phi\rangle$. This result can be compared to the Slater-Condon rule Eq. 3.43 on p. 140. The role of $(1-n_a)$ and $(1-n_b)$ is to test if the corresponding one-particle orbitals are already occupied in $|\Phi\rangle$. If one of the orbitals a or b is already present in $|\Phi\rangle$, the creation operators[1] $c_a^\dagger$ or $c_b^\dagger$ would turn this state into a zero state, for which the matrix element vanishes.

Two-particle operator

For the interaction matrix elements between two Slater determinants $|\Phi_a\rangle \stackrel{\text{def}}{=} \hat{c}_a^\dagger|\Phi\rangle$ and $|\Phi_b\rangle \stackrel{\text{def}}{=} \hat{c}_b^\dagger|\Phi\rangle$ differing by two distinct one-particle orbitals $|\psi_a\rangle$ and $|\psi_b\rangle$, i.e. $a \neq b$, we need to determine matrix elements of the type

$$\langle\Phi_a|\hat{c}_i^\dagger \hat{c}_j^\dagger \hat{c}_k \hat{c}_l|\Phi_b\rangle = \langle\Phi|\hat{c}_a \hat{c}_i^\dagger \hat{c}_j^\dagger \hat{c}_k \hat{c}_l \hat{c}_b^\dagger|\Phi\rangle\,. \tag{J.7}$$

For this matrix element to be non-zero, each annihilator must be paired with a creator of the same orbital.

The matrix element can be evaluated with brute force by commutating all operators so that the creation operators stand to the left of all annihilation operators. Once the matrix elements have this form, they are readily evaluated.

Here, however, we try to be more economical:

1. Let us pair the annihilator $\hat{c}_a$ with one of the creation operators. There are two possibilities: $i = a$ and $j = a$. The possibility $b = a$ has been excluded, because this is the case of two identical Slater determinants, which has been investigated in the previous section. The case $i = j$ does not contribute because the two creation operators stand next to each other and $\hat{c}_j^\dagger \hat{c}_j^\dagger = \hat{0}$.

[1] $\langle\hat{c}_a^\dagger\Phi| = \langle\Phi|\hat{c}_a$

2. For each of the two possibilities there are two cases $b = k$ and $b = l$ where the creator $\hat{c}_b$ is paired with one of the annihilators. As before the cases $a = b$ and $k = l$ do not contribute.

Thus, there are four sets of indices with nonzero value, namely

$$\begin{aligned}
\langle\Phi|\hat{c}_a\hat{c}_i^\dagger\hat{c}_j^\dagger\hat{c}_k\hat{c}_l\hat{c}_b^\dagger|\Phi\rangle &= \Big(\delta_{a,i}\big(\delta_{b,k}\delta_{j,l}+\delta_{b,l}\delta_{j,k}\big)+\delta_{a,j}\big(\delta_{b,k}\delta_{i,l}+\delta_{b,l}\delta_{i,k}\big)\Big)\langle\Phi|\hat{c}_a\hat{c}_i^\dagger\hat{c}_j^\dagger\hat{c}_k\hat{c}_l\hat{c}_b^\dagger|\Phi\rangle \\
&= \delta_{a,i}\delta_{b,k}\delta_{j,l}\langle\Phi|\hat{c}_a\hat{c}_a^\dagger\hat{c}_j^\dagger\hat{c}_b\hat{c}_j\hat{c}_b^\dagger|\Phi\rangle + \delta_{a,i}\delta_{b,l}\delta_{j,k}\langle\Phi|\hat{c}_a\hat{c}_a^\dagger\hat{c}_j^\dagger\hat{c}_j\hat{c}_b\hat{c}_b^\dagger|\Phi\rangle \\
&+ \delta_{a,j}\delta_{b,k}\delta_{i,l}\langle\Phi|\hat{c}_a\hat{c}_i^\dagger\hat{c}_a^\dagger\hat{c}_b\hat{c}_i\hat{c}_b^\dagger|\Phi\rangle + \delta_{a,j}\delta_{b,l}\delta_{i,k}\langle\Phi|\hat{c}_a\hat{c}_i^\dagger\hat{c}_a^\dagger\hat{c}_i\hat{c}_b\hat{c}_b^\dagger|\Phi\rangle \\
&= -\delta_{a,i}\delta_{b,k}\delta_{j,l}\langle\Phi|\hat{c}_a\hat{c}_a^\dagger\left(\hat{c}_j^\dagger\hat{c}_j\right)\hat{c}_b\hat{c}_b^\dagger|\Phi\rangle + \delta_{a,i}\delta_{b,l}\delta_{j,k}\langle\Phi|\hat{c}_a\hat{c}_a^\dagger\left(\hat{c}_j^\dagger\hat{c}_j\right)\hat{c}_b\hat{c}_b^\dagger|\Phi\rangle \\
&\quad +\delta_{a,j}\delta_{b,k}\delta_{i,l}\langle\Phi|\hat{c}_a\hat{c}_a^\dagger\left(\hat{c}_i^\dagger\hat{c}_i\right)\hat{c}_b\hat{c}_b^\dagger|\Phi\rangle - \delta_{a,j}\delta_{b,l}\delta_{i,k}\langle\Phi|\hat{c}_a\hat{c}_a^\dagger\left(\hat{c}_i^\dagger\hat{c}_i\right)\hat{c}_b\hat{c}_b^\dagger|\Phi\rangle \\
&= -\delta_{a,i}\delta_{b,k}\delta_{j,l}(1-n_a)(1-n_b)n_j \quad + \quad \delta_{a,i}\delta_{b,l}\delta_{j,k}(1-n_a)(1-n_b)n_j \\
&\quad +\delta_{a,j}\delta_{b,k}\delta_{i,l}(1-n_a)(1-n_b)n_i \quad - \quad \delta_{a,j}\delta_{b,l}\delta_{i,k}(1-n_a)(1-n_b)n_i \qquad \text{(J.8)}
\end{aligned}$$

In the last step, I exploited that our Slater determinant $|\Phi\rangle$ is an eigenstate of the occupation-number operators

$$\begin{aligned}
\hat{c}_i^\dagger\hat{c}_i|\Phi\rangle &= |\Phi\rangle n_i \\
\hat{c}_i\hat{c}_i^\dagger|\Phi\rangle &= |\Phi\rangle(1-n_i) \qquad \text{(J.9)}
\end{aligned}$$

where n_i are the eigenvalues, which are the occupations of the orbital in $|\Phi\rangle$.

Thus, we obtain

$$\begin{aligned}
\langle\Phi|\hat{c}_a\hat{W}\hat{c}_b^\dagger|\Phi\rangle &= \langle\Phi|\hat{c}_a\left(\frac{1}{2}\sum_{i,j,k,l}W_{i,j,k,l}\hat{c}_i^\dagger\hat{c}_j^\dagger\hat{c}_l\hat{c}_k\right)\hat{c}_b^\dagger|\Phi\rangle \\
&= -\frac{1}{2}\sum_{i,j,k,l}W_{i,j,k,l}\langle\Phi|\hat{c}_a\hat{c}_i^\dagger\hat{c}_j^\dagger\hat{c}_k\hat{c}_l\hat{c}_b^\dagger|\Phi\rangle \\
&= -\frac{1}{2}\sum_j\Big(W_{a,j,j,b}(1-n_a)n_j(1-n_b) - W_{a,j,b,j}(1-n_a)n_j(1-n_b) \\
&\quad -W_{j,a,j,b}(1-n_a)n_j(1-n_b) + W_{j,a,b,j}(1-n_a)n_j(1-n_b)\Big) \\
&= -(1-n_a)(1-n_b)\frac{1}{2}\sum_j n_j\Big(W_{a,j,j,b} - W_{a,j,b,j} - W_{j,a,j,b} + W_{j,a,b,j}\Big) \qquad \text{(J.10)}
\end{aligned}$$

Because of the special form of the interaction $W(\vec{x},\vec{x'}) = W(\vec{x'},\vec{x})$, the terms can be combined pairwise, so that the number of independent terms is reduced from four to two. The definition of the matrix elements Eq. 3.51 from p. 141 is

$$W_{i,j,k,l} \overset{\text{Eq. 3.51}}{\overset{\text{def}}{=}} \int d^4x \int d^4x'\ \varphi_i^*(\vec{x})\varphi_j^*(\vec{x'})W(\vec{x},\vec{x'})\varphi_k(\vec{x})\varphi_l(\vec{x'})\,. \qquad \text{(J.11)}$$

With of $W(\vec{x},\vec{x'}) = W(\vec{x'},\vec{x})$, the interaction $W_{i,j,k,l}$ is symmetric under interchanging simultaneously the first two and the last two indices. Thus, $W_{a,j,j,b} = W_{j,a,b,j}$ and $W_{a,j,b,j} = W_{j,a,j,b}$ and The property $W(\vec{x},\vec{x'}) = W(\vec{x'},\vec{x})$ is an expression of Newton's third law *"actio=reactio"*.

$$\begin{aligned}
\langle\Phi|\hat{c}_a\hat{W}\hat{c}_b^\dagger|\Phi\rangle &= -(1-n_a)(1-n_b)\frac{1}{2}\sum_j n_j\Big(W_{a,j,j,b} - W_{a,j,b,j}\Big) \\
&= (1-n_a)(1-n_b)\frac{1}{2}\sum_{j=1}^{\infty} n_j\Big(W_{a,j,b,j} - W_{a,j,j,b}\Big) \qquad \text{(J.12)}
\end{aligned}$$

The first term ensures, that the result vanishes, if $|\Phi\rangle$ already contains the orbital $|\varphi_a\rangle$ or the orbital $|\varphi_b\rangle$.

Eq. J.12 is the result of the second Slater-Condon rule Eq. 3.43 on p. 140.

J.3 Matrix elements between Slater determinants differing by two orbitals

The procedure is analogous to the above case. We construct the N-electron Slater determinants $\hat{c}_a^\dagger \hat{c}_b^\dagger |\Phi\rangle$ and $\hat{c}_c^\dagger \hat{c}_d^\dagger |\Phi\rangle$ from the same $N-2$ electron Slater determinant $|\Phi\rangle$. All four indices a, b, c, d are pairwise different.

Then we select those terms where all creators are paired with an annihilator of the same orbital. All other terms vanish. Note that the bra related to $\hat{c}_a^\dagger \hat{c}_b^\dagger |\Phi\rangle$ is $\langle\Phi|\hat{c}_b \hat{c}_a$, because $\left(\hat{c}_a^\dagger \hat{c}_b^\dagger\right)^\dagger = \hat{c}_b \hat{c}_a$.

For the one-particle operator, the matrix element vanishes consistent with the third Slater-Condon rule Eq. 3.45, because the one-particle operator can only match one annihilator.

For the two-particle operator, we obtain

$$
\begin{aligned}
& \langle\Phi|\hat{c}_b \hat{c}_a \left(\hat{c}_i^\dagger \hat{c}_j^\dagger \hat{c}_k \hat{c}_l\right) \hat{c}_c^\dagger \hat{c}_d^\dagger |\Phi\rangle \\
= \; & \delta_{b,i}\delta_{a,j}\delta_{k,c}\delta_{l,d} \langle\Phi|\hat{c}_b \hat{c}_a \hat{c}_i^\dagger \hat{c}_j^\dagger \hat{c}_k \hat{c}_l \hat{c}_c^\dagger \hat{c}_d^\dagger |\Phi\rangle \\
+ \; & \delta_{b,i}\delta_{a,j}\delta_{k,d}\delta_{l,c} \langle\Phi|\hat{c}_b \hat{c}_a \hat{c}_i^\dagger \hat{c}_j^\dagger \hat{c}_k \hat{c}_l \hat{c}_c^\dagger \hat{c}_d^\dagger |\Phi\rangle \\
+ \; & \delta_{b,j}\delta_{a,i}\delta_{k,c}\delta_{l,d} \langle\Phi|\hat{c}_b \hat{c}_a \hat{c}_i^\dagger \hat{c}_j^\dagger \hat{c}_k \hat{c}_l \hat{c}_c^\dagger \hat{c}_d^\dagger |\Phi\rangle \\
+ \; & \delta_{b,j}\delta_{a,i}\delta_{k,d}\delta_{l,c} \langle\Phi|\hat{c}_b \hat{c}_a \hat{c}_i^\dagger \hat{c}_j^\dagger \hat{c}_k \hat{c}_l \hat{c}_c^\dagger \hat{c}_d^\dagger |\Phi\rangle \\
\hline
= \; & \delta_{b,i}\delta_{a,j}\delta_{k,c}\delta_{l,d} \langle\Phi|\hat{c}_b \hat{c}_a \hat{c}_b^\dagger \hat{c}_a^\dagger \hat{c}_c \hat{c}_d \hat{c}_c^\dagger \hat{c}_d^\dagger |\Phi\rangle \\
+ \; & \delta_{b,i}\delta_{a,j}\delta_{k,d}\delta_{l,c} \langle\Phi|\hat{c}_b \hat{c}_a \hat{c}_b^\dagger \hat{c}_a^\dagger \hat{c}_d \hat{c}_c \hat{c}_c^\dagger \hat{c}_d^\dagger |\Phi\rangle \\
+ \; & \delta_{b,j}\delta_{a,i}\delta_{k,c}\delta_{l,d} \langle\Phi|\hat{c}_b \hat{c}_a \hat{c}_a^\dagger \hat{c}_b^\dagger \hat{c}_c \hat{c}_d \hat{c}_c^\dagger \hat{c}_d^\dagger |\Phi\rangle \\
+ \; & \delta_{b,j}\delta_{a,i}\delta_{k,d}\delta_{l,c} \langle\Phi|\hat{c}_b \hat{c}_a \hat{c}_a^\dagger \hat{c}_b^\dagger \hat{c}_d \hat{c}_c \hat{c}_c^\dagger \hat{c}_d^\dagger |\Phi\rangle \\
\hline
\overset{c\neq d; a\neq b}{=} \; & \delta_{b,i}\delta_{a,j}\delta_{k,c}\delta_{l,d} \langle\Phi|\hat{c}_b \hat{c}_b^\dagger \hat{c}_a \hat{c}_a^\dagger \hat{c}_c \hat{c}_c^\dagger \hat{c}_d \hat{c}_d^\dagger |\Phi\rangle \\
- \; & \delta_{b,i}\delta_{a,j}\delta_{k,d}\delta_{l,c} \langle\Phi|\hat{c}_a \hat{c}_a^\dagger \hat{c}_b \hat{c}_b^\dagger \hat{c}_d \hat{c}_d^\dagger \hat{c}_c \hat{c}_c^\dagger |\Phi\rangle \\
- \; & \delta_{b,j}\delta_{a,i}\delta_{k,c}\delta_{l,d} \langle\Phi|\hat{c}_a \hat{c}_a^\dagger \hat{c}_b \hat{c}_b^\dagger \hat{c}_c \hat{c}_c^\dagger \hat{c}_d \hat{c}_d^\dagger |\Phi\rangle \\
+ \; & \delta_{b,j}\delta_{a,i}\delta_{k,d}\delta_{l,c} \langle\Phi|\hat{c}_a \hat{c}_a^\dagger \hat{c}_b \hat{c}_b^\dagger \hat{c}_d \hat{c}_d^\dagger \hat{c}_c \hat{c}_c^\dagger |\Phi\rangle \\
\hline
= \; & \delta_{b,i}\delta_{a,j}\delta_{k,c}\delta_{l,d}(1-n_d)(1-n_c)(1-n_a)(1-n_b) \\
- \; & \delta_{b,i}\delta_{a,j}\delta_{k,d}\delta_{l,c}(1-n_d)(1-n_c)(1-n_a)(1-n_b) \\
- \; & \delta_{b,j}\delta_{a,i}\delta_{k,c}\delta_{l,d}(1-n_d)(1-n_c)(1-n_a)(1-n_b) \\
+ \; & \delta_{b,j}\delta_{a,i}\delta_{k,d}\delta_{l,c}(1-n_d)(1-n_c)(1-n_a)(1-n_b)
\end{aligned}
$$

Thus, we obtain

$$
\begin{aligned}
& \langle\Phi|\hat{c}_b \hat{c}_a \left(\frac{1}{2}\sum_{i,j,k,l} W_{i,j,k,l} \hat{c}_i^\dagger \hat{c}_j^\dagger \hat{c}_l \hat{c}_k\right) \hat{c}_c^\dagger \hat{c}_d^\dagger |\Phi\rangle \\
= \; & -\frac{1}{2}\sum_{i,j,k,l} W_{i,j,k,l} \langle\Phi|\hat{c}_b \hat{c}_a \left(\hat{c}_i^\dagger \hat{c}_j^\dagger \hat{c}_k \hat{c}_l\right) \hat{c}_c^\dagger \hat{c}_d^\dagger |\Phi\rangle \\
= \; & -\frac{1}{2}\left(W_{b,a,c,d} - W_{b,a,d,c} - W_{a,b,c,d} + W_{a,b,d,c}\right) \\
& \cdot(1-n_d)(1-n_c)(1-n_a)(1-n_b)
\end{aligned}
$$

Now we exploit that a joint interchange of the first two indices and the last two indices does not change the matrix element, that is $W_{i,j,k,l} = W_{j,i,l.k}$. This is allowed because the interaction is inversion symmetric, that is $V(\vec{x}, \vec{x'}) = V(\vec{x}, \vec{x'})$, which is a special property of the Coulomb interaction.

$$\begin{aligned}
&\langle\Phi|\hat{c}_b\hat{c}_a\left(\frac{1}{2}\sum_{i,j,k,l} W_{i,j,k,l}\hat{c}_i^\dagger\hat{c}_j^\dagger\hat{c}_l\hat{c}_k\right)\hat{c}_c^\dagger\hat{c}_d^\dagger|\Phi\rangle \\
&= -\Big(W_{a,b,d,c} - W_{a,b,c,d}\Big)(1-n_d)(1-n_c)(1-n_a)(1-n_b) \\
&= +\Big(W_{a,b,c,d} - W_{a,b,d,c}\Big)(1-n_d)(1-n_c)(1-n_a)(1-n_b)
\end{aligned}$$

This result corresponds directly to the third Slater-Condon rule Eq. 3.45 on p. 140.

Appendix K

Addenda to the equation of motion for the Green's function

This chapter, I will derive the second equation of motion for the Green's function, which changes the second time argument of the Greens function. The derivation is analogous to that for the equation of motion for the first time argument presented in section 8.1 on p. 265.

The second equation is required, for example, for the arguments (Eq. 3b in [94]) by Kadanoff and Baym.[93, 94] Editor: The connection of the equation of motion with respect to the second time argument with the left-hand equation in Baym needs to be shown here.

$$i\hbar\partial_t \hat{c}^{+}_{H,\zeta}(t) = \hat{\mathcal{U}}(0,t)\left[\hat{c}^{\dagger}_{S,\zeta}, \hat{H}\right]_{-} \hat{\mathcal{U}}(t,0) \tag{K.1}$$

In order to continue, we need the commutator of the creation operator in the Schrödinger picture with the Hamiltonian. For the sake of simplicity, we drop the explicit subscript S denoting the Schrodinger picture. It is implicitly assumed.

$$\hat{H} = \sum_{\alpha,\beta} h_{\alpha,\beta}\hat{c}^{\dagger}_{\alpha}\hat{c}_{\beta} + \frac{1}{2}\sum_{\alpha,\beta,\gamma,\delta} W_{\alpha,\beta,\delta,\gamma}\hat{c}^{\dagger}_{\alpha}\hat{c}^{\dagger}_{\beta}\hat{c}_{\gamma}\hat{c}_{\delta} \tag{K.2}$$

We begin with the one-particle operator

$$\left[\hat{c}^{\dagger}_{\zeta}, \sum_{\alpha,\beta} h_{\alpha,\beta}\hat{c}^{\dagger}_{\alpha}\hat{c}_{\beta}\right]_{-} = \sum_{\alpha,\beta} h_{\alpha,\beta}\Bigg(\underbrace{\hat{c}^{\dagger}_{\zeta}\hat{c}^{\dagger}_{\alpha}}_{-\hat{c}^{\dagger}_{\alpha}\hat{c}^{\dagger}_{\zeta}}\hat{c}_{\beta} - \hat{c}^{\dagger}_{\alpha}\underbrace{\hat{c}_{\beta}\hat{c}^{\dagger}_{\zeta}}_{\delta_{\beta,\zeta}-\hat{c}^{\dagger}_{\zeta}\hat{c}_{\beta}}\Bigg) = \sum_{\alpha,\beta} h_{\alpha,\beta}\hat{c}^{\dagger}_{\alpha}\delta_{\beta,\zeta} = \sum_{\beta} h_{\alpha,\zeta}\hat{c}^{\dagger}_{\alpha} \tag{K.3}$$

and continue with the interaction

$$
\begin{aligned}
\left[\hat{c}_\zeta^\dagger, \frac{1}{2}\sum_{\alpha,\beta,\gamma,\delta} W_{\alpha,\beta,\delta,\gamma}\hat{c}_\alpha^\dagger\hat{c}_\beta^\dagger\hat{c}_\gamma\hat{c}_\delta\right]_- &= \frac{1}{2}\sum_{\alpha,\beta,\gamma,\delta} W_{\alpha,\beta,\delta,\gamma}\Big(\underbrace{\hat{c}_\zeta^\dagger\hat{c}_\alpha^\dagger\hat{c}_\beta^\dagger}_{\hat{c}_\alpha^\dagger\hat{c}_\beta^\dagger\hat{c}_\zeta^\dagger}\hat{c}_\gamma\hat{c}_\delta - \hat{c}_\alpha^\dagger\hat{c}_\beta^\dagger\hat{c}_\gamma\hat{c}_\delta\hat{c}_\zeta^\dagger\Big) \\
&= \frac{1}{2}\sum_{\alpha,\beta,\gamma,\delta} W_{\alpha,\beta,\delta,\gamma}\hat{c}_\alpha^\dagger\hat{c}_\beta^\dagger\Big(\underbrace{\hat{c}_\zeta^\dagger\hat{c}_\gamma}_{\delta_{\zeta,\gamma}-\hat{c}_\gamma\hat{c}_\zeta^\dagger}\hat{c}_\delta - \hat{c}_\gamma\underbrace{\hat{c}_\delta\hat{c}_\zeta^\dagger}_{\delta_{\delta,\zeta}-\hat{c}_\zeta^\dagger\hat{c}_\delta}\Big) \\
&= \frac{1}{2}\sum_{\alpha,\beta,\gamma,\delta} W_{\alpha,\beta,\delta,\gamma}\hat{c}_\alpha^\dagger\hat{c}_\beta^\dagger\Big(\delta_{\zeta,\gamma}\hat{c}_\delta - \hat{c}_\gamma\delta_{\delta,\zeta}\Big) \\
&= \frac{1}{2}\sum_{\alpha,\beta,\delta} W_{\alpha,\beta,\delta,\zeta}\hat{c}_\alpha^\dagger\hat{c}_\beta^\dagger\hat{c}_\delta - \frac{1}{2}\sum_{\alpha,\beta,\gamma}\underbrace{W_{\alpha,\beta,\zeta,\gamma}}_{W_{\beta,\alpha,\gamma,\zeta}}\underbrace{\hat{c}_\alpha^\dagger\hat{c}_\beta^\dagger}_{-\hat{c}_\beta^\dagger\hat{c}_\alpha^\dagger}\hat{c}_\gamma \\
&= \frac{1}{2}\sum_{\alpha,\beta,\delta} W_{\alpha,\beta,\delta,\zeta}\hat{c}_\alpha^\dagger\hat{c}_\beta^\dagger\hat{c}_\delta + \frac{1}{2}\sum_{\alpha,\beta,\gamma} W_{\beta,\alpha,\gamma,\zeta}\hat{c}_\beta^\dagger\hat{c}_\alpha^\dagger\hat{c}_\gamma \\
&= \frac{1}{2}\sum_{\alpha,\beta,\delta} W_{\alpha,\beta,\delta,\zeta}\hat{c}_\alpha^\dagger\hat{c}_\beta^\dagger\hat{c}_\delta + \overbrace{\frac{1}{2}\sum_{\alpha,\beta,\delta} W_{\alpha,\beta,\delta,\zeta}\hat{c}_\alpha^\dagger\hat{c}_\beta^\dagger\hat{c}_\delta}^{\alpha\leftrightarrow\beta,\gamma\leftrightarrow\delta} \qquad \text{(K.4)} \\
&= \sum_{\alpha,\beta,\delta} W_{\alpha,\beta,\delta,\zeta}\hat{c}_\alpha^\dagger\hat{c}_\beta^\dagger\hat{c}_\delta \qquad \text{(K.5)}
\end{aligned}
$$

We exploited that a simultaneous interchange of the first two and, at the same time, the last two arguments leaves the value of the interaction matrix elements unchanged, i.e. $W_{\alpha,\beta,\gamma,\delta} = W_{\beta,\alpha,\delta,\gamma}$. This symmetry follows from the form of the interaction matrix elements defined in Eq. 3.51 on p. 141. Editor: This argument refers to the Coulomb interaction. What about the most general definition as $W(t) = \hat{H}(t) - \hat{h}$?

With the results Eqs. K.3, K.5, we can return to Eq. K.1 and evaluate the time derivative of the annihilator in the Heisenberg picture as

$$
\begin{aligned}
i\hbar\partial_t\hat{c}_{H,\zeta}^+(t) &= \hat{\mathcal{U}}(0,t)\left[\hat{c}_{S,\zeta}^\dagger, \hat{H}\right]_-\hat{\mathcal{U}}(t,0) \\
&\overset{Eqs.\ K.3,K.5}{=} \hat{\mathcal{U}}(0,t)\left(\sum_\alpha h_{\alpha,\zeta}\hat{c}_{S,\alpha}^\dagger + \sum_{\alpha,\beta,\delta} W_{\alpha,\beta,\delta,\zeta}\hat{c}_{S,\alpha}^\dagger\hat{c}_{S,\beta}^\dagger\hat{c}_{S,\delta}\right)\hat{\mathcal{U}}(t,0) \\
&= \sum_\alpha h_{\alpha,\zeta}\hat{c}_{H,\alpha}^+(t) + \sum_{\alpha,\beta,\delta} W_{\alpha,\beta,\delta,\zeta}\hat{c}_{H,\alpha}^+(t)\hat{c}_{H,\beta}^+(t)\hat{c}_{H,\delta}(t) \qquad \text{(K.6)}
\end{aligned}
$$

Now, we can evaluate the time derivative of the Green's function Eq. 7.16. We use the short-hand

notation $\Big\langle \dots \Big\rangle_{T,\mu} \overset{\text{def}}{=} \mathrm{Tr}\{\hat{\rho}^{(W)}_{T,\mu} \dots\}$.

$$
\begin{aligned}
& i\hbar\partial_{t'} G^{\mathcal{C}}_{\alpha,\beta}(t,t') \\
\overset{\text{Eq. 7.16}}{=}\ & i\hbar\partial_{t'}\left[\frac{\theta(t-t')}{i\hbar}\Big\langle \hat{c}_{H,\alpha}(t)\hat{c}^{+}_{H,\beta}(t')\Big\rangle_{T,\mu} - \frac{\theta(t'-t)}{i\hbar}\Big\langle \hat{c}^{+}_{H,\beta}(t')\hat{c}_{H,\alpha}(t)\Big\rangle_{T,\mu}\right] \\
=\ & -\delta(t-t')\Big\langle \hat{c}_{H,\alpha}(t)\hat{c}^{+}_{H,\beta}(t')\Big\rangle_{T,\mu} - \delta(t'-t)\Big\langle \hat{c}^{+}_{H,\beta}(t')\hat{c}_{H,\alpha}(t)\Big\rangle_{T,\mu} \\
+\ & \frac{\theta(t-t')}{i\hbar}\Big\langle \hat{c}_{H,\alpha}(t)\Big(i\hbar\partial_{t'}\hat{c}^{+}_{H,\beta}(t')\Big)\Big\rangle_{T,\mu} - \frac{\theta(t'-t)}{i\hbar}\Big\langle \Big(i\hbar\partial_{t'}\hat{c}^{+}_{H,\beta}(t')\Big)\hat{c}_{H,\alpha}(t)\Big\rangle_{T,\mu} \\
\overset{\text{Eq. K.6}}{=}\ & -\delta(t-t')\Big\langle \Big[\hat{c}_{H,\alpha}(t),\hat{c}^{+}_{H,\beta}(t')\Big]_{+}\Big\rangle_{T,\mu} \\
+\ & \frac{\theta(t-t')}{i\hbar}\Big\langle \hat{c}_{H,\alpha}(t)\Big(\sum_{a} h_{a,\beta}\hat{c}^{+}_{H,a}(t') + \sum_{a,b,d} W_{a,b,d,\beta}\hat{c}^{+}_{H,a}(t')\hat{c}^{+}_{H,b}(t')\hat{c}_{H,d}(t')\Big)\Big\rangle_{T,\mu} \\
-\ & \frac{\theta(t'-t)}{i\hbar}\Big\langle \Big(\sum_{a} h_{a,\beta}\hat{c}^{+}_{H,a}(t') + \sum_{a,b,d} W_{a,b,d,\beta}\hat{c}^{+}_{H,a}(t')\hat{c}^{+}_{H,b}(t')\hat{c}_{H,d}(t')\Big)\hat{c}_{H,\alpha}(t)\Big\rangle_{T,\mu} \\
=\ & -\delta(t-t')\Big\langle \Big[\hat{c}_{H,\alpha}(t),\hat{c}^{+}_{H,\beta}(t')\Big]_{+}\Big\rangle_{T,\mu} \\
+\ & \sum_{a} h_{a,\beta}\left(\frac{\theta(t-t')}{i\hbar}\Big\langle \hat{c}_{H,\alpha}(t)\hat{c}^{+}_{H,a}(t')\Big\rangle_{T,\mu} - \frac{\theta(t'-t)}{i\hbar}\Big\langle \hat{c}^{+}_{H,a}(t')\hat{c}_{H,\alpha}(t)\Big\rangle_{T,\mu}\right) \\
+\ & \sum_{a,b,d} W_{a,b,d,\beta}\left(\frac{\theta(t-t')}{i\hbar}\Big\langle \hat{c}_{H,\alpha}(t)\hat{c}^{+}_{H,a}(t')\hat{c}^{+}_{H,b}(t')\hat{c}_{H,d}(t')\Big\rangle_{T,\mu} - \frac{\theta(t'-t)}{i\hbar}\Big\langle \hat{c}^{+}_{H,a}(t')\hat{c}^{+}_{H,b}(t')\hat{c}_{H,d}(t')\hat{c}_{H,\alpha}(t)\Big\rangle_{T,\mu}\right) \\
\overset{\text{Eq. 8.7}}{=}\ & -\delta(t-t')\delta_{\alpha,\beta} + \sum_{a} h_{a,\beta} G_{\alpha,a}(t,t') \\
+\ & \sum_{a,b,d} W_{a,b,d,\beta}\underbrace{\left(\frac{\theta(t-t')}{i\hbar}\Big\langle \hat{c}_{H,\alpha}(t)\overbrace{\hat{c}^{+}_{H,a}(t')\hat{c}^{+}_{H,b}(t')\hat{c}_{H,d}(t')}^{A}\Big\rangle_{T,\mu} - \frac{\theta(t'-t)}{i\hbar}\Big\langle \overbrace{\hat{c}^{+}_{H,a}(t')\hat{c}^{+}_{H,b}(t')\hat{c}_{H,d}(t')}^{A}\hat{c}_{H,\alpha}(t)\Big\rangle_{T,\mu}\right)}_{\frac{1}{i\hbar}\left\langle \mathcal{T}_{\mathcal{C}}\hat{c}_{H,\alpha}(t)\hat{c}^{+}_{H,a}(t')\hat{c}^{+}_{H,b}(t')\hat{c}_{H,d}(t')\right\rangle_{T,\mu}}
\end{aligned}
\tag{K.7}
$$

Eq. K.7 can be brought into a form similar to the defining equation of the Green's function for non-interacting systems is

EQUATION OF MOTION FOR THE INTERACTING GREEN'S FUNCTION

$$
\sum_{\gamma}\Big(\delta_{\alpha,\gamma} i\hbar\partial_{t'} - h_{\alpha,\gamma}\Big) G^{\mathcal{C}}_{\gamma,\beta}(t,t') =
$$

$$
= -\delta(t-t')\delta_{\alpha,\beta} + \sum_{\gamma}\sum_{b,d}\overbrace{\frac{1}{i\hbar}\mathrm{Tr}\Big\{\hat{\rho}^{(W)}_{T,\mu}\mathcal{T}_{\mathcal{C}}\hat{c}_{H,\alpha}(t)\hat{c}^{+}_{H,\gamma}(t')\underbrace{\hat{c}^{+}_{H,b}(t')\hat{c}_{H,d}(t')}_{\sim\text{density operator}}\Big\}}^{}\, W_{\gamma,b,d,\beta} \tag{K.8}
$$

$$
= -\delta(t-t')\delta_{\alpha,\beta} + \sum_{\gamma}\frac{1}{i\hbar}\mathrm{Tr}\Big\{\hat{\rho}^{(W)}_{T,\mu}\mathcal{T}_{\mathcal{C}}\hat{c}_{H,\alpha}(t)\hat{c}^{+}_{H,\gamma}(t')\underbrace{\sum_{b,d} W_{\gamma,b,d,\beta}\underbrace{\hat{c}^{+}_{H,b}(t')\hat{c}_{H,d}(t')}_{\sim\text{density operator}}}_{\hat{V}_{ee}(t')}\Big\} \tag{K.9}
$$

$\hat{V}_{ee}$ is the operator describing the Coulomb potential from the (other) electrons.

Appendix L

Derivation of Wick's theorem

Wick's theorem[64, 87] her been derived for a time-independent Hamiltonian in section **??** on p. **??**.

Here, I provide a derivation of Wick's theorem. What is shown here is the so-called "generalized Wick's theorem"[87], which is shown here for time-dependent non-interacting Hamiltonians. The generalized Wick's theorem is valid also for finite temperatures and it avoids the problems of "adiabatically switching-on the interaction", which can be problematic if the interaction interchanges ground and excited states.

The gist of Wick's theorem is to map a many-particle expectation value (in Fock space) onto an expression with only one-particle expectation values (in one-particle Hilbert space).

One of the key ingredients for the proof is that the anticommutators between creation and annihilation operators in the interaction picture are numbers, namely the one-particle Green's functions of non-interacting electrons. These anticommutators are worked out in sections L.2 and L.3.

In the following, I will refer to the complex-valued time contour and its time-ordering operator Eq. 6.36. The propagator can be expressed by the time-ordered exponential $\mathcal{T}_\mathcal{C}$ along the contour Eq. 6.37.

One has to remember that the propagator on the complex time contour is, in general, not unitary, Eq. 6.39. Similarly, the creation and annihilation operators in the interaction picture are not hermitian conjugates of each other. The creation operator is therefore indicated as $\hat{a}^+_{l,n}(t)$ instead of $\hat{a}^\dagger_{l,n}(t)$, where the latter is the hermitian conjugate of the annihilator. This is specified in Eq. 6.41 on p. 246 for Heisenberg operators.

The derivation of Wick's theorem shown below is fairly involved. Therefore, I also introduced a simpler derivation, which is limited to time-independent Hamiltonians. It is given below in section 10.2.4 *"Poor-man's derivation of Wick's theorem"* on p. 319. It may be efficient to first study that simplified derivation of section 10.2.4 before investigating the details in their generality provided here.

Editor: Remark: One aspect is worth considering: The perturbation expansion requires that the chemical potential of the interacting system is the same as that of the non-interacting system. The number of electrons in thermal equilibrium may be very different with and without interaction. This implies that the perturbation expansion may proceed through states that are very different from the interacting system of interest. This can be avoided by a suitable time-dependence of the non-interacting Hamiltonian, also along the imaginary time axis. While I have no doubt that the required time-dependence of a global energy shift is permitted, one should carefully check if this is indeed so.

L.1 Field operators in the interaction picture for complex time

FIELD OPERATORS IN THE INTERACTION PICTURE

The creation and annihilation operators $\hat{c}^{+}_{I,\alpha}(t)$, $\hat{c}_{I,\alpha}(t)$ in the interaction picture on a complex time contour $\mathcal{C}$ have the form below in terms of the corresponding creation and annihilation operators $\hat{c}^{\dagger}_{S,\alpha}$, $\hat{c}_{S,\alpha}$ in the Schrödinger picture.

$$\hat{c}^{+}_{I,\alpha}(t) \overset{\text{Eq. L.29}}{=} \sum_{\beta} \hat{c}^{\dagger}_{S,\beta} \, \langle \chi_\beta | \hat{U}(0,t) | \pi_\alpha \rangle \tag{L.1}$$

$$\hat{c}_{I,\alpha}(t) \overset{\text{Eq. L.30}}{=} \sum_{\beta} \langle \pi_\alpha | \hat{U}(t,0) | \chi_\beta \rangle \, \hat{c}_{S,\beta} \tag{L.2}$$

The one-particle orbitals $|\chi_\alpha\rangle$ may be non-orthonormal with an overlap matrix $S_{\alpha,\beta} = \langle \chi_\alpha | \chi_\beta \rangle$. Each orbital has a corresponding projector function $\langle \pi_\alpha | = \sum_\beta S^{-1}_{\alpha,\beta} \langle \chi_\beta |$. The creation and annihilation operators defined for this basisset are $\hat{c}^{\dagger}_{\alpha} = \int d^4x \, \hat{\psi}^{\dagger}(\vec{x}) \langle \vec{x} | \pi_\alpha \rangle$ and $\hat{c}_{\alpha} = \int d^4x \, \langle \pi_\alpha | \vec{x} \rangle \hat{\psi}(\vec{x})$.
The propagator $\hat{U}(t,0)$, which acts in the one-particle Hilbert space, satisfies the time-dependent Schrödinger equation along the contour $\Big[i\hbar\partial_t - \hat{h}(t) \Big] \hat{U}(t,0) = 0$ with the initial condition $\hat{U}(t,t) = \hat{1}$. The propagator can be written as time-ordered exponential.

$$\begin{aligned} \hat{U}(t,0) &= \mathcal{T}_{\mathcal{C}} \mathrm{e}^{-\frac{i}{\hbar} \int_0^t dt \, \hat{h}(t)} \\ \hat{U}(0,t) &= \hat{U}^{-1}(t,0) \end{aligned} \tag{L.3}$$

Note that the propagator is unitary only on the branch of the contour with real-valued time.

L.1.1 Proof for a time-dependent non-interacting Hamiltonian in the complex time plane

Time-dependent one-particle states

Let me choose a complete, orthonormal one-particle basisset $\{|\varphi_n\rangle\}$. The creation and annihilation operators $\hat{a}^{\dagger}_n$, $\hat{a}_n$ and the Slater determinants $|\vec{\sigma}\rangle$ shall be defined with respect to this basisset.

Starting from this basisset $\{|\varphi_n\rangle\}$ as initial states, I construct a set $\big\{|\varphi_n(t)\rangle\big\}$ of time-dependent one-particle states, which satisfy

$$i\hbar\partial_t |\varphi_n(t)\rangle = \hat{h}(t) |\varphi_n(t)\rangle \quad \text{with } |\varphi_n(0)\rangle = |\varphi_n\rangle \tag{L.4}$$

on the complex time contour $\mathcal{C}$. Because the propagator is not unitary, when the time contour deviates from the real-time axis, the orthonormality is not preserved in general. The time-dependent overlap matrix is

$$O_{m,n}(t) \overset{\text{def}}{=} \langle \varphi_m(t) | \varphi_n(t) \rangle \tag{L.5}$$

The states $|\varphi_n(t)\rangle$ are **not** eigenstates of the instantaneous Hamiltonian $\hat{h}(t)$, even when they are eigenstates at $t = 0$. The propagator Eq. 4.32 in the one-particle Hilbert space is then

$$\hat{U}(t,0) \overset{\text{Eq. 4.32}}{=} \sum_{m,n} |\varphi_m(t)\rangle \, \underbrace{O^{-1}_{m,n}(0)}_{\delta_{m,n}} \langle \varphi_n(0)| = \underbrace{\sum_n |\varphi_n(t)\rangle\langle\varphi_n(0)|}_{\mathcal{T}_{\mathcal{C}} \mathrm{e}^{-\frac{i}{\hbar}\int_0^t dt' \, \hat{h}(t')} \quad \text{Eq. 4.43}} \tag{L.6}$$

The inverse overlap matrix present in Eq. 4.32 has been dropped in Eq. L.6, because the orbitals $|\varphi(t)\rangle$ are orthonormal at $t = 0$.

The backward transformation $\hat{U}(0,t) \overset{\text{def}}{=} \hat{U}^{-1}(t,0)$ is

$$\hat{U}(0,t) \overset{\text{Eq. 4.32}}{=} \sum_{m,n} |\varphi_m(0)\rangle\, O^{-1}_{m,n}(t) \langle\varphi_n(t)| \tag{L.7}$$

Thus, the matrix elements of the propagator are

$$\begin{aligned} U_{m,n}(t,0) &\overset{\text{def}}{=} \langle\varphi_m(0)|\hat{U}(t,0)|\varphi_n(0)\rangle \overset{\text{Eq. L.6}}{=} \langle\varphi_m(0)|\varphi_n(t)\rangle \\ U_{m,n}(0,t) &\overset{\text{def}}{=} \langle\varphi_m(0)|\hat{U}(0,t)|\varphi_n(0)\rangle \overset{\text{Eq. L.7}}{=} \sum_j O^{-1}_{m,j}(t) \langle\varphi_j(t)|\varphi_n(0)\rangle \end{aligned} \tag{L.8}$$

The propagator $\hat{U}(t,0)$ acts in the one-particle Hilbert space and so does the Hamiltonian in the time-ordered exponential of Eq. L.6.[1]

Time-dependent many-particle states

From the time-dependent one-particle states $\big|\varphi_n(t)\big\rangle$ defined above, I can construct time-dependent Slater determinants in the form

$$\Phi(\vec{x}_1, \ldots, \vec{x}_N, t) \overset{\text{Eq. 1.88}}{=} \frac{1}{\sqrt{N!}} \sum_{j_1,\ldots j_N=1}^{N} \epsilon_{j_1,\ldots j_N}\, \varphi_{j_1}(\vec{x}_1, t) \cdots \varphi_{j_N}(\vec{x}_N, t) \tag{L.9}$$

where the wave function corresponds to a Slater determinant with N electrons. The time-dependent wave function $|\Phi(t)\rangle$ is a Slater determinant of the time-dependent one-particle orbitals because it is propagated with the non-interacting Hamiltonian.

In this fashion, I construct a time-dependent basisset of Slater determinants $|\Phi_{\vec{\sigma}}(t)\rangle$, which satisfy

$$i\hbar\partial_t |\Phi_{\vec{\sigma}}(t)\rangle = \hat{h}(t)|\Phi_{\vec{\sigma}}(t)\rangle \qquad \text{and} \qquad |\Phi_{\vec{\sigma}}(0)\rangle = |\vec{\sigma}\rangle = \prod_{n=1}^{\infty} \big(\hat{a}^\dagger_{S,n}\big)^{\sigma_n} |\mathcal{O}\rangle \tag{L.10}$$

where $|\vec{\sigma}\rangle$ denotes the Slater determinants in the basis of $|\varphi_n(0)\rangle$.

The propagator in Fock space can then be written as

$$\begin{aligned} \hat{\mathcal{U}}^{(0)}(t,0) &= \sum_{\vec{\sigma},\vec{\sigma'}} \big|\Phi_{\vec{\sigma}}(t)\big\rangle \underbrace{\bar{O}^{-1}_{\vec{\sigma},\vec{\sigma'}}(0)}_{\delta_{\vec{\sigma},\vec{\sigma'}}} \big\langle\Phi_{\vec{\sigma'}}(0)\big| = \underbrace{\sum_{\vec{\sigma}} \big|\Phi_{\vec{\sigma}}(t)\big\rangle\big\langle\Phi_{\vec{\sigma}}(0)\big|}_{\mathcal{T}_{\mathcal{C}} e^{-\frac{i}{\hbar}\int_0^t dt'\, \hat{h}(t')}} \\ \hat{\mathcal{U}}^{(0)}(0,t) &= \hat{\mathcal{U}}^{(0),-1}(t,0) = \sum_{\vec{\sigma},\vec{\sigma'}} \big|\Phi_{\vec{\sigma}}(0)\big\rangle \bar{O}^{-1}_{\vec{\sigma},\vec{\sigma'}}(t) \big\langle\Phi_{\vec{\sigma'}}(t)\big| \\ &\qquad \text{with } \bar{O}_{\vec{\sigma},\vec{\sigma'}} = \big\langle\Phi_{\vec{\sigma}}(t)\big|\Phi_{\vec{\sigma'}}(t)\big\rangle \end{aligned} \tag{L.11}$$

The Hamiltonian in the time-ordered exponential is a one-particle-at-a-time operator in Fock space. The inverse overlap matrix (present in Eq. 4.32) has been dropped, because I required the basisset $|\varphi_n\rangle$ to be orthonormal at time $t = 0$. This, in turn, implies orthonormality, $\bar{O}_{\vec{\sigma},\vec{\sigma'}}(0) = \delta_{\vec{\sigma},\vec{\sigma'}}$, of the Slater determints in this basisset at $t = 0$.[2]

Creation and annihilation operators

Let me define a set of creation and annihilation operators that construct the time-dependent orbitals $|\varphi_j(t)\rangle$. The creation operator $\hat{b}^+_{S,j}(t)$ shall be defined such that

$$|\varphi_j(t)\rangle = \hat{b}^+_{S,j}(t)|\mathcal{O}\rangle \tag{L.12}$$

[1] The non-interacting Hamiltonian and the corresponding operator has the same symbols in the one-particle Hilbert space and in the Fock space.

[2] This orthonormality is preserved along the real-valued time axis, but it does not hold for complex-valued time arguments.

I am using the symbol + rather than † to indicate that $\hat{b}^+_{I,j}(t)$ is not necessarily the hermitian conjugate of the corresponding annihilator, if the contour deviates from the real time axis.

The time evolution of the one-particle orbitals discussed in the section above satisfies

$$|\varphi_j(t)\rangle = \sum_k |\varphi_k(0)\rangle \underbrace{\langle\varphi_k(0)|\varphi_j(t)\rangle}_{U_{k,j}(t,0)} \overset{\text{Eq. L.8}}{=} \sum_k \underbrace{|\varphi_k(0)\rangle}_{\hat{a}^\dagger_{S,k}|\mathcal{O}\rangle} U_{k,j}(t,0) = \sum_k \hat{a}^\dagger_{S,k} U_{k,j}(t,0)\big|\mathcal{O}\big\rangle \quad \text{(L.13)}$$

The comparison of Eq. L.12 and Eq. L.13 suggests[3] the following definition of $\hat{b}^+_{S,k}(t)$

$$\hat{b}^+_{S,j}(t) \overset{\text{def}}{=} \sum_k \hat{a}^\dagger_{S,k} U_{k,j}(t,0) \quad \text{(L.14)}$$

$$\hat{b}_{S,j}(t) \overset{\text{def}}{=} \sum_k U_{j,k}(0,t)\hat{a}_{S,k} \quad \text{(L.15)}$$

The annihilator Eq. L.15 has been defined so that the equal-time anticommutator relation is conserved over time, which is verified as follows:

$$\begin{aligned}\big[\hat{b}^+_{S,m}(t), \hat{b}_{S,n}(t)\big]_+ &= \sum_{j,k} U_{j,m}(t,0)U_{n,k}(0,t) \underbrace{\big[\hat{a}^\dagger_{S,j}, \hat{a}_{S,k}\big]_+}_{\delta_{j,k}\hat{1}} = \sum_j U_{n,j}(0,t)U_{j,m}(t,0)\hat{1} \\ &= \delta_{m,n}\hat{1} \end{aligned} \quad \text{(L.16)}$$

However, the $\hat{b}_{S,j}(t)$ and $\hat{b}^+_{S,j}(t)$ are not hermitean conjugates of each other and $\langle\mathcal{O}|\hat{b}_{S,j}(t) \neq \langle\varphi_j(t)|$!

The new creation operator $\hat{b}^+_{S,j}(t)$ can also be expressed by the (non-interacting) propagator in Fock space. Let me start with the identity in the one-particle Hilbert space.[4]

$$\hat{b}^+_{S,j}(t)|\mathcal{O}\rangle \overset{\text{Eq. L.12}}{=} |\varphi_j(t)\rangle = \hat{\mathcal{U}}^{(0)}(t,0) \underbrace{\hat{a}^+_{S,j}|\mathcal{O}\rangle}_{|\varphi_j(0)\rangle} = \hat{\mathcal{U}}^{(0)}(t,0)\hat{a}^+_{S,j} \underbrace{\hat{\mathcal{U}}^{(0)}(0,t)|\mathcal{O}\rangle}_{=|\mathcal{O}\rangle} \quad \text{(L.17)}$$

This relation between $\hat{b}^+_{S,j}(t)$ and $\hat{a}^\dagger_{S,j}$ can be generalized from the one-particle Hilbert space to arbitrary Slater determinants: On the one hand, the time-dependent Slater determinants can be represented using the time-dependent one-particle orbitals via the definition of Eq. L.9.

$$|\Phi_{\vec{\sigma}}(t)\rangle \overset{\text{Eqs. L.9, L.12}}{=} \prod_{n=1}^{\infty} \Big(\hat{b}^+_{S,n}(t)\Big)^{\sigma_n}|\mathcal{O}\rangle \quad \text{(L.18)}$$

On the other hand, the time-dependent Slater determinants can be obtained by propagating the initial state $|\vec{\sigma}\rangle$.

$$|\Phi_{\vec{\sigma}}(t)\rangle = \hat{\mathcal{U}}^{(0)}(t,0) \underbrace{\prod_{n=1}^{\infty} \Big(\hat{a}^\dagger_{S,n}\Big)^{\sigma_n}|\mathcal{O}\rangle}_{=|\vec{\sigma}\rangle=|\Phi_{\vec{\sigma}}(t=0)\rangle} = \prod_{n=1}^{\infty} \Big(\hat{\mathcal{U}}^{(0)}(t,0)\hat{a}^\dagger_{S,n}\hat{\mathcal{U}}^{(0)}(0,t)\Big)^{\sigma_n} \underbrace{\hat{\mathcal{U}}^{(0)}(t,0)|\mathcal{O}\rangle}_{=|\mathcal{O}\rangle} \quad \text{(L.19)}$$

The comparison provides the identity

$$\hat{b}^+_{S,j}(t) = \hat{\mathcal{U}}^{(0)}(t,0)\hat{a}^\dagger_{S,j}\ \hat{\mathcal{U}}^{(0)}(0,t) \quad \text{(L.20)}$$

The identity for the annihilator $\hat{b}_{S,j}(t)$ is obtained from Eq. L.20 and their anticommutator relations.

$$\hat{b}_{S,j}(t) = \hat{\mathcal{U}}^{(0)}(t,0)\hat{a}_{S,j}\ \hat{\mathcal{U}}^{(0)}(0,t) \quad \text{(L.21)}$$

[3] This is a suggestion rather than a proof, because we showed only that the action on the vacuum state is identical. The proof will follow below.

[4] It is implicitely assumed that the energy of the vacuum state vanishes, which implies $\mathcal{U}(t,0)|\mathcal{O}\rangle = |\mathcal{O}\rangle$.

Some caution is required: The operators $\hat{b}^+_{S,j}(t)$ and $\hat{b}_{S,j}(t)$ are Schrödinger operators and **not** the creation and annihilation operators in the interaction picture: the propagators in the equations above propagate in the opposite direction compared to the transformation Eq. 10.4 into the interaction picture. Rather, we can identify the b-operators in the interaction picture directly with the a-operators in the Schrödinger picture, as shown below:

$$\hat{b}^+_{I,j}(t) \overset{\text{Eqs. 10.4, L.20}}{=} \hat{U}^{(0)}(0,t)\overbrace{\hat{U}^{(0)}(t,0)\hat{a}^\dagger_{S,j}\hat{U}^{(0)}(0,t)}^{\hat{b}^\dagger_{S,j}\quad\text{Eq. L.20}}\hat{U}^{(0)}(t,0) = \hat{a}^\dagger_{S,j} \tag{L.22}$$

$$\hat{b}_{I,j}(t) \overset{\text{Eqs. 10.4, L.21}}{=} \hat{U}^{(0)}(0,t)\overbrace{\hat{U}^{(0)}(t,0)\hat{a}_{S,j}\hat{U}^{(0)}(0,t)}^{\hat{b}_{S,j}\quad\text{Eq. L.21}}\hat{U}^{(0)}(t,0) = \hat{a}_{S,j} \tag{L.23}$$

Now we are ready to translate the creation and annihilation operators in the interaction picture to those in the Schrödinger picture.

- for the creation operator, I obtain

$$\begin{aligned}
\hat{a}^+_{I,n}(t) &\overset{\text{Eq. 10.4}}{=} \hat{U}^{(0)}(0,t)\hat{a}^\dagger_{S,n}\hat{U}^{(0)}(t,0)\\
&\overset{\text{Eq. L.14}}{=} \hat{U}^{(0)}(0,t)\overbrace{\sum_k \hat{b}^+_{S,k}(t)U_{k,n}(0,t)}^{\hat{a}^\dagger_{S,n}}\hat{U}^{(0)}(t,0)\\
&= \sum_k \underbrace{\hat{U}^{(0)}(0,t)\hat{b}^+_{S,k}(t)\hat{U}^{(0)}(t,0)}_{=\hat{b}^+_{I,k}(t)}U_{k,n}(0,t)\\
&\overset{\text{Eq. L.22}}{=} \sum_k \hat{a}^\dagger_{S,k}\,U_{k,n}(0,t)
\end{aligned} \tag{L.24}$$

- and for the annihilation operator, I obtain analogously

$$\begin{aligned}
\hat{a}_{I,n}(t) &\overset{\text{Eq. 10.4}}{=} \hat{U}^{(0)}(0,t)\hat{a}_{S,n}\hat{U}^{(0)}(t,0)\\
&\overset{\text{Eq. L.15}}{=} \hat{U}^{(0)}(0,t)\overbrace{\sum_k U_{n,k}(t,0)\hat{b}_{S,k}(t)}^{\hat{a}_{S,n}}\hat{U}^{(0)}(t,0)\\
&= \sum_k U_{n,k}(t,0)\underbrace{\hat{U}^{(0)}(0,t)\hat{b}_{S,k}(t)\hat{U}^{(0)}(t,0)}_{\hat{b}_{I,k}(t)}\\
&\overset{\text{Eq. L.23}}{=} \sum_k U_{n,k}(t,0)\hat{a}_{S,k}
\end{aligned} \tag{L.25}$$

Eqs. L.24 and L.25 are remarkable results: The field operators in the interaction picture can be represented as superpositions of field operators in the Schrödinger picture.

Editor: The following is a sketch to simplify the derivation above:

$$\begin{aligned}
\underbrace{b^+_{I,k}(t)}_{U^{(0)}(0,t)b^+_{S,k}(t)U^{(0)}(t,0)} &= a^\dagger_{S,k}\\
\Rightarrow b^+_{S,k}(t) &= U^{(0)}(t,0)a^\dagger_{S,k}U^{(0)}(0,t)\\
\Rightarrow b^+_{S,k}(t)|\mathcal{O}\rangle = |\varphi_k(t)\rangle &= \sum_n |\varphi_n(0)\rangle\langle\varphi_n(0)|\varphi_k(t)\rangle = \sum_n |\varphi_n(0)\rangle\langle\varphi_n(0)|\hat{U}(t,0)|\varphi_k(0)\rangle
\end{aligned} \tag{L.26}$$

General (non-orthonormal) basissets

The derivation above used an orthonormal initial basisset. The restriction was not necessary, but has been chosen to keep things simple and move complications out of the picture.

Here, I transform the result to a general basisset of orbitals $|\chi_\alpha\rangle$, which shall be complete, but which need not be orthonormal. The overlap is $S_{\alpha,\beta} = \langle\chi_\alpha|\chi_\beta\rangle$. I am using projector functions $\langle\pi_\alpha|$, which satisfy the biorthogonality condition $\langle\pi_\alpha|\chi_\beta\rangle = \delta_{\alpha,\beta}$. The projector functions may be written as $\langle\pi_\alpha| = \sum_\beta S^{-1}_{\alpha,\beta}\langle\chi_\beta|$.

The creation and annihilation operators $\hat{c}^\dagger_\alpha$, $\hat{c}_\alpha$ of the non-orthonormal basisset $\{|\chi_\alpha\rangle\}$ are transformed onto those $\hat{a}^\dagger_n$, $\hat{a}_n$ of the orthonormal basisset $\{|\varphi_n\rangle\}$ as (I refer to Eq. 3.61 and Eq. 3.64 on p. 142 for an orthonormal basisset and to Eq. B.4 and Eq. B.6 on p. 518 for non-orthonormal basis states.)

$$\begin{aligned}
\hat{c}^\dagger_{S,\alpha} &\overset{\text{Eq. B.6}}{=} \int d^4x\, \hat{\psi}^\dagger_S(\vec{x})\langle\vec{x}|\pi_\alpha\rangle = \sum_n \hat{a}^\dagger_{S,n}\langle\varphi_n|\pi_\alpha\rangle \\
\hat{c}_{S,\alpha} &\overset{\text{Eq. B.6}}{=} \int d^4x\, \langle\pi_\alpha|\vec{x}\rangle\hat{\psi}_S(\vec{x}) \overset{\text{Eq. 3.64}}{=} \sum_n \langle\pi_\alpha|\varphi_n\rangle\hat{a}_{S,n}
\end{aligned} \tag{L.27}$$

and vice versa

$$\begin{aligned}
\hat{a}^\dagger_{S,n} &= \int d^4x\, \hat{\psi}^\dagger_S(\vec{x})\langle\vec{x}|\varphi_n\rangle = \sum_\alpha \hat{c}^\dagger_{S,\alpha}\langle\chi_\alpha|\varphi_n\rangle \\
\hat{a}_{S,n} &= \int d^4x\, \langle\varphi_n|\vec{x}\rangle\hat{\psi}_S(\vec{x}) = \sum_n \langle\varphi_n|\chi_\alpha\rangle\hat{c}_{S,\alpha}
\end{aligned} \tag{L.28}$$

It is important to note that the anticommutator in the non-orthonormal basisset is the overlap of the projector functions!

Let me now work out the field operators in the interaction picture in terms of the Schödinger operators.

$$\begin{aligned}
\hat{c}^\dagger_{I,\alpha}(t) &\overset{\text{Eq. L.27}}{=} \sum_n \hat{a}^+_{I,n}(t)\langle\varphi_n|\pi_\alpha\rangle \\
&\overset{\text{Eq. L.24}}{=} \sum_n \overbrace{\sum_k \hat{a}^\dagger_{S,k}\, \underbrace{U_{k,n}(0,t)}_{\langle\varphi_k|\hat{U}(0,t)|\varphi_n\rangle}}^{\hat{a}^+_{I,n}(t)} \langle\varphi_n|\pi_\alpha\rangle \\
&\overset{\text{Eq. L.28}}{=} \sum_{k,n} \overbrace{\sum_\beta \hat{c}^\dagger_{S,\beta}\langle\chi_\beta|\varphi_k\rangle}^{\hat{a}^\dagger_{S,k}}\langle\varphi_k|\hat{U}(0,t)|\varphi_n\rangle\langle\varphi_n|\pi_\alpha\rangle \\
&= \sum_\beta \hat{c}^\dagger_{S,\beta}\langle\chi_\beta|\hat{U}(0,t)|\pi_\alpha\rangle
\end{aligned} \tag{L.29}$$

$$\begin{aligned}
\hat{c}_{I,\alpha}(t) &\overset{\text{Eq. L.27}}{=} \sum_n \langle \pi_\alpha | \varphi_n \rangle \hat{a}_{I,n}(t) \\
&\overset{\text{Eq. L.25}}{=} \sum_n \langle \pi_\alpha | \varphi_n \rangle \overbrace{\sum_k \underbrace{U_{n,k}(t,0)}_{\langle \varphi_n | \hat{U}(t,0) | \varphi_n \rangle} \hat{a}_{S,k}}^{\hat{a}_{I,n}(t)} \\
&\overset{\text{Eq. L.28}}{=} \sum_{k,n} \langle \pi_\alpha | \varphi_n \rangle \langle \varphi_n | \hat{U}(t,0) | \varphi_k \rangle \overbrace{\sum_\beta \langle \varphi_k | \chi_\beta \rangle \hat{c}_{S,\beta}}^{\hat{a}_{S,k}} \\
&= \sum_\beta \langle \pi_\alpha | \hat{U}(t,0) | \chi_\beta \rangle \hat{c}_{S,\beta}
\end{aligned} \tag{L.30}$$

L.1.2 Sanity check: One-orbital model

The following is a minimal model for many-particle physics. Its one-particle Hilbert space has only a single one-particle orbital. Consequently the Fock space is spanned by only two Slater determinants, namely the vacuum state and the sole one-particle orbital. In this example, we consider the time as complex-valued variable.

One-particle Hilbert space: Consider a one-particle Hilbert space with a single one-particle orbital $|\varphi\rangle$. Let me now also define the time-dependent one-particle orbital, which obeys the Schrödinger equation with the Hamiltonian

$$\hat{h}(t) = |\varphi\rangle \bar{\epsilon}(t) \langle \varphi| \tag{L.31}$$

The Hamiltonian shall only depend on the real part of the time, i.e. $\hat{h}(t) = \hat{h}\big((t+t^*)/2\big)$. Editor: Why is it required that the Hamiltonian depends only on the real part of the time argument?

The Schrödinger equation is

$$\begin{aligned}
i\hbar \left(\frac{dt}{ds}\right)^{-1} \partial_s \Big| \psi\big(t(s)\big) \Big\rangle &= \hat{h}\big(t(s)\big) \Big| \psi\big(t(s)\big) \Big\rangle \\
\Leftrightarrow \qquad i\hbar \partial_t \Big| \psi(t) \Big\rangle &= \hat{h}(t) \Big| \psi(t) \Big\rangle
\end{aligned} \tag{L.32}$$

The solution is

$$\begin{aligned}
\Big| \psi\big(t(s)\big) \Big\rangle &= \Big| \psi\big(t(0)\big) \Big\rangle e^{-\frac{i}{\hbar} \int_0^s ds' \, \frac{dt}{ds} \bar{\epsilon}(t(s'))} \\
\Leftrightarrow \qquad \Big| \psi(t) \Big\rangle &= \Big| \psi(0) \Big\rangle e^{-\frac{i}{\hbar} \int_{\mathcal{C},0}^t dt' \, \bar{\epsilon}(t')}
\end{aligned} \tag{L.33}$$

Let me choose a solution $|\varphi(t)\rangle$ to the Schrödinger equation with specific initial conditions $|\varphi(0)\rangle = |\varphi\rangle$ to define a time-dependent orbital

$$\Big| \varphi(t) \Big\rangle = \Big| \varphi \Big\rangle e^{-\frac{i}{\hbar} \int_{\mathcal{C},0}^t dt' \, \bar{\epsilon}(t')} \tag{L.34}$$

The time-dependent orbital is only normalized for $t = 0$ and the overlap is

$$\begin{aligned}
O(t) = \langle \varphi(t) | \varphi(t) \rangle &= \Big(e^{-\frac{i}{\hbar} \int_{\mathcal{C},0}^t dt' \, \bar{\epsilon}(t')} \Big)^* \langle \varphi | \varphi \rangle e^{-\frac{i}{\hbar} \int_{\mathcal{C},0}^t dt' \, \bar{\epsilon}(t')} = \Big| e^{-\frac{i}{\hbar} \int_{\mathcal{C},0}^t dt' \, \bar{\epsilon}(t')} \Big|^2 \\
&= \exp\left(\frac{1}{\hbar} \mathrm{Im}\Big(\int_{\mathcal{C},0}^t dt' \, \bar{\epsilon}(t') \Big) \right)
\end{aligned} \tag{L.35}$$

The time-dependent orbital remains normalized as long as the time argument remains real valued. As the contour deviates from the real axis, the overlap changes.

The propagator in the one-particle Hilbert space is

$$\hat{U}(t,0) = |\varphi(t)\rangle \underbrace{O^{-1}(0)}_{=1} \langle\varphi(0)| \overset{\text{Eq. L.33}}{=} |\varphi\rangle e^{-\frac{i}{\hbar}\int_0^t dt'\,\bar{\epsilon}(t')} \langle\varphi| \tag{L.36}$$

The back transformation is the inverse of the forward propagator.

$$\begin{aligned}
\hat{U}(0,t) &= |\varphi(0)\rangle O^{-1}(t) \langle\varphi(t)| \\
&= |\varphi(0)\rangle \overbrace{\frac{1}{\left(e^{-\frac{i}{\hbar}\int_0^t dt'\,\bar{\epsilon}(t')}\right)^\dagger \left(e^{-\frac{i}{\hbar}\int_0^t dt'\,\bar{\epsilon}(t')}\right)}}^{O^{-1}(t) \quad \text{Eq. L.35}} \overbrace{\left(e^{-\frac{i}{\hbar}\int_0^t dt'\,\bar{\epsilon}(t')}\right)^\dagger \langle\varphi(0)|}^{\langle\varphi(t)| \quad \text{Eq. L.34}} \\
&= |\varphi(0)\rangle e^{+\frac{i}{\hbar}\int_0^t dt'\,\bar{\epsilon}(t')} \langle\varphi(0)|
\end{aligned} \tag{L.37}$$

Fock space: The Fock space of the one-orbital model contains only two states, the vacuum state $|\mathcal{O}\rangle$ and the one-particle orbital $|\varphi\rangle$. The occupation-number vector of a Slater determinants has only one element, namely $\sigma \in \{0,1\}$. Editor: In the following, I am ignoring the time-dependence of the Hamiltonian.

The creation and annihilation operators are

$$\begin{aligned}
\hat{a}^\dagger &= |\varphi\rangle\langle\mathcal{O}| \\
\hat{a} &= |\mathcal{O}\rangle\langle\varphi|
\end{aligned} \tag{L.38}$$

The Hamiltonian in Fock space is

$$\hat{h} = \bar{\epsilon}\hat{a}^\dagger\hat{a} \tag{L.39}$$

and the Schrödinger equation is

$$i\hbar\partial_t|\Psi(t)\rangle = \hat{h}|\Psi(t)\rangle \tag{L.40}$$

It has the general solution

$$|\Psi(t)\rangle = \hat{\mathcal{U}}^{(0)}(t,0)|\Psi(0)\rangle = |\mathcal{O}\rangle\langle\mathcal{O}|\Psi(0)\rangle + |\varphi\rangle e^{-\frac{i}{\hbar}\bar{\epsilon}t}\langle\varphi|\Psi(0)\rangle \tag{L.41}$$

Let me define the time-dependent Slater determinants by choosing the basis states as initial values. The indices are $\vec{\sigma} \in \{0,1\} = \{\mathcal{O}, \varphi\}$.

$$\begin{aligned}
|\Phi_0(t)\rangle &= |\mathcal{O}\rangle \\
|\Phi_1(t)\rangle &= |\varphi\rangle \underbrace{e^{-\frac{i}{\hbar}\bar{\epsilon}t}}_{U(t,0)}
\end{aligned} \tag{L.42}$$

where $\hat{U}(t,0) = |\varphi\rangle U(t,0)\langle\varphi|$ is the propagator in the one-particle Hilbert space.

When calculating the overlap matrix, we need to take into account that the time argument is complex-valued.

$$\bar{O}(t) = \begin{pmatrix} \langle\Phi_0(t)|\Phi_0(t)\rangle & \langle\Phi_0(t)|\Phi_1(t)\rangle \\ \langle\Phi_1(t)|\Phi_0(t)\rangle & \langle\Phi_1(t)|\Phi_1(t)\rangle \end{pmatrix} = \begin{pmatrix} 1 & 0 \\ 0 & e^{\frac{i}{\hbar}\bar{\epsilon}(t^*-t)} \end{pmatrix} \tag{L.43}$$

The $(1,1)$ overlap matrix element can be expressed by the propagator $\hat{U}^\dagger(t,0)$ in the one-particle Hilbert space as $\bar{O}_{1,1}(t) = \langle\varphi|\hat{U}^\dagger(t,0)\hat{U}(t,0)|\varphi\rangle$. Notice, that the propagator is not unitary, if the time is complex valued.

The propagator has the form

$$\hat{\mathcal{U}}^{(0)}(t,0) = \sum_{\vec{\sigma},\vec{\sigma'}} |\Phi_{\vec{\sigma}}(t)\rangle \bar{O}^{-1}_{\vec{\sigma},\vec{\sigma'}}(0) \langle \Phi_{\vec{\sigma}}(0)| = |\mathcal{O}\rangle\langle\mathcal{O}| + |\varphi\rangle \mathrm{e}^{-\frac{i}{\hbar}\bar{\epsilon}t}\langle\varphi| \tag{L.44}$$

Let me calculate the inverse transformation

$$\begin{aligned}
\hat{\mathcal{U}}^{(0)}(0,t) &= \sum_{\vec{\sigma}} |\Phi_{\vec{\sigma}}(0)\rangle \bar{O}^{-1}_{\vec{\sigma},\vec{\sigma'}}(t) \langle \Phi_{\vec{\sigma'}}(t)| \\
&= |\mathcal{O}\rangle\langle\mathcal{O}| + |\varphi\rangle \underbrace{\mathrm{e}^{-\frac{i}{\hbar}\bar{\epsilon}(t^*-t)}}_{O^{-1}_{\varphi,\varphi}} \underbrace{\mathrm{e}^{+\frac{i}{\hbar}\bar{\epsilon}t^*}\langle\varphi|}_{\langle\varphi(t)|} \\
&= |\mathcal{O}\rangle\langle\mathcal{O}| + |\varphi\rangle \mathrm{e}^{+\frac{i}{\hbar}\bar{\epsilon}t}\langle\varphi|
\end{aligned} \tag{L.45}$$

Notice, that the inverse transformation is not simply the hermitian conjugate, if the time argument is complex-valued.

$$\mathcal{U}^\dagger(t,0) = \mathcal{U}(0,t)\bar{\boldsymbol{O}}(t) \tag{L.46}$$

Let me now turn to the creation and annihilation operators in the interaction picture

$$\begin{aligned}
\hat{a}^+_I(t) &= \overbrace{\Big(|\mathcal{O}\rangle\langle\mathcal{O}| + |\varphi\rangle \mathrm{e}^{+\frac{i}{\hbar}\bar{\epsilon}t}\langle\varphi|\Big)}^{\hat{\mathcal{U}}(0,t)} \overbrace{|\varphi\rangle\langle\mathcal{O}|}^{\hat{a}^\dagger_S} \overbrace{\Big(|\mathcal{O}\rangle\langle\mathcal{O}| + |\varphi\rangle \mathrm{e}^{-\frac{i}{\hbar}\bar{\epsilon}t}\langle\varphi|\Big)}^{\hat{\mathcal{U}}(t,0)} \\
&= |\varphi\rangle \mathrm{e}^{+\frac{i}{\hbar}\bar{\epsilon}t}\langle\mathcal{O}| = \underbrace{\mathrm{e}^{+\frac{i}{\hbar}\bar{\epsilon}t}}_{U(0,t)} \hat{a}^\dagger_S \\
\hat{a}_I(t) &= \overbrace{\Big(|\mathcal{O}\rangle\langle\mathcal{O}| + |\varphi\rangle \mathrm{e}^{+\frac{i}{\hbar}\bar{\epsilon}t}\langle\varphi|\Big)}^{\hat{\mathcal{U}}(0,t)} \overbrace{|\mathcal{O}\rangle\langle\varphi|}^{\hat{a}_S} \overbrace{\Big(|\mathcal{O}\rangle\langle\mathcal{O}| + |\varphi\rangle \mathrm{e}^{-\frac{i}{\hbar}\bar{\epsilon}t}\langle\varphi|\Big)}^{\hat{\mathcal{U}}(t,0)} \\
&= |\varphi\rangle \mathrm{e}^{-\frac{i}{\hbar}\bar{\epsilon}t}\langle\mathcal{O}| = \hat{a}_S \underbrace{\mathrm{e}^{-\frac{i}{\hbar}\bar{\epsilon}t}}_{U(t,0)}
\end{aligned} \tag{L.47}$$

In the interaction picture, the creation and annihilation operators are **not** complex conjugates of each other, unless the time argument is real valued.

The anticommutator of creation and annihilation operators at different times are

$$\Big[\hat{a}^+_I(t), \hat{a}_I(t')\Big]_+ = \Big[\hat{a}^+_S, \hat{a}_S\Big]_+ \underbrace{\mathrm{e}^{-\frac{i}{\hbar}\bar{\epsilon}(t'-t)}}_{=U(0,t)U(t',0)} \tag{L.48}$$

The commutator is readily obtained in this simple example. Let me, nevertheless, now work through the intermediate steps:

The new creation and annihilation operators are defined via the propagator $U(t,0) = \exp\big(-\frac{i}{\hbar}\int_0^t dt'\; h(t')\big)$ of the one-particle problem.

$$\begin{aligned}
\hat{b}^+_S(t) &= \hat{a}^\dagger_S \underbrace{U(t,0)}_{\mathrm{e}^{-\frac{i}{\hbar}\bar{\epsilon}t}} \\
\hat{b}_S(t) &= \underbrace{U(0,t)}_{\mathrm{e}^{+\frac{i}{\hbar}\bar{\epsilon}t}} \hat{a}_S
\end{aligned} \tag{L.49}$$

Let me verify the relation

$$\begin{aligned}
\hat{b}_S^+(t) &= \overbrace{\Big(|\mathcal{O}\rangle\langle\mathcal{O}| + |\varphi\rangle \mathrm{e}^{-\frac{i}{\hbar}\bar{\epsilon}t}\langle\varphi|\Big)}^{\hat{\mathcal{U}}(t,0)} \overbrace{|\varphi\rangle\langle\mathcal{O}|}^{\hat{a}_S^\dagger} \overbrace{\Big(|\mathcal{O}\rangle\langle\mathcal{O}| + |\varphi\rangle \mathrm{e}^{+\frac{i}{\hbar}\bar{\epsilon}t}\langle\varphi|\Big)}^{\hat{\mathcal{U}}(0,t)} \\
&= |\varphi\rangle \mathrm{e}^{-\frac{i}{\hbar}\bar{\epsilon}t}\langle\mathcal{O}| = \hat{a}_S^\dagger \underbrace{\mathrm{e}^{-\frac{i}{\hbar}\bar{\epsilon}t}}_{U(t,0)} \\
\hat{b}_S(t) &= \overbrace{\Big(|\mathcal{O}\rangle\langle\mathcal{O}| + |\varphi\rangle \mathrm{e}^{-\frac{i}{\hbar}\bar{\epsilon}t}\langle\varphi|\Big)}^{\hat{\mathcal{U}}(t,0)} \overbrace{|\mathcal{O}\rangle\langle\varphi|}^{\hat{a}_S} \overbrace{\Big(|\mathcal{O}\rangle\langle\mathcal{O}| + |\varphi\rangle \mathrm{e}^{+\frac{i}{\hbar}\bar{\epsilon}t}\langle\varphi|\Big)}^{\hat{\mathcal{U}}(0,t)} \\
&= |\varphi\rangle \mathrm{e}^{+\frac{i}{\hbar}\bar{\epsilon}t}\langle\mathcal{O}| = \underbrace{\mathrm{e}^{+\frac{i}{\hbar}\bar{\epsilon}t}}_{U(0,t)} \hat{a}_S
\end{aligned} \tag{L.50}$$

$$\begin{aligned}
\hat{a}_I^+(t) &= \hat{\mathcal{U}}^{(0)}(0,t) \overbrace{\underbrace{\mathrm{e}^{+\frac{i}{\hbar}\bar{\epsilon}t}}_{U(0,t)} \hat{b}_S^+(t)}^{\hat{a}_S^\dagger} \hat{\mathcal{U}}^{(0)}(t,0) = \mathrm{e}^{+\frac{i}{\hbar}\bar{\epsilon}t} \hat{b}_I^+(t) = \underbrace{\mathrm{e}^{+\frac{i}{\hbar}\bar{\epsilon}t}}_{U(0.t)} \hat{a}_S^\dagger \\
\hat{a}_I(t) &= \hat{\mathcal{U}}^{(0)}(0,t) \overbrace{\hat{b}_S(t) \underbrace{\mathrm{e}^{-\frac{i}{\hbar}\bar{\epsilon}t}}_{U(t,0)}}^{\hat{a}_S} \hat{\mathcal{U}}^{(0)}(t,0) = \hat{b}_I(t) \mathrm{e}^{-\frac{i}{\hbar}\bar{\epsilon}t} = \hat{a}_S \underbrace{\mathrm{e}^{-\frac{i}{\hbar}\bar{\epsilon}t}}_{U(t,0)}
\end{aligned} \tag{L.51}$$

L.2 Anticommutators of field operators in the interaction picture

For the proof of the generalized Wick theorem in section **??** on p. **??**, we need the anticommutator between creation and annihilation operators in the interaction picture for a time-dependent non-interacting Hamiltonian. In the following, it is shown that the anticommutator is a number (respectively a unit operator in Fock space.) albeit with a value given by the propagator of the non-interacting Hamiltonian.

ANTICOMMUTATORS BETWEEN CREATION AND ANNIHILATION OPERATORS IN THE INTERACTION PICTURE

The anticommutators of the creation and annihilation operators in the interaction picture are given by the matrix elements of the propagator $\hat{U}(t,t')$ in the one-particle Hilbert space. In Fock space, the anticommutators are numbers, that is they are proportional to the identity operator in Fock space.

$$\left[\hat{c}_{I,\alpha}(t_2), \hat{c}^{+}_{I,\beta}(t_1)\right]_+ \overset{\text{Eq. L.56}}{=} \left\langle \pi_\alpha \middle| \hat{U}(t_2,t_1) \middle| \pi_\beta \right\rangle \hat{1} \tag{L.52}$$

$$\left[\hat{c}^{+}_{I,m}(t_1), \hat{c}^{+}_{I,n}(t_2)\right]_+ = \hat{0} \tag{L.53}$$

$$\left[\hat{c}_{I,m}(t_1), \hat{c}_{I,n}(t_2)\right]_+ = \hat{0} \tag{L.54}$$

The one-particle orbitals $|\chi_\alpha\rangle$ may be non-orthonormal with an overlap matrix $S_{\alpha,\beta} = \langle\chi_\alpha|\chi_\beta\rangle$. Each orbital has a corresponding projector function $\langle\pi_\alpha| = \sum_\beta S^{-1}_{\alpha,\beta}\langle\chi_\beta|$. The creation and annihilation operators defined for this basisset are $\hat{c}^\dagger_\alpha = \int d^4x\, \hat{\psi}^\dagger(\vec{x})\langle\vec{x}|\pi_\alpha\rangle$ and $\hat{c}_\alpha = \int d^4x\, \langle\pi_\alpha|\vec{x}\rangle\hat{\psi}(\vec{x})$. The propagator $\hat{U}(t,0)$ satisfies the time-dependent Schrödinger equation along the contour $\left[i\hbar\partial_t - \hat{h}(t)\right]\hat{U}(t,0) = 0$ with the (non-interacting) one-particle Hamiltonian $\hat{h}(t)$. It furthermore satisfies the initial condition $\hat{U}(t,t) = \hat{1}$. The propagator can be written as time-ordered exponential.

$$\begin{aligned}\hat{U}(t,0) &= \mathcal{T}_C \mathrm{e}^{-\frac{i}{\hbar}\int_0^t dt\, \hat{h}(t)} \\ \hat{U}(0,t) &= \hat{U}^{-1}(t,0)\end{aligned} \tag{L.55}$$

Note that the propagator is unitary only on the branch of the contour with real-valued time. [a]

[a] Caution is needed to not confuse $\hat{U}(t_2,t_1$ with the propagator $\hat{\mathcal{U}}^{(0)}(t_2,t_1)$ in Fock space. They differ by the space they act on: $\hat{U}(t_2,t_1)$ acts in the one-particle Hilbert space, while $\hat{\mathcal{U}}^{(0)}(t_2,t_1)$ acts in the Fock space.

The anticommutator relations in the interaction picture are used for Wick's theorem in section **??** on p. **??**.

The proof of Eq. L.52 rests on the finding, that the creation and annihilation operators in the interaction pictures can be expressed in terms of their Schrödinger counterparts as shown in Eq. L.24 and Eq. L.2. The operator $\hat{U}(t,0)$ is the propagator in the one-particle Hilbert space, which differs from the propagator $\hat{\mathcal{U}}^{(0)}(t,0)$ in Fock space.

$$\begin{aligned}\left[\hat{c}_{I,\alpha}(t), \hat{c}^{+}_{I,\beta}(t')\right]_+ &\overset{\text{Eqs. L.1, L.2}}{=} \left[\sum_\gamma \langle\pi_\alpha|\hat{U}(t,0)|\chi_\gamma\rangle\hat{c}_{S,\gamma}, \sum_\delta \hat{c}^\dagger_{S,\delta}\langle\chi_\delta|\hat{U}(0,t')|\pi_\beta\rangle\right]_+ \\ &= \sum_\gamma\sum_\delta \langle\pi_\alpha|\hat{U}(t,0)|\chi_\gamma\rangle \underbrace{\left[\hat{c}_{S,\gamma}, \hat{c}^\dagger_{S,\delta}\right]_+}_{\langle\pi_\gamma|\pi_\delta\rangle \quad \text{Eq. B.8}} \langle\chi_\delta|\hat{U}(0,t')|\pi_\beta\rangle \\ &= \langle\pi_\alpha|\hat{U}(t,0)\underbrace{\sum_\gamma |\chi_\gamma\rangle\langle\pi_\gamma|}_{\hat{1}}\underbrace{\sum_\delta |\pi_\delta\rangle\langle\chi_\delta|}_{\hat{1}}\hat{U}(0,t')|\pi_\beta\rangle \\ &= \langle\pi_\alpha|\hat{U}(t,t')|\pi_\beta\rangle\end{aligned} \tag{L.56}$$

L.3 Commutating a field operator with the density matrix

For the proof of the generalized Wick theorem we need to interchange the order of a creation operator in the interaction picture with the von-Neumann density matrix of a non-interacting system.

$$\hat{c}^{+}_{l,\alpha}(t)\hat{\rho}^{(0)}_{T,\mu} \overset{\text{Eq. L.70}}{=} \sum_{\gamma} \hat{\rho}^{(0)}_{T,\mu}\hat{c}^{+}_{l,\gamma}(t)\left\langle \chi_\gamma \middle| \hat{U}(t,0)\mathrm{e}^{\beta(\hat{h}-\mu\hat{1})}\hat{U}(0,t)\middle|\pi_\alpha\right\rangle \tag{L.57}$$

$$\hat{c}_{l,\alpha}(t)\hat{\rho}^{(0)}_{T,\mu} \overset{\text{Eq. L.71}}{=} \sum_{\gamma} \left\langle \pi_\alpha \middle| \hat{U}(t,0)\mathrm{e}^{-\beta(\hat{h}-\mu\hat{1})}\hat{U}(0,t)\middle|\chi_\gamma\right\rangle \hat{\rho}^{(0)}_{T,\mu}\hat{c}_{l,\gamma}(t) \tag{L.58}$$

where $\hat{U}(t,0)$ is the propagator in one-particle Hilbert space. $\hat{\rho}^{(0)}_{T,\mu}$ is the thermal von-Neumann density matrix of the non-interacting system in the grand canonical ensemble.

Editor: Can this can be shown also for a non-thermal ensemble?

Editor: Is the proof also possible directly in a non-orthonormal basisset?

Assumption: The non-interacting Hamiltonian depends only on the real part of the time. The non-interacting ensemble is determined for the Hamiltonian $\hat{h}(0)$ at time $t = 0$. In the following, I will drop the time argument of the Hamiltonian, when it is zero.

Let the basisset be the eigenstates of the non-interacting Hamiltonian $\hat{h}$. Let me denote the Slater determinants in this basisset in the occupation-number representation as $|\vec{\sigma}\rangle$.

$$\mathrm{e}^{-\beta(\hat{h}-\mu\hat{N})}|\vec{\sigma}\rangle = |\vec{\sigma}\rangle\mathrm{e}^{-\beta\sum_n \sigma_n(\epsilon_n-\mu)} \tag{L.59}$$

$$\Rightarrow \quad \begin{cases} \hat{a}^\dagger_{S,k}\mathrm{e}^{-\beta(\hat{h}-\mu\hat{N})}|\vec{\sigma}\rangle = \hat{a}^\dagger_{S,k}|\vec{\sigma}\rangle\mathrm{e}^{-\beta\sum_n \sigma_n(\epsilon_n-\mu)} \\ \mathrm{e}^{-\beta(\hat{h}-\mu\hat{N})}\hat{a}^\dagger_{S,k}|\vec{\sigma}\rangle = \hat{a}^\dagger_{S,k}|\vec{\sigma}\rangle\mathrm{e}^{-\beta\sum_n \sigma_n(\epsilon_n-\mu)}\mathrm{e}^{-\beta(\epsilon_k-\mu)} \end{cases} \tag{L.60}$$

$$\Rightarrow \quad \begin{cases} \hat{a}_{S,k}\mathrm{e}^{-\beta(\hat{h}-\mu\hat{N})}|\vec{\sigma}\rangle = \hat{a}_{S,k}|\vec{\sigma}\rangle\mathrm{e}^{-\beta\sum_n \sigma_n(\epsilon_n-\mu)} \\ \mathrm{e}^{-\beta(\hat{h}-\mu\hat{N})}\hat{a}_{S,k}|\vec{\sigma}\rangle = \hat{a}_{S,k}|\vec{\sigma}\rangle\mathrm{e}^{-\beta\sum_n \sigma_n(\epsilon_n-\mu)}\mathrm{e}^{+\beta(\epsilon_k-\mu)} \end{cases} \tag{L.61}$$

Combining the equations of each pair yields

$$\hat{a}^\dagger_{S,k}\mathrm{e}^{-\beta(\hat{h}-\mu\hat{N})} = \mathrm{e}^{-\beta(\hat{h}-\mu\hat{N})}\hat{a}^\dagger_{S,k}\mathrm{e}^{+\beta(\epsilon_k-\mu)} \tag{L.62}$$

$$\hat{a}_{S,k}\mathrm{e}^{-\beta(\hat{h}-\mu\hat{N})} = \mathrm{e}^{-\beta(\hat{h}-\mu\hat{N})}\hat{a}_{S,k}\mathrm{e}^{-\beta(\epsilon_k-\mu)} \tag{L.63}$$

Next I use Eqs. L.1 and L.2.

$$\hat{a}^{+}_{l,n}(t) \overset{\text{Eq. L.1}}{=} \sum_k \hat{a}^\dagger_{S,k}U_{k,n}(0,t) \tag{L.64}$$

$$\hat{a}_{l,n}(t) \overset{\text{Eq. L.2}}{=} \sum_k U_{n,k}(t,0)\hat{a}_{S,k} \tag{L.65}$$

to obtain

$$
\begin{aligned}
\hat{a}^+_{l,n}(t)\mathrm{e}^{-\beta(\hat{h}-\mu\hat{N})} &\overset{\text{Eq. } L.1}{=} \sum_k \hat{a}^\dagger_{S,k}\mathrm{e}^{-\beta(\hat{h}-\mu\hat{N})}U_{k,n}(0,t)\\
&\overset{\text{Eq. } L.62}{=} \sum_k \mathrm{e}^{-\beta(\hat{h}-\mu\hat{N})}\hat{a}^\dagger_{S,k}\mathrm{e}^{\beta(\epsilon_k-\mu)}U_{k,n}(0,t)\\
&= \sum_k \mathrm{e}^{-\beta(\hat{h}-\mu\hat{N})}\overbrace{\sum_p \hat{a}^\dagger_{S,p}\underbrace{\sum_q U_{p,q}(0,t)U_{q,k}(t,0)}_{\delta_{p,k}}}^{\hat{a}^\dagger_{S,k}}\mathrm{e}^{\beta(\epsilon_k-\mu)}U_{k,n}(0,t)\\
&= \mathrm{e}^{-\beta(\hat{h}-\mu\hat{N})}\sum_q \underbrace{\sum_p \hat{a}^\dagger_{S,p}U_{p,q}(0,t)}_{\hat{a}^+_{l,q}}\sum_k U_{q,k}(t,0)\mathrm{e}^{\beta(\epsilon_k-\mu)}U_{k,n}(0,t)\\
&\overset{\text{Eq. } L.1}{=} \mathrm{e}^{-\beta(\hat{h}-\mu\hat{N})}\sum_q \hat{a}^+_{l,q}\Big(\sum_k U_{q,k}(t,0)\mathrm{e}^{\beta(\epsilon_k-\mu)}U_{k,n}(0,t)\Big)\\
&\overset{\text{Eq. } L.1}{=} \mathrm{e}^{-\beta(\hat{h}-\mu\hat{N})}\sum_q \hat{a}^+_{l,q}\Big\langle\varphi_q\Big|\hat{U}(t,0)\mathrm{e}^{\beta(\hat{h}-\mu\hat{1})}\hat{U}(0,t)\Big|\varphi_n\Big\rangle
\end{aligned}
\tag{L.66}
$$

$$
\begin{aligned}
\hat{a}_{l,n}(t)\mathrm{e}^{-\beta(\hat{h}-\mu\hat{N})} &\overset{\text{Eq. } L.2}{=} \sum_k U_{n,k}(t,0)\hat{a}_{S,k}\mathrm{e}^{-\beta(\hat{h}-\mu\hat{N})}\\
&\overset{\text{Eq. } L.63}{=} \sum_k U_{n,k}(t,0)\mathrm{e}^{-\beta(\hat{h}-\mu\hat{N})}\mathrm{e}^{-\beta(\epsilon_k-\mu)}\hat{a}_{S,k}\\
&= \mathrm{e}^{-\beta(\hat{h}-\mu\hat{N})}\sum_k U_{n,k}(t,0)\mathrm{e}^{-\beta(\epsilon_k-\mu)}\overbrace{\sum_p \underbrace{\sum_q U_{k,q}(0,t)U_{q,p}(t,0)}_{\delta_{k,p}}\hat{a}_{S,p}}^{\hat{a}_{S,k}}\\
&= \mathrm{e}^{-\beta(\hat{h}-\mu\hat{N})}\sum_k U_{n,k}(t,0)\mathrm{e}^{-\beta(\epsilon_k-\mu)}\sum_q U_{k,q}(0,t)\underbrace{\sum_p U_{q,p}(t,0)\hat{a}_{S,p}}_{\hat{a}_{l,q}(t)}\\
&\overset{\text{Eq. } L.2}{=} \mathrm{e}^{-\beta(\hat{h}-\mu\hat{N})}\sum_q \Big(\sum_k U_{n,k}(t,0)\mathrm{e}^{-\beta(\epsilon_k-\mu)}U_{k,q}(0,t)\Big)\hat{a}_{l,q}(t)\\
&= \mathrm{e}^{-\beta(\hat{h}-\mu\hat{N})}\sum_q \Big\langle\varphi_n\Big|\hat{U}(t,0)\mathrm{e}^{-\beta(\hat{h}-\mu\hat{1})}\hat{U}(0,t)\Big|\varphi_q\Big\rangle\hat{a}_{l,q}(t)
\end{aligned}
\tag{L.67}
$$

Normalizing the Boltzmann factors with the partition sum yields the density operator of the non-inteacting system

$$
\hat{a}^+_{l,n}(t)\hat{\rho}^{(0)}_{T,\mu} = \sum_q \hat{\rho}^{(0)}_{T,\mu}\hat{a}^+_{l,q}\Big\langle\varphi_q\Big|\hat{U}(t,0)\mathrm{e}^{\beta(\hat{h}-\mu\hat{1})}\hat{U}(0,t)\Big|\varphi_n\Big\rangle \tag{L.68}
$$

$$
\hat{a}_{l,n}(t)\hat{\rho}^{(0)}_{T,\mu} = \sum_q \Big\langle\varphi_n\Big|\hat{U}(t,0)\mathrm{e}^{-\beta(\hat{h}-\mu\hat{1})}\hat{U}(0,t)\Big|\varphi_q\Big\rangle\hat{\rho}^{(0)}_{T,\mu}\hat{a}_{l,q}(t) \tag{L.69}
$$

Transformation into a non-orthonormal basisset

Let me now transform from the orthonormal basisset $\{|\varphi_n\rangle\}$ with creation and annihilation operators $\hat{a}^+_{l,n}$ and $\hat{a}_{l,n}$ to a general non-orthonormal basisset $\{|\chi_\alpha\rangle\}$ with creation and annihilation operators

$\hat{c}^+_{l,\alpha}$ and $\hat{c}_{l,\alpha}$.

$$\begin{aligned}
\hat{c}^+_{l,\alpha}(t)\hat{\rho}^{(0)}_{T,\mu} &= \overbrace{\sum_n \hat{a}^+_{l,n}(t)\langle\varphi_n|\pi_\alpha\rangle}^{\hat{c}^+_{l,\alpha}(t)}\hat{\rho}^{(0)}_{T,\mu} \\
&\overset{\text{Eq. L.68}}{=} \sum_{n,q}\hat{\rho}^{(0)}_{T,\mu}\hat{a}^+_{l,q}\Big\langle\varphi_q\Big|\hat{U}(t,0)e^{\beta(\hat{h}-\mu\hat{1})}\hat{U}(0,t)\Big|\varphi_n\Big\rangle\langle\varphi_n|\pi_\alpha\rangle \\
&= \hat{\rho}^{(0)}_{T,\mu}\sum_{q,q'}\hat{a}^+_{l,q}\underbrace{\sum_\gamma\langle\varphi_q|\pi_\gamma\rangle\langle\chi_\gamma|\varphi_{q'}\rangle}_{\delta_{q,q'}}\Big\langle\varphi_{q'}\Big|\hat{U}(t,0)e^{\beta(\hat{h}-\mu\hat{1})}\hat{U}(0,t)|\pi_\alpha\rangle \\
&= \hat{\rho}^{(0)}_{T,\mu}\sum_\gamma\underbrace{\sum_q\hat{a}^+_{l,q}\langle\varphi_q|\pi_\gamma\rangle}_{\hat{c}^+_\gamma(t)}\langle\chi_\gamma|\underbrace{\sum_{q'}|\varphi_{q'}\rangle\Big\langle\varphi_{q'}\Big|}_{\hat{1}}\hat{U}(t,0)e^{\beta(\hat{h}-\mu\hat{1})}\hat{U}(0,t)|\pi_\alpha\rangle \\
&= \sum_\gamma\hat{\rho}^{(0)}_{T,\mu}\hat{c}^+_\gamma(t)\Big\langle\chi_\gamma\Big|\hat{U}(t,0)e^{\beta(\hat{h}-\mu\hat{1})}\hat{U}(0,t)\Big|\pi_\alpha\Big\rangle \qquad \text{(L.70)} \\
\hat{c}_{l,\alpha}(t)\hat{\rho}^{(0)}_{T,\mu} &= \overbrace{\sum_n\langle\pi_\alpha|\varphi_n\rangle\hat{a}_{l,n}(t)}^{\hat{c}_{l,\alpha}(t)}\hat{\rho}^{(0)}_{T,\mu} \\
&\overset{\text{Eq. L.69}}{=} \sum_n\Big\langle\pi_\alpha\Big|\varphi_n\Big\rangle\sum_q\Big\langle\varphi_n\Big|\hat{U}(t,0)e^{-\beta(\hat{h}-\mu\hat{1})}\hat{U}(0,t)\Big|\varphi_q\Big\rangle\hat{\rho}^{(0)}_{T,\mu}\hat{a}_{l,q}(t) \\
&= \sum_q\Big\langle\pi_\alpha\Big|\underbrace{\sum_n|\varphi_n\rangle\langle\varphi_n|}_{\hat{1}}\hat{U}(t,0)e^{-\beta(\hat{h}-\mu\hat{1})}\hat{U}(0,t)\underbrace{\sum_\gamma|\chi_\gamma\rangle\langle\pi_\gamma|}_{\hat{1}}\Big|\varphi_q\Big\rangle\hat{\rho}^{(0)}_{T,\mu}\hat{a}_{l,q}(t) \\
&= \sum_\gamma\Big\langle\pi_\alpha\Big|\hat{U}(t,0)e^{-\beta(\hat{h}-\mu\hat{1})}\hat{U}(0,t)\Big|\chi_\gamma\Big\rangle\hat{\rho}^{(0)}_{T,\mu}\underbrace{\sum_q\langle\pi_\gamma|\varphi_q\rangle\hat{a}_{l,q}(t)}_{\hat{c}_\gamma} \\
&= \sum_\gamma\Big\langle\pi_\alpha\Big|\hat{U}(t,0)e^{-\beta(\hat{h}-\mu\hat{1})}\hat{U}(0,t)\Big|\chi_\gamma\Big\rangle\hat{\rho}^{(0)}_{T,\mu}\hat{c}_{l,\gamma}(t) \qquad \text{(L.71)}
\end{aligned}$$

L.4 Contract the trace

L.4.1 Single step of Wick's theorem

Consider the expectation value $Y = \mathrm{Tr}\Big\{\hat{A}_1\hat{A}_2\ldots\hat{A}_{2M}\hat{\rho}^{(0)}_{T,\mu}\Big\}$ of the time-ordered product of **fermionic** creation and annihilation operators $\hat{A}_j \in \{\hat{c}^+_{l,\alpha}(t), \hat{c}_{l,\alpha}(t)\}$ in the interaction picture as defined in Eq. 10.34.

Before beginning, let me collect the underlying assumptions and the definition of the symbols, so that we can look them up easily.

- The operators $\hat{A}_j$ are fermionic creation and annihilation operators in the interaction picture, i.e $\hat{A}_j \in \{\hat{c}^+_{l,\alpha}(t), \hat{c}_{l,\alpha}(t)\}$.
- The creation and annihilation operators are defined by a one-particle basisset $\{|\chi_\alpha\rangle\}$, i.e. $\hat{c}^\dagger_{S,\alpha}|\mathcal{O}\rangle = |\pi_\alpha\rangle$, which may be non-orthonormal. Each orbital $|\chi_\alpha\rangle$ has a projector function $\langle\pi_\alpha| = \sum_\beta S^{-1}_{\alpha,\beta}\langle\chi_\beta|$, where $S_{\alpha,\beta} = \langle\chi_\alpha|\chi_\beta\rangle$ is the overlap matrix.
- The number of creation and annihilation operators is equal. There are M annihilation operators and M creation operators in the product.

- The time of the operators is increasing from right to left, i.e. $t_1 \geq t_2 \geq \ldots \geq t_{2M}$.

- $\hat{U}(t_2, t_1)$ is the propagator in the one-particle Hilbert space by the time-dependent, non-interacting Hamiltonian $\hat{h}(t)$. That is $\big(\hat{1} i\hbar\partial_t - \hat{h}(t)\big)\hat{U}(t, t') = \hat{0}$ and $\hat{U}(t, t) = \hat{1}$.

- $\hat{\rho}^{(0)}_{T,\mu}$ is the von-Neumann density matrix for the non-interacting Hamiltonian $\hat{h}(t)$ at time $t = 0$, i.e. $\hat{\rho}^{(0)}_{T,\mu} = \frac{1}{Z^{(0)}_{T,\mu}} \mathrm{e}^{-\beta(\hat{h}(0) - \mu\hat{N})}$.

Remember, that the operators $\hat{A}_j$ and $\hat{\rho}^{(0)}_{T,\mu}$ act in the Fock space and $\hat{U}(t, t')$ and the one-particle-reduced density matrix $\hat{\rho}^{(1)(0)}_{T,\mu}$ act on the one-particle Hilbert space. The non-interacting Hamiltonian $\hat{h}(t)$ can be either, an operator in one-particle Hilbert space or a one-particle-at-a-time operator in Fock space.

Now, we are ready to begin with the derivation

$$\begin{aligned}
Y &\overset{\text{Eq. } 10.34}{=} \mathrm{Tr}\Big\{\hat{A}_1\hat{A}_2\ldots\hat{A}_{2M}\hat{\rho}^{(0)}_{T,\mu}\Big\} \\
&= \mathrm{Tr}\Big\{[\hat{A}_1, \hat{A}_2]_+\ldots\hat{A}_{2M}\hat{\rho}^{(0)}_{T,\mu}\Big\} - \mathrm{Tr}\Big\{\hat{A}_2\hat{A}_1\ldots\hat{A}_{2M}\hat{\rho}^{(0)}_{T,\mu}\Big\} \\
&= \mathrm{Tr}\Big\{[\hat{A}_1, \hat{A}_2]_+\ldots\hat{A}_{2M}\hat{\rho}^{(0)}_{T,\mu}\Big\} - \mathrm{Tr}\Big\{\hat{A}_2[\hat{A}_1, \hat{A}_3]_+\ldots\hat{A}_{2M}\hat{\rho}^{(0)}_{T,\mu}\Big\} \\
&\quad + \mathrm{Tr}\Big\{\hat{A}_2\hat{A}_3\hat{A}_1\hat{A}_4\ldots\hat{A}_{2M}\hat{\rho}^{(0)}_{T,\mu}\Big\} \\
&= \underbrace{\sum_{j=2}^{2M}(-1)^j \mathrm{Tr}\Big\{(\hat{A}_2\cdots\hat{A}_{j-1})[\hat{A}_1, \hat{A}_j]_+(\hat{A}_{j+1}\cdots\hat{A}_{2M})\hat{\rho}^{(0)}_{T,\mu}\Big\}}_{X} \\
&\quad - \underbrace{(-1)^{2M}}_{=+1} \mathrm{Tr}\Big\{\hat{A}_2\cdots\hat{A}_{2M}\Big(\hat{A}_1\hat{\rho}^{(0)}_{T,\mu}\Big)\Big\}
\end{aligned} \tag{L.72}$$

As shown in Eq. L.57 and Eq. L.58, the operator $A_1\hat{\rho}^{(0)}_{T,\mu}$ can be expressed as a superposition of terms $\hat{\rho}^{(0)}_{T,\mu}A_1$ with the order interchanged.

$$\hat{c}^+_{l,\alpha}(t)\hat{\rho}^{(0)}_{T,\mu} \overset{\text{Eq. } L.57}{=} \sum_\gamma \hat{\rho}^{(0)}_{T,\mu}\hat{c}^+_{l,\gamma}(t)\Big\langle\chi_\gamma\Big|\hat{U}(t,0)\mathrm{e}^{\beta(\hat{h}-\mu\hat{1})}\hat{U}(0,t)\Big|\pi_\alpha\Big\rangle \tag{L.73}$$

$$\hat{c}_{l,\alpha}(t)\hat{\rho}^{(0)}_{T,\mu} \overset{\text{Eq. } L.58}{=} \sum_\gamma \Big\langle\pi_\alpha\Big|\hat{U}(t,0)\mathrm{e}^{-\beta(\hat{h}-\mu\hat{1})}\hat{U}(0,t)\Big|\chi_\gamma\Big\rangle\hat{\rho}^{(0)}_{T,\mu}\hat{c}_{l,\gamma}(t) \tag{L.74}$$

Cyclic permutation in the trace will bring $\hat{A}_1$ to the front so that the trace has the same structure as Y. Thus, we arrive at a system of equations, which can be resolved for Y.

Notation: We need to distingish several cases, which I distinguish by attaching a superscript $\pm \in \{+, -\}$ and an orbital index α to the result $Y^\pm_\alpha$. The superscript is $\pm = +$ if $\hat{A}_1 = \hat{c}^+_{l,\alpha}(t)$ is a creation operator and it is $\pm = -$ if $\hat{A}_1 = \hat{c}_{l,\alpha}(t)$ is an annihilation operator. In a similar spirit, I will introduce a short-hand notation $X^\pm_\alpha$.

- for $\hat{A}_1 = \hat{c}^+_{l,\alpha}(t)$, I obtain Y^+_α

$$
\begin{aligned}
Y^+_\alpha &\overset{\text{def}}{=} \mathrm{Tr}\Big\{\overbrace{\hat{c}^+_{l,\alpha}(t)}^{\hat{A}_1}\hat{A}_2\ldots\hat{A}_{2M}\hat{\rho}^{(0)}_{T,\mu}\Big\} \\
&\overset{\text{Eq. L.72}}{=} \underbrace{\sum_{j=2}^{2M}(-1)^j\mathrm{Tr}\Big\{(\hat{A}_2\cdots\hat{A}_{j-1})[\hat{A}_1,\hat{A}_j]_+(\hat{A}_{j+1}\cdots\hat{A}_{2M})\hat{\rho}^{(0)}_{T,\mu}\Big\}}_{=:X^+_\alpha} \\
&\quad -\mathrm{Tr}\Big\{\hat{A}_2\cdots\hat{A}_{2M}\overbrace{\sum_\gamma\hat{\rho}^{(0)}_{T,\mu}\hat{c}^+_{l,\gamma}(t)\Big\langle\chi_\gamma\Big|\hat{U}(t,0)e^{\beta(\hat{h}-\mu\hat{1})}\hat{U}(0,t)\Big|\pi_\alpha\Big\rangle}^{\hat{A}_1\hat{\rho}^{(0)}_{T,\mu}\quad\text{Eq. L.57}}\Big\} \\
&= X^+_\alpha - \sum_\gamma\underbrace{\overbrace{\mathrm{Tr}\Big\{\hat{c}^+_{l,\gamma}(t)\hat{A}_2\cdots\hat{A}_{2M}\hat{\rho}^{(0)}_{T,\mu}\Big\}}^{\mathrm{Tr}\left\{\hat{A}_2\cdots\hat{A}_{2M}\hat{\rho}^{(0)}_{T,\mu}\hat{c}^+_{l,\gamma}(t)\right\}}}_{Y^+_\gamma}\Big\langle\chi_\gamma\Big|\hat{U}(t,0)e^{\beta(\hat{h}-\mu\hat{1})}\hat{U}(0,t)\Big|\pi_\alpha\Big\rangle \quad \text{(L.75)}
\end{aligned}
$$

This is a system of coupled equations for the $\{Y^+_\gamma\}$. I bring all terms containing one of the $\{Y^+_\gamma\}$ to the left-hand side of the equation, and multiply both sides with the inverse of the prefactor, which I denote as Z. In Eq. L.76 below[5], I show that the inverse of Z is what I denote as Z^{-1}.

$$
\begin{aligned}
&\Rightarrow \quad \sum_\gamma Y^+_\gamma\underbrace{\overbrace{\Big\langle\chi_\gamma\Big|\hat{U}(t,0)e^{\beta(\hat{h}-\mu\hat{1})}\hat{U}(0,t)\Big|\pi_\alpha\Big\rangle}^{\delta_{\gamma,\alpha}+\left\langle\chi_\gamma\left|\hat{U}(t,0)e^{\beta(\hat{h}-\mu\hat{1})}\hat{U}(0,t)\right|\pi_\alpha\right\rangle}\Big(\hat{1}+e^{\beta(\hat{h}-\mu\hat{1})}\Big)\Big|\pi_\alpha\Big\rangle}_{=:Z_{\gamma,\alpha}} = X^+_\alpha \\
&\overset{\text{Eq. L.76}}{\Rightarrow} \quad Y^+_\gamma = \sum_\alpha X^+_\alpha\underbrace{\Big\langle\chi_\alpha\Big|\hat{U}(t,0)\Big(\hat{1}+e^{\beta(\hat{h}-\mu\hat{1})}\Big)^{-1}\hat{U}(0,t)\Big|\pi_\gamma\Big\rangle}_{Z^{-1}_{\alpha,\gamma}} \\
&\overset{\alpha\to\gamma,\gamma\to\alpha_1}{\Rightarrow} \quad Y^+_{\alpha_1} = \sum_\gamma X^+_\gamma\Big\langle\chi_\gamma\Big|\hat{U}(t_1,0)\Big(\hat{1}+e^{\beta(\hat{h}-\mu\hat{1})}\Big)^{-1}\hat{U}(0,t_1)\Big|\pi_{\alpha_1}\Big\rangle \qquad \text{(L.77)}
\end{aligned}
$$

Notation: In the last step, I renamed the indices (α_1 rather than α) so that I can distinguish the orbital indices α_j of several operators $\hat{A}_j$. Furthermore, I am denoting the time argument of $\hat{A}_j$ with t_j.

[5] I use

$$\sum_\alpha\Big(\sum_\gamma Y^+_\gamma Z_{\gamma,\alpha}\Big)Z^{-1}_{\alpha,\gamma'} = \sum_\alpha\Big(X^+_\alpha\Big)Z^{-1}_{\alpha,\gamma'}$$

where $\boldsymbol{Z}^{-1}$ is the inverse of $\boldsymbol{Z}$ as shown here

$$
\begin{aligned}
&\sum_\alpha Z_{\gamma,\alpha}Z^{-1}_{\alpha,\gamma'} \\
&= \Big\langle\chi_\gamma\Big|\underbrace{\hat{U}(t,0)\Big(\hat{1}+e^{\beta(\hat{h}-\mu\hat{1})}\Big)\hat{U}(0,t)}_{\hat{U}(t,0)\hat{U}(0,t)=\hat{1}}\underbrace{\overbrace{\sum_\alpha\Big|\pi_\alpha\Big\rangle\Big\langle\chi_\alpha\Big|}^{\sum_\alpha|\pi_\alpha\rangle\langle\chi_\alpha|=\hat{1}}\hat{U}(t,0)\Big(\hat{1}+e^{\beta(\hat{h}-\mu\hat{1})}\Big)^{-1}}_{\hat{1}}\hat{U}(0,t)\Big|\pi_{\gamma'}\Big\rangle}_{\hat{U}(t,0)\hat{U}(0,t)=\hat{1}} \\
&= \delta_{\gamma,\gamma'} \qquad \text{(L.76)}
\end{aligned}
$$

$\langle\chi_\gamma|\pi_{\gamma'}\rangle=\delta_{\gamma,\gamma'}$

Let me now turn to X^+_γ. Let $\hat{A}_j = \hat{c}_{l,\alpha_j}(t_j)$ and $\hat{A}_1 = \hat{c}^+_{l,\alpha_1}(t_1)$. I will use Eqs. L.52, L.53 and L.54 from p. 713. The anticommutator of two creation operators vanishes also in the interaction picture, which is taken into account by limiting the sum to annihilators.

$$\begin{aligned} X^+_\gamma &\overset{\text{def}}{=} \sum_{\substack{j=2 \\ \hat{A}_j=\text{annihilator}}}^{2M} (-1)^j \mathrm{Tr}\Big\{(\hat{A}_2\cdots\hat{A}_{j-1})\overbrace{[\hat{c}^+_{l,\gamma}(t_1),\hat{c}_{l,\alpha_j}(t_j)]_+}^{[\hat{A}_1,\hat{A}_j]_+}(\hat{A}_{j+1}\cdots\hat{A}_{2M})\hat{\rho}^{(0)}_{T,\mu}\Big\} \\ &\overset{\text{Eq. L.52}}{=} \sum_{\substack{j=2 \\ \hat{A}_j=\text{annihilator}}}^{2M} (-1)^j \mathrm{Tr}\Big\{(\hat{A}_2\cdots\hat{A}_{j-1})\langle\pi_{\alpha_j}|\hat{U}(t_j,t_1)|\pi_\gamma\rangle(\hat{A}_{j+1}\cdots\hat{A}_{2M})\hat{\rho}^{(0)}_{T,\mu}\Big\} \end{aligned} \tag{L.78}$$

which yields

$$\begin{aligned} Y^+_{\alpha_1} &\overset{\text{Eq. L.77}}{=} \sum_\gamma \overbrace{\sum_{\substack{j=2 \\ \hat{A}_j=\text{annihilator}}}^{2M} (-1)^j \mathrm{Tr}\Big\{(\hat{A}_2\cdots\hat{A}_{j-1})(\hat{A}_{j+1}\cdots\hat{A}_{2M})\hat{\rho}^{(0)}_{T,\mu}\Big\}\Big\langle\pi_{\alpha_j}\Big|\hat{U}(t_j,t_1)\Big|\pi_\gamma\Big\rangle}^{X^+_\gamma} \\ &\qquad\qquad \times\Big\langle\chi_\gamma\Big|\hat{U}(t_1,0)\Big(\hat{1}+e^{\beta(\hat{h}-\mu\hat{1})}\Big)^{-1}\hat{U}(0,t_1)\Big|\pi_{\alpha_1}\Big\rangle \\ &= \sum_{\substack{j=2 \\ \hat{A}_j=\text{annihilator}}}^{2M} (-1)^j \mathrm{Tr}\Big\{(\hat{A}_2\cdots\hat{A}_{j-1})(\hat{A}_{j+1}\cdots\hat{A}_{2M})\hat{\rho}^{(0)}_{T,\mu}\Big\} \\ &\qquad\qquad \times\Big\langle\pi_{\alpha_j}\Big|\hat{U}(t_j,0)\Big(\hat{1}+e^{\beta(\hat{h}-\mu\hat{1})}\Big)^{-1}\hat{U}(0,t_1)\Big|\pi_{\alpha_1}\Big\rangle \end{aligned} \tag{L.79}$$

We find that Y^+_α is expressed by a sum of terms, having a similar structure as $Y^\pm_\alpha$, albeit with less operators in the product. This indicates that the same rule can be applied iteratively to shrink the products in the trace and ultimately make them vanish. What we gain is that a complicated trace in Fock space is replaced by an expression of matrix elements in the one-particle Hilbert space, albeit a lengthy one.

The operator $\big(\hat{1}+e^{\beta(\hat{h}-\mu\hat{1})}\big)^{-1}$ can be identified with one-particle-reduced density matrix $\hat{\rho}^{(1),(0)}_{T,\mu}$ in thermal equilibrium with the initial non-interacting Hamiltonian $\hat{h}(0)$

$$\hat{\rho}^{(1)(0)}_{T,\mu} = f_{T,\mu}(\hat{h}(0)) = \Big(\hat{1}+e^{\beta(\hat{h}-\mu\hat{1})}\Big)^{-1} \tag{L.80}$$

Here, $f_{T,\mu}(\epsilon) \overset{\text{def}}{=} (1+e^{-\beta(\epsilon-\mu)})^{-1}$ is the Fermi distribution.

The prefactor in Eq. L.79 can be identified with the Green's function of the non-interacting Hamiltonian, which is given in Eq. 7.30 (p.258) as

$$\hat{G}^{\mathcal{C},(0)}(t,t') \overset{\text{Eq. 7.30}}{=} \frac{1}{i\hbar}\hat{U}(t,0)\Big\{\underbrace{\theta_\mathcal{C}(t-t')\big(\hat{1}-\hat{\rho}^{(1)(0)}_{T,\mu}\big)}_{\text{electrons}} - \underbrace{\theta_\mathcal{C}(t'-t)\hat{\rho}^{(1)(0)}_{T,\mu}}_{\text{holes}}\Big\}\hat{U}(0,t') \tag{L.81}$$

The prefactor in Eq. L.79 can thus be rewritten as

$$\begin{aligned} \Big\langle\pi_{\alpha_j}\Big|\hat{U}(t_j,0)\Big(\hat{1}+e^{\beta(\hat{h}-\mu\hat{1})}\Big)^{-1}\hat{U}(0,t_1)\Big|\pi_{\alpha_1}\Big\rangle &\overset{t_1\geq t_j}{=} \overbrace{\theta_\mathcal{C}(t_1-t_j)}^{=1 \text{ for } t_1\geq t_j}\Big\langle\pi_{\alpha_j}\Big|\hat{U}(t_j,0)\overbrace{\hat{\rho}^{(1)(0)}_{T,\mu}\Big(\hat{1}+e^{\beta(\hat{h}-\mu\hat{1})}\Big)^{-1}}\hat{U}(0,t_1)\Big|\pi_{\alpha_1}\Big\rangle \\ &\overset{\text{Eq. 7.30}}{=} -i\hbar\Big\langle\pi_{\alpha_j}\Big|\hat{G}^{\mathcal{C}(0)}(t_j,t_1)\Big|\pi_{\alpha_1}\Big\rangle \\ &= -i\hbar\, G^{\mathcal{C}(0)}_{\alpha_j,\alpha_1}(t_j,t_1) \end{aligned} \tag{L.82}$$

The sign factor $(-1)^{j+1}$ in Eq. L.79 can be related to the number of permutations of the indices in the original time-ordered product to bring them into the order $(j, 1, 2, \ldots, j-1, j+1, \ldots, 2M)$ of the final result. There are $j-1$ permutations to bring the index j to the front which gives the desired sign factor $(-1)^{j-1} = (-1)^{j+1}$. This allows one to rewrite the sign factor in the form

$$(-1)^{j+1} = \epsilon_{j,1,2,\ldots j-1,j+1,\ldots,2M} \tag{L.83}$$

where $\epsilon_{j_1,\ldots,2M}$ is the fully antisymmetric tensor.

Thus, the final result for $Y^+_{\alpha_1}$ is

$$Y^+_{\alpha_1} = i\hbar \sum_{\substack{j=2 \\ \hat{A}_j=\text{annihilator}}}^{2M} \epsilon_{j,1,2,\ldots j-1,j+1,\ldots,2M}\, \hat{G}^{\mathcal{C}(0)}_{\alpha_j,\alpha_1}(t_j, t_1)\mathrm{Tr}\Big\{(\hat{A}_2 \cdots \hat{A}_{j-1})(\hat{A}_{j+1} \cdots \hat{A}_{2M})\hat{\rho}^{(0)}_{T,\mu}\Big\} \tag{L.84}$$

Before we continue, let me turn to the second case where $\hat{A}_1$ is an annihilator. The derivation for annihilators and creators is analogous.

- Let me now proceed with the case when $\hat{A}_1$ is an annihilator, that is for $\hat{A}_1 = \hat{c}_{l,\alpha}(t)$. The derivation is analogous to the one above for Y^+. The reader, who wishes to skip this derivation, may proceed to the next subsection *"Summary of one step of Wick's theorem"* on p. 722.

  Similar to the previous case, I am introducing the symbols Y^-_α and X^-_α

$$\begin{aligned}
Y^-_\alpha(t) &\overset{\text{def}}{=} \mathrm{Tr}\Big\{\overbrace{\hat{c}_{l,\alpha}(t)}^{\hat{A}_1}\hat{A}_2 \ldots \hat{A}_{2M}\hat{\rho}^{(0)}_{T,\mu}\Big\} \\
&\overset{\text{Eq. L.72}}{=} \underbrace{\sum_{j=2}^{2M}(-1)^j \mathrm{Tr}\Big\{(\hat{A}_2 \cdots \hat{A}_{j-1})[\hat{A}_1, \hat{A}_j]_+(\hat{A}_{j+1} \cdots \hat{A}_{2M})\hat{\rho}^{(0)}_{T,\mu}\Big\}}_{=:X^-_\alpha} \\
&\qquad -\mathrm{Tr}\Big\{\hat{A}_2 \cdots \hat{A}_{2M} \overbrace{\sum_\gamma \Big\langle \pi_\alpha\Big|\hat{U}(t,0)\mathrm{e}^{-\beta(\hat{h}-\mu\hat{1})}\hat{U}(0,t)\Big|\chi_\gamma\Big\rangle \hat{\rho}^{(0)}_{T,\mu}\hat{c}_{l,\gamma}(t)}^{\hat{A}_1\hat{\rho}^{(0)}_{T,\mu}\quad \text{Eq. L.58}}\Big\} \\
&= X^-_\alpha - \sum_q \Big\langle \pi_\alpha\Big|\hat{U}(t,0)\mathrm{e}^{-\beta(\hat{h}-\mu\hat{1})}\hat{U}(0,t)\Big|\chi_\gamma\Big\rangle \underbrace{\overbrace{\mathrm{Tr}\Big\{\hat{c}_{l,\gamma}(t)\hat{A}_2 \cdots \hat{A}_{2M}\hat{\rho}^{(0)}_{T,\mu}\Big\}}^{\mathrm{Tr}\left\{\hat{A}_2\cdots\hat{A}_{2M}\hat{\rho}^{(0)}_{T,\mu}\hat{c}_{l,\gamma}(t)\right\}}}_{Y^-_\gamma}
\end{aligned} \tag{L.85}$$

This is a system of equations for $\{Y^-_\gamma\}$. I bring all terms containing one of the $\{Y^-_\gamma\}$ to the left hand side of the equation, and multiply both sides with the inverse of the prefactor.

$$\begin{aligned}
&\Rightarrow \quad \sum_\gamma \overbrace{\Big\langle \pi_\alpha\Big|\hat{U}(t,0)\Big(\hat{1}+\mathrm{e}^{-\beta(\hat{h}-\mu\hat{1})}\Big)\hat{U}(0,t)\Big|\chi_\gamma\Big\rangle}^{\delta_{\alpha,\gamma}+\left\langle\chi_\alpha\left|\hat{U}(t,0)\mathrm{e}^{-\beta(\hat{h}-\mu\hat{1})}\hat{U}(0,t)\right|\chi_\gamma\right\rangle} Y^-_\gamma = X^-_\alpha \\
&\Rightarrow \quad Y^-_\gamma = \sum_\alpha \Big\langle \pi_\gamma\Big|\hat{U}(t,0)\Big(\hat{1}+\mathrm{e}^{-\beta(\hat{h}-\mu\hat{1})}\Big)^{-1}\hat{U}(0,t)\Big|\chi_\alpha\Big\rangle X^-_\alpha \\
&\overset{\alpha\to\gamma\to\alpha_1}{\Rightarrow} \quad Y^-_{\alpha_1} = \sum_\gamma \Big\langle \pi_{\alpha_1}\Big|\hat{U}(t,0)\Big(\hat{1}+\mathrm{e}^{-\beta(\hat{h}-\mu\hat{1})}\Big)^{-1}\hat{U}(0,t)\Big|\chi_\gamma\Big\rangle X^-_\gamma
\end{aligned} \tag{L.86}$$

Let me now turn to X_γ^-. Let $\hat{A}_j = \hat{c}^+_{l,\alpha_j}(t_j)$ and $\hat{A}_1 = \hat{c}_{l,\alpha_1}(t_1)$. I will use Eqs. L.52, L.53 and L.54 from p. 713.

$$X_\gamma^- \overset{\text{def}}{=} \sum_{\substack{j=2 \\ \hat{A}_j=\text{creator}}}^{2M} (-1)^j \mathrm{Tr}\Big\{ (\hat{A}_2 \cdots \hat{A}_{j-1}) \overbrace{[\hat{c}_{l,\gamma}(t_1), \hat{c}^+_{l,\alpha_j}(t_j)]_+}^{[\hat{A}_1,\hat{A}_j]_+} (\hat{A}_{j+1} \cdots \hat{A}_{2M}) \hat{\rho}^{(0)}_{T,\mu} \Big\}$$

$$\overset{\text{Eq. } L.52}{=} \sum_{\substack{j=2 \\ \hat{A}_j=\text{creator}}}^{2M} (-1)^j \mathrm{Tr}\Big\{ (\hat{A}_2 \cdots \hat{A}_{j-1}) \overbrace{\langle \pi_\gamma | \hat{U}(t_1,t_j) | \pi_{\alpha_j} \rangle}^{[\hat{A}_1,\hat{A}_j]_+} (\hat{A}_{j+1} \cdots \hat{A}_{2M}) \hat{\rho}^{(0)}_{T,\mu} \Big\} \quad \text{(L.87)}$$

which yields

$$Y^-_{\alpha_1} = \sum_\gamma \Big\langle \pi_{\alpha_1} \Big| \hat{U}(t_1,0) \Big(\hat{1} + \mathrm{e}^{-\beta(\hat{h}-\mu\hat{1})} \Big)^{-1} \hat{U}(0,t_1) \Big| \chi_\gamma \Big\rangle$$

$$\times \overbrace{\sum_{\substack{j=2 \\ \hat{A}_j=\text{creator}}}^{2M} (-1)^j \Big\langle \pi_\gamma \Big| \hat{U}(t_1,t_j) \Big| \pi_{\alpha_j} \Big\rangle \mathrm{Tr}\Big\{ (\hat{A}_2 \cdots \hat{A}_{j-1})(\hat{A}_{j+1} \cdots \hat{A}_{2M}) \hat{\rho}^{(0)}_{T,\mu} \Big\}}^{X^-_\gamma}$$

$$= \sum_{\substack{j=2 \\ \hat{A}_j=\text{creator}}}^{2M} (-1)^j \Big\langle \pi_{\alpha_1} \Big| \hat{U}(t_1,0) \Big(\hat{1} + \mathrm{e}^{-\beta(\hat{h}-\mu\hat{1})} \Big)^{-1} \hat{U}(0,t_j) \Big| \pi_{\alpha_j} \Big\rangle$$

$$\times \mathrm{Tr}\Big\{ (\hat{A}_2 \cdots \hat{A}_{j-1})(\hat{A}_{j+1} \cdots \hat{A}_{2M}) \hat{\rho}^{(0)}_{T,\mu} \Big\} \quad \text{(L.88)}$$

The term with the Boltzmann factor can be expressed by the thermal one-particle-reduced density matrix for the initial non-interacting Hamiltonian $\hat{h}(0)$.

$$\Big(\hat{1} + \mathrm{e}^{-\beta(\hat{h}(0)-\mu\hat{1})} \Big)^{-1} = \hat{1} - f_{T,\mu}(\hat{h}(0)) = \hat{1} - \hat{\rho}^{(1)(0)}_{T,\mu} \quad \text{(L.89)}$$

where $f_{T,\mu}(\epsilon)$ is the Fermi distribution.

The prefactor can then be expressed by the Green's function of the non-interacting system.

$$\Big\langle \pi_{\alpha_1} \Big| \hat{U}(t_1,0) \Big(\hat{1} + \mathrm{e}^{-\beta(\hat{h}-\mu\hat{1})} \Big)^{-1} \hat{U}(0,t_j) \Big| \pi_{\alpha_j} \Big\rangle \overset{t_1 \geq t_j}{=} \overbrace{\theta_\mathcal{C}(t_1-t_j)}^{=1} \Big\langle \pi_{\alpha_1} \Big| \hat{U}(t_1,0) \overbrace{\Big(\hat{1} - \hat{\rho}^{(1)(0)}_{T,\mu} \Big)}^{\left(\hat{1}+\mathrm{e}^{-\beta(\hat{h}-\mu\hat{1})}\right)^{-1}} \hat{U}(0,t_j) \Big| \pi_{\alpha_j} \Big\rangle$$

$$= i\hbar \Big\langle \pi_{\alpha_1} \Big| \hat{G}^{\mathcal{C}(0)}(t_1,t_j) \Big| \pi_{\alpha_j} \Big\rangle$$

$$= i\hbar\, G^{\mathcal{C}(0)}_{\alpha_1,\alpha_j}(t_1,t_j) \quad \text{(L.90)}$$

Let me relate the sign factor $(-1)^{j+1}$ to the number of permutations of the indices in the original time-ordered product to bring them into the order $(1, j, 2, \ldots, j-1, j+1, \ldots, 2M)$ of the final result.

$$(-1)^j = \epsilon_{1,j,2,\ldots,j-1,j+1,\ldots,2M} \quad \text{(L.91)}$$

where $\epsilon_{j_1,\ldots,2M}$ is the fully antisymmetric tensor.

Thus, we obtain the final result for $Y^-_{n_1}$

$$Y^-_{\alpha_1} = i\hbar \sum_{\substack{j=2 \\ \hat{A}_j=\text{creator}}}^{2M} \epsilon_{1,j,2,\ldots,j-1,j+1,\ldots,2M}\, \hat{G}^{\mathcal{C}(0)}_{\alpha_1,\alpha_j}(t_1,t_j) \mathrm{Tr}\Big\{ (\hat{A}_2 \cdots \hat{A}_{j-1})(\hat{A}_{j+1} \cdots \hat{A}_{2M}) \hat{\rho}^{(0)}_{T,\mu} \Big\} \quad \text{(L.92)}$$

Summary of one step of Wick's theorem:

Let me combine the two cases:

$$Y = i\hbar \sum_{j=2}^{2M} \mathrm{Tr}\Big\{ (\hat{A}_2 \cdots \hat{A}_{j-1})(\hat{A}_{j+1} \cdots \hat{A}_{2M}) \hat{\rho}^{(0)}_{T,\mu} \Big\} \times \begin{cases} \epsilon_{j,1,2,\ldots j-1,j+1,\ldots,2M} \;\; \hat{G}^{\mathcal{C}(0)}_{\alpha_j,\alpha_1}(t_j,t_1) & \text{if } A_1 \text{ creator and } A_j \text{ annihilator} \\ \epsilon_{1,j,2,\ldots j-1,j+1,\ldots,2M} \;\; \hat{G}^{\mathcal{C}(0)}_{\alpha_1,\alpha_j}(t_1,t_j) & \text{if } A_j \text{ creator and } A_1 \text{ annihilator} \\ 0 & \text{else} \end{cases} \tag{L.93}$$

In words:

1. The first operator $\hat{A}_1$ is paired with all operators $\hat{A}_j$ of opposite type. That is, when $\hat{A}_1$ is a creation operator it is paired with all $\hat{A}_j$, that are annihilators, and vice versa.
2. Each pair is represented by a Green's function where the annihilator of the pair enters as the left and the creator as the right argument.
3. The order of the indices, after placing Green's function up front (or to the end), enters the fully antisymmetric tensor to determine the sign.
4. A factor $i\hbar$ is introduced.
5. The trace of operators contains two operators less, which made up the Green's function.
6. The product in the trace is still time ordered.

L.4.2 Sequence of Wick's iterations:

So far, we described a single step of Wick's theorem. This step is executed iteratively for the remaining products in the trace, until only $\mathrm{Tr}[\hat{\rho}^{(0)}_{T,\mu}]$ is left, which is a factor 1, that can be ignored.

After all rounds of Wick's theorem have been completed, the result has the form

$$\overbrace{\mathrm{Tr}\Big\{ \hat{\rho}^{(0)}_{T,\mu} \hat{A}_1 \cdots \hat{A}_{2M} \Big\}}^{Y} = (i\hbar)^M \sum_{\vec{P} \in \mathbb{X}} \epsilon_{P_1,\ldots,P_{2M}} \prod_{j=1}^{M} G^{\mathcal{C}(0)}_{\alpha_{P_{2j-1}},\alpha_{P_{2j}}}(t_{P_{2j-1}}, t_{P_{2j}}) \tag{L.94}$$

where the set $\mathbb{X}$ of vectors $\vec{P}$ needs to be specified.

The vectors $\vec{P} \in \mathbb{X}$ map the operator indices from the initial time order onto the operator sequence as they turn up after Wicks theorem. This order is also the time order of the time arguments in the final result.

Let me walk through the rounds of Wicks theorem:

1. In the first round of Wick's theorem, the first operator $\hat{A}_1$ in the trace is paired up with each operator of opposite type, that is creators are paired with annihilators and vice versa. Each pair is converted into a non-interacting Green's function. The result is a sum with M terms each containing one Green's function and a trace with $2M-2$ operators in the trace.
2. In the second round of Wick's theorem, the first of the remaining operators in the trace is paired up with all operators of opposite type. This divides each term of the first round further into $M-1$ terms. After the second round, the sum has $M(M-1)$ terms, each with a product of two Green's functions and a trace with $2M-4$ operators.
3. After the M-th round of Wick's theorem, the sum has $M!$ terms, each consisting of a product of M Green's functions. The trace contains only the von-Neumann density matrix, $\mathrm{Tr}\{\hat{\rho}^{(0)}_{T,\mu}\} = 1$. This is the last round of Wick's theorem.

The final sum contains all complete pairings of operators with a partner of the opposite type. Each of the $M!$ complete pairings occurs exactly once in the sum.

Let me refine the description of the set $\mathbb{X}$ further:

1. The components of the $2M$-dimensional vectors $\vec{P} \in \mathbb{X}$ are integers with $1 \leq P_j \leq 2M$. There are M^M such vectors.
2. The fully antisymmetric tensor filters all vectors out that are not permutations of the initial sequence $(1, 2, \ldots, 2M)$ of operators. There are $(2M)!$ permutations of the initial operator sequence.
3. From the result Eq. L.93 of one round of Wicks theorem, we notice that the annihilation operators occur always as left arguments of a Green's function and the creation operators occur as the right argument. There are $(M!)^2$ vectors $\vec{P}$ with this property: there are $M!$ permutations of the creation operators among each other and $M!$ permutations of the annihilation operators.
4. Two vectors $\vec{P}$, which correspond to an interchange of two (or more) Green's functions in the product, describe the same pairing. To avoid double counting of the same pairing, only one of them can be an element of $\mathbb{X}$. In order to select exactly one vector describing the same pairing, let me require that the even indices, are in ascending order, that is, they maintain the order of creation operator in the initial operator product.

$$P_2 < P_4 < \ldots < P_{2M} \qquad \text{for } \vec{P} \in \mathbb{X} \tag{L.95}$$

Let me summarize this in different words: the indices of the creation operators in the order of the initial product determines the components of $\vec{P}$ with even index. That is, all elements of $\mathbb{X}$ have the same sequence of components P_{2j} with even index $2j$. The components of $\vec{P}$ with odd index refer to the indices of the annihilation operators. These M indices can occur in any order and consequently there are $M!$ terms in the set $\mathbb{X}$.

The selection of the vectors $\vec{P}$ is still a bit clumsy. Bear with me, it will get a little better below...

L.4.3 Wick's theorem for a product that is not time ordered

In the derivation of Wick's theorem, we required in Eq. 10.34 that the operators are already time ordered. This implies that the time ordering $\mathcal{T}_\mathcal{C}$ along the contour has already been performed.

When the time-ordering operator acts on a sequence of operators, it introduces a sign change for every permutation of neighboring fermionic operators. These sign due to the time ordering need to be added to the ones introduced by Wick's theorem.

All these sign changes can described by a fully antisymmetric tensor which monitors the permutations from the order in the operator product to the time-ordered product and further to the order of indices in the final product of Green's functions.

The vector $\vec{P}$ maps the indices in the final product to their arrangement of operators in the initial product before applying the time-ordering operator.

The result of the sequence has the form

$$\mathrm{Tr}\Big\{\hat{\rho}^{(0)}_{T,\mu}\mathcal{T}_\mathcal{C}\hat{A}_1\cdots\hat{A}_{2M}\Big\} \overset{\text{Eq. L.94}}{=} (i\hbar)^M \sum_{\vec{P}\in\mathbb{X}'} \epsilon_{P_1,\ldots,P_{2M}} \prod_{j=1}^{M} G^{\mathcal{C}(0)}_{\alpha_{P_{2j-1}},\alpha_{P_{2j}}}(t_{P_{2j-1}}, t_{P_{2j}}) \tag{L.96}$$

There is a subtle difference between the trace in the equation above and the product Y used earlier in Eq. L.94, namely, the time-ordering operator $\mathcal{T}_\mathcal{C}$ has been inserted. Consequently, the set $\mathbb{X}'$ differs from the set $\mathbb{X}$ used earlier in Eq. L.94, because the vectors map the final sequence of arguments to the initial order of operators, which have no time order.

In the equation above the product $\hat{A}_1\cdots\hat{A}_{2M}$ is **not time ordered**. The time order is established through the time-ordering operator, but then the order of the operators has already changed, i.e.

the indices are no more ascending. Only this, rearranged, product of operators can be used in the expression Y for Wick's theorem.

The insertion of the time-ordering operator maintains the same structure of the result, because the sign changes due to rearrangement of the operators from the initial order to the time order are tracked by the fully antisymmetric tensor.

L.4.4 Alternating order of annihilation an creation operators

It is often convenient to bring the creation and annihilation operators under the time-ordering operator into a specific order, so that the annihilation operators alternate with creation operators.

$$\begin{aligned}\mathcal{T}_{\mathcal{C}}\hat{W}_I(t) &\overset{\text{Eq. } L.97}{=} \frac{1}{2}\sum_{i_1,o_1,i_2,o_2} W_{o_1,o_2,i_1,i_2}\mathcal{T}_{\mathcal{C}}\Big\{\hat{c}^+_{I,o_1}(t^+)\hat{c}^+_{I,o_2}(t^+)\hat{c}_{I,i_2}(t)\hat{c}_{I,i_1}(t)\Big\} \\ &= \frac{1}{2}\sum_{i_1,o_1,i_2,o_2} W_{o_1,o_2,i_1,i_2}\mathcal{T}_{\mathcal{C}}\Big\{\hat{c}_{I,i_1}(t)\hat{c}^+_{I,o_1}(t^+)\hat{c}_{I,i_2}(t)\hat{c}^+_{I,o_2}(t^+)\Big\} \qquad \text{(L.97)}\end{aligned}$$

There are no sign changes.

Inspection of the Green's function in Eq. 10.22 shows that this alternating order is consistent with the order of the operators in the Green's function.

$$\mathrm{Tr}\Big\{\hat{\rho}^{(0)}_{T,\mu}\mathcal{T}_{\mathcal{C}}\prod_{j=1}^{M}\hat{c}_{I,i_j}(t'_j)\hat{c}^\dagger_{I,o_j}(t^+_j)\Big\} \overset{\text{Eq. } L.96}{=} (i\hbar)^M\sum_{\vec{P}\in\mathbb{X}''}\epsilon_{P_1,\ldots,P_{2M}}\prod_{j=1}^{M}G^{\mathcal{C}(0)}_{i_j,o_j}(t'_{\mathcal{P}_j},t^+_j) \qquad \text{(L.98)}$$

The $\mathbb{X}''$ differs from the one used previously because it is the mapping for a different ordering of the initial operator product.

For this specific order of the initial operators, the $2M$-dimensional permutation vectors $\vec{P}$ can be expressed by a set of M-dimensional vectors $\vec{\mathcal{P}}$.

$$\vec{P} = (2\mathcal{P}_1 - 1,\, 2,\, 2\mathcal{P}_2 - 1\,, 4, \ldots, 2\mathcal{P}_M - 1,\, 2M) \qquad \text{(L.99)}$$

$$\epsilon_{\vec{P}} = \epsilon_{2\mathcal{P}_1-1,2,2\mathcal{P}_2-1,4,\ldots,2\mathcal{P}_M-1,2M} \overset{?}{=} \epsilon_{\mathcal{P}_1,\mathcal{P}_2,\ldots,\mathcal{P}_M} = \epsilon_{\vec{\mathcal{P}}} \qquad \text{(L.100)}$$

For a vector $\vec{\mathcal{P}} = (1, 2, \ldots, M)$ the two antisymmetric tensors are equal, i.e. $\epsilon_{\vec{P}} = 1 = \epsilon_{\vec{\mathcal{P}}}$.

Next, I need to show that the interchange of two neighboring components of the vector $\vec{\mathcal{P}}$ involves three interchanges of neighboring components in the corresponding vector $\vec{P}$. Let me demonstrate it for $M = 2$.

$$\begin{array}{ccc}(\mathcal{P}_1,\mathcal{P}_2) & \rightarrow & (\mathcal{P}_2,\mathcal{P}_1)\\ (P_{2\mathcal{P}_1-1},2,P_{2\mathcal{P}_2-1},4) \overset{\text{1st}}{\rightarrow} (2,P_{2\mathcal{P}_1-1},P_{2\mathcal{P}_2-1},4) & \overset{\text{2nd}}{\rightarrow} & (2,P_{2\mathcal{P}_2-1},P_{2\mathcal{P}_1-1},4) \overset{\text{3rd}}{\rightarrow} (P_{2\mathcal{P}_2-1},2,P_{2\mathcal{P}_1-1},4)\end{array} \qquad \text{(L.101)}$$

In both cases the permutation introduces a sign change. Thus, we have shown that $\epsilon_{\vec{P}} = \epsilon_{\vec{\mathcal{P}}}$ if the vector $\vec{P}$ is related to $\vec{\mathcal{P}}$ as described above.

With this choice, the result Eq. L.98 obtains the form

$$\mathrm{Tr}\Big\{\hat{\rho}^{(0)}_{T,\mu}\mathcal{T}_{\mathcal{C}}\prod_{j=1}^{M}\hat{c}_{I,i_j}(t'_j)\hat{c}^\dagger_{I,o_j}(t^+_j)\Big\} \overset{\text{Eq. } L.98}{=} (i\hbar)^M\sum_{\vec{\mathcal{P}}}\epsilon_{\mathcal{P}_1,\ldots,\mathcal{P}_M}\prod_{j=1}^{M}G^{\mathcal{C}(0)}_{i_{\mathcal{P}_j},o_j}(t'_{\mathcal{P}_j},t^+_j) \qquad \text{(L.102)}$$

The set of permutation vectors $\vec{\mathcal{P}}$ is much simpler than the set $\mathbb{X}$: It contains all M-dimensional integer vectors with elements between one and M. The fully antisymmetric tensor selects those vectors that are permutation vectors.

L.4.5 Final form of Wick's theorem

Let me now summarize the final form of Wick's theorem, as it given in Eq. 10.57 on p. 324 of the main text.

WICK'S THEOREM

$$\mathrm{Tr}\Big\{\hat{\rho}^{(0)}_{T,\mu}\mathcal{T}_{\mathcal{C}}\prod_{j=1}^{M}\hat{c}_{l,i_j}(t'_j)\hat{c}^{\dagger}_{l,o_j}(t_j^{+})\Big\}\overset{\text{Eq. L.102}}{=}(i\hbar)^M\sum_{\vec{\mathcal{P}}}\epsilon_{\mathcal{P}_1,\ldots,\mathcal{P}_M}\prod_{j=1}^{M}G^{\mathcal{C}(0)}_{i_{\mathcal{P}_j},o_j}(t'_{\mathcal{P}_j},t_j^{+}) \tag{L.103}$$

The creation and annihilation operators $\hat{c}^{\dagger}_{l,o}$ and $\hat{c}_{l,i}$ are given in the interaction picture with respect to a time-depending, non-interacting Hamiltonian $\hat{h}(t)$. While the Hamiltonian $\hat{h}(t)$ depends only on the real part of the complex-valued time argument, it propagates the wave functions, along a contour $\mathcal{C}$ in the complex time plane.
The time argument t_j^{+} stands for a time, which is infinitesimally displaced forward along the contour relative to the time t_j.
The one-particle basisset defining the creation and annihilation operators may be non-orthonormal.
The density matrix $\hat{\rho}^{(0)}_{T,\mu}$ is the thermal von-Neumann density matrix for the non-interacting Hamiltonian $\hat{h}(t)$ at time $t=0$.
The sum is performed over all M-dimensional vectors with components $\mathcal{P}_j\in\{1,2,\ldots,M\}$. The fully antisymmetric tensor $\epsilon_{\mathcal{P}_1,\mathcal{P}_2,\ldots,\mathcal{P}_M}$ selects the permutation vectors with $\mathcal{P}_j\neq\mathcal{P}_k$.
The non-interacting contour-ordered Green's function $G^{\mathcal{C}(0)}_{i,o}(t',t)$ has been defined in Eq. 7.30 (p.258) as

$$G^{\mathcal{C},(0)}_{i,o}(t',t)\overset{\text{Eq. 7.30}}{=}\frac{1}{i\hbar}\Big\langle\pi_i\Big|\hat{U}(t',0)\Big\{\underbrace{\theta_{\mathcal{C}}(t-t')(\hat{1}-\hat{\rho}^{(1)(0)}_{T,\mu})}_{\text{electrons}}-\underbrace{\theta_{\mathcal{C}}(t'-t)\hat{\rho}^{(1)(0)}_{T,\mu}}_{\text{holes}}\Big\}\hat{U}(0,t)\Big|\pi_o\Big\rangle$$

L.4.6 Why is the time-ordered Green's function important?

As we introduced the Green's function for many particle systems, we have seen that several Green's function could have been defined by adding a solution of the homogeneous Schrödinger equation. As motivation for the time-ordered Green's function, I referred to Wick's theorem. In the derivation above, the contractions are, up to a factor, equal to the time-ordered Green's function and no other type of Green's function, which explains the importance of the time-ordered Green's function.

L.5 Non-interacting grand potential

L.5.1 Grand potential of non-interacting electrons

The grand potential $\Omega^{(0)}_{T,\mu}$ of non-interacting electrons can be obtained from the eigenvalues ϵ_n of the corresponding one-particle Hamiltonian $\hat{h}$. For this purpose, we enter the occupation-number

representation with many-particle eigenstates represented as $|\vec{\sigma}\rangle$.

$$\begin{aligned}
\Omega^{(0)}_{T,\mu} &\overset{\text{Eq. 2.61}}{=} -k_B T \ln \underbrace{\mathrm{Tr}\Big\{ \mathrm{e}^{-\beta(\hat{h}-\mu\hat{N})} \Big\}}_{\text{Trace over Fock space}} \\
&\overset{\text{Eq. 1.97}}{=} -k_B T \ln \sum_{\vec{\sigma}} \mathrm{e}^{-\beta \sum_n \sigma_n(\epsilon_n-\mu)} = -k_B T \ln \sum_{\vec{\sigma}} \prod_n \mathrm{e}^{-\beta\sigma_n(\epsilon_n-\mu)} \\
&= -k_B T \ln \prod_{n=1}^{\infty} \sum_{\sigma_n=0}^{1} \mathrm{e}^{-\beta\sigma_n(\epsilon_n-\mu)} \\
&= -k_B T \ln \prod_{n=1}^{\infty} \Big(1 + \mathrm{e}^{-\beta(\epsilon_n-\mu)}\Big) \\
&= -k_B T \sum_n \ln\Big(1 + \mathrm{e}^{-\beta(\epsilon_n-\mu)}\Big) \\
&= -k_B T \underbrace{\mathrm{Tr}\Big\{ \ln\Big(\hat{1} + \mathrm{e}^{-\beta(\hat{h}-\mu\hat{1})}\Big) \Big\}}_{\text{Trace over 1p Hilbert space}}
\end{aligned} \tag{L.104}$$

In the last line, the trace is performed over the one-particle Hilbert space rather than the Fock space as in the first line.

Pay attention to the interchange of sum and product from the second to the third line: sum and product do not commutate in general.

In terms of the eigenvalues ϵ_n of the Hamiltonian $\hat{h}$, the grand potential is

$$\Omega^{(0)}_{T,\mu} \overset{\text{Eq. L.104}}{=} -k_B T \sum_n \ln\Big(1 + \mathrm{e}^{-\beta(\epsilon_n-\mu)}\Big) \tag{L.105}$$

The function in the above expression has the limiting cases

$$-k_B T \ln\Big(1 + \mathrm{e}^{-\beta(\epsilon_n-\mu)}\Big) = \begin{cases} \epsilon - \mu & \text{for } \beta(\epsilon_n - \mu) \ll 0 \\ 0 & \text{for } \beta(\epsilon_n - \mu) \gg 0 \end{cases} \tag{L.106}$$

L.5.2 Fermi distribution from the grand potential of non-interacting fermions

The mean **occupation**

$$f_n \overset{\text{def}}{=} \sum_{\vec{\sigma}} P_{\vec{\sigma}} \sigma_n \tag{L.107}$$

of a natural orbital can be obtained as the derivative of the grand potential with respect to the corresponding one-particle energy. [6]

[6] Eq. 2.56 defines the grand potential for an interacting or non-interacting system

$$\Omega_{T,\mu} \overset{\text{Eq. 2.56}}{=} \min_{\hat{\rho}^{\nu N}} \Big\{ \overbrace{\mathrm{Tr}[\hat{\rho}^{\nu N}(\hat{h}+\hat{V})]}^{E(\hat{\rho}^{\nu N})} \overbrace{+k_B T\ \mathrm{Tr}\left[\hat{\rho}^{\nu N} \ln\left(\hat{\rho}^{\nu N}\right)\right]}^{-TS(\hat{\rho}^{\nu N})} \overbrace{-\mu \mathrm{Tr}[\hat{\rho}^{\nu N}\hat{N}]}^{-\mu N(\hat{\rho}^{\nu N})} \Big\} \tag{L.108}$$

The variation of the grand potential with respect to the non-interacting Hamiltonian $\hat{h}$ provides

$$d\Omega_{T,\mu} = \mathrm{Tr}\Big(\hat{\rho}^{\nu N}_{T,\mu} d\hat{h}\Big) \tag{L.109}$$

As a consequence of the variational principle, all changes due to induced changes of the density matrix vanish for the equilibirum density matrix. For a one-particle at a time operator as the non-interacting Hamiltonian one may replace the trace over the Fock space by a trace of the one-particle Hilbert space, if we also replace the thermal von-Neumann density matrix by the corresponding one-particle-reduced density matrix.

$$d\Omega_{T,\mu} = \mathrm{Tr}\Big(\hat{\rho}^{(1)}_{T,\mu} d\hat{h}\Big) \tag{L.110}$$

$$f_n = \frac{\partial \Omega^{(0)}}{\partial \epsilon_n} \overset{\text{Eq. } L.105}{=} \left(1 + e^{\beta(\epsilon_n - \mu)}\right)^{-1} \tag{L.113}$$

This defines the **Fermi distribution**

$$f_{T,\mu}(\epsilon) \overset{\text{def}}{=} \left(1 + e^{\beta(\epsilon - \mu)}\right)^{-1} \tag{L.114}$$

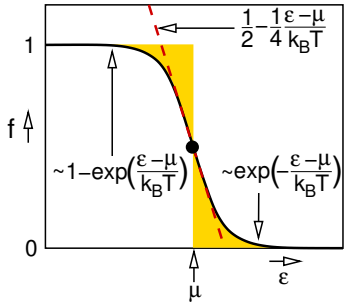


Fig. L.1: Fermi distribution function Eq. L.114 and common limits. (Copy of Fig. L.1)

The Fermi distribution can also be used in operator form to express the thermal one-particle-reduced density matrix of non-interacting electrons by its one-particle Hamiltonian $\hat{h}$

The one-particle-reduced density matrix can be expressed (per definition) in terms of its natural orbitals $|\varphi_n\rangle$ and occupations f_n.

$$\hat{\rho}^{(1)} = \sum_n |\varphi_n\rangle f_n \langle\varphi_n| \tag{L.115}$$

In thermal equilibrium the occupations are given by the Fermi distribution and the natural orbitals are given by the eigenstates of the Hamiltonian $\hat{h}$.

$$\begin{aligned} \hat{\rho}^{(1),(0)}_{T,\mu} &= \sum_n |\varphi_n\rangle f_{T,\mu}(\epsilon_n) \langle\varphi_n| \overset{\text{Eq. } 2.17}{=} \sum_n |\varphi_n\rangle \left(1 + e^{\beta(\epsilon - \mu)}\right)^{-1} \langle\varphi_n| \\ &= \left(\hat{1} + e^{\beta(\hat{h} - \mu)}\right)^{-1} \end{aligned} \tag{L.116}$$

The Hamiltonian is considered here as an operator in one-particle Hilbert space rather than a one-particle-at-a-time operator in Fock space.

Let me now express the non-interacting hamiltonian in terms of its thermal one-particle-reduced density matrix[7]

$$\hat{h} = \mu + k_B T \ln\left\{\left(\hat{1} - \hat{\rho}^{(1),(0)}_{T,\mu}\right)\left(\hat{\rho}^{(1),(0)}_{T,\mu}\right)^{-1}\right\} \tag{L.117}$$

Thus we may identify the one-particle-reduced density matrix with the functional derivative of the thermal grand potential with respect to the non-interacting Hamiltonian. The functional derivative is defined by

$$d\Omega_{T,\mu} = \mathrm{Tr}\left(\frac{\partial \Omega_{T,\mu}}{\partial \hat{h}} d\hat{h}\right) \tag{L.111}$$

so that

$$\hat{\rho}^{(1)}_{T,\mu} = \frac{\partial \Omega_{T,\mu}}{\partial \hat{h}} \qquad \text{or} \qquad f_{n,T,\mu} = \frac{\partial \Omega_{T,\mu}}{\partial \epsilon_n} \tag{L.112}$$

[7] This is possible at any finite temperature. The zero temperature case has to be treated as the low-temperature limit.

This equation is useful for formal considerations. Numerically, this expression is of limited use, because occupations close to zero or one are mapped onto a huge energy window. Small errors in the one-particle-reduced density matrix produce large errors in the hamiltonian further away from the Fermi level.

Eq. L.117 allows one to express the grand potential of non-interacxting electrons as functional of the one-particle-reduced density matrix.

$$\begin{aligned}\Omega^{(0)}_{T,\mu} &\overset{\text{Eq. } L.104}{=} -k_B T \,\mathrm{Tr}\left\{\ln\left(\hat{1} + \mathrm{e}^{-\beta(\hat{h}-\mu\hat{1})}\right)\right\} \\ &\overset{\text{Eq. } L.117}{=} +k_B T \,\mathrm{Tr}\left\{\ln\left(\hat{1} - \hat{\rho}^{(1),(0)}_{T,\mu}\right)\right.\end{aligned} \tag{L.118}$$

The domain for this functional are all N-representable one-particle-reduced density matrices. These are all hermitean matrices with eigenvalues between zero and one.

L.5.3 Grand potential of non-interacting fermions as functional of the non-interacting Green's function

In Eq. 10.89 on p. 337 the grand potential has been expressed as functional of the bare Green's function.

The one-particle-reduced density matrix at time zero can be expressed by the non-interacting Green's function from Eq. 7.30.

$$i\hbar\hat{G}^{\mathcal{C},(0)}(0^+,0) = \hat{1} - \hat{\rho}^{(1),(0)}_{T,\mu} \tag{L.119}$$

Thus, the non-interacting grand potential $\Omega^{(0)}_{T,\mu}$ can be expressed as functional of the non-interacting Green's function.

$$\Omega^{(0)}_{T,\mu} = +k_B T \,\mathrm{Tr}\left\{\ln\left(i\hbar\hat{G}^{\mathcal{C},(0)}(0^+,0)\right)\right. \tag{L.120}$$

Some caution is required: The non-interacting grand potential refers to the initial state defining the ensemble. Thus, it refers to the Hamiltonian at time $t = 0$ or at $t = -i\hbar\beta$, namely the beginning or the end of the contour $\mathcal{C}$.

One-particle-reduced density matrix from Green's function

Editor: This is a short derivation from before I found the more direct one above. It may be relevant elsewhere.

Finally, we may express the one-particle-reduced density matrix by the thermal, non-interacting Green's function

$$\hat{\rho}^{(1)}(t) \overset{\text{Eq. } 8.28}{=} -i\hbar\hat{G}^{\mathcal{C}}(t,t^+) \tag{L.121}$$

The argument t^+ is the time infinitesimally displaced along the contour compared to t.

We can use the equation of motion for the Green's function Eq. 8.8 to determine the step of the Green's function for equal arguments. Let me integrate the equation of motion over an infinitesimal

time window. ($\Delta \Rightarrow 0$)

$$\begin{aligned} i\hbar G^{\mathcal{C}}_{\alpha,\beta}(t+\Delta,t) - i\hbar G^{\mathcal{C}}_{\alpha,\beta}(t-\Delta,t) &= \int_{t-\Delta}^{t+\Delta} dt' \sum_{\gamma} \delta_{\alpha,\gamma} i\hbar \partial_{t'} G^{\mathcal{C}}_{\gamma,\beta}(t',t) \\ &\overset{\text{Eq. 8.8}}{=} \int_{t-\Delta}^{t+\Delta} dt'\, \delta_{\mathcal{C}}(t'-t)\delta_{\alpha,\beta} = \delta_{\alpha,\beta} \\ \overset{\Delta\to 0}{\Rightarrow} \underbrace{-i\hbar G^{\mathcal{C}}_{\alpha,\beta}(t-\Delta,t)}_{\rho^{(1)}} &= \delta_{\alpha,\beta} - i\hbar G^{\mathcal{C}}_{\alpha,\beta}(t+\Delta,t) \end{aligned}$$

$$\underbrace{\delta_{\alpha,\beta} + i\hbar G^{\mathcal{C}}_{\alpha,\beta}(t-\Delta,t)}_{1-\rho^{(1)}} = +i\hbar G^{\mathcal{C}}_{\alpha,\beta}(t+\Delta,t) \tag{L.122}$$

Thus we obtain the empty states from the Green's function, but with the

$$\hat{1} - \hat{\rho}^{(1)(t)}(t) = +i\hbar \hat{G}^{\mathcal{C}}(t^+,t) \tag{L.123}$$

The empty states are obtained from the Green's function by the opposite limit of the two time arguments compared to those for the filled states.

Eq. L.123 holds for any type of Green's function interacting or non-interacting and for all time arguments. Let me now turn to the grand potential.

Appendix M

Code for the construction of Feynman diagrams

While it is important to understand the underpinnings of Feynman diagrams, many of the operations can be performed on the computer. This chapter contains a FORTRAN code that sets up the permutation vectors defining the Feynman diagrams to a specified order. The code determines the linked, topologically inequivalent diagrams together with their symmetry factor and the sign.

M.1 Procedure to exclude disconnected diagrams

The linked-cluster theorem Eq. 11.17 reduces the set of all closed diagrams to the subset of linked clusters. The disconnected diagrams, which need to be sorted out, are easily identified from the drawn diagram itself. Disconnected diagrams can also be identified on the basis of a permutation vector as mentioned in section 11.4 on p. 353. Here, I am sketching a systematic and efficient procedure, which can be used either by hand and which can be put on the computer.

The procedure to discard the disconnected diagrams passes through all vertices of a linked cluster in the diagram and identifies the vertices, which belong to it. If a vertex of the diagram is left over, the diagram is disconnected.

The procedure makes use of the permutation vector $\vec{\mathcal{P}}$ of the diagram. Let the set $\mathbb{B}$ be the linked cluster connected to the first vertex. We maintain an array, which keeps track, which vertices have already been identified as member of $\mathbb{B}$. The array has one entry for each vertex with value true or false

1. We start with the first vertex and complete the Fermi loop that passes through it. This is done by repeating the following two steps until a vertex is encountered that is already marked as member of $\mathbb{B}$.
   (a) The current vertex v_j is marked as member of $\mathbb{B}$
   (b) One proceeds to vertex with number $v_k = \mathcal{P}_j$
   (c) If this vertex has already been marked as member of $\mathbb{B}$, the Fermi loop has been completed and one proceeds to the next step (2) of the procedure described below. If not, one continues with (1.a) to follow along the Fermi loop as sketched above.
2. From the current vertex v_j, one proceeds through the vertices in ascending order of their numbers until a vertex is encountered that is not yet marked as member of $\mathbb{B}$.
3. If, on the one hand, the partner of the odd-even vertex pair containing the current vertex has not been marked as member of $\mathbb{B}$, the diagram at hand is disconnected and not a linked cluster. Thus, the procedure is complete and can be ended.

The reason that one can take the decision to identify a disconnected diagram already at this point, is that each Fermi loop is identified beginning at the vertex having the lowest index.

4. If, on the other hand, the partner of the odd-even vertex pair has already been marked as member of $\mathbb{B}$, the current vertex is connected to $\mathbb{B}$ by an interaction line. Thus, the current member is also part of $\mathbb{B}$. Therefore, one proceeds with step (1.a) to identify the Fermi loop passing through the current vertex.

5. When we arrive at the last vertex, all vertices belong to the same linked cluster $\mathbb{B}$ and the diagram is kept in the set of linked diagrams $\mathbb{L}$.

This procedure identifies a diagram as linked or disconnected in one pass. It can easily be put on the computer. The code is provided in the appendix M on p. 731. The implementation does not implement the procedure as described above, but follows it in spirit.

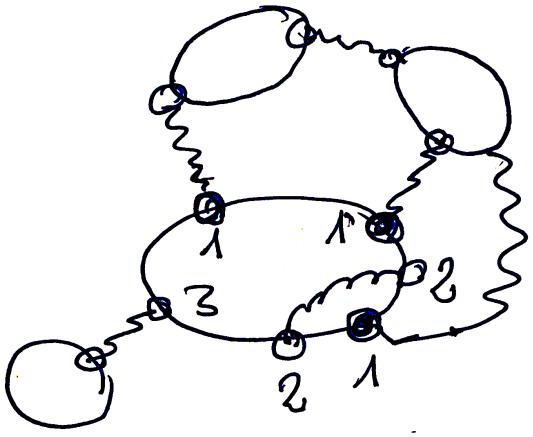
M.2 Procedure to single out skeleton diagrams

A skeleton diagram is one that cannot be cut in two pieces by removing two Green's functions. We notice that the two Green's function to be removed must be part of the same Fermi loop.[1]

For each Fermi loop, we identify subsets of vertices, which are connected externally. An external connection may be an interaction connecting two vertices in the same Fermi loop. An external connection may also lead via interactions and other Fermi loops back to vertices of the original Fermi loop.

This will divide the vertices of the original Fermi loop into subsets, for which the vertices are connected via external connections within each subset but not between different subsets.

Finally we combine the subsets in all possible ways into two groups and see if the vertices of each group are compact. If this is possible, the diagram is not a skeleton diagram. If this is impossible for all the Fermi loops in the diagram, it is a skeleton diagram.



We begin by identifying Fermi loops as in the determination of the sign factor. Then, we establish a network of Fermi loops and interactions. Each vertex v obtains two numbers:

1. one $L_1(v)$ is the loop index of the vertex and

2. the other ($L_2(v)$ is the index of the Fermi loop to which the vertex is connected via the interaction.

[1] When only one Green's function is removed from a Fermi loop, the remaining strand of the Fermi look establishes the connection.

The two arrays determine the loop network $Q(\ell_1, \ell 2)$, which monitors whether two Fermi loops ℓ_1 and ℓ_2 are connected by a single interaction or not. We also count the diagonal elements as "true".

In the next step I identify all vertices of the same Fermi loop, which are connected either by a direct interaction, or via interactions to a common subset of directly connected Fermi loops other than the one currently examined.

The method described here is implemented in the subroutine `skeleton` in the code below.

M.2.1 Skeleton diagrams last

A surprising observation is that in the calculated lists below, the skeleton diagrams occur at the end of the sequence. This has to do with the order of constructing the diagrams.

The following diagrams stand upfront and are not skeleton diagrams

1. A permutation vector beginning with "1" and length greater than 2 has a tadpole (Hartree) insertion

2. A permutation vector beginning with "2" and length greater than 2 has a half-oyster (exchange) insertion .

3. A permutation vector beginning with "3,4,1" and length greater than 4 has a lowest order polarization insertion

4. A permutation vector beginning with "3,4,2" and length greater than 4 has an insertion with two crossing interactions.

M.3 Procedure to single out interaction-skeleton diagrams

We also identify interaction-skeleton diagrams among the particle interaction diagrams. This diagrams fall apart when one or two interaction lines are removed.

We build a table giving the number of interaction between any two Fermi loops.

Fermi loops that are connected by three or more interactions can be merged, because they cannot be separated by removing one or two interaction lines. When two Fermi loops are merged, their contacts are added up. This merging is repeated.

Then inspect the merged groups of Fermi loops. If any of these has only one or two interactions to the outside world, they are polarization insertions and the diagram is not a skeleton diagram.

If it passes this test, it is considered a interaction-skeleton diagram. `Editor: Caution! There is no proof yet that this is a sufficient criterion for a interaction skeleton diagram.`

M.3.1 Insertions

Tadpoles: The diagrams with a permutation vector beginning with $\mathcal{P}(1) = 1$ have a tadpole (Hartree) insertion. Because our construction of the permutation vector begin with the lowest "number" $Z(\vec{\mathcal{P}})$, every diagram having a tadpole diagram anywhere, will have it on the first interaction, so that $\mathcal{P}(1) = 1$. As a result all diagrams having tadpole insertions will stand upfront in the list.

Half-oysters: The diagrams with a permutation vector beginning with $\mathcal{P}(1) = 2$ have a half-oyster (exchange) insertion. The arguments for the tadpole insertions hold also here. Hence, the diagrams having half-oyster insertions follow the ones with tadpole insertions, and preceed all others in the list.

After removing the non-interacting Green's function loop, the remaining expression contains the electrostatic potential of the full density.

M.4 Installation:

Prerequisites are a FORTRAN compiler such as gfortran.

1. Download the code as "diagrams.f90". Be aware of special non-printing symbols when grabbing it from a pdf file.
2. Compile the code with `gfortran -o diagrams.x diagrams.f90`
3. Run the code as `diagrams.x`. You will be asked to provide the order of the diagrams to be calculated.

M.5 Example:

In order to obtain the result for the third order in the interaction execute the following on the command line of a UNIX system.

```
gfortran -o diagrams.x diagrams.f90; echo 3 | diagrams.x > out.dat
```

The resulting file `out.dat` is given below in section M.8.3.

Each line represents a linked Feynman diagram. The first column is the symmetry factor multiplied by the sign of the diagram. Denoted with `p=` is the permutation vector $\vec{\mathcal{P}}$. In order to draw the diagram,

1. start drawing n interaction lines, where n is the order of the diagram.
2. label the vertices so that each interaction line has one odd-numbered vertex and the next higher even-numbered vertex.
3. For each component p_j of the $2n$-dimensional permutation vector draw a bare Green's function line from vertex V_j to vertex V_{p_j}.

M.6 Code Description

- The subroutine **permutationvectors** sets up all $(2n)!$ permutation vectors with length $2n$, where n is the order of the diagrams. It implements the method is described in section 11.2.1 on p. 347.
- The subroutine **loops** determines the sign factor of the diagrams and it identifies disconnected diagrams. If the diagram is not a linked-cluster, the sign factor is set to zero. The routine follows in spirit the method described in section M.1 on p. 731. `Editor: This routine does not exploit the description section M.1 in full: It searches for odd-even pairs from the beginning, rather than from the start of the most recent Fermi loop. It does not stop the search at the first possibility to detect a disconnected cluster, but only at the end.`
- The subroutine **vertexmaps** sets up all $n!2^n$ transformations of permutation vectors, that result in a topologically equivalent diagram. A specific transformation is represented by a vector $\vec{M}$ with the same length $2n$ of the permutation vector.

$$\mathcal{P}'_{M_j} = M_{\mathcal{P}_j} \tag{M.1}$$

- The subroutine **symmetryfactor** determines the symmetry factor `sofd` of a specific diagram and it selects one specific diagram from a set of topologically equivalent diagrams. Internally, all

topologically equivalent diagrams of the current diagram are created using the transformations set up in routine vertexmaps. A sequence for all diagrams is defined. If any of the transformed permutation vectors has a lower value in the sequence, the current diagram is omitted by exiting the routine after setting the symmetry factor `sofd` to zero. If the current diagram is one to be considered, the symmetry factor is determined by identifying the number of mere deformations among all transformations. The symmetry factor is provided as $S(D) =$`sofd`.

- the subroutine **skeleton** determines whether the specified diagram is a skeleton diagram, respectively (two-particle irreducible) 2PI. Skeleton diagrams build up the expansion of the Luttinger-Ward functional.
- the subroutine **polatisatioskeleton** determines whether a supplied skeleton diagram is als irreducible under removal of one or two interaction lines.
- the helper subroutine **onestep** allows to move from one vertex to a neighboring vertex in the diagram. With the identifier 'g', one follows a particle line, whereas with an identifuer "w" one follows the interaction line. The output is the index of the new vertex.

M.7 Source code:

The code `diagrams.f90` can be downloaded from the ΦSX Website `phisx.org`. For the sake of completeness it is included below.

```
      program main
!     ************************************************************************
!     ** determines the permutation vectors defining the topologically       **
!     ** inequivalent, linked feynman diagrams of the specified order        **
!     **                                                                     **
!     ** provide the order of the diagram from standard input (integer)      **
!     **                                                                     **
!     ** interaction lines connect odd numbered vertices with the next higher**
!     ** even numbered index. the j-th component p_j of the permutation      **
!     ** specifies a green's function from vertex j to vertex p_j.           **
!     **                                                                     **
!     ** the value of a diagram is given in                                  **
!     **   p.Bloechl, PhiSX Advanced Solid-State Theory                      **
!     **   http://www2.pt.tu-clausthal.de/atp/phisx.html                     **
!     **                                                                     **
!     ************************************************************************
!     ** COPYRIGHT (C) 2017 PETER BLOECHL, (MODIFIED M.I.T. LICENSE)         **
!     **                                                                     **
!     ** PERMISSION IS HEREBY GRANTED, FREE OF CHARGE, TO ANY PERSON         **
!     ** OBTAINING A COPY OF THIS SOFTWARE (THE "SOFTWARE"), TO DEAL IN THE  **
!     ** SOFTWARE WITHOUT RESTRICTION, INCLUDING WITHOUT LIMITATION THE      **
!     ** RIGHTS TO USE, COPY, MODIFY, MERGE, PUBLISH, DISTRIBUTE, SUBLICENSE,**
!     ** AND/OR SELL COPIES OF THE SOFTWARE, AND TO PERMIT PERSONS TO WHOM   **
!     ** THE SOFTWARE IS FURNISHED TO DO SO, SUBJECT TO THE FOLLOWING        **
!     ** CONDITIONS:                                                         **
!     **                                                                     **
!     ** THE ABOVE COPYRIGHT NOTICE AND THIS PERMISSION NOTICE SHALL BE      **
!     ** INCLUDED IN ALL COPIES OR SUBSTANTIAL PORTIONS OF THE SOFTWARE.     **
!     ** THE SOFTWARE IS PROVIDED "AS IS", WITHOUT WARRANTY OF ANY KIND,     **
!     ** EXPRESS OR IMPLIED, INCLUDING BUT NOT LIMITED TO THE WARRANTIES OF  **
!     ** MERCHANTABILITY, FITNESS FOR A PARTICULAR PURPOSE AND               **
```

```
!       ** NONINFRINGEMENT. IN NO EVENT SHALL THE AUTHORS OR COPYRIGHT HOLDERS **
!       ** BE LIABLE FOR ANY CLAIM, DAMAGES OR OTHER LIABILITY, WHETHER IN AN  **
!       ** ACTION OF CONTRACT, TORT OR OTHERWISE, ARISING FROM, OUT OF OR IN   **
!       ** CONNECTION WITH THE SOFTWARE OR THE USE OR OTHER DEALINGS IN THE    **
!       ** SOFTWARE.                                                          **
!       **                                                                    **
!       ** THIS LICENSE APPLIES ONLY TO THE SECTION OF FORTRAN CODE THAT       **
!       ** CONTAINS THIS LICENSE. IT DOES NOT APPLY TO THE PHISX LECTURE NOTES **
!       ** THAT MAY CONTAIN THE SOFTWARE.                                     **
!       ************************************************************************
        implicit none
        integer(8)             :: order     !order in the interaction
        integer(8)             :: len       !length of permutation vector
        integer(8)             :: nvecx     !X#(permutation vectors)
        integer(8)             :: nmapx
        integer(8),allocatable :: pvec(:,:) !(len,nvecx) permutation vector
        integer(8),allocatable :: map(:,:)  !(len,nmapx)
        integer(8),allocatable :: sofd(:)   !(nvecx) symmetry factor*sign
        integer(8),allocatable :: sgn(:)    !(nvecx)
        logical(4),allocatable :: tskltn(:) !(nvecx) is it skeleton?
        logical(4),allocatable :: tpskltn(:)!(nvecx) is it polarization skeleton?
        integer(8)             :: nvec      !#(permutation vectors)
        integer(8)             :: nmap
        integer(8)             :: i,j
        real(8)                :: svar
!       ************************************************************************
        write(*,fmt='("provide the order of the diagrams (integer):")')
        read(*,fmt=*)order
        write(*,fmt='(40(".",t1,"order of the diagrams",t40,i15)')order
        len=2*order
!
!       ========================================================================
!       == allocate array for permutation vector                              ==
!       == a permutation vector has the length len=2*order                    ==
!       == the number of permutation vectors in this order is factorial(len)  ==
!       ========================================================================
        nvecx=1
        do i=1,len
          nvecx=nvecx*i
        enddo
        allocate(pvec(len,nvecx))
        allocate(sgn(nvecx))
        allocate(sofd(nvecx))

!       ========================================================================
!       == determine all permutation vectors                                  ==
!       ========================================================================
        call permutationvectors(len,nvecx,nvec,pvec)
        write(*,fmt='(40(".",t1,"nr. of all diagrams (=n!)",t40,i15)')nvec
!
!       ========================================================================
!       == count the number of loops (sign of the diagram)                    ==
!       == identify unlinked diagrams (sgn=0)                                 ==
!       ========================================================================
```

```
      do i=1,nvec
        call loops(len,pvec(:,i),sgn(i))
      enddo
!
!     ========================================================================
!     == remove unlinked diagrams                                           ==
!     ========================================================================
      j=0
      do i=1,nvec
        if(sgn(i).eq.0) cycle
        j=j+1
        pvec(:,j)=pvec(:,i)
        sgn(j)=sgn(i)
!        write(*,fmt='("(",20i4,")",i10)')pvec(:,j),sgn(j)
      enddo
      nvec=j
      write(*,fmt='(40(".",t1,"nr. of linked diagrams",t40,i15)')nvec
!
!     ========================================================================
!     == determine symmetry factor (sofd=0 for duplicates)                  ==
!     == sign is integrated into the symmetry factor                        ==
!     ========================================================================
      nmapx=1
      do i=1,order
        nmapx=nmapx*2*i
      enddo
      allocate(map(len,nmapx))
      call vertexmaps(len,nmapx,nmap,map)
      do i=1,nvec
        call symmetryfactor(len,pvec(:,i),nmap,map,sofd(i))
        sofd(i)=sofd(i)*sgn(i)
      enddo
      deallocate(map)
!
!     ========================================================================
!     == remove topologically equivalent diagrams                           ==
!     ========================================================================
      j=0
      do i=1,nvec
        if(sofd(i).eq.0) cycle
        j=j+1
        pvec(:,j)=pvec(:,i)
        sofd(j)=sofd(i)
        sgn(j)=sgn(i)
      enddo
      nvec=j
      write(*,fmt='(40(".",t1,"nr. of top. distinct diagrams",t40,i15)')nvec
!
!     ========================================================================
!     == identify skeleton diagrams                                         ==
!     ========================================================================
      allocate(tskltn(nvec))
      j=0
      do i=1,nvec
```

```
        call skeleton(len,pvec(:,i),tskltn(i))
        if(tskltn(i)) j=j+1
      enddo
      write(*,fmt='(40(".",t1,"nr. of skeleton diagrams",t40,i15)')j
!
!     ==========================================================================
!     == identify polarization skeleton diagrams                              ==
!     ==========================================================================
      allocate(tpskltn(nvec))
      tpskltn(:)=.false.
      j=0
      do i=1,nvec
        if(.not.tskltn(i)) cycle
        call polarizatioskeleton(len,pvec(:,i),tpskltn(i))
      enddo
!
!     ==========================================================================
!     == test sum rule                                                        ==
!     ==========================================================================
      svar=sum(1.d0/abs(sofd(:nvec)))
      do i=1,len/2
        svar=svar*2.d0*real(i,kind=8)
      enddo
      write(*,fmt='(40(".",t1,"sum-rule test 2^n * n! * S(D) ",t40,f15.1)') &
     &             svar
      write(*,fmt='(40(".",t1,"...must reproduce number of linked diagrams")')
!
!     ==========================================================================
!     == print resulting permutation vectors and symmetry factors             ==
!     ==========================================================================
      write(*,*)
      write(*,fmt='("sign, symmetry factor and permutation vectors:")')
      do i=1,nvec
        if(tskltn(i)) then
          if(tpskltn(i)) then
            write(*,fmt='(i8," pi-skltn; sign*sofd=",i8," p=",20i4)') &
     &           i,sofd(i),pvec(:,i)
          else
            write(*,fmt='(i8," skeleton; sign*sofd=",i8," p=",20i4)') &
     &           i,sofd(i),pvec(:,i)
          endif
        else
          write(*,fmt='(i8,"           sign*sofd=",i8," p=",20i4)') &
     &         i,sofd(i),pvec(:,i)
        end if
      enddo
      stop
      end
!
!     ..1.........2.........3.........4.........5.........6.........7.........8
      subroutine vertexmaps(len,nmapx,nmap,map)
!     ******************************************************************
!     ** determine the mappings of vertices that produce topologically **
!     ** equivalent diagrams.                                          **
```

```
!       ** the map array contains all permutations of the vertices among each  **
!       ** other.
!       ************************************************************************
        implicit none
        integer(8),intent(in) :: len    ! #(green's functions)
        integer(8),intent(in) :: nmapx
        integer(8),intent(out):: nmap
        integer(8),intent(out):: map(len,nmapx)
        integer(8),allocatable:: pvec(:,:)
        integer(8)            :: nvecx
        integer(8)            :: nvec
        integer(8)            :: nmap2,imap,jmap,ivec,i,j
!       ************************************************************************
        if(mod(len,2).eq.1) then
          stop 'argument len must be even'
        end if
!
!       == allocate dimension of map array ===================================
        nvecx=1
        do i=1,len/2
          nvecx=nvecx*i
        enddo
        allocate(pvec(len/2,nvecx))
        call permutationvectors(len/2,nvecx,nvec,pvec)
!
!       == construct all permutation of vertices
        nmap=0
        do ivec=1,nvec
          nmap=nmap+1
          do i=1,len/2
            map(2*i-1,nmap)=2*pvec(i,ivec)-1
            map(2*i  ,nmap)=2*pvec(i,ivec)
          enddo
          nmap2=nmap
          jmap=nmap
          do j=1,len/2
            do imap=nmap,nmap2
              jmap=jmap+1
              map(:,jmap)=map(:,imap)
              map(2*j-1,jmap)=map(2*j,imap)
              map(2*j,jmap)=map(2*j-1,imap)
            enddo
            nmap2=jmap
          enddo
          nmap=nmap2
        enddo
        return
        end
!
!       ..1.........2.........3.........4.........5.........6.........7.........8
        subroutine symmetryfactor(len,pvec,nmap,map,sofd)
!       ************************************************************************
!       ** determine symmetry factor                                         **
!       ** a zero value for the symmetry factor is set if a topologically     **
```

```
!      ** equivalent diagram has already been considered.                    **
!      **                                                                    **
!      ** The symmetry factor Sofd is the ratio of mere deformations among   **
!      ** all n!2^n diagrams obtained by remapping the vertices.             **
!      **                                                                    **
!      ** for each diagram there are n!2^n diagrams that give the same value. **
!      ** These diagrams are obtained by remapping the vertices. These       **
!      ** these mappings (1) permutate the interaction lines and             **
!      ** (2) they interchange the two vertices of one interaction.          **
!      **                                                                    **
!      ** A deformation is characterized by the same permutation vector and  **
!      ** is thus the identical diagram. Hence it must not be counted.       **
!      **                                                                    **
!      ** each diagram is converted into a value obtained from the permutation**
!      ** vector. Only those diagrams are retained, for which the            **
!      ** topologically equivalent partners have a higher number than the    **
!      ** diagram itself. This singles out one diagram from each class of    **
!      ** topologically distinct diagrams.                                   **
!      **                                                                    **
!      ************************************************************************
       implicit none
       integer(8),intent(in) :: len         ! #(green's function in the diagram)
       integer(8),intent(in) :: pvec(len)   ! permutation vector
       integer(8),intent(in) :: nmap
       integer(8),intent(in) :: map(len,nmap)
       integer(8),intent(out):: sofd        ! symmetry factor
       integer(8)            :: imap,i
       integer(8)            :: ndef        ! #(deformations)
       integer(8)            :: ovec(len)
       logical(4)            :: tident
       integer(8)            :: order
       integer(8)            :: ndistinct
!      ************************************************************************
       order=len/2
!
!      ========================================================================
!      == initial checks                                                     ==
!      ========================================================================
!      == check that len is even. It is the number of green's functions and  ==
!      == that number is twice the number of interaction lines               ==
       if(mod(len,2).eq.1) then
         stop 'argument len must be even'
       end if
!
!      ========================================================================
!      == loop over all mappings
!      ========================================================================
       do imap=1,nmap
!        == remap vertices ===================================================
         do i=1,len
           ovec(map(i,imap))=map(pvec(i),imap)
         enddo
!
!        ====================================================================
```

```
!       == exclude all diagrams that map onto another one with a smaller count=
!       ========================================================================
        tident=.true.
        do i=1,len
          if(ovec(i).ne.pvec(i)) then
            if(tident.and.ovec(i).lt.pvec(i)) then
              sofd=0 ! is already counted by another pvec
              return
            end if
            exit
          end if
        enddo
      enddo

!     ========================================================================
!     == count mere deformations                                            ==
!     ========================================================================
      ndef=0
      do imap=1,nmap
        do i=1,len
          ovec(map(i,imap))=map(pvec(i),imap)
        enddo
        tident=.true.
        do i=1,len
          if(ovec(i).ne.pvec(i)) then
            tident=.false.
            exit
          end if
        enddo
        if(tident)ndef=ndef+1
      enddo
!
!     ========================================================================
!     == calculate symmetry factor                                          ==
!     ========================================================================
!     == the diagram has ndef deformations. the number of topologically     ==
!     == equivalent diagrams which are not mere deformations is             ==
!     == ndistinct=nmap/ndef.                                               ==
!     == the inverse of symmetry factor is the number of                    ==
!     == topologically equivalent, which are not mere deformations,         ==
!     == divided by the factor n!2^n.                                       ==
!     == Hence, 1/sofd=ndistinct/nmap=1/ndef                                ==
!     ========================================================================
      ndistinct=nmap/ndef
      sofd=ndef !=nmap/ndistinct
      return
      end
!
!     ..1.........2.........3.........4.........5.........6.........7.........8
      subroutine loops(len,pvec,sgn)
!     ************************************************************************
!     **  sgn=1 for an even number of green's function loops                **
!     **  sgn=-1 for an odd number of green's function loops                **
!     **  sgn=0 for a diagram which is not a linked cluster                 **
```

```
!      **                                                                  **
!      ** the sign theorem links the sign of a diagram to the number of    **
!      ** loops formed by Green's functions.                               **
!      **                                                                  **
!      ** the code follows green's function lines and marks each vertex    **
!      ** visited by a loop number. If an un-marked vertex (iloop=0) is    **
!      ** encountered, the code searches for interaction lines, of which one  **
!      ** vertex has been visited and the other not. At such an interaction   **
!      ** the loop index in increased, and loop search  at the unmarked vertex**
!      ** is initiated.                                                    **
!      **                                                                  **
!      ** if interaction lines with two unmarked vertices are left over    **
!      ** the diagram consists of disconnected parts and sgn=0 is set.     **
!      ** otherwise the sign is determined from the the number of loops.   **
!      **                                                                  **
!      ********************************************************************
       implicit none
       integer(8),intent(in) :: len        ! #(greens functions)
       integer(8),intent(in) :: pvec(len)  ! permutation vector of diagram
       integer(8),intent(out):: sgn        ! sign or (zero for linked cluster)
       integer(8)            :: work(len)  ! holds loop indices for each vertex
       logical(4)            :: t1,t2
       integer(8)            :: iloop      ! loop index
       integer(8)            :: ip         ! vertex pointer
       integer(8)            :: i
!      ********************************************************************
       if(mod(len,2).eq.1) then
         write(*,*)'argument len must be even'
         stop 'in loops'
       end if
!
!      ====================================================================
!      == explore diagram for fermi loops                                ==
!      ====================================================================
       work(:)=0
       iloop=1
       ip=1
       work(ip)=iloop
!
1000   continue
!
!      == walk around the first loop of greensfunctions and mark with loop nr.
       do
         ip=pvec(ip)
         if(work(ip).ne.0) exit ! end of Fermi loop encountered
         work(ip)=iloop
       enddo
!
!      == find interaction with one vertex that has been visited and another
!      == one that has not been visited.
       ip=0
       do i=1,len/2
         t1=work(2*i-1).eq.0
         t2=work(2*i).eq.0
```

```
        if(t1.eqv.t2) cycle  ! both are true or both are false.
!       -- set pointer to unmarked vertex ----------------------------------
        if(t1) then
          ip=2*i-1
        else
          ip=2*i
        end if
      enddo
!     == jump back to next fermi-loop search or exit
      if(ip.ne.0) then  ! vertex for fermi-loop search found
        iloop=iloop+1   ! increase loop index
        work(ip)=iloop  ! mark actual vertex
        goto 1000
      end if
!
!     ========================================================================
!     == calculate sgn                                                      ==
!     ========================================================================
      sgn=1
      if(mod(iloop,2).eq.1) sgn=-1
!
!     ========================================================================
!     == check if this is a linked diagram                                  ==
!     ========================================================================
      do i=1,len
        if(work(i).eq.0) then
          sgn=0
          exit
        end if
      enddo
!
      return
      end
!
!     ..1.........2.........3.........4.........5.........6.........7.........8
      subroutine permutationvectors(len,nvecx,nvec,pvec)
!     **************************************************************************
!     ** construct all len-factorial permutation vectors of length len       **
!     ** as described in section 11.1.1 "Construct all permutation vectors"  **
!     ** of P.Bloechl PhiSX Advanced Solid-State Theory                       **
!     **************************************************************************
      implicit none
      integer(8),intent(in)  :: len
      integer(8),intent(in)  :: nvecx           ! X#(permutation vectors)
      integer(8),intent(out) :: nvec            ! #(permutation vectors)
      integer(8),intent(out) :: pvec(len,nvecx) ! permutation vectors
      integer(8)             :: i,j,k,ip1,ip2,isvar
      integer(8)             :: work(len)
!     **************************************************************************
      isvar=1
      do i=1,len
        isvar=isvar*i
      enddo
      if(nvecx.lt.isvar) then
```

```
        stop 'nvecx too small (a)'
      end if
!
!     ========================================================================
!     ==  start the recursive construction with trivial vector (1,2,.., len) ==
!     ========================================================================
      nvec=1
      do i=1,len
        pvec(i,nvec)=i
      enddo
!
!     ========================================================================
!     == construct all other permutation vectors recusively
!     ========================================================================
      do
!
!       == find longest trailing descending sequence ==========================
!       == that is pvec(ip1) > pvec(ip1+1) > pvec(ip1+2) > ... ================
        j=len
        ip1=0
        do j=len,2,-1
          if(pvec(j-1,nvec).gt.pvec(j,nvec)) cycle
          ip1=j-1
          exit
        enddo
        if(ip1.eq.0) exit ! sequence is descending, exit
!
!       == prepare an entry for a new perturbation vector =====================
        nvec=nvec+1
        if(nvec.gt.nvecx) then
          write(*,*)'error report: nvec=',nvec,' nvecx=',nvecx
          stop 'nvec exceeds nvecx (b)'
        end if
!
!       == copy previous permutation vector as non-descending part ============
        pvec(:,nvec)=pvec(:,nvec-1)

!       -- ip1 is the start of the descending series. -------------------------
!       -- identify the smallest component of pvec in the descending sequence -
!       -- that is still larger than the first element of the descending ------
!       -- sequence. ----------------------------------------------------------
        ip2=ip1+1
        do k=ip1+1,len
          if(pvec(k,nvec).lt.pvec(ip1,nvec))exit
          ip2=k
        end do
!
!       -- replace first element of descending seqence ------------------------
        isvar=pvec(ip1,nvec)
        pvec(ip1,nvec)=pvec(ip2,nvec)
        pvec(ip2,nvec)=isvar
!
!       -- change descending sequence into an ascending one -------------------
        work(ip1+1:)=pvec(ip1+1:,nvec)
```

```
        do j=1,len-ip1
          pvec(ip1+j,nvec)=work(len+1-j)
        enddo
      enddo
      return
      end
!
!     ..1.........2.........3.........4.........5.........6.........7.........8
      subroutine skeleton(len,pvec,tskeleton)
!     ****************************************************************************
!     ** test whether diagram is a skeleton diagram                             **
!     ****************************************************************************
      implicit none
      integer(8),intent(in) :: len          ! length of permutation vector
      integer(8),intent(in) :: pvec(len)    ! permutation vector
      logical(4),intent(out):: tskeleton    ! true if pvec is skeleton diagram
      integer(8),allocatable:: loop(:,:)    ! (2,len)
      logical(4),allocatable:: loopnet(:,:) ! (nloop,nloop) loop network
      logical(4),allocatable:: loopchk(:)   ! (nloop)
      integer(8),allocatable:: vconnect(:)  ! (len)
      integer(8),allocatable:: iarr(:)      ! (len)
      logical(4),allocatable:: chkiarr(:)   ! (n)
      logical(4),allocatable:: itchk(:)     ! (nind)
      integer(8)            :: nloop        ! #(loops in the diagram)
      integer(8)            :: nind,isvar
      integer(8)            :: i,j,k,iloop,jloop,n
      logical(4)            :: tchk
!     ****************************************************************************
      tskeleton=.true. ! routine works by identifying non-skeleton diagrams
!
!     ============================================================================
!     == identify loops
!     == loop(1,i) is the loop index of the loop containing vertex i
!     == loop(2,i) is the loop index of the loop connected to vertex i
!     ==          via an interaction
!     ============================================================================
      allocate(loop(2,len))  ! loop index for each vertex
      loop(:,:)=0
      nloop=0
      do i=1,len
        if(loop(1,i).ne.0) cycle
        nloop=nloop+1
        j=i
        do
          loop(1,j)=nloop
          call onestep('g',len,pvec,j)
          if(j.eq.i) exit
        enddo
      enddo
      do i=1,len
        j=i
        call onestep('w',len,pvec,j)
        loop(2,i)=loop(1,j)
      enddo
```

```
!
!      ========================================================================
!      == loop network: loopnet(i,j)="loops i,j are connected by an interaction"
!      ========================================================================
       allocate(loopnet(nloop,nloop))
       do i=1,len
         loopnet(loop(1,i),loop(2,i))=.true.
       enddo
       do iloop=1,nloop
         loopnet(iloop,iloop)=.true.
       enddo
!
!      ========================================================================
!      == determine all out-of-loop connections
!      == two vertices in one Fermi loop have the same value vconnect if
!      == they are connected also via interactions and other Fermi-loops
!      ========================================================================
       allocate(vconnect(len))
       vconnect(:)=0
       allocate(loopchk(nloop))
       do i=1,len
         if(vconnect(i).ne.0) cycle
         vconnect(i)=i
         if(loop(2,i).eq.loop(1,i)) then
!          == direct interaction within the fermi loop ========================
           j=i
           call onestep('w',len,pvec,j)
           vconnect(j)=i
         else
!          == interaction to other fermi loops ================================
!          == loopchk(jloop)=(loop jloop is connected to vertex i)
           loopchk(:)=.false.
           loopchk(loop(2,i))=.true.
!          == complete the loop network except for the original loop loop(1,i)
           tchk=.true.
           do while(tchk) !iterate until done
             tchk=.false.
             do iloop=1,nloop
               if(iloop.eq.loop(1,i)) cycle
               if(.not.loopchk(iloop)) cycle
!              == iloop is in the external loop network connected to vertex i ==
               do jloop=1,nloop  ! is jloop connected to iloop
                 if(jloop.eq.loop(1,i)) cycle
                 if(loopchk(jloop)) cycle  ! is already marked
                 tchk=tchk.or.loopnet(jloop,iloop) ! something changed
                 loopchk(jloop)=loopnet(jloop,iloop)
               enddo
             enddo
           enddo
           do j=1,len
             if(loop(1,j).ne.loop(1,i)) cycle
             if(loopchk(loop(2,j))) vconnect(j)=i
           enddo
         end if
```

```
      enddo
!
!     ========================================================================
!     == vertices, which are connected externally and internally have
!     == the same value of vconnect.
!     ========================================================================
      allocate(iarr(len))
      allocate(chkiarr(len))
      do iloop=1,nloop
!
!       ======================================================================
!       == check if loop "iloop" is 2particle reducible ======================
!       ======================================================================
!       == for each fermi loop, the index iarr points to a vertex
!       == in the same fermi loop, which is connected externally, that is
!       == via interactions and other Fermi loops. The sequence of vertices
!       == pass along the fermi loop in one direction.
        iarr(:)=0
        do i=1,len
          if(loop(1,i).ne.iloop) cycle
          n=0
          j=i
          do
            n=n+1
            iarr(n)=vconnect(j)
            call onestep('g',len,pvec,j)
            if(j.eq.i) exit
          enddo
          exit
        enddo
!
!       == cut the array shorter by removing immediate repetitions ===========
        j=1
        do i=2,n
          if(iarr(i).eq.iarr(j)) cycle
          j=j+1
          iarr(j)=iarr(i)
        enddo
        n=j
!
!       == change the values of iarr so that they are the lowest integers =====
        iarr=-iarr
        k=0
        do i=1,n
          if(iarr(i).gt.0) cycle
          k=k+1
          do j=i+1,n
            if(iarr(j).eq.iarr(i)) iarr(j)=k
          enddo
          iarr(i)=k
        enddo
!
!       == divide the numbers in iarr(:n) into two subsets ====================
!       == (in all possible ways).
```

```
!       == The Fermi loop is 2PI, if both subsets are compact.               ==
!       ==
        nind=maxval(iarr(:n))  ! number of different values in iarr(:n)
        if(nind.eq.1) cycle
        allocate(itchk(nind))
        do i=1,2**(nind-1)  ! loop (true/false) sequences beginnig with true
          itchk(1)=.true.
          do j=1,nind-1
            itchk(j+1)=btest(i,j-1) ! if true, loop j is in subset "1"
          enddo
          do j=1,n
            chkiarr(j)=itchk(iarr(j))  ! is vertex j in group "1"?
          enddo

          isvar=0
          do j=1,n
            if(chkiarr(j).neqv.chkiarr(modulo(j,n)+1)) isvar=isvar+1
          enddo
          if(isvar.eq.2) then ! not a skeleton diagram
            tskeleton=.false.
            return
          end if
        end do ! try next grouping of indices
        deallocate(itchk)
      enddo !iloop

      return
      end
!
!     ..1.........2.........3.........4.........5.........6.........7.........8
      subroutine polarizatioskeleton(len,pvec,tskeleton)
!     ******************************************************************
!     ** test whether diagram is a polarization skeleton diagram       **
!     ** it is skeleton when it is 1WI and 2WI                         **
!     ******************************************************************
      implicit none
      integer(8),intent(in) :: len          ! length of permutation vector
      integer(8),intent(in) :: pvec(len)    ! permutation vector
      logical(4),intent(out):: tskeleton    ! true if pvec is skeleton diagram
      integer(8),allocatable:: loop(:,:)    ! (2,len)
      integer(8),allocatable:: loopnet(:,:) ! (nloop,nloop) loop network
      integer(8)            :: nloop        ! #(loops in the diagram)
      integer(8)            :: i,j
      logical(4)            :: tchk
!     ******************************************************************
!
!     ==================================================================
!     == identify loops
!     == loop(1,i) is the loop index of the loop containing vertex i
!     == loop(2,i) is the loop index of the loop connected to vertex i
!     ==          via an interaction
!     ==================================================================
      allocate(loop(2,len))  ! loop index for each vertex
      loop(:,:)=0
```

```
      nloop=0
      do i=1,len
        if(loop(1,i).ne.0) cycle
        nloop=nloop+1
        j=i
        do
          loop(1,j)=nloop
          call onestep('g',len,pvec,j)
          if(j.eq.i) exit
        enddo
      enddo
      do i=1,len
        j=i
        call onestep('w',len,pvec,j)
        loop(2,i)=loop(1,j)
      enddo
!
!     ================================================================================
!     == loop network: loopnet(i,j)=# interactions between loops i and j
!     ================================================================================
      allocate(loopnet(nloop,nloop))
      loopnet=0
      do i=1,len
        if(loop(2,i).eq.loop(1,i)) cycle
        loopnet(loop(2,i),loop(1,i))=loopnet(loop(2,i),loop(1,i))+1
      enddo
!
!     ================================================================================
!     == merge loops with more than one connecting interactions
!     ================================================================================
      tchk=.true.
      do while(tchk)
        tchk=.false.
        do i=1,nloop
          do j=i+1,nloop
            if(loopnet(i,j).gt.2) then
              loopnet(i,:)=loopnet(i,:)+loopnet(j,:)
              loopnet(j,:)=0
              loopnet(:,i)=loopnet(:,i)+loopnet(:,j)
              loopnet(:,j)=0
              loopnet(i,i)=0
              tchk=.true.
            end if
          enddo
        enddo
        j=0
        do i=1,nloop
          if(sum(loopnet(:,i)).eq.0) cycle
          j=j+1
          loopnet(:,j)=loopnet(:,i)
        enddo
        j=0
        do i=1,nloop
          if(sum(loopnet(i,:)).eq.0) cycle
```

```
            j=j+1
            loopnet(j,:)=loopnet(i,:)
          enddo
          nloop=j
        enddo
        tskeleton=.true.
        do i=1,nloop
          if(sum(loopnet(:,i)).le.2) then
            tskeleton=.false.
            return
          end if
        enddo
        return
        end
!
!       ..1.........2.........3.........4.........5.........6.........7.........8
        subroutine onestep(id,len,pvec,vertex)
        implicit none
        character(1),intent(in)    :: id
        integer(8)  ,intent(in)    :: len
        integer(8)  ,intent(in)    :: pvec(len)
        integer(8)  ,intent(inout) :: vertex
!       ***********************************************************************
        if(vertex.lt.1.or.vertex.gt.len) then
          stop 'error stop in onestep: vertex out of range'
        end if
        if(id.eq.'g') then
          vertex=pvec(vertex)
        else if(id.eq.'w') then
          vertex=vertex+(-1)**(modulo(vertex,2)+1)
        else
          stop 'error stop in onestep: id not recognized'
        end if
        return
        end
```

M.8 Low-order diagrams with symmetry factor and sign

The diagrams marked "pi-skltn" are particle- and interaction-skeleton diagrams, i.e. they are 2-particle reducible and 1- and 2-interaction reducible.

The diagrams marked "skeleton" are particle-skeleton diagrams (2PI), but not interaction-skeleton diagrams.

M.8.1 First order

```
provide the order of the diagrams (integer):
order of the diagrams.................              1
nr. of all diagrams (=n!).............              2
nr. of linked diagrams................              2
nr. of top. distinct diagrams.........              2
nr. of skeleton diagrams..............              2
sum-rule test 2^n * n! * S(D) ........            2.0
```

```
...must reproduce number of linked diagrams

sign, symmetry factor and permutation vectors:
       1 skeleton; sign*sofd=       2 p=   1   2
       2 pi-skltn; sign*sofd=      -2 p=   2   1
```

- The vector $\mathcal{P}_1 = (1, 2)$ is the eyeglass diagram
- The vector $\mathcal{P}_2 = (2, 1)$ is the oyster diagram

M.8.2 Second order

```
provide the order of the diagrams (integer):
order of the diagrams.................              2
nr. of all diagrams (=n!).............             24
nr. of linked diagrams................             20
nr. of top. distinct diagrams.........              5
nr. of skeleton diagrams..............              2
sum-rule test 2^n * n! * S(D) .........          20.0
...must reproduce number of linked diagrams

sign, symmetry factor and permutation vectors:
       1           sign*sofd=      -2 p=   1   3   2   4
       2           sign*sofd=       1 p=   1   3   4   2
       3           sign*sofd=      -2 p=   2   3   4   1
       4 skeleton; sign*sofd=       4 p=   3   4   1   2
       5 pi-skltn; sign*sofd=      -4 p=   3   4   2   1
```

- The vector $\mathcal{P}_4 = (3, 4, 1, 2)$ is the double ring diagram
- The vector $\mathcal{P}_5 = (3, 4, 2, 1)$ is the double exchange diagram

M.8.3 Third order

```
provide the order of the diagrams (integer):
order of the diagrams.................              3
nr. of all diagrams (=n!).............            720
nr. of linked diagrams................            592
nr. of top. distinct diagrams.........             20
nr. of skeleton diagrams..............              6
sum-rule test 2^n * n! * S(D) .........          592.0
...must reproduce number of linked diagrams

sign, symmetry factor and permutation vectors:
       1           sign*sofd=       2 p=   1   3   2   5   4   6
       2           sign*sofd=      -1 p=   1   3   2   5   6   4
       3           sign*sofd=      -1 p=   1   3   4   5   2   6
       4           sign*sofd=       1 p=   1   3   4   5   6   2
       5           sign*sofd=      -2 p=   1   3   5   2   4   6
       6           sign*sofd=       1 p=   1   3   5   2   6   4
       7           sign*sofd=       3 p=   1   3   5   4   2   6
       8           sign*sofd=      -1 p=   1   3   5   6   2   4
       9           sign*sofd=       1 p=   1   3   5   6   4   2
      10           sign*sofd=       2 p=   2   3   1   5   6   4
```

```
      11           sign*sofd=      -3 p=   2   3   4   5   6   1
      12           sign*sofd=      -2 p=   2   3   5   1   6   4
      13           sign*sofd=       1 p=   2   3   5   6   1   4
      14           sign*sofd=      -1 p=   2   3   5   6   4   1
      15 pi-skltn; sign*sofd=       6 p=   3   4   5   6   1   2
      16 pi-skltn; sign*sofd=      -6 p=   3   4   5   6   2   1
      17 skeleton; sign*sofd=      -6 p=   3   5   1   6   2   4
      18 skeleton; sign*sofd=       2 p=   3   5   1   6   4   2
      19 pi-skltn; sign*sofd=      -2 p=   3   5   2   6   4   1
      20 pi-skltn; sign*sofd=       6 p=   3   5   6   2   4   1
```

- The vector $\mathcal{P}_{15} = (3, 4, 5, 6, 1, 2)$ is the particle-particle ladder diagram.
- The vector $\mathcal{P}_{16} = (3, 4, 5, 6, 2, 1)$ is the wheel diagram.
- The vector $\mathcal{P}_{17} = (3, 5, 1, 6, 2, 4)$ is the triple ring diagram
- The vector $\mathcal{P}_{20} = (3, 5, 6, 2, 4, 1)$ is the particle-hole ladder.

The skeleton diagrams are shown in figure M.1 on p. 753

M.8.4 Fourth order

```
provide the order of the diagrams (integer):
order of the diagrams.................              4
nr. of all diagrams (=n!).............          40320
nr. of linked diagrams................          33888
nr. of top. distinct diagrams.........            107
nr. of skeleton diagrams..............             20
sum-rule test 2^n * n! * S(D) ........        33888.0
...must reproduce number of linked diagrams

sign, symmetry factor and permutation vectors:
       1           sign*sofd=      -2 p=   1   3   2   5   4   7   6   8
       2           sign*sofd=       1 p=   1   3   2   5   4   7   8   6
       3           sign*sofd=       1 p=   1   3   2   5   6   7   4   8
       4           sign*sofd=      -1 p=   1   3   2   5   6   7   8   4
       5           sign*sofd=       1 p=   1   3   2   5   7   4   6   8
       6           sign*sofd=      -1 p=   1   3   2   5   7   4   8   6
       7           sign*sofd=      -1 p=   1   3   2   5   7   6   4   8
       8           sign*sofd=       1 p=   1   3   2   5   7   6   8   4
       9           sign*sofd=       1 p=   1   3   2   5   7   8   4   6
      10           sign*sofd=      -1 p=   1   3   2   5   7   8   6   4
      11           sign*sofd=      -1 p=   1   3   4   5   2   7   8   6
      12           sign*sofd=      -1 p=   1   3   4   5   6   7   2   8
      13           sign*sofd=       1 p=   1   3   4   5   6   7   8   2
      14           sign*sofd=      -1 p=   1   3   4   5   7   2   6   8
      15           sign*sofd=       1 p=   1   3   4   5   7   2   8   6
      16           sign*sofd=       1 p=   1   3   4   5   7   6   2   8
      17           sign*sofd=      -2 p=   1   3   4   5   7   6   8   2
      18           sign*sofd=      -1 p=   1   3   4   5   7   8   2   6
      19           sign*sofd=       1 p=   1   3   4   5   7   8   6   2
      20           sign*sofd=      -1 p=   1   3   5   2   4   7   8   6
      21           sign*sofd=      -1 p=   1   3   5   2   6   7   4   8
      22           sign*sofd=       1 p=   1   3   5   2   6   7   8   4
```

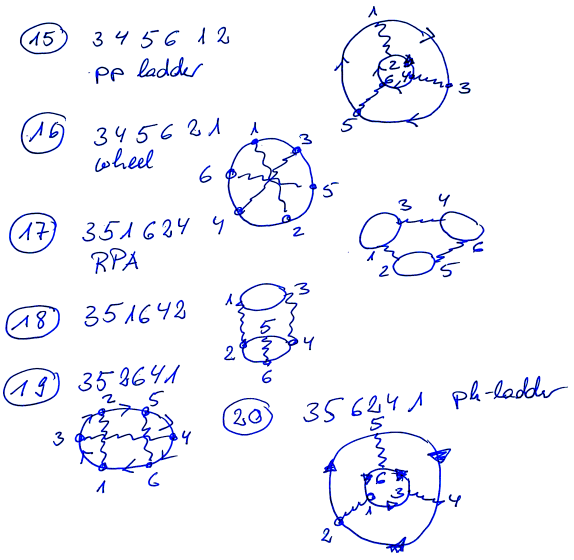


Fig. M.1: Skeleton diagrams of the third order in the interaction.

```
23          sign*sofd=      -2 p=   1   3   5   2   7   4   6   8
24          sign*sofd=       1 p=   1   3   5   2   7   4   8   6
25          sign*sofd=       1 p=   1   3   5   2   7   6   4   8
26          sign*sofd=      -1 p=   1   3   5   2   7   8   4   6
27          sign*sofd=       1 p=   1   3   5   2   7   8   6   4
28          sign*sofd=       1 p=   1   3   5   4   2   7   8   6
29          sign*sofd=      -1 p=   1   3   5   4   7   2   8   6
30          sign*sofd=      -4 p=   1   3   5   4   7   6   2   8
31          sign*sofd=       1 p=   1   3   5   4   7   8   2   6
32          sign*sofd=      -1 p=   1   3   5   4   7   8   6   2
33          sign*sofd=       2 p=   1   3   5   6   2   7   4   8
34          sign*sofd=      -1 p=   1   3   5   6   2   7   8   4
35          sign*sofd=       1 p=   1   3   5   6   4   7   8   2
36          sign*sofd=      -2 p=   1   3   5   6   7   2   4   8
37          sign*sofd=       1 p=   1   3   5   6   7   2   8   4
38          sign*sofd=      -1 p=   1   3   5   6   7   4   8   2
39          sign*sofd=      -1 p=   1   3   5   6   7   8   2   4
40          sign*sofd=       1 p=   1   3   5   6   7   8   4   2
41          sign*sofd=       2 p=   1   3   5   7   2   4   6   8
42          sign*sofd=      -1 p=   1   3   5   7   2   4   8   6
43          sign*sofd=       1 p=   1   3   5   7   2   8   4   6
44          sign*sofd=      -1 p=   1   3   5   7   2   8   6   4
45          sign*sofd=      -1 p=   1   3   5   7   4   2   6   8
46          sign*sofd=       1 p=   1   3   5   7   4   2   8   6
47          sign*sofd=      -1 p=   1   3   5   7   4   8   2   6
48          sign*sofd=       1 p=   1   3   5   7   4   8   6   2
49          sign*sofd=      -1 p=   1   3   5   7   6   2   8   4
50          sign*sofd=       1 p=   1   3   5   7   6   4   8   2
51          sign*sofd=       1 p=   1   3   5   7   6   8   2   4
52          sign*sofd=      -1 p=   1   3   5   7   6   8   4   2
53          sign*sofd=      -1 p=   1   3   5   7   8   2   4   6
54          sign*sofd=       1 p=   1   3   5   7   8   2   6   4
```

```
 55            sign*sofd=       1 p=   1   3   5   7   8   4   2   6
 56            sign*sofd=      -1 p=   1   3   5   7   8   4   6   2
 57            sign*sofd=       2 p=   1   3   5   7   8   6   4   2
 58            sign*sofd=      -2 p=   2   3   1   5   4   7   8   6
 59            sign*sofd=       1 p=   2   3   1   5   6   7   8   4
 60            sign*sofd=       1 p=   2   3   1   5   7   4   8   6
 61            sign*sofd=      -1 p=   2   3   1   5   7   8   4   6
 62            sign*sofd=       1 p=   2   3   1   5   7   8   6   4
 63            sign*sofd=      -4 p=   2   3   4   5   6   7   8   1
 64            sign*sofd=      -1 p=   2   3   4   5   7   1   8   6
 65            sign*sofd=       1 p=   2   3   4   5   7   8   1   6
 66            sign*sofd=      -1 p=   2   3   4   5   7   8   6   1
 67            sign*sofd=      -2 p=   2   3   5   1   7   4   8   6
 68            sign*sofd=       1 p=   2   3   5   1   7   8   4   6
 69            sign*sofd=      -1 p=   2   3   5   1   7   8   6   4
 70            sign*sofd=       2 p=   2   3   5   6   1   7   8   4
 71            sign*sofd=      -2 p=   2   3   5   6   7   1   8   4
 72            sign*sofd=       1 p=   2   3   5   6   7   8   1   4
 73            sign*sofd=      -1 p=   2   3   5   6   7   8   4   1
 74            sign*sofd=       2 p=   2   3   5   7   1   4   8   6
 75            sign*sofd=      -1 p=   2   3   5   7   1   8   4   6
 76            sign*sofd=       1 p=   2   3   5   7   1   8   6   4
 77            sign*sofd=      -1 p=   2   3   5   7   4   1   8   6
 78            sign*sofd=       1 p=   2   3   5   7   4   8   1   6
 79            sign*sofd=      -1 p=   2   3   5   7   4   8   6   1
 80            sign*sofd=       2 p=   2   3   5   7   6   8   4   1
 81            sign*sofd=       1 p=   2   3   5   7   8   1   4   6
 82            sign*sofd=      -1 p=   2   3   5   7   8   1   6   4
 83            sign*sofd=      -1 p=   2   3   5   7   8   4   1   6
 84            sign*sofd=       1 p=   2   3   5   7   8   4   6   1
 85            sign*sofd=      -2 p=   3   4   1   5   7   8   2   6
 86            sign*sofd=       1 p=   3   4   1   5   7   8   6   2
 87            sign*sofd=      -2 p=   3   4   2   5   7   8   6   1
 88 pi-skltn; sign*sofd=       8 p=   3   4   5   6   7   8   1   2
 89 pi-skltn; sign*sofd=      -8 p=   3   4   5   6   7   8   2   1
 90 skeleton; sign*sofd=      -2 p=   3   4   5   7   1   8   2   6
 91 pi-skltn; sign*sofd=       1 p=   3   4   5   7   1   8   6   2
 92 skeleton; sign*sofd=       2 p=   3   4   5   7   2   8   1   6
 93 pi-skltn; sign*sofd=      -1 p=   3   4   5   7   2   8   6   1
 94 pi-skltn; sign*sofd=      -2 p=   3   4   5   7   8   1   6   2
 95 pi-skltn; sign*sofd=       2 p=   3   4   5   7   8   2   6   1
 96 skeleton; sign*sofd=       8 p=   3   5   1   7   2   8   4   6
 97 skeleton; sign*sofd=      -2 p=   3   5   1   7   2   8   6   4
 98 skeleton; sign*sofd=      -4 p=   3   5   1   7   4   8   2   6
 99 skeleton; sign*sofd=       1 p=   3   5   1   7   4   8   6   2
100 skeleton; sign*sofd=       2 p=   3   5   1   7   8   2   6   4
101 skeleton; sign*sofd=      -2 p=   3   5   1   7   8   4   6   2
102 skeleton; sign*sofd=       4 p=   3   5   2   7   1   8   6   4
103 pi-skltn; sign*sofd=      -1 p=   3   5   2   7   4   8   6   1
104 pi-skltn; sign*sofd=      -2 p=   3   5   2   7   8   1   6   4
105 pi-skltn; sign*sofd=       1 p=   3   5   2   7   8   4   6   1
106 pi-skltn; sign*sofd=       8 p=   3   5   7   2   8   1   6   4
107 pi-skltn; sign*sofd=      -4 p=   3   5   7   2   8   4   6   1
```

- The vector $\mathcal{P}_{88} = (3, 4, 5, 6, 7, 8, 1, 2)$ is the particle-particle ladder.
- The vector $\mathcal{P}_{89} = (3, 4, 5, 6, 7, 8, 2, 1)$ is the wheel.
- The vector $\mathcal{P}_{96} = (3, 5, 1, 7, 2, 8, 4, 6)$ is the quadruple ring diagram
- The vector $\mathcal{P}_{106} = (3, 5, 7, 2, 8, 1, 6, 4)$ is the particle-hole ladder.

Appendix N

Second-order perturbation theory

In the chapter 2 on weakly interacting electrons, I have shown in Eq. 2.139 on p.93 how the energy of an general many-particle state into the energy of an ensemble of Slater determinants and an entanglement energy. The motivation for this chapter is to explore the entanglement energy, which is the only energy term that requires Hamilton matrix elements between distinct Slater determinants.

N.1 Perturbation theory

Let me do an error estimate based on second order perturbation theory in the off-site Hamilton matrix elements between pairs of Slater determinants.

I begin with the perturbation expansion by forming the derivatives of the Schrödinger equation with respect to a scale factor λ for the perturbation $\hat{W}$. The Hamiltonian has the form

$$\hat{H}(\lambda) = \hat{h} + \lambda\hat{W} \tag{N.1}$$

The perturbation expansion is obtained from the derivatives of the λ-dependent Schrödinger equation

$$\Big(\hat{h} + \lambda\hat{W}\Big)|\psi_n(\lambda)\rangle = |\psi_n(\lambda)\rangle E_n(\lambda)\ . \tag{N.2}$$

The derivatives are not taken at $\lambda = 0$ but at an arbitrary value of λ. This provides the next order by forming a first derivative on the current order. The λ-dependent quantities are the energies $E_n(\lambda)$ and the wave functions $|\psi_n(\lambda)\rangle$. The λ-dependence is only made explicit where necessary. The first and second derivatives of the Schrödinger equation are

$$\Big(\hat{h} + \lambda\hat{W}\Big)\left|\frac{d\psi_n}{d\lambda}\right\rangle + \hat{W}|\psi_n(\lambda)\rangle \stackrel{\text{Eq. } N.2}{=} \left|\frac{d\psi_n}{d\lambda}\right\rangle E_n(\lambda) + \Big|\psi_n(\lambda)\Big\rangle\frac{dE_n}{d\lambda} \tag{N.3}$$

$$\Big(\hat{h} + \lambda\hat{W}\Big)\left|\frac{d^2\psi_n}{d\lambda^2}\right\rangle + 2\hat{W}\left|\frac{d\psi_n}{d\lambda}\right\rangle \stackrel{\text{Eq. } N.3}{=} \left|\frac{d^2\psi_n}{d\lambda^2}\right\rangle E_n(\lambda) + 2\left|\frac{d\psi_n}{d\lambda}\right\rangle\frac{dE_n}{d\lambda} + \Big|\psi_n(\lambda)\Big\rangle\frac{d^2E_n}{d\lambda^2} \tag{N.4}$$

In addition to the Schrödinger equation, I also need to satisfy the orthonormality.

$$\langle\psi_n(\lambda)|\psi_m(\lambda)\rangle = \delta_{m,n} \tag{N.5}$$

The first two derivatives or the orthonormality condition are

$$\Big\langle\frac{d\psi_n}{d\lambda}\Big|\psi_m\Big\rangle + \Big\langle\psi_m\Big|\frac{d\psi_n}{d\lambda}\Big\rangle \stackrel{\text{Eq. } N.5}{=} 0 \tag{N.6}$$

$$\Big\langle\frac{d^2\psi_n}{d\lambda^2}\Big|\psi_m\Big\rangle + 2\Big\langle\frac{d\psi_m}{d\lambda}\Big|\frac{d\psi_n}{d\lambda}\Big\rangle + \Big\langle\psi_m\Big|\frac{d^2\psi_n}{d\lambda^2}\Big\rangle \stackrel{\text{Eq. } N.6}{=} 0 \tag{N.7}$$

First-order perturbation theory

First-order perturbation yields

$$\underbrace{\langle\psi_m|\Big(\hat{h}+\lambda\hat{W}\Big)}_{E_m\langle\psi_m|}\left|\frac{d\psi_n}{d\lambda}\right\rangle+\langle\psi_m|\hat{W}|\psi_n\rangle\overset{\text{Eq. N.3}}{=}\left\langle\psi_m\middle|\frac{d\psi_n}{d\lambda}\right\rangle E_n+\underbrace{\langle\psi_m|\psi_n\rangle}_{\delta_{m,n}}\frac{dE_n}{d\lambda}$$

$$\Rightarrow\qquad (E_m-E_n)\left\langle\psi_m\middle|\frac{d\psi_n}{d\lambda}\right\rangle\;=\;-\langle\psi_m|\hat{W}|\psi_n\rangle+\delta_{m,n}\frac{dE_n}{d\lambda}\tag{N.8}$$

For $m=n$, Eq. N.8 yields the change of the eigenvalues and for $m\neq n$ it yields the first-order change of the eigenstates.

However, Eq. N.8 does not determine $\langle\psi_n|d\psi_n/d\lambda\rangle$, i.e. $(m=n)$. Considering Eq. N.8, this term is arbitrary, but the real part of this coefficient is determined by the orthonormality condition.

The contribution $\langle\psi_n|d\psi_n/d\lambda\rangle$ is excluded by the normalization condition $\langle\psi_n(\lambda)|\psi_n(\lambda)\rangle=0$, Eq. N.6, which implies $\mathrm{Re}\big[\langle\psi_n|\frac{d|\psi_n\rangle}{d\lambda}\big]=0$. However, only the real part is fixed by the orthonormality condition, while an arbitrary imaginary part may still be added. This imaginary part follows from an arbitrary phase factor $\mathrm{e}^{i\varphi(\lambda)}$ multiplied with the wave function, which preserves the norm, but contributes on additional imaginary term resulting from $\partial_\lambda \mathrm{e}^{i\varphi(\lambda)}=i\frac{\partial\varphi}{\partial\lambda}\mathrm{e}^{i\varphi(\lambda)}$

$$\begin{aligned}\frac{dE_n}{d\lambda}&=\langle\psi_n|\hat{W}|\psi_n\rangle\\ \left|\frac{d\psi_n}{d\lambda}\right\rangle&=\sum_{m;m\neq n}\frac{|\psi_m\rangle\langle\psi_m|}{E_n-E_m}\hat{W}|\psi_n\rangle+|\psi_n\rangle iC_1\end{aligned}\tag{N.9}$$

The real-valued factor C_1 can be chosen arbitrarily, because the norm-conservation determines only the real part of the prefactor of $|\psi_n\rangle$. (I have not extended this argument to degenerate states, where a λ-dependent unitary matrix can be used instead of the λ-dependent phase factor.)

Second-order perturbation theory

The second derivative Eq. N.4 yields

$$\begin{aligned}&\underbrace{\langle\psi_m|\Big(\hat{h}+\lambda\hat{W}\Big)}_{E_m\langle\psi_m|}\left|\frac{d^2\psi_n}{d\lambda^2}\right\rangle-\langle\psi_m\left|\frac{d^2\psi_n}{d\lambda^2}\right\rangle E_n(\lambda)\\ &\qquad=-2\langle\psi_m|\hat{W}\left|\frac{d\psi_n}{d\lambda}\right\rangle+2\langle\psi_m\left|\frac{d\psi_n}{d\lambda}\right\rangle\underbrace{\frac{dE_n}{d\lambda}}_{\langle\psi_n|\hat{W}|\psi_n\rangle}+\underbrace{\langle\psi_m|\psi_n\rangle}_{=\delta_{m,n}}\frac{d^2E_n}{d\lambda^2}\\ \Rightarrow\qquad &(E_m-E_n)\left\langle\psi_m\middle|\frac{d^2\psi_n}{d\lambda^2}\right\rangle=-2\langle\psi_m|\Big(\hat{W}-\langle\psi_n|\hat{W}|\psi_n\rangle\Big)\underbrace{\sum_{p\neq n}\frac{|\psi_p\rangle\langle\psi_p|}{E_n-E_p}\hat{W}|\psi_n\rangle}_{\left|\frac{d\psi_n}{d\lambda}\right\rangle}+\delta_{m,n}\frac{d^2E_n}{d\lambda^2}\end{aligned}\tag{N.10}$$

For $m=n$, I obtain

$$\frac{d^2E_n}{d\lambda^2}=-2\sum_{p\neq n}\frac{\langle\psi_m|\hat{W}|\psi_p\rangle\langle\psi_p|\hat{W}|\psi_n\rangle}{E_n-E_p}\tag{N.11}$$

For $m \neq n$, I obtain

$$\frac{1}{2}\Big\langle \psi_m \Big| \frac{d^2\psi_n}{d\lambda^2} \Big\rangle = \frac{1}{E_n - E_m}\langle\psi_m|\Big(\hat{W} - \langle\psi_n|\hat{W}|\psi_n\rangle\Big)\sum_{p\neq n}\frac{|\psi_p\rangle\langle\psi_p|}{E_n - E_p}\hat{W}|\psi_n\rangle$$
$$= -\frac{1}{E_m - E_n}\Big(\sum_{p\neq n}\frac{\langle\psi_m|\hat{W}|\psi_p\rangle\langle\psi_p|\hat{W}|\psi_n\rangle}{E_n - E_p} - \frac{\langle\psi_m|\hat{W}|\psi_n\rangle}{E_n - E_m}\langle\psi_n|\hat{W}|\psi_n\rangle\Big) \quad \text{(N.12)}$$

The two equations above do not determine the change of the contribution of $|\psi_n\rangle$, which is obtained from the normalization condition $\langle\psi_n(\lambda)|\psi_n(\lambda)\rangle = 0$, which implies

$$\Big\langle \psi_n \Big| \frac{d^2\psi_n}{d\lambda^2} \Big\rangle + 2\Big\langle \frac{d\psi_n}{d\lambda} \Big| \frac{d\psi_n}{d\lambda} \Big\rangle + \Big\langle \frac{d^2\psi_n}{d\lambda^2} \Big| \psi_n \Big\rangle = 0$$
$$\Rightarrow \mathrm{Re}\Big\langle \psi_n \Big| \frac{d^2\psi_n}{d\lambda^2} \Big\rangle = -\Big\langle \frac{d\psi_n}{d\lambda} \Big| \frac{d\psi_n}{d\lambda} \Big\rangle = -\sum_{m;m\neq n}\frac{|\langle\psi_m|\hat{W}|\psi_n\rangle|^2}{(E_n - E_m)^2} \quad \text{(N.13)}$$

$$\frac{1}{2}\Big| \frac{d^2\psi_n}{d\lambda^2} \Big\rangle = +\sum_{m(\neq n)}|\psi_m\rangle\frac{1}{E_n - E_m}\Big(\sum_{p\neq n}\frac{\langle\psi_m|\hat{W}|\psi_p\rangle\langle\psi_p|\hat{W}|\psi_n\rangle}{E_n - E_p} - \frac{\langle\psi_m|\hat{W}|\psi_n\rangle}{E_n - E_m}\langle\psi_n|\hat{W}|\psi_n\rangle\Big)$$
$$- \frac{1}{2}|\psi_n\rangle\sum_{m;m\neq n}\frac{|\langle\psi_m|\hat{W}|\psi_n\rangle|^2}{(E_n - E_m)^2}$$
$$= \sum_{m(\neq n)}|\psi_m\rangle\sum_{p\neq n}\frac{\langle\psi_m|\hat{W}|\psi_p\rangle\langle\psi_p|\hat{W}|\psi_n\rangle}{(E_n - E_p)(E_n - E_m)} - \sum_{m(\neq n)}|\psi_m\rangle\frac{\langle\psi_m|\hat{W}|\psi_n\rangle}{(E_n - E_m)^2}\langle\psi_n|\hat{W}|\psi_n\rangle$$
$$- |\psi_n\rangle\frac{1}{2}\sum_{m;m\neq n}\frac{|\langle\psi_m|\hat{W}|\psi_n\rangle|^2}{(E_n - E_m)^2} + |\psi_n\rangle iC_2 \quad \text{(N.14)}$$

The real-valued factor C_2 can be chosen arbitrarily, because the norm-conservation determines only the real value of the prefactor of $|\psi_n\rangle$. Important is that the phase factor is already included in the wave functions.

Energy and wave function in second-order perturbation theory

So far, we prepared the λ derivatives of energies and wave functions. From now on, we use the Taylor expansion at $\lambda = 0$.

$$E_n(\lambda) = E_n(0) + \lambda\left.\frac{dE_n}{d\lambda}\right|_{\lambda=0} + \frac{1}{2}\lambda^2\left.\frac{d^2E_n}{d\lambda^2}\right|_{\lambda=0} + O(\lambda^3) \quad \text{(N.15)}$$

In the following, I indicate the unperturbed values with $\lambda = 0$ by a bar ontop of the symbol, i.e. $\bar{E}_n = E_n(\lambda = 0)$ and $|\bar{\psi}_n\rangle = |\psi_n(\lambda = 0)\rangle$. I obtain the energies up to second order in λ as

$$E_n(\lambda) = \langle\bar{\psi}_n|\Big(h + \lambda\hat{W}\Big)|\bar{\psi}_n\rangle + \lambda^2\sum_{m;m\neq n}\frac{|\langle\bar{\psi}_m|\hat{W}|\bar{\psi}_n\rangle|^2}{\bar{E}_n - \bar{E}_m} + O(\lambda^3) \quad \text{(N.16)}$$

and the eigenstates as

$$|\psi_n(\lambda)\rangle = |\bar{\psi}_n\rangle + \Big(\sum_{m(\neq n)}\frac{|\bar{\psi}_m\rangle\langle\bar{\psi}_m|}{\bar{E}_n - \bar{E}_m}\Big)\hat{W}|\bar{\psi}_n\rangle - \underbrace{\Big(\sum_{m(\neq n)}\frac{|\bar{\psi}_m\rangle\langle\bar{\psi}_m|}{(\bar{E}_n - \bar{E}_m)^2}\Big)\hat{W}|\bar{\psi}_n\rangle\langle\bar{\psi}_n|\hat{W}|\bar{\psi}_n\rangle}_{\text{correction 1st order energy shift}}$$
$$\underbrace{- |\bar{\psi}_n\rangle\frac{1}{2}\sum_{m(\neq n)}\frac{|\langle\bar{\psi}_m|\hat{W}|\bar{\psi}_n\rangle|^2}{(\bar{E}_n - \bar{E}_m)^2}}_{\text{normalization 1st order}} + \underbrace{\Big(\sum_{m(\neq n)}\frac{|\bar{\psi}_m\rangle\langle\bar{\psi}_m|}{\bar{E}_n - \bar{E}_m}\Big)\hat{W}\Big(\sum_{p\neq n}\frac{|\bar{\psi}_p\rangle\langle\bar{\psi}_p|}{\bar{E}_n - \bar{E}_p}\Big)\hat{W}|\bar{\psi}_n\rangle}_{\text{true second order}} + O(\lambda^3) \quad \text{(N.17)}$$

The wave function agrees with the socond order corrections on Wikipedia `https://en.wikipedia.org/wiki/Perturbation_theory_(quantum_mechanics)` retrieved June 24, 2022.

Second-order perturbation theory with Green's functions

Editor: This section with Green's function is unfinished! The equations are partly incorrect.

Let me use perturbation theory of energies and wave functions to construct the perturbed Green's functions. Here, the discussion is limited to the one-particle Hilbert space, because the Green's function is an operator in the one-particle Hilbert space, and therefore also the perturbation $\hat{W}$ must be in the same space.

$$\hat{G}(\epsilon) = \sum_m \frac{|\psi_m\rangle\langle\psi_m|}{E - E_m} \tag{N.18}$$

In the summations for the perturbation theory the pole is always excluded. This can be achieved by going into the complex plane

$$\hat{G}(\epsilon) = \lim_{\eta\to 0+} \sum_m |\psi_m\rangle \frac{1}{E - E_m + i\eta} \langle\psi_m| \tag{N.19}$$

$$\hat{\bar{G}}(\epsilon) = \sum_m \frac{|\bar{\psi}_m\rangle\langle\bar{\psi}_m|}{E - \bar{E}_m} \tag{N.20}$$

Editor: In the following, the singularities of the Green's functions are not treated properly. In the perturbation expansion, the pole the singular term is removed.

$$E_n(\lambda) = \bar{E}_n + \lambda\langle\bar{\psi}_n|\hat{W}|\bar{\psi}_n\rangle + \lambda^2\langle\bar{\psi}_n|\hat{W}\hat{\bar{G}}(\bar{E}_n)\hat{W}|\bar{\psi}_n\rangle + O(\lambda^3) \tag{N.21}$$

In the following, I will use

$$\partial_\epsilon G(\epsilon) = \partial_\epsilon \sum_m \frac{|\psi_m\rangle\langle\psi_m|}{E - E_m} = -\sum_m \frac{|\psi_m\rangle\langle\psi_m|}{(E - E_m)^2} = -\hat{G}^2(\epsilon) \tag{N.22}$$

$$\begin{aligned}
|\psi_n(\lambda)\rangle &= |\bar{\psi}_n\rangle + \sum_{m;m\neq n} \frac{|\bar{\psi}_m\rangle\langle\bar{\psi}_m|}{\bar{E}_n - \bar{E}_m}\hat{W}|\bar{\psi}_n\rangle \\
&\quad - \sum_{m(\neq n)} |\psi_m\rangle \frac{1}{\bar{E}_m - \bar{E}_n} \sum_{p\neq n} \frac{\langle\bar{\psi}_m|\hat{W}|\bar{\psi}_p\rangle\langle\bar{\psi}_p|\hat{W}|\bar{\psi}_n\rangle}{\bar{E}_n - \bar{E}_p} - \sum_{m(\neq n)} |\psi_m\rangle \frac{1}{\bar{E}_m - \bar{E}_n} \frac{\langle\bar{\psi}_m|\hat{W}|\bar{\psi}_n\rangle}{\bar{E}_n - \bar{E}_m}\langle\bar{\psi}_n|\hat{W}|\bar{\psi}_n\rangle \\
&\quad - |\bar{\psi}_n\rangle \frac{1}{2} \sum_{m;m\neq n} \frac{|\langle\bar{\psi}_m|\hat{W}|\bar{\psi}_n\rangle|^2}{(\bar{E}_n - \bar{E}_m)^2} + O(\lambda^3) \\
&= |\bar{\psi}_n\rangle + \bar{G}(\bar{E}_n)\hat{W}|\bar{\psi}_n\rangle + \bar{G}(\bar{E}_n)\hat{W}\bar{G}(\bar{E}_n)\hat{W}|\bar{\psi}_n\rangle \underbrace{-\bar{G}^2(\bar{E}_n)\hat{W}|\bar{\psi}_n\rangle\langle\bar{\psi}_n|\hat{W}|\bar{\psi}_n\rangle}_{+(\partial_\lambda E_n)\partial_E \hat{\bar{G}}(E)\big|_{\bar{E}_n}\hat{W}|\psi_n\rangle} \\
&\quad - |\bar{\psi}_n\rangle \frac{1}{2}\langle\bar{\psi}_n|\hat{W}\hat{G}^2(\bar{E}_n)\hat{W}|\bar{\psi}_n\rangle + O(\lambda^3) \\
&= |\bar{\psi}_n\rangle + \underbrace{\bar{G}(E_n(\lambda))\hat{W}|\psi_n\rangle}_{\bar{G}(\bar{E}_n)\hat{W}|\bar{\psi}_n\rangle + (\partial_\lambda E_n)\partial_E \hat{\bar{G}}(E)\big|_{\bar{E}_n}\hat{W}|\psi_n\rangle} + \bar{G}(\bar{E}_n)\hat{W}\bar{G}(\bar{E}_n)\hat{W}|\bar{\psi}_n\rangle \\
&\quad - |\bar{\psi}_n\rangle \frac{1}{2}\langle\bar{\psi}_n|\hat{W}\hat{G}(\bar{E}_n)^2\hat{W}|\bar{\psi}_n\rangle + O(\lambda^3)
\end{aligned} \tag{N.23}$$

$$\begin{aligned} & \hat{G}^{-1}(E) = \hat{\tilde{G}}^{-1}(E) - \hat{W} \\ \Rightarrow \quad & \hat{\tilde{G}}(E) = \hat{G}(E) - \hat{\tilde{G}}(E)\hat{W}\hat{G}(E) \\ \Rightarrow \quad & \hat{G}(E) = \hat{\tilde{G}}(E) + \hat{\tilde{G}}(E)\hat{W}\hat{G}(E) \end{aligned} \tag{N.24}$$

N.2 Ensembles of Slater determinants

In the chapter Eq. 2 on weakly interacting systems, I described a division Eq. 2.139 of the total energy of an interacting Hamiltonian into one contribution, which is the energy of an ensemble of Slater determinants, and a rest. The latter has been named the entanglement energy. Here, I use second-order approxmation theory to estimate the entanglement energy.

Let me divide the Hamiltonian $\hat{H} = \hat{h} + \hat{W}$ into a term diagonal in a basis of Slater determinants and the off-diagonal terms as in Eq. 2.139. The off-diagonal terms are then treated in second-order perturbation theory.

$$\hat{H}(\lambda) = \sum_{\vec{\sigma}} |\vec{\sigma}\rangle\langle\vec{\sigma}|\hat{H}|\vec{\sigma}\rangle\langle\vec{\sigma}| + \lambda \sum_{\vec{\sigma},\vec{\sigma}';\vec{\sigma}\neq\vec{\sigma}'} |\vec{\sigma}\rangle\langle\vec{\sigma}|\hat{H}|\vec{\sigma}'\rangle\langle\vec{\sigma}'| \tag{N.25}$$

The perturbation expansion depends on the one-particle basisset used to define the set of Slater determinants. If the Slater determinants are formed from the natural orbitals, the zero-th order contains the mean-field energy of the **thermal Hartree-Fock approximation** (THFA) and the energy due to **correlated occupation-number fluctuations** . The first-order term is responsible for what I call the **entanglement energy**.

The eigenvalues of $\hat{H}(\lambda)$ in second-order perturbation theory are

$$\begin{aligned} E_{\vec{\sigma}}(\lambda) \quad & \stackrel{\text{def}}{=} \quad \langle\Phi_{\vec{\sigma}}(\lambda)|\hat{H}(\lambda)|\Phi_{\vec{\sigma}}(\lambda)\rangle \\ & \stackrel{\text{Eq. } N.16}{=} \langle\vec{\sigma}|\hat{H}|\vec{\sigma}\rangle + \sum_{\vec{\sigma}';\vec{\sigma}\neq\vec{\sigma}'} \frac{|\langle\vec{\sigma}|\hat{H}|\vec{\sigma}'\rangle|^2}{\langle\vec{\sigma}|\hat{H}|\vec{\sigma}\rangle - \langle\vec{\sigma}'|\hat{H}|\vec{\sigma}'\rangle} + O(\lambda^3) \end{aligned} \tag{N.26}$$

The Hamiltonian in the equation above is the full Hamiltonian $\hat{H}(\lambda)$ including off-diagonal terms. The $|\Phi_{\vec{\sigma}}(\lambda)\rangle$ are the eigenstates of the perturbed Hamiltonian $\hat{H}(\lambda)$, that are connected through the perturbation expansion to the Slater determinant $|\vec{\sigma}\rangle$, i.e. $|\Phi_{\vec{\sigma}}(\lambda = 0)\rangle = |\vec{\sigma}\rangle$. The Slater determinants $|\vec{\sigma}\rangle$ are also the eigenstates of the unperturbed Hamiltonian $H(0) = \sum_{\vec{\sigma}} |\vec{\sigma}\rangle\langle\vec{\sigma}|\hat{H}|\vec{\sigma}\rangle\langle\vec{\sigma}|$ Similarly, the eigenvalues $E_{\vec{\sigma}}(\lambda)$ inherit the label from the zeroth-order solutions.

Let me now consider an ensemble $\{P_q, |\Phi_q(\lambda)\rangle\}$, with the λ-dependent eigenstates of the Hamiltonian as micro states $|\Phi_q\rangle$. The states are labeled according to the zeroth-order eigenstates so that $q = \vec{\sigma}$.

The goal is to determine the energy of the ensemble in second-order perturbation theory

$$E = \sum_q P_q E_q(\lambda) \qquad \text{with } \hat{H}(\lambda)|\Psi_q(\lambda)\rangle = |\Psi_q(\lambda)\rangle E_q(\lambda) \tag{N.27}$$

This yields

$$\begin{aligned} E[\{P_{\vec{\sigma}}\}] &= \sum_{\vec{\sigma}} P_{\vec{\sigma}} E_{\vec{\sigma}}(\lambda) = \sum_{\vec{\sigma}} P_{\vec{\sigma}} \langle\vec{\sigma}|\hat{H}|\vec{\sigma}\rangle + \sum_{\vec{\sigma},\vec{\sigma}';\vec{\sigma}\neq\vec{\sigma}'} P_{\vec{\sigma}} \frac{|\langle\vec{\sigma}|\hat{H}|\vec{\sigma}'\rangle|^2}{\langle\vec{\sigma}|\hat{H}|\vec{\sigma}\rangle - \langle\vec{\sigma}'|\hat{H}|\vec{\sigma}'\rangle} + O(\lambda^3) \\ &= \sum_{\vec{\sigma}} P_{\vec{\sigma}} \langle\vec{\sigma}|\hat{H}|\vec{\sigma}\rangle + \frac{1}{2} \sum_{\vec{\sigma},\vec{\sigma}';\vec{\sigma}\neq\vec{\sigma}'} \Big(P_{\vec{\sigma}} - P_{\vec{\sigma}'}\Big) \frac{|\langle\vec{\sigma}|\hat{H}|\vec{\sigma}'\rangle|^2}{\langle\vec{\sigma}|\hat{H}|\vec{\sigma}\rangle - \langle\vec{\sigma}'|\hat{H}|\vec{\sigma}'\rangle} + O(\lambda^3) \end{aligned} \tag{N.28}$$

Thus, the correction to the ensemble energy from second order perturbation theory is

ENTANGLEMENT ENERGY IN SECOND-ORDER PERTURBATION THEORY

The energy difference of an ensemble of Slater determinants $|\vec{\sigma}\rangle$ with fixed probabilities $P_{\vec{\sigma}}$ due to the presence of Hamilton matrix elements between those Slater determinants is, in second-order perturbation theory,

$$\Delta E = \sum_{\vec{\sigma}} P_{\vec{\sigma}} E_{\vec{\sigma}} - \sum_{\vec{\sigma}} P_{\vec{\sigma}} \langle \vec{\sigma} | \hat{H} | \vec{\sigma} \rangle = \frac{1}{2} \sum_{\vec{\sigma},\vec{\sigma}';\vec{\sigma}\neq\vec{\sigma}'} \left(P_{\vec{\sigma}} - P_{\vec{\sigma}'} \right) \frac{|\langle \vec{\sigma} | \hat{H} | \vec{\sigma}' \rangle|^2}{\langle \vec{\sigma} | \hat{H} | \vec{\sigma} \rangle - \langle \vec{\sigma}' | \hat{H} | \vec{\sigma}' \rangle} \tag{N.29}$$

Editor: Can one establish a reasonable link to Möller Plesset perturbation theory? [200]

Appendix O

Further material about Lehmann amplitudes

Editor: Do not read: This is material left over from rewriting the sections on the Lehmann amplitudes.

O.1 Equation of motion for Lehmann amplitudes

Let me represent the Lehmann amplitudes in a non-orthonormal basis of local orbitals $||chi_\alpha\rangle$, with field operators $\hat{c}_\alpha$ and projector functions $|\langle\pi_\alpha|$.

$$
\begin{aligned}
|\psi^{\mathcal{L}a}_{q,q'}(t)\rangle &= \sum_\alpha |\chi_\alpha\rangle\langle\pi_\alpha|\psi^{\mathcal{L}a}_{q,q'}(t)\rangle \\
&= \sum_\alpha |\chi_\alpha\rangle \int d^4x\, \langle\pi_\alpha|\vec{x}\rangle \overbrace{\langle\Phi_q|\hat{\psi}_H(\vec{x},t)|\Phi_{q'}\rangle}^{\langle\vec{x}|\psi^{\mathcal{L}a}_{q,q'}(t)\rangle} \\
&= \sum_\alpha |\chi_\alpha\rangle\langle\Phi_q| \underbrace{\int d^4x\, \langle\pi_\alpha|\vec{x}\rangle\hat{\psi}_H(\vec{x},t)}_{\hat{c}_{H,\alpha}(t)} |\Phi_{q'}\rangle \\
&= \sum_\alpha |\chi_\alpha\rangle \underbrace{\langle\Phi_q|\hat{c}_{H,\alpha}(t)|\Phi_{q'}\rangle}_{\langle\pi_\alpha|\psi^{\mathcal{L}a}_{q,q'}(t)\rangle}
\end{aligned}
\tag{O.1}
$$

Let me now calculate the time derivative

$$
\begin{aligned}
i\hbar\partial_t\big|\psi^{\mathcal{L}a}_{q,q'}(t)\big\rangle &= \sum_\alpha |\chi_\alpha\rangle\big\langle\Phi_q|i\hbar\partial_t\hat{c}_{H,\alpha}(t)\big|\Phi_{q'}\big\rangle \\
&= \sum_\alpha |\chi_\alpha\rangle\big\langle\Phi_q|\big[\hat{c}_{H,\alpha}(t),\hat{H}(t)\big]_-\big|\Phi_{q'}\big\rangle \\
&\overset{\text{Eqs. 8.3,8.4}}{=} \sum_\alpha |\chi_\alpha\rangle\big\langle\Phi_q|\Big(\sum_\beta h_{\alpha,\beta}\hat{c}_{H,\beta}(t) + \sum_{\alpha,\beta,\gamma,\delta} W_{\alpha,\beta,\delta,\gamma}\hat{c}^+_{H,\beta}(t)\hat{c}_{H,\gamma}(t)\hat{c}_{H,\delta}(t)\Big)\big|\Phi_{q'}\big\rangle \\
&= \sum_\alpha |\chi_\alpha\rangle\Big(\sum_\beta h_{\alpha,\beta}\big\langle\Phi_q|\hat{c}_{H,\beta}(t)\big|\Phi_{q'}\big\rangle + \sum_{\beta,\gamma,\delta} W_{\alpha,\beta,\delta,\gamma}\big\langle\Phi_q|\hat{c}^+_{H,\beta}(t)\hat{c}_{H,\gamma}(t)\hat{c}_{H,\delta}(t)\big|\Phi_{q'}\big\rangle\Big) \\
&= \sum_\alpha |\chi_\alpha\rangle\Big(\sum_\beta h_{\alpha,\beta}\langle\pi_\beta|\psi^{\mathcal{L}a}_{q,q'}(t)\rangle \\
&\quad + \sum_{\beta,\gamma,\delta} W_{\alpha,\beta,\delta,\gamma}\big\langle\Phi_q|\hat{c}^+_{H,\beta}(t)\hat{c}_{H,\gamma}(t)\underbrace{\sum_{\bar{q}}|\Phi_{\bar{q}}\rangle\langle\Phi_{\bar{q}}|}_{=1}\hat{c}_{H,\delta}(t)\big|\Phi_{q'}\big\rangle\Big) \\
&= \sum_\alpha |\chi_\alpha\rangle\Big(\sum_\beta h_{\alpha,\beta}\langle\pi_\beta|\psi^{\mathcal{L}a}_{q,q'}(t)\rangle \\
&\quad + \sum_\delta\sum_{\bar{q}}\Big(\sum_{\beta,\gamma} W_{\alpha,\beta,\delta,\gamma}\big\langle\Phi_q|\hat{c}^+_{H,\beta}(t)\hat{c}_{H,\gamma}(t)\big|\Phi_{\bar{q}}\big\rangle\Big)\langle\pi_\delta|\psi^{\mathcal{L}a}_{\bar{q},q'}(t)\rangle\Big)
\end{aligned}
\tag{O.2}
$$

Remark: Where is the exchange contribution? When $\Phi_{q'}$ is an N-particle state, the electrostatic potential is calculated for $N-1$-particle states.

A reasonable approximation would be to discard the elements with $q \neq \bar{q}$.

O.1.1 Lehmann amplitudes and wave functions

Let me mention a number of properties of Lehmann amplitudes

- The Lehmann amplitudes can be expressed in terms of many-particle wave functions as

  - for a one-particle state

$$
\begin{aligned}
|\Psi\rangle &= \int d^4x_1 \underbrace{\hat{\psi}^\dagger(\vec{x}_1)|\mathcal{O}\rangle}_{|\vec{x}_1\rangle}\langle\vec{x}_1|\Psi\rangle \\
\Rightarrow \langle\Psi|\Psi\rangle &= \int d^4x_1\int d^4x'_1\ \langle\Psi|\vec{x}_1\rangle\,\langle\mathcal{O}|\ \underbrace{\hat{\psi}(\vec{x}_1)\hat{\psi}^\dagger(\vec{x'}_1)}_{\delta(\vec{x}_1-\vec{x'}_1)-\hat{\psi}^\dagger(\vec{x'}_1)\hat{\psi}(\vec{x}_1)}\ |\mathcal{O}\rangle\langle\vec{x'}_1|\Psi\rangle \\
&= \int d^4x_1\langle\Psi|\vec{x}_1\rangle\langle\vec{x}_1|\Psi\rangle = \langle\Psi|\Psi\rangle
\end{aligned}
\tag{O.3}
$$

– for a two-particle state

$$
\begin{aligned}
|\Psi\rangle &= \frac{1}{\sqrt{2}} \int d^4x_2 \int d^4x_1 \, \hat{\psi}^\dagger(\vec{x_2})\hat{\psi}^\dagger(\vec{x_1})|\mathcal{O}\rangle \underbrace{\langle \vec{x_1}, \vec{x}_2|\Psi\rangle}_{\Psi(\vec{x}_1,\vec{x}_2)} \\
\Rightarrow \langle\Psi|\Psi\rangle &= \frac{1}{2}\int d^4x_1 \int d^4x_2 \int d^4x_1' \int d^4x_2' \, \langle\Psi|\vec{x}_1\vec{x}_2\rangle\langle\vec{x'}_1,\vec{x'}_2|\Psi\rangle \\
&\quad \times\langle\mathcal{O}|\hat{\psi}(\vec{x}_1) \underbrace{\hat{\psi}(\vec{x}_2)\hat{\psi}^\dagger(\vec{x'}_2)}_{\delta(\vec{x}_2-\vec{x'}_2)-\hat{\psi}^\dagger(\vec{x'}_2)\hat{\psi}(\vec{x}_2)} \hat{\psi}^\dagger(\vec{x'}_1)|\mathcal{O}\rangle \\
&= \frac{1}{2}\int d^4x_1 \int d^4x_2 \int d^4x_1' \int d^4x_2' \, \langle\Psi|\vec{x}_1\vec{x}_2\rangle\langle\vec{x'}_1,\vec{x'}_2|\Psi\rangle \\
&\quad \times\langle\mathcal{O}|\hat{\psi}(\vec{x}_1)\Big(\delta(\vec{x}_2-\vec{x'}_2)\hat{\psi}^\dagger(\vec{x'}_1) - \hat{\psi}^\dagger(\vec{x'}_2) \underbrace{\hat{\psi}(\vec{x}_2)\hat{\psi}^\dagger(\vec{x'}_1)}_{\delta(\vec{x}_2-\vec{x'}_1)-\hat{\psi}^\dagger(\vec{x'}_1)\hat{\psi}(\vec{x}_2)} \Big)|\mathcal{O}\rangle \\
&= \frac{1}{2}\int d^4x_1 \int d^4x_2 \int d^4x_1' \int d^4x_2' \, \langle\Psi|\vec{x}_1\vec{x}_2\rangle\langle\vec{x'}_1,\vec{x'}_2|\Psi\rangle \\
&\quad \times\Big(\delta(\vec{x}_1-\vec{x'}_1)\delta(\vec{x}_2-\vec{x'}_2) - \delta(\vec{x}_1-\vec{x'}_2)\delta(\vec{x}_2-\vec{x'}_1)\Big) \\
&= \frac{1}{2}\int d^4x_1 \int d^4x_2 \, \Big(\langle\Psi|\vec{x}_1\vec{x}_2\rangle\langle\vec{x}_1,\vec{x}_2|\Psi\rangle - \langle\Psi|\vec{x}_1\vec{x}_2\rangle \underbrace{\langle\vec{x}_2,\vec{x}_1|\Psi\rangle}_{-\langle\vec{x}_1,\vec{x}_2|\Psi\rangle}\Big) \\
&= \langle\Psi| \underbrace{\int d^4x_1 \int d^4x_2 \, |\vec{x}_1\vec{x}_2\rangle\langle\vec{x}_1,\vec{x}_2|}_{\hat{1}} |\Psi\rangle = \langle\Psi|\Psi\rangle
\end{aligned}
\tag{O.4}
$$

– for an N-particle state

$$
|\Psi\rangle = \frac{1}{\sqrt{N!}} \int d^4x_1 \ldots \int d^4x_N \, \hat{\psi}^\dagger(\vec{x_N})\cdots\hat{\psi}^\dagger(\vec{x_1})|\mathcal{O}\rangle \underbrace{\langle\vec{x_1},\ldots,\vec{x}_N|\Psi\rangle}_{\Psi(\vec{x}_1,\ldots,\vec{x}_N)} \tag{O.5}
$$

Next we use this representation of the wave functions to express the Lehmann amplitudes by the many-particle wave functions in a real space representation.

$$
\begin{aligned}
\psi^{\mathcal{L}a}_{q,q'}(\vec{x},t) &= \langle\Phi_q(t)|\hat{\psi}(\vec{x})|\Phi_{q'}(t)\rangle \\
&= \underbrace{\frac{1}{\sqrt{(N-1)!}} \int d\vec{x}_1\cdots d\vec{x}_{N-1} \, \Phi_q^*(\vec{x}_1,\ldots,\vec{x}_{N-1},t)\langle\mathcal{O}|\hat{\psi}(\vec{x}_1)\cdots\hat{\psi}(\vec{x}_{N-1})\,\hat{\psi}(\vec{x})}_{\langle\Phi_q(t)|} \\
&\quad \times \underbrace{\frac{1}{\sqrt{N!}} \int d\vec{x'}_1\cdots d\vec{x'}_N \hat{\psi}^\dagger(\vec{x'}_N)\ldots\hat{\psi}^\dagger(\vec{x'}_1)|\mathcal{O}\rangle\Phi_{q'}(\vec{x'}_1,\ldots,\vec{x'}_N,t)}_{|\Phi_{q'}(t)\rangle} \\
&= \frac{1}{(N-1)!}\frac{1}{\sqrt{N}} \int d\vec{x}_1\cdots d\vec{x}_{N-1} \int d\vec{x'}_1\cdots d\vec{x'}_N \Phi_q^*(\vec{x}_1,\ldots,\vec{x}_{N-1},t)\Phi_{q'}(\vec{x'}_1,\ldots,\vec{x'}_N,t) \\
&\quad \times\langle\mathcal{O}|\hat{\psi}(\vec{x}_1)\cdots\hat{\psi}(\vec{x}_{N-1}) \quad \underbrace{\hat{\psi}(\vec{x})\hat{\psi}^\dagger(\vec{x'}_N)}_{\left(\delta(\vec{x}-\vec{x'}_N)-\hat{\psi}^\dagger(\vec{x'}_N)\hat{\psi}(\vec{x})\right)} \quad \ldots\hat{\psi}^\dagger(\vec{x'}_1)|\mathcal{O}\rangle
\end{aligned}
\tag{O.6}
$$

We can commutate the annihilator $\hat{\psi}(\vec{x})$ two the very right, in front of the vacuum state. Each commutation leaves one term with a $delta$-function in place of one creator and one annihilator. Each term removes a different creation operator, say $\hat{\psi}^\dagger(\vec{x}_j)$. We can exploit the antisymmetry of the wave function

$$
\Phi_q\big(\vec{x'}_1,\ldots,\vec{x'}_j,\vec{x'}_{j+1},\ldots,\vec{x'}_N\big) = -\Phi_q\big(\vec{x'}_1,\ldots,\vec{x'}_{j+1},\vec{x'}_j,\ldots,\vec{x'}_N\big) \tag{O.7}
$$

Thus all the terms become identical after renaming the integration variables. Hence

$$\begin{aligned}\psi^{\mathcal{L}a}_{q,q'}(\vec{x},t) &= \frac{1}{(N-1)!}\frac{1}{\sqrt{N}}\int d\vec{x}_1\cdots d\vec{x}_{N-1}\int d\vec{x'}_1\cdots d\vec{x'}_{N-1}\,\Phi^*_q(\vec{x}_1,\ldots,\vec{x}_{N-1},t)\Phi_{q'}(\vec{x'}_1,\ldots,\vec{x'}_{N-1},\vec{x},t)\\ &\quad\times N\underbrace{\underbrace{\langle\mathcal{O}|\hat\psi(\vec{x}_1)\cdots\hat\psi(\vec{x}_{N-1})\hat\psi^\dagger(\vec{x}_{N-1})\ldots\hat\psi^\dagger(\vec{x'}_1)|\mathcal{O}\rangle}_{(N-1)\delta(\vec{x}_N-\vec{x'}_N)\langle\mathcal{O}|\hat\psi(\vec{x}_1)\cdots\hat\psi(\vec{x}_{N-2})\hat\psi^\dagger(\vec{x}_{N-2})\ldots\hat\psi^\dagger(\vec{x'}_1)|\mathcal{O}\rangle}}_{N!\prod_{j=1}^{N-1}\delta(\vec{x}_j-\vec{x'}_j)}\\ &= \sqrt{N}\int d\vec{x}_1\cdots d\vec{x}_{N-1}\,\Phi^*_q(\vec{x}_1,\ldots,\vec{x}_{N-1},t)\Phi_{q'}(\vec{x}_1,\ldots,\vec{x}_{N-1},\vec{x},t)\end{aligned}\tag{O.8}$$

This shows that (and how) the Lehmann amplitudes are the matrix elements between N and $N-1$-particle wave functions.

LEHMANN AMPLITUDES AND MANY-PARTICLE WAVE FUNCTIOINS

$$\psi^{\mathcal{L}a}_{q,q'}(\vec{x},t) = \sqrt{N}\int d\vec{x}_1\cdots d\vec{x}_{N-1}\,\Phi^*_q(\vec{x}_1,\ldots,\vec{x}_{N-1},t)\Phi_{q'}(\vec{x}_1,\ldots,\vec{x}_{N-1},\vec{x},t)\tag{O.9}$$

O.1.2 Spectral function in the average-phase approximation (APA)

Editor: This section is probably superfluous and can be removed.

To make sense of this expression, let me simplify matters and consider the **average-phase approximation (APA)**. The APA has been introduced in section 2.6.1 on p. 78. In the average-phase approximation, the energy eigenstates are Slater determinants. In contrast to the mean-field approximation, however, certain correlations, the **correlated occupation-number fluctuations** , are taken into account.

In the APA, the Hamiltonian has the form

$$\hat H^{APA} = \sum_{\vec\sigma}|\vec\sigma\rangle E_{\vec\sigma}\langle\vec\sigma|\tag{O.10}$$

with the energy expectation values

$$E_{\vec\sigma}\overset{\text{def}}{=}\langle\vec\sigma|\hat H|\vec\sigma\rangle\ .\tag{O.11}$$

The Slater determinants shall be built in a basis of natural orbitals $|\varphi_j\rangle$, the eigenstates of the one-particle-reduced density matrix.

Furthermore, we transform the of field operators from position-and-spin representation into the representation of natural orbitals given in Eq. 3.61 on p. 142

$$\hat\psi^\dagger(\vec{x})\overset{\text{Eq. 3.61}}{=}\sum_j\hat a^\dagger_j\varphi^*_j(\vec{x})\qquad\text{and}\qquad\hat\psi(\vec{x})\overset{\text{Eq. 3.61}}{=}\sum_j\varphi_j(\vec{x})\hat a_j\tag{O.12}$$

$$
\begin{aligned}
\mathcal{A}(\vec{x},t,\vec{x'},t') &\overset{\text{Eq. 9.24}}{=} \frac{1}{2\pi\hbar}\mathrm{Tr}\Big\{\hat{\rho}^{(W)}_{T,\mu}\Big[\hat{\psi}_H(\vec{x},t),\hat{\psi}^+_H(\vec{x'},t')\Big]_+\Big\} \\
&= \frac{1}{2\pi\hbar}\sum_{\vec{\sigma},\vec{\sigma'}} P_{\vec{\sigma}}\Big\{\Big(\langle\vec{\sigma}|\overbrace{\sum_j \varphi_j(\vec{x})\hat{a}_{S,j}}^{\hat{\psi}_S(\vec{x})}|\vec{\sigma'}\rangle \mathrm{e}^{-\frac{i}{\hbar}(E_{\vec{\sigma'}}-E_{\vec{\sigma}})t}\Big)\Big(\langle\vec{\sigma'}|\overbrace{\sum_{j'}\hat{a}^\dagger_{j'}\varphi^*_{j'}(\vec{x'})}^{\hat{\psi}^\dagger(\vec{x'})}|\vec{\sigma}\rangle \mathrm{e}^{-\frac{i}{\hbar}(E_{\vec{\sigma}}-E_{\vec{\sigma'}})t'}\Big) \\
&\qquad +\Big(\langle\vec{\sigma}|\overbrace{\sum_{j'}\hat{a}^\dagger_{j'}\varphi^*_{j'}(\vec{x'})}^{\hat{\psi}^\dagger(\vec{x'})}|\vec{\sigma'}\rangle \mathrm{e}^{-\frac{i}{\hbar}(E_{\vec{\sigma'}}-E_{\vec{\sigma}})t'}\Big)\Big(\langle\vec{\sigma'}|\overbrace{\sum_j \varphi_j(\vec{x})\hat{a}_{S,j}}^{\hat{\psi}_S(\vec{x})}|\vec{\sigma}\rangle \mathrm{e}^{-\frac{i}{\hbar}(E_{\vec{\sigma}}-E_{\vec{\sigma'}})t}\Big)\Big\} \\
&= \frac{1}{2\pi\hbar}\sum_{j,j'}\sum_{\vec{\sigma}} P_{\vec{\sigma}}\Big(\varphi_j(\vec{x})\underbrace{\Big\langle\vec{\sigma}\Big|\hat{a}_{S,j}\overbrace{\hat{a}^\dagger_{S,j}\Big|\vec{\sigma}\Big\rangle}^{|\vec{\sigma'}\rangle}}_{=1-\sigma_j}\underbrace{\overbrace{\Big\langle\vec{\sigma}\hat{a}_j\Big|}^{\langle\vec{\sigma'}|}\hat{a}^\dagger_{j'}\Big|\vec{\sigma}\Big\rangle}_{=(1-\sigma_j)\delta_{j,j'}}\varphi^*_{j'}(\vec{x'})\mathrm{e}^{-\frac{i}{\hbar}\overbrace{(E_{\hat{a}^\dagger_j|\vec{\sigma}\rangle}-E_{\vec{\sigma}})}^{\epsilon^{(\vec{\sigma})}_j}(t-t')} \\
&\qquad +\varphi^*_{j'}(\vec{x'})\underbrace{\langle\vec{\sigma}|\hat{a}^\dagger_{j'}\overbrace{\hat{a}_j|\vec{\sigma}\rangle}^{|\vec{\sigma'}\rangle}}_{=\sigma_j\delta_{j,j'}}\underbrace{\overbrace{\langle\vec{\sigma}\hat{a}^\dagger_{S,j}|}^{\langle\vec{\sigma'}|}\hat{a}_{S,j}|\vec{\sigma}\rangle}_{=\sigma_j}\varphi_j(\vec{x})\mathrm{e}^{-\frac{i}{\hbar}\overbrace{(E_{\hat{a}_j|\vec{\sigma}\rangle}-E_{\vec{\sigma}})}^{-\epsilon^{(\vec{\sigma})}_j}(t'-t)}\Big) \\
&= \frac{1}{2\pi\hbar}\sum_j \varphi_j(\vec{x})\varphi^*_j(\vec{x'})\Big(\sum_{\vec{\sigma}} P_{\vec{\sigma}}(1-\sigma_j)\mathrm{e}^{-\frac{i}{\hbar}\overbrace{(E_{\hat{a}^\dagger_j|\vec{\sigma}\rangle}-E_{\vec{\sigma}})}^{\epsilon^{(\vec{\sigma})}_j}(t-t')} \\
&\qquad +\sum_{\vec{\sigma}} P_{\vec{\sigma}}\sigma_j\mathrm{e}^{-\frac{i}{\hbar}\overbrace{(E_{\hat{a}_j|\vec{\sigma}\rangle}-E_{\vec{\sigma}})}^{-\epsilon^{(\vec{\sigma})}_j}(t'-t)}\Big) \\
&= \int\frac{d\hbar\omega}{2\pi\hbar}\mathrm{e}^{-i\omega(t-t')} \\
&\qquad \times\underbrace{\langle\vec{x}|\sum_j|\varphi_j\rangle\Big\{\sum_{\vec{\sigma}}P_{\vec{\sigma}}\delta\Big(\overbrace{(1-\sigma_j)(E_{\hat{a}^\dagger_j|\vec{\sigma}\rangle}-E_{\vec{\sigma}})-\sigma_j(E_{\hat{a}_j|\vec{\sigma}\rangle}-E_{\vec{\sigma}})}^{\epsilon^{(\vec{\sigma})}_j}-\hbar\omega\Big)\Big\}\langle\varphi_j|\,|\vec{x'}\rangle}_{\hat{\mathcal{A}}(\hbar\omega)} \\
&= \int\frac{d\hbar\omega}{2\pi\hbar}\mathrm{e}^{-i\omega(t-t')}\langle\vec{x}|\underbrace{\Big[\sum_j|\varphi_j\rangle\Big\{\sum_{\vec{\sigma}}P_{\vec{\sigma}}\delta(\epsilon^{(\vec{\sigma})}_j-\hbar\omega)\Big\}\langle\varphi_j|\Big]}_{\hat{\mathcal{A}}(\hbar\omega)}|\vec{x'}\rangle \qquad \text{(O.13)}
\end{aligned}
$$

The energy level $\epsilon^{(\vec{\sigma})}_j$ has been defined for the APA in Eq. 2.122 on p. 85.

Thus, we arrive at the very same frequency-dependent spectral function $\hat{\mathcal{A}}(\hbar\omega)$, which we obtained earlier, in Eq. 2.121 in the chapter 2 on weakly interacting electrons.

$$\hat{\mathcal{A}}(\hbar\omega)=\sum_j|\varphi_j\rangle\Big\{\sum_{\vec{\sigma}}P_{\vec{\sigma}}\delta(\epsilon^{(\vec{\sigma})}_j-\hbar\omega)\Big\}\langle\varphi_j| \qquad \text{(O.14)}$$

For non-interacting electrons, the energy levels are independent of the state, so that each natural orbital contributes only a single delta-peak with unit weight. In the APA, the quasi-particle wave function experiences the surrounding electron distribution, which, in turn, depends on the specific many-particle state at hand. Thus the electron-removal energy for a given quasi-particle wave function may vary, leading to lifetime broadening or side-peaks due to the dynamical behavior of the environment.

In the Hartree-Fock approximation for excited states, which neglects the quasi-particle interactions, the environment is replaced by a mean field, so that a single quasi-particle peak emerges for each natural orbital.

O.1.3 Comparison with Stefanucci

Editor: This section shall define other types of Green's functions such as greater and lesser, reduced and advanced Green's functions and their relations.

In order to crosscheck some equations, I compared with the Book of Stefanucci and vn Leuwen[2]. This section provides the link to other Green's functions such as greater and lesser Green's functions as well as Retarded and advanced Green's functions.

TYPES OF GREEN'S FUNCTIONS

The following equations are only valid for the real-valued time axis.

$$
\begin{aligned}
G^{>}_{\alpha,\beta}(t,t') &\overset{SL6.21}{=} \frac{1}{i\hbar}\mathrm{Tr}\Big\{\hat{\rho}^{(W)}_{T,\mu}\hat{c}_\alpha(t)\hat{c}^{+}_\beta(t')\Big\} \\
&\overset{SL6.73}{=} \frac{1}{i\hbar}\sum_{q,q'}(P_q+P_{q'})\langle\pi_\alpha|\psi^{\mathcal{L}a}_{q,q'}(t)\rangle\big(1-f^{\mathcal{L}a}_{q,q'}\big)\langle\psi^{\mathcal{L}a}_{q,q'}(t')|\pi_\beta\rangle \\
&= -2\pi i\hat{\mathcal{A}}^{(e)}(t,t') \\
G^{<}_{\alpha,\beta}(t,t') &\overset{SL6.22}{=} \frac{-1}{i\hbar}\mathrm{Tr}\Big\{\hat{\rho}^{(W)}_{T,\mu}\hat{c}^{+}_\beta(t')\hat{c}_\alpha(t)\Big\} \\
&\overset{SL6.72}{=} \frac{-1}{i\hbar}\sum_{q,q'}(P_q+P_{q'})\langle\pi_\alpha|\psi^{\mathcal{L}a}_{q,q'}(t)\rangle f^{\mathcal{L}a}_{q,q'}\langle\psi^{\mathcal{L}a}_{q,q'}(t')|\pi_\beta\rangle \\
&= 2\pi i\hat{\mathcal{A}}^{(h)}(t,t') \\
G^{R}_{\alpha,\beta}(t,t') &= \theta(t-t')\frac{1}{i\hbar}\mathrm{Tr}\Big\{\hat{\rho}^{(W)}_{T,\mu}\Big[\hat{c}_\alpha(t)\hat{c}^{+}_\beta(t')\Big]_+\Big\} \\
&\overset{SL}{=} \theta(t-t')\frac{1}{i\hbar}\sum_{q,q'}(P_q+P_{q'})\langle\pi_\alpha|\psi^{\mathcal{L}a}_{q,q'}(t)\rangle\langle\psi^{\mathcal{L}a}_{q,q'}(t')|\pi_\beta\rangle \\
&= -2\pi i\theta(t-t')\Big(\mathcal{A}^{(e)}(t,t')+\mathcal{A}^{(h)}(t,t')\Big) \\
G^{A}_{\alpha,\beta}(t,t') &= \frac{-1}{i\hbar}\theta(t'-t)\mathrm{Tr}\Big\{\hat{\rho}^{(W)}_{T,\mu}\Big[\hat{c}_\alpha(t)\hat{c}^{+}_\beta(t')\Big]_+\Big\} \\
&\overset{SL}{=} \theta(t'-t)\frac{1}{i\hbar}\sum_{q,q'}(P_q+P_{q'})\langle\pi_\alpha|\psi^{\mathcal{L}a}_{q,q'}(t)\rangle\langle\psi^{\mathcal{L}a}_{q,q'}(t)|\pi_\beta\rangle \\
&= +2\pi i\theta(t'-t)\Big(\mathcal{A}^{(e)}(t,t')+\mathcal{A}^{(h)}(t,t')\Big) \\
G^{\mathcal{C}}_{\alpha,\beta}(t,t') &= \frac{1}{i\hbar}\mathrm{Tr}\Big\{\hat{\rho}^{(W)}_{T,\mu}\mathcal{T}_{\mathcal{C}}\hat{c}_\alpha(t)\hat{c}^{+}_\beta(t')\Big\} \\
&\overset{SL}{=} \frac{1}{i\hbar}\sum_{q,q'}(P_q+P_{q'})\langle\pi_\alpha|\psi^{\mathcal{L}a}_{q,q'}(t)\rangle\Big(\theta(t-t')\big(1-f^{\mathcal{L}a}_{q,q'}\big)-\theta(t'-t)f^{\mathcal{L}a}_{q,q'}\Big)\langle\psi^{\mathcal{L}a}_{q,q'}(t)|\pi_\beta\rangle \\
&= -2\pi i\Big(\theta(t-t')\mathcal{A}^{(e)}(t,t')-\theta(t'-t)\mathcal{A}^{(h)}(t,t')\Big) \\
\mathcal{A}^{(tot)}_{\alpha,\beta}(t,t') &= \frac{1}{2\pi\hbar}\mathrm{Tr}\Big\{\hat{\rho}^{(W)}_{T,\mu}\Big[\hat{c}_\alpha(t),\hat{c}^{+}_\beta(t')\Big]_+\Big\} \\
&= \frac{1}{2\pi\hbar}\sum_{q,q'}(P_q+P_{q'})\langle\pi_\alpha|\psi^{\mathcal{L}a}_{q,q'}(t)\rangle\langle\psi^{\mathcal{L}a}_{q,q'}(t)|\pi_\beta\rangle \\
&= \frac{i}{2\pi}\mathrm{sgn}(t-t')\Big(G^{\mathcal{C}}_{\alpha,\beta}(t,t')+\Big(G^{\mathcal{C}}_{\beta,\alpha}(t',t)\Big)^*\Big) \qquad \text{(O.15)}
\end{aligned}
$$

RELATIONS BETWEEN GREEN'S FUNCTIONS

$$
\begin{aligned}
G^{\mathcal{C}}_{\alpha,\beta}(t,t') &= \theta(t-t')G^{>}_{\alpha,\beta}(t,t') + \theta(t'-t)G^{<}_{\alpha,\beta}(t,t') \\
G^{R}_{\alpha,\beta}(t,t') &\overset{SL}{=} \theta(t-t')\Big(G^{>}_{\alpha,\beta}(t,t') - G^{<}_{\alpha,\beta}(t,t')\Big) \\
G^{A}_{\alpha,\beta}(t,t') &\overset{SL}{=} -\theta(t'-t)\Big(G^{>}_{\alpha,\beta}(t,t') - G^{<}_{\alpha,\beta}(t,t')\Big) \\
\hat{A}(t,t') &= \frac{1}{2\pi i}\Big(\hat{G}^{<}(t,t') - \hat{G}^{>}(t,t')\Big)
\end{aligned}
\tag{O.16}
$$

TIME-INVERSION RELATIONS

$$
\begin{aligned}
\hat{G}^{>}(t,t') &= \Big(-\hat{G}^{>}(t',t)\Big)^{\dagger} \\
\hat{G}^{<}(t,t') &= \Big(-\hat{G}^{<}(t',t)\Big)^{\dagger} \\
\Big(\hat{G}^{\mathcal{C}}(t',t)\Big)^{\dagger} &= \Big(\theta(t'-t)\hat{G}^{>}(t',t) + \theta(t-t')\hat{G}^{<}(t',t)\Big)^{\dagger} \\
&= \theta(t'-t)\Big(-\hat{G}^{>}(t,t')\Big) + \theta(t'-t)\Big(-\hat{G}^{<}(t,t')\Big) \\
&= -\theta(t'-t)\hat{G}^{>}(t,t') - \theta(t-t')\hat{G}^{<}(t,t') \neq -\hat{G}^{\mathcal{C}}(t,t') \\
\mathcal{A}^{(h)}_{\alpha,\beta}(t,t') &= \frac{1}{2\pi\hbar}\sum_{q,q'}(P_q + P'_q)\langle\pi_\alpha|\psi^{\mathcal{L}a}_{q,q'}(t)\rangle f^{\mathcal{L}a}_{q,q'}(t)\langle\psi^{\mathcal{L}a}_{q,q'}(t')|\pi_\beta\rangle \\
&= \Big(\frac{1}{2\pi\hbar}\sum_{q,q'}(P_q + P'_q)\langle\pi_\beta|\psi^{\mathcal{L}a}_{q,q'}(t')\rangle f^{\mathcal{L}a}_{q,q'}(t)\langle\psi^{\mathcal{L}a}_{q,q'}(t)|\pi_\alpha\rangle\Big) = \Big(\mathcal{A}^{(h)}_{\beta,\alpha}(t',t)\Big)^{*} \\
\hat{\mathcal{A}}^{(tot)}(t,t') &= \Big(\hat{\mathcal{A}}^{(tot)}(t',t)\Big)^{\dagger} \\
\hat{\mathcal{A}}^{(e)}(t,t') &= \Big(\hat{\mathcal{A}}^{(e)}(t',t)\Big)^{\dagger} \\
\hat{\mathcal{A}}^{(h)}(t,t') &= \Big(\hat{\mathcal{A}}^{(h)}(t',t)\Big)^{\dagger}
\end{aligned}
\tag{O.17}
$$

$$
\begin{aligned}
\hat{G}^{\mathcal{C}}(t,t') &= \theta(t-t')\hat{G}^{>}(t,t') + \theta(t'-t)\hat{G}^{<}(t,t') \\
\Big(\hat{G}^{\mathcal{C}}(t',t)\Big)^{\dagger} &= \Big(\theta(t'-t)\hat{G}^{>}(t',t) + \theta(t-t')\hat{G}^{<}(t',t)\Big)^{\dagger} \\
&= \theta(t'-t)\Big(-\hat{G}^{>}(t,t')\Big) + \theta(t'-t)\Big(-\hat{G}^{<}(t,t')\Big) \\
&= -\theta(t'-t)\hat{G}^{>}(t,t') - \theta(t-t')\hat{G}^{<}(t,t') \\
\hat{G}^{\mathcal{C}}(t,t') + \Big(\hat{G}^{\mathcal{C}}(t',t)\Big)^{\dagger} &= \mathrm{sgn}(t-t')\Big(\hat{G}^{>}(t,t') - \hat{G}^{<}(t,t')\Big) \\
\hat{G}^{\mathcal{C}}(t,t') - \Big(\hat{G}^{\mathcal{C}}(t',t)\Big)^{\dagger} &= \Big(\hat{G}^{>}(t,t') + \hat{G}^{<}(t,t')\Big) \\
\hat{\mathcal{A}}(t,t') &= \frac{i}{2\pi}\mathrm{sgn}(t-t')\Big\{\hat{G}^{\mathcal{C}}(t,t') + \Big(\hat{G}^{\mathcal{C}}(t',t)\Big)^{\dagger}\Big\} \\
\hat{G}^{>}(t,t') &= \theta(t-t')\hat{G}^{\mathcal{C}}(t,t') - \theta(t'-t)\Big(\hat{G}^{\mathcal{C}}(t',t)\Big)^{\dagger} \\
\hat{G}^{<}(t,t') &= \theta(t'-t)\hat{G}^{\mathcal{C}}(t,t') - \theta(t-t')\Big(\hat{G}^{\mathcal{C}}(t',t)\Big)^{\dagger}
\end{aligned}
\tag{O.18}
$$

Appendix P

Dictionary and Symbols

P.1 English-German Dictionary

caveat	Vorbehalt
coincidence	Übereinstimmung
convolution	Faltung
cross section	Wirkungsquerschnitt
esthetics	Ästetik
factorial	Fakultät (mathematische Operation)
faculty	Fakultät (akademische Verwaltungseinheit)
for the sake of ...	um ... willen (gen)
formidable	gewaltig, eindrucksvoll
full width at half maximum	Halbwertsbreite
propagator	Zeitentwicklungsoperator
commutate	kommutieren
rank	Rang
scattering amplitude	Streuamplitude
union	Vereinigung
without loss of generality	ohne Beschränkung der Allgemeinheit
wlog	oBdA (ohne Beschränkung der Allgemeinheit)
work function	Austrittsarbeit

P.2 Explanations

- caveat: Latin, a modifying or cautionary detail to be considered

P.3 Symbols

The list of symbols is not complete, nor is the usage of symbols unique. The list shall give a guidance.
Editor: The notes will not be completely consistent in the choice of symbols. Editor: Later, we may include also a reference to the equations defining the symbols.

Editor: The choice of symbols is a compromise between symbols that are (1) easily differentiated both in printed and hand-written form, that (2) exhibit similarity if there meaning is related, and (3) similarity to symbols commonly used in the literature.

P.4 Mathematical Symbols

- $\forall$ "for all".
- $[A,B]_- = [A,B] = AB - BA$: **commutator** of A and B. A and B may be matrices or operators.
- $[A,B]_+ = AB + BA$: **anti-commutator** of A and B. A and B may be matrices or operators.
- $\vec{a} \times \vec{b}$: **vector product** between two three dimensional vectors $\vec{a}$ and $\vec{b}$.

$$\vec{a} \times \vec{b} = \begin{pmatrix} a_y b_z - a_z b_y \\ a_z b_x - a_x b_z \\ a_x b_y - a_y b_x \end{pmatrix} \tag{P.1}$$

- $\vec{a} \otimes \vec{b}$: **outer product** or **dydadic product** of two vectors $\vec{a}$ and $\vec{b}$.

$$\left(\vec{a} \otimes \vec{b}\right)_{i,j} = a_i b_j \tag{P.2}$$

- $\det|\boldsymbol{A}|$: **determinant** of matrix $\boldsymbol{A}$
- $\mathrm{perm}|\boldsymbol{A}|$: **permanent** of matrix $\boldsymbol{A}$. The permanent is computed like the determinant with the exceptions that all terms are summed up without the sign changes for permutations.
- $\delta_{i,j}$: **Kronecker delta**

$$\delta_{i,j} = \begin{cases} 1 & \text{for } i = j \\ 0 & \text{else} \end{cases} \tag{P.3}$$

- $\delta(\vec{x})$: **Dirac's delta function** defined by

$$\forall_{f(x)} \int dx\, f(x)\delta(x) = f(0) \tag{P.4}$$

  which holds for all differentiable functions $f(x)$. The delta function of a vector is the product of the delta functions of its components.

- $\epsilon_{i_1,\ldots,i_N}$ **Levi-Civita Symbol** or **fully antisymmetric tensor**
- $\theta(x)$: **Heaviside step function**. A subscript defines a special region where the Heaviside is nonzero.
- $\mathrm{sgn}(x)$: sign function.
- $\mathrm{stat}_x F(x)$: value of the function $F(x)$ at its stationary point with respect to x. The stationary point may be a maximum, a minimum or a saddle point.
- $\mathrm{Tr}[\boldsymbol{A}]$: trace of a matrix A.
- $\sum_{x \in \mathbb{X}}$ sum over all elements x in the set $\mathbb{X}$.
- $\sum_{\sigma \in \{\uparrow,\downarrow\}}$ sum of the spin quantum number σ of a spin-$\frac{1}{2}$, which can assume values $\uparrow$ and $\downarrow$. The states are defined by the eigenvalue equations $\hat{S}_z|\uparrow\rangle = |\uparrow\rangle\left(+\frac{\hbar}{2}\right)$ and $\hat{S}_z|\downarrow\rangle = |\downarrow\rangle\left(-\frac{\hbar}{2}\right)$

P.5 Vectors, matrices, operators, functions, etc.

	typed	blackboard
vector	$\vec{a}$	$\vec{a}$
matrix	$\boldsymbol{A}$	$\underline{\underline{A}}$
state	$\|a\rangle$	$\|a\rangle$
operator	$\hat{A}$	$\hat{A}$

Vectors are indicated by a vector arrow such as $\vec{x}$. Matrices are made bold face such as $\boldsymbol{A}$. I have purposely combined two different notation, because this makes the difference optically more evident. I also used the psychological analogy of using an arrow for a one-dimensionally extended object, and "fat symbol" for a two-dimensionally extended object. On the blackboard, I use two underscores for matrices.

Functionals are indicated by an argument in brackets such as $F[y]$, where $y(x)$ is the function in the argument. If function arguments are mixed with normal arguments they are combined as in $F([y], x)$.

Commutators and anticommutators are indicated by brackets. The commutator has a minus sign as subscript or no subscript. An anticommutator always carries a plus sign as subscript.

- rather than using an integer counter for all summations $\sum_{i=1}^{N}$, I often use sums over sets of quantities such as $\sum_{\sigma\in\{\uparrow,\downarrow\}}$ for a sum over spin directions or $\{\sum_{\vec{t}}\}$ for a sum over all lattice translations. When the meaning is obvious, I drop the curly brackets as in $\sum_{\vec{t}}$. The curly brackets should not be dropped for a set of integers, because that would make the expression ambiguous.
- When the summation bounds or integration regions are dropped, "all values" of "the whole range" is implied.

P.6 Generic conventions

- Thermodynamic quantites have arguments related to reservoirs as subscripts.

P.7 Symbols of physical quantities

- t^+ variable t increased by an infinitesimally small, positive number. Useful for discontinuous functions.
- $\hat{c}^+_{H,\alpha}(t)$ creation operator for orbital α in the Heisenberg picture in the complex time plane. Equals $\hat{c}^\dagger_{H,\alpha}(t)$ on the real-time axis.
- $\hat{\rho}^{(1)}$ one-particle-reduced density matrix
- $\hat{\rho}^{(2)}$ two-particle-reduced density matrix
- $\hat{\rho}^{vN}_{T,\mu}$, $\hat{\rho}_{T,\mu}$ von-Neumann density matrix, many-particle density matrix
- $\hat{\rho}^{vN}_{T,\mu}$ von-Neumann density matrix, many-particle density matrix
- $\hat{\rho}^{vN,(0)}_{T,\mu}$, $\hat{\rho}^{(0)}_{T,\mu}$ many-particle density matrix or statistical operator specifically of the non-interacting system
- $\hat{\rho}^{vN,(W)}_{T,\mu}$, $\hat{\rho}^{(W)}_{T,\mu}$ many-particle density matrix or statistical operator specifically of the interacting system

- $Z_{T,\mu}$ partition function of the grand potential
- $Z^{(0)}_{T,\mu}$ partition function of the grand potential specifically for the non-interacting system
- $Z^{(W)}_{T,\mu}$ partition function of the grand potential specifically for the interacting system
- $\Omega_{T,\mu}$ grand potential
- $A_{T,N}$ Helmholtz potential
- $|\mathcal{O}\rangle$ vacuum state
- $|\varnothing\rangle$ zero state
- $\hat{c}^\dagger_\alpha$,$\hat{c}_\alpha$ creation and annihilation operators in a general basisset. Typically they refer local orbitals.
- $\hat{a}^\dagger_n$, $\hat{a}_n$ creation and annihilation operators in a basisset of one-particle eigenstates of the non-interacting Hamiltonian.
- $\hat{\psi}^\dagger(\vec{x})$, $\hat{\psi}(\vec{x})$ creation and annihilation operators in a real-space-and-spin basisset
- $\vec{x}$ composite vector containing a spatial coordinate $\vec{r}$ and a spin index σ.
- $|\vec{x}\rangle$ basis state of the real-space-and-spin representation. Eigenstate to position operator with eigenvalue $\vec{r}$ and of $\hat{S}_z$ with eigenvalue $\frac{\hbar}{2}\sigma$, where σ is the spin index.
- $|\chi_\alpha\rangle$ local orbital. Typically non-orthonormal. When they are orthonormal they can be Wannier orbitals.
- $\langle\pi_\alpha|$ projector function for the orbital $|\chi_\alpha\rangle$
- $|\varphi_j\rangle$: element of a orthonormal one-particle basisset. Often they are natural orbitals or the eigenstates of a one-particle Hamiltonian. Typically they are Bloch states.
- $\left\langle \hat{A} \right\rangle_{T,\mu} = \mathrm{Tr}\left[\hat{\rho}_{T,\mu}\hat{A}\right]$ thermal expectation value of the observable $\hat{A}$ in the grand ensemble.Editor: (legacy notation) Should be $A_{T,\mu}$.
- $\hat{W}$ interaction operator or generally perturbation of an unperturbed Hamilton operator
- $\hat{H}^{(0)}$ unperturbed Hamilton operator
- $\hat{h}$ unperturbed Hamilton operator (without interaction or time dependence)
- $\hat{H}^{(W)}$ Hamilton operator including the interaction or perturbation
- n, $n^{(1)}$ electron density
- E_H Hartree energy
- E_X exchange energy
- E_{xc} exchange-correlation energy
- T kinetic energy
- $\hat{G}(t,t')$ Green's function expressed as operator in the one-particle Hilbert space
- $\hat{D}(\epsilon)$ density of states expressed as operator in the one-particle Hilbert space
- $\hat{U}(t,t')$: propagator in the one-particle Hilbert space
- $\hat{\mathcal{U}}(t,t')$: propagator in the Fock space.

- $\hat{\Sigma}(t,t')$: self energy. Specifically, the proper self energy.
- $\hat{\Sigma}^{red}(t,t')$: reducible self energy.
- $\mathbb{A}_n$ set of all closed, labeled Feynman diagrams of order n in the interaction.
- $\mathbb{L}_n$ set of all closed, labeled, linked Feynman diagrams of order n in the interaction.
- $\mathbb{T}_n$ set of all closed, unlabeled (topologically inequivalent), linked Feynman diagrams of order n in the interaction.
- $\mathbb{S}_n$ set of all closed, unlabeled (topologically inequivalent), skeleton diagrams of order n in the interaction.
- $S(D)$ symmetry factor of an unlabeled diagram D

P.8 Comparison with Fetter Walecka

The Green's function G^{FW} in the Book of Fetter Walecka is related to our definition by

$$G = \frac{1}{\hbar} G^{FW}$$

see Eq. FW-7.1.

P.9 Greek Alphabet

A	α	alpha	N	ν	nu
B	β	beta	Ξ	ξ	ksi
Γ	γ	gamma	O	o,	omicron
Δ	δ	delta	Π	π, ϖ	pi
E	ϵ, ε	epsilon	P	ρ, ϱ	rho
Z	ζ	zeta	Σ	σ, ς	sigma
H	η	eta	T	τ	tau
Θ	θ, ϑ	theta	Υ	υ	upsilon
I	ι	iota	Φ	ϕ, φ	phi
K	κ	kappa	X	χ	chi
Λ	λ	lambda	Ψ	ϕ	phi
M	μ	mu	Ω	ω	omega

Appendix Q

About the PhiSX Series

Q.1 Philosophy of the PhiSX Series

In the ΦSX series, I tried to implement what I learned from the feedback given by the students which attended the courses and that relied on these books as background material.

The course should be **self-contained**. There should not be any statements "as shown easily..." if, this is not true. The reader should not need to rely on the author, but he should be able to convince himself, if what is said is true. I am trying to be as complete as possible in covering all material that is required. The basis is the mathematical knowledge. With few exceptions, the material is also developed in a sequence so that the material covered can be understood entirely from the knowledge covered earlier.

The derivations shall be **explicit**. The novice should be able to step through every single step of the derivation with reasonable effort. An advanced reader should be able to follow every step of the derivations even without paper and pencil.

All **units** are explicit. That is, formulas contain all fundamental variables, which can be inserted in any desirable unit system. Expressions are consistent with the SI system, even though I am quoting some final results in units, that are common in the field.

The equations that enter a specific step of a derivation are noted as **hyperlinks** ontop of the equation sign. The experience is that the novice does not immediately memorize all the material covered and that he is struggling with the math, so that he spends a lot of time finding the rationale behind a certain step. This time is saved by being explicit about it. The danger that the student gets dependent on these indications, is probably minor, as it requires some effort for the advanced reader to look up the assumptions, an effort he can save by memorizing the relevant material.

Important results and equations are highlighted by including them in **boxes**. This should facilitate the preparations for examinations.

Portraits of the key researchers and short biographical notes provide independent associations to the material. A student may not memorize a certain formula directly, but a portrait. From the portrait, he may associate the correct formula. The historical context provides furthermore an independent structure to organize the material.

The two first books are in german (That is the intended native language) in order to not add complications to the novice. After these first books, all material is in English. It is mandatory that the student masters this language. Most of the scientific literature is available only in English. English is currently the language of science, and science is absolutely dependent on international contacts.

I tried to include many graphs and figures. The student shall become used to use all his senses in particular the **visual sense**.

I have slightly modified the selection of the material commonly tought in most courses. Some topics, which I consider of mostly historical relevance I have removed. Others such as the Noether

theorem, I have added. Some, like chaos, stochastic processes, etc. I have not added yet.

Specific remarks for the "Advanced Solid-State Theory"

Editor: check these points for repetitions and eventually integrate into the general set of remarks if possible.

- Often, I provide **outlook** in the solutions to the exercises. This outlook does not aim at a comprehensive description, but rather to connect to prior knowledge or to provide a link to external sources for further reading.
- The exercises aim at treating **minimal models**. In the many-particle description of solids, model systems are often used to study and to describe certain physical effects.
- I took several measures to support students in keeping the **focus** in the learning process. These are (1) **boxes**, highlighting, the most relevant equations. (2) The **index** provides a list of relevant keywords. (3) The **introduction and summaries** of the chapters shall set the material into context.
- Overloaded terminology:
  - In the field the term **vacuum state** is used to denote the ground state such as the Fermi sea. While this use is correct in a world of electrons and holes, it still can be mistaken.
  - the non-interacting part of the Hamiltonian is often called the **kinetic energy**. This stems from the free-electron gas and is an illegal use.

Q.2 About the Author

Prof. Dr. rer. nat Peter E. Blöchl studied physics at Karlsruhe University of Technology in Germany. Subsequently he joined the Max Planck Institutes for Materials Research and for Solid-State Research in Stuttgart, where he developed of electronic-structure methods related to the LMTO method and performed first-principles investigations of interfaces. He received his doctoral degree in 1989 from the University of Stuttgart.

Following his graduation, he joined the renowned T.J. Watson Research Center in Yorktown Heights, NY in the US on a World-Trade Fellowship. In 1990 he accepted an offer from the IBM Zurich Research Laboratory in Ruschlikon, Switzerland, which had just received two Nobel prices in Physics (For the Scanning Tunneling Microscope in 1986 and for the High-Temperature Superconductivity in 1987). He spent the summer term 1995 as visiting professor at the Vienna University of Technology in Austria, from where he was later awarded the habilitation in 1997. In 2000, he left the IBM Research Laboratory after a 10-year period and accepted an offer to be professor for theoretical physics at Clausthal University of Technology in Germany. Since 2003, Prof. Blöchl is member of the Braunschweigische Wissenschaftliche Gesellschaft (Academy of Sciences).

The main thrust of Prof. Blöchl's research is related to ab-initio simulations, that is, parameter-free simulation of materials processes and molecular reactions based on quantum mechanics. He developed the Projector Augmented Wave (PAW) method, one of the most widely used electronic structure methods to date. This work has been cited over 88,000 times. [1] It is among the 100 most cited scientific papers of all times and disciplines[2] , and it is among the 10 most-cited papers out of more than 500,000 published in the 120-year history of Physical Review. [3] Next to the research related to simulation methodology, his research covers a wide area from biochemistry, solid state chemistry to solid state physics and materials science. Prof. Blöchl contributed to 8 Patents and

[1] scholar.google.com, retrieved Apr.23, 2025
[2] R. van Noorden, B. Maher and R. Nuzzo, Nature 514, 550 (2014)
[3] Oct. 15, 2014, search in the Physical Review Online Archive with criteria "a-z".

published about 100 research publications, among others in well-known Journals such as “Nature”. The work of Prof. Blöchl has been cited over 100,000 times, and he has an H-index of 52. [4]

[4] `scholar.google.com`, retrieved Apr.23, 2025

Bibliography

[1] Peter E. Blöchl. ΦSX: Introduction to Solid State Theory. Blöchl, 2017. URL https://phisx.org/.

[2] G. Stefanucci and R. van Leeuwen. Nonequilibrium Many-Body theory of Quantum systems, volume 1. Cambridge University Press, 2013.

[3] A.L. Fetter and J.D. Walecka. Quantum theory of many-particle systems. McGraw Hill, Inc, New York, 1971. URL https://archive.org/details/quantum-theory-of-many-particle-systems-by-alexander-l.-fetter-john-dirk-walecka-physics-z-lib.org.

[4] R.D. Mattuck. A guide to Feynmanns in the many-body problem. McGraw Hill, Inc, New York, 1967.

[5] Peter Fulde. Electron Correlations in Molecules and Solids. Springer, 1995.

[6] Leo P. Kadanoff and Gordon Baym. Quantum Statistical Mechanics. W. A. Benjamin, Inc., New York, 1962.

[7] A. A. Abrikosow, L. P. Gorkov, and I. E. Dzyaloshinski. Methods of Quantum Field Theory in Statistical Physics. Prentice-Hall, Englewood Cliffs, NJ, 1964.

[8] J.W. Negele and H. Orland. Quantum Many-Particle Physics. Westview Press, 1988.

[9] W.-D. Schöne, C. Timm, and W.-D. Schotte. Theoretische festkörperphysik, teil 1. http://kolxo3.tiera.ru/_Papers/TU%20Wien%20Scripta/Physik/Festkoerperphysik/Theoretische_Festkoerperphysik_I_001(de)(189s).pdf, 2001.

[10] A. D. McNaught and A. Wilkinson, editors. IUPAC Compendium of Chemical Terminology. Blackwell Scientific Publications, Oxford, 2 edition, 1997. ISBN 0-9678550-9-8. doi: 10.1351/goldbook. URL https://doi.org/10.1351/goldbook.

[11] E.R. Cohen, T. Cvitas, J.G. Frey, B. Holmström, K. Kuchitsu, R. Marquardt, I. Mills, F. Pavese, M. Quack, J. Stohner, H.L. Strauss, M. Takami, and A.J. Thor, editors. Quantities, Units and Sumbols in Physical Chemistry, IUPAC Green Book. IUPAC and RSC Publishing, Cambridge, 3 edition, 2008. URL http://media.iupac.org/publications/books/gbook/IUPAC-GB3-2ndPrinting-Online-22apr2011.pdf.

[12] Wolfgang Walter. Einführung in die Theorie der Distributionen. BI-Wiss.Verl., 1994.

[13] G.H. Wannier. The structure of electronic excitation levels in insulating crystals. Phys. Rev., 52:191, 1937.

[14] P. E. Blöchl. Projector augmented-wave method. Phys. Rev. B, 50:17953–17979, Dec 1994. doi: 10.1103/PhysRevB.50.17953. URL http://link.aps.org/doi/10.1103/PhysRevB.50.17953.

[15] Peter E. Blöchl. ΦSX: Theoretische Physik I, Klassische Mechanik. Blöchl, 2015. URL https://phisx.org/.

[16] Peter E. Blöchl. ΦSX: Theoretical Physics III, Quantum Theory. Blöchl, 2015. URL https://phisx.org/.

[17] E. Schrödinger. Discussion of probability relations between separated systems. Math. Proc. Cambr. Phil. Soc., 31:555, 1935.

[18] J. Hubbard. Electron correlations in narrow energy bands. Proc. R. Soc. Lond. A, 276:238, 1963. ISSN 0080-4630. doi: 10.1098/rspa.1963.0204.

[19] J. Kanamori. Electron correlation and ferromagnetism of transition metals. Prog. Theor. Phys., 30:275, 1963. doi: doi:10.1143/PTP.30.275. URL http://ptp.oxfordjournals.org/content/30/3/275.

[20] Martin C. Gutzwiller. Effect of correlation on the ferromagnetism of transition metals. Phys. Rev. Lett., 10(5):159, 1963. doi: 10.1103/PhysRevLett.10.159.

[21] Peter E. Blöchl. ΦSX: Quantum Mechanics of the Chemical Bond. Blöchl, 2015. URL https://phisx.org/.

[22] M.J. Rice and E.J. Mele. Elementary excitations of a linearly conjugated diatomic polymer. Phys. Rev. Lett., 49:1455, 1982.

[23] W.P. Su and J.R. Schrieffer. Soliton dynamics in polyacetylene. Proc. Natl. Acad. Sci. USA, 77:5626, 1980.

[24] Peter E. Blöchl. ΦSX: Theoretische Physik II, Elektrodynamik. Blöchl, 2015. URL https://phisx.org/.

[25] J.C. Slater. The theory of complex spectra. Phys. Rev., 34:1293, 1929.

[26] V. Fock. Näherungsmethode zur lösung des quantenmechanischen mehrkörperproblems. Zeitschr. Phys., 61:126, 1930.

[27] V. Fock. "selfconsistent field" mit austausch für natrium. Zeitschr. Phys., 62:795, 1930.

[28] P.W. Anderson. Concepts in Solids; Lectures on the Theory of Solids. W.A. Bejnamin, Inc, New York, 1963.

[29] Per-Olov Löwdin. Quantum theory of many-particle systems. i. physical interpretations by means of density matrices, natural spin-orbitals, and convergence problems in the method of configurational interaction. Phys. Rev., 97:1474, 1955. doi: 10.1103/PhysRev.97.1474. URL http://link.aps.org/doi/10.1103/PhysRev.97.1474.

[30] Ernest R. Davidson. Properties and uses of natural orbitals. Rev. Mod. Phys., 44:451, 1972.

[31] A.J. Coleman. Structure of fermion density matrices. Rev. Mod. Phys., 35:668, 1963. doi: 10.1103/RevModPhys.35.668. URL http://link.aps.org/doi/10.1103/RevModPhys.35.668.

[32] Mark S. Hybertsen and Steven G. Louie. Electron correlation in semiconductors and insulators: Band gaps and quasiparticle energies. Phys. Rev. B, 34:5390, 1986.

[33] Pierre Hohenberg and Walter Kohn. Inhomogeneous electron gas. Phys. Rev., 136:B864, 1964. doi: 10.1103/PhysRev.136.B864. URL http://link.aps.org/doi/10.1103/PhysRev.136.B864.

[34] Walter Kohn and Lu J. Sham. Self-consistent equations including exchange and correlation effects. Phys. Rev., 140:A1133, 1965. doi: 10.1103/PhysRev.140.A1133. URL http://link.aps.org/doi/10.1103/PhysRev.140.A1133.

[35] Kieron Burke, John P. Perdew, and Matthias Ernzerhof. Why semilocal functionals work: Accuracy of the on-top pair density and importance of system averaging. J. Chem. Phys., 109: 3760, 1998.

[36] A. Puzder, M.Y. Chou, and R.Q. Hood. Exchange and correlation in the si atom: A quantum monte carlo study. Phys. Rev. A, 64:22501, 2001.

[37] von Neumann. Mathematische Grundlagen der Qantenmechanik. Springer, Berlin, 1932.

[38] Peter E. Blöchl. ΦSX: Theoretical Physics IV, Statistical Physics. Blöchl, 2015. URL https://phisx.org/.

[39] J. von Neumann. Proof of the quasi-ergodic hypothesis. Proc. Natl. Acad. Sci. USA, 18:70, 1932.

[40] Calvin.C. Moore. Ergodic theorem, ergodic theory, and statistical mechanics. Proc. Natl. Acad. Sci. USA, 112:1907, 2015.

[41] C.E. Shannon. A mathematical theory of computation. Bell. Syst. Techn. J., 22:379, 1948.

[42] E.T. Jaynes. Information theory and statistical mechanics. Phys. Rev., 106:620, 1957.

[43] E.T. Jaynes. Information theory and statistical mechanics ii. Phys. Rev., 108:171, 1957.

[44] T.A. Kaplan and P.N. Argyres. Localized one-electron states in perfect crystals as a consequence of the thermal single-deteiniinant approximation. Phys. Rev. B, 1:2457, 1970.

[45] N. David Mermin. Stability of the thermal hartree-fock approximation. Ann. Phys., 21:99, 1963.

[46] Pinhao Gu and So Hirata. Thermal mean-field theories. J. Chem. Phys., 161:214108, 2024.

[47] So Hirata. Thermal quasi-particle theory. J. Chem, Phys., 161:214109, 2024.

[48] R. McWeeny. Some recent advances in density matrix theory. Rev. Mod. Phys., 32:334, 1960.

[49] Andrea Damascelli, Zahid Hussain, and Zhi-Xun Shen. Angle-resolved photoemission studies of the cuprate superconductors. Rev. Mod. Phys., 75:473–541, Apr 2003. doi: 10.1103/RevModPhys.75.473. URL https://link.aps.org/doi/10.1103/RevModPhys.75.473.

[50] David Bohm and David Pines. A collective description of electron interactions: Iii. coulomb interactions in a degenerate electron gas. Phys. Rev., 92:609, 1953.

[51] M. Gell-Mann and K.Brueckner. Correlation energy of an electron gas at high density. Phys. Rev., 106:364, 1957.

[52] Xinguo Ren, Patrick Rinke, Christian Joas, and Matthias Scheffler. Random-phase approximation and its applications in computational chemistry and materials science. J. Mater. Sci., 47: 7447, 2012. doi: https://doi.org/10.1007/s10853-012-6570-4.

[53] Fabio Carusoa and Feliciano Giustino. The gw plus cumulant method and plasmonic polarons: application to the homogeneous electron gas. Eur. Phys. J. B, 89:238, 2016. doi: https://doi.org/10.1140/epjb/e2016-70028-4.

[54] Johannes Lischner, G. K. Palsson, Derek Vigil-Fowler, S. Nemsak, J. Avila, M. C. Asensio, C. S. Fadley, and Steven G. Louie. Satellite band structure in silicon caused by electron-plasmon coupling. Phys. Rev. B, 91:295113, 2015. doi: 10.1103/PhysRevB.91.205113.

[55] D.M. Ceperley and B.J. Alder. Ground state of the electron gas by a stochastic method. Phys. Rev. Lett., 45:566, 1980.

[56] E.U. Condon. The theory of complex spectra. Phys. Rev., 36:1121, 1930.

[57] Attila Szabo and Neil S. Ostlund. Modern Quantum Chemistry. McGraw-Hill, New York, 1989. ISBN 9780070627390. URL http://store.doverpublications.com/0486691861.html.

[58] G.D. Mahan. Many Particle Physics. Kluwer academic Publishers, 2000.

[59] Stephen Blundell. Magnetism in Condensed Matter. Oxford University Press, 2001.

[60] Malte Schüler, Erik G. C. P. van Loon, Mikhail I. Katsnelson, and Tim O. Wehling. Thermodynamics of the metal-insulator transition in the extended hubbard model. Scipost Phys., 6: 067, 2019.

[61] Y. Zhang and J. Callaway. Extended hubbard model in two dimensions. Phys. Rev. B, 39: 9397, 1989.

[62] George Green. An essay on the application of mathematical analysis to the theories of electricity and magnetism. Arxiv, 0807:0088, 2008.

[63] F. J. Dyson. The radiation theories of tomonaga, schwinger, and feynman. Phys. Rev., 75: 486–502, Feb 1949. doi: 10.1103/PhysRev.75.486. URL https://link.aps.org/doi/10.1103/PhysRev.75.486.

[64] G.C. Wick. The evaluation of the collision matrix. Phys. Rev., 80:268, 1950.

[65] Mariana M. Odashima, Beatriz G. Prado, and E. Vernek. Pedagogical introduction to equilibrium green's functions: condensed-matter examples with numerical implementations. Rev. Bras. Ensino de Fís, 39:e1303, 2017. doi: 10.1590/1806-9126-RBEF-2016-0087. URL https://doi.org/10.1590/1806-9126-RBEF-2016-0087.

[66] E.N. Economou. Green's Functions in Quantum Mechanics. Springer, 1979.

[67] P.W. Anderson. Localized magnetic states in metals. Phys. Rev., 124:41, 1961.

[68] U. Fano. Effects of configuration interaction on intensities and phase shifts. Phys. Rev., 124: 1866–1878, Dec 1961. doi: 10.1103/PhysRev.124.1866. URL https://link.aps.org/doi/10.1103/PhysRev.124.1866.

[69] I.N. Bronstein and K.A. Semendjajew. Taschenbuch der Mathematik. BSB B.G. eubner Verlagsgesellschaft, Leipzig, 1983.

[70] N.G. van Kampen. Contribution to the quantum theory of light scattering. Dan. Mat. Fys. Medd., 26:3, 1951. URL https://www.lorentz.leidenuniv.nl/IL-publications/dissertations/sources/VanKampen_1952.pdf.

[71] Robert van Leeuwen and Gianluca Stefanucci. Equilibrium and nonequilibrium many-body perturbation theory: a unified framework based on the martin-schwinger hierarchy. J. Phys.: Conf. Series, 427:012001, 2013. doi: 10.1088/1742-6596/427/1/012001.

[72] Mathias Wagner. Expansions of non-equilibrium green's functions. Phys. Rev. B, 44: 6104, 1991. doi: 10.1103/PhysRevB.44.6104. URL https://link.aps.org/doi/10.1103/PhysRevB.44.6104.

[73] P.C. Martin and J. Schwinger. Theory of many-particle systems. i. Phys. Rev., 115(6):1342–1373, Sep 1959. doi: 10.1103/PhysRev.115.1342.

[74] V. M. Galitskii and A. B. Migdal. Application of quantum field theory methods to the many body problem. In Sov. Phys. JETP Galitskii and Migdal [78], page 96.

[75] Walter Tarantino, Pina Romaniello, J. A. Berger, and Lucia Reining. Self-consistent dyson equation and self-energy functionals: An analysis and illustration on the example of the hubbard atom. Phys. Rev. B, 96:45124, 2017.

[76] R. Kubo. Statistical-mechanical theory of irreversible processes i. general theory of simple applications to magnetice and conduction problems. J. Phys. Soc. Jap., 12:570, 1957.

[77] L. Hedin, B.I.Lundquist, and S. Lundquist. Beyond the one-electron approximation: Density of states for interacxting electrons. J. Res. Nat'l Bureau of Standards, 74a:417, 1970.

[78] V. M. Galitskii and A. B. Migdal. Application of quantum field theory methods to the many body problem. Sov. Phys. JETP, 7:96, 1958.

[79] V.M. Galitskii. The energy spectrum of a non-ideal fermi gas. Sov. Phys. JETP, 7:104, 1958.

[80] Ferdi Aryasetiawan. The GW approximation and vertex corrections, volume 1 of Advances in Condensed Matter Science, chapter 1, pages 1 – 96. Gordon and Breach Science Publishers, 2000. Booktitle "Strong Coulomb correlations in electronic structure calculations" Ed. V.I. Anisimov.

[81] J.D. Ortiz. Dyson-orbital concepts for description of electrons in molecules. J. Chem. Phys., 153:070902, 2020.

[82] G. Kotliar, S. Y. Savrasov, K. Haule, V. S. Oudovenko, O. Parcollet, and C. A. Marianetti. Electronic structure calculations with dynamical mean-field theory. Rev. Mod. Phys., 78:865–951, Aug 2006. doi: 10.1103/RevModPhys.78.865. URL http://link.aps.org/doi/10.1103/RevModPhys.78.865.

[83] Bengt I. Lundqvist). Single-particle spectrum of the degenerate electron gas i. the structure of the spectral weight function. Phys. Kondens. Materie, 6:193, 1967. doi: 10.1007/BF02422716.

[84] B.I. Lundqvist. Single-particle spectrum of the degenerate electron gas. Phys. Kondens. Materie, 7:117, 1968.

[85] F. Aryasetiawan, L. Hedin, and K. Karlsson. Multiple plasmon satellites in na and al spectral functions from ab initio cumulant expansion. Phys. Rev. Lett., 77:2268, 1996.

[86] C. Metz, Th. Tschentscher, , P. Suortti, A. S. Kheifets, D. R. Lun, T. Sattler, J. R. Schneider, and F. Bell. Three-dimensional electron momentum density of aluminum by (γ, $e\gamma$) spectroscopy. Phys. Rev. B, 59:10512, 1999.

[87] T. Matsubara. A new approach to quantum-statistical physics. Prog. Theor. Phys., 14:351, 1955.

[88] M. Gaudin. Une démonstration simplifiié du théoréme de wick en mécanique statistique. Nucl. Phys., 15:89, 1960.

[89] Abdus Salam. Some speculations on the new resonances. Rev. Mod. Phys., 33:426, 1961.

[90] J. Goldstone. Derivation of the brueckner many-body theory. Proc. Roy. Soc. (London), A239: 267, 1957. doi: doi:10.1098/rspa.1957.0037. URL http://rspa.royalsocietypublishing.org/content/239/1217/267.

[91] Claude Bloch and Cyrano de Dominicis. Un développement du potentiel de gibbs d'un systéme quantique composié d'un grand nombre de particules. Nucl. Phys., 7:459, 1958.

[92] N. E. Bickers and D.J. Scalapino. Conserving approximations for strongly fluctuating electron systems. i. formalism and calculational approach. Ann. Phys., 193:206, 1989. doi: 10.1016/0003-4916(89)90359-X.

[93] Gordon Baym and Leo P. Kadanoff. Conservation laws and correlation functions. Phys. Rev., 124:287, 1961. doi: 10.1103/PhysRev.124.287. URL http://link.aps.org/doi/10.1103/PhysRev.124.287.

[94] G. Baym. Self-consistent approximations in many-body systems. Phys. Rev., 127:1391, 1962. doi: 10.1103/PhysRev.127.1391. URL http://link.aps.org/doi/10.1103/PhysRev.127.1391.

[95] J. M. Luttinger and J. C. Ward. Ground-state energy of a many-fermion system ii. Phys. Rev., 118:1417, 1960. doi: 10.1103/PhysRev.118.1417. URL http://link.aps.org/doi/10.1103/PhysRev.118.1417.

[96] Michael Potthoff. Self-energy-functional approach to systems of correlated electrons. Eur. Phys. J. B, 32:429, 2003. doi: 10.1140/epjb/e2003-00121-8. URL http://link.springer.com/article/10.1140/epjb/e2003-00121-8.

[97] Felix Hofmann, Martin Eckstein, Enrico Arrigoni, and Michael Potthoff. Nonequilibrium self-energy functional theory. Phys. Rev. B, 88:165124, 2013. doi: 10.1103/PhysRevB.88.165124.

[98] Lin Lina and Michael Lindseya. Variational structure of luttinger–ward formalism and bold diagrammatic expansion for euclidean lattice field theory. Proc. Natl. Acad. Sci. USA, 115: 2282, 2018.

[99] M. Potthoff. Non-perturbative construction of the luttinger-ward functional. Condens. Matter Phys., 9:557, 2006. doi: 10.5488/CMP.9.3.557. URL http://www.icmp.lviv.ua/journal/zbirnyk.47/011/abstract.html.

[100] R. Chitra and Gabriel Kotliar. Effective-action approach to strongly correlated fermion systems. Phys. Rev. B, 63:115110, Mar 2001. doi: 10.1103/PhysRevB.63.115110. URL http://link.aps.org/doi/10.1103/PhysRevB.63.115110.

[101] W. Kohn. Nobel Lectures, Chemistry, 1996-2000, chapter Electronic Structure of Matter - Wave functions and Density Functionals, page 213. World Scientific, Singapore, 2003.

[102] Peter E. Blöchl, Thomas Pruschke, and Michael Potthoff. Density-matrix functionals from green's functions. Phys. Rev. B, 88:205139, Nov 2013. doi: 10.1103/PhysRevB.88.205139. URL http://link.aps.org/doi/10.1103/PhysRevB.88.205139.

[103] S. Doniach and E.H. Sondheimer. Green's Functions for Solid State Physicists. The Benjamin/Cummings Publishing Company, INC, Reading, Massachusetts. Reprinted 1998 by Imperial college press, 1974.

[104] P. Nozieres and D. Pines. Electron interactions in solids: General theory. Phys. Rev., 109:741, 1958.

[105] Lars Hedin. New method for calculating the one-particle green's function with application to the electron-gas problem. Phys. Rev., 139:A796–A823, Aug 1965. doi: 10.1103/PhysRev.139.A796. URL http://link.aps.org/doi/10.1103/PhysRev.139.A796.

[106] Robert van Leeuwen, Nils Erik Dahlen, and Adrian Stan. Total energies from variational functionals of the green function and the renormalized four-point vertex. Phys. Rev. B, 74: 195105, 2006.

[107] C.-O. Almbladh, U. von Barth, and R. van Leeuwen. variational total energies from ϕ- and ψ-derivable theories. Int. J. Mod. Phys. B, 13:535, 1999. doi: 10.1142/S0217979299000436.

[108] Mikael Hindgren. Model Vertices Beyond the GW Approximation. Doctoral thesis (compilation), Mathematical Physics, 1997. Defence details Date: 1997-06-07 Time: 10:15 Place: Lecture Hall B, Department of Physics, Lund University, Lund, Sweden External reviewer(s) Name: Rajagopal, A. K. Title: Prof Affiliation: Naval Research Lab., Washington D.C., USA —.

[109] Nils Erik Dahlen and Ulf vonBarth. Variational energy functionals tested on atoms. Phys. Rev. B, 69:195102, May 2004. doi: 10.1103/PhysRevB.69.195102. URL http://link.aps.org/doi/10.1103/PhysRevB.69.195102.

[110] J. Hubbard. The description of collective motions in terms of many-body perturbation theory. Proc. Roy. Soc. A, 240:539, 1957.

[111] L.D. Landau. The theory of a fermi liquid. Sov. Phys. JETP, 3:920, 1957.

[112] L.D. Landau. Oscillations in a fermi liquid. Sov. Phys. JETP, 5:101, 1957.

[113] landau (not done). On the theory of the fermi liquid. Sov. Phys. JETP, 35:70, 1959.

[114] A.A. Abrikosov and I.M. Khalatnikov. The theory of a fermi liquid (the properties of liquid 3he at low temperatures). Rep. Prog. Phys., 22:329, 1959.

[115] Yasutami Takada. Low-energy peak in the one-particle spectral function of the electron gaas at metallic densities. Arxiv, 2407:09746, 2024. URL https://doi.org/10.48550/arXiv.2407.09746.

[116] A.B. Migdal. The momentum distribution of interacting fermi particles. Sov. Phys. JETP, 5: 333, 1957.

[117] T. Giamarchi. Interactions in quantum fluids. Arxiv, 1007:1030, 2010.

[118] V.M. Galitskii. The energy spectrum of a non-ideal fermi gas. Sov. Phys. JETP, 34:104, 1958.

[119] G.A. Sawatzky. Testing fermi-liquid models. Nature, 342:480, 1989.

[120] J.M. Luttinger. Analytic properties of single-particle propagators for many-fermion systems. Phys. Rev., 121:942, 1961. URL https://doi.org/10.1103/PhysRev.121.942.

[121] Hal Tasaki. The hubbard model - an introduction and selected rigorous results. J. Phys.: Condens. Matter, 10:4353, 1998.

[122] L. M. Falicov and J.C. Kimball. Simple model for semiconductor-metal smb and transition-metal oxides. Phys. Rev. Lett., 22:997, 1969.

[123] A.A. Abrikosov. On the anomalous temperature dependence of the resistivity of non-magnetic metals with a weak concentration of magnetic impurities. Sov. Phys. JETP, 21:660, 1965.

[124] H. Suhl. Dispersion theory of the kondo effect. Phys. Rev., 138:A515–A523, Apr 1965. doi: 10.1103/PhysRev.138.A515. URL https://link.aps.org/doi/10.1103/PhysRev.138.A515.

[125] E.H. Lieb and F.Y. Wu. Absence of mott transition in an exact solution of the short-range, one-band model in one dimension. Phys. Rev. Lett, 20:1445, 1968.

[126] J. P. F. LeBlanc, Andrey E. Antipov, Federico Becca, Ireneusz W. Bulik, Garnet Kin-Lic Chan, Chia-Min Chung, Youjin Deng, Michel Ferrero, Thomas M. Henderson, Carlos A. Jiménez-Hoyos, E. Kozik, Xuan-Wen Liu, Andrew J. Millis, N. V. Prokof'ev, Mingpu Qin, Gustavo E. Scuseria, Hao Shi, B. V. Svistunov, Luca F. Tocchio, I. S. Tupitsyn, Steven R. White, Shiwei Zhang, Bo-Xiao Zheng, Zhenyue Zhu, and Emanuel Gull. Solutions of the two-dimensional hubbard model: Benchmarks and results from a wide range of numerical algorithms. Phys. Rev. X, 5:041041, Dec 2015. doi: 10.1103/PhysRevX.5.041041. URL https://link.aps.org/doi/10.1103/PhysRevX.5.041041.

[127] Nevill Mott. Review lecture: Metal-insulator transitions. Proc. R. Soc. Lond. A, 382:1, 1982.

[128] Mario Motta, David M. Ceperley, Garnet Kin-Lic Chan, John A. Gomez, Emanuel Gull, Sheng Guo, Carlos A. Jiménez-Hoyos, Tran Nguyen Lan, Jia Li, Fengjie Ma, Andrew J. Millis, Nikolay V. Prokof'ev, Ushnish Ray, Gustavo E. Scuseria, Sandro Sorella, Edwin M. Stoudenmire, Qiming Sun, Igor S. Tupitsyn, Steven R. White, Dominika Zgid, and Shiwei Zhang. Towards the solution of the many-electron problem in real materials: Equation of state of the hydrogen chain with state-of-the-art many-body methods. Phys. Rev. X, 7:031059, Sep 2017. doi: 10.1103/PhysRevX.7.031059. URL https://link.aps.org/doi/10.1103/PhysRevX.7.031059.

[129] Mario Motta, Claudio Genovese, Fengjie Ma, Zhi-Hao Cui, Randy Sawaya, Garnet Kin-Lic Chan, Natalia Chepiga, Phillip Helms, Carlos Jiménez-Hoyos, Andrew J. Millis, Ushnish Ray, Enrico Ronca, Hao Shi, Sandro Sorella, Edwin M. Stoudenmire, Steven R. White, and Shiwei Zhang. Ground-state properties of the hydrogen chain: Dimerization, insulator-to-metal transition, and magnetic phases. Phys. Rev. X, 10:031058, Sep 2020. doi: 10.1103/PhysRevX.10.031058. URL https://link.aps.org/doi/10.1103/PhysRevX.10.031058.

[130] M. Vanzini, L. Reining, and M. Gatti. Spectroscopy of the hubbard dimer: the spectral potential. Eur. Phys. J. B, 91:192, 2018.

[131] Stefano Di Sabatino. Reduced density-matrix functional theory: Correlation and spectroscopy. PhD thesis, Université Paul Sabatier, 2015. URL https://tel.archives-ouvertes.fr/tel-01230626v2.

[132] F. Gebhard. The Mott Metal-Insulator Transition - Models and Methods. Springer, Heidelberg, 1997. ISBN 3-540-61481-8.

[133] P.W Anderson. New approach to the theory of superexchange interactions. Phys. Rev., 115: 2, 1959.

[134] Assa Auerbach. Interacting electrons and Quantum Magnetism. Graduate Texts in Contemporary Physics. Springer, New York, 1994. doi: doi:10.1007/978-1-4612-0869-3.

[135] H. Bethe. Zur theorie der metalle; i eigenwerte und eigenfunktionen der linearen atomkette. Z. Phys., 71:205, 1931.

[136] L.D. Fadeev and L.A. Takhtajan. What is the spin of a spin wave? Phys. Lett., 85a:375, 1981.

[137] Alois Loidl. Dispersion von bethe-strings. Physik Journal, 19:20, 2020.

[138] Michael O. Marder. Condensed Matter Physics. John Wiley and Sons, 2000. ISBN 0-471-17779-2.

[139] H.P. van de Braak and W.J. Caspers. Ground state properties of finite antiferromagnetic chains. Phys. Stat. Sol., 35:933, 1969.

[140] D. Meyer, T. Wegner, M. Potthoff, and W. Nolting. The asymmetric single-impurity anderson model- the modified perturbation theory. Physica B, 270:225, 1999.

[141] Piers Coleman. Local moments and the kondo lattice. Bolder Summer School 2008 boulderschool.yale.edu, 2008.

[142] J.R. Schrieffer and P.A. Wolff. Relation between the anderson and kondo hamiltonians. Phys. Rev., 149:491, 1966.

[143] Peter Fulde, Joachim Keller, and Gertrud Zwicknagl. Theory of heavy fermion systems. Solid State Phys., 41:1, 1988. doi: 10.1016/S0081-1947(08)60378-1. URL https://doi.org/10.1016/S0081-1947(08)60378-1.

[144] Erich Runge and Gertrud Zwicknagel. Electronic structure calculations and strong correlations: A model study. Ann. Phys., 5:333, 1996. doi: 10.1002/andp.2065080404. URL https://doi.org/10.1002/andp.2065080404.

[145] T. Holstein. Studies of polaron motion. part i. the molecular crystal model. Ann. Phys., 8: 325, 1959.

[146] T. Holstein. Studies of polaron motion: Part ii. the "small" polaron. Ann. Phys., 8:343, 1959.

[147] I. G. Lang and Y. A. Firsov. Kinetic theory of semiconductors with low mobility. Soviet Physics JETP., 16:1301, 1963.

[148] O. Gunnarsson, V. Meden, and K. Schönhammer. Corrections to migdal's theorem for spectral functions: A cumulant treatment of the time-dependent green's function. Phys. Rev. B, 50: 10462, 1994.

[149] David C. Langreth. Singularities in the x-ray spectra of metals. Phys. Rev. B, 1:471, 1970.

[150] Yu A. Firsov and E.K. Kudinov. The polaron state of a crystal. Physics of the Solid State, 43: 447, 2001.

[151] W. P. Su, J. R. Schrieffer, and A. J. Heeger. Solitons in polyacetylene. Phys. Rev. Lett., 42: 1698–1701, Jun 1979. doi: 10.1103/PhysRevLett.42.1698. URL https://link.aps.org/doi/10.1103/PhysRevLett.42.1698.

[152] W. P. Su, J. R. Schrieffer, and A. J. Heeger. Soliton excitations in polyacetylene. Phys. Rev. B, 22:2099–2111, Aug 1980. doi: 10.1103/PhysRevB.22.2099. URL https://link.aps.org/doi/10.1103/PhysRevB.22.2099.

[153] A. J. Heeger, S. Kivelson, J. R. Schrieffer, and W.-P. Su. Solitons in conducting polymers. Rev. Mod. Phys., 60:781, 1988.

[154] E.T. Jaynes and F.W. Cummings. Comparison of quantum and semiclassical radiation theories with application to the beam maser. Proc. IEEE, 51:89, 1963.

[155] V. Weisskopf and E. Wigner. Berechnung der natürlichen linienbreite auf grund der diracschen lichttheorie. Z. Phys., 63:54, 1930.

[156] R. Merlin. Rabi oscillations, floquet states, fermi's golden rule, and all that: Insights from an exactly solvable two-level model. Am. J. Phys., 89:26, 2020. doi: 10.1119/10.0001897. URL https://doi.org/10.1119/10.0001897.

[157] M.G. Burt. An enlightening derivation of so-called fermi's golden rule in quantum mechanics with some new perspectives including quasi adiabatic following. Arxiv, 2006.13180: arxiv2006.13180, 2020.

[158] J. Campbell. Proc. Lond. Math. Soc., 1897.

[159] J. Campbell. Proc. Lond. Math. Soc., 1898.

[160] H. Baker. Proc.Lond. Math. Soc, 34, 1902. Baker-Campbell-Hausdorff theorem.

[161] H. Baker. Proc.Lond. Math. Soc, 35, 1903. Baker-Campbell-Hausdorff theorem.

[162] H. Baker. Proc.Lond. Math. Soc (Ser.2), 3:24, 1905. Baker-Campbell-Hausdorff theorem.

[163] F. Hausdorff. Die symbolische exponentialformel in der gruppentheorie. Ber. Verh. Sächs. Akad. Wiss. Leipzig, 58:19, 1906.

[164] W. Magnus. On the exponential solution of differential equations for a linear operator. Comm. Pure Appl. Math., 7:649, 1954.

[165] Sanwu Wang. Generalization of the thomas-reiche-kuhn and the bethe sum rules. Phys. Rev. A, 60:262–266, Jul 1999. doi: 10.1103/PhysRevA.60.262. URL http://link.aps.org/doi/10.1103/PhysRevA.60.262.

[166] Antoine Georges. The beauty of impurities: Two revivals of friedel's virtual bound-state concept. C.R. Physique, 17:430, 2016. doi: 10.1016/j.crhy.2015.12.005. URL http://dx.doi.org/10.1016/j.crhy.2015.12.005.

[167] Klaas J.H. Giesbertz, Anna-Maija Uimonen, and Robert van Leeuwen. Approximate energy functionals for one-body reduced density matrix functional theory from many-body perturbation theory. Eur. Phys. J. B, 91:282, 2018.

[168] Ebad Kamil, Robert Schade, Thomas Pruschke, and Peter E. Blöchl. Reduced density-matrix functionals applied to the hubbard dimer. Phys. Rev. B, 93:085141, Feb 2016. doi: 10.1103/PhysRevB.93.085141. URL http://link.aps.org/doi/10.1103/PhysRevB.93.085141.

[169] Peter M. W. Gill and John A. Pople. Exact exchange functional for the hydrogen atom. Phys. Rev. A, 47:2383–2385, Mar 1993. doi: 10.1103/PhysRevA.47.2383. URL https://link.aps.org/doi/10.1103/PhysRevA.47.2383.

[170] J.P. Perdew and A. Zunger. Self interaction correction to density-functional approximations for many-electron systems. Phys. Rev. B, 23:5048, 1981.

[171] C.F. v. Weizsäcker. Zur theorie der kernmassen. Z. Phys., 96:431, 1935.

[172] A. Messiah. Quantum Mechanics. Dover, 2000.

[173] Fabien Tran, Peter Blaha, Karlheinz Schwarz, and Pavel Novák. Hybrid exchange-correlation energy functionals for strongly correlated electrons: Applications to transition-metal monoxides. Phys. Rev. B, 74:155108, 2006.

[174] Vladimir I. Anisimov, Jan Zaanen, and Ole K. Andersen. Band theory and mott insulators: Hubbard U instead of stoner I. Phys. Rev. B, 44:943–954, Jul 1991. doi: 10.1103/PhysRevB.44.943. URL http://link.aps.org/doi/10.1103/PhysRevB.44.943.

[175] J.F. Janak. Proof that $\partial e/\partial n_i = \epsilon_i$ in density functional theory. Phys. Rev. B, 18:7165, 1978.

[176] T. Koopmans. über die zuordnung von wellenfunktionen und eigenwerten zu den einzelnen elektronen eines atoms. Physica, 1:104, 1934. doi: 10.1016/S0031-8914(34)90011-2.

[177] J. C. Phillips. Generalized koopmans' theorem. Phys. Rev., 123:420–424, Jul 1961. doi: 10.1103/PhysRev.123.420. URL https://link.aps.org/doi/10.1103/PhysRev.123.420.

[178] Roberto Car and Michele Parrinello. Unified approach for molecular dynamics and density-functional theory. Phys. Rev. Lett, 55:2471, 1985. doi: 10.1103/PhysRevLett.55.2471. URL http://link.aps.org/doi/10.1103/PhysRevLett.55.2471.

[179] L. Verlet. Computer "experiments" on classical fluids i. thermodynamical properties of lennard-jones molecules. Phys. Rev., 159:98, 1967.

[180] H. Kümmel, K.H. Lührmann, and J.G. Zabolitzky. Many-fermion theory in exp(s)- (or coupled cluster) form. Phys. Rep., 36C:1, 1978.

[181] Oktay Sinanoglu. Many-electron theory of atoms and molecules. Proc. Natl. Acad. Sci. USA, 47:1217, 1961. doi: 10.1073/pnas.47.8.1217. URL https://doi.org/10.1073/pnas.47.8.1217.

[182] Pierre Hohenberg and Walter Kohn. Inhomogeneous electron gas. Phys. Rev., 136:B864, 1964. doi: 10.1103/PhysRev.136.B864. URL http://link.aps.org/doi/10.1103/PhysRev.136.B864.

[183] Mel Levy. Universal variational functionals of electron densities, first order density matrixes and natural spin-orbitals and solution of the v-representability problem. Proc. Nat'l Acad. Sci. USA, 76:6062, 1979. URL http://www.pnas.org/content/76/12/6062.abstract.

[184] M. Levy. Electron densities in search of hamiltonians. Phys. Rev. A, 26:1200, 1982.

[185] Elliott H. Lieb. Density functionals for coulomb systems. Int. J. Quantum Chem., 24(3): 243–277, 1983. ISSN 1097-461X. doi: 10.1002/qua.560240302. URL http://dx.doi.org/10.1002/qua.560240302.

[186] J. Harris and R.O. Jones. The surface energy of a bounded electron gas. J. Phys. F: Met. Phys., 4:1170, 1974.

[187] David C. Langreth and John P. Perdew. The exchange-correlation energy of a metallic surface. Sol. St. Commun., 17:1425, 1975.

[188] Olle Gunnarsson and Bengt I. Lundquist. Exchange and correlation in atoms, molecules, and solids by the spin-density-functional formalism. Phys. Rev. B, 13:4274, 1976.

[189] K. Schwarz. Optimization of the statistical exchange parameter α for the free atoms h through nb. Phys. Rev. B, 5:2466, 1971.

[190] I. Lindgren and K. Schwarz. Analysis of the electronic exchange in atoms. Phys. Rev. A, 5: 542, 1972.

[191] Robert O. Jones and Olle Gunnarsson. The density functional formalism, its applications and prospects. Rev. Mod. Phys., 61:689, 1989.

[192] A. D. Becke. Density-functional exchange energy with correct asymptotic behavior. Phys. Rev. A, 38:3098, 1988.

[193] John P. Perdew, Robert G. Parr, Mel Levy, and Jose L. Balduz. Density-functional theory for fractional particle number: Derivative discontinuities of the energy. Phys. Rev. Lett., 49: 1691–1694, Dec 1982. doi: http://dx.doi.org/10.1103/PhysRevLett.49.1691. URL http://link.aps.org/doi/10.1103/PhysRevLett.49.1691.

[194] Mel Levy, John P. Perdew, and Viraht Sahni. Exact differential equation for the density and ionization energy of a many-particle system. Phys. Rev. A, 30:2745–2748, Nov 1984. doi: 10.1103/PhysRevA.30.2745. URL https://link.aps.org/doi/10.1103/PhysRevA.30.2745.

[195] Leonard Kleinman. Reply to "comment on 'significance of the highest occupied kohn-sham eigenvalue' ". Phys. Rev. B, 56:16029–16030, Dec 1997. doi: 10.1103/PhysRevB.56.16029. URL https://link.aps.org/doi/10.1103/PhysRevB.56.16029.

[196] A. Klamt, V. Jonas, T. Bürger, and J.W. Lohrenz. Refinement and parameterization of cosmo-rs. J. Phys. Chem. A, 102:5074, 1998.

[197] M. Dion, H. Rydberg, E. Schröder, D. C. Langreth, and B. I. Lundqvist. Van der waals density functional for general geometries. Phys. Rev. Lett, 92:246401, 2004.

[198] T. Ziegler, A. Rauk, and E.J. Baerends. On the calculation of multiplet energies by the hartree-fock-slater method. Theoret. Chim. Acta. (Berl.), 43:261, 1977.

[199] W. Speier, R. Zeller, and J. C. Fuggle. Studies of total density of states of metals up to 70 ev above E_F. Phys. Rev. B, 32:3597–3603, Sep 1985. doi: 10.1103/PhysRevB.32.3597. URL https://link.aps.org/doi/10.1103/PhysRevB.32.3597.

[200] Christian Møller and M.S. Plesset. Note on an approximation treatment for many-electron systems. Phys. Rev., 46:618, 1934. doi: 10.1103/PhysRev.46.618.

Index

W-skeleton diagram, 414
1PI, 334, 344
2PI, 345, 393

occupation-number fluctuations
    correlated, 93

Abrikosov-Suhl resonance, 436, 461, 462, 515
adiabaticity parameter, 468
adiabatic connection, 671
Anderson model, 225
Anderson impurity, 201
Anderson model, 201, 301, 460
annihilation operator, 81, 134
annihilator, 134
antiadiabatic limit, 468
antisymmetric tensor, 20
APA, 282, 766
atomic level, 26
atomic orbitals, 10
average-phase approximation, 766
average-phase approximation, 282
averaged-phase approximation, 610
averaged-phase approximation, 78

Baker-Haussdorf theorem, 508
band gap, 443
bath, 187, 201
bath Green's function, 188
Bethe sum rule, 512
bi-orthogonality condition, 11
Bloch states, 12
Bloch theorem, 12
Bloch vector, 12
Bohr magneton, 7
Boltzmann entropy, 399, 424
Boltzmann constant, 65
Boltzmann entropy, 70
bond
    ionic, 29
Born approximation
    second-order, 405
boson, 20
boundary conditions
    periodic, 41
branch cut, 290
bubble diagram, 345

Car-Parrinello method, 636
causality, 198
characteristic polynomial, 28
charge background
    neutralizing, 422
charge fluctuations, 84
charge order, 159
charge sum rule, 32, 62, 90, 121
closed diagram, 344
coherence length, 623
colossal magnetoresistance, 444
commutator, 774
conserving approximation, 389
contour derivative, 242
contour integral, 242
contravariant, 12
correlated occupation-number fluctuations, 68, 91, 761
correlation, 61
correspondence principle, 138
Coulomb gauge, 483
Coulomb integral, 555
coupled-cluster theory, 658
covariant, 12
creation operator, 81, 132
crystal momentum, 12

deformation, 362
    mere, 360
degenerate limit, 29
delta function, 774
density
    of momentum, 302
    spin, 45, 562
    total, 45, 562
    two-particle, 61
density-functional theory, 47, 62, 425, 563
    orbital free, 563
density-matrix functional, 60, 71
density functional
    universal, 663, 666
DENSITY MATRIX

ONE-PARTICLE REDUCED, 142
density matrix
one-particle reduced, 52, 665
one-particle reduced, from Green's function, 271
thermal von-Neumann, 66
von Neumann, 64
density of states, 87, 178, 179
jellium model, 42
derivative
Wirtinger, 18
determinant, 774
DFT, 62
diagram, 327, 347
bubble, 345
closed, 344
eyeglass, 349
Green's function, 343
interaction diagram, 343
labeled, 359, 361
linked, 344
open, 332
polarization, 344
ring, 575
self-energy, 344
skeleton, 345
unlabeled, 361
vertex, 344
dimensional bottleneck, 24
Dirac's delta function, 774
Dirac equation, 4
distribution, 8
dot product, 4
double occupancy, 611
double-bubble diagram, 346
double-counting correction, 400
double occupancy, 94, 612
down-folding, 188, 542
dyadic product, 4, 774
Dyson equation, 196, 270
Dyson orbitals, 283

electric constant, 56
electron, 79
electron-addition energies, 84
electron-hole pair, 85
electron-phonon coupling, 470
electron-removal energies, 83
electron affinity, 103, 443
electron gas
degenerate, 41
dilute, 41
emission
spontaneous, 476
energy
entanglement, 610
exchange and correlation, 398
Lehmann, 280
energy sum rule, 32
ensemble, 64, 664
canonical, 664
grand-canonical, 66
thermal, 66
entanglement, 94, 157
entanglement energy, 93, 94, 610, 761
entropy
Boltzmann, 70
Shannon, 65
von Neumann, 65
equilibrium
thermal, 65
ergodic theorem, 65
exchange, 57, 60
exchange-correlation functional, 667
exchange-correlation hole, 670
exchange and correlation
potential energy, 62
potential energy of, 671
self energy, 397
exchange and correlation energy, 398
exchange and correlation functional, 399
exchange energy, 47, 59
exchange hole, 60
exchange interaction, 678
exchange parameter, 158, 450
exchange potential, 59
exciton binding energy, 86
extended Hamiltonian, 76
eyeglass diagram, 346, 349, 353

f-sum rule, 511
Fano model, 225
Fano-Anderson model, 225
Fano model, 202
Fermi distribution, 278
Fermi sea, 79
Fermi's golden rule, 81
Fermi-liquid theory, 575
Fermi-liquid theory, 423
Fermi-momentum, 43
Fermi-surface nesting, 471
fermion, 20
Fermi distribution, 54, 727
Fermi gas
degenerate, 422
Fermi loop, 351, 353
Fermi momentum, 566
ferromagnetism, 125

Feynman diagram, 327
finite linear chain, 211
Floquet theory, 199
fluctuations
    occupation-number, correlated, 68, 91, 761
Fock operator, 617
Fock space, 22, 662
free-electron gas, 41
    Contour Green's function, 257
friction parameter, 636
full-width-at-half-maximum, 183, 208
fully antisymmetric tensor, 774
FWHM, 183, 208

g-factor, 7
gauge potentials, 482
generalized gradient approximations, 681
GGA, 681
grand-canonical ensemble, 66
grand potential, 336, 664
Green's function
    bare, 331, 334
    bath, 188
    dressed, 334
    full, 334
    interacting, 334
    Kohn-Sham, 400
    non-interacting, 334
Green-Kubo formula, 277
GW approximation, 673

Hadamard's lemma, 509
Hamiltonian
    extended, 76
Hartree, 100
Hartree-Fock approximation
    thermal, 761
Hartree-Fock approximation, 91
    thermal, 69, 610, 656
Hartree-Fock method, 47
Hartree atomic units, 100
Hartree energy, 47, 58
Hartree potential, 59
heat bath, 66
Heaviside function, 774
heavy fermion, 460
Heisenberg model, 148, 158, 450
Heisenberg operator, 246
Hellmann-Feyman theorem, 672
Helmholtz potential, 631, 664
hole, 79
hole
    exchange, 60
hole density, 62
hole function, 670
Holstein model, 466
homogeneous electron gas
    contour Green's function, 257
hopping parameter, 26
Hubbard atom, 436
Hubbard band, 104
    lower, 447
    upper, 448
Hubbard model, 25
    extended, 158
Hund's rule, 41, 125
hybridization, 29, 94
hybrid functionals, 674

idempotent, 54
identical particles, 20
imaginary time, 244
incoming index, 317
interaction line, 327, 343
interaction picture, 310
inverse photoemission, 82
ionic bond, 29
ionization potential, 103, 443
irreducible
    one-particle, 334, 344
    two-particle, 345
Ising model, 454

Janak's theorem, 424
Jaynes-Cummings model, 474
jellium model, 25, 41

Kanamori parameter, 101
Kohn-Sham energy, 669
Kohn-Sham Green's function, 400
Kohn-Sham system, 398
Kondo effect, 202, 460
Kondo model, 160, 462
Kondo resonance, 436, 461
Kondo temperature, 202, 541
Kramers-Kronig relation, 213, 214
Kronecker delta, 774
Kubo formula, 418

Lagrange multiplier, 616
Lamb shift, 478, 481
Landé g-factor, 7
Landau parameter, 425
Landau expansion, 424
lattice translation vectors, 12
lattice constant, 33
lattice translation vector
    primitive, 12

left-right correlation, 157, 444
Legendre-Fenchel transform, 665
Lehmann amplitudes, 278
Lehmann energies, 278
Lehmann occupations, 278
Lehmann amplitude
    stationary, 280
    time-dependent, 279
Lehmann amplitudes, 278
Lehmann energy, 280
Lehmann occupation, 278
Lehmann representation, 289
level repulsion, 205, 451, 455
level repulsion, 29, 30, 94, 206, 217
Levi-Civita symbol, 20, 774
life-time broadening, 575
life-time broadening, 229, 231, 291, 430, 431, 478
lifetime broadening, 84
linked-cluster theorem, 353
linked cluster, 344, 354
linked diagram, 344, 354
Lorentzian, 504
Luttinger-Ward functional, 336, 388, 389

macro state, 64, 664
magnetic suszeptibility, 41
magnetic moment
    electron, 7
magnetism, 41
magnetization, 7
magneton
    Bohr, 7
magnetoresistance
    colossal, 444
magnon, 451
magnons, 158
many-body perturbation theory, 309
Markov approximation, 480
Martin-Schwinger hierarchy, 269
maximum-entropy principle, 66
maximum coincidence, 140, 685, 688, 689, 695
MBPT, 309
mean-field theory, 68
mean-field approximation, 78
mean-field energy, 93
mean-field theory, 84
memory kernel, 479
mere deformation, 360
metal-insulator transition, 148, 435, 440, 444
micro state, 64, 664
Migdal-Galitskii-Koltun sum rule, 272, 273, 620
minimal model, 25
momentum density, 302
Mott insulator, 148
Mott-Heisenberg, 447
Mott-Hubbard gap, 440
Mott-Hubbard state, 447
Mott insulator, 104, 435, 444

N-representability, 55
natural orbital, 53, 668
natural orbitals, 92
non-degenerate limit, 29
non-propagating
    Green's function line, 366
non-spin-polarized, 512

occupation, 53, 668, 726
occupation-number fluctuations, 441, 611, 761, 766
    correlated, 68, 91, 610
occupation-number operator, 137
occupation-number representation, 130
on-top value
    exchange hole, 121, 122
one-particle-at-a-time operator, 49
one-particle excitation, 82
one-particle irreducible, 344
one-particle operator, 49
one-particle operator
    one-particle-at-a-time, 50
    true, 50
open-oyster diagram, 346
open diagram, 344
open system, 22
optical spectroscopy, 82
orbital
    natural, 53
outer product, 774
outgoing index, 317
overtone, 199
oyster diagram, 346, 349

pair-correlation function, 670
partial-fraction decomposition, 204
particle reservoir, 66
particle-hole ladder diagram, 406
particle-hole symmetry, 301
particle-particle ladder diagram, 407
particle line, 327, 343
partition function, 66
partition function, 254, 664
Pauli repulsion, 127
Pauli equation, 4
Pauli matrix, 6
Peierls distortion, 34, 470
periodic boundary conditions, 33, 41, 483

permanent, 21, 774
permutation operator, 20
perturbation theory
many-body, 309
photoemission, 82
inverse, 82
plasmaron, 296
plasmon, 158, 596
polarization, 296, 409
circular, 483
polarization insertion, 575
polarization diagram, 344
polarization insertion, 413
polarizibility, 413
reducible, 413
polaron
large, 466
small, 466
polaron binding energy, 468
polaron shift, 468
potential
effective, 669
potential
effective, 618
product
dot, 4
dyadic, 4
inner, 4
outer, 4
scalar, 4
product state, 19
projector function, 10, 11, 26
propagator, 174
interaction picture, 311
pure state, 54
pure state, 93

quantization condition, 13
quantum fluctuations, 451
quantum number
angular momentum, 10
magnetic, 10
principal, 10
spin, 10
quasi-particle, 78, 423
quasi-particle peak, 296
quasi-particle shift, 88, 296
quasi-particle weight, 296
quasi-particle energy, 431
quasi-particle shift, 229
quasi-particle wave functions, 283
quasi-particle weight, 430, 431, 434

Rabi oscillations, 474
Rabi oscillation, 474
random-phase approximation, 89, 408, 676
real-space-and-spin
basisset, 5
reciprocal lattice vectors
primitive, 13
regularization, 257
residue theorem, 183
resolvent, 226
resonance integral, 555
retarded potential, 198
Rice-Mele model, 36
ring diagram, 575
ring necklace, 406
rotating-wave approximation, 475
RPA, 89, 408, 676

S-matrix, 311
satellite, 291, 448
scalar
product
vectors, 4
scattering phase shift, 513
scattering T-matrix, 513
screened interaction, 413
screening, 296, 575
self-consistent field, 424
self-energy insertion, 392
self-energy diagram, 344
self-energy functional, 386
self energy, 198, 265, 269, 600
1PI, 334
exchange and correlation, 397
from downfolding, 190
improper, 334
irreducible, 334
proper, 334
reducible, 325, 334
total, 325
self interaction, 59
Shannon entropy, 65
SIAM, 460
sign factor, 350
sign theorem, 350, 352
singlet
antiferromagnetic correlations, 446
singlet-triplet splitting, 157
singlet state, 150, 164
skeleton diagram, 345
skeleton diagram
self-energy, 393
self energy, 392
skewed coordinates, 12
Slater-Condon rules, 57, 139

Slater determinant, 21
Slater integrals, 624
soliton, 471
spectral function
    two-particle, 86
spectral function, 48, 179, 277, 573
    electron addition, 84
    total, 85
spin density, 45, 562
spin-less fermions, 512
spin-restricted, 512
spinor
    two-component, 4
spin orbital, 4
spontaneous emission, 474
SSH model, 36, 470
state
    macro, 64
    micro, 64
state operator, 241
step function, 774
Su-Schrieffer-Heeger model, 36, 470
sum rule
    charge, 32, 62, 90, 121
    energy, 32
superexchange, 157
susceptibility, 419
symmetry factor, 362

tadpole diagram, 345
tensor
    fully antisymmetric, 774
tensor product, 19
thermal equilibrium, 65
thermal Hartree-Fock approximation, 69
thermal single-determinant approximation, 68, 610
thermodynamically consistent, 389
THFA, 69
Thomas-Reiche-Kuhn sum rule, 511
time
    imaginary, 244
time-ordering operator
    contour, 245
    Dyson's, 178
    Wick, 178, 245
time step, 636
total density, 45, 562
trace theorem, 316
transition rate, 81
triplet state, 150, 164
TSDA, 68
two-particle irreducible, 393
two-particle excitation, 82
two-particle irreducible, 345
two-particle operator, 50

U-tensor, 662
universal, 399
universe
    finite, 8

vacuum level, 82
vacuum state, 49
vacuum permittivity, 56
vacuum state, 22, 129, 130, 134
vector product, 774
Verlet algorithm, 636
vertex, 317, 318, 327, 328, 343
    external, 329, 344
    half, 329
vertex corrections, 416
vertex, renormalized, 416
vertex diagram, 344
von-Neumann density matrix, 64
    thermal, 66

Wannier orbital, 10, 517
wheel diagram, 407
Wick's time-ordering operator, 178, 245
Wigner-Weisskopf approximation, 479
Wigner-Weisskopf theory, 474
Wirtinger derivative, 18, 502

Yukawa potential, 89

Zeeman splitting, 437
zero state, 81
zone scheme
    reduced, 88